

ICASP11

Applications of Statistics and Probability in Civil Engineering

Michael H. Faber, Jochen Köhler & Kazuyoshi Nishijima – EDITORS



 **CRC Press**
Taylor & Francis Group
A BALKEMA BOOK

APPLICATIONS OF STATISTICS AND PROBABILITY IN CIVIL ENGINEERING

This page intentionally left blank

PROCEEDINGS OF THE 11TH INTERNATIONAL CONFERENCE ON APPLICATIONS OF
STATISTICS AND PROBABILITY IN CIVIL ENGINEERING, ZÜRICH, SWITZERLAND, 1–4 AUGUST 2011

Applications of Statistics and Probability in Civil Engineering

Editors

M.H. Faber

*Department of Civil Engineering, Technical University of Denmark
Lyngby, Denmark*

J. Köhler

*Institute of Structural Engineering, Swiss Federal Institute of Technology
Zürich, Switzerland*

K. Nishijima

*Department of Civil Engineering, Technical University of Denmark
Lyngby, Denmark*



CRC Press

Taylor & Francis Group

Boca Raton London New York Leiden

CRC Press is an imprint of the
Taylor & Francis Group, an **informa** business

A BALKEMA BOOK

CRC Press
Taylor & Francis Group
6000 Broken Sound Parkway NW, Suite 300
Boca Raton, FL 33487-2742

© 2011 by Taylor & Francis Group, LLC
CRC Press is an imprint of Taylor & Francis Group, an Informa business

No claim to original U.S. Government works
Version Date: 20111207

International Standard Book Number-13: 978-1-4665-0972-6 (eBook - PDF)

This book contains information obtained from authentic and highly regarded sources. Reasonable efforts have been made to publish reliable data and information, but the author and publisher cannot assume responsibility for the validity of all materials or the consequences of their use. The authors and publishers have attempted to trace the copyright holders of all material reproduced in this publication and apologize to copyright holders if permission to publish in this form has not been obtained. If any copyright material has not been acknowledged please write and let us know so we may rectify in any future reprint.

Except as permitted under U.S. Copyright Law, no part of this book may be reprinted, reproduced, transmitted, or utilized in any form by any electronic, mechanical, or other means, now known or hereafter invented, including photocopying, microfilming, and recording, or in any information storage or retrieval system, without written permission from the publishers.

For permission to photocopy or use material electronically from this work, please access www.copyright.com (<http://www.copyright.com/>) or contact the Copyright Clearance Center, Inc. (CCC), 222 Rosewood Drive, Danvers, MA 01923, 978-750-8400. CCC is a not-for-profit organization that provides licenses and registration for a variety of users. For organizations that have been granted a photocopy license by the CCC, a separate system of payment has been arranged.

Trademark Notice: Product or corporate names may be trademarks or registered trademarks, and are used only for identification and explanation without intent to infringe.

Visit the Taylor & Francis Web site at
<http://www.taylorandfrancis.com>

and the CRC Press Web site at
<http://www.crcpress.com>

Table of contents

Preface	xxvii
Editor's foreword	xxix
Organization	xxxii
Conference organization	xxxiii
Sponsors	xxxvii
 <i>GS_119 — Applications (1)</i>	
Fragility curve of sewerage system due to spatial seismic damaged data <i>S. Nagata & K. Yamamoto</i>	3
A new time-reversal imaging method for active Lamb wave damage monitoring of composite structures <i>S. Yan, N.Z. Zhao & Binbin He</i>	5
Probabilistic concept for the validation of the effectiveness of countermeasures against early-age cracking in massive concrete structures <i>M. Krauß</i>	7
Reliability evaluation of pipelines containing stress corrosion cracking defects <i>W. Zhou & S. Zhang</i>	9
Proportionality of interventions to restore structural safety of existing bridges <i>E. Brühwiler</i>	11
 <i>GS_129 — Applications (2)</i>	
Scenario-based seismic loss estimation for concrete buildings in the central US <i>J. Bai, M. Hueste & P. Gardoni</i>	15
Application of the Monte-Carlo method to determine the time required for construction projects—Influence of ranges and correlations on probability distribution <i>C. Hofstadler</i>	16
Advances in probability density evolution analysis of nonlinear stochastic systems <i>J. Li, J.B. Chen & W.L. Sun</i>	18
Probability density evolution method and polynomial chaos expansion for nonlinear random vibration analysis <i>Y.B. Peng, J. Li & J.B. Chen</i>	20
Reliability-based stochastic control for structures using magnetorheological dampers <i>J. Li, Z. Mei & J.B. Chen</i>	21
 <i>GS_139 — Applications (3)</i>	
Random response of chain structure with parameter uncertainties <i>B.G. Liu, Y. Pan, Y. Ning & Z. Shen</i>	25
A Bayesian acoustic emission source location algorithm: Extended model <i>T. Schumacher & D. Straub</i>	27

Structural reliability criteria in relation to on-line control schemes <i>B.J. Leira</i>	29
Probabilistic anomaly detection in structural monitoring data using a relevance vector machine <i>T. Saito</i>	31
Assessment of fatigue crack growth by cohesive zone elements <i>P. Beaurepaire & G.I. Schuëller</i>	33
Reliability-based design recommendations for FRP-reinforced concrete beams <i>S.E.C. Ribeiro & S.M.C. Diniz</i>	35
<i>GS_318 — Applications (4)</i>	
Simulating two-phase microstructures using level-cut filtered poisson fields and genetic algorithms <i>K. Teferra & E.N. Chatzi</i>	39
Variance Reduction Monte Carlo methods for wind turbines <i>M.T. Sichani, S.R.K. Nielsen & P. Thoft-Christensen</i>	41
A computational study of the buffered failure probability in reliability-based design optimization <i>H.G. Basova, R.T. Rockafellar & J.O. Royset</i>	43
Advanced modeling and simulation tools: From surrogates to copulas <i>M. McCullough, A. Kareem, D.K. Kwon & L. Wang</i>	45
A ground motion record selection procedure utilizing a vector-valued intensity measure for optimized incremental dynamic analysis <i>A.I. Theophilou & M.K. Chryssanthopoulos</i>	47
<i>GS_328 — Applications (5)</i>	
Reliability level of structures designed according to the design codes of the Republic of Belarus <i>Dz. Markouski & V. Tur</i>	51
Classification and moral evaluation of uncertainties in engineering modeling <i>C. Murphy, C.E. Harris, Jr. & P. Gardoni</i>	53
Quantitative safety goals—benefits and limits <i>H.-P. Berg & M. Krauß</i>	54
Evaluating the source of the risks associated with natural events <i>P. Gardoni & C. Murphy</i>	56
Metamodeling of aircraft InfraRed Signature dispersion <i>S. Lefebvre, A. Roblin & G. Durand</i>	57
<i>GS_338 — Applications (6)</i>	
Practical reliability approach to urban slope stability <i>R. Chowdhury & P. Flentje</i>	63
Reliability-based optimization of maintenance and repair for a system of bridges <i>C.-A. Robelin & S.M. Madanat</i>	64
System-level optimization of maintenance and replacement decisions for road networks <i>A. Medury & S.M. Madanat</i>	66
Probability-based reliability assessment for real-time hybrid simulation <i>C. Chen & W. Pong</i>	67
Probabilistic estimates of scenario loss through a two-stage Monte Carlo approach <i>I. Ioannou & M.K. Chryssanthopoulos</i>	69

<i>MS_332 — Applications and new developments of system reliability assessment (theory)</i>	
System reliability of soil slopes by Ditlevsen's bounds <i>J. Zhang, W.H. Tang, L.M. Zhang & H.W. Huang</i>	73
A recursive decomposition algorithm for reliability evaluation of binary system <i>W. Liu & J. Li</i>	76
Seismic reliability analysis of wind turbine systems considering rotation effect <i>K. Huang, J.B. Chen & J. Li</i>	78
Global reliability of large nonlinear structures <i>J.B. Chen, J. Li & J. Xu</i>	79
Structural reliability analysis solved through a SVM-based response surface <i>U. Alibrandi & G. Ricciardi</i>	81
Reliability assessment of parallel systems with brittle elements <i>Y.G. Zhao & Z.H. Lu</i>	82
 <i>MS_114 — Bayesian networks for engineering risk analysis</i>	
Risk-based operation and maintenance of offshore wind turbines using Bayesian networks <i>J.J. Nielsen & J.D. Sørensen</i>	87
On the use of Bayesian networks for Probabilistic Seismic Hazard Analysis <i>N.M. Kuehn, C. Riggelsen & F. Scherbaum</i>	89
Damage assessment of stranding events by means of Bayesian Networks <i>L. Garrè, B.J. Leira, T.-H. Nguyen & J. Amdahl</i>	91
Effect of weather conditions, geography and population density on wildfire occurrence: A Bayesian Network model <i>P. Papakosta & D. Straub</i>	93
Post-earthquake decision-making using influence diagrams <i>M.T. Bensi, A. Der Kiureghian & D. Straub</i>	95
 <i>MS_115 — Bridge traffic loading (1)</i>	
Statistical analyses of Weigh-In-Motion data for bridge live load development <i>T.H.T. Chan & T.J. Miao</i>	99
Recent advances in reliability based assessment of highway bridges <i>A. O'Connor & V. Pakrashi</i>	101
Visualization of live-load probability distribution by Random Number generation and a Reliability Analysis of a bridge girder based on the Traffic Flow Model <i>O. Yoshida</i>	103
Development of live load model for long span bridges <i>E.-S. Hwang, H.-M. Koh & S.W. Lee</i>	105
 <i>MS_125 — Bridge traffic loading (2)</i>	
In-situ dynamic behavior of a railway bridge girder under fatigue causing traffic loading <i>A. Herwig & E. Brühwiler</i>	109
Modelling of highway bridge traffic loading: Some recent advances <i>B. Enright, C.C. Caprani & E.J. OBrien</i>	111
Truck load modeling and bridge code calibration <i>G. Fu & J. You</i>	113

<i>GS_113 — Decision analysis</i>	
Maintenance planning for multi-component systems subject to reliability constraints <i>R. Faddoul, W. Raphael, A.H. Soubra & A. Chateauneuf</i>	117
Post-earthquake reliability assessment of structures subjected to after-shocks: An application to L'Aquila earthquake, 2009 <i>F. Jalayer, D. Asprone, A. Prota & G. Manfredi</i>	119
Supporting decisions on global health and life safety investments <i>M.H. Faber & E. Virguez-Rodriguez</i>	121
Defining guidelines for the application of the marginal life saving costs principle for risk regulation <i>K. Fischer, E. Virguez-Rodriguez, M. Sánchez-Silva & M.H. Faber</i>	123
Adaption of option pricing algorithm to real time decision optimization in the face of emerging natural hazards <i>A. Anders & K. Nishijima</i>	125
<i>MS_116 — Fuzzy analysis and soft computing methods in reliability assessment and optimization (1)</i>	
Bayesian quantification of inconsistent information <i>M. Stein & M. Beer</i>	129
Damage assessment of RC slabs using fuzzy pattern recognition with feature selection <i>H. Furuta, W. Adachi, K. Nakatsu, Y. Nomura & H. Hattori</i>	131
Clustering of multiple system reliability design solutions for decision making <i>E. Zio & R. Bazzo</i>	133
Reliability assessment via differential evolution <i>S. Casciati</i>	134
<i>MS_126 — Fuzzy analysis and soft computing methods in reliability assessment and optimization (2)</i>	
Sensitivity measures for fuzzy numbers based on Artificial Neural Networks <i>S. Pannier & W. Graf</i>	139
A method for the verified solution of finite element models with uncertain node locations <i>A.P. Smith, J. Garloff & H. Werkle</i>	141
An approach on soundings for geotechnical site investigation <i>D. Boumezerane, S. Belkacemi & B. Zlender</i>	143
Strong law of large numbers on the Kôpka D-posets <i>M. Kuková & B. Riečan</i>	144
<i>MS_136 — Fuzzy analysis and soft computing methods in reliability assessment and optimization (3)</i>	
Application of Cokriging method to structural reliability problems <i>W. Zhao & W. Wang</i>	149
On predictive densities in fuzzy Bayesian inference <i>R. Viertl</i>	151
Robustness based design of structures under consideration of generalized uncertainty models <i>J.-U. Sickert, S. Pannier, W. Graf & M. Kaliske</i>	153
<i>GS_238 — Life-cycle analysis</i>	
Optimal next inspection time for bridges based on corrosion deterioration <i>D. De León, C. González-Pérez, V. Bisadi, P. Gardoni, M. Head & S. Hurlebaus</i>	157

Probabilistic estimation of seismic fragility parameters for deteriorated reinforced concrete bridges <i>A. Alipour, B. Shafei & M. Shinozuka</i>	159
Probabilistic bridge network life-cycle connectivity assessment and optimization <i>P. Bocchini & D.M. Frangopol</i>	160
Life-cycle analysis of embodied energy for aging bridges subject to seismic hazards <i>J. Ghosh, C. Tapia & J.E. Padgett</i>	162
<i>MS_215 — Maintenance and safety of aging infrastructure (1)</i>	
Reliability analysis of prestressed concrete bridges located in a marine environment <i>M. Akiyama, D.M. Frangopol & I. Yoshida</i>	167
Optimization of assessment strategies for aging bridges <i>A.D. Orcési & D.M. Frangopol</i>	169
Improved bridge capacity rating methods based on system reliability assessment <i>N. Wang, B.R. Ellingwood & A.-H. Zureick</i>	171
Reliability assessment and life prediction for serviceability of concrete bridges <i>D.-G. Lu, W. Jiang, X.-P. Fan & Y.-X. Yang</i>	173
<i>MS_225 — Maintenance and safety of aging infrastructure (2)</i>	
Using information criteria to classify damage states for structural health monitoring <i>H. Noh, A.C. Cheung & A.S. Kiremidjian</i>	177
A Bayesian approach to the assessment of fracture toughness of reactor components <i>M.D. Pandey & M. Wang</i>	179
A numerical study of maintenance strategy for concrete structures in marine environment <i>K.F. Tee & C.Q. Li</i>	181
Structure lifecycle as a non-stationary random process <i>G. Fu & D. Devaraj</i>	184
<i>MS_118 — Meta-models/surrogate models for uncertainty propagation, sensitivity and reliability analysis (1)</i>	
A numerical comparison of Kriging-based sequential strategies for estimating a probability of failure <i>L. Li, J. Bect & E. Vazquez</i>	187
Sensitivity and reliability analysis of a globe valve using an adaptive sparse polynomial chaos expansion <i>M. Berveiller & G. Blatman</i>	189
Use of HDMR metamodel for seismic fragility analysis <i>I. Zentner, E. Borgonovo & S. Tarantola</i>	190
Metamodel-based importance sampling for the simulation of rare events <i>V. Dubourg, F. Deheeger & B. Sudret</i>	192
Principal component analysis and Least Angle Regression in spectral stochastic finite element analysis <i>G. Blatman & B. Sudret</i>	194
<i>MS_128 — Meta-models/surrogate models for uncertainty propagation, sensitivity and reliability analysis (2)</i>	
A Kriging improvement of the Monte Carlo simulation: AK-MCS method <i>B. Echard, N. Gayton & M. Lemaire</i>	199

RPCM: A strategy to perform reliability analysis using polynomial chaos and resampling—Application to fatigue design <i>A. Notin, J.L. Dulong, P. Villon, N. Gayton, M. Lemaire & H. Jaffal</i>	201
Distribution-based global sensitivity analysis in case of correlated input parameters using polynomial chaos expansions <i>Y. Caniou & B. Sudret</i>	203
Reliability-based design optimization of an imperfect submarine pressure hull <i>V. Dubourg, J.-M. Bourinet, B. Sudret & M. Cazuguel</i>	205
Propagation of variability in railway dynamics simulations <i>G. Perrin, C. Funschilling & B. Sudret</i>	207
<i>GS_123 — Model selection, aggregation and testing for probabilistic seismic hazard assessment (1)</i>	
Learning aggregations of ground-motion models using data <i>C. Riggelsen, N. Gianniotis & F. Scherbaum</i>	211
The collaboratory for the Study of Earthquake Predictability: Perspectives on evaluation and testing for seismic hazard <i>D. Schorlemmer, D.D. Jackson, J.D. Zecher & T.H. Jordan</i>	213
Model selection and uncertainty in earthquake hazard analysis <i>I.G. Main, M. Naylor, J. Greenhough, S. Touati, A.F. Bell & J. McCloskey</i>	214
Benefits of the use of precariously balanced rocks and other fragile geological features for testing the predictions of probabilistic seismic hazard analysis <i>J.G. Anderson, J.N. Brune, M. Purvance, G. Biasi & R. Anooshehpour</i>	216
<i>GS_133 — Model selection, aggregation and testing for probabilistic seismic hazard assessment (2)</i>	
Assessing reliability and skill of earthquake forecasting models in Italy <i>W. Marzocchi</i>	221
On the use of observations for constraining probabilistic seismic hazard estimates—brief review of existing methods <i>C. Beauval</i>	223
Quantification of epistemic uncertainties in probabilistic seismic hazard analysis <i>F. Scherbaum, N. Kuehn, M. Ohrnberger, C. Riggelsen & N. Gianniotis</i>	224
<i>MS_137 — Modelling for Risk management in construction projects</i>	
Acceptance criteria for the spatial variability of the concrete cover depth in a Swiss tunnel <i>V. Malioka, S. Matsch & M.H. Faber</i>	229
Cost and time correlations in linear infrastructure construction <i>Y. Moret & H.H. Einstein</i>	232
Germa, a national research project: Multifactor risk control and management in complex civil engineering projects <i>D. Morand, P. Perret, L. Demilecamps & A. Machu</i>	234
Tunnelling optimization by risk analysis techniques <i>D. Kolic</i>	236
Modeling methodology of the Risk Breakdown Structure for project risk management in construction <i>R. Mehdizadeh, D. Breyse & M. Chaplain</i>	238

How integrated should risk management and quality management be? <i>B. Munier & L. Dehouck</i>	240
<i>MS_135 — Multiple hazards risk assessment and mitigation</i>	
Estimation of damage loss due to hurricane wind and induced surge <i>Y. Li, S.O. Bjarnadottir, A. Ahuja, J.W. van de Lindt & T. Dao</i>	243
Methodological and probabilistic issues in multi-hazard engineering design <i>E. Simiu, F.A. Potra & D. Duthinh</i>	245
Decision-making for civil infrastructure exposed to low-probability, high-consequence hazards: The role of risk-aversion <i>E.J. Cha & B.R. Ellingwood</i>	247
<i>GS_316 — Natural hazards modeling</i>	
Hazard-level specific hurricane event characterization <i>Y. Wang & D.V. Rosowsky</i>	251
A comprehensive approach for online fast hurricane-risk prediction <i>A.A. Taflanidis, A.B. Kennedy, J.J. Westerink, M. Hope, S. Tanaka, J. Smith & K.F. Cheung</i>	253
Optimal seismic design of steel structures using approximate methods <i>A. Zacharenaki, M. Fragiadakis & M. Papadrakakis</i>	256
Development and calibration of central pressure decay models for hurricane simulation <i>F. Liu & W. Pang</i>	259
Reliability analysis of the Swiss avalanche warning system <i>M. Bründl & B. Heil</i>	261
<i>MS_216 — Performance-based design for structures subject to natural hazard (1)</i>	
Probabilistic hazard model of inelastic response of SDOF system based on equivalent linearization technique <i>Y. Mori, S. Kojima & K. Ibuki</i>	265
Performance-based design of structures under Aeolian Hazard <i>M. Ciampoli & F. Petrini</i>	267
Probabilistic and deterministic Soil Structure Interaction (SSI) analysis <i>A. Hashemi, T. Elkhoraibi & F. Ostadan</i>	270
Seismic damage assessment of curved bridges using fragility analysis <i>M. Mohseni & T.R. Norton</i>	272
A framework for performance-based design and assessment of buildings subjected to extreme snow loads <i>A.B. Liel, K.A. Jackson & J.M. Geis</i>	274
<i>MS_226 — Performance-based design for structures subject to natural hazard (2)</i>	
Probabilistic assessment of disproportionate collapse potential of steel moment resisting frames <i>G. Xu & B.R. Ellingwood</i>	279
Life-cycle seismic repair cost assessment and sensitivity analysis <i>A.A. Taflanidis</i>	281
A method for probabilistic seismic design of RC structures <i>P. Franchin & P.E. Pinto</i>	283
A statistical analysis of steel truss temperature data recorded during fire resistance tests <i>D.K. Banerjee, E. Simiu, J.L. Gross & R. Kacker</i>	285

<i>MS_124 — Probabilistic calibration of codes (1)</i>	
Conventional probabilistic models for calibration of codes <i>M. Holický & M. Sykora</i>	289
Comparison of load combination models for probabilistic calibrations <i>M. Sykora & M. Holický</i>	291
Calibration of partial factors for design of concrete structures <i>J. Marková & M. Holický</i>	293
Re-calibration of steel tension members design criteria in AASHTO LRFD bridge design code <i>M. Mohseni & T.R. Norton</i>	295
<i>MS_134 — Probabilistic calibration of codes (2)</i>	
Reliability basis for adopting Eurocodes as South African standards <i>J.V. Retief, C. Barnardo & M. Dithinde</i>	299
Reliability-based design/calibration using enhanced Monte Carlo <i>A. Naess, M.A. Maes & M.R. Dann</i>	301
Calculation of partial safety factors <i>T.T. Poutanen</i>	303
<i>MS_214 — Probabilistic methods for the assessment of existing concrete structures (1)</i>	
Corrosion-crack path based probabilistic model to predict the durability behavior of RC components <i>W.L. Jin & X.Z. Wang</i>	307
Random fields for the modeling of deteriorated structures <i>D.L. Allaix, V.I. Carbone & G. Mancini</i>	308
Semi-probabilistic models for the assessment of existing concrete structures <i>P. Tanner, C. Lara & M. Prieto</i>	309
Target reliability levels for assessment of existing structures <i>M. Sykora, M. Holický & J. Marková</i>	311
<i>MS_224 — Probabilistic methods for the assessment of existing concrete structures (2)</i>	
Monitoring and influence lines based performance indicators <i>A. Strauss, R. Wendner, K. Bergmeister & Dan M. Frangopol</i>	315
Jointless bridges—performance assessment of soil-structure interaction <i>R. Wendner, A. Strauss & K. Bergmeister</i>	318
A semi-probabilistic safety-checking format for seismic assessment of existing RC buildings <i>F. Jalayer, L. Elefante, I. Iervolino & G. Manfredi</i>	320
Stochastic process deterioration modelling for adaptive inspections <i>A. Ohadi & T. Micic</i>	322
<i>MS_234 — Probabilistic methods for the assessment of existing concrete structures (3)</i>	
Development and implementation of a semi-probabilistic procedure for the assessment of the future condition of existing concrete structures <i>J. Gulikers</i>	327
Statistical models for the material parameters of damaged concrete bridges <i>R. Lenner, M. Keuser & T. Braml</i>	329

Safety assessment of existing concrete slab bridges for shear capacity <i>R.D.J.M. Steenbergen, A. de Boer & C. van der Veen</i>	331
 <i>MS_138 — Probabilistic methods in hydraulic and spatial structural analysis</i>	
Forecast analysis of traffic flow through urban road tunnel based on Artificial Intelligent method <i>L. Zhong, J. Wu & H. Xia</i>	337
Non-orthogonal polynomial expansion based approach for structural reliability analysis <i>B. Huang & C. Zhang</i>	339
Application of the sampling theory and methods in random decrement technique <i>W. Shi, Z. Li, H. Wu & Y. Lin</i>	341
Randomness of chloride ion concentration in existing concrete under tidal environment <i>J. Zhang, H. Zheng, L. Wang, J. Zhou & J. Wang</i>	342
 <i>GS_112 — Probabilistic modeling in engineering (1)</i>	
Characterization of random fields at multiple scales: An efficient conditional simulation procedure and applications in geomechanics <i>J.W. Baker, A. Seifried, J.E. Andrade & Q. Chen</i>	347
Performance-based probabilistic capacity models and fragility estimates for reinforced concrete column subject to vehicle collision <i>H. Sharma, P. Gardoni & S. Hurlebaus</i>	349
Adaption of car park loads according to DIN 1055-3 to the current trend of increasing vehicle weights <i>H. Schmidt & M. Heimann</i>	350
Probabilistic modelling of HSC and UHPC slender columns in high-rise buildings <i>H. Schmidt & M. Heimann</i>	352
Estimating marginal densities of materials with multiple anomaly types <i>M.P. Enright & R.C. McClung</i>	354
 <i>GS_122 — Probabilistic modeling in engineering (2)</i>	
Probabilistic fatigue design of composite material for wind turbine blades <i>H.S. Toft & J.D. Sørensen</i>	357
Fragility estimates for the Fabela Bridge in Mexico incorporating vibration field data <i>V. Bisadi, M. Head, P. Gardoni, S. Hurlebaus & D. De Leon Escobedo</i>	359
Probabilistic demand model based on the virtual work method and fragility estimates for offshore wind turbine support structures <i>M. Mardfekri, P. Gardoni & J.M. Roesset</i>	361
Probability-based modeling of chloride-induced corrosion in concrete structures including parameters correlation <i>Z. Lounis, B. Saassouh & J. Zhang</i>	363
Identification of the filament stress transfer length in multifilament yarns using fiber bundle model and chain-of-bundles model <i>R. Rypl, R. Chudoba & M. Vořechovský</i>	365
 <i>GS_132 — Probabilistic modeling in engineering (3)</i>	
Probabilistic wind-borne debris trajectory model for building envelope impact risk assessment <i>M. Grayson, W. Pang & S. Schiff</i>	369
Reliability estimation of deteriorated RC-structures considering various observation data <i>I. Yoshida & M. Akiyama</i>	371

A Bayesian framework to predict deformations during supported excavations based on a semi-empirical method <i>J.-K. Park, P. Gardoni & G. Biscontin</i>	373
Effects of structural uncertainty/variability on the linear and yielding response of a shear frame <i>C.R. Wharton, T.L. Attard, A. Chaudhary & M.P. Mignolet</i>	375
Non-parametric Bayesian updating within the assessment of reliability for offshore wind turbine support structures <i>J.G. Rangel-Ramírez & J.D. Sorensen</i>	377
<i>GS_212 — Probabilistic modeling in engineering (4)</i>	
Software for multi-model reliability analysis <i>M. Mahsuli & T. Haukaas</i>	381
Probabilistic modeling of vehicle impact as accidental action <i>C.U. Kunz</i>	383
Benchmark of random fields simulation methods and links with identification methods <i>X.H. Dang, B. Sudret & M. Berveiller</i>	384
Size effect on probability distribution of fatigue lifetime of quasibrittle structures <i>Jia-Liang Le & Z.P. Bažant</i>	386
<i>MS_117 — Probabilistic modelling of the behaviour of timber in structures (1)</i>	
Comparative risk assessment of secondary structures in wide-span timber structures <i>S. Miraglia, P. Dietsch & D. Straub</i>	391
Evolution of probabilistic analysis of timber structures from second-moment reliability methods to fragility analysis <i>D.V. Rosowsky</i>	394
Performance of timber buildings in earthquakes <i>F. Lam, M. Li, R.O. Foschi, S. Nakajima & T. Nakagawa</i>	397
A new approach to consider moisture induced eigen-stress in timber by load combination <i>M. Häglund & F. Carlsson</i>	399
Probabilistic methods for performance based service life evaluation of wooden components <i>S. Thelandersson, T. Isaksson, M. Häglund & E. Frühwald</i>	401
<i>MS_127 — Probabilistic modelling of the behaviour of timber in structures (2)</i>	
Probabilistic robustness analysis of timber structures—results from EU COST action E55:WG3 <i>P.H. Kirkegaard & J.D. Sorensen</i>	405
Modelling of uncertainties of timber structures due to growth inhomogeneities <i>C. Jenkel, R. Lang & M. Kaliske</i>	407
Structural timber detailing <i>A. Jorissen</i>	409
Multiscale variability of stiffness properties of timber boards <i>G. Fink & J. Kohler</i>	411
Hierarchical modeling of structural timber material properties by means of Bayesian Probabilistic Networks <i>M. Deublein, M. Schlosser & M.H. Faber</i>	413
<i>MS_319 — Probabilistic models and methods for risk assessment of lifeline networks and decision support (1)</i>	
Clustering methods for risk assessment of infrastructure network systems <i>C. Gómez, M. Sánchez-Silva & L. Dueñas-Osorio</i>	417

Regional assessment of hurricane risk to Houston bridge infrastructure <i>N. Ataei, C.D. Arnold & J.E. Padgett</i>	419
Vulnerability of the Swiss electric power transmission grid against natural hazards <i>M. Raschke, E. Bilis & W. Kröger</i>	421
Evaluation of seismic vulnerability of sewerage pipelines based on assessment of the damage data in the 1995 Kobe earthquake <i>G. Shoji, S. Naba & S. Nagata</i>	423
Seismic fragility analysis of telecommunication systems <i>K. Leelardcharoen, J.I. Craig, B.J. Goodno & L. Dueñas-Osorio</i>	425
<i>MS_329 — Probabilistic models and methods for risk assessment of lifeline networks and decision support (2)</i>	
Recursive reliability assessment of radial lifeline systems with correlated component failures <i>J. Rojo & L. Dueñas-Osorio</i>	429
Post-disaster damage detection for pipeline networks by Matrix-based System Reliability analysis <i>W.-H. Kang & J. Song</i>	431
Efficient identification of critical disjoint cut sets and link sets for network reliability analysis <i>H.-W. Lim & J. Song</i>	434
Seismic risk assessment of spatially-distributed systems using ground-motion models fitted considering spatial correlation <i>N. Jayaram & J.W. Baker</i>	436
A FORM-based analysis of lifeline networks using a multivariate seismic intensity model <i>M. Miller, J. Baker, H.-W. Lim, J. Song & N. Jayaram</i>	438
<i>GS_211 — Probabilistic seismic hazard analysis (1)</i>	
Probabilistic design of supplemental dampers for base-isolated bridges <i>A.A. Taflanidis</i>	443
Probabilistic seismic hazard analysis incorporating basin amplification for shallow crustal earthquakes <i>T. Itoi & T. Takada</i>	445
Spatial sensitivity of seismic hazard results to background seismic activity models <i>N. Yilmaz & M.S. Yucemen</i>	448
Stochastic field analyses of the site amplification factors based on observed and inversely analyzed real strong ground motion in Japan <i>M. Fukuda, N. Narita, K. Ogawa, M. Sugai & A. Nozu</i>	450
Development of seismic margin-risk diagram <i>M. Nakajima, Y. Ohtori & K. Hirata</i>	452
<i>GS_221 — Probabilistic seismic hazard analysis (2)</i>	
Orientation dependency of peak ductility demand for seismic performance evaluation <i>K. Goda</i>	455
Methodology and results of a nuclear power plant seismic probabilistic safety assessment <i>M. Richner, S. Tinic, D. Proske, M. Ravindra, R. Campbell, F. Beigi & A. Asfura</i>	456
Redundancy effects on seismic reliability of steel frame structures <i>Q. Li, Q. Zhang, J. Fan & C. Zhang</i>	457
Regression models for predicting the probability of near-fault earthquake ground motion pulses, and their period <i>S.K. Shahi & J.W. Baker</i>	459

Performance-based direct displacement design of engineered timber building in seismic regions <i>Y. Wang, D.V. Rosowsky & W.C. Pang</i>	461
<i>GS_231 — Probabilistic seismic hazard analysis (3)</i>	
Influence of material strength scattering on the ductile response of steel structures <i>M. Gündel, B. Hoffmeister & M. Feldmann</i>	465
A response spectrum based stochastic approach to estimate the peak response of structures subject to seismic pounding <i>A. Giaralis & P.D. Spanos</i>	467
On the schematization of design response spectra as a stochastic model <i>S. Silvestri, G. Gasparini & T. Trombetti</i>	469
A new procedure for probabilistic seismic hazard analysis <i>G. Gasparini, S. Silvestri & T. Trombetti</i>	470
Vector-valued probabilistic seismic hazard analysis of correlated ground motion parameters <i>P. Bazzurro & J. Park</i>	471
<i>MS_236 — Progresses and challenges in probabilistic modeling of tropical storm risks</i>	
Hurricane hazard characterization for performance-based design <i>D.V. Rosowsky, Y. Wang & K.H. Lee</i>	475
Tropical cyclone return periods: Comparison of a stochastic track model with an extreme value analysis of historic data <i>J. Kleinn & T.M. Hall</i>	477
Future typhoon projection using stochastic typhoon model under global climate change <i>T. Yasuda, S. Nakajo, N. Mori, H. Mase, Y. Hayashi & S. Kunitomi</i>	479
Challenges in developing the Florida public hurricane loss model for personal residential and commercial residential structures <i>G.L. Pita, J.-P. Pinelli, T. Johnson, K. Gurley, J. Weekes & S. Hamid</i>	481
Issues of epistemic uncertainty treatment in decision analysis for tropical cyclone risk management <i>M. Graf & K. Nishijima</i>	483
Assessment of hurricane risk and estimates of insured losses using catastrophe modeling <i>S.S. Hamid, J.-P. Pinelli, S.-C. Chen & K. Gurley</i>	485
<i>MS_326 — Recent advances in geotechnical risk and reliability (1)</i>	
Methods for incorporating a variety of site response estimates into seismic hazard maps <i>E.M. Thompson & L.G. Baise</i>	489
Reliability-based design of shallow foundations in cohesionless soils under compression loading: Ultimate limit state <i>S.O. Akbas & F.H. Kulhawy</i>	491
Effect of spatial variability on reliability evaluation of an earth slope <i>Y. Wang, Z.J. Cao & S.K. Au</i>	493
Probabilistic characteristics of strip footing bearing capacity evaluated by random finite element method <i>J. Pieczyńska, W. Pula, D.V. Griffiths & G.A. Fenton</i>	495
Evaluation of reliabilities of drilled shafts using bi-directional pile load test results <i>J.H. Park, D. Kim, K. Kwak, J.H. Lee & M. Chung</i>	497

<i>GS_336 — Recent advances in geotechnical risk and reliability (2)</i>	
Development of a computer-based evaluation system for soil parameters in the reliability design method	501
<i>Y. Watabe, M. Tanaka, T. Nishioka & I. Nozaki</i>	
On risk-based geotechnical site investigation of flood defenses	504
<i>T. Schweckendiek, P.H.A.J.M. van Gelder & E.O.F. Calle</i>	
Challenges in limit equilibrium based slope reliability problems	507
<i>J. Ching, K.-K. Phoon & Y.-G. Hu</i>	
Spatial distributions of strength of an embankment based on synthesis of sounding tests and surface wave method	509
<i>S. Nishimura, Y. Takayama, K. Fujisawa, M. Suzuki & A. Murakami</i>	
Evaluating model uncertainty of a CPT-based model for earthquake-induced soil liquefaction	512
<i>Y.F. Lee, Y.Y. Chi & C.H. Juang</i>	
<i>GS_312 — Reliability methods (1)</i>	
System reliability analysis of fatigue-induced, cascading failures using critical failure sequences identified by selective searching technique	517
<i>N. Kurtz, J. Song, S.-Y. Ok & D.-S. Kim</i>	
Estimation of failure rates of crude product pipelines	520
<i>A.W. Dawotola, P.H.A.J.M. van Gelder, J.J. Charima & J.K. Vrijling</i>	
Reliability analysis with probabilistic and interval variables	523
<i>K. Zaman, M. McDonald, S. Rangavajhala & S. Mahadevan</i>	
Dormant reliability analysis for dam spillways	524
<i>M. Kalantarnia, L. Chouinard & S. Foltz</i>	
On the utilization of monitoring data in an ultimate limit state reliability analysis	526
<i>S. Thöns, M.H. Faber & W. Rücker</i>	
<i>GS_322 — Reliability methods (2)</i>	
Identification of random variables via Markov Chain Monte Carlo: Benefits on reliability analysis	531
<i>F. Lanata & F. Schoefs</i>	
Risk quantification of fatigue-induced sequential failures by Branch-and-Bound method employing system reliability bounds	533
<i>Y.-J. Lee & J. Song</i>	
Reliability analysis of corroding RC members using adaptive Response Surface Method	535
<i>A.N. Kallias & M.I. Rafiq</i>	
Uncertain and unavoidable—reliability estimation in wave and tidal energy systems	537
<i>J. Flinn & C.B. Ferreira</i>	
Post earthquake bridge damage assessment coupling field data and reliability tool	539
<i>M. Torbol, R. Baghaei, J. Kang & M. Feng</i>	
<i>MS_235 — Reliability of marine energy converters</i>	
Reliability of tidal stream turbine blades	543
<i>D.V. Val & L. Chernin</i>	
Reliability of power train components in tidal stream turbines	545
<i>D.V. Val & C. Iliev</i>	

Reliability methodology for evaluating tidal stream devices <i>T.M. Delorm & P.J. Tavner</i>	547
Probabilistic design of wave energy devices <i>J.D. Sørensen, J.P. Kofoed & C.B. Ferreira</i>	549
<i>MS_217 — Risk and reliability analysis for interdependent infrastructure systems (1)</i>	
Seismic risk and hierarchy importance of interdependent lifelines: Methodology and important issues <i>M.N. Alexoudi, K.G. Kakderi & K.D. Pitilakis</i>	553
Modeling cascading failures in ‘systems of systems’ with uncertain behavior <i>E. Zio & G. Sansavini</i>	555
Modeling of restoration process associated with lifeline systems and the interdependency due to a seismic disaster <i>G. Shoji & A. Toyota</i>	557
A new modeling approach for resolving CI interdependency issues <i>C. Nan & W. Kröger</i>	559
<i>MS_227 — Risk and reliability analysis for interdependent infrastructure systems (2)</i>	
Models of interdependence propagation for the fragility assessment of urban networks <i>I. Hernandez-Fajardo & L. Dueñas-Osorio</i>	563
On robust decision-making in interdependent economic and infrastructure systems <i>R. Pant & K. Barker</i>	565
Broadening the discourse on infrastructure interdependence by modeling the “Ecology” of infrastructure systems <i>S. LaRocca, S.D. Guikema, J. Cole & E. Sanderson</i>	567
Geographical vulnerability analysis of interdependent critical infrastructures <i>J. Johansson & H. Hassel</i>	568
<i>GS_219 — Risk assessment (1)</i>	
Revisiting risk management in major infrastructure projects—why a socio-technical systems approach makes sense <i>N.J. Smith, B. Aritua, C. Clegg & R. Challenger</i>	573
Building owners’ requirement for seismic risk communication during structural design <i>K. Hirata & T. Ishikawa</i>	575
Global flood risk assessment of major port cities <i>N. Lind, M. Pandey & J. Nathwani</i>	577
Assessment of risk to life safety in fire compartments using an adaptive response surface methodology <i>C. Albrecht & D. Hosser</i>	579
Effects of uncertainty on the seismic collapse risk of light-frame wood buildings <i>Y.-J. Yin & Y. Li</i>	582
<i>GS_229 — Risk assessment (2)</i>	
Estimation of risk for design of structures exposed to combined effects of hurricane wind speed and storm surge hazards <i>L.T. Phan & E. Simiu</i>	587

Risk assessment for road tunnels in Germany—development and application of quantitative methods <i>F. Heimbecher & B. Kohl</i>	589
Risk assessment for the hazard scenario “Braking action on double track railway bridges” <i>C. Fermaud, F. Stenger, V. Malioka & M. Schenkel</i>	591
Regional risk by reliability analysis <i>M. Mahsuli & T. Haukaas</i>	593
A probabilistic framework for generic fire risk assessment and risk-based decision making in buildings <i>G. De Sanctis, K. Fischer, J. Kohler, M. Fontana & M.H. Faber</i>	595
 <i>MS_218 — Risk assessment and decision support systems for interdependent lifeline infrastructures (1)</i>	
Optimum interface topologies between urban infrastructure systems <i>M. Ouyang, L. Dueñas-Osorio & X. Min</i>	599
Risk assessment of shutdown of water purification plant caused by Tohnankai-Nankai earthquakes tsunami surge <i>M. Nakai & M. Miyajima</i>	601
Disaster restoration support technologies for electric power distribution equipment <i>Y. Shumuta, T. Todou, K. Masukawa & T. Ishikawa</i>	603
Ethical consideration for appropriate structural safety <i>J. Kanda & D.G. Elms</i>	605
Risk assessment and maintenance of existing trunk lines with a new subsidiary system under seismic and deteriorating environments <i>T. Imai & T. Koike</i>	607
 <i>MS_228 — Risk assessment and decision support systems for interdependent lifeline infrastructures (2)</i>	
Seismic risk and hierarchy importance of interdependent lifelines and infrastructures within port facilities: Application in Thessaloniki’s Port (Greece) <i>K.G. Kakderi, M.N. Alexoudi & K.D. Pitilakis</i>	611
A fuzzy comparative model for integrated risk ranking and mitigation prioritization of infrastructures; part 1: Methodology <i>M.B. Javanbarg, C. Scawthorn, J. Kiyono, B. Shahbodaghkhan & S. Takada</i>	614
A fuzzy comparative model for integrated risk ranking and mitigation prioritization of infrastructures; part 2: Application <i>J. Kiyono, M.B. Javanbarg, S. Takada, C. Scawthorn & M. Kobayashi</i>	616
A questionnaire survey to customers on willingness to pay for earthquake countermeasures of water supply system by using risk communication <i>Y. Taniguchi & M. Miyajima</i>	618
 <i>MS_131 — Risk-based assessment of climate change adaptation strategies for infrastructure</i>	
Deterioration of concrete structures in Australia under changing environment <i>M.G. Stewart, X. Wang & M. Nguyen</i>	623
Probabilistic-based assessment of the impacts of climate change on hurricane loss and adaptation strategies <i>S.O. Bjarnadottir, Y. Li & M.G. Stewart</i>	625

Considerations for probabilistic assessment of the effect of global warming on durability of corroding RC structures <i>E. Bastidas-Arteaga, F. Schoefs & M.G. Stewart</i>	627
Development of adaptive flood risk management strategies under uncertainty <i>H. Harvey & J.W. Hall</i>	630
Probabilistic assessment of clay earthfill dams subject to variable precipitation <i>M.-C. Preziosi & T. Micic</i>	632
<i>MS_323 — Robustness of structures (1)</i>	
Robustness of structures—a report on a joint European project <i>M.H. Faber, A.C.W.M. Vrouwenvelder, J.D. Sørensen, M.K. Chryssanthopoulos & H. Narasimhan</i>	637
A threat independent approach to evaluating the robustness of structures <i>S.M. Marjanishvili</i>	640
Risk and robustness of road tunnels <i>D. Diamantidis & M. Holický</i>	642
Progressive collapse in multi-storey steel frames: The effect of varying column spacing <i>V. Janssens & D.W. O'Dwyer</i>	643
Achieving robustness and mitigating risk of disproportionate collapse in building <i>B.R. Ellingwood</i>	645
<i>MS_333 — Robustness of structures (2)</i>	
Probability based assessment of bridge exposed to extraordinary circumstances <i>I. Björnsson, S. Thelandersson & K. Petersen</i>	649
Robust flood defences in a changing environment <i>H.G. Voortman & M. Veendorp</i>	652
Experimental and computational assessment of robustness of steel and reinforced concrete framed buildings <i>J.A. Main, Y. Bao, F. Sadek & H.S. Lew</i>	654
Fragility curve of steel containment failure due to hydrogen deflagration <i>D. Proske & M. Richner</i>	656
Seismic damage probabilities for segmented buried pipelines <i>S. Toprak, E. Nacaroglu & A.C. Koc</i>	657
A reliability-based measure of robustness for concrete structures subjected to corrosion <i>E.S. Cavaco, L.A.C. Neves & J.R. Casas</i>	660
<i>MS_237 — Social perspectives for hazards decision</i>	
Making the case for resilience investments <i>E. Seville, J. Vargo, J. Stevenson & A. Stephenson</i>	665
Rebuilding L'Aquila following the 2009 earthquake: Priorities and perspectives <i>A.B. Liel, R.B. Corotis, J. Sutton, G. Camata, E. Spacone & R. Holtzman</i>	667
The function of regulations and incentives for societal safety <i>A. Lentz & I.B. Kroon</i>	669
Political pitfalls in hazards planning <i>R. Corotis</i>	671
<i>MS_314 — Spatial probabilistic modeling of deterioration and inspection (1)</i>	
Optimization of inspection and monitoring of structures in case of spatial fields of deterioration/properties <i>F. Schoefs, T.V. Tran & E. Bastidas-Arteaga</i>	675

Repair efficiency and Life-Cycle Cost of RC bridge deck maintenance subjected to spatially variable corrosion damage <i>J.A. Mullard & M.G. Stewart</i>	678
A unified probabilistic treatment for in-line inspection with respect to detectability, reportability, false call potential and depth sizing <i>M.A. Maes & M.R. Dann</i>	681
Spatial hierarchical POD model for in-line inspection data <i>M.R. Dann & M.A. Maes</i>	683
 <i>MS_324 — Spatial probabilistic modeling of deterioration and inspection (2)</i>	
Reliability of pipelines under corrosion and mechanical damage <i>F.A.V. Bazán & A.T. Beck</i>	687
The performance of sampling inspections for localized deterioration process <i>S.P. Kuniewski & J.A.M. van der Weide</i>	689
Influence of including spatial variability modelling on whole life management of concrete structures <i>A.J. O'Connor</i>	690
Reliability updating with inspection and monitoring data in deteriorating reinforced concrete slabs <i>D. Straub</i>	692
 <i>MS_334 — Spatial probabilistic modeling of deterioration and inspection (3)</i>	
Spatial deterioration model updating of aging RC structures based on inspection information <i>K.G. Papakonstantinou & M. Shinozuka</i>	697
Statistical analysis of the surfaces of corroded mild steel plates <i>R.E. Melchers, M. Ahammed, R. Jeffrey & G. Simundic</i>	699
Random field modelling of spatial variability in FRP composite materials <i>S. Sriramula & M.K. Chryssanthopoulos</i>	701
Spatial variability of potential fields in reinforced concrete structures <i>S. Kessler, C. Gehlen, D. Straub & M. Huber</i>	703
 <i>GS_317 — Statistical investigations and probabilistic modeling (1)</i>	
Bayesian models for the detection of high risk locations on Portuguese motorways <i>S.M. Azeredo-Lopes & J.L. Cardoso</i>	709
Statistical analysis of mechanical properties of prestressing strands <i>L. Jacinto, M. Pipa, L.O. Santos & L.C. Neves</i>	711
Probabilistic model for damage accumulation in concrete tunnel lining and its application to optimal repair strategy <i>H. Tanaka, O. Maruyama & A. Sutoh</i>	713
Application of extreme value theory to discriminate between failure modes <i>R.E. Melchers</i>	715
Development of state-based Markovian transition probabilities for bridge condition estimation <i>T.M. Reale & A.J. O'Connor</i>	717
 <i>GS_327 — Statistical investigations and probabilistic modeling (2)</i>	
A model for the failure probability of components of electrical substations under seismic load <i>M. Raschke</i>	721

A study of the stochastic properties of auto-correlation coefficients for microtremor data simultaneously observed at two sites <i>H. Morikawa, K. Iiyama & M. Oho</i>	723
A Bayesian approach to analysing structural uncertainties in flood inundation models <i>L. Manning & J.W. Hall</i>	726
Seismic loss modeling of two building portfolios using generalized Pareto model and copula <i>K. Goda & J. Ren</i>	728
ACER function plots as a diagnostic tool for extreme value prediction <i>A. Naess & O. Gaidai</i>	730
 <i>MS_337 — Statistical investigations and probabilistic modeling (3)</i>	
Statistical analysis of NDT results for analysing the efficiency of repair techniques of wharves: The MAREO project <i>F. Benmeddour, G. Villain, X. Dérobert, O. Abraham, F. Schoefs, M. Perrin, S. Bonnet & M. Choinska</i>	735
The $\alpha\delta$ method for reliability modeling and improvement of NDT-tools for Risk Based Inspection (RBI): Application to corroded structures <i>F. Schoefs & J. Boéro</i>	738
Fluctuation Analysis of stochastic physical systems based on Probability Density Evolution Method <i>W.L. Sun, J. Li & J.B. Chen</i>	741
The use of quasi-symmetric point method in probability density evolution method <i>J. Xu, J.B. Chen & J. Li</i>	743
 <i>MS_331 — Stochastic models and simulation of earthquake ground motions</i>	
Seismic risk sensitivity analysis focusing on stochastic ground motion modeling <i>A.A. Taflanidis & C. Vetter</i>	749
Simulation of seismic ground motion time histories from data using a non Gaussian stochastic model <i>I. Zentner, F. Poirion & P. Cacciola</i>	752
Stochastic model for earthquake ground motion using wavelet packets <i>Y. Yamamoto & J.W. Baker</i>	754
Simulation of non-stationary differential support motions accounting for varying soil conditions <i>K. Konakli & A. Der Kiureghian</i>	757
Stochastic simulation of near-fault ground motions for specified earthquake and site characteristics <i>M. Dabaghi, S. Rezaeian & A. Der Kiureghian</i>	759
 <i>GS_222 — Structural reliability (1)</i>	
Variance reducing capacity of concrete conformity control in structural reliability analysis under parameter uncertainties <i>R. Caspeele & L. Taerwe</i>	763
Corrosion effects onto the safety of steel sheet pile walls in marine environment <i>P. Osório, C. Odenbreit, M. Greger & T. Vrouwenwelder</i>	765
Robustness analysis of structural systems considering accidental actions <i>N. Kagh, A. Orcési & C. Cremona</i>	767
A coupling Bayesian/reliability approach for robust updating applications <i>B. Richard, L. Adelaide, A. Orcési & C. Cremona</i>	769

Comparative study of safety formats for nonlinear finite element analysis of concrete structures <i>H. Schlune, M. Plos & K. Gylltoft</i>	771
<i>GS_232 — Structural reliability (2)</i>	
Probabilistic analysis of iced structures <i>J. Marková</i>	775
Probabilistic durability assessment of power-producing facilities <i>M. Holický & J. Marková</i>	777
Uncertainty effects on dynamic response evaluations of wind energy offshore platform <i>K. Kawano, Y. Kimura, K. Nagafuchi & T. Takahashi</i>	779
Seismic risk assessment of building-elevator systems based on simulated ground motion considering long period components and phase characteristics <i>M. Kohiyama & T. Kita</i>	781
Structural reliability analysis of steel sheet-pile seawalls subjected to corrosion in harbour environment <i>J. Boéro, H. Yáñez-Godoy, B. Capra & F. Schoefs</i>	783
<i>GS_311 — Structural reliability (3)</i>	
Reliability-based design optimization via a concurrent process <i>K.W. Liao</i>	787
Efficient method for the probability assessment of ellipsoidal limit state surface <i>S.D. Koduru</i>	789
Modeling structural degradation of RC bridge columns subjected to cumulative seismic damage and their fragility estimates <i>R. Kumar & P. Gardoni</i>	791
Calibration of reliability-based load rating method for New York State <i>M. Ghosn, B. Sivakumar & F. Miao</i>	792
Structural reliability in the fire situation, the effect of active fire safety <i>J.-B. Schleich</i>	794
<i>GS_321 — Structural reliability (4)</i>	
Seismic fragility of RC bridges using the data obtained from nondestructive testing <i>Q. Huang, P. Gardoni & S. Hurlbaas</i>	799
Use of BWIM data for bridge assessment <i>M. Petschacher</i>	800
Harmonic wavelet-based statistical linearization of the Bouc-Wen hysteretic model <i>P.D. Spanos & I.A. Kougioumtzoglou</i>	802
Reliability analysis of stresses in prestressed concrete girder under service live load <i>E.-S. Hwang, I.-R. Paik & S.H. Nguyen</i>	804
Fragility analysis for sensor fault detection of smart structures <i>Y. Kim & J.-W. Bai</i>	806
<i>MS_315 — The treatment of uncertainties in large-scale stochastic systems (1)</i>	
Stochastic responses of Navier-Stokes equations computed with dynamically orthogonal field equations <i>T.P. Sapsis & P.F.J. Lermusiaux</i>	809
Seismic reliability of frame structures with non-Gaussian system properties <i>G. Stefanou & M. Fragiadakis</i>	811

Pile settlement analysis on spatially random soil <i>G. Stefanou, G. Pittos & M. Papadrakakis</i>	812
A response surface method for nonlinear stochastic dynamic analysis <i>U. Alibrandi</i>	813
Estimating seismic performance uncertainty using IDA with progressive accelerogram-wise latin hypercube sampling <i>D. Vamvatsikos</i>	814
 <i>MS_325 — The treatment of uncertainties in large-scale stochastic systems (2)</i>	
The use of homotopy WHEP algorithm for solving stochastic differential equations <i>M.A. El-Tawil</i>	819
Efficient sensitivity analysis of complex engineering problems <i>T. Most</i>	820
Simulation of strongly non-Gaussian stochastic vector processes using translation process theory <i>M.D. Shields & G. Deodatis</i>	822
Computational reliability analysis of Soil-Foundation-Structure Interaction (SFSI) systems <i>Q. Gu, M. Barbato & J.P. Conte</i>	824
 <i>MS_213 — Uncertainty and imprecision in geotechnical and structural engineering (1)</i>	
Error proneness in construction <i>F. Knoll</i>	829
The role of uncertainty in the political process for risk investment decisions <i>H. Bonstrom, R. Corotis & K. Porter</i>	831
Evaluation of the safety criteria of Brazilian Standard NBR 6118 for slender members based on reliability analyses <i>F.R. Stucchi, S.H.C. Santos & R.M. Franco</i>	833
Uncertainty analysis in geotechnical engineering—a comparative study of selected approaches <i>M. Beer, Y. Zhang, S.T. Quek & K.K. Phoon</i>	835
Debris flow impact uncertainty modeling with Grey numbers <i>D. Proske</i>	837
 <i>MS_223 — Uncertainty and imprecision in geotechnical and structural engineering (2)</i>	
Evaluation and implications of soil variability in tunneling <i>M. Huber, P.A. Vermeer & C. Moormann</i>	841
Risks of analyses with lateral earth pressure load <i>P. Koudelka</i>	842
Uncertainty correlation in structural performance assessment <i>J.-A. Goulet & I.F.C. Smith</i>	844
Seismic response evaluations of ground pavement system with uncertainty <i>K. Nagafuchi, K. Kawano & Y. Kimura</i>	846
Resolution and uncertainty analysis in Bayesian FE model updating applied to the damage assessment in a reinforced concrete beam <i>E. Simoen, E. Reynders, G. Lombaert & G. De Roeck</i>	848
 <i>MS_233 — Uncertainty and imprecision in geotechnical and structural engineering (3)</i>	
An extension of limit state functions by parameterized probability measures <i>T. Fetz</i>	853

On the optimal scaling of the Modified Metropolis-Hastings algorithm <i>K.M. Zuev, J.L. Beck & L.S. Katafygiotis</i>	855
Non-specificity modeling of concrete cracking strength using possibility theory <i>J.J. Kim, M.M. Reda Taha & T.J. Ross</i>	856
Likelihood-based representation of imprecision due to sparse point data and/or interval data <i>S. Sankararaman & S. Mahadevan</i>	858
Response bounds for structures with interval stiffness <i>N. Impollonia, S. Zito, G. Muscolino & F. Saitta</i>	859
<i>MS_313 — Uncertainty and imprecision in geotechnical and structural engineering (4)</i>	
Stochastic optimal structural control <i>K. Marti</i>	863
Risk acceptance criteria based on uncertain estimates of structural failure probabilities <i>S.G. Reid</i>	865
Interval finite elements for nonlinear material problems <i>M.V. Rama Rao, R.L. Mullen & R.L. Muhanna</i>	867
Reliability-based design for steel drive-in racks under forklift truck impact <i>H. Zhang, B.P. Gilbert & K.J.R. Rasmussen</i>	869
Reliability analysis of steel scaffold shoring structures <i>H. Zhang, K.J.R. Rasmussen & B.R. Ellingwood</i>	871
<i>GS_111 — Uncertainty, statistics and probability (1)</i>	
Robust simulation for sensitivity analysis of catastrophe risk losses <i>R.J. Murnane, C.E. Taylor, T. Jagger & Z. Hu</i>	875
Propagation of aleatoric uncertainty in light-frame wood shear walls <i>S.M.H. Shirazi & W. Pang</i>	878
Shear strength variability of sandy and fine-grained soils <i>P. Koudelka</i>	881
Correlation in probabilistic simulation <i>M. Vořechovský</i>	883
Computational intelligence techniques with modern applications of fuzzy pattern classification <i>I.F. Iatan</i>	885
<i>GS_121 — Uncertainty, statistics and probability (2)</i>	
Reliability analysis of a brittle fracture due to crack instability using sequential Monte Carlo simulation <i>L.E. Garciano & I. Yoshida</i>	889
Life-cycle assessment and uncertainty in modelling: Introduction of a possible “aid” index <i>E. Garavaglia</i>	891
Mechanical characterisation of lacustrine clay by interpreting spatial variability in CPTU measurements <i>G. Vessia, F. Casini & S. Springman</i>	893
Dynamic response variability of a small span bridge for high speed rail traffic <i>J. Rocha, A.A. Henriques & R. Calçada</i>	896

This page intentionally left blank

Preface

The International Conference on Applications of Statistics and Probability in Civil Engineering (ICASP), one of the two major conferences on statistics, reliability, probability and risk in engineering, is realized through the International Civil Engineering Risk and Reliability Association (CERRA).

CERRA has been formed for the purpose of promoting professional analysis of risk and reliability associated with civil engineering systems, see also <http://www.ce.berkeley.edu/~cerra/>. The principal activity of CERRA is the sponsoring and overseeing of the organization of the ICASP conferences. These conferences have been and will be held about every four years.

The first ICASP conference took place in Hong Kong in 1971 and the latest in Tokyo in 2007. The conferences address all relevant aspects of safety and reliability of civil engineering systems, including probabilistic structural engineering, soil mechanics, and risk analysis. The emphasis is on applications as well as on theory.

This page intentionally left blank

Editor's foreword

Over the last century society has undergone tremendous changes. Developments in science and technology have facilitated the exploitation of resources, development of infrastructure, production and traffic systems—core societal activities of key importance for the safety and welfare as we know it today.

Despite the many positive achievements the societal activities are also associated with risks—risks which need to be managed. In this respect there are still substantial challenges to overcome. Large parts of the world population, under the pressures of harsh environmental conditions and natural hazards, are struggling to maintain their livelihoods. Population growth, increasing land utilization and reducing natural resources necessitate improved efficiency of existing technologies and the development of new ones. Increasing complexity of societal functionalities and interdependencies between infrastructures and urban habitats amplify consequences of malfunctions and failures. Malevolence is yet another hazard with potentially devastating consequences and most recently sustainable development and how to deal with climatic changes have been added to the international list of challenges.

From the perspective of assessing and quantifying risks we as a profession have achieved very substantial progress over the last decades. However, in regard to the broader utilization of risk assessment as a means for societal strategic and operational planning there is still a great need for further development.

With the present conference it is our intention not only to focus on the more traditional technical issues relating to the assessment of reliability and risks for individual structures, facilities and activities but to encourage some emphasis on the societal context of the decision making problems including the interaction between stakeholders. By such a more holistic perspective the aim is to contribute to an enhanced and sustainable allocation of limited resources for the improvement of safety, environment and economy.

The decision problems we are facing are complex and subject to significant uncertainties, however, as stated by Henry Ford; “The best we can do is size up the chances, calculate the risks involved, estimate our ability to deal with them, and then make our plans with confidence”.

The conference comprises 26 mini-symposia and 11 general sessions. The mini-symposia have been organized by researchers, engineers and decision makers who have had the interest, ability and commitment to contribute strategically to the focus of the conference. The general sessions comprise individual contributions organized in accordance with the general themes of the conference. At the time of writing this Foreword we estimate that there will be 359 presentations by about 400 participants representing 39 countries.

These printed proceedings contain the submitted two-page abstracts of the papers presented orally at the conference. The papers themselves are made available to the participant of the conference on DVD. This DVD can also be acquired directly from Balkema (<http://www.taylorandfrancis.com/>).

We would like to take this opportunity to thank first of all the participants of the conference, who made this event interesting and important. Also we would like to thank all the session organizers for their great efforts in suggesting timely and interesting themes and not least for the organization of their sessions. The scientific committee members are warmly thanked for carrying the main workload with regard to the reviewing of the many papers submitted to the conference. ETH and the support staff at ETH have helped the ICASP11 on especially the logistical aspect of the organization and also with valuable advice.

The CERRA board members are thanked for supporting with the nomination for the Allin Cornell Award which was given for the first time at this conference.

A special acknowledgment is forwarded to the sponsors of the conference. Their support underlined the importance of the event. They made it possible to provide financial support for the CERRA Student Recognition Awards and furthermore helped to keep the registration fee low.

We forward our sincere thanks to the members of the organizing committee. Roberto Pascolo is thanked for his expertise and great help on all IT matters arising in the process. Margaretha Neuhaus has

managed the finances and last but not least we want to thank Annette Walzer for keeping the work and progress of preparations on track—firmly and lovingly. The success of the conference rests very much on her efforts.

It has been a great honor for us to lead the organization of ICASP11 and we hope you will find the papers enclosed in this book as interesting as we did—we wish you all enjoyable reading.

Michael Havbro Faber
Jochen Köhler
Kazuyoshi Nishijima
August 2011, Zurich

Organization

KEYNOTE LECTURES

The FuturICT Flagship: Creating Socially Interactive Information Technologies for a Sustainable Future, Dirk Helbling, ETH Zurich.

Risk Based Adaptation to Climate Change, Kjell Eriksson, Det Norske Veritas AS.

Beyond the expected limits of experts – East Japan Earthquake Disaster, Jun Kanda, University of Tokyo.

SESSIONS

Mini-Symposia

Applications and new developments of system reliability assessment (theory), Jie Li, Yan-Gang Zhao.

Bayesian networks for engineering risk analysis, Daniel Straub, Armen Der Kiureghian.

Bridge traffic loading, Colin Caprani, Eugene O'Brien.

Fuzzy analysis and soft computing methods in reliability assessment and optimization, Jan-Uwe Sickert, Michael Beer.

Maintenance and Safety of Aging Infrastructure, Dan M. Frangopol, Yiannis Tsompanakis.

Meta-models/surrogate models for uncertainty propagation, sensitivity and reliability analysis, Bruno Sudret, Jean-Marc Bourinet, Nicolas Gayton, France Marc Berveiller.

Model selection, aggregation and testing for probabilistic seismic hazard assessment, Frank Scherbaum.

Modelling for Risk Management in Construction Projects, Herbert Einstein, Denys Breyse.

Multiple hazards risk assessment and mitigation, Yue Li, John W. van de Lindt.

Performance-Based Design for Structures Subject to Natural Hazard, Marcello Ciampoli, Francesco Petrini.

Probabilistic calibration of codes, Milan Holický.

Probabilistic methods for the assessment of existing concrete structures, Robby Caspele, Luc Taerwe, Stewart Matthews, Giuseppe Mancini.

Probabilistic methods in hydraulic and spatial structural analysis, Bin Huang, Hunan, Zhengnong Li.

Probabilistic modelling of the behaviour of timber in structures, Jochen Köhler, Sven Thelandersson.

Progresses and challenges in probabilistic modeling of tropical storm risks, Kazuyoshi Nishijima, Jean-Paul Pinelli.

Recent advances in geotechnical risk and reliability, Phoon Kok Kwang, Jianye Ching, Charnghsein Juang.

Reliability of marine energy converters, Dimitri V. Val, Jens Peter Kofoed.

Risk and Reliability Analysis for Interdependent Infrastructure Systems, Seth Guikema, Leonardo Duenas-Osorio.

Risk assessment and decision support systems for interdependent lifeline infrastructures, Mohammad Bagher Javanbarg, Charles Scawthorn.

Risk-based assessment of climate change adaptation strategies for infrastructure, Mark G. Stewart, Yue Li, Dimitri Val.

Robustness of Structures, Harikrishna Narasimhan, Ton Vrouwenvelder, John D. Sørensen, Michael H. Faber.

Social perspectives for hazards decision, Ross B. Corotis.

Spatial probabilistic modeling of deterioration and inspection, Daniel Straub, Mark G. Stewart.

Stochastic models and simulation of earthquake ground motions, Armen Der Kiureghian, Sanaz Rezaeian.

The Treatment of Uncertainties in Large-Scale Stochastic Systems, George Stefanou, Manolis Papadrakakis.

Uncertainty and imprecision in geotechnical and structural engineering, Michael Beer, Phoon Kok Kwang, Quek Ser Tong.

General sessions

Applications

Decision analysis

Life-cycle analysis

Natural hazards modeling

Probabilistic modeling in engineering

Probabilistic seismic hazard analysis

Reliability methods

Risk assessment

Statistical investigations and probabilistic modeling

Structural reliability

Uncertainty, statistics and probability

Conference organization

CERRA (2007-2011)

Jun Kanda, President	(Japan)
Michael Faber, Chairman	(Denmark)
Robert Melchers	(Australia)
Samer Madanat	(USA)
Armen Der Kiureghian	(USA)
Lucia Faravelli	(Italy)
Terje Haukaas	(Canada)
Marc Maes	(Canada)
Kok-Kwang Phoon	(Singapore)
John D. Sorensen	(Denmark)
Bruno Sudret	(France)
Wilson Tang	(Hong Kong)

COMMITTEES

Organizing committee

Michael H. Faber, DTU, Denmark
Jochen Köhler, ETH Zurich, Switzerland
Kazuyoshi Nishijima, DTU, Denmark
Ton Vrouwenvelder, TU-Delft, the Netherlands
Eugen Brühwiler, EPFL, Switzerland
Daniel Straub, TUM, Germany
John D. Sørensen, Aalborg University, Denmark

Co implementation team

Annette Walzer, Conference Secretary
Roberto Pascolo, IT
Margaretha Neuhaus, Finance and Controlling

Scientific committee

Agarwal, J., University of Bristol, Bristol, UK
Ammann, W., Global Risk Forum, Davos, Switzerland
Ang, A.H-S., University of California, Irvine, USA
Augusti, G., University La Sapienza, Rome, Italy
Baker, J.W., Stanford University, Stanford, USA
Bazant, Z.P., Northwestern University, Evanston, USA
Bazzurro, P., Air-Worldwide, USA
Beck, J.L., California Institute of Technology, Pasadena, USA
Beer, M., National University of Singapore, Singapore
Bergman, L.A., University of Illinois, Urbana, USA
Biondini, F., Technical University of Milan, Milan, Italy
Bresysse, D., University Bordeaux, Talence, France

Bründl, M., WSL, Davos, Switzerland
 Bucher, C., Vienna University of Technology, Vienna, Austria
 Casas, J.R., Technical University of Catalonia, Barcelona, Spain
 Casciati, F., University of Pavia, Pavia, Italy
 Chen, J., Tongji University, Shanghai, China
 Chryssanthopoulos, M.K., University of Surrey, Guildford, United Kingdom
 Ciampoli, M., University La Sapienza, Rome, Italy
 Conte, J.P., University of California, San Diego, USA
 Corotis, R., University of Colorado, Boulder, USA
 Cremona, C., LCPC, Paris, France
 Dagang, L., Harbin Institute of Technology, Harbin, China
 De Leon, D., Autonomous University of Mexico State, Toluca, Mexico
 Deodatis, G., Columbia University, New York, USA
 Der Kiureghian, A., University of California, Berkeley, USA
 Ditlevsen, O., Technical University of Denmark, Lyngby, Denmark
 Dongping, F., Tsinghua University, Beijing, China
 Duenas-Osorio, L., Rice University, Houston, USA
 Ellingwood, B., Georgia Institute of Technology, Atlanta, USA
 Enright, M.P., Southwest Research Institute, San Antonio, USA
 Estes, A.C., California Polytechnic State University, San Luis Obispo, CA, USA
 Esteva Maraboto, L., Autonomous University of Mexico State, Toluca, Mexico
 Faravelli, L., University of Pavia, Pavia, Italy
 Fontana, M., Swiss Federal Institute of Technology, Zurich, Switzerland
 Frangopol, D.M., Lehigh University, Bethlehem, USA
 Friis Hansen, P., Det Norske Veritas AS, Høvik, Norway
 Furuta, H., Kansai University, Osaka, Japan
 Ghanem, R., University of Southern California, Los Angeles, USA
 Ghosn, M., City University of New York, New York, USA
 Gioffrè, M., University of Perugia, Perugia, Italy
 Goyet, J., Bureau Veritas, Paris, France
 Graubner, C.-A., Technische Universität Darmstadt, Darmstadt, Germany
 Grigoriu, M.D., Cornell University, Ithaca, USA
 Guedes Soares, C., Technical University of Lisbon, Lisbon, Portugal
 Haldar, A., University of Arizona, Tucson, USA
 Hasofer, A.M., University of Melbourne, Melbourne, Australia
 Haukaas, T., University of British Columbia, Vancouver, Canada
 Heinimann, H.-R., Swiss Federal Institute of Technology, Zurich, Switzerland
 Heredia Zavoni, E., Instituto Mexicano del Petróleo, Mexico, Mexico
 Holicky, M., Klokner Institute, Prague, Czech Republic
 Hong, H., University of Western Ontario, Ontario, Canada
 Huang, B., Wuhan University of Technology, Wuhan, China
 Hurni, L., Swiss Federal Institute of Technology, Zurich, Switzerland
 Huysse, L., Southwest Research Institute, San Antonio, USA
 Jacob, B., Laboratoire Central des Ponts et Chaussées, Paris, France
 Jendo, S., Polish Academy of Sciences, Warszawa, Poland
 Kanda, J., University of Tokyo, Tokyo, Japan
 Kareem, A., University of Notre Dame, Notre Dame, USA
 Kiremidjian, A.S., Stanford University, Stanford, USA
 Koh, C.G., National University of Singapore, Singapore
 Koike, T., Tokyo City University, Tokyo, Japan
 Laue, J., Swiss Federal Institute of Technology, Zurich, Switzerland
 Leira, B.J., Norwegian University of Science and Technology, Trondheim, Norway
 Lemaire, M., Institut Francais de Mecanique Avancee, Aubiere, France
 Li, J., Tongji University, Shanghai, China
 Lind, N.C., University of Waterloo, Waterloo, Canada
 Liu, X., Tsinghua University, Beijing, China
 Loh, C.-H., National Taiwan University, Taipei, Taiwan
 Lu, Z.-H., Kanagawa University, Yokohama, Japan

Madanat, S., University of California, Berkley, USA
Maes, M.A., University of Calgary, Calgary, Canada
Mahadevan, S., Vanderbilt University, Nashville, USA
Mazzolani, F., University of Naples, Naples, Italy
Melchers, R., University of Newcastle, Newcastle, Australia
Merz, B., Helmholtz Centre Potsdam, Potsdam, Germany
Moan, T., Norwegian University of Science and Technology, Trondheim, Norway
Mori, Y., Nagoya University, Nagoya, Japan
Muzeau, J.-P., Polytech Clermont-Ferrand, Aubiere, France
Naess, A., Norwegian University of Science and Technology, Trondheim, Norway
Nathwani, J., University of Waterloo, Waterloo, Canada
Nielsen, S.R.K., Aalborg University, Aalborg, Denmark
Nowak, A.S., University of Nebraska, Lincoln, USA
Ohtori, Y., Central Research Institute of Electric Power Industry, Abiko, Japan
Pandey, M., University of Waterloo, Waterloo, Canada
Papadrakakis, M., National Technical University of Athens, Athens, Greece
Phoon, K.K., National University of Singapore, Singapore
Rackwitz, R., Technische Universität München, München, Germany
Rahhal, M.E., Saint-Joseph University, Beirut, Lebanon
Ramon Casas, J., Technical University of Catalunya, Barcelona, Spain
Raphael, W., Saint-Joseph University, Beirut, Lebanon
Reid, S., University of Sydney, Sydney, Australia
Rhyner, J., WSL Institute for Snow and Avalanche Research SLF, Davos, Switzerland
Rosowsky, D.V., Texas A&M University, Texas, USA
Rossetto, T., University College London, London, UK
Schueller, G., University of Innsbruck, Innsbruck, Austria,
Siegrist, M., Swiss Federal Institute of Technology, Zurich, Switzerland
Sobczyk, K., Polish Academie of Sciences, Warsaw, Poland
Song, J., University of Illinois, Urbana, USA
Spanos, P., Rice University, Houston, USA
Spencer, B.F., University of Illinois, Urbana, USA
Stewart, M.G., University of Newcastle, Newcastle, Australia
Sudret, B., Phimeca Engineering, Paris, France
Taerwe, L., Ghent University, Ghent, Belgium
Takada, T., University of Tokyo, Tokyo, Japan
Tang, W.H., Hong Kong University of Science and Technology, Hong Kong
Thelandersson, S., Lund University, Lund, Sweden
Thoft-Christensen, P., Aalborg University, Aalborg, Denmark
Tong, Q.S., National University of Singapore, Singapore
Val, D.V., Heriot-Watt University, Edinburgh, UK
Walker, G., Aon Re Asia Pacific, Australia
Winterstein, S., Stanford University, Stanford, USA
Yamazaki, F., Chiba University, Chiba, Japan
Yucemen, M.S., Middle East Technical University, Ankara, Turkey
Zhao, G., Dalian University of Technology, Dalian, China
Zhao, Y.-G., Kanagawa University, Yokohama, Japan

This page intentionally left blank

Sponsors

Bundesamt für Strassen ASTRA
Federal roads office FEDRO
www.astra.admin.ch



Walt + Galmarini AG
www.waltgalmarini.ch



BKW FMB Energie AG
www.bkw-fmb.ch



Det Norske Veritas AS
www.dnv.com



ETH Zurich
<http://www.ethz.ch/>



OFFICIAL CARRIER



This page intentionally left blank

GS_119 — Applications (1)

This page intentionally left blank

Fragility curve of sewerage system due to spatial seismic damaged data

S. Nagata

Kajima Technical Research Institute, Kajima Corporation, Japan

K. Yamamoto

Urban and Civil Engineering, Tokyo City University, Japan

ABSTRACT: In this paper, the authors studied the fragility function of sewerage pipes and manholes. The fragility function is the maximum ground velocity vs. the damage ratio, which is the ratio of the length of damaged sewerage pipes to the total length of sewerage pipes. And the damage ratio of manholes is the ratio of the number of damaged manholes to the total number of manholes. The digital maps used for this study to estimate the fragility function were drawn up using the GIS on sewerage pipes and manholes damaged during the five recent large earthquakes in Japan.

Sewerage system is one of the most important lifeline systems for an urban society. Functional suspension of sewerage system by seismic damages influences the great impact to the citizen's daily life, business continuity of many companies, public health and so on. For example, in 2004 Mid Niigata Prefecture Earthquake, many people could not use water supply system after restoration during the functional suspension of sewerage system. So, it is very important that the countermeasure against the seismic damages to decrease the effect of the functional suspension of sewerage system is made in advance. And a prospect of the total amount of seismic damages is important to make the restoration plan before earthquake occurrence, too.

In this point of view, we estimate the fragility curve function, which is the maximum ground velocity vs. the damage ratio which is proportion of the total length of damaged pipes to the total length of sewerage pipes, to prospect the amount of damages. And the damage ratio of manholes is the ratio of the number of damaged manholes to the total number of manholes.

In this study, the data base of the sewerage facilities damaged by the recently five great earthquakes in Japan, which are 1995 Hanshin Awaji Great Earthquake, 2004 Mid Niigata Prefecture Earthquake, 2007 Niigata-ken Chuetsu-oki Earthquake, 2007 Noto Hanto Earthquake and 2008 The Iwate-Miyagi Nairiku Earthquake, is constructed with GIS to

estimate the fragility curves function. And damaged sewerage pipe data belong to six cities and one town, which are Kobe city, Nagaoka city, Ojiya city, Kawaguchi town, Kashiwazaki city, Wajima city and Kurihara city.

First, we considered the relation among the damage ratio of sewerage pipes and manholes, the seismic force, the ground factor, the pipe factor, the ground liquefaction factor and so on.

And, we estimated the fragility curve function for physical damage and malfunction. We used the seismic intensity for the maximum ground velocity, and a normal distribution for the basic shape of the fragility curve, as equation (1) shows, with reference to prior research results. (Maruyama and Yamazaki (2009))

$$R(V_i) = C \cdot \Phi \left[\frac{(\ln V_i - \lambda)}{\zeta} \right] \quad (1)$$

$$\varepsilon = \sum_{i=1}^n \left\{ [R_i - R(V_i)]^2 \cdot L_i \right\} \quad (2)$$

where, $R(V_i)$ is an estimated value of the physical damage ratio at a maximum ground velocity of V_i . C , λ and ζ are regression coefficients calculated by

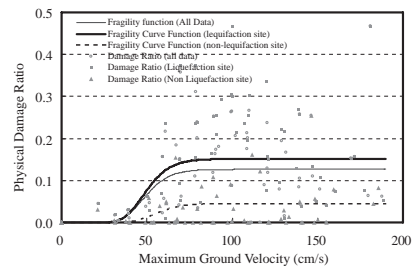


Figure 1. Physical damage ratio of fragility curves of sewerage pipes and sample data used in the calculation of regression.

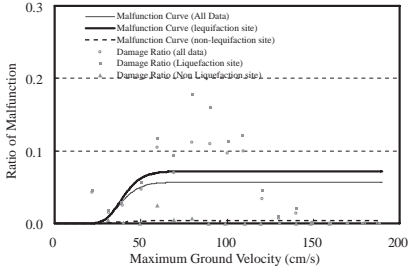


Figure 2. Malfunction curve of sewerage pipes and sample data used in the calculation of regression.

Table 1. Estimated co-efficient of fragility curve of sewerage pipes.

Analysis case	C	λ	ζ	residual error sum of squares	AIC
All Sample Data	0.126	3.898	0.220	0.566	-113.826
Liquifaction site data	0.151	3.907	0.219	1.392	-39.823
Non-Liquifaction site data	0.045	4.022	0.198	0.134	-115.978

Table 2. Estimated co-efficient of malfunction curve of sewerage pipes.

Analysis case	C	λ	ζ	residual error sum of squares	AIC
All Sample Data	0.057	3.651	0.217	0.034	-212.703
Liquifaction site data	0.072	3.680	0.213	0.060	-164.637
Non-Liquifaction site data	0.004	3.652	0.289	0.001	-141.087

Table 3. Estimated co-efficient of fragility curve of manholes.

Analysis case	C	λ	ζ
All Sample Data	0.103	4.066	0.283
Varried depth ($D \geq 2$)	0.153	4.044	0.285
Varried depth ($2 > D$)	0.073	4.028	0.280

minimizing the objective function ε in equation (2) with the quasi-Newton method.

Figures 1 and 2 show fragility curves of physical damage and malfunction of the sewerage pipes calculated by equation (1), while Tables 1 and 2 show regression coefficients of the fragility curves.

And Figures 3 and 4 show fragility curves of physical damage and malfunction of the manholes,

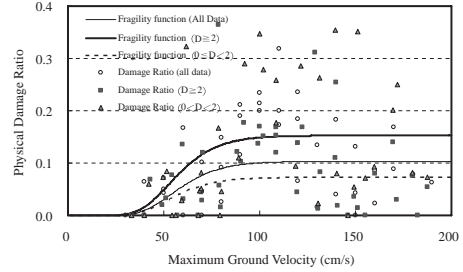


Figure 3. Physical damage ratio of fragility curve of manholes and sample data used in the calculation of regression.

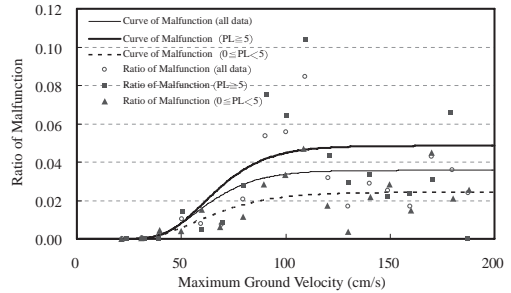


Figure 4. Malfunction curve of manholes and sample data used in the calculation of regression.

Table 4. Estimated co-efficient of malfunction curve of manholes.

Analysis case	C	λ	ζ
All Sample data	0.036	4.133	0.297
Liquifaction site ($PL \geq 2$)	0.049	4.190	0.291
Liquifaction site ($5 > PL$)	0.024	4.163	0.347

while Tables 3 and 4 show regression coefficients of the fragility curves.

REFERENCE

Maruyama Yoshihisa & Yamazaki Fumio (2009). Estimation of Damage Ratio of Water Distribution Pipes Based on Recent Earthquake Damage Data, Proceedings of the 30th JSCE Earthquake Engineering Symposium, pp. 1-9.

A new time-reversal imaging method for active Lamb wave damage monitoring of composite structures

S. Yan & N.Z. Zhao

School of Civil Engineering, Shenyang Jianzhu University, China

School of Civil and Hydraulic Engineering, Dalian University of Technology, China

Binbin He

School of Civil Engineering, Shenyang Jianzhu University, China

ABSTRACT: Lamb wave based non-destructive evaluation methods are widely used for damage detection in engineering structures, in particular, aerospace, civil and marine structures, the response of Lamb waves is correlated to the damage location through estimation of time of arrival of the new peaks (scattered waves). Thus, by employing the wave based methods presence of damage in a structure is detected by looking at the wave parameters affected by the damage. Time reversal is based on the time invariance and spatial reciprocity form of the acoustic waves propagating in any medium. Due to the complex transducer array necessary for time reversal diagnostics of a structure, a modified time reversal method is developed. Theoretical analysis of Lamb wave propagation, actuated by piezoelectric transducers, and experimental comparison with the original time reversal method is used as a basis for validation of the modified time reversal method. Experimental applications of the modified time reversal method are then used in analysis of damage severity classification. A transducer array consisting of piezoelectric discs is used to send and receive A_0 Lamb waves. The modified time reversal method is conducted for each actuator-sensor pair and a damage index is computed. Results show magnitude of the damage index to be directly correlated to the severity of damage within the signal path.

1 INTRODUCTION

There has been a significant increase in the use of solid composites in load-carrying structural components. With the advances in sensor and hardware technologies that can generate and detect Lamb waves, many studies have been proposed to use Lamb waves for detecting defects in composite structures. In particular, many researchers have recognized the potential use of piezoelectric (PZT)

actuators/sensors for Lamb-wave-based structural health monitoring.

The use of Lamb wave based structural health monitoring has shown promise in published research. Lamb waves are of particular interest due to the similarity between their wavelength and the thickness of composite structures generally used and their ability to travel far distances. These two features allow for detection of not only superficial but internal flaws and the ability to examine large areas. Unfortunately, it is difficult to analyze measured responses due to the multimodal and dispersive characteristics of Lamb waves propagation. Signal processing and dispersion curves have typically been used to help the damage detection process and understand the complex Lamb waves. The use of a time reversal method is a new approach developed to mitigate Lamb wave dispersion effects and increase the applicability of Lamb waves for ISHM.

Recently, attention has been paid to the time reversal method developed in modern acoustics to compensate the dispersion of Lamb waves and to improve the signal-to-noise ratio of propagating waves. For instance, a pulse-echo time reversal method, that is, the time reversal method working in pulse-echo mode has been employed to identify the location and size of defects in a plate. However, if there exist multiple defects in a plate, this iterative pulse-echo process tends to detect only the most distinct defect, requiring more sophisticated techniques to detect multiple defects. Furthermore, the pulse-echo process seems impractical for structural health monitoring applications, because a dense array of sensors is required to cover the entire boundary of the plate being investigated.

In the time reversal method, an input signal can be reconstructed at an excitation point (point A) if an output signal recorded at another point (point B) is reemitted to the original source point (point A) after being reversed in a time domain as illustrated.

This time reversibility (TR) of waves is based on the spatial reciprocity and time reversal invariance of linear wave equations. The specific goal of the research described in this paper is to reconstruct the known excitation signal at the original input location through the time reversal process of Lamb waves. In this study, a modified time reversal method is proposed so that the reconstruction of the input signal can be achieved for Lamb wave propagation. The ultimate goal is to use this TR of Lamb waves for damage diagnosis.

This paper presents a Modified Time Reversal Method (MTRM) and evaluation of damage severity within a structure. Development of the MTRM is used as a means to decrease the hardware requirements of structural diagnostics. Theoretical analysis of Lamb wave propagation actuated by piezoelectric transducers, and experimental comparison with the original time reversal method is used as a basis for validation of the modified time reversal method. Experimental applications of the modified time reversal method are then used in analysis of damage severity classification. A composite plate containing impact damage is experimentally investigated by integrating a piezoelectric transducer array onto the plate such that each transducer can be used as both an actuator and a sensor. Increasing levels of damage are simulated by incrementally impacting a composite plate with a steel ball. In diagnosing the health state of the plate, a damage index was used to quantitatively classify the differences between the originally actuated signal and the final signal due to the modified time reversal process. Magnitude of the damage index was used as basis for damage severity evaluation.

2 CONCLUSIONS

This paper has presented a time reversal method to detect the presence of damage within a thin composite plate. A modified time reversal method was developed to enhance the applicability of the process by decreasing the necessary hardware to monitor the health of the structure. Two damage indexing systems, as developed by Park et al (2003 and 2007) and Giurgiutiu (2008), were used to evaluate the effects of severity of damage. It was found that both damage indexing evaluations increased as severity of damage increased, verifying the ability of the modified time reversal method to determine not only the presence of damage, but also the severity.

This evaluation of damage severity is still in the preliminary stages of research and needs further validation. Firstly, a larger array of damage types is necessary to investigate the applicability of using the time reversal method for all damage cases. Furthermore, a more in depth correlation between the actual severity of damage within the plate and the indicated damage severity as indicated by the time reversal method is necessary. In this study, there was little known about the actual extent of damage within the plate although it was assumed that each impact "increased" the damage at the impact location. Further study of the damage indexing systems and their ability to identify increases in damage severity is necessary to determine which method is best to be used in the time reversal method.

Probabilistic concept for the validation of the effectiveness of countermeasures against early-age cracking in massive concrete structures

M. Krauß

Bundesamt für Strahlenschutz, Salzgitter-Lebenstedt, Germany

ABSTRACT: The imperviousness and hence the serviceability of structures subjected to water pressure may be endangered by through cracks. In order to ensure a required serviceability (e.g. tightness in case of ground water pressure) of a massive concrete structure, it is important to control thermal through cracking. However, it is a fact that cracking is a highly scattering phenomenon. Consequently, it is indispensable to perform a reliability-based thermal stress analysis to predict the initiation of thermal cracks by taking the parameters of analysis into consideration as random variables.

The uncertainties depend on the constituents and composition of concrete, on environmental conditions etc. This approach requires a reliability-oriented crack criterion for the forecast of the effectiveness of countermeasures to be realized in the planning and/or execution stage of structure.

This report describes a concept, to evaluate the possibility of thermal cracking in hardening concrete structures in terms of thermal cracking index based on probability theory. The sensitivity of the thermal cracking index—with respect to the variation of the relevant parameters—is investigated with an enhanced Monte-Carlo simulation technique.

By calculation of the probability of thermal cracking, reliability-oriented crack criteria are defined for a wide use in practice. The proposed model can be applied, if reliable estimations of load-independent strains, concrete properties and restraint of the hardening concrete structure as well as of the uncertainties of all parameters are available.

Following this approach, the early-age cracking risk for recently executed railways through structure is evaluated by taking the uncertainty of prediction into account.

The concept presented in this paper, follows the approach of JSCE 2002. The idea of the model is the introduction of the probability of thermal crack occurrence p_{cr} to assess the risk of thermal cracking.

The model defines three different service limit states depending on the requirements of serviceability in terms of tightness. The requirements differ with respect to the required level of reliability.

The probability of thermal crack occurrence can be calculated, if the probability density function of the so-called thermal cracking index γ_{cr} is known. The cracking index is defined as the ratio between the tensile strength f_{ct} and tensile stress level σ_{ct} in structure.

This index can be regarded as a global safety factor against through cracking. As a first approximation, the tensile strength and tensile stress can be regarded as independent and normal distributed random variables.

The classical FORM approach leads to a simple relationship between tensile strength, tensile stress, the associated coefficients of variation $V[f_{ct}]$ and $V[\sigma_{ct}]$ and the probability of thermal crack occurrence p_{cr} . In this paper f_{ct} is regarded as the effective tensile strength in the structure ($f_{cte} = 0.75 f_{ct}$) and C_{cr} denotes the corresponding thermal cracking index. The tensile stresses can be calculated by an arbitrary engineering method like FEM, compensation plane method CPM or one-point method OPM.

An alternative approach for the calculation of the probability density function of γ_{cr} is a Level III—approach and the use of a Monte-Carlo simulation technique.

For this approach it is necessary to define

- a simple and deterministic engineering method for the prediction of restraint stresses in hardening concrete structures;
- a comprehensive model to describe the scatter of material properties of young concrete and other related materials;
- a simple stochastic model to describe the impact of the variance of the climate on the prediction of restraint stresses.

To calculate the restrained stresses with this model, the CPM is used. Following the recommendations of JCSS 2008 a statistical framework

is used to describe the uncertainties of all basic random variables.

The purpose of the study is to verify the effectiveness of the countermeasures taken against early age cracking of the walls of trough. The walls are subjected ground water of differing pressure.

The cracking risk of the walls was proved in the location of maximum restraint level. This point of view enables the transfer of the reliability-oriented analysis of thermal stresses in hardening concrete by means of an OPM. For this purpose, the following models were defined:

- A deterministic model to estimate the temperature development in the walls depending on the expected climates in the execution phase of the through. Three different climates (warm, normal, cold) were taken into consideration.
- Deterministic models to estimate the thermal stresses of the wall with respect to the complex restraint condition (trough and sub-structure, cf. Rostásy & Krauß & Budelmann 2005).
- Definition of a reliability-oriented crack criterion for the assessment of the early-age cracking risk of the walls according to the requirements of serviceability.

Basis for the assessment of the cracking risk is the deterministic calculation of the restrained stresses of the wall. Hardening concrete was regarded as linear-elastic and viscoelastic material. Drying phenomena were not taken into consideration.

For all material properties of wall concrete comprehensive material tests were performed. A statistically validated climate database is used to simulate the time development of ambient temperature.

From a practical point of view the total number of through cracks in all blocks is of particular interest. So the average numbers of cracks per block n_{rm} were calculated in order to evaluate the cracking risk.

The analysis of the crack patterns on-site shows 1.1 cracks per block. The probabilistic analysis shows—depending on the climate—0.8 up to 1.1 cracks per block for the expected value $E[n_{rm}]$. The lower limit of the confidence interval (significance level of 20%) of $E[n_{rm}]$ \inf cal n_{rm} was estimated to 0.3 cracks per block (20%-quantile); the upper limit \sup cal n_{rm} was estimated to 1.4 cracks per block (80%-quantile).

Reliability evaluation of pipelines containing stress corrosion cracking defects

W. Zhou & S. Zhang

The University of Western Ontario, London, Ontario, Canada

ABSTRACT: Stress Corrosion Cracking (SCC) is a major integrity threat to buried oil and gas pipelines worldwide. SCC usually results from a combination of susceptible metallic material, tensile stress and aggressive environmental conditions. A typical SCC defect is characterized by a colony of partly through-wall cracks (i.e. surface-breaking flaws) along the longitudinal direction of the pipeline in response to the hoop stress due to the pipe internal pressure. Once initiated, the individual cracks in the colony will grow and coalesce mainly due to the environmental growth mechanism. The continued growth and coalescence could lead to a single dominant crack that is of sufficient size such that the mechanical growth mechanism (i.e. fatigue) will begin to contribute significantly to the overall growth. It is these long individual cracks within the colony that constitute a significant threat to pipeline integrity.

Inline inspection (ILI) tools are being more and more used on oil and gas pipelines to detect and size SCC defects. Once a defect is found and sized by the ILI tool, the pipeline integrity engineer will evaluate the severity of the defect and decide whether immediate intervention actions are required. If a defect does not require immediate intervention, the remaining life of the pipeline at the defect will be estimated such that a re-inspection/repair interval can be quantified. If reliability-based methodologies are being used in the pipeline integrity management, the re-inspection/repair interval can be determined by evaluating the time at which the time-dependent failure probability (typically on an annual basis) due to the SCC defect exceeds the allowable failure probability.

An efficient methodology was developed in this study to evaluate the time-dependent failure probability of a pressurized oil or gas pipeline containing an SCC defect. Failure is defined as the burst of the pipeline at the defect location due to the pipe internal pressure. The reliability analysis is carried out assuming that the colony of cracks in an SCC defect is represented by a single longitudinally-oriented crack with a semi-elliptical profile. Such an idealization is conservative in that it ignores the

potential stress shielding provided by the smaller cracks surrounding the dominant crack. It is further assumed that the length of the SCC defect does not grow over time since the single crack assumed in this study has incorporated crack coalescence, which is the main mechanism for length growth. The growth of the defect depth was characterized by a superposition model whereby the fatigue growth resulting from cyclic fluctuation of the pipeline internal pressure is superimposed on an environmental growth rate assumed to be uncertain but constant in time. The Paris law was used to evaluate the fatigue growth component of the defect depth. To deal with the variable amplitude loading condition, an equivalent pressure range is evaluated using Miner's rule from the pressure range history that is obtained through rainflow counting.

The limit state function for the reliability analysis is established as the burst pressure at an SCC defect minus the pipe operating pressure. In this study, the Battelle model or "log-secant" approach was employed to calculate the critical defect depth corresponding to burst for given pipe geometry and material properties, defect length and operating pressure. The time to burst, i.e. time required for the defect to grow from its initial depth (depth at the time of defect detection) to the critical depth can then be calculated incrementally by incorporating both the fatigue and environmental growth components. The first-order reliability method (FORM) was used to evaluate the time-dependent probability of burst at the SCC defect.

A numerical example was used to illustrate the above-described methodology. The example is a crude oil pipeline with an outside diameter of 609.6 mm, a pipe wall thickness of 6.3 mm and a nominal operating pressure of 3600 kPa. The specified minimum yield strength of the pipe steel is 359 MPa. A recently run ILI identified an SCC defect with a measured depth of 1.58 mm (i.e. 25% through wall thickness) and a measure length of 100 mm. The reliability indices and corresponding probabilities of burst over a period of 15 years starting from the time of defect detection

were evaluated using the FORM for the example pipeline. The sensitivity factors associated with the random variables were also obtained from the FORM. The results indicate that for this particular example the defect initial depth and Paris law coefficient (C) are associated with the highest and second highest sensitivity factors up to year 5, after which the environmental growth rate and C are associated with the highest and second highest sensitivity factors. It is also interesting to note that the sensitivity factor for the environmental growth

rate changes rapidly from being close to zero at year 1 to approximately 0.7 at year 6 (i.e. the most dominant sensitivity factor).

It should be noted that for simplicity the internal pressure and environmental growth rate were assumed to be time-independent random variables in this study. A more realistic treatment is to characterize the pressure and growth rate as stochastic processes. This will be considered in future studies.

Proportionality of interventions to restore structural safety of existing bridges

E. Brühwiler

Swiss Federal Institute of Technology EPFL, Lausanne, Switzerland

ABSTRACT: The proportionality of interventions on existing structures comprises a comparison between effort (cost) and benefit of interventions with the objective of an efficient use of means. This contribution discusses the evaluation of interventions to restore sufficient structural safety of existing bridges as encountered in real case applications. The considered hazard scenarios include accidental actions and one extreme live load event. For all hazard scenarios, structural safety check could not be fulfilled. Consequently interventions to restore structural safety were developed and their efficiency was analysed by a comparison of risk reduction with respect to safety costs. In addition, safety requirements, operational availability of the structure, magnitude of damage as well as the preservation of material and cultural values were considered. In three of the four cases the safety interventions turned out to be disproportionate. This paper presents a review of the chosen approach and assumed values and numbers used to estimate risk reduction and corresponding safety costs. Finally, issues are raised regarding the decision to implement or not the intervention to restore structural safety.

1 INTRODUCTION

For the examination (often referred to as “assessment”) of existing bridges, most structural engineers apply the codes and in particular load models valid for the design of new bridges. This is a problematic approach since the codes for design and construction of new structures are in principle not or only analogously applicable to existing structures; also, they do not provide a risk-based safety approach.

The professional approach to existing structures is based on an inherent methodology [SIA 269] that essentially includes collecting actual information since the structure exists. The controlling parameters are determined more precisely, and for example, the structural safety of an existing structure is proven using so-called updated values for

actions and resistance. Also, a risk-based safety approach is applied.

In this way, it can often be shown that an existing structure may be subjected to higher solicitation while meeting the safety requirements. Such an approach is needed to avoid rather cost-intensive or even unnecessary maintenance interventions (which are often the result of insufficient knowledge and information about the existing structure).

In cases where the structural safety cannot be verified interventions to restore structural safety need in principle be implemented. However not all safety measures are proportionate, i.e. balanced in terms of invested means for achieved safety. As a matter of fact, the objective is the efficient use of means, in particular financial means. Infrastructure managers have to allocate their means to the most relevant safety problems of a system. They need a systematic approach to be able to objectively evaluate the proportionality of safety measures in situations of insufficient structural safety.

The proportionality of safety interventions on existing structures comprises a comparison between (safety) cost and benefit of interventions in terms of risk reduction.

This paper presents a methodology to evaluate proportionality of safety measures, discusses assumed values and numbers that are used to estimate risk reduction and corresponding safety costs. Application examples will be outlined to illustrate the methodology. Finally, issues are raised regarding the decision to implement or not the intervention to restore structural safety.

2 CASE STUDY 1—VEHICLE IMPACT ON PARAPETS OF A HISTORICAL BRIDGE

Despite the fact that the structural safety of the existing parapets against vehicle impact is not sufficient, the safety intervention consisting in replacing the parapets is disproportionate and shall not be implemented. From a socio-economic

viewpoint the financial means shall more efficiently be invested into different safety related measures which prove to be proportionate.

The study also showed that the probability of occurrence of an impact of a heavy vehicle is in the present case very small such that this hazard scenario may be accepted as an “accepted risk”.

Finally, keeping the existing parapets obviously is the best solution from the viewpoint of preservation of cultural values.

3 CASE STUDY 2—THREE HAZARD SCENARIOS INVOLVING HIGHWAY BRIDGES

The results of this case study may be discussed as follows:

Hazard scenario A—Underpass: Fire of a tank truck: the safety intervention turned out to be clearly disproportionate and only complementary safety measures (like signaling reduced speed) may possibly be taken. This hazard scenario can be considered as an “accepted risk”.

Hazard scenario B—Overpass: Loss of load bearing resistance due to corrosion: the coefficient of efficiency of the safety intervention was larger than 1 and the safety related intervention must in principle be implemented. The values of safety cost and risk reduction were however relatively small and an opposite result could be obtained. It is thus important to identify the values that influence most the result. Also, it is reasonable from the “sound engineering sense” to perform the rehabilitation (and thus the safety related measure) in any case because of the bad condition of the structure.

Hazard scenario C—Viaduct: Failure of railing after impact of a bus: the reduction in risk due to the safety measure is much higher than the safety cost. The safety related intervention is thus clearly proportionate and has to be implemented.

4 CONCLUSIONS

The proportionality of interventions to restore the structural safety of existing bridges was evaluated:

1. The proportionality of safety interventions may be evaluated by means of a comparison of risk reduction (as obtained from the safety interventions) with respect to corresponding safety costs. Relevant information and data have to be updated to consider the specific conditions of the existing structure.
2. The assumptions and available information to estimate cost parameters are of outmost importance. The compensation costs for casualties turn out to be the predominant aspect. Information and data related to cost parameters need to be improved.
3. Evaluation of proportionality of safety interventions may not be based on numerical results alone. Sound engineering judgment and non-monetary values needs to accompany the evaluation.

The case studies also show that application of modern engineering methods for professionally dealing with existing structures lead to more sustainable solutions.

GS_129 — Applications (2)

This page intentionally left blank

Scenario-based seismic loss estimation for concrete buildings in the central US

J. Bai

School of Engineering, California Baptist University, Riverside, CA, USA

M. Hueste & P. Gardoni

Zachry Department of Civil Engineering, Texas A&M University, College Station, TX, USA

ABSTRACT: Existing structures located in the Central United States (US) near the New Madrid Seismic Zone (NMSZ) are at risk of being damaged during a potential seismic event. In particular, a significant seismic event affecting a densely populated area, such as the city of Memphis, Tennessee, could lead to severe damage and significant economic losses. In this study, a scenario-based assessment is conducted for moderate to high intensity earthquakes in this region. Three scenario earthquake magnitudes from moderate to high (5.5, 6.5, and 7.5) are used to provide a better understanding of the expected losses due to different seismic hazard levels. The buildings considered are typical Reinforced Concrete (RC) moment frame buildings in this region. Fragility curves that have been recently developed by Bai et al. (2010) using story-specific demand models are used to represent the seismic vulnerability of the buildings. Story-specific demand models provide a refined approach that includes more building response information than typical demand models, allowing for more accurate estimates of the seismic fragility of multi-story buildings (Bai et al., 2010). When only the maximum interstory drift of a building is considered, as is the case for traditional fragility curve development, the fragility tends to be underestimated; particularly if the interstory drifts for one or more stories are close to the maximum value. A probabilistic framework to assess the structural damage of the selected buildings is used to account for the prevailing uncertainties.

Finally, the corresponding structural losses in dollars due to the scenario earthquake events are estimated. Through this scenario-based approach, critical structures that are expected to have extensive damage can be identified. In addition, decision makers in a region can estimate the economic losses due to potential seismic events and prioritize of mitigation options for high risk structures.

Based on the scenario-based assessment, for the M 5.5 scenario event, all the concrete buildings are expected to have limited structural damage with low total damage factors. The severity of the expected damage increases for higher events. For the M 6.5 event, the majority of the low-rise concrete buildings are expected to have moderate to heavy damage, while the mid-rise buildings are expected to have insignificant to moderate damage. The expected total cost to repair structural damage to the 486 RC frame structures for the M 7.5 event is \$395 million dollars. A major concern for this scenario event is that most RC frame buildings are expected to have heavy damage, with several buildings expected to be in the complete damage range.

It should be noted that this study focuses on a regional seismic loss assessment to determine the expected damage and structural repair costs for an inventory of buildings in order to assess the overall level of damage for the region for three scenario events. Seismic evaluation of individual building structures requires a different approach that considers the individual building configuration, structural and geotechnical details, location, seismicity, etc.

Application of the Monte-Carlo method to determine the time required for construction projects—Influence of ranges and correlations on probability distribution

C. Hofstadler

Institute for Construction Management and Economics, Graz University of Technology, Styria, Austria

ABSTRACT: Construction time is a key part of any building contract and has an influence on construction costs and work execution. Depending on the project phase, the time required for construction is either determined as a rough estimate or calculated precisely. In this respect, the degree of accuracy is dependent upon the mathematical combination of the input parameters. However, input parameters include uncertainties and fuzziness. These input parameter ranges can be accounted for in a non-systematic, deterministic manner. The range of possible construction times can be restricted by establishing both an optimistic and a pessimistic consideration. In most cases, a value between the two defined boundaries is applied. No statement can be made, however, about the accuracy of the value selected.

The type of work, the conditions under which this work is performed, the amount and quality of the work and the construction time required are factors that determine the cost level, and thus pricing. To calculate construction time, the deterministic method is demonstrated for the preliminary planning stage. For this purpose, the equations to be used to perform a rough calculation of construction time are shown (it should be noted that more detailed analyses will always be required at the following stages). Parameters considered in these calculation steps include the duration and output of reinforced concrete works, the average number of workers, daily working time and the total labour consumption rate for reinforced concrete works. Major influences on the output achieved are shown graphically.

The Monte-Carlo method is then applied on the basis of the deterministic calculation mode used initially, using a performing arts centre building as an example. The Monte-Carlo calculation sequence is both described and displayed graphically. This method makes it possible to calculate the probability distribution for the construction time of reinforced concrete works. Formwork, reinforcement and concrete quantities are determined on the basis of the existing building plans and drawings.

Input values to be used for the calculations are estimated on the basis of the existing project documentation, taking account of identifiable site, management, structural and process conditions. For each simulation exercise, distribution functions are selected for the input parameters, and minimum and maximum values are determined, as well as most likely values, as far as reasonably possible. The distribution functions used for the purpose of this paper include isosceles triangles, weighted triangles, rectangular distributions and beta distributions. The @RISK software is used to carry out the calculations. The results are shown as probability distributions for the output parameters defined in a preceding step. The results of several simulations with varying distribution functions are compared to each other and analysed. The parameters to be compared include quantiles (X_5 and X_{95}), standard deviation, mode, skewness and kurtosis. This comparison is to show whether it is useful to apply weighted triangles as distribution functions.

The influence of a reduction in the input parameter range on the probability distributions is also determined. Probability distributions are displayed graphically both for the initial calculations and for the calculations performed after the range reductions. Such range reductions are enabled by a more detailed knowledge of the prevailing site, management, structural and process conditions. The degree of uncertainty and fuzziness can be lowered as a result. This paper should demonstrate and analyse the influence of the input parameter improvement on the results. In the next step, the influence of the above-mentioned four distribution functions on construction time is determined. To compare the simulation results, 50,000 iterations per calculation sequence are performed.

Correlations are introduced to account for any interdependencies. Calculations performed with and without correlations are compared to each other to prove the effects of correlations. Two extreme cases are evaluated within the correlations. On the one hand, positive correlations

are established between selected parameters. On the other, negative correlations are applied consistently. The correlations are applied to the total labour consumption rate, which is one of the key parameters relevant to the determination of construction time. This comparison should show how any incorrectly set correlations may affect the distribution of probability. In addition, the types of distribution functions that show a more or less significant response to correlations should be identified.

The performing arts centre building used as an example to apply the Monte-Carlo method makes it possible to show construction time as a probability distribution, and to state significant values. This probability distribution may also be used as a basis for the decision-making process to determine the construction time that is useful with regard to construction management and economic aspects. In addition, parameters with a major influence on construction time can be identified. The application of probability calculus does not result in a single correct value. Rather, the correlation between the probability of occurrence and the magnitude of the value is reflected (probability distribution). The calculations performed permit the conclusion that virtually no effects of range reductions on mean, modal and median values were found.

By contrast, the reduction in the input parameter ranges resulted in a considerable reduction in both standard deviation and 90% spread.

A significant improvement of the outcomes may be achieved if appropriate construction management measures are taken to more accurately determine the input values. On a related note, clients should, as far as possible, specify construction periods for their projects that are reasonable in terms of construction management and economic factors. This approach creates a good basis to actually achieve the defined project milestones. In this regard, it is crucial to consider the construction management constraints in terms of the number of resources and logistics-related boundary conditions. However, the correct interpretation of probability calculus results will always require expert knowledge with regard to construction management and related economic aspects.

The author is currently conducting further research on the characteristics of distribution functions for consumption rates and structural parameters (such as formwork ratio or reinforcement ratio), as well as on the interdependencies of the risks. The effects of correlations between the input parameters are also being evaluated with respect to their relevance. The results of this research will be published at a later stage.

Advances in probability density evolution analysis of nonlinear stochastic systems

J. Li, J.B. Chen & W.L. Sun

State Key Laboratory of Disaster Reduction in Civil Engineering & School of Civil Engineering,
 Tongji University, Shanghai, P.R. China

1 INTRODUCTION

Stochastic mechanics, particular of nonlinear stochastic system, has gained increasing attention. In the past years, starting with the clarification of the principle of preservation of probability, a family of probability density evolution method (PDEM) has been developed. In the PDEM, a family of generalized density evolution equation was established. This provides a new possibility of tackling nonlinear stochastic systems. Some new advances, extensions and applications of the PDEM, are illustrated in the present paper.

2 GENERALIZED DENSITY EVOLUTION METHOD

The random event description of the principle of preservation of probability

$$\frac{D}{Dt} \int_{\Omega} p_Y(y, t) dy = 0 \quad (1)$$

where $D(\cdot)/Dt$ denotes total derivative. Eq. (1) is the result from the perspective that the probability of a random event is invariant.

A stochastic process can be represented as combinations of random functions

$$\dot{X}_g(t) = \dot{X}_g(\zeta, t) \quad (2)$$

The equation of motion of a MDOF system can thus be written as

$$\mathbf{M}(\Theta)\ddot{\mathbf{X}} + \mathbf{C}(\Theta)\dot{\mathbf{X}} + \mathbf{f}(\Theta, \mathbf{X}) = \mathbf{F}(\Theta, t) \quad (3)$$

where $\mathbf{F}(\Theta, t) = \Gamma \dot{X}_g(\zeta, t)$.

When viewed from the random event description of the principle of preservation of probability combined with the uncoupled physical equation, a completely uncoupled, arbitrary-dimensional density evolution equation can be reached:

$$\frac{\partial p_{Z\Theta}(\mathbf{z}, \theta, t)}{\partial t} + \sum_{j=1}^m \dot{Z}_j(\theta, t) \frac{\partial p_{Z\Theta}(\mathbf{z}, \theta, t)}{\partial z_j} = 0 \quad (4)$$

where Z is the physical quantity of interest.

Although the closed-form solution of general density evolution equation (GDEE) for some simple case is available, the numerical solving procedure is needed for most practical engineering problems. The numerical algorithms for probability evolution theory could be explained as: Select representative points in the probability-assigned space and determination of the assigned probability. Then Solve deterministic dynamical systems. After that, the probability density function of interest could be obtained by solving the GDEE.

3 APPLICATIONS

3.1 Fluctuation analysis of stochastic dynamics Systems

Fluctuation of a nonlinear single-degree-of-freedom system was investigated by the probability density evolution method. The study (Sun et al., 2011) provides evidence that small variation of the natural circular frequency of the structure may induce large fluctuation in structural responses.

3.2 Stochastic response of nonlinear structures

Response analysis of a 2-span 9-story shear frame structure subjected to deterministic ground motion was exemplified. In this example, the Q-SPM was adopted to select the representative points in random-variate space. Totally 20 independent random parameters are involved in the investigation. The coefficients of variation of all random variables in this model are equal to 0.2.

Pictured in Figure 1 is the PDF evolution surface. In Figure 2 shown is the CDF of the extreme value over $[0, 20]$ s compared with the Monte Carlo simulation (MCS). The results show that the global

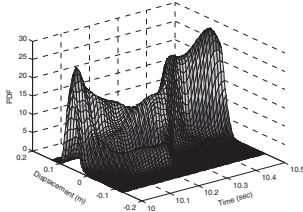


Figure 1. The PDF evolution surface of a dynamical system.

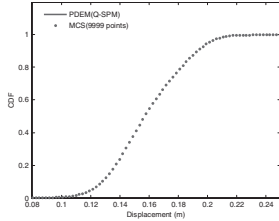


Figure 2. The CDF of the extreme value ($T = 20$ s).

performance and reliability of MDOF nonlinear structures can be captured by the PDEM, which is much more efficient than the traditional MCS. In addition, the computational result by the PDEM is in deterministic sense, different from the MCS which could only give results with random convergence.

3.3 Time-variant life-cycle system reliability: An illustration

Life-cycle reliability of a simply-supported beam with deteriorating materials was carried out.

Because of deterioration of the material, the PDF of the limit state function moves toward the negative direction, i.e. the safety margin is decreasing. This of course means that the reliability will decrease against time. It is remarkable that the reliability decreases in a rapid speed after 35 years of service (Figures 3 and 4).

3.4 The physical stochastic optimal control

Based on the PDEM, a physical stochastic optimal control (PSC) was developed (Li et al., 2010). Different from the traditional stochastic control, the PDEM-based optimal control could achieve optimal effect in the sense of probability. Very recently, a systematic experimental study was conducted validating the proposed method. The results will be published elsewhere.

4 CONCLUSIONS

Combining the random event description of the principle of preservation of probability,

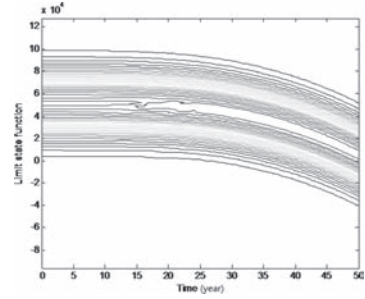


Figure 3. Contour of PDF surface of the limit state function.

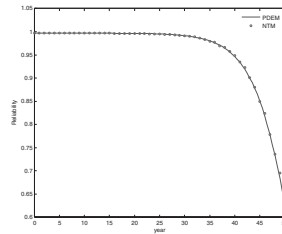


Figure 4. Life-cycle reliability of a simply-supported beam.

the generalized density evolution equations are derived. Numerical procedures for implementation of the probability density evolution method are introduced. Some extensions and applications are discussed or exemplified. Problems need further study include physical modeling of dynamic excitations and multi-scale stochastic physics, etc.

ACKNOWLEDGMENTS

The support of the Natural Science Foundation of China (Grant Nos. 90715083 and 10872148), National Hi-Tech Development Plan (863 Plan) (Grant No. 2008AA05Z413), and the State Key Laboratory of Disaster Reduction in Civil Engineering (Grant Nos. SLDRCE08-A-01 and SLDRCE10-B-02) are greatly appreciated.

REFERENCES

- Li, J. & Chen, J.B. 2009. *Stochastic Dynamics of Structures*, John Wiley & Sons.
- Li, J., Peng, Y.B. & Chen, J.B. 2010. A physical approach to structural stochastic optimal controls. *Probabilistic Engineering Mechanics* 25: 127–141.
- Sun, W.L., Li, J. & Chen, J.B. 2011. Stochastic fluctuation analysis of physical systems based on probability density evolution method. The 11th International Conference on Applications of Statistics and Probability in Civil Engineering, ETH Zurich, Switzerland, 2011, submitted.

Probability density evolution method and polynomial chaos expansion for nonlinear random vibration analysis

Y.B. Peng

State Key Laboratory of Disaster Reduction in Civil Engineering, Tongji University, Shanghai, China
Shanghai Institute of Disaster Prevention and Relief, Tongji University, Shanghai, China

J. Li & J.B. Chen

State Key Laboratory of Disaster Reduction in Civil Engineering, Tongji University, Shanghai, China
School of Civil Engineering, Tongji University, Shanghai, China

ABSTRACT: Due to the challenges arising from the classical analytical methods and numerical techniques for nonlinear random vibration analysis, the solving procedures for nonlinear stochastic structural analysis are investigated in the random vibration analysis if the random excitations acting on systems can be expressed as functions of a set of stochastic variables. For example, the classical perturbation method and the functional series expansion method were generalized to the random vibration of nonlinear oscillator subjected to white noise excitations. As a novel formulation for governing the probability density evolution of stochastic structural systems, the generalized density evolution equation proposed in recent years profoundly reveals the intrinsic connection between deterministic systems and stochastic systems by introducing physical relationships into stochastic systems. It is thus natural to apply the generalized evolution equation in the nonlinear random vibration. In the present paper, an application and a comparative study in the nonlinear random vibration analysis between the generalized density evolution equation implemented with the probability density evolution method (PDEM), the polynomial chaos

expansion (PCE) and Monte Carlo simulations (MCS) are addressed by investigating the stochastic seismic responses of a class of Duffing oscillators. A physical stochastic ground motion model is employed, and represented by a Karhunen-Loeve expansion as the input of the PCE and MCS. Numerical results reveal that the solution processes of the three approaches are identical for the weakly nonlinear systems, and they are approximately identical for the strongly nonlinear systems though the errors resulting from numerical techniques and artificial truncations could be amplified, indicating that the solutions of the PDEM and the PCE are equivalent to that of the nonlinear random vibration analysis in the mean-square sense. The two methods thus can be applied in the classical nonlinear random vibration analysis. It is remarked, moreover, that the PDEM goes a step further than the classical nonlinear random vibration analysis, since the probability density evolution processes of responses and accurate structural reliability assessments can be provided by the PDEM simultaneously. The other methods, however, need much more computational efforts to govern higher order statistics of responses.

Reliability-based stochastic control for structures using magnetorheological dampers

J. Li, Z. Mei & J.B. Chen

State Key Laboratory of Disaster Reduction in Civil Engineering & School of Civil Engineering,
Tongji University, Shanghai, P.R. China

1 INTRODUCTION

The efficacy of vibration mitigation is usually given by the reduction of dynamic responses (particularly peak displacements and peak accelerations) under control compared to those without control. However, what really matters is the reliability of the structures under control subjected to disaster actions.

In this paper, simulation analysis of stochastic control for structures using MR dampers is conducted. Firstly, a dynamic model of a MR damper is developed based on back propagation (BP) neural networks. Secondly, the physical stochastic ground motion model is introduced and 120 earthquake ground motion time histories are generated. Then, simulation analysis of vibration control of a model structure with MR dampers is carried out. Finally, stochastic response analysis and reliability assessment of structural systems with and without control is studied.

2 NEURAL NETWORK MODELING OF MR DAMPER

2.1 Dynamic testing of MR damper

A series of tests were conducted to measure the responses of the MR damper, as shown in Figure 1, under various loading conditions.

2.2 Neural network modeling of MR damper

In this section, BP neural networks are used to emulate the forward dynamics of the MR damper shown in Figure 1 based on the results of the dynamic testing. It is seen that the trained neural



Figure 1. MRD-100-10-type MR damper.

network model can predict the damping force very well and there is relatively good agreement between the neural network outputs and the test data.

3 PHYSICAL STOCHASTIC GROUND MOTION MODEL AND EARTHQUAKE GROUND MOTIONS GENERATED

3.1 Brief introduction of the physical stochastic ground motion model

In the physical stochastic ground motion model (Li & Ai, 2006; Ai & Li, 2009), the effects of engineering site could be regarded as a multi-layer filtering operator. For the sake of clarity, it is modeled as a single-degree-of-freedom (SDOF) system. Using the ground motion at the bedrock as the input process, the absolute response of the SDOF system is namely the process of the ground motion at the surface of the engineering site.

3.2 Earthquake ground motions generated

120 representative time histories of ground acceleration are obtained employing the physical stochastic ground motion model outlined in the preceding section, one of which is shown in Figure 2.

4 SIMULATION ANALYSIS OF VIBRATION CONTROL

4.1 Six-story building model

The model of a six-story, single-bay, building structure is considered, and the number of DOFs

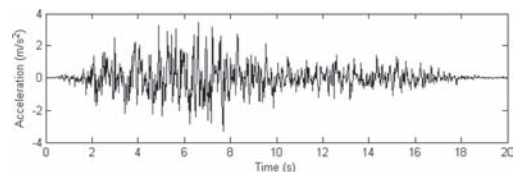


Figure 2. 25th time history of the ground acceleration.

of the model structure is reduced to 6, while still maintaining the important dynamics of the whole model. The structural parameters, like mass matrix, stiffness matrix and damping matrix, can all be obtained through identification.

4.2 *Simulation analysis of vibration control of model structures with and without MR dampers*

Based on the structural parameters of the 6-DOF model identified in section 4.1 and the neural network model of the MR damper established in section 2.2, the simulation analysis of the model structure with and without control is conducted. The statistical values of peak structural responses without control and under passive-off and passive-on control are presented, and the statistical values of maximum control force under passive control are given.

5 STOCHASTIC RESPONSE ANALYSIS OF THE MODEL STRUCTURE

5.1 *Foundations of the Probability Density Evolution Method (PDEM)*

The Probability Density Evolution Method (PDEM) is outlined briefly.

5.2 *Stochastic response analysis of structures with and without control*

In this section, the stochastic response analysis of the structure is carried out based on the results of deterministic dynamic analysis of the structure system according to the PDEM. Typical PDFs of interstory drifts of the first story at different instants of time (3 s, 6 s and 8 s) are given. Additionally, the PDF surface of interstory drift of the first story in the passive-on case (in the time interval from 1.5 to 3.5 s) is presented.

6 RELIABILITY ASSESSMENT OF THE MODEL STRUCTURE

6.1 *The method of dynamic reliability evaluation based on the extreme value distribution*

The method of dynamic reliability evaluation based on the extreme value distribution is introduced in brief.

6.2 *Reliability assessment of structures with and without control*

In the analysis of reliability, the interstory drift angle of each story is used as the performance

Table 1. Reliabilities of the model structure in different cases.

Case	Without control	Passive-off	Passive-on
Reliability	0.9095	0.9958	0.9930

index of the structure, and the maximum value of interstory drift angles should not exceed the threshold. Here, the threshold of interstory drift angles is assumed to be 0.0095 rad. Therefore, the reliabilities of the model structure with and without control are assessed. From the results of the reliability analysis (shown in Table 1), it is clearly seen that the reliability of the model structure with control is bigger than that without control. There is an about 9.5 percent increase in the reliability in the passive-off case, and a 9.2 percent increase is obtained in the passive-on case.

7 CONCLUSIONS

Based on the results of dynamic testing of a MR damper, a BP neural network model of the damper is developed. After briefly introducing the physical stochastic ground motion model, 120 earthquake ground motion time histories are generated, which are used as input ground motions in the analysis of structural vibration control. Then, the simulation analysis of the model structure with and without control is conducted. Additionally, the stochastic response analysis is carried out based on the probability density evolution method. Finally, the reliabilities of the model structure in different cases are carried out through the method of dynamic reliability evaluation based on the extreme value distribution.

ACKNOWLEDGEMENTS

Supports of the Natural Science Foundation of China (Grant No. 10872148), the Hi-tech Development Plan ("863" Plan) of the Ministry of Science and Technology (Grant No. 2008AA05Z413) and the Ministry of Education for New Century Excellent Talents are highly appreciated.

REFERENCES

- Ai, X.Q. & Li, J. 2009. Synthesis method of non-stationary ground motion based on random Fourier spectra. *Earthquake Engineering and Engineering Vibration* 29(2): 7–12. (in Chinese).
- Li, J. & Ai, X.Q. 2006. Study on random model of earthquake ground motion based on physical process. *Earthquake Engineering and Engineering Vibration* 26(5): 21–26. (in Chinese).

GS_139 — Applications (3)

This page intentionally left blank

Random response of chain structure with parameter uncertainties

B.G. Liu, Y. Pan & Y. Ning

Institute of Mechatronic Engineering, Henan University of Technology, Zhengzhou, China

Z. Shen

Zhengzhou Research Institute of Mechanical Engineering, Zhengzhou, China

ABSTRACT: Chain structure systems are a familiar subject matter amongst engineers, and transfer matrix methods (TMMs) are highly useful and efficient for the dynamic analysis of these structures (Lund 1974, Horner & Pillkey 1978, Lee et al., 1993, Kang et al., 1994, Oh 2004, Hsieh et al., 2006). Two kinds of transfer matrix methods are widely used in engineering: the Myklestad-Prohl transfer matrix method (MP-TMM) (Myklestad 1944, Prohl 1945) and the Riccati transfer matrix method (Riccati-TMM) (Horner & Pillkey 1978). The MP-TMM involves the use of simple mathematical equations, making it easy to program, but the method presents numerical difficulties when higher frequencies are calculated and/or when too many degrees of freedom exist. The Riccati-TMM presents no numerical difficulties; thus, it is more frequently used in engineering than the MP-TMM.

In this paper, recurrence perturbation equations based on the Riccati-TMM are derived to calculate the first—and second-order perturbation responses of chain structure systems with uncertain parameters. We call this perturbation method the Riccati perturbation transfer matrix method (Riccati-PTMM). On the basis of the Riccati-PTMM, we provide the detailed equations and steps for calculating the dynamic responses of chain structures with uncertain and random parameters. The equations and steps are used to calculate the mean values and variances of a simply supported Timoshenko beam with random mass density and random section diameter. The results show that the proposed method is enough accurate for engineering problems and much more efficient than Monte Carlo simulation.

The method presented in this paper is a generalisable approach that can be used for lateral and/or torsional dynamic response analysis of chain structure systems with uncertain or random parameters. For concrete problems, as long as the element transfer matrix and the element perturbation equations are given, dynamic analysis can be completed using this method.

1 KEY EQUATIONS

The transfer and recurrence equations of the Riccati-TMM are as follows:

$$\{f\}_i = [S]_i \{e\}_i + \{Q\}_i \quad (1)$$

$$[S]_{i+1} = [u_{11}S + u_{12}]_i [u_{21}S + u_{22}]_i^{-1} = [S_{i1}] [S_{i2}] \quad (2)$$

$$\{Q\}_{i+1} = \{Q_f\}_i - [S]_{i+1} \{Q_e\}_i \quad (3)$$

where $\{f\}_i$ and $\{e\}_i$ are the state vectors at the i th section, and satisfy boundary conditions $\{f\}_1 = \{0\}$ and $\{e\}_1 \neq \{0\}$, respectively; $[u_{11}]_i$, $[u_{12}]_i$, $[u_{21}]_i$, and $[u_{22}]_i$ are the matrixes defined by the transfer relationships of the state vectors between sections i and $i+1$ on element i ; $[S]_i$ is the so-called Riccati transfer matrix; and $\{Q_f\}_i$, $\{Q_j\}_i$, and $\{Q_e\}_i$ are generalised force vectors.

If b_j ($j = 1, \dots, m$) are the uncertain parameters of the chain structure, then they are expressed in the form:

$$b_j = b_{j0} (1 + \varepsilon_j) \quad (j = 1, \dots, m) \quad (4)$$

Response vector $\{e\}_i$ can be described by the following two-order accuracy perturbation equation:

$$\{e\}_i = \{e\}_{i,0} + \sum_{j=1}^m \{e\}_{i,j} \varepsilon_j + \sum_{j=1}^m \sum_{k=1}^j \{e\}_{i,jk} \varepsilon_j \varepsilon_k \quad (5)$$

where $\{e\}_{i,0}$ is the response vectors at section i when $b_j = b_{j0}$ ($j = 1, \dots, m$); and $\{e\}_{i,j}$, $\{e\}_{i,jk}$ are the first—and second-order perturbations of vectors $\{e\}_i$, respectively.

All the other matrixes and vectors are similar to $\{e\}_i$.

Finally, we derive the two-order perturbation transfer relationships as follows:

$$\{f\}_{i,0} = [S]_{i,0} \{e\}_{i,0} + \{Q\}_{i,0} \quad (6a)$$

$$\{f\}_{i,j} = [S]_{i,0} \{e\}_{i,j} + [S]_{i,j} \{e\}_{i,0} + \{Q\}_{i,j} \quad (6b)$$

$$\{f\}_{i,jk} = [S]_{i,0} \{e\}_{i,jk} + [S]_{i,j} \{e\}_{i,k} \quad (6c)$$

$$+(1-\delta_{jk}) [S]_{i,k} \{e\}_{i,j} + [S]_{i,k} \{e\}_{i,0} + \{Q\}_{i,jk}$$

The two-order recurrence perturbation equations are expressed as:

$$[S]_{i+1,0} = [S_{u1}]_{i,0} [S_{u2}]_{i,0} \quad (7a)$$

$$[S]_{i+1,j} = [S_{u1}]_{i,0} [S_{u2}]_{i,j} + [S_{u1}]_{i,j} [S_{u2}]_{i,0} \quad (7b)$$

$$[S]_{i+1,jk} = [S_{u1}]_{i,0} [S_{u2}]_{i,jk} + [S_{u1}]_{i,j} [S_{u2}]_{i,k} \quad (7c)$$

$$+(1-\delta_{jk}) [S_{u1}]_{i,k} [S_{u2}]_{i,j} + [S_{u1}]_{i,jk} [S_{u2}]_{i,0}$$

$$\{Q\}_{i+1,0} = \{Q_f\}_{i,0} - [S]_{i+1,0} \{Q_e\}_{i,0} \quad (8a)$$

$$\{Q\}_{i+1,j} = \{Q_f\}_{i,j} - [S]_{i+1,0} \{Q_e\}_{i,j} - [S]_{i+1,j} \{Q_e\}_{i,0} \quad (8b)$$

$$\{Q\}_{i+1,jk} = \{Q_f\}_{i,jk} - [S]_{i+1,0} \{Q_e\}_{i,jk} - [S]_{i+1,j} \{Q_e\}_{i,k}$$

$$-(1-\delta_{jk}) [S]_{i+1,k} \{Q_e\}_{i,j} - [S]_{i+1,jk} \{Q_e\}_{i,0} \quad (8c)$$

$$\{e\}_{i,0} = [S_{u2}]_{i,0} (\{e\}_{i+1,0} - \{Q_e\}_{i,0}) \quad (9a)$$

$$\{e\}_{i,j} = [S_{u2}]_{i,0} (\{e\}_{i+1,j} - \{Q_e\}_{i,j}) \quad (9b)$$

$$+ [S_{u2}]_{i,j} (\{e\}_{i+1,0} - \{Q_e\}_{i,0})$$

$$\{e\}_{i,jk} = [S_{u2}]_{i,0} (\{e\}_{i+1,jk} - \{Q_e\}_{i,jk}) \quad (9c)$$

$$+ [S_{u2}]_{i,j} (\{e\}_{i+1,k} - \{Q_e\}_{i,k})$$

$$+(1-\delta_{jk}) [S_{u2}]_{i,k} (\{e\}_{i+1,j} - \{Q_e\}_{i,j})$$

$$+ [S_{u2}]_{i,jk} (\{e\}_{i+1,0} - \{Q_e\}_{i,0})$$

where δ_{jk} is the Kronecker delta.

Equations (6)–(9) constitute the perturbation recurrence equations of the Riccati-TMM. This is an approximate method with two-order accuracy.

The detailed equations and calculation steps are provided in the full paper.

2 RANDOM RESPONSE

If ε_j ($j = 1, \dots, m$) are random parameters with zero mean values, and are subject to normal distribution, the mean value and variance of response vector $\{e\}_i$ are as follows:

$$E(\{e\}_i) = \{e\}_{i,0} + \sum_{j=1}^m \sum_{k=1}^m \{\hat{e}\}_{i,jk} E(\varepsilon_j \varepsilon_k) \quad (10)$$

$$Cov(\{e\}_i, \{e\}_i^T) = \sum_{j=1}^m \sum_{k=1}^m \{e\}_{i,j} \{e\}_{i,k}^T E(\varepsilon_j \varepsilon_k) \quad (11)$$

$$+ \sum_{j=1}^m \sum_{l=1}^m \sum_{s=1}^m \{\hat{e}\}_{i,jk} \{\hat{e}\}_{i,ls}^T \times [E(\varepsilon_j \varepsilon_s) E(\varepsilon_k \varepsilon_l) + E(\varepsilon_j \varepsilon_l) E(\varepsilon_k \varepsilon_s)]$$

where

$$\begin{cases} \{\hat{e}\}_{i,jk} = \{\hat{e}\}_{i,kj} = \frac{1}{2} \{e\}_{i,jk} & (j \neq k) \\ \{\hat{e}\}_{i,jj} = \{e\}_{i,jj} \end{cases} \quad (12)$$

3 EXAMPLE AND CONCLUSIONS

Taking a simply supported Timoshenko beam as an example, we assume that mass density ρ and section diameter d of the beam are independent random variables subject to normal distribution, and $E_\rho = 7800 \text{ kg/m}^3$, $\sigma_\rho = 156 \text{ kg/m}^3$; $E_d = 0.2 \text{ m}$, $\sigma_d = 0.004 \text{ m}$. The other parameters are certain: length $L = 10 \text{ m}$ and Young's modulus $E = 2.0 \times 10^{11} \text{ N/m}^2$. The load acting on the middle of the beam is $F = 1000 \sin(50\pi t) \text{ N}$.

The results of the second-order random perturbation are more accurate than those of the first-order random perturbation. The improvements in mean values are also clearly observable. However, in the calculation process, we know that the computations in the second-order random perturbation analysis are more complex. Thus, we propose that engineers use the first-order random perturbation analysis if the accuracy demands are not stringent because the calculation time involved in this approach is considerably shorter than in Monte Carlo random simulation.

The Riccati-PTMM can be used for the two-order perturbation analysis of the dynamic response of chain structures with uncertain or random parameters. The recurrence perturbation equations and steps presented in this paper can be used for lateral and/or torsional response analysis of chain structure systems. For concrete problems, as long as the element transfer matrix and the element perturbation equations are given, dynamic analysis can be completed using this generalisable method.

ACKNOWLEDGEMENT

The authors would like to thank the Committee of the National Natural Science Foundation of China for financial support (Foundation No. 10872064).

A Bayesian acoustic emission source location algorithm: Extended model

Thomas Schumacher

University of Delaware, Newark, DE, USA

Daniel Straub

Technical University Munich, Germany

ABSTRACT: The Acoustic Emission (AE) technique offers the unique opportunity to monitor infrastructure components in real-time and detect sudden changes in the integrity of the monitored element (Grosse and Ohtsu, 2008). AE are stress waves initiated by sudden strain releases from within a solid such as for example crack propagation, material crushing, or bond fracture of two materials in a composite due to over-loading. With networks of piezo-electric sensors mounted to the surface of the structure, stress waves can be detected, recorded, and stored for later analysis. An important step in quantitative analysis methods is the estimation of the stress wave source locations. Since only the time arrivals at each sensor are observed, this represents a nonlinear inverse problem that is commonly solved by iterative procedures whereby a cost function is minimized (Ge, 2003). The main issue of these traditional methods is that sources of uncertainty and variability in the material properties cannot be associated with any of the involved model parameters such as time arrivals, stress wave velocity, sensor locations, etc., essentially treating all parameters as deterministic using mean values.

The authors have developed a Bayesian framework for a probabilistic source location algorithm earlier using Monte Carlo Markov Chain simulation whereby all model parameters are represented by random variables (Schumacher et al., under review). A basic probabilistic model was presented where model parameters were estimated using an example employing observed arrival time data collected from a calibration experiment on a realistic section of a reinforced concrete bridge column (Schumacher, 2006). The probabilistic model is based on Bayesian updating, which can be stated as follows:

$$f_{\Theta}(\theta|x_0) = \frac{L(\theta|x_0)}{c} f_{\Theta}(\theta) \quad (1)$$

where $f_{\Theta}(\theta|x_0)$ represents the posterior distribution of Θ conditioned on observed outcomes x_0 of the random variable X , $L(\theta|x_0) = f_X(x_0|\theta)$ is the likelihood function of parameters θ for observed realizations x_0 of X , c is a normalizing constant, and $f_{\Theta}(\theta)$ is the prior distribution for Θ before additional knowledge is gained. Once the posterior distribution $f_{\Theta}(\theta|x_0)$ for the parameters is obtained, it can be incorporated in a general predictive joint distribution of the form:

$$f_X(x|x_0) = \int_{-\infty}^{\infty} \dots \int_{-\infty}^{\infty} f_X(x|\theta) f_{\Theta}(\theta|x_0) d\theta_1 \dots d\theta_m \quad (2)$$

to predict future events X based on knowledge from past observed realizations x_0 .

In the current study, an extension of the first basic model that was presented by the authors earlier is proposed that uses additional observed information in form of the maximum AE signal amplitude A . The central relationship for the statistical model is based on the relationship between measured arrival times $T_{a[i,j,k]}$, event time $t_{0[i,j]}$, wave slowness $S_{p[i,j]}$, stress wave travel distance $d_{[i,k]}$, and the standard deviations of the errors in the observed arrival times $\sigma_{\epsilon[k]}$, and can be stated as follows:

$$T_{a[i,j,k]} \sim N\left(t_{0[i,j]} + s_{p[i,k]} d_{[i,k]} \cdot \sigma_{\epsilon[i,j,k]}(A_{[i,j,k]}, \alpha)\right) \quad (3)$$

where i , j , and k are the subscripts that stand for event location, event number, and sensor, respectively. Variability in the model is assumed to be associated with the basic source location parameters which are the wave slowness s_p , the observed arrival times t_a , and the event time t_0 . The precision $\tau = \sigma^{-2}$ is assumed to be proportional with the maximum signal amplitude which was observed during the experiment. α is a global parameter that relates the standard deviations of the errors in the

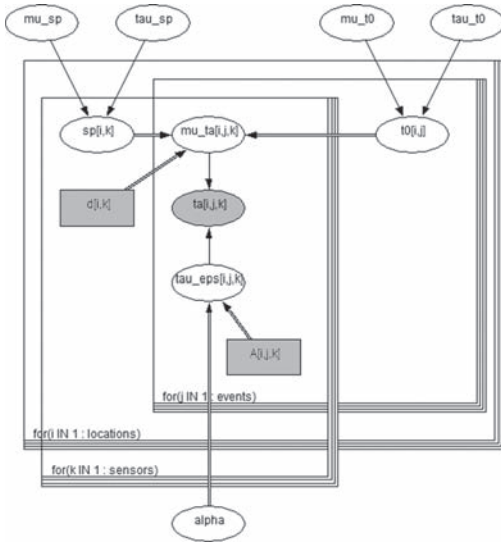


Figure 1. Graphical representation of proposed extended inference model (screenshot from *WinBUGS*).

observed arrival times $\sigma_{e(i,j,k)}$ with the signal amplitude A . In Fig. 1, a graphical representation of the proposed extended model is shown.

A set of data is evaluated using the proposed methodology and the predictions from the proposed extended probabilistic algorithm, the basic probabilistic algorithm presented earlier, and a traditional deterministic algorithm are compared and discussed. It is found that the extended model offers more accurate predictions compared to the

solutions of a traditional deterministic algorithm as well as the basic probabilistic algorithm introduced earlier by the authors (Schumacher et al., under review). Probabilistic algorithms have the additional benefit of providing an improved measure for the uncertainty of the prediction. The application of AE monitoring has often proven difficult because of the presence of noise and changing boundary conditions such as cracks, and the proposed probabilistic approach aims at addressing some of these issues. Implementation of an error term that is different for each sensor is planned in the future and it is expected that this modification will further improve predictions.

REFERENCES

- Ge, M. 2003. Analysis of Source Location Algorithms, Part II: Iterative methods. *Journal of Acoustic Emission*, 21, 29–51.
- Grosse, C.U. & Ohtsu, M. 2008. *Acoustic Emission Testing—Basics for Research-Applications in Civil Engineering*, Berlin & Heidelberg, Germany, Springer Verlag.
- Schumacher, T. 2006. *Acoustic Emission Monitoring of Flexural Tension Reinforcement Anchorage Zones in Full-Scale Bridge Bent Caps*. M.S. M.S. Project Report, Oregon State University.
- Schumacher, T., Straub, D. & Higgins, C. under review. Toward a Probabilistic Acoustic Emission Source Location Algorithm: a Bayesian Approach. *Journal of Sound and Vibration*, submitted on September 20, 2010.

Structural reliability criteria in relation to on-line control schemes

B.J. Leira

*Department of Marine Technology
Norwegian University of Science and Technology, Trondheim, Norway*

1 INTRODUCTION

Control schemes are typically based on minimization of objective functions (or loss functions). These are of different types depending on the specific control algorithm to be applied. Frequently, the loss functions are expressed in terms of costs associated with the response processes and/or the control processes. It is rarely the case that structural reliability criteria as such and the associated cost of structural failure is explicitly taken into account.

In the present paper, a summary of some approaches for incorporation of structural reliability criteria into the control algorithm is first given. Subsequently, the particular case of Linear Quadratic Gaussian (LQG) control is considered for a system with quasistatic response behaviour. A comparison is made between the losses which are obtained by application of the traditional objective function versus one that includes the costs associated with structural failure. Furthermore, a slightly different case where the slowly varying component of the response is controlled by LQG and the rapidly varying component is left unchanged is also considered. This will be relevant e.g. in connection with position control of marine structures.

In relation to formulation of structural response criteria within a specific control scheme, there are at least three possible approaches. The first corresponds to off-line determination of optimal values of specific control parameters based on structural criteria. These optimal values are subsequently applied by the implemented control scheme. The second approach corresponds to monitoring the values of selected structural reliability measures during the load/response process. If these measures exceed certain pre-defined values, a control action is activated or a switch is made to a different control scheme if a first control algorithm has already been activated. The third approach corresponds to making the control action at each time step being dependent on one or more structural reliability measures. These three different types are discussed in the paper.

2 CONTROL SCHEMES INVOLVING STRUCTURAL RELIABILITY CRITERIA

Focus is on dynamic structural response and control schemes which apply to a sequence of stationary conditions. The external excitation is assumed to contain a slowly varying load component (this implies that e.g. earthquake loading is excluded from the present considerations). This will e.g. be the case for structures which are subjected to low-frequency wind or wave forces. Control schemes which make explicit use of structural reliability criteria are considered.

A summary of some relevant control schemes which are described in the literature is first given. These schemes are classified as (i) off-line schemes, see e.g. Tomasula et al. (1996) (ii) reliability monitoring, see e.g. Berntsen et al. (2004) and (iii) on-line schemes, see e.g. Leira et al. (2001) and Berntsen et al. (2009).

3 LINEAR QUADRATIC GAUSSIAN CONTROL (LQG)

Pre-calibration of a well-know control scheme by means of structural failure probability considerations is the main focus of the present paper. The particular case of Linear Quadratic Gaussian (LQG) control is considered. The associated objective function (also referred to as the performance index) is defined. Furthermore, the particular case of quasi-static response where the stiffness of the system dominates is elaborated.

A second “reliability-based” objective function is subsequently introduced which incorporates the costs associated with structural failure. A comparison between the values of the two different objective functions is made, and it is discussed how the parameters of the LQG control scheme can be tuned to give equivalent results to those based on the “reliability-based” objective function.

A slightly different case is also addressed where the response consists of the sum of a slowly varying component and a rapidly varying (high-frequency)

component. The low-frequency component is controlled by LQG while the rapidly varying component is left unchanged. This case will be relevant e.g. in connection with position control of marine structures, see e.g. Berntsen et al. (2009).

The loss function (or performance index) that forms the basis for the LQG control scheme is expressed as:

$$\begin{aligned} J(x) &= E \left[\int_0^T (\alpha x^2 + \beta g^2 u^2) dt \right] \\ &= \int_0^T (\alpha E[x^2] + \beta g^2 E[u^2]) dt \\ &= T \cdot (\alpha E[x^2] + \beta g^2 E[u^2]) \end{aligned} \quad (1)$$

where α is the proportionality factor related to the response cost and β is the proportionality factor associated with the cost of the control action. The substitution of the factor T for the integration operator is due to stationarity of the load and response processes.

Focusing more on the most extreme response levels, it may be considered that there is no cost associated with the response until failure of the structure occurs. The expected response cost is then expressed as the product of the failure cost, C_f , times the probability that such a failure occurs for a given duration T .

The associated loss function can then be expressed as

$$J(x) = (C_f \cdot p_f(T) + T \cdot \beta E[u^2]) \quad (2)$$

The failure probability for a Gaussian response process (for a given duration, T) can be expressed as the probability that the extreme response level exceeds a critical response threshold, x_{cr} . Furthermore, the asymptotic distribution for the extreme response will be of the Gumbel type. The failure probability can then be expressed in terms of the complement of the cumulative Gumbel distribution function.

The cost associated with structural failure is next expressed as a factor R_f times the failure probability. This allows the loss function to be rewritten on the following form:

$$J(x) \sim \left(R_f \cdot F_f(T, R, r, f) + \frac{f^2 r}{(1 + fr)^2} \right) \quad (3)$$

where R is a normalized response threshold, f is a dimensionless control parameter, and r expresses the ratio between the two cost coefficients. This loss function is illustrated for the case that $R_f = 2$, and $r = 1$ in Figure 1.

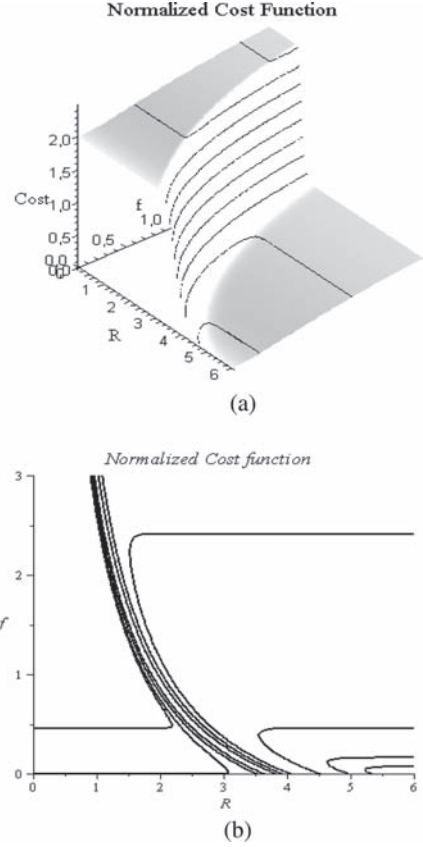


Figure 1. Normalized cost function.

For a specific value of the critical threshold (i.e. R) the value of the control factor f which minimizes the cost function can be identified. A procedure for calibration of the LQG algorithm by means of the failure probability loss function is outlined.

REFERENCES

- Berntsen, P.I.B., Leira, B.J., Aamo, O.M. & Sørensen, A.J. (2004): "Structural reliability criteria for control of large-scale interconnected marine structures", Proc. 23rd OMAE, Vancouver, Canada, 20–25 June.
- Berntsen, P.I.B., Aamo, O.M. & Leira, B.J. (2009): "Ensuring mooring line integrity by dynamic positioning: Controller design and experimental tests", *Automatica*, 45, pp. 1285–1290.
- Leira, B.J., Chen, Q., Sørensen, A.J. & Larsen, C.M. (2001): "Modeling of Riser Response for DP Control", Proc OMAE. 2001, Paper SR-2160, Rio de Janeiro, Brazil.
- Tomasula, D.P., Spencer, B.F. & Sain, M.K. (1996): "Nonlinear Control Strategies for Limiting Dynamic Response Extremes", *Journal of Engineering Mechanics*, Vol. 122, No. 3, March.

Probabilistic anomaly detection in structural monitoring data using a relevance vector machine

T. Saito

Institute of Technology, Shimizu Corporation, Tokyo, Japan

A method for automatically classifying the monitoring data into two categories, normal and anomaly, is developed to remove anomalous data included in monitoring data, making it easier to process the large volume of such data. An RVM is applied to a probabilistic discriminative model with basis functions and their weight parameters whose posterior distribution conditional on the learning data set is given by Bayes' theorem.

The proposed framework is applied to actual monitoring data sets containing anomalous data collected at two buildings in Tokyo, Japan. Examples of the wave time histories are shown in Figure 1, where (a) is a normal earthquake response record, (b) is an anomalous record caused by electrical noise, and (c) is also an anomalous record resulting from human activity (construction work). Data sets that include these two types of anomalous data are bundled as a target of the analysis to develop a more generalized discriminative model that can handle multiple types of anomalous data.

We consider three feature quantities:

- $F_1 = y_f/y_m$
- $F_2 = y_a/y_m$
- $F_3 = y_r/y_m$

where y_m is the maximum absolute value of the waveform, y_f is the maximum absolute value of the waveform low-passed at 2.5 Hz, y_a is the maximum absolute value of the three-second moving average of the waveform, and y_r is the RMS of the waveform. By combining all or some of them, we set four kinds of feature vectors, each of which specifies a model class set, as shown in Table 1.

Then the weights are optimized on the basis of the learning data set by maximizing the evidence: a significant proportion of the weights become concentrated at zero, which means that the terms associated with them are essentially removed. The result is a sparse model with only two relevance vectors in each model class set. These two relevance vectors can be considered representatives of normal and anomalous data, respectively. Table 2 shows the number of relevance vectors, the record number corresponding to each relevance vector and its

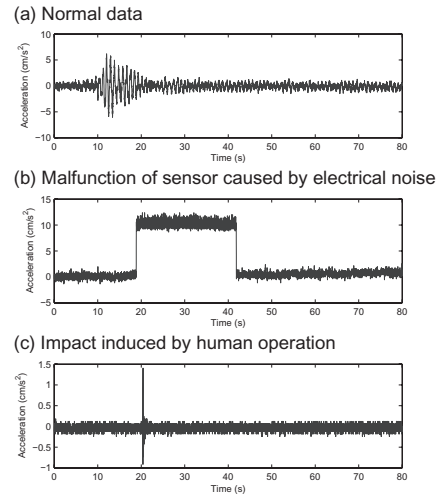


Figure 1. Samples of anomaly in monitoring data.

Table 1. Candidates of model class sets.

Model class set	Feature values used in learning
\mathcal{M}_1	F_1, F_2, F_3
\mathcal{M}_2	F_1, F_2
\mathcal{M}_3	F_1, F_3
\mathcal{M}_4	F_2, F_3

classification as normal/anomaly, the value of the log evidence, the posterior probability of the optimal model in each set, the MAP value of the weight vector, and the standard deviations and correlation coefficient derived from the covariance matrix.

The value of the evidence maximized during optimization represents the relative posterior probability of the optimal model in each set if they are treated as equally probable *a priori*. Thus the appropriateness of each set is evaluated by the maximized evidence. In this study, the evidences in two model class sets maximized during learning have almost equal largest values, demonstrating that they are appropriate.

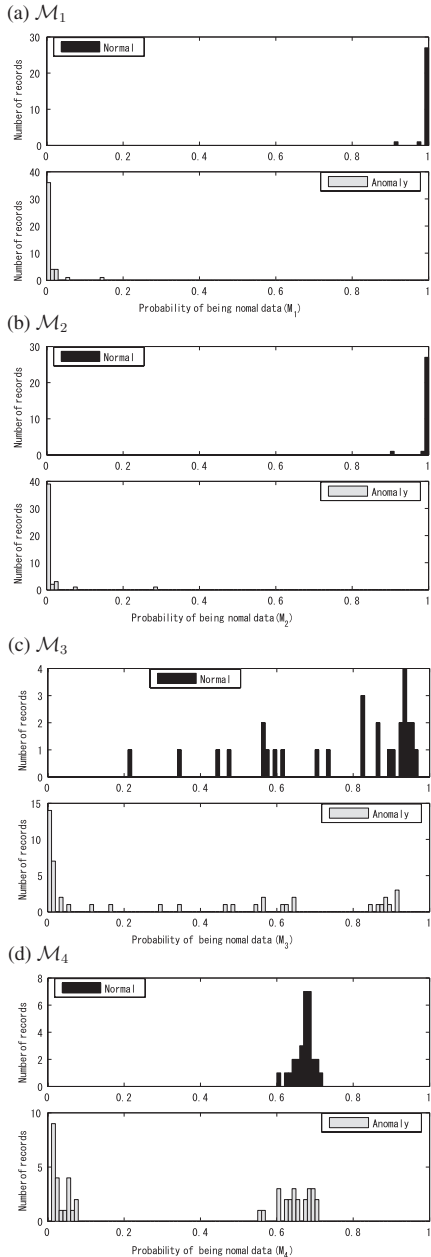


Figure 2. Histograms of output from MAP model in each model class.

The probability of each record being normal is calculated by applying the selected MAP model (that with $\mathbf{w} = \hat{\mathbf{w}}$) in each model class set to the data sets for verification. The results are shown as histograms for both normal and anomalous data in Figure 2. For \mathcal{M}_1 and \mathcal{M}_2 , each of which has a high posterior probability based on the evidence,

Table 2. Results of learning.

	\mathcal{M}_1	\mathcal{M}_2	\mathcal{M}_3	\mathcal{M}_4
Number of RVs	2	2	2	2
Wave No. of RV (1)	46	38	33	68
Normal/anomaly	normal	anomaly	normal	anomaly
Wave No. of RV (2)	51	46	49	69
Normal/anomaly	anomaly	normal	anomaly	normal
Log evidence	62.26	62.19	37.18	24.12
Probability of \mathcal{M}_j (%)	51.82	48.18	0.00	0.00
\hat{w}_1	38.44	-34.87	31.56	-6.35
\hat{w}_2	-37.56	37.65	-32.95	4.26
σ_{w1}	14.22	12.82	7.00	2.01
σ_{w2}	13.61	14.16	7.45	1.22
ρ_{w1w2}	-0.992	-0.993	-0.999	-0.975

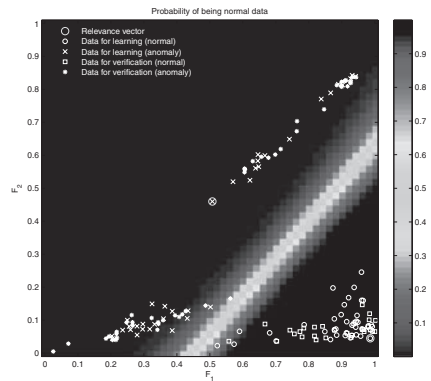


Figure 3. Output from MAP model in \mathcal{M}_2 and learning/verification data.

the probabilities of being normal for normal and anomalous records fall in the region above 90% and below 30% (above 99% and below 1% in most cases), respectively, which shows that these models successfully achieve extremely reliable anomaly detection.

The probability of being normal according to the MAP model in \mathcal{M}_2 is also shown in Figure 3 together with the relevance vectors, the learning data, and the verification data. We can see from this figure that the two relevance vectors are located far from the boundary between normal and anomalous data, and in the center along the boundary.

It is also a significant advantage of the proposed method that we can reasonably judge which combination of feature quantities is optimal by comparing the value of the evidence even if the number of candidate feature quantities is quite large.

Assessment of fatigue crack growth by cohesive zone elements

Pierre Beaurepaire & Gerhart I. Schuëller

Institute of Engineering Mechanics, University of Innsbruck, Innsbruck, Austria

Fatigue is the dominant failure mode of mechanical components subject to alternating loadings, leading to fracture at a stress level much lower than the yield stress of the material. One or several cracks initiate and propagate into the structure, leading to a sudden fracture once a critical length is reached.

Crack propagation can be modeled by the Paris-Erdogan equation (Paris & Erdogan 1963) or any of its further variations. However it is predictive only if a long crack is originally present, which happens seldom in manufactured components. In practical applications, an important part of the fatigue life is spent during crack initiation, which can not be easily modeled.

Cohesive zone elements are an alternative method to account for crack growth by means of finite element simulation. In this context, fracture is considered as a gradual phenomenon, with the progressive separation of the lips of an extended crack. Cohesive elements consist of zero-thickness elements that are inserted between the bulk elements and account for the resistance to crack opening by the mean of a dedicated traction displacement law (see Figure 1).

The cohesive force dissipates, at least partially, the energy related to crack formation. The effects of the fatigue history are modeled using deterioration of the stiffness with time. During the unloading-reloading process, the cohesive law shows an hysteresis loop and a slight decay of the stiffness is introduced to simulate fatigue crack propagation (see Figure 2). In this contribution, the effects of monotonic loadings and cyclic loadings are partially decoupled.

In case of monotonic loading, the formulation proposed by Needleman (Needleman 1987) is used. The stress in the cohesive element is expressed as:

$$T = a \cdot \delta \cdot \exp\left(-\frac{\delta}{b}\right) \quad (1)$$

where δ is the displacement of the nodes of the element, a and b are material parameters. Equation 1 determines the cohesive envelop of the mechanical law.

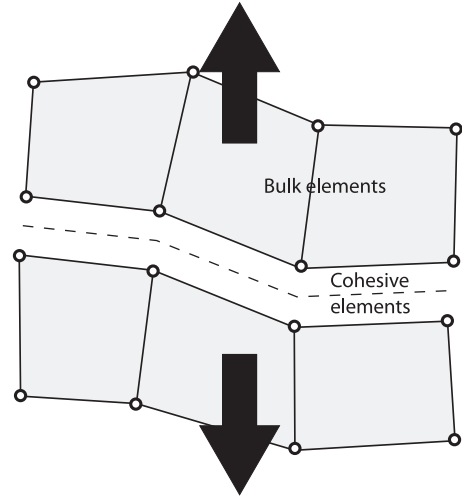


Figure 1. Insertion of cohesive zone elements at the interface of bulk elements.

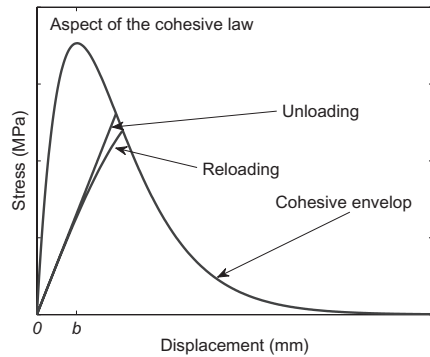


Figure 2. Aspect of the traction displacement law for cohesive elements.

If several unloading-reloading cycles are imposed, the cohesive elements show a loss of stiffness, which is monitored by a damage parameter D :

$$\dot{D} = \alpha \cdot T_n^\beta \cdot \max(T_n - T_0, 0)^\gamma \quad (2)$$

where α , β , γ and T_0 are material parameters.

For high cycle fatigue applications, cycle by cycle finite element simulation of the complete fatigue life would be computationally prohibitive, even for small structures with a limited number of degrees of freedom. A novel algorithm reducing the simulation time with limited loss of accuracy has been developed. It is dedicated to speed-up the fatigue simulations when cohesive zone elements are used. This algorithm is based on successive evaluation of the variation of the damage parameter of the cohesive elements over one (or several) cycles. These values are then used for extrapolation of the damage after a large number of cycle.

McEvily and Illg (McEvily & Illg 1958) conducted an experimental study to determine the crack growth rate of aluminium 2024-T3 in various structures. A crack was introduced in plates with a center hole, which was then undergoing alternating stress. These experiments were modeled using the proposed formulation of the cohesive zone elements. The result from the numerical simulations match experimental data.

Engineers are aware that the fatigue behaviour of components is strongly affected by uncertainties, i.e. nominally identical structures undergoing the same load spectrum present extensive scatter in their fatigue life. Crack initiation and crack propagation can both be seen as uncertain processes. Hence several authors have proposed a probabilistic analysis. The time to crack initiation, the growth rate and the final fracture process might all include uncertainties. Most of the methods available in the literature require to set up several probabilistic models which have to be combined in order to account for all kind of uncertainties inherent to fatigue. Cohesive elements provide an unified framework to describe the whole fatigue life.

Illg (Illg 1956) performed an experimental investigation of the fatigue life of structures subject to various alternating stress levels. The specimens consist of a plate with two notches without initial crack. Hence the fatigue life of the structure depends from the time to crack initiation and from the crack growth rate. The experiments were repeated several time at each stress level. As shows Figure 3, the experimental results are scattered over a wide range of fatigue lives. The uncertainties inherent to fatigue crack initiation and propagation are modeled using random fields for the parameters α , β and γ of Equation (2). A Monte Carlo simulation was performed using 200 samples. As shown in Figure 3, the results from the simulation are in

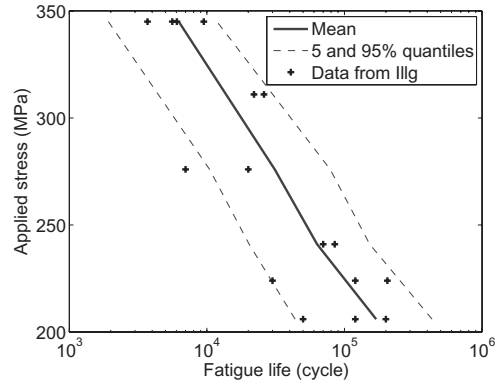


Figure 3. Fatigue life uncertainties. Probabilistic *SN* curve obtained with Monte Carlo simulation. The solid line denotes the mean fatigue life, dash lines denote the 5% and 95% quantiles. Crosses denote the experimental results.

good agreement with the experimental data from (Illg 1956).

A cohesive zone element formulation was developed for modeling fatigue crack growth. It allowed to assess the variability inherent to fatigue crack initiation and propagation using one single probabilistic model. A method to speed up the simulation with acceptable accuracy of the results was developed. The approach has been tested against experimental results available in the literature (Illg 1956, McEvily & Illg 1958). As shown on Figure 3, the numerical results match experimental data.

REFERENCES

- Illg, W. (1956). Fatigue tests on notched and unnotched sheet specimens of 2024 -t3 and 7075 -t6 aluminum alloys and of sae 4130 steel with special consideration of the life range from 2 to 10,000 cycles. Technical report, National Advisory Committy for aeronautics.
- McEvily, A.J. & Illg, W. (1958). The rate of fatigue-crack propagation in two alluminium alloys. Technical report, National Advisory Committy for aeronautics.
- Needleman, A. (1987). A continuum model for void nucleation by inclusion debonding. *J. Appl. Mech.* 54, 525–531.
- Paris, P. & Erdogan, F. (1963). A critical analysis of crack propagation laws. *J. Basic Eng., Trans. ASME* 85, 528–534.

Reliability-based design recommendations for FRP-reinforced concrete beams

S.E.C. Ribeiro & S.M.C. Diniz

Federal University of Minas Gerais, Belo Horizonte, MG, Brazil

ABSTRACT: In recent years, there has been a growing interest on high performance materials such as high-strength concrete and composite materials, among others. These materials may offer higher resistance and greater durability, and, as a consequence, potential gains throughout the life-cycle of the structure. It is well-known that a major problem to the durability of reinforced concrete structures is the corrosion of reinforcing steel. In this light, fiber reinforced polymers (FRP) provide a promising prospect for use as reinforcement in concrete construction.

Although the use of FRP as structural reinforcement can show great promise in terms of durability, the characteristics of these materials have led to new challenges in the design of FRP reinforced concrete (FRP-RC) components. Currently some design recommendations have been developed; however, they have in common the fact of being based on existing recommendations for traditional steel reinforced concrete (RC). In conventional RC beam design, failure is dictated by yielding of steel, thus resulting in a ductile failure. In the case of FRP-RC beams where two brittle materials are involved, a fragile failure is unavoidable. As a result, a change in the RC beam design paradigm (under-reinforced beams) is necessary.

Therefore, due to the increased use of FRP and also due to differences between the mechanical properties of steel and FRP, the reliability of FRP-RC beams shall be evaluated. Most of the suggestions proposed for the design of FRP-RC beams are based on a deterministic point of view. However, since most of the variables involved in the project (mechanical properties, geometric characteristics, loads, etc.) are random, probabilistic methods are required to assessing the reliability of FRP-RC beams.

Current design codes and standards (e.g. ASCE-SEI 7, ACI 318) are based on semi-probabilistic approaches. While it is agreed that the ideal would be to design a structure or structural element for a given probability of failure, the appeal of the semi-probabilistic approach stems from the coupling of design simplicity and the implicit incorporation of probabilistic concepts.

In this paper, a contribution to the development of semi-probabilistic design recommendations for FRP-RC beams is reported. To this end, the investigation presented in Diniz (2007) is extended. The safety levels implicit in the design recommendations of 81 FRP-RC beams designed according to ACI-440 (2006) are assessed. Monte Carlo simulation is used in the computation of the probability of failure of the designed beams with respect to the ultimate flexural strength. Special attention is given to the deterministic procedure for the computation of FRP-RC beam resistance.

The Monte Carlo simulation was implemented in a modular format; initially the probabilistic modeling of the resisting moment was made so that this information could then be used in the corresponding performance criterion. This procedure allowed a better understanding of the behavior of FRP-RC beams subjected to bending. Additionally, it should be noted that the module “Simulation of the Bending Resistance” is independent of any normative criteria. In the reliability analysis approach, the normative criteria are included in the computation of the load statistics. In this way, the procedures presented here can be easily extended to the treatment of other design recommendations for FRP-RC beams.

A comparison between the nominal resisting moment, M_n , and the average resisting moment, μ_{MR} has shown that the concrete compressive strength is the most influential factor in the resulting bending resistance. When the f'_c adopted is 30 MPa, the ratio μ_{MR}/M_n reaches the highest values (1.0464–1.2151), when f'_c is 50 MPa, the ratio μ_{MR}/M_n is in the range 1.0076–1.1542, and when f'_c is 70 MPa, the ratio μ_{MR}/M_n reaches the lowest values (0.9434–1.0813).

Another factor that has great influence on the resisting moment is the FRP reinforcement ratio. For the under-reinforced beams analyzed in this work (FRP ratios between 0.82 and 0.93 ρ_b) the ratio μ_{MR}/M_n reached the highest values (1.0304 to 1.2151), while for the beams in the transition region, the ratio μ_{MR}/M_n is in the range 0.9470 to 1.1204, and reaches the lowest values for the over-reinforced beams (0.9434 to 1.1093).

On the adequacy of the ACI 440 (2006) recommendations, it can be observed that:

- The use of FRP of smaller resistance and lower modulus of elasticity (beams P1) resulted in reduced levels of reliability. Thus the use of materials with these characteristics should be avoided;
- the results of this study point to the possibility that reduced levels of reliability can be achieved, in particular for the combination of higher concrete compressive strength, lower FRP tensile strength and smaller load ratios μ_D/μ_L . This result can be attributed in particular to a lower *in situ* concrete compressive strength relative to the strength measured in cylindrical specimens. In this work a variable factor was used in this conversion; on the other hand, this parameter is taken as fixed in ACI 440, and is equal to 0.85. It should be mentioned that, in the case of RC beams, where these elements are usually designed as under-reinforced beams, such consideration results in a minor effect. However, concrete compressive strength is of fundamental importance in the case of FRP-RC over-reinforced beams. Thus, the use of the procedures of ACI 440 for higher strength concretes should be done with caution;
- the FRP reinforcement ratio has great influence in the reliability levels implicit in the ACI 440 recommendations. The results indicated that under-reinforced beams have reliability rates

reasonably higher than those presented by the beams in the transition region or over-reinforced. It is thus seen that the goal of providing more safety for the failure mode corresponding to the FRP rupture is reached;

- the load ratio has great influence on the reliability levels implicit in the ACI 440 recommendations. In this study it was observed that as the load ratio μ_D/μ_L increases, there is a significant reduction in the probability of failure and consequently an increase in the reliability index. This fact has already been observed by other authors in the context of the development of reliability-based design recommendations; however, it is difficult to be treated within the context of the semi-probabilistic design.

REFERENCES

- ACI Committee 318. 2008. *Building Code Requirements for Structural Concrete (ACI 318-08) and Commentary*. Farmington Hills, Michigan, p. 465.
- ACI Committee 440. 2006. *Guide for the Design and Construction of Structural Concrete Reinforced with FRP Bars*. ACI 440.1R-06.
- ASCE-SEI. 2010. *Minimum Design Loads for Buildings and Other Structures – ASCE/SEI 7-10*, p. 650.
- Diniz, S.M.C. 2007. Reliability Evaluation of FRP Reinforced Concrete Beams. *Computational Stochastic Mechanics – CSM5*, Rhodes, Greece, June 21–23, 2006, Mill Press, pp. 215–225.

GS_318 — Applications (4)

This page intentionally left blank

Simulating two-phase microstructures using level-cut filtered poisson fields and genetic algorithms

Kirubel Teferra

Department of Civil Engineering and Engineering Mechanics, Columbia University, New York, USA

Eleni N. Chatzi

Institute of Structural Engineering, ETH Zürich, Zürich, Switzerland

ABSTRACT: Probabilistic characterization and simulation of morphological structures of random heterogeneous materials is an interdisciplinary research topic spanning the fields of Biology, Medicine, Structural Mechanics, Electrophysics, and many more (Torquato 2002). Once morphological structures are characterized, various physical phenomena, such as uid and contaminant transport, structural mechanical behavior, or chemical reaction processes, can be analyzed. It is often the case that random morphological structures exist at micro—and nano-scales, and attempts have been made to determine Representative Volume Elements (RVEs) through characterization of the random morphologies. Furthermore, a field of micromechanical analyses of heterogeneous materials is emerging in order to quantify the effects that phenomena occurring at the microscale have on observed macroscopic responses, such as the propagation of microcracks, or the determination of Green's functions or RVEs for the use of multi-grid or multi-scale models.

The work that has been done to generate sample microstructures that match specified correlation functions can be divided into two categories. One approach is to apply a perturbation method such as the Metropolis, Markov-Gibbs, Stochastic Optimization, or Simulating Annealing methods, while the other method is to translate an underlying and easily simulated random field to a Binary field by applying a level-cut (Grigoriu 2003; Koutsourelakis and Deodatis 2006). The advantage to the perturbation methods is that they are quite flexible in their capability to match higher order target correlation functions since there is no reliance on an underlying random field. However the major disadvantage to this approach is that a perturbation method must be applied for each sample generated, which is computationally expensive making Monte Carlo Simulation impractical. On the other hand, level-cut translation field models only need to apply a perturbation method once to identify

the properties of the underlying random field that lead to the corresponding target correlation functions when translated. The underlying field is usually a Gaussian field since it is efficiently simulated, thus yielding the method suitable for Monte Carlo Simulation. The drawback to this approach is that since Gaussian fields are completely characterized by their mean and autocorrelation functions, they cannot match more than two target correlation functions. It is well known that third and higher order correlation functions are necessary to accurately characterize many heterogeneous materials (Torquato 2002).

Grigoriu has developed a level-cut filtered Poisson field model that is capable of matching higher order correlation functions due to its ability to incorporate an arbitrary number of parameters (Grigoriu 2003; Grigoriu 2009; Grigoriu 1995). In Grigoriu 2003, he develops the theoretical framework for level-cut filtered Poisson fields and pseudo-analytically matches a target mean and 2-point probability function using a specific filtered Poisson field. In Grigoriu 2009, he outlines a Monte Carlo based procedure to simulate homogeneous and inhomogeneous filtered Poisson fields.

This work is essentially an extension of the work of references Grigoriu 2003; Grigoriu 2009 as it proposes a general methodology to optimize parameters of a filtered Poisson field to match target correlation functions of a Binary random field. This is done through a Monte Carlo based methodology which avoids having to calculate the n th—order probability density function of the underlying filtered Poisson field since it is algebraically and numerically cumbersome to calculate. The parameters of the Filtered Poisson Field are determined using a Genetic Algorithm. Genetic Algorithms are suitable for level-cut translation models since they have few parameters, and it is known that the performance of Genetic Algorithms decreases as the number of parameters increases. Figure 1 is a owchart describing the methodology. The paper

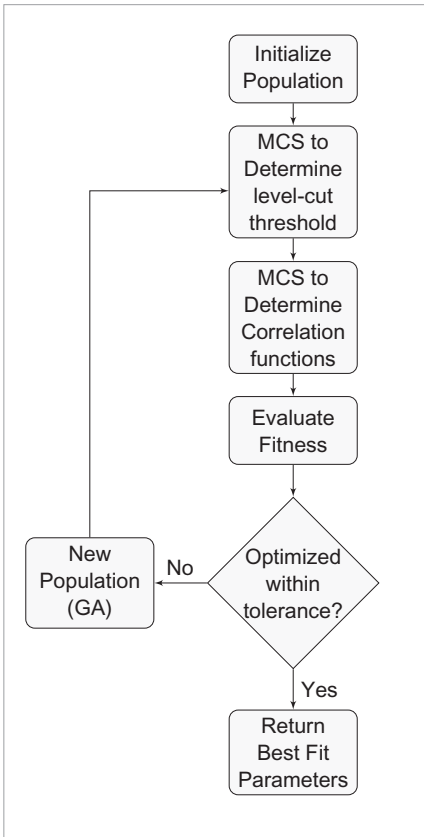


Figure 1. Flowchart of methodology.

concludes with numerical examples where target mean and autocorrelation functions of homogeneous, isotropic and anisotropic Binary fields are matched.

REFERENCES

- Grigoriu, M. (1995). *Applied non-Gaussian Processes*. Prentice Hall.
- Grigoriu, M. (2003). Random field models for two-phase microstructures. *Journal of Applied Physics* 94(6), 3762–3770.
- Grigoriu, M. (2009). Level-cut inhomogeneous filtered poisson field for two-phase microstructures. *International Journal for Numerical Methods in Engineering* 78, 215–228.
- Koutsourelakis & Deodatis, G. (2006). Simulation of multidimensional binary random fields with application to modeling of twophase random media, *Journal of Engineering Mechanics* 132, 619–631.
- Torquato, S. (2002). *Random heterogeneous Materials, Microstructure and Macroscopic Properties*, Springer, New York.

Variance Reduction Monte Carlo methods for wind turbines

M.T. Sichani, S.R.K. Nielsen & P. Thoft-Christensen

Department of Civil Engineering, Aalborg University, Aalborg, Denmark

Development of Variance Reduction Monte Carlo (VRMC) methods has proposed the possibility of estimation of rare events in structural dynamic. Efficiency of these methods in reducing variance of the failure estimations is a key parameter which allows efficient risk analysis, reliability assessment and rare event simulation of structural systems. Different methods have been proposed within the last ten years with the aim of estimating low failure probabilities especially for high dimensional problems. In this paper applicability of four of these methods i.e. Importance Sampling (IS), Distance Controlled Monte Carlo (DCMC), Asymptotic Sampling (AS) and Subset Simulation (SS) are compared to each other on a common problem. The aim of the study is to determine the most appropriate method for application on realistic systems, e.g. a wind turbine, which incorporate high dimensions and highly nonlinear structures.

Assessment of reliability and design of wind turbines require a means for estimation of very low failure probabilities of the system. This task can be tackled from three different points of view. The first class of methods are the extreme value distribution fittings to the extracted data of a wind turbine (Caires & Sterl 2005, Mackay, Challenor & Baha 2010). These data might be taken either from measured responses of a real wind turbine or from epochs of the response simulated by computer. This can be done in combination with some sampling methods such as the epochal method or the Peaks Over Threshold method (POT). It is implicitly assumed that the parent distribution belongs to the domain of attraction of one of the extreme value distributions; therefore the excess values above a given threshold follow a Generalized Pareto (GP) distribution (Naess & Clausen 2001). The required failure probability will be extrapolated from the fitted distribution.

On the other hand the so-called Variance Reduction Monte Carlo simulations (VRMC) might be used for estimating the failure probabilities (Sichani, Nielsen & Bucher a). The applicability and efficiency of the VRMC method on wind turbines is the subject of this study in order to understand advantages and limitations of VRMC methods within the framework of wind turbines.

The VRMC methods enable efficient estimation of the first excursion of the wind turbines within reasonable computation charge. However, they do not provide any means of understanding the evolution of the PDF of the process within time. This is of great interest since it gives a good insight into the statistical characteristics of the system and effect of different components, i.e. controller, on it.

Another approach for estimation of the first excursion probability of any system is based on calculating the evolution of the Probability Density Function (PDF) of the process and integrating it on the specified domain. Clearly this provides the most accurate result among the three class of the methods. The Fokker-Planck-Kolmogorov (FPK) equation is a well-known tool for realizing the evolution of a stochastic process governed by a differential equation. Although solution of the FPK for even low order structural dynamic problems require excessive numerical computations. This confines the applicability of the FPK to a very narrow range of problems. On the other hand the recently introduced Generalized Density Evolution Method (GDEM), (Li & Chen 2006, Chen & Li 2009, Li & Chen 2009), has opened a new way toward realization of the evolution of the PDF of a stochastic process; hence an alternative to the FPK. The considerable advantage of the introduced method over FPK is that its solution does not require high computational cost which extends its range of applicability to high order structural dynamic problems.

Estimation of failure probabilities of a wind turbine model is not a trivial task since it incorporates a highly nonlinear model for which the failure probability is to be estimated within a long time duration e.g. 600 s. However on the structure part, the wind turbine consists of a simple linear model, nonlinearities in such models appear from loading. These stem from two origins namely the nonlinear aerodynamic loads and the presence of a controller. The aerodynamic loads are highly nonlinear functions of the instantaneous wind speed and the pitch angles of the blades which are calculated with different means e.g. Blade Element Momentum theory (BEM) in this study. The pitch-controller introduces additional nonlinearities to the model i.e. due to its saturation state. Next according to the design criterions the

barrier level of a specified failure probability, e.g. 3.8×10^7 (Sichani, Nielsen & Bucher b), is required to be defined. This can most efficiently be estimated if the Cumulative Density Function (CDF) of the failure probability can be derived down to low failure probabilities of the order 10^7 .

The focus of this article is on the VRMC methods. Among the various available methods Importance Sampling (IS) (Bucher 2000, Au & Beck 2001, Macke & Bucher 2003), Distance Controlled Monte Carlo (DCMC) (Pradlwarter, Schuëller & Melnik-Melnikov 1994, Pradlwarter & Schuëller 1997, Pradlwarter & Schuëller 1999), Asymptotic Sampling (AS) (Bucher 2009, Sichani, Nielsen & Bucher a, Sichani, Nielsen & Bucher b), and Subset Simulation (SS) (Au & Beck 2001) are chosen primarily. All of the methods aim at the same subject, i.e. estimation of the low failure probability events. However they tackle the problem from very different points of view. IS moves the so-called sampling density of the problem to the boundaries of the failure region hence generates more samples in this area. The basis of IS is on the Ito stochastic differential equations and specifically on the so-called Girsanov's transformation which allows construction of the so-called Importance Sampling Density (ISD) by adding a deterministic drift to the stochastic excitation. DCMC works more on a logical basis where the idea is to run all the simulation samples simultaneously and find more important simulations, i.e. those which are closer to the boundaries of the safe domain, and artificial increase the outcrossing events by putting more emphasis on these important events. The AS development is based on the asymptotic estimation of failure probabilities (Breitung 1989). Here the advantage of the linear relationship of the safety index for multi-normal probability integrals is considered to estimate low failure probabilities by proper scaling of the probability integral. AS forces more outcrossing by increasing the excitation power, e.g. the standard deviation of the excitation in U-space, in a controlled way. SS takes it basis on the conditional probability estimation. It breaks the problem of a low failure probability estimation into estimation of a multiplication of some higher probabilities. Next a conditional sampler i.e. (modified) Metropolis-Hastings algorithm is used to estimate the conditional probabilities.

Primarily introduced methods are used for failure probability estimation of a Single Degree of Freedom (SDOF) oscillator. Comparison is made on the results of the methods in terms of their accuracy, requirements and computational load. Standard Monte Carlo simulation for the same system is performed for global comparison method accuracy.

This study prevails advantages and disadvantages of each of the methods in application on

Dynamic systems. Next, the method with highest merit is chosen and applied on a wind turbine model developed in previous study.

REFERENCES

- Au, S.K. & Beck, J.L. (2001). First excursion probabilities for linear systems by very efficient importance sampling. *Probabilistic Engineering Mechanics* 16, 193–207.
- Breitung, K. (1989). Asymptotic approximations for probability integrals. *Probabilistic Engineering Mechanics* 4(4), 187–190.
- Bucher, C. (2000). *An importance sampling technique for randomly excited systems discretized by finite elements.*, Volume II. In: Ko J.M., Xu Y.L. editors, *Advances in structural dynamics*. Amsterdam: Elsevier.
- Bucher, C. (2009). Asymptotic sampling for high-dimensional reliability analysis. *Probabilistic Engineering Mechanics* 24, 504–510.
- Caires, S. & Sterl, A. (2005). 100-year return value estimates for ocean wind speed and significant wave height from the era-40 data. *Journal of Climate* 18(7), 1032–1048.
- Chen, J. & Li, J. (2009). A note on the principle of preservation of probability and probability density evolution equation. *Probabilistic Engineering Mechanics* 24, 51–59.
- Li, J. & Chen, J. (2006). The probability density evolution method for dynamic response analysis of non-linear stochastic structures. *Int. J. Numer. Meth. Engng* 65, 882–903.
- Li, J. & Chen, J. (2009). *Stochastic Dynamics of Structures*. Wiley.
- Mackay, E., Challenor, P. & Baha, A. (2010). On the use of discrete seasonal and directional models for the estimation of extreme wave conditions. *Ocean Engineering* 37, 425–442.
- Macke, M. & Bucher, C. (2003). Importance sampling for randomly excited dynamical systems. *Journal of Sound and Vibration* 268, 269–290.
- Naess, A. & Clausen, P. (2001). Combination of the peaks-over-threshold and bootstrapping methods for extreme value prediction. *Structural Safety* 23, 315–330.
- Pradlwarter, H. & Schuëller, G. (1997). On advanced monte carlo simulation procedures in stochastic structural dynamics. *International Journal of Non-Linear Mechanics* 32(4), 753–774(10).
- Pradlwarter, H. & Schuëller, G. (1999). Assessment of low probability events of dynamical systems by controlled monte carlo simulation. *Probabilistic Engineering Mechanics* 14, 213–227.
- Pradlwarter, H., Schuëller, G. & Melnik-Melnikov, P. (1994). Reliability of mdof systems. *Probabilistic Engineering Mechanics* 9(4), 235–243.
- Sichani, M., Nielsen, S. & Bucher, C. (a). Applications of asymptotic sampling on high dimensional structural dynamic problems. *submitted to Structural Safety*.
- Sichani, M., Nielsen, S. & Bucher, C. (b). Efficient estimation of first passage probability of high dimensional non-linear systems. *submitted to Probabilistic Engineering Mechanics*.

A computational study of the buffered failure probability in reliability-based design optimization

H.G. Basova

Turkish Army, Ankara, Turkey

R.T. Rockafellar

Department of Mathematics, University of Washington, Seattle, WA, USA

Department of Industrial and Systems Engineering, University of Florida, Gainesville, FL, USA

J.O. Royset

Operations Research Department, Naval Postgraduate School, Monterey, CA, USA

INTRODUCTION

Engineering structures are subject to uncertain loads, environmental conditions, material properties, and geometry that must be accounted for in the design, maintenance, and retrofit of such structures. The theory of structural reliability provides an analytic framework for assessing the reliability of a structure as measured by its *failure probability*. While the failure probability is of significant importance, it also possesses troublesome properties that raise several theoretical, practical, and computational issues.

First, it only considers two possible states of the structure: failed, i.e., a performance threshold is violated, and safe, i.e., the threshold is not violated. The degree of violation is of no importance within this framework.

Second, the exact computation of the failure probability is rarely possible and commonly used geometric approximations such as the first-order and second-order reliability methods have unknown accuracy and may leave serious design risk undetected.

Third, the sensitivity of the failure probability or its approximations with respect to parameters may be poorly behaving and difficult to compute even if the underlying model of the structure is differentiable with respect to parameters.

Fourth, it is unknown whether the failure probability and its approximations are convex as functions of parameters. For this reason, it may be difficult to obtain a globally optimal design of optimization problems involving the failure probability or its approximations due to their many local minima that are not globally optimal.

The *buffered failure probability* is an alternative measure of reliability that offers several

advantages. The buffered failure probability is handled with relative ease in design optimization problems, accounts for the degree of violation of a performance threshold, and is more conservative than the failure probability. This paper summarizes key properties of the buffered failure probability and compares it with the failure probability.

FAILURE AND BUFFERED FAILURE PROBABILITIES

The failure and buffered failure probabilities are defined in terms a *limit-state function* $g(\mathbf{x}, \mathbf{v})$ that is a function of a vector $\mathbf{x} = (x_1, x_2, \dots, x_n)'$ of *design variables* (with prime ' denoting the transpose of a vector), which may represent member sizes, material type and quality, amount of steel reinforcement, and geometric layout selected by the designer, and a vector $\mathbf{v} = (v_1, v_2, \dots, v_m)'$ of quantities, which may describe loads, environmental conditions, material properties, and other factors the designer cannot directly control. The quantities \mathbf{v} are usually subject to uncertainty and their values are therefore not known a priori. The limit-state function represents the performance of the structure with respect to a specific criterion referred to as a limit state. As commonly done, we describe these quantities by random variables $\mathbf{V} = (V_1, V_2, \dots, V_m)'$ with a joint probability distribution which is regarded as known, although it might need to be estimated empirically. By convention, $g(\mathbf{x}, \mathbf{v}) > 0$ represents unsatisfactory performance of the structure and hence the failure probability is defined by $p(\mathbf{x}) = P[g(\mathbf{x}, \mathbf{V}) > 0]$.

The buffered failure probability is defined as $\bar{p}(\mathbf{x}) = P[g(\mathbf{x}, \mathbf{V}) \geq q_\alpha(\mathbf{x})]$, where $q_\alpha(\mathbf{x})$ is the α -quantile of $g(\mathbf{x}, \mathbf{V})$ and α is selected such that the

superquantile $\bar{q}_\alpha(\mathbf{x}) = E[g(\mathbf{x}, \mathbf{V}) | g(\mathbf{x}, \mathbf{V}) \geq q_\alpha(\mathbf{x})] = 0$. While the buffered failure probability appears more complicated than the failure probability at first sight, it compares favorably with the failure probability in several aspects.

First, we find it highly problematic to apply standard nonlinear optimization algorithms to optimization problems involving $p(\mathbf{x})$ as discussed above. In contrast, problems with $\bar{p}(\mathbf{x})$ is solvable by standard nonlinear optimization algorithms as long as the limit-state function $g(\mathbf{x}, \mathbf{v})$ is continuously differentiable with respect to \mathbf{x} .

Second, the buffered failure probability provides an alternative measure of structural reliability which accounts for the tail behavior of the distribution of $g(\mathbf{x}, \mathbf{V})$, which may be important to risk-averse designers. Hence, designs obtained using $\bar{p}(\mathbf{x})$ may be more desirable than those obtained using $p(\mathbf{x})$.

Third, even if $g(\mathbf{x}, \mathbf{v})$ is convex in \mathbf{x} , $p(\mathbf{x})$ may not be and, hence, it may be difficult to obtain a globally optimal designs when using the failure probability. In contrast, optimization problems involving the buffered failure probability are convex if $g(\mathbf{x}, \mathbf{v})$ and the other constraint and objective functions are convex.

Fourth, optimization problems involving the buffered failure probability facilitates the development of approximation schemes for limit-state functions that are expensive to evaluate.

COMPUTATIONAL METHODS

We present three algorithms for solving design optimization problems involving the buffered failure probability based on sample-average approximations where an expected value is replaced by the corresponding sample average approximation. The first algorithm involves transcription of the design optimization problem into a large-scale optimization problem and the solution of that problem using a standard nonlinear optimization solver. The second algorithm uses the same transcription as the first algorithm, but only considers an adaptively determined subset of variables and constraints during the solution of the large-scale problem. The third algorithm uses an exponential smoothing technique to avoid the transcription into a large-scale optimization problem. The algorithms are attractive due to their simplicity and the fact that they can easily be implemented using standard optimization solvers when the limit-state function $g(\mathbf{x}, \mathbf{v})$ is continuously differentiable with respect to \mathbf{x} . They are also guaranteed to generate globally optimal, locally optimal, and stationary

points under relatively mild assumptions as the sample size in the sample average approximation tends to infinity.

NUMERICAL RESULTS

We consider six engineering design examples from the literature and compare the differences between the failure and buffered failure probabilities in these cases. Example 1 is a simple problem instance with two design variables and two random variables. Example 2 involves the design of the thickness and width of a cantilever beam subject to random yield stress, Young's module, and horizontal and vertical loads. Example 3 deals with the design of the cross-section width and depth of a short column subject to random axial force, bending moment, and yield stress. Example 4 focuses on determining the diameter and thickness of a tubular column under a random load. Example 5 involves the design of a speed reducer under random material properties. The design variables include face width, module of teeth, number of teeth on pinion, and length and diameter of shafts. Example 6 deals with the design of a motor vehicle under a side-impact crash. The design variables include thickness of pillar, floor side, cross member, door beam and door belt line. All design variables are subject to production uncertainties. These examples involve multiple limit-state functions and, hence, we consider a generalization of the failure and buffered failure probabilities to the *system* failure probability and the *system* buffered failure probability. The examples include a mix of explicitly given linear and nonlinear objective and limit-state functions.

We find that the buffered failure probability typically overestimates the failure probability of the structures by a factor of three. Application of the three proposed algorithms yield essentially the same design, but the computational time varies significantly. Algorithm 1 is one to three orders of magnitude slower than Algorithms 2 and 3 due to the large number of variables and constraints that need to be handled by the solver. Its memory requirement is also substantial. Except in Example 2, Algorithm 2 is faster than Algorithm 3 with run times of less than 10 seconds. In Example 2, Algorithm 3 obtains an optimized design in 42 seconds, while Algorithm 2 requires 199 seconds. Overall, the computing times of Algorithms 2 and 3 to solve design optimization problems involving the buffered failure probability are remarkable fast in view of the difficulty associated with optimization problems involving the failure probability.

Advanced modeling and simulation tools: From surrogates to copulas

M. McCullough, A. Kareem & D.K. Kwon
University of Notre Dame, Notre Dame, IN, USA

L. Wang
Technip, Houston, TX, USA

1 INTRODUCTION

In the world of dynamic load effects, advanced modeling and simulation tools are becoming increasingly important in order to handle the non-stationarity and nonlinearity inherent in wind, wave, and earthquake related events. Previous assumptions, while convenient, have proven to over-simplify the complexity of the problems associated with wind engineering. This paper introduces a suite of tools that can be used to model and simulate complex events involving dynamic wind effects on structures and are conveniently applicable to wave and earthquake related load effects as well.

2 SURROGATES

Surrogate data methods can be used as an initial tool to determine whether an event or dataset is non-stationary or where specifically non-stationarity is occurring within the signal. Surrogates have the same Fourier magnitudes of the original signal but have randomized phases. A large number of unique surrogates can easily be created by continuing to simulate random phases. The original time series as well as each surrogate is analyzed in the time-frequency (TF) domain for each of the two methods introduced herein. Wavelet transform produces a time-frequency distribution of energy and has the ability to discern high intensity, short duration frequency components and thus identify transient components of non-stationary processes. Two surrogate methods are explored. The global method simply categorizes the entire signal as stationary or non-stationary, while the local method reveals pockets in time where non-stationarity is occurring.

3 EFFICACY OF AVERAGING INTERVAL FOR NON-STATIONARY WINDS

Several different fixed averaging interval and variable averaging interval approaches are introduced as a

means to determine the turbulence statistics of data based on whether it is stationary or non-stationary. A stationary wind model has been used for many decades with atmospheric boundary-layer winds based on the quasi-static and strip theory for computing wind forces on structures. Based on this stationary wind model, many researchers have used a user-defined fixed averaging interval (FAI) to study boundary-layer winds due to its simplicity. Hurricanes, thunderstorms, and downbursts, however, have non-stationary features that consist of rapid wind speed and directional changes. Therefore, the assumptions associated with the stationary wind model may no longer be appropriate. If the data is non-stationary, which can be determined by the surrogate method, then the traditional FAI approach may not be accurate and detrending may be necessary to decompose the data into the time-varying mean and a fluctuating component. An alternative data driven approach to model non-stationary features of winds and determine turbulence statistics uses fixed averaging intervals with Wavelet Transform (WT) or Empirical Mode Decomposition (EMD). This method, however, is still based around a user-defined FAI. For strong non-stationary wind fields, a user-defined FAI may not be appropriate since the rapid changes in wind speed and direction may be lost using FAI methods since the interval sizes cannot be varied to capture shorter or longer events. Therefore, a variable averaging interval (VAI) approach may be more suitable and will be introduced. In contrast with the user-defined FAI, a VAI approach determines the requisite averaging blocks (windows) based on the measured wind data itself. These three different methodologies, two FAI and one VAI, and their supporting schemes are then evaluated and compared in order to determine the most appropriate framework for capturing the salient features of non-stationary data which can be immediately extended for the dynamic analysis of systems under transient loading. The turbulent wind characteristics, including gust factor and turbulence intensity, are the main focus.

4 CLUSTERING

Clustering is proposed in this paper as a novel approach for developing representative spectra for different wind events. In previous studies, clustering algorithms have been used to classify ocean wave spectra into groups with similar inter-group properties and different intra-group properties. In this manner, the members of each group have similar statistical properties and can be associated with specific events. A similar methodology can be used to classify wind spectra into groups associated with specific wind events. The clustering results for sea waves and wind can be used to predict the wave and wind events that typically occur given the environmental conditions. This will also allow us to see whether correlations exist between the wind and wave environments in a specific location at specific times and a given set of environmental conditions. Determining a set of representative spectra for wind and wave events reveals a great deal about the frequency content of the events, which will help with efficient and effective design of structures to withstand the forces. Application of clustering also includes developing wind statistics from spatially distributed sites to establish a super station.

5 KERNEL DENSITY ESTIMATORS

Similar to clustering, which can be used to predict the specific wind or wave events given the environmental conditions, the kernel density estimation technique can be used to produce the probability distribution functions for wind in the near future given current conditions. Previously, in wind power forecasting, single values were predicted for each time step instead of the entire PDF. Spot or deterministic predictions do not incorporate uncertainty and therefore are difficult to incorporate into risk models. Probabilistic predictions using kernel density estimators show a great deal of promise in the forecasting of wind, which has a great number of uses in structural engineering, especially considering the rise of dynamic and zero-energy buildings.

6 WAVELET BISPECTRUM

Probabilistic prediction of wind pressures on a structure at a specific point using kernel density estimators is a significant research development, but determination of wind pressure correlations on a structure is also of importance when considering cladding design and occupant comfort criteria of tall buildings. Instantaneous wavelet bispectrum together with information theory can be used

to detect the strength and direction of coupling between pressure time histories on buildings. Understanding the strength and direction of coupling between pressure points on a building yields a great deal of information about the nature of the wind fluctuations as they approach the structure. Pressure correlations on a structure have thus far been overly simplified in current models and are in need of refinement.

7 COPULAS

Extreme events have proven difficult to model due to a lack of data and changing environmental factors. Knowledge of extreme events and the statistics associated with them, however, is imperative when considering mitigation options. Copulas have emerged in recent years as a method of determining dependency between variables by formulating a multivariate distribution. Copulas have great potential when applied to extreme event statistics. Specifically, copulas can be used to model the relationship between multiple hazards, where no model yet exists. Multi-hazard mitigation is a growing area of research and being able to understand and model the relationships between events is an important first step.

8 CONCLUSIONS

This study investigates advanced modeling and simulation tools that can be used in wind engineering either together or independently. The surrogate method to determine whether a dataset is stationary or non-stationary can be combined with the averaging interval methods in order to accurately determine the turbulence statistics that can be used to characterize the load effects associated with specific wind events. Clustering can be used to develop representative spectra for various stationary and non-stationary wind events, which can yield insight into the environmental factors generating them. Kernel density estimators is a probabilistic method that can be used to develop short-term wind predictions. Once these are known the coupling between wind pressures on a structure becomes of dominant importance. Instantaneous wavelet bispectra and information theory approaches can be used to better understand the coupling present in wind pressures at different locations on a structure. Finally, copulas can be used to further the research in multi-hazard engineering by developing a model that considers the dependencies between different hazards.

A ground motion record selection procedure utilizing a vector-valued intensity measure for optimized incremental dynamic analysis

Aris I. Theophilou & Marios K. Chryssanthopoulos

University of Surrey, Faculty of Engineering and Physical Sciences, Civil Engineering, Guildford, UK

1 INTRODUCTION

The objective of the present study is to predict the ductility demand of a multi-storey building, within a range of ground motion intensity levels, through incremental dynamic analysis (IDA) (Vamvatsikos and Cornell, 2002). A procedure is developed for optimizing IDA by selecting records from a given dataset. The procedure utilizes a vector-valued intensity measure (IM) which incorporates the normalized spectral area parameter. In the context of performance based earthquake engineering, structural performance is evaluated in terms of damage measures (DMs).

The procedure leads to the same level of accuracy in response prediction for a smaller number of records used, compared to random selection. Conversely, it results in a more accurate response prediction, for the same number of records used.

2 RECORD SELECTION PROCEDURE

The procedure is applied to a single-degree-of-freedom (SDOF) system, which could act as a proxy to a multi-degree-of-freedom system representing the actual structure.

The SDOF system has an elasto-perfectly-plastic force-deformation relationship $f_s(u, \dot{u})$, shown in Figure 1. The yield strength is denoted as f_y , and the maximum deformation response as u_m . Also shown in Figure 1 is the corresponding linear system defined as an elastic system with the same stiffness, together with the maximum elastic deformation u_0 , i.e. the spectral deformation $S_d(T_1)$, and the elastic strength f_0 . The deformation capacity of the bilinear system is assumed to be unlimited, as the purpose is to evaluate the maximum deformation u_m . The yield strength f_y and the elastic strength f_0 are related through the yield reduction factor R_y , given by

$$f_y = \frac{f_0}{R_y} \quad (1)$$

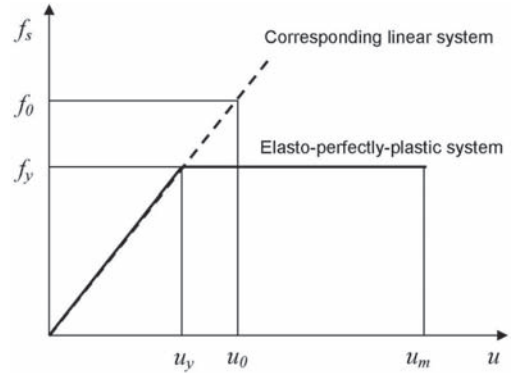


Figure 1. SDOF system force-deformation relationship.

IDA progresses by increasing the yield reduction factor R_y , within a range of intensity levels.

A vector-valued intensity measure (IM) is considered, comprised of the spectral deformation $S_d(T_1)$, the yield reduction factor R_y , and the ‘Normalized Spectral Area’ (NSA) parameter, symbolized as shown below

$$\langle S_d(T_1), R_y, S_{dN}(T_1, T_2) \rangle \quad (2)$$

NSA is evaluated by integration of the deformation spectral area and normalization to the spectral deformation $S_d(T_1)$ at the fundamental period. It is therefore independent of the response spectrum intensity. As a result, it has the potential to capture the effect of the record frequency content and period elongation on the response. The NSA parameter, denoted as $S_{dN}(T_1, T_2)$, is given by

$$S_{dN}(T_1, T_2) = \frac{1}{S_d(T_1) \cdot T_N} \int_{T_1}^{T_2} S_d(T) dT, \quad T_1 < T_2 \quad (3)$$

where T_1 is the fundamental period of the system, $T_N = 1.0$ sec is the unit period, and $S_d(T_1)$ is the response spectrum deformation at T_1 .

The DM investigated is the ductility factor μ_d . It is defined as the maximum inelastic

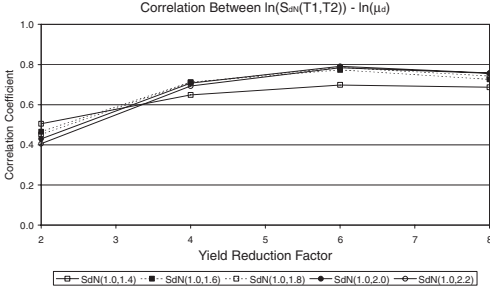


Figure 2. Correlation between $\ln(S_{dN}(T_1, T_2)) - \ln(\mu_d)$.

deformation u_m divided by the yield deformation u_y , expressed as

$$\mu_d = \frac{u_m}{u_y} \quad (4)$$

Having defined both IM and DM to be considered, regression analysis is conducted in order to quantify their functional relationship, including the standard error and the correlation coefficient. For the relationship between $\ln(S_{dN}(T_1, T_2))$ and $\ln(\mu_d)$, the simple linear regression model was found to be suitable.

As observed in Figure 2, the sample correlation coefficient r is seen to increase, as the yield reduction factor R_y increases from 2 to 6, which implies that the proposed IM becomes more efficient. Another observation is that for different yield reduction factors R_y , the peak sample correlation coefficient r corresponds to different integration ranges for the NSA parameter $S_{dN}(T_1, T_2)$.

The initial step in developing the procedure for record selection is to form a suite of records from available databases, according to the design earthquake scenario. Records are then allotted into bins on the basis of their NSA parameter $S_{dN}(T_1, T_2)$. Optimized suites, comprised of a reduced number of records, are then identified from the bins.

3 EXAMPLE

The proposed record selection procedure was applied to a SDOF system of fundamental period $T_1 = 1.0$ sec, which could be considered typical of the fundamental period of a ten storey reinforced concrete frame building. The structure is assumed to be first mode dominated with viscous damping ratio 5%.

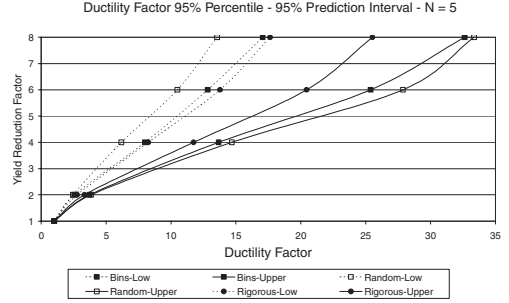


Figure 3. IDA curves for ductility factor 95% percentile, 95% prediction interval, $N = 5$.

In order to compare bin selection to random selection, datasets of a large number of suites were formed using each procedure. The rigorous solution was obtained using a suite comprising of all 34 records. Statistical analysis of the datasets was then carried out, the resulting statistics of which were used in the comparison.

Figure 3 shows the IDA curves for the ductility factor 95% percentile, expressed as a two-sided 95% prediction interval. The ductility factor μ_d is plotted against the intensity measure R_y . For this specific example, the proposed selection procedure based on bin discretization has resulted in prediction intervals up to 35–45% narrower than random selection.

4 CONCLUSIONS

In the present study, IDA was applied in the prediction of the ductility demand of a SDOF system, which is taken as a proxy to a multi-storey building, for a range of ground motion intensity levels. The proposed record selection procedure resulted in a more accurate prediction of structural performance due to future earthquake events, as a result of the higher correlation of DM to the proposed vector-valued IM, compared to random selection.

REFERENCE

Vamvatsikos, D. & Cornell, C.A. 2002. Incremental Dynamic Analysis, *Earthquake Engineering and Structural Dynamics*, Vol. 31, 491–514.

GS_328 — Applications (5)

This page intentionally left blank

Reliability level of structures designed according to the design codes of the Republic of Belarus

Dz. Markouski

Research and Production Enterprise «Modostr», Minsk, Belarus

V. Tur

Brest State Technical University, Brest, Belarus

The results of the investigation devoted to the calibration of the combination factors for loads in persistent design situations, i.e. in normal conditions of use for structures, are presented.

The introduction gives the information about three groups of standards regulating the rules for assessing loads while designing the reinforced concrete structures that are valid in the Republic of Belarus at present. These are

- Eurocode EN 1990—EN 1991;
- Belarusian design code SNB 5.03.01-2000 “Concrete and reinforced concrete structures design”; and
- the USSR design standard SNiP 2.01.07-85 “Loads and actions”.

The Ukrainian standard DBN B.1.2-2-2006 «Loads and actions» is also considered in the article.

The code SNB 5.03.01 and the system of Eurocodes are 100% harmonized in respect of loads assessment in design. However, the majority of provisions stated in SNiP 2.01.07-85 contradict the standards ISO 2394 and EN 1990 that are also valid in Belarus. For example, there are inconsistencies in the classification of actions, in values of partial factors for loads, in combination rules for loads for ultimate as well as serviceability limit state design of structures.

The aim of the present paper is to estimate the level of design reliability of structures (provided by using a system of safety factors and combination factors for loads) in persistent design situations, according to each standard mentioned above. The following problems are solved for this purpose:

- the state functions for structural elements that allow considering different ratios of permanent, live, and snow loads, are formulated;
- the probabilistic models of basic variables contained in the state functions are formulated;
- an estimation of reliability level of structures, designed in accordance with standards EN, SNB,

SNiP, and DBN, is performed by the 1st order reliability method. Moreover, different systems of safety factors and combination factors as well as the difference in combination rules for loads are taken into account.

The second part of the article is “Comparison of the approaches to assessing loads in the design codes”.

The rules for deriving design combinations of loads on structures in persistent design situations are presented here. The case when permanent, live, and snow loads are imposed, is considered.

It should be stipulated that coefficients γ and ψ have disparate treatment and mathematical concept within the bounds of corresponding standards. As well there are distinctions in loads classification and in method of setting characteristic values of loads and actions.

It is noted that there is a significant difference between the approaches to setting characteristic values of loads. The safety factor for permanent loads γ_G in Eurocode has a greater value, but it should be used together with combination coefficient ξ that is not specified in the other two standards. Another important difference comes from the fact that within the bounds of SNiP the factor γ_G has a physical meaning of overload factor, and its value is assigned using this consideration.

A striking difference in approaches to setting characteristic values for snow loads should be noted: in EN 1991-1-3 the characteristic value is the value which on average is exceeded once in 50 year. An analogous approach is accepted in Ukrainian standard DBN. Meanwhile, within the bounds of SNiP, the characteristic value of a snow load is the mean value of 1 year maximums.

The third part of the article is “Reliability methods and models”.

For estimating reliability level of structural elements, which is provided by the system of partial factors and combination factors, the following procedure is applied. It is based on the 1st order

reliability method (FORM) as well as the method of quickest descent (which are both used for analysis of probabilistic state functions of structures and for estimation of the values of reliability indices), and the Ferry Borges—Castanheta model and Turkstra's rule (for probabilistic modeling of loads and combinations of loads).

The value of target reliability index for structures is accepted $\beta = 4.7$ for the reference period $T = 1$ year in accordance with EN 1990. Normal distribution is adopted for modeling permanent loads, Gumbel distribution—for modeling variable loads, Normal distribution—for load effect uncertainties, LogNormal distribution—for modeling resistance of structural elements.

In general form the probabilistic state function $g(\mathbf{X})$ characterizes safety margin of a structural element (ultimate limit state). It contains a system of factors giving the relative importance of each load among other loads. The probabilistic models of basic variables characterize resistance of structural elements, permanent loads, variable live and snow loads, as well as uncertainty in load effect model. They have been developed subject to the nature of these actions and to their expected duration.

The probabilistic models of *live load* are developed basing on the investigation of statistical parameters of loads on structures in residential buildings presented in JCSS Probabilistic Model Code.

The probabilistic models of *snow load* are based on the results of the current statistical investigation

of long-term data collected from 18 weather stations which are spread proportionally on the territory of Belarus. Moreover the zoning of the territory by characteristic values of snow load is also taken into account.

The probabilistic model of the *resistance of structural elements* R is developed for flexural reinforced concrete members basing on the experimental and theoretical investigation.

The forth part of the article “Reliability levels comparison” shows the reliability diagrams. We conclude that provided the proposed probabilistic models of basic variables are valid the system of partial safety factors and combination factors stated in Eurocode gives the required level of reliability of designed structures in most of the design situations. However in some cases reliability of structures in persistent design situations does not meet the requirements of RC2 reliability class; and the actual average reliability level corresponds to the minimum recommended level. At the same time the rules for assessing actions on structures in accordance with SNiP 2.01.07-85 *do not meet* modern reliability and safety of structures requirements.

It has been shown that the level of reliability of structures designed according to USSR and Ukrainian standards is significantly lower than the required level, and that the probability of failure for structures can exceed maximum permissible values up to 100 times.

Classification and moral evaluation of uncertainties in engineering modeling

C. Murphy & Charles E. Harris Jr.

Department of Philosophy, Texas A&M University, College Station, TX, USA

P. Gardoni

Zachry Department of Civil Engineering, Texas A&M University, College Station, TX, USA

Keywords: Modeling; Uncertainty; Ethics

Models are typically used by engineers to quantify the level of likelihood or probability of the occurrence of specific events or set of consequences. Probability is used due to the lack of certainty about whether a specific event will occur (or not), as well as its place, time, and magnitude. Our paper focuses specifically on the case of natural hazards, defined here as a potentially damaging or destructive natural event that might occur in the future. Given the occurrence of a natural hazard, uncertainty surrounds the behavior and response of a structure or infrastructure. Finally, uncertainties are typically associated to basic characteristics of a structure or infrastructure. Such uncertainties include the variability in material properties (e.g., characteristics of soil, steel, or concrete), geometry, and external boundary conditions (e.g., loads or physical constraints).

In this paper we first discuss the role of engineering in society and the role of modeling in engineering. We then provide a taxonomy of the kinds

of uncertainty that should be accounted for when constructing and implementing a model. There are three stages where uncertainty must be treated in modeling: (1) the development of a model; (2) the application or implementation of a model; and (3) the analysis of the results of a model. We distinguish between aleatory and epistemic, as well as endodoxastic, and metadoxastic uncertainties. Finally, we develop criteria for evaluating how each kind of uncertainty should be treated. Our discussion distinguishes between science and engineering in terms of what constitutes the distinctive kind of knowledge sought in each domain, the function of models in each field, and the role and responsibilities of scientists and engineers. We argue that uncertainty can be acceptable or not, depending on how a given uncertainty impacts the ability of engineers to meet their responsibilities: (1) to respond to the societal need which a given project is addressing, and (2) to promote safety and justice.

Quantitative safety goals—benefits and limits

H.-P. Berg & M. Krauß

Bundesamt für Strahlenschutz, Salzgitter-Lebenstedt, Germany

ABSTRACT: A safety assessment is a systematic process to verify that applicable safety requirements are met in all phases of the life cycle of a plant. Safety analysis is a key component of a safety or risk assessment. Safety analysis incorporates both probabilistic and deterministic approaches, which in main cases are seen as complementary tools to each other.

In particular quantified risk and hazard analysis techniques are emerging as powerful tools for the safety management of different types of hazardous plants such as the process industry and the nuclear industry where these approaches are already applied since nearly twenty years.

Although the concept in general, i.e. a probabilistic approach to risk quantification, remains similar, there are apparent variations in methodological practices and particularly in the range of applications, focus and emphasis in the implementation of these tools for the different industries.

There is an apparent variation between quantified risk and hazard analysis in the process industry and probabilistic safety assessment in the nuclear industry. Compared to the relatively narrower range of applications of these tools in the process industry a more extensive use is made by the nuclear industry in implementing probabilistic safety assessment at the design and operational stages of nuclear power plants including plant changes.

Although several approaches applying quantitative criteria are already in force and experiences are available, there is much debate about the concept of acceptable risk. The question what level of risk should be tolerated and who determines acceptability is still controversial in the area of safety management. The importance of communicating is illustrated by the differential in willingness to tolerate risks from different sources, independent from benefit considerations, and the differential in willingness to accept types of risks between different groups of individuals.

The concept that some level of risk is tolerable is fundamental to risk assessment and risk management. Without the definition of such a tolerable risk criterion, risk assessment may be hampered in terms of decision making and formulation of

risk management strategies. The setting of and adherence to precise and rigid criteria, however, does not acknowledge the limitation in accuracy of methodologies, nor does it allow for appropriate consideration of the benefits against which the acceptability of the risk may be assessed in each case.

Furthermore, the extent of compliance with any risk criteria should not be the sole basis for evaluating the success of risk management measures. Other criteria include the extent of risk and risk reductions achieved, the cost of risk reductions in social, economic and environmental terms, and the cost effectiveness of control measures. As such, while debate will probably continue on the appropriateness of quantitative risk criteria as a measure of tolerability, future applications of quantitative risk assessment will greatly benefit from focusing more on the assessment process itself and the interpretation of the quantitative safety criteria as a target guideline.

As demonstrated by the wide spectrum of applications, the fact is illustrated that in the nuclear industry the use of PSA for other than compliance with formal criteria dominates. Some countries which operate nuclear power plants apply numerical safety objectives/criteria/rules/goals. The role and interpretation of such quantitative guidelines vary from country to country.

One main opinion on quantitative safety goals is that they should not be used within a regulatory framework of strict acceptance or non-acceptance criteria but should be considered as one factor in arriving at regulatory judgement. However, the safety goal approach partially can answer the old question “how safe is safe enough?”

Risk acceptance criteria are used in a so-called ALARP regime, which means that the risk should be reduced to a level that is as low as reasonable practicable. In literature a discussion is presented about the suitability of such criteria. Some authors argue not using risk acceptance criteria and the emphasis should be more on the generation of alternatives and analysis of these in order to provide decision support, balancing all pro and cons of the alternatives. From a social point of view, a risk acceptance criterion is meant to be a tool for

achieving a desired solution, and is then a frame condition in decision-making for a firm, but is not necessarily a frame condition for society.

On the other hand, society level criteria, intermediate level criteria and technical level criteria (even there are named or used differently in different industries and/or countries) are already in force in the nuclear field, process industry, aviation and other transportation means).

Whenever, on the basis of risk assessments, decision alternatives have been identified and compared regarding the expected value of benefits or losses, the risks must be considered in regard to their acceptability. One way of determining quantitative risk criteria is to consider probabilistic safety assessment. It is far from self-evident how probabilistic safety criteria should be defined and used. On one hand, experience indicates that safety goals are valuable tools for the interpretation of results of a probabilistic safety analysis, and they tend to enhance the realism of a risk assessment. On the other hand, strict use of probabilistic criteria is usually avoided.

A major problem is the large number of different uncertainties in PSA model, which make it difficult to demonstrate the compliance with a probabilistic criterion. Therefore, sometimes the safety goals are expressed as a band of either consequence or frequency.

Furthermore PSA results can change a lot over time due to scope extensions, revised operating experience data, method development, or increase of level of detail, mostly leading to an increase of the frequency of the calculated risk. This can

cause a problem of consistency in the judgements. Another concern is, that the introduction of predetermined criteria may give the wrong focus to risk assessment activities, i.e. on meeting risk criteria rather than on obtaining overall safe and effective solutions and measures.

Risk management and safety management, based on the results of risk analysis, provide the ability to support the process of decision making both for the industries and the respective regulatory bodies.

Therefore, the need for the development of risk criteria, which would support risk informed decision-making, is expressed worldwide. However, risk acceptance is also correlated to the cultural context, even if, e.g., the European Commission is acting in determining or harmonizing quantitative safety goals for different industrial fields because risk acceptance criteria are already used in process and other industries for many years. One example is the project "Safety and Reliability of Industrial Products, Systems and Structures" (SAFEREL-NET), launched by the European Commission to investigate risk criteria already used in the EU for the population living in the vicinity of hazardous facilities. Other current attempts are dedicated to railway and road safety.

A common thinking has been that risk analysis and assessments cannot be conducted in a meaningful manner without the use of such criteria. Ideally, the strength of such criteria as a decision support tool is that they make interpretation of the results of a risk assessment explicit and traceable.

Evaluating the source of the risks associated with natural events

P. Gardoni

Zachry Department of Civil Engineering, Texas A&M University, College Station, TX, USA

C. Murphy

Department of Philosophy, Texas A&M University, College Station, TX, USA

Keywords: Risk; Natural Hazards; Uncertainty; Ethics

Tornadoes, hurricanes, droughts, and earthquakes are example of natural events that pose risks to society. As typically defined, risk refers to a set of scenarios, their associated probability of occurrence and consequences. Such natural events pose risks because they may occur and bring potentially damaging and destructive consequences. Devising and implementing effective natural hazard risk mitigation efforts represents one of the most important challenges to the international community. One of the key issues for risk mitigation is determining which risks are acceptable and which are not, so that the risks to address with mitigation measures can be prioritized.

The first objective of this paper is to show that we cannot simply apply to risks associated with natural events insights and frameworks for moral evaluation developed in the literature by considering ordinary risks, technological risks and the risks posed by anthropogenic climate change. The second objective of this paper is to identify and develop

a framework for the moral evaluation of the source of the risks associated with natural events, or the actions which sustain and impact such risks. Our discussion concentrates on the way the construction and modification of the built and natural environments can alter the probability of occurrence of natural events and the character and magnitude of the impact that such events have. We then argue for the need to develop a standard of reasonable care for decisions about the built and modified natural environment, which accounts for technical and resource constraints, as well as the place of natural hazard mitigation in public policy.

The proposed standard is of direct value to the decision- and policy-makers for optimal resource allocation for the mitigation of natural hazards. It will provide criteria for prioritizing risks to address and for identifying when mitigation action should be taken and which mitigation actions are most appropriate, including societal considerations.

Metamodeling of aircraft InfraRed Signature dispersion

S. Lefebvre, A. Roblin & G. Durand

Theoretical and Applied Optics Department, ONERA Chemin de la Hunière, Palaiseau Cedex, France

ABSTRACT: Existing computer simulations of aircraft InfraRed Signature (IRS) do not account for the dispersion induced by uncertainty on input data such as aircraft aspect angles and meteorological conditions. As a result, they are of little use to estimate the detection performance of optics systems: in that case, the scenario encompasses a lot of possible situations that must indeed be addressed, but cannot be singly simulated. In this paper, a three-step methodological approach for predicting simulated IRS dispersion of imperfectly known aircraft is proposed. The first step is a sensitivity analysis. The second step consists in a Quasi-Monte Carlo survey of the code output dispersion. In the last step, two metamodels of the IRS simulation code are constructed and compared: a neural network one and a kriging one. A metamodel will allow carrying out thorough computationally demanding tasks, such as those required for optimization of an optics sensor. This method is illustrated in a typical scenario, and gives satisfactory estimation of the infrared signature dispersion.

INTRODUCTION AND METHODOLOGY

Progress made during the last fifty years in optics sensors enhanced the use of IR detection for scientific, surveillance and military applications. IR sensors enable to detect targets that cannot be set apart from their surroundings in the visible spectral range, thanks to their emitted heat. This explains why knowledge of aircraft IR emission is compulsory: for example in order to assess their detection probability and thus their susceptibility, and why IR signature analysis is important. For many reasons, the experimental approach is generally not feasible to evaluate the IRS, and computer programs are therefore extremely valuable tools. Existing computer simulations of aircraft IRS do not account for the dispersion induced by uncertainty on input data, they are thus of little use to estimate the detection performance of IR optics systems: in that case, the scenario encompasses a lot of possible situations that cannot be singly simulated.

For an aircraft in a given atmospheric environment, the first order effects on the IRS relate to the spectral range, the presentation geometry, the aircraft speed and the engine power setting. Several sources of variability lead to a dispersion of the values likely to be observed: weather, aircraft aspect angles, aircraft type, optical properties. These uncertainties in the input data propagate through the simulation model to the output data. Therefore, the simulated result is no longer a single IRS value, but an interval of possible IRS which should include the IRS measured at a given instant.

ONERA has developed for thirty years a simulation of aircraft IRS, CRIRA, initiated by Gauffre 1981. Using CRIRA, we aim at defining a general methodology for predicting simulated IRS dispersion of imperfectly known aircraft and non-detection probabilities for typical thresholds. A black box representation is associated to the IRS computer simulation code $f: Y=f(X_1, \dots, X_n)$ where the n X_i denote the uncertain input factors of the code, and Y is the output of the simulation. A well-known tool to estimate non-detection probabilities is the Monte Carlo stochastic sampling. The main drawback of this method is the slow convergence, scaling asymptotically with the inverse square root of the number of samples and starting from what is often a large initial error. It is therefore not uncommon to need more than one million samples to guarantee an accuracy better than one percent. The computational cost can thus be prohibitive. Alternative approaches have been developed, in order to speed up the convergence, such as Quasi-Monte Carlo method. The convergence rate depends on the problem's dimension n , which can be lowered by focusing exclusively on really significant input factors, according to their impact on the code output dispersion. We thus propose a three-step methodological approach for predicting simulated IRS dispersion of imperfectly known aircraft. The first step is a sensitivity analysis, which identifies inputs that have negligible influence on the IRS and can be set at a constant value. The second step consists in a Quasi-Monte Carlo survey of the code output dispersion. In the last step, several metamodels

of the IRS simulation code are constructed and compared: a neural network one and a kriging one. The test case is based on the use of our own aircraft IRS computation code for a standard air-to-ground detection scenario, namely a daylight air-to-ground full-frontal approach by a generic aircraft flying at low altitude.

RESULTS

We consider a daylight air-to-ground approach in a mid latitude region by a generic aircraft, flying at low altitude (800–1200 ft) without afterburning. The infrared sensor is located on the ground, at a twenty kilometers distance from the aircraft, in the flight direction. The aircraft is supposed to be spatially unresolved by the sensor. Many inputs of CRIRA are uncertain: from twenty up to sixty. For this scenario, twenty eight input data are uncertain: nine describe IR optical properties of the various aircraft surfaces, seven are related to flight conditions and to aspect angles of the aircraft, twelve are related to atmospheric conditions.

Three factors are qualitative, the others are quantitative. Other inputs such as aircraft geometry or engine properties are supposed to be perfectly known.

Our computer simulation of aircraft IRS is complex, and linear regression models give poor predictions, we thus preferred nonlinear modeling, more precisely neural network and kriging metamodells as described respectively in Hastie et al. 2001 and Santner et al. 2003. The choice of a MLP or a gaussian process as a nonlinear metamodel of our simulation of IRS was made in comparison with other kinds of metamodells, such as splines.

The sensitivity analysis shows that 90% of the IRS variance is explained with only four factors. As we do not want to leave off potentially important factors, we keep the nine most significant variables before going on to the next stage. All the other variables are set at a constant value before proceeding to the next step: the IRS dispersion estimation with low discrepancy sequences. Given the computation time, we limit the number of numerical experiments to a thousand for this step, and set N to 10240.

The input data of the metamodells are the nine most significant factors of the previous subsection, they are reduced and centered. We have compared the predictions of several single-layer perceptrons, with 500, 2000, 4000 or 6000 training samples, and 5, 7 or 10 hidden neurons. The decay parameter has been set at 0.01, according to a preliminary study. The best results were obtained with a single-layer perceptron with

10 hidden neurons and 4000 training samples. We have built six Universal Kriging metamodells with nugget effect, one for each combination of ihaze and model levels. Ten models were built in each case, five with 250 training samples, and five with 500, and we chose the best according to IRS prediction performances. One of the main asset of kriging is that the metamodel prediction is associated to confidence intervals, thanks to the prediction variance σ_{UK}^2 . An adaptive construction could thus be performed without expensive bootstrap estimation. However, σ_{UK}^2 is quite large, and not very informative, and we have six different kriging metamodells, making the set up of an adaptive construction difficult in practice. We have decided to focus on adaptive neural network in a first step.

This construction is based on Gazut et al. 2008 results: the main idea is to add some points associated to imprecise predictions to the learning sample. To do so, we start with the 500 first points of our whole sample, we estimate the variance of predictions for 50000 potential new learning points by bootstrap, and we add the 100 points that correspond to the largest variance σ . We iterate, until 1500 new points have been added.

Large IRS are not very interesting for the study of the optics sensor performances, it would thus be interesting to focus on small IRS values when downsizing the learning sample with an adaptive construction. We performed a first attempt on the specific interval $[0.16, 160]$. We applied the same adaptive procedure but added the proposed points to the learning sample only when their mean prediction value μ satisfies:

$$\begin{cases} 0.16 < \mu - k\sigma \\ \mu + k\sigma < 160 \end{cases}$$

Three values of parameter K were compared: 0.5, 1 and 2, and best results were obtained with $k = 2$. Another construction was tested, a mixed one: at each step, the 10 points with the larger predicted variance were added, even if the previous conditions were not satisfied, in order to globally improve our metamodel. The adaptive single-layer perceptron metamodel, based on a 2000 points learning set, and the kriging one, based on 2250 training samples, enable to obtain very satisfying estimations of $|IRS|$ empirical cumulative distribution function and 1% and 5% quantiles. First results of focusing the adaptive construction of neural networks on a specific range of IRS are conclusive, and work is in progress to deal with adaptive kriging and sparse polynomial chaos metamodells.

REFERENCES

- Gauffre, G. (1981). Aircraft infrared radiation modeling. *Rech. Aerosp.* 4, 245–265.
- Gazut, S., Martinez, J.M., Dreyfus, G. & Oussar, Y. (2008). Towards the optimal design of numerical experiments. *IEEE Trans. on Neural Netw.* 19, 874–882.
- Hastie, T., Tibshirani, R. & Friedman, J. (2001). *The Elements of Statistical Learning*. New York: Springer.
- Santner, T., Williams, B. & Notz, W. (2003). *The Design and Analysis of Computer Experiments*. Springer.

This page intentionally left blank

GS_338 — Applications (6)

This page intentionally left blank

Practical reliability approach to urban slope stability

Robin Chowdhury & Phil Flentje

Faculty of Engineering, University of Wollongong, Wollongong, New South Wales, Australia

ABSTRACT: Urban slope stability presents diverse problems, ranging from first-time failures to reactivated landslides and from minor, localized slope movements to catastrophic events. Short-term goals include the identification of recent slope failures and areas of low or marginal stability and performing site-specific studies, so that remediation or preventive slope management can be carried out effectively. Long-term goals include investigating the variability of important influencing factors, assessing local and regional uncertainties and carrying out required analyses in order to minimize slope failure hazards, mitigate associated risks and plan future development on a rational basis.

Assessing urban slope stability requires consideration of significant uncertainties including those associated with shear strength and pore water pressure. For site-specific studies, there is considerable merit in adopting a reliability approach within a probabilistic framework based on widely accepted geotechnical models. Regional slope stability studies are facilitated by using a GIS-based approach. Considerable effort is required to prepare regional data-sets including topography and geology and to develop a comprehensive landslide inventory. There are some similarities and several differences between site-specific approaches on the one hand and regional approaches on the other. Thus it is vitally important to demonstrate the connection between the two types of analysis for a given region.

In this paper an innovative approach is introduced to show that a regional hazard study can be interpreted in terms of reliability indices corresponding to different hazard zones. Mean factors of safety associated each hazard zone may be calculated under different assumptions of uncertainty

and considering different magnitudes of pore water pressure. A GIS-based regional study developed on the basis of various data-sets may be interpreted in terms of traditional performance indicators with which geotechnical engineers are familiar. This approach has allowed a further validation of a well-documented regional study made for a study area in an urban region of New South Wales, Australia. Key aspects of that study are summarized in the full paper.

Reference is made to a comprehensive knowledge-based approach for assessing failure susceptibility and hazard. Important details of the method and approach are summarized in the full paper. A section of the hazard zoning map is shown. Moreover, the assessed quantitative values of failure susceptibility (likelihood or probability of failure) for each hazard zone are presented. The corresponding reliability index values for each zone are estimated based on the assumption of a suitable probability distribution. Estimates of the mean safety factor associated with each hazard zone are made under different assumptions of coefficient of variation of the factor of safety. Also the factors of safety are calculated for different values of pore water pressure ratio. The results are reasonable and credible and provide further validation of the comprehensive regional study. This approach is a practical application of reliability analysis within a probabilistic framework. In fact it demonstrates that the reliability process can be usefully applied in reverse and that the results of a quantitative regional study can be presented in a systematic way in terms of performance indicators used in conventional site-specific studies, deterministic and probabilistic. Significant future extensions of this approach are mentioned in the full paper.

Reliability-based optimization of maintenance and repair for a system of bridges

C.-A. Robelin & S.M. Madanat

University of California, Berkeley, CA, USA

ABSTRACT: The objective of bridge management optimization models is to determine optimal maintenance and repair (M&R) decisions, based on the knowledge of the current condition of the system through inspections, and on the prediction of future condition through the use of deterioration models. The optimization can be formulated as a Markov decision process (Madanat 1993, Jiang et al., 2000). In these methods, the deterioration is described by a Markov chain, with the state representing the condition of the facility. The main advantage of these models is that they enable the use of standard and efficient optimization techniques. As a consequence, these models have been used to solve the system-level problem, i.e. to determine optimal M&R decisions for a system of facilities (Hawk 1994, Golabi and Shepard 1997, Smilowitz and Madanat 2000). The system-level optimization can be solved using linear programming. The limitation of the Markovian models is the memoryless assumption, according to which the probability for the condition of a facility to transition from an initial state A to a lower state B does not depend on the time spent in state A or on the history of deterioration and maintenance. Although the assumption of history independence may be valid for certain bridge states, namely those where the deterioration is primarily governed by mechanical processes, it has been shown empirically that it is unrealistic for bridge states where the deterioration is primarily governed by chemical processes (Mishalani and Madanat 2002). Moreover, these optimization models are based on a top-down approach, which is only feasible for systems of relatively homogeneous facilities.

Deterioration models in which the history of deterioration is taken into account exist and have been used in bridge M&R decisions optimization, considering one facility (Mori and Ellingwood 1994), or a system of homogeneous facilities (Kong and Frangopol 2003). However, due to the complexity of their underlying deterioration models, these optimization methods use a very limited number of decision variables in order to remain tractable. To the knowledge of the authors, there

does not exist a system-level bridge management optimization method that has more than a few decision variables and that is based on a deterioration model that takes into account the history of deterioration and maintenance.

The system-level optimization presented in this article is based on the results of the facility-level optimization discussed in Robelin & Madanat (2007). The facility-level problem uses a Markovian deterioration model that accounts for aspects of the history of deterioration and maintenance. These aspects are: the time since the performance of the latest maintenance action and the type of that action. Such a model represents a compromise between simple Markovian deterioration models that allow the use of standard optimization techniques, and detailed mechanistic deterioration models whose complexity prevents efficient optimization of maintenance and replacement decisions. The optimization formulation at the facility-level consists of minimizing the cost of maintenance and replacement, subject to a reliability constraint.

A possible extension of this formulation at the system-level can correspond to minimizing the cost of maintenance and replacement for all facilities, subject to a reliability constraint for each facility. However, a more suitable formulation in the context of reliability-based optimization is to minimize the highest probability of failure threshold, subject to a budget constraint. Consequently, the optimal policy results in adopting a common value of the probability of failure threshold for all facilities. Such a result is intuitive, since it necessitates an equitable budget allocation across the entire network. In addition, the paper also provides a formal proof of optimality in the case where the probabilities of failure thresholds are allowed to be continuous.

In order to ascertain the validity of the continuous case results for a discrete state space of threshold probabilities, a numerical case study is implemented. The numerical application considers a system of 742 heterogeneous bridges. The deterioration of each bridge deck is modeled according to Frangopol, Kong & Gharaibeh

(2001), and maintenance and replacement cost information is adapted from Kong & Frangopol (2003). A system of heterogeneous bridges is created by changing the parameters provided in these papers within reasonable ranges. The facility-level optimization problem is first solved for each facility, for various values of the threshold of probability of failure. Given a user-defined budget, the optimal value of the threshold of probability of failure is determined as the smallest probability of failure such that the cumulative system-level M&R costs do not exceed the budget. With the help of this parametric study, it is shown that the results obtained in the discrete-case implementation of the solution seem to be valid approximations of the continuous-case results.

In addition, the proposed solution methodology is such that the computational complexity of the system-level problem is low. Namely, the fact that the threshold of probability of failure is the same for all facilities at system-level optimum reduces the optimization problem for n facilities to n independent facility-level problems. Therefore, the complexity is proportional to the number of facilities in the system, i.e. $O(n)$. For each facility, the facility-level optimization problem is solved a small number of times. Since the time to solve one facility-level problem is of the order of a few seconds on a personal computer, typical values of computation times for the system-level problem are five hours per thousand facilities. These computation times indicate that the proposed system-level optimization method can be applied to systems of the size of that managed by a state Department of Transportation in the United States. For example, if applied to the system managed by Caltrans, composed of 24,000 bridges (California Department of Transportation 2006), the optimization would require a computation time of approximately five days, which is very short when compared with the time scale of maintenance and replacement decisions.

REFERENCES

- California Department of Transportation (2006). *Structure Maintenance and Investigations*. California Department of Transportation. Caltrans, <<http://www.dot.ca.gov/hq/structure/strmaint/>> (Oct 09, 2006).
- Frangopol, D.M., Kong, J.S. & Gharaibeh, E.S. (2001). Reliability-based management of highway bridges. *Journal of Computing in Civil Engineering* 15(1), 27–34.
- Golabi, K. & Shepard, R. (1997). Pontis: a system for maintenance optimization and improvement for U.S. bridge networks. *Interfaces* 27(1), 71–88.
- Hawk, H. (1994). *Bridgit: Technical Manual*. Toronto, Canada: National Engineering Technology Corporation.
- Jiang, M., Corotis, R.B. & J.H. Ellis (2000). Optimal life-cycle costing with partial observability. *Journal of Infrastructure Systems* 6(2), 56–66.
- Kong, J.S. & Frangopol, D.M. (2003). Life-cycle reliability-based maintenance cost optimization of deteriorating structures with emphasis on bridges. *Journal of Structural Engineering* 129(6), 818–828.
- Madanat, S.M. (1993). Optimal infrastructure management decision under uncertainty. *Transportation Research, Part C* 1(1), 77–88.
- Mishalani, R.G. & Madanat, S.M. (2002). Computation of infrastructure transition probabilities using stochastic duration models. *Journal of Infrastructure Systems* 8(4), 139–148.
- Mori, Y. & Ellingwood, B. (1994). Maintaining reliability of concrete structures. ii: Optimum inspection/repair. *Journal of Structural Engineering* 120(3), 846–862.
- Robelin, C.A. & Madanat, S.M. (2007). History-dependent optimization of bridge maintenance and replacement decisions using markov decision processes. *Journal of Infrastructure Systems* 13(3), 195–201.
- Smilowitz, K. & Madanat, S.M. (2000). Optimal inspection, maintenance and rehabilitation policies for networks of infrastructure facilities under measurement and forecasting uncertainty. *Journal of Computer-Aided Civil and Infrastructure Engineering* 15(1), 5–13.

System-level optimization of maintenance and replacement decisions for road networks

A. Medury & S.M. Madanat

University of California, Berkeley, CA, USA

ABSTRACT: Transportation infrastructure management refers to the process of allocating a limited set of resources to a system of deteriorating facilities for maintenance, rehabilitation and replacement (MR&R) activities. It is a decision-support tool used by agencies to inform effective policy implementation. The decision-making process requires a multi-objective approach involving adequate recognition of agency budget as well as the costs incurred by the users in the form of vehicle wear-and-tear. In addition, MR&R activities on road networks can also cause significant delays to travelers (because of loss in capacity, detours, etc.). According to one estimate, more than 60 million vehicles per hour per day of capacity were lost due to work zone activity on the National Highway System over a two week period in the United States in 2001 (Wunderlich and Hardesty 2003). Hence, the impact of rehabilitation activities, especially in saturated traffic flow conditions, can be severe, and it is important to address and incorporate these user concerns into the decision-process as well.

Most studies in the infrastructure management literature have approached the decision-making process as a problem of optimal allocation of limited financial resources (Golabi et al., 1982, Smilowitz and Madanat 2000, Kuhn and Madanat 2005). On the other hand, while work zone scheduling problems consider the impact of rehabilitation activities by explicitly accounting for network properties, the underlying financial planning is often not investigated (Fwa and Muntasir 1998, Chang et al., 2001). Hence, there is a need for a cohesive framework in network-level infrastructure management systems, which can effectively incorporate both, budget allocation and work zone scheduling problems.

In this paper, a bottom-up methodology is proposed in order to investigate the significance of network configurations and the resulting

interdependencies between facilities in pavement management. A two-stage system-level methodology, represented as an integer programming formulation, is devised to solve a finite planning horizon problem. The first stage corresponds to a resource allocation problem, while the second stage is a scheduling problem involving different construction scenarios and network constraints. In particular, the capacity losses due to construction activities are subjected to an agency-defined network capacity threshold. Finally, a Pareto optimal frontier involving different capacity thresholds and budget levels is developed to facilitate multi-objective decision-making. The proposed methodology is illustrated with the help of a parametric study on a stylized network configuration.

REFERENCES

- Chang, Y., Sawaya, O. & Ziliaskopoulos, A. (2001). A tabu search-based approach for work zone scheduling. *Proceedings, Transportation Research Board 80th Annual Meeting (CD-ROM), Paper No. 01-2950.*
- Fwa, T.C.R. & Muntasir, A. (1998). Scheduling of pavement maintenance to minimize traffic delays. *Transportation Research Record 1650*, 28–35.
- Golabi, K., Kulkarni, R. & Way, G. (1982). A statewide pavement management system. *Interfaces 12(6)*, 5–21.
- Kuhn, K.D. & Madanat, S.M. (2005). Model uncertainty and management of a system of infrastructure facilities. *Transportation Research Part C 13(5–6)*.
- Smilowitz, K. & Madanat, S. (2000). Optimal inspection, maintenance and rehabilitation policies for networks of infrastructure facilities. *Computer Aided Civil and Infrastructure Engineering 15(1)*, 5–13.
- Wunderlich, K. & Hardesty, D. (2003). A snapshot of summer 2001 work zone activity based on information reported on state road closure and construction websites. EDL #13793, National Transportation Library, FHWA, U.S. Department of Transportation.

Probability-based reliability assessment for real-time hybrid simulation

C. Chen & W. Pong

School of Engineering, San Francisco State University, San Francisco, CA, USA

ABSTRACT: Real-time hybrid simulation provides an economic and efficient technique to experimentally evaluate performances of structures with rate-dependent devices under earthquakes. It divides a structural system into different substructures, where the experimental substructure(s) are physically tested in the laboratory and the analytical substructure(s) are numerically modeled using finite element program. An integration algorithm is utilized to solve the structural dynamics and determine the displacement response for the substructures. The coupling between the experimental and analytical substructures is achieved by maintaining the compatibility and equilibrium at the interfaces between these substructures. Real-time hybrid simulation thus enables the system response to be considered while testing only part of the structure. It therefore allows the structural engineering researchers to address the rate effects in large-structures in limited size laboratories. The development of performance-based design procedures for structures with rate-dependent devices requires that the device's behavior be well understood, the performance of the structural system with the devices be evaluated, and the design procedure be verified. These requirements can be economically met by performing real-time hybrid simulation of structural systems with these devices.

Servo-hydraulic actuators are often used to apply the command displacements to the experimental substructures in a real-time hybrid simulation. However, the servo-hydraulic dynamics will lead to a time delay between the time that the actuator receives the command and the time that the actuator reaches the desired position. Compensation methods are often used to reduce the effect of actuator delay, but cannot eliminate the actuator control error in real-time hybrid simulation. It is therefore necessary to conduct reliability assessment for real-time hybrid simulation results with the presence of actuator control errors.

Tracking indicator is developed by researchers to quantify the accumulative effect of actuator delay during a real-time hybrid simulation. It is

based on the enclosed area of the hysteresis in the synchronized subspace plot between the command and measured displacements. The tracking indicator provides useful information about the lag or lead in the actuator response to the command. The inevitable actuator error a real-time hybrid simulation will lead to nonzero value of tracking indicator. The definition of tracking indicator however does not specify the ranges of values to differentiate reliable and unreliable the real-time hybrid simulation results.

This paper presents a probability-based tracking indicator to evaluate the reliability of real-time hybrid simulation results. The statistic analysis of the actuator control error is first investigated through real-time tests with predefined displacements. The actuator control errors are shown to follow normal distribution with zero means. The standard deviation however is observed to be affected by the compensation methods used in the tests. To provide a probability-based tracking indicator that can be applied for real-time hybrid simulation using different compensation methods, the authors propose to use the equipment accuracy to determine the standard deviation for the normal distribution model of the actuator control error.

The probability-based tracking indicator is then derived using the normal distribution assumption of the actuator control error. With selected values of probability, a value range for the tracking indicator can be calculated based on the command displacement and the assumed normal distribution. The reliability of real-time hybrid simulation results is then assessed by comparing the value of tracking indicator from the experimental results with the calculated value range. Real-time hybrid simulation results for a two-story four-bay steel moment resisting frame with magneto-rheological fluid dampers in passive-on mode are used to demonstrated the application of the proposed probability-based tracking indicator. It is shown that the proposed probability-based tracking indicator can provide an effective tool to evaluate the reliability of the real-time hybrid simulation results.

REFERENCES

- Bayer, V., Dorka, U.E., Fullekrug, U. & Gschwilm, J. 2005. On real-time pseudo-dynamic sub-structure testing: algorithm numerical and experimental results. *Aerospace Science and Technology* 9(3): 223–232.
- Blakeborough, A., Williams, M.S., Darby, A.P. & Williams, D.M. 2001. The development of real-time substructure testing. *Philosophical Transactions of the Royal Society of London A* 359:1869–1891.
- Bonnet, P.A., Lim, C.N., Williams, M.S., Blakeborough, A., Neild, S.A., Stoten, D.P. & Taylor, C.A. 2007. Real-time hybrid experiments with Newmark integration, MCSmd outer-loop control and multi-tasking strategies. *Earthquake Engineering and Structural Dynamics* 36(1):119–141.
- Chen, C. & Ricles, J.M. 2008. Development of direct integration algorithms for structural dynamics using discrete control theory. *Journal of Engineering Mechanics* accepted for publication.
- Chen, C. & Ricles, J.M. 2008. Stability analysis of SDOF real-time hybrid testing systems with explicit integration algorithms and actuator delay. *Earthquake Engineering and Structural Dynamics* 37(4): 597–610.
- Chen, C. & Ricles, J.M. 2009. Analysis of Actuator Delay Compensation Methods for Real-Time Testing.” *Engineering Structures* 31(11): 2643–2655.
- Chen, C. & Ricles, J.M. 2010. Tracking error-based servo-hydraulic actuator adaptive compensation for real-time hybrid simulation. *Journal of Structural Engineering*, 136(4): 432–440.
- Chen, C., Ricles, J.M., Marullo, T. & Mercan, O. 2009. Real-time hybrid testing using the unconditionally stable explicit CR integration algorithm. *Earthquake Engineering and Structural Dynamics* 38(1): 23–44.
- Chen, C., Ricles, J.M., Sause, R. & Christenson, R. 2010. Experimental Evaluation of an Adaptive Actuator Control Technique for Real-Time Simulation of a Large-Scale Magneto-Rheological Fluid Damper. *Smart Material and Structures* 19(2).
- Christenson, R., Lin, Y.Z., Emmons, A. & Bass, B. 2008. Large-scale experimental verification of semi-active control through real-time hybrid simulation. *Journal of Structural Engineering* 134(4):522–534.
- Darby, A.P., Blakeborough, A. & Williams, M.S. 1999. Real-time substructure tests using hydraulic actuators. *Journal of Engineering Mechanics* 125: 1133–1139.
- Darby, A.P., Blakeborough, A. & Williams, M.S. 2002. Stability and delay compensating for real-time substructure testing. *Journal of Engineering Mechanics* 128(12): 1276–1284.
- Horiuchi, T., Inoue, M., Konno, T. & Namita, Y. 1999. Real-time hybrid experimental system with actuator delay compensation and its application to a piping system with energy absorber.” *Earthquake Engineering and Structural Dynamics*, vol. 28, no. 1), pp. 1121–1141, 1999.
- Horiuchi, T. & Konno, T. 2001. A new method for compensating actuator delay in real-time hybrid experiment. *Philosophical Transactions of the Royal Society of London A* 359: 1893–1909.
- Jung, R.Y., Shing, P.B., Stauffer, E. & T. Bradford. 2007. Performance of a real-time pseudodynamic test system considering nonlinear structural response. *Earthquake Engineering and Structural Dynamics* 36(12): 1785–1809.
- Karavasilis, T.L., Ricles, J.M. & Chen, C. 2010. HybridFEM: A program for nonlinear dynamic time history analysis and real-time hybrid simulation of large structural systems. *ATLSS Report*, Lehigh Univ., Bethlehem, PA.
- Lee, K.S., Fan, C.P., Sause, R. & Ricles, J.M. 2005. Simplified design procedure for frame buildings with viscoelastic or elastomeric dampers. *Earthquake Engineering and Structural Dynamics* 34(10): 1271–1284.
- Lehigh RTMD User Manual, <http://www.nees.lehigh.edu/index.php?page=rtmd-user-s-manual>, 2010.
- Mercan, O. 2007. Analytical and experimental studies on large scale, real-time pseudodynamic testing. *Ph.D. Dissertation*, Department of Civil and Environmental Engineering, Lehigh University, Bethlehem, PA.
- Mercan, O. & Ricles, J.M. 2007. Stability and accuracy analysis of outer loop dynamics in real-time pseudodynamic testing of SDOF systems. *Earthquake Engineering and Structural Dynamics* 36(11): 1523–1543.
- Nakashima, M., Kato, H. & Takaoka, E. 1992. Development of real-time pseudodynamic testing. *Earthquake Engineering and Structural Dynamics* 21(1): 79–92.
- National Science Foundation. Issues and research needs in simulation development, a report of a workshop on hybrid simulation development, September 13, 2007, Chicago.
- Soong, T.T. & Spencer, Jr. B.F. 2002. Supplemental energy dissipation: state-of-the-art and state-of-the-practice. *Engineering Structures* 24: 243–259.
- Wallace, M.I., Sieber, J., Neild, S.A., Wagg, D.J. & Krauskopf, B. 2005. Stability analysis of real-time dynamic substructuring using delay differential equation models. *Earthquake Engineering and Structural Dynamics* 34(15):1817–1832.
- Wu, B., Wang, Q., Shing, P.B. & Ou, J. 2007. Equivalent force control method for generalized real-time substructure testing with implicit integration. *Earthquake Engineering & Structural Dynamics* 36(9): 127–1149.

Probabilistic estimates of scenario loss through a two-stage Monte Carlo approach

Ioanna Ioannou & Marios K. Chryssanthopoulos

Faculty of Engineering and Physical Sciences, University of Surrey, Guildford, Surrey, UK

1 INTRODUCTION

In recent years, there is increased interest by decision makers in seismic loss estimates accompanied by statements of confidence. This may be addressed by the distinct treatment of inherent uncertainties (aleatory) from those that could be, theoretically at least, reduced (epistemic). The present study captures these two sources of uncertainty and quantifies their effects by developing a two loop Monte Carlo methodology which can be applied under general conditions (Ioannou 2010). In particular, the proposed procedure can be utilized with vulnerability obtained by any of the commonly accepted methodologies (e.g. empirical, analytical, hybrid or methods based on engineering judgment) and damage-to-loss relationships. The methodology is presented here for the estimation of financial loss sustained by a single building given particular levels of ground motion intensity, in a scenario loss approach. The probabilistic loss estimates can be used to make informed decisions regarding the financial resiliency of the building owner or to aid in forming effective seismic mitigation policies for building stocks.

2 METHODOLOGY

Scenario loss is estimated by bringing together vulnerability and exposure analysis through a two-loop Monte Carlo procedure. The inner loop accounts for the aleatory uncertainties in the two components and results in a single distribution for scenario loss in the form:

$$P(L > l | im) = \sum_{i=0}^n P(L > l | ds_i) p_{DS|IM}(ds_i | im) \quad (1)$$

where $P(L > l | im)$ is the complementary cumulative distribution function (CCDF) of the l given intensity im ; $P(L > l | ds_i)$ is the CCDF of loss l given a damage state ds_i ; $p_{DS|IM}(ds_i | im)$ is the probability

of being in ds_i given im and n is the total number of damage states.

The outer loop accounts for the epistemic uncertainties in the vulnerability and exposure by randomizing the damage probability matrix and damage-to-loss functions. This results in a family of distributions for the loss in the form:

$$P(L > l | im) = \sum_{i=0}^n P(L > l | ds_i) p_{DS|IM}(ds_i | im) \quad (2)$$

where the bold letters indicate that the terms are now randomized due to epistemic uncertainty.

3 CASE STUDY

The proposed methodology is illustrated on a three-storey steel moment resisting frame, which is considered to be used as a school/college. The vulnerability and exposure of the structural and non-structural elements are expressed in terms of the widely used lognormal fragility curves and the normal distributions truncated below zero, respectively.

The 90% confidence intervals obtained through the developed procedure by randomising only the lognormal mean λ of the fragility curves are compared in Fig. 1 with the corresponding intervals obtained by a simple method employed by Aslani and Miranda (2005). For the specific building considered herein, the simplified method is conservative (i.e. it results in wider bounds) and gives a reasonably close results to the methodology developed in the present study. Clearly, its main advantage is that it requires much less computational effort than the two-loop Monte Carlo procedure.

Figure 2 shows the confidence bounds obtained by randomising parameters λ and μ (5% and 95% curves labelled 'random: λ, μ '), which capture epistemic uncertainties in vulnerability and exposure, contrasted with the single curve (curve labelled 'deterministic: λ, μ' ') which accounts for aleatory

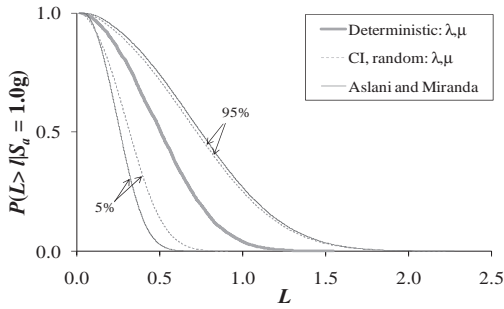


Figure 1. The 90% confidence intervals of the CCDF distributions of the loss for $S_a = 1.0$ g based on the method proposed here and the approach of Aslani and Miranda (2005) for ‘random λ ’.

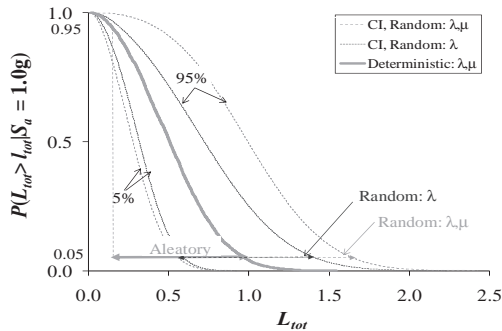


Figure 2. 90% confidence intervals (for ‘random λ ’, ‘random λ, μ ’) of the CCDF of the total loss given $S_a = 1.0$ g and the CCDF corresponding to the ‘deterministic: λ, μ ’ case.

Table 1. Ranges and the associated width values representing the aleatory and epistemic uncertainty associated with the total scenario loss (Vose, 2008).

$S_a^{(g)}$	Aleatory uncertainty		Epistemic uncertainty	
	Deterministic: λ, μ	Random: λ	Random: λ	Random: λ, ζ
1.0 g	$0.23 \leq L_{tot} \leq 0.87$ (0.64)	$0.60 \leq L_{tot} \leq 1.41$ (0.82)	$0.56 \leq L_{tot} \leq 1.65$ (1.08)	

uncertainties only. Presented in this form, the separate treatment of the epistemic and aleatory uncertainties allows their contribution to the overall uncertainty to be assessed through the intuitive method proposed by Vose (2008). The band widths determined through this approach are summarised in Table 1.

The same method may be adopted in order to differentiate between the epistemic uncertainty contributions. This is attempted by contrasting the

interval width values corresponding to the overall epistemic uncertainty (‘random: λ, μ ’) with the width values expressing the epistemic uncertainty affecting only the vulnerability (‘random: λ ’). The values of the relevant band widths are also presented in Table 1.

4 CONCLUSIONS

A two-loop Monte Carlo methodology has been presented for the estimation of a family of loss distributions for a single building. The proposed methodology explicitly treats the aleatory and epistemic uncertainties both vulnerability and exposure. Therefore, the economic loss can be presented in terms of a value and a range at any desired level of confidence. The methodology can be implemented using fragility curves obtained by any of the commonly accepted procedures. Its applicability was demonstrated for the case of a three-storey steel moment resisting frame used as a school/college. The results were first compared with those from a simplified procedure, in order to establish its validity. For the examined building, it was shown that epistemic uncertainty was the main contributor to the overall uncertainty of the loss estimates. It was also observed that levels of epistemic uncertainty in vulnerability played a more significant role than their counterparts attributed to exposure.

Clearly, the conclusions from this simple example cannot be generalized, and more research is needed in a number of key areas. It is also worth noting that the present study has honed into vulnerability and exposure, thus narrowing the focus and avoiding overall comparisons that would include the influence of uncertainty on the hazard. Notwithstanding, the proposed methodology suggests ways in which a desirable level of transparency can be established in quantifying uncertainty in loss estimation studies. It is believed that this should prove useful in improving consistency and transferability of results, an essential step towards the acceptance and more widespread use of probabilistic loss estimates by relevant stakeholders and decision makers.

REFERENCES

Aslani, M. & Miranda, E. 2005. *Probabilistic Earthquake Loss Estimation and Loss Disaggregation in Buildings*. Department of Civil and Environmental Engineering, Stanford University.

Ioannou, I. *Quantification of the Uncertainty in the Seismic Damage and Economic Loss for a Single Building*. PhD Thesis. University of Surrey, UK.

Vose, D. 2008. *Risk Analysis: A Quantitative Guide*. Chichester, England, John Wiley & Sons, Ltd.

*MS_332 — Applications and new developments
of system reliability assessment (theory)*

This page intentionally left blank

System reliability of soil slopes by Ditlevsen's bounds

J. Zhang

State Key Laboratory of Underground Engineering of Minister of Education and Department of Geotechnical Engineering, Tongji University, Shanghai, China

W.H. Tang & L.M. Zhang

Department of Civil and Environmental Engineering, The Hong Kong University of Science and Technology, Hong Kong SAR, China

H.W. Huang

State Key Laboratory of Underground Engineering of Minister of Education and Department of Geotechnical Engineering, Tongji University, Shanghai, China

1 INTRODUCTION

Slope failure is one of the most serious natural hazards threatening society. Many theoretical models have been developed for slope failure prediction. Yet, due to challenges in accurately determining the parameters of the theoretical models, prediction of slope failure is still very challenging. To account for the uncertainty in slope stability analysis, probabilistic methods have been developed for slope stability analysis in the past decades. As a slope may have many potential slip surfaces, the failure probability of a slope is different from that of a single slip surface. This is often known as the system failure probability problem.

Ditlevsen's bounds (Ditlevsen 1979) and Monte Carlo simulation are widely used for calculating system failure probability. Ditlevsen's method is often usually reasonably accurate and is often computationally more efficient than Monte Carlo simulation. However, when the number of failure modes considered is large, Ditlevsen's bounds are often too wide to be practical significance. In the slope reliability problem, each probable slip surface represents a possible failure mode. When the number of slip surfaces to be considered is large, Ditlevsen's bounds may not be directly applicable.

The objective of this paper is thus to suggest a method to calculate the failure probability of a slope efficiently using the Ditlevsen's bounds even when the number of potential slip surfaces is large. The paper consists of two parts: the methodology for system failure probability is first introduced, followed by an illustrative example with discussions about factors affecting system failure probability calculation.

2 METHODOLOGY

Although there might be a large number of potential slip surfaces in a slope, the factors of these slip surfaces are often highly correlated. For a group of highly correlated slip surfaces, the failure probability of the group of slip surfaces can be approximated by the failure probability of the most critical slip surface in this group, which is called a representative slip surface here. As the number of representative slip surfaces is usually significantly less than the number of possible slip surfaces, it is then possible to estimate the system failure probability using Ditlevsen's bounds based on the representative slip surfaces.

Suppose there are n representative slip surfaces. Let E_i denote the event that the slope will slide along the i th slip surface, E denote the event of slope failure, and $P(E)$ denote the probability of slope failure. As slope sliding along slip surface can be considered as slope failure, the slope can be considered as a series system. Thus, the problem of calculating the failure probability of a slope can be considered as calculating the failure probability of a series system. While calculating the exact value of failure probability of a series system is often very difficult, equations for estimating the bounds of the system failure probability has been suggested in the literature

$$\left\{ P(E_1) + \sum_{i=2}^n \max \left[P(E_i) - \sum_{j=1}^{i-1} P(E_i E_j), 0 \right] \right\} \leq P(E) \\ \leq \left\{ P(E_1) + \sum_{i=2}^n \left[P(E_i) - \max_{j < i} P(E_i E_j) \right] \right\} \quad (1)$$

where $P(E_i)$ = the failure probability corresponding to the i th failure mode, i.e., the probability of sliding along the i th slip surface; and $P(E_i E_j)$ = the probability that the i and j th limit state functions are violated simultaneously, i.e., the probability of sliding along slip surfaces i and j in the same time.

In Eq. (1), $P(E_i)$ can be assessed via methods such as First Order Reliability Method (FORM) and Monte Carlo simulation. Calculating $P(E_i E_j)$, which is the intersection of two failure events, is generally not easy. A weak form of Eq. (1) was due to Ditlevsen (1979), who suggested that lower and upper bounds of $P(E_i E_j)$ be calculated as follows:

$$\max[a, b] \leq P(E_i E_j) \leq a + b \text{ for } \rho_{ij} > 0 \quad (2a)$$

$$0 \leq P(E_i E_j) \leq \min[a, b] \text{ for } \rho_{ij} < 0 \quad (2b)$$

where a and b are defined as

$$a = \Phi(-\beta_i) \Phi\left(-\frac{\beta_j - \rho_{ij} \beta_i}{\sqrt{1 - \rho_{ij}^2}}\right) \quad (3a)$$

$$b = \Phi(-\beta_j) \Phi\left(-\frac{\beta_i - \rho_{ij} \beta_j}{\sqrt{1 - \rho_{ij}^2}}\right) \quad (3b)$$

in which β_i and β_j = reliability indices corresponding to failure modes i and j , respectively; and ρ_{ij} = correlation coefficient between the factors of safety of slip surfaces i and j . Substituting the bounds in Eqs. (2a) and (2b) into Eq. (1), the upper and lower bounds for $P(E)$ can then be estimated. In this way, the complex problem of estimating system failure probability is reduced to problems of estimating failure probabilities corresponding to various single limit states as well as the correlation coefficients among various failure modes.

3 EXAMPLE

Congress Street Cut is analyzed to illustrate the suggested method for failure probability calculation. Congress Street Cut was located mainly in saturated clays and failed in an undrained manner in 1952 dur-

Table 1. Statistics of uncertain variables.

	s_{u1}	s_{u2}	s_{u3}
Mean	136	80	102
Std	50	15	24
Distribution	Normal	Normal	Normal

ing the construction of Congress Street in Chicago. The slip surface passed through four different layers of soil, i.e., a sandy fill overlaying three saturated clay layers. The cohesion of the sandy fill was zero. Let s_{u1} , s_{u2} , and s_{u3} denote the average undrained shear strengths of the three clay layers, and ϕ denote the average friction angle of the sandy fill. As the slope stability is insensitive to ϕ , only s_{u1} , s_{u2} , and s_{u3} are considered as uncertain variables. The statistics of the uncertain variables are shown in Table 1.

For the Congress cut, rotational failure mechanism dominates. To calculate the system failure probability of the slope, 4096 circular slip surfaces are first generated, as shown in Fig. 1. The slip surfaces differ in the entry point, exit point as well as the radius. Among the 4096 slip surfaces, three representative slip surfaces governing the system failure probability are identified, as shown in Fig. 2. Compared with the 4096 samples in Fig. 2, the number of slip surfaces is greatly reduced. The reliability indices as well as the correlation coefficients among the factors of safety of the three slip surfaces are also shown in Fig. 2. The failure probability corresponding to the most critical slip surfaces is 9.11×10^{-3} . With Ditlevsen's method, the system failure probability is in the range of $9.51-9.62 \times 10^{-3}$. The failure probability of the most critical slip surface is smaller than that of the system failure probability.

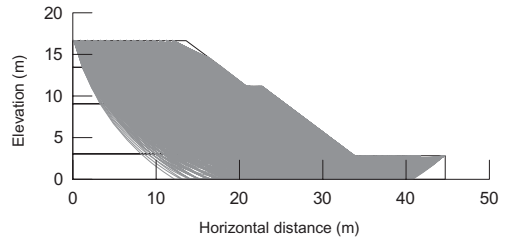


Figure 1. 4096 potential slip surfaces considered in the system reliability analysis.

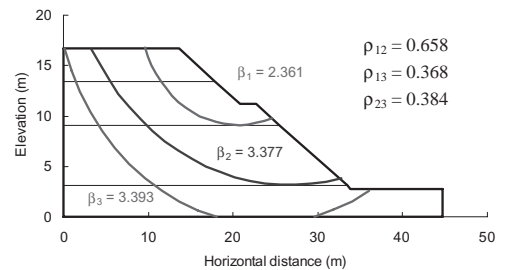


Figure 2. Representative slip surfaces identified based on the potential slip surfaces in Fig. 1.

Parametric studies are then carried out to investigate factors affecting the system failure probability calculation. It is found:

1. In order to identify the representative slip surfaces governing the slope failure, the number of potential slip surfaces must be sufficiently large. Also, all possible potential failure modes should be considered; otherwise the system failure probability will be underestimated.
2. The system failure probability will be larger than the failure probability of the most critical slip surface when the several representative slip surfaces have similar failure probabilities; otherwise, the system effect may not be obvious.
3. It is possible to estimate the bounds solely based on the failure probability of the most critical slip surface. Since the effect of other slip surfaces are not considered, the failure probability estimated in this way is wider than those obtained based on the Ditlevsen's bounds.

REFERENCE

- Ditlevsen, O. 1979. Narrow reliability bounds for structural systems. *Journal of Structural Mechanics, ASCE* 7(4): 453-472.

A recursive decomposition algorithm for reliability evaluation of binary system

Wei Liu & Jie Li

State Key Laboratory of Disaster Reduction in Civil Engineering, Tongji University, Shanghai, China
Department of Building Engineering, Tongji University, Shanghai, China

ABSTRACT: A binary system is a system with two states, operative and failed states. Many practical systems are binary system, such as node-pair network system, K -terminal network system, k -out-of- n : G system and weighted k -out-of- n : G system. Although many algorithms are proposed for the reliability evaluation of these systems, the goal of almost all the algorithms is to find the accurate solution. However, because of the complexity of the problem, it is not available to give the accurate solution of some complex systems in an acceptable time. For the complex system, a good idea is to give an approximate reliability which satisfies a prescribed error bound. In 1978, Dotson firstly proposed a real time disjoint of minimal paths for node-pair network system and gave an illumination to calculate the approximate value of network reliability. Later in 2002, Li & He presented a path-based recursive decomposition algorithm (PRDA) for node-pair network system by introducing the concept of structural function and combining Dotson algorithm with computer storage skills. In 2007, Liu & Li modified the PRDA and improved its efficiency.

In this paper, a general recursive decomposition algorithm based on the structural function (RDASF), a generalization of PRDA from the node-pair network system to the general binary system, is proposed. Firstly, a system structural function and a system complementary structural function are introduced. The minimal successful event (MSE) and the minimal failed event (MFE) are defined and three theorems are proved using Boolean laws. Based on these theorems, RDASF is derived to give the reliability of binary system. Taking a MSE of the system as decomposition policy and using the Boolean laws of set operation and the probabilistic operation principal, a recursive decomposition process is constructed. During the decomposition process, the Disjoint Minimal Successful Event (DMSE) set and the disjoint minimal failed event (DMFE) set are enumerated gradually. As the result, the probabilistic inequality can be used to give the results which

satisfy a prescribed error bound without obtaining all DMSEs or DMFEs. Meanwhile, the accurate value will be given when the decomposition process ends. A simple example is studied using the RDASF and the DMSEs and the DFSEs are enumerated gradually.

The proposed algorithm is applied to four typical system analysis, including node-pair network system, K -terminal network system, k -out-of- n : G system and weighted k -out-of- n : G system. It finds that, for the general binary system, if DMFE are obtained during the decomposition, all MSEs should be given before decomposition, or it cannot judge whether a decomposed system is an f -system or not. However, for the practical system, whether a decomposed system is an f -system or not can be judged based on its physical background. As the result, not all MSEs are needed before decomposition which reduces the computation time and store space. Moreover, for the system in which all elements failures are mutually s -independent, two reduction techniques, a parallel reduction technique and a series reduction technique (Page, 1988; 1989), are introduced to speed up the algorithm.

Figure 1 is an example in Liu and Li's paper. It is a network with 17 nodes and 32 edges. The edges failures are mutually s -independent. Let all edges reliabilities be 0.9. Considering different error bound, the results using RDASF are shown in Table 1. It is shown in table 1 that the computation time and the number of decomposed disjoint events increases as the error bound decreases. Moreover, when the error bound is between 0.001

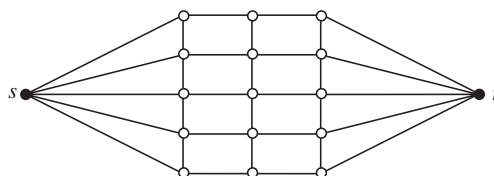


Figure 1. A network in Liu and Li's paper.

Table 1. Results for the network in figure 1.

Error bound	Reliability	Computed event number	
		DMP	DMC
0	0.999930	17,523	15,637
0.0001	0.999901	954	48
0.0002	0.999861	537	14
0.0005	0.999728	355	5
0.001	0.999492	193	1

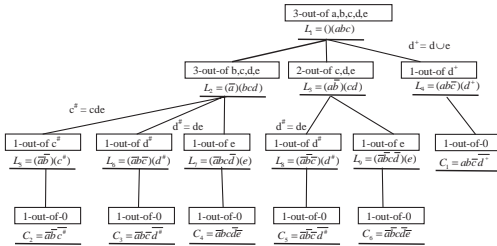


Figure 2. Process of decomposing a 3-out-of-5:G system. (For any DMSE, the value in the first bracket is the coefficient in front of current structural function while the coefficient in the second bracket represents a MSE of current system).

and 0.0001, the computation time and the number of decomposed disjoint events for the approximate solution is much less than those to give the accurate value. For example, when error bound is 0.0001, the computation time is only 0.34 s, 17.7% of those to give the accurate value. Also, the number of decomposed disjoint events is 1002, only 3% of that to give the accurate value.

In Figure 2, a 3-out-of-5:G system in which the elements failures are mutually s -independent is used to illuminate the process of the RDASF.

REFERENCES

Dotson, W.P. & Gobien, J.O. 1979. A new analysis technique for probability graphs. *IEEE Transactions on Circuits & Systems*, 26:855–865.

Jer-Shyan Wu & Rong-Jaya Chen. 1994. An Algorithm for Computing the Reliability of Weighted- k -out-of- n systems, *IEEE Transactions on Reliability*, 43(2):327–328.

Kuo, S.-Y. Lu, S.-K. & Yeh, F.-M. 2002. OBDD-Based Evaluation of K -Terminal Network Reliability. *IEEE Transactions on Reliability*, 51(4):443–450.

Li, J. & He, J. 2002. A Recursive Decomposition Algorithm for Network Seismic Reliability Evaluation. *Earthquake Engineering and Structural Dynamics*, 31: 1525–1539.

Liu Wei & Li Jie. 2009. An improved recursive decomposition algorithm for reliability evaluation of lifeline networks, *Earthquake Engineering and Engineering Vibration*, 2009, 8(3):409–419.

Myron Lipow, 1994. A Simple Lower Bound for Reliability of k -out-of- n :G Systems, *IEEE Transactions on Reliability*, 43(4):656–658.

Page, L.B. & Perry, J.E. 1988. A practical implementation of the factoring theorem for network reliability, *IEEE Transactions on Reliability*, 37(3):259–267.

Page, L.B. & Perry, J.E. 1989. Reliability of directed networks using the factoring theorem, *IEEE Transactions on Reliability*, 38(4):556–562.

Yong Chen & Qingyu Yang. 2005. Reliability of Two-Stage Weighted- k -out-of- n Systems with Components in Common, *IEEE Transactions on Reliability*, 54(3):431–440.

Zhang hong, Zhao Liancang et al. 2005. A new algorithm of Computing K -terminal network reliability. *Science Technology and Engineering*, 5(7):387–399.

Seismic reliability analysis of wind turbine systems considering rotation effect

K. Huang, J.B. Chen & J. Li

State Key Laboratory of Disaster Reduction in Civil Engineering, Tongji University, Shanghai, China

As the power of wind turbines increasing rapidly, the wind turbine structure is also growing. Based on the theory of finite element, tower and blades of wind turbines are discretized and equations of motion of blades and tower have been established. In order to ensure the safety and lower the cost, the tower was designed as variable cross section. This model tries to build an accurate model by starting with the relationship between the radius and the deflection. For efficient modeling and accurate dynamic analysis of a wind turbine, a finite element model based on the Kane's dynamics equations, which is in the field of flexible multi-body dynamics theory, is recommended since it takes the coupling relationship between the space rotating movement of blades and the elastic distortion into considered. Then the impact of blade rotation on the stiffness is considered.

Then the stochastic earthquake loads were modeled. In order to calculate the stochastic dynamic response and reliability of the structure under random earthquake loads, especially nonlinear stochastic dynamic response, not only the power spectrum model of ground motion, but also the acceleration of ground motion time history is needed. Therefore, it becomes an important issue to generate a random ground motion using the power spectral density function. Stochastic harmonic function representations and their properties are studied. As the distributions of the random frequencies are consistent with the target power spectral density function, the power spectral density of the stochastic harmonic process is identical to the target power spectral density. It is proved that the stochastic harmonic process is asymptotically normally distributed. Compared to existing representations of stochastic process, very few stochastic harmonic components can capture the exact target power spectral density. This greatly reduces the number of the random variables and thus eases the difficulty of stochastic dynamics. Take the Clough-Penzien spectral as an example, 200 time histories of the stochastic ground motion acceleration were generated.

Based on the generalized density evolution equation (GDEE), the extreme value distribution could be evaluated through constructing a

virtual stochastic process. The idea of equivalent extreme-value event and accordingly a new approach to evaluate the structural system reliability are employed. Elaborated investigations show that correlative information among the component random events is inherent in the equivalent extreme-value event. Since the probability density function of the equivalent extreme value could be obtained through the probability density evolution method, the idea of equivalent extreme-value event leads to a new uniform approach to evaluate the structural system reliability for both static and dynamic problems. Particularly, the investigation points out that computation of the dynamic reliability essentially involves dealing with infinite-dimensional correlation information and that is why the widely-used out-crossing process theory could be only an approximate and somewhat empirical reliability evaluation rather than an exact approach.

More researches were done focusing on the effect of the rotation rate of blades. In order to consider the coupling among different parts of the wind turbine system, assuming that the tower has little impact on blades, we take the response of the rotating blades as another external incentive. The 1.25 MW pitch-regulated wind turbine system model with representative dimensions are adopted in the dynamic reliability analysis under earthquake loads. Investigating the characteristic behavior of wind turbine systems under random dynamic loads, the seismic analysis is carried out with a series of artificial random seismic waves. The reliability of the wind turbine systems is evaluated by the probability density evolution method (PDEM). Some features of the stochastic dynamic responses and reliabilities of the wind turbine system are observed and discussed. The results show that the natural frequency of rotating blades is increasing with the rotation speed. The blades have great impactation on the response of tower. The obtained EVD is obviously different from the widely used regular distribution with the same mean and standard deviation. The results demonstrate that the PDEM is applicable and efficient in the stochastic dynamic response and reliability analysis.

Global reliability of large nonlinear structures

J.B. Chen, J. Li & J. Xu

State Key Laboratory of Disaster Reduction in Civil Engineering & School of Civil Engineering,
 Tongji University, Shanghai, P.R. China

1 INTRODUCTION

Seismic response analysis and reliability evaluation of structures are of paramount importance and have attracted many endeavors from the community of earthquake engineering and stochastic mechanics. However, even very recently Wen (2004) stated that “the reliability of such design to withstand damage and collapse was unknown and undefined.”

The probability density evolution method (PDEM) provides a new possibility for the problem (Li & Chen, 2009). In the present paper, an explicit representation of stochastic ground motion is inserted into the PDEM. On this basis, the global reliability of structures can be evaluated by introducing the thought of equivalent extreme value event.

2 PROBABILITY DENSITY EVOLUTION METHOD BASED GLOBAL RELIABILITY

2.1 Dynamic reliability of nonlinear structures

In general stochastic dynamical systems, the first-passage reliability is defined as

$$R(T) = \Pr\{Z(t) \in \Omega_s, 0 \leq t \leq T\} \quad (1)$$

where $Z(t)$ is the physical quantity upon which failure of the structure is specified.

An approach for reliability evaluation is through the integral of extreme value distribution. As a matter of fact, we can always define an extreme value corresponding to the failure criterion in Eq. (7) (Chen & Li, 2007). For instance, if one consider the maximum absolute value of $Z(t)$, extreme value of the response $Z(t)$ reads $Z_{\text{ext}}(T) = \max_{0 \leq t \leq T} |Z(\Theta, t)|$, where the extreme value $Z_{\text{ext}}(T)$ is a random variable. Eq. (1) is now equivalent to

$$R(T) = \Pr\{Z_{\text{ext}}(T) \leq Z_B, 0 \leq t \leq T\} \quad (2)$$

Thus, the reliability is given by $R(T) = \int_{\Omega_B} p_{Z_{\text{ext}}}(z, T) dz$, where $p_{Z_{\text{ext}}}(z, T)$ is the PDF of $Z_{\text{ext}}(T)$.

Our task is now to evaluate the extreme value distribution $p_{Z_{\text{ext}}}(z, T)$. To this end, we construct a virtual stochastic process $Y(\tau) = \phi(Z_{\text{ext}}, \tau)$ such that $Y(0) = 0$, $Y(\tau_c) = Z_{\text{ext}}$. For instance, if $Y(\tau) = Z_{\text{ext}}(\Theta) \sin \omega \tau$, where $\omega = (2k + 0.5)\pi$, k is an integer, then the condition is satisfied as $\tau_c = 1$.

Now, (Y, Θ) is a probability preserved system and thus a GDEE governing evolution of the joint PDF of (Y, Θ) , denoted by $p_{Y\Theta}(y, \theta, \tau)$, can be obtained (Li & Chen, 2009).

$$\frac{\partial p_{Y\Theta}(y, \theta, \tau)}{\partial \tau} + \dot{Y}(\theta, \tau) \frac{\partial p_{Y\Theta}(y, \theta, \tau)}{\partial y} = 0 \quad (3)$$

Solving this equation under the specified initial and boundary condition will yield $p_{Y\Theta}(y, \theta, \tau)$ and then $p_Y(y, \tau) = \int p_{Y\Theta}(y, \theta, \tau) d\theta$. Thus, we have $p_{Z_{\text{ext}}}(z, T) = p_Y(y = z, \tau_c)$.

Thus, dynamic reliability evaluation is transformed to a one-dimensional integral.

2.2 Global reliability evaluation

The application of the ideas described in the preceding sub-section to global reliability evaluation is of none essential additional difficulties. The ideas are illustrated by the following reliability problem.

$$R(T) = \Pr\left\{\bigcap_{j=1}^m \left(|Z_j(t)| \leq b_j, t \in [0, T]\right)\right\} \quad (4)$$

Likewise, when an equivalent extreme value is defined as $Z_{\text{ext}}(T) = \max_{\substack{0 \leq t \leq T \\ 1 \leq i \leq m}} |Z_i(t)/b_i|$, then the same procedure is carried out as described in Section 2.1. The PDF of $Z_{\text{ext}}(T)$ can then be obtained and the system reliability in Eq. (4) can be finally evaluated through a one-dimensional integral $R(T) = \int_0^1 p_{Z_{\text{ext}}}(z, T) dz$.

3 STOCHASTIC HARMONIC FUNCTION IN SPECTRAL REPRESENTATION

Recently, a stochastic harmonic function is proposed for representation of stochastic process

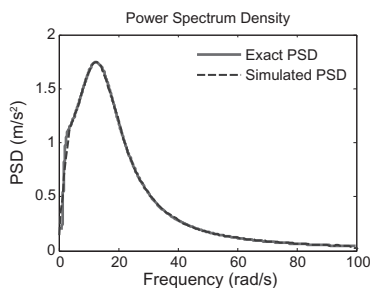


Figure 1. Comparison between simulated power spectrum and original power spectrum.

(Chen & Li, 2011). It is proved that the power spectral density of the stochastic harmonic process is identical to the target power spectral density. For the Clough-Penzien spectrum, Figure 1 shows the comparison when only ten terms are included.

4 NUMERICAL EXAMPLE

Stochastic seismic response and global reliability evaluation of a 9-story shear frame under stochastic seismic excitation are carried out. The masses from top to bottom are 3.442, 3.278, 3.056, 2.756, 2.739, 2.739, 2.739 and 2.692 ($\times 105$ kg), respectively. The lateral stiffness are 0.89, 0.96, 1.85, 1.92, 1.60, 1.60, 1.62, 1.63 and 1.47 ($\times 10^8$ N/m), respectively. Rayleigh damping is adopted such that the damping matrix is given by $\mathbf{C} = a\mathbf{M} + b\mathbf{K}$, where $a = 0.2643\text{s}^{-1}$, $b = 0.0071\text{s}$. In the case nonlinearity is involved in the restoring forces, the Bouc-Wen model is adopted. The parameters in the hysteretic model are: $\alpha = 0.04$, $A = 1$, $n = 1$, $q = 0.25$, $p = 1000$, $d_\psi = 5$, $\lambda = 0.5$, $\psi = 0.05$, $\beta = 100$, $\gamma = 20$, $d_v = 2000$, $d_\eta = 2000$ and $\zeta = 0.99$.

The global reliability of the nonlinear structure is evaluated. The results by MCS are taken as the validation. The extreme value distribution (EVD) of the response over the time interval $[0, 20$ s] is pictured in Figure 2(a). Simultaneously shown in Figure 2(a) are the PDFs of the normal, lognormal and EVD-I distribution with the second-order statistics identical to the computed EVD. It is found that the computed EVD is different from the widely used regular distributions, indicating that it might be imprudent to use regular distributions in reliability evaluation. Figure 2(b) shows the comparison between the CDF of the extreme value of the response over the time interval $[0, 20$ s] by the PDEM and MCS, where perfect accordance could be observed again. It is demonstrated that the PDEM is of high accuracy and efficiency for global seismic reliability assessment of complex nonlinear structures.

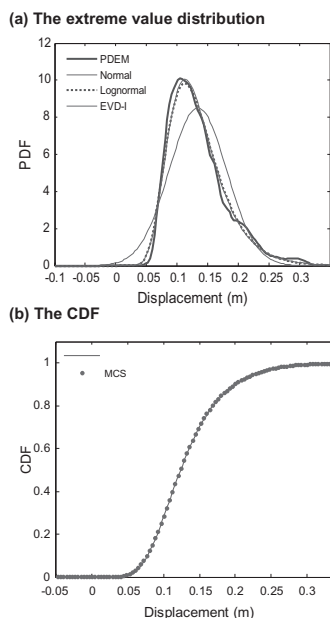


Figure 2. The EVD and CDF of extreme values under stationary excitation ($T = 20$ s).

5 CONCLUSION

Stochastic seismic response analysis and global reliability evaluation of nonlinear structures are of paramount importance. In the present paper, the probability density evolution method combined with the new spectral representation is taken to implement seismic response analysis and global reliability evaluation. The results show that the hybrid method is of accuracy and efficiency for stochastic seismic response analysis and global reliability evaluation of nonlinear structures.

The support of the Natural Science Foundation of China (Grant Nos. 90715083 and 10872148), National Hi-Tech Development Plan (863 Plan) (Grant No. 2008AA05Z413), and the State Key Laboratory of Disaster Reduction in Civil Engineering (Grant Nos. SLDRCE08-A-01 and SLDRCE10-B-02) are greatly appreciated.

REFERENCES

- Chen, J.B. & Li, J. 2011. Stochastic Harmonic Function and Spectral Representations. *Chinese Journal of Theoretical Applied Mechanics*, in press.
- Li, J. & Chen, J.B. 2009. *Stochastic Dynamics of Structures*, John Wiley & Sons.
- Wen, Y.K. 2004. Probabilistic aspects of earthquake engineering. In: Bozorgnia, Y. & Bertero, V.V. (ed.) *Earthquake Engineering*. Boca Raton: CRC Press.

Structural reliability analysis solved through a SVM-based response surface

Umberto Alibrandi & Giuseppe Ricciardi

Department of Civil Engineering, University of Messina, Italy

ABSTRACT: Recently it has been largely recognized that a realistic analysis of the structural systems should take into all the unavoidable uncertainties appearing in the problem at hand. In this context a powerful tool is represented from the structural reliability theory (Ditlevsen & Madsen 1999) which gives a rational treatment of the uncertainties and which allows the assessment of the evaluation of the safety of structures in presence of uncertain parameters.

To evaluate the failure probability in the most general case it is necessary to solve numerically a multidimensional integral, which is computationally demanding. Usually approximate methods are used such as the First and the Second Order Reliability Methods (FORM/SORM) or the Monte Carlo Simulation (MCS). The latter has great robustness properties, but it is computationally demanding, especially in the range of the very small failure probabilities. The computational cost can be reduced by using the Response Surface Methodology (RSM), which builds a surrogate model of the target limit state function, defined in a simple and explicit mathematical form (Bucher & Burgound 1990). Once the Response Surface (RS) is built, it is no longer necessary to run demanding finite element analyses.

In this paper we consider a specific type of response surface methodology, based on the

Support Vector Method (SVM) and the theory of the statistical learning (Vapnik 1998). Using the SVM the reliability problem is treated as a classification approach (Hurtado & Alvarez 2003) and extensive numerical experimentation has shown that each type of limit state can be adequately represented; however it could require an high number of support points. In this work we show that using a suitable strategy for the choice of the support points, it is possible to obtain a good approximation of the limit state without high computational complexity. A simple numerical examples shows the accuracy and effectiveness of the presented procedure references.

REFERENCES

- Bucher, C. & Burgound, U. 1990. A fast and efficient response surface approach for structural reliability problems. *Structural Safety* 7: 57–66.
- Ditlevsen, O. & Madsen, H.O. 1999. *Structural Reliability Methods*, Wiley.
- Hurtado, J.E. & Alvarez, D.A. 2003. Classification Approach for Reliability Analysis with Stochastic Finite-Element Modeling, *J. Struct. Engrg.*, 129(8), 1141–1149.
- Vapnik, V. 1998. *Statistical Learning Theory*, Wiley.

Reliability assessment of parallel systems with brittle elements

Y.G. Zhao

Kanagawa University, Yokohama, Japan

Z.H. Lu

Central South University, Changsha, China

1 INTRODUCTION

The evaluation of a system reliability for parallel system with brittle elements is generally difficult problem if the distributions of random variables of the member strength are different and non-normal. In the present paper, In the present paper, the performance function of a parallel system with brittle elements is investigated and system reliability assessment is conducted based on the investigation on the distribution of the performance function.

2 PERFORMANCE FUNCTION OF PARALLEL SYSTEMS

In general, for a brittle parallel system with n elements as shown in Fig. 1, Order the strength R_1, R_2, \dots, R_n from small to large, and denote X as the ordered random variables, that is

$$\mathbf{X} = (X_1, X_2, \dots, X_n) = \text{Order}(R_1, R_2, \dots, R_n) \quad (1)$$

Since the elements are brittle, the element with the minimum strength will broke when its strength is less than S/n , and the element with the second minimum strength will broke when its strength is less than $S/(n-1)$, and so on, therefore, the performance function of the parallel system can be expressed as

$$G(\mathbf{X}) = \max(X_i - \frac{S}{n-i+1}, i = 1, \dots, n) \quad (2)$$

As shown in the equations above, since the system performance function $G(\mathbf{X})$ will not be smooth although the performance function of a component is smooth, it is difficult to obtain the sensitivity of the performance function, the derivative-based FORM would not be applicable. In the present paper, Dimension Reduction Integration (DRI) for system reliability evaluation is investigated. The first few moments of the system performance function are obtained by DRI, from

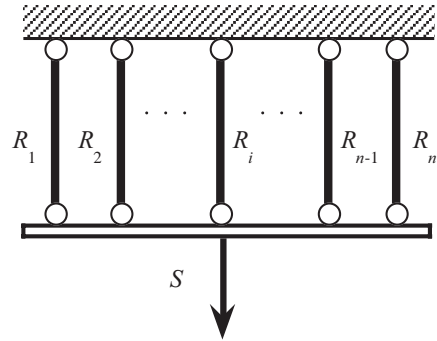


Figure 1. Parallel systems with n elements.

which the moment-based reliability index based on the fourth moment standardization function and failure probability can be evaluated without Monte Carlo simulations.

3 DIMENSION REDUCTION INTEGRATION FOR MOMENTS OF PERFORMANCE FUNCTION

For a performance function $Z = G(\mathbf{X})$, Xu and Rahman (2004) proposed generalized multivariate dimension-reduction method, in which the n -dimensional performance function is approximated by the summation of a series of, at most, D -dimensional functions ($D < n$). Let $L(\mathbf{u} = \{G[T^{-1}(\mathbf{u})]\}^k$ in Eq. (7), by the bivariate dimension reduction method (Xu and Rahman 2004), the k th order moment of G is evaluated as

$$\begin{aligned} \mu_{kG} &= E\{G[T^{-1}(\mathbf{U})]^k\} \cong E\{L(\mathbf{U})\} \\ &= \sum_{i < j} \mu_{L2ij} + (n-2) \sum_i \mu_{Li} + \frac{(n-1)(n-2)}{2} L_0 \end{aligned} \quad (3)$$

where

$$\mu_{Li} = \sum_{r=1}^m P_r L(0, \dots, 0, u_r, 0, \dots, 0) \quad (4)$$

$$\mu_{L2ij} = \sum_{r_1=1}^m \sum_{r_2=1}^m P_{r_1} P_{r_2} L(0, \dots, 0, u_{r_1}, 0, \dots, u_{r_2}, 0, \dots, 0) \quad (5)$$

where u_r and P_r are estimating points and the corresponding weights. (Zhao and Ang 2003).

Finally, the mean, standard deviation, the skewness, and the kurtosis of a performance function $G(\mathbf{X})$ with n random variables can be obtained using the moments above.

4 APPROXIMATE DISTRIBUTION OF THE PERFORMANCE FUNCTION OF THE PARALELL SYSTEM

After the first three or four moments of $G(\mathbf{X})$ are obtained, the reliability analysis becomes a problem of approximating the distribution of a specific random variable with its known first three or four moments. The fourth moment standardization function is expressed as (Zhao and Lu 2007)

$$Z_s = S(U, \mathbf{M}) = -l_1 + k_1 U + l_1 U^2 + k_2 U^3 \quad (6)$$

where l_1, k_1 and k_2 are coefficients.

The PDF of $Z = G(\mathbf{X})$, can be obtained as

$$f_Z(z) = \frac{1}{\sigma} \phi(u) \left| \frac{dz_s}{du} \right| \quad (7)$$

where

$$u = S^{-1} \left(\frac{z - \mu_G}{\sigma_G} \right) \quad (8)$$

Then the corresponding reliability index is expressed as

$$\beta = -\Phi^{-1}(P_f) = -S^{-1}(-\beta_{2M}, \mathbf{M}) \quad (9)$$

5 NUMERICAL EXAMPLES

Four examples are conducted. The histograms of the performance function obtained using Monte Carlo simulation (MCS) are depicted with the PDF of the performance function defined by the first four moments using the Cubic normal distribution. Example 1 is shown in Fig. 2 from which one can see that although the performance function is not smooth, the histograms have good behaviors and the PDF should be smooth. The first four moments of the performance functions obtained by the two methods are also compared from which one can see that the results obtained by DRI are quite close to those obtained by MCS.

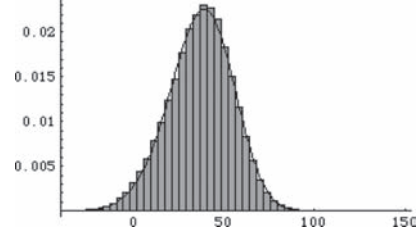


Figure 2. Histogram and PDF for example 1.

6 CONCLUSIONS

1. The performance function of parallel system with brittle elements is investigated and system reliability assessment is conducted based on the investigation on the distribution of the performance function.
2. A Dimension Reduction Integration based moment method for system reliability evaluation is investigated. The method directly calculates the reliability indices based on the first few moments of the performance function of a structure. It does not require the reliability analysis of the individual failure modes; also, it does not need the iterative computation of derivatives, nor the computation of the mutual correlations among the failure modes, and does not require any design points. Thus, the proposed moment method should be more effective for the system reliability evaluation of complex structures than currently available methods.
3. Although the performance function of parallel systems are not smooth, the histograms have good behaviors and the PDF of the system performance function should be smooth, and the histograms can be approached by the PDF defined by the first four moments.
4. The accuracy of results, including the first four moments of the performance function, and the probability of failure, obtained with the proposed method has been thoroughly examined by comparisons with large sample Monte Carlo simulations (MCS).

REFERENCES

Xu, H. & Rahman, S. (2004). "A generalized dimension-reduction method for multidimensional integration in stochastic mechanics." *Int. J. Numer. Meth. Engrg.*, 61(12), 1992–2019.

Zhao, Y.G. & Ang, Alfredo H-S. System reliability assessment by method of moments, *Journal of Structural Engineering, ASCE, Vol. 129, No. 10, 1341–1349, 2003.10.*

Zhao, Y.G. & Lu, Z.H. (2007), Fourth moment standardization for structural reliability assessment, *J. Structural Engineering, ASCE, Vol. 133, No. 7, 916–924.*

This page intentionally left blank

*MS_114 — Bayesian networks for engineering
risk analysis*

This page intentionally left blank

Risk-based operation and maintenance of offshore wind turbines using Bayesian networks

J.J. Nielsen & J.D. Sørensen

Department of Civil Engineering Aalborg University, Aalborg, Denmark

ABSTRACT: Operation and maintenance are large contributors to the cost of energy for offshore wind turbines. One large contributor is the large number of component failures which leads to a need for corrective maintenance and lost energy production. More optimal planning and preventive maintenance methods are used could be introduced to reduce the overall costs. This will give costs due to inspections and preventive repairs, but the costs due to corrective maintenance can be reduced. Optimal planning could be based on risk-based methods, where the total costs through the lifetime are minimized.

In this paper, long time planning is considered, i.e. which years to make inspections. A simple decision rule for preventive repairs is included; if a damage is detected at an inspection, it is repaired. The problem of deciding when to make inspections is intractable in the unreduced form, and therefore, an approximation is necessary. In this paper, Bayesian networks are used for making the decisions, and the inspection plans are updated whenever new information is received.

It is assumed that the considered component is exposed to deterioration, which can be described by a damage model. A dynamic Bayesian network can then be build to model the damage growth probabilistic, see (Straub 2009). The networks are made with a time slice for each year, and the lifetime is set to 20 years. The Bayesian network can be updated efficiently whenever new information from inspections becomes available.

Two different approaches are used for finding the optimal decisions regarding inspection times. In the first method, a threshold value for the failure probability is chosen, and inspections are always made before this value is reached. Inspection results are entered into the network, and thereby the failure probability is updated at each time step. The Bayesian network for this method is shown in Figure 1, where three time steps are shown. Monte Carlo sampling is performed for different threshold values in order to find the total expected costs for each value, such that the optimal value could be found.

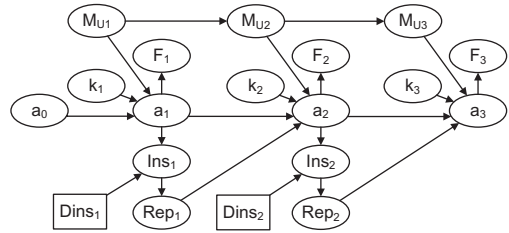


Figure 1. Bayesian network for the threshold approach with nodes: a_i : damage size, k_i , M_{Uj} : model parameters, F_i : failure probability, Ins_i : inspection result, Rep_i : repair decision, and $Dins_i$: decision on inspection.

The other method uses a Limited Memory Influence Diagram (LIMID) where cost and decision nodes are included directly in the Bayesian network, see (Lauritzen and Nilsson 2001). The method is an approximation because the decision nodes only include the direct parents in the policy tables; thus the decisions have to be updated each time new information is entered in the network, in order to make the optimal decisions. The Bayesian network for this case is shown in Figure 2. For this method, the expected costs can be calculated directly from the network, but only approximately, and Monte Carlo sampling is used to find the correct expected costs.

The methods are demonstrated through an application example, where a component with failure rate 0.1/year and a damage model based on Paris law is considered. For both methods, Monte Carlo sampling is performed, and the network is updated one time step at a time, and the decisions are made according to the two methods.

For the threshold method, Monte Carlo sampling is performed with different thresholds for the failure probability, and the expected costs are shown in Figure 3. The threshold value 0.05 is found to give smallest expected costs for this example, but if the specific costs for inspections, repairs, and failures were different, another value could be optimal.

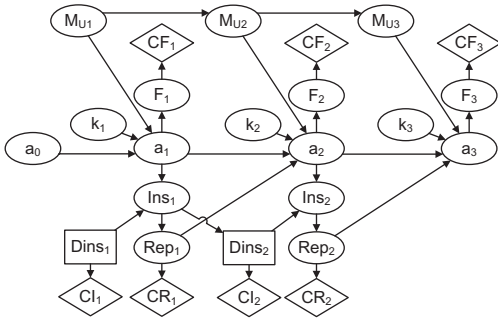


Figure 2. Bayesian network for the LIMID approach with nodes: CF_i ; cost of failure, CI_i ; cost of inspection, CR_i ; cost of repair, and see figure 1 for the rest.

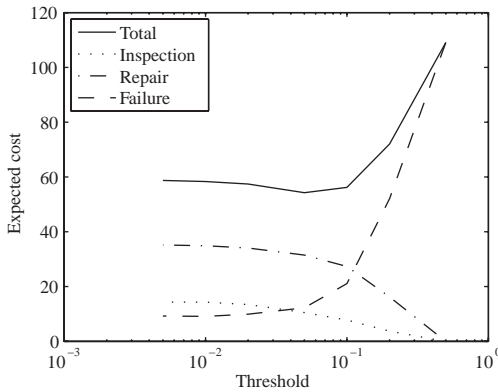


Figure 3. Costs for different thresholds.

Table 1. Expected costs for threshold and LIMID approach. Costs are shown for a threshold 0.05, which gives minimum expected costs for this strategy.

Case	Total	Inspection	Repair	Failure
Threshold	54.3	10.5	31.5	12.3
LIMID	54.0	11.6	31.9	10.5

For the LIMID, the approximative total expected cost found directly from the network was 64.5, but the correct total expected cost found using Monte Carlo sampling was 54.0. This difference is caused by the fact that the policies are updated each year, and for the direct calculation of the expected costs it is assumed that the policies calculated in year zero are used throughout the lifetime.

In Table 1, the costs for both methods are shown. The total costs are found to be almost equal, and therefore, the methods are considered to be equally good. The downside of the threshold method is that Monte Carlo sampling has to be performed initially in order to find the optimal threshold value to use, but then the computations are very simple during the lifetime. For the LIMID, no Monte Carlo sampling has to be performed in order to use the method, but the computations needed during the lifetime is less simple, and problems could arise if more complicated problems are modeled.

ACKNOWLEDGEMENTS

The work presented in this paper is part of the project “Reliability-based analysis applied for reduction of cost of energy for offshore wind turbines” supported by the Danish Council for Strategic Research, grant no. 2104-08-0014. The financial support is greatly appreciated.

REFERENCES

- Lauritzen, S.L. & Nilsson, D. (2001). Representing and solving decision problems with limited information. *Management Science* 47(9), 1235–1251.
- Straub, D. (2009). Stochastic modeling of deterioration processes through dynamic bayesian networks. *Journal of Engineering Mechanics* 135(10), 1089–1099.

On the use of Bayesian networks for Probabilistic Seismic Hazard Analysis

N.M. Kuehn, C. Riggelsen & F. Scherbaum

Institute of Earth and Environmental Sciences, University of Potsdam, Potsdam, Germany

The goal of Probabilistic Seismic Hazard Analysis (PSHA) is to estimate the annual rate of exceedance of a particular ground motion level A , $\nu(Z > A)$. Here, the ground-motion parameter Z describes a quantity that is of engineering interest, such as peak ground acceleration (PGA) or the response spectrum. In the calculation of the annual exceedance rate $\nu(Z > A)$, all uncertainties are taken care of. This relates to both epistemic (i.e. associated with the lack of knowledge) and aleatory (i.e. associated with intrinsic variability) uncertainties. Aleatory uncertainties are for example the time, location and magnitude of a future earthquake. In particular, it is important to take into account the intrinsic variability of ground-motion, since this largely controls the shape of the hazard curve (Bommer and Abrahamson, 2006), in particular for low exceedance frequencies. Epistemic uncertainties are for example different parameter values or different models. From a statistical point of view, the difference is that aleatory uncertainty is integrated out, while epistemic uncertainty is retained in the calculation of hazard curves. Hence, aleatory variability controls the shape of the hazard curve, while epistemic uncertainty leads to different hazard curves (a distribution of hazard curves) (Abrahamson and Bommer, 2005).

The annual rate of exceedance of a particular ground-motion level A is calculated via the so-called hazard integral

$$\nu(Z > A) = \nu(M_{\text{Min}}) \int_M \int_R f_M(m) f_R(r) \Pr(Z > A | m, r) dr dm, \quad (1)$$

where $f_M(m)$ and $f_R(r)$ denote probability density functions for magnitude and distance, respectively, and $\nu(M_{\text{Min}})$ is the earthquake occurrence rate. The integration over M and R is carried out from the minimum to the maximum magnitude and from the minimum to the maximum distance. $\Pr(Z > A | m, r)$ is the conditional probability that an earthquake with magnitude m in a distance r generates a ground motion Z that is larger than A . It can be easily calculated from the probability density function of Z by integrating from A to ∞ .

As one can see in equation (1), calculation of the hazard integral involves probabilities on many levels. In practical applications, the calculation of hazard curves becomes even more complicated. For example, a common choice for the probability density function for magnitudes, $f_M(m)$, is a doubly truncated exponential function (the Gutenberg-Richter distribution), which includes the parameters b and M_{Max} . These are usually not known exactly, so one has to account for their uncertainty, which makes $f_M(m)$ a conditional probability, $f_M(m|b, M_{\text{Max}})$. Furthermore, often there are competing models, so one also has to condition on the model.

A good tool to deal with uncertainties and conditional probabilities are graphical models (e.g. Koller and Friedman, 2009). In particular, Bayesian networks, a special kind of graphical models, allow for fast inference and calculation of conditional probabilities given different evidence. They also allow to estimate conditional probabilities when there is no information about individual variables available. This makes it useful for PSHA, where many parameters are only known with considerable uncertainty.

To develop a graphical model for PSHA, we start out with the ground-motion parameter of interest, Z , since we are mainly interested in its conditional distribution. The distribution of Z is affected by several earthquake source, path and site parameters, most notably magnitude M and distance R , but also the style-of-faulting FM and the average shear wave velocity in the upper 30 m, V_{s30} . Hence, for each of these variables X there is an arc $X \rightarrow Z$ in the model. If we want to model additional dependencies of Z on other variables, we just add the corresponding node and arc to the model. If we have reason to believe that some of the “predictor” variables X are not independent, we can easily model this dependency by adding an arc between these variables.

There is considerable uncertainty about the exact form of the dependency of Z on the other parameters such as magnitude, distance r , V_{s30} . Hence, the distribution of Z also depends on the model used. This can be represented by an additional parent of

Z in the graph. The above considerations define the conditional distribution of the ground-motion parameter of interest,

$$\Pr(Z) = \Pr(Z|M, R, FM, V_{S30}, MOD). \quad (2)$$

We now assume that the magnitudes are distributed according to a truncated exponential distribution with (unknown) parameters b and M_{Max} . Thus, the magnitude distribution is

$$\Pr(M) = \Pr(M|b, M_{Max}). \quad (3)$$

This is represented by two arcs $b \rightarrow M$ and $M_{Max} \rightarrow M$ in the graphical model.

The whole graphical model is depicted in Figure 1. Here, the joint distribution of all variables X is

$$\Pr(X) = \Pr(Z|M, R, V_{S30}, FM, MOD) \Pr(M|b, M_{Max}) \Pr(R) \Pr(V_{S30}) \Pr(FM) \Pr(b) \Pr(M_{Max}), \quad (4)$$

from which it is easy to calculate the marginal probability $\Pr(Z)$. The probabilities $\Pr(R)$, $\Pr(V_{S30})$, $\Pr(FM)$, $\Pr(b)$, and $\Pr(M_{Max})$ represent the initial uncertainties/variabilities of these parameters.

One can either calculate $\Pr(Z)$ including the uncertainties for all the other variables (which corresponds to the mean hazard), or keeping some parameters fixed at a certain level (which corresponds to individual branches of the hazard curve distribution).

The parameters of the model, i.e. the individual probability distributions, can be either set by experts, calculated based on existing models/physical reasoning, or determined from data. Then, it is possible to calculate any conditional distribution of interest. In particular, one can compute

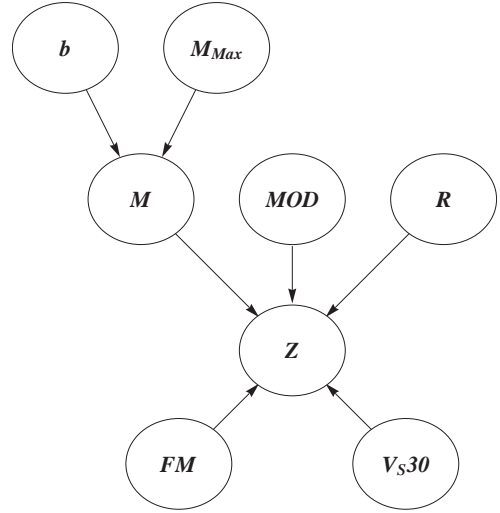


Figure 1. Conceptual graphical hazard model.

the conditional distribution of the ground-motion parameter of interest Z , given evidence or no evidence of the other parameters. This conditional distribution is directly linked to the seismic hazard.

REFERENCES

- Abrahamson, N.A. & Silva, W.J. (2008). Summary of the Abrahamson & Silva NGA Ground-Motion Relations, *Earthquake Spectra* **24**, 67–97.
- Bommer, J.J. & Abrahamson, N.A. (2006). Why Do Modern Probabilistic Seismic-Hazard Analyses Often Lead to Increased Hazard Estimates?, *Bull. Seism. Soc. Am.* **96**, 1967–1977.
- Koller, D. & Friedman, N. (2009). *Probabilistic Graphical Models: Principles and Techniques*, MIT Press.

Damage assessment of stranding events by means of Bayesian Networks

L. Garrè, B.J. Leira, T.-H. Nguyen & J. Amdahl

Department of Marine Technology, NTNU, Trondheim, Norway

ABSTRACT: Grounding and stranding of tankers are some of the main causes of pollution to the sea environment, due to the usually large amount of oil which is spilled if rupture of the tanks should occur.

In the present paper the so-called stranding scenario is considered. This scenario begins when the dynamic grounding phase has passed: the ship is steadily stranded on the seabed (the indenter) at a given location along her bottom. At this location the ground reaction force acts and causes a penetration in the ship's bottom structure. In this situation the ship has reduced operability and is exposed to the environment, mainly waves and tide. In the present work only the latter is considered, and specifically ebb tide. In this case, the reaction force increases with time and the ship experiences a further settling on the indenter, with consequent increase of the penetration. In past accidents this situation has been proved to be rather critical, as rupture of tanks and subsequent spill of cargo and/or global collapse of the hull girder can take place, depending on the local characteristics of the indenter.

Contrary to other types of accidents, the damage for such situations is not directly visible. This is due to a difficult, if not impossible, access and investigation of the bottom area until the ship is actually removed from the stranding location. Damages due to grounding can differ considerably depending on the characteristics of the indenter: from a local cutting/sliding type of damage caused by sharp indenters to an extended crushing type of damage caused by blunt and large shoals.

For the above reasons, tools for the assessment of the structural damage in the stranding situations, with particular focus on penetration of the indenter into the ship bottom and reduction of the flexural capacity of the hull girder, are of primary importance. This is particularly true in the frame of rapid emergency response and salvage engineering, as mitigating actions must account for the specific type of damage which is taking place during the stranding scenario. Since the development of the damage depends on the type of indenter, also this item should be estimated. Moreover, the

assessment must necessarily be based on a set of external indicators or measurements which are directly available at the stranding site.

In this respect, the present work adopts a procedure for the identification of the type of indenter along with the assessment of its penetration into the bottom. This procedure is based on measurements of the draughts of the ship at the stranding site at different tide levels during ebb tide. Parallel with these readings, also the reaction forces are estimated and the obtained quantities compared with a suitable database associated with different types of indenter. The appropriate indenter and the corresponding penetration are then estimated according to a best fit of the observed quantities and the database.

In order to facilitate the identification, also a categorization of possible indenters into classes of similar indenters is introduced. This categorization can be used in conjunction with the identification procedure in order to assign a stranding scenario which is being observed to a certain class.

Clearly, the assessment of the damage must be carried out in a variety of potential stranding situations, i.e. different types of indenters and different locations along the bottom of the ship. This is required in order to establish a framework for near-real-time decision support and intervention which is to be applied in real situations. In addition to this, uncertainties affect the measurements. These considerations call for the adoption of a probabilistic framework.

In the present study Bayesian Networks provide this framework. The reason for using BNs is the availability of well-established built-in inference algorithms and the possibility to formally include different sources of uncertainties. Moreover, BNs are versatile and usually easy to model and decision making can be modeled as well. This last aspect makes BNs extremely attractive for the present context, with respect to evaluation of emergency plans such as de- or re-weighting of the ship, lifting, pull-out strategies and so on.

It is outlined that, in line with common BN terminology, the identification procedure needs to be

divided into a diagnostic and a causal estimation of the penetration. The first makes use of the measurements of draughts, whereas the second takes advantage of causal relationships between the penetration and the contact force applied to the bottom. These relationships depend on the local features of the seabed and in the present paper are represented by curves of force versus penetration. These curves are obtained from finite element simulations of a variety of possible stranding events and constitute the previously mentioned database of cases.

Following the diagnostic approach, inference of the level of penetration is made in the BN on the basis of the history of the draught measurements during tide. From there on, at each new tide level, the diagnostic inference back-propagates in the

BN through the causal modeling and updates the posterior probability density function of the class of indenter.

In order to test the BN, estimates of the class of indenters and of the penetration are obtained using histories of draught measurements generated artificially with simulations of stranding onto different indenters. It is seen that, in most of the tested cases, the BN estimates the right class of indenter with a probability higher than 60% within 1 m of ebb tide variation. Moreover, also the level of penetration is usually satisfactorily estimated for each tide level simulated.

Considering the preliminary stage of the study and the level of details, the performance of the BN is deemed satisfactory and further extensions seem promising.

Effect of weather conditions, geography and population density on wildfire occurrence: A Bayesian Network model

P. Papakosta & D. Straub

Engineering Risk Analysis Group, Technische Universität München, München, Germany

ABSTRACT: Wildfires are common in geographic areas where the climate is sufficiently moist for vegetation growth but also features extended dry hot periods, such as the Mediterranean area. Besides climate, human interventions, such as land clearing activities, also play an important role in the occurrence of wildfires.

The research on wildfire occurrence addresses the questions on when, where and why wildfires are triggered and start to grow. The answer to these questions requires understanding of the interrelations among biotic and abiotic factors and multidisciplinary approaches are thus needed for modeling fire risk.

The interdisciplinary approach to natural hazard risk modeling can be supported efficiently by Bayesian Networks (BN). Based on acyclic graphs, BN enable to model the probabilistic dependence among a large number of variables influencing the risk. The causalities expressed by the arcs between the variables make BN not only convenient for graphical communication of the interrelations between the influencing factors (qualitative part), but also include, through conditional probability tables, a quantitative probabilistic model (Jensen & Nielsen 2007). Dlamini (2009) developed a BN model for wildfire occurrence, which is used to analyze the influence of 12 biotic and abiotic variables on wildfire occurrence in Swaziland, including land cover, elevation, mean annual rainfall and mean annual temperature.

In this paper, we attempt to construct a BN model for wildfire occurrence, which includes the effect of weather, vegetation and humans and deals with the problem of non observable variables. In contrast to Dlamini (2009), our BN model is based on continuous (3 hr or 6 hr) weather data and can thus serve for prediction purposes. The Fine Fuel Moisture Code of the Canadian Fire Weather Index (Van Wagner 1987) is utilized in the BN to model the effect of weather conditions on the fire occurrence. The model is applied to the Greek Mediterranean island of Rhodes.

The introduced BN to estimate wildfire occurrence rates is based on temporal and spatial data

(Figure 1). Here, the spatial reference of the model is the municipality level (administrative unit), to account for the available data (i.e. fire records that are available only for a municipality without geo-reference). The temporal reference is one day. Therefore, the BN represents the factors influencing wildfire occurrence in a municipality (as specified by the corresponding node) during a particular day.

The nodes of the model represent variables influencing wildfire occurrence. Grey nodes represent the variables used for the calculation of the daily fuel moisture and are treated separately in the parameter estimation.

Every node has a number of discrete mutually exclusive states, meaning that continuous random variables (such as Area or Human population density) are discretized.

The nodes Municipality, Area and Human population density are deterministic, and can be determined from spatial and demographic data. Land cover has labeled states that are related to fuel type.

The node FFMC (Fine Fuel Moisture Code) represents the continuous variable fuel moisture.

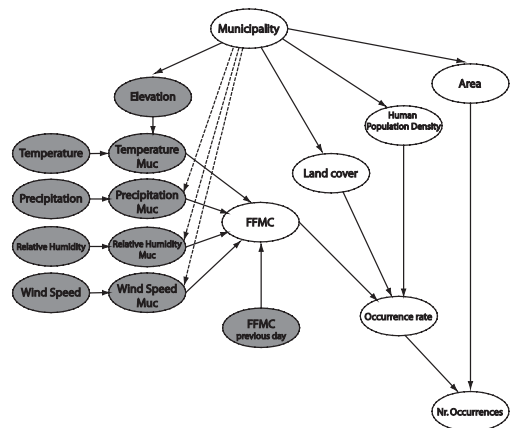


Figure 1. Bayesian Network for fire occurrences.

The node is a child of the weather variables (temperature, wind speed, relative humidity and precipitation) and the fuel moisture of the previous day. The daily values of FFMC are calculated deterministically.

The node Occurrence rate represents the mean number of wildfire occurrences per day and km². In this model, the rate is a function only of land cover, human population density and FFMC, which includes all weather related variables. The occurrence rate is not observable (hidden variable) and is estimated based on historical data.

The parameters of the BN are determined through the EM algorithm. The numerical implementation is carried out with the Hugin software. In total 109.994 records, corresponding to daily values for 7 years (2000; 2004–2009), each for 43 municipalities, are used for parameter estimation.

The main result of the parameter estimation is the probability mass function of the occurrence rate conditional on the FFMC, the land cover and the human population density.

Figure 2 shows the mean occurrence rate for different ranges of human population density. The occurrence rate increases with increasing values of human population density.

FFMC is found to have only slight influence on the occurrence rate. To facilitate interpretation of this result, Figure 3 shows calculated FFMC values for year 2000, together with daily precipitation and the observed number of fires. The FFMC values are generally high, and the only large changes occur during and after rainfall events.

The results show that for the investigated area, FFMC is only a weak indicator for the rate of wildfire occurrence. This might be explained by the fact that FFMC was developed for the climate and vegetation specific to Canada. In Rhodes, precipitation

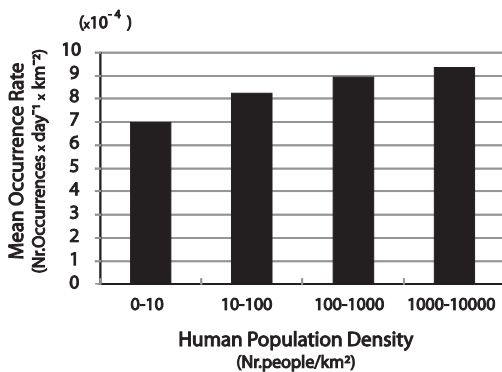


Figure 2. Mean fire occurrence rate and human population density.

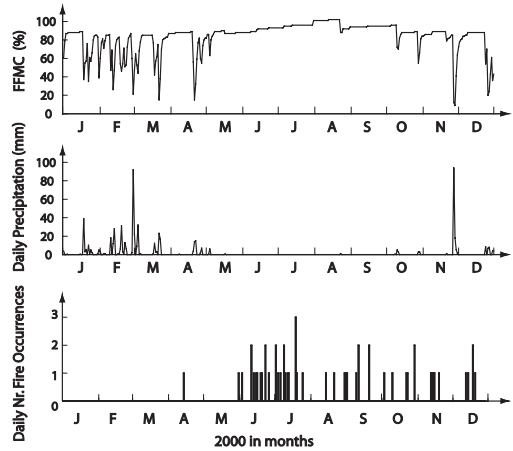


Figure 3. FFMC values at a representative municipality, together with observed precipitation at the weather station and total number of wildfire occurrences on the island for year 2000.

events are rare from May to September (Figure 3). As a result, the FFMC remains high (>80%) during this period, in which most of the wildfires occur. However, it is also observed from Figure 3 that the meteorological conditions have a clear effect on the occurrence of fires. The model must therefore be improved by utilizing more expressive meteorological indicators.

Once an improved description of meteorological conditions is established, the proposed Bayesian Network model, since it is based on daily weather data, can serve for prediction purposes and early warning. In addition, it can be continuously updated with new observations of weather conditions and wildfire occurrences, leading to an improved model in the future. Future work towards these goals includes the validation of the model and linking a GIS to the model for better visualization of the results to support the management of wildfire prevention measures.

REFERENCES

- Dlamini, W.M. (2009): A Bayesian belief network analysis of factors influencing wildfire occurrence in Swaziland. In: *Environmental Modeling & Software*, pp. 1–10.
- Jensen, F.V. & Nielsen, T.D. (2007): *Bayesian Networks and Decision Graphs*. Springer, NY, USA.
- Van Wagner, C.E. (1987): *Development and structure of the Canadian Forest Fire Weather Index System*. Forestry Technical Report 35. Canadian Forestry Service, Ottawa, Ontario, Canada. Available online: <http://warehouse.pfc.forestry.ca/HQ/19927.pdf>

Post-earthquake decision-making using influence diagrams

Michelle T. Bensi & Armen Der Kiureghian
University of California, Berkeley, USA

Daniel Straub
Technische Universität München, Germany

INTRODUCTION

A Bayesian network (BN) is a probabilistic graphical model that represents a set of random variables and their probabilistic dependencies. BNs are graphical and intuitive, facilitate information updating, can be used for identification of critical components within a system, and can be extended by decision and utility nodes into influence diagrams (IDs) to solve decision problems. These characteristics and capabilities make the BN-ID useful for assessing and responding to hazards posed to civil infrastructure systems. The goal of this paper is to demonstrate how IDs can be used to solve decision problems in the aftermath of an earthquake affecting a civil infrastructure system. We develop preliminary IDs to solve a specific problem involving the post-earthquake inspection and shutdown of the components of a system. Specifically, we focus on a post-earthquake scenario in which an earthquake has occurred and placed seismic demands on the components of an infrastructure system. Immediately following the earthquake, the owner/decision-maker must quickly decide, for each component of the system, whether to keep it open or shut it down, or to conduct an inspection before deciding on the fate of the component. The owner must make these decisions in an evolving state of information as observations about the earthquake and its effects are being made. Because of finite resources, the owner cannot simultaneously inspect all components. Therefore, for components for which inspections are required, the owner must choose the inspection order.

We begin with a brief introduction to BNs. Then, we provide an introduction to IDs as well as their more general counterpart: limited memory influence diagrams (LIMID). Later, we develop a framework for using IDs in post-earthquake decision-making related to the inspection and shutdown decisions. We develop this framework for both component- and system-level decision-making. We also establish a heuristic

for prioritizing post-earthquake inspections. The paper ends with an example application.

INTRODUCTION TO BAYESIAN NETWORKS

A BN is a directed acyclic graphical model consisting of a set of nodes representing random variables and a set of links representing probabilistic dependencies, typically causal relationships. BNs are useful for answering probabilistic queries when one or more variables are observed. Probabilistic inference in BNs takes two forms: forward (predictive) analysis and backward (diagnostic) analysis. Forward analysis calculates the probability distribution of any node in the BN based on the assumed prior marginal probability mass functions (PMFs) of the root nodes and the conditional PMFs of all other nodes. Backward analysis involves the computation of the posterior probability distribution of a node given observations on one or more nodes in the BN. While many analysis techniques are able to perform forward analysis, the power of BNs lies in the ease with which they facilitate information updating, i.e. backward analysis. Inference algorithms are available that efficiently perform calculations in BNs. A variety of exact and approximate algorithms is available; many of these are implemented in software (DSL 2007; Hugin Expert A/S 2008).

INTRODUCTION TO INFLUENCE DIAGRAMS

BNs can be extended by decision and utility nodes to solve decision problems. The resulting graphical model is known as an influence diagram (ID). An ID can generally be viewed as a compact representation of the same information contained in a decision tree. Detailed description of IDs can be found in Kjaerulff & Madsen (2008) and Jensen & Nielsen (2007). The ID encodes both the probability

model and the decision problem structure, which represents a sequence of observations, outcomes, and decision alternatives. Solving a decision problem via ID amounts to (1) calculating the expected utility associated with each decision alternative, and (2) selecting the optimal decision strategy, i.e. the strategy that maximizes expected utility from the perspective of the decision-maker. Like a BN, an ID consists of nodes representing discrete random variables (hereafter called chance nodes) that are connected by directed links and are associated with conditional probability tables. An ID differs from a BN because it includes utility and decision nodes. A utility node represents the value associated with a specific decision(s) and/or the outcome of a chance node(s). A utility node has no states; instead it is assigned a utility value as a function of the states of its parent variables. A decision node encodes alternative actions available to the decision maker. It is defined by a finite set of states corresponding to the decision alternatives

A LIMID differs from an ID due to the relaxation of the no-forgetting assumption associated with IDs. Rather than considering that all preceding decisions are known at the time a decision is made, only the states of nodes that are direct parents to the decision node are assumed to be known. Because LIMIDs do not require a temporal ordering on decisions, the possible combinations of orders on decision alternatives can be extremely large. Rather than explicitly considering all combinations and possible orders of decision alternatives, (locally) optimal solutions are determined using an iterative procedure known as *single policy updating*. The result is an approximate solution, see Lauritzen & Nilsson (2001).

INFLUENCE DIAGRAM FOR POST-EARTHQUAKE DECISION-MAKING

Within the context of the aforementioned inspection-shutdown decision, we consider two decision problems. First we consider decision-making at the component-level without addressing system-level effects. Then we consider decision-making when accounting for system-level effects.

The decision to shut down or reduce the capacity of a component is made under competing objectives: on the one hand the owner does not wish to lose revenue by unnecessarily shutting down or reducing the operating level of a component that may not have experienced serious damage, while on the other hand the owner does not want to incur a liability by making an unsafe decision, i.e. keeping the component open when it may have sustained serious damage. To reduce the uncertainty associated with this decision, the

owner may elect to conduct an inspection of the component, incurring a certain cost, which will yield information about the state of the component. The decision to close or not close the component will then be made after receiving information gained from the inspection.

Immediate post-event decisions regarding post-event inspection and closure of components should ideally be made at the system level. Consideration of losses at the system level allows the decision framework to account for redundancies in the system. To facilitate prioritization of post-earthquake inspections of components at the infrastructure system level, we define a value of information-based heuristic. The *value of information* is a concept commonly employed in decision analysis to quantify the amount of resources a decision-maker is willing to expend to acquire more information before making a decision. The heuristic assumes that, at each stage, the decision-maker is looking for the “next best component” to inspect. Using the LIMID methodology, the inspection prioritization order evolves as new information becomes available, e.g. from ground motion measurements and information from structural health monitoring sensors, and as inspections are performed and decisions are made regarding the shutdown of components. The information propagates through the LIMID to provide an up-to-date probabilistic characterization of the system model and decision structure. At any stage, the recommendations regarding component inspections may differ from those made at a previous stage. Thus, the LIMID provides the decision-maker with guidance on optimal decisions relating to inspection and component closure, at any point in time, based on all available information up to that time.

The above methodology is demonstrated through an example application.

REFERENCES

- Bensi, M. (2010). “A Bayesian Network Methodology for Infrastructure Seismic Risk Assessment and Decision Support.” Ph.D., University of California, Berkeley, Berkeley, CA.
- DSL. (2007). *GeNIe 2.0 by Decision Systems Laboratory* (<http://genie.sis.pitt.edu/>).
- Hugin Expert A/S. (2008). *Hugin Researcher API 7.0* (www.hugin.com). Hugin Expert A/S, Denmark.
- Jensen, F.V., and Nielsen, T.D. (2007). *Bayesian Networks and Decision Graphs*. Springer-Verlag, New York.
- Kjaerulff, U.B. and Madsen, A.L. (2008). *Bayesian Networks and Influence Diagrams: A Guide to Construction and Analysis*. Information Science and Statistics, Springer Science+Business Media, LLC, New York.
- Lauritzen, S.L. and Nilsson, D. (2001). “Representing and Solving Decision Problems with Limited Information.” *Management Science*, 47(9), 1235–1251.

MS_115 — Bridge traffic loading (1)

This page intentionally left blank

Statistical analyses of Weigh-In-Motion data for bridge live load development

T.H.T. Chan

Faculty of Built Environment and Engineering, Queensland University of Technology, Brisbane, Australia

T.J. Miao

Department of Civil & Structural Engineering, The Hong Kong Polytechnic University, Hung Hom, Hong Kong

ABSTRACT: This paper discusses the statistical analyses used to derive bridge live loads models for Hong Kong from a 10-year Weigh-In-Motion (WIM) data. The statistical concepts required and the terminologies adopted in the development of bridge live load models are introduced. This paper includes studies for representative vehicles from the large amount of WIM data in Hong Kong. Different load affecting parameters such as gross vehicle weights, axle weights, axle spacings, average daily number of trucks etc are first analyzed by various stochastic processes in order to obtain the mathematical distributions of these parameters. As a prerequisite to determine accurate bridge design loadings in Hong Kong, this study not only takes advantages of code formulation methods used internationally but also presents a new method for modelling collected WIM data using a statistical approach.

1 INTRODUCTION

The ability to weigh vehicles as they travel at a highway speed has become known as Weigh-in-Motion (WIM) technology. Using a WIM system, virtually a 100% sample of traffic data for statistical purposes can be obtained. The information can be transmitted immediately in real time, or at some future time, to locations remote from the WIM site via conventional communications networks. At present, WIM systems are used for enforcement primarily to identify individual vehicles that are suspected of being in violation of weight or size laws and for locating sites where relatively large numbers of probable weight, speed, or size violations occur. Relevant departments of the Hong Kong SAR Government (known as Hong Kong Government before 1997) decided to install WIM systems in Hong Kong several years ago, and a large amount of WIM data has been obtained. These WIM data can be analyzed to understand the real traffic status for comparison with bridge design live load models

in use in Hong Kong to test overloading. These WIM data can also supply basic information, such as traffic flow, and heavy vehicle distribution to plan road networks. Bridge loading models are very closely related to gross vehicle weights, axle weights, axle spacings and average daily number of trucks. If the mathematical distributions of these parameters are obtained accurately, bridge live load models can subsequently then be easily formulated. WIM systems can provide a great amount of real traffic data to assist in determine these parameters. The problem is how to determine these parameters from the measured WIM data. It is impossible to determine these parameters in a load model if the tremendous amount of WIM data is not described statistically.

This paper discusses the methodologies, analytical concepts and the statistical models derived from the analysis of a 10-year WIM database described in (Miao 2001). The statistical analysis approach used in this paper is an effective method to obtain the Cumulative Distribution Function (CDF) of related parameters such as gross vehicle weight, axle weight, axle spacing and so on. These obtained parameters are the base of formulating the bridge live load models (Miao and Chan 2002). This approach can provide a distinct CDF and a required value of any parameter under a given probability level.

2 STATISTICAL PROCEDURE

The statistical procedure adopted to estimate the maximum values of the gross vehicle weight and axle weight in bridge design life includes the following:

1. WIM data collecting and handling
2. Selection of Statistical Processes and Estimation of the corresponding Statistical Parameters
3. Grouping of the recorded WIM data
4. Simulation of the selected Stochastic Processes.

3 STATISTICAL PROCESS SELECTION

The distributions considered include the followings:

- i. Normal Distribution (ND)
- ii. Weibull Distribution (WD)
- iii. Filtered Weibull Process (FWP)
- iv. Gamma Distribution (GD)
- v. Logarithmic Normal Distribution (LND)
- vi. Extreme Value Distribution—Type I (EVD)
- vii. Inverse Gaussian Distribution (IGD)
- viii. Filtered Poisson Process (FPP).

The Monte Carlo method is then used to simulate the distributions of maximum value stochastic processes of a series of given stochastic processes. The expected value and standard deviation for Gross Weight, Axle Weight, Headway, Time Interval are then determined.

4 MAXIMUM VALUE ESTIMATION

After identifying the stochastic processes for each bridge loading related parameters, the distribution parameters of every domain can be obtained. The maximum value of vehicle gross weight and axle weight for a design return period of bridge life can then be determined. The Kolmogorov-Smirnov approach is used again to check whether Normal, Lognormal, Weibull, Gamma, Extreme Value Type-I and the Inverse Gauss Distribution describe the maximum value distributions of the gross weight and axle weight respectively. It is interesting to note that the maximum value of gross weight and axle weight during bridge design life, say 120 years, calculated according to the above approach are very close to their legal limitations of Hong Kong which are 42 tons for gross weight and 10 tons for axle weight TDHK (1997).

5 CONCLUSIONS

To meet the demands, the loading carried by a heavy vehicle will be getting heavier and heavier, a bridge design loading should meet the needs

of this development. The maximum gross vehicle weight within a bridge design life, say 120 years, should be obtained and considered in the development of bridge design loading models. The statistical analysis approach used in this paper is an effective method to obtain the cumulative distribution function (CDF) of related parameters such as gross vehicle weight, axle weight, axle spacing and so on. These obtained parameters are the base of formulating the bridge live load models. This approach can provide a distinct CDF and a required value of any parameter under a given probability level.

The WIM data from Hong Kong has been statistically analyzed in this paper as an example of the proposed method. The mathematical distributions of gross vehicle weights, axle weights and headway are obtained accordingly. The maximum values of axle weight and gross vehicle weight are compound stochastic processes. Their mathematical distributions are also obtained. Then the maximum gross weights and axle weights within bridge design life under a probability level are then calculated. It is interesting to notice that the maximum value of gross weight and axle weight during bridge design life, say 120 years, calculated according to the above approach are very close to their legal limitations of Hong Kong.

ACKNOWLEDGEMENT

The work described in this paper was supported by a grant from the Research Grants Council of the Hong Kong Special Administrative Region, PRC (Project No. PolyU 5033/02E). The statistical research and the random process for the gross vehicle, axle weight, axle spacing and so on are based on the WIM data provided by the Highways Department of the Hong Kong SAR Government. The support provided by the Queensland University of Technology is also gratefully appreciated.

Recent advances in reliability based assessment of highway bridges

A. O'Connor

Department of Civil, Structural and Environmental Engineering, Trinity College Dublin, Ireland

V. Pakrashi

Department of Civil and Environmental Engineering, University College Cork, Cork, Ireland

ABSTRACT: Often in bridge assessment the failure of a deterministic assessment at some limit state is taken to imply that the structure requires either rehabilitation or replacement. There is however a third option, probability-based safety assessment, which is often ignored by bridge owners/managers but which if considered can lead to considerable savings by avoiding the need for costly repair or rehabilitation. The principles of probabilistic assessment are no different than the techniques used in code derivation. A minimum safety index is specified for the structure, dependent upon its importance, expected failure mode etc. and at each limit state the computed level of safety of the structure is required to exceed this minimum. Therefore probabilistic assessment can be related to the derivation of a bridge specific code for the structure. The approach benefits from a lack of generalisation inherent in design codes without compromising the level of safety of the structure. A logical progression from probabilistic assessment of individual structures is the concept of safety based maintenance management. The basic premise lies in acceptance of the concept that when it becomes impossible or too costly to maintain bridges to their as-built standard, bridge owners must at least ensure that the bridges fulfil specified requirements of structural safety. Safety based bridge maintenance management is attractive as it enables bridge owners/managers to extend service lifetimes by reducing or postponing costly major rehabilitation projects. Instead focused repairs are performed on specific critical components of the structure to ensure the overall level of safety remains above the minimum requirement. The critical structural components are determined from deterministic assessment. Significantly, at no stage in the process is the required level of safety compromised. Central to the process of probability-based safety assessment is accurate modelling of the resistance and load. Original structural drawings and material records may be employed to provide information

on the distributions of the material variables and consequently the parameters governing structural resistance. Bayesian updating of these distributions may be performed using results of bridge inspections, testing etc. Modelling of the loads to which the structure is subjected is often performed using codified assessment models or site surveys of loading. It is critical to assess random variables as accurately as possible to reduce the level of uncertainty. Of all loads to be modeled, by far the most variable are live loads, traditionally prescribed based upon subjective assumptions of the maximum expected axle, vehicle or combination of vehicles. These assumptions led to conservative and/or inconsistent design load effects and consequently, inconsistency in safety levels among structures. Using of Weigh in Motion (WIM) data in probabilistic safety assessment reduces uncertainty in the load-modelling process. Statistical parameters governing traffic flow at site may be accurately recorded and modelled and realistic estimates of load effects can be obtained through realistic simulations of multiple transverse and longitudinal presences. The response of the structure is also modelled with greater accuracy as the WIM system enables computation of the actual influence surface for the structure. Therefore the actual structural behaviour, incorporating any damage or change of structural system is modelled rather than that as idealised from finite element models or theory. It is however important to recognise that just as probability-based assessment attempts to model structural resistance degradation with time, some effort is required to allow for evolution of traffic with time. This paper presents through example the benefit of some of the aforementioned recent advances for reliability based safety assessment and maintenance management of highway bridges.

From a schematic viewpoint, bridge maintenance management through reliability based assessment is fundamentally hierarchical by resource and information limitations. Three main

zones—a) Inspection and Testing, b) Computation and c) Decision Making interact with each other to reach to an optimised decision. Often, selected parts of this scheme are used for actual decision making based on available cost and/or time resources.

Time variant live traffic loads require statistical modelling to determine the magnitude of their characteristic effects. The levels of extreme values of these loads are associated with a return period against a certain intensity taking place with a given degree of confidence in terms of statistical significance. This degree of statistical significance and consequently the return period or the intensity of the action at a given intensity vary when evolution of increasing traffic load over time is taken into account. It is thus important to establish the description of such load in terms of extreme value distributions and concentrate on the statistical description of the tails, or the extremes of such distributions. Typically, the Gumbel family of distributions (*Gumbel*, *Frechet* and *Weibull*) are fitted to measured data, recorded over a period of time. WIM systems are directly employed for the acquisition of this data.

Subsequent extrapolation of these fitted distributions for a specified return period yields the characteristic value to be used for time variant loads. The difference in distributions contained within the Gumbel family lies in their tail behaviour, i.e., whether they are bounded or unbounded in the extreme.

The importance of fitting the tail from WIM observations is noted. The same histogram may appear to exhibit a reasonable fit on the whole to a number of very different distributions. However, it is the goodness of fit of the tail that governs the site-specific characteristic loading with probabilistic descriptions. Consequently, fitting the tail very significantly affects the reliability index of the structure in an as-built condition. Additionally, as shown in the figure, a non-parametric fit may exhibit an excellent fit even on the tails but should be used with caution due to its high dependence on the measured data. The parameters of traffic loading can be significantly changed with time bringing about a complete change in the statistical description of traffic loading. Such a situation is usually

accompanied with an increase in average loading and a decrease in the return period of extreme loads with time. Additionally, it is also possible that the information on the extremes is only partial. Significantly compromised measurement would give rise to unrealistic assessment values and consequently the acceptance of a dataset should be carried out with care. However, even in the presence of acceptable datasets the choice of statistical description of measured quantities remains critically importance.

An important application of reliability analysis can be related to the problem of sensitivity analysis and over-parametrisation of the number of variables involved. The sensitivity analysis results on the parameters of reliability index, when compared and ranked, can provide indication of the critical parameters that contribute maximum to the establishment of the reliability index if the bridge. Additionally, it also allows quantifying the relative participation of each parameter. When the parameters are from the resistance side, such information can be used for choosing locations and methods of testing or health monitoring of structures. When the parameters are from the loading side, to be specific for traffic loading, appropriate limits on maximum loads can be set in conjunction with other intervention methods to appropriately manage the safety of bridges. However, when a structure is overparametrised with too many variables, the sensitivity analysis may mask important participation ratios due to the division of participation into too many numbers of parameters. Consequently, care is required while choosing the number of parameters, even if a large number can be modeled from observed WIM data.

Another important aspect of employing WIM data can be related to a realistic estimate of often intangible cost to the road user for any intervention on the bridge. The cost to the road user is generated due to a loss of time, a detour or both. The cost of detour per unit length or loss of unit time is directly related to the class of vehicle with respect to its weight. An appropriate description of the frequency of vehicles above a certain weight directly affects and improves the realistic calculations of cost to the bridge user when such information is readily not available.

Visualization of live-load probability distribution by Random Number generation and a Reliability Analysis of a bridge girder based on the Traffic Flow Model

O. Yoshida

Yoshida Engineering Laboratory, Chiba City, Japan

This paper makes a proposal method for setting the live-load probability distribution using random vehicle weights. Traffic Flow Models which are propounded in Japanese “Fatigue design Guide Line for Road Bridges” are adopted. In those models, vehicles are classified into eight categories and have hierarchal component percentages. Each category has separate weight probability distribution. Random Numbers are generated for each category in accordance with the probability distributions and the component percentage. They are merged and shuffled. Thus a random arrayed motorcade is built for each Traffic Flow Model. An assumption is herein introduced that the generated motorcade samples have the similar probability distribution to that of traffic loads in the whole bridge life.

Reliability assessment examples for the Plate-Girder Bridge are carried out using these probability characteristics, being compared with allowable stress design. Thus, an interrelation of the allowable stress design method and Reliability Theory is identified for each Traffic Flow Model. In other words, allowable stress design method can be converted to Reliability assessment method practically on the premise of Traffic Flow classification.

In order to simulate the sequential vehicles on the bridge, random numbers are generated for the vehicle categories in accordance with the probability distributions and the component percentages.

Generated samples are merged and shuffled. Thus a random arrayed motorcade is built for each Traffic Flow Model. An assumption is herein introduced that the generated motorcade samples have the similar probability distribution to that of traffic loads in the whole bridge life.

Figure 1 shows the histogram of all samples in case of Traffic Flow class-E, as the example of the heaviest traffic.

Serial vehicle weight of the random arrayed motorcade is counted until its summed length reaches the loading length. Repeating this from the head to the next sequentially, the summed weights are divided by the loading length. Thus the distributed load intensities are derived. Therefore

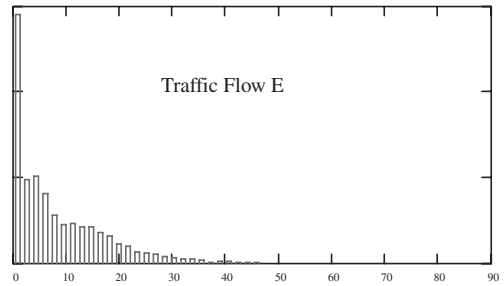


Figure 1. Histogram of all samples (ton).

its probability distribution characteristics are obtained.

Figure 2 shows the histograms of distributed load intensities of Traffic flow C. The dotted line is the Normal distribution fit line which has the mean value and the standard deviation of Traffic flow C.

Several fractile values of distributed loads are calculated and compared with the nominal load value of the Japanese design code “Specification of Highway Bridges”. Through those simulations, regulations of uniform load reduction for the span length and for the transverse direction can be explained theoretically. Using these characteristics, the expectations on several fractile percentages are calculated. They are shown in Figure 3, together with the nominal uniform load value of the Japanese design code. This Figure 3 shows the relative position between the simulated expectation and the nominal load value.

Among these results, we can know that the nominal load value corresponds to which percentages expectation value. For example, traffic flow C line of 90% fractile is the nearest to the nominal load line. And it may not sound strange to our empirical recognition that nominal load may be 90% fractile or so.

The reduction effect of the fractile value according to the loading width exists on the same reason as loading length. Then, the problem can be

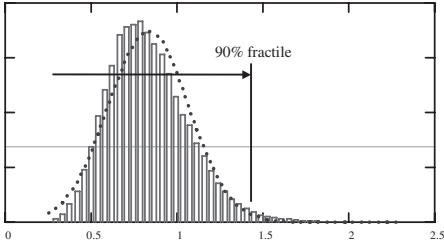


Figure 2. Histogram of distributed load (tonf/m/lane).

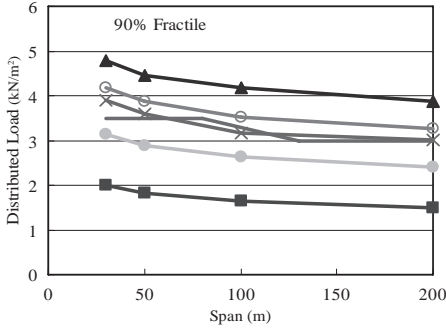


Figure 3. Distributed load on loading length.

analyzed such as the loading length is multiplied by the lane number.

Figure 4 shows the reduction coefficients of the fractile value by number of lanes, when 90% fractile of traffic flow C is selected.

The allowable stress of SM400 steel is regulated, based on the yielding stress divided by about 1.7. The variance of the yield stress of actually supplied steel material in Japan is researched and reported in the reference 3). The probability distribution characteristics can be set using this data.

Figure 5 was described as Normal distributions by these reported yield stress data.

In case of 30 m span, the probability distributions of each load share and yield stress are shown in Figure 6.

In attempt to realize the tangible analysis example, several example model bridges (Plate girder span = 30–60 m) are taken.

The Reliability assessment for the bridges designed by the allowable stress method is carried out.

The Reliability Index based on the second moment equation is introduced, using these probability distributions. By the results, the calculated Reliability Indexes gradually increases along the increase of span length. It is caused by the reduction of live-load share. More economical design can be introduced if the Reliability Index is kept constant.

The allowable stress design method can be converted to Reliability assessment method practically on the premise of Traffic Flow classification.

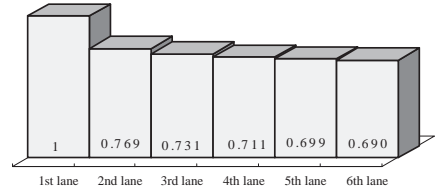


Figure 4. Reduction of fractile value by number of lanes.

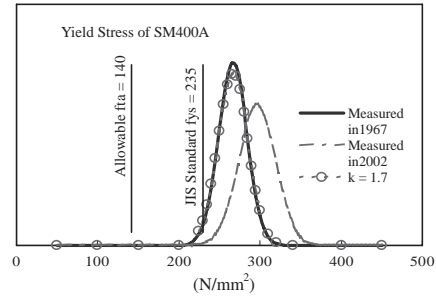


Figure 5. Distribution of yield stress.

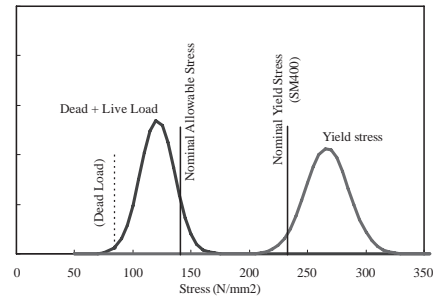


Figure 6. Probability distributions of reliability assessment (Traffic Flow C).

The role of the infrastructure responds to the social demands. From that standpoint, traffic flow is the most important factor for Bridge designing. Social role of a bridge is to meet the traffic demand. The width and the geometric alignment of the bridge are decided based on the traffic grade. Therefore, traffic load should be decided considering the traffic grade, in the same sense. When the heavier traffic grade is expected than the standard one, the bridge must be strengthened in accordance with that. And, if the percentage of the heavy vehicle is expected smaller than the standard, the bridge must economically be designed.

The allowable stress design method is widely rooted as a de-facto standard. Many an engineer shall be able to address the reliability design by an accessible method. Then the reliability technology shall develop higher being used by many engineers, and make a social contribution greatly.

Development of live load model for long span bridges

E.-S. Hwang

Kyung Hee University, Yongin, Korea

H.-M. Koh

Seoul National University, Seoul, Korea

S.W. Lee

Kyung Hee University, Yongin, Korea

This paper deals with the development of live load model for long span bridges using Weigh-In-Motion (WIM) system and a comparison with the current live load model from various countries. The live load model in Korea Bridge Design Code (KBDC) was developed about 40 years ago for short and medium span bridges less than 200 m. In 2006, Design Guideline for Steel Cable Bridges (DGSCB) was developed for use with bridges longer than 200 m. However, heavy truck data is limited and the live load model doesn't reflect the current status of heavy traffic. New live load model was proposed based on Weigh-In-Motion (WIM) data for short and medium span bridges and plan to be adopted in 2011. To be consistent with new load model, live load model for long span bridges need to be developed. A WIM system was installed and has been operated for more than ten months to collect real traffic data. To estimate the maximum effect, the fictitious traffic jam model is assumed, which consider only truck traffic with minimum headway distances between front and rear trucks. To calculate the actual load effects, two long span bridges (one cable stayed and one suspension bridge) are selected. Load effects of main members such as cable, pylon and stiffening girder

are calculated and compared with various live load models in the world, such as AASHTO LRFD, Korean Bridge Design Code and Japanese Code from Honshu-Shikoku Bridge Authority. The structural analysis models of selected bridges have been developed by MIDAS and RM software. For the verification of the model, DL-24 load model in KBDC is applied to Incheon Bridge model and the live load model in DGSCB is applied to Leeshunsin Bridge. The results are compared with original design results. There is a maximum 8% error from original design values for Incheon Bridge, which proves the adequacy of the model. Results for Leeshunsin Bridge verify the adequacy of the analysis model.

To determine the maximum load effects, it is assumed that fictitious traffic jam situation is happened and all trucks without any cars or small vehicles in between are located with bumper to bumper with minimum headway distance. Spacing between the last axle of the front truck and first axle of the rear truck is assumed as 3 m. Then from the series of trucks maximum intensity of truck weights are determined by calculating the uniformly distributed load intensity considering the influence line as shown in Figure 3. The maximum load intensity



Figure 1. Incheon Bridge, Cable stayed Bridge, Main span length = 800 m.



Figure 2. Leeshunsin Bridge, Suspension bridge, Main span length = 1545 m.

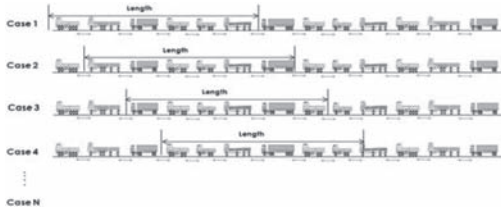
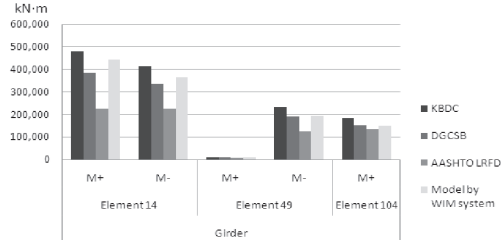
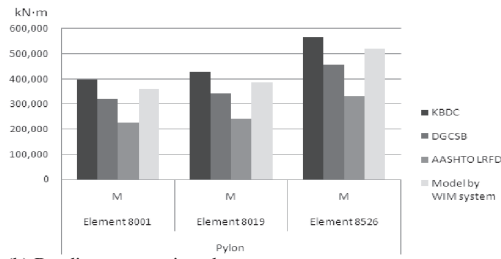


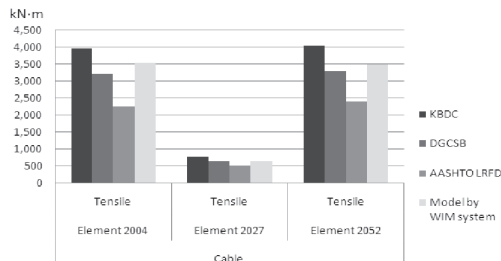
Figure 3. Traffic jam simulation of truck through the length of influence line.



(a) Bending moment in stiffening girder



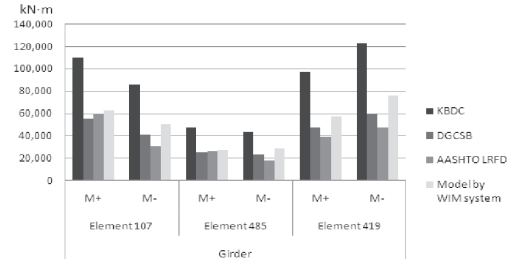
(b) Bending moment in pylon



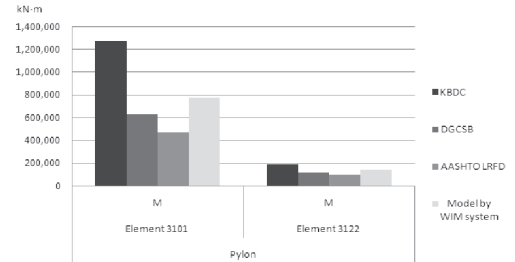
(c) Tension force in cable

Figure 4. Analysis results of Incheon Bridge.

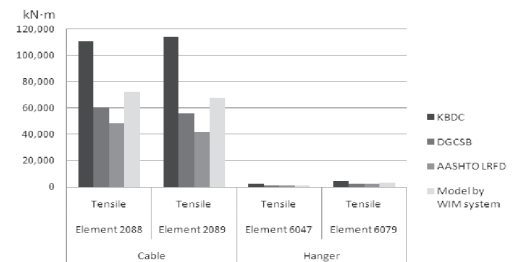
is calculated by total weights of trucks in influence length divided by the influence length for each section as cable, pylon and stiffening girder. Figure 4 and Figure 5 show the comparison between live load model in various live load models and model from traffic jam model. Results show that the traffic jam model generally shows smaller values than KBDC model but higher values than DGSCB. Also AASHTO LRFD model show much less



(a) Bending moment in stiffening girder



(b) Bending moment in pylon



(c) Tension force in main cable and hanger cable

Figure 5. Analysis results of Leeshunsin Bridge.

values than other models. In the future, nominal load model and load factors should be determined with longer term data and additional WIM data.

MS_125 — Bridge traffic loading (2)

This page intentionally left blank

In-situ dynamic behavior of a railway bridge girder under fatigue causing traffic loading

A. Herwig

EMPA—Swiss Federal Laboratories for Materials Science and Technology, Dübendorf, Switzerland

E. Brühwiler

EPFL—Ecole Polytechnique Fédérale, Lausanne, Switzerland

ABSTRACT: Stresses in bridges due to traffic loading need to be determined as accurately as possible for reliable fatigue safety verification. In particular, the dynamic traffic effect due to running vehicles has to be considered in a realistic way. In-situ measurements of the dynamic behavior of a one-track railway bridge have been performed to analyze the complex elastic dynamic system consisting of running trains—railway track—bridge structure. The main causes for dynamic effects for fatigue relevant bridge elements have been identified to be the vertical track position, i.e. track irregularities. The dynamic behavior has been modeled with sufficient accuracy using simple models when fatigue relevant dynamic effects are studied. The results of this study allow for the consideration of realistic dynamic amplification factors for fatigue verification.

1 INTRODUCTION

For the examination of existing bridges, dynamic amplification factors for updated traffic loads need to be derived for the deterministic verification of each the structural safety, serviceability and fatigue safety. This paper concentrates on realistic dynamic amplification factors to be deduced considering elastic structural behavior of bridge elements under fatigue loading.

Stresses in the fatigue vulnerable steel reinforcement of concrete railway bridges due to traffic loading have to be determined as accurately as possible for reliable and realistic fatigue safety verification. Therefore, the dynamic traffic effect due to running trains has to be considered in detail.

The aim of this paper is to show that the complex elastic dynamic system consisting of running train—railway track—bridge may be modeled with sufficient accuracy using simple models when fatigue relevant dynamic effects are studied. These simple models may then allow the study of the

effect of other velocities and increased trainloads on fatigue relevant bridge elements.

In view of this objective, dynamic measurements are conducted on a one-track railway bridge. First, the measured behavior is compared with the dynamic behavior of a model taking into account only train velocity. Then the dynamic behavior due to railway-track irregularities is investigated with simple models.

2 MAIN RESULTS AND DISCUSSION

Modeling of dynamic behavior: The presented study shows that the dynamic behavior as measured from a prestressed concrete bridge girder is well represented by simple models which allow identifying fatigue relevant dynamic effects. It may be noticed that the dynamic bridge behavior has no significant influence on the dynamic behavior of the car because of the high difference in stiffness between the car suspensions and the bridge structure. Also, it is sufficient to represent the first vibration mode of the bridge girder. The bridge structure may be attributed to a rigid base for the car, and car and bridge may be modeled separately.

Fatigue relevant dynamic actions: Track irregularities are found to be the main cause leading to amplifications of the bridge dynamic response. Typical cases are local settlements in the transition zone embankment-bridge or a difference in elevation of the railway track due to a rail joint (misalignment) or bad welding. The wheel force variation due to railway track depressions leads to an almost immediate bridge response.

As observed in the measurements and simulations, the dynamic amplification factor varies with varying train velocity. A maximum occurs at the resonance speed for maximum car excitation due to track irregularities. High contact force amplitude leads to high action effect amplitudes. Maximum dynamic wheel forces do however not necessarily

occur always at the location leading to maximum action effect such as the bending moment.

It should be noted that maximum dynamic amplifications due to both train velocity and track irregularities should actually not just be added to obtain the total dynamic amplification factor, since it is rather unlikely that the maximum dynamic effect of both effects occurs at the same time for the occasional case of a carriage with a high fatigue relevant load.

Fatigue relevant action effect: The action effect of interest (i.e. the maximum moment) is caused by more than one bogie. It must not be expected that all the bogies increase due to dynamic effects their contact force at the same time. Consequently for fatigue loading, the sum of the contact forces leads to lower amplification factors than those for single bogies.

For the investigation of the fatigue safety, the dynamic effect of high traffic loads rather than medium or lightweight cars running at high speeds are of interest.

Dynamic amplification factors for high traffic loads are distinctly lower than for trains with lighter carriages as has been shown by many investigations. In particular, wheel force amplification and corresponding action effects (forces) in the bridge element due to track irregularities decrease with increasing weight of carriage [Herwig 2008, Ludescher & Brühwiler 2009] and it may be deduced:

- In the case of dynamic amplification due to *excitation from train movement* (train velocity), maximum dynamic effects occur only with regular axle spacing in narrow velocity domains. Other velocities lead to moderate dynamic effects. Here the effect of carriage weight is less pronounced.
- In the case of dynamic effects due to *track irregularities*, one needs to consider that the track quality varies over time, and since the overloaded carriage (as leading action) is an *occasional* event, it is reasonable to consider track irregularities as a quasi-permanent state.

Application: As a consequence and since the static load considered in the FLS verifications is extreme (high), the dynamic amplification factor according to EN 1991-2 may be reduced accordingly. At fatigue limit state FLS, frequent values of dynamic action effects are considered to represent service load conditions. Based on the foregoing considerations, the following dynamic amplification factor φ_{FLS} is suggested [SB4.3.3 2007]:

$$\varphi_{FLS} = 1 + 0.5(\varphi' + 0.3\varphi'') \quad (1)$$

with φ' and φ'' according to EN 1991-2.

3 CONCLUSIONS

The following conclusions are valid for the investigated bridge as well for fatigue relevant shorter bridges:

- The dynamic behavior of a bridge can be represented by simple models when fatigue relevant action effects are studied. It is sufficient to represent the first vibration mode of the bridge girder.
- Track irregularities are the most important cause for fatigue relevant dynamic amplifications of action effects. This effect occurs at each train passage for each car.
- Dynamic amplification factors for elastic structural behavior at fatigue limit state shall consider the effects of two main parameters involved, i.e. (1) train velocity and (2) track irregularity.

The investigated prestressed concrete bridge girder itself is actually only little fatigue vulnerable due to its relatively long span and the fully prestressed concrete cross section. Since the investigated bridge was rather stiff, the assumptions on the modeling are however applicable for bridges of shorter spans.

Modelling of highway bridge traffic loading: Some recent advances

B. Enright & C.C. Caprani

Dublin Institute of Technology, Dublin, Ireland

E.J. O'Brien

University College Dublin, Dublin, Ireland

1 INTRODUCTION

In recent years, the improved quality and increasing use of weigh-in-motion (WIM) technology (Jacob & O'Brien 2005) has meant that more accurate measurements of vehicle weights are now available for relatively long periods of time. These extensive measurements can be used to refine probabilistic bridge loading models for the assessment of existing bridges, and to monitor the implications for bridge design of trends in vehicle weights and types. Site-specific bridge assessment, based on measured traffic, can lead to very significant cost reductions for maintenance (O'Connor & Enevoldsen 2009).

Different approaches can be used for the estimation of lifetime maximum bridge loading from WIM data. One approach is to fit a statistical distribution to the calculated load effects for the measured traffic, and to use these distributions to estimate characteristic lifetime maximum effects (Nowak 1993). An alternative approach adopted by many authors is to use Monte Carlo (MC) simulation (O'Connor & O'Brien 2005), and this is the approach described here. In the MC simulation approach, statistical distributions for vehicle weights, inter-vehicle gaps and other characteristics are derived from the measurements, and are used as the basis for the simulation of traffic, typically for some number of years. It is thus possible to simulate vehicles and combinations of vehicles that have not been observed during the period of measurement. Lifetime maximum loading can be estimated by simulating traffic for periods of 1000 years or more, or by extrapolation from the results of shorter simulation runs. Both options are discussed in the paper, and statistical techniques are presented which improve the extrapolation process. Recent advances in the probabilistic analysis of dynamics and their effect on lifetime loading are also discussed.

2 MONTE CARLO SIMULATION

The paper presents details of extensive WIM measurements that have been collected at five European

sites in recent years and significant numbers of extremely heavy vehicles were recorded. For Monte Carlo simulation, it is necessary to use a set of statistical distributions based on observed data for each of the random variables being modelled, and gross vehicle weight (GVW) is particularly important. A "semi-parametric" method proposed by O'Brien et al. (2010) uses the measured histogram in the lower GVW range where there are sufficient data, and models the upper tail with a parametric fit. This ensures much greater accuracy of the probabilities in the tail region. Bridge load effects for the spans considered here are very sensitive to wheelbase and axle layout. In the simulation model described by Enright (2010), empirical distributions are used for the maximum axle spacing within each vehicle class. The axle position at which this maximum spacing occurs varies, and is also modelled using empirical distributions. Lateral distribution of load in multi-lane traffic is incorporated in the simulation model by using lane factors which have been derived from finite element analysis of typical short to medium span bridges. These lane factors depend on the type of construction used, and on the load effect (moment, shear) being considered.

The availability of relatively large amounts of WIM data make it practical to compare daily maximum load effects estimated from simulation with those calculated from the measured traffic. Results for load effects from the simulation show good agreement with those calculated from measured data.

For short to medium span bridges with two same-direction lanes of traffic, loading events featuring one truck in each lane (either side-by-side or staggered) are particularly important. Various patterns of correlation are evident in the WIM data, and these patterns are difficult to model using conventional techniques. An alternative multi-dimensional smoothed bootstrap approach has been developed (Enright 2010) which avoids many of the difficulties associated with existing approaches. This approach draws sample traffic scenarios from the measured data, and the GVWs, gaps and speeds that define each scenario are modified by adding some "noise"

using variable-bandwidth kernel functions (Scott 1992). This method has been found to provide a good fit to load effects calculated from measured traffic.

Long-run simulations make it possible to examine in detail the types of loading events that give rise to the characteristic load effects. Bridge loading for the spans and sites considered is governed by single-truck and 2-truck events.

3 STATISTICAL TECHNIQUES FOR EXTRAPOLATION

Extrapolation directly from measured data or from short simulation runs remains a valuable technique for predicting lifetime maximum loading. A composite distribution statistics (CDS) model is presented which separates loading event by type (one-truck, two-truck etc.) and combines extreme value distributions fitted to the load effects for each type.

Since many codes define characteristic values as a probability of exceedance in the design life of the structure (for example, the Eurocode's 5% probability of exceedance in 50 years definition), it is not a distribution of characteristic values that is of interest, but the distribution of lifetime load effect. Therefore focus should be centred on the estimation of the lifetime distribution of load effect, from which the characteristic value can then be derived. Predictive likelihood is a method for estimation which allows both for sampling and modelling uncertainties. It is based on the maximization of the likelihood of both the data and a predictand (possible prediction value). Caprani & OBrien (2010) have applied this method to the bridge loading problem and showed that the traditional return period approach yields different results to the direct estimate of the characteristic value from the lifetime distribution of load effect (Caprani & OBrien 2006).

4 ALLOWING FOR DYNAMIC INTERACTION

The dynamic amplification factor (DAF) is defined as the ratio of total to static load effect, where total load effect results from the truck and bridge interacting dynamically. Total and static load effects are related through the DAF, which is not constant as all loading events differ both dynamically and statically. However, there remains a degree of correlation between these statistical variables. The recent statistical theory of multivariate extreme values has been applied to this problem to extrapolate these correlated variables to their design lifetime values (Caprani 2005). Their ratio at this level is therefore

the level of dynamic interaction applicable for the bridge design lifetime. This has been termed the assessment dynamic ratio (ADR) in recognition that it does not arise from any one single loading event. A sample application of the statistical analysis for ADR indicates a DAF of about 1.06 which is significantly less than the DAF allowed for in the Eurocode and has particular importance for the majority of bridges that are of short- to medium-length since it is currently assumed that the governing loading scenario for these bridges is that of free-flowing traffic with associated dynamic effects. Analysis shows that the threshold bridge length above which congested, rather than free-flowing, traffic governs lifetime maximum bridge loading depends on the type of load effect, and for hogging bending moment on a two-span bridge, this threshold bridge length is found to be as low as 33 m.

REFERENCES

- Caprani, C.C. (2005), Probabilistic analysis of highway bridge traffic loading, PhD Thesis, School of Architecture, Landscape and Civil Engineering: University College Dublin, Ireland.
- Caprani, C.C. & OBrien, E.J. (2006b), 'Statistical Computation for Extreme Bridge Traffic Load Effects', In: B.H.V. Topping, ed. Proc. 8th Int. Conf. on Computational Structures Technology, Civil-Comp Press, Stirling, Scotland, Paper No. 139.
- Caprani, C.C. & OBrien, E.J. (2010), 'The Use of Predictive Likelihood to Estimate the Distribution of Extreme Bridge Traffic Load Effect', *Structural Safety*, 32 (2, March), 138–144, doi: <http://dx.doi.org/10.1016/j.strusafe.2009.09.001>
- Enright, B. (2010), Simulation of traffic loading on highway bridges, PhD Thesis, School of Architecture, Landscape and Civil Engineering: University College Dublin, Ireland.
- Jacob, B. & OBrien, E.J. (2005), 'Weigh-In-Motion: Recent developments in Europe', In: E.J. OBrien, B. Jacob, A. González, & C.-P. Chou, eds. Fourth International Conference on Weigh-In-Motion (ICWIM4), Taipei, Taiwan, National Taiwan University.
- Nowak, A.S. (1993), 'Live load model for highway bridges', *Structural Safety*, 13, 53–66.
- OBrien, E.J. & Caprani, C.C. (2005), 'Headway modelling for traffic load assessment of short- to medium-span bridges', *The Structural Engineer*, 83 (16), 33–36.
- OBrien, E.J., Enright, B. & Getachew, A. (2010), 'Importance of the Tail in Truck Weight Modeling for Bridge Assessment', *Journal of Bridge Engineering*, ASCE, 15 (2), 210–213, doi: [http://dx.doi.org/10.1061/\(ASCE\)BE.1943-5592.0000043](http://dx.doi.org/10.1061/(ASCE)BE.1943-5592.0000043)
- O'Connor, A. & Enevoldsen, I. (2009), 'Probability-based assessment of highway bridges according to the new Danish guideline', *Structure and Infrastructure Engineering*, 5 (2), 157–168.
- Scott, D.W. (1992), *Multivariate density estimation: theory, practice, and visualization*, New York: Wiley.

Truck load modeling and bridge code calibration

G. Fu

*Guangdong University of Technology, Guangzhou, China,
Fuzhou University, Fuzhou, China,
Tongji University, Shanghai, China,
Wayne State University, Detroit, US*

J. You

Tongji University, Shanghai, China

1 INTRODUCTION

The AASHTO LRFD Bridge Design Specifications has advanced bridge design to structural reliability based practice. In developing these specifications, failure risks involved were controlled by prescribing appropriate load and resistance factors. On the other hand, this first generation of reliability based specifications can be further improved.

The design life of bridges is relatively long compared with the available measured load data. For example, the AASHTO LRFD specifications specifies 75 years as the target life span of highway bridges, but until several years ago there had been very few weight data for trucks in operation, which can be reliably used for code calibration. Accordingly common practice to understand and cover long term loads is to employ statistical inference or projection based on short term data. Using short term load data to predict or project to a remote future maximum load is exercised for specification calibration and development, as for the AASHTO LRFD bridge design specifications. However, the approaches used have not been adequately evaluated or validated due to lack of long term data, which is important for the structures' safety governed by these codes. This issue is focused here, taking advantage of now available long term truck weight data obtained using the weigh-in-motion (WIM) technique.

2 A NEW APPROACH

A new projection approach is proposed in this paper for reliable prediction, based on the understanding

of importance of the load probability distribution's high tail. This approach significantly reduces the mathematical temporal length for projection and thus increases prediction reliability, shown here in application examples. In addition, the projection approach is proposed to be evaluated in each application, using quantitative indices. The application of temporal prediction can now be guided using these quantitative indices about its validity and appropriateness.

3 CONCLUSIONS

This paper focuses on the issue of reliably predicting or projecting the future maximum load statistics with application to truck loads on highway bridges. In the past, very limited truck weight data were available and statistical inference could not be performed to a high quality. With more truck weight data being made available now, a new projection approach is developed here based on a larger amount of data. It has been compared with other methods reported in the literature. Results show that the new approach can produce reliable projected statistics for the expected life span of bridges, such as 75 or 100 years. For general application of this method, two error indices also have been developed in this paper to estimate the range of variation associated with such a projection. Comparison using long term data shows that these error indices can realistically indicate the real errors. This tool will allow the user to evaluate application of the proposed method for the particular data used.

This page intentionally left blank

GS_113 — Decision analysis

This page intentionally left blank

Maintenance planning for multi-component systems subject to reliability constraints

R. Faddoul & W. Raphael

École supérieure d'ingénieurs de Beyrouth (E.S.I.B.) Saint-Joseph University, Beirut, Lebanon

A.H. Soubra

Institut de Recherche en Génie Civil et Mécanique, St-Nazaire, France

A. Chateauneuf

Polytech, Clermont-Ferrand, France

ABSTRACT: Markov Decision Processes (MDPs) are commonly used for optimization of inspection, maintenance, and rehabilitation (IM&R) of deteriorating assets and machinery. This is especially the case for civil engineering infrastructures where management optimization systems based on MDPs are by far the most widespread and accepted decision support tools (Golabi and Shepard 1997, 1982, Dekker 1996). Most of the existing MDP models found in the specialized literature consider only the minimization of IM&R costs generated by single component systems. However, real world structures are often multi-component systems. Moreover limits are usually imposed by the society (often in the form of formal regulatory constraints) on the acceptable risk associated with the failure of civil engineer structures.

Regardless of the type of the model used for IM&R optimization of single component systems, its extension to the multi-component systems case is far from being straightforward. This is mainly due to the interdependences that may exist among the components within the system. These interdependences can be either structural/functional, stochastic or economic (Thomas 1986, Dekker *et al.*, 1997, Durango-Cohen and Sarutipand 2007).

The aim of this paper is the optimization of inspection, maintenance and rehabilitation of multi-component systems. It is supposed that the optimization is constrained by a fixed imposed minimum reliability of the whole system during each time period during the entire time horizon thus creating a structural dependence between the decisions related to each of the components.

The problem of searching for optimal decisions for several simultaneous but independent sequences of decisions over a finite time horizon under reliability constraints can be modeled as a multidimensional MDP. Then, the state space

of the system will be a Cartesian product of the state spaces of its components. This is due to the fact that one must take into account the effect of the interaction of decisions in each chain on the whole problem through the system reliability constraint. Such an approach is computationally intractable even for very small number of components. For example, considering the case where each chain has only seven different possible states at the beginning of each time period (in POMDPs the number of possible states can be in the order of hundreds of thousands); the number of possible combinations for a 15 component system becomes $7^{15} = 4.7 \times 10^{11}$. Clearly, the intractable complexity of constrained MDPs originates from the interdependence generated by the constraints. Therefore, a natural approach to solve the problem will be to try to find a new formulation of the same problem without the constraints being explicit.

Linear programming is usually used to solve parallel MDPs subject to global resource constraints for each of the time periods (Golabi *et al.*, 1982, Murakami and Turnquist 1985, Smilowitz and Madanat 2000, Madanat *et al.*, 2006). This methodology however has a major limitation; namely, it is restricted to homogenous systems (with respect to costs, activities types and deterioration). i.e. the different components of the system have to be essentially the same.

Following Faddoul *et al.* (2010) a Lagrangian relaxation technique is used for the extension of existing dynamic programming methods from single component systems to multi-component level. By using the Everett theorem we present a proposition which is used by the methodology to separate the initial combinatorial problem into k smaller sub-problems (k being the number of components).

We discuss the existence of an optimality gap *i.e.* an optimal solution satisfying exactly the constraints does exist but the proposed methodology may not be able to find it. In that case, a set of values of λ^n that respect the constraints does not exist. An optimality gap in Lagrange relaxation optimization is due to the non-convexity of the problem (Fisher 1981).

The proposed methodology uses existing single component MDP or POMDP methodologies using discrete-space dynamic programming for IM&R or M&R optimization. As opposed to the existing methodologies, the components of the system do not have to be similar. Thus, different sets of feasible maintenance actions, different sets of feasible inspection techniques, different models for deterioration over time and different direct and indirect costs can be assigned to each component. The existence of an appropriate set of Lagrange multipliers is discussed and a procedure for finding these multipliers is presented. The methodology is illustrated by using a Generalized Partially Observable Markov Decision Process having a decision tree composed of a sequence of two decisions at the beginning of each time period; namely an inspection decision followed by a maintenance action decision.

A numerical example concerning the optimization of inspection, maintenance and rehabilitation of a five component bridge is presented.

REFERENCES

- Bazaraa, M.S., Sherali, H.D. & Shetty, C.M. 2006. *Non-linear programming: theory and algorithms*. John Wiley and Sons, third edition, chap 9.
- Corotis, R.B., Ellis, J.H. & Jiang, M. 2005. Modeling of risk-based inspection, maintenance and life-cycle cost with partially observable Markov decision process. *Structure and Infrastructure Engineering*, **1**, 75–84.
- Dekker, R., Wildeman, R. & van der Duyn Schouten, F. 1997. A review of multi-component maintenance models with economic dependence. *Mathematical Methods of Operation Research*, **45**(3), 411–435.
- Dekker, R. 1996. Applications of maintenance optimization models: a review and analysis. *Reliability Engineering and System Safety*, **51**(3):229–240.
- Durango-Cohen, P. & Sarutipand, P. 2007. Capturing interdependencies and heterogeneity in the management of multifacility transportation infrastructure systems. *Journal of infrastructure systems*, **13**(2), 115–123.
- Everett III, H. 1963. Generalized Lagrange multiplier method for solving problems of optimum allocation of resources. *Operations Research*, **11**(3), 399–417.
- Faddoul, R., Raphael, W. & Chateaneuf, A. 2009a. A generalized partially observable Markov decision process updated by decision trees for maintenance optimisation. *Structure and Infrastructure Engineering*, **5**.
- Faddoul, R., Raphael, W., Chateaneuf, A. & Soubra, A.-H. 2009b. Processus généralisé de décision markovien partiellement observable utilisant les arbres de décisions. Proceedings of the *41st Journées de Statistique*, 2009, Bordeaux (France), in French.
- Faddoul, R., Raphael, W., Chateaneuf, A. & et Soubra, A. 2010. Processus de décisions markoviens parallèles soumis à des contraintes budgétaires. *Fiabilité des Matériaux et des Structures 2010 6èmes Journées Nationales de Fiabilité* – Toulouse – France.
- Fisher, M.L. 1981. The Lagrangian relaxation method for solving integer programming problems. *Management science*, **27**(1), 1–18.
- Golabi, K., Kulkarni, R. & Way, G. 1982. A statewide pavement management system. *Interfaces*, **12**(6), 5–21.
- Golabi, K. & Shepard, R. 1997. Pontis: a system for maintenance optimization and improvement of US bridge networks. *Interfaces*, **27**(1):71–88.
- Madanat, S., and Ben-Akiva, M. 1994. optimal inspections and repair policies for infrastructure facilities. *Transp. Sci.*, **28**(1), 55–62.
- Madanat, S, Park, S. & Khun, K. 2006. Adaptive optimization and systematic probing of infrastructure system maintenance policies under model uncertainty. *Journal of infrastructure systems*, **12**(3), 192–198.
- Murakami, K. & Turnquist, M. 1985. A dynamic model for scheduling maintenance of transportation facilities. *Transportation research record*, 1030, transportation research board, Washington, D.C., 8–14.
- Smilowitz, K. & Madanat, S. 2000. Optimal inspection and maintenance and rehabilitation policies for networks of infrastructure facilities under measurement and forecasting uncertainty. *J. Comput. – Aided Civ. Infrastruct. Eng.*, **15**(1), 5–13.
- Thomas, L.C. 1986. A survey of maintenance and replacement models for maintainability and reliability of multi-item systems. *Reliability engineering*, **16**, 297–309.

Post-earthquake reliability assessment of structures subjected to after-shocks: An application to L'Aquila earthquake, 2009

F. Jalayer, D. Asprone, A. Prota & G. Manfredi

Department of Structural Engineering, University of Naples Federico II, Italy

1 INTRODUCTION

The inspection and management of civil structures after the occurrence of a severe earthquake event is subjected to considerable challenges. The post-earthquake deterioration as a result of the sequence of after-shocks may obstacle significantly eventual inspections and/or re-occupancy of these structures. In fact, a significant main-shock is often followed by a number of after-shock events (usually smaller in moment magnitude) which take place in a limited area (i.e., the after-shock zone) around the epicenter of the main event. This sequence of after-shock events can last in some cases for months. Although these events are smaller in magnitude with respect to the main event, they can prove to be destructive on the structure. This is due to both the significant number of after-shocks (in some cases up to 6000) and to the fact that the structure has probably already suffered damage from the main event.

The occurrence of main-shock events is often modeled by a homogenous Poisson stochastic process with time-invariant rate. However, the sequence of after-shocks are characterized by a rate of occurrence that decreases as a function of time elapsed after the earthquake. The first few days after the occurrence of main-shock can be very decisive as there is urgent need for re-occupancy of the building (for rescue or for inspection) while the mean daily after-shock rate is quite considerable.

The present study presents a procedure for calculating the time-dependent probability of exceeding the limit states corresponding to various discrete performance objectives. A simple cyclic stiffness deteriorating single degree of freedom (SDOF) model of the structure is used in order to study the damages induced as a result of a sequence of after-shocks. The time-decaying model parameters are estimated for the L'Aquila 2009 after-shock sequence using a Bayesian updating framework based on the Italian generic sequence as prior information. As a criteria for assessment of the decisions regarding re-entrance for inspections purposes, the (time-dependent) probability of

exceeding the limit state of life-safety in a 24-hour interval is compared to an acceptable threshold. The less severe limit states of severe damage and onset of damage can be used in a similar manner in order to make decisions regarding the re-occupancy and serviceability of the structure.

2 METHODOLOGY

The objective of this methodology is to calculate the time-dependent probability of exceeding various discrete limit states in a given interval of time for a given structure subjected to a sequence of after-shocks. The methodology presented herein for the evaluation of the limit state probability in a given time interval can be used for decision making between different viable actions such as, re-entry/evacuation, re-occupancy/shutting down. This methodology starts from the state of the structure after it is hit by a main-shock. Therefore, given that the main shock wave-forms are available, the damages undergone by the structural model can be evaluated. The clustering of earthquakes usually occurs near the location of the main-shock also referred to as the after-shock zone. Therefore, it is assumed that for the sequence of earthquakes including the main-shock and after-shock events, each point within the after-shock zone is equally likely to be the epicenter of an earthquake event. The aftershock clusters should be eventually classified based on their generating source, should they belong to different fault structures, as in the case of L'Aquila Earthquake. An important characteristic of the sequence of after-shocks following the main-shock is that the rate of after-shocks dies off quickly with time elapsed since the main-shock. The time-decaying parameters of the aftershock sequence are estimated by applying a Bayesian updating framework to the L'Aquila 2009 sequence based on the Italian generic after-shock model as prior information. The methodology presented is of an adaptive nature; that is, with occurrence of more after-shock events, the state of the structure can be updated by evaluating the damages

undergone by the structural model subjected to the sequence of main-shock and after-shocks.

3 NUMERICAL EXAMPLE

The methodology presented is applied to an existing structure as a case study.

The Bayesian updating framework is used in order to calculate the parameters of the aftershock occurrence rate for the sequence of after-shocks following the L'Aquila earthquake of 6th April 2009 with moment magnitude equal to $M_m = 6.3$.

In order to calculate the failure probabilities due to the sequence of after-shock events, a set of ground motion records (consisting of main-shocks and after-shocks) are chosen. Each ground motion record is applied sequentially k times on the equivalent SDOF model with cyclic stiffness degrading behavior. The probability of failure given that a sequence of k after-shocks has occurred is calculated following the procedure explained in previous section. For each sequence of k earthquakes, the maximum displacement response of the equivalent SDOF system is calculated.

The probability of exceeding the limit state of collapse in a day (24 hours) has been. The results are plotted in Figure 1 where they are compared against an acceptable mean daily collapse rate of $2 \times 10^{-3}/365$, as a proxy for life safety considerations. This threshold value is on average equivalent to an acceptable mean annual rate of collapse equal to 2×10^{-3} . This verification is done for ensuring life safety for the building occupants.

It can be observed that the low-residual structure is immediately below the acceptable threshold for life-safety limit state; whereas, the high-residual

case does not verify the acceptable threshold up to around one week elapsed after the occurrence of the main-shock. After 7 days, due to the decreasing rate of occurrence of after-shocks, the structure verifies against the life-safety limit state threshold.

4 CONCLUSIONS

A simple methodology is presented for calculating the probability of exceeding a limit state in a given interval of time elapsed after the occurrence of the main-shock event. This procedure employs an after-shock model based on the modified Omori law in order to model the time-decay in the mean daily rate of the occurrence of significant after-shocks. The seismic after-shock hazard at the site of the structure is calculated by setting the main-shock moment magnitude as the upper limit for magnitude and is updated using the Bayes formula given that the small-amplitude spectral acceleration of the main-shock at the fundamental period of the structure is known. Comparing the time-variant probability of collapse in a 24-hour period of time against an acceptable threshold, it can be observed that the strongly damaged structure could be occupied after a certain amount of days has elapsed after the occurrence of the main-shock while the lightly damaged structure could be occupied immediately. This type of verification can be useful for evaluation of re-occupancy risk for the structures located in a zone prone to after-shocks, based on the life-safety criterion. In fact, the necessary time elapsed after the main-shock for the structure to verify the life-safety requirements is calculated as a function of different values of residual to collapse displacement capacity ratio.

REFERENCES

- Asprone, D. Jalayer, F., Prota, A. & Manfredi, G. 2010. Proposal of a probabilistic model for multi-hazard risk assessment of structures in seismic zones subjected to blast for the limit state of collapse, *Structural Safety*, Volume 32, Issue 1, pp. 25–34.
- Lolli, B. & Gasperini, P. 2003. Aftershocks hazard in Italy Part I: Estimation of time-magnitude distribution model parameters and computation of probabilities of occurrence. *Journal of Seismology*, 7:235–257.
- Reasenber, P. & Jones, L. 1994. Earthquake aftershocks: Update, *Science*, 265:1251–1252.
- Yeo, G. & Cornell, C.A. 2009. A probabilistic framework for quantification of aftershock ground-motion hazard in California: Methodology and parametric study, *Earthquake Engineering and Structural Dynamics*, 38(1):45–60.

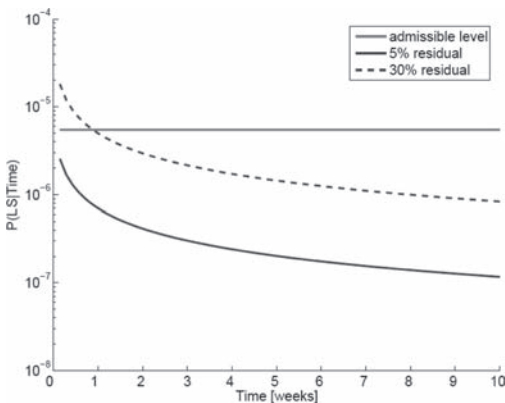


Figure 1. Probability of exceeding the collapse limit state in a day.

Supporting decisions on global health and life safety investments

M.H. Faber

Institute of Structural Engineering, ETH Zürich, Switzerland

E. Virguez-Rodriguez

Urban and Regional Sustainability Research Center, Universidad de los Andes, Bogotá, Colombia

Health and life safety are not only preferences of individuals but are globally considered to comprise important demographic indicators concerning the state of societal development. Individual societies and their developments are often analyzed and assessed in terms of cohort life tables, the life expectancy at birth, as well as indexes like the Human Development Index (HDI) which at national scales combines the status of health with economic capacity and education.

Decision making with regard to allocation of available societal resources into activities aiming to improve health and life safety is an issue of strategic importance. Moreover, in the realm of limited resources and the pressure from the necessity of sustainable developments, it is evident that this decision problem is not a trivial one; we all would like to have better health and life safety. However, the question is: how much investments aiming for an improvement in life safety can we afford from a societal perspective?

The Life Quality Index (*LQI*) was proposed some 15 years ago by Nathwani, Pandey and Lind. The philosophy behind the *LQI* is that the preference of a society in regard to investments into health and life safety improvements may be described in terms of the life expectancy at birth, the Gross Domestic product per capite and the ratio between working time and leisure time. Whereas the *LQI* was originally proposed on the basis of socio-economic theoretical considerations its validity has been empirically justified subsequently. The *LQI* facilitates the assessment of decisions with regard to their conformity with societal preferences in regard to life safety investments. Based on the *LQI* it is possible to derive the so-called marginal life saving costs, i.e. the necessary and affordable expenditures which should be invested into saving one additional life. Alternative approaches from the field of economics such as contingent life value evaluations have been found to yield results similar to those of the *LQI*.

Until now societal decision making in regard to health and life safety investments is mostly

approached from a national perspective. Individual nations make decisions on how to allocate their resources for the better of their citizens. However, there are issues of health and life safety which clearly go beyond the borders of the individual nations and this concern e.g. sustainable global developments and management of disease and global catastrophic risks, including mitigation of losses due to climatic change. Decisions on such issues ultimately should be made on behalf of the global Earth society; a problem of allocation and prioritization of globally available and shared resources. The question in this problem setting remains, how to decide on how much we as a global society can afford and should invest into health and life safety improvements?

In the present paper this question complex is addressed taking basis in the idea that the *LQI* might provide a basis not only for decision making in regard to health and life safety investments at national scale, but also at global or supra-national scale. The paper starts out by addressing the general problem context of resource allocation for health and life safety management. Here the context of decision making at supra-national scale is analyzed, by concerning how shared resources can be distributed to different recipient nations and prioritized between different activities of health and life safety improvements.

Subsequently the basic philosophy and theory behind the *LQI* principle application is provided focused on the derivation of the Societal Willingness to Pay (*SWTP*) from the *LQI* net benefit criterion, i.e. requiring that any societal activity shall lead to an increase in the *LQI*, and the Societal Value of a Statistical Life (*SVSL*) as indicators of the amount of societal resources that must be invested on behalf of health and life safety. Thereafter, the assessment of the demographical statistics and indicators required for the formulation of the *LQI* are presented. Finally the available empirical evidence for the *LQI* as a societal preference for the population of the Earth is produced (see Table 1) and discussed.

Table 1. SVSL and ESVSL for the year 2008 expressed in current thousand US Dollars for different discount rates.

Region	Discount rate			
	1%	2%	3%	4%
Canada	\$ 8.110	\$ 6.301	\$ 5.064	\$ 4.186
United States	\$ 6.464	\$ 5.060	\$ 4.091	\$ 3.397
China	\$ 362	\$ 285	\$ 232	\$ 193
Brazil	\$ 1.186	\$ 926	\$ 747	\$ 618
Australia	\$ 11.258	\$ 8.711	\$ 6.977	\$ 5.752
Mozambique	\$ 36	\$ 29	\$ 24	\$ 20
Mali	\$ 57	\$ 46	\$ 38	\$ 32
Dem. Republic of Congo	\$ 16	\$ 13	\$ 10	\$ 9
World (World Life Table)	\$ 984	\$ 775	\$ 629	\$ 524

Through the analysis of statistical demographical data for all nations in the world it is found that the application of the *LQI* at Earth scale can be justified from the observation that 71 countries, representing more than 70% of the population of Earth, have developed in accordance with

the preference underlying the *LQI* principle. i.e. the joint development of health and life safety, economy and necessary time to work can be explained through the preference for investments into life safety described by the *LQI*. Moreover, when assessing the demographical indicators required for the application of the *LQI* principle, using data representing the Earth as one global society and analyzing these indicators for different years it is found that the development of the Earth society also conforms very well to the *LQI* preference.

Based on the assessments made it appears that there are possibilities to enhance decision making concerning management of global problems with impact on health and life safety. The assessed Earth Societal Willingness To Pay (*ESWTP*) could provide a guidance on necessary and affordable investments into life risk reductions, however, whether the *ESWTP* or the usual nation specific *SWTP* apply in a given situation must be carefully assessed with a view to whether indeed the resources and the health and life safety risks of concern are shared.

Defining guidelines for the application of the marginal life saving costs principle for risk regulation

K. Fischer

Institute of Structural Engineering, ETH Zurich, Switzerland

E. Virguez-Rodriguez

Urban and Regional Sustainability Research Center, Universidad de los Andes, Bogotá, Colombia

M. Sánchez-Silva

Department of Civil and Environmental Engineering, Universidad de los Andes, Bogotá, Colombia

M.H. Faber

Institute of Structural Engineering, ETH Zurich, Switzerland

Societal resources for life saving activities are scarce and need to be invested in the most efficient risk reduction measures available. This can be guaranteed by comparing the marginal life saving costs to the Societal Willingness To Pay (*SWTP*) for a marginal increase in life safety, i.e. the level of expenditure that society is willing to invest into saving an additional life.

Societal preferences for life saving investments can be quantified with the aid of the Life Quality Index (LQI) first introduced by Nathwani et al. (1997). The LQI is a societal utility function composed of the GDP per capita g , the life expectancy e and an exponent q defining the trade-off between wealth (as a requisite for consumption) and leisure time. Based on the LQI net benefit criterion, requiring that any societal activity shall lead to an increase in the LQI, the following threshold criterion for investments into life safety can be derived:

$$-dg \geq SWTP = \frac{g}{q} \frac{de}{e} \approx \frac{g}{q} C_x d\mu \quad (1)$$

For technical problems typically only the marginal mortality reduction $d\mu$ can be quantified. de/e is then calculated by multiplying the mortality change with a demographic constant C_x .

The idea behind the societal acceptance criterion (1) is that safety investments shall be increased until the marginal life saving costs $-dg$ are equal to the *SWTP* for the marginal increase in life expectancy de achieved by the investment. Investments below the threshold in (1) are not acceptable while higher values for $-dg$ are possible, but inefficient from a life saving point of view. The criterion is

thus based on efficiency considerations: Life safety investments are required (only) until further investments are not efficient any more. As pointed out by Faber and Maes (2009), this leads to different absolute levels of life safety deemed to be acceptable, depending on the available best practice for risk reduction: Low absolute levels of safety are accepted in areas where safety measures are expensive compared to high acceptable safety in areas where low-cost risk reduction measures are available. This uneven distribution of life safety is, however, consistent with the aim of optimal resource allocation for life saving measures.

The LQI net benefit criterion can be seen as the state-of-the-art method to establish quantitative risk acceptance criteria, being applicable to all areas where resources for life saving activities have to be allocated. The theoretical foundations of the LQI are already well-established and have been discussed in peer-reviewed literature. A big fraction of this discussion has been aimed to understand the assessment of life safety benefits in terms of mortality reduction. Yet when it comes to applying the LQI net benefit criterion to real-world decision problems, a number of issues arise concerning the assessment of the marginal life saving costs implied by the safety measures to be evaluated. The aim of the present paper is to establish guidelines on how to carry out such an assessment for different applications.

The criterion given in equation (1) is based on yearly values for $-dg$ and the *SWTP*. If costs and benefits accrue at different points in time they need to be discounted before comparison. In practical applications of the LQI principle therefore the same problems arise as in classical

societal cost-benefit analysis: The results are highly dependent on the definition of costs and benefits as well as the choice of discount rate and the time horizon of the decision. In the present paper we focus on the last issue, on the question to what extent future consequences have to be accounted for in the acceptance criterion. The aim is to establish guidelines on how to define the time horizon of the decision when marginal life saving costs and societal acceptance shall be evaluated for regulatory purposes. An extended discussion also on the other issues mentioned above will be published in an upcoming journal paper (Fischer et al., (2011)).

First we introduce the general problem of evaluating risk reduction measures. We distinguish between public decision-makers deciding on behalf of society and private decision-makers maximizing their own utility. Acceptability of life saving investments is based on societal preferences and thus needs to be imposed on the decision problem of the individual decision-makers as a boundary condition. This is shown in Figure 1 where the derivation of the *SWTP* for life safety is illustrated in the lower part, defining an acceptance threshold for the (pure monetary) optimization shown in the upper part. A short discussion on how societal life saving costs should be defined is provided in the paper.

This clear distinction between individual optimization and societal risk acceptance is the basis for the choice of discount rate used for calculating the acceptance criterion: As risk acceptance is a societal issue, a societal discount rate has to be applied for discounting both life saving costs and benefits. The choice of discount rate will be discussed more in detail in Fischer et al. (2011).

The focus of the present paper is to give guidelines on how the time horizon of regulatory

decisions has to be defined. The choice of time horizon determines to what extent future costs and benefits are taken into account when evaluating societal risk acceptance based on the LQI net benefit criterion. This can have a strong influence especially when regarding preventive risk reduction measures where high discrete initial investments are necessary to achieve a continuous future life safety benefit until the end of the safety measure's service life. In this case the required safety investments are highly dependent on the time horizon chosen.

Finally we discuss two possible means of risk management that can be chosen in the context of code-making, namely the definition of design and assessment criteria versus required absolute levels of safety. The two approaches have different implications regarding the distribution of life safety within the population of regulated structures.

As a result of the discussion we conclude which general principles have to be followed when performing an assessment of acceptability based on the LQI net benefit criterion. The idea is to provide guidelines for a consistent application of the LQI principle to a variety of regulatory decisions.

REFERENCES

- Faber, M.H. & Maes, M.A. (2009). Sustainable strategic and operational management of life safety. In *4th International Forum on Engineering Decision Making - IFED*.
- Fischer, K., Virguez-Rodriguez, E., Sanchez-Silva, M. & Faber, M.H. (2011). On the assessment of marginal life saving costs for risk acceptance criteria. *To be published*.
- Nathwani, J.S., Lind, N. & Pandey, M. (1997). *Affordable Safety by Choice: The Life Quality Method*. Waterloo: University of Waterloo.

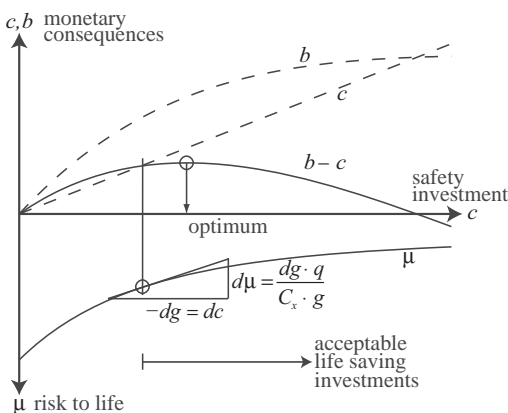


Figure 1. The LQI net benefit criterion as a boundary condition for optimization.

Adaption of option pricing algorithm to real time decision optimization in the face of emerging natural hazards

A. Anders & K. Nishijima

Institute of Structural Engineering, ETH Zurich, Zurich, Switzerland

1 INTRODUCTION

Formal decision analysis in engineering often requires that a sequence of decisions has to be jointly optimized; i.e. the decision at each decision phase must be optimized based on the information available up to the current decision phase as well as on the consideration of all possible outcomes and decisions undertaken in the future. Important examples of such decision analysis include inspection planning of deteriorating structures (see e.g. Straub (2004)), quality control of manufactured products (e.g. Nishijima & Faber (2007)) and decision support for real time decisions in the face of emerging natural hazards (Nishijima et al., (2008), (2009)).

For the formulation of this type of decision problems, the pre-posterior decision framework provides the philosophical basis (Raiffa & Schlaifer (1961)). It has been applied, among others, in civil engineering for the examples mentioned above. The framework is general and the formulation of decision problems based on the framework is straightforward; however, the analytical solutions to the decision problems are available only in limited cases (see e.g. Chapter 12 in DeGroot (1970)). Quite often, the solutions are not available even numerically without any approximations to the problems. This is due to the large number of combinations of the decision alternatives and the realizations of random phenomena at all decision phases, which must be considered in the optimization. Thus, the original decision problems are often simplified; e.g. by reducing the number of decision phases and/or decision alternatives at each decision phase; otherwise, with coarse discretization of the sample space of the random phenomena. However, the adaptation of appropriate simplifications requires trial-and-errors, and the validation of the simplifications is often difficult. On the other hand, the coarse discretization of the sample space may result in significant errors. The lack of algorithms for the solutions to the decision problems without these approximations (i.e. simplification and coarse discretization) significantly undermines the possibility to apply the pre-posterior decision framework in practice.

2 PROPOSED APPROACH

Focusing on the real time decision optimization in the face of emerging natural hazards, the present paper proposes an approach for solving the decision problems without such approximations. The proposed approach takes basis in a method originally developed for option pricing in financial mathematics; the Least Squares Monte Carlo method (LSM method) proposed by Longstaff & Schwartz (2001).

From a viewpoint of decision analysis, the LSM method is seen as a Monte Carlo (MC) simulation based method, which estimates the maximum expected value of the utility in sequential decision problems. In general, the LSM method is composed of three steps: Generate a set of realizations of the underlying random phenomena by Monte Carlo simulations; estimate the conditional expected values of the utility at each decision phase by least squares regressions as a function of the current state of the random phenomena; and determine the optimal decision rule. In order to facilitate the concept of the LSM method to real time decision problems in engineering as described above, several extensions are required due to the nature of the decision problems; e.g. (1) the underlying random processes are characterized by higher-order Markov processes, whereas the original LSM method assumes first-order Markov processes, and (2) the expected values of the utility corresponding to terminal decisions are not analytically known, and thus the evaluation of the expected values of the utility requires additional Monte Carlo simulations. The adaption of the LSM method and its extensions with these respects constitute the proposed approach in the present paper.

3 EXAMPLE

For the purpose of illustrating the use and advantages of the proposed method, the example investigated in Nishijima et al. (2009) is re-examined. Note in the present paper, the main focus is the solution to the decision problem, whereas

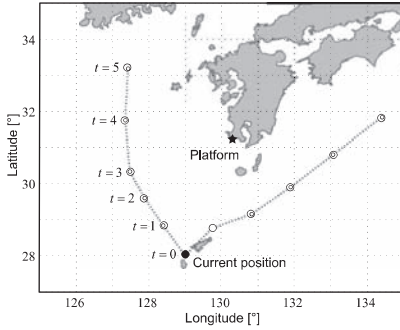


Figure 1. Two realizations of the transition of a typhoon and the location of the platform (Nishijima et al. (2009)).

Nishijima et al. (2009) focus on the formulation of the decision framework, the solution to the decision problem and its efficiency are not examined in detail. The example considered here is a decision situation in which a decision maker is faced to decide whether or not the operation of an offshore platform should be shut down in the emergence of a typhoon event. Figure 1 shows two realizations of the typhoon path relative to the platform (indicated by dashed lines with circles).

4 RESULTS

Following the LSM method with the proposed extensions, the optimal decision at time zero is identified as “evacuation”. In the example, various types of basis functions (Linear, Chebyshev, Legendre, weighted Laguerre and Power polynomials) with different polynomial degrees are examined in the least squares regressions. It is found that the estimated value of the minimized expected cost is insensitive to the choice of the basis functions and the polynomial degree.

In Figure 2, the convergences of the estimated value of the minimized expected cost are shown for the case of first-order polynomials. It is seen that (1) the estimated value of the minimized expected cost is biased low with respect to the number M of the realizations in the Monte Carlo simulations for the evaluation of the expected costs corresponding to the terminal decisions, and converges as the number M increases, and (2) the estimated value converges at $b = 2 \cdot 10^5$ realizations of typhoon path simulations. The computational time is approximately 2 hours with a standard PC with $b = 2 \cdot 10^5$ and $M = 50$.

5 CONCLUSION

The present paper (1) introduces the Least Squares Monte Carlo method (LSM method) which is

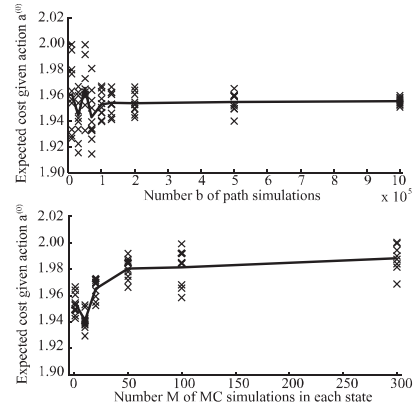


Figure 2. (top) Convergence as a function of the number b of generated typhoon paths ($M = 1$); (bottom) Convergence as a function of the number M of the MC simulations ($b = 2 \cdot 10^5$).

originally developed for option pricing, (2) points out that the method is useful to pre-posterior type of engineering decision problem, and (3) proposes extensions of the LSM method for the application to an engineering decision problem; i.e. real time decision making in the face of emerging natural hazards. The performance of the proposed approach is investigated with an example, and it is shown that it is applicable in practice from a computational point of view. Possible improvements and applications are briefly discussed.

REFERENCES

DeGroot, H. 1970. *Optimal Statistical Decisions*, John Wiley & Sons, Inc.

Longstaff, F.A. & Schwartz, E.S. 2001. Valuing American Options by Simulation: A Simple Least-Squares Approach, *The Review of Financial Studies*, 14 (1), pp. 113–147.

Nishijima, K. & Faber, M.H. 2007. Bayesian approach to proof loading of quasi-identical multi-components structural systems, *Civil Engineering and Environmental Systems*, 24 (2), pp. 111–121.

Nishijima, K., Graf, M. & Faber, M.H. 2008. From Near-Real-Time Information Processing to Near-Real-Time Decision Making in Risk Management of Natural Hazards, *Proceedings EM08, Inaugural International Conference of the Engineering Mechanics Institute*, Minneapolis.

Nishijima, K., Graf, M. & Faber, M.H. 2009. Optimal evacuation and shut-down decisions in the face of emerging natural hazards, *ICOSSAR2009*, Osaka, Japan.

Raiffa, H. & Schlaifer, R. 1961. *Applied Statistical Decision Theory*. Cambridge, Cambridge University Press.

Straub, D. 2004. *Generic approaches to risk based inspection planning for steel structures*, Department of Civil, Environmental and Geomatic Engineering, Zurich, ETH Zurich.

*MS_116 — Fuzzy analysis and soft computing methods
in reliability assessment and optimization (1)*

This page intentionally left blank

Bayesian quantification of inconsistent information

M. Stein

Department of Civil & Environmental Engineering, National University of Singapore, Singapore

M. Beer

Centre for Engineering Sustainability, School of Engineering, University of Liverpool, Liverpool, UK

Whenever decision making in engineering is based on results from a numerical analysis, it is essential that the available information is reflected properly in these results. This requires a realistic modeling of the available information without distorting it or ignoring certain aspects.

In engineering practice, the information basis usually consists of plans, drawings, measurements, observations, experiences, expert knowledge, codes and standards, and so on. Hence, it is frequently not certain or precise but rather imprecise, diffuse, fluctuating, incomplete, fragmentary, vague, ambiguous, dubious, or linguistic. This type of inconsistent information requires a generalized uncertainty model to minimize the risk from modeling errors under uncertainty in engineering computations and prognoses. Shortcomings, in this regard, may lead to biased computational results with an unrealistic accuracy and may therefore lead to wrong decisions with the potential for associated serious consequences. Uncertainty modeling has thus already become an engineering task of great importance and interest. Besides the traditional probabilistic models including Bayesian statistics, a variety of non-probabilistic models exist. These include, for instance, intervals, convex models, fuzzy sets, theory of rough sets, evidence theory, theory of fuzzy random variables, interval probabilities, and imprecise probabilities. The selection of an appropriate uncertainty model out of this variety of choices demands the investigation of the sources of the uncertainty; the underlying nature dictates the model. Since uncertainty typically appears in a hybrid form with different characteristics simultaneously, a unifying approach to model hybrid uncertainty originating from a variety of different sources simultaneously is required.

A mixed probabilistic/non-probabilistic model requires an extension from the classification concept of aleatory and epistemic uncertainty towards a classification which distinguishes between probabilistic and non-probabilistic characteristics. Such a classification is given with uncertainty and imprecision. While uncertainty refers to probabilistic characteristics, non-probabilistic

characteristics are summarized as imprecision. A sound mathematical representation of imprecision is achieved with set—theoretical models.

In addition to a general model which includes both uncertainty and imprecision, suitable quantification methods to adjust the model according to the available information in each particular case are required. Therefore, methods of traditional mathematical statistics and Bayesian statistics are merged with statistics for imprecise data and set-theoretical methods.

In the present study, fuzzy probability theory (Beer, 2009a) is selected for the simultaneous treatment of uncertainty and imprecision. The fuzzy probabilistic model provides a high degree of generality and flexibility, as it combines probabilistic modeling with fuzzy modeling. It enables to take into account an entire set of plausible probabilistic models complying with the underlying information. This is mathematically realized with the aid of fuzzy variables for the distribution parameters and for the description of the distribution type. The associated fuzzy probability distribution functions $\tilde{F}_{\tilde{x}}(x)$ represent a bunch of plausible traditional distribution functions with fuzzy parameters as bunch parameters; their functional values are fuzzy numbers.

For the evaluation of crisp statistical data, the entire framework of traditional statistics with parametric and non-parametric estimation and test methods may be utilized. Fuzzy modeling is used to numerically represent non-statistical information such as linguistic assessments, single uncertain measurements, and vagueness in expert opinions. The membership functions can be specified with various basic concepts and according to further suggestions and explanations from literature (Viertl 1996, Möller & Beer 2004, Klir 2006). The quantification of subjective uncertainty with a probabilistic character in conjunction with statistical data can be covered with Bayesian methods, which incorporate the subjectivity via prior distributions assumed on the basis of experience from previous pertinent investigations. For the quantification of imprecise data, respective statistical

methods extended to set-valued sample elements are available (Kruse & Meyer 1987, Viertl 1996, Beer 2009b).

The available quantification methods are yet insufficient to cover all practical cases. So far, the combination of Bayesian methods with imprecise information has not been investigated extensively. Developments in this direction, summarized with the term fuzzy Bayes methods, have been published in (Viertl & Hareter 2004, Viertl 2008). This approach involves averaging elements regarding the propagation of the imprecision during the update. In the present study we pursue an alternative approach to reflect the imprecision of the input information in the predicted distribution in compliance with the fuzzy probabilistic model in (Beer 2009a).

Bayesian statistics as a copula that combines traditional statistics with subjective components is extended to dealing with imprecise data and imprecise prior expert knowledge. The Bayesian theorem is used as a starting point. This provides the following options for the development of fuzzy Bayes methods.

One option covers the case where no component in the Bayesian theorem is affected by fuzziness as in the standard Bayesian approach, but where fuzziness is induced by the parameter estimation. Another option covers the case of an imprecise likelihood function, where according to prior information the type of the distribution of the random variable cannot be specified precisely. The third option covers the case where fuzziness is induced due to imprecision in the prior distribution. Option four is concerned with the scenario of a Bayesian update with imprecise data. The four basic options can be combined with each other to build further quantification options in the gaps between the basic options. Herein we focus on the latter two options and their combination.

The Bayesian approach extended to inconsistent information is demonstrated by means of an

example. It is shown, that the Bayesian update with imprecise information retains the attractive properties of the standard Bayesian approach. The imprecision of the input information is reflected as imprecision in the estimation results without being averaged out. Hence, the predicted distribution exhibits both uncertainty and imprecision.

ACKNOWLEDGEMENTS

The authors gratefully acknowledge the financial support by National University of Singapore through the Ministry of Education Academic Research Fund, Grant No. R246000234133.

REFERENCES

- Beer, M. 2009a. Fuzzy Probability Theory In: Meyers, R. (ed.), *Encyclopedia of Complexity and Systems Science*, Vol. 6, 4047–4059, New York: Springer.
- Beer, M. 2009b. Engineering quantification of inconsistent information, *Int. J. Reliability and Safety*, 3(1/2/3): 174–197.
- Klir G.J., 2006. *Uncertainty and information: foundations of generalized information theory*. Hoboken: Wiley-Interscience.
- Kruse, R. & Meyer, K., 1987. *Statistics with Vague Data*. Dordrecht, Reidel.
- Möller, B. & Beer, M. 2004. *Fuzzy Randomness—Uncertainty in Civil Engineering and Computational Mechanics*. Springer, Berlin.
- Viertl, R., 1996. *Statistical Methods for Non-Precise Data*. CRC Press, Boca Raton, New York, London, Tokyo.
- Viertl, R. & Hareter, D. 2004. Generalized Bayes-theorem for non-precise a-priori distribution, *Metrika*, 59 (3): 263–273.
- Viertl, R. 2008. Foundations of Fuzzy Bayesian Inference. *Journal of Uncertain Systems*, 2 (3):187–191.

Damage assessment of RC slabs using fuzzy pattern recognition with feature selection

Hitoshi Furuta, Wataru Adachi & Koichiro Nakatsu
Department of Informatics, Kansai University, Takatsuki, Japan

Yasutoshi Nomura
Department of Mechanical Engineering, Ritsumeikan University, Kusatsu, Japan

Hiroshi Hattori
Graduate School of Engineering, Kyoto University, Kyoto, Japan

1 INTRODUCTION

In this study, an attempt is made to develop a damage assessment system of Reinforced Concrete (RC) slabs by using the pattern recognition technology with the ability of feature selection. The damage of RC slabs is evaluated with the aid of digital photos and pattern recognition. Here, the fuzzy ensemble classifier system is introduced into the pattern recognition process so as to improve the recognition performance even for the case with insufficient data. Several numerical examples are presented to illustrate the efficiency of the proposed method.

2 PROPOSED METHOD

The structures of the proposed fuzzy ensemble classifier system are shown in Figure 1. The fuzzy ensemble classifier system has two types of fuzzy rule-based systems. One is the fuzzy classifier that is used for final classification, and the other is the fuzzy ensemble that selects a fuzzy classifier from an input pattern. Both fuzzy rule-based classification systems consist of a set of fuzzy if-then rules. However, the consequent parts of the fuzzy if-then rules are different.

The proposed fuzzy ensemble classifier system consists of fuzzy classifiers, neural network and SVM classifiers and fuzzy ensemble system. Fuzzy

classifiers, neural network and SVM classifiers are constructed according to each feature. Those are used to construct classifiers based on various characters. The fuzzy ensemble system estimates weight value to each classifier result. The best classifier result is selected from the classifiers results using this weight value.

3 DAMAGE ASSESSMENT OF BRIDGE DECKS

Cracks in a digital image of concrete deck are detected in accordance with the following procedure: First, the digital images undergo a geometric transformation to extract a rectangular part containing a crack zone. The binarization is a method for transforming grayscale image pixels into either black or white pixels by selecting a threshold. Because the crack zone exists in only a small part of digital image, and also the brightness is not uniform through the crack zone due to the uneven lighting, the extracted rectangular part is divided into smaller blocks. The method proposed by Ohtsu is applied to the block unit to determine the threshold for binary-coding processing. Then, each block is divided into sub-blocks and the binary-coding processing is applied to each sub-block. In these binary images some noise such as spots and holes are reduced after the binary-coding processing. The aim of thinning processing is to reduce the crack zone pixels to lines with one pixel width. The crack pattern can be easily recognized by such a thinning processing. Finally, the smoothing processing such as the reduction of insufficient points and the addition of missing line are implemented. After all of these processing, the crack pattern is obtained and used for extracting the characteristics of digital images (Figure 4).

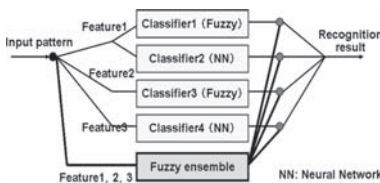


Figure 1. Proposed ensemble classifier system.

Feature extraction of cracks is conducted from binary images. However, binary images are compressed to 50×50 pixels rectangle because original binary images have 1782×1220 pixels and therefore take a lot of time to construct classifiers. The features that are extracted from the binary images are the density of cracks, the average and variance of each part and the cross pointing and branch pointing.

In the density of cracks, black pixels are searched for from top left to bottom right of the binary images and the box of 7×7 pixels is made centering on black pixels. The number of black pixels in this box is used as the feature of density of cracks. In the average and variance, the average value and the variance value of the number of black pixels in each area are used, where the binary image was divided into the four regions. In the cross pointing and branch pointing, the numbers of cross point and branch point are used.

Table 1 shows that fuzzy classifier with 4 fuzzy sets and neural network classifier using the density as the feature provide the highest performance as 81% among the classifiers. For the case with the feature of mean and variance, SVM with Gaussian kernel function provides the highest value of 78.4%. For the case with the feature of crossing point, F4 and NN show the highest performance of 83.8%. This 83.8% is the highest recognition value among all the cases. Table 1 also implies that each classifier shows different performance for the three cases of feature selection. Moreover, the selection of feature influences the



Figure 2. Digital image.



Figure 3. Binary image.

Table 1. Recognition result.

Feature	Density (Cracks)				
	F3	F4	NN	P-SVM	G-SVM
Recognition rate	59.5%	81.1%	81.1%	70.3%	70.3%
Feature	Average . Variance (Cross division)				
	F3	F4	NN	P-SVM	G-SVM
Recognition rate	73.0%	59.5%	59.5%	73.0%	78.4%
Feature	Cross pointing . Branch pointing				
	F3	F4	NN	P-SVM	G-SVM
Recognition rate	70.3%	81.1%	83.8%	70.3%	70.3%

F3: Fuzzy classifier (3 dimension membership function)

F4: Fuzzy classifier (4 dimension membership function)

NN: Neural network classifier

P-SVM: SVM with polynomial kernel function classifier

G-SVM: SVM with gaussian kernel function classifier

Table 2. Recognition result by ensemble system.

Features	Density (Cracks)		Average Variance (Cross division)	Cross pointing Branch pointing	
	F4	NN		F4	NN
Each classifier	F4	NN	G-SVM	F4	NN
Recognition rate	81.1%	81.1%	78.4%	81.1%	83.8%
Ensemble system	FE		NE		
Recognition rate	89.2%		89.2%		

FE: Fuzzy ensemble system

NE: Neural ensemble system

recognition performance even by using the same classifier. In this study, it is intended to improve the recognition performance by using the recognition result in the construction of ensemble system. The result is presented in Table 2. From Table 2, it is seen that both fuzzy ensemble and neural ensemble systems can improve the recognition performance to 89.2%. Considering that the highest recognition value by a simple classifier is 83.8%, it can be considered that the proposed ensemble classifier method can improve the recognition performance effectively.

Comparing the results of fifteen classifiers, it can be confirmed that there are differences at the recognition rate by the difference of the features even with the classifiers using the same algorithm. The ensemble classifier system is constructed based on these fifteen classifiers, and the highest recognition performance of 92% is achieved. Details of the recognition result of each classifier will be shown in the next section, and the characteristic of each classifier is considered.

4 CONCLUSIONS

In this study, the classifiers were constructed according to the features that are extracted from digital photos of RC bridge decks and such algorithms as fuzzy logic, neural network and support vector machine. From the numerical experiments, it is confirmed that the recognition results of these classifiers are quite different. By using the proposed ensemble classifier system, it is possible to select the appropriate classifiers effectively from these classifiers and to improve the recognition performance effectively.

Clustering of multiple system reliability design solutions for decision making

E. Zio

*Ecole Centrale Paris—Supelec, Paris, France, Chair “Systems Science and Energetic Challenge”
European Foundation for New Energy—EDF
Politecnico di Milano, Dipartimento di Energia, Milano, Italy*

R. Bazzo

Politecnico di Milano, Dipartimento di Energia, Milano, Italy

ABSTRACT: The process of solving a multiobjective optimization problem for system reliability design leads to a discrete approximation of the Pareto Front and corresponding Pareto Set of design solutions. On this basis, the decision maker (DM) is requested to select one or more preferred solutions.

The selection task by the DM can be difficult when the Pareto Front contains a large number of solutions; to make the task feasible, only a small number of solutions representative of the Pareto Front should be offered for selection to the DM.

In this work, a procedure is proposed for reducing the set of solutions in a Pareto Front to a small number of representative ones. The procedure is made of two main steps. First, the set of optimal solutions constituting the Pareto Front and Set is partitioned in a number of clusters (here also called “families”) of solutions sharing common features. The clustering is performed by considering the geometrical distance between solutions in the objective values space; three clustering algorithms are analyzed: k-means [1], c-means [2] and subtractive clustering [3]; the latter is concluded to be most apt to the task. The second step consists in selecting for each family (or cluster) the representative solution (the “head of the family”) on the basis of the distance from the ideal solution, which optimizes all objectives simultaneously; by so doing, the DM is provided with the best performing solutions.

The procedure is applied to a system reliability design problem of literature, with three objectives: system availability to be maximized, system cost and weight to be minimized [4].

Level Diagrams [5] are used to graphically represent, analyse and interpret the Pareto Fronts and Sets considered in the analyses.

This work has been partially funded by the Foundation pour une Culture de Sécurité Industrielle of Toulouse, France, A0-2009-04.

REFERENCES

- [1] Bandyopadhyay, S. & Maulik, U. (2002). An Evolutionary Technique Based on K-Means Algorithm for Optimal Clustering in R^N , *Information Science*, 146: 221–237.
- [2] Bezdek, J. (1974). “Cluster Validity with Fuzzy Sets,” *J. Cybernetics*, 3 (3):58–71.
- [3] Chiu, S. (1994). Fuzzy Model Identification Based on Cluster Estimation, *Journal of Intelligent & Fuzzy Systems*, 2 (3): 1240–1245.
- [4] Taboada, H. & Coit, D. (2007). Recent Developed Evolutionary Algorithms for the Multi-Objective Optimization of Design Allocation Problems, *Proceedings of the 5th International Conference on Quality & Reliability (ICQR5)*, Chiang Mai, Thailand.
- [5] Blasco, X., Herrero, J.M., Sanchis, J. & Martínez, M. (2008). A New Graphical Visualization of n-Dimensional Pareto Front for Decision-Making in Multiobjective Optimization, *Information Science*, 178: 3908–3924.

Reliability assessment via differential evolution

S. Casciati

Department DARC, University of Catania, Italy

The methods of risk and reliability analysis in civil engineering applications mainly developed during the last three decades and they are increasingly gaining importance as decision support tools (Faber & Stewart 2003). In particular, the Reliability-Based Design Optimization (RBDO) methods drive the selection of the design parameters by seeking the best compromise between cost and safety. When the non-deterministic nature of the input data is explicitly considered in the structural optimization problem, the adoption of suitable algorithms in order to evaluate the reliability constraints is required. The structural reliability assessment can be pursued either by stochastic simulations or by moment methods. Since the Monte Carlo simulations are computationally expensive, the moment methods, such as the first and second order reliability methods (FORM and SORM), are usually preferred due to their simplicity and efficiency. Nevertheless, their computational cost is still high with respect to deterministic optimization and it represents the main obstacle to the application of RBDO methods to practical engineering structures. The original formulations of these traditional approaches for structural reliability calculations can be conveniently revisited in light of the most recently emerging soft computing techniques in order to overcome their limitations and to improve their performance.

Differential Evolution (DE) algorithms are heuristic methods for the direct search of the global optimum of an objective function. With respect to the classical gradient based algorithms, they do not require any assumption on the differentiability of the objective function and they lead to results which are independent of the initial guess. The null gradient condition is replaced by a convergence criterion which is satisfied when the optimal points retrieved from two successive iterations fall very close to each other in the solution space. Therefore, such a family of algorithms is particularly suitable to solve optimization problems which are characterized by strong nonlinearities. In general, the adoption of an evolutionary strategy to solve an optimization problem allows more freedom in the selection of the objective function formulation, whose gradient has not to be computed. The main

criticism usually raised against these techniques is related to their computational effort, but the DE procedure originally proposed by Storn & Price (1997) significantly shortens the implementation runtime with respect to the common genetic algorithms, by making use of simple sum and difference operations to perform the cross-over and the mutation tasks. In Casciati (2008), it is shown that the convergence can be reached within a reasonable number of iterations even when the DE procedure is applied to high dimensional problems. The main advantages of this procedure include its easiness of implementation, its readiness of adaptability for the solution of different optimization problems, and its high rate of convergence. In this paper, an optimization algorithm of differential evolution type is employed for the reliability assessment in RBDO problems.

Several approaches were proposed in literature to tackle the RBDO problem. A recent overview of the subject can be found in Aoues & Chateaneuf (2010), where a benchmark study is also developed to enable a comparison of the numerical performance and accuracy of the different RBDO methods. The benchmark study consists of a set of examples using mathematical and finite element models. Its aim is to define the validity domain of each method and to lead to the choice of the most suitable approach depending on the engineering structure to be solved. In the present work, it is used to prove that the validity domain of the one-level RBDO method based on the Karush-Kuhn-Tucker (KKT) conditions of the first order reliability method (Rackwitz 2002) can be significantly enlarged by exploiting the differential evolution technique as solution strategy. Indeed, when the RBDO problem is characterized by a strong nonlinearity of the limit state function, an unsatisfactory performance of the KKT approach is achieved by adopting a traditional optimization framework based on a Sequential Quadratic Programming (SQP) algorithm. Indeed, a high sensitivity to the initial point leads to an initial increase of the objective function when the algorithm starts far away from the optimal point. Furthermore, a numerical instability of the optimization algorithm and a consequent lack of convergence occur as the

nonlinearity of the limit state function increases. These issues suggest to resort to evolutionary techniques which are, in general, capable to reach the optimal solution with simplicity in theory and easiness of programming, even when a highly nonlinear and partly non-differentiable objective function which exhibits many local minima is considered. Whereas the gradient methods operate on a single potential solution and look for some improvements in its neighborhood, the global optimization techniques, represented herein by the so called evolutionary methods, maintain large sets (populations) of potential solutions and apply to them some recombination and selection operators. In particular, the DE approach is adopted as a robust statistical, parallel direct search method for cost function minimization. Besides its good convergence properties, the attractiveness of the method also consists of requiring only few input parameters which remain fixed throughout the entire optimization procedure. The influence of the initial guess on the results is removed by applying the procedure to a population of NP equally important $(N + D)$ -dimensional vectors, instead of referring only to a single nominal parameter vector. At the start of the procedure (i.e., generation $P = 0$), the population of vectors is randomly chosen from an uniform probability distribution. For the following $(P + 1)$ generation, new vectors are generated according to a mutation scheme. With respect to other evolutionary strategies, the mutation is not performed based on some separately defined Probability Density Functions (PDF), but it is solely derived from the positional information of three randomly chosen distinct vectors in the current population. The trial parameter vector is built by adding the weighted difference between two randomly chosen population vectors to a third random vector. This scheme provides for automatic self-adaptation and eliminates the need to adapt the standard deviations of a PDF. As it is commonly done in the evolutionary strategies, a discrete recombination or cross-over is then introduced to increase the diversity of the new parameter vectors. The latter ones are eventually compared with the members of the current population and they are chosen as their replacements in the next generation only when they lead to an improvement of the objective function value toward the search direction.

The formulation of a pertinent objective function is crucial to the design process and the multiple objectives have to be adequately weighted.

Such an approach can be naturally extended to include also a robustness requirement as discussed in (Casciati 2007) and (Casciati & Faravelli 2008). The differential evolution strategy is applied to solve some of the mathematical problems proposed by the benchmark study. In particular, the efficacy of the method is discussed with reference to problems characterized by cost functions with different degrees of nonlinearities and problems characterized by multiple limit states. The results show that the DE strategy is quite reliable in terms of finding the solution. Nevertheless, several counteractions need to be performed along the optimization process in order to avoid local minima and to limit the computational burden. Two further improvements, such as the adoption of response surface approximations for the performance functions to avoid large finite element computations and the fragmentation of the design space in sub-domains to decrease the number iterations to convergence, are considered as possible themes for future work.

REFERENCES

- Aoues, Y. & Chateaneuf, A. 2010. Benchmark study for reliability-based design optimization. *Structural and Multidisciplinary Optimization* 41: 277–294.
- Casciati, S. 2007. Including structural robustness in reliability-oriented optimal design. In George Deodatis and Pol D. Spanos (eds.), *Computational Stochastic Mechanics; Proc. CSM-5 Fifth International Conference, Rhodes, 21–23 June, 2006*. Rotterdam: Millpress. 157–161.
- Casciati, S. 2008. Stiffness identification and damage localization via differential evolution algorithms. *Journal of Structural Control and Health Monitoring* 15(3): 436–449.
- Casciati, S. & Faravelli, L. 2008. Building a Robustness Index. In Michael Faber (ed.): *Action TU0601 Robustness of Structures; Proceedings of the 1st Workshop, ETH Zurich, 4–5 February 2008*. Zurich: Reprozentrale ETH Honggerberg, 49–56.
- Faber, M.H. & Stewart, M.G. 2003. Risk assessment for civil engineering facilities: critical overview and discussion. *Reliability Engineering and System Safety* 80: 173–184.
- Rackwitz, R. 2002. Optimization and risk acceptability based on the life quality index. *Structural Safety* 24: 297–331.
- Storn, R. & Price, K. 1997. Differential evolution—a simple and efficient heuristic for global optimization over continuous spaces. *Journal of Global Optimization* 11: 341–359.

This page intentionally left blank

*MS_126 — Fuzzy analysis and soft computing methods
in reliability assessment and optimization (2)*

This page intentionally left blank

Sensitivity measures for fuzzy numbers based on Artificial Neural Networks

S. Pannier & W. Graf

Institute for Structural Analysis, Technische Universität Dresden, Dresden, Germany

The simulation based design process of engineering structures is a complex task, especially, when multiple input variables have to be handled. Versatile tools are on hand to optimize the structure or assess the reliability by means of black-box programs. But most often, engineers long for an deepened insight into the specific problem to get an idea about the underlying reality. Therefore, data mining tools can be applied, which enable to detect structures in some predetermined point sets. These point sets are generated with an initial design of experiment, a random sampling or can be the results of a prior optimization or reliability runs. However, the aim is to reason dependencies between variables, mostly between input and result variables. An important issue is to determine the influence of individual input variables in view of specific result variables. This is done by determining the sensitivity of input variables (Helton, Johnson, Sallaberry & Storlied 2006).

Even though, first approaches of sensitivity analysis are rather old, the improvement of sensitivity measures is still of main interest in research. An ordinary form of determining sensitivity statements is the evaluation of gradients in a point of interest, which are denoted as local sensitivity measures (Saltelli, Ratto, Tarantola & Campolongo 2006). On account of the fact, that first sensitivity analysis were applied in experimental investigation, the gradients were not available. To appraise the influence of inputs on the outputs anyway, individual input variables are varied in specified ranges, one at a time. This sensitivity analysis is adopted in numerical investigations and still in broad application (Saltelli, Ratto, Tarantola & Campolongo 2006). Those methods are appropriate for linear problems with non-interacted input variables. Thus, their application for industry-relevant problems may be questionable (Saltelli, Ratto, Tarantola & Campolongo 2006).

A more general approach offers the approach of global sensitivity measures (GSM) since they enable to capture even non-linear interacted characteristics in the functional relationship of input and result variables. Global in this sense means, that

opposite to local sensitivity measures the sensitivity is not assessed for specific points but rather for the input spaces. Thereby, the spreading of input variables has to be incorporated appropriately in the sensitivity approach. For the determination of global sensitivity measures several approaches are available. In general, two strategies can be distinguished. The first strategy assesses the structural response itself by means of evaluating the variance. Therefore, the function decomposition is introduced and in consequence respective variances are evaluated. Well known approaches are, inter alia, fast Fourier transform and Sobol indices. The latter is said to provide the best results for complex computational models (Reuter & Liebscher 2008). The second strategy assesses the first partial derivatives of the function in the integral mean and can be considered as an extension of local sensitivity measures. First concepts were introduced by (Morris 1991) and further improvements were presented by (Campolongo, Cariboni & Saltelli 2007, Kucherenko, Rodriguez-Fernandez, Pantelides & Shah 2009, Sobol' & Kucherenko 2009).

Generally, precise statements about sensitivity are not available, since sensitivity is not defined strictly. Only measures, evaluating different nuances of the function under investigation, are available. They assess multiple characteristics and, in consequence, provide diverse results about the sensitivity. Thus, determining all important measures and ponder about the appropriateness in view of the specific problem will enable a reasonable assessment about the influence of input parameters.

In result of a global sensitivity analysis, a singleton sensitivity measure for each input dimension is obtained. All information about the nonlinear, complex functional relation of input and result variables is condensed to a single value. This is reasonable for a high number of input variables (e.g. more than 100). But, for low dimensional problems (e.g. up to 30) a more detailed insight is preferable. Therefore, the approach of sectional sensitivity measures is introduced in (Pannier & Graf 2010). The idea is to partition the sensitivity measure per input dimension additionally and determine the

global sensitivity section-wise. In result, statements about the functional relationship of input and result variables can be concluded.

In this paper, the focus is set on the consideration of uncertain input quantities in the sensitivity analysis. Even though, variance measures for functions of interest and expectations for their first partial derivatives are evaluated, the input quantities are not uncertain quantities (e.g. design ranges of an optimization task). Thus, the definition of sensitivity measures has to be extended in order to enable the consideration of uncertainty models to specify input quantities. First attempts for random variables are done in (Sobol' 2005), here, sensitivity measures for fuzzy sets are introduced. Though, in (Hanss, Hurlebaus & Gaul 2002, Moens & Vandepitte 2007) sensitivity and interval sensitivity are presented, here, a more general definition is given, focusing especially on global sensitivity measures. On the basis of GSM and the incorporation of random variables in GSM, an approach for fuzzy sensitivity measures can be deduced. In view of applicability of those measures, details about numerical implementation are provided.

While sophisticated sensitivity approaches provide worthwhile results, their computational expense hinders sometimes the applicability for industry-relevant problems. Thus, sensitivity analysis may be coupled with metamodels. Here, artificial feedforward neural networks are applied. Neural networks are capable to reason unknown dependencies between variables on the basis of a set of initial information. Thereby, properties like data storage, derivability and numerical efficient evaluation of artificial neural networks can be used to determine global sensitivity measures. In this paper the focus is on weighting based sensitivity measures. While in (Montaño & Palmer 2003) an overview about existing weighting based sensitivity measures is provided, here, some new weighting based sensitivity measures are introduced.

In summary, in this paper different soft computing methods are applied—in detail sensitivity, analysis fuzzy sets and artificial neural networks—in order to obtain information about the importance of uncertain input quantities. Thereby, the definition of sensitivity measures is extended to allow for a consideration of fuzzy numbers as input quantities. However, the consideration of uncertainty characteristics will affect statements about the importance of respective input quantities. These sensitivity statements are in favor, since the uncertain input variables are the basis for reliability assessments and robust optimizations. Beside formal definitions for sensitivity measures under consideration of uncertain input quantities, solution statements for the numerical realization are presented. Furthermore, artificial neural networks are utilized to determine sensitivity

statements. Thereby, new weighting based as well as activation-weighting based sensitivity measures are introduced. On the basis of suggested numerical implementations, features of the sensitivity measures are demonstrated by way of a principle example and the applicability is underlined by means of an industry-relevant example.

ACKNOWLEDGEMENTS

The authors gratefully acknowledge the courtesy of BMW AG. Furthermore, we acknowledge the contribution of Bernd Zwingmann on this topic.

REFERENCES

- Campolongo, F., Cariboni, J. & Saltelli, A. (2007). An effective screening design for sensitivity analysis of large models. *Environmental Modelling & Software* 22, 1509–1518.
- Hanss, M., Hurlebaus, S. & Gaul, L. (2002). Fuzzy sensitivity analysis for the identification of material properties of orthotropic plates from natural frequencies. *Mechanical Systems and Signal Processing* 16(5), 769–784.
- Helton, J., Johnson, J., Sallaberry, C. & Storied, C. (2006). Survey of sampling-based methods for uncertainty and sensitivity analysis. *Reliability Engineering and System Safety* 91, 1175–1209.
- Kucherenko, S., Rodriguez-Fernandez, M., Pantelides, C. & Shah, N. (2009). Monte carlo evaluation of derivative-based global sensitivity measures. *Reliability Engineering and System Safety* 94, 1135–1148.
- Moens, D. & Vandepitte, D. (2007). Interval sensitivity theory and its application to frequency response envelope analysis of uncertain structures. *Computer Methods in Applied Mechanics and Engineering* 196, 2486–2496.
- Montaño, J.J. & Palmer, A. (2003). Numeric sensitivity analysis applied to feedforward neural networks. *Neural Computing & Application* 12, 119–125.
- Morris, M.D. (1991). Factorial sampling plans for preliminary computational experiments. *Technometrics* 33(2), 161–174.
- Pannier, S. & Graf, W. (2010). Sectional sensitivity measures with artificial neural networks. In 9th *LS-DYNA user meeting*, Bamberg, pp. I–I–21.
- Reuter, U. & Liebscher, M. (2008). Global sensitivity analysis in view of nonlinear structural behavior. In 7th *LS-DYNA user meeting*, Bamberg, pp. F–I–02.
- Saltelli, A., Ratto, M., Tarantola, S. & Campolongo, F. (2006). Sensitivity analysis practices: Strategies for model-based inference. *Reliability Engineering and System Safety* 91, 1109–1125.
- Sobol', I. (2005). Global sensitivity indices for nonlinear mathematical models. Review. *Wilmott Magazine* 1, 56–61.
- Sobol', I. & Kucherenko, S. (2009). Derivative based global sensitivity measures and their link with global sensitivity indices. *Mathematics and Computers in Simulation* 79, 3009–3017.

A method for the verified solution of finite element models with uncertain node locations

A.P. Smith & J. Garloff

Faculty of Computer Science, University of Applied Sciences (HTWG) Konstanz, Konstanz, Germany

H. Warkle

Faculty of Civil Engineering, University of Applied Sciences (HTWG) Konstanz, Konstanz, Germany

Many sources of uncertainty exist in models for the analysis of structural mechanics problems, including measurement imprecision and manufacturing imperfections. An uncertain quantity is often assumed to be unknown but bounded, i.e. lower and upper bounds for the parameter can be provided (without assigning any probability distribution). These quantities can therefore be represented by intervals, and interval arithmetic, e.g. [1, 8], can be used to track uncertainties throughout the whole computation, yielding an interval result which is guaranteed to contain the exact result.

The Finite Element Method (FEM) is a frequently used numerical method in structural mechanics. However, its accuracy is affected by discretisation and rounding errors and model and data uncertainty. The source of parametric uncertainty (sometimes also called data uncertainty) is the lack of precise data needed for the analysis. In the FEM, parameters describing the geometry, material, and loads may be uncertain. Parametric uncertainty may result from a lack of knowledge (*epistemic uncertainty* or *reducible uncertainty*), e.g. loads are not exactly known, or an inherent variability (*aleatory uncertainty* or *irreducible uncertainty*) in the parameters, e.g. material parameters are only known to vary within known bounds, cf. [5].

In the case of a problem where some of the physical model parameters are uncertain, the application of the FEM results in a system of linear equations with numerous interval parameters which cannot be solved conventionally—a naive implementation in interval arithmetic typically delivers result intervals that are excessively large. The interval arithmetic approach has been variously adapted to handle parameter uncertainty in the application of the FEM to problems in structural mechanics, e.g. [2, 6, 7, 9, 12]. Most of these papers consider the case of affine parametric dependency. Typically, more advanced models involve polynomial or rational parameter dependencies, in which case the coefficients of the systems

of linear equations to be solved are polynomial or rational functions of the parameters. In [4, 14] we present approaches to solve such systems, employing a general-purpose fixed-point iteration using interval arithmetic [10], an efficient method for bounding the range of a multivariate polynomial over a given box based on the expansion of this polynomial into Bernstein polynomials [3, 13], and interval tightening methods. Most of the problems treated in the cited works only exhibit uncertainty in either the material values or the loading forces. The problem that the lengths of the bars of a truss system are uncertain, due to fabrication errors or thermal changes, is considered in [6]. However, in real-life problems, not only the lengths are uncertain but also the positions of the nodes are not exactly known. A statically-determinate problem with uncertain node locations was successfully solved in [14].

The approach presented here permits a structural truss problem where *all* of the physical model parameters are uncertain to be treated. Not only the material values and applied loads, but also the positions of the nodes are assumed to be inexact but bounded and are represented by intervals.

Our new method begins by computing starting guaranteed interval enclosures for the node displacements which are relatively wide. These solution intervals are iteratively tightened by performing a monotonicity analysis of all the parameters coupled with a solver for interval systems of linear equations. A parametric system of linear equations can alternatively be viewed as an interval system; its solution set is larger, but easier to compute. During the construction of a set of related interval systems of equations governing the possible monotonicity of the node displacements with respect to each parameter, it is necessary to implement several optimisations in order to minimise the occurrence of each parameter and reduce the well-known dependency effect from interval arithmetic. A simple solver can be employed to

determine in which orthants of \mathbf{R}^n these solution sets lie, which corresponds to monotonicity information. This information is used to reduce the range of parameters by iteratively subdividing and performing a local monotonicity analysis.

The method is illustrated with a simple mechanical truss structure. In somewhat more than half of all cases, a solution component is found to be monotone (over the whole parameter domain) with respect to a particular parameter. Several of the solution components are also locally monotone near the minimum or maximum. It is shown that exploitation of the monotonicity information yields a significant tightening of the displacement intervals.

ACKNOWLEDGEMENT

We gratefully acknowledge support from the State of Baden-Württemberg, Germany.

REFERENCES

- [1] Alefeld, G. & Herzberger, J. (1983). *Introduction to Interval Computations*. Academic Press, New York.
- [2] Corliss, G., Foley, C. & Kearfott, R.B. (2007). Formulation for reliable analysis of structural frames. *Reliable Computing* 13, 125–147.
- [3] Garloff, J. & Smith, A.P. (2008). Rigorous affine lower bound functions for multivariate polynomials and their use in global optimisation. In *Proceedings of the 1st International Conference on Applied Operational Research*, Tadbir Institute for Operational Research, Systems Design and Financial Services, *Lecture Notes in Management Science* 1, pp. 199–211.
- [4] Garloff, J., Popova, E.D. & Smith, A.P. (2009). Solving linear systems with polynomial parameter dependency in the reliable analysis of structural frames. In *Proceedings of the 2nd International Conference on Uncertainty in Structural Dynamics*, Sims, N. & Worden, K. (eds.), Sheffield, UK, pp. 147–156.
- [5] Moens, D. & Vandepitte, D. (2005). A survey of non-probabilistic uncertainty treatment in finite element analysis. *Computational Methods in Applied Mechanics and Engineering* 194, 1527–1555.
- [6] Muhanna, R.L., Erdolen A. & Mullen, R.L. (2006). Geometric uncertainty in truss systems: an interval approach. In *Proceedings of the 2nd International Workshop on Reliable Engineering Computing, NSF Workshop on Modeling Errors and Uncertainty in Engineering Computations*, Muhanna, R.L. & Mullen, R.L. (eds.), Savannah, Georgia, USA, pp. 475–481. Available under <http://www.gtsav.gatech.edu/workshop/rec06/REC'06Proceedings.pdf>
- [7] Muhanna, R.L., Zhang, H. & Mullen, R.L. (2007). Interval finite elements as a basis for generalized models of uncertainty in engineering mechanics. *Reliable Computing* 13, 173–194.
- [8] Neumaier, A. (1990). *Interval Methods for Systems of Equations*. Cambridge Univ. Press, London.
- [9] Neumaier, A. & Pownuk, A. (2007). Linear systems with large uncertainties, with applications to truss structures. *Reliable Computing* 13, 149–172.
- [10] Popova, E.D. (2007). Solving linear systems whose input data are rational functions of interval parameters. In *Numerical Methods and Applications 2006*, T. Boyanov et al. (eds.), *Lecture Notes in Computer Science* 4310, Springer, Berlin, Heidelberg, pp. 345–352. Extended version available under <http://www.math.bas.bg/~epopova/papers/05PreprintEP.pdf>
- [11] Popova, E.D. (2007). Computer-assisted proofs in solving linear parametric problems. In *IEEE-Proceedings of SCAN 2006, 12th GAMM-IMACS International Symposium on Scientific Computing, Computer Arithmetic and Validated Numerics*, Luther, W. & Otten, W. (eds.), Duisburg, Germany, pp. 35–43.
- [12] Popova, E.D., Iankov, R. & Bonev, Z. (2006). Bounding the response of mechanical structures with uncertainties in all the parameters. In *Proceedings of the 2nd International Workshop on Reliable Engineering Computing, NSF Workshop on Modeling Errors and Uncertainty in Engineering Computations*, Muhanna, R.L. & Mullen, R.L. (eds.), Savannah, Georgia, USA, pp. 245–265.
- [13] Smith, A.P. (2009). Fast construction of constant bound functions for sparse polynomials. *Journal of Global Optimization* 43(2–3), 445–458.
- [14] Smith, A.P., Garloff, J. & Werkle, H. (2009). Verified solution for a simple truss structure with uncertain node locations. In *Proceedings of the 18th International Conference on the Application of Computer Science and Mathematics in Architecture and Civil Engineering*, Gürlebeck, K. & Könke, C. (eds.), Weimar, Germany.

An approach on soundings for geotechnical site investigation

D. Boumezerane & S. Belkacemi

Ecole Nationale Polytechnique d'Alger, Civil Engineering Department, Algiers, Algeria

B. Zlender

University of Maribor, Faculty of Civil Engineering, Maribor, Slovenia

ABSTRACT: Geotechnical site investigation is generally carried out in two steps. The first step, consisting of preliminary soundings, guides subsequent site characterization. The number of soundings, required to adequately characterize a site, is set on the basis of the engineering judgement following the preliminary investigation, and is affected by the geologic context, the area topography, the project type, and the knowledge of the neighbouring areas.

A Fuzzy Inference System (FIS) is used to determine the optimal number of soundings to carry out on site for geotechnical investigations of common projects. Certain number of parameters influences the quantity of required boreholes for a given site. We can quote the geology of the site, the type of project, the topography and available information about adjoining sites. These parameters are generally expressed linguistically depending on the Engineer's judgment. Each parameter influences the density (number) of soundings to execute.

The parameters like the site geologic nature, site topography and project type, which may affect the number of soundings, are described and considered as INPUT parameters, while the density (number) of boreholes to obtain is taken as an OUTPUT parameter of the system. The theory of fuzzy sets allows handling parameters having vague or doubtful information as well as treating problems presented under linguistic or qualitative form. Each parameter of entry (INPUT) of the system indicates if more or less soundings are required. The construction of the Fuzzy Inference System permits to implement the rules considered, by taking into account their weights, and to evaluate the final decision. An application on an existing site investigation is used as calibration of the FIS. It permits to determine the number of soundings needed for a new site.

An analysis of the FIS input and output is completed using Monte Carlo simulations. The results of the FIS are analyzed by simulating number of realizations of input parameters. The random numbers are generated with uniform probability distributions for each parameter of entry.

Each entry parameter is replaced by a vector (of values) composed of random numbers generated using uniform probability distributions. Monte Carlo simulations are used for this purpose. The set "Known-Geology" varying between [0,100] is replaced by a random vector $r(k)$ which elements are uniformly distributed in terms of probability. The same reasoning is completed with "Complexity" of local geology and "Similarity" of preliminary results, their values are replaced by the randomly generated vectors $q = (j)$ and $t = (m)$. The "Project type" fuzzy set's support varying from 1 to 10 is taken with the same length as a vector $s(l)$ randomly generated also. When information is available about the geotechnical parameters of the ground [1, 3000] kg/cm² we use a vector $p(i)$ which elements are comprised between [1,3000]. The number of elements for each vector is set upon Monte Carlo simulations.

Given the input vectors with uniform probability distributions for each one we search for the probability distributions of the FIS output (results). We look by this way to predict how the results will behave, or what will be their tendency if almost all the possibilities of input are taken into account.

The obtained results are expressed in form of histograms and probability distributions. The results are fitted with non-parametric probability distribution and with a "t location-scale" function which seems to have a good agreement in this case. The obtained distributions of output results inform about their tendency in general and help taking decisions about the density of soundings on site.

Strong law of large numbers on the Kôpka D-posets

M. Kuková

Department of Mathematics, Faculty of Natural Sciences, Matej Bel University, Banská Bystrica, Slovakia

B. Riečan

Institute of Mathematics and Informatics, Slovak Academy of Sciences, Banská Bystrica, Slovakia

ABSTRACT: MV algebras play the same role in many-valued logic as Boolean algebras in two-valued logic. Therefore the development of probability theory on MV-algebras is important, especially on MV—algebras with product ([7], [8]). Of course, F. Kôpka introduced the D—posets with product (see [4,5]), which are a generalization of MV-algebras with product ([7,8]). In the paper the strong law of large numbers is proved under some weaker assumptions as it was realized in [10] (without the assumption of weak σ —distributivity of the given MV-algebra).

Definition 1 The structure $(D, \leq, -, 0, 1)$ is called D-poset if the relation \leq is a partial ordering on D, 0 is the smallest and 1 is the largest element on D and

1. $b - a$ is defined iff $a \leq b$,
2. if $a \leq b$ then $b - a \leq b$ and $b - (b - a) = a$,
3. $a \leq b \leq c \Rightarrow$
 $\Rightarrow c - b \leq c - a, (c - a) - (c - b) = b - a$.

Definition 2 Let $(D, \leq, -, 0, 1)$ be a D-poset. It is called the Kôpka D-poset, if there is a binary operation $*$: $D \times D \rightarrow D$, which is commutative, associative and has the following properties:

1. $a * 1 = a, \forall a \in D$;
2. $a \leq b \Rightarrow a * c \leq b * c, \forall a, b, c \in D$;
3. $a - (a * b) \leq 1 - b, \forall a, b \in D$.

Definition 3 A state on a D-poset D is any mapping $m : D \rightarrow [0, 1]$ satisfying the following properties:

1. $m(1) = 1, m(0) = 0$;
2. $a_n \nearrow a \Rightarrow m(a_n) \nearrow m(a), \forall a_n, a \in D$;
3. $a_n \searrow a \Rightarrow m(a_n) \searrow m(a), \forall a_n, a \in D$.

If D is a lattice (with respect to the ordering \leq), then m is called σ -additive, if $m(a \vee b) = m(a) + m(b)$ whenever $a \wedge b = 0$.

Definition 4 Let $J = \{(-\infty, t); t \in R\}$. An observable on D is any mapping $x : J \rightarrow D$ satisfying the following conditions:

1. $A_n \nearrow R \Rightarrow x(A_n) \nearrow 1$;
2. $A_n \searrow \emptyset \Rightarrow x(A_n) \searrow 0$;
3. $A_n \nearrow A \Rightarrow x(A_n) \nearrow x(A)$.

Theorem 1 Let $x : J \rightarrow D$ be an observable, $m : J \rightarrow [0, 1]$ be a state. Define a mapping $F : R \rightarrow [0, 1]$ by the formula $F(t) = m(x((-\infty, t)))$: Then F is a distribution function.

Denote by $B(R)$ the family of all Borel subsets of the real line R. Since F is a distribution function, there exists exactly one probability measure $\lambda_F : B(R) \rightarrow [0, 1]$ such that $\lambda_F((a, b)) = F(b) - F(a)$ for any $a, b \in R, a < b$.

Definition 5 Observables x_1, \dots, x_n are called independent, if

$$m(x_1((-\infty, t_1)) * x_2((-\infty, t_2)) * \dots * x_n((-\infty, t_n))) = m(x_1((-\infty, t_1))) \cdot m(x_2((-\infty, t_2))) \cdot \dots \cdot m(x_n((-\infty, t_n)))$$

for any $t_1, t_2, \dots, t_n \in R$.

Denote $\Delta_t^n = \{(u_1, u_2, \dots, u_n) \in R^n; u_1 + u_2 + \dots + u_n < t\}$ and $M = \{\Delta_t^n; t \in R\}$. There has been proved the existence of a mapping $h_n : \Delta_t^n \rightarrow D$ such that the mapping $z : J \rightarrow D$ defined by the equality $z((-\infty, t)) = h_n(\Delta_t^n)$ is an observable in [9]. Moreover the following theorem ([9], Theorem 2) has been proved:

Theorem 2 Let x_1, \dots, x_n be independent observables, F_1, \dots, F_n be the corresponding distribution functions, $\lambda_{F_1}, \dots, \lambda_{F_n}$ the corresponding probability measures. Then there exists exactly one observable $z : J \rightarrow D$ such that $z((-\infty, t)) = \lambda_{F_1} \times \lambda_{F_2} \times \dots \times \lambda_{F_n}(\Delta_t^n)$, where $\lambda_{F_1} \times \lambda_{F_2} \times \dots \times \lambda_{F_n} : B(R^n) \rightarrow [0, 1]$ is the product of the probabilities $\lambda_{F_1}, \lambda_{F_2}, \dots, \lambda_{F_n}$.

Definition 6 The observable $z : J \rightarrow D$ introduced in Theorem 2 is the sum $z = x_1 + \dots + x_n$ of independent observables x_1, \dots, x_n . Moreover, the arithmetic mean \bar{x} of x_1, \dots, x_n is defined by the equality

$$\bar{x}(-\infty, t) = \frac{1}{n}(x_1 + \dots + x_n)(-\infty, t) = (x_1 + \dots + x_n)(-\infty, nt).$$

Definition 7 Let $(x_i)_{i=1}^\infty$ be a sequence of independent observables on a σ -complete Kôpka D-poset D with a σ -additive state m . We say that this sequence converges m -almost everywhere to zero, if the following equality holds:

$$\lim_{l \rightarrow \infty} \lim_{k \rightarrow \infty} \lim_{i \rightarrow \infty} m\left(\bigwedge_{n=k}^{k+i} x_n\left(\left(-\frac{1}{l}, \frac{1}{l}\right)\right)\right) = 1,$$

where $x((\alpha, \beta)) = x((-\infty, \beta)) - x((-\infty, \alpha])$ and

$$x((-\infty, \beta]) = \bigwedge_{n=1}^\infty x((-\infty, \alpha + \frac{1}{n})) \forall \alpha, \beta \in R$$

Definition 8 Let $x : J \rightarrow D$ be an observable, $a \in R$. Then we define the observable $x - a : J \rightarrow D$ by the formula $(x - a)((-\infty, t)) = x((-\infty, t + a))$.

Theorem 3 Let D be a σ -complete Kôpka D-poset with σ -additive state $m : D \rightarrow [0, 1]$, let $(x_n)_{n=1}^\infty$ be a sequence of square integrable observables such that $\sum_{n=1}^\infty \frac{\sigma^2(x_n)}{n^2} < \infty$. Then the sequence of observables

$$\frac{1}{n} \sum_{i=1}^n (x_i - E(x_i))$$

converges m -almost everywhere to 0.

REFERENCES

- [1] Chang, C.C. (1958). Algebraic analysis of many-valued logics. *Trans. Amer. Math. Soc.* 88, 467–490.
- [2] Dvurečenskij, A. & Pulmannová, S. (2000). *New trends in quantum structures*. Kluwer, Dordrecht.
- [3] Foulis, D.J. & Bennett, M.K. (1994). Effect algebras and un-sharp quantum logics. *Found. Phys.* 24, 1325–1346.
- [4] Kôpka, F. (2004). D-posets with meet function. *Advances in Electrical and Electronic Engineering* 3, 34–36.
- [5] Kôpka, F. (2008). Quasi product on Boolean D-posets. *Int. J. Theore. Phys.* 47, 26–35.
- [6] Kôpka, F. & Chovanec, F. (1994). D-posets. *Math. Slovaca* 44, 21–34.
- [7] Montagna, F. (2000). An algebraic approach to propositional fuzzy logic. *J. Logic Lang. Inf* 9, 91, 124.
- [8] Riečan, B. (1999). On the product MV-algebras. *Tatra Mt. Math. Publ.* 16, 143–149.
- [9] Riečan, B. & Lašová, L. (2009). On the probability theory on the Kôpka D-posets. *Developments in Fuzzy Sets, Intuitionistic Fuzzy Sets, Generalized Nets and Related Topics. Volume I: Foundations*, IBS PAN- SRI PAS, Warsaw.
- [10] Riečan, B. & Mundici, D. (2002). Probability on MV-algebras. In: *Handbook of Measure Theory* (E. Pap. ed.), Elsevier Science, Amsterdam, 869–909.
- [11] Riečan, B. & Neubrunn, T. (1997). *Integral, Measure, and Ordering*. Kluwer, Dordrecht.

This page intentionally left blank

*MS_136 — Fuzzy analysis and soft computing methods
in reliability assessment and optimization (3)*

This page intentionally left blank

Application of Cokriging method to structural reliability problems

Wei Zhao & Wei Wang
Harbin Institute of Technology, China

1 INTRODUCTION AND BACKGROUND

Approximation methods are widely used in structural reliability analysis because they are simple to create and provide explicit functional relationships between the responses and variables instead of the implicit limit state function. These methods include the Response Surface Method (RSM), Artificial Neural Networks (ANN) and so on. Recently, the kriging method which is a semi-parameter interpolation technique that can be used for deterministic optimization and structural reliability has been recognized as an alternative to the traditional Response Surface Method.

The kriging method is presented as an alternative approximation method to RSM for the design and analysis of computer experiments since the interpolation of the sampled data is carried out using a maximum likelihood estimation procedure, which allows for the capturing of multiple local extrema. However, the accuracy of a kriging model depends greatly on the number of sample data points used and their locations in multidimensional space. In order to fully exploit the advantages of kriging models, a large number of sample data points must be distributed within the design space. When the limit state function is high-dimensional, this sampling process can be very costly and even impractical in design and computation.

As surrogate models are known to become inefficient as dimension increased, a third method using a cokriging (gradient-enhanced kriging) formulation is presented. It uses a sample limited cokriging approach. This formulation was set up to overcome the large computational cost needed to build a surrogate model. Actually, the cokriging method is an extension of the kriging method that incorporates the gradient information in addition to primary function values when generating approximation models. But its application to a structural reliability problem has not been realized.

Against this background, this paper explores the use of the cokriging method for structural reliability problems and gives some examples and discussion.

2 THE COKRIGING METHOD FOR THE STRUCTURAL RELIABILITY

In this paper, a new method—the cokriging method, which is an extension of kriging, is proposed to calculate the structural reliability. cokriging approximation incorporates secondary information such as the values of the gradients of the function being approximated. The authors describe two basic approaches to construct the cokriging model. The gradient information can be directly built into the cokriging formulation, which we called the *direct cokriging* method. Alternatively, the gradient information can be included in an augmented kriging model by adding new points to the sample database that are obtained using a linear Taylor series expansion about the points at which the gradients were computed, which we called the *Database Augmentation* or the *indirect cokriging* method. The authors use the *indirect cokriging* method, which can be divided mainly into three stages: First, a design of experiment method such as grid sample design can be selected to form the necessary experimental points. Secondly, the surrogate model of the limit state function has been constructed. And then, the structural reliability method—FORM has been chosen to find the design point corresponding to the reliability index, after the iterative process, the reliability results will be obtained.

For Database Augmentation, the additional points from the Taylor Series expansion can be located at various points in space relative to the sample points. One might consider four different schemes to augment the database.

Scheme 1 adds one point “diagonally” (i.e. or) for each sample point in the original design space. So, only one point is added in the neighborhood of each sample point. In total, the number of added, approximate points is the number of sample points, n . Scheme 2 adds both and and this scheme would effectively triple the size of the database. Scheme 3 adds one approximate sample point along each design variable axis for each sample point in the design space. In total, the number of sample points, n , times the dimensionality of

the design space, d . Similarly, scheme 4 adds twice the number of points as Scheme 3. In scheme 4, two additional points located at and relative to a sample point along each design variable axis are added. The number of total points added is then $2n$ in a d -dimensional design space with n sample points. These last two schemes dramatically increase the computing cost, so we choose the previous two schemes in this paper to make comparisons.

In this paper, the author presents two numerical examples to compare the kriging method with the cokriging method. In order to verify the efficiency and accuracy of the cokriging method, especially in the high-dimensional problems, the examples are selected to have an explicit limit state function with three random variables, and five random variables.

The sampling quality is essential to obtain an accurate model. Classical sampling is space-filling and including grid design, orthogonal design and uniform design. The grid distribution is the most common in engineering, however, it should be used with great care, because truncated grids are to be avoided and grids in high dimension require unreachable sample sizes. Both the orthogonal design and the uniform design can reduce the number of samples to some extent and the results are acceptable. The author uses them to replace the grid design in the examples above and compares them in the giving tables.

3 CONCLUSIONS AND FUTURE RESEARCH

In this paper, the method of improving the accuracy of the approximations that are used for the limit state function in structural reliability analysis while reducing the amount of design space information was presented. This was achieved by incorporating

gradient information and Taylor Series expansion into the kriging approximation technique.

The authors explore the use of the cokriging method for structural reliability problems and make comparisons between the results obtained by kriging method and those from the cokriging method based on some numerical examples. It can be deduced that the cokriging approach can gain similar results with a much smaller number of samples without significantly sacrificing the accuracy. In another word, when using the same number of sample points, the accuracy of results obtained by the cokriging method will be improved. When the dimensions increase, the improvement will be more visible. Therefore, the cokriging is a viable alternative to the kriging on the computation of reliability. In the cokriging model, the authors present four database augmenting schemes and compares two of them. The results shows that scheme 2 may be better than scheme 1, but the computing cost is higher. One realizes that there is always a trade-off between the accuracy of the approximation and the computing cost. This trade study represents an interesting future research topic. The section of the discussion concerning the design of experiments shows that the grid design requires unreachable sample sizes, especially in high dimensions. Instead, both the orthogonal design and the uniform design can reduce the number of samples and the results are satisfactory at least in the examples mentioned in this paper.

Although the approximation method based on the cokriging technique has shown a good potential in structural reliability problems, it is in the very beginning stage. Some implementation issues associated with the approach such as the experimental design, the database augmenting scheme, varying the step size for the design variables with sample points and nugget effect at added points, have been presented and represent topics for future research.

On predictive densities in fuzzy Bayesian inference

R. Viertl

Department of Statistics and Probability Theory, Vienna University of Technology, Wien, Austria

INTRODUCTION

In case of fuzzy data compare (Bandemer 2006) and (Klir & Yuan 1995) Bayesian statistical analysis has to be generalized in order to be able to update the a-priori information. This is possible by a generalization of Bayes' theorem which is also able to take care of fuzzy a-priori information. The resulting aposteriori distribution is a fuzzy probability distribution on the parameter space Θ . For continuous stochastic model and continuous parameter space the a-posteriori distribution is represented by a so-called *fuzzy probability density*. Based on fuzzy a-posteriori densities the generalization of predictive densities is necessary.

In standard Bayesian inference for stochastic model $X \sim f(\cdot|\theta)$; $\theta \in \Theta$, a-priori density $\pi(\cdot)$, and data $D = (x_1, \dots, x_n)$ the a-posteriori density $\pi(\cdot|D)$ on Θ is obtained by Bayes' theorem

$$\pi(\theta|D) = \frac{\pi(\theta) \cdot \ell(\theta; D)}{\int_{\Theta} \pi(\theta) \cdot \ell(\theta; D) d\theta} \quad \forall \theta \in \Theta, \quad (1)$$

where $\ell(\theta; D)$ is the likelihood function. The likelihood function is for complete data $D = (x_1, \dots, x_n)$ given by

$$\ell(\theta; x_1, \dots, x_n) = \prod_{i=1}^n f(x_i | \theta) \quad \forall \theta \in \Theta. \quad (2)$$

In this standard case the predictive density for X , denoted by $p(x|D)$, is given by its values

$$p(x|D) = \int_{\Theta} f(x|\theta) \cdot \pi(\theta|D) d\theta \quad \forall x \in M_X, \quad (3)$$

where M_X is the observation space of X , i.e. the set of possible values for X .

FUZZY INFORMATION

In the context of this paper two kinds of fuzzy information appear: Fuzzy observations x_i^* of X , and

fuzzy a-priori information concerning the parameter θ . The last one is expressed by a fuzzy a-priori distribution, frequently given by a fuzzy probability density $\pi^*(\cdot)$ on the parameter space Θ .

Fuzzy one-dimensional observations can be described by fuzzy numbers. These are defined by generalizations of indicator functions, so-called *characterizing functions* $\xi(\cdot)$.

Definition 1: A characterizing function $\xi(\cdot)$ of a fuzzy number x^* is a real function of one real variable x obeying the following:

1. $\forall \delta \in (0; 1]$ the so-called δ -cut $C_{\delta}(x^*) := \{x \in \mathbb{R} : \xi(x) \geq \delta\} = [a_{\delta}; b_{\delta}] \neq \emptyset$
2. The support of $\xi(\cdot)$, $supp[\xi(\cdot)] := \{x \in \mathbb{R} : \xi(x) > 0\}$ is contained in a compact interval

Fuzzy numbers are an appropriate mathematical description of non-precise data.

Fuzzy probability densities on Θ are fuzzy valued functions $\pi^*: \Theta \rightarrow \mathcal{F}(\mathbb{R}_+)$ obeying certain regularity conditions, where $\mathcal{F}(\mathbb{R}_+)$ is the set of all fuzzy numbers with $supp[\xi(\cdot)] \subseteq [0; \infty]$.

In order to define fuzzy probability densities the concept of integration of fuzzy valued functions is necessary.

Let $(\Omega, \mathcal{S}, \mu)$ be a measure space. The generalized integral of a fuzzy valued function $f^*: \Omega \rightarrow \mathcal{F}(\mathbb{R}_+)$ is defined based on the so-called δ -level functions $\underline{f}_{\delta}(\cdot)$ and $\overline{f}_{\delta}(\cdot)$ $\forall \delta \in (0; 1]$. For $\omega \in \Omega$ and $\delta \in (0; 1]$ δ -cut of $f^*(\omega)$ is a compact interval denoted by $[\underline{f}_{\delta}(\omega); \overline{f}_{\delta}(\omega)]$. For variable ω the functions $\underline{f}_{\delta}(\cdot)$ and $\overline{f}_{\delta}(\cdot)$ are the δ -level functions.

Assuming all δ -level functions are integrable with finite integrals

$$a_{\delta} := \int_{\Omega} \underline{f}_{\delta}(\omega) d\mu(\omega) \quad \text{and} \quad b_{\delta} := \int_{\Omega} \overline{f}_{\delta}(\omega) d\mu(\omega), \quad (4)$$

the generalized fuzzy valued integral $\int_{\Omega} f^*(\omega) d\mu(\omega)$ is the fuzzy number x^* whose characterizing function $\xi(\cdot)$ is given by the so-called construction lemma for characterizing functions of fuzzy numbers, i.e.

$$\xi(x) := \sup \left\{ \delta \cdot \mathbb{1}_{[a_\delta, b_\delta]}(x) : \delta \in [0;1] \right\} \quad \forall \quad x \in IR. \quad (5)$$

For details compare (Viertl 2011).

Definition 2: A fuzzy probability density $f^*(\cdot)$ on the measure space (Ω, S, μ) is a fuzzy valued function obeying the following:

1. $supp[f^*(\omega)] \subseteq [0; \infty] \quad \forall \quad \omega \in \Omega$
2. $\int_{\Omega} f^*(\omega) d\mu(\omega)$ is a fuzzy number x^* such that for the characterizing function $\xi(\cdot)$ of x^* the following holds: $1 \in C_1[\xi(\cdot)]$

BAYES' THEOREM FOR FUZZY A-PRIORI DENSITIES AND FUZZY DATA

The generalization of Bayes' theorem to the situation of fuzzy a-priori density and fuzzy data is possible and yields a fuzzy a-posteriori density $\pi^*(\theta|D^*)$ on the parameter space Θ . For details see (Viertl 2008) and (Viertl 2011).

Based on the fuzzy a-posteriori density $\pi(\theta|D^*)$ the predictive density from section 1 has to be generalized, i.e. the integral becomes

$$p^*(x|D) = \int_{\Theta} f(x|\theta) \cdot \pi^*(\theta|D^*) d\theta. \quad (6)$$

This is an integral of a fuzzy valued function $f(x|\theta) \cdot \pi^*(\theta|D^*)$. There are different possibilities to define the generalized fuzzy valued predictive density $p^*(x|D^*)$ on the observation space M_X .

FUZZY PREDICTIVE DENSITIES

The first idea is to apply the generalized integration from section 2, i.e.

$$p^*(x|D^*) := \int_{\Theta} f(x|\theta) \cdot \pi^*(\theta|D^*) d\theta \quad \forall \quad x \in M_X. \quad (7)$$

Indeed by this definition a fuzzy probability density $p^*(x|D^*)$ is obtained.

But there is another possibility based on classical densities on the parameter space. Let D_δ be

the set of all classical probability densities $g(\cdot)$ on Θ obeying

$$\underline{\pi}_\delta(\theta) \leq g(\theta) \leq \bar{\pi}_\delta(\theta) \quad \forall \quad \theta \in \Theta. \quad (8)$$

Then the fuzzy value of the generalized predictive density for $x \in M_X$ is defined via the family of nested compact intervals $[a_\delta; b_\delta] \quad \forall \quad \delta \in (0;1]$ in the following way:

$$\begin{aligned} b_\delta &:= \sup \left\{ \int_{\Theta} f(x|\theta) g(\theta) d\theta : g(\cdot) \in D_\delta \right\} \\ a_\delta &:= \inf \left\{ \int_{\Theta} f(x|\theta) g(\theta) d\theta : g(\cdot) \in D_\delta \right\} \end{aligned} \quad (9)$$

The characterizing function $\psi_x(\cdot)$ of $p^*(x|D^*)$ is obtained by the construction lemma:

$$\psi_x(y) := \sup \left\{ \delta \cdot \mathbb{1}_{[a_\delta; b_\delta]}(y) : \delta \in [0;1] \right\} \quad \forall \quad y \in IR \quad (10)$$

Remark 1: Since the a-posteriori density is a fuzzy probability density it follows that the set D_1 is nonempty and therefore by the above construction a fuzzy probability density on M_X is obtained.

The last construction seems to be more appropriate because it is more connected to the stochastic concept of predictive distributions.

Remark 2: For precise data and classical a-priori distributions the results coincide with the standard results from Bayesian inference.

REFERENCES

- Bandemer, H. (2006). *Mathematics of Uncertainty - Ideas, Methods, Application Problems*. Berlin: Springer.
- Klir, G. & Yuan, B. (1995). *Fuzzy sets and fuzzy logic: theory and applications*. Upper Saddle River: Prentice Hall.
- Viertl, R. (2008). Foundations of fuzzy bayesian inference. *Journal of Uncertain Systems 2 (No. 3)*, 187–191.
- Viertl, R. (2011). *Statistical Methods for Fuzzy Data*. Chichester: Wiley.

Robustness based design of structures under consideration of generalized uncertainty models

J.-U. Sickert, S. Pannier, W. Graf & M. Kaliske

Institute for Structural Analysis, Technische Universität Dresden, Germany

While the terms reliability and safety level are well-defined, an overall mathematical formulation of the linguistic well-known term “robust structure” is missing so far. Many approaches provide only qualitative construction rules which are inappropriate to compare diverse designs. More extensive approaches on the basis of the uncertainty model randomness are reviewed in Zang et al. (2005). The here proposed approach contributes to the discussion how to quantify robustness in order to compare different structural designs within a computer oriented design process.

An appropriate measure is introduced, which considers different approaches of robustness, like the incorporation of uncertain parameters and the consideration of unforeseen events, within an unified concept. Thus, the robustness measure evaluates consequences of uncertainty on structural behavior, the effect of local failure on global structural resistance as well as the influence of variations in load and alteration processes on the structural reliability. The proposed robustness measure could be applied independently of the measure utilized for quantification of the uncertainty. Thus, it is possible to consider uncertainty of two kinds—variability and imprecision—within the robustness assessment approach. Due to the different sources of variability and imprecision, the imprecise probability concept “fuzzy randomness” is adopted. Consequently, the structural analysis results in fuzzy random structural responses, whereas the reliability analysis leads to a time-dependent fuzzy failure probability. Some basically remarks concerning fuzzy randomness are summarized in the paper.

In general, uncertainty exists in loading, material characteristics and geometry of structures. The sources of this uncertainty may be classified into inherently non-deterministic nature of the regarded structure and information deficit. The uncertainty because of the inherently non-deterministic nature is referred to as aleatory uncertainty. It is irreducible, random, and objective assessable. In contrast, information deficit leads to epistemic uncertainty (imprecision) which can be reduced by means of

collecting more data, better understanding of the problem, strict quality control and further information retrieval actions. Nevertheless, epistemic uncertainty cannot be prevented completely.

Aleatory uncertainty, also referred to as randomness, occurs as a result of heterogeneity. It may be assessed with the aid of random results of a test if the test provides crisp sample elements and is repeatable on an almost unlimited number of occasions under constant boundary conditions. This is an almost unreachable state, because the boundary conditions are (apparently) subject to arbitrary fluctuations, a comprehensive system overview is lacking, the number of observations are only available to a limited extend, or the sample elements are of doubtful accuracy (non-precise). Therefore, imprecision results in addition to the randomness. Imprecision is modelled with the uncertainty model fuzziness because of the fact that its nature is not conform with the frequentist view on probability.

Joining both randomness and fuzziness in a proper manner, a fuzzy random variable \tilde{U} can be defined on the basis of fuzzy bunch parameters. The bunch parameter representation enables a decoupling of fuzziness and randomness, which provides the basis for the numerical realization of uncertain structural analysis and reliability assessment. The bunch parameter vector contains typical parameters of probability distribution functions which are specified as fuzzy variables, such as fuzzy mean and fuzzy standard deviation, for example.

The aim of the described robustness measure, e.g. introduced in Graf et al. (2010), is to provide a measure, which captures different meanings of robustness simultaneously and is independent of the applied uncertainty model. To meet these requirements, uncertain structural analysis is repeatedly performed considering selected stress processes and local failure events in order to determine a robust structure in the sense that the structure will resist a high number of different—also extreme—load and alteration processes. In result, the design variants are evaluated by means of the robustness measure on the basis of selected

uncertain structural responses. The application of the robustness measure requires quantification of the uncertainty of input and response variables. The uncertainty of variables can be quantified by means of uncertainty measures. This procedure represents the mapping of an uncertain variable onto a deterministic value M . Different uncertainty measures for fuzzy, random and fuzzy random variables are introduced.

To manage the high computational effort due to the repetition of the uncertain structural analysis, an algorithm for the robustness based design is presented. The computational cost of a fuzzy stochastic structural and reliability analysis is almost completely caused by the nonlinear structural analysis. Thus, the most effective measure to increase the numerical efficiency is to replace the costly deterministic computational model by a fast approximation solution based on a reasonable amount of initial deterministic computational results. The fuzzy stochastic analysis can then be performed with that surrogate model, which enables the utilization of an appropriate sample size for the simulation. The surrogate model is designed to describe a functional dependency between the structural parameters and the structural responses in the form of a response surface approximation.

For response surface approximation a variety of options exist, see e.g. Pannier et al. (2009). The suitability of the particular developments primarily depends on the properties of the computational model. Due to the very general properties of the FE analysis in structural analysis, which can hardly be limited to convenient cases, a high degree of generality and flexibility of the approximation is needed. In this context, an artificial neuronal network, provides a powerful basis for response surface approximation. This can extract information from initial deterministic computational results and can subsequently reproduce the structural response based on the extracted information only. According to the universal function approximation theorem, artificial neural networks are capable of uniformly approximating any kind of nonlinear functions over a compact domain of definition to any degree of accuracy. There is virtually no restriction for a response surface approximation with the aid of artificial neural networks.

The applicability of the robustness based design approach is demonstrated by means of an example. The investigated building has a rectangular plan whose dimensions are 10.80×20.40 m². In Mandara et al. (2009) the results of the vulnerability evaluation have been published. Thereby, a three-dimensional FE model of the structure has been created considering floors like rigid diaphragms in the horizontal plane. Two nonlinear static analyses and a set of linear and nonlinear

time history analyses have allowed to evaluate the vulnerability of the structure in the as-built condition and the effectiveness of the upgrading interventions. The time history analysis has shown an excessive deformability of the original structure, not compatible with the structural safety and immediate occupancy requirement after seismic events, see Mandara et al. (2009). The assumed upgrading interventions are aimed at reducing the lateral floor displacements of the structure by means of steel braces fitted with additional energy dissipation devices. Such devices connect the original structure at the first floor level with rigid steel braces and act due to the relative displacements occurring between the original structure and the steel braces. The study has been carried out considering the connection with purely viscous devices.

Nonlinear time-history analyses of the simplified 2-DOF system have then been performed considering the seismic input of El Centro (1940), Calitri (1980) and Taiwan (1999) earthquakes, scaled to peak ground acceleration (PGA) value of 0.25 g. For each seismic input, the fuzzy maximum displacement \tilde{u}_{TD} at the top of the structure has been calculated on the basis of fuzzy displacement-time dependencies.

The results of the structural analyses are applied for the robustness assessment. Thereby, the uncertain maximum top displacements are evaluated for different viscosities and bracing systems. The three considered earthquakes represent three load cases.

ACKNOWLEDGEMENTS

The authors gratefully acknowledge the financial support of the German Research Foundation (DFG).

REFERENCES

- Graf, W., Sickert, J.-U., Pannier, S. & Kaliske, M. (2010). Robust design with uncertain data and response surface approximation. In M. Beer, R. Muhanna, and R. Mullen (Eds.), *4th International Workshop on Reliable Engineering Computing*, pp. 554–574. Research Publ.
- Mandara, A., Ramundo, F. & Spina, G. (2009). Seismic upgrading of r.c. structures with innovative bracing systems. In F. Mazzolani (Ed.), *Proceedings of PROHITEC*, London. Taylor & Francis Group.
- Pannier, S., Sickert, J.-U. & Graf, W. (2009). Patchwork approximation scheme for reliability assessment and optimization of structures. In H. Furuta, D.M. Frangopol, and M. Shinozuka (Eds.), *Safety, reliability and risk of structures, infrastructures and engineering systems*, pp. 1–8. CRC Press/Balkema.
- Zang, C., Friswell, M. & Mottershead, J. (2005). A review of robust optimal design and its application in dynamics. *Computers & Structures* 83(4–5), 315–326.

GS_238 — Life-cycle analysis

This page intentionally left blank

Optimal next inspection time for bridges based on corrosion deterioration

D. De León & C. González-Pérez

Universidad Autónoma del Estado de México, Toluca, Estado de México, Mexico

V. Bisadi, P. Gardoni, M. Head & S. Hurlebaus

Zachry Department of Civil Engineering, Texas A&M University, College Station, TX, USA

As the traffic demands grow constantly, and some vehicle bridges deteriorate due to corrosion, bridge agencies require non expensive procedures to schedule cost-effective maintenance programs. Also, due to the growing demand of safe and sustainable procedures to keep the bridges within acceptable operating conditions, new maintenance criteria based on life-cycle performance are required to assess the bridge conditions and recommend practical measures to provide a satisfactory care to the bridges, specially the oldest ones.

In this paper a reliability-based formulation is proposed for prediction of the next inspection time including the epistemic uncertainty on the corrosion initiation time and as a means to generate safe and sustainable bridge maintenance procedures. For the identification of the bridge integrity state where little or no follow up has been previously made, the prediction of damage state contains a great deal of epistemic uncertainty. The impact of this epistemic uncertainty on the prediction of corrosion initiation time is appraised for the purpose of weighting, later on, the cost/benefit of further and more detailed studies.

The concept of risk involves the failure probability and the failure consequences of the structure (Ang and De Leon, 2005). In the case of bridges, the consequences become critical as an important part of infrastructure systems in a region or country (Agarwal, 2003).

The bridge reliability is calculated in terms of a damage index that depends on the bridge corrosion deterioration and the corrosion impact is calculated as a function of the moment capacity reduction (cracking moment) and the evolution of the bridge failure probability.

As the acceptable failure probability is used as the safety threshold, this failure probability is calculated from the minimization of the annual expected life-cycle cost including the possibility of the bridge replacement. This replacement condition

is important because, given the interruption period of bridge operations after the collapse, the regular income is deferred and, whenever the money value changes with time, the income is reduced.

The cracking moment capacity is calculated according to standard procedures and the concrete strength, the prestressed steel area and the bridge live load are considered as random variables.

Finally, the bridge is modeled as a single component, being the beam under corrosion the main element, the limit state is described by the event where the beam moment capacity is exceeded by the maximum acting moment.

The bridge failure probability evolves as the corrosion develops in the girder and, as the bridge is under heavy and frequent vehicles loading, the tension stresses trend to accelerate the cracking process in the girder. The evolution of the bridge reliability index may be used to recommend a time to inspect, the bridge condition. If, after inspection, enough evidences of bridge deterioration are found, maintenance or repair works should be undertaken.

The proposed formulation is applied to a Mexican bridge and the

The acceptable value of the annual reliability of 2.78 is reached by the bridge reliability at the time range between 5.5 and 10.5 years, after corrosion initiation, for the coefficient of variation of corrosion initiation time, of 0.1. Cost/benefit studies may be used to weight the cost of narrowing this range against the benefit of making more precise predictions of the bridge inspection time.

The bridge importance will move the acceptable reliability index to higher or lower thresholds. Also, the corrosiveness of the location environment, and stresses demand on the bridge, may produce that the girder deteriorates faster and the recommended time to inspect and potentially maintain the bridge may be shorter.

Improvements and upgrading works to the bridge are not considered here.

The bridge age may play an important role as the corrosion may be initiated faster than for other newer bridges. Further studies, with other spans, ages and importance level, may help to produce general guidelines for bridge maintenance, where corrosion is the major damaging factor, in Mexico.

Ang, A. De Leon, D. & Modeling and Analysis of Uncertainties for Risk-Informed Decisions in Infrastructures Engineering. *Journal of Structure and Infrastructure Engineering*, 1(1), 2005, 19–31.

REFERENCES

Agarwal, J. Protecting existing structures against unforeseen events, In: *Procs. of Applications of Statistics and Probability in Civil Engineering*, Der Kiureghian, Madana & Pestana (eds), Millpres, Netherlands, 2003, 775–780.

Probabilistic estimation of seismic fragility parameters for deteriorated reinforced concrete bridges

A. Alipour, B. Shafei & M. Shinozuka

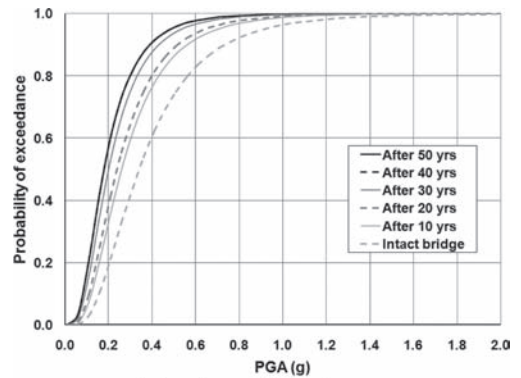
Department of Civil and Environmental Engineering, The Henry Samueli School of Engineering,
University of California, USA

ABSTRACT: Chloride-induced corrosion in Reinforced Concrete (RC) bridges is a mechanism caused by the intrusion of chloride ions into concrete. This mode of corrosion is more probable when RC bridges are located in coastal regions and exposed to aggressive environmental conditions. Because of the penetration of chloride ions in structural members, the chloride content of concrete gradually increases and when the concentration of chloride ions in the pore solution on the vicinity of reinforcing bar reaches a threshold value, the chloride-induced corrosion initiates.

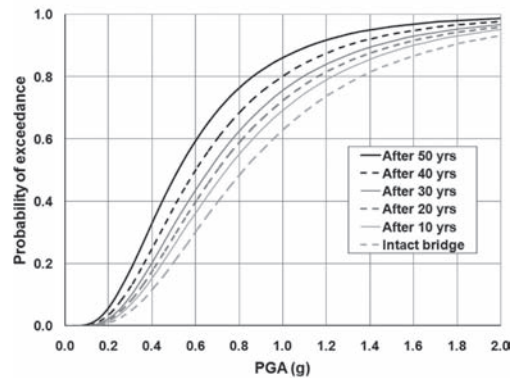
Chloride transport mechanism in concrete is a complex phenomenon that may occur in several forms, such as ionic diffusion, capillary suction, and permeation. The rate of this mechanism depends on the characteristics of concrete, degree of pore saturation, chloride binding capacity, free chloride content, and exposure conditions. By increasing the duration of time through which a bridge is exposed to aggressive conditions, the deterioration process of reinforcing bars can get relatively fast. This results in cracking or spalling of RC members and may lead to severe reduction in serviceability of bridges.

The time between corrosion initiation and serviceability failure is usually smaller than the required time for corrosion to initiate. Therefore, the realistic estimation of corrosion initiation time has a significant role in the accurate performance prediction of RC bridges over time. In the present paper, an integrated computational framework is proposed to simulate the penetration of chloride ions into concrete. Towards this goal, the effects of various parameters, such as water to cement ratio, ambient temperature, relative humidity, age of concrete, free chloride content, and chloride binding capacity, are considered to calculate the chloride content in different time intervals. It can be seen that by increasing the time during which a bridge is exposed to the aggressive conditions, the deterioration process of reinforcing bars can become relatively fast. This causes the cracking and spalling of the concrete in addition to reduction in the mass

and effective cross section of the reinforcing bars. Based on obtained results, structural performance of a set of short-, medium-, and long-span bridges with different structural attributes are evaluated using probabilistic lifetime fragility analysis over a life cycle of 30 years and the effects of variation in corrosion initiation time on the fragility parameters are investigated.



(a) at least slight damage state



(b) at least moderate damage state

Figure 1. Time-dependant fragility curves for deteriorated bridges under study.

Probabilistic bridge network life-cycle connectivity assessment and optimization

P. Bocchini & D.M. Frangopol

Department of Civil and Environmental Engineering, ATLSS Engineering Research Center Lehigh University, Bethlehem, PA, USA

Lifelines and, in particular, transportation networks play a critical role in the economy of any nation. Moreover, after the strike of extreme events, such as earthquakes and floods, the high resilience of the civil infrastructure systems is required for the prompt response of the emergency activities and for the recovery of the region in the following months. For these reasons, the research interest on this kind of network is rapidly increasing (Liu & Frangopol 2006, Gao et al., 2010, Golroo et al., 2010, Bocchini & Frangopol 2011b). In fact, even if the individual components of the network (e.g. bridges) need to be thoroughly designed, monitored, and maintained, it is the performance of the overall network that determines the major impact on the economy and the safety of a region subject to an extreme event (in terms of the ability to evacuate, bring help, and restore the socio-economic activities).

The reliability of the individual components of a network and, in turn, of the entire network itself is subject to degradation along its life-cycle. To contrast this unavoidable degradation, preventive and corrective maintenance actions are applied to the network components. The goal of the research presented in this paper is to develop a comprehensive numerical tool that assists the planning process for maintenance interventions on the bridges of a network. While previous papers (Bocchini & Frangopol 2011a, Bocchini et al., 2011) focused on the performance of the network in terms of its ability of distributing the traffic flows and avoiding traffic disruptions and congestions in an ordinary scenario, this paper focuses on *connectivity* as metric for the network performance. In fact, after an extreme event that disrupts the network, the prompt intervention and all the first aid activities rely on the possibility to reach every point of the region using the highway system.

The original results presented in this paper are based on a model for the simulation of the network traffic flow that accounts for the in/out of service state of the bridges and their correlation. The time-dependent reliability of the individual

bridges is also accounted for and its effect on the reliability profile (in terms of connectivity) of the entire network along the life-cycle is assessed.

The concepts of preventive (PM) and required maintenance (RM) are considered and integrated into the analysis. Preventive maintenance includes the interventions that are scheduled at predefined time instants and that are aimed at keeping the bridge performance at a high level all along the life-cycle. These interventions can be proficiently planned and optimized at the network level. Required maintenance (also called “corrective maintenance”) indicates the recovery actions and the minor interventions that are performed when a bridge has just reached a limit state or when it is going to reach a distress state imminently.

The design variables of the problem are the years of application of the preventive maintenance actions on each bridge of the network. If the maximum number of applications that are considered for each bridge is n_{MPM} and the number of bridges belonging to the network is n_B , the total number of design variables is $n_{MPM} \cdot n_B$.

The bridge network is described according to graph theory. The edges of the network represent the highway segments and their traffic flow capacity. Each edge is unidirectional, therefore each two-way highway segment is represented by two edges. Edges connect an origin node to a destination node and can be carried and/or overcrossed by bridges. The nodes represent the points of access to the network and they usually coincide with the cities and the points of change in the highway traffic flow capacity.

The first objective of the optimization is the maximization of the network connectivity. The proposed probabilistic analysis is based on simulation and the connectivity has to be computed for each sample, as well as for each considered time instant along the life—cycle. The connectivity matrix $C_i(t)$ of sample i at time t is an $n_N \times n_N$ matrix where each row represents an origin node and each column represents a destination node, n_N being the total number of nodes of the network.

Each element of the matrix is equal to 1 if it is possible to go from the relative origin node to the relative destination node; otherwise it is equal to 0. The value of the connectivity index $C_i(t)$ is then obtained as summation of all the elements of the matrix $C_i(t)$. Finally, the objective to be maximized $netconn$ is computed as:

$$netconn = \min_t \left[\frac{\sum_{i=1}^{n_S} C_i(t) - C^0}{C^{100} - C^0} \right] \quad (1)$$

where n_S is the total number of samples, C^{100} and C^0 are the values of the connectivity index when all the bridges are in service and out of service, respectively. The second objective of the optimization is the minimization of the total maintenance cost, including PM and RM on every bridge.

Several constraints are implemented in the analysis. The first is on the design variables: PM actions have to take place within a prescribed time horizon. Second, the total maintenance cost has to be less or equal to the available funding. Finally, the number of PM actions has to be lower or equal to a prescribed limit.

By means of genetic algorithms (GAs), the maintenance on the various individual bridges of the network can be prioritized and the optimal maintenance schedule can be found. The objectives of the optimization are in general conflicting. For instance the minimization of the total maintenance cost would lead to opposite choices with respect to the optimization of the network performance. For this reason, multi-objective GAs provide a whole front of Pareto-optimal solutions among which decision makers can choose the one that better fits the needs of the region, according to economic constraints and engineering judgment.

The large amount of uncertainty involved in the problem at hand (i.e. time-dependent reliability of the network, effects of the maintenance actions, correlation among the bridge in/out of service states) is accounted for using stochastic models, Latin hypercube sampling, and random field simulation.

The transportation network shown in Fig. 1 is used to validate the proposed approach and the resulting Pareto-optimal front is shown in Fig. 2. The numerical application shows that the proposed methodology identifies the best maintenance strategy in terms of both schedule and number of interventions. Moreover, the most important bridges are automatically identified and the available funding is allocated accordingly.

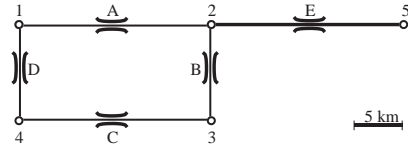


Figure 1. Transportation network layout. Numbers indicate nodes (i.e. cities), segments indicate highway segments, and letters indicate bridges.

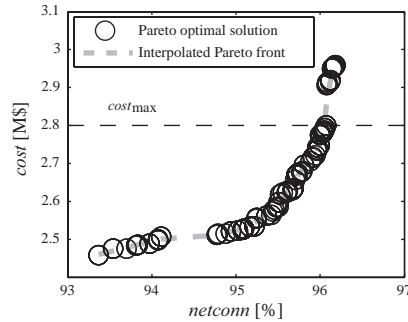


Figure 2. Pareto front. Each circle represents a PM schedule for each bridge of the network. Solutions that yield a cost above the threshold denoted by $cost_{max}$ are not feasible.

REFERENCES

- Bocchini, P. & Frangopol, D.M. 2011a. A probabilistic computational framework for bridge network optimal maintenance scheduling. *Reliability Engineering and System Safety*, 96(2), 332–349.
- Bocchini, P. & Frangopol, D.M. 2011b. A stochastic computational framework for the joint transportation network fragility analysis and traffic flow distribution under extreme events. *Probabilistic Engineering Mechanics*, 26(2), 182–193.
- Bocchini, P., Frangopol, D.M. & Deodatis, G. 2011. Computationally efficient simulation techniques for bridge network maintenance optimization under uncertainty. In *Computational Stochastic Mechanics (Deodatis & Spanos eds.)*, (pp. 93–101). Research Publishing Services, Singapore, in press.
- Gao, L., Xie, C. & Zhang, Z. 2010. Network-level multi-objective optimal maintenance and rehabilitation scheduling. In *Proceedings of the 89th Annual Meeting of the Transportation Research Board of the National Academies*, Washington, DC, USA.
- Golroo, A., Mohaymany, A.S. & Mesbah, M. 2010. Reliability based investment prioritization in transportation networks. In *Proceedings of the 89th Annual Meeting of the Transportation Research Board of the National Academies*, Washington, DC, USA.
- Liu, M. & Frangopol, D.M. 2006. Optimizing bridge network maintenance management under uncertainty with conflicting criteria: Life-cycle maintenance, failure, and user costs. *J of Struct Eng, ASCE*, 132(11), 1835–1845.

Life-cycle analysis of embodied energy for aging bridges subject to seismic hazards

Jayadipta Ghosh, Citlali Tapia & Jamie E. Padgett

Department of Civil and Environmental Engineering, Rice University, Houston, TX, USA

ABSTRACT: The deteriorating health of existing bridge infrastructure indicates the potential increased risk of structural damage not only under operational but also extreme loading conditions, such as seismic events. Such damage results not only in threats to public safety or economic consequences, but also requires an increased amount of energy spent on subsequent repair, restoration, or replacement, as well as rerouting of traffic. In recent years there has been an increasing interest in the life-cycle analysis of infrastructure, for managing infrastructure systems, prioritizing investments, and selecting upgrades. These analyses of lifetime cost, energy usage, or emissions typically neglect the contribution of extreme events. Furthermore natural hazard risk mitigation planning has evolved independently, without explicit consideration of many of these impact metrics. However, the required additional energy usage from natural hazard damage, such as earthquake damage, conflicts with goals of sustainable bridge and transportation infrastructure adopted by many US departments of transportation, and its quantification can aid in rational prioritization and selection of seismic retrofit cognizant of energy expenditures.

This paper poses a framework to probabilistically estimate life-cycle embodied energy associated with seismic risk, while considering the time-evolving fragility of aging bridge systems (Figure 1). The scope

of the embodied energy estimation includes the risk of energy expenditure from labor and materials used for bridge repair or replacement due to seismic exposure. A non-homogeneous Poisson process model is introduced to assess the cumulative risk of embodied energy usage involved in the repair processes along the service life of the aging bridge. This model integrates hazard potential, bridge vulnerability or fragility curves, and probabilistic repair models and their associated embodied energy estimates. In contrast to the typical assumption of constant seismic fragility, time-dependent fragility curves are developed to capture the effects of continued corrosion deterioration of multiple bridge components considered in the life-cycle analysis.

A case study is presented for representative multiple span continuous steel girder bridges to evaluate the embodied energy of the corroded bridge system given lifetime exposure to seismic hazards (Figure 2). Along with the net values of life cycle estimates, the contribution of major repair items are also evaluated as shown in Table 1.

Although the decreasing of total embodied energy should be addressed for these major

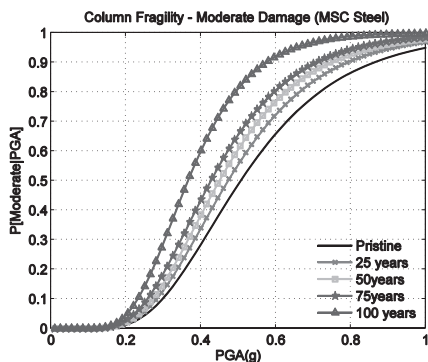


Figure 1. Time-dependent fragility curves for deteriorating bridge columns.

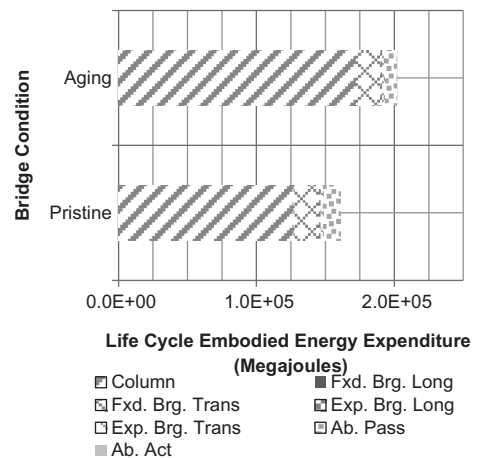


Figure 2. Expected values of life-cycle embodied energy for pristine and aging MSC steel bridge.

Table 1. showing contribution of major repair/ replacement procedures to life-cycle embodied energy.

Repair procedure	Bridge condition	Embodied energy (MJ)	% Contribution
Column replacement	Pristine	4.29×10^3	2.6%
	Aging	4.55×10^3	2.25%
Fixed bearing replacement	Pristine	1.21×10^3	0.75%
	Aging	1.29×10^3	0.63%
Expansion bearing replacement	Pristine	1.91×10^4	12%
	Aging	1.91×10^4	9.5%
Demolish and replace bridge	Pristine	1.33×10^5	82.8%
	Aging	1.74×10^5	86.3%

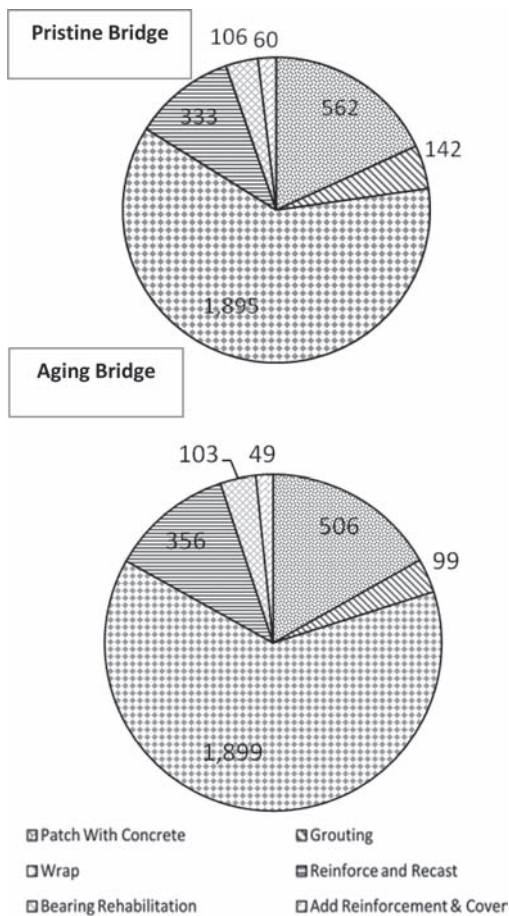


Figure 3. Contribution of localized repair procedures to the life-cycle embodied energy (MJ).

repair procedures, greater effort should be placed on making more commonly performed localized minor repairs—such as grouting and wrapping—sustainable. This is as shown in Figure 3 for localized repair procedures which contribute the most to life-cycle embodied energy estimates.

The case study findings highlight the importance of capturing the time evolving deteriorated structural condition when evaluating the expected embodied energy estimates, as well as the impact of uncertainty propagation in the life-cycle analysis and effect of variation of input models on the distribution of lifetime energy usage. Given the ongoing need to develop indicators to measure the level of sustainability of a structure, system, or region, the proposed framework is also anticipated to help guide the selection of rehabilitation or retrofit measures for bridge infrastructure based on target sustainability metrics related to energy usage.

REFERENCES

- Alcorn, Andrew, Embodied Energy and CO2 Coefficients for New Zealand Building Materials, Centre for Building Performance Research Report, March 2003.
- ASCE. (2009). "ASCE: Infrastructure Fact Sheet." <http://www.infrastructurereportcard.org/sites/default/files/RC2009_bridges.pdf>
- Ghosh, J. & Padgett, J.E. (2010). "Aging Considerations in the Development of Time-Dependent Seismic Fragility Curves." *Journal of Structural Engineering*, In Press doi:10.1061/(ASCE)ST.1943-541X.0000260.

This page intentionally left blank

*MS_215 — Maintenance and safety
of aging infrastructure (1)*

This page intentionally left blank

Reliability analysis of prestressed concrete bridges located in a marine environment

M. Akiyama

Tohoku University, Sendai, Miyagi, Japan

D.M. Frangopol

Lehigh University, Bethlehem, PA, USA

I. Yoshida

Tokyo City University, Tokyo, Japan

ABSTRACT: Corrosion may significantly influence the long-term performance of Reinforced Concrete (RC) and Prestressed Concrete (PC) structures, particularly in aggressive environments. Corrosion of reinforcement in concrete components may lead to loss of strength due to reduction in steel area and unserviceability. Reliability analysis includes probabilistic information from all resistance, loading and modeling variables influencing the assessment process and provides a rational criterion for the comparison of the consequences of decision making under uncertainty (Frangopol 2009). Therefore, it is necessary to assess the remaining safe and service life of deteriorating structures in aggressive environments using structural reliability theory.

For existing structures, the uncertainties associated with predictions can be reduced by the effective use of information obtained from visual inspections and field test data. This information helps engineers to improve accuracy on structural condition prediction. In addition, recently, novel monitoring techniques, such as instrumented-based non-destructive methods, have become more attractive. These techniques are based on the measurement of physical quantities in space and time and they provide, consequently, an objective and more realistic assessment of structural performance (Frangopol et al., 2008). The proper handling of the provided monitoring data is one of the main challenges in structural health monitoring. A necessary monitoring period and possible interruption period has to be investigated. Also, the advantage of structural health monitoring over simple inspection or manual measurements needs to be demonstrated.

This paper presents a probabilistic framework for estimating the time-dependent reliability for existing PC structures in a marine environment.

Since, non-Gaussian variables are usually involved in life-cycle reliability assessment of concrete structures, an approximate approach for updating is needed. In this study, nonlinear filtering technique denoted Sequential Monte Carlo Simulation (SMCS) is used (Yoshida 2009, Akiyama et al., 2010) as shown in Figure 1.

Chloride concentration distribution representing the relationship between the chloride content and the distance from concrete surface obtained by coring test is used as observational information in SMCS. Based on the manual measurement by concrete coring, a chloride penetration curve can be established. Meanwhile, probes for automatic monitoring of chloride penetration into concrete have been developed and adopted in real concrete structures (Gjørv 2009). This study assumes that chloride concentration at various depths below the concrete surface is provided by automatic monitoring.

Chloride concentration obtained by ordinary MCS is used as standard observational information. To consider the variability in time of measured chloride concentration, white Gaussian noise with a mean equal of 0.0 and a standard deviation of 0.5 or 5.0 is added to chloride concentration obtained by MCS. The reliability of PC bridge girders is updated under the following conditions.

- AMA: Automatic monitoring A (monitoring period = continuous during the lifetime of structure)
- AMB: Automatic monitoring B (monitoring period = one month, and time interval between monitorings T_m (interruption periods) = 1 year, 5 years, 10 years, or 15 years)
- MM: Manual measurement by concrete coring (time interval between inspections T_m = 1 year, 5 years, 10 years, or 15 years)

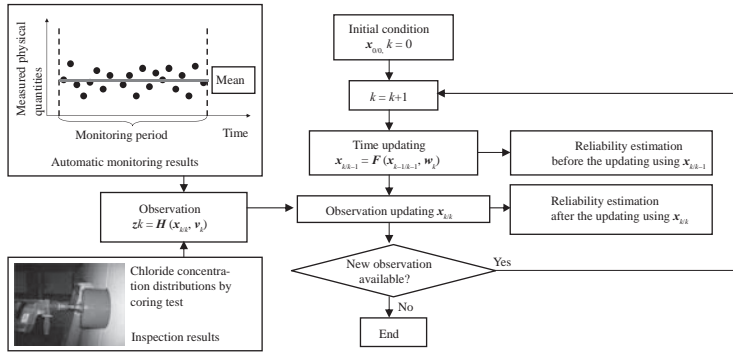


Figure 1. Flowchart of reliability estimation by SMCS using inspection or monitoring results.

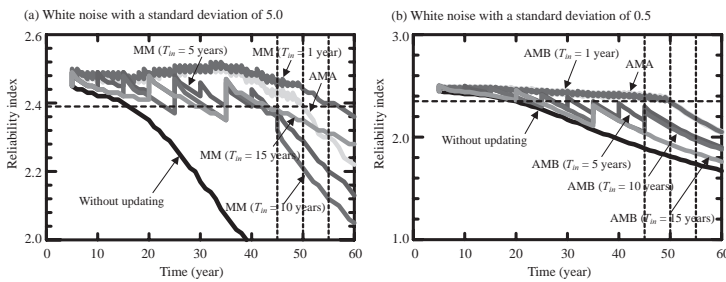


Figure 2. Effect of the time interval of automatic monitoring and manual measurement on time-dependent reliability of PC bridge girders.

The effect of the differences between manual measurement and automatic monitoring, time intervals, and the degree of variability of measured chloride concentrations on the time-dependent reliability of PC bridge girders is shown in Figure 2. When PC bridges are located in aggressive environments, structural performance decreases with time. To evaluate the time-dependent reliability accurately, updating of random variables using the inspection and/or monitoring results is needed.

If measured chloride concentrations include the large variability in time, reliability of PC bridge girder by manual measurement of coring test even with time interval of inspection of 1 year is very different from that by AMA. Since measured chloride concentrations during monitoring period (i.e., one month) in AMB are averaged and used as observational information, time-dependent reliability updated by AMB is insensitive to variability of chloride concentrations. However, time interval between monitorings T_{in} (interruption periods) needs to be very small to obtain the similar updated estimates of reliability as that provided by AMA. A lifetime cost optimization planning of structures requires the efficient application of monitoring in time (Frangopol & Liu 2007). Optimal time intervals between monitorings

(interruption periods) should be investigated based on the life-cycle cost under uncertainty.

REFERENCES

- Akiyama, M., Frangopol, D.M. & Yoshida, I. 2010. Time dependent reliability of existing RC structures in a marine environment using hazard associated with airborne chlorides. *Engineering Structures* 32: 3768–3779.
- Frangopol, D.M. 2009. Life-cycle performance, management, and optimization of structural systems under uncertainty: Accomplishments and challenges. Keynote paper. *Proceedings of the Tenth International Conference on Structural Safety and Reliability, ICOS-SAR2009*. Osaka, Japan.
- Frangopol, D.M. & Liu, M. 2007. Maintenance and management of civil infrastructure based on condition, safety, optimization, and life-cycle cost. *Structure and Infrastructure Engineering* 3(1):29–41.
- Frangopol, D.M., Strauss, A. & Kim, S. 2008. Use of monitoring extreme data for the performance prediction of structures: General approach. *Engineering Structures* 30: 3644–3653.
- Gjørv, O.E. 2009. Durability design of concrete structures in severe environments. Taylor & Francis. New York, USA.
- Yoshida, I. 2009. Data assimilation and reliability estimation of existing RC structure. *Computational Methods in Structural Dynamics and Earthquake Engineering 2009*, Rhodes, Greece: CD281.

Optimization of assessment strategies for aging bridges

A.D. Orcési

French Institute of Science and Technology for Transport, Development and Networks, Paris, France

D.M. Frangopol

Lehigh University, Bethlehem, PA, USA

Maintenance of aging bridges is a challenge for stakeholders since failure leads, most of the time, to drastic social, environmental and/or economic consequences. Under uncertainty and limited financial resources, bridge owners need efficient tools to decide when maintenance strategies should be applied (Estes & Frangopol 2001, Estes et al., 2004, Frangopol & Liu 2007, Orcesi et al., 2010, Orcesi & Cremona 2011, Orcesi & Frangopol 2011a,b, Frangopol 2011).

Choosing between preventive maintenance, essential maintenance and major rehabilitation is a crucial issue for aging bridges under uncertainties and financial constraints (Estes & Frangopol 1999, Orcesi & Frangopol 2011c,d). Optimal decisions on maintenance/rehabilitation have to be made based on accurate assessment of the structural performance. A model using lifetime functions to assess the probability of survival of aging bridges is proposed. The impact of inspecting the structure is modeled by updating the probability density function (PDF) of time to failure. Depending on the type of inspection, the uncertainty associated with the inspection result varies. Visual inspections are associated with greater uncertainties than in-depth inspections. Therefore, in the case of visual inspections, the information provided is less accurate and the updating of the PDF of time to failure is less effective. An event-tree based optimization procedure handling conflicting criteria is proposed. Expected inspection, maintenance and failure costs are minimized in a conflicting way. This methodology should enable to find the optimal lifetime inspection strategy for an aging bridge.

In this paper, the case of in-depth inspection related to the fatigue of steel girders is chosen as an illustrative example. In theory, only two outcomes are possible after each inspection: either the structural component survives or it has already failed. However, in practice, inspections are subject to various uncertainties and the probabilities of (i) non detection and (ii) false alarm have to be considered to fully characterize inspection outcomes. Figure 1

illustrates schematically this concept for each of the N inspections considered during the service life of a structure. At each inspection, four feasible alternatives are considered. Indeed, inspection of a bridge component can indicate (Orcesi and Frangopol 2011b) no damage when there is no damage (branch 1), damage when there is no damage (branch 2), no damage when there is damage (branch 3), and finally damage when the component is damaged (branch 4).

By repeating the analysis shown in Figure 1 for each of the inspection times, the event-tree analysis can be conducted for the N inspections during the service life of the structure.

It is noted that branches 1 and 3 in Figure 1 are associated with a probability of false alarm (PoFA) and a probability of no detection, respectively (Orcesi & Frangopol 2011b). Considering the specific case of flaws detection in fatigue steel details, the probability of no detection can be due to human error in case of a visual inspection (VI). When considering in-depth inspection such as

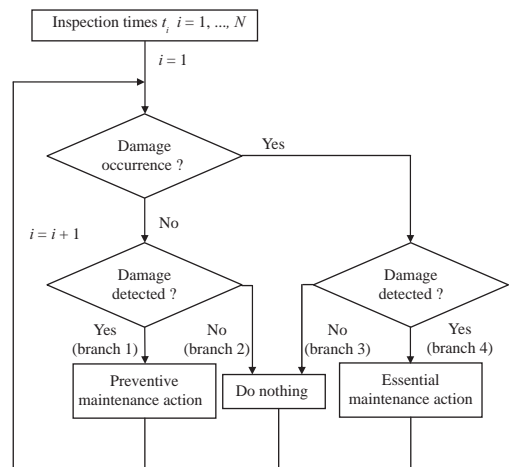


Figure 1. Event-tree based framework for bridge component inspections.

magnetic particle inspection (MPI) and ultrasonic inspection (UI), the probabilities of no detection and false alarm can be quantified by considering the probability of detection (PoD) curves for different types of inspections as proposed by (Chung et al., 2006).

The objective of the optimization process is to determine optimal inspection times and types (assumed herein to be no inspection (NI), VI, MPI and UI). A bi-objective optimization process is considered to minimize both the sum of the expected inspection and rehabilitation costs (denoted $E[C_{m,1}]$) and the sum of the expected failure and preventive maintenance costs (denoted $E[C_{m,2}]$). Optimal solutions are Pareto solutions obtained by using genetic algorithms. The bridge considered in the illustrative example is a reinforced concrete slab supported by nine standard-rolled, compact steel girders. The benefit of preventive maintenance (PM) is clearly demonstrated. This is due to the fact that the expected cost of failure is dramatically decreased when PM is applied. Also, the impact of probabilities of false alarm on the maintenance decision is investigated.

The framework proposed in this paper enables to determine optimal inspection strategies for fatigue details of steel bridges. Several inspection types are considered and optimal inspection strategies are determined. In this paper, the impact of probabilities of false alarm on the maintenance decision is investigated and the benefit of preventive maintenance is shown. It is noted that this model is practical and does not require expensive computational time. It is a promising approach for bridge owners who need efficient management tools. It is also noted that the approach can be adapted to degradation phenomena which are different from the fatigue of steel details.

ACKNOWLEDGEMENT

The support from (a) the National Science Foundation through grant CMS-0639428, (b) the Commonwealth of Pennsylvania, Department of Community and Economic Development, through the Pennsylvania Infrastructure Technology Alliance (PITA), (c) the U.S. Federal Highway Administration Cooperative Agreement Award DTFH61-07-H-00040, and (d) the U.S. Office of Naval Research Contract Number N-00014-08-0188 is gratefully acknowledged. The opinions and conclusions presented in this paper are those of the authors and do not necessarily reflect the views of the sponsoring organizations.

REFERENCES

- Chung, H.-Y., Manuel, L. & Frank, K.H. 2006. Optimal Inspection Scheduling of Steel Bridges Using Non-destructive Testing Techniques. *Journal of Bridge Engineering*, ASCE, 11(3): 305–319.
- Estes, A.C. & Frangopol, D.M. 1999. Repair optimization of highway bridges using system reliability approach. *Journal of structural Engineering*, ASCE, 125(7): 766–775.
- Estes, A.C. & Frangopol, D.M. 2001. Minimum expected cost - oriented optimal maintenance planning for deteriorating structures: Application to concrete bridge decks. *Reliability Engineering & System Safety*, Elsevier, 73(3): 281–291.
- Estes, A.C., Frangopol, D.M. & Foltz, S.D. 2004. Updating reliability of steel miter gates on locks and dams using visual inspection results. *Engineering Structures*, Elsevier, 26(3): 319–333.
- Frangopol, D.M. 2011. Life-Cycle Performance, Management, and Optimization of Structural Systems under Uncertainty: Accomplishments and Challenges. *Structure and Infrastructure Engineering*, Taylor and Francis (eds), 7(6): 389–413.
- Frangopol, D.M. & Liu, M. 2007. Maintenance and management of civil infrastructure based on condition, safety, optimization and life-cycle cost. *Structure and Infrastructure Engineering*, Taylor and Francis (eds), 3(1): 29–41.
- Orcesi, A.D. & Cremona, C.F. 2011. Optimization of Maintenance Strategies for the Management of the National Bridge Stock in France. *Journal of Bridge Engineering*, ASCE, 16(1): 44–52.
- Orcesi, A.D. & Frangopol, D.M. 2011a. Optimization of bridge maintenance strategies based on structural health monitoring information. *Structural Safety*, Elsevier, 33(1): 26–41.
- Orcesi, A.D. & Frangopol, D.M. 2011b. The Use of Lifetime Functions in the Optimization of Nondestructive Inspection Strategies for Bridges. *Journal of Structural Engineering*, ASCE, doi:10.1061/(ASCE)ST.1943-541X.0000304, 137(4), in press.
- Orcesi, A.D. & Frangopol, D.M. 2011c. Probability-Based Multiple-Criteria Optimization of Bridge Maintenance Using Monitoring and Expected Error in the Decision Process. *Structural and Multidisciplinary Optimization*, Springer, 2010, doi:10.1007/s00158-010-0613-8 (in press).
- Orcesi, A.D. & Frangopol, D.M. 2011d. A stakeholder probability-based optimization approach for cost-effective bridge management under financial constraints. *Engineering Structures*, Elsevier, doi:10.1016/j.engstruct.2010.12.035 (in press).
- Orcesi, A.D., Frangopol, D.M. & Kim, S. 2010. Optimization of bridge maintenance strategies based on multiple limit states and monitoring. *Engineering Structures*, Elsevier, 32(3): 627–640.

Improved bridge capacity rating methods based on system reliability assessment

N. Wang, B.R. Ellingwood & A.-H. Zureick
Georgia Institute of Technology, Atlanta, Georgia, USA

ABSTRACT: Condition assessment and safety verification of existing bridges may be prompted by changes in traffic patterns; concern about faulty building materials or construction methods; discovery of a design/construction error after the structure is in service; concern about deterioration discovered during routine inspection; and damage following extreme load events. Condition assessment and decisions as to whether a bridge requires posting currently are addressed through analysis, load testing, or a combination of these methods. In the United States, the rating process is described in the American Association of State Highway and Transportation Officials (AASHTO) *Manual for Bridge Evaluation, First Edition* (AASHTO 2008), which permits ratings to be determined through allowable stress, load factor, or load and resistance factor methods, the latter of which is keyed to the AASHTO *LRFD Bridge Design Specifications, Fourth Edition* (AASHTO, 2007) and has a reliability basis (Minervino et al., 2004). These three rating methods may lead to different rated capacities and posting limits for the same bridge (Wang et al., 2009), a situation that cannot be justified from a professional engineering viewpoint and one that has potentially serious implications with regard to the safety of the public and the economic well-being of businesses and individuals who may be affected by bridge postings or closures. The economics of bridge upgrading or posting makes it imperative to determine condition assessment criteria and methods (either by analysis or by testing) that are tied in a rational and quantitative fashion to public safety and functional objectives.

This paper summarizes a recently completed multi-year coordinated research program of bridge analysis and load testing aimed at improving the current bridge rating process using structural reliability methods (Ellingwood et al., 2009). A sample of bridges with steel or reinforced concrete girders that are typical of those that are candidates for possible posting, with ages ranging from 20 to 50 years, were selected from the Georgia bridge management system database (these bridges are believed to be typical of non-interstate bridges

in regions of low seismicity in North America). Finite element models of these bridges were developed; subsequently, the bridges were instrumented and load-tested to validate their finite element modeling (O'Malley et al., 2009). Following the analysis and validation phase, these bridges were used in a system reliability analysis. Virtual load tests were conducted using the finite element models to determine the fragility of typical older bridge systems designed using what would now be considered archaic (and inadequate) loads. The uncertainties associated with material properties, dimensions and modeling error were propagated through the FE analysis using Monte Carlo simulation with Latin Hypercube Sampling. It was found that such bridges typically have capacities that are substantially in excess of what the AASHTO rating procedures would indicate. Moreover, their reliability indices in the *in situ* condition may equal or exceed the reliability targets stipulated for new bridges in the AASHTO *LRFD Bridge Specifications* (AASHTO 2007). These reliability analyses suggest that many older bridges are posted unnecessarily. The research program has led to several recommendations for improvements in current bridge rating methods that facilitate the incorporation of *in situ* test data in the rating process in a format that is consistent with the LRFR option in the *Manual for Bridge Evaluation* (AASHTO 2008).

REFERENCES

- American Association of State Highway and Transportation Officials 2007. *AASHTO LRFD Bridge Design Specifications, 4rd Edition*. American Association of State Highway and Transportation Officials, Washington, DC.
- AASHTO Highways Subcommittee on Bridges and Structures (2008). *Manual for Bridge Evaluation, First Edition*. American Association of State Highway and Transportation Officials, Washington, DC.
- Ellingwood, B.R., Zureick, A.-H., Wang, N. & O'Malley, C. 2009. Condition assessment of existing bridge structures, Task 4 - State of the art of bridge condition assessment. *Report of GDOT Project RP 05-01*. Georgia Department of Transportation, Atlanta, GA.

- Minervino, C., Sivakumar, B., Moses, F., Mertz, D. & Edberg, W. 2004. New AASHTO guide manual for load and resistance factor rating of highway bridges, *Journal of Bridge Engineering*, 9(1): 43–54.
- O'Malley, C., Wang, N., Ellingwood, B.R. & Zureick, A.-H. 2009. Condition assessment of existing bridge structures: Report of Tasks 2 and 3 - Bridge Load Testing Program. *Report of GDOT Project RP 05-01*. Georgia Department of Transportation, Atlanta, GA.
- Wang, N., Ellingwood, B.R., Zureick, A.-H. & O'Malley, C. 2009. Condition assessment of existing bridge structures: Report of Task 1 – Appraisal of state-of-the-art of bridge condition assessment. *Report of Project GDOT No. RP05-01*, Georgia Department of Transportation, Atlanta, GA.

Reliability assessment and life prediction for serviceability of concrete bridges

D.-G. Lu, W. Jiang, X.-P. Fan & Y.-X. Yang
 Harbin Institute of Technology, Harbin, China

1 INTRODUCTION

Aging reinforced concrete bridges have been subjected to not only in-service loading but also an aggressive environment. These may cause the degradation of structural resistance, and affect not only the safety of the bridges, but also their serviceability characterized by concrete cracking and the excessive member deflection. Many of existing reinforced concrete bridges in China have been in the ill condition state due to concrete carbonation and reinforcement corrosion. Owing to the social needs for using these existing bridges, especially for the public and transportation safety, it is very urgent to assess the safety and serviceability, to predict the remaining service life and to monitor the health of some key bridges.

In this paper, the time-dependent reliability of deteriorated reinforced concrete bridges for the serviceability limit states is analyzed based on the original design situations and the inspection data. The first-passage probability method is utilized to calculate the reliability index for the concrete crack limit state and member deflection limit state. The hazard curves for the two limit states mentioned above also are obtained, as shown in Figure 1. The service load reference period for assessment is determined by the principle of equal exceedance probability, and then, the target reliability index in service is derived from the target reliability index in design according to the principle of equal exceedance probability and the service load reference period. The calculated time-dependent reliability index is compared to the target reliability index in service to check if the bridge is in the serviceability state or not, as shown in Figure 2. Finally, the time for the concrete girders to be unserviceable due to concrete crack and member deflection is predicted based on the design and inspection data. The results of this study can be used to aid bridge engineers and asset managers to develop a risk-informed and cost-effective strategy in the management of corrosion-affected concrete bridges.

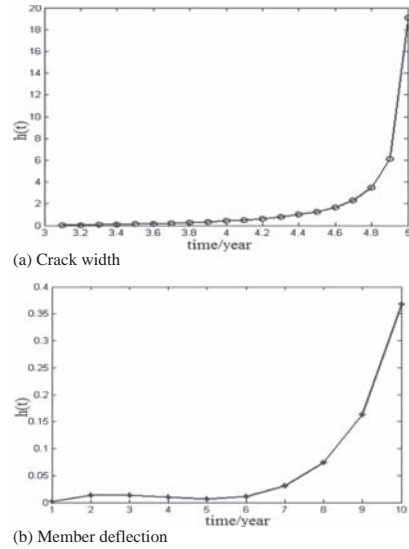


Figure 1. Hazard function curves of serviceability.

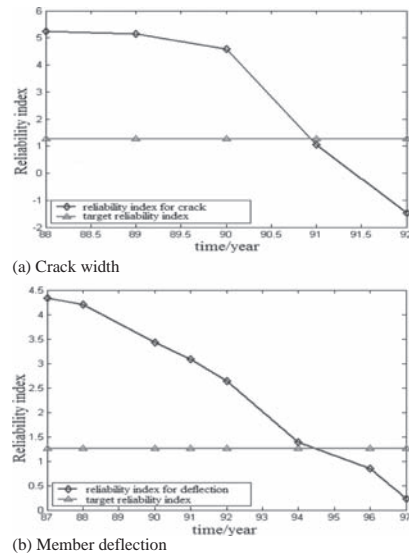


Figure 2. Reliability assessment of serviceability.

REFERENCES

- Akgul, F. & Frangopol, D.M. 2005. Lifetime performance analysis of existing reinforced concrete bridges. I: Theory. *Journal of Infrastructure Systems*, 11(2): 122–128.
- Akgul, F. & Frangopol, D.M. 2005. Lifetime performance analysis of existing reinforced concrete bridges. II: Application. *Journal of Infrastructure Systems*, 11(2): 129–141.
- Ciampoli, M. 1998. Time dependent reliability of structural systems subject to deterioration. *Computers & Structures*, 67: 29–35.
- Enright, M.P. & Frangopol, D.M. 1998. Service-life prediction of deteriorating concrete bridges. *Journal of Structural Engineering*, 124(3): 309–317.
- Enright, M.P. & Frangopol, D.M. 1999. Reliability-based condition assessment of deteriorating concrete bridges considering load redistribution. *Structural Safety*, 21: 159–195.
- Gonzalez, J.A. et al. 1996. Some questions on the corrosion of steel in concrete. Part two: Corrosion mechanism and monitoring, service life prediction and protection methods. *Material Structural*, 29: 97–104.
- Gong, J.X. & Zhao, G.F. 1999. Reliability analysis for deteriorating structures. *Chinese Journal of Building Structures*, 19(5): 43–51. (in Chinese).
- Li, C.Q. 1995. Computation of the failure probability of deteriorating structural systems. *Computers & Structures*, 56(6): 1073–109.
- Li, C.Q. et al. 2005. Time-dependent reliability method to assess the serviceability of corrosion-affected concrete structures. *Journal of Structural Engineering*, 131(11): 1674–1680.
- Melchers, R.E. 1999. *Structural Reliability Analysis & Prediction* (Second Edition). *John Wiley & Sons*.
- Mori, Y. & Ellingwood, B.R. 1993. Reliability-based service-life assessment of aging concrete structures. *Journal of Structural Engineering*, 119(5): 1600–1621.
- Vu, K.A.T. & Stewart, M.G. 2000. Structural reliability of concrete bridges including improved chloride-induced corrosion models. *Structural Safety*, 22: 313–333.

*MS_225 — Maintenance and safety
of aging infrastructure (2)*

This page intentionally left blank

Using information criteria to classify damage states for structural health monitoring

H. Noh, A.C. Cheung & A.S. Kiremidjian
Stanford University, Stanford, CA, USA

1 INTRODUCTION

The ability to detect damage in a structure using remote sensors has far-reaching ramifications for structural engineering (Chang 2007). Real-time detection of damage would allow for substantial savings in maintenance costs as well as increased performance and safety. In addition, following a major catastrophe such as an earthquake, structural health monitoring would allow emergency response and repair crews to focus immediately on the most heavily damaged structures.

One method to detect damage is to apply statistical pattern recognition methods to structural responses to ambient vibrations and extract a damage sensitive feature (DSF) whose value migrates as the damage occurs to the structure. Nair et al. (2006) showed that autoregressive (AR) coefficients extracted from structural acceleration responses are suitable DSFs. Structural responses are collected from the structure in various damage states including undamaged state. The DSFs extracted from the undamaged structure is referred to as baseline. Then, the number of clusters in the mixed set of DSFs is identified as the number of damage states present in the data set. In general, determining the optimum number of clusters present in a given data set is a difficult problem.

In this paper, we investigate methods using different information criteria, including Akaike information criteria (AIC), AIC3, minimum description length (MDL), and Olivier et al.'s φ_β criterion, for clustering DSF values into each damage state. We hypothesize that there will be one cluster of DSFs for each damage scenario plus the baseline case. Then those methods are applied to both simulated data and field data in order to compare their performance. Among the investigated information criteria, the criterion developed by Olivier et al. (1999) performed most accurately for estimating the number of damage states in the data set.

2 THEORY

A good estimator for the optimal number of clusters must balance closely fitting the model to the

data and reducing the complexity of the model. To prevent over-fitting, a penalty term is added to the optimization function. The information criteria considered in this paper are based on the likelihood function of the model plus some penalty term. We can calculate the optimal number of clusters by minimizing the information criteria over the number of estimated clusters. The four information criteria that we investigate in this paper are defined as follows.

The Akaike information criterion (AIC), which is given by Akaike (1973) as

$$AIC(k) = -2 \times (\log - \text{likelihood}) + 2 \times k \quad (1)$$

where k is the number of estimated clusters. However, as the $-2 \times (\log - \text{likelihood})$ result becomes larger, the penalty term becomes increasingly insignificant. For large data sets, there is a high probability that the log-likelihood values will grow large.

Bozdogan (1993) argued that the penalty factor of 2 is not correct for finite mixture model based on the asymptotic distribution of the likelihood ratio for comparing two models with different parameters. Instead, he suggested using 3 as the penalty factor. This information criterion is referred to as AIC3.

The idea of using the minimum description length (MDL) for model selection was developed by Rissanen (1978). As the estimation error, he used the length of the Shannon-Fano code for the data, which implies the complexity of the data given a model in information theory. The idea is to choose the model that results in the minimum description length (or the minimum of the combination of the model complexity and the estimation error). MDL uses $k \log(\sqrt{n})$ as the penalty where, n is the number of data. It is assumed that $\log(\sqrt{n})$ represents the precision for each parameter of any given model.

Olivier et al. (1999) developed a new information criterion, φ_β , which is given as

$$\varphi_\beta(k) = -2 \times \left(\begin{array}{l} \text{conditional log - likeli-} \\ \text{hood given parameters} \end{array} \right) + kn^\beta \log(\log(n)) \quad (2)$$

where n is the total number of points in the data set and $0 < \beta < 1$ is a parameter that is input by the user to scale the information criterion. Olivier et al. (1999) derived desirable lower and upper bounds for β , which are

$$\frac{\log(\log(n))}{\log(n)} < \beta < 1 - \frac{\log(\log(n))}{\log(n)} \quad (3)$$

3 VALIDATION

These information criteria are first applied to a set of simulated data to verify their performance, and then applied to two sets of field data collected from the structures subjected to systematically increasing extent of damage.

The results for numerically simulated data are shown in Figure 1. $\varphi_{\beta, \min}$, $\varphi_{\beta, \text{avg}}$, and $\varphi_{\beta, \text{max}}$ corresponds to φ_{β} criteria with different β values—lower bound, average of lower and upper bound, and upper bound, respectively. For comparison, $-2 \times (\log\text{-likelihood})$ values are also shown in Figure 1. In general, the φ_{β} criterion with $\beta = 0.3$ or 0.4 produces reasonable results.

Two different structures undergoing progressive damage tests are considered. The first is the Z24 Bridge in Switzerland subjected to settlement in one pier. The other is a three-story benchmark steel frame in Taiwan subjected to the reduced flange width of the ground floor columns. Only the results for the Taiwanese benchmark structure are presented in this abstract. Figure 2 shows the values of various information criteria over cluster estimates of 1 through 5. The result of AIC is very similar to that of AIC3, thus omitted in the figure for simplicity. The AIC3, MDL, and φ_{β} with β set at its lower bound are not significantly different than the $-2 \times (\log\text{-likelihood})$, and all of them overestimate the number of clusters. On the other hand, setting β at its upper bound penalizes additional complexity too harshly and, as a result, underestimates the

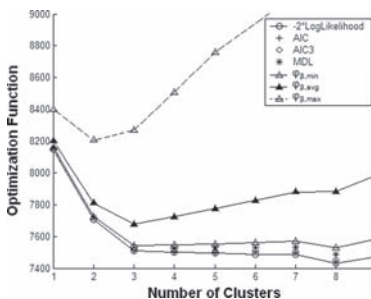


Figure 1. Estimated optimum number of clusters for simulated data using different information criteria.

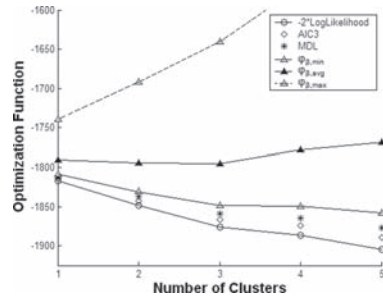


Figure 2. Estimated optimum number of clusters for Taiwanese benchmark structure.

number of clusters. However, using an average of the upper and lower bounds for β to compute φ_{β} results in a minimum value for three clusters, which is the true number of damage scenarios.

4 CONCLUSIONS

Olivier et al.'s φ_{β} criterion works noticeably better than other similar information criteria in identifying optimal number of clusters for both simulated and field data. However, identifying a suitable β parameter is important. We conclude that taking an average of the upper and lower bound is a good starting point for β , and this method works well in identifying the number of clusters.

REFERENCES

Akaike, H. 1973. Information theory and an extension of the maximum likelihood principle. In B.N. Petro & F. Csaki (eds), *Second International Symposium on Information Theory*: 267–281. Budapest: Akademiai Kiado.

Bozdogan, H. 1993. Choosing the number of component clusters in the mixture-model using a new information complexity criterion of the inverse Fisher information matrix. In O. Opitz, B. Lausen & R. Klar (eds.), *Information and Classification, Concepts, Methods and Applications*: 40–54. Berlin: Springer.

Chang, F.-K. (ed.) 2007. *Proceedings of the 6th International Workshop on Structural Health Monitoring, Stanford, 11–13 September 2007*. Lancaster: DEStech Publications.

Nair, K.K., Kiremidjian, A.S. & Law, K.H. 2006. Time Series-Based Damage Detection and Localization Algorithm with application to the ASCE Benchmark Structure. *Journal of Sound and Vibration* 291(2): 349–368.

Olivier, C., Jouzel, F., & EL Matouat, A. 1999. Choice of the number of component clusters in mixture models by information criteria. *Proceedings of the 12th conference on Vision Interface, Trois-rivieres, Canada, 18–21 May 1999*.

Rissanen, J. 1978. Modeling by the shortest data description. *Automatica* 14: 465–471.

A Bayesian approach to the assessment of fracture toughness of reactor components

M.D. Pandey & M. Wang

University of Waterloo, Waterloo, ON, Canada

ABSTRACT: Zirconium alloys are susceptible to a stable cracking process called delayed hydride cracking (DHC), which can compromise the integrity of pressurized components in the nuclear reactor. For example, pressure tubes in CANDU¹ reactors are susceptible to DHC when hydrogen concentration in the alloy exceeds a threshold in the vicinity of stress raisers, such as flaws or cracks (Sagat et al., 1994). Fracture mechanics based models and experimental data have shown that the DHC initiation takes place when the applied stress intensity at a stress raiser exceeds a threshold value, denoted as K_{IH} . This is also referred to as DHC initiation toughness of zirconium alloy, an intrinsic material property that provides protection against the DHC of flaws in the zirconium alloy.

The DHC initiation toughness, like any other toughness related material property, exhibits considerable variability due to micro-structural variations, effect of neutron irradiation and operation temperature (Pandey and Radford 2008). In order to monitor variability and possible changes over time, material surveillance programs are adopted by the nuclear industry. As an example, a surveillance pressure tube is removed at a 5–10 year interval from an operating reactor and fracture toughness related properties, such as K_{IH} , are evaluated (CSA 2005).

The assessment of material property data obtained from testing of specimens taken from a surveillance pressure tube is considered satisfactory, so long as K_{IH} exceeds a lower bound specified by the CSA Standard N285.8 [Clause D.6.2], such as

$$K_{IH} = \begin{cases} 4.5 \text{ MPa}\sqrt{\text{m}} & \text{(radial-axial direction)} \\ 15.0 \text{ MPa}\sqrt{\text{m}} & \text{(radial-transverse direction)} \end{cases} \quad (1)$$

The variability in K_{IH} is evident from experimental data collected from surveillance pressure tubes removed from various CANDU reactors in Canada over the past several years (Sagat et al., 1994), as shown in Section 2.

The current deterministic approach to define the lower bound and assess K_{IH} from data is somewhat restrictive, as it does not account for variability associated with K_{IH} in a logical manner. Therefore, the industry and the regulator are interested in developing a probabilistic definition and interpretation of lower bound K_{IH} .

The next important task is the interpretation of new material surveillance data, collected from operating reactors, in relation to the defined lower bound. Material surveillance data are typically obtained from the testing of samples taken from components removed from the reactor. Since fracture toughness is considered as a random variable, reasonable variability in the test data is anticipated. Although new data are mostly expected to exceed the lower bound, there is a possibility that a few data points could be lower than the lower bound K_{IH} . This is reasonable, since a random variable can take any value in its entire range. Thus, a few low values of K_{IH} cannot be considered to invalidate the lower bound, rather new information should be used to revise the confidence associated with it. Actual value of lower bound should be revised, only when the associated confidence level has severely eroded by new sample of data.

The paper proposes that the lower bound should be defined as X_{qp} , which is a q th percentile of the fracture toughness (X) distribution estimated at a p th confidence level. The interpretation of the lower bound is that the fracture toughness (K_{IH}) in the population is expected to exceed the lower bound X_{qp} with probability $(1-q)$. Furthermore, the lower bound should be estimated from a sample of data at p % confidence level. For example, $X_{10/95}$ means 10% of the population is expected to have X less than this value and there is a 95% confidence associated with the sample estimate of lower bound. In other words that if several samples are drawn and lower bound estimated from each sample, 95% of estimated lower bounds will exceed the value of $X_{10/95}$. Conceptually, this definition is similar to that of the “best estimate” used in probabilistic risk analysis (PRA) literature in the nuclear engineering.

The objectives of this paper are to (1) propose the definition and method of estimation of the

¹CANada Deuterium Uranium, trademark of Atomic Energy of Canada Limited.

lower bound threshold fracture toughness (K_{III}), (2) develop a Bayesian method to update the lower bound and evaluate its sensitivity to potential new values, and (3) prepare control charts that can be used for fitness for service disposition of new data.

The paper presents a probabilistic definition of the lower bound K_{III} , and its Bayesian interpretation to address both aleatory and epistemic uncertainties. The paper proposes a new method to update the lower bound K_{III} as new surveillance data become available from the testing of components removed from operating reactors. A concept of a control chart is introduced to support the disposition of new surveillance data. The main advantage of the proposed approach is that it provides a practical, risk-informed basis for fracture toughness assessment of pressurized components. The proposed method is generic, and it can be

applied to assessment of civil and mechanical engineering structures and components.

REFERENCES

- Canadian Standard Association (2005). Technical Requirements for In-Service Evaluation of Zirconium Alloy Pressure Tubes in CANDU Reactors. CSA – N285.8.[4].
- Pandey, M.D. and Radford, D.D. (2008). A Statistical Approach to the Prediction of Pressure Tube Fracture Toughness. *Int. J. Nuclear Engineering and Design*, 238(12), 3218–3226.
- Sagat, S., Coleman, C.E., Griffiths, M. and Wilkins, B.J.S. (1994). The effect of fluence and irradiation temperature on delayed hydride cracking in Zr–2.5 Nb. 10th Int. Symposium Zirconium in the Nuclear Industry, ASTM STP 1245, 35–61.

A numerical study of maintenance strategy for concrete structures in marine environment

K.F. Tee & C.Q. Li

University of Greenwich, Kent, UK

ABSTRACT: Reinforced concrete structures located in marine environment are susceptible to chloride induced steel corrosion in concrete, which causes severe structural deterioration and ultimate structural collapse. Corrosion-induced structural deterioration is a gradual process, consisting of a number of phases during the service life of reinforced concrete structures. These include corrosion initiation, concrete cracking, delamination and the ultimate collapse due to loss of strength of the structure. This paper presents a numerical method for developing a maintenance strategy based on risk-cost optimization of corrosion affected concrete structures during the whole life of service. The associated risks for concrete cracking, delamination and rupture are quantified based on Monte Carlo simulation. The proposed methodology can help the management in making optimal decisions concerning the intervention to ensure the safe and serviceable operation of the structures. This will, in turn, result in better asset and capital utilization.

1 INTRODUCTION

Maintenance of civil infrastructure systems aims to fulfill a large number of technical requirements under economical constraints. Initial construction costs are not the only costs that must be considered in infrastructure system design. In some cases, the maintenance costs on a system can exceed the initial costs. Asset managers need to be able to develop the optimal strategy regarding inspection as well as maintenance works or rehabilitation works.

The main objective of this paper is to formulate a maintenance strategy based on risk-cost optimization of the structure during its whole service life. A performance based model is proposed to determine each phase of service life of corrosion-affected reinforced concrete structures. The proposed methodology is comprehensive and quantitative, comprising structural response for corrosion-induced cracking, delamination and rupture of a structural member. The associated risks for each phase of service life are quantified based on Monte Carlo simulation. The overall objective of

the maintenance strategy is to minimize the whole life cost without compromising the structural safety during the operation of the structure. A numerical example will be provided to illustrate the application of the maintenance strategy with a view to prevent unexpected failures of the structure during its whole service life. The proposed methodology can help the management in making correct decisions concerning the intervention to ensure the safe and serviceable operation of the structures. This will, in turn, result in better asset and capital utilization.

2 THEORY

Crack width is a parameter of the most practical significance for the design and assessment of reinforced concrete structures. Crack width can be expressed as

$$w(t) = \frac{4\pi d_s(t)}{\frac{(1-v_c)(a/b)\sqrt{\alpha} + (1+v_c)(b/a)\sqrt{\alpha}}{2\pi b f_t} E_{ef}} \quad (1)$$

The practical performance criteria related to concrete cracking of reinforced concrete structures is to limit the crack width to an acceptable level. In the theory of structural reliability, this criterion is expressed in the form of a limit state function and the probability of structural failure due to concrete cracking and delamination can be determined by (Melchers 1999).

$$p_c(t) = P[G(w_{cr}, w, t) \leq 0] = P[w(t) \geq w_{cr}(t)] \quad (2)$$

$$p_d(t) = P[G(w_d, w, t) \leq 0] = P[w(t) \geq w_d(t)] \quad (3)$$

Eventually, the rebar corrosion in concrete will lead to the rupture at the critical cross-section of a structural member. The probability of failure for structural rupture can be expressed as

$$p_r(t) = P[G(R, R_a, t) \leq 0] = P[R_a(t) \geq R(t)] \quad (4)$$

The attainment of a limit state at each phase, i.e. cracking, delamination and rupture, is quantified by a probability p_c , p_d and p_r , respectively. Clearly only when p_c or p_d is greater than an acceptable limit respectively will the corresponding maintenance be warranted to achieve cost effectiveness. Similarly, p_r has to be smaller than an acceptable limit to eliminate undue risk of rupture. With these constraints, the time and number of maintenances can be determined through conventional minimization in terms of a total cost, C_T . Mathematically this can be expressed as (Li et al., 2007).

$$C_T(t_L) = \sum_{i=1}^{n_c} C_c(t_c) \cdot p_c(t_c) + \sum_{i=1}^{n_d} C_d(t_d) \cdot p_d(t_d) + C_r(t_L) \cdot p_r(t_L) \quad (5)$$

Subject to

$$p_c(t_c) \geq p_{c,a}, \quad p_d(t_d) \geq p_{d,a}, \quad p_r(t_L) \leq p_{r,a} \quad (6)$$

3 WORKED EXAMPLE

To illustrate the application of the proposed methodology for a maintenance strategy, a reinforced concrete seawall is used as an example. Assume that a segment of the long wall is selected for investigation. The wall has a dimension of 1000 (wide) \times 2000 (high) \times 150 (thick). Table 1 shows the total cost and associated risk for different number of maintenance due to cracking and delamination with service life of 70 years. For service life of 70 years, the total cost is 8.49 relative to the initial construction cost of the structure when $n_c = 1$ and $n_d = 1$. The high total cost is due to the high probability of rupture (0.9986) and the high cost of structural rupture.

The outputs of the optimization are shown in Table 2 based in minimum total cost. Thus, for instance, if the structure is designed for 100 years, the maintenance strategy is $n_c = 2$ and $n_d = 5$ with

Table 1. Total cost and (associated risk) for different number of maintenance due to cracking and delamination with service life of 70 years.

	$n_c = 1$	$n_c = 2$	$n_c = 3$	$n_c = 4$	$n_c = 5$
$n_d = 1$	8.49 (0.9986)	7.93 (0.9186)	4.97 (0.5124)	2.22 (0.1325)	1.45 (0.0191)
$n_d = 2$	6.07 (0.6634)	2.80 (0.2155)	1.54 (0.0360)	1.39 (0.0041)	–
$n_d = 3$	1.73 (0.0655)	1.38 (0.0081)	–	–	–

Table 2. Outputs of optimization from the maintenance strategy for the example structure based on minimum total cost.

Service life	Minimum total cost	Maintenance strategy	p_r
70	1.38	$n_c = 2; n_d = 3$	0.0081
75	1.43	$n_c = 1; n_d = 4$	0.0056
80	1.51	$n_c = 3; n_d = 3$	0.0092
85	1.57	$n_c = 2; n_d = 4$	0.0063
90	1.65	$n_c = 1; n_d = 5$	0.0043
95	1.77	$n_c = 3; n_d = 4$	0.0072
100	1.87	$n_c = 2; n_d = 5$	0.0049
105	2.02	$n_c = 4; n_d = 4$	0.0081
110	2.16	$n_c = 3; n_d = 5$	0.0056
115	2.37	$n_c = 7; n_d = 3$	0.0046
120	2.54	$n_c = 4; n_d = 5$	0.0063
125	2.77	$n_c = 3; n_d = 6$	0.0043
130	3.06	$n_c = 5; n_d = 5$	0.0072
135	3.35	$n_c = 4; n_d = 6$	0.0049
140	3.70	$n_c = 1; n_d = 8$	0.0067
145	4.13	$n_c = 5; n_d = 6$	0.0056
150	4.61	$n_c = 2; n_d = 8$	0.0076

the minimum total cost of 1.87 relative to the initial construction cost of the structure. The associated confidence for the remaining safe life is 0.0049.

4 CONCLUSION

A practical methodology is proposed for the prevention of failures based on risk-cost optimized maintenance strategy for the management of whole life operation of the concrete structure. The proposed methodology is comprehensive and quantitative, comprising structural response for corrosion-induced cracking, delamination and rupture of a structural member. Stochastic models for failure mechanism of concrete cracking, delamination and rupture are developed and the associated risks are quantified based on Monte Carlo simulation. The overall objective of the maintenance strategy is to minimise the whole life cost without compromising the structural safety during the operation of the structure. Tradeoffs between risks, cost and frequency of repairs are examined through a life cycle cost analysis to determine the most cost effective option. It has been found that there exists an optimal number of maintenances for cracking and delamination that returns the minimum total cost for the structure in its whole service life. It can be concluded that the proposed maintenance strategy can help structural engineers, operators, and asset managers make decisions with regards to repairs of corrosion-affected concrete structures.

REFERENCES

- Li, C.Q., Mackie, R.I. & Lawanwisut, W. 2007. A risk-cost optimized maintenance strategy for corrosion-affected concrete structures. *Computer-Aided Civil and Infrastructure Engineering* 22: 335–346.
- Melchers, R.E. 1999. *Structural Reliability Analysis and Prediction*. Chichester: John Wiley and Sons.

Structure lifecycle as a non-stationary random process

G. Fu

Guangdong University of Technology, Guangzhou, China

Fuzhou University, Fuzhou, China

Tongji University, Shanghai, China

Wayne State University, Detroit, USA

D. Devaraj

Wayne State University, Detroit, USA

ABSTRACT: Structural components or systems deteriorate and renew with time. Deterioration and renewal modeling is an important step in management operation of structures. In the popular bridge management system Pontis, a stationary Markov Chain model is used to describe bridge element deterioration and renewal. The core part of this model is its transition probability matrix, which describes the deterioration process using a probability measurement for the likelihood that the element deteriorates or renews (transits) from a condition state to another. Namely, those elements that deteriorate faster are assigned higher transition probabilities from a better condition state to a worse one. Elements also renew according to the action of maintenance, repair, and/or replacement. It is interesting though to point out that this approach does not take into account the age of the element. In other words, an older bridge element is assigned the same transition probabilities from better conditions to worse ones as a much younger one, because only one transition probability matrix is used in the stationary Markov Chain. In addition, inaccuracy in transition probability matrix estimation can cause large errors for prediction over the lifecycle.

This paper presents a new model of non-stationary Markov Chain as a random process to take into account the element's age. Therefore, a number of such matrices are used to model the entire lifecycle of the bridge element's deterioration process.

The following formulation is developed for estimating or identifying the non-stationary transition probability matrices for each bridge element:

$$\text{Minimize } \sum_{i=1, \dots, N} |Y_i - \text{Predicted}[Y_i, P(A_i)]|^2 \quad (1)$$

$$\text{Subject to } \sum_{k=1, 2, \dots, S} p_{jk}(A_i) = 1 \quad \text{for all } j \quad (2)$$

$$0 \leq p_{jk}(A_i) \leq 1 \quad \text{for all } k \text{ and } j \quad (3)$$

where N is the total number of condition transition data pairs used; Y_i is the condition state vector right after the i th transition for the corresponding data pair; Predicted $[Y_i, P(A_i)]$ is the predicted condition state vector for the same element involved in the i th transition, using the transition probability matrix $P(A_i)$ depending on the element's age A_i . The symbol $|x|$ means the magnitude or modulus of vector x . The transition probabilities p_{jk} for $j, k = 1, 2, \dots, S$ are the elements of matrix P , and S is the total number of possible states for that element. The constraints for them to satisfy in Equations 2 to 3 are for consistency that was violated in the Pontis approach.

A fitting scheme is also proposed here to estimate the non-stationary transition probabilities depending on age. In addition, a new screening scheme is formulated in this study for initial data screening to filter inconsistent raw data. Application of the proposed model to Michigan bridge inspection data shows improved modeling results. This approach was also applied to the bridge condition rating data in the National Bridge Inventory format and thereby produced more realistic predictions.

REFERENCES

- AASHTO Pontis Technical Manual, Release 4.4, 2004.
- Fu, G. and Devaraj, D. "Methodology of Homogeneous and Non-homogeneous Markov Chains for Modeling Bridge Element Deterioration", Final Report to Michigan Department of Transportation, Center for Advanced Bridge Engineering, Department of Civil and Environmental Engineering, Wayne State University, August 2008, MDOT Research Report 1520.
- Fu, G. and Moses, F. "Application of Lifetime System Reliability", Preprint No. 52-1, American Society of Civil Engineers - Structures Congress'86, New Orleans, LA, Sept. 15-18, 1986, p. 281.

MS_118 — Meta-models/surrogate models for uncertainty propagation, sensitivity and reliability analysis (1)

This page intentionally left blank

A numerical comparison of Kriging-based sequential strategies for estimating a probability of failure

L. Li, J. Bect & E. Vazquez

Department of Signal Processing and Electronic Systems, Supélec, Gif-sur-Yvette, France

In many engineering problems, it is important to estimate the probability of a system to be operated under dangerous conditions due to uncertainty on some design parameters or input factors. The performance of a system is usually quantified by a real valued function $f: \mathbb{X} \rightarrow \mathbb{R}$, where $\mathbb{X} \subseteq \mathbb{R}^d$ is the space of uncertain design parameters or input factors. Usually, f is not given in closed form, but can however be evaluated pointwise using computer simulations of the system. Given a probability distribution $P_{\mathbb{X}}$ on \mathbb{X} , and a threshold $T \in \mathbb{R}$, our objective is to estimate the probability $\alpha(f) = P_{\mathbb{X}}(\{x \in \mathbb{X} : f(x) > T\})$ of the excursion set of f above T . The probability $\alpha(f)$ can be estimated using the Monte-Carlo estimator

$$\alpha_m := \frac{1}{m} \sum_{i=1}^m \mathbf{1}_{\{f(X_i) > T\}}, \quad (1)$$

where the X_i s are independent random variables with distribution $P_{\mathbb{X}}$, $\mathbf{1}_{\{f(X_i) > T\}}$ is the excess indicator which equals to one when $f(X_i) > T$ and zero otherwise, and m is the Monte-Carlo sample size.

However, it is well-known that α_m converges to α very slowly when m increases. When dealing with complex engineering problems (for instance, in aeronautics), the total budget of evaluations of f may be limited due to the cost of the evaluation of the performance function. Therefore, it is very useful to develop methods that will make it possible to estimate a probability of failure with a good accuracy and a small number of evaluations of the performance function.

There exist two main approaches to deal with this problem in the literature. One approach is based on approximating the contour $S(f) = \{x \in \mathbb{X} : f(x) = T\}$ by a simple geometrical shape. The most popular methods are the first- and second-order reliability methods (FORM and SORM) [see, e.g., Bjerager (1990)]. However, the accuracy of the approximation depends on the actual shape of $S(f)$ and its resemblance to the approximated shape: in general, they do not provide statistically consistent results. Another category of methods utilizes a cheap meta-model to approximate the expensive

function f , followed by a Monte-Carlo sampling method applied to the meta-model. The strategies compared in this paper belong to this group.

This paper recalls the stepwise uncertainty reduction algorithm (SUR) proposed in Vazquez & Bect (2009), which is in essence a Bayesian sequential search algorithm similar to the algorithm EGO in Jones et al. (1998) for finding a global optimum of a function. More precisely, the SUR strategy is based on the sequential maximization of the one-step lookahead expected mean square error $J_{SUR} = \mathbb{E}\{(\alpha(f) - \hat{\alpha}_n)^2 | \mathcal{F}_{n-1}\}$ where $\hat{\alpha}_n$ is an estimator of $\alpha(f)$, and \mathcal{F}_{n-1} represents the information that has been learned about f after $n-1$ evaluations. Implementation details are provided in the full paper.

The SUR strategy is then compared, on the basis of numerical experiments, to other Bayesian sampling strategies; namely, the targeted integrated mean square error (tIMSE) method of Picheny et al. (2008), the contour approximation strategies of Ranjan et al. (2008) and Bichon et al. (2008), and the AK-MCS method of Echard et al. (2010).

The average performance of the criteria recalled is first evaluated using simulated sample paths of a Gaussian process. A mean-square error (MSE) criterion is adopted to measure the performance after N evaluations:

$$MSE(\hat{\alpha}_N) = \frac{1}{M} \sum_{l=1}^M (\hat{\alpha}_N^l - \alpha_m)^2, \quad (2)$$

where $M = 4000$ is the number of simulated sample paths and $\hat{\alpha}_N^l$ is the probability of failure estimated on the l th path.

Figure (1) shows the result of a numerical comparison of SUR with other criteria proposed in the literature, in terms of mean-square estimation error (MSE). The SUR strategy turns out to be the most efficient. The tIMSE strategy of Picheny et al. (2008), presented here with its tuning parameter set to the empirically best value ($\sigma_{\varepsilon}^2 \approx 0$), also has good performances. The other strategies are less efficient but provide interesting alternatives because of their smaller computational cost.

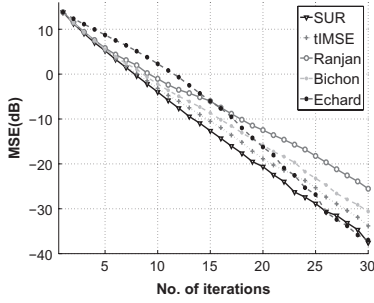


Figure 1. Comparison of different criteria in terms of *MSE*.

Table 1. Comparison of the convergence to α_m for different dimension d , total number of evaluations N , where $n_0 = 5d$, $\gamma = .001$.

Criteria	Dimension d				Parameters
	2	6	10	50	
J_{SUR}	37	66	65	275	–
J_{IMSE_1}	51	67	75	271	$\sigma_\epsilon^2 = 10^{-6}$
J_{IMSE_2}	> 100	> 120	> 150	> 320	$\sigma_\epsilon^2 = 1$
J_{RANJ}	48	69	79	272	$\alpha = 2$
J_{BIC}	46	65	77	272	$\alpha = 2$
J_{ECH}	43	63	73	270	–

Then we apply all criteria on a benchmark example in structural reliability. The objective is to estimate the probability of failure of a so-called *four-branch series system* [see e.g. Schueremans (2001), Deheeger (2008)]. A failure happens when the system is working under the threshold $T = 0$. The performance function $f: \mathbb{R}^2 \rightarrow \mathbb{R}$ is two-dimensional. In our experiments, we will extend this test function to a d -dimensional function by considering a number $(d-2)$ of non-influent variables.

To evaluate the rate of convergence, we define n_γ as the number of evaluations needed before the relative error of the estimation stabilizes in an interval of width 2_γ around α_m :

$$n_\gamma = \min \left\{ n \geq n_0; \forall k \geq n, \frac{|\hat{\alpha}_{n_0+k} - \alpha_m|}{\alpha_m} < \gamma \right\} \quad (3)$$

Table 1 presents the total number of evaluations $N = n_0 + n_\gamma$ for all criteria in different dimensions. We can see that the SUR strategy is more efficient than other criteria in low dimensional cases. When the dimension of the input space increases, all criteria tend to have similar performance. It is also noticed that all estimators converge to α_m with the

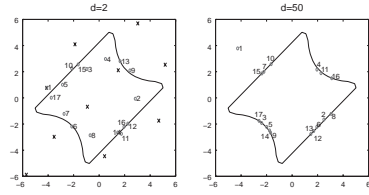


Figure 2. The first 16 points (red circle) evaluated using sampling criterion J_{SUR} , in dimension $d = 2$ (on the left) and $d = 50$ (on the right). Numbers near circles indicate the order of evaluation. The location of the $n_0 = 10$ points of the initial design are indicated by cross for $d = 2$.

required accuracy, except in the case of the criterion J_{IMSE_2} with $\sigma_\epsilon^2 = 1$. We found that this convergence problem is caused by the estimation error on the parameters of the covariance function.

Here we only show the design of 16 points chosen by SUR strategy in different dimensions in Figure (2). However, designs from other criteria and in different dimensions are also provided in the full length paper.

Encouraged by these promising results, our next stage of work will to apply the SUR strategy to more realistic high dimensional industrial problems.

REFERENCES

- Bichon, B.J., M.S. Eldred, L.P. Swiler, S. Mahadevan & J.M. McFarland (2008). Efficient global reliability analysis for nonlinear implicit performance functions. *AIAA Journal* 46(10), 2459–2468.
- Bjægerager, P. (1990). On computational methods for structural reliability analysis. *Structural Safety* 9, 76–96.
- Deheeger, F. (2008). *Couplage mécano-fiabiliste: ²SMART – méthodologie d’apprentissage stochastique en fiabilité*. Ph.D. thesis, Université Blaise Pascal – Clermont II.
- Echard, B., N. Gayton & M. Lemaire (2010). Kriging-based monte carlo simulation to compute the probability of failure efficiently: AK-MCS method. In *6èmes Journées Nationales de Fiabilité, 24–26 mars, Toulouse, France*.
- Jones, D.R., M. Schonlau & W.J. Welch (1998). Efficient global optimization of expensive black-box functions. *J. Global Optim.* 13, 455–492.
- Picheny, V., D. Ginsbourger, O. Roustant, R. Haftka & N. Kim (2008). Adaptive design of experiments for accurate approximation of a target region. In *European Network for Business and Industrial Statistics*.
- Ranjan, P., D. Bingham & G. Michailidis (2008). Sequential experiment design for contour estimation from complex computer codes. *Technometrics* 50(4), 527–541.
- Schueremans, L. (2001). *Probabilistic evaluation of structural unreinforced masonry*. Ph.D. thesis, Catholic University of Leuven.
- Vazquez, E. & J. Bect (2009). A sequential bayesian algorithm to estimate a probability of failure. In *15th IFAC Symposium on System Identification*.

Sensitivity and reliability analysis of a globe valve using an adaptive sparse polynomial chaos expansion

Marc Berveiller & Géraud Blatman

EDF R&D—Department MMC, Site des Renardières, Moret sur Loing Cedex, France

A globe valve is a type of valve used for isolating a piping part inside a circuitry. It generally consists of a movable element and a stationary seat which are relatively moved in order to create flow shut-off. The choice of material is crucial due to the presence of many constraints (pressure, temperature, corrosion, etc.). Among others, the rod has to resist to a possible high water pressure inside the circuit, and valve tightness has to be ensured. Three quantities of interest are of interest in this study, namely the maximum displacement of the rod and two contact pressures located at different parts of the globe valve.

In practice, the material properties of the system components are not exactly known and the model responses are therefore affected by uncertainty. Then it is of major interest to quantify the respective influence of the various input parameters on the model output (sensitivity analysis). Moreover, it is important to assess the probability of failure of the system (reliability analysis).

Sensitivity and reliability analysis may be carried out using standard methods based on intensive simulation schemes, such as Monte Carlo

simulation. However these methods reveal time consuming for our study since a single model evaluation takes about 3 minutes. In order to reduce the computational cost, one uses the so-called *polynomial chaos* (PC) *expansion* technique. The latter consists in replacing the random vector of model responses by a decomposition onto a basis made of orthonormal polynomials. In this context, the problem is reduced to the estimation of a finite set of coefficients, which may be achieved using a non intrusive regression scheme. However, the number of unknown PC coefficients blows up when increasing the degree of the decomposition, hence a possible unaffordable computational cost.

To overcome this difficulty, an iterative procedure based on *Least Angle Regression* (LAR) is used in order to build up a *sparse* PC approximation, i.e. a representation that contains a small number of nonzero terms, which may be computed by means of few model evaluations. Eventually sensitivity and reliability analysis of the system may be carried out at a negligible cost by post-processing the sparse PC expansion.

Keywords: adaptive sparse polynomial chaos expansion, Least Angle Regression, globe valve, sensitivity analysis, reliability analysis

Use of HDMR metamodel for seismic fragility analysis

I. Zentner

Laboratory for the Mechanics of Aging Industrial Structures, LaMSID UMR EDF-CNRS, France

E. Borgonovo

Department for Decision Sciences, Bocconi University, Italy

S. Tarantola

Institute for the Protection and Security of the Citizen, Joint Research Centre of the European Commission, Italy

Industrial (FEM-) models used for seismic vulnerability analysis contain generally an important number of DOFs and are computationally intensive since complex damage models and failure modes have to be considered. This is why the choice of an accurate metamodel is crucial for uncertainty propagation and sensitivity analysis. Moreover, we have to account for stochastic input, that is the stochastic processes modelling seismic ground motion. Indeed, in many real-life problems, the stochastic input is often characterized by a single parameter (or sometimes a couple of parameters) that cannot entirely describe the random phenomenon. This paper addresses the use of High Dimensional Model Representation (HDMR) for the construction of such metamodels. We develop an ANOVA-HDMR based metamodel that can be used for seismic vulnerability analysis. The terms of the decomposition are evaluated by means of state-dependent regression model, recently proposed by Ratto et al., 2007. The results of this paper demonstrate that ANOVA-HDMR decomposition provides a convenient framework to account for stochastic uncertainties.

High Dimensional Model Representation (HDMR) is a generic tool for modeling high dimensional input-output system behavior. It consists in decomposing a function into terms of increasing dimensionality that can be used for principally two purposes:

- Construction of a computational model from field data or creation of metamodels,
- Identification of key model parameters and sensitivity analysis.

HDMR has been initially introduced by Sobol', 1993 for the purpose of sensitivity analysis and further investigated in (Sobol', 2003). Different approaches have been proposed in literature since for evaluating the HDMR terms: these are

principally cut-HDMR and ANOVA-HDMR. The latter is also referred to as Random sampling (RS)-HDMR. Defining the model

$$Y = f(X) \in \mathbb{R}, \quad (1)$$

where f is an analytical expression or a "black box" code, Y is the model output and $X = (X_1, X_2, \dots, X_p)$ are the uncertain parameters that are modeled by independent random variables. HDMR consists in decomposing a function $f(X)$ in terms of increasing dimensionality yielding an expression of the form:

$$f(X) = f_0 + \sum_i f_i + \sum_{1 \leq i < j \leq p} f_{ij} + \dots + f_{12 \dots p}, \quad (2)$$

where the total number of summands is 2^p . The use of HDMR for metamodeling is based on the observation that in most physical models, higher order interaction terms are negligible. This means that that the series (2) could be truncated to a reduced number of low order terms (in general first and second order terms are sufficient) without considerable loss of precision.

However, in many real-life applications, all of the output variability cannot always be explained by the set of chosen input parameters. Let us consider the truncated HDMR:

$$f(X) = f_0 + \sum_i f_i + \sum_{1 \leq i < j \leq p} f_{ij} + \epsilon. \quad (3)$$

In this expression, we have put $\epsilon = \epsilon_c + \epsilon_r$, where ϵ_c models the contribution of neglected higher order terms while ϵ_r represents the contribution due to effects not explained by the model parameters. The truncated terms can be modelled by a Gaussian random variable, considering them as a sum of a large number of independent centred random

variables (Ratto et al., 2007). The unexplained effects, due to stochastic input may be obtained as noise terms. When noise is not dependant on the parameter values (homoscedastic behavior), then it is easy to evaluate its characteristics from data and to introduce it into the model. This is unfortunately not the case for seismic analysis where the the variance of the noise depends on on the parameter values. The following sections give a description of how the parameter dependent noise is handled here. One of the advantages of the ANOVA-HDMR is the independence of the decomposition terms. This allows for a step by step evaluation of the functional terms using only input output samples, making the method very versatile from a practical viewpoint. It namely allows here to treat parametric and stochastic uncertainties separately. The terms corresponding to uncertain model parameters are evaluated using the ANOVA-HDMR as described in the paper while terms related to stochastic input ϵ_r , that is uncertainty not explained by the model parameters, are introduced in a second time as described in this paper.

The metamodel allows us to evaluate fragility curves at very low cost. Moreover, we address the topic of sensitivity analysis of both seismic capacity and fragility curves. Indeed, when the quantities of interest are not variances but probabilities, then the use of other importance measures than the Sobol' indices might be more meaningful. Indeed, moment independent importance measures, as introduced in (Borgonovo, 2007), are more appropriate for addressing the issue of importance ranking when probabilities and not variance is considered. Two sets of importance measures emerged (Borgonovo et al., 2010): The first set quantifies the relevance of an uncertain parameter to capacity. In this case, one can rely on the moment independent importance measure introduced in (Borgonovo, 2007). In the second case, when the fragility curve is the decision-criterion, then one needs importance measures for the whole cdf. Such importance measures are introduced in (Borgonovo et al., 2010, Zentner et al., 2010) as extension of the importance measures for densities.

REFERENCES

- Borgonovo, E. A new uncertainty importance measure. *Reliability Eng. & System Safety* 92, 771–784, 2007.
- Borgonovo, E. Pellegrini, A. Zentner, I. Tarantola, S. de Roc-quigny, E. Importance measures for seismic fragility assessment. *Work in progress*, 2010.
- Ellingwood, B.R. & Kinali, K. Quantifying and communicating uncertainty in seismic risk assessment. *Structural Safety* 31(2), 2009.
- Hamburger, R.O. Foutch, D.A. & Cornell, C.A. Translating Research to Practice: FEMA/SAC Performance-based Design Procedures. *Earthquake Spectra* 19(2), 1992.
- Iooss, B. & Ribatet M. Global sensitivity analysis of computer models with functional inputs. *Reliability Eng. & System Safety* 94, 1194–1204, 2009.
- Marrel, A. Joint metamodeling for sensitivity analysis of continuous and stochastic inputs of a computer code. *Procedia Social and Behavioural Sciences* 2, 7706–7707, 2010.
- Rabitz, H. Alis, Ö. Shorter, J. & Shim K. Efficient input-output model representations. *Computer Physics Communications* 117, 11–20, 1999.
- Ratto, M. & Pagano, A. Recursive algorithms for efficient identification of smoothing spline ANOVA models. *Manuscript*, 2010.
- Ratto, M. Pagano, A. & Young, P. State Dependent Parameter metamodeling and sensitivity analysis. *Computer Physics Communications* 177, 863–876, 2007.
- Sobol', I.M. Sensitivity estimates for nonlinear mathematical models. *Mathematical Modelling and Computational Experiments* 1, 407–414, 1993.
- Sobol', I.M. Theorems and examples on high dimensional model representation. *Reliability Eng. & System Safety* 79, 187–193, 2003.
- Storlie, C.B. Swiler, L.P. Helton, J.C. & Sallaberry, C.J. Implementation and evaluation of nonparametric regression procedures for sensitivity analysis of computationally demanding models. *Reliability Eng. System Safety* 94, 1735–1763, 2009.
- Storlie, C.B. Bondell, H.D. Reich, B.J. & Zhang, H.H. Surface Estimation Variable Selection, and the Non-parametric Oracle Property, *Statistica sinica*, in press, 2010.
- Storlie, C.B. & Helton, J.C. Multiple predictor smoothing methods for sensitivity analysis: Description of techniques, *Reliability Eng. System Safety* 93, 28–54, 2008.
- Zentner, I. Borgonovo, E. Pellegrini, A. & Tarantola, S. Use of moment independent importance measures in the framework of seismic fragility assessment. *Procedia Social and Behavioural Sciences* 2, 7774–7775, 2010.

Metamodel-based importance sampling for the simulation of rare events

V. Dubourg

Clermont Université, IFMA, EA 3867, Laboratoire de Mécanique et Ingénieries, Clermont-Ferrand, France
 Phimeca Engineering, Centre d'Affaires du Zénith, Cournon d'Auvergne, France

F. Deheeger

Phimeca Engineering, Centre d'Affaires du Zénith, Cournon d'Auvergne, France

B. Sudret

Clermont Université, IFMA, EA 3867, Laboratoire de Mécanique et Ingénieries, Clermont-Ferrand, France
 Phimeca Engineering, Centre d'Affaires du Zénith, Cournon d'Auvergne, France

ABSTRACT: Reliability analysis consists in the assessment of the level of safety of a system. Given a probabilistic model (a random vector \mathbf{X} with *probability density function* (PDF) f) and a performance model (a function g), it makes use of mathematical techniques in order to estimate the system's level of safety in the form of a failure probability. A basic approach, which makes reference, is the Monte-Carlo simulation technique that resorts to numerical simulation of the performance model through the probabilistic model. Failure is usually defined as the event $F = \{g(\mathbf{X}) \leq 0\}$, so that the failure probability is defined as follows:

$$p_f = \mathbb{P}(F) = \mathbb{P}(\{g(\mathbf{X}) \leq 0\}) = \int_{g(\mathbf{x}) \leq 0} f(\mathbf{x}) d\mathbf{x} \quad (1)$$

Introducing the failure indicator function $\mathbb{1}_{g \leq 0}$ being equal to one if $g(\mathbf{x}) \leq 0$ and zero otherwise, the failure probability turns out to be the mathematical expectation of this indicator function with respect to the joint probability density function f of the random vector \mathbf{X} . The Monte-Carlo estimator is then derived from this convenient definition. It reads:

$$\hat{p}_{fMC} = \hat{\mathbb{E}}_f[\mathbb{1}_{g \leq 0}(\mathbf{X})] = \frac{1}{N} \sum_{k=1}^N \mathbb{1}_{g \leq 0}(x^{(k)}) \quad (2)$$

where $\{x^{(1)}, \dots, x^{(N)}\}$ $N \in \mathbb{N}^*$ is a set of samples of the random vector \mathbf{X} . According to the central limit theorem, this estimator is asymptotically unbiased and normally distributed with variance:

$$\sigma_{\hat{p}_{fMC}}^2 = \text{V}[\hat{p}_{fMC}] = \frac{p_f(1-p_f)}{N} \quad (3)$$

In practice, this variance is compared to the unbiased estimate of the failure probability in order to decide whether it is accurate enough or not. The *coefficient of variation* is defined as $\delta_{\hat{p}_{fMC}} = \sigma_{\hat{p}_{fMC}} / \hat{p}_{fMC}$. Given N , this coefficient dramatically increases as soon as the failure event is too rare ($p_f \rightarrow 0$) and proves that the Monte-Carlo estimation technique intractable for real world engineering problems for which the performance function involves the output of an expensive-to-evaluate black box function—e.g. a finite element code. Note that this remark is also true for too frequent events ($p_f \rightarrow 1$) as the coefficient of variation of $1 - \hat{p}_{fMC}$ exhibits the same property.

In order to reduce the number of simulation runs, different alternatives to the brute-force Monte-Carlo method have been proposed and might be classified as follows.

One first approach consists in replacing the original experiment by a *surrogate* which is much faster to evaluate. Among such approaches, there are the well-known first and second order reliability methods (e.g. Ditlevsen and Madsen, 1996; Lemaire, 2009), quadratic response surfaces (Bucher and Bourgund, 1990) and the more recent meta-models such as *support vector machines* (Hurtado, 2004; Deheeger and Lemaire, 2007), *neural networks* (Papadrakakis and Lagaros, 2002) and *kriging* (Kaymaz, 2005; Bichon et al., 2008). Nevertheless, it is often difficult or even impossible to quantify the error made by such a substitution.

The other approaches are the so-called *variance reduction techniques*. In essence, these techniques aim at favoring the Monte-Carlo simulation of the failure event F in order to reduce the estimation variance. These approaches are more robust because they do not rely on any assumption

regarding the functional relationship g , though they are still too computationally demanding to be implemented for industrial cases. For an extended review of these techniques, the reader is referred to the book by Rubinstein and Kroese (2008).

In this paper an hybrid approach is developed. It is based on both *margin meta-models*—e.g. kriging (Santner et al., 2003) or P-SVM (Platt, 1999), and the importance sampling technique. It is then applied to an academic structural reliability problem involving a linear finite-element model and a two-dimensional random field.

ACKNOWLEDGEMENTS

The first author was funded by a CIFRE grant from Phimeca Engineering S.A. subsidized by the ANRT (convention number 706/2008). The financial support from the ANR through the KidPocket project is also gratefully acknowledged.

REFERENCES

- Bichon, B., Eldred, M., Swiler, L., Mahadevan, S. & McFarland, J. (2008). Efficient global reliability analysis for nonlinear implicit performance functions. *AIAA Journal* 46(10), 2459–2468.
- Bucher, C. & Bourgund, U. (1990). A fast and efficient response surface approach for structural reliability problems. *Structural Safety* 7(1), 57–66.
- Deheeger, F. & Lemaire, M. (2007). Support vector machine for efficient subset simulations: 2SMART method. In *Proc. 10th Int. Conf. on Applications of Stat. and Prob. in Civil Engineering (ICASP10), Tokyo, Japan*.
- Ditlevsen, O. & Madsen, H. (1996). *Structural reliability methods* (Internet (v2.3.7, June-Sept 2007) ed.). John Wiley & Sons Ltd, Chichester.
- Hurtado, J. (2004). An examination of methods for approximating implicit limit state functions from the viewpoint of statistical learning theory. *Structural Safety* 26, 271–293.
- Kaymaz, I. (2005). Application of kriging method to structural reliability problems. *Structural Safety* 27(2), 133–151.
- Lemaire, M. (2009). *Structural Reliability*. John Wiley & Sons Inc.
- Papadrakakis, M. & Lagaros, N. (2002). Reliability-based structural optimization using neural networks and Monte Carlo simulation. *Comput. Methods Appl. Mech. Engrg.* 191(32), 3491–3507.
- Platt, J. (1999). Probabilistic outputs for support vector machines and comparisons to regularized likelihood methods. In *Advances in large margin classifiers*, pp. 61–74. MIT Press.
- Rubinstein, R. & Kroese, D. (2008). *Simulation and the Monte Carlo method*. Wiley Series in Probability and Statistics. Wiley.
- Santner, T., Williams, B. & Notz, W. (2003). *The design and analysis of computer experiments*. Springer series in Statistics. Springer.

Principal component analysis and Least Angle Regression in spectral stochastic finite element analysis

G. Blatman

EDF, R&D Division, Site des Renardières, Moret-sur-Loing, France

B. Sudret

Clermont Université, IFMA, EA 3867, Laboratoire de Mécanique et Ingénieries, Clermont-Ferrand, France
Phimeca Engineering, Centre d'Affaires du Zénith, Couron d'Auvergne, France

Polynomial chaos (PC) expansions allow one to represent explicitly the random response of a mechanical system whose input parameters are modelled by random variables. The PC coefficients may be efficiently computed using non intrusive techniques such as projection (Ghiocel and Ghanem 2002) or least squares regression (Berveiller, Sudret, and Lemaire 2006). However, the required number of model evaluations (*i.e.* the computational cost) increases with the PC size, which itself dramatically increases with the number of input variables when the common truncation scheme of the PC expansion is applied (*i.e.* retain all the multivariate polynomials of total degree not greater than a prescribed p). To overcome this problem, an iterative procedure based on Least Angle Regression for building up a *sparse* PC approximation (*i.e.* a PC representation containing a small number of significant coefficients) was devised in (Blatman and Sudret 2010b, Blatman and Sudret 2010a). This method allows an automatic enrichment of both the PC basis and the experimental design (*i.e.* the set of model evaluations to be performed). It has to be noticed though that LAR-PC was mainly devoted to *scalar* model responses, *e.g.* the maximal Von Mises stress in a finite element calculation. In case of *vector-valued* model responses, it is necessary to build up separate LAR-PC meta-models for each output variable, which may reveal cumbersome when the model response has a large dimension, *e.g.* a discretized field such as the Von Mises stresses at all the integration points of all elements.

Consider a mechanical system described by a numerical model \mathcal{M} which can be analytical or more generally algorithmic (*e.g.* a finite element model). Suppose that this model has M uncertain input parameters which are represented by *independent* random variables $\{X_1, \dots, X_M\}$ gathered in a random vector X with prescribed joint probability density function $f_X(x)$. Hence the model

response denoted by $Y = \mathcal{M}(X)$ is also random. Throughout this paper, a *vector valued* response $Y = \{Y_1, \dots, Y_K\}$, $K \geq 2$ is considered. Provided that the quantity $\mathbb{E}[\|Y\|^2]$ is finite (where $\|\cdot\|$ denotes the usual Euclidean norm), random vector Y may be expanded onto the so-called *polynomial chaos* (PC) *basis* (Soize and Ghanem 2004). In this setup, characterizing the random response Y is equivalent to computing all the coordinates of the response in the PC basis, *i.e.* the PC coefficients.

This can be achieved using an Ordinary Least Squares (OLS) scheme (Berveiller, Sudret, and Lemaire 2006, Sudret 2007). This method requires the choice of a *truncation* of the infinite PC series *ab initio*. However, the required number of model evaluations (*i.e.* the computational cost) increases with the PC size, which itself dramatically increases with the number of input variables when the common truncation scheme of the PC expansion is applied (*i.e.* retain all the multivariate polynomials of total degree not greater than a prescribed p). This can lead to intractable calculations in high dimensions for a computationally demanding model \mathcal{M} .

An adaptive strategy has been proposed in (Blatman and Sudret 2010b, Blatman and Sudret 2010a) in order to overcome this difficulty. It is based on the *Least Angle Regression* (LAR) (Efron, Hastie, Johnstone, and Tibshirani 2004) algorithm, which is an iterative variable selection method in statistics. LAR is aimed at selecting those basis polynomials that have the greatest impact on the response component Y , among a possibly large set of candidates. LAR eventually provides a *sparse* PC approximation, *i.e.* which only contains a small number of terms compared to a classical full representation. LAR reveals efficient to build up accurate sparse PC approximations of scalar model responses. In case of a vector-valued response $Y = \{Y_1, \dots, Y_Q\}$, the procedure should be applied componentwise. However such a strategy

may be cumbersome in case of a large number K of response components (e.g. a discretized field such as the Von Mises stresses at all the integration points of a finite element model).

In order to decrease the computational effort, we propose to perform a *principal component analysis* (PCA) of the vector random response, allowing one to capture the main stochastic features of the response by means of a small number K' of (non physical) variables compared to the original number K of output components. This allows a relatively small number of calls to the adaptive LAR procedure in order to characterize the original random response Y . The computational flowchart of the LAR-PCA algorithm is sketched in Figure 1.

The LAR-PCA procedure is tested on an academic problem, namely the analysis of a truss structure subjected to point loads (Figure 2). The problem involves ten input random variables (namely the Young's moduli and the cross-section areas of the bars as well as the point loads), and the model random response Y is the vector of nodal displacements which is here of size 26, since the model comprises 13 nodes with two degrees of freedom, namely the horizontal and vertical components of displacement.

The gPC-LAR approach is first used for each single nodal vertical displacement (an experimental design of 300 computer experiments is used).

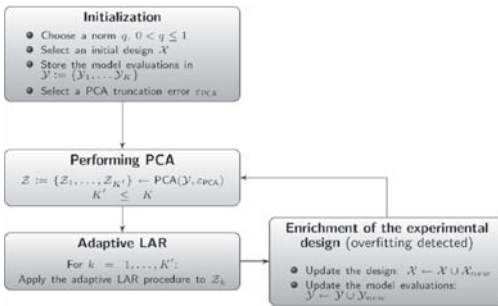


Figure 1. Computational flowchart of the PCA-LAR procedure.

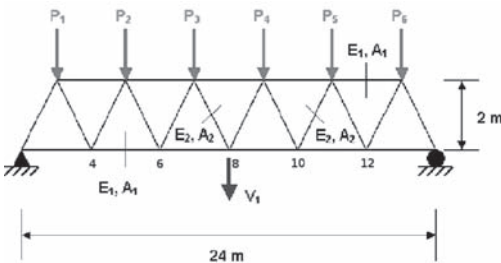


Figure 2. Truss structure comprising 23 members.

Eventually the gPC-PCA approach is run, which makes it possible to get the PC expansion of the vector of all nodal displacements from a reduced number of gPC-LAR analysis (corresponding to the number of retained eigenvalues in the PCA decomposition). It is observed that rather accurate estimates of statistical moments and quantiles of nodal displacements are obtained from a *single* gPC analysis corresponding to the first principal component (one single eigenvalue) of the PCA decomposition. Moreover, it appears that the PDF are almost exactly superposed to the reference solution, which means again that the result obtained using one single eigenvalue in the analysis is already very accurate.

A similar efficiency is expected to solve problems featuring smooth random fields (e.g. fields made of mechanical tensors such as stresses and strains). This will be the scope of further investigations.

REFERENCES

Berveiller, M., Sudret, B. & Lemaire, M. (2006). Stochastic finite elements: a non intrusive approach by regression. *Eur. J. Comput. Mech.* 15(1-3), 81-92.

Blatman, G. & Sudret, B. (2010a). Adaptive sparse polynomial chaos expansion based on Least Angle Regression. *J. Comp. Phys.* submitted for publication.

Blatman, G. & Sudret, B. (2010b). Efficient computation of global sensitivity indices using sparse polynomial chaos expansions. *Reliab. Eng. Sys. Safety* 95(11), 1216-1229.

Efron, B., Hastie, T. Johnstone, I. & Tibshirani, R. (2004). Least angle regression. *Annals of Statistics* 32, 407-499.

Ghiocel, D. & Ghanem, R. (2002). Stochastic finite element analysis of seismic soil-structure interaction. *J. Eng. Mech.* 128, 66-77.

Soize, C. & Ghanem, R. (2004). Physical systems with random uncertainties: chaos representations with arbitrary probability measure. *SIAM J. Sci. Comput.* 26(2), 395-410.

Sudret, B. (2007). *Uncertainty propagation and sensitivity analysis in mechanical models – Contributions to structural reliability and stochastic spectral methods.* Habilitation à diriger des recherches, Université Blaise Pascal, Clermont-Ferrand, France. Available at <http://bruno.sudret.free.fr/docs/HDR%20Sudret.pdf>

This page intentionally left blank

MS_128 — Meta-models/surrogate models for uncertainty propagation, sensitivity and reliability analysis (2)

This page intentionally left blank

A Kriging improvement of the Monte Carlo simulation: AK-MCS method

B. Echard, N. Gayton & M. Lemaire

*Clermont Université, Institut Français de Mécanique Avancée, EA 3867,
Laboratoire de Mécanique et Ingénieries, Clermont-Ferrand, France*

Structural analyses in industry commonly involve complex computational models such as finite element methods. Despite the advances in computer technology, these models may require extremely long lasting computation times (several minutes to several hours) which can become a delicate issue in the case of structural reliability analyses. In fact, the study of reliability demands very numerous repeated calls to the mechanical model in order to evaluate accurately the probability of failure. Consequently, reducing this number of calls has become an important domain of research in reliability in order to bring this concept to industrial applications. To do so, meta models (or surrogate models) are a well-recognised solution. Commonly, a meta-model aims at approximating the response of the model thanks to a design of experiments, *i.e.* a few evaluations of the model. Then, the computational expensive model is replaced by its metamodel and classic reliability methods such as Monte Carlo simulation, are then conducted on it. Quadratic Response Surfaces (Gayton et al., 2003) and Polynomial Chaos (Ghanem and Spanos 1991) are examples of these surrogate models. Other meta-models such as Support Vector Machine (Hurtado 2004) have a different objective. They perform a classification which consists, in the case of reliability, in identifying, among a population, the negative performance function values and the positive ones. These classification surrogate models are found to be extremely efficient as they focus only on the sign and not the value of the performance function. In fact, to calculate the probability of failure, only the sign of the performance function is needed and more information on the model's response is not required (unless sensibilities are to be calculated). This article focusing on the efficient evaluation of the probability of failure, we propose a new classification method based on the stochastic metamodel called Kriging (or Gaussian Process).

Developed for geostatistics in the fifties and sixties by Krige and then theorised by Matheron

(1973), Kriging presents several interesting differences with the other metamodels. First, it is an exact interpolation method, *i.e.* the points of the design of experiments are interpolated. This is an interesting property as mechanical models such as Finite Element Models give same results if run twice with the same inputs. In addition to this, thanks to its stochastic property, Kriging provides not only a predicted value in a point but also an estimation of the uncertainty on the prediction (Kriging variance) which can be used to identify the most uncertain prediction among a population. This characteristic can be used to develop active learning method as the metamodel can be improved step by step. In fact, Kriging has been used intensively in optimisation problems in the nineties with active learning methods such as the Efficient Global Optimisation EGO by Jones et al. (1998).

The first applications of Kriging to reliability are rather recent (Romero et al., 2004, Kaymaz 2005). At first, Kriging was not performed in fully active learning methods. The methods were in several iterations however Kriging variance was not used to determine the next most interesting point to evaluate. Furthermore, Kriging is used as an approximation metamodel. Following this, Bichon et al. (2008) propose a first active learning method inspired by EGO and the Kriging contour estimation method by Ranjan et al. (2008). The method is found to be extremely efficient as it enables to focus on the evaluation of points in the vicinity of the limit state. However, it still uses Kriging as an approximation metamodel. Indeed, the limit state is approximated in the whole design space and therefore, even in regions where configurations show very weak densities of probabilities and have negligible effects on the probability of failure.

This article proposes an active learning method which uses Kriging as a classification surrogate model and not an approximation one. The method is called AK-MCS for Active learning method combining Kriging and Monte Carlo

Simulation. It consists in predicting by Kriging the performance function's signs of a Monte Carlo population thanks to a design of experiments composed of only a few evaluated points. A learning function called U is proposed in this paper to select wisely these points among the population which, if evaluated, would improve the most the quality of the Kriging classification model. In fact, the learning function is able thanks to the Kriging variance to identify the point whose prediction's sign is the most uncertain. By adding it to the design of experiments, the updated classification model is then more accurate and consequently the probability of failure too.

In this paper, AK-MCS is performed on two examples. The first one is chosen for its high non-linear and non-convexity limit state in 2D. Several populations are tested to show that AK-MCS gives accurate results on the probability of failure for any Monte Carlo population. The second example is a truss structure with 10 random variables. AK-MCS is compared to Monte Carlo simulation and results of polynomial chaos metamodel from literature. It is proved to guarantee a great accuracy on the probability of failure with less calls to the performance function than the approximation metamodels.

This research was supported by the French Agence Nationale de la Recherche under the project APPRoFi (Approche Mécano Probabiliste pour la conception Robuste en Fatigue), which is gratefully acknowledged by the authors.

REFERENCES

- Bichon, B.J., Eldred, M.S., Swiler, L.P., Mahadevan, S. & McFarland, J.M. (2008, October). Efficient Global Reliability Analysis for nonlinear implicit performance functions. *AIAA Journal* 46, 2459–2468.
- Gayton, N., Bourinet, J.M. & Lemaire, M. (2003). CQ2RS: a new statistical approach to the response surface method for reliability analysis. *Structural Safety* 25(1), 99–121.
- Ghanem, R.G. & Spanos, P.D. (1991). *Stochastic Finite Elements: A Spectral Approach*. Springer, Berlin.
- Hurtado, J.E. (2004, July). An examination of methods for approximating implicit limit state functions from the viewpoint of statistical learning theory. *Structural Safety* 26(3), 271–293.
- Jones, D.R., Schonlau, M. & Welch, W.J. (1998, December). Efficient Global Optimization of expensive black-box functions. *Journal of Global Optimization* 13(4), 455–492.
- Kaymaz, I. (2005, April). Application of Kriging method to structural reliability problems. *Structural Safety* 27(2), 133–151.
- Matheron, G. (1973). The intrinsic random functions and their applications. *Advances in Applied Probability* 5(3), 439–468.
- Ranjan, P., Bingham, D. & Michailidis, G. (2008, November). Sequential experiment design for contour estimation from complex computer codes. *Technometrics* 50(4), 527–541.
- Romero, V.J., Swiler, L.P. & Giunta, A.A. (2004, April). Construction of response surfaces based on progressive-lattice-sampling experimental designs with application to uncertainty propagation. *Structural Safety* 26(2), 201–219.

RPCM: A strategy to perform reliability analysis using polynomial chaos and resampling—Application to fatigue design

A. Notin, J.L. Dulong & P. Villon

Laboratoire Roberval de Mécanique, Université de Technologie de Compiègne, Compiègne, France

N. Gayton & M. Lemaire

Laboratoire de Mécanique et Ingénieries, Université de Clermont-Ferrand, Clermont-Ferrand, France

H. Jaffal

Pole Ingénierie, Simulation et Conception CETIM, Senlis, France

ABSTRACT: In materials science, fatigue is the progressive and localized structural damage that occurs when a material is subjected to cyclic loading. If the loads are above a certain threshold, microscopic cracks will begin to form at the surface. Eventually a crack will reach a critical size, and the structure will suddenly fracture. The shape of the structure will significantly affect the fatigue life. For example, square holes or sharp corners will lead to elevated local stresses where fatigue cracks can initiate. According to the ASTM (American Society for Testing and Materials), the fatigue life (N_f) is defined as the number of stress cycles that a specimen sustains before the failure occurs. Fatigue is a random process in essence. The randomness comes from the loading process and the fatigue resistance of material. Monte Carlo simulation methods are commonly used to solve this kind of problems. Even if these methods have strong advantages (Papadrakakis and Papadopoulos 1996, Stefanou and Papadrakakis 2004), they usually become computer time-consuming as the complexity and the size of the embedded deterministic models increase. In order to find an alternative to Monte Carlo simulations, the so-called Spectral Stochastic Finite Element Method (SSFEM) has been developed in the early 90's by Ghanem and Spanos (1991) to solve structural mechanics problems featuring spatially random parameters. The model response (*i.e.* the vector of nodal displacements) is expanded onto a particular basis of the probability space, made of Hermite polynomials, called the polynomial chaos (Ghanem and Spanos 1991, Puig et al. 2002, Soize and Ghanem 2004, among others).

In the industry, the prediction and the validation of the fatigue resistance of a structural component is crucial in the assessment of its reliability. Structural reliability methods allow computing

the reliability index and the probability of failure (Ditlevsen and Madsen 2007, Lemaire 2009). Applications of the stochastic finite elements method to structural reliability have been shown (Sudret and Der Kiureghian 2002, Choi et al. 2004). Besides, according to Walz and Riesch-Oppermann (2006), the use of confidence bounds provide “*important information on the accuracy of failure probability predictions in the light of the uncertainties of the available data base*”. Taking into account that in the industry new data's can be very expensive to obtain the use of resampling techniques provides an additional tool to obtain more information without new mechanical computations (Efron 1979, Efron and Tibshirani 1993, Gayton et al. 2003, Lemaire 2009). From a general point of view, the objective of this paper is to demonstrate the contribution of resampling techniques in polynomial chaos based approaches. Such metamodelling technique requires the truncation of the PC representation. It is well known that the number P of basis functions may be prohibitively large when the number of input random variables M increases. Indeed, when truncating the PC expansion, only the basis polynomials of total degree not greater than p are retained. In practice, the degree p is chosen a priori. Such an assessment is of crucial importance since the accuracy of the results of an uncertainty or a reliability analysis will directly depend on the *goodness-of-fit* of the response surface. That is why the estimation of the approximation error is essential. It has to be noted that the error estimation should not require additional model evaluations (since the latter may be computationally expensive), but rather reuse the already performed computer experiments. To tackle this problem, we propose a new approach coupling polynomial chaos expansions and confidence intervals. This approach, which we call

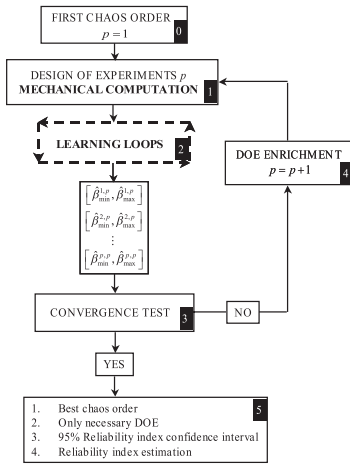


Figure 1. Resampling Polynomial Chaos Method procedure.

RPCM (Resampling Polynomial Chaos Method), aims at exploring an existing database to find the best chaos order which allows to reach the reliability index. The idea behind the RPCM method comes from the work by Gayton et al. (2003) who have introduced the use of Bootstrapping techniques for reliability analysis and Lemaire (2006) who has first mentioned the contribution of confidence intervals for PC expansions.

ACKNOWLEDGEMENTS

This work is supported by the CETIM (Centre Technique des Industries Mécanique—France) and the Roberval research center at the University of Technology of Compiègne. The author would like to thank the French National Research Agency for its support through APProFi project.

REFERENCES

Choi, S., Grandhi, R. & Canfield, R. (2004). Structural reliability under non-gaussian stochastic behaviour. *Computers and Structures* 82, 1113–1121.

Ditlevsen, O. & Madsen, H. (2007). *Structural reliability Methods*. Chichester, UK: Wiley. Edition 2.3.7: Internet edition.

Efron, B. (1979). Bootstrap methods: Another look at the jackknife. *The Annals of Statistics* 7, 1–26.

Efron, B. & Tibshirani, R.J. (1993). *An introduction to the bootstrap*. New York: Chapman Hall.

Gayton, N., Bourinet, J. & Lemaire, M. (2003). Cq2rs: a new statistical approach to the response surface method for reliability analysis. *Structural Safety* 25, 99–121.

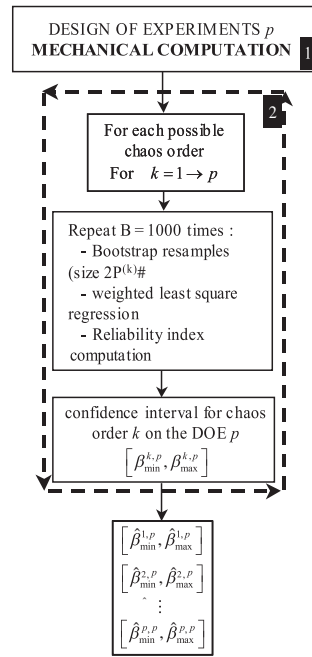


Figure 2. Details on the learning loop (Step 2).

Ghanem, R. & Spanos, P. (1991). *Stochastic finite elements: a spectral approach*. New York: Springer-Verlag. Revised Edition published by Dover in 2003.

Lemaire, M. (2006). Implementation of parametric reliability methods in industrial applications. In *Integrating Structural Analysis and Reliability*, P.K. Das, editor: 3rd ASRANet colloquium, Glasgow, U.K.

Lemaire, M. (2009). *Structural Reliability—Static Mechanical coupling*. ISTE.

Papadrakakis, M. & Papadopoulos, V. (1996). Robust and efficient methods for stochastic finite element analysis using monte carlo simulation. *Computer Methods in Applied Mechanics and Engineering* 134, 325–340.

Puig, B., Poirion, F. & Soize, C. (2002). Non-gaussian simulation using hermite polynomial expansion: convergences. *Prob. Engr. Mech.* 17, 253–264.

Soize, C. & Ghanem, R. (2004). Physical systems with random uncertainties: chaos representations with arbitrary probability measure. *SIAM Journal on Scientific Computing* 26(2), 395–410.

Stefanou, G. & Papadrakakis, M. (2004). Stochastic finite element analysis of shells with combined random material and geometric properties. *Computer Methods in Applied Mechanics and Engineering* 193, 139–160.

Sudret, B. & Der Kiureghian, A. (2002). Comparison of finite element reliability methods. *Probabilistic Engineering Mechanics* 17, 337–348.

Walz, G. & Riesch-Oppermann, H. (2006). Probabilistic fracture mechanics assessment of flaws in turbine disks including quality assurance procedures. *Structural Safety* 28, 273–288.

Distribution-based global sensitivity analysis in case of correlated input parameters using polynomial chaos expansions

Y. Caniou & B. Sudret

Clermont Université, IFMA, EA 3867, Laboratoire de Mécanique et Ingénieries, Clermont-Ferrand, France
 Phimeca Engineering, Centre d’Affaires du Zénith, Courmon d’Auvergne, France

Global sensitivity analysis aims at studying how uncertainty in the model input variables can influence the uncertainty in the model output. Methods based on the decomposition of the variance of the output are the most famous techniques for the sensitivity analysis (Saltelli et al., 2004). Considering the following model:

$$Y = \mathcal{M}(X), X = (X_1, \dots, X_n) \quad (1)$$

with n uncertain input variables, variance-based methods allow one to decompose the total variance V of Y into *partial variances*, which leads to sensitivity indices such as Sobol’ first order and total indices after some normalization.

The computation of the conditional moment $\text{Var}[\mathbb{E}[Y | X_i]]$ is required. The numerical cost of a variance-based method is then the number of evaluations of the model \mathcal{M} , which can be over a million. When \mathcal{M} is not an analytical function but a numerical model such as a finite element code, each evaluation can last from a few seconds to a few hours and it is obviously impossible to run it so many times.

Metamodeling techniques enable to build an accurate representation $\hat{\mathcal{M}}$ of the model \mathcal{M} via only a limited number of model evaluations. In this paper we will focus on a technique called *polynomial chaos expansion*. The approach consists in the approximation of the random response Y of a model \mathcal{M} into a suitable finite-dimensional basis $\{\psi_\alpha(X), \alpha \in A\}$ as follows:

$$Y \approx \hat{M}(X) = \sum_{\alpha \in A} a_\alpha \psi_\alpha(X) \quad (2)$$

where the ψ_α ’s are multivariate orthogonal polynomials with respect to the input joint PDF $f_X(x)$ and the a_α ’s are coefficients to be computed. α denotes the multi-indices that define the polynomials and:

$$|\alpha| = \sum_{i=1}^n \alpha_i \quad (3)$$

In practice, we select multivariate orthogonal polynomials ψ_α of a total degree not greater than a maximal degree p :

$$A = \left\{ \alpha : |\alpha| = \sum_{i=1}^n \alpha_i \leq p \right\} \quad (4)$$

The size of the basis is determined by:

$$P = \binom{n+p}{p} \quad (5)$$

Experience shows that especially when considering a high degree p , most of the a_α ’s are 0. To avoid the computation of all the originally possibly null co-efficients, the *adaptive sparse polynomial chaos approximations based on Least Angle Regression* is used (Blatman 2009). This technique uses the LAR algorithm (Efron, Hastie, Johnstone & Tibshirani 2004) that calculates the most significant coefficients until the target accuracy is reached. Then the metamodel $\hat{\mathcal{M}}$ may be evaluated at low cost for suitable postprocessing such as sensitivity analysis (Sudret 2008).

In this paper, we investigate a new *moment-independent uncertainty importance measure* originally introduced in Borgonovo 2007. It is defined by the shift between the conditional distribution of the output $f_Y(y)$ and its conditional distribution when X_i is known $f_{Y|X_i}(y)$:

$$s(X_i) = \int_{D_Y} |f_Y(y) - f_{Y|X_i}(y)| dy \quad (6)$$

It corresponds to the area between the two probability density functions as shown in Figure 1. The importance measure δ_i is defined by:

$$\delta_i = \frac{1}{2} \mathbb{E}[s(X_i)] \quad (7)$$

where $\mathbb{E}[s(X_i)]$ represents the expected value of $s(X_i)$ over the domain of variation of X_i and where the

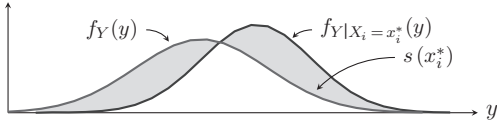


Figure 1. Shift between $f_Y(y)$ and $f_{Y|X_i}(y)$.

coefficient $\frac{1}{2}$ is introduced for normalization. This global sensitivity indicator assesses the influence of input uncertainty on the entire output distribution without any reference to a specific moment of the output. In addition, this moment independent importance measure can also be properly defined when the input parameters $\{X_1, \dots, X_N\}$ are dependent.

Traditionally, the dependence structure of the input parameters is taken into account using correlation coefficients such as the Bravais-Pearson correlation coefficient ρ , or the Spearman rank correlation coefficient ρ_s . These two coefficients offer good results provided the correlation is linear or monotonic but show limitations in the case of complex dependence structures. The *copula theory* (Nelsen 1999) allow a more comprehensive modelling of the dependence structure.

The main equation that rules the copula theory is the Sklar's theorem. Let H be the joint distribution function with margins F and G . Then there exists a copula function C such that for all x, y in \mathbb{R} :

$$H(x, y) = C(F(x), G(y)) \quad (8)$$

Provided the margins are continuous, the copula is unique and defined by:

$$C(u, v) = H(F^{-1}(u), G^{-1}(v)) \quad (9)$$

In other words, the copula is what remains of a multidimensional distribution ($n \geq 2$) once the effect of the marginal distributions has been erased. Thus, a copula can be seen as a *dependence function*.

In this paper, we propose a methodology to address sensitivity analysis on models with

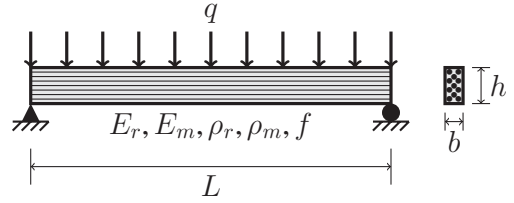


Figure 2. Composite beam under dead weight.

dependent input parameters based on three ingredients:

- the moment-independent uncertainty importance measure δ_p ,
- the polynomial chaos expansion,
- and the copula theory.

The methodology is applied to a multilevel nested modelling of a composite beam under dead weight illustrated in the Figure 2.

The example investigated illustrates the strong role the dependence structure the parameters could have on sensitivity analysis and point out the informations offered by an indicator adapted to problems with dependent variables.

REFERENCES

- Blatman, G. (2009). *Adaptive sparse polynomial chaos expansions for uncertainty propagation and sensitivity analysis*. Ph.D. thesis, Blaise Pascal University-Clermont II, Ecole Doctorale Sciences Pour l'Ingénieur.
- Borgonovo, E. (2007). A new uncertainty importance measure. *Reliab. Eng. Sys. Safety* 92, 771–784.
- Efron, B., T. Hastie, Johnstone, I. & Tibshirani, R. (2004). Least Angle Regression. *Annals of Statistics* 32, 407–499.
- Nelsen, R.B. (1999). *An introduction to Copulas*. Lecture Notes in Statistics. Springer.
- Saltelli, A. et al. (2004). *Sensitivity analysis in practice*. John Wiley & Sons, Ltd.
- Sudret, B. (2008). Global sensitivity analysis using polynomial chaos expansions. *Reliab. Eng. Sys. Safety* 93, 964–979.

Reliability-based design optimization of an imperfect submarine pressure hull

V. Dubourg

Clermont Université, IFMA, EA 3867, Laboratoire de Mécanique et Ingénieries, Clermont-Ferrand, France
Phimeca Engineering, Centre d'Affaires du Zénith, Courmon d'Auvergne, France

J.-M. Bourinet

Clermont Université, IFMA, EA 3867, Laboratoire de Mécanique et Ingénieries, Clermont-Ferrand, France

B. Sudret

Clermont Université, IFMA, EA 3867, Laboratoire de Mécanique et Ingénieries, Clermont-Ferrand, France
Phimeca Engineering, Centre d'Affaires du Zénith, Courmon d'Auvergne, France

M. Cazuguel

DCNS, Ingénierie Navires Armés, Lorient Cedex, France

INTRODUCTION

In order to ensure that their design is safe enough, mechanical engineers and other stake-holders usually cope with uncertainty using *partial safety factors*. Such factors are usually prescribed in specific standards depending on the field of application and are calibrated with respect to both experience and scatter of environmental, material and structural properties. However, they might either introduce an excessive degree of conservatism or on the contrary, they might lack exhaustivity about the servicing conditions of the system to be designed. This is the reason why Reliability-Based Design Optimization has gained much attention in the past decades as it allows one to consider explicitly uncertainty in the design optimization procedure.

RBDO aims at designing the system in a robust manner by minimizing some cost function c with respect to a set of characteristic design parameters θ (e.g. means) under *reliability constraints* instead of the original *deterministic constraints*. The reliability-based optimal design θ^* of interest is thus defined as the following minimizer:

$$\theta^* = \arg \min_{\theta \in D_\theta} c(\theta) : \begin{cases} f_i(\theta) \leq 0, i = 1, \dots, n_c \\ \mathbb{P}(g_l(X(\theta)) \leq 0) \leq P_{fl}^0, l = 1, \dots, n_p \end{cases} \quad (1)$$

where D_θ is the admissible design space, $\{f_i, i = 1, \dots, n_c\}$ are classical deterministic constraints that either do not put the system's safety

at stake or involves partial safety factors in order to cope with some unconsidered failure scenarii, $\{\mathbb{P}(g_l(X(\theta)) \leq 0) \leq P_{fl}^0, l = 1, \dots, n_p\}$ are the so-called reliability constraints involving the vector of uncertain variables X and the maximum failure probabilities that are tolerated by the code of practice $\{P_{fl}^0, l = 1, \dots, n_p\}$. Note that, in this paper, X is distributed according to its joint probability density function $f_X(\cdot, \theta)$ which is parameterized by the design parameters θ .

METHODOLOGY

In essence, RBDO methods have to mix optimization algorithms together with reliability calculations. The classical approach known as “*double loop*” consists in nesting the computation of the probability of failure with respect to the current design within the optimization loop. Crude or advanced simulation methods are not applicable to industrial models (e.g. finite element models) due to the associated computational burden. In contrast, methods based on the approximation of the reliability (e.g. FORM) may not be applicable to real-world problems. The interested reader may refer to the book by Tsompanakis et al. (2008) which provides a complete review of existing approaches.

In order to try to circumvent the aforementioned drawbacks of existing approaches, an original method has been developed. It is based on both the adaptive construction of a *kriging meta-model* for the original time-consuming mechanical model (Santner et al., 2003), and the use of the *subset*

simulation technique for the efficient and accurate computation of the failure probability (Au and Beck, 2001) and its associated sensitivities w.r.t. the design variables (Song et al., 2009). The strategy is briefly described in this paper before the application to the design of imperfect submarine pressure hulls. The interested reader may find some more detailed explanations in a forthcoming paper (?).

RELIABILITY-BASED DESIGN OF AN IMPERFECT SUBMARINE PRESSURE HULL

The design study addressed in this paper is inspired from Dubourg et al. (2008). It aims at finding the optimal dimensions of a single bay of a ring-stiffened cylinder representative of a submarine pressure hull under external hydrostatic pressure. The single bay is illustrated in Figure 1. The stochastic model accounts for uncertainties in the material properties, in the amplitudes of its imperfections and in the design parameters (e, h_w, e_w, w_f, e_f). The imperfections of the hull are supposed distributed over the two most critical buckling modes in a first simplified approach: the overall and interframe buckling modes. They are also supposed to be triggered by two typical shapes of imperfection, respectively: *out-of-roundness* and *out-of-straightness* whose amplitudes are denoted by A_n and A_m . These imperfections are illustrated in Figure 1 for the case studied in this paper where $n = 2$ and $m = 14$.

The collapse pressures are determined by means of closed-form and semi-analytical formulas that are commonly used for preliminary design in the submarine industry (e.g. the BS5500). These pressures are then compared to an arbitrary reference diving pressure in order to define the limit-state functions for the reliability constraint. The reliability-based optimal design is defined as the one

that minimizes the expected “hull weight” / “water displacement” ratio.

The algorithm is run for three different minimum reliability constraints $\beta_0 = \{3.00, 4.50, 6.00\}$ and convergence is achieved within a few hundred evaluations of the mechanical model. The optimal designs are compared to the FORM-based optimal designs from Dubourg et al. (2008). The results provided in this paper provides a first sound basis for a future application involving a higher fidelity non-linear shell finite element model.

ACKNOWLEDGEMENTS

The first author was funded by a CIFRE grant from Phimeca Engineering S.A. subsidized by the ANRT (convention number 706/2008). The financial support from DCNS is also gratefully acknowledged.

REFERENCES

- Au, S. & Beck, J. (2001). Estimation of small failure probabilities in high dimensions by subset simulation. *Prob. Eng. Mech.* 16(4), 263–277.
- BS5500. Unfired fusion-welded pressure vessels. British Standard Institutions.
- Dubourg, V., Noifalisse, C. & Bourinet, J.-M. (2008). Reliability-Based Design Optimization: An application to the buckling of imperfect shells. In *4th ASRANet colloquium*, Athens, Greece.
- Santner, T., Williams, B. & Notz, W. (2003). *The design and analysis of computer experiments*. Springer series in Statistics. Springer.
- Song, S., Lu, Z. & Qiao, H. (2009). Subset simulation for structural reliability sensitivity analysis. *Reliab. Eng. Sys. Safety* 94(2), 658–665.
- Tsompanakis, Y., Lagaros, N. & Papadrakis, M. (Eds.) (2008). *Structural design optimization considering uncertainties*. Taylor & Francis.

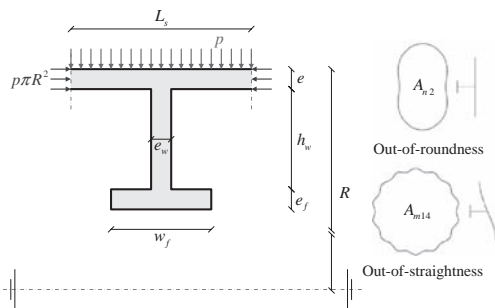


Figure 1. Single bay reference structure—Types and amplitudes of imperfections.

Propagation of variability in railway dynamics simulations

G. Perrin & C. Funfschilling

UR Navier, Marne-la-Vallée, France

SNCF, Innovation and Research Department, Paris, France

B. Sudret

Phimeca, Paris, France

The track/vehicle system contains several sources of variability: variability of the mechanical parameters of a train among a class of vehicles (mass, stiffness and damping of different suspensions), variability of the contact parameters (friction coefficient, wheel and rail profiles) and variability of the track design and quality. This variability plays an important role on the security, on the ride quality, and thus on the certification criteria.

When using simulation for conception and certification purposes, it seems therefore crucial to take into account the variability of the different inputs. In particular, by making homologation become probabilistic, we accept the possibility of exceeding a normalized threshold, but this risk has to be computed and monitored. The probabilistic standardization has thus to define thresholds but also the corresponding tolerated risks of exceedance.

A method to take into account the input variability in the railway dynamic modelling is proposed.

The first step is to formulate the railway stochastic problem from classical railway dynamic problem.

When a stochastic model is considered, it is very interesting to calculate most of the statistical content of the quantities of interest, such as mean values, deviations, probability density functions, as well as probabilities of exceeding thresholds P_f .

Nevertheless, the track/vehicle system being very non-linear, every statistical moments of the output cannot be computed directly: the variability has to be propagated through the model using uncertainty propagation methods.

There are two families of methods to propagate the variability in mechanical models (Soize 2005): the parametric methods, which only consider input uncertainties, and can be used on analytical models as well as on black-box codes, and the non-parametric methods, which consider both input and model uncertainties. The commonly used railway dynamic codes (Vampire, Simpack, ...) being commercial codes in which the constitutive

equations are not available, parametric methods are chosen. Uncertainties from the model itself are thus not considered in this description.

As a Vampire simulation (Vampire being much faster than Simpack and Vocolin) of a train on a classical track of several kilometers lasts around 100 seconds, the simulation time becomes a key point in the propagation of the variability.

Moreover, when probabilities of exceeding thresholds are of interest, the tail of the distribution has to be characterised very precisely. Fiability methods have been developed in order to compute more efficiently these probabilities, by focusing on these tails without computing the whole probability density function. FORM/SORM methods are the most classical methods to the assesment of P_f . If the model is analytical, differentiable, and depends on a limited number of input, Algorithms such as Rackwitz Fiessler give access to very good assesments of P_f from only a few dozen of simulations. Nevertheless, in railway simulations, the model response is very fuzzy, and the number of sources of uncertainty may be very high, which makes these methods become unsuitable. On the contrary, subset methods seem to be very promising.

In addition, to optimize the conception or the maintenance of the track and of the vehicle, it is interesting to compute the importance factors of the different inputs on the outputs. In this context, polynomial chaos expansion methods may be very efficient. Based on projections of the values of interest on known and chosen orthonormal polynomial basis, these methods aim at building a meta-model for each component of the output to substitute the long and costly mechanical codes. Hence, inputs and outputs are directly linked thanks to an analytical model, which allows many time benefits. Once computed, the meta-model allows to calculate more easily importance and sensitivity factors, such as Sobol indices.

This methodology can thus be applied to the analysis of the influence of the wheel/rail contact variability on a railway certification criterion. The wheel and rail profiles are fully parameterized thanks to analytical functions. A set of measured profiles are rebuilt and the parameters distributions and their dependencies are determined. These input characteristics are then propagated through the deterministic multi-body model thanks to polynomial chaos expansion methods. Finally, the

stochastic content of the certification criterion is analysed.

REFERENCE

- Soize, C. (2005). A comprehensive overview of a non-parametric probabilistic approach of model uncertainties for predictive models in structural dynamics. *Journal of sound and vibration* 288, 623–652.

*GS_123 — Model selection, aggregation and testing
for probabilistic seismic hazard assessment (1)*

This page intentionally left blank

Learning aggregations of ground-motion models using data

Carsten Riggelsen, Nikos Gianniotis & Frank Scherbaum

Institute of Earth and Environmental Science, Geophysics/Seismology, Potsdam University, Potsdam, Germany

INTRODUCTION

An ensemble is a collection of models where each model has been set-up or trained to solve the same problem. One of the main motivations for using an ensemble, rather than a single model, is the superior performance in terms of generalisation error. In the paper we wish to highlight certain ideas behind ensemble methods and motivate why such methods are relevant in the context of ground motion model (GMM) aggregation. GMMs are an important component of PSHA. GMM uncertainty is an important factor controlling the exceedence frequency of e.g. peak ground acceleration (PGA) (Bommer & Abrahamson 2006). Several GMMs have been proposed, and these differ considerably in the way they have been derived, resulting in different functional forms and in the number and kind of predictor variables used to characterize the earthquake source, path and site effects.

In PSHA it is crucial to take into account the so-called *epistemic* uncertainty that arises from the inadequacy of any single model being able to perfectly capture all aspects of ground motion. This is particularly important when we are interested in a region for which no dedicated GMM has been developed. In the de facto guideline for PSHA (colloquially referred to as the SSHAC guidelines—Senior Seismic Hazard Analysis Committee) a significant emphasis is put on incorporating all opinion diversity in the levels of experts and models. However, the recommendations do not detail how this should be implemented.

ENSEMBLE METHODS

Motivation

In ML, ensemble learning has been an active area of research that has yielded many important results and algorithms for combining models in a principled way. The main motivation for employing ensembles in machine learning is the improved generalisation ability that they exhibit over single models. Justification of how this gain arises may be obtained from different viewpoints:

1. Ensembles augment the hypothesis space (Dietterich 2000, Polikar 2006): Each model is a candidate hypothesis from the space of all possible hypotheses i.e. the space of all possible parametrisations of the model. It may occur however that no model from the space of all possible models, is capable of adequately fitting the data at hand. In this case, our hypothesis space is simply not “rich” enough. However, using multiple models in the form of an ensemble can augment the hypothesis space and allow us to adequately represent the data.
2. Statistical viewpoint: Imagine a classification task where an ensemble of models classifies data items either as class 0 or 1. Each model is given an input and it predicts a class, independently of the other models. The prediction of the ensemble is taken to be the class predicted by most models. Thus, the ensemble commits an error, only if the majority of models is incorrect, which leads to better prediction performance (Kuncheva, Whitaker, Shipp & Duin 2000). Similarly ensembles perform well in regression tasks in terms of generalisation provided the individual regression models commit uncorrelated errors (Rosen 1996, Liu & Yao 1999).
3. Ensembles may help alleviate other types of problems (Polikar 2006): For instance, in a classification task where data appear in large volumes, training a single classifier may be a computationally demanding task. A viable solution is to split the data into manageable subsets and train one classifier per subset and subsequently combine all trained classifiers into an ensemble.

Popular ensemble methods include Bagging (Breiman 1996), Adaboost (Freund & Schapire 1996) and Mixture of Experts (Jordan & Jacobs 1994).

Ensemble methods in the context of GMMs

In ensemble methods, as presented in ML, data drive both the learning of the individual models and their combination into an ensemble. This is not entirely the aim in our case; rather, we are provided with several physically plausible predictive models

of ground motion, but acknowledge the fact that no single GMM captures the full truth. Contrary to ensemble methods, data are not allowed to alter the “physics” of these individual models, however, they are allowed to dictate the combination of the GMMs.

Often we may be interested in predictions about a region for which no dedicated GMM has been developed. In this case, we do not expect any GMM to give accurate predictions, i.e. to generalise well in the new region. Nevertheless, we hope that data available for this new region in question, can guide us on how to aggregate the available GMMs into an ensemble that can then be used for obtaining predictions. As a first step in the paper we investigate the following types of aggregation techniques: mixture models, conditional mixture models and linear Gaussian models. The full version of the paper presents experimental results on aggregating 12 GMMs from the literature on data that originate from the Europe/Middle East. The ensembles are trained via the Expectation Maximisation algorithm or MCMC methods.

CONCLUSION

The paper presents a first investigation into introducing ensemble methods in the context of GMMs. While in ML there exist established techniques that prescribe how to combine models into an ensemble (i.e. type of combination such as linear combination, mixture of experts, etc.) and how to train the ensemble, it is not yet understood how to aggregate GMMs into an ensemble. GMMs are not merely regression models that predict ground motion; physical considerations are incorporated during their development. Forming an ensemble by taking a linear combination of GMMs needs to be justified, since a linear combination does not necessarily yield a physically plausible model. Future

research will explore the problem of forming GMM ensembles that are physically sound.

ACKNOWLEDGEMENTS

We wish to thank Elise Delavaud for preparing the data, and for providing the GMMs, including correct references. Thanks to Nicolas Kühn for comments on the draft manuscript. Data were provided by T. Allen. Carsten Riggelsen is funded by DFG project RI 2037/2-1 and Nikos Gianniotis is funded by BMBF project PROGRESS.

REFERENCES

- Bommer, J. & Abrahamson, N. (2006). Why do modern probabilistic seismic-hazard analyses often lead to increased hazard estimates? *Bulletin of the Seismological Society of America* 96 (6), 1967–1997.
- Breiman, L. (1996). Bagging predictors. *Machine Learning* 24, 123–140.
- Dietterich, T. (2000). Ensemble methods in machine learning. In *Multiple Classifier Systems*, Volume 1857 of *Lecture Notes in Computer Science*, pp. 1–15. Springer Berlin / Heidelberg.
- Freund, Y. & Schapire, R.E. (1996). Experiments with a new boosting algorithm. In *ICML*, pp. 148–156.
- Jordan, M.I. & Jacobs, R.A. (1994). Hierarchical mixture of experts and the EM algorithm. *Neural Computation* 6, 181–214.
- Kuncheva, L., Whitaker, C., Shipp, C. & Duin, R. (2000). Is independence good for combining classifiers? In *International Conference on Pattern Recognition*, Volume 2, pp. 168–171. IEEE Computer Society.
- Liu, Y. & Yao, X. (1999). Ensemble learning via negative correlation. *Neural Networks* 12 (10), 1399–1404.
- Polikar, R. (2006). Ensemble Based Systems in Decision Making. *Ieee Circuits And Systems Magazine* 6(3), 21–45.
- Rosen, B. (1996). Ensemble learning using decorrelated neural networks. *Connection Science* 8, 373–384.

The collaboratory for the Study of Earthquake Predictability: Perspectives on evaluation and testing for seismic hazard

D. Schorlemmer

Southern California Earthquake Center, University of Southern California, Los Angeles, USA

David D. Jackson

Department of Earth and Space Sciences, University of California Los Angeles, USA

Jeremy D. Zechar

Swiss Seismological Service, ETH Zurich, Zurich, Switzerland

Thomas H. Jordan

Southern California Earthquake Center, University of Southern California, Los Angeles, USA

ABSTRACT: The Collaboratory for the Study of Earthquake Predictability (CSEP) aims to increase the understanding of earthquake predictability and earthquake physics through a global collaboration. CSEP promotes rigorous earthquake predictability experiments in various tectonic environments and has so far established 4 earthquake forecast testing centers around the world. Within these centers, more than 100 earthquake forecast models in 6 testing regions are being evaluated using a rigorous and truly prospective testing procedure. Centers are operating in Los Angeles (US), Wellington (NZ), Tokyo (JP), and Zurich (CH), covering many different regions and tectonic environments: California, New Zealand, Western Pacific, Japan, and Italy. In addition to regional earthquake forecast testing, CSEP has started a global testing program which is targeting the magnitude range of destructive earthquakes that are relevant for seismic hazard and risk.

The current testing program is the first link in the chain of facilities that aim to test comprehensively models of seismic hazard and risk (and their underlying hypotheses). To complement the current

activities, CSEP is developing methods to assess the reliability of earthquake early warning algorithms, to understand the uncertainties and limits of earthquake source inversions, and to gauge the accuracy of ground motion prediction models. Because most earthquake forecasting models are composed of various hypotheses and assumptions about earthquake physics and/or earthquake occurrence, the underlying assumptions and hypotheses need to be tested separately. CSEP researchers are working on creating testable models for many seismological hypotheses, e.g. characteristic earthquakes and relations between maximum magnitude and fault length.

The open, collaborative structure of CSEP involves many research institutions (e.g., SCEC, ERI, GNS, ETH, INGV, etc.). CSEP is also collaborating with large modeling efforts like the Uniform California Earthquake Rupture Forecast (UCERF3) and the Global Earthquake Model (GEM). We present the ongoing activities, first results, and give perspectives for the future development of CSEP and its global collaboration.

Model selection and uncertainty in earthquake hazard analysis

I.G. Main, M. Naylor, J. Greenhough, S. Touati & A.F. Bell

University of Edinburgh, School of GeoSciences, Edinburgh, Scotland

J. McCloskey

University of Ulster, School of Environmental Sciences, Coleraine, Northern Ireland

SUMMARY

According to a recent UN report, seismic risk from large earthquakes continues to increase globally in line with infrastructure and population increase in developing nations. This implies the vulnerability is not decreasing relative to increased exposure. Specific examples include recent devastating earthquakes in Haiti and Sumatra in areas of known seismic hazard, but clearly this is part of a much wider problem. Seismologists and engineers can play a key role in public engagement, in communicating known best practice to local planners and practitioners on appropriate mitigation strategies, and in fundamental research to quantify seismic hazard in a probabilistic way.

All probabilistic hazard forecasts are subject to epistemic (systematic) and aleatory (statistical) uncertainty. To date it has been assumed that the major uncertainties in probabilistic seismic hazard analysis are due to uncertainties in ground motion attenuation. As new strong ground motion data become available, and site response is better characterized locally in advance of major earthquakes, this uncertainty will reduce. Here we address the generic problem of quantifying the effect of sampling bias and statistical error in determining earthquake recurrence rates from seismic catalogues.

We find even simple parameters such as mean event rate converge to a central limit much slower than would be expected for a Gaussian process. The residuals in the frequency-magnitude distribution instead follow a Poisson distribution to a good approximation at all magnitudes, and converge to the Gaussian limit only very slowly.

We also examine the statistical significance of a range of hypotheses for the occurrence rate of extreme events, including the pure Gutenberg-Richter law, the tapered Gutenberg-Richter law, and the characteristic earthquake hypothesis. For the former two we find the best-fitting distribution for the global earthquake population can be changed by a single large event and its aftershocks. In regional studies it is currently not possible to

reject the Gutenberg-Richter hypothesis in favour of the characteristic earthquake model within the Poisson counting error, even when visually the extreme events appear as significant outliers on a log frequency-magnitude plot.

The epistemic and aleatory uncertainties described here must also be taken into account in assessing the skill of time-dependent hazard models relative to the uncertainties in time-independent models, or in comparison with higher-order null hypotheses that include triggering.

Epistemic uncertainty

Perhaps the greatest source of systematic bias in earthquake hazard analysis is the very slow rate of the process relative to the scale of a human lifetime, so that the large, damaging events are always insufficiently sampled by instrumental, historical and even palaeoseismic data. Average earthquake recurrence intervals for such events are typically from hundreds to tens or even hundreds of thousands of years. In most cases the absence of a large event implies that hazard is typically underestimated from fitting the Gutenberg-Richter law to frequency-magnitude data. On the other hand, if a large event occurs by chance near the start of a catalogue the hazard from the largest events will be overestimated.

Fig. 1 illustrates the temporal sampling effect by studying the effect of the occurrence of the M_w 9.3 2004 Boxing-day earthquake in Sumatra on global earthquake occurrence statistics using the global CMT catalogue. This event was the largest in the modern era of digital recording, and extended the Gutenberg-Richter trend significantly (Fig. 1a). This mega-earthquake and its aftershocks did not significantly change the mean monthly event rate for all magnitudes, which had converged from below by about 1996, and was not strongly affected by Sumatran mega-earthquake and its aftershocks (Fig. 1b).

The standard deviation in monthly event rate is still around 1/3 of the mean (Fig. 2b), and

increasing. Clearly global earthquake frequency data are not yet exhibiting the inverse square root convergence of a Gaussian process.

Aleatory uncertainty

Fig. 1a illustrates how the random or statistical scatter in the data increases significantly for the rare, large events. We can estimate this source of statistical error and the magnitude scatter using synthetic models for the seismic process. Fig. 2 shows the results of 1000 randomly-drawn samples of 500 events each drawn from 500,000 events sampled from a parent Gutenberg-Richter frequency-magnitude distribution. The multiple small samples cover the same magnitude range as the single large sample, but the horizontal cut off at a minimum of one event in each bin ($\log F = 0$ on Fig. 2a) introduces a magnitude scatter that spans five magnitude units. This horizontal

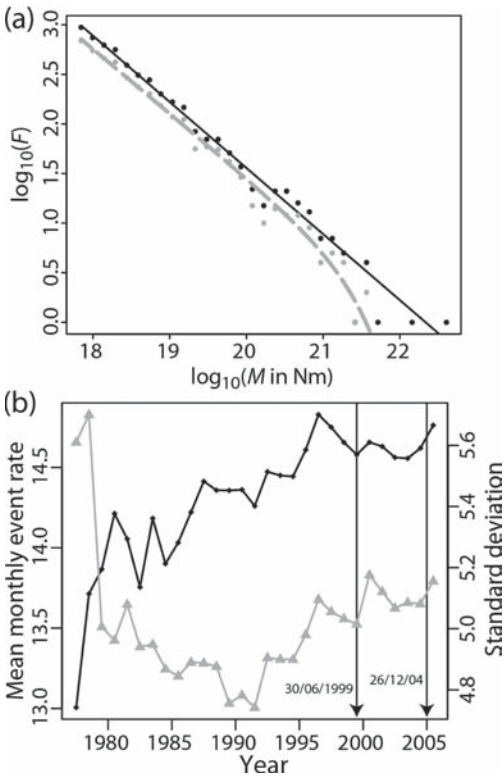


Figure 1. (a) Frequency of occurrence of earthquakes in the CMT catalogue prior to (lower curve) and after (upper straight line) the 2004 Sumatra Boxing day earthquake. (b) Mean event rate (black) and its standard deviation (grey) for earthquakes above a seismic moment magnitude of 5.8, after Main et al. (2008, Nature Geoscience 1, p. 142).

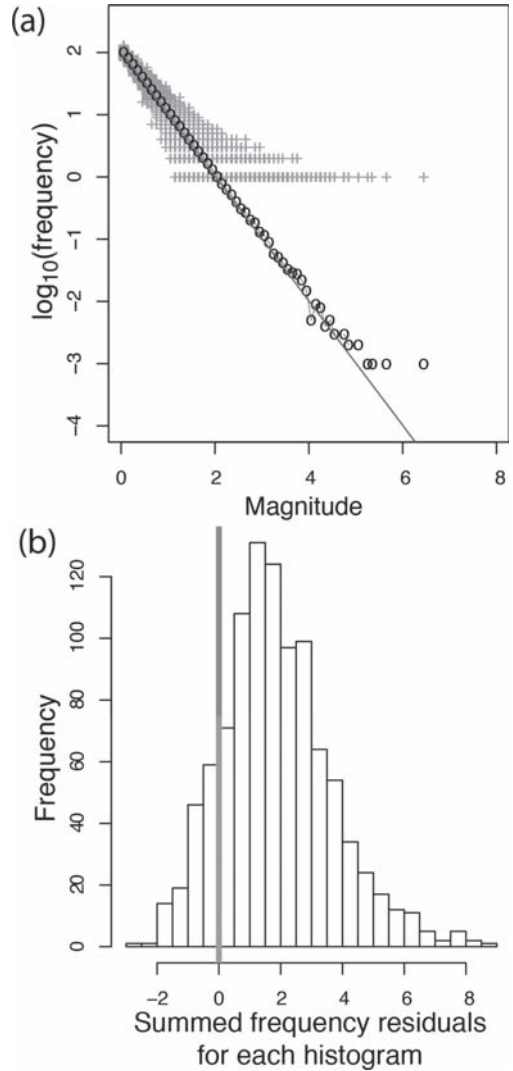


Figure 2. (a) Synthetic incremental frequency-magnitude distributions for 1000 samples of 500 earthquakes (crosses) and the whole data set (circles) sampled from an unbounded Gutenberg-Richter law (solid line), after Naylor et al. (2009, *Geophys. Res. Lett.* 36, L20303). (b) Histogram of residuals for the frequency at a given magnitude from the data in (a).

cut-off also leads to a significant bias at higher magnitudes, expressed by a skew in the distribution range to the right of the parent distribution's line in Fig. 2b. In contrast the single realization of 500,000 events shows much less horizontal scatter, except for the largest few points that deviate from the trend, indicating the eventual statistical convergence of a larger sample.

Benefits of the use of precariously balanced rocks and other fragile geological features for testing the predictions of probabilistic seismic hazard analysis

J.G. Anderson, J.N. Brune, M. Purvance & G. Biasi

Nevada Seismological Laboratory, University of Nevada, Reno, NV, USA

R. Anooshehpour

US Nuclear Regulatory Commission, Washington, DC, USA

EXTENDED ABSTRACT

Probabilistic Seismic Hazard Analysis (PSHA) attempts to answer a simple question: at what rates are different levels of strong ground motion exceeded? The reliability of PSHA results depends on the quality of the input. Primary interest is in exceedance rates of less than 10^{-2} per year so instrumental verification is not possible. However, in some Places Precariously Balanced Rocks (PBRs), with ages of $\sim 10^4$ years, can be used to test the predictions of exceedance rates in this range of interest. A PBR is a type example of a Fragile Geological Feature (FGF) that is suitable for testing PSHA. Another potentially valuable class of FGF is speleothems, since their preservation in caves is not dependent on climate.

The output of a PSHA is a calculated (ground motion) exceedance rate curve, $\lambda_c(Y)$, that estimates the number of times per year that an earthquake motion will exceed the amplitude Y . If the Poisson model holds, the probability of exceeding Y in a time interval of duration T is:

$$P(Y, T) = 1 - \exp(-\lambda_c(Y)T) \quad (1)$$

In this paper, $P(Y, T)$ is called a (ground motion) exceedance probability curve. A generalized expression for $\lambda_c(Y)$ is:

$$\lambda_c(Y) = \iint n(M, \mathbf{x}) \Phi(y \geq Y | \hat{Y}(M, R(\mathbf{x})), \sigma_T) dM dx \quad (2)$$

The term $\Phi(y \geq Y | \hat{Y}(M, R(\mathbf{x})), \sigma_T)$ is developed from a Ground Motion Prediction Equation (GMPE), and gives the probability that an earthquake with magnitude M at location x will cause a ground motion that equals or exceeds Y . The median value of Y from the GMPE is $\hat{Y}(M, R(\mathbf{x}))$, and σ_T is the standard deviation. Equation 2 is valid for any functional form of Φ , which is a function

of Y , decreasing monotonically from 1.0 for $Y = 0$, through 0.5 for $Y = \hat{Y}(M, R(\mathbf{x}))$, towards 0.0 as Y continues to increase. The seismicity model, $n(M, \mathbf{x}) dM dx$, gives the number of earthquakes per year in a magnitude range of width dM and an area (or volume) of size dx . $R(\mathbf{x})$ is the distance from the earthquake at location x to the site of interest. For a finite fault, x is defined as in the GMPE. The integrals in Equation 2 are over relevant magnitudes and the relevant volume of the Earth. The exceedance rate curve is thus estimated from a model, and must be treated as a scientific prediction, subject to testing.

The exceedance rate curve is tested by the PBRs using vector-valued PSHA, incorporating sophisticated modeling of the physics of overturning. The two dimensional description of the method is easy to visualize. The rock is parameterized by the angle, α , between vertical and the line from the center of gravity to the rocking point, and the moment of inertia. Given these parameters, the probability of the rock being toppled by ground motions is parameterized as a function of the peak acceleration (PGA) and the acceleration response spectral value at a period of 1 second (SA(1 sec)). Equation 2 is generalized so that Y is a vector consisting of these two parameters, and the rate of toppling as a function of vector Y is calculated as the product of the probability of toppling and the vector exceedance rate curve. The integral over the toppling rate surface gives the overall toppling rate. Multiplied by the age of the precarious feature, the probability of the feature surviving is calculated. If the probability of surviving is very small, then the hazard estimate is inconsistent. Using this approach, several studies have found numerous examples of PBRs that are inconsistent with the 2008 USGS National Hazard Map.

Testing a specific $\lambda_c(Y)$ by an appropriate FGF may thus be considered a forward problem, and is relatively straightforward. Identifying the cause of

an inconsistency, in contrast, is an inverse problem and may not have a unique solution.

The way to resolve it is by modifying the input to Equation 2. We consider it given that there must be a solution, because there must be a “true” hazard curve for existing precarious rocks that is consistent with the continued existence of the rock. It follows that the “true” hazard is determined from the “true” input.

Up to this point, we have approached the inverse problem from a largely empirical, and intuitive, perspective. We start with knowledge of the input and an understanding of how changes to the input will affect the hazard curve. From this we identify the features of the input that are most likely to resolve the inconsistency.

The following is a brief summary of different input features that have been called into question by PBR observations in different locations.

Few observations control the GMPEs at large magnitudes and small distances. Precarious rocks on the foot wall of normal faults suggest that GMPEs overestimated the mean ground motions for those conditions. Similarly, precarious rocks are consistent with the hypothesis that transtensional segments of strike-slip faults have relatively lower ground motions than other segments.

Consideration of the PBRs in the Mojave Desert near the San Andreas fault led the recognition that GMPE development makes an ergodic assumption: the uncertainty at a single station is estimated from the scatter of ground motions over a network of stations. An approximate way to resolve this problem is to truncate the large-amplitude tails of the GMPEs, although justification for this step is lacking.

Seismicity models for PSHA often include background, area source zones. Precarious rocks suggest that the methodology of estimating seismic activity in background zone of the US National Seismic Hazard Map contributes the discrepancy with precarious rocks in a zone between the Elsinore and San Jacinto faults and in the Mojave desert.

Precarious rocks above two faults in southern California are inconsistent with the activity rates assigned to those faults, suggesting that geologists reevaluate the strength of the evidence for the assigned slip rates. Precarious rocks in another region of southern California may help identify, or rule out, which fault broke in a poorly-known earthquake early in the history of the region.

When the PSHA uses multiple weighted models to incorporate epistemic uncertainty, it is possible to test each of the contributing hazard curves for consistency with the FGF, and use the results to evaluate the probability each branch is valid and to learn about the character of input models that are consistent with the rocks.

Eventually, following the lead of the Southern California Earthquake Center, we consider it possible that the practice of PSHA will switching to scenario-based models. By this method, possible fault ruptures are identified, and realistic synthetic seismograms are calculated from each—thus replacing the GMPE. By this approach, the details of the regional crustal structure can be realistically incorporated. PBRs that are known to have survived specific historical earthquakes can be tested by synthetic time series of those earthquakes, which tests whether the synthetic ground motions are realistic. Such tests may also constrain whether specific faults consistently rupture in a preferred direction.

Finally, we accept that in some cases, it is necessary to live with discrepancies between PSHA and PBRs. This is necessary when resolving the discrepancy requires collecting detailed data on site and regional conditions, and collecting that data is cost prohibitive.

Considering the many ways PBRs have suggested improvement to the input of PSHA in southern California, we suggest that studying PBRs and resolving discrepancies has the potential to result in widespread and general improvement of PSHA.

As the prediction of PSHA for any ground motion amplitude is the result of an integral over all possible earthquake sources, improvements in the input that resolve inconsistencies at any point on the hazard curve will affect the entire hazard curve, both at the site of the test and at nearby sites. Tests at low probabilities afforded by PBRs are particularly important for two distinct reasons. One is that the resolution of tests at high probabilities is low. The other is that low-probability hazards to critical facilities are very important. Thus we conclude that to gain confidence in PSHA inputs and statistical assumptions it is important to use PBRs to test hazard curves at low probabilities whenever data is available.

This page intentionally left blank

*GS_133 — Model selection, aggregation and testing
for probabilistic seismic hazard assessment (2)*

This page intentionally left blank

Assessing reliability and skill of earthquake forecasting models in Italy

W. Marzocchi

Istituto Nazionale di Geofisica e Vulcanologia, Roma, Italy

We review very recent initiatives aimed at testing Earthquake Occurrence (EO) models in Italy. All the material presented here has been published or is under consideration for publication in scientific journals.

Earthquake forecasting is a basic component of any kind of seismic hazard assessment at different time scales (decades, years, days). This means that the success of a seismic hazard model indispensably depends, among others, on the use of reliable and skillful earthquake forecasting models. In a nutshell, a forecasting model has to produce forecasts/predictions compatible with the future seismicity, and the forecasts/predictions have to be precise enough to be usable for practical purposes (i.e., they need a good skill). Moreover, if a set of reliable models is available, it is important to know what is the “best” one(s), i.e., the one(s) with the highest skill.

The evaluation of these pivotal features characterizing each forecasting/prediction model is the primary goal of the Collaboratory Studies for Earthquake Predictability (CSEP; <http://www.cseptesting.org>; Jordan 2006). CSEP provides a rigorous framework for an empirical evaluation of any forecasting and prediction model at different time scales (from 1 day to few years). Basically, the CSEP experiment compares forecasts produced by several EO models in testing centers with real data observed in the testing regions after the forecasts have been produced (Schorlemmer et al., 2007, Zechar et al., 2010). CSEP can be considered the successor of the Regional Earthquake Likelihood Model (RELM) project. While RELM was focusing on California, CSEP extends this focus to many other regions (New Zealand, Italy, Japan, North- and South-Western Pacific, and the whole World) as well as global testing centers (New Zealand, Europe, Japan). The CSEP experiment in Italy (Marzocchi, Schorlemmer & Wiemer 2010) has started on Aug. 1, 2009. The coordinated international experiment has two main advantages: the evaluation process is supervised by a scientific international committee, not only by the modelers themselves; the cross-evaluation of a model in different regions of the world can facilitate its evaluation in a much shorter period of time.

The CSEP experiments are truly prospective, i.e., they are meant to compare forecasts and future seismicity. Of course this testing phase may require many years to be completed. Meanwhile, we can get some preliminary information about the forecasting capability of models through a retrospective test (Werner et al., 2010). Retrospective tests do not represent the optimum strategy to test models and forecasts because some sort of retrospective (conscious or unconscious) adjustment or overfit can never be rule out. On the other hand, this testing phase aims at showing unreliable models (models that produce unreliable forecasts) and the retrospective skill of the forecasts of each model, providing a first preliminary objective ranking of the EO models.

The results of retrospective tests carried out in Italy have been very recently used to build the “best” EO model for the next ten years (Marzocchi, Amato, Akinci, Chiarabba, D’Agostino, Lombardi & Pantosti 2011); the model will be used by Civil Protection to prioritize risk reduction strategies across Italy in the next few years. Once the reliability and skill of the EO models have been checked in the retrospective experiments, we have merged the ten-years forecasts of the reliable models, weighting them according to their retrospective skill. A remarkable feature of this approach is the reduction of the subjectivity introduced by expert opinions.

Despite we emphasize here the paramount importance of the testing process, we also remark that, in some case, there might be difficulties for its implementation. In general, the choice of the “best” model to be applied in hazard assessment may be less straightforward than expected. Marzocchi and Zechar 2011 discussed in detail this point for two of the most important initiatives in California: RELM and the Uniform California Earthquake Rupture Forecast (UCERF). We believe that this discussion can be painlessly extrapolated to almost all hazard approaches commonly used. In a nutshell, Marzocchi and Zechar 2011 emphasize the role of expert opinion that may be very helpful to achieve a general agreement on one consensus model, assembling different pieces of scientific information; on the other hand, the use of expert opinion generates

untestable models. In general, each forecasting and hazard endeavor is characterized by a balance between scientific and practical components. These are not necessarily opposing forces but they do influence the approach for building or selecting the best model. That said, it is easy to foresee a wider application of the testing procedures in hazard assessment, probably embracing also the Ground Motion Prediction Equations (GMPEs). The basic idea behind this larger application is that every reduction of subjectivity implies in parallel a reduction of possible controversies. Testing is behind science and even though nowadays it turns to be not always possible, it has to represent the ultimate goal of each hazard assessment.

REFERENCES

- Jordan, T. (2006). Earthquake predictability, brick by brick. *Seismol. Res. Lett.* 77, 3–6.
- Marzocchi, W., Amato, A., Akinci, A., Chiarabba, C., D'Agostino, N., Lombardi, A. & Pantosti, D. (2011). A ten-years earthquake occurrence model for Italy. *Bull. Seismol. Soc. Am.*, submitted.
- Marzocchi, W., Schorlemmer, D. & Wiemer, S. (2010). Preface to the special volume “An earthquake forecast experiment in Italy”. *Ann. Geophys.* 53, 3.
- Marzocchi, W. & Zechar, J. (2011). Earthquake forecasting and earthquake prediction: different approaches for obtaining the best model. *Seism. Res. Lett.*
- Schorlemmer, D., Gerstenberger, M., Wiemer, S., Jackson, D. & Rhoades, D. (2007). Earthquake likelihood model testing. *Seismol. Res. Lett.* 78, 17–29.
- Werner, M., Zechar, J., Marzocchi, W. & Wiemer, S. (2010). Retrospective tests of the long-term earthquake forecasts submitted to CSEP-Italy predictability experiment. *Ann. Geophys.* 53, 11–30.
- Zechar, J., Gerstenberger, M. & Rhoades, D. (2010). Likelihood-based tests for evaluating spaceratemagnitude earthquake forecasts. *Bull. Seismol. Soc. Am.* 100, 1184–1195.

On the use of observations for constraining probabilistic seismic hazard estimates—brief review of existing methods

Céline Beauval

ISTerre/LGIT, IRD-UJF-CNRS, Grenoble, France

As probabilistic methods are now the standard for estimating long-term seismic hazard, it is tempting and legitimate to use as much as possible past observations to validate (or cast doubt) on PSHA estimations. Dealing with the output of a Probabilistic Seismic Hazard (PSH) calculation, these observations can be of at least three types: strong-motion recordings, intensity assignments and fragile geological structures. Probabilistic seismic hazard estimates by definition correspond to rare phenomena. For example, the ground-motion with return period 475 years, currently still in use for conventional building, has a 10% probability of being exceeded at least once in a 50 yrs-time window. In other words, this ground-motion has

a mean occurrence rate of 1 every 475 years. In nuclear safety, the design ground-motions of reference correspond to much longer return periods. Here, the aim is to encourage the use of ground motions, intensities, or other observations, to derive methods to compare observed occurrences with probabilistic estimations. We discuss advantages and shortcomings of existing testing techniques, and encourage future authors to perform such studies with full transparency on the hypotheses underlying any of the testing methods. Otherwise, results might be over-interpreted, and in the case of validating or rejecting probabilistic hazard maps to be used in building regulation, consequences can be tremendous.

Quantification of epistemic uncertainties in probabilistic seismic hazard analysis

F. Scherbaum, N. Kuehn, M. Ohrnberger, C. Riggelsen & N. Gianniotis
Institute of Earth and Environmental Science, University of Potsdam, Potsdam, Germany

ABSTRACT: The quantification of epistemic uncertainties is still a major challenge in seismic hazard analysis. Uncertainties in the context of selecting ground-motion models and judging their appropriateness for example are known to often dominate seismic hazard assessments at low probability levels. Current practice is primarily based on using logic trees which is conceptually limited to exhaustive and mutually exclusive model sets. For a discussion of issues related to these aspects see for example Bommer and Scherbaum (2008). A major issue is caused by the fact that within the standard logic tree framework, models are commonly judged from a purely descriptive, model based perspective, in other words on a categorical or nominal scale (Scherbaum et al., 2005). Due to the absence of distance metrics for nominal scales (Stevens, 1946), a quantitative comparison of model proximity is impossible and model redundancy can only be dealt with in an ad-hoc fashion. As a practical consequence for seismic hazard analysis, this invites creating unintended inconsistencies regarding the weights on the corresponding hazard curves. On the other hand, for human experts it is usually difficult to judge from a value-based perspective, which would require to confidently express degrees-of-beliefs in particular numerical ground-motion values. In a previous paper (Scherbaum et al., 2010) we have demonstrated for ground-motion models how the model and the value-based perspectives can be partially reconciled by using high-dimensional information-visualization techniques.

The key idea is to represent ground-motion models in terms of high-dimensional feature vectors. These feature vectors can be thought of as spanning a two-dimensional model manifold in a high-dimensional space. The structure of this manifold can be analysed through a combination of SOM (Kohonen, 2001) and Sammon's mapping (Sammon, 1969). Here, in extension of our earlier work we use an information-theoretic distance metric (Cover and Thomas, 2006) to express the mutual relationship between ground-motion models (Scherbaum et al., 2009) for the construction of

the SOMs. This allows the representation of epistemic uncertainties on ground-motion models in terms of “*model proximity maps*” which quantify the relative information loss between ground-motion models on a continuous interval scale.

This paves the way for a radical paradigm change. Instead of viewing the set of candidate ground-motion models in a seismic hazard study as a set of mutually exclusive and collectively exhaustive categorical set of models, which is a rather strong assumption, we consider it more appropriate to consider the set of candidate models as a set of samples from a continuous model domain. One possible way to quantify such a model domain could be in terms of a finite region of a model proximity map. Each model could then be seen as representing a particular part of the complete model region.

Making the conceptual transition from treating a set of candidate models as categories on a categorical scale to which subjective probabilities are assigned as illustrated by the vertical bars in (Fig. 1a) to seeing models as points in a model continuum also provides a new look at the problem of model redundancy. For ground-motion

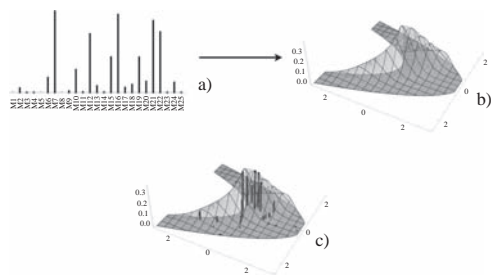


Figure 1. Sketch of the consequences of the conceptual transition to a model continuum for the weighting. Instead of a set of discrete weights for the categorical perspective (a), for the continuous model the weights become a weight surface on the model domain (b). Individual model weights can be seen as samples of this weight surface (c).

models, the problem of model redundancy may arise in cases where ground-motion models have been constructed from partially overlapping data sets or even on identical data set but for different functional forms. On the nominal scale, model redundancy can only be dealt with in an adhoc way by down weighing those models assumed to be affected.

On the continuous model domain, however, epistemic uncertainty is no longer defined as a discrete set of weights, but by a continuous weighting function over the domain (Fig. 1b). The degree-of-belief values on the individual models in the logic tree perspective are then nothing else than scaled samples of this weighting function at the locations given by the location of the models on the proximity map (Fig. 1c).

Reusing a dataset or a part of a data set for a new model will generate a new model vector location in the vicinity of already existing ones. During the generation of the SOM, this will pull in more prototype vectors into that region but will not pose any conceptual problem, since in the continuous model domain the distance between models is taken into account. As a consequence, on a continuous model domain model redundancy can be easily dealt with in a systematic way.

In the present study we explore ways to reconcile the basic idea of logic trees to work with a finite set of models with the notion that these models can be seen as samples from a model continuum. We illustrate the concept for ground-motion models only, but we do not see a reason why this could not be applied to other aspects of a hazard model. The basic idea is to represent the models as finite-length model feature vectors. As a consequence of this transformation, the task of weighting individual models on a purely nominal scale is transformed into the problem of defining a weight “surface” function on the model manifold. This function represents a PDF of the epistemic uncertainty on the model manifold. The condition that the weights have to sum up to 1 translates into the condition that the volume under the surface (taken over the model manifold) has to be one. Using a tessellation of the model manifold with the cell centers defined by the individual model representation vectors,

the cell size of each vector is proportional to the area this model exclusively represents on the model manifold. Therefore it could directly be used to normalize the degree-of-belief values which an expert may have given to a ground-motion model to the area it exclusively represents on the model region.

Representing models as discrete high-dimensional feature vectors opens up new roads of dealing with epistemic uncertainties in seismic hazard analysis. We admit that there is still a lot of roadwork ahead to make this roads passable but we believe it is definitely worth exploring.

REFERENCES

- Bommer, J.J. & Scherbaum, F. (2008). The use and misuse of logic-trees in Probabilistic Seismic Hazard Analysis, *Earthquake Spectra*, **24**(4), 997–1009.
- Cotton, F., Scherbaum, F., Bommer, J.J. & Bungum, H. (2006). Criteria for selecting and adjusting ground-motion models for specific target regions: application to Central Europe and rock sites, *Journal of Seismology*, **10**, 137–156, DOI: 110.1007/s10950-10005-19006-10957.
- Cover, T.M. & Thomas, J.A. (2006). *Elements of information theory* (2. ed.): Wiley & Sons Inc.
- Kohonen, T. (2001). *Self-organizing maps*. Berlin-Heidelberg-New York Springer Verlag.
- Sammon, J.W. (1969). A nonlinear mapping for data structure analysis, *IEEE Trans. on Computers*, **C-18**(5), 401–409.
- Scherbaum, F., Bommer, J.J., Bungum, H., Cotton, F. & Abrahamson, N.A. (2005). Composite ground-motion models and logic trees: methodology, sensitivities, and uncertainties, *Bulletin of the Seismological Society of America*, **95**(5), 1575–1593.
- Scherbaum, Frank, Elise Delavaud, & Carsten Riggelsen (2009). Model Selection in Seismic Hazard Analysis: An Information-Theoretic Perspective, *Bulletin of the Seismological Society of America*, **99**(6), 3234–3247.
- Scherbaum, F., Kuehn, N., Ohrnberger, M. & Koehler, A. (2010). Exploring the Proximity of Ground-Motion Models Using High-Dimensional Visualization Techniques, *Earthquake Spectra in press*.
- Stevens, S.S. (1946). On the theory of scales of measurement, *Science*, **103**(2684), 677–680.

This page intentionally left blank

*MS_137 — Modelling for Risk management
in construction projects*

This page intentionally left blank

Acceptance criteria for the spatial variability of the concrete cover depth in a Swiss tunnel

Vasiliki Malioka

Ernst Basler + Partner, Division of Safety and Security, Zollikon, Switzerland

Stefan Matsch

Ernst Basler + Partner, Division of Infrastructure and Transportation Systems, Zurich, Switzerland

Michael H. Faber

ETH Zurich, Risk and Safety, Zurich, Switzerland

1 INTRODUCTION

In what concerns the construction of large concrete structures, a problem often faced is the lack of providing the owner of the structure with a reliable forecast of the structural performance. Uncertainties involved in the design and construction stages deem the performance of the realized structure uncertain in terms of the fulfillment of the owner's requirements.

Research concentrated on the assessment of the performance of existing structures, neglecting the fact that if structures were more sufficiently controlled at the beginning of their structural lives several of the faced serviceability and economical problems could have been avoided or treated with reduced costs. The decision problem faced by owners of large scale concrete structures, upon their completion, is their acceptability upon the fulfillment of a number of requirements. The current practice is that few properties, e.g. compressive strength, are measured upon completion of the structure and its acceptability is based on a standard set of requirements. A structure though is exposed during its service life to several factors that affect its performance in time. Faber & Rostam (2001) pointed out the necessity of providing owners with a realistic forecast of the future structural performance based on information made available at the handing over phase of newly built structures. Within this context, owners' requirements shall have the form of acceptance criteria, related to the quality control of the final structure, upon fulfillment of which the contractor could be released from his contractual obligations.

Latest advances in research provide the tools for setting up such acceptance criteria. Focus has been given mostly on acceptance criteria for the temporal and local effects of deterioration

processes. However, a variation of the concrete characteristics is expected from the design stages, while the variability of batches and workmanship during the construction of a structure add to this. Furthermore, factors such as the concentration of harmful substances differ among the various locations of a concrete structure since they are exposed to different environments. The consistent consideration of the spatial variations in the realized structure have lately started to be a focus point e.g. Faber & Gehlen (2002), Malioka & Faber (2006), Straub et al. (2009). In Malioka (2009) an approach is presented on how acceptance criteria for the spatial variation of the as-built concrete material properties may be formulated on the basis of the owners' requirements, how they can be assessed and communicated.

In the present paper a methodical framework for setting up quality control acceptance criteria is summarized aiming to present the modeling and application advantages but also limitations of the approach. Measurements of the concrete cover depth of a Swiss road tunnel are then used for the presentation of an application of the framework. The acceptance criteria are formulated focusing on the future structural performance of a tunnel segment subjected to corrosion due to carbonation.

2 METHODOLOGICAL FRAMEWORK

It is proposed that the owner requirements for the service life performance shall be formulated in terms of the probability that more than a percentage of a structural zone is in a certain condition state at a reference time i.e. after a period of time in service. This facilitates comparison of the performance of a given structure with specified requirements. At the same time, the formulation

enables to account for the spatial variability of the uncertain parameters that are decisive for the service life durability performance.

A prerequisite for the assessment of the spatial variability is the division of the structure into homogeneous zones and then into individual elements. That allows the assessment of two types of spatial variability, namely the within and the between the elements variability. These can be assessed by testing of the as-built material properties in the structure. The two types of spatial variability are assessed in terms of sample statistics and their compliance or not to the specified requirements can easily be proved.

The division of the structure to homogeneous zones follows from the consideration of a number of initial condition indicators, e.g. age, exposure environment etc. The further division into individual elements is based on a study of the namely correlation radius or length that is a measure of the distance within which strong correlation persists. Various aspects and limitations regarding the assessment of the correlation radius are discussed in the paper.

The probabilistic characteristics of the deterioration process at each element are assessed using the DuraCrete (2000) model that describes the degradation process and its progress in time. The condition states of the individual elements are interdependent due to common influencing parameters in the system. This stochastic dependency is accounted in the assessment of the spatial characteristics of deterioration through the use of common influencing parameters as explained in e.g. Faber et al. (2006) and Straub et al. (2009). Conditional on the realization of the common influencing parameters, the elements constituting a specific homogeneous zone are considered to behave statistically independent in terms of their deterioration characteristics.

The random variables in the model are identically distributed for all individual elements. Their distribution characteristics have parameter values (mean and standard deviation) according to the initial condition indicators based on which the homogeneous zone of consideration has been defined. Spatially distributed material properties are represented in the model by uncertain random variables i.e. their mean value is not constant but is an uncertain variable itself. In that way the within and between the elements variability are directly incorporated in the model. In the paper it is discussed how the statistical characteristics of the spatially distributed variables can be assessed from measurements performed in the considered zone.

From the probabilistic modeling of the degradation process over time, a prior probability density function of the probability of degradation of one

element is established by Monte Carlo simulation over the random variables representing statistical and model uncertainties. Using this prior probability, the probability of distributed degradation is estimated for a percentage of the examined zone being in a condition state of interest. Provided that this probability fulfils the acceptance criteria set by the owner, the spatial variability of the concrete material property can be accepted. The proposed framework has the advantage that all possible combinations of the within and between the elements variability can be calculated prior to any measurements i.e. prior to the submission of the structure. These combinations are illustrated in the form of iso-contours for different acceptability levels. That enables the direct assessment of the acceptance of the structure upon its submission or at any construction stage when measurements are made available.

3 APPLICATION IN THE ST. GOTTHARD TUNNEL

An application of the presented framework is provided in the St. Gotthard road tunnel in Switzerland. The bidirectional traffic tunnel with an approximate length of 16.4 km is one of the longest road tunnels in the world. It is shown how the quality control acceptance criteria are formulated and then assessed for the purpose of quality control of the concrete cover depth. A homogeneous zone of the false ceiling of the tunnel, lying approximately in the middle of the tunnel, is examined. The statistical characteristics of the concrete cover depth are assessed based on measurements carried out during an inspection, Ernst Basler + Partner (2004). The future performance of the structure in terms of the carbonation progress is assessed. For different acceptability levels that could be set by the owner, it is examined whereas the spatial variability of the concrete cover depth is acceptable or not.

REFERENCES

- DuraCrete (2000). Statistical quantification of the variables in the limit state functions. BRITE EU-RAM Project no. 1347, Document BE95-1347/R9.
- Ernst Basler + Partner (2004). *Gottard Strassentunnel: Untersuchungen der Zwischendecke, Messtechnische Untersuchungen (Potentialmessungen) und statische Überprüfung*. Client: Swiss Federal Roads Office (FEDRO; ASTRA in German).
- Faber, M.H. & Gehlen, C. (2002). Probabilistischer Ansatz zur Beurteilung der Dauerhaftigkeit von bestehenden Stahlbetonbauten. *Journal of Beton- und Stahlbetonbau*, 97. Heft 8: 421–429. ISSN 0005-9900, Ernst & Sohn.

- Faber, M.H. & Rostam, S. (2001). Durability and Service Life of Concrete Structures-The Owners Perspective. *Proceedings: International Conference on Safety, Risk and Reliability-Trends in Engineering*, IABSE. Malta, 21–23 March 2001, pp. 369–374.
- Malioka, V., Leeman, A., Hoffmann, C. & Faber, M.H. (2006). *Spatial variability of concrete properties within a building component (Streuung der Betzoneigenschaften in bauwerken)*. Research report on the appointment of the FEDRO (ASTRA) Working Group on Bridge Research (AGB2002/027).
- Malioka, V. (2009). *Condition Indicators for the Assessment of Local and Spatial Deterioration of Concrete Structures*. PhD Thesis, Swiss Federal Institute of Technology (ETH), Chair of Risk and Safety, Zurich.
- Straub, D., Malioka, V. & Faber, M.H. (2009). A framework for the asset integrity management of large deteriorating concrete structures. *Structure and Infrastructure Engineering*, 5(3), pp. 199–213.

Cost and time correlations in linear infrastructure construction

Y. Moret & H.H. Einstein

Massachusetts Institute of Technology, Cambridge, MA, USA

ABSTRACT: Cost and time overruns in construction occur often. Many internal and external factors may play a role. The objective of this paper is to investigate the effect of cost and/or time correlations between construction entities. Several studies in building construction have shown that construction costs are correlated and produce larger standard deviations of total cost compared to assuming independence. This paper expands on these findings by investigating the effect of cost and time correlations in linear infrastructure (rail lines, highways and similar) construction.

Total construction cost is obtained by summing all project costs while total construction time is obtained by summing the times along the critical path. To represent correlated costs or correlated times, one needs correlation models, which in turn are based on correlation matrices (coefficients) and marginal probability distributions. The NORTA correlation model and the Spearman correlation coefficient are used here, while the marginal distributions are lognormal for cost and triangular for time, both skewed toward the higher values.

The central part of this paper is the identification of correlation types that need to be considered in linear infrastructure construction. As a matter of fact, these correlations also apply to any networked construction project; however, in order to stay with concrete and practical issues the following will be related to linear infrastructure projects such as rail lines or highways. Such projects consist of four major structure types, namely, tunnels, viaducts (bridges), embankments and cuts. The construction of each of these structures consists of one to several activities for which correlations might have to be considered:

- Tunnel: One activity—excavation and support of one meter tunnel.
- Viaduct: Several activities—pier foundation, pier, deck section, abutment, technical block.
- Embankment: Several activities—clearing, improvement, filling, capping, sub-ballast.
- Cut: Several activities—clearing, excavation, capping, sub-ballast.

The following four cost correlations and one cost-time correlation are identified in the construction of rail lines and highways:

1. Correlation between the costs of a repeated activity in a structure. The costs of repeated activities are expected to be positively correlated because of the repetitiveness of the processes. A good example of repeated activities occurs in tunnels, where activities can be independent, perfectly correlated (same cost for each repeated activity) or partially correlated at an intermediate level, i.e. the cost per meter is randomly selected for each meter, and if one cost per meter is above average, the next cost per meter will tend to be also above average.
2. Correlation between the costs of different activities in a structure. The cost of different activities in a structure are expected to be positively correlated because these activities might be subject to the same type of constraints. Such possibly correlated activities occur in viaduct construction. They will be described later in this abstract.
3. Correlation between the costs of activities in adjacent structures. Typical adjacent structures are cuts and embankments in a cut and embankment sequence, cuts and tunnels at the tunnel's portals, and embankments and viaducts at the viaduct's ends. The costs of activities in adjacent structures are expected to be positively correlated because they might be sharing construction activities.
4. Correlation between the costs of the same activities in the same type of structures. Positive correlations between the cost of same type of structures (e.g. between tunnel I and tunnel J) are expected if geology is similar. Since the cost distribution of e.g. a tunnel is a function of the geology, similar geologies produce similar cost distributions.
5. Correlation between the cost and time of the same activity in a structure. Correlations between cost and time of an activity do occur regularly. It is expected that the cost and the time of an activity are positively correlated. In fact, if an activity lasts longer than the average time, one can expect the cost of the activity to be also

larger than average. However, if activities are done in parallel, they may not increase the total duration (time of critical path activities) but increase cost.

Practically speaking one needs to simulate construction of these typical structures by simulating cost and time of the pertinent activities. This is done through a construction simulation model based on an extension of the Decision Aids for Tunneling. To investigate the effect of correlation, the construction model needs to be combined with the correlation model mentioned above. With this, one can make cost/time predictions of infrastructure projects considering the various types of correlation.

Two examples cases are described to demonstrate the effect of correlations: the construction of a viaduct is simulated first modeling correlation type 2, the correlation between the costs of different activities in a structure, and then correlation types 5, the correlation between the cost and time of the same activity in a structure. The viaduct is a 395 m long viaduct of the Portuguese High Speed Rail network.

In correlation type 2, the construction of the pile set, the footing and the pier may be similarly constrained by site access. These activities can, therefore, be independent (no site access constraint) or partially positively correlated if constrained by site access, i.e. if pile set cost is high, footing and pier costs are also high. In the example case study we assume that pile set, footing and pier, which form a unit, are correlated with correlation 0.8. Modeling correlation type 2 and comparing the total cost and total time distributions with those assuming independence shows an increase of 8.3% in the standard deviation of the total cost. A sensitivity analysis investigates the impact of the viaduct length, i.e. the number of units, on the standard deviation of the total cost. Simulations with 2, 9, 30, 50, 100 units show that the means and the standard deviations increase with number of units. Most importantly the total cost standard deviation when modeling correlation increases faster than that when modeling independence. For 100 units,

the standard deviation of the correlated costs is 15.5% larger than the one of independent costs. When comparing this to the aforementioned difference of 8.3% for a nine-unit viaduct it is evident that length (i.e. the number of activities) plays an important role.

In correlation type 5, the cost and the time of each activity are correlated, whilst costs are independent of one another and times are independent of one another. In the example case study the correlation is assumed equal to 0.8. The results show that the total cost and the total time distributions are equal to those modeling independence. However, the correlation between total cost and total time is equal to 0.38. Similarly to correlation type 2, a sensitivity analysis investigates the impact of the viaduct length on the correlation between total cost and total time. Of particular interest is the result that with increasing number of units in the viaduct, i.e. increasing length of the viaduct, the correlation between total cost and total time increases. The final important result shows that despite the correlation between the total cost and the total time, the means, the 80th and the 95th percentiles of the total cost are equal to the case modeling independent cost and time. This indicates that correlation between cost and time of each activity does not impact the marginal distributions of the total cost and total time.

The investigation underlying this paper shows that four types of cost correlations and one cost-time correlation play a role when determining infrastructure cost. The standard deviation of total cost can substantially increase if activities are correlated and this becomes more significant as the number of correlated activities (generally associated with the length of the structure) increases.

All this is incorporated in a construction simulation model, which allows one to make cost/time predictions for linear infrastructure projects. The examples shown in this paper stem from work on an application to High Speed Rail lines of RAVE in Portugal.

Germa, a national research project: Multifactor risk control and management in complex civil engineering projects

D. Morand

Paris-Est Marne-la-Vallée University, Marne la Vallée, France

P. Perret

Artelia, Saint Denis, France

L. Demilecamps

Vinci Construction France, Nanterre, France

A. Machu

IOSIS, Montreuil, France

ABSTRACT: Notable development in civil and urban engineering (such as projects involving public and private) as well as the difficulties and accidents during the project (or after commissioning of works), have marked the evolution of the profession of Civil Engineering in recent decades.

The evolution of regulation and legislation (public-private partnerships, expansion of activities of project management to decentralize ...), the involvement of local politics may constrain or modify any project and the multiplicity of actors also contributed to a more complex project control and risk management.

These projects sometimes led to serious failures (technical, financial or commercial) to a questioning of traditional objectives (cost, schedule and performance) or specifically related (environment, sustainable development, industrial accidents, ...) or their final abandonment.

That's why the project management and management of project risks have become a major issue for many organizations.

Germa is a national research project aiming with risk and control in complex civil engineering projects. Our proposal aims to carry on the performances improving in engineering field in its role of the management of complex projects in civil engineering. The methodology of the project will integrate risks related to this complexity of projects.

A first analysis, conducted from spectacular damages for major projects in recent years, lead us to believe that:

- The lack of basic knowledge database increases the cost of insurance
- The current regulatory framework is inadequate for large projects

- The impact of these damages is such that at any time the insurers may refuse to get involved in projects.

Between all actors of the life cycle of a project, knowledge bases and practices (methods and tools) in the risk management of risk is quite fragmented and compartmentalized. Studies relating to project risk in the construction sector are still scarce and fragmentary. The main stakeholders in the world of civil engineering world remain uninvolved in methodological developments and do not actually change their behaviors and their relationship to the projects.

Our research is using a 3D-approach: phase, impact and stakeholder.

Decomposition of the project into different phases can be done at different levels of detail. In our study, we estimated that the following events delineate the significant phases with respect to risk management: decision to start, general design, building permit, call for tenders, contracts signing, preliminary works, main works, acceptance of works.

Many studies have attempted to establish a typology of risk (in terms of causes, impacts ...). In order to limit the scope of our research, we finally considered 8 impacts: financing, project economics, delay, user safety, worker safety, environmental, technical, operability.

The owner is responsible for the work, the result of a set of actions to be undertaken to reach an objective. He aims to identify needs and to define the work that will satisfy those needs. He will also identify and mobilize the resources necessary to carry out the work. He finally checks the conformity of the work done.

Three main stakeholders are considered: the owner, which function is assured by the owner himself but also by the developer, the operator, the user, the client; the project management and engineering, assumed by the person or entity that is responsible for the design and the realization of a work; the realization, corresponding to the construction of the building.

Our approach considers the incidence of the risk management on the functional level of the relations between owners, project managers, designers and civil engineering firm. It approaches the incidence of the generic risk management from the point of view of the insurance. The present research aims to analyze the risk management according to the stage of the project (project definition, design, building license, contracting, work, end of project), the type of impact (cost, delay, safety, environment,

technics, ...) and the concerned stakeholder (owner, project manager, firm). We have presented the result with a three-dimensional matrix.

Main results of our research are:

- A large literature review
- The definition of a fictional stakeholder (the project it-self)
- The edition of a methodological guide
- The definition of a risk observatory.

These results are presented in the full article. Another important result is the development of a 'training package'.

This research was undertaken by a multi-field team (universities, project managers and designers, civil engineering firm) and it has been funded by French National Research Agency and by the cluster Advancity.

Tunnelling optimization by risk analysis techniques

D. Kolic

Neuron Consult ZT, Pasching-Linz, Austria

INTRODUCTION

Experience based design knowledge is especially used and applied in early project phases as conceptual and preliminary design. During these two early design phases very important design decisions have to be made that have direct and dominant impact on the final cost estimation and overall project budget of each structure, by underground structures as well. Therefore one new approach and methodology of influence in early design phases has been developed in last years. It is based on the implemented design decisions and is already used on several on-going tunnelling project performed as SCL (NATM) tunnels or TBM driven tunnels. The methodology “FAUST” uses evaluation of predicted procedures that may happen during project development and construction from conceptual design toward final construction works. It enables the optimization of different tunnel options and methodologies as well and is based on the final economic evaluation of tunnel variants.

STRUCTURES FOR STRAIT CROSSINGS

Comparison of different structural options will usually be performed on few interesting but

different crossing locations in micro and/or macro region. Usual problem with such comparisons comes from the use of unit prices that are of questionable decent and usually are not coming from some other comparable strait crossing structure.

Strait crossings are still rare structures and experience made on one of them could not be fully taken over to another strait crossing. For the Fehmarn belt crossing different crossing options have been developed comparing basically bridge, bored tunnel and an immersed tube options providing different traffic capacities (Fig. 1).

OPTIMIZATION MODULE “FAUST”

The module FAUST is dedicated basically to tunnel structures. It implies series of negative scenarios that may happen within one tunnelling project concerning surrounding conditions as geology and water, tunnel structural capacity and different design decisions and solutions, influences from construction and hazards during construction procedure. Project risks are implemented over negative scenarios about possible influences that may disturb planned procedure or can have direct influence on the structural elements or construction methodology. This analysis and optimization can

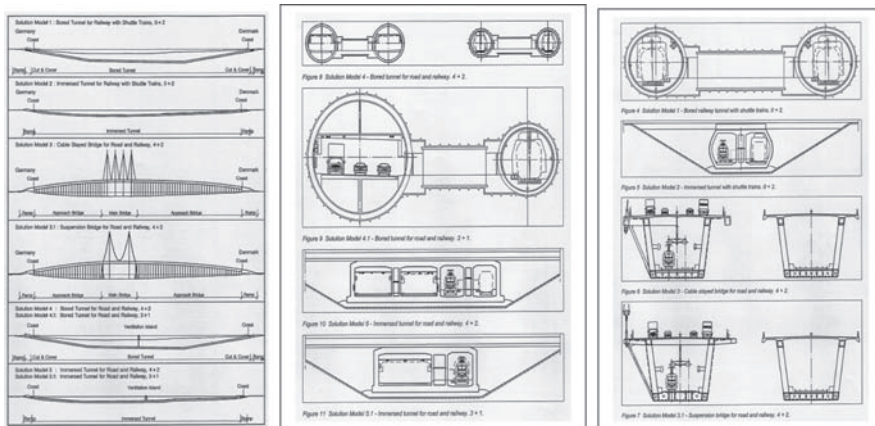


Figure 1. Fehmarn belt: overview of tunnel and bridge options for a 19 km long crossing (Jensen 2000).

Table 1. Fehmarn Belt, Danemark-Germany: total predicted construction cost overview.

Opt. Nr.	Type of structure	Overall estimated constr. costs Mill. [€]	Relation [%]	Additional		Overall predicted		Relat.		Constr. costs per m ² traff. surface min/max [€/m ²]
				Costs Min Mill. [€]	Costs Max Mill. [€]	con. costs Min Mill. [€]	con. costs Max Mill. [€]	Min [%]	Max [%]	
1	Bored tunnel 0+2	3.391,0	118	508,7	644,3	3.899,7	4.035,3	15	19	15.404/ 15.939
2	Immersed tube 0+2	3.545,0	123	602,7	780,0	4.147,7	4.325,0	17	22	18.657/ 19.455
3	Cable stayed bridge 4+2	3.040,0	106	668,8	760,0	3.708,8	3.800,0	22	25	6.691/ 6.856
3.1	Suspension bridge 4+2	3.573,0	124	750,3	1.071,9	4.323,3	4.644,9	21	30	7.815/ 8.396
4	Bored tunnel 4+2	4.420,0	154	1.060,8	1.326,0	5.480,8	5.746,0	24	30	9.240/ 9.687
5	Immersed tube 4+2	3.780,0	132	907,2	1.209,6	4.687,2	4.989,6	24	32	8.846/ 9.416
4.1	Bored tunnel 3+1	2.992,0	104	448,8	568,5	3.440,8	3.560,5	15	19	9.004/ 9.317
5.1	Immersed tube 3+1	2.874,0	100	574,8	718,5	3.448,8	3.592,5	20	25	10.103/ 10.524

be applied in very early project phases. Estimation of overall construction costs is based on the structural concepts and used structural elements and pertinent construction methodology. Regular cost estimation covers the part we know as “basic costs”. There is another amount of costs called “additional costs” that comes from unexpected, undefined or unknown reasons. This part of costs is responsible for massive cost overruns and has its base in: weak project planning, rough estimations in early project phases, unknown project scenarios that come with the higher level of the project size, but also in political decisions, making project more attractive for investors, in giving reasons to start the project and in generally making the project more feasible. The module “FAUST” consists of qualitative and quantitative part of analysis and uses experienced based knowledge collected on other tunnelling projects for defining negative risk scenarios for analyzed project and pertinent project phase and further they are economical valued as additional costs.

The intention to analyse Fehmarn belt crossing cost estimation results comes from very low dispersion of cost estimation results for completely different structural options. It was to be expected that some differences may influence overall construction cost results because the present analysis

has been performed in the very early project development phase. The evaluation of known project circumstances has been limited on collected published information but still some of investigation gave relatively clear picture about dominant expected influences on this crossing location and partly from other similar project locations in vicinity where similar projects have been developed and constructed within last 30 years.

CONCLUSION

Herewith presented capacity of the module “FAUST” shows the ability to predict the total construction project costs of tunnelling strait crossing options. The method is based on the evaluation of the negative risk scenarios based on the character of the structural solution and on the information about the conditions on the location of the crossing. Negative risk scenarios have been developed for the specific tunnel project options but are based on the experience of similar conditions or limitations on other known and available tunnel projects. The quality of estimation and prediction is based on the range and quality of available project information.

Modeling methodology of the Risk Breakdown Structure for project risk management in construction

R. Mehdizadeh, D. Breyse & M. Chaplain

Université Bordeaux, I2M, Department of Civil and Environmental Engineering (GCE), Talence Cedex, France

Project Risk Management (PRM) is aimed at reducing the probability of failure to reach the project objective at a residual, identified and acceptable level.

Main objectives of the project usually are cost, time and quality. “Quality” can cover the functionality of the product, but also other dimensions, like the worker safety or environmental impacts. In the following, we will consider:

- *project risk* as a measure of consequences (positive or negative) for the project, which can result for the occurrence of uncertain events,
- *risk event (RE)* as any fact or event whose occurrence can have some impact/consequence on at least one of the objectives of the project,
- *risk category (RC)* as a way to group several risk events. Any category can be split into subcategories when wanting a more detailed view or, reversely, grouped with other categories when wanting a more general view.

The hierarchical description of risks can be based on the risk breakdown structure—RBS, which offers a global view on the risks (Chapman, 2001) and is a very adequate tool for risk management:

- a. since each stakeholder can have his own view on the project, RBS can be helpful, at any stage of the project in offering different pictures of the same state of knowledge, making certain that the various pictures remain consistent,
- b. the RBS can “live” with the project, its branches being more or less developed (or replaced with others) when some risk categories become more or less important. At each stage of the project and for each possible user, explicit rules must justify the selection of the appropriate RBS,
- c. the time evolution of the tree also concerns the rules according to which the project risks are calculated.

The RBS however suffers several drawbacks, the main one being that there is no consensus on how to develop it. A detailed study has shown (Mehdizadeh et al., 2010) that lack of clarity and inconsistencies are not uncommon. There is in

general no clear definition of the meaning of risk categories, and the same words can cover different items. Another difficulty comes from the definition of the rules enabling the transfer of qualitative/quantitative information on risks across the tree. The sensitivity of the results to the rules deserves a careful study.

Our aim is to develop a methodology which profits of all advantages of RBS, without suffering its usual drawbacks. Therefore, the challenges are to ensure: (a) consistency of the picture and between several pictures, (b) possibility of evolution, (c) ability to select a more appropriate picture according to explicit criteria. Of course, the methodology must be both general enough to cover all construction projects and specific enough to be adapted to a given particular project. Once more, RBS is a convenient tool, since it suffices, keeping the same frame, to develop the branches corresponding to a specific context (i.e. tunnel works or railway infrastructure). The idea will be that of « *tailor-made RBS* » (Mehdizadeh et al., 2010).

The methodology is based on:

- a. Establishing a taxonomy of risk events RE and risk categories RC, based on an extensive review of existing literature.
- b. Identifying a database of elementary trees, or micro-trees MT, which highlight how each risk category can be subdivided into subcategories.
- c. Synthesizing the knowledge base, which includes the risk events, the risk categories and the micro-trees, by building a matrix which formalizes all possible hierarchical links.
- d. Defining a series of criteria which enable one to quantify the “quality” of a RBS. The issue of quality is central, since there is not an “optimal RBS” but RBSs which are more or less adapted to a given situation and objective.
- e. Elaborating a strategy for building a RBS which satisfies the main requirements, which are expressed in a given situation.
- f. The last step will be to define the rules enabling the transfer of information (frequencies/probabilities and magnitude/impact) from the bottom to the top of the RBS.

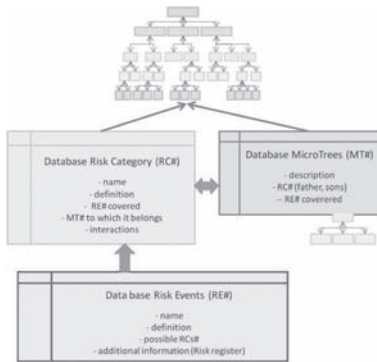


Figure 1. Relations between the 3 components of the database.

We developed a knowledge base containing three interactive components (Fig. 1):

- a library of Risk events RE,
- a library of Risk categories RC,
- a library of Micro-trees MT.

Risk events

The RE database must answer two questions: that of the identification of RE, that must be consistent in terms of level of detail and that of their classification which consists in defining all RCs to which the RE can belong. One practical difficulty is that the RC database is developed in parallel, thus requiring many iterative checks, Table 1 represents a small part of the RE database.

Risk categories and micro-trees

The development of the RC database raises the same type of questions as that of the RE database. The bibliographical analysis has lead to more than 300 RC, but they have been reviewed in detail, such as to ensure consistency and to avoid a factorial multiplication of the possibilities. It is only through many comparisons and iterations that we could define a limited number of categories and elementary trees that cover a very large percentage of existing trees. At the end of the process, the database contains a list of MT and a list of RC, with all belonging relations defining:

- For any MT, all RC it contains,
- For any RC, to which MT it can belong (who are all the possible father nodes).

These rules ensure the propagation of information from the bottom level to the top level in the RBS. For the existing database, it also appears that some of the RC are not further decomposed (they never are a “father node”). These RC are “bottom categories” to which RE can be directly attached.

Table 1. Abstract of the RE list.

Delay payment to contractor during project implementation phase
Failure of equipment during construction
Lack of qualified staff working for contractor
Financial difficulties of contractor
Change in management system of the owner of the project
Unpredicted increase of needed material price in implementation phase
Improper intervention of government during contract phase

For all others RC, it is only through propagation that RE are attached.

The authors are fully aware that the solution is not unique and that our choices are somehow subjective, but they result from a long maturation process, during which the criteria for decisions were: elimination of useless solutions, reduction of the possibilities, consistency checking.

BUILDING RBS PROCESS—A MULTISCALE AND DYNAMIC VIEW

Three criteria define what is a “good” RB to compute several notes for comparison between RBSs.

- a. a RBS must be developed at a “convenient” level (neither too much nor too little),
- b. a RBS must decompose the risks in agreement with the users view (what are his objectives? on what performance does he wants to focus?),
- c. a RBS must decompose the risks such as to highlight the more important ones. The focus is given of contrast between “high risks” and “low risks”.

It is finally on the basis of five notes (with three notes for the second criterion) that all RBS can be compared and the best ones selected, using a final multicriteria decision process. At the present stage of development of this work, the propagation rules of risk values throughout the RBS have not yet been fixed, but they will be implemented so as to make possible the propagation of quantitative information, as well as that of qualitative information, like that of a Likert scale.

REFERENCES

Chapman, R.J. 2001. The controlling influences on effective risk identification and assessment for construction design management, *Int. J. of Project Management*, 19, 147–160.

Mehdizadeh, R., Breyse, D., Chaplain, M. & Niandou H. 2010. A methodology for building taylor's made RBS for project risks management in construction, 5th Asranet conf., Edimburgh, 14–16 june 2010.

How integrated should risk management and quality management be?

Bertrand Munier

GRID and IAE de Paris, Sorbonne's Business School, France

Laurent Dehouck

GRID and Ecole Normale Supérieure de Cachan, France

Most project managers are proud to announce that they have an integrated system of managing quality and risk as well as safety. Such an integrated vision rests on classical technical engineering determinism. This paper shows that this type of alleged integration is bound to lead to erroneous steps of prevention/protection. Consequently, bad results will happen more than could have been obtained. Project's life is too uncertain, engineer and manager's brain too bounded to secure construction project objectives. Thus, actually, ex-ante plans on delays, costs and quality are not completely executed. Results can over or under perform expectations.

We argue that this integration is simply a historical misconception that has led to mistakes. To avoid the latter the authors develop basic principles of risk management, which should be regarded as necessary specifications of any admissible method of risk management.

The first one is a probabilistic view of the world. It is not an easy change because it breaks the common managerial culture of perfect control and managerial "misconception of chance". Project risk should not be considered as being only detrimental because it overlooks most of the time residual risks and hence assurance cost.

Project risk evaluation methods should enable to compare different risks on a single dimension providing an operational approach to manage tradeoffs between project actors at all project stages. It should therefore refer to some practical metric (interval scale).

To create such a project risk governance, one need also a person in charge of organizing all this sense making. It should remain on the direct

authority of the project chief and has to coordinate all along the project lifetime risk taking behaviors in accordance with an project risk appetite framed by the project owner.

It is easy to note differences between these three fundamental requirements of risk management and quality management quoting the famous 14 principles (Deming, 1982) and its fundamental premises: understanding past variations; trust people giving up numerical goals. Moreover, Deming's total quality improvement processes rest on two sequential action's categories: (i) to enhance system stability (ii) to reduce systemic errors. In this framing, risk management is reduced to minimize defaults, because something has been done inadequately and should be corrected. It is in sharp contrast to our three precedent basic principles.

The authors then show that the major presently used methods of risk management do not meet such requirements in general: Failure Mode and their Effects Analysis (FMEA), Bow-Tie models, Risk Matrices.

To conclude, a clear revision is called for. The recently published norm ISO 31000 may be a relevant guide toward such a revision, as it lays down principles of risk management.

The issue, however, goes beyond principles and encompasses the question of the tools to use. If current tools do not fit the requirements presented above, are other tools available and do they comply with the principles put forward in this paper? It is particularly impressive that the norm ISO 31010 lists 31 tools, which, by far, are not all in compliance with the principles put forward by the mother norm ISO 31000.

*MS_135 — Multiple hazards risk assessment
and mitigation*

This page intentionally left blank

Estimation of damage loss due to hurricane wind and induced surge

Y. Li, S.O. Bjarnadottir & A. Ahuja

Department of Civil and Environmental Engineering, Michigan Technological University, USA

J.W. van de Lindt & T. Dao

Department of Civil, Construction, and Environmental Engineering, University of Alabama, USA

ABSTRACT: Residential buildings in coastal areas are often at risk to more than one natural hazard, such as hurricanes, coastal inundation or river flooding. While the United States (US) averaged \$1.6 billion in hurricane damage annually from 1950–1989, this figure rose dramatically between 1989–1995, to approximately \$6 billion annually (Pielke & Pielke 1997). The average annual normalized hurricane damage in the US was about \$10 billion in recent years, with more than \$150 billion in damage in 2004 and 2005 (Pielke et al., 2008). Greater than 75% of declared Federal disasters are a result of flooding. As of 2003, approximately 53% of the US population, or 153 million people, lived in coastal counties (Crosset 2008). This is an increase in population of 33 million since 1980, and it is estimated that the US coastal population will increase by another 12 million by 2015 (W & PE 2003). Increases in population and the wealth of this population lead an increased risk in potential hurricane losses. In addition to loss due to hurricane wind, hurricane-induced surge caused significant damage to residential buildings. The National Weather Service (2009) estimates that 60% of Hurricane Katrina's losses can be attributed to hurricane-induced surge; this emphasizes the importance of a comprehensive hurricane risk assessment model.

Although current design codes do consider load combinations, these are generally for non-environmental (natural hazard) loading and focus on dead and live loads and then their combination with each environmental load individually. In this paper, a methodology for loss analysis for combined wind and surge is proposed in this paper. Correlations between hurricane and wind-induced surge are considered. A simple rectangular residential building is used to demonstrate the methodology.

The loss due to hurricane wind including rainwater intrusion and hurricane-induced surge are both determined using assembly-based vulnerability (ABV), including extensive wind field modeling, rainwater intrusion modeling, and loss

modeling with the ABV. In their study they applied the ABV approach developed by Porter (2000) for earthquake engineering based on specific structural and non-structural details of a single woodframe building. These details included the dimensional and quantitative information for all the damageable components within the house.

The numerical hurricane model considers the location of a community, or subdivision, or houses in proximity to a hurricane path and wind field model. This can be accomplished by applying the Rankine vortex model (Liu 1991). Hurricane properties including intensity, size, and track are considered in the model to be used in the wind loss estimate. ASCE-7 (2005) wind loading is applied to a detailed finite element model of the building. Loss to the residential building due to rainwater intrusion during the hurricane is estimated using five damage states, which then can be converted to a percentage loss in terms of replacement values. Variation of such loss estimation is determined. The loss due to the hurricane wind including rainwater intrusion is computed using the method of Dao and van de Lindt (2010).

Buildings within a kilometer or two of the coastline may also be affected by storm surge during hurricanes. This type of damage was widespread in hurricane Katrina in 2005. In the present study the regressive model developed by Irish et al. (2008) is used to determine the statistical distribution of storm surge height for a given hurricane defined by several size and intensity parameters. A hurricane-induced surge model which includes the effect of the intensity and size of the hurricane as well as other hurricane properties such as central pressure, and the associated uncertainties is used in this paper. Although wave action can certainly result in damage immediately on the coastline, the present work is limited to flood damage as a result of hurricane storm surge using the flood loss estimation methodology of Taggart & van de Lindt (2009).

Table 1 shows the maximum wind speed (V_{\max}), the radius to maximum wind speed (R_{\max}), surge height, and the loss for each hurricane. The loss

Table 1. Combined loss from wind and surge.

Hurricane ID	V_{max}	R_{max}	Mean surge height	Combined loss
	m/s	km	m	Ratio to house value
1	43.5	20	1.20	0.238
2	54.4	11	1.59	0.318
3	66.0	19	2.65	0.444
4	43.5	26.5	1.26	0.239
5	54.4	43	2.02	0.372
6	66.0	40.3	2.68	0.492
7	43.5	33	1.32	0.292
8	54.4	74	2.40	0.436
9	66.0	56	2.91	0.567

due within the table is presented for wind, surge, and for the combined loss.

Combining the ABV for flood due to surge, wind damage, and rainwater intrusion requires consideration of which damageable components would essentially be counted twice within the framework. In the approach presented here, the probability of exceeding a particular level of loss for the example building is determined as a function of hurricane intensity and size. The method for estimating loss due to combined wind and surge in hurricanes may be used for design code assessment and proposals, retrofit of buildings in the coastal areas, disaster planning purposes, and potentially for insurance underwriting.

REFERENCES

ASCE-7 2005. Minimum Design Loads for Buildings and Other Structures. (ASCE Standard 7-05), *Am. Soc. of Civil. Engineers*, Reston.

Crosset, K.M., Culliton, T.J., Wiley, P.C. & Goodspeed, T.R. 2004. Population Trends along the Coastal United States. Administration: Silver Spring, MD.

Dao, T.N. & van de Lindt, J.W. 2010. Methodology for Wind-Driven Rainwater Intrusion Fragilities for Light-Frame Wood Roof Systems, *Journal of Structural Engineering*, 136, 700–706.

Irish, J.L., Resio, D.T. & Ratcliff, J.J. 2008. The Influence of Storm Size on Hurricane Surge. *Journal of Physical Oceanography*, 38, 2003–2013.

Liu, H. 1991. A Handbook for Structural Engineers. Prentice Hall, Englewood Cliffs, New Jersey.

National Weather Service (NWS) 2009. Flood Losses: Compilation of Flood Loss Statistics. [cited 2010 August 04]; Available from: http://www.weather.gov/oh/hic/flood_stats/Flood_loss_time_series.shtml

Pielke, R.A.J. & Pielke, R.A.S. 1997. Hurricanes: Their nature and impacts on society. Wiley, U.K.: Chichester.

Pielke, R.A., Gratz, J., Landsea C.W., Collins, D., Saunders, M.A. & Musulin, R. 2008. Normalized hurricane damage in the United States: 1900–2005. *Nat Hazards Reviews*, ASCE, 9, 1, 29–42.

Porter, K.A. 2000. Assembly-based vulnerability of buildings and its uses in seismic performance evaluation and risk-management decision-making. Doctoral dissertation, Stanford University, Stanford CA.

Taggart, M. & van de Lindt, J.W. 2009. Performance-Based Design of Residential Wood-Frame Buildings for Flood Based on Manageable Loss, *Journal of Performance of Constructed Facilities*, ASCE, 23, 2, 56–64.

Woods & Poole Economics, Inc. (W&PE). 2003. 2003 Desktop Data Files. W&PE, Washington, DC.

Methodological and probabilistic issues in multi-hazard engineering design

E. Simiu, F.A. Potra & D. Duthinh
 National Institute of Standards and Technology, Gaithersburg, MD, USA

1 INTRODUCTION

There is a growing interest in the development of procedures for the design of structures exposed to multiple hazards. The goal is to achieve safer and more economical or “greener” designs than would be the case if the demands on structures were calculated independently for each individual hazard and an envelope of those demands were used for member sizing. To date a number of useful, if mostly ad-hoc, approaches to multi-hazard design have been proposed. However, a broad, multidisciplinary foundation for multi-hazard design remains to be developed. We argue that such a foundation should include probabilistic, structural analysis, optimization, and structural reliability components.

It has recently been determined by the authors that ASCE 7 Standard provisions on design of structures in regions subjected to strong winds and earthquakes can be unconservative.

The authors have also shown that modern optimization procedures applied to multi-hazard design, notably interior point methods, can help to achieve significant reductions in materials and energy consumption while maintaining requisite safety levels.

2 PROBABILITIES OF EXCEEDANCE OF LIMIT STATES FOR REGIONS WITH STRONG WIND AND SEISMIC HAZARDS

One explanation for the development of the current ASCE 7 Standard provisions on structural

design for regions with strong wind and seismic hazards is the belief that such provisions should be determined strictly by the fact that the probability of simultaneous occurrence of such hazards is negligible. Actually the provisions should be determined, in addition, by the fact that

$$P(s_1 \cup s_2) = P(s_1) + P(s_2) \tag{1}$$

where \cup denotes union, $P(s_1)$ and $P(s_2)$ are, respectively, the annual probabilities of the events s_1 and s_2 that the wind and seismic loads are larger than those required to induce the limit states associated with design for wind and earthquakes, and $P(s_1 \cup s_2)$ is the annual probability of the event that s_1 or s_2 occurs. It follows from Eq. 1 that $P(s_1 \cup s_2) > P(s_1)$ and $P(s_1 \cup s_2) > P(s_2)$. If $P(s_1) = P(s_2)$ the increase is twofold. Such an increase can occur, for example, for lower-floor columns of buildings or towers. A case study that considers a water tower (Fig. 1) is presented in some detail.

3 OPTIMIZATION

Optimization under N hazards ($N > 1$) is a means of integrating the design so that the greatest possible economy is achieved while satisfying specified safety-related and other constraints. We consider a set of n variables (i.e., a vector) (d_1, d_2, \dots, d_n) characterizing the structure. In a structural engineering context we refer to that vector as a *design*. Under a single hazard, we subject those variables to a set of m constraints

$$g_1(d_1, d_2, \dots, d_n) \leq 0, g_2(d_1, d_2, \dots, d_n) \leq 0, \dots, g_m(d_1, d_2, \dots, d_n) \leq 0 \tag{2}$$

Examples of constraints are minimum or maximum member dimensions, design strengths, and allowable drift and accelerations. A design (d_1, d_2, \dots, d_n) that satisfies the set of m constraints is called *feasible*. Optimization of the structure consists of selecting, from the set of all feasible designs, the design denoted by $(\bar{d}_1, \bar{d}_2, \dots, \bar{d}_n)$



Figure 1. Schematic of water tower structure.

that minimizes a specified *objective function* $f(d_1, d_2, \dots, d_n)$. The objective function may represent, for example, the weight or cost of the structure. The selection of the optimal design is a nonlinear programming problem (NLP). We consider structures whose configuration is specified, and whose design variables consist of member sizes.

In multi-hazard design each hazard $i (i=1, 2, \dots, N)$ imposes a set of m_i constraints. Typically the optimal design under hazard i is not feasible under (i.e., does not satisfy the constraints imposed by) hazard $j \neq i$ e.g., the optimal design that satisfies the drift constraints under one hazard may not satisfy drift constraints under another hazard). Common engineering practice is to obtain separately feasible designs d^i corresponding to each hazard $i (i = 1, 2, \dots, N)$. Those designs are used to construct an envelope d such that the constraints imposed under all hazards are satisfied. Such a design will in general be suboptimal.

The NLP is more difficult to solve in the multi-hazard case. However, recent progress in the field of nonlinear programming (in particular interior point methods) now renders the solution of complex multi-hazard problems a practical possibility.

4 CONCLUSIONS

Wind engineering in a multi-hazard context has features that concern optimization, probabilistic, and structural design aspects in ways not currently addressed by building codes. We provide an overview of research and results that allow design of structures subjected to wind and earthquakes to be performed more rationally, resulting in structures that are safer and more economical than was heretofore possible.

Decision-making for civil infrastructure exposed to low-probability, high-consequence hazards: The role of risk-aversion

E.J. Cha & B.R. Ellingwood

Georgia Institute of Technology, Atlanta, GA, USA

ABSTRACT: Quantifying risk to civil infrastructure requires two components: probability of a potentially damaging event and the corresponding consequence of the damage, measured in financial or human terms. Although the limit state probability (or reliability index) itself has provided a sufficient measure of risk in the development of first-generation probability-based limit states design codes [Ellingwood, 2000; Ellingwood and Wen, 2005], a more complete consideration of the consequences of failure will need to be included to advance the new paradigm of performance-based engineering and risk-informed evaluation and decision regarding civil facilities. Various decision models, such as cost-benefit analysis, expected utility theory, cumulative prospect theory, life quality index-based analysis, and capability-based analysis, have been developed and implemented in various contexts during the past two decades to incorporate both probability and consequence in decision-making [Tversky and Kahneman, 1992; Nathwani, Lind, and Pandey, 1997; Goda and Hong, 2008; Murphy and Gardoni, 2007]. The application of such models to decision-making involving low-probability, high-consequence events affecting civil infrastructure requires a fundamental understanding of risk acceptance and how it affects individual and group choices. Risk acceptance attitudes determine the willingness of individuals, groups and institutions to assume or transfer (socialize) risk, and affect the manner in which stakeholders value the limit state probability as well as the consequence of failure. Risk-aversion is an important aspect of risk acceptance [Keeney and Raiffa, 1976]; risk-averse decision-makers tend to overestimate possible losses and limit state probabilities, especially for low-probability, high-consequence events, and thus resist choosing a decision alternative which a traditional quantitative risk assessment (e.g., minimum expected cost analysis) suggests is near-optimal. A substantial amount of evidence suggests that individuals, in particular, do not evaluate the probabilities and consequences of rare events rationally in actual decision processes. Moreover, the

level of irrationality increases as the consequences of the event increase or become less certain at the same time that the probability of occurrence of the event decreases. Similar irrational patterns can be observed in decision-making of groups or institutions when the probable maximum losses exceed capital resources. Risk aversion is a major contributor to irrational behavior in decision-making; its roots and how it affects the irrationality in decision processes are not fully understood, especially in the context of dealing with low-probability, high-consequence events affecting civil infrastructure.

This paper explores the nature of risk aversion embedded in decisions regarding safety of civil infrastructure subjected to low-probability, high-consequence natural hazards such as earthquakes, hurricanes, or flooding using analytical and statistical approaches. Insights are achieved by examining the nature of risk aversion and how it is understood in the insurance industry and, from this examination, drawing inferences that are applicable to civil infrastructure decision-making regarding rare events. In the insurance industry, the concept of a volatility multiplying factor, defined as the ratio of insurance premiums to claims, has been introduced to price risks [Walker, 2008]. The volatility multiplying factor is determined based on dynamic financial analysis considering average annual losses, targeted average annual return on initial capital, and probability of insolvency, and increases as the magnitude of covered losses increases or the coefficient of variation of annual losses increases. The volatility factor reflects the willingness of the insurance company to tolerate the underwritten risks or, in other words, how risk-averse the insurance company is in underwriting risks from damages from natural hazards and other catastrophic events, such as earthquakes or hurricanes, or flooding. Since corporate risk aversion is embedded in the volatility multiplying factor, the nature of risk-aversion (at least as viewed by a corporate entity) can be inferred from it and can be utilized to guide the development of possible value systems for other large civil infrastructure-related decisions. The process is illustrated with the structural design

of a 9-story steel moment-resisting frame building, allowing the role of risk aversion to be examined in the context of a practical structural engineering problem involving risk-informed decision-making.

REFERENCES

- Ellingwood, B.R. 2000. LRFD: implementing structural reliability in professional practice. *Engrg. Struct.* 22(2):106–115.
- Ellingwood, B.R. & Wen, Y.K. 2005. Risk-benefit-based design decisions for low-probability/high consequence earthquake events in Mid-America. *Prog. Struct. Engng. Mater.* 7:56–70.
- Goda, K. & Hong, H.P. 2008. Application of cumulative prospect theory: implied seismic design preference. *Structural Safety* 30(6):506–516.
- Keeney, R.L. & Raiffa, H. 1976. *Decisions with multiple objectives: Preferences and value tradeoffs*. New York: Wiley.
- Murphy, C. & Gardoni, P. 2007. Determining public policy and resource allocation priorities for mitigating natural hazards: a capability-based approach. *Science and Engineering Ethics* 13:489–504.
- Nathwani, J.S., Lind, N.C. & Pandey, M.D. 1997. *Affordable safety by choice: the Life Quality Method*. IRR, Ontario, Canada: University of Waterloo.
- Tversky, A. & Kahneman, D. 1992. Advances in Prospect Theory: Cumulative representation of uncertainty. *Journal of Risk and Uncertainty* 5: 297–323.
- Walker, G.R. 2008. Earthquake Insurance: An Australian Perspective. *Australian Journal of Structural Engineering* 8(1):39–48.

GS_316 — Natural hazards modeling

This page intentionally left blank

Hazard-level specific hurricane event characterization

Y. Wang & D.V. Rosowsky

Department of Civil and Environmental Engineering, Rensselaer Polytechnic Institute, Troy, NY, USA

ABSTRACT: This paper suggests a methodology for hazard-specific/risk-consistent hurricane event characterization. Typically, the hurricane hazard is described in terms of maximum wind speed V_{\max} (at the eye-wall), since damage descriptors associated with intensity scales (e.g., the Saffir-Simpson Hurricane Scale) and collateral hazards (e.g., hurricane surge) are related most often to maximum wind speed. However, recent studies have shed light on the importance of storm size (i.e., radius of maximum winds, R_{\max}) in describing the hurricane wind field and thus the spatial extent of potential damage. The large losses from several recent hurricanes underscore the need for better understanding the impact of storm size on damage. To that end, we seek to develop parameter combinations (e.g., V_{\max} and R_{\max}) that define “characteristic” risk-consistent hurricane events in one particular geographic region. A simulation framework is developed to generate 10,000 years of simulated hurricane events and a synthetic hurricane wind speed database for the state of Texas, using state-of-the-art hurricane modeling techniques and information extracted from historical hurricane data. The resulting 10,000 years database, which includes information developed for every zip-code in Texas, includes time of hurricane passage, maximum gradient wind speed and surface wind speed. Using this simulation framework, selected parameters (i.e., intensity and size parameters) are recorded for each hurricane at the time of landfall along the Texas coast. Using a hurricane decay model specifically calibrated for this location, parameters V_{\max} and R_{\max} at inland locations also are recorded. The critical values of V_{\max} and R_{\max} are then selected to jointly describe the intensity and spatial extent of hurricanes and the joint histogram is developed. Finally, these variables are statistically characterized and a suite of the characteristic hazard events (V_{\max} and R_{\max} combinations) corresponding to certain hazard levels are identified. The proposed methodology for event-based hurricane hazard characterization, when coupled with a hurricane damage model, can be used for regional loss estimation and other spatial impact analyses. The proposed approach also can be used to develop characteristic hazard

definitions (and event descriptions corresponding to specific hazard levels) for use in performance-based engineering applications.

REFERENCES

- Batts, M.E., Cordes, M.R., Russell, L.R., Shaver, J.R., and Simiu, E. (1980), *Hurricane Wind Speeds in the United States*, NBS Building Science Series 124, U.S. Department of Commerce, National Bureau of Standards, Washington, DC.
- Caton, P.G.F. (1975), “Standardized map of hourly mean wind speed over the United Kingdom and some implication regarding wind speed profiles,” *Proceedings: 4th International Conference on Wind Effects on Buildings and Structures*, London, UK, pp. 7–21.
- Darling, R.W.R. (1991), “Estimating probabilities of hurricane wind speeds using a large scale empirical model,” *Journal of Climate*, 4(10):1035–1046.
- Federal Emergency Management Agency (FEMA) (2003). HAZUS-MH Multi-Hazard Loss Estimation Methodology, Hurricane Model Technical Manual. Washington, DC.
- Georgiu, P.N. (1985), *Design Wind Speeds in Tropical Cyclone-Prone Regions*, Ph.D. Dissertation, Department of Civil Engineering, University of Western Ontario, Canada.
- Heneka, P. (2008), “A damage model for the assessment of storm damage to buildings,” *Engineering Structures*, 30(12):3603–3609.
- Ho, F.P., Su, J.C., Hanevich, K.L., Smith, R.J. and Richards, F. (1987), *Hurricane Climatology for the Atlantic and Gulf Coasts of the United States*, NOAA Technical Report NWS 38.
- Huang, Z., Rosowsky, D.V. and Sparks, P.R. (2001), “Hurricane simulation techniques for the evaluation of wind-speeds and expected insurance losses,” *Journal of Wind Engineering and Industrial Aerodynamics*, 89(7–8):605–617.
- HURDAT (2005), http://www.aoml.noaa.gov/hrd/hurdat/Data_Storm.html, Atlantic Oceanographic and Meteorological Laboratory (AOML), National Oceanic and Atmospheric Administration (NOAA).
- Irish, J.L., Resio, D.T. and Ratcliff, J.J. (2008), “The influence of storm size on hurricane surge,” *Journal of Physical Oceanography*, 38(9):2003–2013.
- Jelesnianski, C.P., Chen, J. and Shaffer, W.A. (1992), *SLOSH Sea, Lake, and Overland Surges from Hurricanes*, NOAA Technical Report NWS 48, Silver Spring, Maryland.

- Khanduri, A.C. and Morrow, G.C. (2003), "Vulnerability of buildings to windstorms and insurance loss estimation," *Journal of Wind Engineering and Industrial Aerodynamics*, 91(4):455–467.
- Lee, K.H. and Rosowsky, D.V. (2007), "Synthetic hurricane wind speed records: development of a database for hazard analysis and risk studies," *Natural Hazards Review*, ASCE, 8(2):23–34.
- Legg, M.R., Nozick, L.K. and Davidson, R.A. (2010), "Optimizing the selection of hazard-consistent probabilistic scenarios for long-term regional hurricane loss estimation," *Structural Safety*, ASCE, 32(1): 90–100.
- Phan, L.T. and Simiu, E. (2008), "A Methodology for developing design criteria for structures subjected to combined effects of hurricane wind speed and storm surge," *Proceedings: 4th International Conference on Structural Engineering and Mechanics (ASEM 08)*, Jeju, Korea, pp. 1510–1524.
- Rosowsky, D.V., Sparks, P.R. and Huang, Z. (1999), *Wind Field Modeling and Hurricane Hazard Analysis*, Report to the South Carolina Sea Grant Consortium, Department of Civil Engineering, Clemson University, SC.
- Sparks, P.R. (2003), "Wind speeds in tropical cyclones and associated insurance losses," *Journal of Wind Engineering and Industrial Aerodynamics*, 91(12–15):1731–1751.
- Sparks, P.R. and Huang, Z. (1999), "Wind speed characteristics in tropical cyclones," *Proceedings: 10th International Conference on Wind Engineering*, Copenhagen, Denmark.
- Vickery, P.J. and Twisdale, L.A. (1995), "Wind-field and filling models for hurricane wind-speed prediction," *Journal of Structural Engineering*, ASCE, 121(11):1700–1709.
- Vickery, P.J., Skerlj, P.F., Steckley, A.C. and Twisdale, L.A. (2000a), "Hurricane wind field model for use in hurricane simulations," *Journal of Structural Engineering*, ASCE, 126(10):1203–1221.
- Vickery, P.J., Skerlj, P.F. and Twisdale, L.A. (2000b), "Simulation of hurricane risk in the U.S. using empirical track model," *Journal of Structural Engineering*, ASCE, 126(10):1222–1237.
- Wang, Y. (2010), *Studies on Hazard Characterization for Performance-Based Structural Design*, Ph.D. Dissertation, Department of Civil Engineering, Texas A&M University, USA.
- Watson C. and Johnson, M. (2004), "Hurricane loss estimation models: Opportunities for improving the state of art," *Bulletin of the American Meteorological Society*, 85:1713–1726.

A comprehensive approach for online fast hurricane-risk prediction

A.A. Taflanidis, A.B. Kennedy, J.J. Westerink, M. Hope & S. Tanaka
University of Notre Dame, Notre Dame, IN, USA

J. Smith
US Army Engineer Research and Development Center, Vicksburg, MS, USA

K.F. Cheung
University of Hawaii at Manoa, Honolulu, HI, USA

1 INTRODUCTION

Hurricane surge risk assessment has received a lot of attention the past years, in response to 2005 and 2008 hurricane seasons. Conventional approaches are based on parametric or non-parametric analysis of data from historical storms or on simulation of hurricane design events. A different methodology, frequently referenced as the Joint Probability Method (JPM), relies on a simplified description of hurricane scenarios through a small number of model parameters. Characterization of the uncertainty in these parameters, through appropriate probability models, leads then to a probabilistic characterization of the hurricane risk. This probabilistic approach is gradually emerging as the standard tool for hurricane risk evaluation (Resio et al., 2009). One of the greater recent advances in this field has been the development and adoption of high-fidelity numerical simulation models for reliable and accurate prediction of surge responses for a specific hurricane event (Resio and Westerink 2008). These models permit a detailed representation of the hydrodynamic processes, albeit at the cost of greatly increased computational effort (Westerink et al., 2008).

In this work an efficient computational framework is developed for evaluation of hurricane risk for coastal regions with particular emphasis on online risk estimation. This framework is based on the parameterization of each hurricane scenario by five model parameters and the development of response surface approximations as a surrogate model for efficient estimation of the surge response for any potential hurricane scenario.

2 FRAMEWORK

Each hurricane event is approximately described by only five variables: (i) the location of landfall x_j ;

(ii) the angle of impact at landfall θ ; (iii) the central pressure c_p ; (iv) the forward speed during final approach to shore v_f ; and (v) the radius of maximum winds R_m . These variables ultimately constitute the model parameters vector, \mathbf{x} , describing each hurricane scenario. The variability of the hurricane track and characteristics prior to landfall is approximately addressed by appropriate selection of the hurricane track history prior to landfall, so that important anticipated variations are efficiently described.

In this setting, let \mathbf{z} denote the vector of response quantities of interest throughout the entire region of significance. Such response quantities include the (i) the still water level (SWL), the (ii) wave breakup level (WBL), or (iii) the significant wave height H_s along with the corresponding period of wave oscillation T_s . The response vector \mathbf{z} for a specific hurricane scenario, described by the model parameter vector \mathbf{x} , may be accurately estimated by numerical simulation, once an appropriate high fidelity model is established. Since the high-fidelity model requires extensive computational effort for each analysis, a surrogate model is also developed for simplification of the risk evaluation. This surrogate model is based on information provided by a number of pre-computed evaluations of the computationally intensive high-fidelity model, and ultimately establishes an efficient approximation to the entire response vector for each hurricane scenario, $\hat{\mathbf{z}}$.

Hurricane risk is finally expressed in terms for the response $\hat{\mathbf{z}}$; if $p(\mathbf{x})$ is the probability model describing the uncertainty in the hurricane model parameters, then each risk component R_j is expressed by the stochastic integral

$$R_j = \int_X h_j(\mathbf{x}) p(\mathbf{x}) d\mathbf{x} \quad (1)$$

where X corresponds to the region of possible values for \mathbf{x} and $h_j(\cdot)$ is the risk occurrence measure

that is related to $\hat{\mathbf{z}}$ and ultimately depends on the definition for R_j . Through appropriate selection of $h(\cdot)$ all potential hurricane risk quantifications can be addressed through this framework. Note that for online risk estimation during an approaching event, the probability model $p(\mathbf{x})$ may be ultimately selected through information provided by the National Weather Service (NWS). Finally the risk integral (1) is estimated by *stochastic simulation*; using a finite number, N , of samples of \mathbf{x} simulated from $p(\mathbf{x})$, an estimate for R_j is

$$\hat{R}_j = 1/N \sum_{k=1}^N h(\mathbf{x}^k) \quad (2)$$

where vector \mathbf{x}^k denotes the sample of the uncertain parameters used in the k th simulation. Based on the surrogate model this estimation can be efficiently performed and whenever the prediction for $p(\mathbf{x})$ are updated (as the hurricane approaches landfall) the estimate (2) may be also updated.

3 APPLICATION TO ONLINE RISK ESTIMATION FOR OAHU

3.1 High fidelity modeling and simulations

The surge and wave responses in this study are accurately calculated by a combination of the ADCIRC and SWAN numerical models. ADCIRC solves the shallow-water equations for water levels and the momentum equations for currents while SWAN solves for wave action density which evolves in time, geographic space and spectral space. SWAN+ADCIRC are fully integrated into a comprehensive modeling system allowing full interaction between model components and highly efficient parallel implementation. The computational domain developed for the high-fidelity simulation of the hurricane response in this study, encompasses a large portion of the northern Pacific Ocean and extends from 0 (equator) to 35 degrees north and from 139 to 169 degrees west. The grid incorporates 1,590,637 nodes and 3,155,738 triangular elements. For the numerical simulation, SWAN applies 10 minute time steps while ADCIRC applies 1 second time steps. A SWAN+ADCIRC simulation runs in 16 wall clock minutes per day of simulation on 1024 cores on Diamond, a 2.8 GHz dual quad core based machine. For the wave breakup 750 transects are considered around the island and for each transect a matrix of combinations of wave height and water level is created. One dimensional Boussinesq model analysis is then performed for all these parameter combinations, yielding a prediction for the wave

runup along each transect (Demirbilek et al. 2009). These results are then used through a simple two dimensional interpolation scheme, to provide an estimate of maximum inundation distance along that transect for any input for wave or water level required for the risk assessment.

3.2 Surrogate modeling

Based on information from the NWS on historical storms, a suite of 300 hurricane scenarios is created, chosen so that they cover most future hurricane events that are anticipated to have significant impact on Oahu. The response for these storms is then computed by the ADCIRC+SWAN model, a process which required ultimately more than 500,000 computational hours, and all results of interest were stored. Using the information from these pre-computed storms as support points a moving least squares response surface surrogate model is built. This surrogate model facilitates a computationally efficient prediction of the response, in particular the still water level \hat{z}_{sj} and significant wave height \hat{H}_{sj} , for any desired hurricane scenario and *simultaneously* for all locations of interest around the island. The interpolation scheme discussed previously for the wave breakup is then be used to additionally calculate the wave breakup for each transect using as input the previous predictions for \hat{z}_{sj} and \hat{H}_{sj} .

3.3 Online risk assessment tool

A risk assessment tool is finally developed for the online hurricane risk estimation. The tool accepts as input the parametric configuration for the most probable hurricane track as well as the estimate for time till landfall, used in the current version to select $p(\mathbf{x})$. Based on this input and the pre-computed information from the high fidelity simulations, the surrogate response surface approximation is used to predict either the output for the most probable hurricane or the hurricane risk, estimated as the threshold with a pre-specified probability of exceedance. In the latter case $N = 2000$ is used for the stochastic simulation (2). The outputs from the risk estimation are graphically presented as contours for the SWL and WBL around the island. The total time needed for the tool to provide the required output is less than 2 min on a 3.2 GHz single core processor with 2 GB of RAM, which illustrates that it can be efficiently used for online risk evaluation.

REFERENCES

Demirbilek, Z., Nwogu, O.G., Ward, D.L. & Sanchez, A. 2009. Wave transformation over reefs: evaluation of

- one dimensional numerical models. Report ERDC/CHL TR-09-1, US Army Corps of Engineers.
- Resio, D., Irish, J. & Cialone, M. 2009. A surge response function approach to coastal hazard assessment – part 1: basic concepts. *Natural Hazards* 51(1): 163–182.
- Resio, D.T. & Westerink, J.J. 2008. Modeling of the physics of storm surges. *Physics Today* 61(9): 33–38.
- Westerink, J.J., Luettich, R.A., Feyen, J.C., Atkinson, J.H., Dawson, C., Roberts, H.J., Powell, M.D., Dunion, J.P., Kubatko, E.J. & Pourtaheri, H. 2008. A basin-to channel-scale unstructured grid hurricane storm surge model applied to southern Louisiana. *Monthly Weather Review* 136(3): 833–864.

Optimal seismic design of steel structures using approximate methods

A. Zacharenaki

*Institute of Structural Analysis & Seismic Research, School of Civil Engineering,
National Technical University of Athens, Athens, Greece*

M. Fragiadakis

Department of Civil and Environmental Engineering, University of Cyprus, Nicosia, Cyprus

M. Papadrakakis

*Institute of Structural Analysis & Seismic Research, School of Civil Engineering,
National Technical University of Athens, Athens, Greece*

ABSTRACT: A new approach for the performance-based seismic design of buildings using a structural optimization framework is proposed. Incremental Dynamic Analysis (IDA), one of the most powerful seismic performance estimation methods, requires numerous nonlinear response history analysis and thus often is not practical for the seismic design of buildings. To overcome the increased computing cost of IDA we adopt an approximate seismic performance estimation tool, known as Static Pushover to IDA (SPO2IDA). The SPO2IDA tool is nested within the framework of a Genetic Algorithm resulting to an efficient tool for seismic design. The Genetic Algorithm is able to locate the most efficient design in terms of the minimum weight of the structure. A three and a nine-storey steel moment resisting frames are used to demonstrate the design algorithm proposed. The proposed methodology leads to the efficient building designs within reasonable computing time and therefore is suitable for practical design applications.

1 INTRODUCTION

Advancements in structural optimization have made possible the move from traditional trial-and-error design procedures towards fully automated ones using a structural optimization search-engine. For complex and realistic nonlinear structural design problems, evolutionary-based optimizers are the only reliable approach, since most mathematical programming algorithms will converge to a local optimum or may not converge at all. A review paper discussing alternative seismic design frameworks using structural optimization tools can be found in Fragiadakis & Lagaros (2011).

This study discusses an alternative seismic design approach that can be nested in a structural optimization algorithm. Incremental Dynamic Analysis (IDA) (Vamvatsikos & Cornell 2002), a resource—demanding but powerful seismic performance estimation method is replaced by an approximate and suitable for design purposes method, known as Static Pushover to Incremental Dynamic Analysis (SPO2IDA) (Vamvatsikos & Cornell 2005, 2006). SPO2IDA is employed to provide quickly an estimate of the demand at various performance levels. A Genetic Algorithm is used to handle the resulting seismic design problem. A three and a nine storey steel moment-resisting frames (SMRF) are used to demonstrate the efficiency of the proposed seismic design approach.

2 STRUCTURAL PERFORMANCE ESTIMATION

According to the Incremental Dynamic Analysis (IDA) method the mathematical model of the structure is subjected to a suite of ground motion records incrementally scaled to different levels of seismic intensity. This method provides a thorough insight of the structural capacity at the cost of increased computational resources. This fact paves the way of using cost-efficient methods to obtain the structural demand and capacity.

To avoid the costly IDAs, approximate performance estimation methods can be also adopted within a structural optimization environment. The approximate method here adopted is SPO2IDA where the static capacity curve is approximated with a quadrilinear curve and the extracted properties of the approximated curve are given

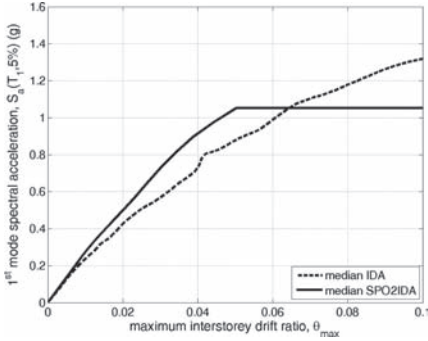


Figure 1. Median IDA curve and its SPO2IDA approximation. The curves refer to the optimal design obtained using the proposed GA-based design procedure for the three-storey SMRF.

as input to the SPO2IDA tool. The fractile IDAs are instantaneously recreated in normalized coordinates of the strength reduction factor R versus the ductility μ . The final approximate IDAs are obtained after a series of calculations on the available R - μ data (Fragiadakis & Vamvatsikos, 2010). A comparison of the actual median IDA curve and its corresponding SPO2IDA approximation is shown in Figure 1.

3 METHODOLOGY

A discrete deterministic-based structural optimization problem (DBO) is formulated as:

$$\begin{aligned} &\min F(\mathbf{S}) \\ &\text{subject to } g_j(\mathbf{S}) \leq 0 \quad j = 1, \dots, m \\ &\quad s_i \in R^d \quad i = 1, \dots, n \end{aligned} \quad (1)$$

where $F(\mathbf{S})$ = objective function to be minimized; R^d = a given set of discrete values; and s_i ($i = 1, \dots, n$) = the design variables that can take values only from this set.

For the structures considered the objective function is their total material weight and the design variables are the cross sections of the members, chosen from tables of commercially available sections. The constraints are used to satisfy the requirements set by European design provisions. The ultimate purpose of the design problem at hand is to find the best combination of cross sections that leads to minimum total weight. The steps of the proposed methodology are briefly summarized:

1. Initialization step: Random generation of an initial population of vectors of the design variables x^j ($j = 1, \dots, n_{pop}$).

Table 1. Optimum designs for the two SMRF buildings.

Case study	Volume	Optimal design	
	m ³	inches	
3 SMRF	24	W33 × 118, W21 × 44, W14 × 22	W27 × 84, W14 × 26,
9 SMRF	175.8	W40 × 167, W40 × 167, W36 × 160, W36 × 135, W33 × 141, W21 × 50, W14 × 43,	W40 × 149, W36 × 160, W33 × 118, W27 × 84, W14 × 30, W14 × 22

2. Analysis step (Fitness evaluation): Firstly, perform checks that do not require analysis to ensure that the design complies with the “strong-column-weak-beam” philosophy and any detailing requirements. Subsequently, perform linear elastic analysis to obtain the demand for the non-seismic load combinations and then perform Static Pushover for the seismic actions. Use the SPO2IDA tool to obtain the demand. Assign penalties on the constraints if the design violates them.
3. Selection, Generation and Mutation step: Apply the GA operators to create the next population ψ ($j = 1, \dots, n_{pop}$).
4. Final check: If a prespecified number of generations has been reached stop, else go back to step 2.

4 RESULTS AND CONCLUSIONS

The performance-based optimal seismic design with the use of the SPO2IDA method has been adopted on a three and nine steel moment-resisting frames (SMRF). The resulting designs are summarized in Table 1. The Genetic Algorithm (GA) was implemented for the solution of the design problem leading to efficient optimal solutions through an iterative procedure. Our results reveal the efficiency of the proposed approach for the design of first-mode dominated structures reducing considerably the computing time and therefore resulting to a powerful and efficient seismic design approach.

REFERENCES

- Fragiadakis, M. & Vamvatsikos, D. 2010. Fast performance uncertainty estimation via pushover and approximate IDA. *Earthquake Engineering & Structural Dynamics* 39(6): 683–703.

- Fragiadakis, M. & Lagaros, N. 2011. An overview to structural seismic design optimization frameworks, *Computers & Structures* (in press).
- Vamvatsikos, D. & Cornell, C.A. 2002. Incremental Dynamic Analysis. *Earthquake Engineering & Structural Dynamics* 31(3): 491–514.
- Vamvatsikos, D. & Cornell, C.A. 2005. Direct estimation of the seismic demand and capacity of MDOF systems through Incremental Dynamic Analysis of an SDOF Approximation. *ASCE Journal of Structural Engineering* 131(4): 589–599.
- Vamvatsikos, D. & Cornell, C.A. 2006. Direct estimation of the seismic demand and capacity of oscillators with multi-linear static pushovers through Incremental Dynamic Analysis. *Earthquake Engineering & Structural Dynamics* 35(9): 1097–1117.

Development and calibration of central pressure decay models for hurricane simulation

Fangqian Liu & Weichiang Pang

Department of Civil Engineering, Clemson University, Clemson, SC, USA

1 INTRODUCTION

According to the post hurricane reconnaissance reports compiled by the National Hurricane Center (NHC), structural damage and loss of lives due to hurricanes are closely related to the condition of the storms at landfall. Not only the coastal regions, but cities and towns located several hundred of kilometers inland were also affected by hurricanes. Development of better models to predict pre- and post-landfall behavior of hurricanes is essential for accurate prediction of hurricane risk. One of the key components in hurricane simulation is the filling-rate model (also known as the decay model), which describes the post landfall decay rate of hurricanes.

2 DECAY MODELS

In this study, a central pressure decay model was derived using central pressure and track information in the hurricane database (HURDAT). Similar to the model proposed by Vickery and Twisdale (1995), the new filling rate model utilizes the post landfall time as a key predictor for the decay rate:

$$\Delta P(t) = (P_a - P_{co}) \exp(a \times t) \quad (1)$$

where P_c is the central pressure at t hour after landfall, a is the decay coefficient given as: $a = a_0 + \varepsilon$. The values of the filling rate coefficients, a_0 , were determined using historical data. For modeling purpose, hurricanes were grouped into four classes based on the travel direction and distance: (1) hurricanes entering the land from sea (landfalling hurricanes), (2) hurricanes traveling from the coast to sea (exiting hurricanes), (3) hurricanes traveling along or parallel to the shoreline (along-shore hurricanes), and (4) hurricanes travelling relatively far into the land and away from the shoreline (inland hurricanes). The coastal areas of North America are divided into five geographic regions for modeling the decay behavior of landfalling hurricanes (Figure 1): Gulf Coast (GC), Florida



Figure 1. Geographic regions for modeling the decay rate of landfalling and inland hurricanes.

(FL), East Coast (EC), North East (NE), and Mexico (MX).

When a hurricane moves further inland, it typically travels at a slower speed and decays at a slower rate. In order to determine the boundary for the inland region, equation 1 was used to compute the central pressure deficit curve of each historical hurricane record. The positions of hurricane eye for nineteen hurricanes at the moment when the decay rate (or slope of the decay curve) changes abruptly were used to define the boundary between the inland and the coastal regions.

Least-square fitting was used to obtain the decay rate (parameter a) for each geographic region. The error term, ε , of each decay model was calculated as the difference between the model and the actual decay rates recorded in HURDAT. The error terms were modeled using the Johnson Unbounded Distribution. The fitted decay coefficients are summarized in Table 1 and the associated error terms are summarized in Table 2.

3 MODEL COMPARISON

Using the decay coefficients and error terms derived for different regions (Tables 1 and 2), central pressures and gradient wind speeds for all historical hurricanes that made landfall in the US

Table 1. Central pressure decay parameters.

Region	Model format	Parameter a
Along-Shore	$y = (a+\epsilon) \times t + 1$	0.00137
Exiting	$y = (a+\epsilon) \times t + 1$	0.00879
Gulf Coast	$y = \exp[(a+\epsilon) \times t]$	-0.03408
East Coast	$y = \exp[(a+\epsilon) \times t]$	-0.03183
North-East	$y = \exp[(a+\epsilon) \times t]$	-0.02656
Florida	$y = (a+\epsilon) \times t + 1$	-0.01035
Inland	$y = \exp[(a+\epsilon) \times t]$	-0.02010
Great Lake	$y = (a+\epsilon) \times t + 1$	-0.00186
Mexico	$y = \exp[(a+\epsilon) \times t]$	-0.02402

* t is the time after the storm enters the region of interest.
 * ϵ is the modeling error (see Table 3 for more details).

Table 2. Modeling error terms for the new decay model.

Region	Johnson system distribution parameters			
	γ	η	ϵ	λ
Along-Shore	0.202	0.942	-0.012	0.017
Exiting	-1.181	0.898	-0.037	0.055
Gulf Coast	-0.712	0.933	-0.011	0.018
East Coast	-0.427	0.452	-0.011	0.006
North-East	-0.003	0.270	-0.019	0.002
Florida	-0.198	0.540	-0.003	0.013
Inland	-1.250	0.936	-0.037	0.018
Great Lake	-0.217	0.391	-0.000	0.009
Mexico	-2.033	0.830	-0.045	0.011

*Type of Johnson System Distribution is unbounded S_{μ} .

were computed and compared to historical data in HURDAT. Ten cities located at a distance approximately equal to 50 km away from the coastline are selected and the cumulative density function (CDF) of the gradient wind speeds are plotted in Figure 2 (Five of them are shown here). As can be seen, the gradient wind speeds estimated using the new model follow the general pattern of the historical wind speeds better than that of an existing decay model.

4 SUMMARY AND CONCLUSIONS

Building on the foundation of previous hurricane central pressure decay models, a new scenario-based multi-region decay model was developed and calibrated using the information in HURDAT. In the new model, the decay behavior of a hurricane at a given time step is described using one of the four cases (landfalling, along-shore, exiting, and inland hurricanes). Through an evaluation of the wind speeds computed using the new and a previous decay model, it has been shown that the previous model, which does not consider the heading direction of hurricanes (e.g. exiting and along-shore) generally underestimated the wind speeds at both near-shore and inland locations in East Coast and North-East Coast regions, but overestimated the wind speeds in Florida region. It has been shown that the new model can be used to produce better wind speed predictions than that of the earlier decay models. This multi-region decay model can be implemented into hurricane simulation frameworks for long-term hurricane simulation.

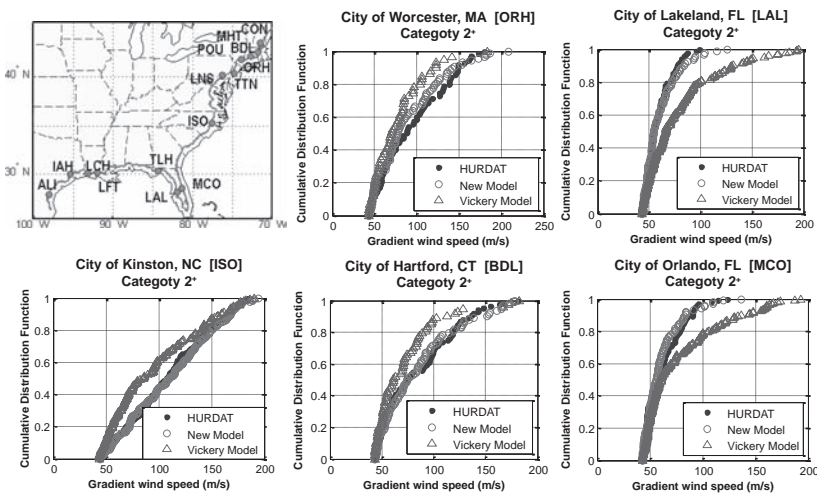


Figure 2. Cumulative distribution of gradient wind speeds for cities located approximately 50 km from the coastline.

Reliability analysis of the Swiss avalanche warning system

M. Bründl & B. Heil

WSL Institute for Snow and Avalanche Research SLF, Davos, Switzerland

The establishment of monitoring networks for various measurements relevant for management of natural hazards and the enhancements of forecast models in the past 25 years have tremendously enhanced the possibility to warn against natural hazards (Bründl et al., 2004; Romang et al., 2009). Electronic, software-based warning systems are currently being established in this field. However, there is a lack of experience in observing the reliability of such systems.

The WSL Institute for Snow and Avalanche Research (SLF) operates the national warning centre for avalanches in Switzerland. In order to provide consistent avalanche warning, SLF uses a wide variety of data acquired automatically by measurement stations and manually by field observers. In addition to that, meteorological models and the deterministic snow cover model SNOWPACK (Lehning et al., 1999) deliver basic information for avalanche forecasting. The combination of data with the expertise of the avalanche forecasters at SLF allows for a dependable and continuous warning against avalanches issued twice a day during the winter. However, little is known about the reliability of the complex system consisting of monitoring networks, server infrastructure, software, and the humans involved in the warning process.

In order to develop a concept for the systematic reliability analysis of early warning systems, we have conducted an analysis of the performance of the Swiss avalanche warning system. Thereby, the following four research questions were asked: (1) What is the constructional design of the avalanche warning system? (2) Which methods are applicable for reliability analyses of warning systems? (3) Which components are the least reliable in the avalanche warning system? (4) How can a concept for reliability analysis of early warning systems look like?

In order to answer the above mentioned research questions, a system sketch of the avalanche warning system was drawn. After a literature review of established methods for reliability assessment, the method of Fault Tree Analysis (FTA) was chosen for analysing its reliability.

The avalanche warning system was continuously developed over the last decades by integrating

enhancements and new developments. This helped keeping the system up to date, eased data interpretation and allowed for an adaptation of the dissemination of the avalanche bulletin to modern technologies. However, due to the various changes in the system components, its configuration became more and more complex.

During the FTA, a total of 75 primary failures was found. The fault tree was validated in terms of syntactically and semantically correctness. This ensured that every event has been linked to a well-defined primary event. In order to analyze the fault tree qualitatively, minimal cut sets (MCS) were generated. Therefore, a recursive algebraic method was used. A MCS is a primary failure or a set of primary failures, which—if occurring—will result in the top event. A relatively high number of 44 MCS of order 1 were found. 16 MCS were of order 2, whereas 13 MCS of order 3 were revealed. To get deeper insights into the MCSs failure probability, all order 1 MCS were complemented with qualitative danger levels ranging from 1 to 3, with danger level 3 expressing the highest criticality. Influencing factors for the danger level were on the one hand the estimated failure probability and on the other hand the expected time needed to solve the problem. The estimations were made by IT specialists at SLF with long-time experience in maintaining the various system components. During this analysis, one MCS was estimated to have danger level 3.

As a validation of the results of the fault tree analysis we used a failure database containing all major problems of the avalanche warning system since the winter 1999 / 2000. The entries of this database were regularly logged by the technical support team of SLF. 276 failures were recorded during the last ten years. No significant positive or negative trend in the frequency of faults during this period can be observed, which means that the system's failure probability did not change over the last 10 years.

A frequency analysis summarizing the number of failures per system component revealed interesting results (see Fig. 1). The two most critical system components (found with FTA) caused failures relatively often. The bulletin editor triggered

*MS_216 — Performance-based design for structures
subject to natural hazard (1)*

This page intentionally left blank

Probabilistic hazard model of inelastic response of SDOF system based on equivalent linearization technique

Y. Mori & S. Kojima

Nagoya University, Nagoya, Japan

K. Ibuki

Obayashi Co., Ltd., Tokyo, Japan

1 INTRODUCTION

Predictors of seismic structural demands (such as interstorey drift ratios) that are less time consuming than nonlinear dynamic analysis (NDA) are useful for structural performance assessment and design. Several techniques for realizing such predictors have been proposed using the results of a nonlinear static pushover analysis (e.g., Yamanaka, et al., 2003). These techniques often use the maximum response of an inelastic oscillator (computed via NDA) that is “equivalent” to the original frame

In reliability-based seismic design of a structure, it is necessary to express the maximum response of the inelastic oscillator probabilistically. In practice, such information could be obtained using simple methods such as an equivalent linearization technique (EqLT, e.g., Shimazaki 1999) using an elastic response spectrum. Design spectra are being developed on the basis of probabilistic approaches such as a uniform hazard spectrum (UHS) and a conditional mean spectrum (CMS, Baker & Jayaram 2008).

A UHS is obtained by plotting the response with the same (i.e., uniform) exceedance probability for a suite of elastic oscillators with different natural periods, T_1 , and hence, a UHS does not represent any specific ground motion. There exists some correlation among the spectral responses of elastic oscillators to a ground motion (e.g., Baker & Jayaram 2008); however, perfect correlation is implicitly assumed in the use of a UHS. In such a scenario, the response could be overestimated via EqLT when a very rare event is considered.

The correlation among the spectral responses could be considered by using a CMS, which is the mean spectrum conditional to the event that the spectral displacement of an elastic oscillator with a certain period, T_c , equals the displacement with, say, 10% exceedance probability in 50 years. However, guidelines for the selection of T_c are not well established.

2 HAZARD MODEL OF $S_D^I(T)$

2.1 Probabilistic model of seismic hazard

It is assumed that the basic information on the seismic hazard is expressed by the suite of probability distributions of the maximum spectral displacement of elastic oscillators in n years, $S_{Dn}^E(T;h)$. Such information can be obtained through a seismic hazard analysis, which generally involves the following steps.

1. Simulate the occurrence of earthquakes at the faults that could cause a strong ground motion at the site for the next n years.
2. Estimate the response spectrum at the site for each earthquake considering the variability and the correlation among the residuals from the spectrum estimated by an attenuation formula.
3. At each natural period, take the maximum response among the ground motions estimated in Step (2) as the sample of the maximum response in n years.
4. Repeat Steps (1)–(3) many times to obtain the probability distribution functions of the n -year maximum displacement, $S_{Dn}^E(T;h)$.

In this research, the seismic hazard at the city hall of Nagoya, which is located in the central part of Japan, is estimated and used in the following analysis.

The seismic hazard is estimated by analyzing 4,000 samples for 50-year seismic activities. An acceleration response spectrum for each ground motion at the site is estimated by the attenuation formula proposed by An-naka, et al. (1997). The corresponding displacement response spectrum is estimated by multiplying the acceleration response spectrum with $(T_1/2\pi)^2$. It is assumed that the residuals of a response spectrum are lognormally distributed with the coefficient of variation (c.o.v.) equal to 0.5 and with the correlation coefficient

proposed by Baker & Jayaram (2008), which are taken into account in Step (2).

2.2 Approximate estimate of $S_D^I(T)$ using UHS/CMS

The exceedance probability of the maximum displacement of an inelastic oscillator in 50 years is estimated by the CS method using either the UHS or the CMS. It is assumed that the damping factor is 0.05; the yield base shear coefficient of the inelastic oscillator, C_y , is 0.3 or 0.5; the elastic natural period is 0.3, 0.5, 1.0, or 1.5 s; and the second stiffness ratio, k_2 , is 0.0 or 0.03. The probability is compared with “accurate” one estimated by employing the following steps:

- i. Apply the CS method in the $T - S_D$ coordinate to the response spectrum of each ground motion during each period of 50 years (see Step (2)) to estimate the maximum response of an inelastic oscillator to that ground motion.
- ii. Take the maximum response within each period of 50 years as the sample of the 50-year maximum value.

There are many cases in which the use of the EqLT with a UHS provides fairly accurate estimates, especially when the elastic natural period is longer than or equal to 1.0 s. The error becomes smaller when $k_2 = 0.03$. However, when $T_1 = 0.3$ or 0.5 s, the error in the estimation obtained using a UHS becomes large. When $T_1 = 0.3$, the correlation coefficient is relatively small, which is far from the perfect correlation implicitly assumed in the UHS. The error is more noticeable when $C_y = 0.5$.

The estimates obtained using a CMS are fairly accurate when the elastic natural period is longer than or equal to 1.0 s. However, it always provides an estimate that is optimistic by 10% to 25% when $T_1 = 0.3$ or 0.5. The error is especially noticeable when $C_y = 0.3$ and $k_2 = 0$.

2.3 New approximation method

The use of the CMS presented in the previous section is based on the condition that the spectral displacement at T_1 is equal to the value with 10% exceedance probability in 50 years. However, there could be many other possible events with “10% exceedance probability in 50 years.” An inelastic

oscillator with an elastic natural period of T_1 could reach its maximum value in 50 years when the spectral response at a period longer than T_1 takes a larger value than the response with 10% exceedance probability in 50 years. If such possible events are ignored, the response could be underestimated and a large error could occur.

Considering such observations, a new approximation method is proposed here assuming that T_c is a random variable uniformly distributed between T_1 and T_{eqUHS} , where T_{eqUHS} is the equivalent natural period estimated using the UHS. Then, the response is estimated as the expected value in terms of T_c .

The response of the inelastic oscillators corresponding to the 10% exceedance probability in 50 years estimated by the proposed method is discussed. When $T_1 = 0.3$ or 0.5, the accuracy improves considerably compared to that of the method using a single CMS with $T_c = T_1$. The error is fairly minor except for the case in which $C_y = 0.3$ and $k_2 = 0.03$. It is interesting to note that when an EqLT using the CMS with random T_c provides an estimate with a noticeable error, an EqLT using the UHS provides a fairly accurate estimate, and vice versa.

At the end of the paper, some of the results are further investigated using a generic model expressed in a stationary standard normal stochastic process.

REFERENCES

- An-naka, T., F. Yamazaki and F. Katahira, 1997. “Attenuation formula for maximum ground motion and response spectrum based on 87 ground motions observed by Japan Meteorological Agency” *Proc. 24th Meeting of Earthquake Engineering*, 161–164. (in Japanese).
- Baker, J.W. and N. Jayaram, 2008. “Correlation of spectral acceleration values from NGA ground motion models,” *Earthquake Spectra*, 24(1), 299–317.
- Shimazaki, K., 1999. “Evaluation of structural coefficient D_s by displacement response estimation using the equivalent linear method,” *J. Structural & Construction Engineering*, 516, 51–57. (in Japanese).
- Yamanaka, T., Y. Mori and M. Nakashima, 2003. “Estimation of displacement response of multi-story frame considering modal shape after yielding,” *Summaries of Technical Papers of Annual Meeting, AIJ*, B-1, 563–564. (in Japanese).

Performance-based design of structures under Aeolian Hazard

M. Ciampoli & F. Petrini

Department of Structural and Geotechnical Engineering, Sapienza University of Rome, Rome, Italy

1 INTRODUCTION

During the last decades, the risk assessment of structures under wind actions has been the subject of many researches. It has been recognized that Performance-Based Design represents the most rational way of assessing and reducing the risks of engineered facilities and infrastructures also in Wind Engineering.

The probabilistic procedure illustrated in (Augusti & Ciampoli 2008, Ciampoli et al., 2009) represents a general theoretic setup for the assessment of the performances of structures subject to wind actions. It has been developed in the framework of the so-called Performance-Based Wind Engineering (PBWE), and derived by extending the approach proposed for Performance-Based Seismic Design (PBSD) by the researchers of the Pacific Earthquake Engineering Research Centre (Porter 2003).

In this paper, the procedure is briefly described, and applied to an example case: the assessment of the occupant comfort for a high-rise building. The occupant comfort is related to the perception of building vibrations under wind actions. Specific emphasis is put on the proper characterization of the random variables governing the problem.

2 THE PROCEDURE FOR PERFORMANCE-BASED WIND ENGINEERING

In assessing the Aeolian risk of structures, different sources of uncertainty can be distinguished by considering the free-field conditions in the environment and the wind-structure interaction. Specific attention has to be given to the choice and probabilistic characterization of the minimum number of parameters that are needed to characterize the wind field and the structural response. In what follows, the parameters that characterize the wind field in the environment (the free-field conditions) are grouped in the *Intensity Measure* vector (**IM**); the parameters that characterize the structural behavior are grouped in the vector of *Structural Parameters* (**SP**); the parameters modeling the wind-structure interaction are grouped in the vector of *Interaction Parameters* (**IP**). The two

groups of parameters **IM** and **SP** are considered uncorrelated; on the contrary, the interaction parameters **IP** are strongly dependent on both the environmental **IM** and structural **SP** parameters.

The central objective of the procedure is the assessment of the adequacy of the structure through the probabilistic description of a set of decision variables (*DVs*). Each *DV* is a measurable attribute that represents a specific structural performance, which can be defined in terms of the interest of the users or the society. In Wind Engineering, typical *DVs* are the number of lives that are lost during windstorms, the economic losses resulting from windstorms, the exceeding of a (collapse or serviceability) limit condition, the discomfort of the occupants, etc.

Regardless the target performance, the structural risk can be conventionally measured by the probability of exceeding a relevant value of the corresponding *DV* (Ciampoli et al., 2009):

$$G(DV) = \iiint G(DV|DM) \cdot f(DM|EDP) \cdot f(EDP|IM, IP, SP) \cdot f(IP|IM, SP) \cdot f(IM) \cdot f(SP) \cdot dDM \cdot dEDP \cdot dIM \cdot dIP \cdot dSP \quad (1)$$

where *EDP* is a scalar engineering demand parameter, representing the structural response (e.g. the inter-storey drift) and *DM* is a scalar damage measure (e.g. the damage to the partitions and claddings in a building as a function of the inter-storey drift). The formal extension to vectors **DM** and **EDP** is straightforward.

By means of Equation 1, the problem of risk assessment is disaggregated into the following elements:

- site-specific *hazard analysis*, that requires the assessment of the joint probability density function $f(\mathbf{IM})$;
- *structural characterization*, that requires the assessment of the joint probability density function $f(\mathbf{SP})$;
- *interaction analysis*, that requires the assessment of the conditional probability density function $f(\mathbf{IP}|\mathbf{IM}, \mathbf{SP})$;

- *structural analysis*, aimed at assessing the probability density function of the structural response $f(EDP|\mathbf{IM}, \mathbf{IP}, \mathbf{SP})$ conditional on the parameters characterizing the wind field, the wind-structure interaction and the structural properties;
- *damage analysis*, that gives the damage probability density function $f(DM|EDP)$ conditional on EDP ;
- finally, *loss analysis*, that requires the assessment of $G(DV|DM)$, where $G(\cdot)$ is a complementary cumulative distribution function.

If the performance is expressed by the fulfillment of a limit state, and the limit state condition in terms of an EDP , the whole procedure can be simplified, assuming $DV = EDP$, and Equation 1 becomes:

$$G(EDP) = \int \int \int G(EDP|\mathbf{IM}, \mathbf{IP}, \mathbf{SP}) \cdot f(\mathbf{IP}|\mathbf{IM}, \mathbf{SP}) \cdot f(\mathbf{IM}) \cdot f(\mathbf{SP}) \cdot d\mathbf{IM} \cdot d\mathbf{IP} \cdot d\mathbf{SP} \quad (2)$$

3 AEOLIAN RISK ASSESSMENT

The PBWE procedure briefly described in Section 2 is applied to assess the comfort of the building occupants. The selected EDP is the peak acceleration a_L^p at the top of the building in across-wind direction. The comfort is evaluated by comparison of the EDP with the threshold values given in CNR (2008). The risk is conventionally evaluated in terms of the complementary cumulative distribution function $G(EDP)$, as indicated by Equation 2. The characteristics of the considered random parameters are reported in Table 1.

In Figure 1 the complementary distribution function $G(a_L^p)$ evaluated by Monte Carlo

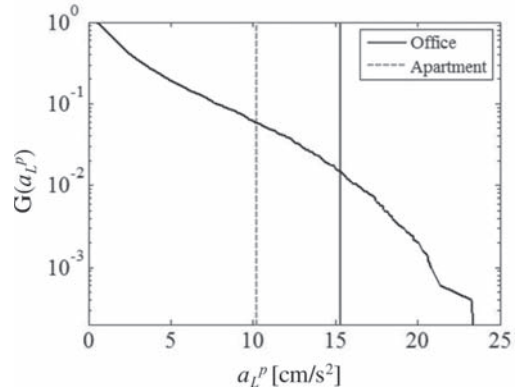


Figure 1. Complementary cumulative distribution function of a_L^p (Monte Carlo simulation 5000 runs).

simulation (5000 runs) is reported: the corresponding annual probabilities of exceeding the human perception thresholds for apartment and office building vibrations are 0.0576 and 0.0148 respectively.

4 CONCLUDING REMARKS

A general probabilistic framework for the Performance-Based Design of structures subject to wind action is applied to an example case. The main objective of the procedure is the assessment of the adequacy of the structure with specific reference to the occupant comfort evaluated in terms of the motion perception of building vibrations due to wind. The examined structure is a 74 storey steel building; the assumed DV is the peak value of the across-wind acceleration at the top of the building.

Table 1. Characteristics of the considered random variables.

	Variable		Distribution type and parameters
IM	V_{10} [m/s]	Mean wind velocity at 10 m height	Weibull PDF
	θ [deg]	Direction of mean wind velocity	Derived from the NIST wind velocity database
	z_0 [m]	Roughness length	Lognormal PDF
SP	ξ	Structural damping	Lognormal PDF
IP	g_r	Peak factor	Gaussian PDF
	C_V, C_D	Aerodynamic coefficients	Gaussian PDF

REFERENCES

- AIJ-Guidelines (2004). *Guidelines for the evaluation of habitability to building vibration*. Architectural Institute of Japan, Maruzen, p. 132. (in Japanese).
- Augusti, G. & Ciampoli, M. 2008. Performance-Based Design in risk assessment and reduction. *Probabilistic Engineering Mechanics*, 23: 496–508.
- Ciampoli, M. Petrini, F. & Augusti, G. 2009. A Procedure for the Performance-Based Wind Engineering. In: *Proc. Tenth international conference on structural safety and reliability (ICOSSAR'09)*, Osaka, Japan. Boca Raton: CRC press.
- CNR (Consiglio Nazionale delle Ricerche), 2008. *CNR-DT 207/2008: Istruzioni per la valutazione delle azioni e degli effetti del vento sulle costruzioni*. Rome, Italy: CNR (in Italian).
- Porter, K.A. 2003. An Overview of PEER's Performance-Based Engineering Methodology. In: *Proc. Ninth International Conference on Applications of Statistics and Probability in Civil Engineering (ICASP9)*, San Francisco, USA. Rotterdam: Millpress.
- Spence, S.M.J., Giofrè, M. & Gusella, V. 2008. Influence of higher modes on the dynamic response of irregular and regular tall buildings. In: *Proc. 6th International Colloquium on Bluff Bodies Aerodynamics and Applications (BBAA VI)*, Milan, Italy. Available at: <http://bbaa6.mecc.polimi.it/uploads/validati/pst024.pdf> [Accessed 10 September 2010].

Probabilistic and deterministic Soil Structure Interaction (SSI) analysis

A. Hashemi, T. Elkhoraibi & F. Ostadan
Bechtel National, Inc., San Francisco, USA

Soil-structure interaction (SSI) dominates the seismic response of stiff structures on relatively soft soil sites. Typical examples include nuclear facilities and civil infrastructures such as tunnels, dams and lock-head structures. Currently most SSI analyses are performed deterministically incorporating limited range of variation in soil and structural properties. This is mainly due to the fact that the computational cost of performing SSI analysis has been prohibitive for the incorporation of comprehensive probabilistic approaches. As such, bounding deterministic approaches have been preferred by the industry and accepted by the regulatory agencies. However, the need for a probabilistic-based approach to the SSI analysis is becoming clear with the advances in performance-based engineering and the utilization of fragility analysis in the decision making process whether by the owners or the regulatory agencies. Probabilistic SSI analysis is the more robust approach to evaluate the performance of the facility which is often decided on a probabilistic basis.

This paper demonstrates the use of both probabilistic and deterministic SSI analysis methodologies to identify important engineering demand parameters (EDPs) in the structure. Note that the term deterministic SSI analysis should not be taken as a single analysis with prescribed values for soil and structural properties. Rather, the deterministic approach examined here is consistent with ASCE 4-98 and performance-based provisions of ASCE 43-05 methodology targeted to determining an upper bound (often interpreted as one-standard deviation higher than the median or roughly an 80th percentile) seismic response. In both deterministic and probabilistic approaches, the analysis begins at the rock level using the low frequency and high frequency rock input motions obtained from Probabilistic Seismic Hazard Analysis (PSHA) and the site response analysis is conducted with randomized soil profiles and accompanying soil nonlinearity curves. The deterministic approach utilizes three strain-compatible soil profiles (Lower Bound (LB), Best Estimate (BE) and Upper Bound (UB)) determined based on the variation

of strain-compatible soil profiles obtained from the site response analysis and uses SSI analysis to determine a *conservative* estimate of the required response as the envelope of the SSI results from LB, BE and UB soil cases. In contrast, the probabilistic SSI analysis propagates the uncertainty in the soil and structural properties and provides rigorous estimates for the statistical distribution of the response parameters of interest.

An example site-structure system representative of a nuclear industry practice (Figure 1) on a deep soil site is used as a case study to illustrate the probabilistic SSI approach and compare it to the deterministic SSI methodology. The SSI analysis results are provided for both methods using the input ground motion at 10,000 year return period. Note that the design level defined for performance-based seismic design of nuclear buildings is

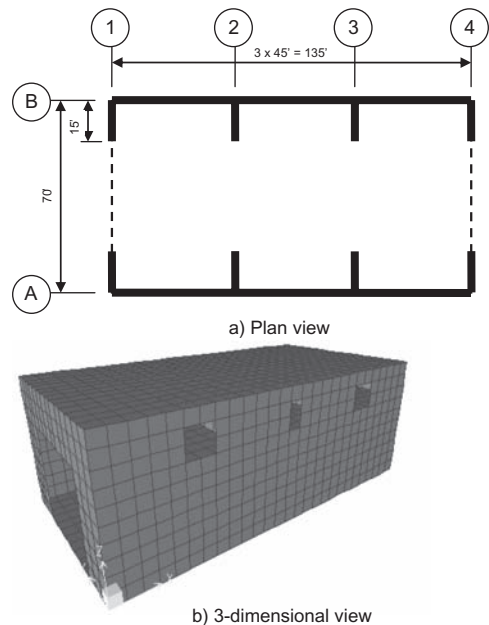


Figure 1. Example structure.

typically defined using a response spectra between 10,000 year and 100,000 year return period using prescribed frequency dependent design [weight] factors, ASCE (2005). However, the applicability of these factors to the full probabilistic SSI analysis results is not clear. Therefore, 10,000 year return period is used for consistent comparison between the deterministic and probabilistic SSI analysis results.

The EDPs evaluated are the shear wall forces and In-Structure-Response Spectra (ISRS) for the example structure. Application of the probabilistic SSI analysis in fragility function calculation and further in quantitative risk assessment (e.g. annual probability of failure calculation) using Integrated Soil Structure Fragility Analysis (ISSFA) methodology, Hashemi & Elkhoraibi (2009), is demonstrated and contrasted with deterministic based seismic margin analysis methodology.

For selected nodes on the base mat and roof of the example structure, the ISRS are calculated and presented using both deterministic and probabilistic SSI methodology. The deterministic ISRS is compared with percentiles of the probabilistic ISRS as shown in Figure 2.

The shear demand forces in the critical section of the wall are also determined both deterministically (envelope of LB, BE, and UB cases) and probabilistically for each of the 30 LHS cases and their distribution is illustrated in Figure 3(a). Figure 3(b) shows the cumulative density function (CDF) of the probabilistic results and the CDF of a corresponding log-normal distribution with the mean and standard deviation calculated from the probabilistic SSI results, as well as the results obtained from deterministic SSI analysis.

The ISRS comparisons indicate that for the example structure, the application of the

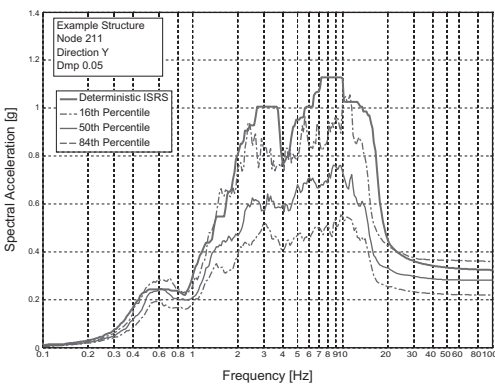


Figure 2. Comparison of the deterministic and probabilistic ISRS at node 211 (Basemat) in the transverse (Y) direction.

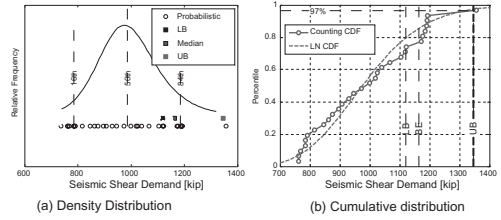


Figure 3. Probabilistic and deterministic shear demand distribution for the critical wall section (1 kip = 4.448 kN).

deterministic SSI analysis methodology results in an overly conservative ISRS, especially at the peak ISRS values. This finding has important implications since the calculated deterministic ISRS are typically used for seismic qualification of the non-structural components, piping and equipment and constitute a significant portion of the plant construction qualification costs.

The force comparisons shown indicates that for the example structure, the deterministic SSI analysis forces correspond to a 97th percentile demand force instead of the generally stated conservative target of 80th percentile. This finding suggests much larger margin in the design of structural members than previously thought.

In summary, the implementation of the performance based deterministic and probabilistic SSI analysis are demonstrated and contrasted for a representative example structure and the following conclusions are summarized:

- For the example structure, the deterministic SSI analysis overestimates the shear wall forces resulting in a 97th percentile design force. This finding indicates larger design margins than previously thought when using deterministic SSI analysis.
- For the example structure, the deterministic SSI analysis overestimates the ISRS, especially at the peak spectral values with significant potential implications for piping and equipment seismic qualification in nuclear facilities.
- The comparison between deterministic based and probabilistic fragility functions and annual probabilities of failure indicates that simplified deterministic methods generally produce results within the same order of magnitude from those of the probabilistic results and bounded by the 16th% and 84th% confidence intervals on the probabilistic results. However, the perceived conservatism of the simplified seismic margin analysis is doubtful.

Note that before the presented results can be further generalized, additional studies are needed including cases with embedded structures and shallow soil sites.

Seismic damage assessment of curved bridges using fragility analysis

Mehdi Mohseni & Terri R. Norton
University of Nebraska-Lincoln, Omaha, NE, USA

ABSTRACT: In presented study, an existing multispan curved bridge with continues composite girders is investigated for horizontal earthquake excitations. Based on the complex modal behavior of irregular bridge structures, such as curved bridges, their seismic response might be greatly affected by changing analysis assumptions. Using fragility analysis, a comprehensive damage assessment of the bridge structure has been done for different qualitative damage levels.

The radius of horizontal curve is 162 m constantly, providing almost 75 degrees of rotation. Bridge deck is rigidly connected to driven H-section steel piles at both abutments while sitting on radially fixed bearing devices at central pier and guided bearing devices at two adjacent piers. Three double rectangular column piers are standing on 1.2 m thick pile caps on a group of driven H section steel piles. In considering live load effects, four design lanes are assumed as the maximum bridge function regards to deck width. The four-span bridge structure is designed according to AASHTO guide specifications for horizontally curved steel girder highway bridges.

Statistically generated bridge samples were used in probabilistic evaluation of bridge structure. For this reason, 60 different bridge models were generated applying various geometry, material properties and load conditions. A nonlinear three dimensional dynamic analysis was performed for each bridge model using a randomly selected ground motion record with random direction.

To evaluate generated bridge models, 60 different ground motions for New Madrid seismic zone were applied in this study. Applying finite element method, all dissimilar 3D models were subjected to nonlinear direct integration time history analysis. Furthermore, P-delta effect and justified damping ratio were taken into account in each analysis.

Latin hypercube method has been used to generate uncorrelated random bridge models. Applying this method facilitates using smaller number of samples with respect to Monte Carlo simulation technique, while covering the entire sample space.

Variable parameters consist of ground motion direction, soil properties, damping, dead load/mass factor, live load factor, bearings properties

and material properties. Probability distribution type and related parameters for each random variable were selected according to previous studies and bridge construction documents.

In general, fragility curves illustrate the probability of exceeding demand (D) by capacity (C) of the structure for different damage levels. This probability can be expanded for a variety of intensity measures which is a ground motion characteristic.

To determine this probability, seismic demand and capacity of each component should be defined. Probabilistic seismic demand models (PSDM) can be developed by using analysis results of bridge samples.

Figure 1 shows probabilistic seismic demand model (PSDM) for column curvature ductility. In this figure, maximum curvature ductility in columns is plotted against PGA (in terms of g) in a logarithmic scale. The best linear regression equation is taken as the seismic demand model for the column curvature ductility.

The capacity of monitored bridge components should be expressed for each considered damage state. Four qualitative damage states—slight, moderate, extensive and complete damages—were assumed to evaluate functionality of the bridge components and structure. The capacity of bridge

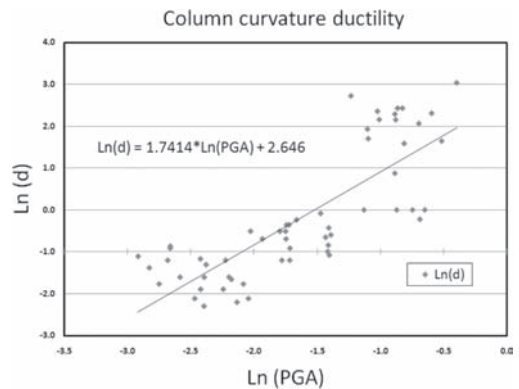


Figure 1. Probabilistic seismic demand model for column curvature ductility.

components can be obtained by using analytical methods, empirical data or even engineering judgments. In this research, medians and dispersion capacity values (S_c, β_c) for bridge components at each damage level were selected according to previous studies.

Figure 2 shows concluded fragility curves for moderate damage state for each observed component. In each curve, vertical coordinate declares the probability of passing damage level criteria for given pick ground acceleration. In this particular bridge, high rigidity of fixed and guided bearing devices led to a safe behavior of these elements while increased damage in other components such as pier columns, effectively. Based on nonlinear analysis results, most damages in columns were observed at pier no. 1 and 3, even though pier no. 3 is almost 35% shorter than pier no. 2. It is noticeable that different skew angles between each pier cap and roadway centerline makes the bridge structure more irregular and unpredictable.

Results of each single analysis announce high dependency on ground motion direction. To improve the accuracy of analysis results, a seismic hazard analysis for the bridge site is recommended. By identifying possible earthquake sources, magnitudes and directions, more dependable probabilistic distribution can be selected for ground motions. As an example, current uniform distribution for

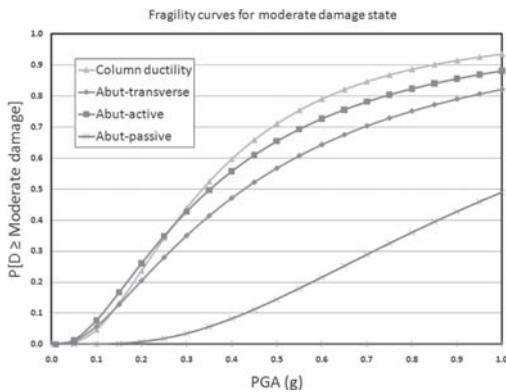


Figure 2. Fragility curves for moderate damage state.

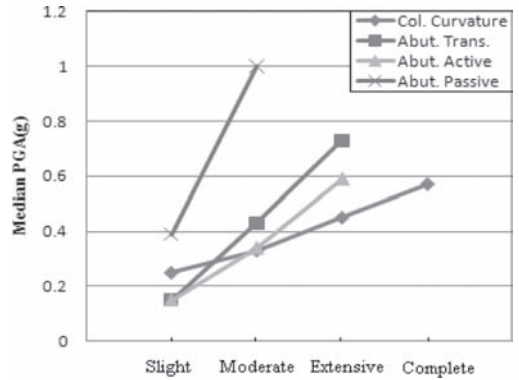


Figure 3. Median PGA values for each damage state (g).

earthquake direction (0 to π radians) could be represented by a normal distribution function using specified direction as the mean value.

For the complete damage state, abutment damages are not applicable, although excessive damage in pier columns can lead to collapse of bridge structure. It has been observed that even large displacement of abutments in active, passive, and transverse direction cannot terminate the bridge operation for a long time and be considered as a complete or extensive damage.

According to concluded fragility curves, transverse and active deformation of abutments are the most vulnerable issues for slight damage state, while for higher damage levels column curvature ductility acts as the critical damage in bridge structure (Fig. 3). Confidently, the repair or replacement of columns is considerably more expensive than repair of abutments. Hence, using isolation bearings could effectively reduce plastic damages in columns and associated repair cost.

Compared to straight multispan bridges, this examined curved bridge declared more sensitivity to some analysis assumptions such as ground motions. For future research/design purposes, it is recommended to analyze curved bridges for different directions of ground motion if a comprehensive fragility analysis is not practically feasible.

A framework for performance-based design and assessment of buildings subjected to extreme snow loads

A.B. Liel, K.A. Jackson & J.M. Geis

*Department of Civil, Environmental and Architectural Engineering,
University of Colorado, Boulder, CO, USA*

1 MOTIVATION

Extreme snow loading can cause significant damage to buildings and even collapse, requiring costly repairs, interrupting business, damaging building contents, and potentially endangering life safety. While past storms have caused few deaths in the U.S., snow-related damage and building closure can have significant societal and economic impacts on businesses and communities. In many cases, snow loads dominate roof design.

This paper describes a framework for performance-based snow engineering that enables explicit consideration of the risks of snow-induced failure in decisions about structural design. Performance-based engineering is a methodology for design and assessment of engineered facilities, which ensures that building performance under normal and extreme loads meets the needs of owners, occupants and the public (Krawinkler and Miranda 2004). Goals for building performance are used to inform decisions about design to reduce life-cycle costs and mitigate risks. However, efforts to develop performance-based methods have focused primarily on seismic and, more recently, wind engineering, and potential applications to snow engineering have not yet been fully developed. The performance-based framework for extreme loads developed here builds on this past research to account probabilistically for the many sources of uncertainty in the magnitude and distribution of roof snow loads and their impact on structural behavior and response.

The metrics of building performance obtained can inform decisions about structural design and assessment to mitigate the impacts of snow loads. This information is particularly important for structures for which the consequences of snow-related failure are high, either because of the large number of potential building occupants (as in arenas or theaters), or because of the high costs of business interruption if the building is damaged or evacuated (as in some manufacturing facilities). Performance-based snow engineering can also advance understanding of the relationship between

critical design variables and building performance for improving the consistency of code provisions conventional design practice. The importance of considering uncertainties in snow engineering is intensified by global climate change, which has altered geographic distributions, frequencies and severities of snowstorms (U.S. CCSP 2008).

2 FRAMEWORK FOR PERFORMANCE-BASED SNOW ENGINEERING

The theoretical framework for performance-based snow engineering is modular, separating hazard analysis, structural analysis, damage assessment, and loss and risk analysis. Key components of each module are described below, highlighting conceptual challenges that arise in development of probabilistic assessment methods for snow engineering.

2.1 *Characterization of ground snow hazard*

A ground snow hazard curve, like a seismic hazard curve, describes the mean annual frequency of exceeding the ground snow load of specified intensity at a particular site. The site-specific ground snow hazard curve is a function of weather patterns, site location and elevation and snow density, which can vary substantially according to geography and season. Ground snow hazard curves can be constructed where sufficiently detailed historic climate and weather data is available. Characterization of the ground snow hazard is a crucial input to the evaluation of structural response and building performance limit states.

2.2 *Roof snow loads*

In this study, roof snow loads are defined as a conversion factor on the ground snow load. These conversion factors, which relate ground snow load at a particular time to the snow load on the building at the same time, are different from those typical presented in building codes and other design

documents, which relate the maximum ground snow load in a season to the maximum roof load in the season and may occur at different times. Characterization of all roof snow loads, not only yearly maxima, allows us to combine roof snow load models with the probabilistic characterization of ground snow hazard to predict structural response under any level of snow load to obtain a comprehensive prediction of risk.

Roof snow loads depend on the snow load on the ground, as well as the exposure (accounting for terrain and wind conditions), building thermal properties (specifically the amount of insulation, measured by the roof's thermal resistance), roof material (e.g. shingled roofs tend to have higher snow loads than metal roofs) and geometry (slope). Drift loads will depend on wind speed and direction, the density of snow, obstructions (e.g. gables, parapets, mechanical equipment), and roof configuration (slope, multi-levels etc.).

In this study, a model has been developed to predict the distribution of roof snow loads as a function of ground snow load. Roof snow loads can then be determined through Monte Carlo simulations which generate realizations of the roof snow load, depending on the ground snow load and the uncertainty in the roof snow load resulting from snow transport, drift distribution and formation and weather conditions.

2.3 Evaluation of structural response

The outcome of the roof load probability models is a set of possible realizations of roof snow load for each value of ground snow load of interest. Each realization produces a different magnitude and distribution of roof load to which the structure will be subjected. Accordingly, each of these different loading scenarios leads to a different prediction of structural response. Structural response can then be evaluated at a variety of different levels of ground snow loads to obtain predictions ranging from very low to high snow loads for a particular structure. The variability in roof deflection associated with each level of ground snow load is associated with uncertainties in prediction of roof snow load. Besides roof deflection, other structural response parameters of interest may include the ratio of stress in critical member to yield stress and roof failure.

2.4 Assessment of limit state probabilities of exceedance

Building performance limit states of interest are related to the potential consequences building

owners or society wish to avoid. Snow loads can cause structural and nonstructural damage, economic losses due to costs associated with repairing snow-related damage, downtime and business interruption or collapse. Broadly speaking, building owners and occupants are interested in assessments of safety (*i.e.* collapse risks) and downtime and economic losses, which facilitate life-cycle assessment of design decisions. Therefore, metrics for performance-based snow engineering may include (i) repair costs exceeding $X\%$ of building replacement cost, (ii) building closure or downtime exceeding Y days, or (iii) the risk of structural collapse. Limit states related to significant beam deflection (*i.e.* the onset of significant damage) are illustrated in this paper for a case study building.

3 NEXT STEPS

This framework for performance-based snow engineering can be used to quantify the behavior and reliability of structures subject to extreme snow loading, advancing risk-informed decisions about snow design. It is applicable to a wide variety of structures and, by extension, vulnerable lifeline systems. Assessments of building performance under snow loads improves understanding of the key sources of uncertainty governing snow design and the impacts of snow design decisions and code provisions on structural response and other limit states of interest to building owners.

Future research will explore the application of this methodology to complex real structures, focusing on long-span light-frame metal structures that have been shown to be particularly vulnerable to snow-related building damage.

REFERENCES

- Krawinkler, H. & Miranda, E. 2004. Performance-Based Earthquake Engineering. In Y. Bozorgnia, and B.V. eds., *Earthquake Engineering: From Engineering Seismology to Performance-Based Engineering*, CRC Press: Boca Raton.
- United States. Climate Change Science Program. Subcommittee on Global Change Research. Weather and Climate Extremes in a Changing Climate. June 2008. <<http://downloads.climatechange.gov/sap/sap3-3/sap3-3-final-all.pdf>>

This page intentionally left blank

*MS_226 — Performance-based design for structures
subject to natural hazard (2)*

This page intentionally left blank

Probabilistic assessment of disproportionate collapse potential of steel moment resisting frames

Guoqing Xu

Georgia Institute of Technology, Atlanta, GA, USA

Bruce R. Ellingwood

The Raymond Allen Jones Chair in Civil Engineering, School of Civil and Environmental Engineering, Georgia Institute of Technology, Atlanta, GA, USA

ABSTRACT: Disproportionate (or progressive) collapse has become an increasingly important building structure performance issue following the collapses of the Alfred P. Murrah Federal Building in Oklahoma City in 1995 and the World Trade Center in 2001. Unified guidelines for providing progressive collapse resistance for new Federal building construction and major modernization projects in the United States recently have been issued (DoD 2009). These guidelines utilize, among other strategies, the alternative path method (APM) of analysis (Ellingwood & Dusenberry 2005), in which the robustness of a structure is assessed analytically by notionally removing major gravity load-bearing elements (columns, bearing walls), one at a time, and determining whether the damaged structure can sustain the local damage without further collapse. As currently implemented, however, these robustness assessment methods are entirely deterministic in nature, and do not take into account uncertainties in structural demands and resisting capacities subsequent to initiating damage (Stevens et al., 2008). Moreover, most recent research on the collapse resisting capacity of frames and their connections utilizes deterministic methods (e.g., Khandelwal & El-Tawil, 2007), although large variation of the capacities are known to exist. Little research has been conducted on the effects of these uncertainties on robustness assessment of structures.

In this paper, the robustness of moment-resisting steel frames that were typical of construction in seismic regions prior to the 1994 Northridge earthquake is assessed probabilistically, taking into account the uncertainties in the collapse demands and the resisting capacities of the connections in the frames. A failure mode involving fracture in the weld metal connecting the beam and column flanges was identified as the dominant failure mode in pre-Northridge steel moment resisting connections. A probabilistic model for this failure mode under scenarios involving sudden column

loss is developed with a J-integral characterization of fracture demand (Rice 1968), coupled with detailed finite element simulations. The main factors (e.g. initial flaw size and yielding strength of beam sections) affecting the fracture are modeled probabilistically and incorporated into the simulations through Latin hypercube sampling. The probability distribution of the connection strength is then derived by comparing the probabilistic fracture demands with the statistical result of the weld fracture toughness reported by Kaufmann & Fisher (1997) and Patterson et al. (1998). The probabilistic connection behavior model is verified by comparing to connection test results from the SAC project (FEMA 2000). The capability of such connections to develop catenary action following damage (Byfield 2004; Khandelwal & El-Tawil 2007) and its contribution to subsequent collapse behavior of the connections also is examined. Following the development and validation of the connection model, the robustness of several steel frames designed in the SAC project is assessed separately by (1) the deterministic method utilizing the requirements in the new *Unified Facilities Criteria* (2009) and (2) a system reliability analysis method in which the uncertainties in gravity loads and resisting capacities described by the probabilistic connection model are taken into account. The importance of considering uncertainties in connection behavior is investigated by comparing the assessment results from these two methods. The results of this analysis offer insight on the contribution of connection behavior to disproportionate collapse risk of steel frame buildings.

REFERENCES

- Byfield, M.P. (2004). "Design of steel framed buildings at risk from terrorist attack." *The Structural Engineer*, 82(22), 31–38.

- Department of Defense (DoD). (2009). Unified Facilities Criteria (UFC 4-023-03, July 14, 2009): *Design of Buildings to Resist Progressive Collapse*, Washington, D.C.
- Ellingwood, B.R. & Dusenberry, D.O. (2005). "Building Design for Abnormal Loads and Progressive Collapse." *Computer-Aided Civil and Infrastructure Engineering*, 20(3), 194–205.
- Federal Emergency Management Agency (FEMA). (2000). FEMA 355D: *State of the Art Report on Connection Performance*, Washington, D.C.
- Kaufmann, E.J. & Fisher, J.W. (1997). *Failure analysis of welded steel moment frames damaged in the Northridge earthquake*. Building and Fire Research Lab., National Inst. of Standards and Technology, Gaithersburg, Md.
- Khandelwal, K. & El-Tawil, S. (2007). "Collapse Behavior of Steel Special Moment Resisting Frame Connections." *Journal of Structural Engineering*, 133(5), 646–655.
- Patterson, S., Vaillancourt, H. & Kuntz, T. (1998). "Variability and statistical bounds of the strength and fracture toughness of common structural steel shapes and weld metals used in welded moment frame building construction." *Proc., Int. Conf. on Welded Constr. in Seismic Areas*, American Welding Society.
- Rice, J.R. (1968). "A Path Independent Integral and the Approximate Analysis of Strain Concentration by Notches and Cracks." *Journal of Applied Mechanics*, 35, 379–386.
- Stevens, D., Crowder, B., Hall, B. & Marchand, K. (2008). "Unified progressive collapse design requirements for GSA and DOD." *Proc., SEI Structures Congress 2008*, Vancouver, BC.

Life-cycle seismic repair cost assessment and sensitivity analysis

A.A. Taflanidis

University of Notre Dame, Notre Dame, IN, USA

1 INTRODUCTION

Life-cycle loss estimation in earthquake engineering requires proper integration of (i) approaches for treating the uncertainties related to the seismic hazard and to the structural behavior over the entire life-cycle of the building, (ii) methodologies for evaluating the structural performance using socio-economic criteria, as well as (iii) algorithms appropriate for stochastic analysis (Taflanidis and Beck 2009). One of the most important components of this process is appropriate modeling of earthquake losses. Initial methodologies for this task expressed these losses in terms of the global reliability of the structural system. Recent advances in performance-based engineering quantify, more accurately, repair cost, casualties, and downtime in relation to the structural response, using fragility curves to develop such a relationship. In this context, approaches have been developed that approximately describe the nonlinear structural behavior by the static pushover response and/or estimate earthquake losses in terms of global response characteristics. Other researchers have developed more thorough analytical tools to evaluate seismic vulnerability on a more-detailed level. According to this methodology, the nonlinear time-history response of the structure under a given seismic excitation is used to calculate damages in a component level. This paper discusses a probabilistic framework for assessment and sensitivity analysis of the life-cycle repair cost, based on such an earthquake loss estimation methodology.

2 LIFE-CYCLE SEISMIC COST ASSESSMENT

For evaluation of seismic cost adoption of appropriate models is needed for the structural system itself, the earthquake excitation and for loss evaluation. The combination of the first two models provides the structural response and in the approach adopted here this is established in terms of nonlinear time-history analysis. The loss evaluation model quantifies, then, earthquake performance in economic terms based on that response.

The characteristics of these models are not known with absolute certainty, though. Uncertainties may pertain to the properties of the structural system, to the variability of future seismic events, or to parameters related to the fragility of the system components. For explicitly incorporating these uncertainties in the modeling process, let $\theta \in \Theta \subset \mathbb{R}^{n_\theta}$, denote the augmented vector of model parameters where Θ represents the space of possible model parameter values. Vector θ is composed of *all* the model parameters for the individual structural system, excitation, and loss evaluation, models. The uncertainty in these model parameters is then quantified by assigning a probability model $p(\theta)$ to them, which incorporates our available prior knowledge about the system and its environment into the modeling process.

In this setting, the overall cost, for a specific structural configuration and seismic excitation, described by θ , is denoted by $h(\theta)$. The expected life-cycle is then simply given by the expected value of $h(\theta)$ over the chosen probability models

$$C = \int_{\Theta} h(\theta)p(\theta)d\theta \tag{1}$$

Since the models adopted for characterization of the earthquake losses can be complex, i.e. may involve a large number of model parameters and various sources of nonlinearities, the expected value (1) cannot be calculated, or even accurately approximated, analytically. An efficient alternative approach is to estimate this integral by *stochastic simulation*. In this case, using a finite number, N , of samples of θ simulated from some importance sampling density $q(\theta)$, an estimate for (1) is given by the *stochastic analysis*:

$$\hat{C} = 1/N \sum_{j=1}^N h(\theta^j)p(\theta^j)/q(\theta^j) \tag{2}$$

where vector θ^j denotes the sample of the uncertain parameters used in the j^{th} simulation and $\{\theta^j\}$ corresponds to the entire sample set. Though appropriate selection of system and probability models, this approach efficiently takes into account all uncertainties about the properties, excitation

and performance of the structural system through the specified lifetime.

This framework may be also extended to additionally investigate the sensitivity of the seismic risk with respect to each of the uncertain model parameters. This sensitivity analysis is based on the novel ideas discussed in (Taflanidis 2009). Foundation of this methodology is the definition of an auxiliary probability density function that is proportional to the integrand of the life-cycle cost integral

$$\pi(\boldsymbol{\theta}) \propto h(\boldsymbol{\theta})p(\boldsymbol{\theta}) \quad (3)$$

Comparison between the marginal distribution $\pi(\theta_i)$ and the prior distribution $p(\theta_i)$ expresses the *probabilistic* sensitivity of the seismic risk with respect to θ_i . Uncertainty in all other model parameters and stochastic excitation is explicitly considered by appropriate integration of the joint probability distribution $\pi(\boldsymbol{\theta})$ to calculate the marginal probability distribution $\pi(\theta_i)$. As quantitative metric to characterize this sensitivity the relative information entropy, between probability distributions $\pi(\theta_i)$ and $p(\theta_i)$ is used and a computationally efficient sampling-based approach is discussed for evaluation of this entropy (Taflanidis 2009).

3 LOSS ESTIMATION METHODOLOGY

For estimating earthquake losses the comprehensive methodology described in (Goulet et al., 2007) is adopted; the components of the structure are grouped into damageable assemblies. Each assembly consists of components of the structural system that have common characteristics with respect to their vulnerability and repair cost. For each assembly j different damage states are designated and a fragility function is established for each damage state. These functions quantify the probability the component has reached or exceeded its k th damage state, conditional on some engineering demand parameter which is related to the time-history response of the structure (for example, peak transient drift, peak acceleration, maximum plastic hinge rotation, etc.). Damage state 0 is used to denote an undamaged condition. A repair cost is then assigned to each damage state, which corresponds to the cost needed to repair the component back to the undamaged condition. The expected losses in the event of the earthquake is then calculated based on this information. This approach can be extended to evaluating the cost of injuries and fatalities, or downtime cost.

4 GROUND MOTION MODEL

This life-cycle assessment framework requires development of a probabilistic model of the entire ground motion time history that will adequately describe the uncertainty in future earthquake events. A stochastic ground motion modeling methodology is adopted for this task. This model is based on modulating a stochastic sequence through time-domain and frequency domain models. The parameters of these models are correlated to earthquake (type of fault, moment magnitude and epicentral distance) and site characteristics (shear wave velocity, local site conditions) by appropriate predictive relationships. Description of the uncertainty for the earthquake characteristics and the predictive relationships leads then to a complete probabilistic model for future ground-motion time-histories. In particular, a point-source stochastic ground motion model (Boore 2003) is adopted in this study for this purpose.

5 ILLUSTRATIVE EXAMPLE

The framework was illustrated in an illustrative example for a three-storey reinforced-concrete office building. The detailed assessment of the repair cost, per floor and per damageable assembly, provided a valuable insight into the seismic performance and vulnerabilities of the structure. With respect to the sensitivity analysis, the seismic hazard characteristics, i.e., the magnitude and epicentral distance, were recognized as the most important parameters influencing the total repair cost, whereas interesting differences were identified between the sensitivity results with respect to the different damageable components.

REFERENCES

- Boore, D.M. 2003. Simulation of ground motion using the stochastic method. *Pure and Applied Geophysics* 160: 635–676.
- Goulet, C.A., Haselton, C.B., Mitrani-Reiser, J., Beck, J.L., Deierlein, G., Porter, K.A. & Stewart, J.P. 2007. Evaluation of the seismic performance of code-conforming reinforced-concrete frame building-From seismic hazard to collapse safety and economic losses. *Earthquake Engineering and Structural Dynamics* 36(13): 1973–1997.
- Taflanidis, A.A. 2009. Stochastic subset optimization with response surface methodologies for stochastic design. In, *1st International Conference on Soft Computing Technology in Civil, Structural and Environmental Engineering, Madeira, Portugal, 1–4 September*.
- Taflanidis, A.A. & Beck, J.L. 2009. Life-cycle cost optimal design of passive dissipative devices *Structural Safety* 31(6): 508–522.

A method for probabilistic seismic design of RC structures

P. Franchin & P.E. Pinto

Sapienza University of Rome, Rome, Italy

1 INTRODUCTION

This paper presents a method for performance-based seismic design of RC structures which is based on explicitly probabilistic design constraints in terms of mean annual frequencies (MAFs) of exceedance of chosen performance-levels/limit-states. The method, which is an approximate one, rests on the validity of two basic results of earthquake engineering: the closed-form expression for the MAF of exceedance of a limit-state from (Cornell *et al.*, 2002) and the well-known, so-called (empirical) “equal-displacement” rule. Limits of validity of the above results are clearly recognised and are inherited by this proposal. The approximation of the method is explored with reference to a 15-storey RC plane frame structure.

2 METHODOLOGY

The method iteratively modifies a design solution until it satisfies multiple probabilistic constraints, i.e. constraints on the MAFs of multiple performance-levels (e.g. light damage, collapse, etc), employing the gradients of the MAFs with respect to the design variables. By virtue of the assumed validity of the “equal-displacement” rule, the iteration process is carried out on a (cracked) elastic model of the structure whose deformed shape, as obtained from multi-modal response spectrum analysis, is taken as a proxy for the true inelastic shape. The assumption of elasticity allows explicit analytical evaluation of the gradients of the MAFs, needed in the search algorithm employed to find a design that satisfies the constraints, a fact that increases manifold the computational effectiveness of the procedure. Flexural reinforcement is designed only when the iteration process on the cross-section dimensions has ended. Shear reinforcement is capacity-designed as the last step.

2.1 Gradients of the MAF

The “SAC/FEMA” closed-form expression of the mean annual frequency of exceedance λ of a structural limit-state reads (Cornell *et al.*, 2002):

$$\lambda = \lambda_{IM} \left(IM_{\hat{D}=\hat{C}} \right) \exp \left[\frac{1}{2} \frac{k^2}{b^2} \left(\beta_D^2 + \beta_C^2 \right) \right] = k_0 \left(\frac{\hat{C}}{a} \right)^{\frac{k}{b}} \exp \left[\frac{1}{2} \frac{k^2}{b^2} \left(\beta_D^2 + \beta_C^2 \right) \right] \quad (1)$$

where $IM_{\hat{D}=\hat{C}} = \left(\hat{C}/a \right)^{1/b}$ is the intensity measure (IM) value that induces a median demand \hat{D} equal to the median limit-state capacity \hat{C} , while $\beta_D = \sigma_{\ln D}$ and $\beta_C = \sigma_{\ln C}$ are the demand and capacity dispersions. The above expression holds under the assumption that demand and capacity distribute lognormally with median demand varying with the IM according to the power law $\hat{D} = aIM^b$, and that the MAF of the IM (hazard) approximates as $\lambda_{IM}(x) = k_0 x^{-k}$.

Under the assumed validity of the equal-displacement rule, the response of the structure depends only on the elastic properties of its elements, i.e. the section axial and flexural stiffnesses, EA and EI. For RC structures the effect of cracking on flexural stiffness is taken care of by means of reduction factors. Cross-section dimensions are grouped into a vector \mathbf{d} . The gradient of the MAF in Eq. (1) with respect to the design variables \mathbf{d}_1 can be expanded as:

$$\nabla_{\mathbf{d}_1} \lambda = \frac{\partial \lambda}{\partial k_0} \frac{\partial k_0}{\partial \mathbf{d}_1} + \frac{\partial \lambda}{\partial k} \frac{\partial k}{\partial \mathbf{d}_1} + \frac{\partial \lambda}{\partial a} \frac{\partial a}{\partial \mathbf{d}_1} + \frac{\partial \lambda}{\partial b} \frac{\partial b}{\partial \mathbf{d}_1} \quad (2)$$

The paper presents analytical expressions for the terms in (2).

2.2 Search algorithm

The performance constraints that the structure must comply with are expressed in terms of λ of the limit-state violations for a number of limit-states of interest, e.g. a serviceability limit-state, such as light damage (LD), and a safety-related one, such as collapse prevention (CP). For example (the limits on the frequencies being arbitrary):

$$\lambda_{LD} \leq \lambda_{LD}^* = 1/100 \text{ years} \quad (3)$$

$$\lambda_{CP} \leq \lambda_{CP}^* = 1/2500 \text{ years} \quad (4)$$

When working with multiple constraints it is useful to normalize each of them according to: $\tilde{\lambda} = \lambda / \lambda^* - 1$. This allows to define the governing constraint at each iteration, as that having the largest value of $\tilde{\lambda}$. At the end of the process only one of the constraints is satisfied in equality, while the remaining ones are satisfied with more or less wide margins.

The search for a feasible design solution, i.e. the problem of finding a zero for the $\tilde{\lambda} = \tilde{\lambda}(\mathbf{d})$ function, is carried out by means of a quasi-Newton method, transforming it into the problem of finding a minimum for $\tilde{\lambda}^2$, where the gradient $\nabla_{\mathbf{d}} \tilde{\lambda}^2 = \mathbf{0}$. In practice, since the feasible design must also satisfy a number of other practical constraints related, e.g., to construction (column tapering, minimum section dimensions, etc), the problem is cast in the form of a constrained optimization:

$$\begin{cases} \min_{\mathbf{d}} s = \tilde{\lambda}^2 \\ \text{subject to } \mathbf{c} \leq 0 \end{cases} \quad (5)$$

where the vector $\mathbf{c}(\mathbf{d}) = \mathbf{A}\mathbf{d} + \mathbf{b} \leq 0$ collects the n constraints $c_i(\mathbf{d})$ which are formulated to take upon positive values whenever the corresponding constraint is violated.

2.3 Reinforcement design

Design of longitudinal reinforcement is carried out for a “seismic” combination of gravity loads and a seismic action characterized by a given average return period, chosen to limit structural damage (yielding) for frequent earthquakes. Design of longitudinal reinforcement is carried out for a seismic action with an average return period related to the λ_{LD}^* limit on the light damage performance-level.

Capacity design procedure, not strictly required for the relative flexural strength of beams and

columns, since drifts are explicitly limited in the method, is a good practice that would certainly reduce the uncertainty associated with the drift prediction and increase the reliability of the proposed method. Capacity design is clearly employed for determining the shear strength of members and joints. The distribution of flexural reinforcement along the height is carried out aiming at a as uniform as possible ratio of moment demand to capacity (see also Figure 1, where this is shown with reference to the example application).

3 VALIDATION

The method has been implemented in a MATLAB® code that employs the built-in optimization functions (in particular the constrained minimization algorithms in `fmincon`) and performs response spectrum analysis of linear elastic frames, computing both response and its sensitivity. Validation of the obtained design is carried out by means of inelastic time-history analysis within the finite-element code OPENSEES (McKenna and Fenves, 2001). A meaningful comparison of the risk value obtained by means of linear analysis at the end of the design iteration process with the “exact” value must take into account the inter-analyst dispersion of “exact” values computed by different analysts employing different sets of records. To obtain an estimate of the distribution of “exact” risk values the bootstrap (Efron and Tibshirani, 1993) technique has been used.

4 CONCLUSIONS

As far as it is allowed by the limited validation that has been carried out, it is feasible to design in an explicitly probabilistic manner a RC frame structure on the basis of two basic approximations: the so-called “Cornell” closed-form for seismic risk and the well-known “equal-displacement” rule. This latter rule appears to maintain its approximate validity also for MDOF structures, on the condition that the reinforcement design is carried out to provide the structure with a “uniform” distribution of the actual to required strength ratio, in order to maintain similarity of the deformation pattern between the elastic and inelastic response regimes.

Current efforts are focusing on relaxing the reliance on the equal displacement rule, introducing an intermediate single-step iteration on stiffnesses to account for the influence of the designed strength (reinforcement) on the cracked stiffness, as well as of axial force.

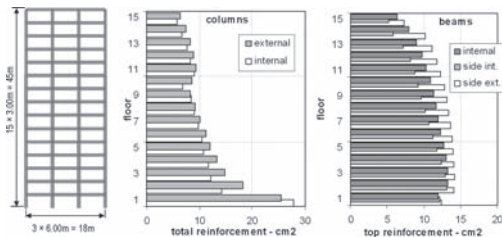


Figure 1. Geometry and reinforcement of the fifteen-storied RC plane frame.

A statistical analysis of steel truss temperature data recorded during fire resistance tests

Dilip K. Banerjee, Emil Simiu & John L. Gross

National Institute of Standards and Technology, Building and Fire Research Laboratory, Gaithersburg, Maryland

Raghu Kacker

National Institute of Standards and Technology, Information Technology Laboratory, Gaithersburg, Maryland

ABSTRACT: The performance of composite floor steel trusses in fires is a function of the steel temperatures within the trusses. For any given specified fire and composite system design, the temperatures depend on three factors that vary randomly with position: (1) the thermal behavior of the concrete slab, (2) the thermal behavior of the spray applied fire resistive material (SFRM), and (3) the thickness of the SFRM spray. Models of the dependence of steel truss temperatures on these three factors are needed to predict the temperatures within the truss and, therefore, the performance of the trusses corresponding to those temperatures. To develop the models it is necessary to make use of the measured temperature data. Such measurements were obtained in four Standard Fire Tests (2 full scale and 2 half scale) conducted at the Underwriters Laboratories fire testing facility using two furnaces. The furnaces were heated by 80 individual floor mounted burners following the American Society for Testing and Materials (ASTM) E119 standard time-temperature curve, and furnace temperatures were monitored at 24 locations in the larger furnace and 16 locations in the smaller furnace. Time-temperature data were collected at specific locations along the truss near the top chord, at mid height of the web, and at the bottom chord.

A first step in the development of statistical models for the three factors mentioned earlier is

an approximate analysis of the dependence of the influence of thermal mass of the concrete slab on the temperatures recorded at a particular location on the steel truss. The analysis indicates that this influence is small at the level of the lower truss chord. Therefore, the variability of the temperatures at that level can be assumed approximated as due only to the joint effect of the variability of the SFRM properties and thickness. Once the effect of the thermal mass of the slab is understood on the basis of measurements obtained on the lower chord, it is possible to estimate the influence of the thermal mass of the slab on recorded steel temperatures by analyzing data measured close to the slab and at mid-truss level. This estimation requires the subtraction of the effect of the variability of the spray properties and thickness from the total observed variability.

In the present study, experimentally recorded temperature data collected during the fire resistance tests are analyzed to understand the influence of the concrete slab and the spray applied fire resistive material (SFRM) on the temperature profile in the steel truss. It was shown that the effect of the SFRM thickness on steel temperatures was more pronounced at the lower chord than it was at the level of the mid web. The conclusions of this work help to clarify the correlation of the variability in temperature data with the thermal mass of the concrete.

This page intentionally left blank

MS_124 — Probabilistic calibration of codes (1)

This page intentionally left blank

Conventional probabilistic models for calibration of codes

M. Holický & M. Sykora

Czech Technical University in Prague, Klokner Institute, Prague, Czech Republic

1 INTRODUCTION

Probabilistic models of basic variables used in various studies of structural reliability are significantly different. Obviously, the reliability studies may then lead to dissimilar results and undesirable discrepancies in recommendations concerning partial safety factors, combination factors and other reliability elements.

The present paper aims to summarize and propose conventional probabilistic models in order to enable an efficient comparison of reliability studies of various structural members made of different materials (steel, concrete, composite). Proposed models represent average values of action and material properties, common structural conditions and normal quality control. As an example reliability a generic steel member is analysed considering the recommended probabilistic models.

2 CONVENTIONAL PROBABILISTIC MODELS

The following conventional models of basic variables are intended to be used as prior theoretical models that could be accepted for general reliability studies and calibration procedures in connection with foreseen revisions of codes for structural design. The models may also be applied as prior models in the framework of Bayesian updating.

The theoretical models may be used in time-invariant reliability analyses of simple structural members. In addition, parameters describing time-variant properties of selected actions are provided for time-variant reliability analyses.

Table 1 includes the three fundamental categories of basic variables (actions, material strengths and geometric data) supplemented by the uncertainty factors for action effects and structural resistance. The data indicated in Table 1 represent conventional

Table 1. Conventional models of basic variables.

Name	Sym. X	Dist.	Mean μ_X	St.dev. σ_X	Prob. $F_X(x_k)$
Permanent action	G	N	g_k	$0.03-0.10\mu_X$	0.5
Imposed load (5y.)	Q	Gum	$0.2q_k$	$1.1\mu_X$	0.995
Imposed l. (50 y.)	Q	Gum	$0.6q_k$	$0.35\mu_X$	0.953
Wind (1 y.)	W	Gum	$0.3w_k$	$0.5\mu_X$	0.999
Wind (50 y.)	W	Gum	$0.7w_k$	$0.35\mu_X$	0.890
Snow (1 y.)	S	Gum	$0.35s_k$	$0.70\mu_X$	0.998
Snow (50 y.)	S	Gum	$1.1s_k$	$0.30\mu_X$	0.437
Yield strength steel	f_y	LN	$f_{yk} + 2\sigma_X$	$0.07-0.10\mu_X$	0.02
Ultim. streng. steel	f_u	LN	$\kappa \mu_{fy}^*$	$0.05\mu_X$	–
Concrete strength	f_c	LN	$f_{ck} + 2\sigma_X$	$0.10-0.18\mu_X$	0.02
Yield streng. reinf.	f_y	LN	$f_{yk} + 2\sigma_X$	30 MPa	0.02
IPE profiles	A, W, I	N	$0.99x_{nom}$	$0.01-0.04\mu_X$	0.73
L-sections, rods	A, W, I	N	$1.02x_{nom}$	$0.01-0.02\mu_X$	0.16
Cross-section	b, h	N	b_k, h_k	$0.005-0.01$ m	0.5
Cover of reinforce.	a	BET	a_k	$0.005-0.015$ m	0.5
Additional eccentr.	e	N	0	$0.003-0.01$ m	–
Model unc. load	θ_E	LN	1	$0.05-0.10$	–
Model unc. resist.	θ_R	LN	$1-1.25$	$0.05-0.20$	–

*the coefficient κ can be considered as follows— $\kappa = 1.5$ for structural carbon steel; $\kappa = 1.4$ for low alloy steel; and $\kappa = 1.1$ for quenched and tempered steel, JCSS (2006).

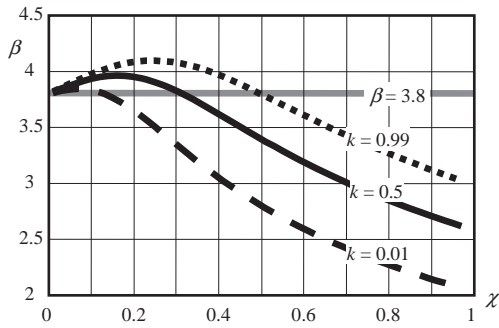


Figure 1. Variation of the reliability index with the load ratio.

models only, which may not be adequate in specific cases (e.g. wind actions on high-rise buildings).

3 NUMERICAL EXAMPLE

As an example reliability of the generic steel member exposed to snow and wind loads is analysed using the proposed conventional models. The steel member is designed according to relationship (6.10) given in EN 1990 (2002). The load ratio χ of the total characteristic variable load effect to the total characteristic load effect is considered. The variable load ratio is defined as the characteristic wind action over the characteristic snow load $k = w_k/s_k$. Failure probability is estimated considering the reference period of 50 years. Combination of the time-variant loads is approximated by the rule proposed by Turkstra (1970).

The results of the reliability analysis given in terms of the reliability index β , EN 1990 (2002), are shown in Figure 1. The reliability index is plotted as a function of the load ratio for three values of the variable load ratio— $k = 0.01$ (snow load only), $k = 0.5$ (dominant snow load) and $k = 0.99$ (the snow and wind loads of similar effects). Target value of the reliability index $\beta = 3.8$ recommended in EN 1990 (2002) for the ultimate limit states of buildings designed for a 50-year working life is also indicated in Figure 1. It follows that the reliability index significantly varies with the load ratio and decreases below the target level with an increasing load ratio. The predicted reliability level is lower for a single snow load as compared with the combinations of the actions.

4 CONCLUDING REMARKS

The proposed conventional models of basic variables, intended primarily for comparative studies,

are indicative and should be applied in normal conditions only. In the reliability analysis of a particular structure probabilistic models should be specified taking into account actual loading, structural conditions, and relevant experimental data. When considering the proposed models, the following remarks should be taken into account:

1. Actual variability of self-weight and other permanent loads may vary in the broad range from 0.03 up to 0.10; as a first approximation the permanent load may be described by the normal distribution having the mean $\mu_G = g_k$ and coefficient of variation $V_G = 0.1$.
2. 50-year maxima of the sustained imposed load may be described by the Gumbel distribution having the indicative mean $\mu_{p,50} = 0.6q_k$ and coefficient of variation $V_{Q50} = 0.35$ (for an office area of a middle size and middle level of action variability).
3. 50-year maxima of a wind action may be described by the Gumbel distribution having the indicative mean $\mu_{w50} = 0.7w_k$ and coefficient of variation $V_{w50} = 0.35$.
4. 50-year maxima of a snow load may be described by the Gumbel distribution having the indicative mean $\mu_{s50} = 1.1s_k$ and coefficient of variation $V_{s50} = 0.3$.
5. The probabilistic models for material properties and geometric data indicated in Table 1 correspond to a normal quality control.
6. Input data for a reliability analysis should always be carefully specified with respect to actual conditions of a structure.

ACKNOWLEDGEMENTS

The study has been conducted at the Klokner Institute, Czech Technical University in Prague, in the framework of the research project GA103/08/1527 Global safety formats for design of concrete structures, supported by the Czech Science Foundation. Results of the research project TA01031314 Optimisation of Safety and Reliability for Existing Bridges have been utilised.

REFERENCES

- EN 1990: 2002. *Eurocode - Basis of structural design*. Brussels: CEN.
- JCSS 2006. *JCSS Probabilistic Model Code*. Zurich: Joint Committee on Structural Safety.
- Turkstra, C.J. 1970. *Theory of Structural Design Decisions*, SM Studies Series No. 2. Ontario, Canada: Solid Mechanics Division, University of Waterloo.

Comparison of load combination models for probabilistic calibrations

M. Sykora & M. Holický

Czech Technical University in Prague, Klokner Institute, Prague, Czech Republic

1 INTRODUCTION

1.1 Motivation

Civil engineering structures are, as a rule, exposed to combinations of time-variant loads. Selection of an appropriate model for the load combination is one of the key issues of probabilistic calibrations of reliability elements in codes.

Models for load combinations are often based on the rule proposed by Turkstra (1970). Another widely used model is based on rectangular wave renewal processes with fixed durations of load pulses proposed by Ferry Borges & Castanheta (1971)—“FBC models”.

Alternatively random load fluctuations in time can often be described by rectangular wave renewal processes with random durations between renewals and random durations of load pulses. Such processes seem to be applicable for a wide range of loads on structures. In reliability analyses an upper bound on the failure probability is mostly used.

The paper is aimed at comparison of these techniques.

1.2 Basic assumptions

Basic variables used in the analysis include:

- Time-invariant resistance and geometry variables, permanent actions and model uncertainties,
- Time-variant actions $Q_i(t)$ such as climatic actions, imposed loads etc., that can be described by stationary, ergodic and regular processes.

2 GENERAL COMPARISON

General comparison of the considered approaches is provided focusing on differences among the approaches with respect to:

- Applicability of standard reliability methods available in commercial software products,
- Accuracy of the techniques for different combinations of intermittent and sustained loads,

- Derivation of partial factors of basic variables,
- Applicability in case of non-stationary conditions.

3 NUMERICAL EXAMPLE

3.1 Basis of analysis

The approaches are applied in probabilistic reliability analysis of representative steel portal frames designed according to Eurocodes. Intermittent snow load and always present wind action are considered. Models for the climatic loads and material properties are based on meteorological data for six locations in Germany and data collected from producers of rolled profiles, respectively.

3.2 Reliability analysis

Reliability index β obtained by the probabilistic analysis for the six locations is indicated in Figure 1. Two basic cases are distinguished:

1. Snow and wind loads are of comparable effects (particularly for Bremen, but also for Münster and Aachen): Turkstra’s rule rather overestimates reliability level. However, the differences between Turkstra’s rule and FBC models are small (up to 0.3 in terms of β). The upper bound for intermittent renewal processes is in some cases rather conservative (reliability index lower by about 0.1–0.4 compared to FBC models).
2. Snow is dominant (particularly for Braunlage): differences among the approaches are small since load combination aspects are insignificant.

Reliability index as a function of the load ratio χ (characteristic variable over characteristic total load effect) is shown in Figure 2 for Berlin.

It follows from Figure 2 that the difference between Turkstra’s rule and FBC models is insignificant, for the whole range of the load ratio up to 0.1. For $\chi < 0.4$ the upper bound becomes overly conservative (difference up to 0.8).

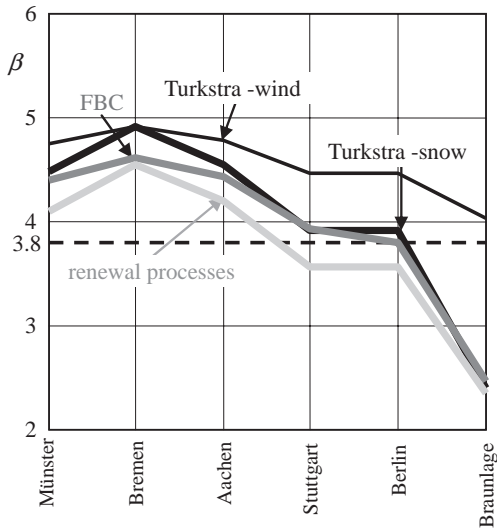


Figure 1. Reliability index for different locations.

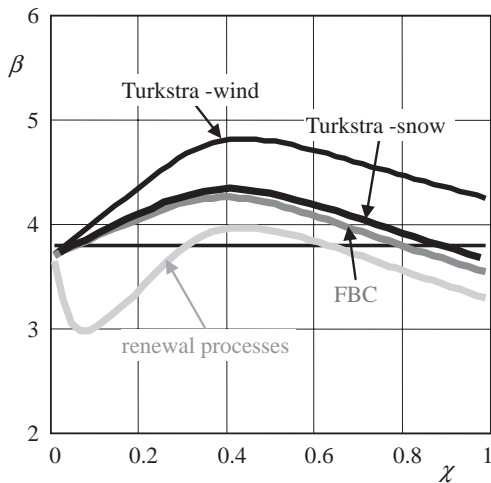


Figure 2. Reliability index as a function of χ (Berlin).

Partial factors of basic variables are then derived using the three approaches. It appears that for the time-invariant variables, Turkstra's rule and FBC models lead to nearly same partial factors while somewhat higher values are obtained for intermittent renewal processes. Different partial factors are estimated for time-variant loads; however, influence on design is insignificant.

4 CONCLUSIONS

Selection of an appropriate model for the load combination may be one of the key issues of

probabilistic calibrations. Comparison of the considered approaches indicates that:

1. Turkstra's rule:
 - Reliability can be assessed by any method for the time-invariant analysis.
 - The rule may lead to overestimation of an actual reliability, but the error is insignificant.
 - Estimation of partial factors is straightforward.
2. FBC models:
 - Analysis is usually based on the Rackwitz-Fiessler algorithm that may not be available in software products.
 - The exact solution is found if time-variant loads are well described by FBC models.
 - Estimation of partial factors may be complicated.
3. Intermittent renewal processes:
 - An upper bound on failure probability can be evaluated by any system reliability method; however, it is not available in software products.
 - Estimation of partial factors is straightforward if a dominant load case is identified.

Numerical example reveals that:

- Differences between Turkstra's rule and FBC models are insignificant,
- When time-invariant variables are dominant, the upper bound becomes conservative.
- Turkstra's rule rather overestimates significance of the leading action while intermittent renewal processes overestimate significance of time-invariant variables when time-invariant variables are dominant.

For common calibration studies, Turkstra's rule is recommended. Results can be verified by the analysis based on FBC models.

ACKNOWLEDGEMENTS

The study has been conducted at the Klokner Institute CTU within the project GACR 103/09/0693 Assessment of Safety and Risks of Technical Systems. Results of the project LG11043 Probabilistic Reliability and Risk Assessment of Structures have been utilised.

REFERENCES

- Ferry Borges, J. & Castanheta, M. 1971. *Structural Safety*, Course 101 (2nd ed.). Lisbon: Laboratorio Nacional de Engenharia Civil.
- Turkstra, C.J. 1970. *Theory of Structural Design Decisions*, SM Studies Series No. 2. Ontario, Canada: Solid Mechanics Division, University of Waterloo.

Calibration of partial factors for design of concrete structures

J. Marková & M. Holický

Klokner Institute CTU, Prague, Czech Republic

ABSTRACT: The Eurocodes are currently applied as exclusive standards for the design of structures in several CEN Member States including the Czech Republic. National choice of the Nationally Determined Parameters (NDPs) is specified in the National Annexes. Presently available information indicates that most European countries have accepted the values of partial factors and other reliability elements recommended in EN 1990 (2002) for the basis of structural design. About half of the countries accepted the expression A (6.10) for combinations of actions for verification of ultimate limit states (ULS of type STR) and others twin expressions B (6.10a,b). Both alternatives (6.10) or (6.10a,b) are also allowed to be applied in some countries including the Czech Republic. In few countries modified twin expressions C (6.10a,b) are used where in the first expression permanent actions are considered only. Moreover, alternative D is considered here where the partial factor of variable actions $\gamma_Q = 1 + \chi$ depends on the ratio χ between characteristic variable actions to total actions. This rule was partly applied for imposed loads in the Czech original standards for basis of structural design.

Some countries which preferred the twin expressions (6.10a,b) decided to increase the value of reduction factor ξ for non dominant permanent actions from the recommended value 0,85 up to 0,93 diminishing the difference in application of both alternative load combinations. Therefore, the reliability of structures designed according to the nationally implemented Eurocodes may differ from country to country what is allowed by EC as a matter of their national safety.

Combined effects of reliability differentiation provided in EN 1990 (2002) and reduced material factors recommended in EN 1992-1-1 (2004) are also analysed. Nationally selected parameters of some CEN Member States are taken into account. A reinforced concrete beam and a column exposed to permanent and two variable loads designed according to recommendations of Eurocodes are analyzed using probabilistic methods of structural reliability.

EN 1990 (2002) allows a design directly based on the probabilistic methods. In accordance with

the principles of these methods the basic variables are considered as random variables with appropriate distributions. It is verified that a limit state of a member is exceeded with a probability lower than the target value p_t

$$P(g(X) < 0) < p_t \quad (1)$$

where $g(X)$ denotes the limit state function, for which the inequality $g(X) < 0$ indicates that the limit state is exceeded. The condition (1) may be replaced by the inequality $\beta > \beta_t$, where β denotes the reliability index. EN 1990 (2002) recommends the target probability $p_t = 7,24 \times 10^{-5}$ corresponding to the reliability index $\beta_t = 3,8$ for 50 year design working life.

The limit state function of the reinforced concrete beam is based on equation (2) given as

$$g(X) = K_R (A_s f_s (h - a - 0,5 A_s f_y / (b \alpha_c f_c))) - K_E (G + Q + W) \quad (2)$$

and in the case of short column the limit state function is based on equation (3)

$$g(X) = K_R (A_s f_y + 0,8 A_c f_c) - K_E (G + Q + W) \quad (3)$$

The limit state functions (2) and (3) include coefficients of model uncertainty K_R and K_E , which take into account model uncertainty of resistance and action effects.

Probabilistic models of the basic variables are given in tables in full conference paper, based on materials of JCSS (2001) and previous research of the Klokner Institute (KI CTU).

Selected results of the reliability analysis of the beam are illustrated in Figures 1 to 3.

An effect of alternative load combination rules A to D of a beam is illustrated in Figure 1 for basic production quality.

Obviously the combination B leads to a better balanced reliability than the combination rule A. Combination B and newly proposed combination D are practically equivalent.

Combination C with parameters NDPs selected in some CEN countries where the value of partial factor for permanent load is $\gamma_G = 1, 2$ in exp. (6.10a_{mod}) and

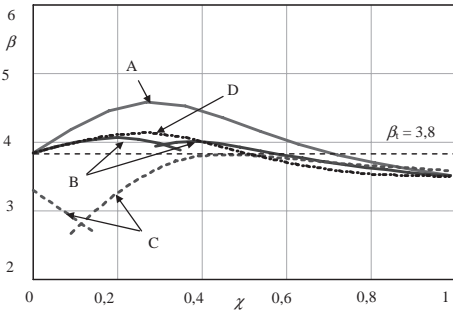


Figure 1. Variation of the reliability index β of the beam with the load ratio χ ($\rho = 1\%$), for the basic production quality and load combinations A to D.

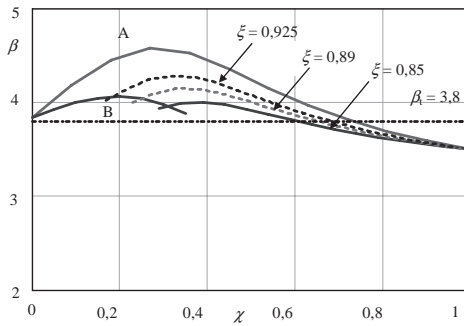


Figure 2. Variation of the reliability index β of the beam with the load ratio χ for the basic production quality and load combinations A and B (for $\xi = 0,85, 0,89$ and $0,925$).

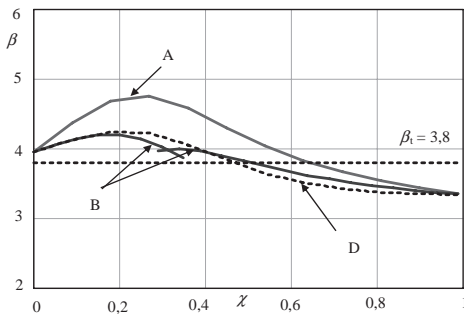


Figure 3. Variation of the reliability index β of the beam with the load ratio χ ($\rho = 1\%$), for the increased production quality and load combinations A, B and D.

$\gamma_G = 1,0$ in exp. (6.10b), for variable loads $\gamma_Q = 1, 5$, for concrete $\gamma_c = 1, 45$ and for reinforcement $\gamma_s = 1, 2$ leads to a rather low reliability level of the beam. It should be noted here that the target reliability accepted by these countries for the reliability class RC2 has been reduced and the reliability index $\beta_1 = 3, 3$ is considered only for structures in class RC2.

Figure 2 shows the significance of national decision concerning the value of reduction factor ξ in alternative B, exp. (6.10b), on the reliability of the beam which is approaching the alternative A.

Variation of the reliability index β of the beam with the load ratio χ ($\rho = 1\%$), increased production quality and load combinations A, B and D is shown in Figure 3.

Alternative rules for load combinations provided in EN 1990 (2002) may lead to considerably different reliability levels of designed structures. The most uniform distribution of reliability level is provided by the combination rule B (6.10a,b) or proposed combination rule D. The national selection of rule C leads to significantly low structural reliability level.

Alternative rules for load combinations provided in EN 1990 (2002) may lead to considerably different reliability levels of designed structures. The most uniform distribution of reliability level is provided by the combination rule B (twin expression (6.10a,b)), or proposed combination rule D. The national selection of combination rule C lead to a significantly low structural reliability level.

Reliability level of the beam designed with reduced partial factors recommended in EN 1992-1-1 (2004) for increased production quality appears to be lower for prevailing variable loads.

Reliability of reinforced concrete members depend on reinforcement ratio (the reliability of a beam increases with increasing reinforcement ratio while of a column decreases). The partial factors should be, therefore, adequately differentiated.

The load combinations and partial factors given in the present generation of Eurocodes should be further harmonised on the basis of calibration studies and analyses of nationally selected NDPs.

ACKNOWLEDGEMENT

This study is a part of the project No. 103/09/0693 Assessment of Safety and Risks of Technical Systems supported by GACR.

REFERENCES

- EN 1990, 2002. Basis of structural design. CEN. pp. 87.
- EN 1992-1-1. 2004. Design of concrete structures - General rules and rules for buildings. CEN. pp. 125.
- Holický M. & Retief J.V. 2008. Reliability assessment of alternative Eurocode and South African load combination schemes for structural design. *Journal of South African Institution of Civil Engineering*. Vol. 47.
- JCSS. 2001. Probabilistic model code. <http://www.jcss.ethz.ch>
- Marková, J. 2006. Reliability differentiation for design of reinforced concrete members. In: *Safety and Reliability for Managing Risk*, pp. 1511–1514.

Re-calibration of steel tension members design criteria in AASHTO LRFD bridge design code

Mehdi Mohseni & Terri R. Norton
 University of Nebraska-Lincoln, Omaha, NE, USA

ABSTRACT: Providing a reasonable balance between cost and safety of structures has always been the major concern in developing design codes and specifications. A more conservative design will enhance the structural safety along with increasing cost of the construction. Evidently, re-calibration of existing design criteria, even those with reliability analysis backbone is unavoidable due to numerous technical improvements and change in cost factors. In fact, the latest dependable experimental data for both load and resistant parameters should be considered for any re-evaluation of current design criteria. However, simplification of design equations offers more conservative criteria in most cases.

The objective of this study is re-calibrating steel tension members design criteria in AASHTO LRFD bridge design code based on the latest applicable load and resistance models.

Most predominant applying loads on highway bridges; dead load and live load (including dynamic effect) have been considered as random variables due to the uncertainty in the actual amount of each applied load. Table 1 shows utilized load models with their distribution functions and related random parameters based on the latest existing statistical data.

According to cumulative distribution functions for recorded vehicular dynamic load allowance, IM, for through trusses, deck trusses, and rigid steel frames, the average Coefficient of Variation (COV) is considerably larger than calculated COV for steel or concrete girders ($V = 1.25$ vs. $V = 0.71$ for steel girders and $V = 0.56$ for P/C AASHTO concrete girders). This high ratio of COV leads to

a lower reliability index for designed steel tension members rather than steel or concrete girders.

To develop resistance models for steel tension members both yielding and fracture failures are considered. Applied models in current study include discretization factor, d , in addition to material, M , geometry, G , and professional, P , factors:

$$R = GMPd \quad (1)$$

Table 2 illustrates latest suggested resistance parameters for steel tension members in yielding and fracture. Statistical parameters are based on collected data from thousands of tested steel products, made by major suppliers in North-America during 1999 and 2000.

According to AASHTO LRFD Bridge Design Code, the factored resistance, P_r shall be taken as the smallest value of the yield and fracture resistance of the section:

$$P_r = \phi_y F_y A_g \quad (2-a)$$

$$P_r = \phi_u F_u A_n U \quad (2-b)$$

where F_y and F_u are the yield and fracture strength of steel, A_g and A_n are the gross and net cross sectional area of the member, and U is the reduction factor due to the shear lag effect in connections. Resistance factors, ϕ_y and ϕ_u , insure a safer design by considering uncertainty of the predicted yield and fracture resistance of steel members.

Table 1. Load components random parameters.

Distribution function	DC	DW	LL	IM
	normal	normal	lognormal	lognormal
Bias factor	1.04	1.40	1.30	0.52
Coef. of var.	0.09	0.25	0.12	1.125

Table 2. Resistance statistical parameters.

Steel section	Yielding*		Fracture*	
	λ_R	V_R	λ_R	V_R
WWF	1.18	0.070	1.28	0.077
Rolled W	1.09	0.081	1.19	0.080
HSS (class C)	1.36	0.103	1.20	0.088
HSS (class H)	1.32	0.094	1.24	0.084

* For tested steel equivalent to M270/A702 Grade 50 ($F_y = 50$ ksi, $F_u = 65$ ksi).

To evaluate reliability of current AASHTO criteria, Monte-Carlo simulation technique has been employed in this study.

For yielding mode, where the failure is specifying a ductile behavior, a minimum reliability index equal to 3.0 has been chosen. However, higher target reliability should be taken for fracture mode due to undesired brittle failure. Considering target reliability index equal to 4.5, maintains the probability of fracture failure, securely low enough.

Figure 1 shows the reliability curves for yielding of Rolled W sections (with minimum β values) in current AASHTO code. In presented diagrams, horizontal axis shows the dead load to total load ratios, and vertical axis declares the calculated reliability index, β , for a specific section and different load modification factors, η . It was observed that steel sections with lower bias factor or higher coefficient of variation experience lower reliability indices. Based on analysis results, it is concluded that using current $\phi_y = 0.95$ is relatively conservative (minimum reliability indices in practical dead to live load ratios with $\eta = 1.0$ is around 3.5).

Similarly, Figure 2 demonstrates calculated reliability indices for Rolled W sections considering variation of load ratios and load modification factor, η . As it can be seen, effective minimum reliability index for sections is significantly less than target reliability index $\beta_r = 4.5$.

To increase existing reliability of fracture design equation, increasing nominal percentage of dynamic load allowance is examined up to 75%. Figure 3 shows new reliability curves for Rolled W sections with minimum values among all sections. This correction has modified reliability indices to a minimum reliability equal to 4.3 for shorter spans and about 5.3 for longer spans.

In conclusion, results of executed reliability analysis on current yield and fracture design

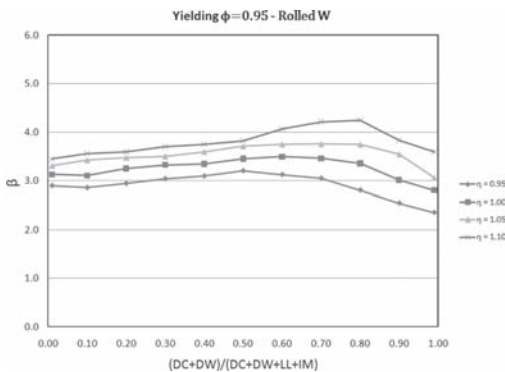


Figure 1. Reliability analysis results for yielding equation using current AASHTO criteria: Rolled W.

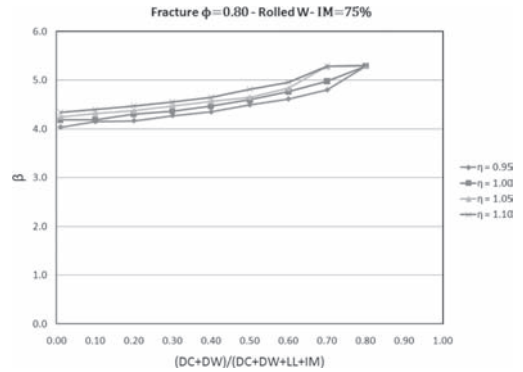


Figure 2. Average reliability indices for all four sections designed for fracture for corrected IM percentage (IM = 75%).

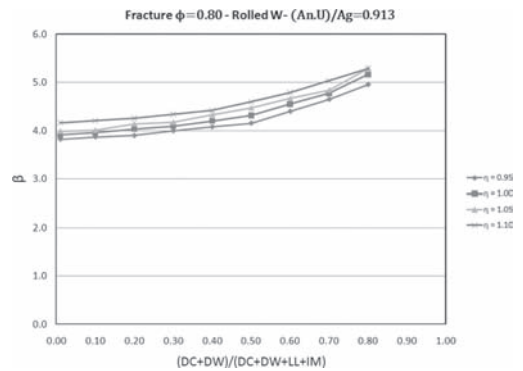


Figure 3. Reliability analysis results for fracture equation using current AASHTO criteria: Rolled W.

equations, validate a conservative design for yielding mode, while declare an unsafe performance of mentioned elements for fracture situation. Thus, by suggesting 75% nominal vehicular dynamic load allowance, instead of conventional 33% nominal value, the reliability indices are pushed up to $\beta = 4.3$. Also a new resistance factor for yielding of the gross section, $\phi_y = 1.00$, has been evaluated and suggested for design purposes.

MS_134 — Probabilistic calibration of codes (2)

This page intentionally left blank

Reliability basis for adopting Eurocodes as South African standards

J.V. Retief, C. Barnardo & M. Dithinde
 Stellenbosch University, Stellenbosch, South Africa

1 INTRODUCTION

The development and implementation of Eurocode EN 1990 as head standard for a unified approach in structural design and as basis for harmonisation of European practice represent the most recent demonstration of the utility of the principles of structural reliability.

The merit of accepting Eurocode as reference for the next generation of South African standards for structural design is generally accepted locally. Due to wide differences in construction, environmental and institutional conditions, such implementation of Eurocode requirements and procedures into South African standards is not a straightforward process. The only rational manner in which standards from elsewhere could be adopted, adapted and calibrated for a specific set of conditions is to base the process on the principles of structural reliability.

Various initiatives are in progress or have recently been completed in applying selected standards and parts of Eurocode as adopted or adapted South African standards. The paper describes the way in which calibration procedures are used to assess action combinations schemes and associated partial factors, and for structural resistance procedures with special reference to geotechnical design (Dithinde 2007), concrete and water retaining structures (Holický et al., 2009 & 2010).

2 FUNDAMENTAL RELIABILITY MODEL

2.1 Representation of reliability requirement

The reliability performance function $g(X)$ of the limit state is expressed as a function of the basic variables of resistance (R); permanent actions (G) and variable actions (Q) as follows:

$$g(X) = R - (G + Q) = 0 \quad (1)$$

FORM solutions of Equation (1) in terms of χ given in Equation (2) versus GSF given in

Equation (3); and characteristic values (X_k) for a given target level of reliability β_T can be expressed as the function $f\{GSF; \chi\}$.

$$\chi_{mean} = \frac{\mu_Q}{\mu_G + \mu_Q};$$

$$\chi_k = \frac{k_Q}{k_G(1 - \chi_{mean}) + k_Q \chi_{mean}} \chi_{mean} \quad (2)$$

$$GSF_{mean} = \frac{\mu_R}{\mu_G + \mu_Q};$$

$$GSF_k = \frac{k_R}{k_Q} \frac{\chi_k}{\chi_{mean}} GSF_{mean} \quad (3)$$

where μ_X represents the mean value of the basic variable X and $k_X = X_k / \mu_X$.

2.2 Basic case for South African practice

The probability models for basic variables used in calibrating SANS 10160-1989 are given in Table 1 (Kemp et al., 1987). These basic variables are used for the first assessment of revised procedures referenced to EN 1990. The target reliability $\beta_T = 3$ applies to South Africa (Milford 1988).

2.3 Design verification functions

The general expression for design verification related to Equation (1) is given in Equation (4), with the basic expression for γ_R given by Equation (5).

Table 1. Representative basic variables for South African conditions.

Variable X	Distribution	μ_X / X_k ($1 / k_X$)	V_X	p_k (%)
Permanent load G	Normal	1.05	0.10	68
Office floor Q	Gumbel	0.96	0.25	36
Resistance [5% characteristic]	Lognormal	[1.28]	0.15	[5]

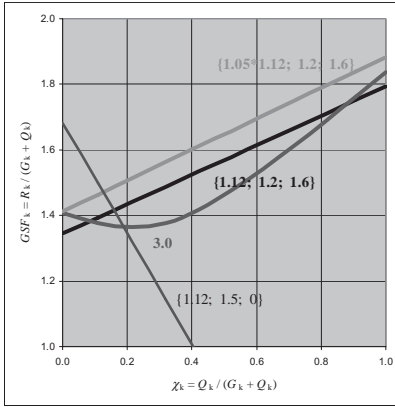


Figure 1. Comparison of SABS 0160-1989 design function to reliability requirement for office floor load and $\beta_T = 3$.

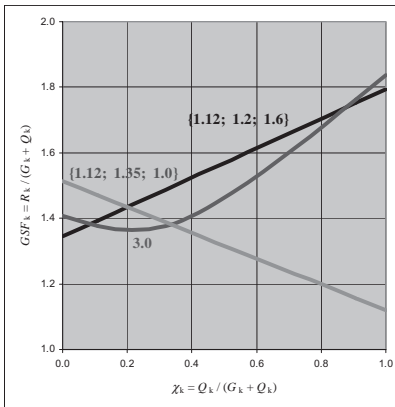


Figure 2. Comparison of SANS 10160-1:2010 design function to reliability requirement for office floor load and $\beta_T = 3$.

$$R_k / \gamma_R - (\gamma_G G_k + \gamma_Q Q_k) \geq 0 \quad (4)$$

$$\gamma_R = EXP(\alpha_R \beta_T V_R - 1.64 V_R) \quad (5)$$

where $\alpha_R = 0.8$ is the sensitivity factor for resistance.

The design function can then be compared to the reliability requirement for SABS 0160-1989, shown in Figure 1 and SANS 10160-1:2010 shown in Figure 2. In addition to $\gamma_R = 1.12$ from Equation (5), the effect of adjusting γ_R by a factor of 1.05 is also shown.

3 CONCLUSIONS

The general methodology presented here is to separately determine the reliability requirement for

structural performance and the design verification procedure. Such comparison provides a clear overall view of the efficiency of the design verification functions. The influence of the various partial factors can conveniently be inspected by the calibration procedure presented here.

Matching the advanced, comprehensive set of Eurocodes to the specific South African needs and conditions require careful assessment. The set of calibration exercises presented in this paper confirms the utility of using structural reliability as the basis for such transference, adoption or adaptation.

The more explicitly the design procedures are based on the principles of reliability, the easier it is to perform (re)calibration. Assessment of the procedures from EN 1990 was relatively straightforward. For EN 1992-1-1 it is more problematic, since the reliability based applications are imbedded in the procedures. For EN 1997 principles of reliability are not implemented explicitly at all, which is a complication in transferring standardised procedures.

Structural reliability not only provides a proper basis for the development of standards for structural design, but also enhances the degree of harmonisation and consistency that can be achieved, whilst allowing for calibration to very specific conditions of safety levels, the local economy and environmental conditions.

REFERENCES

- Dithinde, M. (2007). *Characterisation of model uncertainties for reliability-based design of piled foundations*. PhD Thesis, University of Stellenbosch.
- EN 1990:2002. Basis of structural design. European Committee for Standardization (CEN) Brussels.
- Holický, M., Retief, J. & Wium, J. (2009). *Probabilistic design for cracking of concrete structures*. Van Gelder, Proske & Vrijling (Editors): Proceedings 7th IPW, Delft, Netherlands. 25–26 November 2009.
- Holický, M., Retief, J.V. & Wium, J.A. (2010) Partial factors for selected reinforced concrete members: Background to a revision of SANS 10100-1. SAICE Journal, Vol. 52, No. 1.
- Kemp, A.R., Milford, R.V. & Laurie, J.A.P. (1987). Proposals for a comprehensive limit states formulation for South African structural codes. The Civil Engineer in SA 29 (9), 351–360.
- Milford, R.V. (1988). Target safety and SABS 0160 load factors. The Civil Engineer in South Africa, 30(10), 475–481.
- SABS 0160-1989. The general procedures and loading to be adopted in the design of buildings. SABS, Pretoria.
- SANS 10160-2010. Basis of structural design and actions for buildings and industrial structures. SABS, Pretoria. Part 1 Basis of structural design. Part 5 Basis for geotechnical design and actions.

Reliability-based design/calibration using enhanced Monte Carlo

A. Naess

Centre for Ships and Ocean Structures & Department of Mathematical Sciences,
 Norwegian University of Science and Technology, Trondheim, Norway

M.A. Maes & M.R. Dann

Department of Civil Engineering, University of Calgary, Calgary, Canada

1 INTRODUCTION

A new Monte Carlo (MC) based method for estimating system reliability was recently developed by Naess et al. (2009). The aim of this method is to reduce computational cost while maintaining the advantages of crude MC simulation, specifically, its ease in dealing with complex systems. The key idea is to exploit the regularity of tail probabilities to enable an approximate prediction of far tail failure probabilities based on small Monte-Carlo sample results obtained for much more moderate levels of reliability.

The fundamentals of the Naess et al. (2009) method are as follows. A safety margin $M = G(X_1, \dots, X_n)$ expressed in terms of n basic variables, is extended to a parameterized class of safety margins using a scaling parameter λ ($0 \leq \lambda \leq 1$):

$$M(\lambda) = M - (1 - \lambda)E(M) \quad (1)$$

The failure probability is then assumed to behave as follows:

$$p_f(\lambda) = \text{Prob}(M(\lambda) \leq 0) \underset{\lambda \rightarrow 1}{\approx} q(\lambda) \exp\{-a(\lambda - b)^c\} \quad (2)$$

where the function $q(\lambda)$ is slowly varying compared with the exponential function $\exp\{-a(\lambda - b)^c\}$. Clearly, the target failure probability $p_f = p_f(1)$ can be obtained from values of $p_f(\lambda)$ for $\lambda < 1$. It is easier to estimate the failure probabilities $p_f(\lambda)$ for $\lambda < 1$ accurately than the target value itself, since they are larger and hence require less simulations. Fitting the parametric form (2) for $p_f(\lambda)$ to the estimated values would then allow us to provide an estimate of the target value by extrapolation. The viability of this approach is demonstrated by both analytical and numerical examples in Naess et al. (2009) and Naess et al. (2010).

2 USING ENHANCED MONTE CARLO TO OPTIMIZE A DESIGN PARAMETER

A general situation, typical in the context of calibration of design specifications, consists of having the safety margin controlled by a design check function $c(x_{1c}, x_{2c}, \dots, x_{nc}, \alpha)$ involving characteristic values x_{ic} of each basic variable X_i , and where α acts as a design factor which “controls” the reliability of the structure or component. Admissible designs are such that $c(\alpha) \geq 0$. Minimal acceptable designs are marked by $c(\alpha) = 0$, an assumption which is made throughout this paper. Often the design check function c is selected to be the same mathematical function as G but this is not required—all that matters is that the resulting safety margin $M(\alpha) = G(X_1, \dots, X_n | c(x_{1c}, \dots, x_{nc}, \alpha) = 0)$ is monotonic with respect to α in its approach to the target α_T . Hence the objective is to determine α_T as follows:

$$\alpha_T: \text{Prob}(G(X_1, \dots, X_n | c(x_{1c}, \dots, x_{nc}, \alpha) = 0) \leq 0) = p_{fT} \quad (3)$$

Typically now p_{fT} is a very small target probability and hence the behavior of p_f as a function of α is similar to a deep tail estimation problem so that it is reasonable to assume that:

$$p_f(\alpha) \underset{\alpha \rightarrow \alpha_T}{\approx} q(\alpha) \exp\{-a(\alpha - b)^c\} \quad (4)$$

where $q(\alpha)$ is slowly varying compared to the exponential expression. This function is used for optimized fitting and prediction of α_T .

3 EXAMPLE: COMPONENT LOAD FACTOR CALIBRATION

The example in the following two sections all have simple explicit limit state functions in terms of the

basic random variables. The computational issue is therefore minor and no effort has been made to investigate the possibility of implementing more effective sampling strategies. If the proposed method were to be used in combination with computationally demanding procedures involving e.g. a FE method for calculating the sample, it would be necessary in general to use more effective sampling strategies than the brute force procedure used here.

In this first example, the 10-bar truss structure shown in Figure 1 is studied. An enhanced Monte-Carlo reliability analysis of this truss is given in Naess et al. (2009). Here a load factor for a transversal load P is calibrated in order to achieve a target reliability of $(1 \cdot 10^{-6})$ with respect to the horizontal sway of the truss. The ten truss members are cut from three different aluminum rods with cross-sectional areas A_1 , A_2 and A_3 , as shown in Figure 1.

The structure is subjected to external loads P as shown in Figure 1. The horizontal displacement D at the upper right hand corner of the truss structure can be written as:

$$D(A_1, A_2, A_3, B, E, P(\alpha)) = \frac{BP(\alpha)L}{A_1A_3E} \times \left\{ \frac{4\sqrt{2}A_1^3(24A_2^2 + A_3^2) + A_3^3(7A_1^2 + 26A_2^2)}{D_T} + \frac{4A_1A_2A_3 \frac{20A_1^2 + 76A_1A_2 + 10A_3^2}{D_T}}{4\sqrt{2}A_1A_2A_3^2 \frac{25A_1 + 29A_2}{D_T}} \right\} \quad (5)$$

where $D_T = 4 A_2^2(8 A_1^2 + A_3^2) + 4\sqrt{2} A_1A_2A_3(3A_1 + 4A_2) + A_1A_3^2(A_1 + 6A_2)$ and E is Young's modulus. The random variable B accounts for model uncertainties. It is assumed that A_1 , A_2 , A_3 , B , P , E are independent basic random variables. Their properties are summarized in Table 1. Also shown

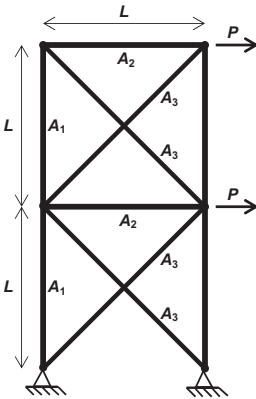


Figure 1. Ten-bar truss structure.

Table 1. Basic variables.

	Mean value	COV	Probability distribution	Characteristic value in (21)
A_1	$1.0 \cdot 10^{-2} \text{ m}^2$	0.05	Normal	1% quantile
A_2	$1.5 \cdot 10^{-3} \text{ m}^2$	0.05	Normal	1% quantile
A_3	$6.0 \cdot 10^{-3} \text{ m}^2$	0.05	Normal	1% quantile
B	1.0	0.10	Normal	Mean
E	$6.9 \cdot 10^4 \text{ MPa}$	0.05	Lognormal	1% quantile
P	based on (21)	0.10	Gumbel	95% quantile
d_0	0.1 m	—	—	—
L	9.0 m	—	—	—

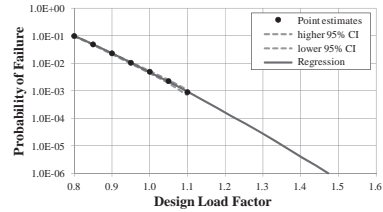


Figure 2. Sample size 10^5 —weighted regression.

are the characteristic values used in the design check Equation (7).

The safety margin

$$M(\alpha) = d_0 - D(A_1, A_2, A_3, B, E, P(\alpha)) \quad (6)$$

and the design check constraint is

$$c(\alpha) = d_0 - D(A_{1c}, A_{2c}, A_{3c}, B_c, E_c, \alpha P_c(\alpha)) \quad (7)$$

where α represents the transversal load factor.

Figures 2 show the optimized fitted parametric curve to the empirical data in a log plot for sample size 10^5 . Applying the proposed procedure with a sample of size 10^5 gives the estimated value of $\alpha_T = 1.47$ with a 95% confidence interval (1.46, 1.48). CPU time 40 seconds on a standard laptop computer.

A crude Monte Carlo simulation using $3 \cdot 10^9$ samples verifies that $\alpha_T = 1.46$ for $p_{Tc} = 10^{-6}$ to within 2.5% at 95% confidence. This requires a computation time of about 24h on a laptop computer.

REFERENCES

- Naess, A., Leira, B.J. & Batsevych, O. 2009. System reliability analysis by enhanced Monte Carlo simulation. *Structural Safety*, 31: 349–355.
- Naess, A., Leira, B.J. & Batsevych, O. 2010. Efficient Reliability Analysis of Structural Systems with a high Number of Limit States”, *Proc. 29th International Conference on Ocean, Offshore and Arctic Engineering*, Paper no. OMAE2010-21179, Shanghai, China, 2010.

Calculation of partial safety factors

T.T. Poutanen

Tampere University of Technology, Tampere, Finland

1 INTRODUCTION

The current calculation of structural reliability is undetermined. The calculation is based on independent combination EN 1990 (2002), Gulvanessian et al. (2002), Ranta-Maunus et al. (2001), but loads are sometimes combined without a combination factor i.e. dependently. The author has explained earlier, Poutanen (2010a,b), that the loads are dependent.

This paper set out two methods: a normalized convolution equation method and a quantile sum method of calculating the safety factors dependently. As a comparison, a convolution equation method is presented to calculate the safety factors independently. The present independent calculation is unsafe, i.e. the design reliability is less than the target reliability, and the partial safety factors are too small.

Usually the safety factors are calculated indirectly through a reliability index β . It is not needed in the calculation explained here and therefore the conceptual error of the reliability index is avoided.

The eurocode is used here as a model code and the basic assumptions are selected equal to this code except for the independent loads.

1.1 Setting the basic parameters

The basic distribution parameters $\mu_G, \sigma_G, \mu_Q, \sigma_Q, \mu_M, \sigma_M$ are obtained from the actual distribution functions, the coefficients of variation and the design point. The parameters of the failure state are obtained by multiplying or dividing these distributions with the safety factors.

2 CONVOLUTION METHOD

The convolution equation is the basic equation to combine distributions. It is needed here to combine two loads and to combine the load and the material property. A convolution equation makes a combination of independent distributions. The load and the material property are independent and the normal convolution equation can be used. However, the loads must be combined dependently. The author has explained, Poutanen

(2010a,b), that the combination load distribution crosses the crossing point of the partial load distributions. Therefore the combination distribution based on the convolution equation must have alteration called here normalization. It means that the deviation obtained from the convolution equation is changed so that the combination distribution crosses the crossing point of the partial distributions.

3 QUANTILE SUM METHOD

As the Monte Carlo method is used to combine dependent loads, one seed number is given to all loads, i.e. the combination distribution is obtained by adding up the partial distributions by quantiles. It stipulates us to convert this idea to an analytic form. The load G and Q are combined by adding up the quantile values of the partial loads.

4 MATERIAL FACTORS OF THE EUROCODE

This example deals with the material safety factors γ_M at a base case of the eurocode: The material safety factors γ_M are presented in Figure 1 as a

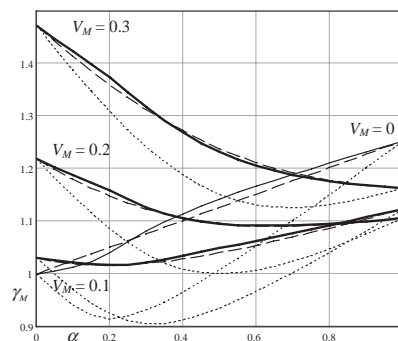


Figure 1. Material safety factors γ_M , as the coefficient of variation V_M is 0, 0.1, 0.2 and 0.3. Solid lines apply dependent combination calculated by using the deviation method, dashed lines apply quantile sum calculation, dotted lines denote independent combination according to the current hypotheses.

function of the load ratio α , assuming that all variability is included in the listed variability values. The solid lines apply to dependent calculation based on the deviation normalization. The dashed lines apply to the values calculated by the quantile sum method and the dotted lines to independent combination.

The factors γ_M are assumed constant in current codes, i.e. these curves are assumed horizontal. Thus the the current codes have a considerable textural variation.

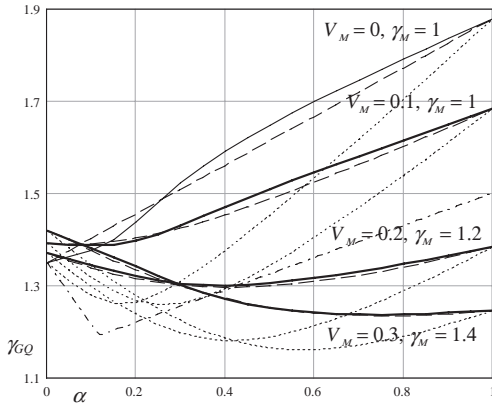


Figure 2. Load safety factors γ_{GQ} , as a function of load ratio α (variable load to all loads) in four materials: ideal material, $V_M = 0$; steel, $V_M = 0.1$; glue lam, $V_M = 0.2$ and sawn timber, $V_M = 0.3$, solid lines denote dependent combination with deviation normalization, dashed lines quantile sum calculation; dotted lines independent calculation according to the current hypotheses; the dash-dotted line denotes the load factor γ_{GQ} of the current Finnish eurocode.

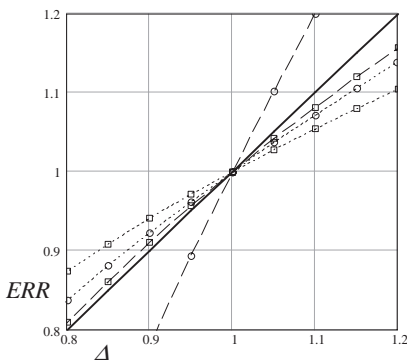


Figure 3. Error, ERR , in the design equation is equal to the error Δ in the safety factor as shown by the solid straight line. Other lines denote the reliability index β . Dashed lines denote permanent load and dotted lines variable load. The circled lines denote $V_M = 0.1$ values and boxed ones $V_M = 0.3$ values.

5 LOAD FACTORS OF THE EUROCODE

γ_M -values were calculated above when γ_G and γ_Q are fixed. In this example, we do the opposite and calculate the γ_{GQ} -values, presented in Figure 2, as γ_M -values are fixed.

6 RELIABILITY INDEX

The safety factor is a good reliable criterion for assessing the error of the calculation. The reliability index is often used for this purpose but it includes a bias which is demonstrated in Figure 3.

7 CONCLUSIONS

Four conclusions can be drawn:

The safety factors γ_G , γ_Q , and γ_M are wrongly calculated when the action consists of two (or more) partial loads, as the loads are assumed independent but should be calculated dependently. Due to this error the total reliability is up to ca 20% too small.

The combination rules 6.10a,mod and 6.10a,b of EN 1990 (2002) have two safety factors for the permanent load γ_G which result from independent load combination. Therefore, these combination rules should be deleted.

The reliability index β estimates the design error wrongly outside the target safety. Therefore this index should be used carefully.

A safety factor moves the implied distribution from the location defined by the design point to an appropriate location. The design point value may be selected in a way the distribution is in the appropriate location and the safety factor is not needed.

REFERENCES

EN 1990. 2002. Eurocode – Basis of structural design.
 Gulvanessian H., Calgareo J-A. & Holicky M. 2002. *Designer's Guide to EN 1990, Eurocode: Basis of structural design*, Thomas Telford Publishing Ltd, London.
 Ranta-Maunus A., Fonselius M., Kurkela J. & Toratti T. 2001. *Reliability analysis of timber structures*, VTT research notes 2109, Espoo, Finland.
 Poutanen T. 2010a. *Safety factors and design codes*, Joint IABSE – fib Conference, Dubrovnik, Croatia, May 3–5, 2010.
 Poutanen T. 2010b. *Dependent versus independent loads in structural design*, CIB-W18/43–101–1, Nelson, New Zealand, October 23–26, 2010.

*MS_214 — Probabilistic methods for the assessment
of existing concrete structures (1)*

This page intentionally left blank

Corrosion-crack path based probabilistic model to predict the durability behavior of RC components

W.L. Jin

Institute of Structural Engineering, Zhejiang University, Hangzhou, China

X.Z. Wang

Hanjia design group Co., Ltd., Hangzhou, China

Institute of Structural Engineering, Zhejiang University, Hangzhou, China

ABSTRACT: Taking account to the stochastic and time-dependent behaviors of existing concrete structures in service environment, an improved Path Probability Model (PPM) is established to predict the process of corrosion, crack and load capability degradation of existing reinforced concrete structures with time. The time-dependent probability distribution of reinforcement corrosion ratio, crack width and load capability loss of RC concrete in carbonation, chloride penetration or coupling-effect environment can be simulated effectively by numerical calculation. Therefore

it enable the computer simulation of the whole deterioration process of RC element from harmful mediums erosion, corrosion initiation of reinforcement, corrosion induced concrete crack and load capability reduction. Behavioral parameters involve percentage of corroded steel samples, steel corrosion ratio, area percentage of cracked concrete, and crack width and load capability reduction factor. These prediction results are proved reasonable and effective by statistics information from field data of existing concrete structures.

Random fields for the modeling of deteriorated structures

D.L. Allaix, V.I. Carbone & G. Mancini

Department of Structural and Geotechnical Engineering, Politecnico di Torino, Torino, Italy

ABSTRACT: The assessment of existing structures is generally a complex task, due to the uncertainties related mainly to the deterioration processes and the consequent mechanical behaviour. When dealing with reinforced concrete structures subject to corrosion of the reinforcement, the prediction of the evolution of the safety level is very important for the planning of maintenance and repair interventions.

Clearly, the effectiveness of these interventions depends on the analytical models adopted for the prediction of the time dependent corrosion of reinforcement and the probabilistic models of the model parameters.

Therefore it is necessary to develop a model which describes several aspects, including, the transport mechanisms of chlorides into the concrete cover, the on-set of corrosion and the development in time of the structural effects of corrosion.

Models for the prediction of the initiation of corrosion due to chloride ingress are available in literature, describing the problem from the analytical (Boddy et al., 1999, Kassir & Ghosn 2002, Luping & Gulikers 2007) and numerical point of view (Zhao et al., 1994, Martín-Pérez et al., 2001, Shim, 2002).

Guidance for the description of the randomness of the material and environmental parameters involved in the diffusion process has been also developed (Lay & Schießl 2003, fib 2006). Extensive research has been conducted in order to estimate the effect of the randomness of the main parameters (i.e. diffusion coefficient, surface chloride concentration and depth of the concrete cover) on corrosion initiation (Tikal'sky et al., 2005, Val & Trapper 2008, Ann et al., 2009).

Hence the structural effects of corrosion (Geocisa & Torroja Institute) have to be described in probabilistic terms.

The paper is focused on the probabilistic analysis of the effects of the corrosion process, when the spatial variability of the relevant parameters is considered. The attention is also focused on the random field models and their application for the assessment of the existing structures. For the purpose, a numerical discretization procedure based on Karhunen-Loeve series expansion and the finite element method is applied (Allaix & Carbone 2010).

The ingress of chlorides into the concrete structure is modeled by a 2D numerical model, which takes into account the point to point variability of material properties and environmental conditions.

Then, the effect of corrosion in terms of reduction of the mechanical properties of the reinforcing steel and cracking and spalling of the concrete cover are investigated.

REFERENCES

- Allaix, D.L. & Carbone, V.I. 2010. Numerical discretization of stationary random processes. *Probabilistic Engineering Mechanics*, 25: 332–347.
- Ann, K.Y., Ahn, J.H. & Ryou, J.S. 2009. The importance of chloride content at the concrete surface in assessing the time to corrosion of steel in concrete structures. *Construction and Building Materials*, 23: 239–245.
- Boddy, T., Bentz, E., Thomas, M.D.A. & Hooton, R.D. 1999. An overview and sensitivity study of multi-mechanistic chloride transport model. *Cement and Concrete Research*, 29: 827–837.
- Fib 2006. Model code for service life design. *Fib bulletin* 34.
- Geocisa & Torroja Institute. A validated users manual for assessing the residual service life of concrete structures, Innovation project CONTECVET (IN309020I).
- Kassir, M.K. & Ghosn, M. 2002. Chloride-induced corrosion of reinforced concrete bridge decks. *Cement and Concrete Research*, 32: 139–143.
- Lay, S. & Schießl, P. 2003. Service life models. *Life Cycle Management of Concrete Infrastructures for Improved Sustainability LIFECON*.
- Luping, T. & Gulikers, J. 2007. On the mathematics of time-dependent apparent chloride diffusion coefficient in concrete. *Cement and Concrete Research*, 37: 589–595.
- Martín-Pérez, B., Pantazopoulou, S.J. & Thomas, M.D.A. 2001. Numerical solution of mass transport equations in concrete structures. *Computers & Structures*, 79: 1251–1264.
- Tikal'sky, P.J., Pustka, D. & Marek, P. 2005. Statistical variations in chloride diffusion in concrete bridges. *ACI Structural Journal*, 102: 481–486.
- Val, D.V. & Trapper, P.A. 2008. Probabilistic evaluation of initiation time of chloride-induced corrosion. *Reliability Engineering and System Safety*, 93: 364–372.
- Zhao, C., Xu, T.P. & Valliappan, S. 1994. Numerical modelling of mass transport problems in porous media: a review. *Computers & Structures*, 53: 849–860.

Semi-probabilistic models for the assessment of existing concrete structures

P. Tanner, C. Lara & M. Prieto

Instituto Eduardo Torroja de Ciencias de la Construcción (IETcc-CSIC), Madrid, Spain

1 INTRODUCTION

The rules set out in the Spanish Technical Building Code (CTE 2006) for the evaluation of existing structures establish a framework for general assessment. They envisage a phased procedure in which the accuracy of resistance models and models simulating the effect of actions from phase to phase is enhanced by improving design assumptions through updates of the initial general data.

The most accurate way to find actual load and resistance would be to conduct a probabilistic analysis using site data. This is a time-consuming process, however, calling for a working knowledge of probabilistic methods, that may not be suited to everyday use by practising engineers. A simplified semi-probabilistic method for safety assessment should therefore be developed. This method should be based on the same partial factor formulation as adopted in structural design codes, in which the representative values for the variables and the partial factors can be modified on the basis of updated information.

While the (CTE 2006) procedure formally includes such an assessment method, the lack of any specific information in the code on the aforementioned modifications limits its applicability. The present study therefore aims to develop tools for the safety assessment of existing sound and deteriorated concrete structures using semi-probabilistic calculations.

2 DEVELOPMENT OF PRACTICAL TOOLS

The issues that must be addressed to develop tools for assessing the safety of existing sound concrete structures with semi-probabilistic calculations include:

- The state of uncertainty associated with the rules set out in the existing structural design standards;
- The level of reliability implicitly required in such standards;

- The effect of altering the variables studied on structural reliability for more effective information update planning;
- The combination of test results and prior knowledge;
- The effect of the updated information on the semi-probabilistic models used for assessment.

The proposed application of semi-probabilistic tools designed for the safety assessment of sound reinforced concrete (RC) structures to the assessment of corrosion-deteriorated structures requires addressing two additional tasks:

- The quantification of the uncertainties associated with the resistance models for corrosion-deteriorated RC structures;
- The analysis of the effect of these uncertainties on structural reliability and the semi-probabilistic models used for assessment.

3 WORK DONE

3.1 *Uncertainties and reliability associated with design rules*

In the approach adopted in this paper, the level of reliability required is equivalent to the reliability associated with structures that are strictly compliant with the structural safety requirements set out in the Spanish codes on the basis of design, actions on structures and resistance of RC structures. A procedure was therefore established to determine the probabilities of failure implicitly accepted by Spanish standards governing the design of building structures (Tanner et al., 2007). The survey involved selecting a series of hypothetical but realistic standard structural elements (roof girders, floor beams and columns) made from different constituent materials. For RC members, for instance, such a set consisted of 240 roof girders, 450 floor beams and 22320 columns. All these members were strictly designed to code rules and analyzed for reliability. The 5% fractile of the reliability index obtained for roof and floor concrete beams, as well as for columns, may

be regarded to be the level of reliability implicitly required by the codes presently in place.

3.2 Combination of information

A simple approach based on Bayesian statistics is proposed for combining prior information on the variables involved in the assessment of existing RC structures with empirical findings. A phased procedure is defined to determine the predictive distributions and updated distribution parameter values for the action and resistance variables for which prior distributions were deduced by (Tanner et al., 2007).

3.3 Updated models

Updating information about a variable by gathering site-specific data to reduce the associated uncertainties affects both the characteristic value of the variable considered and the respective partial factor. The effect of this change of information on the characteristic value can be deduced by applying statistical methods to the experimental results found and using any previously available information (section 3.2). Partial factors are represented in terms of the coefficients of variation of the associated variables to estimate how they are impacted by the change in information on these variables. By way of example, Figure 1 shows the partial factor for reinforcing steel resistance, γ_s , versus the coefficient of variation for reinforcement tensile strength, $V_{F_{ys}}$.

3.4 Application of updated semi-probabilistic models

The procedure for applying site-specific semi-probabilistic models can be divided into the six steps listed below:

1. Statistical evaluation of the data gathered.
2. Combination of test results and prior information.
3. Determination of the updated parameters for the probability density function.
4. Calculation of the coefficient of variation for variables whose uncertainties are reflected in the partial factors to be updated.
5. Determination of the updated partial factor as a function of the associated updated coefficient of variation.
6. Verification of structural reliability with updated semi-probabilistic models.

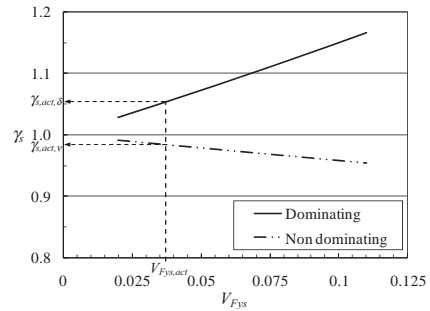


Figure 1. Partial factor for reinforcing steel resistance, γ_s , versus the coefficient of variation for reinforcement tensile strength, $V_{F_{ys}}$.

3.5 Corrosion-damaged structures

In general, structural resistance may be described by models comprising three types of variables, respectively addressing the dimensions of the members and their derived quantities, the relevant properties of the constituent materials, and the uncertainties associated with the resistance models applied. Structural reliability depends on all these variables. The main effects of the corrosion of steel bars in reinforced concrete (RC) structures are known and may be quantified, and models for estimating the residual load bearing capacity of corrosion-damaged structures are described in the literature (Contecvet 2001). No information is available, however, on the uncertainties associated with such models. On the basis of test results from the literature (Rodriguez et al., 1995), the probabilistic parameters for model uncertainty variables are deduced for simplified models used to find the bending capacity of RC beams with corroded reinforcement bars. Their effect on the reliability of such members is also discussed.

REFERENCES

- Contecvet 2001. *A validated Users Manual for assessing the residual service life of concrete structures*. EC Innovation Program IN309021.
- CTE 2006. *CTE DB-SE. Código Técnico de la Edificación. Documento Básico: Seguridad Estructural*. Madrid: Ministerio de Vivienda.
- EN 1990:2002. *Eurocode—Basis of structural design*, Brussels: European Committee for Standardization, CEN.
- Rodriguez, J., Ortega, L.M. & Casal, J. 1995. *Relation between corrosion and load bearing capacity on concrete beams*. Brite Euram Project BREU-CT-0591.
- Tanner, P., Lara, C. & Hingorani, R. 2007. *Seguridad estructural. Una lucha con incertidumbres. Hormigón y Acero*, No. 245, pp. 59–78, Madrid, ISSN 0439-5689.

Target reliability levels for assessment of existing structures

M. Sykora, M. Holický & J. Marková

Czech Technical University in Prague, Klokner Institute, Prague, Czech Republic

1 INTRODUCTION

At present existing structures are mostly verified using simplified deterministic procedures based on the partial factor method commonly applied in design of new structures. Such assessments are often conservative and may lead to expensive repairs. More realistic verification of actual performance of existing structures can be achieved by probabilistic methods when uncertainties of basic variables are described by appropriate probabilistic models.

Specification of the target reliability levels is required for the probabilistic assessment of existing structures. In addition the target reliabilities can be used to modify the partial factors for a deterministic assessment. It has been recognised that it would be uneconomical to specify for all existing structures the same reliability levels as for new structures.

The target reliability levels recommended in EN 1990 (2002) and ISO 13822 (2003) are related to consequences of failure only. More detailed classification is given in ISO 2394 (1998) where relative costs of safety measures are also taken into account. The target reliability levels provided in these documents are partly based on calibrations to previous practice and should be considered as indicative.

ISO 13822 (2003) indicates a possibility to specify the target reliability levels by optimisation of the total cost related to an assumed remaining working life. The submitted paper attempts to apply this approach for existing structures.

2 OST OPTIMISATION

According to Ang & De Leon (1997) the underlying economics is of concern and importance in the upgrading of existing structures. From an economic point of view, the objective may be to minimise the total working-life cost.

Based on previous studies concerning existing structures, the expected total costs C_{tot} may be generally considered as the sum of the expected costs of inspections, maintenance, repairs and costs related to failure of a structure. The decision parameters

to be optimised in the assessment may influence resistance, serviceability, durability, maintenance, inspection, repair strategies etc.

3 REQUIREMENTS ON HUMAN SAFETY

The cost optimisation is aimed to find the optimum decision from the perspective of an owner of the structure. However, society commonly establishes limits for human safety. Steenbergen & Vrouwenvelder (2010) proposed to consider the acceptable maximum probability to become a victim of structural failure approximately 10^{-5} per year and derived the target reliability indices to assure minimum human safety. This procedure is adopted in the present study, but the acceptable maximum probability to become a victim of structural failure is here considered as 10^{-6} per year in accordance with ISO 2394 (1998).

4 NUMERICAL EXAMPLE

Application of the optimisation procedure is illustrated by the example of reliability assessment of a generic member of the existing building with the remaining working life $t_r = 15$ or 30 years, assuming moderate costs of safety measures and moderate failure consequences. The probabilistic models of basic variables recommended by JCSS (2006) are applied in the reliability analysis.

To derive generally applicable target reliability levels indicating whether the structure should be repaired or not, the limiting value of d_{olim} of the rate d_0 (resistance before repair over resistance required by Eurocodes) is found from the following relationship:

$$E[C_{\text{tot}}'(d_{\text{olim}}, t_r)] = E[C_{\text{tot}}''(d_{\text{opt}}, t_r)] \quad (1)$$

where C_{tot}' = total costs in case of no repair; C_{tot}'' = total costs in case of repair; and d_{opt} = optimum value of decision parameter d (resistance after repair over resistance required by Eurocodes) minimising the total cost C_{tot}'' . For $d_0 < d_{\text{olim}}$ the reliability level of an existing structure is too low and the decision is to repair

Table 1. Overview of target reliabilities for the considered structure.

Code, method	Remaining 15 years	working life 30 years
EN 1990	4.1	4.0
ISO 13822	3.8	3.8
ISO 2394	3.1	3.1
Optimisation β_0	3.3	3.1
Optimisation β_1	3.5	3.5

the structure as the optimum repair strategy yields a lower total cost. For $d_0 > d_{0\text{lim}}$ the present state is accepted from an economic point of view.

The minimum acceptable reliability index is:

$$\beta_0 = \max [\beta(d_{0\text{lim}}, t_r); \beta_{\text{hs}}(t_r)] \quad (2)$$

where $\beta(\cdot)$ = reliability index; and $\beta_{\text{hs}}(\cdot)$ = reliability index for minimum human safety.

When the repair is necessary (actual reliability index is less than β_0), the total cost C_{tot} is optimised and the optimum value d_{opt} and optimum reliability index are found:

$$\beta_1 = \max [\beta(d_{\text{opt}}, t_r); \beta_{\text{hs}}(t_r)] \quad (3)$$

Table 1 provides a comparison of the target reliabilities estimated for the considered structure using different procedures in structural codes, or based on the total cost optimisation and the requirements on human safety. A great scatter is observed, for instance for $t_r = 15$ years, the reliability index varies within the range from 2.5 to 4.1. It should be noted that EN 1990 (2002) recommends considerably greater values that seem to be applicable primarily for new structures. Also ISO 13822 (2003) provides a rather high reliability level. ISO 2394 (1998) indicates values similar to the target reliability levels obtained by the optimisation concerning the decision on repair of a structure (β_0).

5 CONCLUSIONS AND RECOMMENDATIONS FOR STANDARDISATION

The following conclusions may be drawn from the present study:

- It is uneconomical to require all existing structures comply fully with the target reliability levels for new structures. Lower target reliability levels can be used if they are justified on the basis of social, cultural, economical, and sustainable considerations,
- Decisions in the assessment can result in acceptance of an actual state or in the repair of a structure; two target reliability levels are thus needed—the minimum level below which the

structure is unreliable and should be repaired (β_0), and the level indicating an optimum repair strategy (β_1).

- The probabilistic cost optimisation provides useful background information for specification of these levels,
- In the optimisation the total failure consequences including direct and indirect consequences should be taken into account,
- Minimum levels for human safety should not be exceeded,
- The target reliability levels are primarily dependent on the failure consequences and on the marginal cost per unit of a decision parameter; repair costs independent of the decision parameter and remaining working life are less significant.

The results of this study may be implemented in practical design using the partial factor method as follows:

- The characteristic values of the basic variables including time-variant loads remain independent of the remaining working life (in accordance with EN 1990 (2002));
- The design values are specified on the basis of an appropriate reliability index assessed for relevant costs of safety measures and failure consequences,
- The partial factors are determined considering specified design values and unchanged characteristic values of basic variables.

ACKNOWLEDGEMENTS

The study has been conducted at the Klokner Institute, Czech Technical University in Prague, in the framework of the research project GACR 103/09/0693. Results of the research project COST OC08059 have been utilised.

REFERENCES

- Ang, A.H.S. & De Leon, D. 1997. Determination of optimal target reliabilities for design and upgrading of structures. *Structural Safety* 19(1): 91–103.
- EN 1990: 2002. *Eurocode - Basis of structural design*. Brussels: CEN.
- ISO 13822: 2003. *Bases for design of structures - Assessment of existing structures*. Geneva: ISO TC98/SC2.
- ISO 2394: 1998. *General principles on reliability for structures*. Geneva, Switzerland: ISO.
- JCSS 2006. *JCSS Probabilistic Model Code*. Zurich: Joint Committee on Structural Safety.
- Steenbergen, R.D.J.M. & Vrouwenvelder, A.C.W.M. 2010. Safety philosophy for existing structures and partial factors for traffic loads on bridges. *Heron* 55(2): 123–139.

*MS_224 — Probabilistic methods for the assessment
of existing concrete structures (2)*

This page intentionally left blank

Monitoring and influence lines based performance indicators

A. Strauss, R. Wendner & K. Bergmeister

Institute of Structural Engineering, University of Natural Resources and Life Sciences, Vienna, Austria

Dan M. Frangopol

Lehigh University, Bethlehem, PA, USA

ABSTRACT: Monitoring is of most practical significance for the design and assessment of new and existing engineering structures. Practical experience and observations show that monitoring can provide the basis for new code specifications or efficient maintenance programs. Moreover, monitoring systems can avoid considerable costs of repairs and inconvenience to the public due to interruptions. This gives rise to the need for a thorough investigation to achieve an effective implementation of recorded monitoring data in numerical or analytical structural models that allow the detection of a deviant behavior from the proposed and the detection of initial deterioration processes. This study attempts to derive a concept for the effective incorporation of monitoring information in numerical models based on the concept of model correction factors. In particular, these studies are performed on the abutment free bridge structure S33.24 that has been proof loaded and monitored since December 2008. A merit of models derived based on monitoring data is that it is directly related to performance indicators that can be used for the assessment of the existing structural capacity and for an efficient life cycle analysis.

1 INTRODUCTION

In general, there is a high interest in construction towards more sustainable, cost efficient and robust design concepts. An increase in this can be observed in recent years at least partly motivated by steadily increasing budgetary constraints regarding the construction of new infrastructure as well as the maintenance and rehabilitation of existing ones. Jointless bridge structures are considered to be susceptible to degradation, more durable and cost efficient than “traditional” construction types.

Nevertheless, a proper functioning of joint less bridge structures depends on the accuracy of design models and design specifications that have to focus on the following main influence factors apart from

the chosen boundary conditions: (a) traffic loads and constraint loads resulting from earth pressure, (b) partial settlements and (c) the time dependent creep and shrinkage processes. Currently based on international experiences and a series of research projects a new guideline (RVS Entwicklung) is being developed with the aim of (a) specifying the appropriate load models for critical loads like earth pressure and temperature (gradient) and (b) giving general rules for a functional design. In order to study and advance design principles of this guideline that guarantees a cost effective structural performance over the planned life time, there is the requirement for intensive numerical simulations, based on monitored structural properties, and for the definition of performance indicators, as proposed by (Okasha and Frangopol 2011) for the early detection of deviations from the intended structural behaviour.

Therefore, this paper attempts to derive a concept for the effective incorporation of monitoring information in numerical models based on the concept of influence lines and model correction factors. In particular, the studies are performed on the abutment free bridge structure S33.24 that has been proof loaded and monitored since December 2008.

A merit of a monitoring associated model is that it is directly related to performance indicators that can be used for the assessment of the existing structural capacity and for an efficient life cycle analysis.

In particular, the paper treats (a) principles of finite element modeling of the pile founded joint less bridge S33.24, (b) the fiber optical sensor layout for the efficient description of the structural behavior during the erection, before and during traffic loading, and during the proof loading procedure, (c) the proof loading procedure for model updating, (d) the sensor associated influence line concept as bases for the model correction concept, and (e) the model correction procedure used for the determination of performance indicators in

order to provide the basis for an efficient structural life cycle analysis.

2 JOINTLESS MARKTWASSER BRIDGE S33.24

2.1 Geometry

The joint less Marktwasser Bridge S33.24 is a fore-shore bridge leading to a recently erected Danube crossing which is part of an important highway connection to and from Vienna. The structure actually consists of two structurally separated bridge objects, the wider one of which allows for five lanes of highway traffic. The S33.24 is a three-span continuous plate structures with span lengths of 19.50 m, 28.05 m and 19.50 m as is shown in Figure 1.

2.2 Monitoring system

As the design and the performance of jointless structures depend not only on dead load and the traffic loads but especially on constraint loads resulting from temperature, earth pressure and creep/shrinkage processes an integrative monitoring concept had to be developed covering the superstructure, its interaction with the reinforced earth dam behind the abutment and the dilatation area above the approach slabs. In total 5 different sensor systems consisting of strain gages, temperature sensors and extensometers were permanently installed, see also (Strauss et al., 2010; Wendner et al., 2010)

2.3 Proof Loading Procedure (PLP)

Proof load tests have been performed in 2010. The results of these proof loadings serve for the calibration of the static linear model and the verification of the assumed structural behavior. The concept for the proof loading procedure was developed with the following goals in mind. Firstly defined load situations with significant structural response were to ensure a proper model calibration mainly with respect to the boundary conditions. As a consequence three 40 to trucks (see Figure 2 and Table 1) with known axle loads were positioned in 16 static scenarios. The trucks were positioned

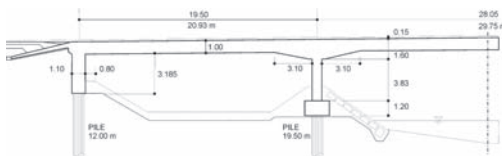


Figure 1. Longitudinal Cut of S33.24.

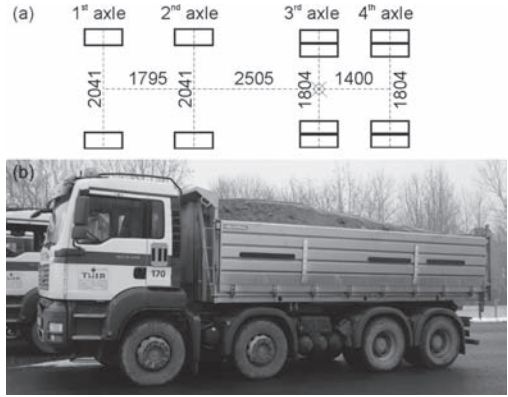


Figure 2. Proof loading vehicle (a) geometric distances between truck wheels, (b) side view of the ~40 to loaded truck.

Table 1. Axle loads of trucks 1 to 3.

	Truck 1 [kg]	Truck 2 [kg]	Truck 3 [kg]
1st axle	8,440	7,600	8,140
2nd axle	7,850	7,680	7,800
3rd axle	12,960	13,160	13,550
4th axle	12,300	12,390	12,810
Total	41,550	40,830	42,300

independently as well as in the most unfavorable configurations on lanes 1 to 3.

2.4 Influence line and model factor based performance indicators

The paper presents principles for the finite element modeling and monitoring based assessment of joint less bridges. In particular, the model correction factor and the influence line concept has been applied on the joint-less bridge S33.24. This approach allows the definition of model correction factors associated level I performance indicators, and of cross section and material properties associated level II performance indicators.

ACKNOWLEDGMENTS

The support of the National Science Foundation through the Eurostars—Project E!4351 Reliability Lifecycles Assessment Concrete Structures RLACS to the University of Natural Resources and Life Sciences, Vienna. The opinions and conclusions presented in this paper are those of the authors and do not necessarily reflect the views of the sponsoring organization.

REFERENCES

- Frangopol, D.M. & Liu, M. "Maintenance and management of civil infrastructure based on condition, safety, optimization, and life-cycle cost." *Structure and Infrastructure Engineering* 3(1): 29–41, 2007.
- Okasha, N.M. & Frangopol, D.M. "Integration of Structural Health Monitoring in a System Performance Based Life Cycle Bridge Management Framework." *Structure and Infrastructure Engineering*: (in press), 2011.
- Strauss, A., Wendner, R., Bergmeister, K. & Frangopol, D.M. "Monitoring based analysis of an concrete frame bridge "Marktwasser bridge." *Third International fib Congress*. Washington, DC, USA: 11, 2010.
- Wendner, R., Strauss, A., Bergmeister, K. & Frangopol, D.M. "Monitoring Based Evaluation of Design Criteria for Concrete Frame Bridges." *IABSE Symposium 2010*. Venice, Italy, IABSE, AIPC, IVBH. **Report Vol. 97**: 7, 2010.

Jointless bridges—performance assessment of soil-structure interaction

R. Wendner, A. Strauss & K. Bergmeister

Institute of Structural Engineering, University BOKU, Vienna, Austria

ABSTRACT: In structural bridge engineering maintenance strategies and thus budgetary demands are highly influenced by the quality of design in general as well as the chosen construction type in particular. As bridge owners nowadays are including life-cycle cost analyses in their decision processes regarding the overall design structural detailing with respect to robustness, durability and efficiency is becoming increasingly important, e.g. pushing jointless bridge structures. However efforts to reduce maintenance costs over the expected lifetime by adopting well established design principles lead to unknown risks, e.g. associated with boundary conditions. Monitoring solutions can reduce the associated risk by constant supervision of critical structural characteristics and substitute experience by advanced data analyses methodologies. This paper focuses on the analysis of monitoring data obtained by an integrative multi-sensor-monitoring system targeting the soil-structure interaction of frame bridges. In particular deformations in the transition area to the earth dam are analyzed with respect to design assumptions yielding probabilities of exceedance.

1 INTRODUCTION

In structural bridge engineering the quality of design and the choice of a suitable construction type are the dominant influence factors on maintenance strategies and planning. In general life cycle costs associated with a certain structure can be estimated by analyses of all individual structural members with regard to loading, resistance, exchangeability, accessibility and resulting economic costs due to limitations in usage during repair. This information can serve for the optimisation of maintenance strategies and thus minimization of overall costs. Nowadays bridge owners and planers are increasingly extending this strategy towards optimizing structural details and ensuring cost-efficient design. Structural members prone to damage and degeneration

are likely to be substituted by more durable and robust solutions thus reducing the likelihood of necessary and costly rehabilitation and maintenance works.

One of these construction types are frame structure which are typically applied as overpasses with one to three spans and span lengths of ordinarily less than 30 m. Through their lack of bridge equipment susceptible to degradation they are assumed to be more durable than “traditional” construction types. However, by leaving behind well-established design solutions unknown risks arise.

2 CASE STUDY—S33.24

In course of this paper the chosen design solution of the recently erected 67 m long three span jointless frame bridge S33.24, see Fig. 1, is being assessed with respect to the soil structure interaction.

One of the greatest challenges during design of the S33.24 was a functional solution for the transition area between structure (abutment) and earth dam. Figure 2 shows the final design of this detail including a reinforced earth body, a gap element between abutment wall and soil and an inclined slab.

The soil body directly behind the abutment wall is reinforced with geotextiles (see Fig. 2, marker 4). In combination with a soft gap element fixed to the abutment wall (marker 5) the amount of earth pressure against the abutment wall is reduced from full passive earth pressure to active earth pressure or less.

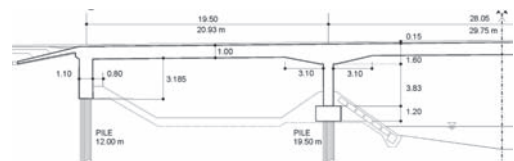


Figure 1. Longitudinal Cut of S33.24.

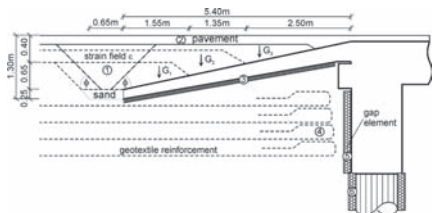


Figure 2. Structural detail of transition area behind abutment.

3 PERFORMANCE ASSESSMENT

The time dependent performance of jointless bridge structures is defined by (a) the bearing capacity of the superstructure, (b) serviceability related characteristics of structural response, and (c) the traffic safety and comfort with respect to the condition of the pavement. The latter aspect is highly influenced by the amount of displacements introduced by the structure in the transition area behind the abutments as well as these areas' structural detailing.

During design of the Marktwasser Bridge only the active earth pressure was accounted for in order to reduce constraint loads and thus increase efficiency of the concrete deck slab as well as columns. The assumption is only justified if the constructive detailing of the abutment area is functional, see Fig. 2. According to the design hypothesis the combination of reinforced earth dam with a soft gap element should limit relative displacements to a level which can be accommodated by the gap element. The monitoring based assessment of this concept yields limit state equation $G_6(t)$ for an admissible gap closure u_{lim} at the level of the extensometer

$$G_6(t) = u_{lim} - u_A(t) \quad (1)$$

In Fig. 3 the temporal development of $G_6(t)$ for three limits $u_{lim} = 0, 2, 4$ mm is plotted. If no gap closure is accepted the design criterion is constantly violated denoting a compression of the gap element already during construction works. Realistic thresholds of 2 mm and 4 mm respectively result in transgressions during summer of the first monitoring year for the 2 mm limit, whereas no violation for the higher limit is observed.

Due to changes in sampling frequency after the end of construction works and singular instances of power loss within the first year of monitoring, probabilities of exceedance p_E are determined based on short term extreme values—daily and weekly minima of $G_6(t)$ and the empirical definition of probability. With respect to the daily minima a probability of exceeding the design specification of $p_E = 24.2\%$ is determined, whereas the weekly minima are result in $p_E = 27.5\%$.

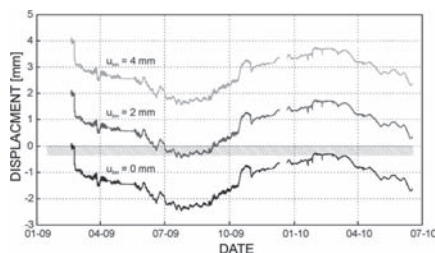


Figure 3. Development of earth pressure related limit state over time for $u_{lim} = 0, 2, 4$ mm.

4 CONCLUSIONS

The design of structures following new design principles motivated e.g. by economic considerations based on the life cycle cost concept is associated with uncertainties. The application of monitoring systems in combination with suitable assessment strategies increases understanding regarding structural response under varying load situations and thus ensures safe, efficient and durable future constructions.

Within this contribution a general methodology for the performance evaluation of new design principles based on limit state equations and the determination of probabilities of exceeding the design specifications has been presented. The proposed methodology has been applied to a recently erected three-span jointless frame structure which had been instrumented with an integrative monitoring system. In particular design assumptions regarding the soil structure interaction influencing the detailing of the transition area between abutment and earth dam as well as the build-up of earth pressure against the abutment walls have been investigated.

Future research regarding a performance prediction over time based on the proposed approach will in combination with risk assessment strategies allow for a quantitative evaluation of design concepts with respect to an acceptable risk level.

ACKNOWLEDGEMENTS

This research was conducted with the financial support of ASFINAG and BMVIT within the research project “Monitoring and analysis of integral bridge structures” and with the financial support of the Austrian research funding agency FFG within the EUREKA Eurostar research project “Risk Lifetime Assessment of Concrete Structures”. The opinions and conclusions presented in this paper are those of the author and do not necessarily reflect the views of the sponsoring organizations.

A semi-probabilistic safety-checking format for seismic assessment of existing RC buildings

F. Jalayer, L. Elefante, I. Iervolino & G. Manfredi

Department of Structural Engineering, University of Naples Federico II, Naples, Italy

1 INTRODUCTION

The performance assessment of existing buildings is particularly important in the process of decision-making for retrofit, repair and re-occupancy of existing buildings. With respect to new construction, the seismic assessment of existing buildings is characterized by the presence of uncertainties in the structural modeling parameters. The current European code-based procedures seem to address the uncertainties present in the structural modeling, by dividing the mean material properties by a factor larger than unity, known as the confidence factor. The confidence factor, which is classified based on discrete levels of knowledge about the building, seems to create an overall margin of safety in the performance assessments without specifically addressing the modeling uncertainties.

As an alternative to the CF approach in code-based recommendations, a probabilistic and performance-based approach, adopted in the American Department of Energy Guidelines DOE-1020 and in SAC-FEMA guidelines, is chosen in this work. This approach, that is also known as the *Demand and Capacity Factor Design* (DCFD) [Cornell et al., 2002] for its similarity with the Load and Resistance Factor Design (LRFD), takes into account the overall effect of the various types of uncertainties on a global structural performance parameter. An important feature of this safety-checking format is that it reduces to an analytic closed-form solution which could be calibrated for potential code implementations.

2 METHODOLOGY

A representation of the DCFD safety-checking format which is particularly suitable for code-implementation is described herein. For the case of dynamic analyses, the DCFD safety-checking format compares the (factored) structural performance parameter to a less than unity quantity in order to provide a certain level of confidence x in the assessment:

$$\hat{Y} \cdot \gamma \cdot e^{\frac{1}{2} \frac{k}{b} \beta_{\gamma|s_a}^2} \leq e^{-\Phi^{-1}(x) \sqrt{\beta_{\gamma|s_a}^2 + \beta_{UC}^2}} \quad (1)$$

where $\Phi^{-1}(x)$ is the inverse Gaussian cumulative distribution function (CDF) for percentile x . γ is a bias factor and β_{UC} represents the over-all effect of structural modeling uncertainties. \hat{Y} represents the structural performance parameter calculated based on the median material properties obtained from the test results and nominal values for the structural detailing parameters. For instance, \hat{Y} can be calculated by performing linear least squares as a function of the first-mode spectral acceleration based on the set of records. The bias factor γ represents the (usually larger-than-unity) factor that once multiplied by the nominal value \hat{Y} leads to the median value $\eta_Y(P_o)$ for the structural performance parameter for an admissible probability value P_o :

$$\gamma = \frac{\eta_Y(P_o)}{\hat{Y}} \quad (2)$$

where P_o is an acceptable threshold for structural failure probability and $\eta_Y(P_o)$ is the median structural performance parameter corresponding to the acceptable probability P_o . κ is the slope coefficient for linear regression (in the logarithmic space) of spectral acceleration hazard versus spectral acceleration and b is the slope coefficient for linear regression (in the logarithmic space) of the structural performance parameter Y versus spectral acceleration. The term $\beta_{\gamma|s_a}$ measures the effect of record-to-record (ground motion) variability on the total dispersion in the structural performance parameter given spectral acceleration.

In the static case, safety-checking can be performed by calculating a given percentile $x\%$ of the structural performance parameter Y and by verifying whether it is less than or equal to unity:

$$\hat{Y} \cdot \gamma \cdot e^{\Phi^{-1}(x) \beta_Y} \leq 1 \quad (3)$$

where γ is a bias factor and β_Y is the standard deviation of the structural fragility curve. \hat{Y} represents

the structural performance parameter calculated for the structural model corresponding to the median material properties based on the test results and nominal values for the structural detailing parameters. The bias factor γ represents the (usually larger-than-unity) factor that once multiplied by the nominal value \hat{Y} leads to the median value η_Y . γ can be calculated as:

$$\gamma = \frac{\eta_Y}{\hat{Y}} \quad (4)$$

where η_Y is the median value for the structural performance variable Y .

3 NUMERICAL EXAMPLE

As the case-study, the parameters of the analytical safety-checking formats presented herein for both static and dynamic analyses are estimated for an existing reinforced concrete school structure located in Avellino (Italy). These parameters are estimated using an efficient small-sample simulation-based Bayesian method (Jalayer et al., 2010). Two groups of structural modeling uncertainties are considered, the uncertainty in the mechanical property of materials and the uncertainty in the structural construction details. In particular, the structural construction details include, stirrup spacing, concrete cover, anchorage and splice length. In order to take into account the uncertainty in the representation of the GM, a set of 30 records based on Mediterranean events are chosen. The probability distributions for the uncertain parameters are updated according to the increasing knowledge levels (KL) defined in the Eurocode 8 (CEN 2003). Since the results of tests and inspections actually available for the frame in question did not exactly match the Eurocode 8 definition of the KL's, the test and inspection results used herein are simulated based on three different simplified hypotheses: (a) 100% of the test results verify the design values indicated in the original documents (b) 50% of the test results verify the design values (c) 0% of the test results. The estimated parameters are tabulated.

For the static analyses, it is observed that the β_Y values remain quasi-invariant with respect to the hypotheses regarding the outcome of the tests and inspections. However, they reduce as the knowledge level increases. Moreover, based on the prior distributions considered herein, considering the structural modeling uncertainties influences the structural reliability up to 15%. The bias factor γ remains more-or-less invariant with respect to the KL; however, it changes as a function of the percentage of the test and inspection results that verify the nominal value. For example, γ is approximately equal to 1.40, 1.20

and 1.0 for percentages verified equal to 100%, 50% and 0%, respectively.

For the dynamic analyses, it is observed that the values for β_{UC} reduce with increasing the KL. The bias factor γ which is observed to be more-or-less invariant with respect to the KL, is approximately equal to 1.50, 1.30 and 1.0 for 0%, 50% and 100% of the test and inspections verifying the nominal tests and inspections.

4 CONCLUSIONS

A semi-probabilistic safety-checking format for the existing buildings is proposed. It is demonstrated how the parameters of a simplified analytic safety-checking format arranged similar to Load-Resistance Factor Design (LRF) for different knowledge levels (KL) considering dynamic analyses can be estimated for a case-study structure. An analogous analytic safety-checking format is proposed for static analyses.

In perspective, the probability-based analytical safety-checking formats calibrated for the case-study building herein, are potentially suitable candidates for implementation in the guidelines for existing buildings. It should be mentioned that in order to make accurate performance assessments, the best way to approach would be to carry out case-specific assessments based on the outcome of the tests and inspections. However, these probability-based analytical safety-checking formats and their tabulated parameters can offer significant improvements in the assessment of existing buildings with respect to the current CF approach; they can serve as a less-than-ideal, approximate solution with a rigorous basis.

REFERENCES

- CEN, European Committee for Standardisation TC250/ SC8/ [2003]. "Eurocode 8: Design Provisions for Earthquake Resistance of Structures, Part 1.1: General rules, seismic actions and rules for buildings," PrEN1998-1.
- Cornell, C.A., Jalayer, F., Hamburger, R.O. & Foutch, D.A. [2002]. "The probabilistic basis for the 2000 SAC/FEMA steel moment frame guidelines", *ASCE Journal of Structural Engineering*, Vol. 128, No. 4, pp. 526-533.
- Department of Energy (DOE). [1994]. "Natural Phenomena Hazards Design and Evaluation Criteria for Department of Energy Facilities", DOE-STD-1020-94, U.S. Department of Energy, Washington, D.C.
- Federal Emergency Management Agency (FEMA) [2000d]. "Pre-Standard and Commentary for the Seismic Rehabilitation of Buildings" FEMA 356, Washington, D.C.
- Jalayer, F., Elefante L., Iervolino, I. & Manfredi, G. [2010]. "Knowledge-based Performance Assessment of Existing RC Buildings", In press, *Journal of Structural Engineering*.

Stochastic process deterioration modelling for adaptive inspections

A. Ohadi & T. Micic

City University London, UK

ABSTRACT: In many developed countries management of infrastructure, such as highway bridges, includes a well defined and rather prescriptive routine aiming to ensure reliable service to the public. However, due to the intrinsic uniqueness of infrastructure and diversity of processes records that are kept by the owners are substantial but not highly usable. Furthermore, in recent years, modern technology has enabled greater variety of monitoring techniques and therefore availability of data from sensors, video imaging, etc. is rapidly increasing. Thus, the long established infrastructure inspection processes can be reviewed to reconcile quality and diversity of site specific data, physical behaviour models and technology.

While inspection regimes are often strictly prescribed, many issues can be identified with such approach:

- Quality of data that results from inspections is rather poor and difficult to store,
- Inspection data can rarely be used for quantitative analysis,
- It is difficult to include alternative inspection techniques over the lifecycle,
- Quantitative information about the detection performance for different inspection techniques is not available,
- Mapping of outcomes of the inspection to optimization of maintenance and repair is, at best, attempted by random variable modelling
- There is a very limited scope for structure specific inspection regime that would provide more usable data.

It is worth focusing on a sample infrastructure such as bridges. Due to widely acknowledged uncertainties present the probabilistic methodology has been used for modelling and optimization. In many applications random variable modelling has been implemented and probability of failure would have been evaluated using standard procedures, Frangopol et al. (2004). Unfortunately, such approach reveals inconsistencies as random variable modelling is not sophisticated enough to account for fundamental differences in properties over the lifecycle and in specific environmental conditions.

For example we can consider Figure 1 where 2 structures are considered with distinct deterioration paths (DET1 and DET2). We also identify two inspection techniques (INS1 and INS2) that have distinct deterioration detection domains. Several issues can be identified here:

- quality of data that we receive from inspections will be highly variable over time,
- there will be need to distinguish tolerances from the different inspection techniques
- time horizon for implementation of different techniques can be very uncertain, etc.

As it stands the inspection regimes do not acknowledge that, in early years, current inspection techniques have very low deterioration detection likelihood. That is why we consider implementation of stochastic process modelling.

Thus, the procedure over the lifecycle would need to evolve like this:

- i. An initial deterioration profile is established on the basis of expert judgement.
- ii. For the initial deterioration profile we select the inspection technique and the inspection interval.
- iii. Selected inspection is carried out.
- iv. On the basis of inspection outcome we update the deterioration profile.
- v. We select the subsequent inspection technique and the inspection interval.

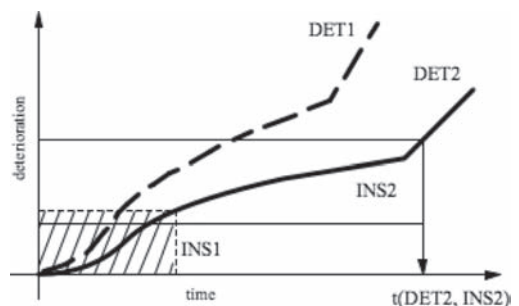


Figure 1. General status for infrastructure subject to inspections and deterioration.

Since deterioration process of any structures is non-negative, increment and continuous phenomena, Gamma process is an appropriate process for deterioration presentation.

In mathematical terms for the gamma process modelling, we first consider a random variable X that has a gamma distribution with the shape parameter $\alpha > 0$ and scale parameter $\beta > 0$. Its probability density function is given by:

$$Ga(x | \alpha, \beta) = \frac{\beta^\alpha}{\Gamma(\alpha)} x^{\alpha-1} \exp(-\beta x)$$

where

$$\Gamma(a) = \int_{z=0}^{\infty} z^{a-1} e^{-z} dz$$

Then the Gamma process formulation is:

$$\left\{ \begin{array}{l} P(X(0) = 0) = 1 \\ X(\eta) - X(t) \approx Ga(\alpha(\eta) - \alpha(t), \beta) \text{ for } \eta > t \geq 0 \\ X(t) \text{ has independent increments} \end{array} \right\}$$

An advantage of modelling deterioration using Gamma processes is that the required mathematical calculations are relatively straightforward.

For a sample deterioration process we first take advantage of the power law formulation

$$\alpha(t) = ct^b.$$

Since, c and β are unknown, they need to be established by using expert judgement or statistics. For simplicity we have implemented the method of moments. To demonstrate the approach we consider a simple circular bar element (16 mm diameter) that could be a part of bridge deck reinforcement.

After the method of moments was applied, in Table 1 we present the Gamma process parameters following different inspection times.

Expert judgement is an appropriate method for parameter estimation in early years however it is envisaged to be used only in early years. Figure 2, shows the percentage loss of section using gamma process representation from the inspection outcomes in year 13.

Figure 3 represents two sample density functions from time horizons that would reveal the progress of deterioration and could be considered at selected time intervals.

By implementing standard formulations, cumulative measure of deterioration, as indicated by the shaded are in Figure 5, can be evaluated. This estimate can be carried out for a desired interval and used to identify most effective inspection technique.

Table 1. Gamma process parameters that are obtained after inspection.

Time	β	c	$\alpha(t)$
0	—	—	—
9	β_{expj}	c_{expj}	$\alpha(t)_{expj}$
13	14.3	20.5	2.665
17	8.45	11.57	1.966
21	1.72	2.13	0.447

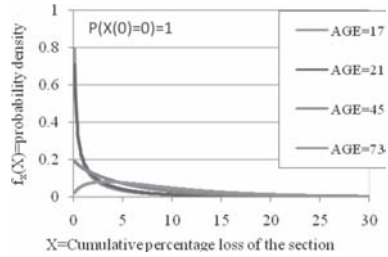


Figure 2. Gamma process representation following the inspection at year 13.

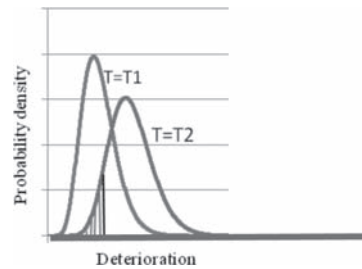


Figure 3. Cumulative measure of deterioration following Gamma process modelling.

Ultimately, at the scale of a country wide network of, say highway bridges, it is expected that the number of inspections carried out would be noticeably reduced and that the new procedures would represent a significant reduction in costs of inspections. At the same time this reduction in inspection costs is envisaged to actually improve the efficiency of maintenance and scheduling of repair.

From the results we see an opportunity to establish adaptive inspection regime that would account much better for:

- Structure specific deterioration path,
- Site specific environment,
- In service inspection outcomes,
- Inspection technique effectiveness,
- Planning for the future, etc.
- Maintenance planning,
- Repair scheduling.

This page intentionally left blank

*MS_234 — Probabilistic methods for the assessment
of existing concrete structures (3)*

This page intentionally left blank

Development and implementation of a semi-probabilistic procedure for the assessment of the future condition of existing concrete structures

J. Gulikers

Ministry of Infrastructure and The Environment, Centre for Infrastructure, Utrecht, The Netherlands

1 INTRODUCTION

In an increasing number of contracts on projects of the Dutch Ministry of Infrastructure there is a trend to gradually shift responsibilities regarding maintenance and management of infrastructure facilities towards the contractor for a time period of 10 to 30 years. In order to allow for a proper assessment of the financial risks involved, an evaluation of the actual condition level of the structures involved is urgently required. Such an evaluation will provide the starting point for a prediction of the condition development until end of contract and end of design service life and to consider when and which maintenance measures are to be taken.

With respect to chloride-induced reinforcement corrosion a simplified calculation procedure has been developed with takes into account the variability of cover depth and concrete cover quality, Gulikers (2009). The objective is that this procedure can be used by contractors and asset managers to provide a quantified condition rating of a concrete structure.

2 DEVELOPMENT OF A PRAGMATIC SEMI-PROBABILISTIC APPROACH

As most parameters included in a mathematical model are of a stochastic nature an assessment based on calculations using mean values may prove to be too optimistic. Consequently a probabilistic approach could be helpful to obtain a more realistic assessment of the actual and future condition of a structure or its components. On the other hand it should be borne in mind that in practice a full probabilistic approach is not feasible in view of the lack of reliable statistical information on the most relevant model parameters, e.g. the ageing exponent n and the critical chloride content, C_{crit} . Moreover, for practitioners a more pragmatic approach is considered to be of more interest provided that the basic considerations are properly

understood as to prevent the method to be used as a black box exercise.

The semi-probabilistic approach considers the critical chloride content C_{crit} and the thickness of the concrete cover c as the only stochastic variables. In view of the use by practitioners, i.e. a non-scientific community, for C_{crit} a lognormal distribution is arbitrarily chosen with $\mu C_{crit} = 0.60\%$ and $\sigma C_{crit} = 0.20\%$, CUR (2009).

A reliable impression on the statistical distribution of the concrete cover c can be obtained by performing cover measurements on site. A statistical treatment of the data obtained will result in values for μc and σc , and an adequate type of distribution. In this paper for reasons of simplicity a normal distribution will be assumed for the concrete cover thickness, although care should be exercised as negative values could be encountered.

Knowing the mathematical relationship between chloride content C and probability of corrosion initiation P_p , measured chloride profiles can easily be translated into probability profiles. Assuming a lognormal distribution for C_{crit} this results in profiles as shown in Figure 1. In addition the

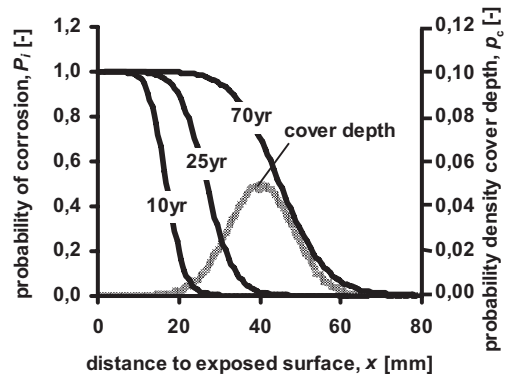


Figure 1. Calculated probability profiles including probability density function of cover depth ($\mu c = 40$ mm; $\sigma c = 8$ mm; N).

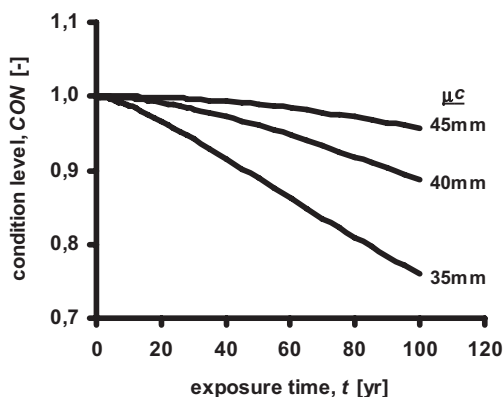


Figure 2. Calculated development of the condition level CON over time for $\mu c = 35, 40$, and 45 mm; $\sigma c = 8$ mm.

variability of the thickness of the concrete cover is demonstrated.

By combining data on measured chloride profiles and cover depths, the probability of corrosion initiation can then be calculated. In practice this can easily be accomplished by multiplying the mean probability of corrosion initiation at a certain depth interval $(x + \Delta x)$ with the relative amount of steel reinforcement embedded within this interval $(x < c < x + \Delta x)$. If the development of chloride ingress over time can be predicted, eventually this results in a prediction of the development of probability of corrosion over time. The translation into a condition level CON is achieved through:

$$CON(t) = 1 - P_i(t) \quad (1)$$

Figure 2 shows the calculated result for the condition level CON obtained for $C_s = 2.0\%$, $C_i = 0.1\%$; $D_a(14 \text{ yr}) = 0.5 \cdot 10^{-12} \text{ m}^2/\text{s}$; $n = 0.50$ for 3 values of

the average cover depth $\mu c = 35, 40$ and 45 mm ($\sigma c = 8$ mm).

3 CONCLUDING REMARKS

A basis for a pragmatic approach for quantitative condition assessment has been developed. The approach is aimed at practitioners without scientific knowledge on chloride ingress and probabilistics. Although the method seems to be straightforward it is foreseen that major modifications have to be implemented in due course. At present the approach has been applied in a number of projects, however the number of concrete profiles available for analysis has been limited. This is partly due to the fact that the concrete structures to be assessed hardly show any visual damage resulting from reinforcement corrosion although most of the structures have been in service for more than 40 years. Consequently, the necessity for extensive chloride profiling is not present. The experience obtained so far with this approach will be evaluated with contractors and consultants.

For practice this mathematical exercise of condition assessment is only one part; the experience of the inspector will always remain decisive in the overall evaluation.

REFERENCES

- Fib. 2006. Model Code for Service Life Design, bulletin 34 Lausanne.
- CUR, 2009. Guideline 1 Durability of structural concrete with respect to chloride-induced reinforcement corrosion, Gouda (in Dutch).
- Gulikers, J. 2009. Guideline for the determination of condition and residual service life of existing concrete structures, Rijkswaterstaat, Utrecht (in Dutch).

Statistical models for the material parameters of damaged concrete bridges

R. Lenner & M. Keuser

Institute of Structural Engineering at the University of the German Armed Forces, Munich, Germany

T. Braml

Munich, Re, Munich, Germany

ABSTRACT: With the aging infrastructure it has become very important in the recent years to inspect and reevaluate existing structures. Due to the increasing age, many of these structures, bridges in particular, show some level of deterioration. In most countries, bridges are visually inspected in regular intervals. In Germany, for example, these intervals are set at every three years for a small (routine) visual inspection and at every six years for a general (in-depth) inspection. From these inspections it is apparent that a large number of bridges exhibit a certain degree of deterioration due to the aging and service demands. These detrimental effects must be considered in the structural assessment in order to ensure both public safety and the safety of the structure itself. A particularly attractive tool for such assessment is the reliability analysis, which takes in account the true nature of the structure, because it incorporates reliable data obtained during the inspection. The damage varies in magnitude, extent, and type—for example a bridge can bear just localized concrete spalls or exhibit large areas of spalls with extensive cracking and exposed corroded reinforcement. The inspector on site has to make a call and subjectively evaluate the deterioration in order to assess the further serviceability of the bridge. With better and more accurate data, the level of reliability of the structure can be assessed with higher accuracy and can further dictate actions that need to take place, such as strengthening, posting load limits or closing the bridge down.

In most cases, however, there is no time or tools available to calculate the reliability of a bridge accurately, either during or after the inspection. Therefore a method for a rapid bridge assessment incorporating detrimental effects has been developed by the Institute of Structural Engineering at the University of German Armed Forces in Munich—Braml (2010), Braml & Keuser (2009). It utilizes a probabilistic approximation assessment. With the help of geometric measurements

and quantified damage assessment from the inspection, the reliability analysis utilizing FORM (First Order Reliability Method) and SORM (Second Order Reliability Method) provides results, which help to correctly estimate the condition of the structure. As a first pioneered example reinforced concrete bridges have been evaluated.

The method is based on a number of subsequent steps. As a first step standardized levels of damage for concrete and reinforcing steel were set based on the damage intensity in order to provide a basis for the analysis and further comparison. As a next step, ultimate limit state functions for each failure mode were described. In essence, these limit state functions express axial, bending and shear failure. Subsequently, each limit state was normalized to a dimensionless format. The main advantage of the dimensionless functions is the normalized influence of each variable. It is then possible to transfer results from one generalized analysis to various structures. For the given normalized limit state a reliability index was calculated as a function of all possible damage effects combination. As a result, a matrix of reliability indices and associated damage levels was developed. The main advantage is that a reliability index can be quickly determined using this matrix, without actually performing the probabilistic approximation, for any reinforced concrete bridge that has quantified damage according to the standardized levels. The complete procedure and its development process are shown in Braml (2010). As a final result, based on desired performance of the structure, the reliability index dictates necessary actions.

For the described method it is important to have calibrated stochastic models which describe the properties of damaged members and materials. To this point, most of the stochastic models for concrete, reinforcing steel and geometric measurements, from for example JCSS (2002), Strauss (2006), Wisniewski (2007), Strauss et al. (2006), were focused on new elements and materials.

Only a few publications were describing models of deteriorated materials for a use in the probabilistic assessment. One example is Capra (2003) that determined coefficient of variation for corroded steel as $v_{d,As} = 25\%$. As a result new procedures and methods for calibrating and developing probabilistic models of damaged materials and elements are in development.

The paper focuses on the models associated with the bending ultimate limit state of a reinforced concrete member. The deterioration of reinforced concrete elements can be fundamentally divided in three categories—concrete, concrete with impact to reinforcing bars, and reinforcement damage. In particular the properties of damaged concrete, such as compressive strength and geometric measurements, are of an interest of this paper. The detrimental effects need to be evaluated in the respect of their influence of on the median value, standard deviation and the distribution function of the aforementioned variables.

For a probabilistic assessment of existing structures adjusted statistical models that reflect the true state of that structure are important. Furthermore, these models are necessary for each failure mode. The paper gives an overview of the calibration process that was used for modifying and redeveloping the statistical model for concrete and geometric values. For clarity only some of the results were presented, while the rest in can be found in a full detail in Braml (2010). It must be noted, that the given general recommendations are intended for a non-site specific assessment, or as developed for the rapid assessment method. Whenever there is actual inspection data available the models should be adjusted accordingly.

Further actions in the field of refining the probabilistic models should include experimental verification of the suggested mathematically derived

stochastic models and introduction of additional limit states—such as service or fatigue.

Only work to this point has been done on limited types of structures, such as reinforced concrete bridges, which suggests there is room for further expansion of this assessment method to broader variety of structures and construction materials.

REFERENCES

- Braml, T. 2010. *Zur Beurteilung der Zuverlässigkeit von Massivbrücken auf der Grundlage der Ergebnisse von Überprüfungen am Bauwerk*. Doctoral Thesis. German University of Armed Forces. Düsseldorf: VDI – Verlag.
- Braml, T. & Keuser, M. 2009. Beurteilung der Tragfähigkeit von geschädigten Stahlbetonbrücken auf der Grundlage der Ergebnisse einer Bauwerksprüfung, *Beton-und Stahlbetonbau* 104, Heft 5, pp. 256–267, Berlin: Ernst & Sohn Verlag.
- Capra, B. & Sellier, A. & Hamsa, S. 2003. Reliability assessment of a reinforced concrete beam subjected to corrosion. *Applications of Statistics and Probability in Civil Engineering*. Edited: Kiureghian, D., Madanat, Pestena. Rotterdam.
- Joint Committee on Structural Safety (JCSS). 2002. *Probabilistic Model Code 12th draft*. <http://www.jcss.ethz.ch>
- Strauss, A. 2003. *Stochastische Modellierung und Zuverlässigkeit von Betonkonstruktionen*. Doctoral Thesis, Institute for Structural Engineering, Universität für Bodenkultur, Wien.
- Strauss, A., Kala, Z., Bergmeister, K., Hoffmann, S. & Novak, D. 2006. Technologische Eigenschaften von Stählen im europäischen Vergleich, *Stahlbau* 75, Heft 1, pp. 55–60, Ernst & Sohn Verlag, Berlin.
- Wisniewski, D.F. 2007. *Safety formats for the assessment of concrete bridges with special focus on precast concrete*. Doctoral Thesis, Department of Civil Engineering, University of Minho, Portugal.

Safety assessment of existing concrete slab bridges for shear capacity

Raphaël D.J.M. Steenbergen

TNO Structures and Safety, Delft, The Netherlands

Ane de Boer

Ministry of Infrastructure and Environment, Utrecht, The Netherlands

Cornelis van der Veen

Delft University of Technology, Delft, The Netherlands

1 INTRODUCTION

For a large part of the existing buildings and infrastructure the design life has been reached or will be reached in the near future. This is because a huge part of the existing stock has been built in the sixties of the previous century. These structures need to be reassessed in order to investigate whether the safety requirements are met. In general, the safety assessment of an existing structure differs from that of a new one, see Diamantidis (2001) and Vrouwenvelder (1996). The main differences are:

1. Increasing safety levels usually involves more costs for an existing structure than for structures that are still in the design phase. The safety provisions embodied in safety standards have also to be set off against the cost of providing them, and on this basis improvements are more difficult to justify for existing structures. For this reason and under certain circumstances, a lower safety level is acceptable.
2. The remaining lifetime of an existing building is often less than the standard reference period of 50 or 100 years that applies to new structures. The reduction of the reference period may lead to reductions in the values of representative loads.

In this paper, the safety philosophy for existing structures is discussed, resulting in the required β -values as been derived in Steenbergen and Vrouwenvelder (2010) and Vrouwenvelder and Scholten (2010). Based on this, for existing bridges under traffic load, the partial safety factors for the shear force assessment are derived using a full probabilistic approach.

2 EXISTING STRUCTURES

The required β -values are presented for two types of decision. First we have the level β_u below which

the structure is unfit for use. If this safety level is not reached, the authorities have to send immediately a notification that the structure has to be closed and to be adapted. Second, we have the safety level β_r for repair of existing structures.

Establishing safety targets for existing structures, both economic arguments and limits for human safety play a role. For existing structures normally a shorter design life is employed, however, as shown in Steenbergen and Vrouwenvelder (2010), this does not provide arguments for a reduction of β . If only economic optimization is considered and the failure probability increases approximately linear in time, it makes sense to use the same target reliability index regardless the design life time; as it is more economical to invest in safety measures if one can profit from it for a longer period of time. Therefore, a shorter design live does not provide an argument for a reduction of β .

The reason that from an economical point of view the required safety level for existing structures is lower than for new structures is the following: increasing the safety level usually involves more costs for an existing structure than for structures that are still in the design phase. The β -value is here the result of an economic optimization of the total building costs and the product of the damage costs and the probability of failure. For existing structures therefore a lower β -value is to be applied than for new structures. In Steenbergen and Vrouwenvelder (2010) and Vrouwenvelder and Scholten (2010), based on economical arguments, for the level β_u below which existing structures are unfit for use is proposed: $\beta_u = \beta_n - 1.5$. For Eurocode consequence class 2 a reduction by 1.5 means a shift from $\beta = 3.8$ to $\beta = 2.3$ and for the wind dominated cases from $\beta = 2.8$ to $\beta = 1.3$ (life time basis).

For repair a safety level β_r was defined $\beta_n < \beta_r < \beta_u$, leading to $\beta_r = \beta_n - 0.5$.

However the limits for human safety may never be exceeded. The maximum allowable annual probability of failure may not be exceeded.

Table 1. Lower β limits for human safety.

CC	β for a 15 year design life
1	1.1
2	2.5
3	3.3

Table 2. β -values for existing structures.

CC	Minimum reference-period	new		repair		unfit for use	
		β_n		β_r		β_u	
		wn	wd	wn	wd	wn	wd
1 A	1 year	3.3	2.3	2.8	1.8	1.8	0.8
1B	15 year	3.3	2.3	2.8	1.8	1.8	1.1*
2	15 year	3.8	2.8	3.3	2.5*	2.5*	2.5*
3	15 year	4.3	3.3	3.8 ¹⁾	3.3*	3.3*	3.3*

wn = wind not dominant

wd = wind dominant

(*) in this case is the minimum limit for human safety decisive;

1) in the Dutch Code, this value is relaxed to 3.6 because in the old Dutch Code $\beta=3.6$ was the highest safety level for new structures.

Too short life times may lead to unacceptable large probabilities of failure. In Steenbergen and Vrouwenvelder (2010) it has been shown that for short reference periods the limits for human safety become determining and, instead of raising partial factors for short periods, it is derived that for CC2 and CC3 a minimum design life time of 15 year is to be required in design.

In Table 1, the lower limit for the β -values for the three consequence classes are shown. The β -values are given at the minimum design life of 15 years. A complete derivation can be found in Steenbergen and Vrouwenvelder (2010).

Based on both the economical arguments and the limits for human safety the β -values for existing structures are established. This leads to the values in Table 2 indicating the values for β in the cases of repair and unfitness for use. In this Table, according to the Dutch Code NEN-8700, consequence class 1 from EN 1990 has been subdivided into 1 A and 1B, these classes are the same except for the fact that in 1 A no danger for human life is present.

3 PARTIAL FACTORS

In this paper probabilistic calculations are performed in order to establish the partial factors for

the load that are needed to obtain the required reliability for the shear force assessment of existing concrete slab bridges with a relatively small span under traffic load. Considered is a period of 15 years with loading by dead weight and traffic load. Other loads play a minor role in the design and assessment of traffic bridges. The limit state function is as follows:

$$Z = R - m_G G - m_T T$$

In this expression, R is the resistance of a structural element being here the shear strength, $m_G G$ is the effect of the dead load and $m_T T$ is the effect of the traffic load, where m_G and m_T represent model uncertainties. For the traffic load T the statistical distribution as obtained from weigh in motion (WIM) measurements for small spans has been implemented. For the shear strength the EN-1992 model is used. It gives for the design value of the shear strength τ_i :

$$\tau_{i,d} = \tau_{i,rep} / \gamma_m \text{ with } \gamma_m = 1.5 \text{ and}$$

$$\tau_{i,rep} = 0.18 \cdot k \cdot (100 \cdot \rho_l \cdot 0.85 \cdot f_{ck})^{1/2}$$

The statistical distribution belonging to the shear strength is obtained from experiments. From CEB-bulletin 224, "Model uncertainties" the following expression of the stochastic parameter τ_i results:

$$\tau_i = f_M \cdot 0.163 \cdot \{1 + (0.22/h)^{1/2}\} \cdot (\omega_0 \cdot 0.82 \cdot 0.85 \cdot f_c')^{1/3}$$

The factor f_M is lognormally distributed with a mean value of 1.0 and a coefficient of variation of 0.12. The cube compressive strength f_c' has a standard deviation of 10 N/mm². For CC3 for different parameters combinations the β -values are calculated for the EN 1990 formats 6.10a and 6.10b. A series of calculations have been performed in order to derive that load factors γ_G and γ_T that guarantee the required β -values for all different parameter combinations. These values of γ_G and γ_T are collected in Table 3.

Table 3. Load factors for existing structures.

	Reference period [year]	Obtained β	Partial factor		
			Weight γ_G	Weight $\xi \gamma_G$	Traffic γ_T
Repair	15	3.8	1.30	1.15	1.30
Disapproval	15	3.4	1.25	1.10	1.25

In Steenbergen and Vrouwenvelder (2010) it is proven that these factors are also valid for other failure mechanisms of existing bridges.

4 CONCLUSIONS

In this article a theoretical background of the safety assessment of existing structures has been presented. For existing concrete slab bridges under traffic load, adapted partial factors have been established using full probabilistic calculations.

These are now being used for the reassessment of existing bridges.

REFERENCES

- Steenbergen, R.D.J.M. & Vrouwenvelder, A.C.W.M. Safety philosophy for existing structures and partial factors for traffic load on bridges, *Heron* 55 no. 2, 2010.
- Vrouwenvelder, A.C.W.M. & Scholten, N.P.M. Assessment Criteria for Existing Structures, *Structural Engineering International* 1/2010.

This page intentionally left blank

*MS_138 — Probabilistic methods in hydraulic
and spatial structural analysis*

This page intentionally left blank

Forecast analysis of traffic flow through urban road tunnel based on Artificial Intelligent method

Luo Zhong, Jun Wu & Hongxia Xia

School of Computer Science and Technology, Wuhan University of Technology, Wuhan, China

ABSTRACT: Artificial Intelligent Technology provides us invaluable opportunities for effectively exploiting massive information resources. Along with the development of Artificial Intelligent Technology, some excellent methods have been developed to find exact or approximate solutions of optimal problems, which include Neural Network (NN), Support Vector Machines (SVM), Genetic Algorithm (GA) and so on. Obviously, whatever Artificial Intelligence is very useful for massive Data mining. As we know, how to monitor and predict the traffic flow through urban road tunnel is a particular point in the traffic project of city. If this problem can be solved effectively, it would be significantly helpful for improving the quality of urban traffic service nowadays. In the present paper, an introduction on forecast analysis of traffic flow through urban road tunnel based on artificial intelligent method is presented. With reference to experimental data and artificial intelligent method, a new type of analyzing model is set up for solving the problem of Data mining and knowledge discovery that will happen in forecasting traffic flow through urban road tunnel. Given its effectiveness in solving the problem, more optimal and better forecasting results can be obtained. Finally, examples show that this method is effective in predicting traffic flow through urban road tunnel.

1 INTRODUCTION

In recent years the urban road transportation condition more and more was crowded, the transportation question has nearly become one of the most common problem but also the most difficulty which exists during the daily life. It is important to get the information which would assist to alleviate the municipal and crowded traffic flow, to optimize the urban road transportation network movement. The data mining is bought to the intelligent transportation domain research area which could promote the efficiency of the massive traffic

flow data.^[1] The massive primary data value lies in is possibly hiding some unknown knowledge, may give the people to think provides more useful information which would give helpful decision-making or prediction to the next moment.

Along with the data acquisition technology development and information technology development, the data quantity is more and more huge, the attribute are also more and more complicated, how obtains the effective knowledge from these data is precisely the question which the data mining needs to solve. At present, this research area already become correlation domain and so on the Database, Information Management System, Artificial Intelligence and Policy-making support research topics.

2 METHOD & MODELING

2.1 Data mining process

Data mining has attracted a great deal of attention in the information industry and in society as a whole in recent years, due to the wide availability of huge amounts of data and the imminent need for turning such data into useful information and knowledge. The information and knowledge gained can be used for application ranging from market analysis, fraud detection, and customer retention, to production control and science exploration. Data mining involves an integration of techniques from multiple disciplines such as database and data warehouse technology, statistics, machine learning, high-performance computing, pattern recognition, neural networks, data visualization, information retrieval, image and signal processing, and spatial or temporal data analysis.

The approaches to classification, such as k-nearest-neighbor classifiers, case-based reasoning, genetic algorithms, rough sets, and fuzzy logic techniques which vest in the Artificial Intelligence method area are widely used. Methods for prediction, includes linear regression, nonlinear regression, and other regression-based models.^[2]

The following preprocessing steps which be shown in Fig. 1 may be applied to the data to help improve the accuracy, efficiency, and scalability of the prediction process.

2.2 Artificial neural networks

Neural networks are composed of simple elements operating in parallel. These elements are inspired by biological nervous systems. As the neural network in nature, the network function is determined by the connections between elements. A neural network can be trained to perform a particular function by adjusting the values of the weights between the elements.^[3] Commonly neural networks are adjusted, or trained, so that a particular input leads to a specific target output.

2.3 ANN modeling of traffic flow

The ANN modeling consists of two steps: First step is to train the network; second step is to test the network with data, which were not used for training. The processing of adaptation of the weights is called learning. During the training stage the network uses the inductive-learning principle to learn from a set of examples called the training set.^[6-7] Learning methods can be classified as supervised and unsupervised learning. In supervised learning, for each input neuron there is always an output neuron.

However, for the unsupervised learning it is enough only to have input neurons. The network selected here uses a back-propagation algorithm. The back-propagation learning algorithm is one of the most important historical developments in neural networks. It has reawakened the scientific and engineering community to the modeling and processing of many quantitative phenomena using neural networks. This learning algorithm is applied to multilayer feed-forward networks consisting of processing elements with continuous and differentiable activation functions. Such networks associated with the back-propagation learning algorithm are also called back-propagation networks.^[8] Given training set of input–output pairs, the algorithm provides a procedure for changing the weights in a back-propagation network to classify the given input patterns correctly.

3 APPLICATION

During this experiment, SQL provides the data which contains the urban road tunnel. It is capa-

ble to carry on the forecasting analysis to the per day traffic data in the database. Firstly, the urban road tunnel control system could give us the Transportation condition demonstration contact surface which is shown as the Figure 3. It is easy to do the Real-time monitoring. On the other hand, the accurate number of the traffic flow of the urban road tunnel could never be found easily and quickly. Because of these results, we have to forecast the number of the traffic flow in order to control the urban road tunnel safely and efficiently.

Obviously it is helpful of using the history data under the ANN model to get the forecasting result. As the Figure 4 shown, after a certain interval, the control system can count the left flow and the right flow which is the Traffic Statistics Parameters Module of the urban road tunnel control system. Then the database could provide the history data of the previous traffic flow which is seemed as the Table 1 shown.

As the part of the data formats are shown in Figure 4, it has 5 attributes which contains time, left lane traffic flow per hour, right lane traffic flow per hour, 5 sum of traffic flow 5. Then from these 5 attributes, choose the input for the ANN modeling. To deal with the forecasting problem can train the network by the data base which contain the data from 2010-2-1 1:00:00 to 2010-2-7 23:00:00, and then use the ANN algorithm. Finally, the forecasting output data follow closely matches the real data which is statistical by then. Figure 5 shows the comparison between the forecasting result and statistical sum data.

4 CONCLUSIONS

In this paper, we presented the implementation of data mining with Artificial Neural Network. After building modeling, making algorithm, and overview the structure of the forecasting system, we can have a traffic flow forecasting model. Then it is able to make attribute, selection data, and forecast result. This model fully uses data mining technology to optimal the massive data, and the experiment on the urban road tunnel shows that its forecast efficient.

Non-orthogonal polynomial expansion based approach for structural reliability analysis

Bin Huang & Chao Zhang

School of Civil Engineering & Architecture, Wuhan University of Technology, Wuhan, P.R. China

The study on the safety of engineering structures attracted more and more modern engineers. In order to evaluate the structural safety quantitatively, one needs to calculate the probability of failure in time-invariant component reliability analysis, or a multifold integral in the view of mathematics. For most practical problems, it is usually difficult, and in some cases even impossible, to reach the exact evaluation of this integral while the dimension of multifold integral is large, and the performance function is a highly non-linear function of random quantities with non-Gaussian distribution. While research is ongoing, various approximate methods, such as the first- and second-order reliability methods (FORM/SORM), moment methods, simulation methods and response surface methods are developed to estimate the failure probability.

In this paper a new class of computational methods, referred to as recursive stochastic finite element methods based on non-orthogonal polynomial expansion, is presented for predicting the reliability of structural systems subject to random loads, material properties, as well as geometry. The idea of recursive approach on random multivariate functions, originally developed by the authors for statistical moment analysis, has been extended for reliability analysis in the current paper. The proposed reliability methods include the determination of the initial coefficients of the non-orthogonal polynomial terms of the random vector, which represents the unknown static response, the redefining of the random response based on the assumption of new polynomial basis, and the conduction of Galerkin projection scheme. Afterwards, in terms of the obtained explicit polynomial expansion of the random response, the failure probability of performance function can be evaluated by FORM/SORM if multi MPPs are not exist, or calculated through the Monte Carlo simulation. In the end, two numerical examples including a random cantilever beam and random wedge are conducted to illustrate the effectiveness of the proposed method.

Main points involved in the paper are inductively displayed in the following.

1 NON-ORTHOGONAL POLYNOMIAL EXPANSION

The present paper suggests using the following non-orthogonal polynomial expansion to denote the random response vector, d , as

$$d(X, \alpha) = d_0(X)\varphi_0 + \sum_{i=1}^{\infty} d_i(X)\varphi_1(\alpha_i) + \sum_{i=1}^{\infty} \sum_{j=1}^i d_{ij}(X)\varphi_2(\alpha_i, \alpha_j) + \sum_{i=1}^{\infty} \sum_{j=1}^i \sum_{k=1}^j d_{ijk}(X)\varphi_3(\alpha_i, \alpha_j, \alpha_k) + \dots \quad (1)$$

where $\varphi_n(\alpha_i, \alpha_j, \dots)$ denotes the multi-dimensional, non-orthogonal polynomial, the first four terms can be written as

$$\begin{cases} \varphi_0 = 1 \\ \varphi_1(\alpha_i) = \alpha_i \\ \varphi_2(\alpha_i, \alpha_j) = \alpha_i, \alpha_j \\ \varphi_3(\alpha_i, \alpha_j, \alpha_k) = \alpha_i, \alpha_j, \alpha_k \end{cases} \quad (2)$$

2 RECURSIVE APPROACH OF STATIC PROBLEMS

$$\left(K_0 + \sum_{i=1}^n \alpha_i K_i \right) \left(d_0 \varphi_0 + \sum_{i=1}^n d_i \varphi_1(\alpha_i) + \sum_{i=1}^n \sum_{j=1}^i d_{ij} \varphi_2(\alpha_i, \alpha_j) + \dots \right) = f_0 + \sum_{i=1}^n f_i \alpha_i$$

where

$$K_i = 0 \quad (i = n_1 + 1, \dots, n); \quad f_i = 0 \quad (i = 1, \dots, n_1) \quad (3)$$

In accordance with equation (3), a series of deterministic recursive equations can be determined by perturbation technique.

3 GARLEKIN PROJECTION SCHEME

The expression of stochastic nodal displacement response is reassumed to be

$$d = \beta_0 d_0 \varphi_0 + \beta_1 \left(\sum_{i=1}^n d_i \varphi_1(\alpha_i) \right) + \beta_2 \left(\sum_{i=1}^n \sum_{j=1}^i d_{ij} \varphi_2(\alpha_i, \alpha_j) \right) + \beta_3 \left(\sum_{i=1}^n \sum_{j=1}^i \sum_{k=1}^j d_{ijk} \varphi_3(\alpha_i, \alpha_j, \alpha_k) \right) + \dots \quad (4)$$

The undetermined parameters β_i in the redefined stochastic polynomial expansions can be calculated through enforcing the Galerkin condition which makes the stochastic residual error $\mathbf{e}(\alpha) \in \mathbb{R}^n$ to be orthogonal to the basis vector Φ_i in a probability space spanned by independent random variables α_i as expressed in Eq. (5).

$$\langle \Phi_k^T, \mathbf{e}(\alpha) \rangle = 0 \quad (k=0, \dots, m) \quad (5)$$

where $\langle \cdot \rangle$ denotes the operator of mathematical expectation.

Then, by solving the m equations, the unknown coefficients $\beta_0, \beta_1 \dots \beta_m$ can be easily determined.

4 DEFINITION OF FAILURE PROBABILITY

$$P_f = \int_{R(\alpha) < 0} R(\alpha) f(\alpha_1, \alpha_2 \dots \alpha_n) d\alpha_1 d\alpha_2 \dots d\alpha_n \quad (6)$$

where $f(\alpha_1, \alpha_2 \dots \alpha_n)$ is the joint probability distribution function of the orthogonal random variables $\{\alpha_1, \alpha_2 \dots \alpha_n\}$.

5 CALCULATION OF MULTIFOLD INTEGRAL

At first, it is expected to use well established computational schemes such as those of FORM/SORM to evaluate the reliability index, once an explicit expression is available for the structural response. Secondly, Monte-Carlo simulation method can be used to implement the computation of reliability by the obtained output response.

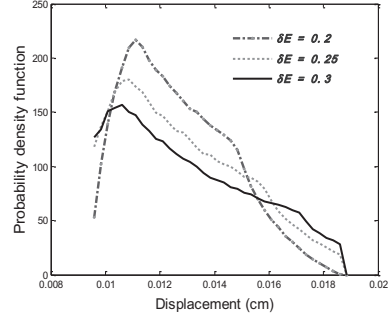
6 EXAMPLES

For example 1, some results of failure probability of random cantilever beam are listed in Table 1.

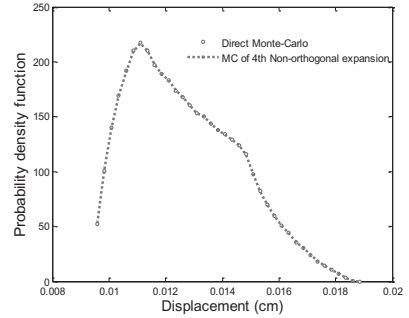
The static reliability problem of a random wedge under gravity and hydraulic pressure is illustrated

Table 1. Failure probabilities of random beam from 4 different methods.

Methods	$\sigma_E = 1e-5$		$\sigma_E = 0.1$	
	$\delta_l = 0.12$	$\delta_l = 0.179$	$\delta_l = 0.12$	$\delta_l = 0.179$
FORM	5.37e-4	2.55e-2	8.90e-3	4.19e-2
SORM	2.94e-4	2.01e-2	4.68e-3	3.12e-2
MC	3.3e-4	1.87e-2	4.53e-3	2.98e-2
DMC	3.5e-4	1.84e-2	4.36e-3	2.81e-2



(a) Different Covs of elastic modulus



(b) DMC vs MC ($\delta_E = 0.2$)

Figure 1. PDF curves of horizontal displacement at the top of wedge.

by example 2. The PDF curves of output random responses in some cases are shown in Figure 1 here.

Through the conducted numerical analysis, we can conclude that, taking advantage of the explicit expressions of random responses determined by recursive stochastic finite element method, the approximation approaches for reliability calculation, such as FORM/SORM, can be successfully used to evaluate the failure reliability if the solution is convergent and no multi most probable points occur. Further, taking into account that the computation amount of the failure reliability based on Monte-Carlo simulation is acceptable since the obtained explicit performance functions are provided, the proposed Monte-Carlo simulation is a good choice when the performance function is of strong nonlinearity or even has multi peaks.

Application of the sampling theory and methods in random decrement technique

Wenhai Shi

College of Architectural and Civil Engineering, Wenzhou University, Wenzhou, Zhejiang Province, China

Zhengnong Li & Honghua Wu

College of Civil Engineering, Hunan University, Changsha, Hunan Province, China

Ye Lin

The Spine Surgery, The 2nd Affiliated Hospital and Yuying Children's Hospital of Wenzhou Medical College, Wenzhou, Zhejiang Province, China

1 INTRODUCTION

The Random Decrement (RD) technique was explored initially and developed heuristically by Cole (1968, 1971). However, a strict theoretical proof for the RD technique was not proposed until 1982 by Vandiver, who established the general relationship between the auto-correlation function and the auto RD signature for a linear and time-invariant dynamic system. Then, Bedewi (1986) expanded the work of Vandiver to theoretically develop the multiple-signal RD technique for a linear Multiple-Degree-Of-Freedom (MDOF) dynamic system. Huang (1999) and Chiu (2004) expanded the mathematical derivation of relations between the RD signatures and the corresponding free vibration responses from displacement response to velocity response and acceleration response.

The RD technique provided a simple and direct method, instead of the FFT based method, to implement data analysis of vibration systems excited by random forces. Therefore, it has been widely implemented in modal and damping ratio parameter identification of civil engineering field. For example, Li (1998) and Shi (2010) applied the RD technique to identify the damping ratio parameter of structures. Kijewski (2002) and Chiu also made detailed discussions about the application problems of random decrement technique.

In the extraction of RD signature from measured data the signal interception threshold selection is critical. Generally, the structure response signal length is certain. The obtained sub-signal number will decrease with a large selected threshold value, correspondingly, the effective averaging times will decrease and lead to a worse average value results. On the contrary, if the threshold value is too small, although the averaging times increased, the signal section quality obtained will be worse and also lead to a worse RD signature. Therefore, in practical

application, both the suitable amplitude of threshold value and the amount of the averaging times need to be guaranteed (generally takes above 500~1000 times). Obviously, if the measured response signal is insufficient, the application of RD technology will meet great difficulty. On the other hand, when the selected segments number is very large, a more accurate structure vibration characteristic will be obtained, but lead to a greater computational work, therefore, there appeared the problem of how to extract the representative sampling segments in order to reduce the computation time by only extracting appropriate number of sampling segments.

This paper presents the application of sampling theory and methods on RD method for parameter identification of linear dynamic system. When dealing with parameters identification problem, the RD technique supplies an easy and powerful tool for extracting meaningful signals from measured random structural responses and has frequently been used in various fields. However, there are some problems, for instance, the sampling segments quantity is insufficient or too much, or the recognition precision is not satisfied to implement a good data analysis.

This paper unified pps sampling, stratified sampling, two-stage sampling and systematic sampling separately with the RD technique, then accordingly proposed the RD techniques based on above sampling methods, and developed corresponding formulations to produce a stable random decrement signature in some extent.

The results of four simulation examples indicate that in different vibration parameter recognition situations, the above provided RD technique based on different sampling methods could improve the quality of RD signature obviously, and lead to a quite accurate identification of vibration parameters of structural system under the effective use of all measured sampling segments.

Randomness of chloride ion concentration in existing concrete under tidal environment

Junzhi Zhang, Hui Zheng, Liangying Wang, Jianmin Zhou & Jiandong Wang
 College of Architecture and Civil Engineering, Zhejiang University of Technology, Hangzhou, P.R. China

ABSTRACT: Under the natural chloride environment, the free chloride ion concentration of concrete in different depths from the concrete surface is actually a random variable, randomness of these concentrations including concentration of surface concrete and bar' surface will decide randomness characteristic of initial corrosion time of steel bar in concrete and durability life of concrete elements.

Based on the measured values including concrete protective lawyers and free chloride ion concentration in an existing concrete of hydraulic gates under strong tidal estuary of the Qiantang River, the randomness of free chloride ion concentrations of surface concrete and bar' surface is analyzed in this paper, and the distribution parameters and distribution function are studied.

The studied background engineering built in 1980 is existing concrete sluice gates which are located in the natural strong tidal estuary of the Qiantang River and has been used to exceed 26 years. There are 5 holes with RC deck-girder gates which clear width is 3.00 m. Combining sampling with dismantling sluice, the concrete sample of the gates are been sampled in February 2007. The length of every concrete core sample is the thickness of gate that is insight into the gate. The marked "A" sample is located 200 cm height upper the base plate of the sluice and the marked "B" sample is located below gates.

The concrete protective layers of gates are measured based on samples, there is steel wire in concrete gates which diameter is 4 mm, and the average thickness of concrete of gates and of concrete protective layers of gates are 68.3 mm and 15.63 mm, respectively. The probability mode thickness can be analyzed in probability check method, the result show that the thickness of concrete protective layer is a normal distribution function.

By the measuring method above, the distribution of free chloride ion concentration in concrete of the existing gate can be analyzed. Figure 1 is the distribution map of free chloride ion concentration in concrete core A4~A6 and B4~B6.

Shown in figure 2 is the mean of free chloride ion concentration in concrete core A4~A6 and B4~B6.

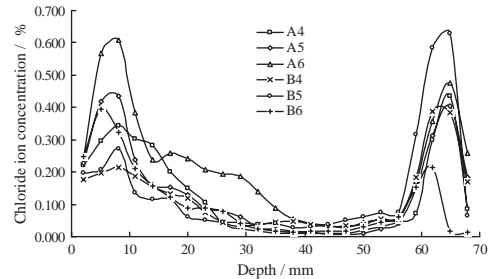


Figure 1. Distribution of free chloride ion concentration in concrete cores.

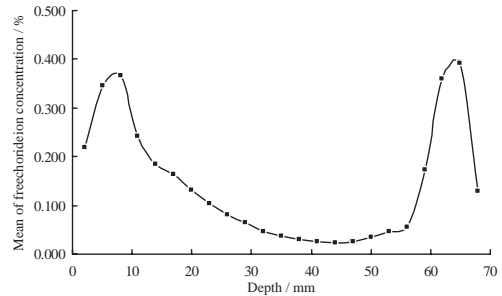


Figure 2. Mean of free chloride ion concentration in concrete cores A4~A6 and B4~B6.

Based on the free chloride ion concentration in concrete cores, the steady decrease phase of mean of free chloride ion concentration in concrete begins at 10 mm or so.

The analysis result show the probability distribution of free chloride ion concentration in identical depth conforms to a log normal distribution. For example, the probability distribution function of free chloride ion concentration at 20 mm depth of all cores concrete is:

$$f(x) = \frac{1}{0.4248 \times \sqrt{2\pi}} \exp\left(-\frac{(\ln x + 2.1204)^2}{2 \times 0.4248^2}\right) \quad (1)$$

The standard deviation and variation coefficients of free chloride ion concentration of

concrete cores A4~A6 and B4~B6 can be analyzed. Figure 3 is standard deviations with depths at cores A4~A6.

Figure 4. is standard deviation with depths at cores B4~B6.

According to analysis for calculation results above, the absorption of capillary is the main seepage action of chloride ions in concrete surfaces at the strong tidal estuary of the Qiantang River, and the randomness of seepage action is strong and the erosion is unstable. The largest variation coefficient of free chloride ion concentration in different depths reaches 0.73 where is 2~3 mm depth from surface sides. The absorption of capillary decreases gradually when the erosion depth is larger than 10 mm, and the seepage is trending to diffuse. The content mean of chloride ions has the general trend to decrease steadily, and the variation coefficients of content distribution of chloride ions are 0.20~0.45.

The analysis results show the concrete protective layer is a normal distribution, and the free chloride ion concentration of surface concrete and bar's surface are a log normal distribution. The main seepage action of chloride ions in concrete surfaces is the absorption of capillary at the strong tidal estuary of the Qiantang River, and the mean of free chloride ion concentration in concrete cores

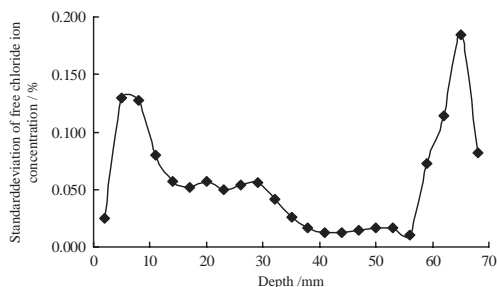


Figure 3. Relationship between standard deviations of free chloride ion concentration and different depths at cores A4~A6.

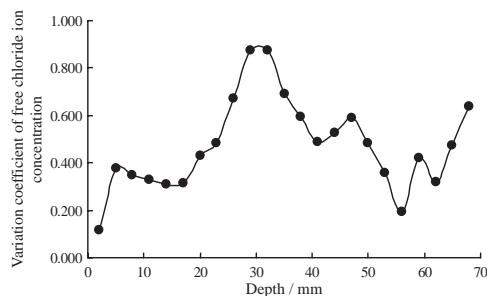


Figure 4. Relationship between variation coefficients of free chloride ion concentration and different depths at cores B4~B6.

increases with depth of surface concrete, but the steady decreases depth of mean of free chloride ion concentration in concrete is about 10 mm.

Keywords: Chloride ion, concentration, concrete, distribution

ACKNOWLEDGEMENT

The presented work was supported by the National Natural Science Foundation of China under project number 50879079.

REFERENCES

- Andrea Boddy (1999). An overview and sensitivity study of a multimechanistic chloride transport model, *Cement and Concrete Research* (29): 827-837.
- Wu, J. and Wu, S.X. (2004). Stochastic model of chloride ion concentration at steel-concrete interface in marine environment, *Journal of Hohai University* (Natural Sciences) 32(1), 38-41, in Chinese.
- Zhang, J.Z., Huang, H.Z. and Zou, C.R. *et al.* (2008) Study on carbonization durability for hydraulic concrete structures under the estuary environment in the Qiantang River, *Yangzte River* 39(2), 37-39, in Chinese.

This page intentionally left blank

GS_112 — Probabilistic modeling in engineering (1)

This page intentionally left blank

Characterization of random fields at multiple scales: An efficient conditional simulation procedure and applications in geomechanics

Jack W. Baker & Andrew Seifried

Department of Civil and Environmental Engineering, Stanford University, Stanford, CA, USA

Jose E. Andrade & Qiushi Chen

Department of Civil Engineering and Applied Mechanics, California Institute of Technology, Pasadena, CA, USA

ABSTRACT: This paper describes an approach to account for the multi-scale nature of soil by using a multi-scale hierarchical Monte Carlo simulation framework. The behavior of particulate media, such as sands, is encoded at the granular-scale, and so methods for accurately predicting soil behavior must rely on methods for up-scaling such behavior across relevant scales of interest. Multi-scale analysis is known to be especially important under strain localization, penetration or liquefaction conditions, where a classical constitutive description may no longer apply. A probabilistic framework across multiple scales is needed to efficiently model and simulate multiscale fields of spatially varying material properties and to consistently compute the behavior of the material in a multi-scale model. From a material modeling standpoint, the multi-scale framework is facilitated here using a hierarchical conditional simulation procedure. With this approach, a more accurate material description at finer scales is pursued only when needed, such as in the presence of strong inhomogeneities. Monte Carlo simulation is used to simulate material properties at an initial coarse scale, and that initial simulation is adaptively refined at finer scale materials whenever necessary, conditional upon previously simulated coarse scale data. Here the background of the multiscale geomechanics motivation is summarized, the mathematics of this simulation approach is developed, and then several example calculations are shown to bring insights regarding the approach and its potential application in problems where multi-scale effects are important. Details regarding open-source software documenting these calculations are also provided.

1 INTRODUCTION

Many geotechnical engineering problems are multi-scale in nature because of inhomogeneities existing at different length-scales in geomaterials.

Information pertaining to granular systems, including inhomogeneities, is encoded at the granular scale and propagated up to the field scale. Their effect on the global performance of geosystems at the field scale, such as oil reservoirs, can be profound as it has been shown that these features can serve as flow barriers, reducing the effective permeability of the reservoir by orders of magnitude (Holcomb and Olsson 2003; Sternlof et al., 2006).

When characterizing fields of soil properties while accounting for uncertainty, consideration of spatial dependence is of great importance, and much effort has been devoted to this problem. Often, spatially dependent random fields are modeled spectrally. Another common approach is to use a correlation coefficient between the unknown values of a soil property at two points, and the correlation decreases with increasing distance between the points. While spectral-based simulation approaches are often preferable for random field simulation due to their stability and computational tractability, here a sequential correlation-based approach is valuable if one desires to do adaptive refinement as described below, because it is not necessary to specify a priori the locations requiring fine-scale resolution; one can simply add additional fine scale data, conditional upon all previously simulated data, as the need arises.

2 SIMULATIONS APPROACH

A sequential conditional simulation adopted here. First an arbitrary location in the grid is selected and a simulation is generated from the standard Gaussian distribution. Subsequent locations are simulated conditional upon all previous simulations. The needed distributions are easy to obtain when the field is Gaussian. This conditional simulation approach is ideally suited for multiscale analysis because it is possible to selectively produce fine-scale simulations that are conditional upon an



Figure 1. Adaptively refined grid at a slightly larger scale.

original set of coarse-scale simulations. Simulations of non-Gaussian fields are obtained using a post-processing transformation of a simulated Gaussian field. This approach is widely used today, is seen to be reasonable in many situations (Goovaerts 1997; Phoon 2006), and has been adopted by the authors in past research (Andrade et al., 2008; Baker and Faber 2008; Chen et al., 2010).

For multiscale simulations, one proposed approach is to first produce simulated properties at the coarsest scale of interest and then iteratively simulate at finer scales, conditional on the coarse-scale random field simulations. This iterative simulation approach has recently been previously used by the authors (Chen et al., 2010), and has the advantage that fine-scale simulations are produced only at locations where they are needed. For example, if the coarse scale random field simulation produces a region of weak or potentially unstable material, then additional simulations at progressively finer scales can ‘fill in’ more detail at this critical region. Or if the finite element analysis for soil instabilities indicates that strains are localizing in a particular band, then supplemental random field simulations can be generated and the finite element mesh can be updated to incorporate the needed fine-scale details in this particular region. The only input needed is how to identify the locations where refinement would produce the most benefit for later analyses. Figure 1 shows a simulation of a 30×20 coarse scale field with 30% of grid points refined by identifying regions of strong heterogeneities in the coarse scale simulation.

3 CONCLUSIONS

This manuscript outlines a modeling approach used to simulate spatially correlated fields of random variables, and refine the discretization adaptively (i.e., without pre-specifying the refinement

locations prior to beginning the simulations). The procedure relies on transforming the random variables of interest to Gaussian random variables, and then relying on the properties of Gaussian fields to simulate additional values conditional upon previously specified variable values. The procedure has been implemented for the analysis of geomechanics problems, but is applicable to other problems where spatially varying random variables are used as inputs. The software used to produce these results is easily adaptable for other geometries and refinement strategies, and the source code has been provided on the authors’ website for use by other researchers.

ACKNOWLEDGEMENTS

This work was supported by the National Science Foundation under NSF grant number CMMI 0727121 to Stanford University and grant number CMMI 0726908 to Northwestern University. Any opinions, findings and conclusions or recommendations expressed in this material are those of the authors and do not necessarily reflect the views of the National Science Foundation.

REFERENCES

- Andrade, J.E., Baker, J.W. and Ellison, K.C. (2008). “Random porosity fields and their influence on the stability of granular media.” *International Journal for Numerical and Analytical Methods in Geomechanics*, 32(10), 1147–1172.
- Baker, J.W. and Faber, M. (2008). “Liquefaction risk assessment using geostatistics to account for soil spatial variability.” *Journal of Geotechnical and Geoenvironmental Engineering*, 134(1), 14–23.
- Chen, Q., Seifried, A., Andrade, J.E. and Baker, J.W. (2010). “Characterization of random fields and their impact on the mechanics of geosystems at multiple scales.” *International Journal for Numerical and Analytical Methods in Geomechanics (in review)*, ((in review)).
- Goovaerts, P. (1997). *Geostatistics for natural resources evaluation*. Applied geostatistics series., Oxford University Press, New York.
- Holcomb, D.J. and Olsson, W.A. (2003). “Compaction localization and fluid flow.” *Journal of Geophysical Research*, 108(B6), 2290.
- Phoon, K. (2006). “Modeling and Simulation of Stochastic Data.” *GeoCongress 2006*, ASCE, Atlanta, Georgia, USA, 17.
- Sternlof, K.R., Karimi-Fard, M., Pollard, D.D. and Durlofsky, L.J. (2006). “Flow and transport effects of compaction bands in sandstone at scales relevant to aquifer and reservoir management.” *Water Resources Research*, 42(7), 7425.

Performance-based probabilistic capacity models and fragility estimates for reinforced concrete column subject to vehicle collision

Hrishikesh Sharma, Paolo Gardoni & Stefan Hurlbaeus

Zachry Department of Civil Engineering, Texas A&M University, College Station, TX, USA

ABSTRACT: The infrastructure and transportation facilities have increased rapidly over the years. This has been accompanied by the increase in the number of vehicle collisions with structure. This type of collisions leads to the damage and often total collapse of the structure. There is need to protect the structures against such collisions. In the Reinforced Concrete (RC) structures, columns are usually the most vulnerable members exposed to such collisions. The columns in the lower story of the building, column of a bridge, electric poles are such members susceptible to vehicle collision. The existing design guidelines and provisions for protection of these members against collision of vehicles are not adequate. The desired behavior and the associated performance levels of the structure during a vehicle collision are not defined. The capacity of the RC column to withstand a vehicle collision and the demand imposed on it is not available. The current provisions do not take into account the uncertainty associated with the vehicle collision. There is a need to address these issues for the safety and protection of the infrastructure and transportation facilities and smooth operation of the system.

The proposed work addresses these issues. In this paper dynamic shear capacity models are developed to accurately estimate the capacity of the

RC column during vehicle collision. The different developed capacity models are associated with the different desired behavior and the corresponding performance levels of the RC column during vehicle collision. The probabilistic formulation used to develop the dynamic shear capacity model accounts for the uncertainties associated with the collision of vehicles with RC column. The proposed model is able to accurately predict the dynamic shear capacity of the RC column subject to vehicle collision during different performance levels. A framework is developed to estimate the fragility of the RC column subject to vehicle collision. The fragility estimate of a bridge RC column is made using the developed models during different performance levels. This estimate is used to predict the reliability of the structure for a performance level during vehicle collision.

The developed probabilistic dynamic shear capacity models can be used for a performance-based design of structures such as buildings, bridges. It can be used to estimate the adequacy of a structure to sustain a collision event and make recommendations for repair and retrofit. The state of knowledge can be applied to study similar cases of collision such as ship collision to a barge, projectile collision into concrete walls; and develop adequate models.

Keywords: Bridge Vehicle Collision, Capacity, Probabilistic Model, Demand, Fragility Estimates, Performance-Based Design

Adaption of car park loads according to DIN 1055-3 to the current trend of increasing vehicle weights

Holger Schmidt & Martin Heimann

Institute for Concrete and Masonry Structures, Technische Universität Darmstadt, Germany

Structures must be built in such a way that construction costs are kept to a minimum while meeting the structure's requirements with sufficient reliability both at the serviceability limit state (SLS) and the ultimate limit state (ULS). However, this demanding task can be accomplished only if the loads acting on a structure during its entire useful life are realistically considered in the calculation using suitable stochastic models and converted into easy to use standard load values. In this respect the forecast of future trends of loads varying with time is a difficult task subject to great uncertainties which, depending on the kind of influence, requires a critical review of standard load values at regular intervals.

The load data for multi-storey car parks currently available for building practice in the form of regulations under German standard DIN 1055-3 (2006) are based on load measurements and theoretical studies carried out by Marten (1975) back in the nineteen seventies. The annual new registrations recorded by the Kraftfahrt-Bundesamt (2007) KBA (Federal Motor Transport Authority) demonstrate, however, that average as well as maximum car weights have increased markedly since then. Based on data of the Kraftfahrt-Bundesamt (2007b), Figure 1 illustrates the trend in individual weight categories of all motor vehicles registered in Germany since 1989.

This illustration shows that in addition to the increase in weight in the medium category range (from 1400 kg–1700 kg up to 1700 kg–2500 kg) there was noticeable growth in vehicles with a maximum gross vehicle weight of >2500 kg. The load values for multi-storey car parks currently defined in German standard DIN 1055-3 (2006) therefore cannot ensure sufficient reliability of the loaded structural components and lead to insufficient safety in structural design.

To take the current trend of rising vehicle weights into account, the authors carried out load measurements at the *Hauptwache* multi-storey car park in Frankfurt am Main, Germany, and compared the results with data provided by the Kraftfahrt-Bundesamt (Federal Motor Transport

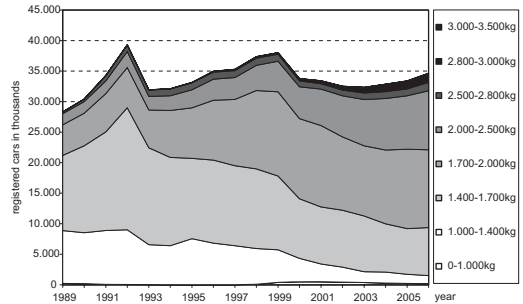


Figure 1. Trend in maximum gross vehicle weight since 1989 [Kraftfahrt-Bundesamt (2007b)].



Figure 2. Load measurements at the Hauptwache multi-storey car park in Frankfurt am main.

Authority). Vehicle weights were determined by means of a mobile wheel load scale, whereby the weight of front and back axles, the number of car occupants and vehicle fluctuation were measured. The load measurements were taken in the months of July to October 2009. Vehicles were weighed on leaving the car park, including the added load and weight of people. Figure 2 shows by way of example a vehicle during load measurement.

The distribution function of vehicle weights obtained from the load measurements made it possible to calculate uniformly distributed car park loads as a function of the reference area with the help of numerical simulations. On this basis the

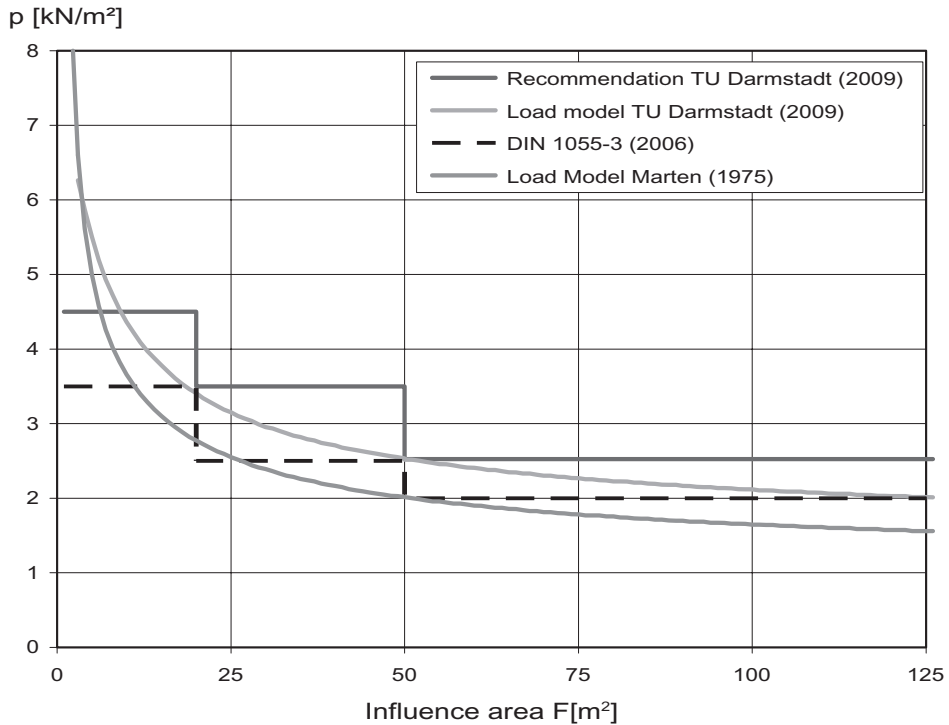


Figure 3. Annual extreme values of equivalent loads based on Marten (1975), Schmidt & Heimann (2009) and DIN 1055-3 (2006).

requisite annual extreme values for multi-storey car parks were determined for implementation in the standard.

Figure 3 compares the current annual extreme values of equivalent loads from Schmidt & Heimann (2009) with the values based on load measurements made by Marten (1975). In line with Marten (1975) and with reference to the CEB recommendation, the 95% quantile of the extreme value distribution with a reference period of one year, taking into account the load concentration factor f_s^* , is used to determine the design load. Using the 98% quantile would lead to only insignificantly higher loads, due to the small variation coefficient of the extreme value distribution.

As expected, the updated load values are higher than the load values given by German standard DIN 1055-3 (2006) which were based on measurements taken in the years 1972/1973. The design loads proposed by the authors [$A \leq 20 \text{ m}^2$ or $L \leq 5 \text{ m}$ ($q = 4.5 \text{ kN/m}^2$), $A \leq 50 \text{ m}^2$ or $L \leq 9 \text{ m}$ ($q = 3.5 \text{ kN/m}^2$) and $A > 50 \text{ m}^2$ or $L > 9 \text{ m}$ ($q = 2.5 \text{ kN/m}^2$)] are appropriate for realistically representing the bending moments of floor slabs in multi-storey car parks. The proposed design loads are however not suited to covering local shear force effects of axle loads close to supports.

Accordingly it is recommended for the shear force proof to use uniformly distributed design loads together with an axle load of 20 kN in unfavourable load position. This approach agrees in principle with the method of proof in bridge building and is suited for describing realistically also shear force effects of car park occupancies.

REFERENCES

- DIN 1055-3:2006-03: Einwirkungen auf Tragwerke – Teil 3: Eigen und Nutzlasten für Hochbauten, März 2006, DIN Deutsches Institut für Normung e.V.
- Kraftfahrt-Bundesamt: „Fahrzeugzulassungen - Bestand, Gewichtsklassen, Sitzplätze 01.01.2007“, Statistische Mitteilungen, September 2007.
- Kraftfahrt-Bundesamt: „Jährliche Neuzulassungen von Personenkraftwagen nach zulässigem Gesamtgewicht 1989-2006“, Januar 2007.
- Kraftfahrt-Bundesamt: „Der Fahrzeugbestand am 1. Januar 2008“, Pressemitteilung 4/2008, Januar 2008.
- Marten, K.: „Zur Festlegung wirklichkeitsnaher Nutzlasten und Lastabminderungsfaktoren“, Dissertation, Darmstadt 1975.
- Schmidt, H.; Heimann, M.: „Anpassung der Nutzlasten für Parkhäuser nach DIN 1055-3 an die aktuelle Entwicklung gestiegener Fahrzeuggewichte“, Forschungsbericht F09-15-2009, TU Darmstadt 2009.

Probabilistic modelling of HSC and UHPC slender columns in high-rise buildings

Holger Schmidt & Martin Heimann

Institute for Concrete and Masonry Structures, Technische Universität Darmstadt, Germany

For realistic modelling of the load bearing behaviour of slender RC columns, material and geometric nonlinearities have to be considered. Material nonlinearity means the stiffness reduction with increasing load intensity and geometric nonlinearities result from second order effects. Due to the load dependant material behaviour (moment-curvature-relationship) a sudden stability failure may occur long before material strength is exceeded. In these cases we speak of stability failure due to load dependant stiffness reduction. For correct analysis of the described phenomena the use of realistic material laws are inevitable. This applies not only to the stress-strain-relationships of concrete and reinforcing steel, but also to the tension stiffening effect (TS). The computer program developed by Six (2003) takes into account these phenomenon accurately which has been proven by several recalculations of experiments. The reliability analysis presented in the current study concentrates on short (slenderness $\lambda = 0$) and slender (slenderness $\lambda = 100$) high strength concrete columns, with a nominal compression strength of $f_{ck} = 100$ MPa.

The results of the reliability analysis are illustrated in Fig. 1. This figure illustrates the reliability index in the domain of the eccentricity ratio e/h . Additionally the target reliability index $\beta_{Target} = 4.7$ for a reference period of 1 year according to Eurocode 1 is marked. The short columns with slenderness $\lambda = 0$ (cross-section analysis) reveal a sufficient reliability level of $\beta = 4.7$ for the eccentricity ratio $e/h = 0.1$. With increasing eccentricity (transition from pure compression to bending) the reliability index declines to 4.2 at an eccentricity ratio of $e/h = 2.0$. This value lies in the accepted range of variation according to Eurocode 1. The different ratios of the nominal live load to dead load Q_k/G_k have almost no influence on the results. The slender column type with slenderness $\lambda = 100$ on the other hand show a significant reduction of the reliability index for medium eccentricity ratios e/h . The lowest value of $\beta = 3.5$ is reached at $e/h = 0.4$ and $Q_k/G_k = 0.25$. At eccentricity ratio $e/h = 0.4$ only stiffness determining variables such as concrete modulus of elasticity, tensile strength

(Tension Stiffening Effect) and the cross-section height are of major influence, what is a clear sign of stability failure. This serious reliability gap is not acceptable, since the stability failure occurs without any prior notice by e.g. increasing deflection and crack formation. The reason for this safety gap is that the partial safety factors γ_c and γ_s in the design format of Eurocode 2 can not reduce the design bearing capacity R_d in the case of stability failure since the failure occurs long before either the design yielding point of steel f_{yd} or design concrete strength f_{cd} are reached. The problem can be solved by applying a safety format which operates with only one single partial safety factor γ_R on the resistance side according to Eurocode 2—Part 2 (Concrete Bridges). The American Standard ACI 318-05 (2005) also works with only one strength reduction factor γ on the resistance side and therefore avoids a safety gap in case of stability failure. Fig. 1 shows that with the safety format according to Eurocode 2—Part 2 a very balanced reliability level can be achieved and therefore this safety format is strongly recommended by the authors for the design of slender columns.

Meanwhile the concrete-technological developments allow for an unerring production of ultrahigh-performance concrete (UHPC) with a compressive strength of more than 150N/mm². Fig. 2 shows

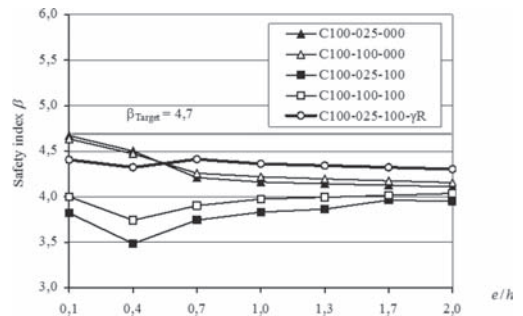


Figure 1. Reliability Index β for high strength concrete columns C100 ($f_{ck} = 100$ MPa) versus load eccentricity ratio e/h (caption: Concrete strength— $Q_k/G_k - \lambda$).

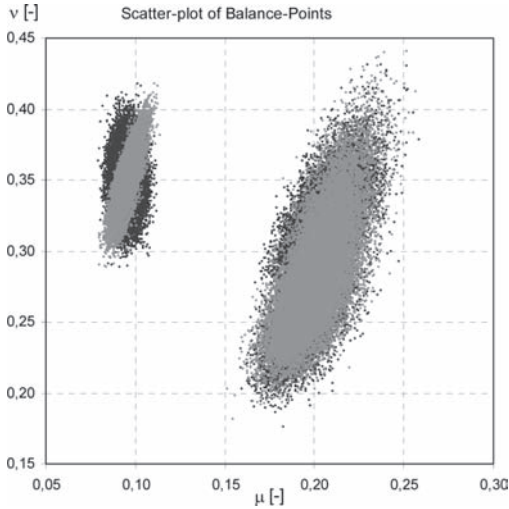


Figure 2. Scatter-plot of Balance Points for C150 (left side) and C30 (right side) concrete under the influence of shrinkage (black/grey dots); slenderness $\lambda = 0$.

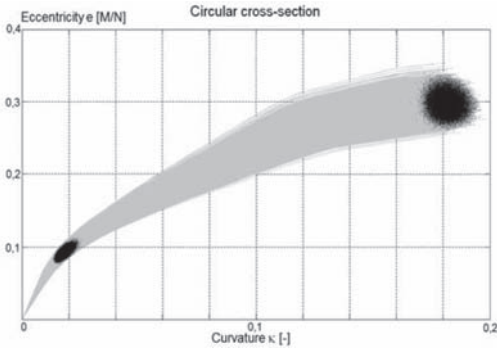


Figure 3. Eccentricity-Curvature diagram of a circular cross-section; Concrete C150; slenderness $\lambda = 0$; scatter-plot on the left side: crack starting point; scatterplot on the right side: load-carrying capacity.

exemplarily a scatter plot of the balance points of a circular cross-section for C150. The data are extracted from a specific M-N-diagram which is based on numerical simulation. The plot identifies the influence of shrinkage of the UHPC on the load-carrying capacity of a circular cross-section towards NSC. The distribution changes only in case of UHPC into a likely more multivariate distribution. Therefore the influence of shrinkage

is significantly and has to be considered in a probabilistic model of UHPC.

In addition, the illustration of the stiffness behaviour of a circular cross-section by means of an moment-curvature-diagram gives an explanation of the variation of the stiffness in dependence of the load effect. Fig. 3 draws the eccentricity of the internal force (ratio $e = M/N$ with $N = -2000$ kN) over the curvature of a circular cross-section. The changing stiffness with increasing eccentricity is identified by the trend of the curves. The dots on the left side describe the crack origin of the respective cross-section. The dots on the right side show the load-carrying capacity. In this case the yield strength point and the point of yield of the reinforcing steel subjected to compression are not reached. It can be seen that the variation of the curvature increases with increasing concrete compression. This can be traced back on the influence of dispersion of the concrete.

The knowledge of structural reliability of innovative UHPC column systems is mandatory because applications of this high-end building material could be executed without sufficient construction experiences. Moreover, the knowledge which is given for normal- and high-strength concrete cannot be simply transferred to UHPC. On the basis of the results of this research project, innovation potentials and limits of applicability of UHPC will be defined.

REFERENCES

- ACI Committee 318, "Building Code Requirements for Structural Concrete (ACI 318-05) and Commentary (318R-05)," American Concrete Institute, Farmington Hills, Mich., 2005.
- EN 1991-1-1, Eurocode 1: Actions on Structures, Part 1-1: General Actions—Densities, self weight, imposed loads for buildings, European Committee for Standardization, April 2002.
- EN 1992-1-1, Eurocode 2: Design of concrete structures - Part 1-1: General rules and rules for buildings, European Committee for Standardization, 2002.
- EN 1992-2, Eurocode 2: Design of concrete structures - Part 2: Concrete Bridges, European Committee for Standardization.
- JCSS Probabilistic Model Code Part 3: Resistance Models, Joint Committee of Structural Safety, 2001.
- Six, M.: „Sicherheitskonzept für nichtlineare Traglastverfahren im Betonbau“. Heft 534 des Deutschen Ausschusses für Stahlbeton DAfStb. Berlin: Beuth Verlag, 2003.

Estimating marginal densities of materials with multiple anomaly types

M.P. Enright & R.C. McClung

Southwest Research Institute, San Antonio, TX, USA

The fatigue life of fracture-critical metal alloys can be strongly influenced by material anomalies that may appear during the manufacturing process. If undetected, the anomalies can initiate growing fatigue cracks that may lead to premature failure of the component. The corresponding probability of fracture is dependent on a number of random variables, including the size, orientation, and occurrence frequency associated with a specified anomaly type (among other factors).

Some materials may have more than one type of anomaly (pores and inclusions, for example) which can introduce a number of additional random variables that must be characterized and treated for probabilistic assessments. If the crack formation and growth lives associated with the dependent random variables are known for all of the various anomaly types, the component probability of fracture can be assessed using established system reliability methods. However, these lives are often difficult to obtain in practice for multiple-anomaly materials because the test specimens typically are not isolated to a single anomaly type. Even when the component failures can be traced to a specific anomaly type, there is a potential overlap among the failures of different anomaly types which can be classified as the problem of competing risks.

If the failures associated with different anomaly types are independent and sufficient failure data are available, the marginal densities associated with them can be estimated using nonparametric statistical methods. Once the failure probabilities associated with the individual anomaly types are known, they can be used to calibrate probabilistic models for each anomaly type. The resulting calibrated probabilistic models can then be used to predict the behavior of the component with different numbers and types of anomalies.

In this paper, a probabilistic framework is presented that provides treatment for multiple types of anomalies in fracture-critical gas turbine engine

materials. It is based on previous work that has been extended to address the overlap among anomaly type failure modes using the method of Kaplan-Meier combined with the data-smoothing technique recommended by Meeker and Escobar. The framework is illustrated for risk prediction of a nickel-based superalloy. The results can be used to predict the risk of general materials with multiple types of anomalies.

REFERENCES

- Aalan, O., 1978. Nonparametric estimation of partial transition probabilities in multiple decrement models. *The Annals of Statistics* 6(3): 534–545.
- Cai, J. & Prentice, R.L. 1995. Estimating equations for hazard ratio parameters based on correlated failure time data. *Biometrika* 82: 151–164.
- Chen, B.E., Kramer, J.L., Greene, M.H. & Rosenberg, P.S. 2008. Competing risks analysis of correlated failure time data. *Biometrics* 64: 172–178.
- Enright, M.P. & Huysse, L. 2006. Methodology for probabilistic life prediction of multiple anomaly materials. *AIAA Journal* 44 (4): 787–793.
- Gaynor, J.J., Feuer, E.J., Tan, C.C., Wu, D.H., Little, C.R., Straus, D.J., Clarkson, B.D. & Brennan, M.F. 1993. On the use of cause-specific failure and conditional failure probabilities: examples from clinical oncology data. *Journal of the American Statistical Association* 88(422): 400–409.
- Kaplan, E.L. & Meier, P. 1958. Nonparametric estimation from incomplete observations. *Journal of the American Statistical Association* 53: 457–481.
- Meeker, W.Q. & Escobar, L.A. 1998. *Statistical Methods for Reliability Data*, John Wiley: New York.
- Moeschberger, M.L., and Klein, J.P. 1995. Statistical methods for dependent competing risks. *Lifetime Data Analysis* 1: 195–204.
- Nelson, W. 1972, Theory and application of hazard plotting for censored failure data. *Technometrics* 14: 945–966.

GS_122 — Probabilistic modeling in engineering (2)

This page intentionally left blank

Probabilistic fatigue design of composite material for wind turbine blades

H.S. Toft

Aalborg University, Department of Civil Engineering, Aalborg, Denmark

J.D. Sørensen

Aalborg University, Department of Civil Engineering, Aalborg, Denmark
 Riso-DTU, Wind Energy Division, Roskilde, Denmark

In the present paper a probabilistic design approach to fatigue design of wind turbine blades is presented.

Wind turbine blades normally consist of a main spar and an aerodynamic shell, see Figure 1. The purpose of the main spar is to carry flapwise loading whereas the aerodynamic shell primary gives the blade the correct aerodynamic profile and support for loads in the edgewise direction. The aerodynamic shell and the main spar webs in the blade are normally made of composite material such as glass fiber reinforced epoxy along with sandwich material.

The uncertainty related to the fatigue properties of composite material is in the present paper estimated using public available test results. Fatigue tests with both constant amplitude and variable amplitude are studied in order to determine the physical uncertainty on the fatigue strength and the model uncertainty on Miners rule for damage accumulation.

Composite material differs from many other materials because the fatigue strength is dependent on the mean stress and differs in tension and compression. The influence of the mean stress on the fatigue strength is normally taken into account by estimating SN-curves for different R-ratio's and arranging these in a constant life diagram. The R-ratio is defined by:

$$R = \frac{\sigma_{\min}}{\sigma_{\max}} \quad (1)$$

where σ_{\min} and σ_{\max} are the minimum and maximum stress in a fatigue cycle, respectively. In Figure 2 a constant life diagram estimated from constant amplitude fatigue tests with geometry R04MD is shown.

The model uncertainty on Miner rule for linear damage accumulation is estimated based on variable amplitude fatigue tests with the Wisper

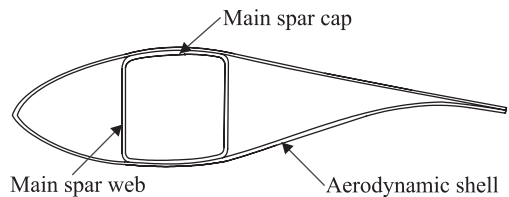


Figure 1. Typical cross-section of a wind turbine blade.

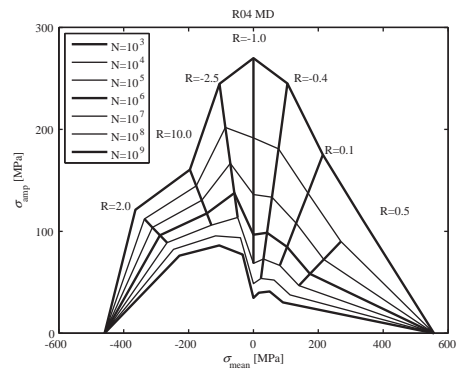


Figure 2. Constant life diagram for geometry R04MD.

and Wisperx spectrum. The estimated accumulated damage at failure is shown in Table 1. The results show that Miners rule gives a non-conservative estimate on the accumulated damage at failure.

The reliability of a wind turbine blade is in the present paper estimated for both out-of-plane and in-plane loading. The reliability estimation assumes that the blade is designed to the limit according to three different wind turbine design standards:

- IEC 61400-1
- Det Norske Veritas (DNV)
- Germanischer Lloyd (GL)

Table 1. Accumulated damage at failure, geometry R04MD.

Geometry	Spectrum	Tests	Mean	Std.
R04MD	Wisper	10	0.90	0.54
R04MD	Wisperx	13	0.28	0.20
R04MD	Reverse Wisper	2	0.20	–
R04MD	Reverse Wisperx	10	0.32	0.16
R03UD	Wisper	18	0.35	0.13

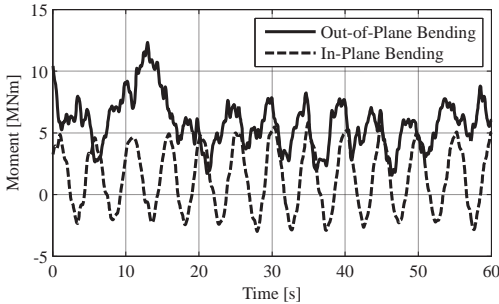


Figure 3. Time series for in-plane and out-of-plane bending moment for a pitch controlled 5 MW wind turbine at 13 m/s.

The three design standards differ in the way the fatigue strength is specified. However, also the partial safety factors and fatigue load changes between the three standards. In the present paper the IEC-standard is modified slightly for which reason it is denoted IEC-mod.

The reliability of the wind turbine blade is estimated using a limit state equation for the out-of-plane and in-plane loading, respectively. Figure 3 shows the typical response for the two load types. It is seen that the in-plane bending moment has a very regular behavior which is dominating by gravity loading of the blade. The out-of-plane bending moment has on the other hand has a more irregular behavior which is dominated by turbulence in the wind. Also, the blade passing the tower influences the out-of-plane bending moment. The fatigue cycles obtained from Rainflow-counting corresponds for the in-plane bending moment mainly to $R = -0.4$ and $R = -1.0$, whereas the out-of-plane bending moment mainly corresponds to $R = 0.1$ and $R = -0.4$.

In a numerical example the reliability is estimated using the three different design standards. The fatigue load is obtained from aeroelastic simulation of the NREL 5 MW reference wind turbine which is pitch controlled. The estimated annual reliability index β and annual probability of failure P_F for the last year of service ($t = 20$ years) are shown in Table 2. The table shows that the reliability is

Table 2. Estimated annual reliability index and probability of failure in the last year of service for the different standards.

Standard	Geometry	Load	β	P_F
IEC-Mod.	R04MD	Out-of-plane	3.12	$9.1 \cdot 10^{-4}$
IEC-Mod.	R04MD	In-plane	3.20	$6.9 \cdot 10^{-4}$
IEC-Mod.	R03UD	Out-of-plane	3.01	$1.3 \cdot 10^{-3}$
IEC-Mod.	R03UD	In-plane	3.32	$4.5 \cdot 10^{-4}$
DNV	R04MD	Out-of-plane	3.58	$1.7 \cdot 10^{-4}$
DNV	R04MD	In-plane	3.41	$3.2 \cdot 10^{-4}$
DNV	R03UD	Out-of-plane	3.01	$1.3 \cdot 10^{-3}$
DNV	R03UD	In-plane	3.32	$4.5 \cdot 10^{-4}$
GL	R04MD	Out-of-plane	2.26	$1.2 \cdot 10^{-2}$
GL	R04MD	In-plane	2.27	$1.2 \cdot 10^{-2}$
GL	R03UD	Out-of-plane	2.16	$1.5 \cdot 10^{-2}$
GL	R03UD	In-plane	4.19	$1.4 \cdot 10^{-5}$

Table 3. Summary of estimated annual reliability indices for the three standards.

Standard	Mean β	Std. β
IEC-Mod.	3.16	0.13
DNV	3.33	0.24
GL	2.72	0.98

slightly higher for in-plane loading compared to out-of-plane loading. This is due to the smaller physical uncertainty on the gravity load compared to the wind load which is dominating for the out-of-plane loading. The reliability obtained for geometry R04MD and R03UD differs slightly for the IEC-Mod standard. However, a larger variation is observed for the DNV standard and for the GL standard a significant variation in the estimated reliability is observed.

In Table 3 the mean and standard deviation for the annual reliability index are shown for each of the three standards. In the background documentation to IEC 61400-1 a target annual reliability index on $\beta = 3.09$ is specified corresponding to an annual probability of failure on $P_F = 10^{-3}$. From table 3 it is seen that the reliability obtained in the present study is slightly higher for IEC-Mod. and DNV whereas a lower reliability is obtained for GL.

The variation in the reliability index between the four cases considered is smallest for the IEC-Mod standard, where the full constant life diagram is used. A higher variation in the reliability is observed for the DNV standard which uses a constant life diagram based on three R-ratio's ($R = 0.1$, $R = -1$, $R = 10$). For the GL standard which uses the simple shifted Goodman diagram a large variation in the estimated reliabilities is observed.

Fragility estimates for the Fabela Bridge in Mexico incorporating vibration field data

V. Bisadi, M. Head, P. Gardoni & S. Hurlebaus

Zachry Department of Civil Engineering, Texas A&M University, TX, USA

D. De Leon Escobedo

Universidad Autónoma del Estado de México, Toluca, Estado de México, Mexico

Past experience shows that bridges with single column concrete piers are vulnerable to earthquakes in the transverse direction. This paper estimates the fragility curves for the Fabela Bridge, a five-span concrete bridge with single column concrete piers in Toluca, Mexico. The elevation of the bridge is shown in Figure 1. There are three traffic lanes on the bridge. The columns of the bridge are continuous to the deck and form two frames at the second and fourth spans of the bridge in the longitudinal direction. There are four in-span joints in the bridge with the distance of 5 m from the columns at the first, third and fifth spans of the bridge. The heights of columns A, B, C and D are 5.90 m, 6.87 m, 7.55 m and 7.28 m, respectively and the diameter of all the columns are 2 m. Shallow foundations with the length of 9 m and width of 6 m support the columns of the bridge.

Deterioration of bridge components change their stiffness during time. Therefore, the real stiffnesses of the bridge components might be different from those obtained from the design drawings. To get more realistic estimations of the structural properties of the bridge, the properties obtained from design drawings of the Fabela Bridge are updated based on the data from field vibration tests. Field vibration data are the recorded transverse accelerations from two accelerometers installed on the deck of the bridge. One of the accelerometers is installed on the deck at the top of Column B and

the other one is installed 20 m away from the first one near the center of the bridge. Installed accelerometers record the accelerations with 0.005 seconds sampling time. The data from vibration tests are processed to obtain the vibration frequencies of the first four transverse modes that excite the bridge at the location of the accelerometers.

An analytical nonlinear model of the bridge is created in OpenSees (2009) and the preliminary structural properties are assigned to the bridge components in the model based on the information available in design drawings. Then, the structural properties used in the model are updated by matching the vibration frequencies of the analytical model and the vibration frequencies obtained field from vibration tests. The matching process is conducted using Markov Chain Monte Carlo (MCMC) method. The updated structural properties are also used in the probabilistic capacity and demand models of the Fabela Bridge.

Probabilistic capacity and demand models are developed for the bridge based on the framework developed by Gardoni et al. (2002, 2003). Updated structural properties are used to develop probabilistic capacity and demand models for the Fabela Bridge. Fragility curves are estimated based on the developed probabilistic capacity and demand models. Two modes of failure are considered in the development of probabilistic models: deformation failure of bridge columns and shear failure

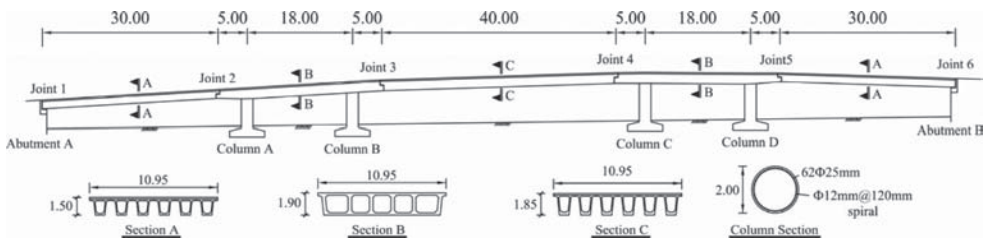


Figure 1. Elevation of the Fabela Bridge (dimensions are in m unless otherwise mentioned).

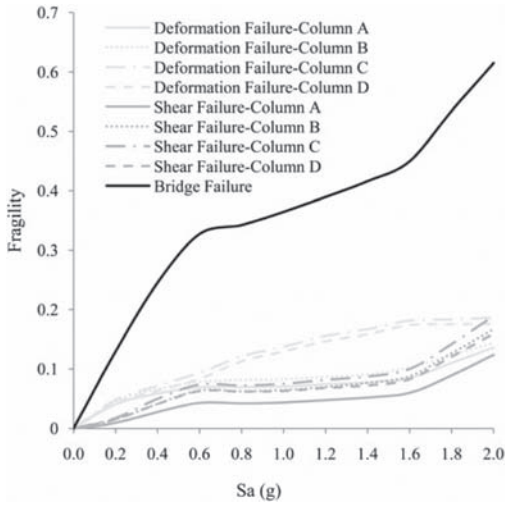


Figure 2. Fragility curves for the Fabela Bridge.

of bridge columns. Because there are 31 random variables in the capacity and demand models and running Monte Carlo simulations with that number of random variables is time-consuming, an importance analysis is conducted to find the variables that have large effects on the limit state functions and the other variables are considered in the analyses with a point estimation equal to their mean values. Fragility of each column of the Fabela Bridge in deformation and shear failure modes is estimated and also the fragility curve for whole the bridge structure is developed.

Figure 2 shows the estimated fragility curves for the Fabela Bridge. Results show that bridge columns are more vulnerable to deformation failure that is a ductile mode of failure than shear failure that is a brittle mode of failure. Also, the fragility curves show that columns C and D that are taller than columns A and B are more vulnerable to deformation failure.

REFERENCES

- Gardoni, P., Der Kiureghian, A. & Mosalam, K.M. (2002). Probabilistic capacity models and fragility estimates for reinforced concrete columns based on experimental observations. *J. Eng. Mech.*, 128(10), 1024–1038.
- Gardoni, P., Mosalam, K.M. & Der Kiureghian, A. (2003). Probabilistic seismic demand models and fragility estimates for RC bridges. *J. Earthquake Eng.*, 7(Sp. Issue 1), 79–106.
- McKenna, F. & Fenves, G.L. (2009). Open system for earthquake engineering simulation. Pacific earthquake engineering research center.

Probabilistic demand model based on the virtual work method and fragility estimates for offshore wind turbine support structures

M. Mardfekri, P. Gardoni & J.M. Roesset

Zachry Department of Civil Engineering, Texas A&M University, College Station, TX, USA

Extensive installation of offshore wind farms for electricity production in the United States and abroad has raised a new concern about the analysis and design of offshore wind turbine support structures. Reliable power production operation of a wind turbine is one of the key factors to reduce the cost of energy. Providing adequate reliability can help reduce the need for costly repairs and downtime. Furthermore, an accurate assessment of the reliability of wind turbines can be used for a reliability-based optimal design that minimized construction and maintenance costs while maintaining minimum reliability requirements. An important criterion for the design of a wind turbine support structure is to meet the serviceability criteria of the turbine. The proper operation of wind energy converters relies on the limited movement of the turbine installed at the top of the wind turbine tower.

Therefore, in this paper a probabilistic model is developed to predict the deformation demand on wind turbine support structures due to the operation of the turbine, and wind and wave loading. An existing deterministic model is corrected by adding a correction term to capture the inherent bias and model error arising from an inaccurate model form or missing variables. The correction term and the model error are assessed using data obtained from detailed three dimensional nonlinear finite element analyses of a set of wind turbine systems considering different design parameters. Fragility of the support structure is then defined as a conditional probability of not meeting a specified deformation performance level. Existing simplified methods for the analysis of the support structure and foundation of wind turbines have limitations in the modeling of the nonlinear behavior of the foundations. Three dimensional nonlinear finite element analyses provide a more rigorous and accurate modeling of the soil mass, pile and their interaction, but they are computationally expensive and time consuming. The proposed probabilistic demand model provides an

accurate framework for predicting the deformation of support structure properly accounting for the underlying uncertainties, and for estimating the vulnerability of the wind turbine support structure without the need of conducting complicated nonlinear finite element analyses.

A set of representative configurations are selected to generate virtual experiments later used to calibrate the proposed probabilistic demand models. The representative configurations are selected by conducting an experimental design to maximize the information content of the cases run and minimize the computational costs associated with running 3D nonlinear finite element analyses.

Finite element models are developed in ABAQUS to simulate the dynamic response of the support structure of typical offshore wind turbines, subjected to wind, wave and turbine operational loading. The finite element model of the support structure is constructed such that it is able to account for the nonlinearity of the soil behavior and soil-structure interaction.

Wave loading is modeled using a linear irregular wave model which is commonly used to model stochastic ocean waves. Morison's equation is used to determine the hydrodynamic forces.

Wind turbulence is simulated using the computer program TurbSim. The aerodynamics of the turbine is simulated by the aid of the computer program FAST (Fatigue, Aerodynamics, Structures, and Turbulence). The result of this simulation is the operational loading on the tower, which is used in the finite element model of the support structure as an external loading in addition to wave loading.

A probabilistic demand model is developed, following Gardoni et al. (2002, 2003), by adding a correction term to a selected existing deterministic demand model. The proposed demand model for given material properties, structural dimensions, and boundary conditions, \mathbf{x} , and for a given wind and wave loading, \mathbf{w} , can be formulated as

$$D(\mathbf{x}, \mathbf{w}, \Theta) = \hat{d}(\mathbf{x}, \mathbf{w}) + \gamma(\mathbf{x}, \mathbf{w}, \theta) + \sigma \varepsilon \quad (1)$$

where $\hat{d}(\mathbf{x}, \mathbf{w})$ = selected deterministic demand model, $\gamma(\mathbf{x}, \mathbf{w}, \theta)$ = correction term for the bias inherent in the deterministic model, $\sigma \varepsilon$ = model error, $D(\mathbf{x}, \mathbf{w}, \theta)$ = probabilistic demand model, $\mathbf{w} = (w_1, w_2)$, w_1 = mean wind speed, w_2 = significant wave height, $\Theta = (\theta, \sigma)$, θ = vector of unknown model parameters, σ = standard deviation of the model error, and ε = random variable with zero mean and unit variance.

In this paper, fragility is defined as the probability that the deformation demand exceeds a deformation threshold C for given wind and wave conditions. Following the conventional notation in structural reliability theory (Ditlevsen and Madsen, 1996), the fragility of the support structure, $F(\mathbf{w}, \Theta)$, will be defined as

$$F(\mathbf{w}, \Theta) = P[g(\mathbf{x}, \mathbf{w}, \Theta) \leq 0 | \mathbf{w}] \quad (2)$$

where $g(\mathbf{x}, \mathbf{w}, \Theta)$ = a mathematical model describing the limit state for the corresponding “failure” mode of the support structure. The limit state function is defined as

$$g = C - D(\mathbf{x}, \mathbf{w}, \Theta) \quad (3)$$

where $D(\mathbf{x}, \mathbf{w}, \Theta)$ is obtained from Eq. (1).

We consider different performance level criteria for displacement at the top of the tower as deterministic capacity model. Displacement threshold for the tower top is the maximum displacement, exceeding which may cause a temporary shutdown of the turbine, different damage levels or even collapse of the support structure. Since, these criteria are different for each wind turbine and usually determined by the manufacturer based on the characteristics of the rotor mounted at the top of

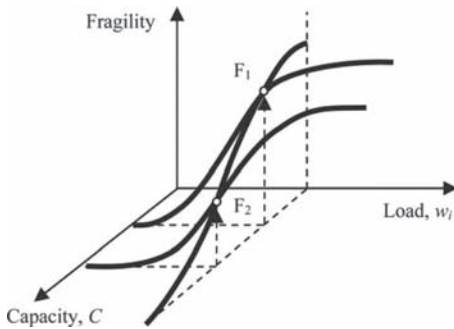


Figure 1. Schematic diagram for the fragility of wind turbine.

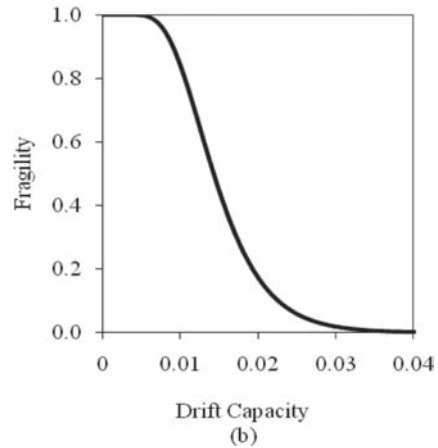
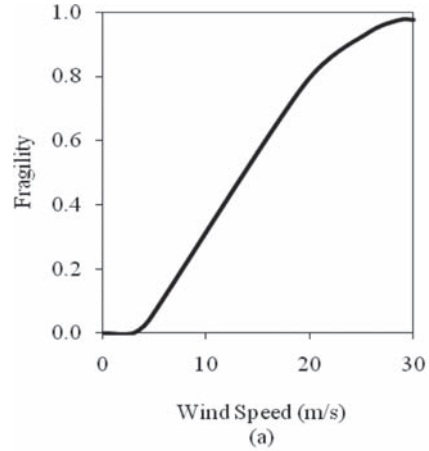


Figure 2. Fragility estimate of an offshore wind turbine for a) a drift capacity of 1.0% and b) a wind speed equal to 21 m/s.

the support structure, the fragility estimates are parameterized with respect to C . Fig. 1 shows how the fragility changes with respect to the wind or wave load and C . Fig. 2 shows the estimation of fragility for an example wind turbine.

REFERENCES

- Ditlevsen, O. & Madsen, H.O. (1996). *Structural reliability methods*, Wiley, New York.
- Gardoni, P., Der Kiureghian, A. & Mosalam, K.M. (2002). “Probabilistic Capacity Models and Fragility Estimates for RC Columns Based on Experimental Observations.” *J. Engrg. Mech.*, ASCE, 128(10), 1024–1038.
- Gardoni, P., Mosalam, K.M. & Der Kiureghian, A. (2003). “Probabilistic Seismic Demand Models and Fragility Estimates for RC Columns.” *Journal of Earthquake Engineering* 7(1), 79–106.

Probability-based modeling of chloride-induced corrosion in concrete structures including parameters correlation

Z. Lounis, B. Saassouh & J. Zhang

National Research Council Canada, Canada

In porous solids, such as Reinforced Concrete (RC) structures, chlorides can penetrate into concrete via different physical mechanisms, such as diffusion, capillary absorption, etc. which lead to the corrosion of the steel reinforcement. The corrosion of the steel reinforcement leads to concrete fracture through cracking, delamination and spalling of the concrete cover, reduction of concrete and reinforcement cross sections, loss of bond between the reinforcement and concrete, and reduction in strength and ductility. As a result, the safety and serviceability of concrete structures are reduced.

In practice, the design of durable concrete structures is mainly based on specifying a minimum concrete cover depth (depending on the environmental exposure), a maximum water-to-cement ratio (to achieve low chloride diffusivity), and as well the use of more corrosion resistant reinforcing steels.

Chloride diffusion is the transfer of mass by random motion of free chloride ions in the pore solution, resulting in a net flow from regions of higher to regions of lower concentration. Since in the field, chloride ingress occurs under transient conditions, Fick's second law of diffusion can be used to predict the time variation of chloride concentration for one-dimensional flow. In the modeling of chloride ingress as Fickian process, the following assumptions are made:

- The phenomena of capillary flow, chloride binding (chemical reaction that some of the chlorides within the concrete) are not considered.
- Using Crank's solution for a plane sheet assumes dealing with plane isotropic concrete structures (one dimensional diffusion)
- The diffusion coefficient and surface chloride concentration are assumed constant
- The initial concentration of chlorides in the concrete is negligible.
- Interaction with other ions and with electrical double layer is ignored.

As for the corrosion, it can be described as a two stage process: (i) corrosion initiation; and (ii) corrosion propagation. The corrosion initiation

stage corresponds to the process of chloride ions (chlorides) ingress into concrete (and/or carbonation) while the steel remains passivated. The corrosion propagation stage starts after the initiation of active corrosion. The corrosion initiates when the amount of chloride (in contact with the steel) is high in such a way to destroy the passivation of the steel.

In concrete mix design, it is well understood that both the water/cement (w/c) ratio and chemical compositions of cementing binding materials, particularly the use of supplementary mineral admixtures, such as silica fume and slag, are key factors for the development of high performance concrete with good properties. The use of low w/c ratio directly reduces the porosity and refines the pore structure, and therefore reduces the permeability of concrete and other transport indices such as D .

The lowering of w/c ratio and use of mineral admixtures lead to the beneficial effect of reducing chloride diffusion coefficient; however, they may have parting effects on the chloride resistance of embedded steel. The effect of reducing w/c ratio would increase the chloride threshold level, because a low w/c ratio helps to stabilize the micro-environment at the depth of the reinforcement as the moisture permeability decreases. The effect of using mineral admixtures, on the other hand, may reduce the chloride threshold.

Despite the potential negative effect of reducing the chloride diffusivity by using mineral admixtures on the chloride threshold value, the penetration of chlorides is the controlling factor for passivity of the embedded steel over the possible drop of pH value by using mineral admixtures. It implies that although the use of mineral admixtures can have adverse effects on the chloride threshold values, however, this negative effect is outweighed by their positive impacts on the reduction of the chloride diffusion coefficient.

Most of the cases treated in the literature assume that the parameters of the diffusion model are independent. For the purpose of this study, a weak to medium correlation between D and C_{th} in

the range of +20% to -20% can be assumed. The negative correlation reflects the effect of changing the w/c ratio; i.e. reducing w/c ratio decreases D but increases C_{th} . The positive correlation reflects the possible effect of using mineral admixtures in decreasing D and C_{th} .

However, a considerable level of uncertainty may be associated with one or more parameters of the diffusion process and corrosion initiation. This uncertainty in the model output could have serious consequences in terms of over-estimation of service life, inadequate planning of inspection and maintenance and increased life cycle costs.

The objective of this paper is twofold: (i) present a practical approach for probabilistic modeling of chloride-induced corrosion of carbon steel reinforcement in concrete structures based on the first-order reliability method (FORM); and (ii) Evaluate the impact of parameters correlation on the probability of corrosion.

The FORM approach enables to take into account the uncertainties in the parameters that govern the physical models of chloride ingress into concrete and corrosion of carbon steel, including chloride diffusivity, concrete cover depth, surface chloride concentration and threshold chloride level for onset of corrosion, as well as the correlation between chloride diffusivity and threshold chloride

level. The governing parameters are modelled as random variables with different levels of correlation and the probability of corrosion is determined and compared to the predictions obtained by more rigorous approaches, such as second-order reliability method (SORM) and Monte Carlo simulation (MCS).

The FORM approach is applied to predict the level of corrosion in the top layer of reinforcing carbon steel of a highway bridge deck that was exposed to chlorides from deicing salts. It is found that the first order reliability method provides accurate results and is more efficient than Monte Carlo simulation (for the same amount of data) and remains conservative compared to the SORM method, despite the high nonlinearity of the performance function. The results illustrate the accuracy and efficiency of FORM when compared to SORM and MCS. For many examples tested (by varying the mean values and the coefficients of variation) that consider the correlation between C_{th} and D, the variation in the probability of corrosion does not exceed 4% in all the cases (e.g. carbon steel, severe exposure, other depth values, etc.) Hence, the impact of the correlation between chloride diffusivity and chloride threshold value, on the probability of corrosion is marginal and can be ignored.

Identification of the filament stress transfer length in multifilament yarns using fiber bundle model and chain-of-bundles model

R. Rypl & R. Chudoba

Institute of Structural Concrete, RWTH Aachen University, Germany

M. Vořechovský

Institute of Structural Mechanics, Brno University of Technology, Czech Republic

INTRODUCTION

Textile fabrics are increasingly applied as a reinforcement of concrete structures in civil engineering realizations. In composites, however, the yarns are not fully penetrated by the matrix. The bond between filaments and matrix develops only in the outer region of the yarn cross section and a large fraction of filaments without any contact to the matrix is still present. The filament-filament frictional stress is much lower than the bond shear stress transmitted by the outer bond filament-matrix. Nevertheless, the effect of the inner bond on the macroscopic performance of a reinforced tensile specimen cannot be neglected. While the outer bond affects the behavior locally at the length scale of a crack distance, the inner bond influences the failure process at the length scale of a structural element with sufficiently large stress transfer (or anchorage) length. As a consequence, the interaction and damage effects for both outer and inner bond require a detailed mechanical characterization. While it is possible to study and characterize the interaction between a single filament and the matrix experimentally using the pull-out test, it is impossible to directly test the *in-situ* filament-filament interaction. In the present paper the available theoretical framework of statistical fiber bundle models is utilized with the goal to provide a method for identifying the filament-filament interaction within the yarn using the data from a specifically designed tensile test setup. The key idea of the present approach is to exploit the fact that the *in-situ* filament-filament interaction significantly affects the length-dependent strength of the yarn. The effect of friction between filaments becomes significant when the specimen length is larger than the stress transfer length, i.e. the length at which a broken filament recovers its stress. Such a yarn structure gets fragmented into a chain-of-bundles and behaves like a pseudo-composite.

This conference contribution promotes a recent journal paper (Chudoba, Vořechovský & Rypl 2011).

STATISTICAL MODELS

Throughout the study, the only source of randomness considered is the variability in local filament strength. Filaments have elastic response until sudden (brittle) failure upon reaching their strength. The local random strength (or breaking strain) X at a certain point over the filament length is considered to follow the Weibull distribution:

$$F_X(x) = P(X \leq x) = 1 - \exp\left[-\left(\frac{x}{s}\right)^m\right] \quad (1)$$

With these assumptions for a single filament a qualitative profile of the MSEC of a multifilament yarn can be expected as shown in Figure (1). Two different mechanisms of load transfer in a yarn can be distinguished depending on the yarn length. The two regions are separated by the yarn length l_b^*

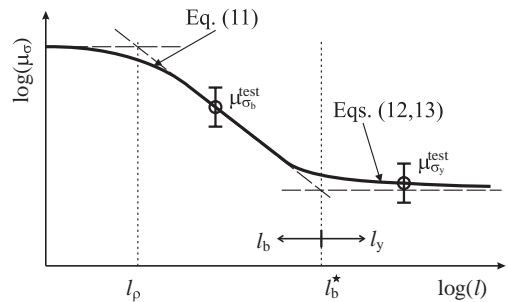


Figure 1. Mean size-effect curve in logarithmic scale with three distinguished asymptotes.

at which the fiber fragmentation can occur. Here, we implicitly assume that the autocorrelation length l_ρ of a random strength process along the filament is less than l_b^* at which the mechanism is changed. The two main regimes can be characterized as follows:

- For the range of lengths $l < l_b^*$, the yarn is acting as a bundle or a set of parallel, independent filaments with identical Weibull strength distribution. Its size effect behavior is described in the classical work by (Daniels 1945) and was later corrected by (Smith 1982). In such a bundle, a filament is assumed to break only once within its length and the associated released force is redistributed evenly among the surviving fibers.
- With an increasing length, the filament-filament friction can recover the stress released upon a filament break and allows for the fragmentation of a single filament along its length. Such a length l_b^* marks the transition from the bundle behavior to the behavior of a chain-of-bundles. The slope of the MSEC for $l > l_b^*$ gets reduced and in the limit asymptotically approaches the slope $-1/(n_r m)$, where n_r is the number of filaments in the bundle.

EVALUATION OF THE EFFECTIVE BUNDLE LENGTH

Now let us assume that two sets of strength data $\mu_{\sigma_b}^{\text{test}}$ and $\mu_{\sigma_y}^{\text{test}}$ are available for two respective test lengths falling into the different length ranges described in Section (2), i.e. $l_b^{\text{test}} < l_b^*$ and $l_y^{\text{test}} > l_b^*$. Apart from the known specimen lengths and the measured mean strengths, the knowledge of the value of Weibull modulus m of the tested material and the value of the autocorrelation length l_ρ is required. The estimation of the transitional length l_b^* is then performed using the following procedure:

1. From the mean strength $\mu_{\sigma_b}^{\text{test}}$ estimated as the average strength for the length l_b^{test} and the filament parameters l_ρ and m the scaling parameter s_b of the Weibull distribution for the tested length is obtained as:

$$s_b = \mu_{\sigma_b}^{\text{test}} \cdot \left[m^{-1/m} \cdot c + n_r^{-2/3} \cdot m^{-(1/m+1/3)} \exp\left(-\frac{1}{3m}\right) \lambda \right]^{-1} \quad (2)$$

2. With the scaling parameter s_b at hand, the corresponding standard deviation γ_{σ_b} gives

$$\gamma_{\sigma_b} = s_b \cdot m^{-1/m} \sqrt{c_m \cdot (1 - c_m)}. \quad (3)$$

with $c_m = \exp\left(-\frac{1}{m}\right)$.

3. The obtained bundle characteristics are scaled to the unknown length l_b^* using the fact that all quantiles of the Weibull distribution are scaled in the same way:

$$\mu_{\sigma_b}^* = \mu_{\sigma_b}^{\text{test}} \cdot \frac{f(l_b^*)}{f(l_b^{\text{test}})} \quad \text{and} \quad \gamma_{\sigma_b}^* = \gamma_{\sigma_b}^{\text{test}} \cdot \frac{f(l_b^*)}{f(l_b^{\text{test}})}.$$

Here, $f(\cdot)$ stands for the scaling function.

4. The chaining effect involved in the experimental data is now expressed for the unknown bundle length l_b^* :

$$H_{n_b, n_r}(x) = 1 - [1 - G(x)]^{n_b}, \quad x \geq 0, \quad (4)$$

where $H_{n_b, n_r}(x)$ and $G(x)$ are the distribution functions of the chained yarn and a single bundle, respectively, and n_b is the number of serially coupled bundles in the yarn.

5. The set of non-linear equations is then solved for l_b^* using numerical root finding methods.

ACKNOWLEDGEMENTS

The work has been supported by the German Science Foundation under the project number CH276/1-1. Additionally, the work of the first and third authors has also been supported by the Czech Science Foundation under the projects no. 103/09/H085 and P105/10/J028. This support is gratefully acknowledged.

REFERENCES

- Chudoba, R., Vořechovský, M. & Rypl, R. (2011). Identification of the effective bundle length in a multifilament yarn from the size effect response. *Journal of Composite Materials*, in press.
- Daniels, H.E. (1945). The statistical theory of the strength of bundles of threads. i. *Proceedings of the Royal Society of London. Series A, Mathematical and Physical Sciences* 183(995), 405–435.
- Smith, R.L. (1982). The asymptotic distribution of the strength of a series-parallel system with equal load-sharing. *The Annals of Probability* 10(1), 137–171.

GS_132 — Probabilistic modeling in engineering (3)

This page intentionally left blank

Probabilistic wind-borne debris trajectory model for building envelope impact risk assessment

Michael Grayson, Weichi Pang & Scott Schiff
Civil Engineering Department, Clemson University, Clemson, SC, USA

1 INTRODUCTION

This paper presents a probabilistic debris flight trajectory model adapted from the deterministic 6-Degree-of-Freedom (6-DoF) model presented by Richards et al. 2008, in which both the aleatoric (inherent) and epistemic (knowledge-based) uncertainties will be considered in the proposed probabilistic model. While the inherent randomness (aleatoric uncertainty) in the debris flight trajectory is irreducible due to the wind turbulence, variation in wind direction, gustiness of the wind event and so forth, the proposed probabilistic model seeks to address these uncertainties through the application of the appropriate statistical methods. The proposed probabilistic model will provide an effective method for predicting debris trajectories in a three-dimensional (3D) space, which is imperative when performing regional building envelope impact risk assessment in which a large amount of debris sources and targets must be considered in the simulation.

2 DETERMINISTIC TRAJECTORY MODEL

An understanding of the orientation of the debris principal axes (i.e., X_p , Y_p , Z_p) with respect to the fixed translating axes (i.e., X_G , Y_G , Z_G) is necessary for the transition of the deterministic trajectory model to the probabilistic trajectory model. The orientation of the debris in relation to the translating ground axes is defined by three position angles: pitch (α), yaw (β), and roll (ϕ) with respect to the X-axis.

The angle of attack (ϵ) and the tilt angle (γ) are the debris flow angles that are observed between the debris relative velocity, and the debris principal Y_pZ_p -plane and the debris principal X_pZ_p -plane, respectively. Results from wind tunnel tests performed by Richards et al. (2008) clearly illustrated that the normal force, which is the only significant force for plates, is a function of the angle of attack and the tilt angle.

Due to the dependence of the force and moment coefficients on the calculation of the angle of

attack and the tilt angle within the Richards et al. (2008) debris trajectory model, it was appropriate that the randomness required for a probabilistic model would be incorporated into the deterministic model at these points. Therefore, the angle of attack and the tilt angle were modified within the deterministic debris trajectory model to use the calculated values of the flow angles obtained from the deterministic model as the mean value, which was then utilized to sample from a statistical distribution at the start and end of each time step.

3 PROBABILISTIC TRAJECTORY MODEL

Limited experimental data on the statistical distribution of the debris flow angles during flight required that certain assumptions be made at the outset of the transition to a probabilistic debris trajectory model. Due to the range of the flow angles as defined by Richards et al. (2008), it was assumed that the flow angles had an equal chance of occurring on either side of the mean as calculated by the deterministic debris trajectory model; therefore this warranted the assumption that the

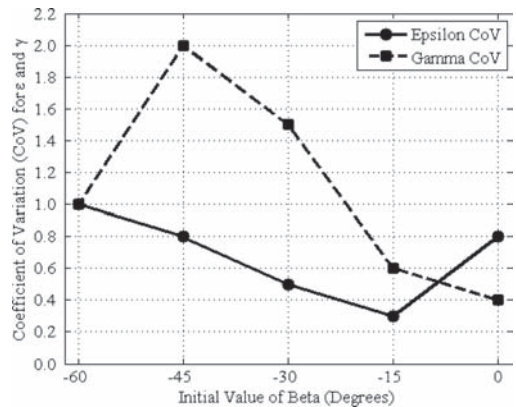


Figure 1. Graphical representation of the coefficients of variation for the angle of attack (ϵ) and the tilt angle (γ) determined by the parametric study.

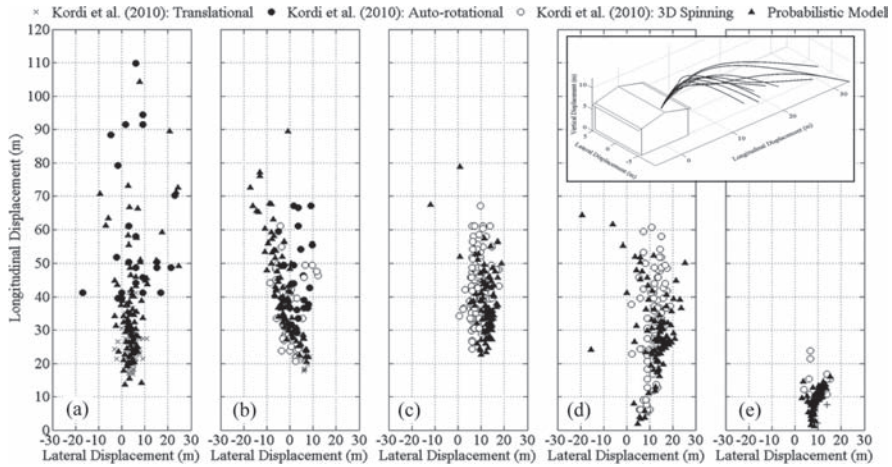


Figure 2. Comparison of simulated ground impact locations of 1.2 m × 2.4 m × 12.7 mm roof sheathing panel to test data provided by Kordi et al. (2010) for wind directions of (a) 0°, (b) 15°, (c) 30°, (d) 45°, (e) 60°.

appropriate statistical distribution was a normal distribution for both flow angles.

In order to determine appropriate values of the Coefficient of Variation (CoV) for a normal distribution, a parametric study was performed by varying the coefficients of variation for the angle of attack and the tilt angle in increasing increments of 0.1 from a minimum CoV = 0.1 up to a maximum CoV = 2 for five wind directions: 0°, 15°, 30°, 45° and 60°. Figure 1 depicts the values of the coefficients of variation for the debris flow angles as determined by the parametric study. Note that the values of the initial yaw (β_0), used to represent the change in the wind direction in the model, are negative in Figure 1 to replicate the experimental setup of Kordi et al. (2010) within the probabilistic trajectory model.

Typically, numerical models that utilize a uniform horizontal wind flow are unable to account for the variations in the velocity field due to the aerodynamics of the building and the local velocities; therefore, by sampling from a normal distribution with flow angle CoVs that produce results that correspond with test data produced by the scaled failure model tests of Visscher & Kopp (2007) and Kordi et al. (2010), the aleatoric uncertainty is encapsulated within the CoV terms.

The values of the CoV of the angle of attack and the tilt angle were verified by plotting the simulated ground impact locations to the test data provided by Kordi et al. (2010). The modes of flight

identified by Visscher & Kopp (2007) and Kordi et al. (2010) (e.g., translational, auto-rotational, and 3D spinning) were not tracked in this study; however, regardless of the mode of flight illustrated during the simulated flight of the roof sheathing panels, there is good agreement between the simulated ground impact locations and that provided by Kordi et al. (2010). Figure 2 illustrates ten simulations of a full-scale roof sheathing panel performed utilizing the probabilistic debris trajectory model.

4 CONCLUSION

A deterministic 6-DoF debris trajectory model has been modified to perform as a probabilistic model in this paper. By adapting the model to provide results that match physical test data, both the aleatoric and epistemic uncertainty have been addressed by incorporating error usually associated with uniform horizontal flow debris trajectory models into the coefficients of variation used to sample the angle of attack and the tilt angle of a roof sheathing panel from a normal distribution. The proposed probabilistic model provides an effective method for predicting debris trajectories in a 3D space, which is imperative when performing regional building envelope impact risk assessment in which a large amount of debris sources and targets must be considered in the simulation.

Reliability estimation of deteriorated RC-structures considering various observation data

Ikumasa Yoshida

Department of Urban and Civil Engineering, Tokyo City University, Tokyo, Japan

Mitsuyoshi Akiyama

Department of Civil and Environmental Engineering, Tohoku University, Sendai, Japan

1 INTRODUCTION

Reliability estimation for existing structures with physical model is discussed. It is essential to update the physical model with reflecting observation or inspection data for an existing structure. The reliability has to be estimated based on the updated model. That is, however, more difficult than that of newly constructed structures. The updated PDF is not expressed in simple form in general. The complexity of the solution in Bayesian updating arises from nonlinearity of the state, observation equations and/or non-Gaussian PDF of related uncertainties. Approximate solutions of the problem can be found by several approaches. Monte Carlo (MC) approach attracts more and more attention because of its versatility. This line of methods is referred by many terms, but, in this paper, the term Sequential MCS (SMCS) is used. The methodology can be extended to reliability estimation quite easily. Its outline is illustrated in Figure 1.

Accuracy estimation is one of the important issues when MC approach is adopted. Specially

SMCS approach has a problem known as degeneracy. Effective sample size is introduced to predict the accuracy of estimated limit state exceeding probabilities. The proposed method is demonstrated through a numerical example of reliability analysis on deteriorating RC structures.

2 NUMERICAL EXAMPLE AND ACCURACY OF ESTIMATED PROBABILITIES

It is shown how the proposed method can be used to predict stochastic deterioration relating to the long-term chloride corrosion in a reinforced concrete bridge pier. It is assumed that the bridge is located at 0.1 km from coastline in Niigata city of Japan.

Figure 2 shows limit state probabilities over time, which are updated 30 years after construction by visual inspection and/or chloride concentration profiling. Three limit states, 1) initiation of corrosion of rebar, 2) initiation of concrete crack, 3) degradation of member strength, are considered. The random variables of the model are updated by the assumed observation data set. Consequently the limit state probabilities are also updated.

In Case 1 which uses visual inspection rank I (no crack is observed on concrete surface) as observation data, the probabilities of all limit states are decreased after the observation updating. In Cases 2 and, 3, the probabilities are increased after the updating naturally since rank II, III means observation of crack on concrete surface. It is noted the probabilities are updated though the information obtained by visual inspection is too small to identify model parameters. This difficulty in inverse or parameter identification problem is well known as ill-posedness or multicollinearity problem. In addition to visual inspection result I, chloride concentrations through depth by coring test are considered as observation data in case 4, 5 and 6.

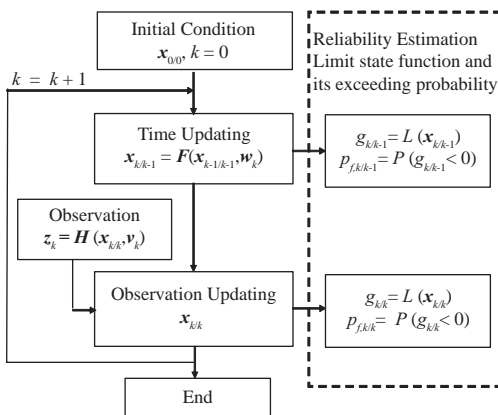


Figure 1. Flowchart of the proposed method.

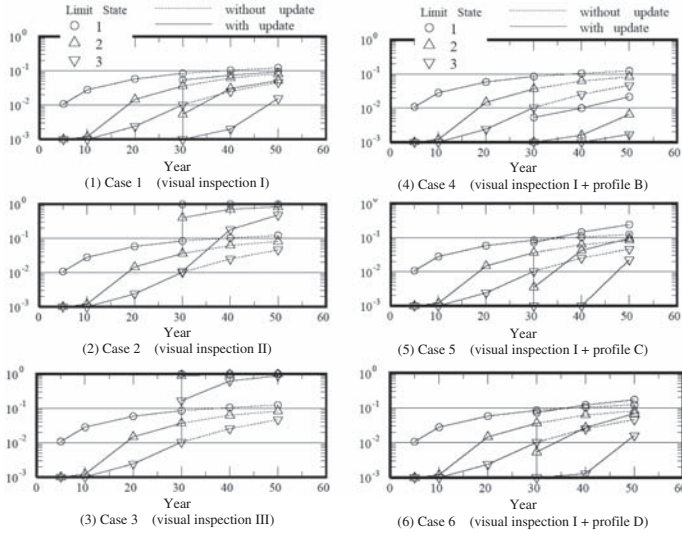


Figure 2. Three kinds of limit state probabilities over time.

3 DEGENERACY IN SMCS

SMCS has a problem known as degeneracy or sample impoverishment, which causes reduction of accuracy.

COV (Coefficient of Variance) of probability p estimated by ordinary MCS can be predicted by

$$COV = \sqrt{\frac{1-p}{np}} \tag{1}$$

where n is the number of sample in MCS. This equation is obtained assuming that each sample is perfectly independent. Equation (1) indicates theoretical lower limit of COV of a probability calculated by SMCS. The degree of degeneracy can be estimated by following indicator, effective number N_{eff} .

$$N_{eff} = \frac{1}{\sum_{i=1}^n (a_k^{(j)})^2} \tag{2}$$

When likelihood of all samples are same, we have $a_k^{(j)} = 1/n$, consequently $N_{eff} = n$. When likelihood of one specific sample is 1.0 and those of the other are 0.0 as opposite extreme case, we have $N_{eff} = 1$. Effective sample ratio is introduced for numerical experiments of accuracy, which is defined by

$$R_{eff} = \frac{N_{eff}}{n} \tag{3}$$

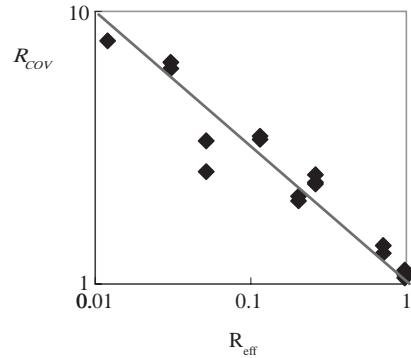


Figure 3. Effective Sample Ratio R_{eff} and R_{COV} Ratio to Theoretical lower limit COV.

In order to examine the accuracy depending on the degeneracy level R_{eff} , the calculation of probabilities updated by SMCS is repeated 100 times with different seed of random number. COV of estimated probabilities is calculated based on the 100 estimated probabilities. Sample size of SMCS is 10000. Parameter R_{COV} that shows efficiency or accuracy is introduced and defined as ratio of obtained COV to the theoretical COV. Changing the standard deviation, type of observation, we obtained many pairs R_{eff} and R_{COV} , which are shown in Figure 3. The obtained R_{COV} is almost proportional to effective sample ratio R_{eff} in logarithmic space. It indicates that we can predict accuracy level, namely, COV of probabilities calculated by SMCS, substituting effective number N_{eff} obtained by Eq. (2) into Eq. (1).

A Bayesian framework to predict deformations during supported excavations based on a semi-empirical method

J.-K. Park, P. Gardoni & G. Biscontin

Zachry Department of Civil Engineering, Texas A&M University, College Station, USA

ABSTRACT: Evaluating the magnitude and distribution of ground movements adjacent to a supported excavation is an important part of the design process when excavating in an urban environment. Structural design methods, empirical/semi-empirical methods, theoretical limit state soil mechanics methods, and numerical modeling methods have been increasingly applied to the design of excavation support systems to achieve safe and cost effective systems.

Empirical/semi-empirical methods are the most commonly used to predict the induced ground movements due to a supported excavation. However, empirical/semi-empirical methods have five limitations. First designs based on empirical/semi-empirical methods can be overly conservative in sensitive design scenarios, especially when dealing with layered soil conditions and complex geometries. Second, much of the current empirical/semi-empirical methods have evolved from important empirical observations carried out since the 1940's with the construction of subway systems in Berlin, Chicago, New York, and Oslo. The construction material, method and stiffness of support systems have been improved to both enhance the safety and reduce ground movements. Third, empirical/semi-empirical methods do not account for the characteristics of the site-specific soil and loading conditions. Fourth, the empirical/semi-empirical methods have incomplete linkage between horizontal displacements and surface settlements. Fifth, they do not account for the uncertainty in the estimates of the deformations and therefore they cannot be used to assess the degree of safety of a design. A method is needed to calibrate and update empirical/semi-empirical methods based on site-specific measurement data as they become available during the excavation process.

This paper presents a Bayesian framework to update the predictions of ground movements in the later stages of excavation based on recorded deformation measurements. The posterior statistics of the unknown soil properties and model parameters are computed using an efficient Markov Chain Monte Carlo (MCMC) simulation

method. Markov chains are generated with the likelihood formulation of the probabilistic models based on the initial points and a prior distribution until a convergence criterion is met. The proposed approach provides better estimates of the deformations during supported excavations and properly account for the relevant uncertainties so that the actual reliability of the supported excavation system can be assessed.

Analysis of excavation-induced ground movements generally consists of the following four steps: (1) estimate the maximum horizontal displacement, $\delta_{h,max}$; (2) estimate the deformation ratio, $\theta_R = \delta_{h,max} / \delta_{v,max}$, where $\delta_{v,max}$ is the maximum surface settlement; (3) calculate $\delta_{v,max}$; and (4) estimate the surface settlement profile. In this paper, we have used Clough and O'Rourke (1990) chart to estimate $\delta_{h,max}$, $\delta_{v,max}$ and Kung et al. (2007) equations to estimate a surface settlement profile. A mathematical description of these curves is needed to update the predictions of the ground movements in the later stages of excavation based on recorded deformation measurements. The Box and Cox transformation is used to define analytical expressions for the curves in Clough and O'Rourke chart.

A probabilistic model that describes the deformation at the k th excavation stage can be written as

$$D_k = \hat{d}_k(\boldsymbol{\theta}_{CO}) + \sigma \varepsilon_k, \quad k = 1, \dots, m \quad (1)$$

where, D_k = the measured $\delta_{h,max}$ or $\delta_{v,max}$, \hat{d}_k = the deformation estimate by Clough and O'Rourke (1990) chart, $\boldsymbol{\theta}_{CO} = (\theta_{Sub}, \theta_{Sub}, \theta_R)$ = a set of unknown parameters, $\sigma \varepsilon_k$ = the model error, σ = the unknown standard deviation of the model error, ε_k = a random variable with zero mean and unit variance. In assessing the probabilistic model, the following three assumptions are made: (a) the model variance σ^2 is independent of $\boldsymbol{\theta}$ (homoskedasticity assumption), (b) ε_k follows the normal distribution (normality assumption), (c) ε_k at two different excavation stages are uncorrelated.

However, Clough and O'Rourke (1990) chart only gives the normalized maximum horizontal

displacement and the surface settlement as deformation estimates. Both the location of the maximum horizontal displacement and its profile cannot be estimated from the chart, so the arbitrary forms of the distribution function for deformations are needed to be compared with the field measurement inclinometer reading data taken at regular intervals. In this study, the focus was on the assessment of the three dimensional deformation shapes that develop perpendicular and parallel to an excavation.

The form of the fitting function (shown in Figure 1) for the three dimensional deformation shapes is established through numerous trial-and-error analyses after checking with different forms of distribution function with an objective of maintaining simple functional form and easily understandable for the engineers. The three dimensional ground movement distribution around the excavated area is predicted using a combination of fitting function, an assessment of the maximum ground deformation, and knowledge of the geometry of the excavation.

The proposed probabilistic approach is applied to an actual supported excavation project for the Robert H. Lurie Medical Research Building in Evanston, Illinois. The prior distribution models are selected depending on the range of the parameters. The means are based on the previous research results. The standard deviations are based on an assumed value for the coefficient of variation.

The predicted values capture accurately the horizontal displacement (as shown in Figure 2), the settlement profile and the location of the maximum surface settlement (as shown in Figure 3).

A Bayesian approach is used to assess the unknown soil parameters by updating prior information based on site specific field measurement data. The updated model parameters are then used to develop new and more accurate predictions of the deformations in the subsequent stages until the end of the excavation project.

The key advantage of this proposed approach for practicing engineers is that they can use a

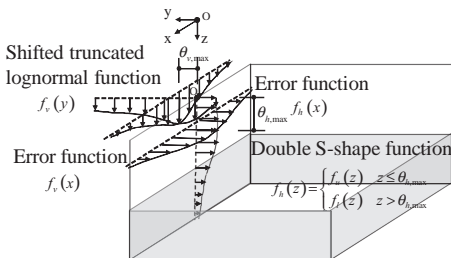


Figure 1. Each function describing the three-dimensional ground movements.

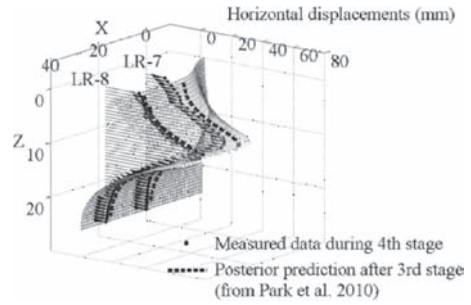


Figure 2. Comparison of measured and predicted horizontal displacements based on posterior estimates for Lurie case (after stage 3).

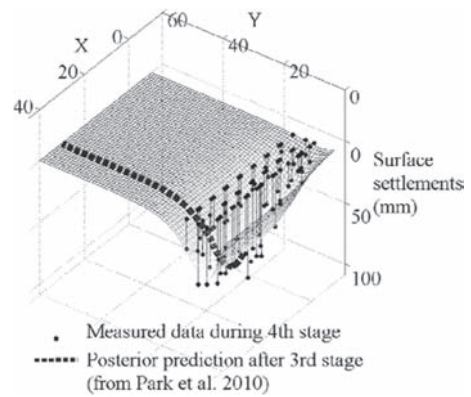


Figure 3. Comparison of measured and predicted surface settlements based on posterior estimates for Lurie case (after stage 3).

semi-empirical chart together with a simple calculation, to evaluate three-dimensional displacement profiles without the need for constitutive laws and complex calculations. The proposed approach can also be used for an adaptive reliability-based optimal design of the excavation system in which the design is modified after each excavation stage to minimize costs and maintain a minimum reliability requirement.

REFERENCES

Clough, G.W. & O'Rourke, T.D. (1990). "Construction Induced Movements of Insitu Walls." Design and Performance of Earth Retaining Structures, L.A.H. Philip Lambe, ed., ASCE, Ithaca, New York, 439-470.

Kung, G.C., Juang, C.H., Hsiao, E.L. & Hashash, Y.A. (2007). "Simplified model for wall deflection and ground-surface settlement caused by braced excavation in clays." Journal of Geotechnical and Geoenvironmental Engineering, 133(6), 731-747.

Effects of structural uncertainty/variability on the linear and yielding response of a shear frame

C.R. Wharton & T.L. Attard
 University of Tennessee, Knoxville, TN, USA

A. Chaudhary & M.P. Mignolet
 Arizona State University, Tempe, AZ, USA

This investigation focuses on the development and exemplification of a comprehensive methodology for the inclusion of uncertainty in mass, stiffness, and post-yield properties in nonlinear dynamic analysis of structures exhibiting yielding. The maximum entropy-based nonparametric approach (Soize, 2000, 2008, Mignolet & Soize, 2008) is proposed here for the statistical modeling of these uncertainties while the post-yield analysis is carried out using a recently introduced material degradation model (Attard, 2005, Attard & Mignolet, 2008).

The structure chosen to exemplify the methodology is the 4-story shear frame of Figure 1 analyzed in physical coordinates.

The mass and stiffness matrices of the system of Figure 1(b) exhibit specific topological constraints implying that:

- a. the off-diagonal elements of the mass matrix;
- b. the 13, 14, and 24 elements of the stiffness matrix are zero, and
- c. relations exist between the diagonal and off-diagonal elements of the stiffness matrix.

In fact, these topological constraints imply that there is only one random mass and one random stiffness per degree of freedom that need to be specified. The inclusion of these particular constraints within the maximum entropy framework is first performed. It leads to a nonparametric uncertainty modeling approach that maintains the topology observed here. A comparison is next made between the responses of uncertain linear shear frames satisfying and violating the topological constraints. Surprisingly, it is found that the power spectra of the responses, see Figure 2 are extremely close suggesting for this structure that a slight violation of the topology by the uncertainty model has only a small effect.

Next, yielding was introduced in the computations using a recently formulated degradation

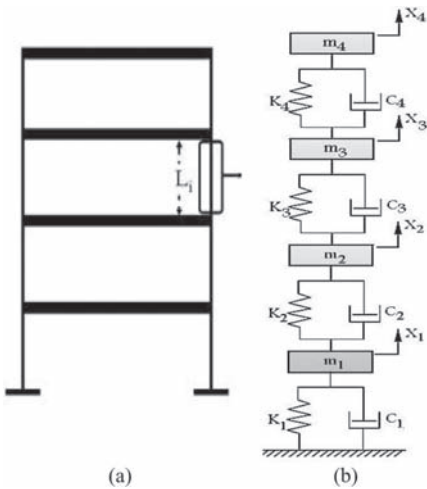


Figure 1. (a) 4-story shear frame. (b) 4 degree of freedom lumped mass model of (a). From Attard & Mignolet (2008).

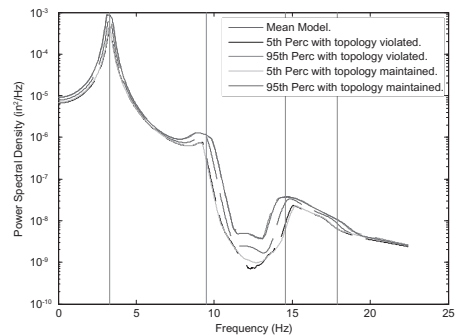


Figure 2. Comparison of the non parametric approach considering the topology and disregarding it. Power spectral density of the top floor displacement and its 5th and 95th percentiles. The vertical lines indicate the natural frequencies. Uncertainty in stiffness.

model and uncertainty was introduced in the mass matrix (option 1), linear stiffness matrix (option 2), and linear stiffness matrix and post-yield behavior (option 3) using the topology preserving nonparametric approach. For each option, the nonlinear yielding response of 100 shear frames to random ground motions characterized by the same spectrum was determined. This population of response records was then analyzed and it was found that:

1. the *mean* response of the shear frames is very similar to the response of the mean, deterministic structure but that,
2. a large scatter in the response does occur due to even a small uncertainty level (e.g. 8%–10%) in the mass and stiffness properties, see Figure 3 and Table 1,
3. the variability of the post yield characteristics (e.g. displacement after yield, post-yield stress) are noticeably more affected by the uncertainty in stiffness than in mass and that both the uncertainties in the linear stiffness matrix and the post-yield behavior are important factors, see Figure 3, and Table 1,
4. the variability in the overall response, i.e. in the power spectral density of the physical response of a particular floor, is affected quite similarly by the mass and stiffness uncertainties as in the linear case with a small effect of the presence

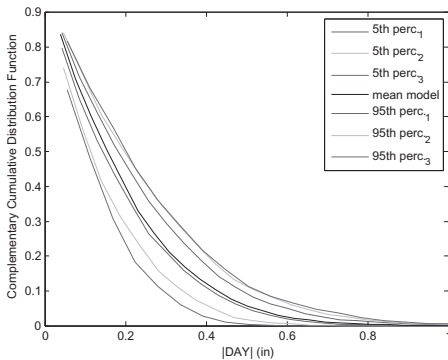


Figure 3. Complementary cumulative distribution function of the displacement after yield of the bottom floor (in magnitude); mean and 5th and 95th percentiles for all uncertainty options (1 = mass matrix, 2 = linear stiffness matrix, 3 = Young's modulus).

Table 1. Probabilities for the displacement after yield of the bottom floor column to exceed 0.5 for the three uncertainty options and the mean model.

Mean model	5th perc. mass	95th perc. mass	5th perc. stiff.	95th perc. stiff.	5th perc. young	95th perc. young
0.0570	0.0501	0.0934	0.0166	0.1138	0.0034	0.1172

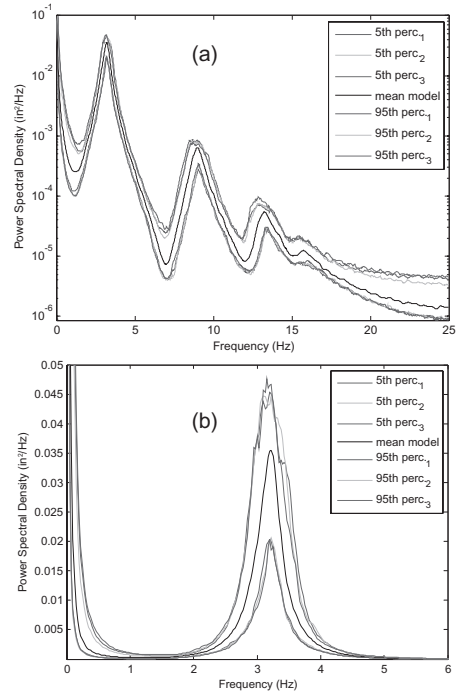


Figure 4. Power spectral density of the response of the top floor; mean and 5th and 95th percentiles for all three uncertainty options (1 = mass matrix, 2 = linear stiffness matrix, 3 = Young's modulus). (a) Log-linear scales, (b) linear-linear scales.

or absence of uncertainty in the post-yield characteristics, see Figure 4.

REFERENCES

Attard, T.L. 2005. Post-yield material nonlinearity: optimal homogeneous shear-frame sections and hysteretic behavior. *International Journal of Solids and Structures* 42: 5656–5668.

Attard, T.L. & Mignolet, M.P. 2008. Random plastic analysis using a constitutive model to predict the evolutionary stress-related responses and time passages to failure. *Journal of Engineering Mechanics* 134: 881–891.

Mignolet, M.P. & Soize, C. 2008. Nonparametric stochastic modeling of linear systems with prescribed variance of several natural frequencies. *Probabilistic Engineering Mechanics* 23: 267–278.

Soize, C. 2000. A nonparametric model of random uncertainties on reduced matrix model in structural dynamics. *Probabilistic Engineering Mechanics* 15: 277–294.

Soize, C. 2008. Construction of probability distributions in high dimension using the maximum entropy principle: Applications to stochastic processes, random fields and random matrices. *International Journal for Numerical Methods in Engineering* 76: 1483–1611.

Non-parametric Bayesian updating within the assessment of reliability for offshore wind turbine support structures

J.G. Rangel-Ramírez

Aalborg University, Denmark

J.D. Sørensen

Aalborg University and RISØ-DTU, Denmark

ABSTRACT: Monitoring systems for Offshore Wind Turbines (OWT) have been developed due to the desire to increase the reliability, availability, efficiency and competitiveness of wind industry. Information from the monitoring systems can be used to update the prior knowledge about uncertain variables, resulting in a more accurate assessment of structural reliability during the life cycle. Further, the information can be used to update the operation and maintenance planning.

Classical Bayesian Updating (CBU) is a widespread updating approach for decision makers. The parametric form and simplicity of handling the information are the main advantages of CBU. However, when multi-parametric updating is considered, the CBU approach is not a straightforward option anymore; not only for the parametric treatment but also for integrating it into assessment of the reliability. Non-Parametric Bayesian Updating (NPBU) can be used for multi-parametric updating. However, the resulting updating distribution is not easily integrated in a reliability assessment and should e.g. be integrated in the reliability analysis through an orthogonal polynomial approximation model. In NPBU discrete approximations or simulation approaches are used. Gibbs Sampling (GS) is a sample technique belonging to Monte Carlo Markov Chain (MCMC) methods and represents a better approach for addressing more intricate and/or hierarchical arrangements of the unknown parameters.

In this paper, NPBU is used for assessment of reliability for offshore wind turbine support structures. For integrating the new information into the Structural Reliability Analysis, a third-order Hermite-Chaos polynomial approximation is used. Applications of discrete updating and the GS approach are shown.

The inference of univariate models through Bayesian statistics can be carried out by just applying the Bayesian updating formula:

$$f_{\psi}(\psi | \hat{z}) = \frac{f_z(\hat{z} | \psi) f_{\psi}(\psi)}{\int_{\psi} f_z(\hat{z} | \psi) f_{\psi}(\psi) d\psi} \quad (1)$$

where $f_{\psi}(\psi)$ is the prior distribution of the vector ψ of statistical parameters and represents the beliefs concerning the statistical parameters of the probability density function (PDF) $f_z(Z)$ of the stochastic variables Z . The predictive distribution of Z is representing the current predictions of the probabilistic distribution of Z and can be calculated with:

$$f_z(z | \hat{z}) = \int_{\psi} f_z(z | \psi) f_{\psi}(\psi | \hat{z}) d\psi \quad (2)$$

where $f_z(z | \hat{z})$ is the predictive distribution function of z conditional on the new samples \hat{z} .

The Discrete semi (or non-) conjugated updating (DSCU) technique belongs to the non-parametric updating techniques. It avoids correlation inherited by mixing the priors' notation for multi-parameter density functions. Moreover, DSCU is more efficient for numerical implementation compared with the entire evaluation of equation (1). The relative posterior discrete density function is calculated by

$$\nu_d(\psi_m | \hat{z}_1, \hat{z}_2, \dots, \hat{z}_n) = \frac{p(\psi_m, \hat{z}_1, \hat{z}_2, \dots, \hat{z}_n)}{\sum_{i_1, \dots, i_m} p(\psi_{i_1, i_2, \dots, i_m}, \hat{z}_1, \hat{z}_2, \dots, \hat{z}_n)} \quad (3)$$

where $p(\psi_m, \hat{z}_1, \hat{z}_2, \dots, \hat{z}_n)$ is the joint probability distribution of the parameters $\psi_m = (\psi_1, \psi_2, \dots, \psi_m)$ to be updated using the sample $\hat{z} = (\hat{z}_1, \hat{z}_2, \dots, \hat{z}_n)$. m refers to the number of parameters.

As a part of MCMC algorithms, GS represents a suitable simulation technique to estimate the posterior probability density function. Compared to crude Monte Carlo simulation, the GS algorithm uses a more elaborated iterative sampling technique but is still rather simple. In essence, simulation of sequences of samples with parameters $\psi^{(s)} = \{\psi_1^{(s)}, \psi_2^{(s)}, \dots, \psi_m^{(s)}\}$, $\psi^{(s+1)} = \{\psi_1^{(s+1)}, \psi_2^{(s+1)}, \dots, \psi_m^{(s+1)}\}$ is based on the following recursive algorithm:

1. $\psi_1^{(s+1)} \sim p(\psi_1 | \psi_2^{(s)}, \dots, \psi_m^{(s)}, \hat{z}_1, \hat{z}_2, \dots, \hat{z}_n);$
2. $\psi_2^{(s+1)} \sim p(\psi_2 | \psi_1^{(s+1)}, \dots, \psi_m^{(s)}, \hat{z}_1, \hat{z}_2, \dots, \hat{z}_n) \dots$
3. $\psi_m^{(s+1)} \sim p(\psi_m | \psi_1^{(s+1)}, \psi_2^{(s+1)}, \dots, \psi_{m-1}^{(s+1)}, \hat{z}_1, \hat{z}_2, \dots, \hat{z}_n) \dots$
4. $\psi^{(s+1)} = \left\{ \psi_1^{(s+1)}, \psi_2^{(s+1)}, \dots, \psi_m^{(s+1)} \right\}$
5. Initializing
 $\psi_1^{(s+2)} \sim p(\psi_1 | \psi_2^{(s+1)}, \dots, \psi_m^{(s+1)}, \hat{z}_1, \hat{z}_2, \dots, \hat{z}_n)$

In this work, the one dimensional case with third order chaos expansion the series is used and calculated in an optimization scheme where the least-square error obtained from the k -central moments is minimized. The ‘‘Wiener-Hermite chaos’’ polynomial function is used assuming the underlying stochastic process is Gaussian. The Gaussian stochastic process can be approximated by the following series:

$$\begin{aligned}
 X(\omega) = & a_0 H_0 + \sum_{i_1=1}^{\infty} a_{i_1} H_1(\xi_{i_1}(\omega)) \\
 & + \sum_{i_1=1}^{\infty} \sum_{i_2=1}^{i_1} a_{i_1, i_2} H_2(\xi_{i_1}(\omega), \xi_{i_2}(\omega)) \\
 & + \sum_{i_1=1}^{\infty} \sum_{i_2=1}^{i_1} \sum_{i_3=1}^{i_2} a_{i_1, i_2, i_3} H_3(\xi_{i_1}(\omega), \xi_{i_2}(\omega), \xi_{i_3}(\omega)) + \dots,
 \end{aligned} \tag{3}$$

The term $H_n(\xi_1, \dots, \xi_n)$ is the Hermite-Chaos term of order n in the standard Gaussian variables (ξ_1, \dots, ξ_n) with zero mean and unit variance.

The design equation for a single offshore wind turbine (not within a wind farm) can be written:

$$\begin{aligned}
 G(z) = & 1 - \frac{\nu FDF T_L}{K_c} \int_{U_{in}}^{U_{out}} \left[(1 - N_w p_w) D(m; \sigma_{\Delta\sigma}(U, z)) \right. \\
 & \left. + p_w \sum_{j=1}^{N_w} D(m; \sigma_{\Delta\sigma, j}(U, z, j)) \right] f_U(U) dU
 \end{aligned} \tag{4}$$

where ν is the number of stress cycles per year, FDF is the fatigue design factor, T_L is the design life time, K_c is characteristic value of K (material parameter in SN-curve), U_{in} and U_{out} are the cut-in and –out wind speeds, m is the Wöhler exponent in SN-curve, $f_U(U)$ is the probability density function of mean wind speed U , z is a design parameter and D represents the expected value of fatigue damage for the all stress ranges given a mean wind speed U and standard deviation of stress ranges $\sigma_{\Delta\sigma}$. To assess the reliability for wind turbines within a wind farm the following limit state equation is used:

$$\begin{aligned}
 & g(t) = \Delta \\
 & - \frac{\nu t}{K} (X_w X_{SCF})^m \int_{U_{in}}^{U_{out}} \int_0^{\infty} \left[(1 - N_w p_w) D(m; \sigma_{\Delta\sigma}(U, z)) \right. \\
 & \left. + p_w \sum_{j=1}^{N_w} D(m; \sigma_{\Delta\sigma, j}(U, z, j)) \right] f_{\sigma_u}(\sigma_u | U) f_U(U) d\sigma_u dU
 \end{aligned} \tag{5}$$

with

$$\sigma_{u, j} = \sqrt{\frac{X_{wake} U^2}{(1.5 + 0.3 d_j \sqrt{U/c})^2} + \sigma_u^2} \tag{6}$$

Δ , X_w , X_{SCF} and X_{wake} represent the uncertainties related with the Miner rule of damage accumulation, wind load effects, local stress concentration and analysis, and the uncertainty related to the wake turbulence conditions coming from surrounding wind turbines. t is the reference time and f_{σ_u} is the probability density function for free flow.

As an example a welded detail in a wind turbine support structure is considered and the support structure is assumed to have a design lifetime, $T_L = 20$ years. The fatigue life T_F for the component is assumed to be 40 years ($FDF = 2$). It is assumed that a meteorological mast provides samples of the variables representing the uncertainty related with the wind and wake condition, X_w and X_{wake} . Figure 1 shows results where it is assumed that the reliability is updated each year sequentially using the information obtained the latest year.

The results in this paper show the influence on the time dependent updated reliability when non-parametric and classical Bayesian approaches are used. Further, the influence on the reliability of the number of updated parameters is illustrated.

The phenomenological uncertainty is reduced with the new information, coming from the external measurements and condition monitoring of OWT. The illustrative examples show the impact of Bayesian updating methods in the assessment of reliability and a clear influence of the chosen prior and updating approach.

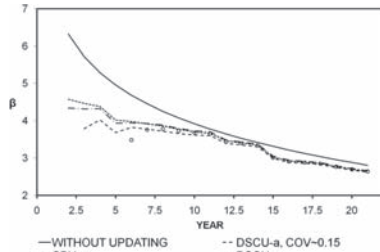


Figure 1. Reliability indices of the assessment of reliability of the general cases 1–4 and 7.

GS_212 — Probabilistic modeling in engineering (4)

This page intentionally left blank

Software for multi-model reliability analysis

M. Mahsuli & T. Haukaas

University of British Columbia, Vancouver, BC, Canada

In the past, a central objective in the structural reliability community has been the development of accurate and efficient reliability methods. FORM, SORM, response surface methods, and sampling schemes are among the significant accomplishments. The authors of this paper contend that, at this time, a renewed focus on modelling rather than analysis is necessary.

In current practice, engineering analyses are often carried out with simplified analytical models. When applicable, such models will remain essential to foster basic physical understanding and to check the results from more complex analysis. However, such models are often associated with unknown predictive capability. In fact, many models are developed with a conservative philosophy, *i.e.*, to achieve designs that are “on the safe side.”

Conversely, modern engineering, exemplified by performance-based structural engineering, aims at making predictive estimates for complex phenomena. For example, the losses associated with future earthquakes are sought. The structural reliability community has an important role to play in this new paradigm.

A central postulation in this paper is that reliability methods in conjunction with multiple sophisticated probabilistic models is a powerful alternative to analytical probabilistic integration. In fact, the proposed reliability-based approach can be viewed as an alternative to the “PEER integral” and similar analytical integration techniques.

In the approaches that are most popular at present, the models are often formulated as conditional probabilities. For example, damage models (often presented as fragility curves) estimate the probability of exceeding various damage states for a given ground shaking intensity.

An alternative strategy is called unified reliability analysis, in which each model produces measurable parameter realizations, not probabilities. In other words, given realizations of the random variables that describe the parameter and model uncertainty, a unique realization of the response is produced.

This paper discusses the unified reliability approach and presents a new comprehensive computer program to carry out such analyses.

The program is called **Rt** and is freely available at www.inrisk.ubc.ca. An array of software features and potential applications are presented in this text, while another paper at this conference presents specific models and a comprehensive risk analysis for the Metro Vancouver region in Canada.

Ongoing work is aimed at creating a library of advanced probabilistic models for hazards, infrastructure, and consequences within the **Rt** framework. Many models are already implemented.

In this paper, a series of modelling, analysis, and software features are presented and discussed. The reader is encouraged to visit the aforementioned website for up-to-date information about models and analysis options.

It is the authors’ experience that the suggested use of reliability methods—*e.g.* in performance-based engineering—triggers some trepidation in many engineers. Consequently, an important motivation for the **Rt** software is to make multi-model reliability analysis available to the broad civil engineering community. To the extent that this is possible, it is achieved by developing a user-friendly and robust software application. To this end, the user interface for **Rt** contains four “panes” as shown in Figure 1. In respective panes, the user creates and modifies models, parameters, functions, and analysis settings. The Central Pane is the largest in Figure 1 and provides four visualization example plots. In addition to the shown Google Maps®, which is interactive, the Central Pane is able to provide a number of other valuable plots.

The analysis module in **Rt** contain the tools necessary to conduct reliability and optimization analysis. To run a reliability analysis, the user creates (or auto-generates) objects with the algorithms that are necessary for that analysis. For instance, FORM requires objects that search for the design point, determine the step size and direction in the search, and check the convergence, among other things. Importantly, the analysis settings can be changed during run-time. As a case in point, the parameters of the Armijo step size rule are readily changed in the Properties Pane during a FORM analysis.

Currently, the analysis options available in **Rt** are FORM, a limited curvature-based SORM,

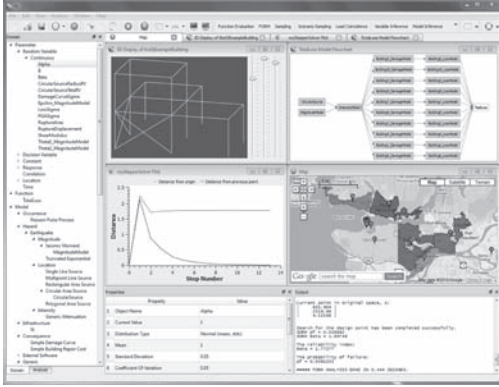


Figure 1. Screenshot of the graphical user interface of *Rt*.

various sampling schemes, and load combination analysis (one sampling-based and one based on load coincidence theory). An analysis strategy that has proved robust and effective in the authors' reliability analyses is:

1. Carry out sampling about the mean value of the random variables and generate histograms of the responses. A typical result is shown in Figure 2, where the relative frequency diagram, comparable with the PDF of the response, is complemented with the cumulative frequency diagram, which is comparable with the CDF of the response. The histograms provide rough estimates of loss probabilities, *etc.*
2. From the histogram, determine the response threshold for which a more accurate probability is sought and carry out FORM at this threshold. Figure 3 shows a FORM-convergence plot from *Rt*. In this figure, the upper red line shows the distance from the trial point to the origin in the standard normal space of random variables. The lower blue line gives the distance from the previous trial point. The plot shows that this particular FORM analysis did not converge because of the limit-state function was not continuously differentiable. This is remedied by smoothing techniques; which is presented in the companion paper at this conference.
3. At the design point from FORM analysis, carry out an importance sampling analysis to verify and possibly amend the result from FORM. Figure 4 shows a plot of the coefficient of variation of the probability result. The plot demonstrates how the sampling result becomes more accurate as more samples are accumulated.

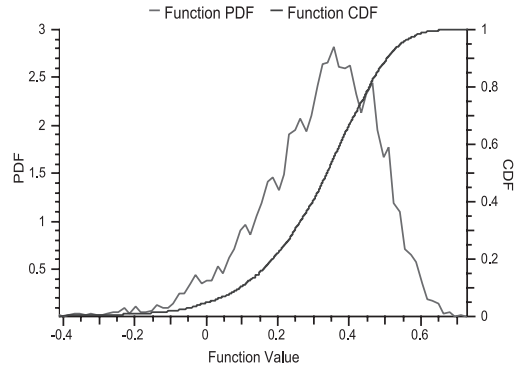


Figure 2. Output from *Rt* for a histogram sampling analysis.

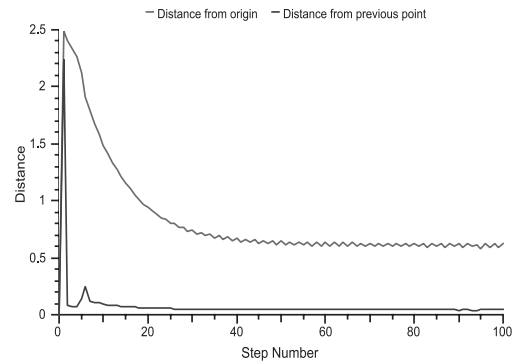


Figure 3. Output from *Rt* for a FORM analysis.

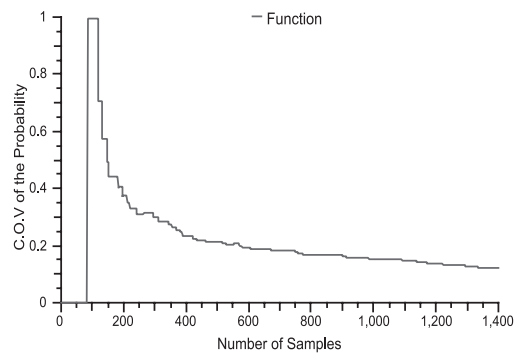


Figure 4. Output from *Rt* for a sampling reliability analysis.

These are only a few of the features of *Rt*. The reader is encouraged to visit www.inrisk.ubc.ca and to read the authors' two papers at this conference for more information.

Probabilistic modeling of vehicle impact as accidental action

Claus U. Kunz

Bundesanstalt für Wasserbau, Karlsruhe, Germany

ABSTRACT: Accidental actions are rare events but may injure the load bearing capacity of structures and become a threat to their users and uninvolved persons. Accidental actions are characterized by a short duration and a rare occurrence probability during the lifetime of a structure. Therefore the use of probabilistic methods seems adequate. In case of both ship impact and road vehicle impact to piers of bridges crossing a travel course the former deterministic design practice for bridges has been improved towards advanced probabilistic analyses and derived design values according to Eurocode basics.

Comprehensive studies concerning load-indentation for inland waterway ships have included static and dynamic model tests as well as numerical analyses. Different contact situations such as head-on collision (frontal impact) and skew (lateral) impact have been investigated. The load-indentation of road vehicles, cars and trucks, have been found out of analysing crash tests and by literature reviews. The probabilities of the impact loads have been based on the traffic patterns such as mass frequencies, velocity frequencies and distributions of impact angles and have lead to impact models. For road vehicle traffic it was found that only trucks are dominating the collision problem because cars and other light vehicles will be retained by guardrails which are placed along critical stretches of the main roads and motorways.

The accident scenarios, both for ship and for road vehicle impact, were based on accident analyses and have been described by mathematical models so as to estimate the load probabilities and the collision probabilities. Road vehicles on a carriageway may have a different physical behaviour from ships in a fairway but from probabilistic point of view the probabilistic behaviour seems to

be quite similar in accidental situations. So it was obvious to use the same procedure for determining the load probability and the same model for evaluating the collision probability.

For this parameters which determine the impact force had been considered such as the stiffness of the colliding object, the mass distribution of the waterway or road traffic, the distribution of ship or truck velocities, the distribution of impact angles and the distribution of the severity of the impact. The combination of these factors and their probabilities lead to a probabilistic load function. As second function the travel course distributions and the geometries of the hit structures have been considered. The combination of the probability of the impact loads and the probability of bridge collisions, both for ship impact and road vehicle impact to bridge piers, result in particular impact distribution functions where the collision load is referred to an exceedance probability. To determine the risk level the value of the representative accidental action is derived by an exceedance probability of $p_{\bar{u}} = 10^{-4}$ per year and structural element. This risk level enables to compare the safety of traffic systems and—more over—the safety level of different accidental actions. By these impact distribution functions for ship impact and road vehicle impact have been estimated in a probabilistic way, design loads are determined for individual projects and lead to recommendations for new codes, i.e. EN 1991-1-7 (2006), Actions on Structures—Accidental Actions, or in the adjacent German National Annex.

The probabilistic method for the determination of impact loads as accidental actions enables to consider uncertainties within the data. More over the probabilistic procedure will lead to a harmonization of other accidental actions.

Benchmark of random fields simulation methods and links with identification methods

X.H. Dang & B. Sudret

Clermont Université, IFMA, EA 3867, Laboratoire de Mécanique et Ingénieries, Clermont-Ferrand, France
Phimeca Engineering S.A., Centre d'affaires du Zénith, Couron, France

M. Berveiller

EDF R&D, Site Renardières, Moret-sur-Loing cedex, France

INTRODUCTION

Modelling spatial variability of material properties becomes crucial in the analysis of mechanical systems, especially when some micromechanical approaches are introduced into the analysis. The discretization of Gaussian random fields of known properties is now well-established and the simulation of non Gaussian fields is also addressed in the literature (Bocchini & Deodatis 2008). Of cutting edge importance is now the *identification* of random fields from real data. The paper addresses the simulation of 2D random fields using a 2D extension of the *circulant embedding* method and the *spectral* method. Then the synthetic data is used for identification.

The paper is divided into two parts: the first one proposes a benchmark of discretization methods for Gaussian random fields. The circulant embedding and spectral methods are also compared with the classical discretization method known as Expansion Optimal Linear estimation (EOLE) (Li & Der Kiureghian 1993), Karhunen-Loeve (Sudret 2007), direct simulation (Schlather 2009). The second part of the paper benchmarks identification method of Gaussian stationary random fields called *periodogram* method.

SIMULATION METHODS

Circulant embedding method

This method exploits the special characters of a *circulant matrix* whose eigenvalues and vectors are closely related to the Fourier transform. The basic idea is to embed the original domain into a larger domain such that the field covariance matrix associated to some grid discretization is a circulant matrix, *i.e.* has special algebraic properties that facilitate the simulation of a field realization in the

embedding domain. Then the part of the trajectory related to the original domain is extracted. The computational time is again considerably reduced by the use of the Fast Fourier Transform.

Spectral method

The spectral method is based on the Power Spectra Density (PSD) estimation computed by the Fourier transform of the covariance function. The combination of the definition of PSD and Parseval's theorem leads to a relationship between the discretized PSD and the modules of the components in the spectral domain. The phases are chosen as uniform random variables in $[0, 2\pi]$. The inverse Fourier transform yields a realization of the random field in the original time domain. This approach uses the Fast Fourier Transform, so that the computing time is considerably reduced.

IDENTIFICATION METHOD

The identification method called *periodogram* which uses the spectral representation of the random field for the estimation of the *periodogram* from the real data. It links directly to the spectral simulation method by the use of the power spectral density. It was presented in (Stoica & Moses 1997) and (Li 2005). The parameters of the random field are computed by fitting the periodogram using classical regression. The computational time is considerably reduced by the use of the FFT.

REFERENCES

- Bocchini, P. & Deodatis, G. (2008). Critical review and latest developments of a class of simulation algorithms for strongly non-Gaussian random fields. *Prob. Eng. Mech.* 23(4), 393–407.

- Li, J. (2005). *Spectral estimation*. Gainesville, FL 32611, USA: Department of Electrical and Computer Engineering - University of Florida.
- Li, C. & Der Kiureghian, A. (1993). Optimal discretization of random fields. *J. Eng. Mech.* 119(6), 1136–1154.
- Schlather, M. (2009). Simulation and analysis of random fields. Technical report, Department of Mathematics and Statistics, Lancaster University, UK.
- Stoica, P. & Moses, R. (1997). *Basic definitions and the spectral estimation problem*. Prentice Hall.
- Sudret, B. (2007). *Uncertainty propagation and sensitivity analysis in mechanical models – Contributions to structural reliability and stochastic spectral methods*. Habilitation à diriger des recherches, Université Blaise Pascal, Clermont-Ferrand, France, 173 pages.

Size effect on probability distribution of fatigue lifetime of quasibrittle structures

Jia-Liang Le

Department of Civil Engineering, University of Minnesota, Minneapolis, USA

Zdeněk P. Bažant

Department of Civil Engineering and Environmental Engineering Northwestern University, Evanston, USA

ABSTRACT: The design of various engineering structures, such as buildings, infrastructure, aircraft, ships, as well as microelectronic components and medical implants, must ensure an extremely low probability of failure (such as 10^{-6}) during their service lifetime. Such a low probability is beyond the means of histogram testing. Therefore, one must rely on some physically based probabilistic model for the statistics of structural lifetime. This study focuses on the structures consisting of quasibrittle materials, which are brittle materials with inhomogeneities that are not negligible compared to structure size (exemplified by concrete, fiber composites, tough ceramics, rocks, sea ice, bone, wood, and many more at micro- or nano-scale). This paper presents a new theory of the lifetime distribution of quasibrittle structures failing at the initiation of a macrocrack from one representative volume element of material under cyclic fatigue. The formulation of this theory begins with the derivation of the probability distribution of critical stress amplitude by assuming that the number of cycles and the stress ratio are prescribed. The Paris law is then used to relate the probability distribution of critical stress amplitude to the probability distribution of fatigue lifetime. The theory naturally yields a power-law relation for the stress-life curve (S-N curve), which agrees well with Basquin's law. The theory indicates that quasi-brittle structures must exhibit a marked size effect on the mean structural lifetime under cyclic fatigue and consequently a strong size effect on the S-N curve. It is shown that the theory matches the experimentally observed systematic deviations of lifetime histograms of engineering and dental ceramics from the Weibull distribution.

MOTIVATION

The problem of rational determination of safety factors and prediction of lifetime for quasibrittle

structures of various sizes is analyzed, and the challenges and opportunities are discussed. The paramount importance of reliability analysis is obvious if one notes that the load factors and under-strength (capacity reduction) factors, still essentially empirical and physically poorly understood, represent much larger corrections to deterministic calculations than the typical errors of modern computer analysis of structures.

This study is motivated by the fact that an effect of particular concern for structural reliability and lifetime predictions is the transition from quasi-plastic to brittle response with increasing structure size, and the associated effect of structure type and geometry (or brittleness). Such transition typically occurs in quasibrittle materials, which include concrete, fiber-polymer composites, tough ceramics, rocks, sea ice, wood, etc., at normal scale and many more at the scale of MEMS and thin films, and are the sole focus of this study. The structures made of such materials are characterized by a fracture process zone that is not negligible compared to the cross-section dimensions of structure. Recent studies (Bažant & Pang 2006, Bažant & Pang 2007, Bažant, Le & Bazant 2009, Le, Bažant & Bazant 2009, Le & Bažant 2010b) showed that, due to the non-negligible size of fracture process zone (material inhomogeneities), the cumulative distribution functions (cdf's) of strength and creep lifetime of quasibrittle structures failing at fracture initiation vary with the structure size and geometry. In this study, we investigate the size effect on the type of probability distribution of fatigue lifetime and its consequence on the stress-life curve.

SUMMARY OF MAIN RESULTS

This study shows that the probability distribution of fatigue lifetime depends on structure size and geometry. The size effect on mean fatigue lifetime (at fixed stress amplitude and stress ratio) must be

considered to deviate from the power-law predicted by the classical two-parameter Weibull theory.

It is shown that the cumulative distribution function (cdf) of fatigue strength, defined as the critical stress amplitude that causes a structure to fail for a given number of cycles and a fixed stress ratio, can be derived from the fracture mechanics of nano-cracks propagating through a nanoscale element by tiny jumps over numerous activation energy barriers on the surface of the free energy potential of the lattice, caused by crack length jumps by one atomic spacing. A statistical hierarchical model, previously used for the derivation of cdf of static strength of one representative volume element (RVE) (Bažant & Pang 2007, Le & Bažant 2010b), is adopted to link the statistics of fatigue strength at nano- and macroscales. The model shows that the cdf of fatigue strength of one RVE can be approximated as a Gaussian distribution onto which a Weibull tail is grafted at $P_f \approx 10^{-4} - 10^{-3}$.

To derive the cdf of fatigue lifetime, i.e. the critical number of cycles that causes a structure to fail for a given stress amplitude, one needs the Paris law (Paris & Erdogan 1963), which describes the growth rate of a fatigue crack as a function of stress amplitude. The Paris law has been successfully applied to many quasibrittle structures as an empirical law (Bažant & Xu 1991, Kawakubo 1995, Hoshide 1995). Recently, the Paris law was physically justified by the equality of energy dissipation of moving macro-scale FPZ and all the nano-cracks inside the FPZ (Le & Bažant 2010a). With the Paris law, one can directly relate the fatigue strength to the fatigue lifetime. Thus the cdf of fatigue lifetime can be calculated from the cdf of fatigue strength of one RVE. Based on the weakest-link model, in which the structure is statistically modelled as a chain of RVEs, the cdf of fatigue lifetime of a structure is shown to depend on structure size and geometry.

The derived cdf of fatigue strength is verified by the optimum fitting of histograms of fatigue lifetime of various quasibrittle materials such as engineering and dental ceramics (Sakai & Fujitani 1989, Sakai & Hoshide 1995, Studarta, Filser, Kochera & Gauckler 2007). The histogram, on the Weibull scale, is separated by a localized kink into two segments. The two-parameter Weibull distribution cannot fit both segments simultaneously. The present theory gives perfect fits, and the location of the kink physically characterizes the quasi-brittleness of the structure.

As a consequence of the size effect on the cdf of fatigue lifetime, the mean fatigue lifetime must also be size-dependent. This implies a marked size effect on the stress-life curve (S-N curve). It is shown that, in a bi-logarithmic plot, the

S-N curve must shift horizontally to the left as the structure size increases. This is important for design since it allows one to determine the mean lifetime of full-scale structures, such as large concrete structures, as well as large composite aircraft frames and ship hulls, under relatively low stress amplitude from the laboratory tests on prototypes under a relatively high stress amplitude.

REFERENCES

- Bažant, Z.P., Le, J.-L. & Bazant, M.Z. (2009). Scaling of strength and lifetime distributions of quasibrittle structures based on atomistic fracture mechanics. *Proc. Nat'l Acad. Sci., USA* 106, 11484–11489.
- Bažant, Z.P. & Pang, S.D. (2006). Mechanics based statistics of failure risk of quasibrittle structures and size effect on safety factors. *Proc. Nat'l. Acad. Sci., USA* 103, 9434–9439.
- Bažant, Z.P. & Pang, S.D. (2007). Activation energy based extreme value statistics and size effect in brittle and quasibrittle fracture. *J. Mech. Phys. Solids* 55, 91–134.
- Bažant, Z.P. & Xu, K. (1991). Size effect in fatigue fracture of concrete. *ACI Material J.* 88, 390–399.
- Hoshide, T. (1995). Proof testing and subsequent fatigue characteristics in ceramics. In *Cyclic Fatigue in Ceramics, Elsevier Science B.V. and The Society of Materials Science*, Japan, pp. 207–232.
- Kawakubo, T. (1995). Fatigue crack growth mechanics in ceramics. In *Cyclic Fatigue in Ceramics, Elsevier Science B.V. and The Society of Materials Science*, Japan, pp. 123–137.
- Le, J.-L. & Bažant, Z.P. (2010a). Scaling of probability distribution of fatigue lifetime of quasibrittle structures. Technical report, Northwestern University, Evanston, Illinois.
- Le, J.-L. & Bažant, Z.P. (2010b). Unified nano-mechanics based probabilistic theory of strength, scaling, static crack growth and lifetime of quasibrittle structures. Technical report, Northwestern University, Evanston, Illinois.
- Le, J.-L., Z.P. Bažant, & Bazant, M.Z. (2009). Crack growth law and its consequences on lifetime distributions of quasibrittle structures. *J. Phys. D: Applied Physics* 42, 214008.
- Paris, P.C. & Erdogan, F. (1963). A critical analysis of crack propagation law. *J. Basic Engrg.* 85, 528–534.
- Sakai, T. & Fujitani, K. (1989). A statistical aspect on fatigue behavior of alumina ceramics in rotating bending. *Engrg. Frac. Mech.* 34, 653–664.
- Sakai, T. & Hoshide, T. (1995). Statistical aspect on fatigue fracture of structural ceramics under cyclic loads. In *Cyclic Fatigue in Ceramics, Elsevier Science B.V. and The Society of Materials Science*, Japan, pp. 189–206.
- Studarta, A.R., Filser, F., Kochera, P. & Gauckler, L.J. (2007). Fatigue of zirconia under cyclic loading in water and its implications for the design of dental bridges. *Dent. Mater.* 23, 106–114.

This page intentionally left blank

*MS_117 — Probabilistic modelling of the behaviour
of timber in structures (1)*

This page intentionally left blank

Comparative risk assessment of secondary structures in wide-span timber structures

S. Miraglia

Università degli Studi di Napoli “Federico II”, Naples, Italy
 Engineering Risk Analysis Group, TU München, Germany

P. Dietsch

Chair for Timber Structures and Building Construction, TU München, Germany

D. Straub

Engineering Risk Analysis Group, TU München, Germany

ABSTRACT: During the past ten years, several collapses of wide span roofs occurred in Northern Europe under high snow loads. Many of these roofs were built with timber elements (solid or glulam timber). The failures most likely originated from errors made during the design phase, followed by errors made during the execution, while failures due to material deficiencies or maintenance were relatively uncommon. This is consistent with an extensive study by Ellingwood (1987) that compiled results from a series of investigations on failed structures during the years 1979–1985.

The goal of this study is to investigate the behavior of a wide span timber roof with a secondary structure designed according to three different structural configurations, which were already the subject of a previous deterministic analysis carried out by Dietsch & Winter (2010), and to compare the performance of the three different configurations with respect to reliability, robustness and risk. The risk assessment is performed by considering (probabilistically) all possible failure scenarios of purlin elements in the roof. In this initial study, failure of the primary beams is not considered. The assessment accounts for the possibility of systematic errors (which are modeled by weakened sections that occur randomly in the secondary structure) in order to include the possibility of a systematic weakening of the structure, which can be due to errors in the production and/or construction process.

The investigated roof covers an area of $\ell \times w = 30.0 \times 20.0 \text{ m}^2$ and is supported by 6 primary pitched cambered beams at a distance of 6.0 m (see Figure 1). The secondary elements (purlins) are mounted on the primary elements, which feature a pitch angle of 10° . The three different configurations were chosen as: (a) purlins

designed as simply supported elements; (b) purlins designed as continuous beams; (c) purlins designed as lap-jointed beams.

The purlins are made from solid structural timber, with strength class C24, feature a cross section of $b \times h = 100 \times 200 \text{ mm}^2$ and the distance between the axis of the purlins is chosen so that the utilization factor according to EC5 (2004) is in the range $0.9 < \eta < 1$. The resulting distances between purlins are: a) 1 m, b) 1.2 m and c) 1.6 m.

The risk associated with structural failure of the secondary system is considered to be proportional to the failed area of the roof A_F . Since there is no interest in computing absolute values of the risk, the risk can be defined as:

$$Risk = E[A_F] = \int_0^{A_{roof}} a f_{A_F}(a) da \quad (1)$$

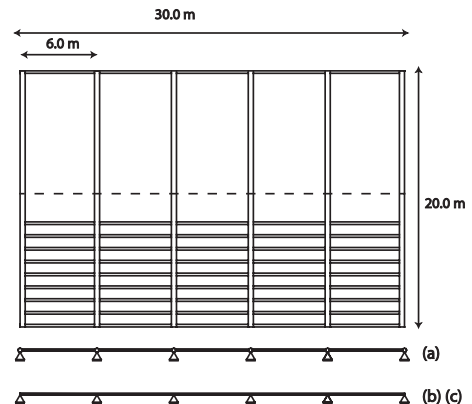


Figure 1. Geometry of the roof (Dietsch and Winter 2010).

where $E[A_F]$ denotes the expectation operation and $f_A F(a)$ is the probability density function (PDF) of the failed area.

The main failure mechanism is bending failure as a function of snow load on the ground Q , shape factor C (snow load on the roof), timber specific weight G , permanent load P and bending strength R_j (at cross section j). It is assumed that the resistance of the elements is not time-dependent and the strength along the purlin changes according to the Isaksson model (Thelandersson et al., 2003, Köhler 2007). Failure of a purlin leads to changes in the static scheme for configurations (b) and (c) (Figure 2).

Therefore, upon failure of one or more sections, the change in the static configuration is considered in order to account also for progressive failures.

Computations are performed with Monte Carlo Simulations (MCS), that enable the evaluation of the full distribution of the damaged area, while the sensitivity of the results on the probabilistic model is assessed by means of First-Order Reliability Method (FORM).

Figure 1 shows the computed CDF of the failed area A_F conditional on the system having failed F and on the absence of systematic errors, $\bar{D}, F_{A_F|F, \bar{D}}(a)$: a failure in the structural system with simply supported purlins (a) results in smaller damages than the other configurations. In the statically indeterminate configurations, progressive collapse mechanisms lead to a larger number of purlin failures once the first section has failed.

EN 1991-1-7 includes a requirement that a failure should not lead to a failed area in excess of 15% of the total area. To check this “robustness” criterion, we calculate the probability that the failed area exceeds 15% of the total area given a failure, Table 1.

Finally, the computed risk, which is defined as the expected size of the failed area $E[A_F]$ in Eq. (1), is summarized in Table 2.

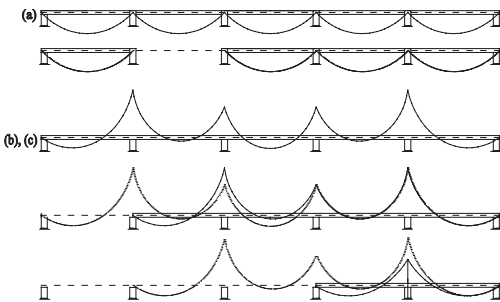


Figure 2. A possible failure scenario for the three configurations.

Table 1. Probability of the failed area exceeding 15% of the total area upon failure (for $\Pr(D) = 0.1$).

	$1-F(A_F = 15\% F)$
(a) Simply supp.	0.027
(b) Continuous	0.035
(c) Lap-Jointed	0.032

Table 2. Expected value of area failed (%).

	$E[A_F]$ $\Pr(D) = 1\%$	$E[A_F]$ $\Pr(D) = 10\%$
(a) Simply supp.	$1.3 \cdot 10^{-3}$	$1.4 \cdot 10^{-3}$
(b) Continuous	$0.8 \cdot 10^{-3}$	$0.9 \cdot 10^{-3}$
(c) Lap-Jointed	$0.8 \cdot 10^{-3}$	$0.9 \cdot 10^{-3}$

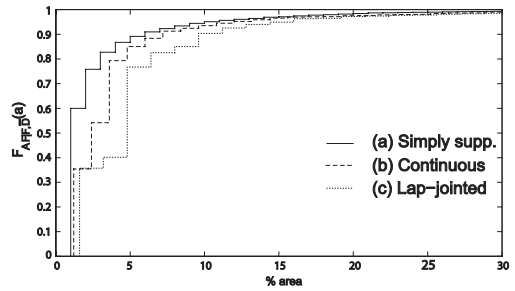


Figure 3. $F_{A_F|D}(a)$ for the three systems without systematic weakening.

From the robustness requirement, it could be argued that structural system configuration (a), consisting of simply supported purlins, is the optimal one, because a failure in this configuration leads to the smallest failed area (Figure 3) and it has the lowest probability of not fulfilling the 15%-area requirement (Table 1).

However, the risk calculated for configuration (a) is higher than for configurations (b) and (c), which are statically indeterminate (Table 2). This is due to the fact that the probability of system failure is higher for configuration (a), even though the consequences are lower. Therefore, it is argued that despite the fact that configuration (a) is more robust, this study indicates that configurations (b) and (c) are more optimal. In addition, configuration (c) is the cheapest, thus supporting this choice of this configuration from a risk (or rather expected cost) perspective. This points to a general problem in the definition of robustness, which is beyond the scope of this paper, namely that a more robust system might often be less optimal from a risk analysis point-of-view.

REFERENCES

- Dietsch, P. & Winter, S. (2010). Robustness of Secondary Structures in wide-span Timber Structures. Proceedings WCTE 2010, Riva del Garda, Italy.
- Ellingwood, B. (1987). Design and Construction error Effects on Structural Reliability. *Journal of Structural Engineering*, 113(2): 409–422.
- EN 1995-1-1. (2004). Eurocode 5: Design of Timber Structures: Part 1–1 General- Common rules and rules for buildings, European Committee for Standardization (CEN), Brussels.
- Koehler, J. (2007). Reliability of Timber Structures. IBK Bericht 301, ETH Zurich, Switzerland.
- Thelandersson, S. & Larsen, H.J. (2003). *Timber Engineering*, Wiley & Sons, England.

Evolution of probabilistic analysis of timber structures from second-moment reliability methods to fragility analysis

D.V. Rosowsky

Department of Civil and Environmental Engineering, Rensselaer Polytechnic Institute, Troy, NY, USA

ABSTRACT: Over the last two decades, significant advances have been made in the areas of probabilistic modeling of timber mechanical properties, structural analysis models for wood-frame structural systems, and stochastic modeling of structural and environmental loads. Collectively, this work has formed the scientific underpinning for modern limit-states timber design codes (e.g., in Europe, the United States, Canada, Japan, and elsewhere). Thus, it is fair to say that strength-based (limit states) design of structures in general, and timber structures in particular, is well developed and only incremental work is needed to keep these codes current. Advanced second-moment reliability techniques and Monte Carlo simulation (and variance reduction techniques) have been adequate for the development of today's probability-based limit states design codes, which are largely member-based with only a relatively simplistic treatment of multi-member systems. With increased attention being paid to economic loss as a limit state deserving of concurrent attention with life safety, especially following extremely costly natural disasters in the last two decades, there are efforts throughout the international engineering communities to move toward a philosophy of multi-objective performance-based (also called objective-based) design. Coupled with this activity has been a move toward fragility analysis techniques to uncouple the hazard (e.g., seismic, wind) from the structural system response, thereby enabling more efficient probabilistic analysis and inference. Fragility techniques are also increasingly being accepted by those in the design communities (especially seismic design) and are likely to form the basis for next generation performance-based design procedures for all hazards. This paper describes this philosophical transition and reports on advances in fragility-based techniques that relate directly to the performance-based design of timber structures.

REFERENCES

- AF & PA/ASCE 16 (1996). "Standard for Load and Resistance Factor Design (LRFD) for Engineered Wood Construction," American Forest & Paper Association, American Wood Council, Washington, DC.
- ASCE (2006). "Minimum Design Loads for Buildings and Other Structures," ASCE Standard 7-05, American Society of Civil Engineers, Reston, VA.
- Barrett, J.D. & Foschi, R.O. (1978). "Duration of Load and Probability of Failure in Wood," *Canadian Journal of Civil Engineering*, 5(4):505-532.
- Bulleit, W.M., Rosowsky, D.V., Fridley, K.J. & Criswell, M.E. (1993). "Reliability of Wood Structural Systems," *Journal of Structural Engineering*, ASCE, 119(9):2629-2641.
- Cobeen, K., Russell, J. & Dolan, J.D. (2004). "Recommendations for Earthquake Resistance in the Design and Construction of Woodframe Buildings," CUREE Report No. W30, CUREE-Caltech Woodframe Project, Consortium of Universities for Earthquake Engineering, Richmond, CA.
- Ellingwood, B.R. (1994). "Probability-Based Codified Design for Earthquakes," *Engineering Structures*, 16(7):498-506.
- Ellingwood, B., Galambos, T.V., MacGregor, J.B. & Cornell, C.A. (1980). "Development of a Probability Based Load Criterion for American National Standard A58," Special Publication No. SP-577, National Bureau of Standards, Washington, DC.
- Ellingwood, B. & Rosowsky, D. (1991). "Duration of Load Effects in LRFD for Wood Construction," *Journal of Structural Engineering*, ASCE, 117(2):584-599.
- Ellingwood, B.R., Rosowsky, D.V., Li, Y. & Kim, J.H. (2004). "Fragility Assessment of Light-Frame Wood Construction Subjected to Wind and Earthquake Hazards," *ASCE Journal of Structural Engineering*, 130(12):1921-1930.
- Filiatrault, A. & Folz, B. (2000). "Performance-Based Seismic Design of Wood Framed Buildings," *ASCE Journal of Structural Engineering*, 128(1):39-47.
- Foschi, R.O. & Yao, F.Z. (1986). "Another Look at Three Duration of Load Models," Report by Working Commission W18 - Timber Structures, International Council for Building Research Studies and Documentation, Florence, Italy.
- Foschi, R.O., Folz, B.R. & Yao, F.Z. (1989). "Reliability-Based Design of Wood Structures," Structural Research Series, Report No. 34, Department of Civil Engineering, University of British Columbia, Vancouver, Canada.
- Gerhards, C.C. (1979). "Time-Related Effects of Loading on Wood Strength: a Linear Cumulative Damage Theory," *Wood Science*, 11(3):139-144.

- Green, D.W. & Evans, J.W. (1987). "Mechanical Properties of Visually Graded Lumber, Volumes 1-8," United States Department of Agriculture, Forest Service, Forest Products Laboratory, Madison, WI.
- Kim, J.H. & Rosowsky, D.V. (2005a). "Fragility Analysis for Performance-Based Seismic Design of Engineered Wood Shearwalls," *ASCE Journal of Structural Engineering*, 131(11):1764-1773.
- Kim, J.H. & Rosowsky, D.V. (2005b). "Incorporating Nonstructural Finish Effects and Construction Quality in a Performance-Based Framework for Wood Shearwall Design," *Structural Engineering and Mechanics*, 21(1).
- Lee, K.H. & Rosowsky, D.V. (2005). "Fragility Assessment for Roof Sheathing Failure in High Wind Regions," *Engineering Structures*, 27:857-868.
- Lee, K.H. & Rosowsky, D.V. (2006). "Fragility Curves for Woodframe Structures Subject to Lateral Wind Loads," *Wind & Structures*, 9(3):217-230.
- Melchers, R.E. (1999). *Structural Reliability: Analysis and Prediction*, John Wiley & Sons, NY.
- Murphy, J.F. (ed.) (1988). "Load and Resistance Factor Design Specifications for Wood Construction—a Pre-Standard Report," American Society of Civil Engineers, New York, NY.
- Pang, W., Rosowsky, D.V., Pei, S. & van de Lindt, J.W. (2010). "Simplified Direct Displacement Design of Six-Story Woodframe Building and Pretest Seismic Performance Assessment," *ASCE Journal of Structural Engineering*, 136(7):813-825.
- Philpot, T.A., Rosowsky, D.V. & Fridley, K.J. (1993). "Serviceability Design in LRFD for Wood," *Journal of Structural Engineering*, ASCE, 119(12):3649-3667.
- Rosowsky, D.V. (1993). "Stochastic Models for Structural Lumber Properties," *Probabilities and Materials: Tests Models and Applications*, Proceedings of the PROBAMAT Workshop, Cachan, France, published by Kluwer Academic Publishers, The Netherlands, pp. 119-129.
- Rosowsky, D.V. (1996). "Probabilistic Methods in Engineered Wood Design in North America," Keynote Lecture, *Proceedings: European Workshop on the Application of Probability and Statistics in Wood Mechanics*, Bordeaux, France, February 1996.
- Rosowsky, D.V. (2002). "Reliability-Based Seismic Design of Wood Shearwalls," *ASCE Journal of Structural Engineering*, 128(11):1439-1453.
- Rosowsky, D.V. & Bulleit, W.M. (2002). "Load Duration Effects in Wood Members and Connections: Order Statistics and Critical Loads," *Structural Safety*, 24:347-362.
- Rosowsky, D.V. & Cheng, N. (1999). "Reliability of Light-Frame Roofs in High-Wind Regions. II: Reliability Analysis," *Journal of Structural Engineering*, ASCE, 125(7):734-739.
- Rosowsky, D.V., Cheng, N. & Huang, Z. (1999). "Probabilistic Modeling of Wind Loads on Light-Frame Roof Components in Hurricane-Prone Regions," *Proceedings: Asian-Pacific Symposium on Structural Reliability and its Applications (APSSRA 99)*, Taipei, Taiwan, February 1999, pp. 490-504.
- Rosowsky, D. & Ellingwood, B. (1991). "System Reliability and Load Sharing Effects in Light Frame Wood Construction," *Journal of Structural Engineering*, ASCE, 117(4):1096-1114.
- Rosowsky, D. & Ellingwood, B. (1992). "Reliability of Wood Floor Systems Subjected to Stochastic Loads," *Wood and Fiber Science*, 24(1):47-59.
- Rosowsky, D.V. & Ellingwood, B.R. (2002). "Performance-Based Engineering of Wood Frame Housing: a Fragility Analysis Methodology," *ASCE Journal of Structural Engineering*, 128(1):32-38.
- Rosowsky, D.V. & Fridley, K.J. (1992). "Moisture Content and Reliability-Based Design for Wood Members," *Journal of Structural Engineering*, ASCE, 118(12):3466-3472.
- Rosowsky, D.V. & Fridley, K.J. (1993). "Reliability-Based Design of Wood Members Subject to Ponding," *Journal of Structural Engineering*, ASCE, 119(11):3326-3343.
- Rosowsky, D.V., Fridley, K.J. & Hong, P.Y. (1996). "Reliability-Based System Factor for Serviceability Design of Wood Floors," *Wood and Fiber Science*, 28(3):356-368.
- Rosowsky, D.V., Gromala, D.S. & Line, P. (2004). "Keeping Pace with Evolving Load Standards: Recalibration of LRFD for Wood," *Proceedings: 8th World Conference on Timber Engineering (WCTE 2004)*, Lahti, Finland, June 2004.
- Rosowsky, D.V., Gromala, D. & Line, P. (2005a). "Reliability-Based Code Calibration for Design of Wood Members Using Load and Resistance Factor Design," *ASCE Journal of Structural Engineering*, 131(2):338-344.
- Rosowsky, D.V. & Lee, K.H. (2007). "Macro and Micro-Zone Snow Models for Probabilistic Design," *Proceedings: 10th International Conference on the Application of Statistics and Probability in Civil Engineering (ICASP10)*, Tokyo, Japan, July 2007.
- Rosowsky, D.V. & Kim J.H. (2002). Task 1.5.3-*Reliability Studies*, CUREE Publication No. W-10, Consortium of Universities for Research in Earthquake Engineering, Richmond, CA.
- Rosowsky, D.V. & Reinhold, T.A. (1999). "Rate-of-Load and Duration-of-Load Effects for Wood Fasteners," *Journal of Structural Engineering*, ASCE, 125(7):719-724.
- Rosowsky, D.V., Walsh, T.G. & Crandell, J.H. (2003). "Reliability of Residential Woodframe Construction from 1900-to-Present," *Forest Products Journal*, 53(4):19-28.
- Rosowsky, D.V., Yu, G. & Bulleit, W.M. (2005b). "Reliability of Light-Frame Wall Systems Subject to Combined Axial and Transverse Loads" *ASCE Journal of Structural Engineering*, 130(9):1444-1455.
- van de Lindt, J.W. & Rosowsky, D.V. (2004). "Strength-Based Reliability of Wood Shearwalls Subject to Wind Load," *ASCE Journal of Structural Engineering*, 131(2):359-363.
- van de Lindt, J.W., Huart, J.N. & Rosowsky, D.V. (2005). "Strength-Based Seismic Reliability of Wood Shearwalls Designed According to AF&PA/ASCE 16," *ASCE Journal of Structural Engineering*, 131(8):1307-1312.
- van de Lindt, J.W., Rosowsky, D.V., Filiatrault, A., Symans, M.D. & Davidson, R.A. (2008). "The

- NEESWood Project: Progress on the Development of a Performance-Based Seismic Design Philosophy for Mid-Rise Woodframe Construction," *Proceedings: 2008 World Conference on Timber Engineering (WCTE 2008)*, Miyazaki, Japan, June 2008.
- Yu, G. & Rosowsky, D.V. (2003). "Reliability Analysis of Light-Frame Wall Systems Using a Portfolio Approach," *Proceedings: 9th International Conference on Applications of Statistics and Probability in Civil Engineering (ICASP9)*, San Francisco, CA, July 2003.
- Wang, Y., Rosowsky, D.V. & Pang, W. (2010). "Performance-Based Procedure for Direct Displacement Design of Engineered Wood-frame Structures," *ASCE Journal of Structural Engineering*, 136(8):978–988.

Performance of timber buildings in earthquakes

Frank Lam, Minghao Li & Ricardo O. Foschi
University of British Columbia, Vancouver, Canada

Shiro Nakajima & Takafumi Nakagawa
Building Research Institute, Tsukuba, Japan

ABSTRACT: Performance of timber buildings in earthquakes depends on many factors including the strength, stiffness and ductility of individual components such as shear walls and diaphragms, the structural layout of the components, the available structural redundancy, the carried mass, and the characteristics of the seismic events. Reliability-based evaluation of the seismic performance of timber buildings should consider the uncertainties inherent in ground motions and the structural capacity. It requires a robust computer model with reasonable accuracy and computational efficiency as well as an efficient reliability evaluation tool to estimate failure probabilities. This paper presents a reliability-based approach to assess the performance of timber buildings by coupling the use of a verified structural model PB3D to perform time history analyses of buildings and the first order reliability method (FORM) as well as the importance sampling (IS) method.

The PB3D structural model, as shown in Fig. 1, is composed of shear wall systems and roof/floor systems. The shear wall system consists of vertical wall posts between horizontal diaphragms and

diagonal nonlinear springs to take into account the contributions of bracing elements (sheathing panels or diagonal bracing members) to the shear wall resistance. The load-deformation characteristics of the nonlinear springs are represented by a simplified but mechanics-based shear wall model called “pseudo-nail” model. The “pseudo-nail” model uses a nail connection analogue to represent the load-drift hysteresis of a wood shear wall. Floor and roof diaphragms are modeled by beam elements and brace elements. By adjusting the stiffness of brace elements, the in-plane stiffness of roof/floor can be considered. In this study, the PB3D was verified against shake table test results of two post-and-beam timber buildings.

The peak inter-story drift (PID) response was used to formulate the performance function of timber buildings, which is

$$G = \delta - \Delta(a_G, r, M, F_d, \epsilon) \quad (1)$$

where δ is the building inter-story drift capacity and Δ is essentially an implicit function of PID demand. This function should involve a lot of

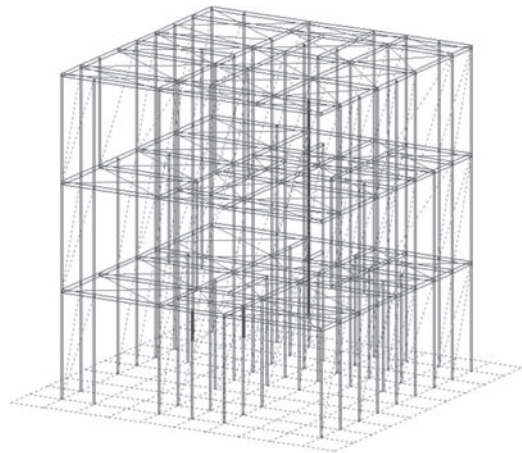


Figure 1. A three-story post-and-beam timber building and the PB3D model.

uncertainties such as the characteristics of ground motions (peak ground acceleration or spectral acceleration and frequency content, duration of shaking, etc.), structural mass M ; design factors F_d (shear wall design, building eccentricity, etc.) and others. To convert Eq. (1) to an explicit performance function, polynomials were used to fit the structural response surface and the fitting error was also considered as a source of uncertainty. Once the explicit performance function is obtained, given the distributions of random variables or design factors, the reliability index β can be estimated by FORM. Considering the high nonlinearity of the performance function, IS method was further used by centering the sampling distribution near the design point, i.e., a region of most importance or likelihood of non-performance.

Case studies of reliability evaluations were conducted on a two-story building and a three-story building which were used for the "PB3D" model verification. A total of ten Japanese historical earthquake records were used to general the structural response database over the domain of random variables and design factors. For the two-story building, the performance function

considered uncertainties of seismic intensity (PGA), structural mass M and the RS fitting errors. For the three-story building, it considered seismic intensity PGA, a design factor F_d called the lateral force resisting factor (LFRF) which is defined as the ratio between the amount of designed shear walls and the seismic code minimum requirement, and the RS fitting errors. Given the assumption on seismic hazard, the reliability results indicated clearly the influence of the structural mass and shear wall design on the seismic safety levels of the buildings with respect to different performance expectations.

In general, the procedure presented in this paper provided a very useful tool to evaluate the seismic performance of timber buildings. The major computational demand is to establish the seismic response database although a reduced number of seismic simulations which are performed on the discrete points of random variables. The performance function can take into account the uncertainties of seismic hazard as well as some important design parameters. By doing so, the optimization of seismic design can be achieved by satisfying specified target reliabilities.

A new approach to consider moisture induced eigen-stress in timber by load combination

M. Häglund & F. Carlsson

Division of Structural Engineering, Lund University, Sweden

ABSTRACT: This paper presents results on moisture induced stress (MIS) in timber. It is argued that MIS may be considered as an ordinary load to be combined with other structural actions, for example snow load. Climatic variations of moisture results in variable stress gradients within timber elements and therefore it is characteristically closer related to external actions than to material strength. This insight is not new and over the last years ideas to consider moisture effects on the load side instead of reduction of strength have been proposed within the engineering community. In order to further explore this approach, effects of load combination of MIS and snow load are investigated. Based on measured snow depths and calculated MIS at four different locations in Sweden it is suggested that the load combination factor for MIS is set to 0.2. It was also found that this factor as a function of relative snow load is practically indifferent to whether a Weibull stress or a maximum cross-sectional stress approach for MIS is used.

It is well known that moisture influences strength properties and that variation of moisture content (MC) cause induced eigen-stresses (i.e. stresses not originating from external forces) due to internal restraint of hygro-expansion. Timber researchers and designers have been interested in moisture induced stresses (MIS) for a long time and during later years it has been suggested that MIS may be considered as an ordinary load to be compared with other structural loads, such as snow load. One essential concern for such an approach is how the MIS load should be combined with other variable loads when applicable (i.e. when external loading causes tensile stresses, e.g. in the perpendicular to grain direction in a curved or tapered beam, see Figure 1).

This paper presents and suggests a MIS load combination factor when MIS and snow load are combined. The procedure is based on daily measured snow depths and calculated MIS at four different locations in Sweden. The paper is based on three main parts: climate and moisture transport, moisture induced stress, and statistical analysis of the developed stresses. In accordance with most

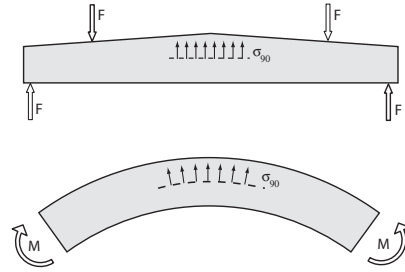


Figure 1. Example of mechanical loading of two timber elements that create tensile stresses perpendicular to grain. In combination with eigen-stress caused by moisture variation the load effect is increased. Interaction with snow load will for example occur if the beams are part of a roof supporting construction.

models found in the literature, it is assumed that the total strain may be expressed as summation of mechanically different strains (Eq. (1)).

$$\dot{\epsilon} = \dot{\epsilon}_e + \dot{\epsilon}_{ms} + \dot{\epsilon}_u = \frac{\dot{\sigma}}{E} + \sigma(m|\dot{u}| + b\dot{u}) + \alpha\dot{u} \quad (1)$$

where $\epsilon_e = \sigma / E$ is elastic, $\epsilon_{ms} = \sigma(m|\dot{u}| + b\dot{u})$ is mechano-sorptive, and $\epsilon_u = \alpha\dot{u}$ is hygro-expansion. α is the hygro-expansion coefficient; m and b are mechano-sorption coefficients; σ is the stress; E is the elastic modulus; u is the moisture content (in per cent by weight).

Modern building codes use a design criterion similar to Eq. (2), which is expressed in the Eurocode notation with partial safety factors (γ) and combination factors (ψ). These parameters are calibrated to attain predetermined formal probabilities of failure.

$$\sum_{j \geq 1} (\gamma_{Gj} \sigma_{Gj}) + \gamma_{Q1} \sigma_{Q1} + \sum_{i \geq 2} (\gamma_{Qi} \psi_i \sigma_{Qi}) \leq k_{mod} \frac{f_k}{\gamma_M} \quad (2)$$

Influence of moisture is today accounted for by a general reduction of strength by a coefficient k_{mod} (note that effects of duration of load are also included in this coefficient). It has however been

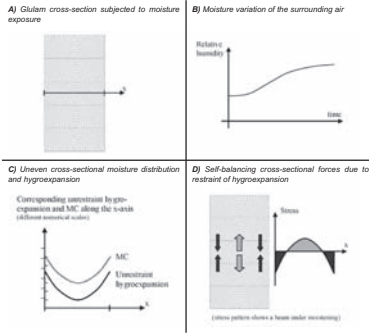


Figure 2. Exemplifying schematic illustrations of how variation of moisture induces cross-sectional stress in timber beams. A glulam beam in A is subjected to variation of relative humidity in the surrounding air according to B. This will lead to higher MC near the surface which in turn causes a corresponding unrestraint hygroexpansion profile as shown in C (i.e. if the beam was to be cut in numerous slices perpendicular to the x-axis, all slices would be able to expand freely and independently of each other). However, unrestraint hygroexpansion is not possible in an actual beam since the internal restraint of expansion prevents it; instead internal section forces develop to self-balance compressive and tensile stress components as schematically shown in D.

argued that moisture impact instead should be considered by adding a variable load that can be combined with other structural loads such as snow or live; in other words, the design criterion for multiple loads would in principle be like in Eq. (3).

$$\sum_{j \geq 1} (\gamma_{Gj} \sigma_{Gj}) + \gamma_{Q1} \sigma_{Q1} + (\gamma_{Q2} \psi_2 \sigma_{Q2})_{\text{moisture action}} + \sum_{i \geq 3} (\gamma_{Qi} \psi_i \sigma_{Qi}) \leq k_{DOL} \frac{f_k}{\gamma_M} \quad (3)$$

One step in order to develop the idea of treating MIS as an additional load is to determine the load combination factor ψ_{MIS} which should be chosen to fulfill Eq. (4).

$$\gamma_G G_k + \gamma_{Q1} Q_{snow,k} + \psi_{MIS} \gamma_{Q2} Q_{MIS,k} = \gamma_G G_k + \gamma_{Q1} Q_{snow+MIS,k} \quad (4)$$

The combined load $Q_{sbiv+MIS,k}$ is determined by probability based analysis (involving a simulation procedure of daily time coherent values) after which ψ_{MIS} can be calculated according to Eq. (5).

$$\psi_{MIS} = \frac{\gamma_{Q1} Q_{snow+MIS,k} - \gamma_{Q1} Q_{snow,k}}{\gamma_{Q2} Q_{MIS,k}} = \left[\begin{array}{l} \gamma_{Q1} = 1.5 \\ \gamma_{Q2} = 1.5 \end{array} \right] = \frac{(Q_{snow+MIS,k} - Q_{snow,k})}{Q_{MIS,k}} \quad (5)$$

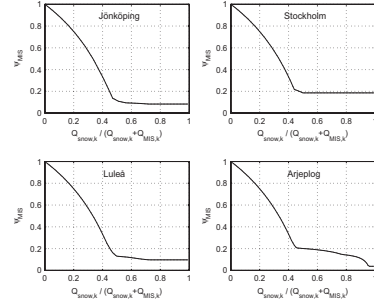


Figure 3. Load combination factor ψ_{MIS} as a function of the relative snow load (according to Eq. (5) and usage of time coherent daily values).

Since the load effect of the variable loads depends on the structural arrangement (for example the type of beam), the combination factor is here determined as a function of the relative snow load $Q_{snow,k} / (Q_{snow,k} + Q_{MIS,k})$ in order to cover all possible combinations on a stress based level. The snow load distribution in time was assumed proportional to the snow depth. The combined load $Q_{sbiv+MIS,k}$ was determined from the summation of Q_{snow} and the maximum calculated tensile MIS of a $90 \times 270 \text{ mm}^2$ uncoated glulam cross-section located indoors in Stockholm, Jönköping, Luleå and Arjeplog. This procedure consists of linear scaling of the complete time series of measure snow depths and calculated MIS in order to fulfill $Q_{snow,k} / (Q_{snow,k} + Q_{MIS,k}) = A$, where A was varied between 0 and 1 in steps of 0.01. The combined load $Q_{sbiv+MIS,k}$ could then be determined by combinations of the time coherent daily values from the linearly scaled series of snow depth and MIS.

RESULTS AND DISCUSSION

The results are shown in Figure 3 which reveals a fairly constant load combination factor at high relative snow loads (as a result of the statistical distribution in time of the two loads). From a design point of view this is favorable since a constant value would mean no approximation. For the load combination in Eq. (5), only relative snow loads above 0.5 is of interest since snow is the leading load; in other words, the range of applicability for the displayed function value of ψ_{MIS} is for $Q_{snow,k} / (Q_{snow,k} + Q_{MIS,k}) > 0.5$ only. Based on these results it is therefore suggested that the load combination factor for moisture induced stress when snow is the leading load is set as $\psi_{MIS} = 0.2$.

Probabilistic methods for performance based service life evaluation of wooden components

S. Thelandersson, T. Isaksson, M. Häglund & E. Frühwald
 Division of Structural Engineering, Lund University, Sweden

ABSTRACT: A performance-based service life design format based on climatic exposure on one hand and “biological wood resistance” on the other hand is presented in this paper. Limit states for onset of mould growth and rot decay are defined. Performance models were applied to assess risk for onset of mould growth and decay under natural outdoor climate. The results indicate that quantitative models can be used as a powerful tool for durability design of wood in the building envelope and in exterior applications. It is demonstrated that the uncertainty originating from climate variability between years and between different geographical locations is significant.

1 INTRODUCTION

One of the key issues in wood construction is durability. Traditionally, durability design of wooden components and structures is based on experience and adherence to good building practice, sometimes formalised in terms of implicit prescriptive rules. Therefore, the design cannot be optimised and any change of design will be associated with uncertain risks.

A proposed principle for a performance-based service life design model is illustrated in Figure 1. The problem is here described in terms of climatic exposure on one hand and resistance of the material on the other hand. The design model is based on a clearly defined limit state, which could be onset of mould growth or decay alternatively a specified acceptable degree of mould growth or decay. The performance requirement in a certain situation could e.g. be that onset of mould growth is not accepted during a specified service life. Since most factors affecting the performance are associated with uncertainty, the probability of non-performance must be assessed so that it can be limited to an accepted maximum level.

2 PERFORMANCE MODELS

A key element in this approach is the performance model (limit state criterion), which shall be able to

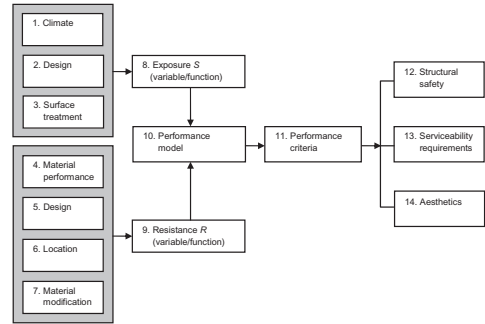


Figure 1. Principle for performance-based service life design of wood elements.

predict violation of the limit state as a function of all relevant influencing parameters.

A dose-response model is used to describe the limit state function for *onset of mould growth* which can be written as

$$g(\phi, T, D_{cr}) = D_{cr} - \sum_{i=1}^N D_{\phi}(\phi_i) D_T(T_i) \quad (1)$$

where

ϕ_i = average relative humidity for day i

T_i = average temperature for day i

D_{ϕ} = dose component related to relative humidity ϕ

D_T = dose component related to temperature T

D_{cr} = critical dose corresponding to onset of mould growth, depending on the material

N = number of days of the time period considered.

Mould growth on spruce and pine sapwood under different climate conditions has been investigated by Viitanen (1996) and the model used here has been calibrated against his test data. More details of the model described by Equation 1 can be found in Isaksson et al. (2010).

The limit state for *onset of rot decay* is defined with reference to decay level 1 “slight attack” according to the standard EN 252 (1989). The limit state function is also here based on a dose-response

model, where the dose is given as a function of wood moisture content and temperature. Starting with a time series of interconnected values of daily average moisture content u_i and temperature T_i for day i the accumulated dose D_N for N days can be calculated from

$$D_N = \sum_{i=1}^N D_u(u_i) \cdot D_T(T_i) \quad (2)$$

where

$D_u(u_i)$ is the dose related to moisture content and

$D_T(T_i)$ is the dose related to temperature ($^{\circ}\text{C}$)

Further details about the model for decay can be found in Thelandersson et al. (2011). Both performance models are based on the simple fact that the fungi spores need favorable moisture and temperature conditions during a sufficiently long period of time in order to germinate and grow.

3 RESULTS

The effect of climate variability on the risk for mould growth was investigated assuming that planed spruce sapwood is exposed to outdoor relative humidity and temperature. Climate data (time series of temperature and relative humidity) from the Swedish Meteorological and Hydrological Institute (SMHI) for 47 years (1961–2007) was used as input. The maximum annual dose describing the risk for mould growth was calculated for each of the 47 years and for 8 sites in Sweden. The results are presented in terms of a relative annual dose D_{rel} where $D_{rel} = 1$ corresponds to the limit state for onset of mould growth. Each year was considered

isolated in the sense that the effects from previous years were not regarded. In this way variability between years with different climate can be evaluated. Cumulative distribution functions (CDF:s) for the eight sites are presented, see Figure 2. More details about the method behind Figure 2 can be found in Häglund et al. (2010).

A similar procedure was used to evaluate relative risk of rot decay depending on geographical site as well as relative risk depending on detail design in exterior wood applications. Results and methods are described in the full paper.

4 CONCLUSIONS

It was demonstrated that the risk of mould growth as well as rot decay can be assessed with the help of performance models describing how microbiological development is affected by moisture and temperature conditions. The uncertainty originating from climate variability between years, between different geographical locations and due to detail design is significant. This provides a basis to develop design tools where the influence of climate conditions, detailed design, choice of material, etc. can be considered in a rational way similar to that used in structural design. It will also enable an assessment of uncertainties in the factors affecting service life performance, which is needed to estimate the reliability for a given design. Knowledge about reliability is an important element in the decision process but is more or less disregarded in today's practice for service life design of wood.

REFERENCES

- Häglund, M., Isaksson, T. & Thelandersson, S. 2010. Onset of mould growth - the effect of climate variability and different geographical locations. International Research Group on Wood Protection, IRG/WP10-20446, Biarritz, France.
- Isaksson, T., Thelandersson, S., Ekstrand-Tobin, A. & Johansson, P. (2010). Critical conditions for onset of mould growth under varying climate conditions. *Building and Environment* **45**(7):1712–1721.
- Viitanen, H. (1996). Factors affecting the development of mould and brown rot decay in wooden materials and wooden structures. Dissertation, SLU Uppsala, Sweden.
- Thelandersson, S., Isaksson, T., Suttie, E., Frühwald, E., Toratti, T., Grull, G., Viitanen, H. & Jermer, J. (2011). Quantitative design guideline for wood outdoors above ground. International Research Group on Wood Protection, IRG/WP11-20xxx, Queenstown, New Zealand.

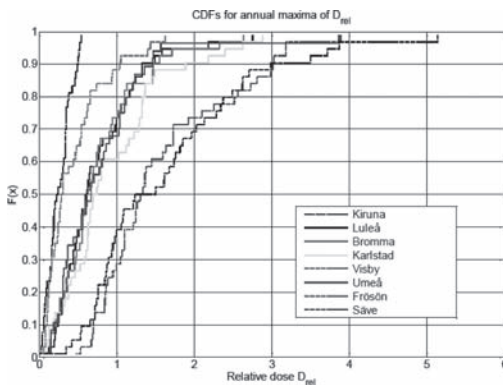


Figure 2. Cumulative distribution functions (CDF) for annual maxima of D_{rel} at eight sites. Onset of mould growth is initiated when $D_{rel} > 1$. Material: Resawn spruce sapwood.

*MS_127 — Probabilistic modelling of the behaviour
of timber in structures (2)*

This page intentionally left blank

Probabilistic robustness analysis of timber structures—results from EU COST action E55:WG3

P.H. Kirkegaard & J.D. Sørensen

Department of Civil Engineering, Aalborg University, Denmark

ABSTRACT: Timber is an efficient building material, not least in regard to its mechanical properties but also because it is a highly sustainable material considering all phases of the life cycle of timber structures: production, use and decommissioning. Timber is a widely available natural resource throughout Europe; with proper management, there is a potential for a continuous and sustainable supply of raw timber material in the future. Timber is a light material and compared to its weight the strength is high; the strength to weight ratio in grain direction is even higher than for steel. However, considering its beneficial properties, timber is still not used to its full potential in the building and construction sector. Many building developers, architects and structural engineers do not consider timber as a competitive building material compared with concrete, steel or masonry. Attributes such as high performance regarding reliability, serviceability and durability are generally not associated with timber as a building material.

One of the main reasons for this is that timber is a highly complex material; it actually requires a significant amount of expertise to fully appreciate the potential of timber as a structural building material. There are also a number of issues which need to be further researched before timber can achieve the same recognition as a high quality building material such as steel and concrete. These issues are the focal point of the EU COST Action E55—‘Modelling of the performance of timber structures’ (Köhler 2006). The objectives of the project are achieved according to three main research activities: the identification and modelling of relevant load and environmental exposure scenarios, the improvement of knowledge concerning the behaviour of timber structural elements and the development of a generic framework for the assessment of the life-cycle vulnerability and robustness of timber structures. Recently results achieved by working group 3 (WG3) are related to the subtasks: definition of structural robustness of timber structures (Branco and Neves 2009; Sørensen, Rizzuto et al., 2009), quantification of robustness and methods of assessing robustness

of timber structures (Cizmar, Rajcic et al., 2010) (Kirkegaard and Sørensen 2008; Kirkegaard and Sørensen 2008; Kirkegaard and Sørensen 2009; Kirkegaard, Sørensen et al., 2009; Cizmar, Rajcic et al., 2010; Kirkegaard, Sørensen et al., 2010) as well as methods of designing for robustness of timber structures (Dietsch and Munch-Andersen 2009; Dietsch and Winter 2009; Munch-Andersen and Dietsch 2009). The present paper outlines these recent results from the working group 3.

REFERENCES

- Branco, J. & Neves, L. (2009). *Earthquakes and robustness for timber structures*. Joint Workshop of COST Actions TU0601 and E55, Zurich, ETH Zurich.
- Cizmar, D., Rajcic, V. et al. (2010). *Robustness analysis of big span glulam truss structure*. Structures & Architecture, Guimaraes, Portugal.
- Cizmar, D., Rajcic, V. et al. (2010). *Robustness analysis of timber truss structure*. WCTE 2010, Trentino, Italy.
- Dietsch, P. & Munch-Andersen, J. (2009). *Robustness considerations from failures in two large-span timber roof structures*. Proceedings of the Joint Workshop of COST Actions TU0601 and E55, Ljubljana, Slovenia.
- Dietsch, P. & Winter, S. (2009). *Assessment of the Structural Reliability of all wide span Timber Structures under the Responsibility of the City of Munich*. 33rd IABSE Symposium, Bangkok, Thailand.
- Kirkegaard, P.H. & Sørensen, J.D. (2008). *Collapse Analysis of Timber Structures*. The Ninth International Conference on Computational Structures Technology, Athens, Greece, Civil-Comp Press.
- Kirkegaard, P.H. & Sørensen, J.D. (2008). A Probabilistic Approach for Robustness Evaluation of Timber Structures. Aalborg University: Department of Civil Engineering: 22.
- Kirkegaard, P.H. & Sørensen, J.D. (2009). *System reliability of timber structures - ductility and redundancy*. Joint Workshop of COST Actions TU0601 and E55, Zurich, ETH Zurich.
- Kirkegaard, P.H., Sørensen, J.D. et al. (2009). *Robustness Evaluation of Timber Structures with Ductile Behaviour*. The Twelfth International Conference on Civil, Structural and Environmental Engineering Computing, Madira, Portugal, Civil-Comp Press.

- Kirkegaard, P.H., Sørensen, J.D. et al. (2010). *Robustness Evaluation of Timber Structures - Results from EU COST Action E55:WG3*. Structures & Architecture, Guimaraes, Portugal.
- Koehler, J. (2006). Modelling of the performance of timber structures. *Proposal for a new COST Action E55*, Institute of Structural Engineering IBK Swiss Federal Institute of Technology ETH.
- Munch-Andersen, J. & Dietsch, P. (2009). *Robustness considerations from failures in two large span timber roof structures*. Joint Workshop of COST Actions TU0601 and E55, Zurich, ETH Zurich.
- Sørensen, J.D., Rizzuto, E. et al. (2009). *Robustness - theoretical framework*. Joint Workshop of COST Actions TU0601 and E55, Zurich, ETH Zurich.

Modelling of uncertainties of timber structures due to growth inhomogeneities

C. Jenkel, R. Lang & M. Kaliske

Institute for Structural Analysis, Technische Universität Dresden, Germany

Although a large practical knowledge on wood is available, the numerical simulation of timber structures has been unattended in the past. In order to understand constitutive relationships and to enable new kinds of application of the material wood in engineering, the numerical simulation by means of FEM is required. Therefore, modelling of the different characteristics of wood is of major importance.

Material models for the simulation of timber structures have been developed at the Institute for Structural Analysis. For the description of the elastic behaviour in the range of small strains, a cylindrically anisotropic linear elastic material model has been developed. The ductile failure under compression is described by a multi-surface-plasticity formulation (Resch and Kaliske 2010). Brittle failure under shear and tensile loading, especially perpendicular to grain is captured by cohesive elements (Schmidt and Kaliske 2009). Besides, the naturally grown material wood is characterized by growth inhomogeneities, which affect the load bearing behaviour of timber structures. The inhomogeneities considered in this contribution are caused by branches, which lead to so-called knots in timber and a local deviation of the grain course in the area of the knots.

Based on the developed material formulations, knots are captured in the numerical structural model. Thereby, two methods are considered. In the first one, e.g. applied in (Baño et al., 2010), knots are modelled explicitly. The knots of a certain structural part made of timber (Figure 1a) are captured by the applied FE-mesh (Figure 1b). To describe the geometry of the knots as accurately as possible, different types of elements, e.g. tetrahedron or hexahedron-elements, can be utilized. With regard to a large number of simulations with knots, which differ in number, position, size and shape, and the consideration of the imprecision of model parameters, the computational effort is increasing by meshing the knots explicitly. Since a local coordinate system can be assigned to every integration point of the finite elements (GAUSS points), it is possible to describe the knots and surrounding

material by the integration points (Figure 1c). The meshing effort is minimized because a regular FE-mesh can be applied for arbitrary knot geometries. The method is characterized by a “smeared” distinction of knots and surrounding wood. The method has already been applied in several areas of engineering like micro mechanics (Zohdi and Wriggers 2005). In the contribution, both models, explicit and smeared description of knots, are described detailed and compared by an example.

The branches in a tree lead to a deviation of the fibre orientation. In the contribution, a model for the numerical generation of the grain course is introduced. The approach is based on principal stresses. The idea behind the formulation is the minimization of shear stresses in natural growth. The fibres are always orientated in the direction of the principal stresses resulting from the main load case of a tree. The theory was first applied in (Mattheck 1997) in two-dimensional FE-formulation utilizing an orthotropic material model and was enhanced for a three-dimensional FE-formulation with an cylindrically anisotropic material model in (Resch and Kaliske 2005).

In a FE-analysis, the investigated structure or structural part is loaded by a defined main exposure, e.g. constant tension. At the beginning, an isotropic material behaviour is assumed and the principal stresses are computed. Subsequently, the local coordinate systems of the elements are generated by the directions of the principal stresses, whereas the longitudinal direction is set in the direction of the maximum principal stress. With the updated fibre directions of the finite elements, the principal stresses are computed again and the local coordinate systems of the finite elements are

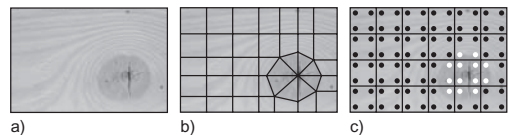


Figure 1. Discrete and smeared consideration of knots.

adapted stepwise. The procedure is repeated until the alteration of the shear stresses converges to a defined tolerance. Thus, the fibre direction is generated by an iterative procedure (see Figure 2). The process is shown by an example. Thereby, the concepts of the explicit modelling of the knots by the FE-mesh and the modelling by the integration points are applied in comparison.

To obtain insight into the effect of branches on the load bearing behaviour, (numerical) parameter studies have to be performed, whereas the determining parameters, like number, position, size and shape of the knots, are changed. Within complex timber structures, these properties are varying, which can be captured by applying adequate uncertainty models. Beside these model parameters, the material properties utilized in the numerical models are strongly varying due to the natural growth. This variation of material properties has to be considered in the structural analysis as well. Additionally, geometrical parameters, external loads and environmental conditions cannot be captured and described exactly by deterministic values.

Imprecise data has to be modelled on the basis of the available information and to be included in the structural analysis to gain not only idealised results of the load bearing behaviour. The consideration of the uncertainty of data is of increasing relevance in Civil Engineering.

Traditionally, the imprecision of data is described by the uncertainty model randomness within a structural analysis. Parameters are modelled by random variables and captured in the numerical simulation, e.g. applying a Monte-Carlo simulation. Applying randomness, a sufficient number of samples obtained under constant reproduction conditions is required to determine the related type of probability distribution. However, the available amount of data is often limited, especially considering the material properties of wood.

Therefore, the uncertainty model fuzziness is applied in this contribution. The model is based on the fuzzy set theory, introduced amongst others in (Klir and Folger 1988). Fuzziness can be utilized to describe objective and subjective uncertainty. Beside the insufficient data basis, informal

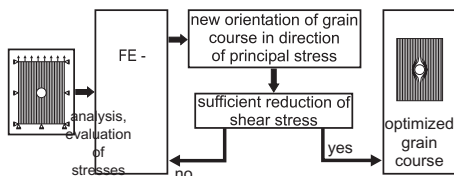


Figure 2. Process chart of fibre course adaption.

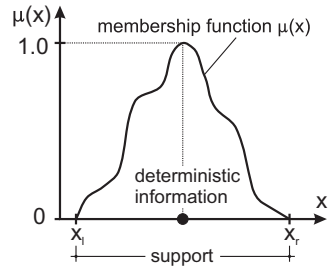


Figure 3. Example for a fuzzy number.

uncertainty resulting of an deficit in information and lexical uncertainty based on linguistic statements, e.g. in terms of expert knowledge, can be taken into account by the data model (Möller and Beer 2004). Figure 3 exemplarily shows a fuzzy number. Simplifying, it can be understood as an assessed interval. A numerical structural analysis under consideration of fuzzy parameters, referred to as fuzzy analysis, is introduced. In a fuzzy analysis, fuzzy input parameters are mapped onto fuzzy results by a deterministic computational model, i.e. the FE models introduced in the contribution.

The methods are illustrated by an example. Thereby, the interfaces between the branches and the surrounding wood are considered, since they are not crisp but blurry, i.e. fuzzy. The knot size is modelled by a fuzzy number and the effect on the load bearing behaviour is investigated in the numerical simulation.

REFERENCES

- Baño, V., Arriaga, F., Soilán, A. and Guaita, M. (2010). F.e.m. Analysis of the strength loss in timber due to the presence of knots. In *World Conference on Timber Engineering*, Riva del Garda.
- Klir, G.J. and Folger, T.A. (1988). *Fuzzy Sets, Uncertainty, and Information*. Prentice Hall, New Jersey.
- Mattheck, C. (1997). *Design in der Natur*. Rombach Verlag, Freiburg.
- Möller, B. and Beer, M. (2004). *Fuzzy Randomness—Uncertainty in Civil Engineering and Computational Mechanics*. Springer-Verlag, Berlin.
- Resch, E. and Kaliske, M. (2005). Bestimmung des Faserverlaufs bei Fichtenholz. *Leipzig Annual Civil Engineering Report 10*, 117–130.
- Resch, E. and Kaliske, M. (2010). Three-dimensional numerical analyses of load-bearing behavior and failure of multiple double-shear dowel-type connections in timber engineering. *Computers and Structures 88*, 165–177.
- Schmidt, J. and Kaliske, M. (2009). Models for numerical failure analysis of wooden structures. *Engineering Structures 31*, 571–579.
- Zohdi, T.I. and Wriggers, P. (2005). *Introduction to Computational Micromechanics*. Springer-Verlag, Berlin.

Structural timber detailing

André Jorissen

University of Technology in Eindhoven (TU/e) and SHR Timber Research in Wageningen, The Netherlands

ABSTRACT: In timber detail design interfaces are used like metal dowel type fasteners, ring and plate fasteners, glue, shear blocks of wood or other materials. In the detail different elements or group of elements are jointed together. In the detail load has to be transported or a closure has to be formed. The detail has a meaning. The detail is necessary to create a structure and/or to point out that one is changing into the other.

Structurally, the fasteners used in the detail may transform load or are just used for positioning. Structural timber detail design should aim at transporting loads by contact areas where the fasteners just have a positioning function. This is however not always possible and the fasteners have to transfer the load. This paper describes some historical, cultural and principle design aspects of timber detailing.

Furthermore, some connections with (single) dowel type fasteners loaded in shear and/or withdrawal are analysed regarding strength and stiffness. Furthermore a basic probabilistic approach is chosen to describe the variability in strength values when the variability in the parameters involved (wood density, fastener diameter, etc.) is known.

1 INTRODUCTION

Ancient structures give an inside guide to the society in which they were erected. Examples can still be found around the world although, due to wood being vulnerable to decay, hardly any wooden artefacts still exist from periods more than 1000 years ago.

Modern (timber) design is less pronounced in telling you something about (differences in) society. An architectural walking tour in e.g. modern Kuala Lumpur is very interesting: high rise buildings with facades breath the culture of this city. The inside, even most of the furniture, can be found at many places around the earth. This is not astonishing knowing that many (architectural) designers work all around the world never succeeding (completely) in expressing the culture of the different locations.

2 TIMBER DETAIL DESIGN APPROACH

All timber connections in old timber structures transfer load by bearing, which is a very effective way of load transfer. However, the principle of load transfer by bearing is hardly possible for connections under tension. For these connections, mechanical fasteners, of which the most applied are the dowel type fasteners, are applied.

3 CONNECTIONS WITH LOAD CARRYING DOWEL TYPE FASTENERS

Traditionally these fasteners are laterally loaded. Johansen [1] started the development of a strength calculation model based on embedment and metal (steel) yielding. This model was extended by Meyer [2] into the model used for most timber codes nowadays.

More recently calculation models for screws loaded in tension, for which the selftapping (full treated) screws as shown in Figure 1 are designed, have been developed, mainly at Karlsruhe University of Technology [3].

Examples of the load carrying connections with laterally loaded dowel type fasteners are the connections with slotted-in steel plates. In the paper these connections are analysed more in detail regarding strength and variability.

Connections with dowel type fasteners loaded in axial tension (+ shear) are very effective and suitable for timber to timber connections. The withdrawal capacity of (long) full threaded screws is much higher than the lateral capacity. Connections with inclined screws have been developed with an optimal inclination angle α , defined in figure 1, between 45 and 55 degrees.

4 SOME BASIC PROBABILISTIC ANALYSES

The load carrying capacity is calculated with basic design equations, which are given in the paper. However, the result is deterministic and does not reflect the variability in the parameters (e.g. timber density) involved.

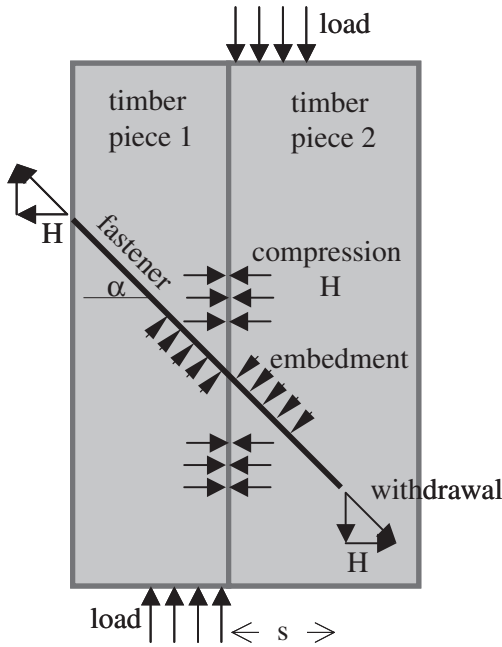


Figure 1. Connection with inclined fastener loaded in withdrawal and shear.

In this section basic probabilistic analyses are carried on the variability of the load carrying results based on the assumption that the stochastic parameters and variables are independent and normally distributed. Furthermore a linearization according to equation (1) is used.

$$F = F(x_{i,0}) + \sum (x_i - x_{i,0}) \frac{\partial F}{\partial x_i}(x_{i,0}) \quad (1)$$

In which $x_{i,0}$ = the value of the variable or parameter for starting the linearization.

5 CONCLUSIONS

For both the connections with dowel type fasteners and slotted in steel plates as well as for

the connections with axially loaded screws the (variation) in the diameter of the dowel type fastener is very important for the variation in the load carrying capacity.

Apparently, the variation in the load carrying capacity is higher than the variation in the individual parameters and properties. For the connections with fasteners in withdrawal the variation increases up to 30% although the variation in the individual parameters and properties is less or equal to 20%. For laterally loaded fasteners the variation in load carrying capacity is about 22%, only slightly higher than the variation in the parameters involved. This difference, and the fact that the expected variation in load carrying capacity is higher for fasteners in withdrawal, might be considered for the future EN 1995-1-1 (Eurocode 5) development. A higher material factor γ_m for screws loaded in withdrawal, compared to γ_m for connections with dowel type fasteners loaded in shear, in $F_d = \frac{F_k}{\gamma_m} k_{mod}$ might be appropriate.

REFERENCES

- [1] Johansen, K.W. Theory of timber connections, International Association of Bridge and Structural Engineering, Publication 9:249-262, 1949.
- [2] Meyer, A. Die Tragfähigkeit von Nagelverbindungen bei statischer Belastung, Holz als Roh- und Werkstoff, 15 Jg. Heft 2, S. 96-109, 1957.
- [3] Blass, H.J. & Bejtka, I. Screws with continuous threads in timber connections, proceedings of Joints in Timber Structures, pp. 193-201, Rilem Publications S.A.R.L, PRO 22, 2001.
- [4] EN, 1995-1-1, including amendment A1, Eurocode 5 – Design of timber structures – part 1-1: General – common rules and rules for buildings, CEN, Brussels, 2007/2008.
- [5] Jorissen, A. Double shear timber connections with dowel type fasteners, PhD thesis, Delft University of Technology, ISBN 90-407-1783-4, Delft University Press, 1998.

Multiscale variability of stiffness properties of timber boards

Gerhard Fink & Jochen Kohler

Institute of Structural Engineering, ETH Zurich, Switzerland

1 INTRODUCTION

The efficient use of materials in structures requires that strength and stiffness related material properties can be predicted with sufficient accuracy. Timber is a natural grown building material. Thus, compared to other building materials, timber properties demonstrate higher variability. Due to the highly in-homogeneous structure of timber, this variability is pronounced not only between different structural elements but also within single elements. A major reason for this is the presence of knots and knot clusters in structural timber.

In the present paper the variability of strength and stiffness related properties of timber is analyzed and described. Thereby it is particularly focused on the influence of knots and knot clusters on the timber stiffness. The analysis takes basis in material property assessments of a sample of 30 timber board specimen. Each board is subdivided into sections with and without knot clusters. For each of these sections the stress-strain relationship is measured and the stiffness is estimated. Based on the stiffness estimates a hierarchical model for the multi-scale variability of stiffness is developed that includes an explicit representation of the stiffness variability between boards and the stiffness variability within boards. The parameters of the model are presented together with the corresponding uncertainties. The presented model can be used e.g. as an input for a more refined probabilistic representation of the load bearing capacity of glued laminated timber.

2 EXPERIMENTAL ANALYSIS

30 randomly selected specimens of the strength grade L25 are analyzed. Thereby the dimensions and the position of all significant knots are measured. Knots with a diameter less than 10 mm are neglected.

Furthermore, a nondestructive tension test is performed. Therefore each board is subdivided into two types of sections: Knot sections (*KS*) and clear wood sections (*CWS*). *KS* represent the sections containing knot clusters or single major

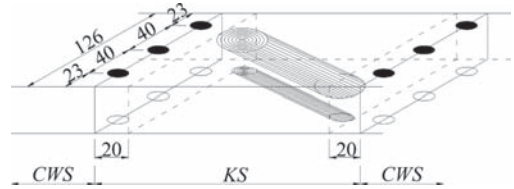


Figure 1. Illustration of the LED-arrangement around a knot cluster.

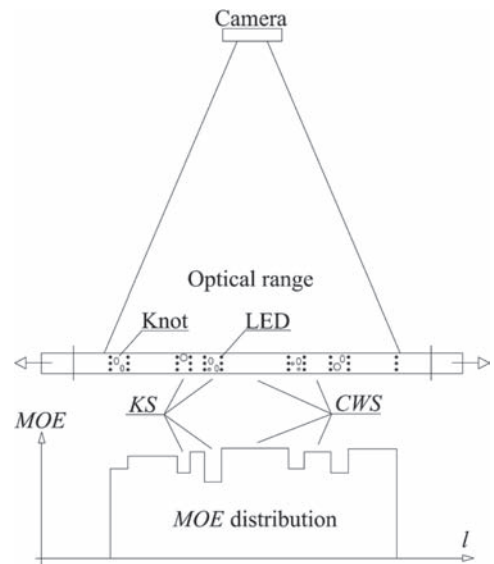


Figure 2. Illustration of the experimental set-up.

knots and *CWS* represent the sections between the *KS*.

At the beginning and at the end of a *KS* three high frequent infrared light emitting diodes (LEDs) are mounted. In Figure 1 the LED-arrangement (black circles) around a *KS* is illustrated.

The boards are clamped in a tension machine and loaded with an axial tension force. During the tension test the LED's send light impulses with a frequency of 20 Hz. The position of the LED's during the tension test is measured with an infrared camera. Figure 2 illustrates of the test procedure.

Table 1. Estimated parameters of the stiffness model and there coefficient of variations.

Parameter	μ_{WS}	$\mu_{\tau, \rho_{WS}}$	$\sigma_{\tau, \rho_{WS}}$	$\mu_{\epsilon, ij_{WS}}$	$\sigma_{\epsilon, ij_{WS}}$	μ_{CWS}	$\mu_{\tau, \rho_{CWS}}$	$\sigma_{\tau, \rho_{CWS}}$	$\mu_{\epsilon, ij_{CWS}}$	$\sigma_{\epsilon, ij_{CWS}}$	c	k	ν
Expected value	9.150	0	0.138	0	0.120	9.410	0	0.144	0	0.0684	150	5.99	0.0125
COV	0.0017	–	0.1308	–	0.0579	0.0016	–	0.1337	–	0.0648	–	0.126	0.132

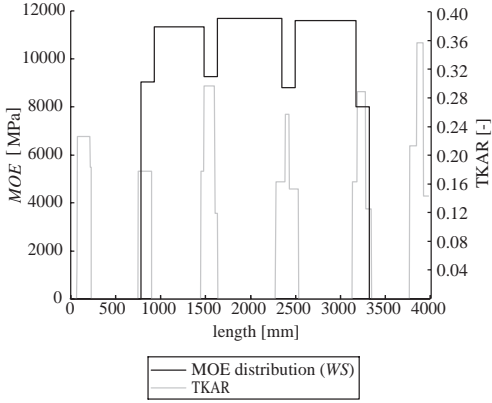


Figure 3. Example of the *MOE* distribution over the length and TKAR distribution (board 5010).

The properties of the *KS* depend on parameters, such as size of the knots and/or the knot arrangement. Thus, the probabilistic characteristic of the properties of the *KS* are difficult to describe. Therefore a weak section (*WS*) with a unit length $c = 150 \text{ mm}$ is introduced.

The established stiffness of each *WS* is compared with an established knot parameter. Therefor the so-called total knot area ratio (TKAR) is used. In Isaksson (1999) the TKAR is defined as the sum of the projected knot areas located within 150 mm of the timber length, divided by the cross-sectional area. Therefor the visible surfaces of the knots are mapped. The three-dimensional shape of each knot is idealized by a frustrum. In Figure 3 the TKAR-value for each part of the board and the *MOE* distribution over the length with *WS* are illustrated for board 5010.

3 HIERARCHICAL STIFFNESS MODEL

In the following a hierarchical model for the variability of the stiffness properties is described and the statistical model parameters are identified based on the sample described before.

The model is summarized in Equation 1 and Equation 2 whereas the sections $j = \{1, 3, 5, \dots, n\}$ are considered to be *WS* and the sections $j = \{2, 4, 6, \dots, n-1\}$ are considered to be *CWS* (n denotes the number of sections within one board). Further a strong correlation between the average values of the *MOEs* of all *WS* within one board and average values of the *MOEs* of all *CWS* within one board is identified. This is considered by the correlation of the variables $\tau_{i, WS}$ and $\tau_{i, CWS}$.

$$MOE_{ij} = \begin{cases} \exp(\mu_{WS} + \tau_{i, WS} + \epsilon_{ij, WS}) & \text{for } j = \{1, 3, 5, \dots, n\} \\ \exp(\mu_{CWS} + \tau_{i, CWS} + \epsilon_{ij, CWS}) & \text{for } j = \{2, 4, 6, \dots, n-1\} \\ \rho(\tau_{i, WS}, \tau_{i, CWS}) = 0.787 \end{cases} \quad (1)$$

The distance d between the *WS* is represented by a gamma distribution. The length of the *WS* is constant with $c = 150 \text{ mm}$. Thus, the length of each section is described with the following equation:

$$l_{ij} = \begin{cases} c = 150 \text{ mm} & \text{for } j = \{1, 3, 5, \dots, n\} \\ d - c & \text{for } j = \{2, 4, 6, \dots, n-1\} \\ \text{with } d \sim \Gamma(k, \nu), \rho(k, \nu) = 0.959 \end{cases} \quad (2)$$

The estimated parameters of the stiffness model and there coefficient of variations are given in Table 1.

REFERENCE

Isaksson, T. 1999. Modelling the Variability of Bending Strength in Structural Timber, Report TVBK-1015, Lund Institute of Technology, PhD.

Hierarchical modeling of structural timber material properties by means of Bayesian Probabilistic Networks

M. Doublein, M. Schlosser & M.H. Faber
Institute of Structural Engineering, ETH Zurich, Switzerland

1 OVERVIEW & APPROACH

For the utilization of timber as a construction material it is essential to adequately take into account all uncertainties which are connected to the statistical grading process. The complex nature of timber and the susceptible production environments require that many of the factors which are influencing the material properties have to be implemented into the grading models as aleatory uncertainties. For the representation of the above-mentioned uncertainties in the modeling of timber material properties it is proposed to utilize a probabilistic hierarchical approach. Material properties in general can be modeled at different levels of resolution in a hierarchical manner. This approach is applied to the context of modeling the material properties of structural timber. The different scales considered in this context are shown in Figure 1.

The present paper addresses the influence of different origins (sources) as well as the cross-sectional dimensions on the probabilistic characteristics of the timber material properties. Probabilistic models are first established in order to characterize the relevant timber material properties. A hierarchical model is then developed to represent the influences of source and cross-sectional dimensions on the probabilistic models of the material properties. Conditional probabilities are assessed given observations of the influencing variables, i.e. origin and dimensions. The general methodical framework builds on the construction of a Bayesian Probabilistic Network (BPN). Marginal probability distributions of the material properties can easily be assessed on this basis. The construction of the BPN is based on Bayesian regression analysis which describes the causal interrelationships and the logical constellation of the network components. In addition to the information of the origin and cross-sectional dimensions, non-destructive tests results using a modern grading device, the GoldenEye 706, are incorporated as input variables into the BPN. Thus, the proposed methodology provides a new basis for the development of an alternative approach to the present methods for

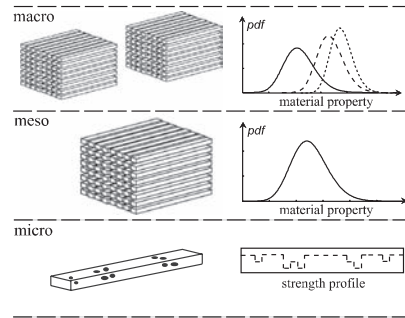


Figure 1. Levels for hierarchical modeling of timber material properties (Köhler, 2006).

machine strength grading and determination of characteristic values of graded timber material.

2 MATERIALS & TESTING

The ultimate tension strength (f_t), the tension modulus of elasticity (moe) and the timber density (ρ) are considered as relevant timber material properties. In total 447 specimens are sampled from three different regions of Switzerland: *Mittelland*, *Jura* and *Berner Oberland*, denoted as $S1$, $S2$ and $S3$, respectively. Furthermore, the sample consists of three different cross sections referred to as $X1$, $X2$ and $X3$. The grading machine GoldenEye 706 is used for non-destructive measurements of the material properties. After machine grading the specimens are tested destructively in tension according to EN 408 at the ETHZ laboratories.

3 DEVELOPMENT OF BPN

The proposed BPN as shown in Figure 2 takes into account prior information concerning the material properties of the particular sources or cross sections and facilitates updating of this information with additional evidences provided by measurements from the grading machine.

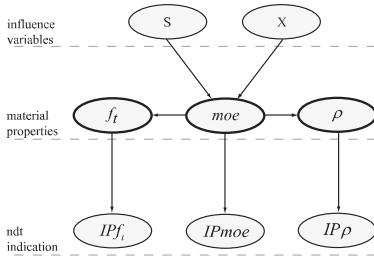


Figure 2. Proposed Bayesian Probabilistic Network.

The conditional probability distributions of the material properties can be assessed based on the indicating properties assessed by the grading machine. By means of probability papers and based on the assessments of the sample log-likelihoods it is validated if the chosen distribution functions are appropriate to represent the underlying experimental data. Estimates of the first and second distribution parameters are established by means of the Maximum Likelihood Method, which is providing also information about the variance and correlations of the parameters (Benjamin & Cornell, 1970). Probability density functions are assessed for the different cross sections and for the various combinations of sources and cross sections. Based on these probability density functions the discrete conditional probability tables of the BPN's material property nodes are derived. For the representation of the relationship between destructive test results and the indications achieved from the grading machine Bayesian linear regression analysis forms a consistent and adequate methodical framework. Conditional on the combination of source and cross section different regressions models are established for the relationships between the material properties themselves and between the material properties and the corresponding machine indications.

The structure of the network represents the grading process during the production process of structural timber. The core elements of the network are the material properties since every graded batch of timber has to fulfill defined criteria in regard to characteristic values.

An example for the conditional probability tables for the ultimate tension strength with stepwise arbitrarily chosen evidence for the influence variables is shown in Table 1. The major influence on the probability distributions appears as soon as non-destructive indications for the material properties are available.

4 CONCLUSIONS

The complex nature of timber, the different production environments as well as the current practice

$P(f_i)$	no evidence	$e_{S,2}$	$e_{X,3}$	$e_{IP\rho,5}$	$e_{IPmoe,4}$	$e_{IPf_i,5}$
5 – 15 MPa	0.17	0.13	0.09	0.03	0.04	0.00
15 – 25 MPa	0.39	0.36	0.34	0.23	0.11	0.00
25 – 35 MPa	0.26	0.29	0.31	0.34	0.32	0.01
35 – 45 MPa	0.12	0.16	0.18	0.26	0.34	0.26
45 – 55 MPa	0.05	0.07	0.08	0.14	0.22	0.72

Table 1. Marginal probability tables for the ultimate tension strength with stepwise added evidences (e.g. $e_{S,2}$ means that evidence is given for the second state of the node S).

and state of knowledge imply that timber material properties are associated with significant uncertainties. In order to represent these uncertainties consistently a probabilistic hierarchical approach is proposed for the modeling of the timber material properties.

The proposed hierarchical model is established based on a BPN which takes into account prior information about the sources and cross-sectional dimensions of the timber. Furthermore, non-destructive measurements using a modern grading device are utilized to provide additional predictive information about the material properties. Given the source and the cross-sectional dimensions of the timber specimens, the proposed network is capable of updating the conditional probability density functions of the timber material properties with additional evidences provided by measurements from the grading machine.

The proposed method for the modeling the material properties seems to have potential for real-time quality control procedures which then may be utilized during the production process of timber elements or engineered timber products. The model is capable to be updated frequently and as a consequence, allows dynamic adaptations of the grading machine settings to account for quality fluctuations of the raw material. Supplementary information can be implemented into the proposed network straightforwardly by extending the structure of the network with additional nodes and updating the interrelationships as well as the probability distribution functions of the variables.

REFERENCES

- Benjamin, J.R. & Cornell, C.A. (1970). *Probability, statistics and decisions in civil engineering*, Mc Graw - Hill Book Company.
- CEN, EN14081:2006. parts 1-4 *Timber structures - Strength graded structural timber with rectangular cross section*; European Committee for Standardization; Brussels, Belgium.
- Köhler, J. (2006). *Reliability of Timber Structures*.

*MS_319 — Probabilistic models and methods
for risk assessment of lifeline networks
and decision support (1)*

This page intentionally left blank

Clustering methods for risk assessment of infrastructure network systems

C. Gómez & M. Sánchez-Silva

Department of Civil and Environmental Engineering, Universidad de los Andes, Bogotá, Colombia

L. Dueñas-Osorio

Department of Civil and Environmental Engineering, Rice University, Houston, TX, USA

ABSTRACT: Infrastructure networks are essential to the socioeconomic development of any country; therefore, studying networks' performance is important to support decisions about risk mitigation, future development, investments and maintenance policies that lead to efficient and reliable operation. Therefore, managing the risk associated to both external (e.g. earthquakes, hurricanes, floods) and internal (operational difficulties) events over essential lifeline systems (public services, transportation and telecommunications) is a primary need of the public and private sectors related to the operation of this infrastructure.

The paper pursues the following objectives: first, to discuss the conceptual aspects and the benefits of using a hierarchically-based representation of a network for reliability analysis; and secondly, beyond a previous paper by the authors, to present a deeper treatment of the different techniques that can be used for this purpose and to focus on reliability analysis within the elements of the hierarchical representation. Special emphasis is given to the effectiveness of this approach within the context of risk-based decision-making.

COMPLEXITY OF INFRASTRUCTURE NETWORKS

The modeling of infrastructure systems and their performance assessment (e.g., reliability estimations) require considering these systems as networks (i.e., collections of interconnected components). One of the main issues in the treatment of complex networks is that, usually, the complexity of the computations over these networks increases exponentially with the number of elements. Besides the natural complexity in the modeling and analysis of such systems, additional intricacy appears when dealing with probabilistic events that affect their purpose and objectives.

In order to maintain and improve network performance under the effect of uncertainties it

is required to make reliability assessments which are relevant for decision-making; this implies evaluating the probability that the system operates above a pre-specified performance threshold taking into account every possible state. Studies requiring the identification of all possible failure scenarios become a problem known as NP-hard due to the enormous number of possible states that have to be considered. Therefore, alternative solutions that allow both sufficient accuracy in the reliability estimation and relevant information for decision about interventions and operation are required. Several approximate methods, network reductions and varied simulation techniques are used in practical applications where an analytical solution is available only for special cases, not available or an exhaustive treatment is prohibitive.

MANAGING COMPLEXITY THROUGH A SYSTEMS APPROACH

A systems approach to network modeling and analysis has been recently proposed by the authors as an alternative to gain conceptual insight on systems' structure and to reduce the computational cost of network reliability analysis. In such approach, a network system is recursively decomposed into subsystems and described hierarchically obtaining different models of the network in terms of the subunits that compose it at different scales. Then, models with different scope and precision are available depending upon the level of abstraction where analyses are performed.

Using this strategy, a compromise between precision and relevance can be found because the scope of the decision and the level of description of the network are closely related. This means that an intermediate (simplified) network representation, obtained from the hierarchical description of the system, may provide enough evidence for the decision at hand, reducing the computational burden of modeling the entire network. This way of

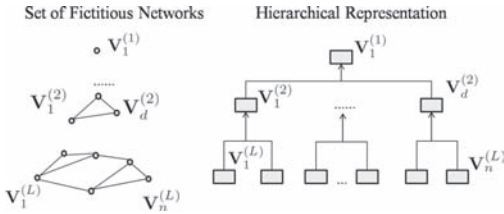


Figure 1. Fictitious networks and hierarchical representation of infrastructure systems.

rearrangement of information (i.e., how clusters are embedded in others in order to give rise to a larger system) leads to a more manageable use of available data, enhancing decision-making capacities.

Figure 1 shows three levels of the hierarchical representation of a network system. Each hierarchy level has an associated fictitious network that represents the system in terms of its subsystems at a specified scale.

CLUSTERING AS A TOOL FOR NETWORK DECOMPOSITION

Identifying patterns around which communities of elements can be grouped is commonly known as clustering and it is useful to address large and complex problems. The existence of algorithms that intelligently detect structures within datasets makes clustering a natural way to proceed with the proposed network decomposition. In the context of statistical learning, clustering is known as an unsupervised multiple classification problem, i.e., a dataset is to be classified into k classes without using any information such as class-labels or a *correct* partitioning to guide the algorithm to an optimal solution. Considering this approach, community structures within an infrastructure system can be revealed without *a priori* knowledge of their existence but rather unraveling them from the intrinsic properties of the system.

Although clustering is a well-known paradigm in computational sciences it has not been considered as a way to perform risk-based decision-making on physical systems (i.e., infrastructure networks), therefore, a revision of different clustering methods and their implications in this context is provided. In addition to the study of algorithms themselves, other issues are taken into account: first, the validity of the obtained partitionings, which is important because clustering (as an unsupervised learning technique) does not count on information about correct classification; and second, the satisfaction of conceptual considerations given by the systems approach, which are not necessarily evaluated by computational algorithms.

RELIABILITY ASSESSMENT

Connectivity reliability is a relevant performance indicator for the case of infrastructure systems, for it accounts for the possibility that users have access to a specific service (e.g., water supply). This measure is based on the probability that either two nodes, a subset, or the whole network gets disconnected after single element failure. In this paper, an origin-destination connectivity approach is considered, therefore, it is proposed that the failure probability is calculated for the fictitious networks at each level of the hierarchy; since the failure probabilities of the detected subsystems (clusters) are unknown, they must be calculated by solving the same connectivity failure probability problem for the network that constitutes each subsystem. Consequently, at the top of the hierarchy, computational complexity increases due to the evaluation of large subsystems, whereas at the bottom of the hierarchy it increases due to the evaluation of many small subsystems.

An illustrative example of computing connectivity reliability for a real infrastructure system (i.e., a transportation network) is presented. This example exhibits the proposed methodology including: partitioning initialization, recursive application of clustering methods throughout the hierarchy, cluster numerical and conceptual validation, failure probability assessment for network representation at different levels and computation of subsystem internal failure probabilities.

CONCLUSIONS

The definition and advantages of the hierarchical approach are presented along with a set of considerations that need to be taken into account to perform a computational partitioning of infrastructure network systems. A study of diverse approaches to computational network partitioning and clustering methods is presented, including additional considerations such as conceptual constraints that must be satisfied as well as clustering initialization and validation methods. The details for a hierarchy-based probabilistic analysis of network performance is presented, enabling reliability computations for the system taking into account internal failure probabilities of the subsystems detected by the intelligent algorithms.

The adjustable level of abstraction achieved by the hierarchical representation of the network system enables the decision-maker to balance the specificity and relevance of the information at hand (e.g., in disaster situations); this allows for an adequate management of the tradeoff between computational complexity and level of detail.

Regional assessment of hurricane risk to Houston bridge infrastructure

N. Ataei, C.D. Arnold & J.E. Padgett
Rice University, Houston, TX, USA

ABSTRACT: Previous studies have concluded that given current estimates of hazard exposure, nearly 60,000 miles of coastal highways in the United States are exposed to regular coastal storm, flood, surge, and wave (Chen et al., 2007). Bridges are among the most important links in the transportation network, whose failure during extreme events may result in significant direct and indirect losses as well as affect post-event recovery and restoration of a region. The susceptibility of coastal bridges to damage during hurricanes has been illustrated in past events, such as in Mississippi and Louisiana during Hurricane Camille (1969), in Florida during Hurricane Ivan (2004), in Hokkaido, Japan during the Songda Typhoon (2004), in Haiti during Hurricane Dennis (2005), and in Louisiana during Hurricane Katrina (2005). In particular, Hurricane Ike in 2008 revealed the potential vulnerability of Houston/Galveston area infrastructure and has motivated investigation of the risk to regional bridge infrastructure in future events.

This paper presents a risk assessment of Houston/Galveston area bridge infrastructure to provide new insight into the spatial distribution of potential damage and major transportation routes potentially affected to support risk mitigation planning for the region. This assessment provides a first phase of risk assessment of the bridge infrastructure, emphasizing damage potential from hurricane induced storm surge and wave loading as well as potential functionality inhibition from inundation. Scenario hurricane events are considered in this first phase to illustrate the bridge reliability analysis approach considering the distributed effects of surge and flood from hurricanes. First, a detailed inventory analysis of the region is conducted and a new database of Houston bridge infrastructure is developed to enable hurricane risk assessment. Figure 1 shows a sample statistics of bridges in the area by age. This database documents bridge details lacking elsewhere to support risk assessment of bridge inventory, including such characteristics

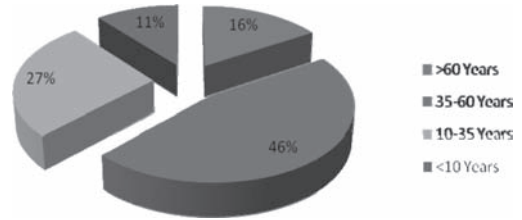


Figure 1. Classification of bridges in the case study area by age.

required for bridge capacity and demand analysis as bridge elevation, superstructure-substructure connection type, number and type of girders, among others.

A total of 136 water crossing bridges near the Galveston Bay are considered in the analysis. The recent AASHTO specifications for coastal bridges vulnerable to coastal storms (AASHTO 2008) employed for the estimation of wave forces on bridge deck, since its accuracy has been validated based on experimental test data. Based on relatively large database, probability density functions for the capacity and demand of each bridge is estimated, taking into account uncertainties associated with both structural properties and hurricane induced wave and surge loads. These conditional reliability estimates, or bridge fragility curves, are used in an assessment of regional bridge performance given input of storm surge and flood elevation across the Houston region for scenario hurricane events. Figure 2 shows the probability of failure for the deck unseating mode of failure for Hurricane Ike wave and surge hind-cast.

The scenario results provide a basis for advanced reliability analyses using high fidelity finite element modeling or nonlinear dynamic analyses by highlighting the potentially susceptible bridges in the region. Furthermore, this work forms the foundation for a more holistic regional risk assessment considering likelihood of hazard occurrence or integration with transportation network analyses.



Figure 2. Probability of failure of bridges in Houston/Galveston for the Hurricane Ike scenario.

REFERENCES

AASHTO. (2008). *Guide Specifications for Bridges Vulnerable to Coastal Storms*, American Association of State Highway and Transportation Officials (AASHTO).

Chen, Q., Wang, L., Zhao, H. and Douglass, S.L. (2007). "Prediction of storm surges and wind waves on coastal highways in hurricane-prone areas." *Journal of Coastal Research*, 23(5), 1304–1317.

Vulnerability of the Swiss electric power transmission grid against natural hazards

Mathias Raschke, Evangelos Bilis & Wolfgang Kröger
Laboratory for Safety Analysis, ETH Zurich, Zürich, Switzerland

ABSTRACT: The synchronized European electric power transmission grid is one of the most complex networks and the Swiss transmission grid is central part of it. Natural phenomena, such as the occurrence of earthquakes or winter storms, may damage/destroy grid components and disrupt the normal operation of the electric-power infrastructure. A disruption may possibly propagate through the network and lead to problems in other areas, besides the geographical area directly affected by the natural phenomenon.

This paper delineates the modelling of the earthquake and storm risk of a power transmission grid. The different model parts “hazard”, “vulnerability” and “response” of the grid are explained with focus on the implemented statistical methods. The novel probabilistic winter storm model is explained in detail.

We present our approach to estimate the risk of the transmission grid in Switzerland (Fig. 1) from earthquake and winter storm. This includes the adaptation of an existing model of earthquake hazard in and around Switzerland and the earthquake failure functions for substation elements. Furthermore we have introduced a statistical model of max stable random fields to model large area winter storms. We neglect the concrete local wind hazard in the model but considered dependencies between the locations and the local

wind risk appropriately. This approach could be useful for further researches.

We model the risks as realistically as possible and the results are not in contradiction to empirical observations. Nevertheless the models could be improved. The safety shut down of generating units is considered for example in our actual research. The advantages of our model compared with the former researches are explained in the relevant sections. The main items are the most realistic occurrence models for the endangering events and the more detailed model of the grid reaction including physics of power flow, operator reaction and hidden failure. The resulting risk estimation can be validated well by empirical data, but this weakness concerns all former published models too. Beside this, the methodological advantages of the presented models do obviously not depend on the empirical validation.

The estimated risks have special characteristics. The occurrence frequency of winter storm events with a grid failure is relatively high but only small events with few failed elements are generated. This results in an exponential shape of the cumulative frequency. In contrary to this, earthquake caused failure events are very rare but events with a large number of failed grid elements are caused rather by an earthquake than by a winter storm. The cumulative occurrence frequency of earthquake caused failure events are heavy tailed (Fig. 2).

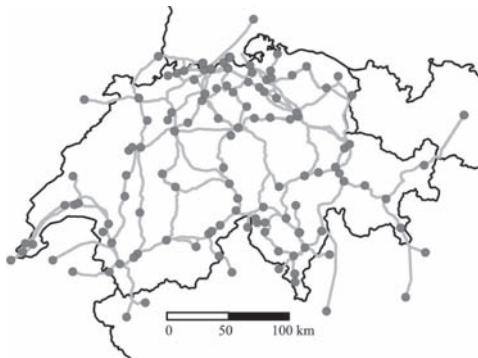


Figure 1. Transmission grid of Switzerland.

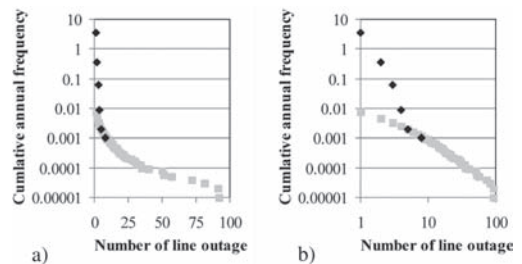


Figure 2. Comparison of modelled earthquake and winter storm risk of transmission grid of Switzerland: a) Outage of power lines, b) Outage of power lines with logarithmic unit.

Furthermore it is remarkable how stable the whole UCTE grid works after disaster impact. The power flow has not converged to a solution (according to the NEPLAN calculation) in few of the 100'000 repetitions of a year of earthquake occurrence. The element failures caused by storms (1000 repetitions

of a year) have never caused an instable power flow. But we could consider only the possible failure in Switzerland although a winter storm concerns larger regions of Western and Central Europe.

Details of the research can be found in the paper.

Evaluation of seismic vulnerability of sewerage pipelines based on assessment of the damage data in the 1995 Kobe earthquake

G. Shoji & S. Naba

University of Tsukuba, Ibaraki, Japan

S. Nagata

Kajima Technical Research Institute, Tokyo, Japan

ABSTRACT: Economical and societal activities in a mega city strongly depend on the function of lifeline systems such as water treatments and so forth. However, there is few research associated with the seismic damage evaluation on sewerage pipelines. The related management sectors (Investigation Committee on Sewerage Damage Assessment on Large-Scale Earthquake, ICSDALE, at Ministry of Land, Infrastructure, Transport and Tourism 2006) present the manuals for seismic countermeasures and frameworks for damage prediction based on the assessment of the sewerage damage on the recent large earthquakes. We evaluate the relation between the sewerage damage and the estimated seismic hazards which indices are peak ground velocity (PGV) and seismic intensity (IJ) based on the analysis of the data in the 1995 Kobe earthquake with respect to diameters of pipelines, types of pipelines, microtopography and occurrence of sand boiling. We quantify the seismic damage by the ratio of the functional disrupted length L_d with the length of related sewerage pipelines L and the ratio of the number of physical damages N_p with L .

Figure 1 shows the relation between cumulative functional disrupted length L_d (CL_d) and PGV with respect to diameters of pipelines (D), types

of pipelines, microtopography and occurrence of sand boiling. From Figure 1a, CL_d on D of 250 mm (—) is the longest and those of 200 mm (—) and 300 mm (—) are second and third ones. The damage on D of 250 mm (—) starts to occur at PGV of 31.9 cm/s and more than 10 km of CL_d occurs beyond PGV of 83.2 cm/s and the CL_d increases rapidly from CL_d of 15.0 km to 59.7 km when PGV varies from 101.2 cm/s to 150.2 cm/s. CL_d on D of 200 mm (—) increases gradually up to CL_d of 8.7 km when PGV varies from 55.1 cm/s to 155.4 cm/s and the rate of the increase on CL_d changes at PGV of 101.2 km.

Fromures Figure 1b, CL_d on hume pipe (—) is the longest and that on tile pipe (---) is second one. The damage on hume pipe (—) starts to occur at PGV of 31.9 cm/s and the CL_d increases up to 67.1 km at PGV of 158.3 cm/s. The CL_d increases rapidly from 16.3 km to 66.5 km when PGV varies from 101.2 cm/s to 150.2 cm/s. The damage on tile pipe (---) starts to occur at PGV of 59.0 cm/s and the CL_d increases rapidly from 1.4 km to 9.1 km when PGV varies from 101.5 cm/s to 115.9 cm/s and again CL_d increases from 10.1 km to 13.2 km around the range of PGV from 145 cm/s to 150 cm/s.

From the analyses, we attempt to develop seismic fragility curves (SFCs) by using L_d/L and

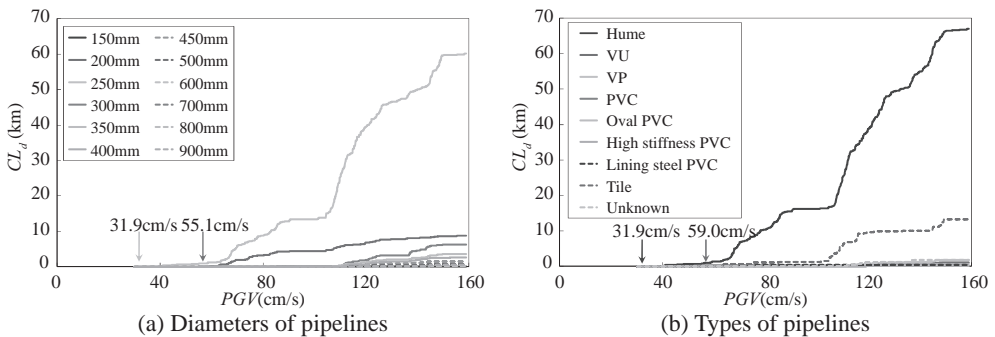


Figure 1. Relation between PGV and functional disrupted length L_d .

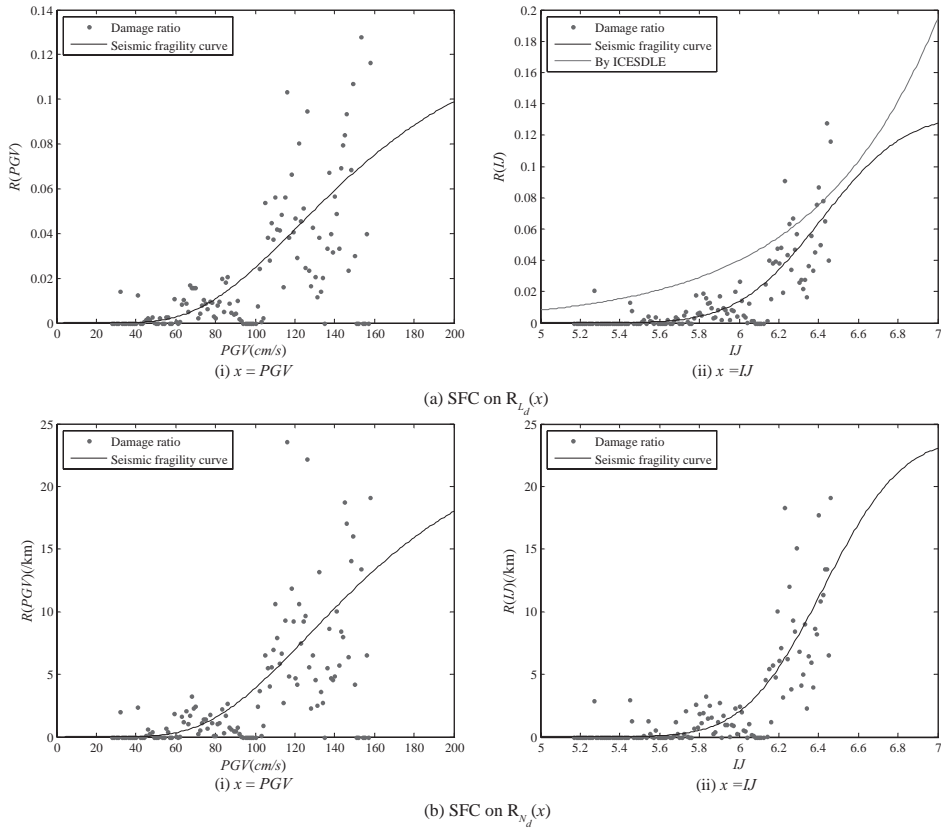


Figure 2. Models of seismic fragility curve estimated by our SHD.

Table 1. Calculated regression coefficients calculated by our SHD.

(a) Functional disrupted ratio						
Regression coefficients						
	C	λ	ζ	μ	σ	Constrains
PGV	0.13	4.99	0.44	162.55	75.13	$\zeta > = 0.44$
IJ	0.13	-	-	6.42	0.33	$\sigma > = 0.33$
(b) Physical damage ratio						
Regression coefficients						
	C	λ	ζ	μ	σ	Constrains
PGV	24.17	5.02	0.42	165.37	72.64	$\zeta > = 0.42$
IJ	23.82	-	-	6.43	0.31	$\sigma > = 0.31$

N_p/L . They are modeled based on logarithmic normal cumulative distribution function (CDF) in the case of $x = PGV$ or normal CDF in the case of $x = IJ$.

Figure 2 shows developed fragility curves. Table 1 shows calculated regression coefficients and the constrains in the regressions. First, $R_{L_d}(PGV)$ starts to increase nearly at PGV of 50.6 cm/s, and increases gradually up to over 0.06 at PGV of 150 m/s. $R_{L_d}(IJ)$ also starts to increase nearly at IJ of 5.63, and gradually up to over 0.06 at IJ of 6.4. $R_{N_d}(PGV)$ starts to increase nearly at PGV of 50.0 cm/s, and increases gradually up to over 11.9 at PGV of 150 cm/s. $R_{N_d}(IJ)$ also starts to increase nearly at IJ of 5.62, and gradually up to over 10.9 at IJ of 6.4.

Second, from comparing our seismic fragility curve with the curve proposed by ICSDALE, both the SFC by this study and that by ICSDALE also monotonously increase from IJ of 5.0 to 6.6. The value of SFC by this study is 1.2 times of that by ICSDALE at IJ of 6.4. It indicates that the ratio of functional disrupted length L_d is larger than that of physical damaged length L_d^p .

Seismic fragility analysis of telecommunication systems

K. Leelardcharoen, J.I. Craig & B.J. Goodno
Georgia Institute of Technology, Atlanta, GA, USA

L. Dueñas-Osorio
Rice University, Houston, TX, USA

Past earthquake experiences reveal that telecommunication systems are extremely vulnerable to seismic hazard. They suffer from physical damage to their facilities and from a surge of communication services demand. Physical damage results in reduced redundancy and capacity of the system while abnormally high demands tend to overload system capacity. Moreover, because typical telecommunication systems are not designed for extreme high volume of calls, network congestion becomes a potential threat to system performance. Timely communication is impossible during congested regimens; and if these conditions prevail, then they affect adequate operation of other infrastructures and slow down emergency or recovery activities. By understanding the mechanisms that enable functionality-based failure to evolve, performance of telecommunication systems and their dependent infrastructures can be improved. Previous studies recognize the problem of congestion, but do not include their effects on system performance assessment. Only physical seismic performance of equipment, buildings, and transmission lines are considered by lifeline engineers. In order to account for both physical damage and traffic congestion in performance estimation of telecommunication system under seismic conditions, a new procedure for constructing system functionality curves of typical telecommunication systems is proposed.

The seismic fragility analysis presented in this paper deals with capacity problems of the telecommunication infrastructure due to dramatic increases in call demands and reduction in topological and structural capacity triggered by seismic hazards. The procedure starts from seismic evaluation of individual network components. The concepts of system reliability and fault tree analysis are used to construct fragility function of network components from their critical contents. These component fragility functions mathematically represent failure of individual components due to earthquakes.

This paper distinguishes communication demands into three sources—(1) communication among subscribers within earthquake affected areas, (2) communication between emergency service agencies and subscribers in earthquake affected areas, and (3) Communication attempts from subscribers outside the earthquake affected area—to simulate the effect of abnormally high communication demand after earthquakes for seismic performance analysis of telecommunication infrastructure. The recognition of the demand sources allows flexibility in modeling of the congestion effects in different demographic areas (e.g. rural and metropolitan area). The proposed probabilistic models representing communication demand after earthquakes are developed based on the teletraffic theory, a classical traffic theory for telecommunication. While Poisson process is used to model normal day demand, the seismic-induced demand is modeled by renewal process.

The basic concepts of teletraffic theory are also used to evaluate system performance. This paper employs network blocking probability, a ratio of unsuccessful call attempts to overall attempts across the network, as performance measurement of telecommunication systems. This allows both physical failure and congestion of network components to contribute to system performance of seismic impaired telecommunication systems. In order to capture the inherent randomness and uncertainties, the seismic performance assessment of a telecommunication system is presented in terms of fragility functions. The fragility analysis of telecommunication network consists of three major steps; (1) determine component blocking probability, (2) determine network blocking probability, and (3) determine probability of exceeding a performance limit state. The Monte Carlo simulation method (MCS) is used in this paper to probabilistically obtain solution of the fragility functions (Fig. 1).

To illustrate the application of the proposed methodology, the analysis is performed on a

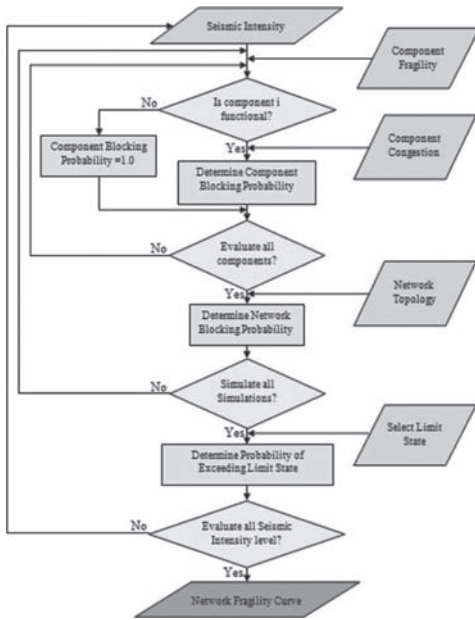


Figure 1. Fragility analysis of telecommunication network.

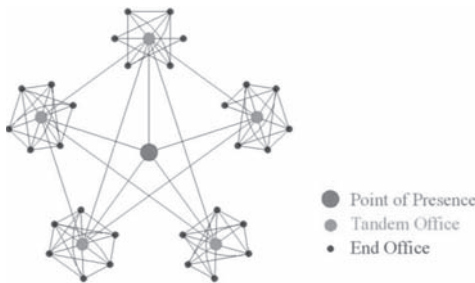


Figure 2. A simplified 30-end-office telecommunication network with 5 tandem offices and 75% redundancy.

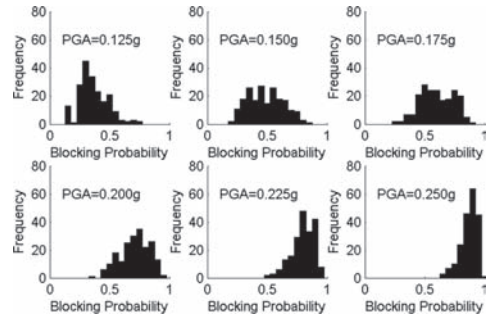


Figure 3. Histogram of network blocking probabilities of a simplified telecommunication network (Fig. 2), subjected to uniform seismic hazard at PGA = 0.125 g, 0.150 g, 0.175 g, 0.200 g, 0.225 g, and 0.250 g.

synthesized network, representing a simplified telecommunication network in a metropolitan area (Fig. 2). The seismic fragility analysis example comprehensively demonstrates the application of the proposed procedure. The example also presents the results of intermediate steps required to obtain fragility function of telecommunication systems (Fig. 3). The proposed methodology provides a framework for probabilistic seismic performance assessment of existing or prospective telecommunication systems. Such an assessment provides quantitative information which can be used to evaluate seismic mitigation actions on a telecommunication network. The method can also be used in the study of infrastructure interdependencies.

*MS_329 — Probabilistic models and methods
for risk assessment of lifeline
networks and decision support (2)*

This page intentionally left blank

Recursive reliability assessment of radial lifeline systems with correlated component failures

J. Rojo

Department of Statistics, Rice University, Houston, TX, USA

L. Dueñas-Osorio

Department of Civil and Environmental Engineering, Rice University, Houston, TX, USA

The increasing susceptibility of lifeline systems to failure due to aging and external hazards requires efficient methods to quantify their reliability and related uncertainty. Monte Carlo simulation techniques for network-level reliability and uncertainty assessment accommodate component correlations and topological complexity without high computational demands but at the expense of reduced accuracy. In contrast, available analytical approaches provide accurate reliability assessments but for limited topologies with component correlations at the expense of high computational complexity. This study introduces a recursive closed-form technique to obtain the entire probability distribution of a reliability metric of customer service availability (CSA) for radial lifeline systems with *component failure correlations*. The flexibility of correlation inclusion is enabled by a novel recursive algorithm that does not perform the recursive operations explicitly, but rather it recursively transfers knowledge about which operations need to be performed. This approach halves the computation time relative to a naïve reliability assessment implementation. In addition, this study demonstrates that correlation inclusion transforms a problem solvable in polynomial time as a function of problem size into a problem only solvable in exponential time, yielding a fundamental insight for computing in civil engineering. Such tool for radial topologies also applies to other systems upon pertinent modifications, including bridges and wind turbines, while providing infrastructure owners an efficient tool to inform operation and maintenance decision making.

It is clear that a desirable approach to study lifeline system reliability should be fast and yield not only average values or moment-based bounds, but also the entire probability distribution of multi-valued system-level reliability metrics. Hence, this work specifically discusses a methodology to satisfy such computational needs by constructing the probability mass function (PMF) of a basic adequacy reliability metric for general radial lifeline systems that measures the number of customers

retaining service relative to the total number of customers. Since adequacy relates to the existence of sufficient facilities and paths within the lifeline systems to satisfy consumer demands, this concept is applicable to infrastructures of different nature and size. The PMF of the proposed adequacy reliability metric is a probability law with a nested sum of products structure. This formulation requires a combinatorial exploration of all possible surviving network component sets to construct the multi-valued customer service availability metric (CSA) introduced here. However, an efficient recursive algorithm is likely to exploit the structure of the CSA formulation even when the failure among network components is *correlated*—an analytical task not yet addressed in the literature. This is because a recursive algorithm for *uncorrelated* component failures has already been shown to run in $O(M^3)$ time by performing a polynomial number of operations, where the “big O ” notation represents the asymptotic growth rate of the algorithm’s running time as a function of the number of network nodes M . A recursive formulation that exploits the knowledge of the nested operations is the key to halve the number of operations of exponential time naïve reliability solutions in the presence of correlated components.

A radial *distribution* system consists of supply nodes that deliver commodities to end users within a shared service territory. The system in Figure 1 shows typical radial power delivery networks as sample lifeline systems. This network represents the portion of a power system between distribution substations and transformers at tapping points, and consist of main feeders emanating from low voltage substations (supply buses), and lateral segments that branch out from main feeders to reach load points with different number of customers.

Let f^{ij} denote the j^{th} lateral branching point of the i^{th} main feeder of a radial network, where $i = \{1, 2, \dots, I\}$, $j = \{1, 2, \dots, J_i\}$, I is the number of main feeders in the circuit, and J_i is the number of branching points per main feeder i . Let b_{ij} be the number of individual lateral segments

emanating from branching point f_{ij} and let n_{ijl} be the number of customers served by load point LP_{ijl} , where $l = \{1, 2, \dots, b_{ij}\}$. Using this notation, the total number of load points in the system is $M = \sum_{i=1}^I \sum_{j=1}^{J_i} b_{ij}$. The service availability of customers at load point LP_{ijl} can be described by a binary random variable X_{ijl} , indicating which users retain service when the equipment or lines in the lateral segment that contain the $(i,j,l)^{th}$ end point do not fail with probability p_{ijl} , and the $(i,j)^{th}$ path linking the supply station (bus) with branching point f_{ij} does not fail with probability v_{ij} .

The reliability of the main feeder segments that form path (i,j) (which has reliability v_{ij}) is denoted as $v_{i,j-1,j}$, where $j-1$ and j are the j^{th} starting and end points of main feeder segments, respectively, $j-1 = \{0, 1, 2, \dots, J_i - 1\}$ with $j-1 = 0$ denoting the substation bus, and $j = \{1, 2, \dots, J_i\}$ as before. To illustrate this notation, consider feeder 2 ($i = 2$) in Figure 1. Let's select an arbitrary path, such as the path between the supply point (bus bar) and the end of the feeder at branching point $f_{2,3}$. This path has a reliability $v_{2,3}$, which depends on the reliability of the main feeder segments $v_{2,0,1}$, $v_{2,1,2}$ and $v_{2,2,3}$.

Building upon counting arguments, an unconditional estimate of the probability $P(CSA = s/N | IM)$, where s is the number of customers served, N the total number of customers and IM a hazard intensity level, is the following:

$$P\left(CSA = \frac{s}{N} | IM\right) = \sum_{k^* \in K_s} \int_{-\infty}^{\infty} \left(\prod_{r=1}^M \alpha_r(x)^{k_r} \prod_{r=1}^M (1 + ar(x) - 1\phi(x)) dx \right) \quad (1)$$

where $\phi(x)$ is the standard normal probability density function that helps reaching conditional independence from x , and the α_r terms are a

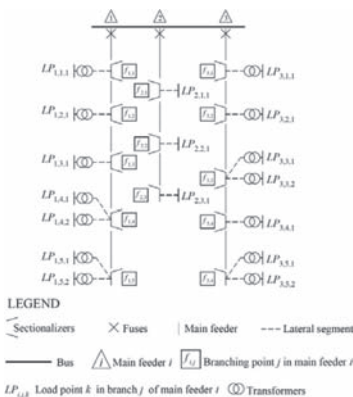


Figure 1. Simplified 17-node radial topology of typical power systems at the distribution level.

function of x because $\alpha_r = p_r/(1-p_r)$ and each p_r is a reliability function that depends on the normal random variable X associated with the Dunnett-Sobel class correlation structure. This correlation structure has shown errors up to 10% in bridge applications, which are manageable, although further studies are required to assess the error in spatially distributed systems. Data from smart grid systems will contribute to the assessment of component correlation structures in the future. Also, in Equation (1), $K_s \subseteq K$ includes the totality of 2^M possible state vectors k^* that capture all possible failure realizations. Equation (1) requires the integration over all values of x before the summation takes place. Hence, performing a recursion is impossible since it operates directly over the sum of products, and Equation (1) will thus require an exponential amount of time for its computation.

A conceptual solution to improve the computation time of Equation (1) is the main contribution of the present manuscript. The idea is not to perform the operations of the recursion, but only to keep track cumulatively of the indices of the elements that carry over once the recursion is initialized. Without loss of generality, assume s takes values in the set $S = \{0, \dots, M\}$, which implies each load point is a single customer. The R function (recursion function) for $s = 1$ is $R(1, K_1) = \alpha_1 + \alpha_2 + \dots + \alpha_M$. Then, instead of performing the recursion to obtain $R(2, K_2)$ as a function of $R(1, K_1)$, its element indices are stored as $R(2, K_2) = \alpha_1\alpha_2 + \alpha_1\alpha_3 + \dots + \alpha_1\alpha_M + \alpha_2\alpha_3 + \dots + \alpha_{M-1}\alpha_M$. Note that each s level has as many terms as its binomial coefficient choosing s out of M . Once the R function is found for all $s \in S$, then the integration of Equation (1) takes place halving the time of a naive implementation, while highlighting the intrinsic computational complexity of adding correlation to otherwise polynomial time solutions (Figure 2). The magnitude assessment of the correlation effects in CSA estimates constitutes ongoing research work.

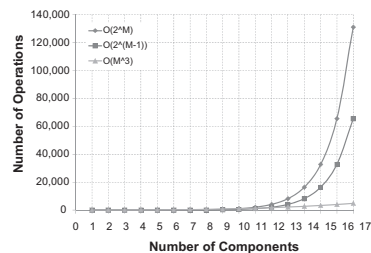


Figure 2. Computational complexity in number of operations for radial system reliability assessment. Results show a naive implementation with component correlations $O(2^M)$, a recursive approach without correlations $O(2^M(M-1))$, and the proposed recursive-informed correlated components approach $O(M^3)$.

Post-disaster damage detection for pipeline networks by Matrix-based System Reliability analysis

W.-H. Kang & J. Song

University of Illinois at Urbana-Champaign, Urbana, IL, USA

1 INTRODUCTION

This study aims to develop efficient system reliability methods to facilitate uncertainty quantification of post-disaster network flows and damage detection of pipeline networks. First, a system reliability method is developed to quantify the uncertainties in the flow quantities of pipeline networks for a given earthquake scenario. The method improves the efficiency of the Matrix-based System Reliability (MSR) method (Kang *et al.*, 2008, Song & Kang 2009, Lee *et al.*, 2010) by using an event-tree-based selective search scheme. Second, a system reliability method is proposed to estimate the conditional probabilities of water pipeline damage given post-disaster flow monitoring data, based on the Bayesian framework introduced in Poulakis *et al.*, (2003) and the MSR method. Since finding such conditional probabilities is even more time-consuming than system uncertainty quantification, the proposed method finds the optimal problem size for efficient and accurate stochastic damage detection using a selective expansion scheme. Both methods are applied to a water distribution network with 15 pipelines subjected to an earthquake event, and the results are compared to those by existing system reliability methods and Monte Carlo simulations (MCS).

2 PROPOSED SYSTEM RELIABILITY METHODS

The MSR-based system uncertainty quantification method (Lee *et al.*, 2010) is further developed for a lifeline network with a large number of component damage scenarios. In order to overcome the computational challenge of the MSR method in dealing with large system problems, the method constructs the vectors of the system state probabilities efficiently by selectively searching elements that correspond to the system states with higher likelihoods. This allows us to obtain probability distributions and statistical parameters of network flow quantities efficiently, using the convenient matrix-based framework.

Based on a Bayesian framework (Poulakis *et al.*, 2003), a stochastic system damage detection method is proposed to compute the conditional probability that a component is damaged given post-disaster network flow monitoring data. To overcome the computational challenges in estimating such conditional probabilities, the method uses a selective expansion scheme which reduces the number of system states by combining damage states of selected components. This method achieves an optimal matrix-based representation of the problem for efficient damage detection.

3 APPLICATION TO A WATER PIPELINE NETWORK

The methods are applied to the water pipeline network shown in Figure 1. The network consists of 15 pipes (links), 11 nodes, one inflow location, and three outflow locations. It is assumed that for the inflow rate $0.1 \text{ m}^3/\text{sec}$, the rate of each outflow for undamaged condition is $0.0333 \text{ m}^3/\text{s}$. The flow rates of the undamaged pipes can be computed using

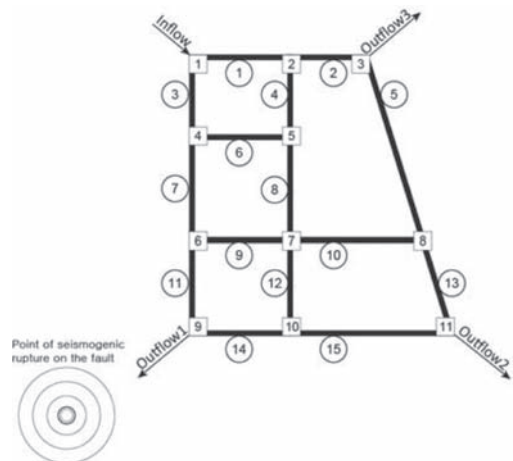


Figure 1. A water pipeline network with 15 components.

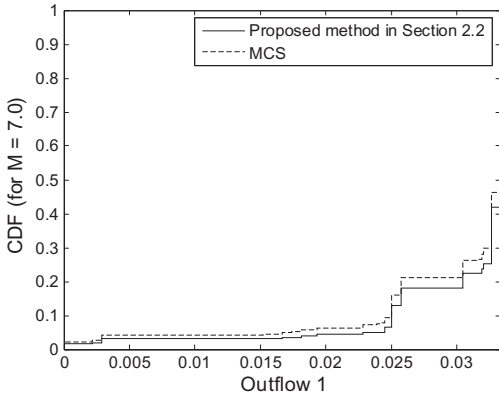


Figure 2. Cumulative distribution functions of Outflow 1.

water flow rate equilibrium equations at the nodes. Each pipe has four damage states represented by 0%, 25%, 50%, and 100% water loss, and has the corresponding component quantities. The probabilities of the damage states are computed using the repair rate in the HAZUS technical manual, a ground motion attenuation relationship, and water loss distribution models in the literature.

The cumulative frequency diagram of Outflow 1 is estimated using the proposed uncertainty quantification method (Figure 2). Comparison with the cumulative frequency diagram obtained by MCS (10^5 samples) confirms the reasonable accuracy of the proposed method. It is noted that the proposed method needed only two minutes while the MCS required one hour using a personal computer. The proposed method evaluated the outflows of the network for only 13,008 system states among around a billion. This demonstrates that the proposed method can perform uncertainty quantification for a large system accurately without evaluating the probabilities and system quantities for too many system states.

Suppose, after an earthquake event with $M = 7.0$ occurs, the three outflow rates are observed as 1.20×10^{-2} , 2.05×10^{-2} and 1.21×10^{-3} m³/s (from Outflow 1 to 3). Using the Bayesian method developed in this paper, one can calculate the updated probabilities that the pipes are damaged and thus experience any loss of water flow rate. In order to account for various uncertainties in the problem (e.g. measurement error, and model errors), the errors of water flow rate prediction are described as zero-mean Gaussian random variables with the standard deviations σ assumed to be 1% of the inflow rate 0.1 m³/s.

To test the accuracy of the proposed method, we evaluate the updated probabilities completely (i.e. without the selective expansion scheme) using a

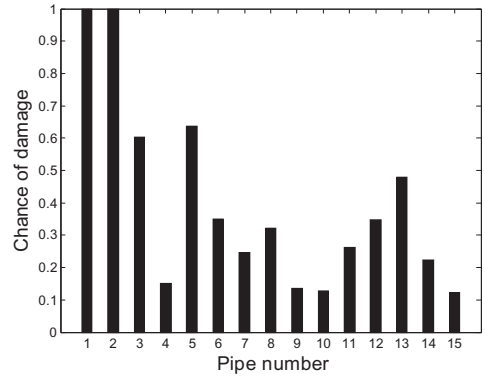


Figure 3. Component damage probabilities based on the complete vector of the updated probabilities obtained by a supercomputer ($\sigma = 1\%$ of inflow).

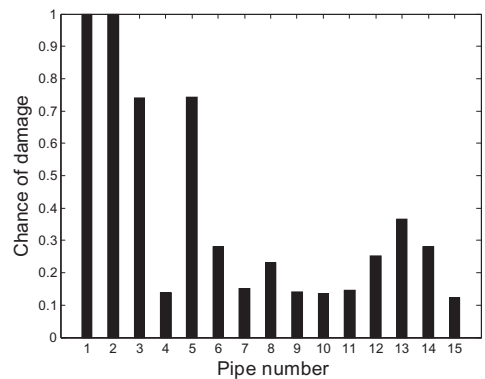


Figure 4. Component damage probabilities based on the incomplete vector of the updated probabilities obtained by the proposed method ($\sigma = 1\%$ of inflow).

supercomputer, which requires a total of $4^{15} (\approx 10^9)$ flow analyses. By summing up the updated probabilities corresponding to the damage of each component, the component damage probability is calculated (see Figure 3). Next, the same analysis is conducted by a personal computer, using the efficient method proposed in this paper. In the analysis, only 6 out of 15 components with complete damage states were used for accurate results. The results in Figure 4 show a good agreement with those in Figure 3. MCS was not able to detect damaged components effectively despite a large number of samples and exceedingly large computational time.

4 CONCLUSION

In this study, two efficient system reliability methods are developed to facilitate uncertainty

quantification of post-disaster network flow and damage detection. The developed methods were successfully applied to a water pipe network consisting of 15 pipelines. Comparison of the results with those by Monte Carlo simulations and the MSR method demonstrated the accuracy and efficiency of the proposed methods.

REFERENCES

- Kang, W.-H., Lee, Y.-J., Song, J. & Gencturk, B. 2010. Further development of matrix-based system reliability method and applications to structural systems. *Structure and Infrastructure Engineering: Maintenance, Management, Life-cycle Design and Performance*, in print (doi:10.1080/15732479.2010.539060).
- Lee, Y.-J., Song, J., Gardoni, P. & Lim, H.-W. 2011. Post-hazard flow capacity of bridge transportation network considering structural deterioration of bridges. *Structure and Infrastructure Engineering: Maintenance, Management, Life-cycle Design and Performance* 7(7): 509–521.
- Poulakis, Z., Valougeorgis, D. & Papadimitriou, C. 2003. Leakage detection in water pipe networks using a Bayesian probabilistic framework, *Probabilistic Engineering Mechanics* 18: 315–327.
- Song, J. and Kang, W.-H. 2009. System reliability and sensitivity under statistical dependence by matrix-based system reliability Method. *Structural Safety* 31(2): 148–156.

Efficient identification of critical disjoint cut sets and link sets for network reliability analysis

H.-W. Lim & J. Song

University of Illinois at Urbana-Champaign, Urbana, IL, USA

1 INTRODUCTION

Reliability analysis of urban infrastructure networks for transportation, telecommunication, and utility services of electricity, water, sewage and gas is complex in nature due to a large number of network components, network topology and component/system interdependency. Thus, risk assessment is often performed by repeated computational simulations based on random samples of hazard intensity measures and corresponding component status, which may hinder rapid risk assessment and risk-informed decision making for hazard mitigation.

This paper presents a new method to improve the process for identifying disjoint cut sets and link sets by use of a non-sampling-based algorithm, the recursive decomposition algorithm (RDA). This new method, termed as “selective” RDA identifies critical disjoint cut sets and link sets, i.e. sets with higher probabilities with a priority so that one can calculate the probabilities of network connection or disconnection with a fewer number of disjoint sets. The identified critical sets can be also used to compute component importance measures to quantify the contributions of network components to the network disconnection events.

2 RDA AND SELECTIVE IDENTIFICATION OF CRITICAL DISJOINT CUT SETS/LINK SETS

The RDA recursively decomposes the network into sub-graphs until there remain no paths between the source and terminal nodes in all the sub-graphs. Each path found in the network and sub-graphs becomes disjoint link sets after merging with the coefficient sets for the sub-graphs and thus contributes to the network reliability while the coefficient sets for the sub-graphs containing no paths are disjoint cut sets and contribute to the system failure probability (Li & He 2002). If *disjoint* paths are identified, the network reliability can be calculated by summing up the probabilities of individual disjoint paths or link sets.

For a large network, the upper and lower bounds of the network reliability and failure probability can be calculated by use of the partial sets of disjoint cut sets and link sets identified by considering the desired level of accuracy because it might be difficult to enumerate all disjoint cut sets and link sets.

$$\sum_{i=1}^{n_{L,i}} P(L_i) \leq R \leq 1 - \sum_{i=1}^{n_{C,i}} P(C_i) \tag{1}$$

$$\sum_{i=1}^{n_{C,i}} P(C_i) \leq F \leq 1 - \sum_{i=1}^{n_{L,i}} P(L_i)$$

where L_i and C_i are the i -th disjoint link set and cut set of G , respectively. $n_{L,i}$ and $n_{C,i}$ are the numbers of the identified disjoint link sets and cut sets, respectively.

In this paper, the original RDA is improved by two stages and the improved method will be termed as “selective” RDA. First, while the original RDA does not account for component reliabilities in identifying shortest paths, the disjoint cut sets and link sets, which will be identified afterwards, are different depending on the shortest paths and thus the shortest paths will have a significant impact on the system reliability convergence. A method is developed to identify the most reliable path by modifying the distance based Dijkstra’s Algorithm (Ahuja *et al.*, 1993) into the probability based algorithm.

Second, the question is which sub-graph should be first investigated on their connectivity. In the original RDA, the connectivity is sequentially investigated following the original component numbering choice and thus the cut sets and link sets are identified on the sub-graph order basis. However, they could not be critical sets because they are identified regardless of their probability. The selective RDA identifies the sub-graph with the maximum probability of the coefficient of the sub-graphs and check whether it is connected or disconnected.

As a result, disjoint cut sets are identified in the descending order in terms of their probability. This

method will make the bounds obtained by the RDA will converge faster than the original approach.

3 APPLICATION OF SELECTIVE RDA TO LIFELINE RISK ASSESSMENT

The selective RDA can be used for risk assessment of lifeline networks. In this paper, first the failure probabilities of components, e.g., stations at nodes or pipelines between nodes, are estimated based on 1) the inter-event/intra-event uncertainties and spatial correlation for intra-event uncertainties on the seismic demand side, and 2) the uncertainties in the seismic capacity of the components based on the HAZUS fragility model (FEMA 2008). Next, the probability of each disjoint set is computed by a multi-variate normal probability algorithm developed by Genz (1992). Using the estimated probabilities of the identified disjoint cut sets and link sets, the upper and lower bounds of the network reliability or failure probability are calculated by Equation 1.

In order to measure the relative importance of components, the conditional probability importance measure (CIM), which is proposed by Song & Kang (2009), can be used. The CIM is approximately obtained based on the identified disjoint link sets as

$$CIM_i = \frac{\sum_{j=1}^{n_{C,i}} P(E_i C_j)}{\sum_{j=1}^{n_{C,i}} P(C_j)} \quad (2)$$

where E_i is the component failure event of interest. On the other hand, by using the identified disjoint link sets, the CIM is approximated as

$$CIM_i = \frac{1 - P(\bar{E}_i) - \sum_{j=1}^{n_{L,i}} P(L_j) + \sum_{j=1}^{n_{L,i}} P(\bar{E}_i L_j)}{1 - \sum_{j=1}^{n_{L,i}} P(L_j)} \quad (3)$$

4 NUMERICAL EXAMPLE

The selective RDA is demonstrated by the reliability analysis of a simple gas transmission network of Shelby County in Tennessee, USA for an earthquake scenario with a magnitude M_w of 7.7 at the epicenter N35.3° and W90.3° as shown in Figure 1.

Figure 2 clearly shows that the bounds by the selective RDA converge much faster than those by

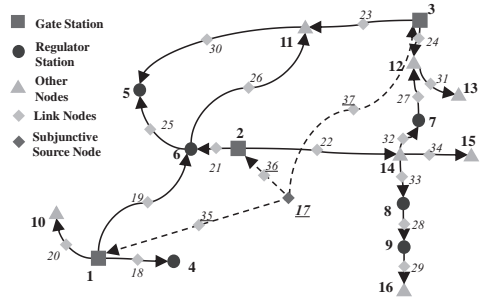


Figure 1. Simplified gas transmission network in Shelby County, Tennessee.

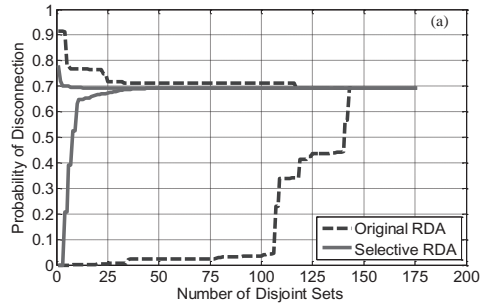


Figure 2. The bounds on the probability of disconnection obtained by the original and selective RDAs in terms of number of identified disjoint sets.

the original RDA. Specifically, the numbers of the total identified sets needed by the selective RDA to achieve the bound widths of 1% and 5% are only about 27% and 10% of those in the original RDA. The CIM's shows that pipelines contribute more to the disconnection and that CIM's can be calculated with considerable accuracy even with limited number of identified cut sets and link sets.

REFERENCES

Ahuja, R.K., Magnanti, T.L. & Orlin, J.B. 1993. *Network Flow: Theory, Algorithms, and Applications*. Upper Saddle River, New Jersey: Prentice-Hall.

Federal Emergency Management Agency (FEMA). 2008. *HAZUS MH-MR3 Technical Manual*. Washington D.C.: FEMA.

Genz, A. 1992. Numerical computation of multivariate normal probabilities. *Journal of Computational and Graphical Stat.*: 141-149.

Li, J. & He, J. 2002. A recursive decomposition algorithm for network seismic reliability evaluation. *Earthquake Engineering and Structural Dynamics* 31(8): 1525-2539.

Song, J. & Kang, W.-H. 2009. System reliability and sensitivity under statistical dependence by matrix-based system reliability method. *Structural Safety* 31(2): 1584-1593.

Seismic risk assessment of spatially-distributed systems using ground-motion models fitted considering spatial correlation

Nirmal Jayaram

Risk Management Solutions Inc., CA, USA

Jack W. Baker

Stanford University, CA, USA

ABSTRACT: Ground-motion models are commonly used in earthquake engineering to predict the probability distribution of the ground-motion intensity at a given site due to a particular earthquake event. These models are often built using regression on observed ground-motion intensities, and are fitted using either the one-stage mixed-effects regression algorithm proposed by Abrahamson and Youngs (1992) or the two-stage algorithm of Joyner and Boore (1993). In their current forms, these algorithms ignore the spatial correlation between intra-event residuals. Recently, Jayaram and Baker (2010) and Hong et al. (2009) observed that considering spatial correlation while fitting the models does not impact the model coefficients that are used for predicting median ground-motion intensities, but significantly increases the standard deviation of the intra-event residual and decreases the standard deviation of the inter-event residual. These changes have implications for risk assessments of spatially-distributed systems, because a smaller inter-event residual standard deviation implies lesser likelihood of observing large ground-motion intensities at all sites in a region.

This manuscript explores the impact of considering spatial correlation on the residual standard deviations in situations where the ground-motion model is fitted using only a few recordings or closely-spaced recordings, which is often the case in low to moderately seismic regions such as the eastern United States. This is done by refitting the Campbell and Bozorgnia (2008) ground-motion model (subsequently referred to as the CB08 model) to predict spectral accelerations at six different periods (0, 1, 2, 4, 7.5, 10 seconds) with and without consideration of spatial correlation, using earthquakes with a small to moderate number of recordings or closely-spaced recordings. Figure 1 shows the changes in the residual standard deviations after refitting the CB08 model using subsets of earthquakes with a

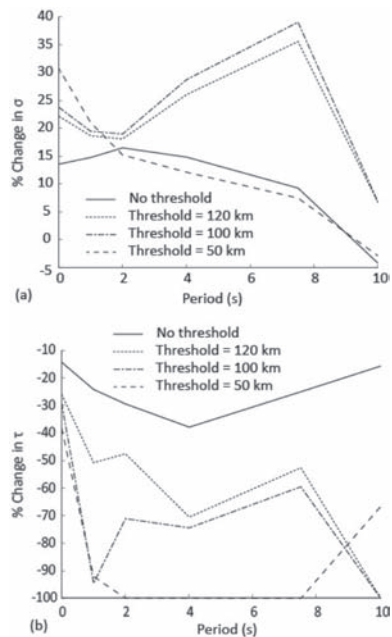


Figure 1. Impact of the average site-separation distance on (a) σ (b) τ .

specified maximum average separation distance between recordings. In general, the consideration of spatial correlation results in an increase in the intra-event residual standard deviation (σ) and a decrease in the inter-event residual standard deviation (τ). These changes are more significant when smaller average separation distance thresholds are used, with an exception being the change in the long-period σ 's when the threshold is set at 50 km.

Figure 2 shows the changes in the residual standard deviations after refitting the CB08 model using subsets of earthquakes with a specified maximum number of recordings. In this case, the

impact of considering spatial correlation does not increase monotonically with a reduction in the threshold number of sites (large changes are seen when the threshold is set at 200).

Ignoring spatial correlation while fitting the ground-motion model does not significantly affect the estimates of the ground-motion medians or the standard deviation of the total residuals, and therefore hazard and loss analyses for single structures will produce accurate results if the existing ground-motion models are used. Risk assessments for spatially-distributed systems, however, are influenced by the standard deviation of the inter-event and the intra-event residuals and not just by the medians and the standard deviation of the total residuals. This is illustrated using sample risk assessments for a hypothetical portfolio of hundred \$1,000,000 buildings in the San Francisco Bay Area located on a 10 by 10 grid with a grid spacing of 20 km. The risk assessment is carried out using the values of σ and τ estimated in this work with and without consideration of spatial correlation for two cases: (a) case 1: ground-motion model fitted using all the NGA database records used by CB08 (b) case 2: ground-motion model fitted using earthquakes where the average station-station separation distance is less than 100 km. In both cases, the CB08 median model co-efficients are used for estimating median intensities, since the objective of this manuscript is to demonstrate the impact of

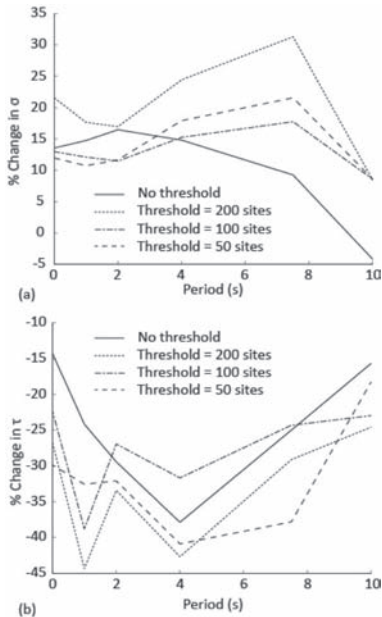


Figure 2. Impact of the number of recordings on (a) σ (b) τ .

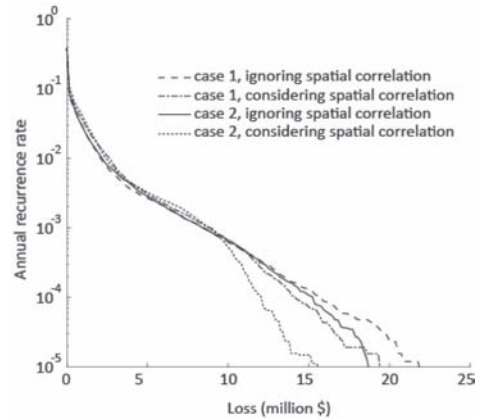


Figure 3. Risk assessment for a hypothetical portfolio of buildings performed using ground-motion models developed with and without the proposed refinement.

the changes in the standard deviations on the risk estimates. The resulting loss exceedance curves are shown in Figure 3.

It can be seen from Figure 3 that the recurrence rates of extreme losses are overestimated while using the standard deviations obtained without consideration of spatial correlation. The difference between the risk estimates obtained with and without consideration of spatial correlation is higher in case 2 than in case 1 directly as a consequence of the more significant differences in the values of σ and τ in case 2.

Overall, this work serves to illustrate the need to consider spatial correlation in the regression for ground-motion models in upcoming projects such as the NGA east project.

REFERENCES

- Abrahamson, N.A. & Youngs, R.R. (1992). A stable algorithm for regression analyses using the random effects model. *Bulletin of the Seismological Society of America* 82(1), 505–510.
- Campbell, K.W. & Bozorgnia, Y. (2008). NGA ground motion model for the geometric mean horizontal component of PGA, PGV, PGD and 5% damped linear elastic response spectra for periods ranging from 0.01 to 10 s. *Earthquake Spectra* 24(1), 139–171.
- Hong, H.P., Zhang, Y. & Goda, K. (2009). Effect of spatial correlation on estimated ground-motion prediction equations. *Bulletin of the Seismological Society of America* 99(2A), 928–934.
- Jayaram, N. & Baker, J. (2010). Considering spatial correlation in mixed-effects regression, and impact on ground-motion models. *Bulletin of the Seismological Society of America* 100(6), 3295–3303.
- Joyner, W. & Boore, D. (1993). Methods for regression analysis of strong-motion data. *Bulletin of the Seismological Society of America* 83(2), 469–487.

A FORM-based analysis of lifeline networks using a multivariate seismic intensity model

M. Miller & J. Baker

Stanford University, Stanford, CA, USA

H.-W. Lim & J. Song

University of Illinois Urbana-Champaign, Urbana, IL, USA

N. Jayaram

Risk Management Solutions Inc., CA, USA

ABSTRACT: Governmental organizations, private firms, and others in seismically active regions are interested in how reliable lifeline networks will be in the event of an earthquake. Assessing risk in these networks is more complicated than assessing risk for individual sites using traditional Probabilistic Seismic Hazard Analysis (PSHA) because of interdependencies among different system links, as well as correlations among ground motion intensities across a region. The focus of this paper is three-fold: (1) to construct a multivariate probability distribution of seismic intensities at many locations in an example network, by analyzing simulated earthquake data, (2) to develop a framework based on the First Order Reliability Method (FORM) to calculate network flow capacity after a disaster, and (3) to illustrate the importance of more accurately describing joint distributions of ground motion intensities when computing lifeline network reliability. This proposed approach provides probability distributions of network flow capacity given an earthquake, and also quantifies the importance of each lifeline component, which would allow system administrators to identify the most critical links in their lifeline systems and prioritize network upgrades. The example results indicate that neglecting the correlation of the ground motions can result in gross overestimation or underestimation of the probability of achieving a given system flow.

1 INTRODUCTION

Officials deciding how to mitigate risk to their lifeline networks, whether through maintenance, retrofitting, new construction, or other policies, face uncertainty in network demands as well as capacity. Assessing risk for a network is yet more complex

than that of a single site, because of interactions among network components. For example, there is no simple closed-form equation that can be evaluated to find network performance, such as maximum flow capacity, even if the ground motion intensities at each location are known. A further complication is that the demands due to ground motions are correlated among a region, and similar bridge construction methods or codes can lead to a correlation among structural capacities too, as described by Lee & Kiremidjian (2007) among others.

A common choice for assessing network performance is Monte Carlo Simulation (MCS), such as used by Crowley & Bommer (2006), and Jayaram & Baker (2010). However, this method does not directly determine which components or uncertainties have the most impact on the overall failure probability, nor the most likely failure scenario.

This paper proposes the use of the First-Order Reliability Method (FORM) to determine probabilities of exceeding certain levels of performance loss in a sample San Francisco Bay Area (USA) transportation network. FORM overcomes the limitations of MCS described above because it naturally provides a “design point,” i.e. most probable set of values of the random variables that causes a failure (Der Kiureghian 2005). However, the error in FORM increases with the nonlinearity of the problem and the number of random variables. Furthermore, FORM traditionally uses a closed-form limit state expression. The proposed approach overcomes some obstacles traditionally prohibiting researchers from using FORM for network reliability analyses.

First, the network is focused to 38 main links in the SF Bay Area. Second, careful mathematics enable the demand and capacity uncertainty

to be captured by only two random variables per location, which is less than that required by some other analysis approaches. The selected random variables are a) the natural logarithm of the spectral intensity demand, $\ln S_a$, and b) a parameter that captures the combined effect of uncertainty in both the damage state and the flow capacity for a given demand, ε_T . These two variables enable the calculation of traffic flow across each link. Using only the random variables $\ln S_a$ and ε_T , total maximum network flow capacity can be estimated. The formulation presented is also carefully selected to create a smooth limit state function, which is critical for the gradient-based algorithm used by FORM to find the design point. Third, the analysis captures the complex network performance by linking to an external subroutine that efficiently calculates the network flow at each iteration, while finding the design point. This subroutine takes the place of an explicit limit state function.

In addition, this paper presents a multivariate seismic intensity model, which is crucial because FORM traditionally requires that the random variables can be completely parameterized by a standard probability distribution. The seismic intensity in this paper is modeled as:

$$\ln(S_{a_{ij}}) = \ln(\bar{S}_{a_{ij}}) + \sigma_{ij}\varepsilon_{ij} + \tau_j\eta_j \quad (1)$$

where $S_{a_{ij}}$ is the spectral acceleration at a period of 1 s at site i during earthquake j , $\bar{S}_{a_{ij}}$ is the median predicted spectral acceleration that is a function of period, magnitude, distance, shear wave velocity, and other local conditions, and the other terms comprise residual terms as described by Jayaram & Baker (2009).

While researchers such as Jayaram & Baker (2008) have shown close matching of the residual terms to a normal distribution, the term $\ln \bar{S}_{a_{ij}}$, in contrast, is a nonlinear function of many variables, including magnitude and distance to the fault. There is no clear reason why the composite $\ln S_a$ values will follow any particular distribution, however results below indicate that a normal distribution predicts the log spectral intensity values well. The following sections describe how a 38-dimensional probability model can then be created to describe the joint distribution of ground shaking intensity at each component location. This result, combined with the previously described methods, allows for a risk assessment of this sample network under a probabilistic scenario of future earthquakes.

2 RESULTS AND CONCLUDING REMARKS

The seismic intensity model developed in this paper results from an analysis of thousands of

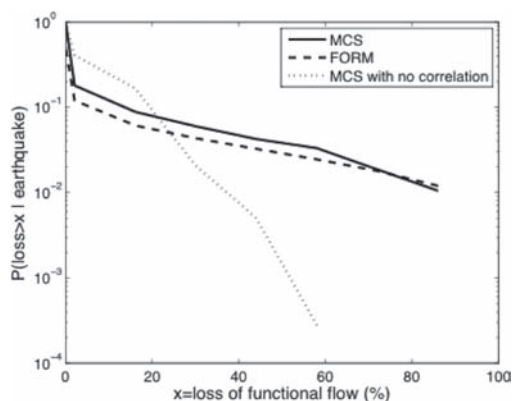


Figure 1. $P(\text{loss} > x \mid \text{earthquake})$ where x is the relative to the case with more network flow loss of maximum network flow between the start and end nodes.

simulated earthquakes in the San Francisco Bay Area generated by MCS, ending in fitting a multivariate Normal distribution to the logarithms of the spectral intensities at all component locations. Figure 1 shows the probability of exceedance for different loss levels of maximum flow capacity, given an earthquake.

Figure 1 also highlights the dramatic difference in the computed network performance if correlation in ground motion intensities is neglected.

Although MCS is less restrictive in the form of modeling parameters, FORM more efficiently provides importance factors and design points.

The importance factors help identify critical network components and weaknesses. This information helps support the decision of officials determining if and where to improve their lifeline networks.

ACKNOWLEDGEMENTS

The authors would like to thank Professor Kiremidjian at Stanford University and Caltrans for providing the network data. Thanks also to B. Shen at the University of Illinois Urbana-Champaign for cataloging the bridges in order to determine the “weakest” bridge on each link. M. Miller thanks the support of NSF and Stanford Graduate Fellowship Program. J. Baker and J. Song thank NSF for funding under grant numbers CMMI 0952402 and CMMI 1031318 respectively.

REFERENCES

- Crowley, H. & Bommer, J.J. 2006. Modelling seismic hazard in earthquake loss models with spatially distributed exposure. *Bulletin of Earthquake Engineering* 4(3): 249–273.

- Der Kiureghian, A. 2005. First- and second-order reliability methods. Chapter 14 in *Engineering design reliability handbook*, E. Nikolaidis, D.M. Ghiocel and S. Singhal, Edts., CRC Press, Boca Raton, FL.
- Jayaram, N. & Baker, J.W. 2008. Statistical tests of the joint distribution of spectral acceleration values. *Bulletin of the Seismological Society of America* 98(5): 2231–2243.
- Jayaram, N. & Baker, J.W. 2009. Correlation model for spatially-distributed ground-motion intensities. *Earthquake Engineering & Structural Dynamics* 38(15): 1687–1708.
- Jayaram, N. & Baker, J.W. 2010. Efficient sampling and data reduction techniques for probabilistic seismic lifeline risk assessment. *Earthquake Engineering & Structural Dynamics* 39: 1109–1131.
- Lee, R. & Kiremidjian, A. 2007. Uncertainty and Correlation for Loss Assessment of Spatially Distributed Systems. *Earthquake Spectra* 23: 753–770.

GS_211 — Probabilistic seismic hazard analysis (1)

This page intentionally left blank

Probabilistic design of supplemental dampers for base-isolated bridges

A.A. Taflanidis

University of Notre Dame, Notre Dame, IN, USA

1 INTRODUCTION

Applications of seismic isolation techniques to bridges have gained significant attention over the last decades. This configuration provides with enhanced capabilities for energy dissipation during earthquake events while also accommodating thermal movements during the life-cycle of operation of the bridge. It is associated though with large displacement, especially (but not only) under near fault earthquake ground motions, which may lead to inelastic deformations and to seismic pounding of the deck between adjacent spans or to the abutments. For controlling such vibrations, application of seismic dampers has been proposed (Makris and Zhang 2004). One of the main challenges in the design of such dampers has been the explicit consideration of the nonlinear behavior of the isolators and the dampers in the design process as well as proper modeling of soil-structure interaction. Another challenge has been the efficient consideration of the variability of future ground motions. This work investigates an end-to-end simulation based, probabilistic framework that addresses all aforementioned challenges, allowing consideration of complex models for describing the bridge behavior and the seismic hazard under near-fault seismic excitations.

2 BRIDGE MODEL

A two-span, straight bridge is considered, supported on the abutments and the intermediate pier through seismic isolators. Each span of the bridge is modeled as a rigid body. For appropriately addressing at the design stage the impact between adjacent spans, soil-structure interaction characteristics and the nonlinear behavior of isolators and dampers, nonlinear dynamic analysis is used for evaluating the bridge response. The interaction with the abutment and the dynamic characteristics of the latter are incorporated in the analysis by modeling each abutment as a mass connected to the ground by a spring and a dashpot, with stiffness and damping properties that are related to the local soil

conditions. The vibration behavior of the isolators, the dampers and the pier is incorporated by appropriate nonlinear models (Makris and Zhang 2004; Taflanidis et al., 2008). Impact between adjacent spans, or to the abutments, is approximated as a Hertz contact force with an additional non-linear damper to account for energy losses during contact (Muthukumar and DesRoches 2006).

3 NEAR FAULT EXCITATION MODEL

For describing near-fault excitation a comprehensive stochastic model is used (Taflanidis et al., 2008); according to it the high-frequency and long-period components of the motion are independently modeled and then combined to form the acceleration time history. The fairly general, point source stochastic method is selected for modeling the higher-frequency component. This method is based on a parametric description of the ground motion's radiation spectrum $A(f;M,r)$, which is expressed as a function of the frequency, f , for specific values of the earthquake magnitude, M , and epicentral distance, r . The duration of the ground motion is addressed through an envelope function $e(t;M,r)$, which again depends on M and r . The acceleration time-history for a specific event magnitude, M , and source distance, r , is obtained according to this model by modulating a white-noise sequence by $e(t;M,r)$ and subsequently by $A(f;M,r)$. For describing the pulse characteristic of near-fault ground motions, the simple analytical model developed by Mavroeidis and Papageorgiou (2003) is selected, with pulse characteristics that can be related to M and r as well (Bray and Rodriguez-Marek 2004). The *stochastic model* for near-fault motions is finally established by combining the above two components.

4 RISK ASSESMENT, OPTIMAL DESIGN AND SENSITIVITY ANALYSIS

The characteristics of the models for the seismically isolated bridge and for earthquake excitations are

not known with absolute certainty. Uncertainties may pertain to (i) the properties of the bridge system, for example, related to stiffness or damping characteristics and traffic loads; to (ii) the variability of future seismic events, i.e., the moment magnitude or the epicentral distance; or even to (iii) the predictive relationships about the near-fault pulse characteristics. For explicitly incorporating these uncertainties in the modeling process, let $\boldsymbol{\theta} \in \Theta \subset \mathfrak{R}^{n_\theta}$, denote the augmented vector of model parameters for the structural system and the excitation models, where Θ represents the space of possible model parameter values. The uncertainty in these model parameters is then quantified by assigning a probability model $p(\boldsymbol{\theta})$ to them, which incorporates our available prior knowledge about the system and its environment into the model and it addresses future variability for both the seismic hazard, as well as for the bridge system and its performance. Also, let the vector of controllable system parameters, referred to herein as *design variables*, be $\boldsymbol{\varphi} \in \Phi \subset \mathfrak{R}^{n_\varphi}$, where Φ denotes the admissible design space.

Finally, the seismic performance of the bridge, for specific design $\boldsymbol{\varphi}$ and model description $\boldsymbol{\theta}$, is characterized by the performance measure $h(\boldsymbol{\varphi}, \boldsymbol{\theta})$, which ultimately quantifies performance according to the designer criteria. In this stochastic setting, the overall performance is then described by the following *stochastic integral* that corresponds to the expected value of $h(\boldsymbol{\varphi}, \boldsymbol{\theta})$ and ultimately quantifies seismic risk.

$$C(\boldsymbol{\varphi}) = \int_{\Theta} h(\boldsymbol{\varphi}, \boldsymbol{\theta}) p(\boldsymbol{\theta}) d\boldsymbol{\theta} \quad (1)$$

Since the models adopted for the bridge and the excitation are complex this multi-dimensional integral (1) cannot be calculated, or even accurately approximated, analytically. An efficient alternative approach is to estimate the integral by *stochastic simulation*; Using a finite number, N , of samples of $\boldsymbol{\theta}$ drawn from some importance sampling density $p_{is}(\boldsymbol{\theta})$, an estimate for (1) is given by

$$\hat{C}(\boldsymbol{\varphi}) = 1/N \sum_{i=1}^N h(\boldsymbol{\varphi}, \boldsymbol{\theta}_i) p(\boldsymbol{\theta}_i) / p_{is}(\boldsymbol{\theta}_i) \quad (2)$$

where vector $\boldsymbol{\theta}_i$ denotes the sample of the uncertain parameters used in the i th simulation. The robust stochastic design is finally established by selecting the design variables that minimize $C(\boldsymbol{\varphi})$, and is expressed through the *stochastic optimization*

$$\boldsymbol{\varphi}^* = \arg \min_{\boldsymbol{\varphi} \in \Phi} C(\boldsymbol{\varphi}) \quad (3)$$

where any additional deterministic constraints, related, for example, to location or space constraints

for the dampers are incorporated into the definition of admissible design space Φ . The novel two-stage optimization approach (Taflanidis and Beck 2008), based on the innovative Stochastic Subset Optimization (SSO) algorithm, is used in this study to efficiently perform this optimization.

This framework may be also extended to additionally investigate the sensitivity of the seismic risk with respect to each of the uncertain model parameters. An efficient approach is presented for this task, founded on information-based principles (relative entropy) and performed through simulation of samples from an auxiliary density, proportional to the integrand of the seismic risk integral (1).

5 ILLUSTRATIVE EXAMPLE

An illustrative example is presented that considers the design of nonlinear viscous dampers for protection of a two-span bridge. The fragility of the bridge system due to seismic pounding but also against failure modes related to pier shear and abutment deformations is considered as the performance measure quantifying seismic risk. The addition of the dampers is shown to provide considerable risk reduction, especially with respect to the fragility against seismic pounding. Results from the probabilistic sensitivity analysis show that the excitation properties have the highest importance in affecting seismic risk and that the inclusion of the dampers does alter the sensitivity characteristics.

REFERENCES

- Bray, J.D. & Rodriguez-Marek, A. 2004. Characterization of forward-directivity ground motions in the near-fault region. *Soil Dynamics and Earthquake Engineering* 24: 815–828.
- Makris, N. & Zhang, J. 2004. Seismic response analysis of a highway overcrossing equipped with elastomeric bearings and fluid dampers. *Journal of Structural Engineering* 130(6): 830–845.
- Mavroeidis, G.P. & Papageorgiou, A.P. 2003. A mathematical representation of near-fault ground motions. *Bulletin of the Seismological Society of America* 93(3): 1099–1131.
- Muthukumar, S. & DesRoches, R. 2006. A Hertz contact model with non-linear damping for pounding simulation. *Earthquake Engineering & Structural Dynamics* 35: 811–828.
- Taflanidis, A.A. & Beck, J.L. 2008. An efficient framework for optimal robust stochastic system design using stochastic simulation. *Computer Methods in Applied Mechanics and Engineering* 198(1): 88–101.
- Taflanidis, A.A., Scruggs, J.T. & Beck, J.L. 2008. Probabilistically robust nonlinear design of control systems for base-isolated structures. *Journal of Structural Control and Health Monitoring* 15(3): 697–719.

Probabilistic seismic hazard analysis incorporating basin amplification for shallow crustal earthquakes

T. Itoi & T. Takada

Graduate School of Engineering, University of Tokyo, Tokyo, Japan

1 INTRODUCTION

In the conventional Probabilistic Seismic Hazard Analysis (PSHA), Residual of an Empirical Ground Motion Prediction Equation (GMPE) is generally regarded as aleatory uncertainty. On the other hand, ground motion simulation techniques, e.g. the stochastic Green's function method, have been widely used for practical procedure, which can predict a ground motion time history instead of ground motion intensity measures. However, it is not clarified how to treat uncertainty in the simulation. This study investigates the consistency between uncertainty evaluated by accumulating the effects of source parameters and that of an empirical GMPE.

2 RESIDUAL OF EMPIRICAL GMPE

Ground motion intensity measure IM , e.g. peak velocity, at engineering bedrock can be evaluated as summation of three factors as follows:

$$\log IM = f_{source} + f_{Path} + f_{Basin} \quad (1)$$

where f_{source} , f_{Path} and f_{Basin} are respectively the source term, the path term and the basin amplification term. The effect of the path term f_{Path} is assumed to be negligible for near-field ground motions. Then, covariance between intensity measures of two distant sites is calculated as follows:

$$\begin{aligned} \text{Cov}[IM_1, IM_2] &= \text{Cov}[f_{Source1} + f_{Basin1}, f_{Source2} + f_{Basin2}] \\ &= \text{Cov}[f_{Source1}, f_{Source2}] + \text{Cov}[f_{Basin1}, f_{Basin2}] \end{aligned} \quad (2)$$

Ground motion simulation is conducted for a shallow crustal earthquake (M_w 6.5) by the stochastic Green's function method. Peak velocities are calculated as maximum of two horizontal components of simulated ground motions. The log residual $\varepsilon(x_i)$ of simulated peak velocities $V_{sim}(x_i)$ from the median attenuation \bar{V}_{pre} is calculated as follows:

$$\varepsilon(x_i) = \log_e(V_{sim}(x_i)/\bar{V}_{pre}) \quad (3)$$

Figure 1 shows spatial distribution of the residual $\exp(\varepsilon_i)$, which indicates the spatial correlation. Normalized auto-covariance function R_{Source} can be modeled as a function of distance h (km) between receivers as follows:

$$R_{Source}(h) = e^{-(h/27.9)^2} \cdot J_0(h/10.8) \quad (4)$$

Next, basin amplification for peak velocities all over Japan is evaluated as shown in Figure 2.

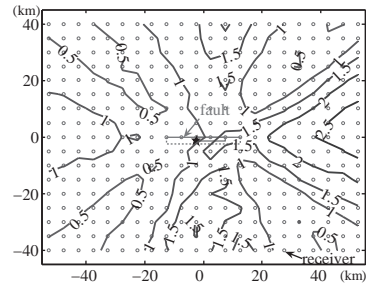


Figure 1. Fault geometry, receiver location and spatial distribution of residual simulated peak velocity.

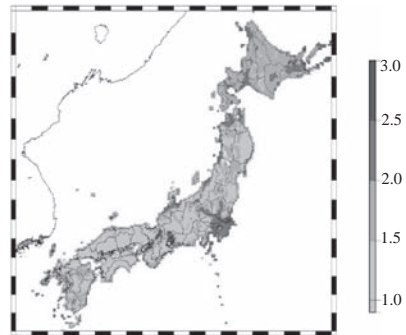


Figure 2. Basin amplification of peak velocity in Japan calculated by one-dimensional multiple reflection theory (from seismic bedrock to engineering bedrock).

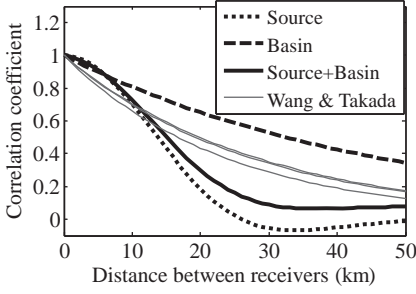


Figure 3. Comparison between numerically evaluated spatial correlation and empirical spatial correlation.

Normalized auto-covariance function R_{Basin} is modeled as a function of distance between receivers h (km) as follows:

$$R_{Basin}(h) = \exp(-h/46.8) \quad (5)$$

From Equation (2), a normalized covariance function between two sites R_{12} is calculated as follows:

$$R_{12} = \frac{\sigma_{Source}^2 R_{Source} + \sigma_{Basin}^2 R_{Basin}}{\sigma_{Source}^2 + \sigma_{Basin}^2} \quad (6)$$

Figure 3 compares a numerical spatial correlation R_{12} by Equation (6) with empirical macrospatial correlation models obtained by Wang & Takada (2005) for crustal earthquakes. Combined spatial correlation R_{12} is comparable to empirical models.

3 SIMPLE CORRECTION METHOD FOR SITE-DEPENDENT BASIN AMPLIFICATION

Basin amplification is modeled as a function of $D_{1.5}$, depth to the rock with shear wave velocity 1.5 km/s, as follows:

$$\log_e(V_{amp}) = \max(0, 0.180 \log_e(D_{1.5}) - 0.530) \quad (7)$$

Then, a site-specific peak velocity $PGV(i)$ at a specified site is assumed to be obtained by a multiplying basin amplification correction factor $f_{Ba}(i)$ to a predicted peak velocity PGV_{Atm} by an empirical GMPE (Si & Midorikawa 1999) as follows:

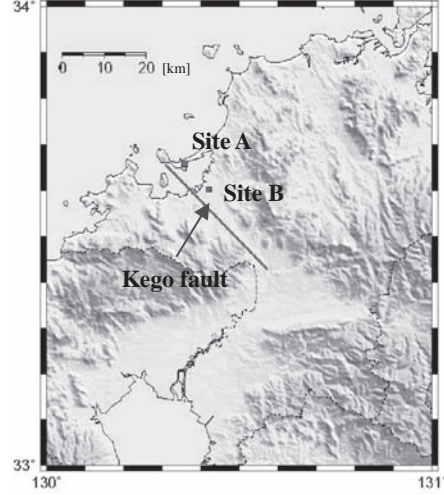


Figure 4. Geometry of Kego fault (Kyushu, Japan) and site location.

$$PGV(i) = f_{Ba}(i) \cdot PGV_{Atm} \quad (8)$$

$$f_{Ba}(i) = c \cdot V_{amp}(i) \quad (9)$$

where c ($= 0.667$) is a constant evaluated from observed records.

4 NUMERICAL EXAMPLES

The target area is Fukuoka city in Japan as shown in Figure 4, which is located just above Kego fault (Mw 6.7). Seismic hazard analysis for peak velocity of engineering bedrock are conducted at two distant sites (A & B) shown in Figure 4. Four procedures are employed for calculation as shown in Table 1.

Figure 5 compares hazard curves for peak velocity at an individual site between different procedures. Methods (i), (ii) and (ii') are comparable to each other at exceedance probability of more than 10^{-2} in 50 years, while the peak velocity predicted by the method (iii) is about twice as large as the other three. This result indicates the accuracy of GMPE is improved by considering a site-specific basin amplification. Figure 6 compares the probability of simultaneous non-exceedance at both sites for peak velocities. The results show the similar tendencies to the result for a single site in Figure 5.

Table 1. Comparison of four different procedures for PSHA.

Ground motion prediction	Spatial correlation
(i) Stochastic Green's function method + 1D multiple reflection theory	—
(ii) Empirical attenuation (Si & Midorikawa 1999; $\sigma_i = 0.41$) + basin amplification factor (Equation (8))	Numerical model for source directionality (Equation (4))
(ii') Empirical attenuation (Si & Midorikawa 1999; $\sigma_i = 0.41$) + basin amplification factor (Equation (8))	Numerical model for source directionality (Equation (4))
(iii) Empirical attenuation (Si & Midorikawa 1999) ($\sigma_{Att} = 0.53$)	Empirical mode (Wang & Takada, 2005)

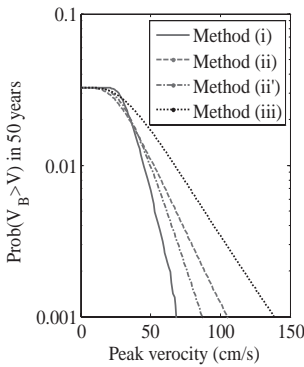


Figure 5. Seismic hazard curve for peak velocity by different procedures. (site B)

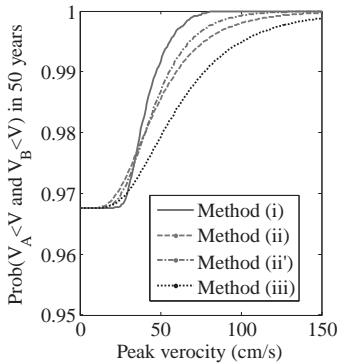


Figure 6. Probability of simultaneous non-exceedance at both sites evaluated by different procedures.

5 CONCLUSIONS

Residual of an empirical GMPE was investigated by numerical simulation. A correction factor of an empirical GMPE incorporating site-specific basin amplification was proposed for shallow crustal earthquakes. Seismic hazard analysis was demonstrated by an empirical GMPE as well as by ground motion simulation. The correction factor for site-specific basin amplification was shown to improve the accuracy of an empirical GMPE.

REFERENCES

- Si, H.J. Midorikawa, S. 1999. New Attenuation Relationships for Peak Ground Acceleration and Velocity Considering Effects of Fault Type and Site Condition, *Journal of Structural and Construction Engineering (Transactions of AIJ)*: 523: 63–70. (in Japanese with English abstract).
- Wang, M. Takada, T. 2005. Macrospatial Correlation Model of Seismic Ground Motions, *Earthquake Spectra* 21(4): 1137–1156.

Spatial sensitivity of seismic hazard results to background seismic activity models

N. Yilmaz

Earthquake Department, Disaster and Emergency Management Presidency, Ankara, Turkey

M.S. Yucemen

Civil Engineering and Earthquake Studies Departments, Middle East Technical University, Ankara, Turkey

ABSTRACT: In the probabilistic seismic hazard procedures, the past earthquake records that can not be associated with any one of the specific faults are treated as background seismic activity. Contribution of background seismic activity to seismic hazard is generally calculated by using two different models, namely: background area source with uniform seismicity and spatially smoothed seismicity model.

The spatially smoothed seismicity model developed by Frankel (1995) assumes that future earthquakes will occur in the vicinity of past earthquakes. In this model, earthquakes that are not assigned to major seismic sources are assumed to be potential seismic sources and are spatially distributed to cells of a grid. In the alternative model, background area sources are delineated and over these background area sources seismic characteristics are assumed to be spatially homogeneous.

In this study, sensitivity of seismic hazard results to the models used to describe background seismic activity is investigated. For this purpose, two case studies are carried out for a large (a country) and a small region (a province). These two case studies involve Jordan and the Bursa province, which is located in Turkey. Seismic databases are compiled for these two regions. In compiling these databases the raw data in the earthquake catalogs are processed as follows: Magnitudes reported in different scales are converted to a common magnitude scale (scale homogenization). Earthquake clusters are identified and dependent events (fore and after shocks) are eliminated by defining appropriate space and time windows (declustering). So an alternative database containing only main shocks is obtained to ensure statistical independence.

Using the resulting seismic databases, seismicity parameters are determined for background seismic activity and seismic hazard analyses are carried out by using both spatially smoothed seismicity model and background area source with uniform seismicity. Spatial variation of the differences between

the seismic hazard values obtained from these two models is examined. For this purpose maps displaying the spatial variation of the differences in PGA values obtained from the spatially smoothed seismicity model and the background area source with uniform seismicity are plotted for return periods of 475 and 2475 years. In order to construct these maps differences between the PGA values obtained from these two models are calculated at each grid point covering the whole region under consideration by using the following equation:

$$\text{Difference}(\%) = \left(\frac{\text{PGA}_s - \text{PGA}_b}{\text{PGA}_b} \right) \times 100 \quad (1)$$

where, PGA_s and PGA_b denote the PGA values estimated from spatially smoothed seismicity model and background area source with uniform seismicity, respectively. The difference with negative sign (–) means that background area source with uniform seismicity gives higher PGA values than the spatially smoothed seismicity model and that with positive sign (+) represents the opposite trend. Here, because of space limitation only one difference map is presented for each case study. Figure 1 displays the spatial variation of this difference for Jordan, whereas in Figure 2 the difference map is given for Bursa, corresponding to the alternative case where only main shocks are considered and the database is adjusted for incompleteness. In both maps the return period is 2475 years, since the differences are more significant for this return period. In these maps epicenters of earthquakes are also plotted. Difference maps corresponding to 475 years return period and additional maps showing the influence of other alternative assumptions are also displayed in the main paper.

In the case of Bursa province the influence of the assumptions with respect to catalog completeness and dependence are also reflected to the difference maps. The maximum PGA values obtained from

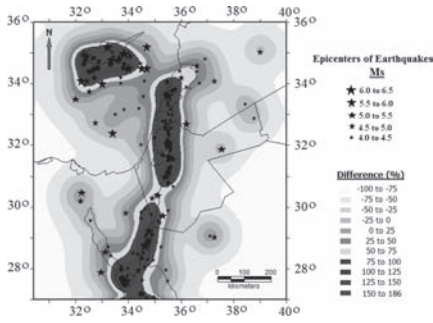


Figure 1. Map showing the spatial variation of the difference between PGA values obtained by using spatially smoothed seismicity model and background seismic source with uniform seismicity for a return period of 2475 years and epicenters of earthquakes (Jordan).

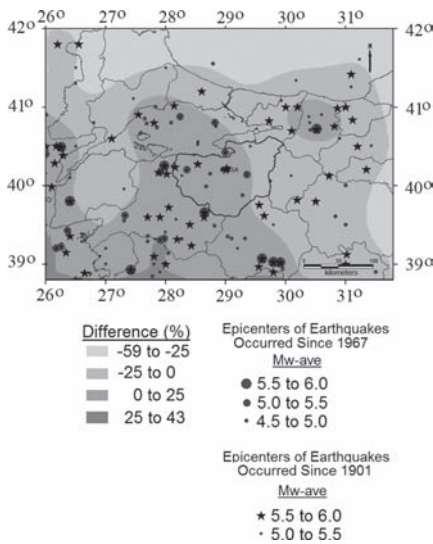


Figure 2. Map showing the spatial variation of the difference between the PGA values obtained from spatially smoothed seismicity model and background area source with main shocks and database adjusted for incompleteness for a return period of 2475 years; and epicenters of earthquakes considered in the spatially smoothed seismicity model (Bursa).

the analyses carried out by using the background area source with uniform seismicity and spatially smoothed seismicity model of Frankel (1995) for return periods of 475, 1000, and 2475 years are presented in Tables 1 and 2, respectively.

Based on the results of these two case studies, it is observed that for background seismic activity, the use of spatially smoothed seismicity model or the alternative background area source with uniform seismicity affects the results. Spatially smoothed

Table 1. Maximum PGA values (in g) obtained from background area source with uniform seismicity (Bursa).

Catalog type	Correction for incompleteness	Return period (Year)		
		475	1000	2475
All earthquakes	No	0.18	0.22	0.29
	Yes	0.19	0.24	0.31
Only main shocks	No	0.14	0.19	0.24
	Yes	0.16	0.20	0.26

Table 2. Maximum PGA values (in g) obtained from spatially smoothed seismicity model of Frankel (Bursa).

Catalog type	Correction for incompleteness	Return period (Year)		
		475	1000	2475
All earthquakes	No	0.24	0.29	0.37
	Yes	0.27	0.34	0.42
Only main shocks	No	0.19	0.24	0.31
	Yes	0.20	0.25	0.33

seismicity model gives higher seismic hazard values at the regions where the epicenters of earthquakes cluster. On the other hand, nearly a spatially uniform seismic hazard distribution is obtained in the case of background area source with uniform seismicity. Therefore, background area source model with uniform seismicity is expected to give higher seismic hazard values compared to the spatially smoothed seismicity model for sites located far away from clustering regions of past earthquake epicenters; i.e. where the epicenters of earthquakes are scarce or no earthquakes have occurred in the past.

The analyses carried out for the background seismic activity by using both models with different combinations of assumptions on earthquakes in the catalog with respect to completeness and dependence yield different seismic hazard values. Therefore, the validity of the results obtained for background seismic activity depends also on the reliability of the earthquake catalog compiled, the method used to identify main shocks and completeness of the catalog with respect to small magnitude earthquakes.

REFERENCE

Frankel, A. 1995. Mapping seismic hazard in the Central and Eastern United States, *Seismological Research Letters*, 66(4): 8–21.

Stochastic field analyses of the site amplification factors based on observed and inversely analyzed real strong ground motion in Japan

Muhtar Fukuda

Nagoya Sangyo University, Japan

Nobuhiko Narita, Katsuro Ogawa & Michiyo Sugai

Nagoya Sangyo University, Japan

Atsushi Nozu

The Port and Airport Research Institute, Japan

The present paper reports the results of stochastic field analyses of amplifications of actual strong ground motions, caused by real earthquakes, observed and estimated in the Japanese archipelagos.

Although significance of amplifications of strong ground motions has been well recognized, their distributions have not been explored or clarified sufficiently, especially in deep hard bed rock grounds in which ordinary engineering boring investigations are usually not performed.

However, objective stochastic field studies are available now, after strong motion networks, such as K-NET, have been established over the Japanese archipelagos. These networks can observe and record real strong ground motions influenced not only by local soil deposit but also by firm ground, which are usually beyond the reach of engineering boring investigations in Japanese practice. As a result, newly observed data show that the amplifications of real strong ground motions are evidentially heterogeneous not only due to the heterogeneity of local soil deposit but also due to the heterogeneity of firm ground, whose statistical properties are not sufficiently incorporated in the existing hazard maps for on coming the Toh-Nankai great earthquake or the others. Such hypothesis leads to overestimations of strong ground motions in some areas and underestimations in another areas, which counterwork optimum earthquake disaster mitigation plan under the Japanese economical and social conditions such as the long-term slow economic growth, population ageing, the rapid fall in population or so on. The information in the record data had to be utilized for establishing better earthquake disaster mitigation or prevention plans in this country.

On the other hands, information in the record cannot directly be utilized in conventional sto-

chastic analyses theories due to the indispensable random behaviors of the amplifications in natural ground layers at each observation point. A lot of theoretical scientific papers are published based on Kriging methods to clarify stochastic fields of the amplification. However, these studies cannot be applied to data of the newly observed and inversely analyzed real strong ground motions, because some errors adhere to the real data. It should be noted here that the objectively estimated amplifications are not completely identical in each observation point. The amplifications can only be calculated as an average value from the variable observed real strong ground motions recorded during real earthquakes. While error indexes such as variances or standard deviations can also be calculated with the averages, these indexes are found to be far from negligible, and to be, as well as the average values, vary from point to point in the stochastic random field. As most of the recent theoretical studies have not been take such indexes of the errors into the analyses, their methods can only be applied to ideal data, but cannot derive practical parameters in Kriging analyses from those records with errors adhere to the real data.

Then the present paper proposes utilizing some Kriging methods, which can make account of the errors in the analyses, and reports their consequent practical results of the stochastic analyses.

As a result, the followings are clear from the present study.

1. The amplifications can be modeled better in log-normal Gaussian stochastic fields than in normal Gaussian fields.
2. The stochastic distributions of the site amplification factors are not to be white noise within the central area Japan.

3. The Sills are larger for lower frequencies and smaller for higher frequencies except those for the very small frequencies; the accuracies of Kriging interpolations will generally be higher for higher frequencies and lower for lower frequencies especially where interpolated points do not exist nearer the observation points.
4. The ranges are estimated to distribute around 20 km though it is based on rough assumption.
5. Stochastic field can be reasonably estimated showing the difference of probabilistic distributions in coastal zones and those in mountainous zones.
6. As is predicted in an engineering sense, the roughly estimated ranges in deep firm ground are much longer than those in softer soil parameters in shallow soil ground.
7. The estimated ranges of the site amplification factors are longer for lower frequencies and shorter for higher frequencies. This result in Figure 5 is also very good accordant with a well known fact; the earthquake strong motions of lower frequencies do not attenuate more drastically than those of higher frequencies.

Development of seismic margin-risk diagram

M. Nakajima, Y. Ohtori & K. Hirata

Central Research Institute of Electric Power Industry, Abiko-shi, Chiba-ken, Japan

Seismic margin of structures (systems and components) is extremely important index and information when we evaluate and account seismic safety of critical structures, systems and components quantitatively. For example, some electric power companies evaluate the seismic margin of each plant in back-check of nuclear power plants in Japan because the seismic safety of nuclear power plants is a great concern for the Japanese people after the 2007 Niigata Chuetsu-Oki Earthquake.

The seismic margin of structures is usually defined as a structural capacity margin corresponding to design earthquake ground motion. However, there is little agreement as to the definition of the seismic margin and we have no knowledge about a relationship between the seismic margin and seismic risk (annual failure probability) which is obtained in PSA (Probabilistic Safety Assessment).

The purpose of this paper is to discuss a definition of structural seismic margin and to develop a diagram which can identify a relation between seismic margin and seismic risk.

The main results of this paper are summarized as follows:

- i. The seismic margin which is defined based on the fact that intensity of earthquake ground motion has been developed (Figure 1) because it is more appropriate than the conventional definition (i.e., the response-based seismic margin) for the following reasons:
 - seismic margin based on earthquake ground motion is invariant where different typed structures are considered,

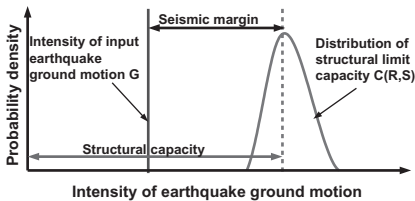


Figure 1. Schematic illustration of seismic margin definition based on intensity of earthquake ground motion.

- stakeholders can understand the seismic margin based on the earthquake ground motion better than the response-based one.
- ii. By defining structural seismic margin based on the intensity of earthquake ground motions, we have developed a seismic margin-risk diagram (Figure 2). The diagram represents a relationship between a deterministic structural capacity (acceleration capacity) and a probabilistic seismic risk.

This diagram facilitates us to judge easily whether we need to perform detailed probabilistic risk analysis or only deterministic analysis, given that the reference risk level although information on the uncertainty parameter β is not obtained.

- iii. Numerical simulations based on the developed method for four sites in Japan have been performed. The structural capacity-risk diagram differs depending on each location because the diagram is greatly influenced by seismic hazard information for a target site.

Furthermore, the required structural capacity corresponding to the given risk level is not affected by the uncertainty parameter β . This indicates that we have a possibility of rationalizing the seismic PSA.

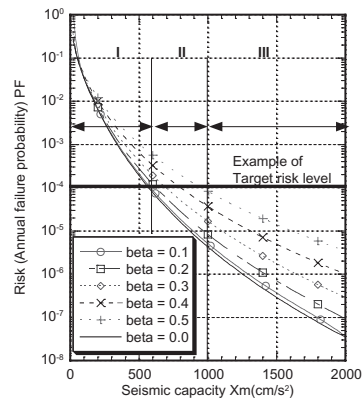


Figure 2. Developed seismic margin (structural capacity)-risk diagram which relates deterministic seismic margin to probabilistic seismic risk.

GS_221 — Probabilistic seismic hazard analysis (2)

This page intentionally left blank

Orientation dependency of peak ductility demand for seismic performance evaluation

K. Goda

University of Bristol, Bristol, UK

ABSTRACT: Protection of lives and mitigation of seismic damage are primarily achieved through adequate seismic provisions in the national building codes. The current provisions specify a seismic load level for structural design based on a uniform-hazard elastic response spectrum, which is obtained from probabilistic seismic hazard analysis. Although the majority of uncertain aspects are taken into account in probabilistic seismic hazard analysis, variability associated with the orientation of ground motion measures, which is treated ambiguously in the national building codes, can be an important factor in assessing reliability of engineered structures. In particular, the orientation effects due to directivity-pulse of near-fault ground motions are significant (Tothong et al., 2007).

Despite the popularity of characterizing the orientation of elastic seismic demand, the orientation effects of inelastic seismic demand have not been investigated extensively. The main objective of this study is to examine the orientation dependency of the peak ductility demand of inelastic single-degree-of-freedom (SDOF) systems with known strength by accounting for record-to-record variability of ground motions. The adopted method, known as a constant strength approach, is useful for evaluating the seismic performance of existing structures (FEMA 2005). By comparing the peak ductility demand in recording directions with those in the maximum/minimum response directions (Hong & Goda 2007) and the major/minor principal directions (Arias 1970, Penzien & Watabe 1975), it will be shown that the peak ductility demand depends on how input ground motions are defined in terms of record orientation. Moreover, the observed orientation dependency can be attributed to the response spectral shape effects of rotated ground motion records in different directions (Luco & Bazzurro 2007).

The results have an important implication in the current earthquake engineering practice, as

they suggest that separate peak ductility demand models should be developed and used for different ground motion measures to evaluate the seismic performance of existing structures consistently without bias. For instance, the International Building Code 2009 recommends the definition of a representative horizontal ground motion in the maximum response direction. The peak ductility demand in the maximum response direction for a given relative seismic excitation level is generally smaller than that in recording directions. Therefore, if an elastic seismic demand model in the maximum response direction is combined with a peak ductility demand model in recording directions (this is the most common orientation considered in developing a peak ductility demand model), the inelastic seismic demand would be overestimated.

REFERENCES

- Arias, A. 1970. A measure of earthquake intensity. In *Seismic Design for Nuclear Power Plants*: 438–483. MIT Press: Cambridge.
- FEMA, 2005. *Improvement of nonlinear static seismic analysis procedures*. Washington DC: Federal Emergency Management Agency.
- Hong, H.P. & Goda, K. 2007. Orientation-dependent ground-motion measure for seismic-hazard assessment. *Bull. Seism. Soc. Am.* 97: 1525–1538.
- Luco, N. & Bazzurro, P. 2007. Does amplitude scaling of ground motion records result in biased nonlinear structural drift responses? *Earthquake Eng. Struct. Dyn.* 36: 1813–1835.
- Penzien, J. & Watabe, M. 1975. Characteristics of 3-dimensional earthquake ground motion. *Earthquake Eng. Struct. Dyn.* 3: 365–373.
- Tothong, P., Cornell, A.C. & Baker, J.W. 2007. Explicit directivity-pulse inclusion in probabilistic seismic hazard analysis. *Earthquake Spectra* 23: 867–891.

Methodology and results of a nuclear power plant seismic probabilistic safety assessment

Martin Richner, Sener Tinic & Dirk Proske
Axpo AG, Nuclear Power Plant Beznau, Switzerland

Mayasandra Ravindra, Robert Campbell & Farzin Beigi
ABS Consulting, Irvine, USA

Alejandro Asfura
APA Consulting, Walnut Creek, USA

ABSTRACT: The most recent results and insights gained from Seismic Level 2 PSA study of the Beznau NPP are shown. Beznau is the oldest operating PWR worldwide. The plant was extensively backfitted during the last years, especially with respect to seismic events. The paper shows the recent results of the probabilistic seismic hazard study performed for the four NPPs in Switzerland. This so called PEGASOS study was performed according to the SSHAC procedures (NUREG/CR-6372) at the highest elaborated Level 4. Switzerland is an area of low to moderate seismicity and the PEGASOS study was the first one of that kind performed for a NPP at that high level. The paper also presents the methods, results and conclusions of the Beznau Seismic PSA. Some examples illustrate how plant safety was improved based on the results of the seismic PSA. The paper discusses the role of the seismic capacity of the containment with respect to the large early release frequency (LERF). In addition, the calculated results indicate that seismic events are important contributors to the core damage frequency (CDF) and to the LERF even in areas of low to moderate seismicity. Based on the PEGASOS seismic hazard results, an out-look is given on the reactor building seismic capacity required for Advanced Light Water Reactors (ALWRs).

REFERENCES

ABSG (2007a). ABS Consulting Inc. for NOK, “Probabilistic Seismic Response Analyses for Beznau Safety Related Buildings”, Rev. 1.

ABSG (2007b). ABS Consulting Inc. for NOK, “Seismic Fragility Evaluation of Structures and Equipment at Beznau Unit 2”, Rev. 1.

ABSG (2007c). Consulting Inc., “RISKMAN® PRA Software Manual”, Version 10.0.

ABSG SASSI. ABSG Computer Code SASSI Version 1.0.

Basler & Hofmann, (1984). “Beznau NPP, Site-Specific Seismic Hazard Functions for Probabilistic Risk Assessment”.

ETH Zurich (1977). “Seismic Hazard Maps of Switzerland”.

EPRI (1991). NP-6041-SL “A Methodology for Assessment of Nuclear Power Plant Seismic Margin”, Rev. 1.

GeorRisk (2000). GeoRisk Earthquake Research Institute Ltd., “Seismic Hazard Assessment at Paks NPP Site”.

NAGRA (2004). “Probabilistic Seismic Hazard Analysis for Swiss Nuclear Power Plant Sites (PEGASOS Project)”.

NOK (1999). and PLG Inc. “Beznau Unit 2, Full-Power Probabilistic Risk Assessment (BERA)”, KKB511D127, Rev. 2 dated December 1999.

NOK (2002). and Westinghouse. “Beznau Unit 2, Full-Power PSA (BERA) – Level 2”, KKB511D147, Rev. 1.

NUREG/CR-6372 (1997). “Senior Seismic Hazard Analysis Committee, Recommendations for PSHA, Guidance on Uncertainty and Use of Experts”.

PLG Inc. (1989). PLG-0511, “Beznau Station Risk Assessment – Plant with NANO”, 1989.

PLG Inc. (1998). PLG-1208, “Beznau Unit 2, Shutdown and Low-Power Probabilistic Risk Assessment (BESRA)”.

Redundancy effects on seismic reliability of steel frame structures

Quanwang Li, Qinming Zhang, Jiansheng Fan & Can Zhang
 Department of Civil Engineering, Tsinghua University, Beijing, China

1 INTRODUCTION

The importance of structural redundancy has been long recognized by structural engineers. Especially after the 1994 Northridge and 1995 Kobe earthquake, a lot of research work has been conducted showing that, besides structural configuration, there are some other factors contributing to redundancy effects, including load and resistance uncertainty, member ductility and strength correlation.

A new structural redundancy factor was recommended in NEHRP (2003) and adopted in ASCE-7 (2005), which is primarily a function of the number of moment frames in the direction of earthquake excitation force. Correspondingly, structural systems are classified into redundant or non-redundant and a uniform penalty factor of 1.3 is assigned to the lateral design force of the latter. However, the uniform penalty on lateral design force fails to account for the large differences in configuration, ductility capacity and strength correlation within each classification, and obviously could lead to poor designs.

This paper attempts to quantify the effects of structural redundancy on the seismic reliability of structural systems considering the variability, uncertainty and correlation of member strength and variation of ductility capacity. The probabilistic effect of redundancy on the reliability of an ideal parallel system was firstly presented. And a nonlinear beam-column connection model, which accounts for the strength degradation, stiffness deterioration and finite ductility capacity, was developed and used in the 3D nonlinear pushover analysis to investigate the effects of structural

redundancy on the seismic reliability of structural systems with finite ductility capacity.

2 MEASUREMENT OF STRUCTURAL REDUNDANCY

In this paper, the frame structure with only 1 moment-resisting frame is viewed as non-redundant, and the frame structure with n moment-resisting frames is measured to be redundant of $(n-1)$ degree (RD). Take the 3-story frame structure shown in Fig. 2 as an example. According to the measurement of structural redundancy mentioned above, the structure is redundant to the 1st degree in x direction and to the 4th degree in y direction.

3 EFFECTS OF STRUCTURAL REDUNDANCY ON SEISMIC RELIABILITY OF FRAME STRUCTURES WITH INFINITE DUCTILITY

Each moment-resisting frame has a resistance of R_i , which is modeled by a log-normal distribution with mean value of μ_R and standard deviation of σ_R . The correlation coefficient between R_i is assumed to be identically ρ . The seismic load effect is also described by log-normal distribution with mean value of μ_S and standard deviation of σ_S .

Defining the over-strength factor (η) as the ratio between the mean value of the structural resistance and the mean value of seismic load

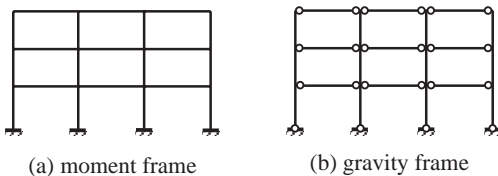


Figure 1. Moment frame and gravity frame.

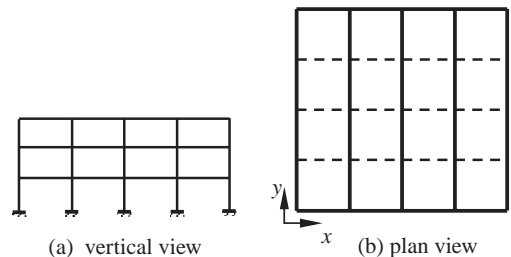


Figure 2. Moment frame and gravity frame.

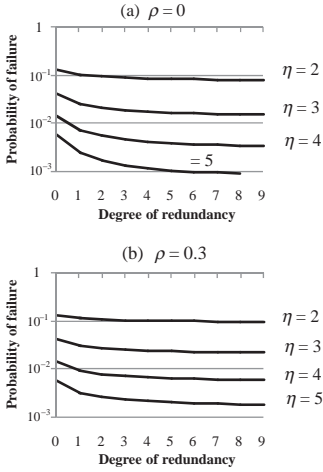


Figure 3. Failure probability of system.

effect ($\eta = \mu_R / \mu_S$), the seismic reliability of frame structures with n moment-resisting frames can be written as:

$$P_f = \Phi \left(\frac{-\ln(\eta) + \frac{1}{2} V_{Ri}^2 \left(\frac{1}{n} + \frac{n-1}{n} \rho \right) - \frac{1}{2} \ln(1 + V_S^2)}{\sqrt{V_{Ri}^2 \left(\frac{1}{n} + \frac{n-1}{n} \rho \right) + \ln(1 + V_S^2)}} \right) \quad (1)$$

where V represents the Coefficient Of Variation (COV) and $\Phi(\cdot)$ is the standard normal cumulative function.

To assess the resistance of a moment-resisting frame (R_i), a structural model of 3-story 4-bay steel frame was established in Open Sees. The yield strength and the elastic modulus of steel were modeled by normal variables with mean values of 57.6 ksi and 29000 ksi, and a COV of 0.15 and 0.04 respectively. Through 2D nonlinear pushover analysis, the mean value and standard deviation of the resistance of a moment frame were found to be 0.37 g and 0.063 g respectively, so $V_{Ri} = 0.17$. The seismic load effect has a COV of 35%.

The values obtained from Eqn. (1) for different over-strength factor (η) are shown in Fig. 3.

4 SEISMIC RELIABILITY OF FRAME STRUCTURES WITH FINITE DUCTILITY CAPACITY

To study the effect of member ductility, a connection model capable of experiencing strength deterioration was established as shown in Fig. 4

Through 3D pushover analysis, the resistance of the frame structure was assessed for different degree of redundancy and Ductility Capacity

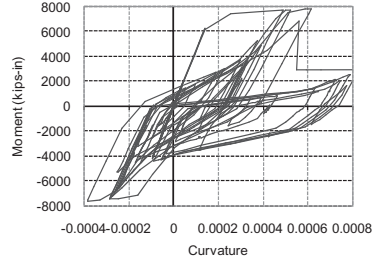


Figure 4. Moment-curvature history of a beam-column connection with ductility capacity of 4.5.

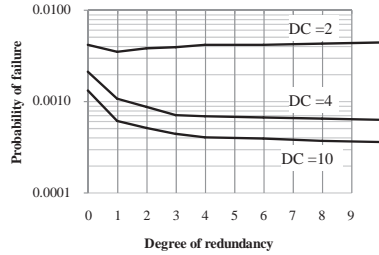


Figure 5. Failure probability of system as function of redundancy degree for different ductility capacity.

(DC). The probabilities of failure of the structural system were computed and plotted in Fig. 5.

5 CONCLUSIONS

From the results obtained in the above analysis, it is conclude that:

1. To take advantage of structural redundancy, the uncertainty in seismic load effects should be lowered;
2. Under current uncertainty level in seismic load effect, the over-strength ratio should be greater than 3 and the strength correlation coefficient should be less than 0.3 to take advantage of redundancy based on its “probabilistic effect”;
3. A minimum member ductility capacity is required to take advantage of structural redundancy, and it should be no less than 4 from this study.
4. As for the strength-related limit state, increasing the ductility capacity from moderate (4 for example) to high (10 for example), the improvement in structural reliability is insignificant.
5. Arranging more than 4 moment-resisting frames in a frame structure leads to an immaterial improvement in the structural reliability, regardless of the over-strength ratio and member ductility capacity.

Regression models for predicting the probability of near-fault earthquake ground motion pulses, and their period

Shrey K. Shahi & Jack W. Baker

Department of Civil and Environmental Engineering, Stanford University, Stanford, CA, USA

ABSTRACT: Near-fault earthquake ground motions containing large velocity pulses are known to cause severe demands on structures and geotechnical systems, but the probability of occurrence of these pulses in future earthquakes is not well understood. Using a database of past ground motions that have been classified as containing or not containing velocity pulses, this paper develops calibrated regression models to predict the occurrence of velocity pulses in future ground motions, as well as the nature of the pulses if they do exist. The regression model selection procedure indicates that useful predictors of pulse occurrence include source-to-site geometry variables such as the length of rupture between the epicenter and location of interest, and the closest distance from the location of interest to the fault rupture. It is observed that the period of any resulting velocity pulse is related primarily to the earthquake magnitude, but other predictive parameters are also considered and discussed. Both empirical regression tests and theoretical seismology explanations are given as to why the chosen predictor variables are important and meaningful. Some comparisons with previous similar models are also presented. The resulting predictive models can be incorporated into probabilistic seismic hazard analysis calculations. These results demonstrate the potential importance of quantitatively considering occurrence of near-fault pulses, and facilitate seismic reliability calculations that explicitly consider near-fault ground motion pulses.

INTRODUCTION

Near fault ground motions may sometime contain a strong pulse at the beginning of the velocity time history. This pulse-like feature is primarily caused by forward directivity effects and are observed when the fault ruptures towards the site at a speed close to the propagation velocity of the shear waves (Somerville et al., 1997, Somerville 2003, Spudich and Chiou 2008). These ground motions referred as “pulse-like” in this paper place extreme demands on structures and are known to be the cause of extensive damage in previous earthquakes (e.g., Bertero et al., 1978, Anderson and Bertero 1987, Hall et al., 1995, Iwan 1997, Alavi and Krawinkler 2001, Menun and

Fu 2002, Makris and Black 2004, Mavroeidis et al., 2004, Akkar et al., 2005, Luco and Cornell 2007). Pulse-like ground motions have higher elastic spectral acceleration (S_a) compared to ground motions without the pulse-like feature. The current ground motion models which are used to perform probabilistic seismic hazard analysis (PSHA) do not account for the amplification in S_a caused by these ground motions. Thus the PSHA results computed using the current ground motion models results in under-prediction of hazard at near fault sites, where pulse-like ground motion are expected.

Along with amplifying S_a , pulses also cause larger inelastic multi degree of freedom (MDOF) response. Traditional intensity measures like S_a at the fundamental period of the structure are inadequate in capturing the larger nonlinear response of MDOF systems excited by pulse-like ground motions (Baker and Cornell 2008), which makes characterizing the risk from pulse-like ground motion difficult. The importance of accounting for the effect of pulse-like ground motion in design code has long been recognized, but the methods to account for pulses used currently are relatively ad-hoc. We need deeper understanding of how these pulse-like ground motions affect both the hazard and the risk before we can properly account for their effect in future design codes.

PROBABILITY OF PULSE

Pulse-like ground motions caused by forward directivity effects are observed at near fault sites, but not all near fault sites experience pulse-like ground motion. This makes it important to estimate the probability of observing a pulse in order to correctly do PSHA calculations for near fault sites. Forward directivity is a physical phenomenon with well known causes, but it is hard to predict the occurrence of pulse-like ground motion at a site because of incomplete information about the source, site and the path of wave propagation that cause this phenomenon. Due to this lack of knowledge it is useful to develop a statistical model which agrees with the observations. We follow the approach of Iervolino and Cornell (2008) and model the occurrence of pulse by a random variable (I) which takes the value 1 if pulse is observed at the site and 0 if pulse is not

observed at the site (these type of variables are also called indicator variables).

PULSE PERIOD

The period of the pulse-like feature is an important parameter, as the ratio of pulse period and the structural period can be used to determine the structure's response (Anderson and Bertero 1987, Alavi and Krawinkler 2001, Mavroeidis et al., 2004). The amplification of S_a due to presence of pulse also occurs in a small band of period close to the period of the pulse, this makes predicting pulse period an important part of hazard and risk computations. Several models have been proposed in the past for predicting the period of pulse-like ground motion (e.g., Mavroeidis and Papageorgiou 2003, Bray and Rodriguez-Marek 2004, Akkar et al., 2005). We decided to model this relationship again as the classification algorithm of Shahi and Baker (2010) used for this study identifies pulses in different orientation. With the new dataset we have information from many pulses in different orientation at the same site, something which was not available for previous studies.

CONCLUSION

In this paper we study and develop predictive equations for the probability of observing pulse-like ground motion at a site and the period of the pulse expected at a site. Pulse-like ground motions classified by Shahi and Baker (2010) were used to fit predictive relationships. Statistical techniques were used to find appropriate functional forms for the models and effort was made to develop parsimonious models which are easy to interpret and thus can lead to better understanding of the overall phenomenon.

Separate relationships were developed for strike-slip and non-strike-slip faults and these relationships were very different from each other. In case of probability of pulse model, the difference was primarily due to the difference in the geometry of the fault ruptures and the different parameters used to define the source-to-site geometry. In case of the pulse period model, different parameters appear to influence the pulse period from strike-slip and non-strike-slip faults. Along with having immediate practical use for hazard and risk estimation, the trends and differences between the predictive equations developed here can be useful in further understanding properties of pulse-like ground motions.

REFERENCES

Akkar, S., Yazgan, U. & Gulkan, P. (2005). Drift estimates in frame buildings subjected to near-fault ground motions. *Journal of Structural Engineering* 131(7), 1014–1024.

Alavi, B. & Krawinkler, H. (2001). Effects of near-fault ground motions on frame structures. Technical Report Blume Center Report 138, Stanford, California.

Anderson, J.C. & Bertero, V. (1987). Uncertainties in establishing design earthquakes. *Journal of Structural Engineering* 113(8), 1709–1724.

Baker, J.W. & Cornell, C.A. (2008). Vector-valued intensity measures for pulse-like near-fault ground motions. *Engineering Structures* 30(4), 1048–1057.

Bertero, V., Mahin, S. & Herrera, R. (1978). Aseismic design implications of near-fault San Fernando earthquake records. *Earthquake Engineering & Structural Dynamics* 6(1), 31–42.

Bray, J.D. & Rodriguez-Marek, A. (2004). Characterization of forward-directivity ground motions in the near-fault region. *Soil Dynamics and Earthquake Engineering* 24(11), 815–828.

Hall, J.F., Heaton, T.H., Halling, M.W. & Wald, D.J. (1995). Near-source ground motion and its effects on flexible buildings. *Earthquake Spectra* 11(4), 569–605.

Iervolino, I. & Cornell, C.A. (2008). Probability of occurrence of velocity pulses in near-source ground motions. *Bulletin of the Seismological Society of America* 98(5), 2262–2277.

Iwan, W. (1997). Drift spectrum: measure of demand for earthquake ground motions. *Journal of Structural Engineering* 123(4), 397–404.

Luco, N. & Cornell, C.A. (2007). Structure-specific scalar intensity measures for near-source and ordinary earthquake ground motions. *Earthquake Spectra* 23(2), 357–392.

Makris, N. & Black, C.J. (2004). Dimensional analysis of bilinear oscillators under pulse-type excitations. *Journal of Engineering Mechanics* 130(9), 1019–1031.

Mavroeidis, G.P., Dong, G. & Papageorgiou, A.S. (2004). Near-fault ground motions, and the response of elastic and inelastic single-degree-of-freedom (SDOF) systems. *Earthquake Engineering & Structural Dynamics* 33(9), 1023–1049.

Mavroeidis, G.P. & Papageorgiou, A.S. (2003). A mathematical representation of near-fault ground motions. *Bulletin of the Seismological Society of America* 93(3), 1099–1131.

Menun, C. & Fu, Q. (2002). An analytical model for near-fault ground motions and the response of SDOF systems. In *Proceedings, 7th U.S. National Conference on Earthquake Engineering*, Boston, MA, p. 10. Earthquake Engineering Research Institute.

Shahi, S.K. & Baker, J.W. (2010). An empirically calibrated framework for including the effects of near-fault directivity in probabilistic seismic hazard analysis. *Bulletin of the Seismological Society of America* (under review).

Somerville, P.G. (2003). Magnitude scaling of the near fault rupture directivity pulse. *Physics of the earth and planetary interiors* 137(1), 12.

Somerville, P.G., Smith, N.F., Graves, R.W. & Abrahamson, N.A. (1997). Modification of empirical strong ground motion attenuation relations to include the amplitude and duration effects of rupture directivity. *Seismological Research Letters* 68(1), 199–222.

Spudich, P. & Chiou, B.S.J. (2008). Directivity in NGA earthquake ground motions: Analysis using isochrone theory. *Earthquake Spectra* 24(1), 279–298.

Performance-based direct displacement design of engineered timber building in seismic regions

Y. Wang & D.V. Rosowsky

Department of Civil and Environmental Engineering, Rensselaer Polytechnic Institute, Troy, NY, USA

W.C. Pang

Department of Civil Engineering, Clemson University, Clemson, SC, USA

ABSTRACT: This paper reports on a study to extend a recently proposed direct displacement design (DDD) procedure for mid-rise engineered wood frame structures and develop a set of factors for use in the procedure to meet specified performance levels with certain target probabilities. Representative index multi-story building configurations were selected from the archetype buildings developed for the FEMA ATC-63 project. Seismic hazard levels and performance requirements recommended by ASCE 41-06 and modified for use in the recently completed NEES-Wood project were used. The archetype buildings, originally designed using current force-based design (FBD) procedures, were re-designed using the simplified direct displacement design procedure (also described herein) with a range of non-exceedance probability adjustment factors (C_{NE}). Specifically, the design inter-story shear forces and the sheathing nail spacings were determined for each structure designed using C_{NE} . Nonlinear time-history analysis (NLTHA) was performed for each archetype structure under the 2%/50 year seismic hazard level and peak inter-story drift distributions were developed. The non-exceedance probability at the 4% drift limit was then plotted against building height and design charts were developed for each different value of C_{NE} . Given the building height, target drift and desired non-exceedance probability, engineers/designers can select the appropriate minimum value of C_{NE} using these charts. Thus, a probability-based, multi-objective performance-based procedure for the seismic design of mid-rise wood frame structures is described.

REFERENCES

- American Society of Civil Engineers (ASCE) (2005). *Minimum Design Loads for Buildings and Other Structures* (ASCE/SEI 7-05), American Society of Civil Engineers, Reston, VA.
- American Society of Civil Engineers (ASCE) (2006). *Seismic Rehabilitation of Existing Buildings* (ASCE/SEI 41-06), American Society of Civil Engineers, Reston, VA.
- Applied Technology Council (2008). *Quantification of Building Seismic Performance Factors*, ATC-63 Project Report, FEMA P695. Washington, DC, in preparation.
- Camelo, V., Beck, J. & Hall, J. (2001). *Dynamic Characterization of Woodframe Structures*, CUREE Report W-11, Task 1.3.3, Consortium of Universities for Research in Earthquake Engineering, Richmond, CA.
- Christovasilis, I.P., Filiatrault, A. & Wanitkorkul, A. (2007). *Seismic Testing of a Full-Scale Two-Story Wood Light-frame Building: NEESWood Benchmark Test*, NEESWood Report NW-01, State University of New York at Buffalo, NY.
- Christovasilis, I.P., Filiatrault, A., Constantinou, M.C. & Wanitkorkul, A. (2009). "Incremental Dynamic Analysis of Woodframe Buildings," *Earthquake Engineering and Structural Dynamics*, 38(4):477–496.
- Ellingwood, B.R., Rosowsky, D.V. & Pang, W.C. (2008). "Performance of Light-frame Wood Residential Construction Subjected to Earthquakes in Regions of Moderate Seismicity," *ASCE Journal of Structural Engineering*, 134(8): 1353–1363.
- Filiatrault, A. & Folz, B. (2002). "Performance-Based Seismic Design of Wood Framed Buildings," *ASCE Journal of Structural Engineering*, 128(1): 39–47.
- Filiatrault, A., Christovasilis, I., Wanitkorkul, A. & Folz, B. (2006). "Displacement-Based Seismic Design of Light-Frame Wood Buildings," *Proceedings of the 9th World Conference on Timber Engineering*, Portland, OR.
- Filiatrault, A., Wanitkorkul, A., Christovasilis, I.P., van de Lindt, J., Symans, M., Rosowsky, D. & Davidson, R. (2007). "Experimental Seismic Performance Evaluation of a Full-scale Woodframe Building," *Proceedings of the 2007 Structures Congress*, Long Beach, CA.
- Fischer, D., Filiatrault, A., Folz, B., Uang, C-M. & Seible, F. (2001). *Shake Table Tests of a Two-Story Woodframe House*, CUREE Report W-06, Task 1.1.1, Consortium of Universities for Research in Earthquake Engineering, Richmond, CA.
- Folz, B. & Filiatrault, A. (2001). "Cyclic Analysis of Wood Shear Walls," *ASCE Journal of Structural Engineering*, 127(4): 433–441.

- Folz, B. & Filiatrault, A. (2004a). "Seismic Analysis of Woodframe Structures I: Model Formulation," *ASCE Journal of Structural Engineering*, 130(9): 1353–1360.
- Folz, B. & Filiatrault, A. (2004b). "Seismic Analysis of Woodframe Structures II: Model Implementation and Verification," *ASCE Journal of Structural Engineering*, 130(9): 1426–1434.
- International Code Council (ICC) (2006). *International Building Code*, Building Officials and Code International Code Council Inc., Country Club Hills, IL.
- Krawinkler, H. (1999). "Challenges and Progress in Performance-based Earthquake Engineering." *International Seminar on Seismic Engineering for Tomorrow*, Tokyo, Japan.
- Pacific Earthquake Engineering Research Center (PEER) (2000). "PEER Strong Motion Database," <http://peer.berkeley.edu/smcat>
- Pang, W.C. & Rosowsky, D.V. (2009). "Direct Displacement Procedure for Performance-based Seismic Design of Mid-rise Woodframe Structures," *Earthquake Spectra*, 25(3): 583–605.
- Pang, W.C., Rosowsky, D.V., Pei, S. & van de Lindt, J.W. (2010). "Performance-Based Shear Wall Design of Six-Story Neeswood Capstone Building via Simplified Direct Displacement Design Procedure," *Proceedings of the 2010 Structures Congress*, Orlando, FL.
- Pardoen, G., Waltman, A., Kazanjy, R., Freund, E. & Hamilton, C. (2003). *Testing and Analysis of One-story and Two-story Shearwalls under Cyclic Loading*, CUREE Report W-25, Task 1.4.4, Consortium of Universities for Research in Earthquake Engineering, Richmond, CA.
- Priestley, M.J.N. (1998). "Displacement-based approaches to rational limit states design of new structures," Keynote Address, *Proceedings of the 11th European Conference on Earthquake Engineering*, Paris, France.
- van de Lindt, J.W. (2005). "The Next Step for ASCE 16: Performance-Based Design for Woodframe Structures," *Proceedings of the 1st Invitational Workshop on Performance-Based Design of Wood-frame Structures*, <http://www.engr.colostate.edu/pbd>
- van de Lindt, J.W. & Liu, H. (2006). "Correlation of Observed Damage and FEMA 356 Drift Limits: Results from One-Story Wood-frame House Shake Table Tests," *Proceedings of the 2006 Structures Congress*, St. Louis, MO.

GS_231 — Probabilistic seismic hazard analysis (3)

This page intentionally left blank

Influence of material strength scattering on the ductile response of steel structures

M. Gündel, B. Hoffmeister & M. Feldmann

Institute for Steel Structures, RWTH Aachen University, Germany

1 INTRODUCTION

The exploitation of the capability of steel structures to dissipate energy by means of plastic deformations is a common and effective design strategy to achieve a high resistance against exceptional loads like earthquake. The crucial point in this design method is the prediction and control of the formation of plastic mechanisms with regard to their location and to their ultimate resistance combined with the prevention of brittle or other sudden failure modes. To this end so called capacity design rules are applied, where brittle parts of the structure are designed with a sufficient overstrength compared to the plastic limits of ductile members and thus enabling the development of the intended plastic mechanisms.

The overstrength used in the capacity design needs to cover the differences between the nominal plastic resistances of members obtained with the nominal values of yield strength and member dimensions and the real resistances which include the influence of strain hardening, cross-sectional dimensions and the real yield strength of the material. In particular the scattering of the yield strength, which in reality is usually significantly higher than the nominal value, is of high importance. Current European material standards however provide no requirements with regard to a limitation of the upper yield strength values.

2 MATERIAL STRENGTH SCATTERING

In the recently finished research project OPUS—founded by the Research Found for Coal and Steel—two European steel producers provided more than 13000 material data sets from three plants including yield stress, tensile strength, ultimate elongation and nominal thickness. The data were obtained from HE-, IPE- and UPN-sections in steel grade S235M, S275M, S355M and S460M produced according to EN10025. The data were grouped according to steel grade and flange thicknesses (3 to 16 mm and 16 to 40 mm).



Figure 1. Office building MRF: Fundamental period = 1.27 s.

The statistical evaluation of the yield strength led to coefficient of variations mainly between 0.05 and 0.07. These results are in good agreement with data from literature (Faber et al., 2001). The ratio from mean values to nominal value depended strongly on the steel grade: for S235 it was 1.40, for S275 between 1.20 and 1.32, for S355 between 1.12 and 1.28, for S460 between 1.08 and 1.13. Therefore, for low steel grades already the ratio from mean value to nominal value was significantly higher than the overstrength factor of 1.25 proposed in EN1998-1.

3 NONLINEAR DYNAMIC ANALYSIS

To investigate the influence of material scattering on the seismic performance, four typical steel structures were analysed: 5-storey office building braced either (i) by moment resisting frames or (ii) by concentric braces, 4-storey industrial building braced either (iii) by moment resisting frames or (iv) by concentric braces. In the first step the buildings were designed for ordinary loads according to EN1991 and E1993 considering dead load, imposed load, wind and snow loads. Afterwards the initial design was extended by adopting requirements for moderate seismic loads according to EN1998-1 by the lateral force method ($a_g = 0.1$,

Table 1. Seismic failure criteria.

Criteria	Limit	Reference
Roof drift	2.5% (ind.)	FEMA356
Storey drift	2.5% (ind.)	FEMA356
Ultimate rotation	$6\theta_y$ (limit)	EN1998-3
Ultimate def. in compression	$4\Delta_c$ (limit)	EN1998-3
Ultimate def. in tension	$7\Delta_t$ (limit)	EN1998-3

θ_y = chord rotation at yielding, for $0.3 < N/N_{pl} < 0.5$:
 $\theta_y^* = \theta_y (1 - N/N_{pl})$ acc. to FEMA350
 Δ_c = axial deformation of the brace at buckling load
 Δ_t = axial deformation of the brace at tensile yielding load.

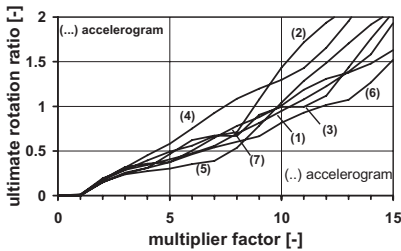


Figure 2. Office building MRF: maximum ultimate rotation ratio in the IDA's (nominal material properties).

Soil type C, 3% damping). Finally, non-linear time-step analyses were carried out on 2-D models for probabilistic investigations. The considered failure criteria in the non-linear analysis are summarized in Table 1.

In the analyses of MRF-structures the scattering of deformation parameters as roof drift and element rotation for different material samples was moderate (COV = 0.03 to 0.07). The scattering between different accelerograms were obviously predominant (COV = 0.16 and 0.17, Fig. 3). As ultimate rotation was the dominant failure criterion (see previous section), the failure probability of the structures seems to be nearly independent from material scattering. In contrast to this observation connection and foundation forces were highly correlated with the yield stress of the adjacent dissipative element (Fig. 4). The differences between particular accelerograms were however very small.

Similar results were also obtained for concentrically braced frames. The scattering of global and local deformation parameters for different material samples within one accelerogram was significant lower than the scattering between different accelerograms. The evaluation of connection and foundation forces adjacent to bracings (dissipative elements) show similar tendencies as for the MRF: correlation to the actual yield strength and low scattering between different accelerograms.

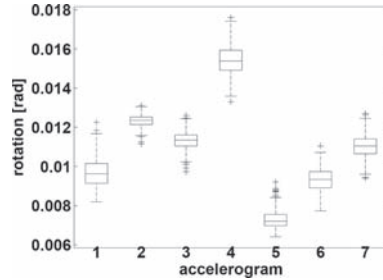


Figure 3. Office building MRF: Box plot of column foot rotation (material properties as random variables, multiplier 10).

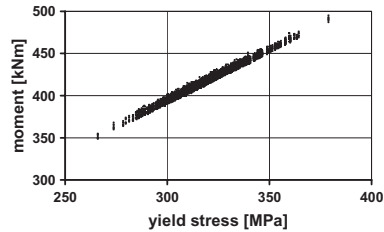


Figure 4. Office building MRF: maximum moment at joint vs. yield stress (beam connection, multiplier 10).

4 CONCLUSIONS

Based on the results of four reference structures—office and industrial building braced by MRF and CBF—following conclusions are made:

- The global and local deformation behaviour of the investigated steel structures is less dependent on material scattering.
- The scattering of global and local deformation behaviour of the structure due to different accelerograms is predominant.
- Connection and foundation forces correlate strongly with the yield stress of adjacent dissipative elements, but they are nearly independent to the scattering of the seismic action.

ACKNOWLEDGEMENT

The research leading to these results has received funding from the Research Program of the Research Fund for Coal and Steel RFSR-CT-2007-00039.

REFERENCES

Faber, H.M. et al., 2001. JCSS Probabilistic Model Code. Joint Committee on Structural Safety. www.jcss.ethz.ch
 Feldmann, M., Schäfer, D. & Eichler, B. 2009. Vorhersage duktilen Festigkeitsversagens von Stahlbauteilen mit Hilfe schädigungsmechanischer Methoden. Stahlbau, 78: 784–794. doi: 10.1002/stab.200910094.

A response spectrum based stochastic approach to estimate the peak response of structures subject to seismic pounding

A. Giaralis

City University London, London, UK

P.D. Spanos

Rice University, Houston, TX, USA

ABSTRACT: Field observations in the aftermath of various major seismic events have indicated that pounding between closely spaced structures and structural components/secondary equipment within structures contributes significantly to the overall earthquake-induced structural damage and to the associated economic loss (e.g. Kasai and Maison 1997).

In this paper, a stochastic approach recently proposed in Giaralis & Spanos (2010) is adopted to estimate the peak response of certain nonlinear systems used to model structures and secondary equipment protected from seismic pounding. Specifically, structural systems whose lateral motion due to strong ground shaking is confined in both directions by rigid barriers fixed to the ground are considered. Suppose that during a preliminary aseismic design stage such a system is modeled as a linear Single-Degree-Of-Freedom (SDOF) oscillator characterized by a mass m , a stiffness k and a viscous damping coefficient c . Further, assume that certain measures are taken to mitigate the pounding hazard associated with seismic events by means of appropriate protective material/devices fixed to the barrier allowing a clearance δ from the structure. Such provisions may be applicable to protect the deck of single-span bridges from collision with the abutments along their longitudinal direction (e.g. Zhu et al., 2002); the foundations of base-isolated structures from pounding to the surrounding soil (e.g. Komodromos 2008); and sensitive equipment housed in buildings from hitting against their containers and/or solid objects (e.g. Wolf & Skrikerud 1980). Herein, both linear, and stiffening springs described by the “Hertzian” law (spring force proportional to the deformation raised to the power of $3/2$) are used to account for the overall increase of stiffness in the considered model for $|x| > \delta$ as depicted in Figure 1. The parameter α gauges the severity in the nonlinearity of the differential equation of motion governing the deformation x of the structure.

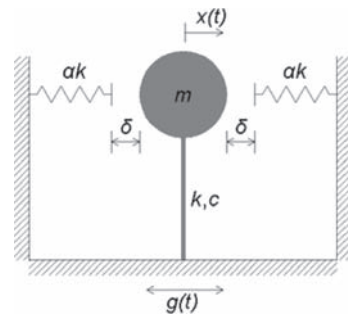


Figure 1. Model of the considered structural system subject to two-sided pounding on springs following Hooke's (linear) law and Hertz's law.

Following Giaralis & Spanos (2010), this paper considers processes $g(t)$ compatible with the given seismic design spectrum in conjunction with the method of statistical linearization to derive effective linear properties of the above described nonlinear elastic systems. For illustrative purposes, the elastic spectrum of the European EC8 aseismic code (CEN 2004) for peak ground acceleration $0.36 g$ ($g = 981 \text{ cm/sec}^2$), ground type B and damping ratio $\zeta = 5\%$ is used as a paradigm of an input seismic spectrum shown in Figure 2. An efficient numerical scheme is utilized to derive a non-parametric power spectrum representing a stationary stochastic process of finite duration which is compatible in a stochastic sense with the given design spectrum. In Figure 2 the power spectrum of a stationary process of 20 s duration which is compatible with the considered EC8 design spectrum is shown.

Next, the thus derived power spectrum is used in conjunction with the statistical linearization method to determine equivalent linear properties (ELPs) (i.e. equivalent ratio of critical damping ζ_{eq} and equivalent natural period T_{eq}) for linear SDOF structures characterized by a damping ratio ζ_n and a natural period T_n pounding on linear and Hertzian

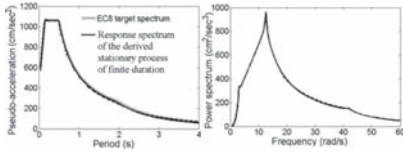


Figure 2. Power spectrum compatible with the considered EC8 target/design spectrum.

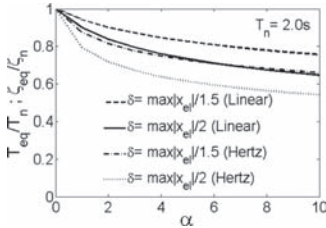


Figure 3. Effective linear properties of various viscously damped linear SDOF systems pounding on springs following the linear (Hooke's) and the Hertz's laws.

springs as shown in Figure 1. Pertinent numerical results are shown in Figure 3 for structures with $T_n = 2$ s. Note that these ELPs corresponding to the considered nonlinear structural systems depend explicitly on the assumed design spectrum. In this context, the obtained ELPs are used in conjunction with the EC8 spectrum of Figure 2 to estimate the peak response of the considered nonlinear systems in the context of response spectrum-based dynamic analyses as shown in Figure 4. In particular, consider a specific linear structure of natural period T_n and damping ratio $\zeta_n = 5\%$ exposed to the EC8 elastic design spectrum (vertical broken lines) pounding on linear or Hertzian springs characterized by the parameter α assuming a clearance δ . One can move, following the horizontal arrows, to a vertical solid line which corresponds to a (ζ_{eq}, T_{eq}) pair of ELPs obtained by the statistical linearization based methodology herein adopted and “read” the related spectral ordinate. In this respect, the adopted approach provides estimates of the maximum response of the nonlinear systems subject to a seismic response spectrum without resorting to numerical integration of the governing nonlinear equations of motion. Furthermore, Monte Carlo simulations involving an ensemble of 100 non-stationary EC8 design spectrum compatible accelerograms obtained by means of a wavelet-based methodology (Giaralis and Spanos 2009) are conducted to confirm that the average peak response of the considered nonlinear systems compares reasonably well with that of the ELPs.

In view of the numerical results included in this study, it is envisioned that the adopted statistical linearization based approach can be used to minimize at a preliminary design stage, at least, the seismic pounding hazard. Future work can include

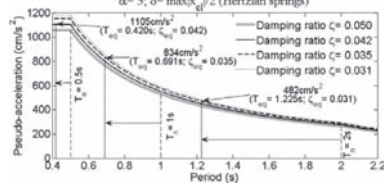
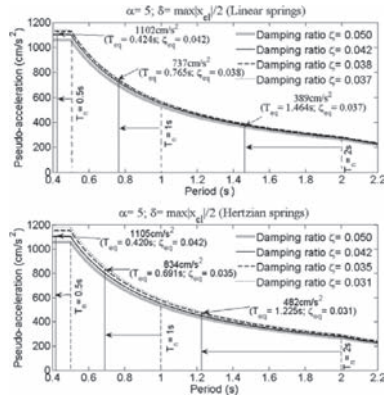


Figure 4. Estimation of the peak response of various viscously damped linear SDOF systems pounding on springs following the linear (Hooke's) and the Hertz's laws.

the incorporation of more sophisticated nonlinear hysteretic models (e.g. Jankowski 2005, Muthukumar & Des Roches 2006) to account for the energy absorption during impact combined with appropriate statistical linearization schemes.

REFERENCES

- CEN, Eurocode 8: *Design of Structures for Earthquake Resistance - Part 1: General Rules, Seismic Actions and Rules for Buildings. EN 1998-1: 2004*. Comité Européen de Normalisation, Brussels, 2004.
- Giaralis, A. & Spanos, P.D. 2009. Wavelet-based response spectrum compatible synthesis of accelerograms-Eurocode application (EC8). *Soil Dynamics and Earthquake Engineering* 29: 219–235.
- Giaralis, A. & Spanos, P.D. 2010. Effective linear damping and stiffness coefficients of nonlinear systems for design spectrum based analysis. *Soil Dynamics and Earthquake Engineering* 30: 798–810.
- Jankowski, R. 2005. Non-linear viscoelastic modeling of earthquake-induced structural pounding. *Earthquake Engineering and Structural Dynamics* 34: 595–611.
- Kasai, K. & Masai, B.F. 1997. Building pounding damage during the 1989 Loma Prieta earthquake. *Engineering Structures* 19: 195–207.
- Komodromos, P. 2008. Simulation of the earthquake-induced pounding of seismically isolated buildings. *Computers and Structures* 86: 618–626.
- Muthukumar, S. & DesRoches, R. 2006. A Hertz contact model with non-linear damping for pounding simulation. *Earthquake Engineering and Structural Dynamics* 35: 811–828.
- Wolf, J.P. & Skrikerud, P.E. 1980. Mutual pounding of adjacent structures during earthquakes, *Nuclear Engineering and Design* 57: 253–275.
- Zhu, P., Abe, M. & Fujino, Y. 2002. Modelling three-dimensional non-linear seismic performance of elevated bridges with emphasis on pounding of girders, *Earthquake Engineering and Structural Dynamics* 31: 1891–1913.

On the schematization of design response spectra as a stochastic model

S. Silvestri, G. Gasparini & T. Trombetti

Department DICAM, University of Bologna, Bologna, Italy

ABSTRACT: This paper focuses on the identification of the characteristics that a group of earthquake inputs must possess in order to be associated to a given exceedance probability, for seismic design applications. The identification of the characteristics of the “group of uniform hazard time-histories” is deeply rooted upon their probabilistic identification and is here made with reference to the elastic response spectral ordinates, takes advantage of the information carried by the

“epsilon” parameter, and is rooted on a separate treatment of the aleatory (intrinsic) variability and the epistemic uncertainty considered in the hazard analysis. The response spectra of the time-histories are described as a stochastic model: both (1) the probabilistic distribution functions of the spectral ordinates of given hazard (which depend on the period) and (2) the autocorrelation function of the spectral ordinates are obtained.

A new procedure for probabilistic seismic hazard analysis

G. Gasparini, S. Silvestri & T. Trombetti

Department DICAM, University of Bologna, Bologna, Italy

ABSTRACT: In the Performance-Based Seismic Design framework, the development of an appropriate “Probabilistic Seismic Hazard Analysis” which allows to statistically characterize the seismic input at the site of an engineering project becomes of crucial importance. The objective of the hazard analysis is to compute, for a given site over a given observation time, the probability of exceeding any particular value of specified ground motion parameters. This paper proposes a new

hazard analysis procedure which is based on the same assumptions of the Cornell’s widely upheld approach, but is alternative to this. The peculiarities of the proposed procedure resides (i) in that it leads to the determination of the probability functions (CDF and PDF) of the selected ground motion parameter (PGA, PGV, ...), and (ii) in that the occurrence of seismic events may be schematized either with the widely-used Poisson process or with more general Non-Poissonian models.

Vector-valued probabilistic seismic hazard analysis of correlated ground motion parameters

P. Bazzurro & J. Park

AIR Worldwide Corporation, USA

ABSTRACT: After many years of development in academia, performance-based earthquake engineering (PBEE) has become a common tool in industry for assessing the response of buildings and other structures subjected to seismic loading. Studies based on PBEE are used by a variety of stakeholders. Building owners, for example, use the results of these studies to decide whether to retrofit buildings and/or whether to invest in earthquake insurance. Lending institutions use them to decide whether to grant or deny a loan. Insurers use them to decide whether to underwrite earthquake insurance for a structure at a particular site and to determine an appropriate premium. Regardless of the application, it is critical that estimates of the likelihood that a structure's response exceeds a given level of severity, ranging from the onset of damage to incipient collapse, be as accurate as reasonably possible.

The three main aspects of PBEE are (1) evaluation of seismic hazard, (2) assessment of the response of the structure for any given level of ground shaking, and (3) computation of consequences potentially induced by any state of damage predicted by the response analysis. Such consequences are usually measured in terms of monetary losses, downtime and casualties. To increase the accuracy of the response prediction, engineers have recently taken advantage of the computational capabilities of modern computers by building more realistic two-dimensional and three-dimensional numerical models. The response of these complicated models is better gauged by monitoring multiple behavioural metrics, such as maximum interstorey drifts in both the longitudinal and transverse directions, and the maximum story acceleration along the height of the structure. To predict the values of such response measures, multiple intensity measures (IMs) of the ground motion in both horizontal (and sometimes vertical) directions are necessary. Hence, many researchers have recognized the need for estimating the joint site hazard of the predicted ground motion parameters of interest, which is a complicated task since these parameters are generally correlated.

The seminal methodology to evaluate joint seismic hazard, which was co-authored by the PI of this proposal, was introduced in 1998 and was called Vector Probabilistic Seismic Hazard Analysis (VPSHA). This method, which is herein called the “direct method”, is based on numerical integration of the joint Gaussian distribution of ground motion parameters generated at a site by an earthquake of given characteristics. Despite the long availability of the methodology, VPSHA has been rarely used in practice mainly because the three VPSHA computer programs in existence (Bazzurro 1998, Thio 2003, Gülerce & Abrahamson 2010) have inadequate documentation, are limited to two parameters, and are unable to identify the scenarios that control the joint hazard via the so-called “disaggregation” procedure. These shortcomings have severely hindered their use. To circumvent these problems, engineers have used scalar PSHAs for single ground motion parameters that are combinations of multiple ones (e.g. the geometric mean of the spectral accelerations at the first period of vibration in the two main horizontal directions of a building).

To help promoting the use of VPSHA, this study develops a methodology, herein called the “indirect approach”, which allows the computation of the joint hazard using any standard scalar PSHA software. In addition, the method makes use of the covariance matrix of the ground motion parameters for which the joint hazard is sought, and the disaggregated scalar site hazard for all the ground motion parameters considered. The empirically-derived covariance matrix for many ground motion parameters is currently available in the literature. This indirect approach to VPSHA is more computationally efficient as compared to the direct method based on the integration of multivariate Gaussian distributions. The indirect method can accommodate up to five or six random variables with current desktop computer limitations without significant loss of accuracy and can disaggregate the joint hazard. Note that the direct integration method, which is analyzed in this study only for the purposes of validating

the proposed indirect approach, can only handle up to three variables, and requires extremely costly computations. The computationally efficient indirect method could be easily coupled with the hazard and disaggregation results from USGS scalar hazard maps or OpenSHA to produce joint hazard estimates at any site.

Gülerce, Z. & Abrahamson, N.A. 2010. Vector-valued Probabilistic Seismic Hazard Assessment for the Effects of Vertical Ground Motions on the Seismic Response of Highway Bridges, *Earthquake Spectra*, (Accepted in publication).
Thio, H.K. 2003. Personal communication, URS Corporation, Pasadena, CA, July.

REFERENCES

Bazzurro, P. 1998. Probabilistic Seismic Demand Analysis, Ph.D. Dissertation, Dept. of Civil and Environmental Engineering, Stanford University, Stanford, CA, August.

*MS_236 — Progresses and challenges in probabilistic
modeling of tropical storm risks*

This page intentionally left blank

Hurricane hazard characterization for performance-based design

D.V. Rosowsky & Y. Wang

Department of Civil and Environmental Engineering, Rensselaer Polytechnic Institute, Troy, NY, USA

K.H. Lee

Energo Engineering, Inc., Houston, TX, USA

ABSTRACT: This paper presents advances in probabilistic modeling of hurricane wind fields and their incorporation into both short-term (near real-time) and long-term hurricane risk analysis simulation models. Output from the short-term model can be used in advance of an approaching hurricane to make decisions about evacuation, resource staging, hardening of selected facilities or routes, and so forth. Output from the long-term model can be used to characterize hurricanes for purposes of individual structure or portfolio risk analysis, as the basis for risk-consistent design basis wind speeds (e.g., performance-based design), or to characterize hurricane events (rather than simply maximum wind speeds) for purpose of spatial risk analysis or performance-based assessment of a portfolio of structures. Examples of each are presented and suggestions for future work are discussed. Also included is a brief discussion of modeling the joint hurricane wind-surge hazard.

REFERENCES

- Batts, M.E., Cordes, M.R., Russell, L.R., Shaver, J.R. and Simiu, E. (1980), *Hurricane Wind Speeds in the United States, NBS Building Science Series 124*, U.S. Department of Commerce, National Bureau of Standards, Washington, DC.
- Caton, P.G.F. (1975), "Standardized map of hourly mean wind speed over the United Kingdom and some implication regarding wind speed profiles," *Proceedings: 4th International Conference on Wind Effects on Buildings and Structures*, London, UK, pp.7–21.
- Darling, R.W.R. (1991), "Estimating probabilities of hurricane wind speeds using a large scale empirical model," *Journal of Climate*, 4(10):1035–1046.
- Federal Emergency Management Agency (FEMA) (2003). HAZUS-MH Multi-Hazard Loss Estimation Methodology, Hurricane Model Technical Manual. Washington, DC.
- Georgiu, P.N. (1985), *Design Wind Speeds in Tropical Cyclone-Prone Regions*, Ph.D. Dissertation, Department of Civil Engineering, University of Western Ontario, Canada.
- Heneka, P. (2008), "A damage model for the assessment of storm damage to buildings," *Engineering Structures*, 30(12):3603–3609.
- Ho, F.P., Su, J.C., Hanevich, K.L., Smith, R.J. and Richards, F. (1987), *Hurricane Climatology for the Atlantic and Gulf Coasts of the United States*, NOAA Technical Report NWS 38.
- Huang, Z., Rosowsky, D.V. and Sparks, P.R. (2001), "Hurricane simulation techniques for the evaluation of wind-speeds and expected insurance losses," *Journal of Wind Engineering and Industrial Aerodynamics*, 89(7–8):605–617.
- HURDAT (2005), http://www.aoml.noaa.gov/hrd/hurdat/Data_Storm.html, Atlantic Oceanographic and Meteorological Laboratory (AOML), National Oceanic and Atmospheric Administration (NOAA).
- Irish, J.L., Resio, D.T. and Ratcliff, J.J. (2008), "The influence of storm size on hurricane surge," *Journal of Physical Oceanography*, 38(9):2003–2013.
- Jelesnianski, C.P., Chen J. and Shaffer W.A. (1992), *SLOSH Sea, Lake, and Overland Surges from Hurricanes*, NOAA Technical Report NWS 48, Silver Spring, Maryland.
- Khanduri, A.C. and Morrow G.C. (2003), "Vulnerability of buildings to windstorms and insurance loss estimation," *Journal of Wind Engineering and Industrial Aerodynamics*, 91(4):455–467.
- Lee, K.H. and Rosowsky, D.V. (2007), "Synthetic hurricane wind speed records: development of a database for hazard analysis and risk studies," *Natural Hazards Review*, ASCE, 8(2):23–34.
- Legg, M.R., Nozick, L.K. and Davidson, R.A. (2010), "Optimizing the selection of hazard-consistent probabilistic scenarios for long-term regional hurricane loss estimation," *Structural Safety*, ASCE, 32(1): 90–100.
- Phan, L.T. and Simiu, E. (2008), "A Methodology for developing design criteria for structures subjected to combined effects of hurricane wind speed and storm surge," *Proceedings: 4th International Conference on Structural Engineering and Mechanics (ASEM 08)*, Jeju, Korea, pp. 1510–1524.
- Rosowsky, D.V., Sparks, P.R. and Huang, Z. (1999), *Wind Field Modeling and Hurricane Hazard Analysis*, Report to the South Carolina Sea Grant Consortium, Department of Civil Engineering, Clemson University, SC.

- Sparks, P.R. (2003), "Wind speeds in tropical cyclones and associated insurance losses," *Journal of Wind Engineering and Industrial Aerodynamics*, 91(12-15):1731-1751.
- Sparks, P.R. and Huang, Z. (1999), "Wind speed characteristics in tropical cyclones," *Proceedings: 10th International Conference on Wind Engineering*, Copenhagen, Denmark.
- Vickery, P.J. and Twisdale, L.A. (1995), "Wind-field and filling models for hurricane wind-speed prediction," *Journal of Structural Engineering*, ASCE, 121(11):1700-1209.
- Vickery, P.J., Skerlj, P.F., Steckley, A.C. and Twisdale, L.A. (2000a), "Hurricane wind field model for use in hurricane simulations," *Journal of Structural Engineering*, ASCE, 126(10):1203-1221.
- Vickery, P.J., Skerlj, P.F. and Twisdale, L.A. (2000b), "Simulation of hurricane risk in the U.S. using empirical track model," *Journal of Structural Engineering*, ASCE, 126(10):1222-1237.
- Wang, Y. (2010), *Studies on Hazard Characterization for Performance-Based Structural Design*, Ph.D. Dissertation, Department of Civil Engineering, Texas A&M University, USA.
- Watson, C. and Johnson, M. (2004), "Hurricane loss estimation models: Opportunities for improving the state of art," *Bulletin of the American Meteorological Society*, 85:1713-1726.

Tropical cyclone return periods: Comparison of a stochastic track model with an extreme value analysis of historic data

J. Kleinn

Aspen Re, Zurich, Switzerland

T.M. Hall

NASA Goddard Institute for Space Studies, New York, USA

1 INTRODUCTION

Stochastic event sets of tropical cyclones are frequently used for risk assessment. These data sets represent thousands of years of hypothetical events with the same overall statistics as the historic data. Having such large data sets allows the performance of risk assessment at return periods much longer than the length of the historic data set. The purpose of this paper is to present a stochastic event set for the Atlantic basin together with several validation techniques. The validation techniques are based on the intensity of landfalls along the US coast.

This paper presents a stochastic event set for the Atlantic basin together with several possible ways of validating a stochastic event set. One of the methods is based on extreme value statistics by estimating a best fit together with confidence bounds, which can then be compared to the historic data. The other methods are based on estimating the uncertainty in the stochastic event set. One of these two methods is based on resampling the time period of the historic data set from the stochastic event set and the other is based on reconstructing the stochastic model and leaving out part of the original data.

2 DATA

Historic data from 1950–2008 is used in this study is from the 6-hourly HURDAT database of Atlantic hurricanes (Landsea et al., 2004). Data for this time period is used for the development of the stochastic event set as well as for its validation. This time period is assumed to be complete and not suffer from storm count underestimation.

The stochastic event set is ongoing work and based on Hall and Jewson (2007). The stochastic model consists of a stochastic tropical cyclone genesis process, a stochastic storm track simulation, and a stochastic intensity simulation along the

tracks. This yields in a 6-hourly data set of tropical storms representing thousands of years.

The last data point before landfall (storm track crossing the coast line) is used as landfall intensity for both data sets. Only the time period 1950–2008 from HURDAT is used in the validation of the stochastic event set to be consistent with the data used for the stochastic event set itself.

3 GPD WITH CONFIDENCE INTERVALS

Extreme value statistics consists of a set of methods useful for the analysis of rare and extreme events. For the analysis of hurricane landfall intensity, the General Pareto Distribution (GPD) is used. The GPD is a so-called peaks-over-threshold method (POT) using all data over a certain threshold. Scale and shape parameter of the GPD are fitted by a maximum-likelihood approach and the threshold is set so that the amount of data used for the fit is maximized and the fit only changes marginally with increasing threshold. While extreme value statistics allows the estimation of return periods for return levels (i.e. landfall intensity), the uncertainty of such an estimation grows rapidly for time periods beyond the length of the data used. Therefore the GPD is not a replacement of a stochastic event set.

The estimation of confidence bounds by profile likelihood is only possible if enough data is available and if the GPD fit is of good quality. This is a limitation, especially for smaller landfall regions and regions of low historic activity.

If the data of the stochastic event set lies within the confidence bounds of the GPD fit, we can say that the two data sets cannot be statistically distinguished. In other words, the stochastic event set fits the historic data within the confidence limits.

4 SAMPLING OF STOCHASTIC EVENT YEARS

By re-sampling the number of years of the historic data set (59 years in our case) from the stochastic

data set, we can estimate another set of confidence bounds. The figure shows 10,000 sets of data, each as long as the historic data and each randomly sampled from the stochastic event set. Also shown are the associated 5% and 95% confidence bounds. These bounds represent the sampling uncertainty of the stochastic model. If the historical curve is all inside these confidence bounds, then the historical landfall set can be seen as one possible representation of the much larger set of stochastic landfall. In this case the stochastic model landfall is validated.

This procedure evaluates the realism of the stochastic model, but it does not provide uncertainty estimates on the model's mean landfall rates. For this a different sampling procedure is needed.

5 REPEATED CONSTRUCTION OF THE STOCHASTIC MODEL

To estimate the uncertainty of the stochastic model we perform a generalized jackknife procedure. We re-build the stochastic model a number of times, each time leaving out randomly 12 of the 59 data years (~20%). By this method, the sensitivity of the model's mean rates to sampling error in the underlying data is tested. This method is computationally very intensive, since the stochastic model has to be built over and over again.

6 RESULTS

Figures 1–2 show all of the methods for landfalls along the entire US coast. Figure 1 shows the

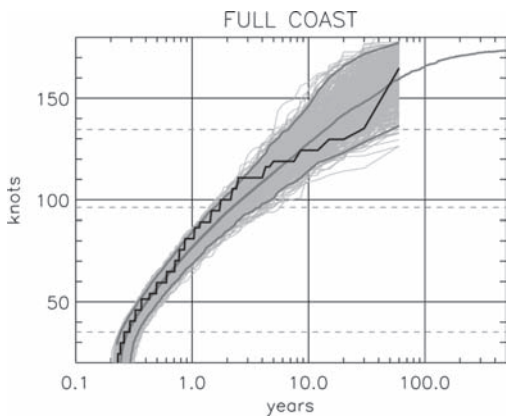


Figure 1. Landfall intensities and return periods along the US coast from historic HURDAT data for 1950–2008 (blue), the entire data of the stochastic event set (green), samples of 59 years of the stochastic event set (yellow), and the 5% and 95% confidence bounds of the samples (red).

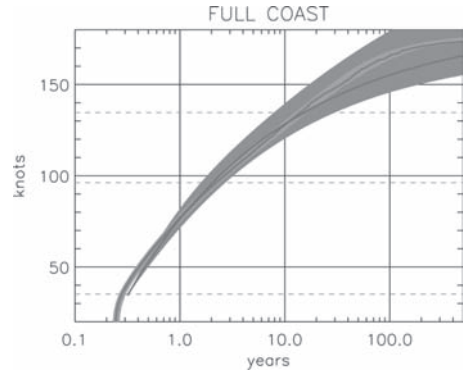


Figure 2. Landfall intensities and return periods along the US coast from the entire data of the stochastic event set (green line). The green surface is determined by the repeated construction of the model with random 20% data drops. The red line is the GPD fit of the historic data of 1950–2008 and the orange surface represents the 95% confidence bounds of the GPD fit.

historic HURDAT data for 1950–2008, the entire data of the stochastic event set, samples of 59 years of the stochastic event set, and the 5% and 95% confidence bounds of these samples. Figure 2 shows the entire data of the stochastic event set with the model uncertainty being determined by the repeated construction of the model with random 20% data drops. Figure 2 also includes the GPD fit of the historic data of 1950–2008 and the the 95% confidence bounds of the GPD fit.

7 CONCLUSIONS

The three different validation techniques show that the stochastic event set generally matches the historic data with regard to US landfall intensities. The uncertainty of the model (represented by the random drop out) is much less than the uncertainty of the extreme value fit or the uncertainty of the resampling.

REFERENCES

Hall, T.M. and Jewson, S. 2007. Statistical modeling of North Atlantic tropical cyclone tracks. *Tellus*, 59A, 486–498, doi:10.1111/j.1600-0870.2007.00240.x

Landsea, C.W., Anderson, C., Charles, N., Clark, G., Dunion, J., Fernandez-Partagas, J., Hungerford, P., Neumann, C. and Zimmer, M. 2004. The Atlantic hurricane database re-analysis project: Documentation for the 1851–1910 alterations and additions to the HURDAT database. “Hurricanes and Typhoons: Past, Present and Future”, R.J. Murnane and K.-B. Liu, Eds., Columbia University Press, 177–221.

Future typhoon projection using stochastic typhoon model under global climate change

T. Yasuda, S. Nakajo, N. Mori & H. Mase

Disaster Prevention Research Institute, Kyoto University, Japan

Y. Hayashi

Graduate School of Engineering, Kyoto University, Japan

S. Kunitomi

Kunitomi Co., Ltd., Japan

ABSTRACT: Intensity of tropical cyclones (typhoons, hurricanes and cyclones) in the future will possibly increase with the increase of sea surface temperature, as reported in the fourth assessment report of Intergovernmental Panel on Climate Change (IPCC AR4, 2007). Intensity enhancement of tropical cyclone, in other words, increase of wind speeds and decrease of atmospheric depressions cause severe coastal disasters due to extreme waves and storm. Thus, it is necessary to evaluate the future climate change effects on typhoons. A deterministic evaluation of storm surges in a particular bay is difficult because the data of typhoons, causing damages on a specific region, are very few. Since extreme analyses are necessary for disaster reduction planning, the number and intensity of projected typhoons by a single GCM does not provide enough information, therefore a stochastic typhoon model (STM) is necessary for engineering purposes.

The purpose of this study is to establish a STM for estimating characteristics of typhoons from cyclogenesis to cyclolysis in both present and future climate conditions in order to evaluate coastal hazard risks. Differences of statistical characteristics between the present and the future typhoons were estimated from projections by a GCM under a climate change scenario and are taken into account in the stochastic modelling of future typhoons based on the climate change signal. The STM is used to estimate the probability of future typhoon hazard for Japanese major bay area.

The present study reports on the STM from cyclogenesis to cyclolysis without distinction of season based on the observed typhoon track data (so-called best track data, BT) to assess the accuracy and bias tendencies of GCM projections. BT contains 1468 observed typhoons from 1951 to 2005 in the northwest Pacific.

Two-dimensional probabilistic density functions (2D-pdf) are estimated for each area of ($1^\circ \times 1^\circ$)

in the target area Ocean (0°N – 70°N , 100°E – 200°E) from the BT. The 2D-pdf consists of an input value and its local variation. Such analysis was evaluated for track direction, velocity, central atmospheric pressure, cyclogenesis and cyclolysis. We employed principal component analysis to estimate the 2D-pdfs. Finally, the STM employs the Monte Carlo simulation which generates typhoons by combining statistical 2D-pdf information.

The MRI-AGCM3.1S is an atmospheric GCM with T959L60 and is newly developed by Meteorological Research Institute, Japan (Kitoh et al., 2009). Time slice experiments were conducted for three climate periods of 1979–2003 (present climate), 2015–2030 (near future climate) and 2075–2099 (future climate) with different sea surface temperatures (SSTs). SSTs are used as one of external forcing of the AGCM as a bottom boundary condition. Observed SST from the UK Met Office Hadley Centre (HadISST) is used for the present climate experiment, and ensemble mean SSTs from CMIP3 multi-model projections of SRES A1B are employed for the future climate experiments. Indicative typhoon data was selected key features of typhoons such as typhoon tracks, central atmospheric pressures and maximum wind velocities every 6 hours. Although it is difficult to represent typhoon magnitude perfectly, the biases are consistent to the estimated changes between present and future climates produced by a dynamical model. Therefore we applied the changes in typhoon characteristics, predicted by the GCM to the proposed STM.

The STM has applied to hindcast (present climate) by using BT data from 1951 to 1995. Figure 1 shows the annual mean numbers of typhoon transit; the panel (a) is for BT data by RSMC-TTC and (b) is for STM result for 10,000 years. Although the STM simulation has a little bias in genesis area compared to the observation, trajectory pattern of typhoons is well reproduced.

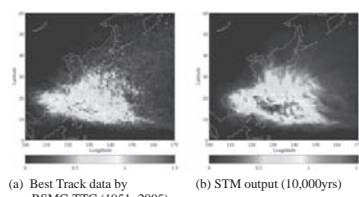


Figure 1. Typhoon track density in the Northwest Pacific.

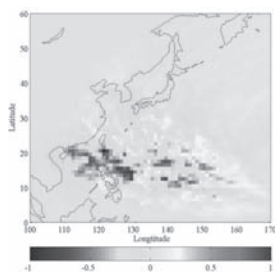


Figure 2. Difference of typhoon track density between future and present in the Northwest Pacific.

For example, some typhoons go straight toward China and some other typhoons turn to northeast near Taiwan. It was confirmed that the mean values of probabilistic properties of typhoons (e.g. landed number, central pressure and moving speed) approaching near the Osaka bay (134.5E~135.5E, 34 N~35 N) simulated by the present stochastic model agreed fairly well with those of analyzed typhoons.

The future characteristic of typhoon is discussed by using the proposed STM with the assumed probabilistic information of future climate. Thus the question arises how the future typhoon information should be taken into account. The analysis of typhoon data of GCM is conducted, first. Then, the transformation of BT data based on future GCM analysis is evaluated as an expected future typhoon data set.

It was found that future typhoons projected from the MRI-AM20 have large biases and it is therefore difficult to use the typhoon data directly to evaluate as the base data set of STM. To utilize the changes in typhoon characteristics projected by GCM, the locations of cyclogenesis and cyclolysis of BT data are changed proportionally according to the lognormal pdf's change. The modified future typhoon track may be extended or shortened which will change the timing and location of landfall in Japan. The stochastic procedure in the future experiment uses the modeled future typhoon tracks as input data on a grid of 1° by 1°.

Due to the shift of cyclogenesis location, number of typhoon around 10 N~20 N is decreased in the west side and is increased east side of the Northwest Pacific Ocean. As a result, typhoon

transit density decreases in the Philippine Sea and decreases a little in the East China Sea. There is about 0.3 decreases around the west Japan. It will be discussed in detail.

From the Monte Carlo simulation, the number of possible typhoon events will decrease in Japanese major bay areas. This is expected because the number of future cyclogenesis is given smaller than present climate. However, the number of future cyclogenesis is decreased about 21% in the whole domain but number of future typhoon is decreased 30%. This is the influence of shift of typhoon tracks and cyclolysis.

The lowest central atmospheric pressures of the typhoons passing over major bays will stay approximately the same in the future. One of the most significant results is the suggestion that for all three major bays the possibility of intense typhoons with central atmospheric pressure lower than 960 hPa will increase in the future. Although the average typhoon intensity will not change, extreme conditions will become more severe.

A stochastic typhoon model (STM) for estimating characteristics of typhoons from cyclogenesis to cyclolysis was established and its performance verified in the present climate. Differences between statistical characteristics of the present and the future typhoons were estimated from projections by an AGCM under a climate change scenario and are taken into account in the stochastic modelling of future typhoons as a climate change signal. The Monte Carlo simulation of the STM conducted a 10,000 year dataset of typhoons for the present and for the future, respectively. It was found that the number of typhoons that would hit Japan will decrease by about 30 percent but the mean value of the central atmospheric pressures will not change significantly. An important point is that the arrival probability of stronger typhoons will increase in the future climate scenario.

REFERENCES

- IPCC. 2007. Climate Change 2007: The Physical Science Basis, Working Group I Contribution to the Fourth Assessment Report of the Intergovernmental Panel on Climate Change. *Cambridge University Press*: Cambridge, UK; p. 996
- Kitoh, A., Ose, T., Kurihara, K., Kusunoki, S. & Sugi, M. KAKUSHIN Team-3 Modeling Group. 2009. Projection of changes in future weather extremes using super-high-resolution global and regional atmospheric models in the KAKUSHIN Program: Results of preliminary experiments. *Hydrological Research Letters*, 3, 49–53. doi:10.3178/hrl.3.49.
- Yasuda, T., Mase, H. & Mori, N. 2010. Projection of future typhoon landing on Japan based on a stochastic typhoon model utilizing AGCM projections. *Hydrological Research Letters*, 4, 65–69, doi:10.3178/HRL.4.65.

Challenges in developing the Florida public hurricane loss model for personal residential and commercial residential structures

G.L. Pita, J.-P. Pinelli & T. Johnson

Department of Civil Engineering, Florida Institute of Technology, Melbourne, FL, USA

K. Gurley & J. Weekes

Department of Civil Engineering, University of Florida, Gainesville, FL, USA

S. Hamid

Department of Finance, Florida International University, Miami, FL, USA

1 INTRODUCTION

1.1 *Florida before hurricane Andrew*

Building wind vulnerability started to be a concern to both state agencies and the insurance industry in the 1950's. Some counties began with the gradual enactment of building codes to standardize the construction practices while the insurance industry began to analyze exposure and make underwriting with econometric methods based on time series of past catastrophe losses.

There were mainly two codes in use in Florida before the 1990's, the South Florida Building Code in Miami-Dade and Broward counties and the Standard Building Code in most of the rest of the State. Although the SFBC was the most stringent code in Florida, this was uncorrelated with compliance and enforcement from many builders, design professionals and inspectors. To a lesser extent, some of the code stringency was eroded for almost three decades.

On the insurance industry side loss projection methods relied solely on recent historical claim data to set the premiums for hurricane peril and for the estimation of average annual losses. By the 1980's and 1990's up to 30 years of past losses were used for the homeowner policies ratemaking, depending on the company available information. In the late 1980's, the Insurance Services Office (ISO) tuned the existing technique by splitting hurricane and non-hurricane losses for ratemaking; the method was called the "excess wind procedure". The method predicted an "excess" catastrophe loss of \$80 million, for 1992.

1.2 *Florida after hurricane Andrew*

Hurricane Andrew in 1992 changed the perception that Floridians had of the building stock vulnerability. The damage resulted in \$16 billion

in insured losses and \$26.5 billion in total losses expressed in 1992 dollars. The aftermath revealed that the losses could have been significantly reduced if (1) builders, professionals and inspectors had at least complied with and enforced the existing building code, and (2) if the loss projection method accepted by the insurance industry would have considered vulnerability more thoroughly.

To address these problems, the obvious shortcomings of the "excess wind procedure" method led the ISO in 1996 to replace it by computer simulation methods. In addition, the state of Florida responded vigorously in all fronts, including:

- The adoption of a single building code, The Florida Building Code, which saw light in 2001 and was made effective on March 1, 2002. Studies indicate that the losses due to hurricanes have decreased since the enactment of the FBC.
- The creation of the Florida Commission on Hurricane Loss Methodology (FCHLM), to mediate between the insurance industry and the state of Florida, to set a method for the rate filing process and to review and certify loss models. The FCHLM is now the "gold standard for the review of hurricane models for producing property insurance-loss costs" serving not only Florida but helping all hurricane-prone states by providing a wealth of information that is useful to ease the acceptance process of loss models.
- The creation of a not-for-profit insurer of last resort, Citizens Property Insurance Corporation to provide property insurance for home-owners who cannot obtain insurance elsewhere.
- The development of a state of the art catastrophe model, the Florida Public Hurricane Loss Model (FPHLM), to predict insurance losses in Florida.

This paper focuses on this later development.

2 SCOPE OF THE PAPER

The paper starts with a description of the different component of the FPHLM. The authors follow with a description of the modeling approach. The differences between the two approaches followed for the low rise personal and commercial residential, and the mid/high-rise commercial residential buildings are highlighted. In the case of the low rise buildings, the buildings are modeled as a whole, while in the case of the mid/high rise buildings, the buildings are treated as an aggregation of apartment units.

Next, the exposure studies carried out for both personal and commercial residential structures are reported.

The paper then describes how the two modeling approaches are applied in the derivation of the vulnerability functions of the buildings. In the case of the low rise buildings, overall structures vulnerabilities are derived, while in the case of mi/high rise buildings apartment external vulnerabilities are derived.

Finally, the integration of these vulnerabilities in the actuarial model to compute insured losses is described.

3 VALIDATION

The validation challenge is that all components of the model, i.e. atmospheric, engineering, and actuarial, need to be validated independently and then a validation of all components working together is also necessary. These validations are dependent on the availability of reliable insurance data. The validation of the LB and MHB modules are more difficult due to the scarcity of available data. However, the modelers were able to compare the results of the model against claim data from one insurance company, for Hurricane Wilma. The data contained 3436 LB policies and 237 MHB policies.

In the case of the LB claims, the FPHLM over predicted the losses by 17%, while in the case of the MHB claims, the FPHLM under predicted the losses by 1%.

4 CONCLUSIONS

This paper describes the development of wind vulnerabilities for personal residential and commercial residential buildings, including low-rise and mid/high-rise structures.

The work reported here includes several novel approaches regarding the treatment of building vulnerabilities. These include a new interior damage model based on an estimate of water intrusion, and water propagation. Sensitive points include the estimate of vertical rain fall, rain duration, conversion of vertical rainfall into horizontal rainfall and correlation of water intrusion with interior and contents damage. Another novel approach is a modular description of mid/high rise buildings of any shape and size, which are treated as an aggregation of apartment units.

Access to meteorological data and damage and claim data are important for the validation and calibration of these new vulnerability models. Preliminary validation results are extremely encouraging.

ACKNOWLEDGMENTS

This research is supported by the State of Florida through an Office of Insurance Regulation grant to the Florida International University International Hurricane Research Center. The opinions, findings, and conclusions expressed in this presentation are not necessarily those of the FLOIR. The research is also funded by the Center of Excellence for Hurricane Damage Mitigation & Product Development at Florida International University.

Issues of epistemic uncertainty treatment in decision analysis for tropical cyclone risk management

M. Graf & K. Nishijima

Institute of Structural Engineering, ETH Zurich, Switzerland

1 INTRODUCTION

During the last few decades the probabilistic modeling of natural hazards and their risks generally has experienced significant improvement and many successes not only in methodology, but also in their applications. Important applications include risk/reliability-based structural design, determination of design loads in building design codes, insurance loss estimations of engineered facilities and portfolios, and risk mapping to facilitate efficient resource allocations for risk reduction measures.

Sharing the common methodologies and similar data sets in the modeling, however, models developed based on these often result in significantly different assessments of risks. These differences come from the use of different data sets, different modeling schemes, and different specification of the modeling schemes. In spite of the presence of advanced statistical techniques, the identification of *the* best modeling scheme and *the* best specification are difficult, hence, these are often highly subjective, presumably contributing to the large variability of the risk assessments.

This type of variability is generally understood as epistemic uncertainty, which arises from the lack of sufficient data and/or knowledge. Note that in contrast to the epistemic uncertainty, randomness in nature is called aleatory uncertainty. The general treatment of both types of uncertainty in risk assessment and formal decision analysis has been, since decades, an issue of attention in civil engineering and other fields. Presently, the general framework for the treatment of the uncertainties is readily available, see e.g. Paté-Cornell (1996).

However, in practice the epistemic uncertainty is often ignored, mixed up with aleatory uncertainty otherwise treated in ad hoc manners, which can lead to erroneous assessment of risks. Such examples are investigated in detail in Nishijima et al. (2008). Exceptions for these are found in the state-of-the-art projects for seismic hazard assessment for nuclear facilities at Yucca mountain in USA and in Switzerland (PEGASOS project). In these projects epistemic uncertainties are explicitly and consistently taken into account in the

assessment of the seismic hazards. In regard to tropical cyclones, a unique study has been undertaken to quantify the variability of the risk assessment results using different models, taking basis in the areas of Florida and North Carolina in USA. (Watson and Johnson, 2004).

1.1 Challenging issues

The ultimate objective of probabilistic modeling and risk assessment is to facilitate decision makers to identify optimal decisions. Seen in this light, together with the current status described above, the following issues are addressed as future tasks in regard to the tropical cyclone risk management: (1) Separation of aleatory and epistemic uncertainties; (2) Quantification of epistemic uncertainty; (3) Implementation of these uncertainties in the formal framework for risk assessment and decision analysis.

1.2 Focus in the paper

As a first step for challenging these tasks, the present paper focuses on the assessment of the hazard variability that comes from the use of different modeling schemes and data sets, and the specification of the modeling schemes; which is addressed as a part of the second task “quantification of epistemic uncertainty”. A general framework for the uncertainty treatment in risk assessment and decision analysis is introduced, whereby accounting for the tasks mentioned above. The typhoon risk model developed by the group of the authors is introduced (Graf et al., 2009). This model is used as the reference typhoon model, based on which several variants of the modeling schemes and the specification of the schemes are developed and systematically investigated.

2 REFERENCE TYPHOON MODEL AND ALTERNATIVE MODELS

The referenced typhoon model (Graf et al., 2009) consists of two parts; a hazard model and a

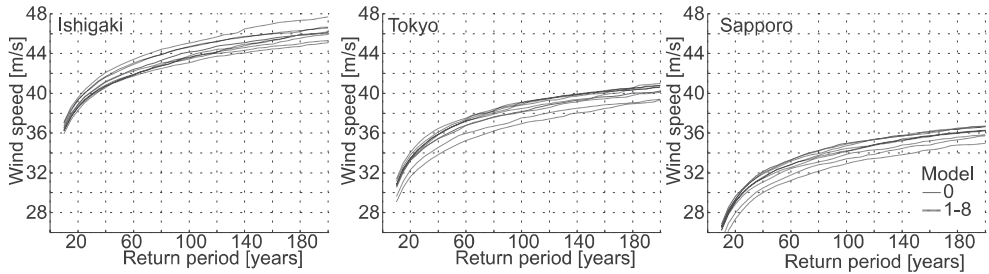


Figure 1. Maximum wind speeds as a function of return period for Ishigaki (left), Tokyo (centre) and Sapporo (right) for the different alternative models.

vulnerability model. The hazard model describes the probabilistic nature of the entire life-time of typhoons and associated wind fields from their occurrence to dissipation. The hazard model is composed of four sub-models; i.e. occurrence model, transition model, wind field model and surface friction model.

To investigate the variability due to the different modeling schemes and their specifications in the transition model, eight different alternative models are established. The variables considered here are: discretization in time and space, the order of Markov chains for the transition, and different data sets.

3 VARIABILITY OF HAZARD ASSESSMENT BETWEEN ALTERNATIVE MODELS

Using the alternative models for the transition, and the other parts of the typhoon model developed by the group of the authors, Monte Carlo simulations are performed to investigate the variability of the hazard assessment.

The maximum 10-minute sustained wind speeds for each typhoon event are considered. The wind speeds are simulated at several locations in Japan. Based on the simulations, the maximum wind speeds are estimated as a function of return period.

Figure 1 shows the maximum wind speeds at Tokyo, Sapporo and Ishigaki, which are obtained from the different alternative models. The maximum wind speeds obtained from the different alternative models differs by 2 to 3 [m/s] at the return period of 100 years. The variation increases at locations of higher latitudes.

4 CONCLUSIONS

The present paper addresses three challenging issues in tropical cyclone risk management from the perspective of the treatment of uncertainty. These are: (1) Separation of aleatory and epistemic uncertainties. (2) Quantification of epistemic uncertainty. (3) Implementation of these uncertainties in the formal framework for risk assessment and decision analysis.

As a first step for challenging these issues, quantification of the variability of hazard assessment results due to different alternative models is investigated.

Taking basis in the typhoon model developed by the group of the authors, eight different alternative models are systematically developed (i.e. no subjective “tuning-up”). The variability of the 100-year return period wind speed at Tokyo is approximately 3 m/s.

REFERENCES

- Graf, M., Nishijima, K. and Faber, M.H. (2009). *A Probabilistic Typhoon Model for the Northwest Pacific Region*, APCWE 7, Taipei.
- Nishijima, K., Maes, M. and Faber, M.H. (2008). *Probabilistic assessment of extreme events subject to epistemic uncertainties*, ASME 27th International Conference on Offshore Mechanics and Arctic Engineering, OMAE2008, Estoril, Portugal.
- Paté-Cornell, M.E. (1996). *Uncertainties in risk analysis: Six levels of treatment*, Reliability Engineering & System Safety, 54 (2–3), pp. 95–111.
- Watson, C.C. and Johnson, M.E. (2004). *Hurricane loss estimation models: Opportunities for improving the state of the art*. Boston, MA, US, American Meteorological Society.

Assessment of hurricane risk and estimates of insured losses using catastrophe modeling

Shahid S. Hamid

Department of Finance and International Hurricane Research Center, Florida International University, FL, USA

Jean-Paul Pinelli

Department of Civil Engineering, Florida Institute of Technology, FL, USA

Shu-Ching Chen

Department of Computer and Information Science, Florida International University, FL, USA

Kurt Gurley

Department of Civil and Coastal Engineering, University of Florida, FL, USA

1 INTRODUCTION

Recent hurricanes have created a crisis in the homeowner insurance market. There is great uncertainty about the nature of the risk and the potential losses. To help assess such risk, predict insured losses for personal and commercial residential properties, and to help evaluate rate filings, the Florida Office of Insurance Regulation contracted a group of interdisciplinary university researchers to develop the Florida Public Hurricane Loss Model (FPHLM). This paper discusses the nature and use of a public catastrophe model to assess hurricane risk and estimate potential losses. It briefly explains the model design and then presents estimates of the average annual insured residential losses and probable maximum insured losses for the state of Florida. It also presents scenario-based loss estimates for Category 1 and 5 hurricanes land-falling at various locations in the state.

The model can generate inputs used by insurance companies. The Average Annual Loss (AAL) estimates are typically used by insurance companies as input in the rate making process, and are also used by state regulators to help evaluate rate filings. The PML provides the loss estimate for a variety of return periods. It is in the interest of society, government, and the economy that insurance companies have the ability to cover massive potential losses. The PML provides loss estimates for such large events, and hence provides insight into how much reinsurance is needed.

2 CAT MODELING METHODOLOGY

Development of the FPHLM required collaboration of several disciplinary teams: a meteorological

team developed a hurricane wind model, Powell et al. (2005); an engineering team developed the building vulnerability and exposure model, Pinelli et al. (2010, 2008, 2004); an actuarial and insurance team translated the building physical damage to insurance loss; and a computer team integrated the different components into a user-friendly and stable computer platform, Chen et al. (2009). An overall discussion of the model and related statistical issues is provided in Hamid et al. (2010a, 2010b).

Both the meteorology and engineering components provide outputs that constitute critical inputs into the insured loss model. The meteorology component provides the probability distribution of winds for each zip code centroid or geocoded location. These are 3-second peak gust winds corrected for the terrain roughness. The component performs simulations to generate a stochastic set representing 50,000 years of activity. Models have been developed to determine translational velocity, central pressure, radius of maximum winds etc. The storms retained in the simulations include both hurricane events at Florida landfall and bypassing hurricanes that produce open terrain winds >30 mph on land in at least one zip code.

The tracks of historical hurricanes have been shifted probabilistically to generate tracks and intensities for the simulated hurricanes. The initial seeds for the storms are derived from the HURDAT data base produced by the Hurricane Research Division of NOAA. Each simulated storm has an estimated track and intensity and a set of modeled wind fields at successive time intervals. The wind field model generates the open terrain 1-minute maximum sustained wind speeds for the storm at various locations (e.g., population-weighted zip codes centroids) along its track. These 1-minute

maximum sustained winds are then converted to 3-second peak gust winds corrected for terrain roughness by using the gust wind model and the terrain roughness model. Higher terrain roughness reduces surface winds, and peak gust winds can be 30% to 35% higher than the sustained winds. For each zip code centroid, an accounting is then made of all the simulated storms that pass through it, Hamid (2010b).

The end product of the engineering component for personal residential properties are damage probability matrices that are used as input in the insured loss model, Pinelli et al. (2010, 2004). Each column of the damage matrix shows the probability distribution across damage levels for a given wind speed, and matrices are provided for building, contents, appurtenant structures and additional living expenses. Vulnerability matrices are provided for these construction type, and include masonry, frame, mobile home, and unknown. Separate vulnerability functions are generated for commercial residential properties. Within each construction type, the damage matrices are specific to the roof types (hip or gable) and number of stories. Since policy data may not provide this level of specificity, weighted matrices are used, where the weights are the proportion of different parameters such as roof cover, roof types, number of stories, and opening protection in a given region as determined by a survey of the building stock existing in the state of Florida. Furthermore, the year of construction is used as a proxy for construction quality and to account for the building codes. A total of over 1,000 matrices are created to cover different combinations of structural type, region, and quality. And regional differences in the vulnerability matrices capture the regional differences in the building code and construction practices.

The actuarial component produces loss estimates such as the average annual loss, and the maximum probable loss for a given event over a given time period; Hamid (2010b). The insurance policy exposure data for both personal and commercial residential properties are used. They are extracted from the Florida Catastrophe Fund policy data set. The loss cost estimates do not include expenses, risk loads, investment income, premium reserves, taxes, assessments, or profit margins. The model produces pure loss costs. The modeled loss costs also do not include storm surge losses.

3 SELECTED RESULTS

Average annual loss costs (AAL) were estimated for the state of Florida based on the 2007 exposure

data. The zero deductible statewide average annual losses are approximately \$5.9 billion for combined personal and residential properties. It should be noted that the zero deductible loss is the ground-up loss. A 100-year hurricane is expected to produce about \$64 billion in residential losses.

Simulations were also done to estimate “what if scenarios” of land falling hurricanes at various locations in Florida for personal residential properties only. The worst case scenario, e.g., a 1 in a 1000 year event, resulted in over \$100 billion in insured losses in South Florida. More typically, a Cat 5 hurricane land falling in Miami and proceeding west will produce estimated gross personal residential loss of \$47 billion, while an identical hurricane landing in Tampa and proceeding east will produce \$60 billion in estimated gross loss. It is also shown that the topography of Southeast and Central West Florida are a source of higher risk and vulnerability.

REFERENCES

- Chen, S.C., Chen, M., Zhao, N., Hamid, S., Chatterjee, K. & Armella, M. 2009. Florida Public Hurricane Loss Model: Research in Multi-Disciplinary System Integration Assisting Government Policy Making. *Government Information Quarterly* 26(2): 285–294.
- Hamid, S., Kibria, B.M.G, Gulati, S., Powell, M., Annane, B., Cocke, S., Pinelli, J.P., Gurley, K. & Chen, S.C. 2010a. Predicting Losses of Residential Structures in the State of Florida by the Public Hurricane Loss Evaluation Models. *Statistical Methodology* 7 (5): 552–573.
- Hamid, S., Pinelli, J.P., Chen, S.C. & Gurley, K. 2010b. Catastrophe Model Based Assessment of Hurricane Risk and estimates of Potential Insured Losses for the State of Florida. *Natural Hazard Review*, in press.
- Pinelli, J.P., Gurley, K., Pita, G., Torkian, B., Hamid, S. & Subramanian, C. 2010. Damage Characterization: Application to Florida Public Hurricane Loss Model. *Natural Hazard Review*, in press.
- Pinelli, J.P., Gurley, K., Subramanian, C., Hamid, S. & Pita, G. 2008. Validation of a probabilistic model for hurricane insurance loss projections in Florida. *Reliability Engineering and System Safety International Journal* 93(12): 1896–1905.
- Pinelli, J.P., Simiu, E., Gurley, K., Subramanian, C., Zhang, L., Cope, A., Filliben, J.J. & Hamid, S. 2004. Hurricane Damage Prediction Model for Residential Structures. *Journal of Structural Engineering (ASCE)*, 130(11): 1685–1691.
- Powell, M., Soukup, G., Cocke, S., Gulati, S., Morisseau-Leroy, N., Hamid, S., Dorst, N. & Axe, L. 2005. State of Florida Hurricane Loss Projection Model: Atmospheric Science Component. *Journal of Wind Engineering and Industrial Aerodynamics* 93: 651–674.

*MS_326 — Recent advances in geotechnical
risk and reliability (1)*

This page intentionally left blank

Methods for incorporating a variety of site response estimates into seismic hazard maps

E.M. Thompson & L.G. Baise

Department of Civil and Environmental Engineering Tufts University, Medford, MA, USA

EXTENDED ABSTRACT

Many different site response proxies have been proposed for estimating the site response amplifications with varying degrees of precision and spatial coverage. Site response data may be vector or raster spatial data and may be either period-dependent or period-independent. We study both the spatial coverage and the accuracy of these different methods. Vector data are typically either point data, such as individual velocity surveys, or polygon data, such as mapped surficial geology (Wills and Clahan 2006). Raster data include topographic slope (δ) (Wald and Allen 2007).

The site response proxies with the greatest spatial coverage are the raster datasets, which can be estimated globally. However, the accuracy of these proxies varies by region because the correlations are developed on a different or smaller region.

The most accurate site response proxies are those based on in situ measurements of S -wave velocity (V_S), but these point data require spatial interpolation for mapping, such as kriging. As distance between the location of the estimate and the nearest measurement increases, the accuracy of the interpolation/extrapolation decreases. Thus, the accuracy of estimating the site response proxy must also be accounted for when incorporating site effects into seismic hazard maps.

In this paper, we use the square-root-of-impedance (SRI) method (Joyner et al., 1981) rather than the widely used time averaged V_S to 30 m depth ($V_{S,30}$) (Borcherdt 1994) because the V_S profiles contain valuable information for site response beyond the single value of $V_{S,30}$. We also use the procedure described by Zhao et al. (2006) to estimate the fundamental site frequency (f_0) from horizontal-to-vertical spectral ratios (H/V).

We present two case studies that illustrate two different approaches for combining multiple estimates of period-dependent site effects. First, we investigate the Kobe, Japan, sedimentary basin where a large number of V_S profiles are available. In this first case study, we focus on incorporating mapped surficial geology into a geostatistical model for spatial interpolation, known as kriging with a trend.

The second case study (Parkfield, USA), many V_S profiles have been measured at strong motion stations. Here, we focus on how we can use the measured ground motions to quantify the estimation and model uncertainties in this region and use this information to compute a weighted mean of the different estimates of site effects, where the weight is inversely proportional to the variance of the individual amplification estimates.

This result of this method is illustrated in Figure 1 which plots the predicted site response amplifications for a variety of periods: (a) 0.2 sec, (b) 0.5 sec, (c) 1.0 sec, and (d) 4.0 sec. The 0.5 sec period predicted amplifications are controlled by local V_S surveys period in the vicinity of the strong motion stations. The influence of the topographic slope method increases as the distance to the measured data increases because the variance of the kriged estimate of the amplification increases. At larger periods (1.0 sec and 4.0 sec) the geology polygons have more influence on the predicted amplifications.

The Kobe and Parkfield case studies illustrate how the data that are available for mapping site response are highly variable from one region to the next. Both of these regions, however, are relatively extensive datasets because most regions will not have the amount of geotechnical data available here. In regions where data are more scarce, the first option is to use the Wald and Allen (2007) method to estimate the site response amplifications from topographic slope. This requires the least effort, and provides a first order approximation of the site response. As additional effort is invested (either in analyzing satellite imagery or geologic mapping), and additional data are collected (either in geotechnical exploration or ground motion records), the accuracy and reliability of the site response map is improved. The major challenge to seamlessly combining multiple estimates of period-dependent site effects is to account for the uncertainties of each estimate, which is both a function of location and period. In Kobe, where the data consists of velocity profiles and surficial geology, kriging with a trend is able to produce a map that combines these two types of data. In Parkfield, the data are

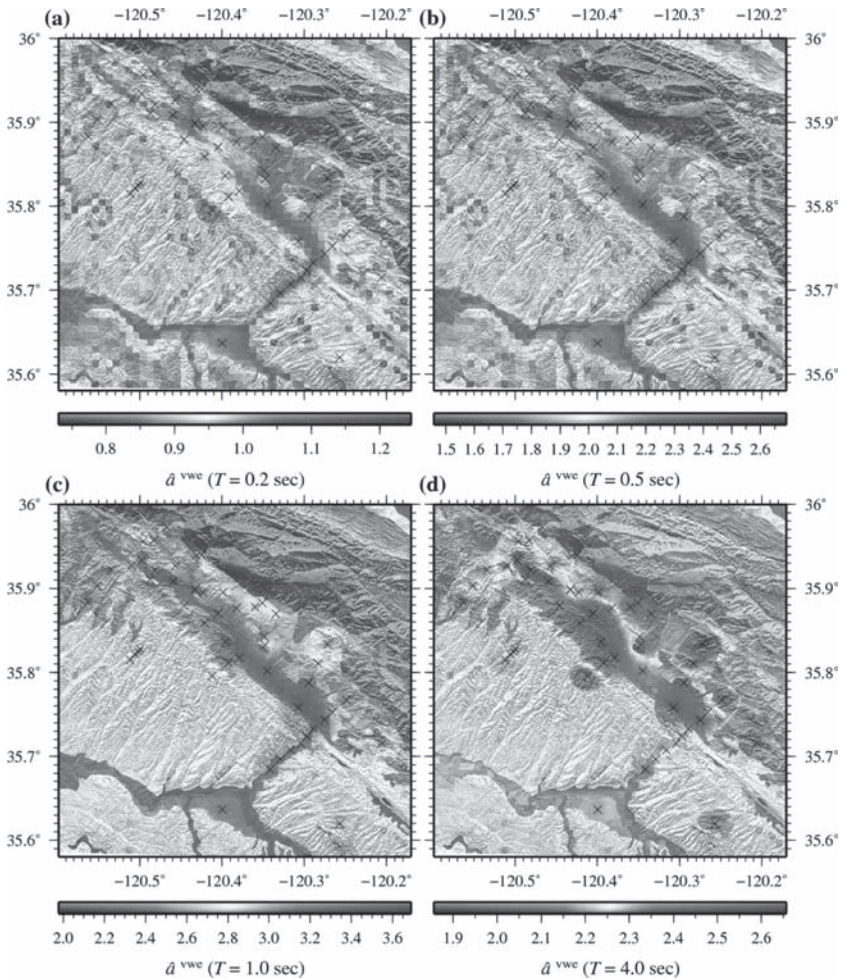


Figure 1. Map of the site response amplifications that integrate four different explanatory variables: f_0 , SRI, surficial geology, and topographic slope. The period dependence of the amplifications is illustrated by showing the maps for a variety of different periods: (a) $T=0.2$ sec, (b) $T=0.5$ sec, (c) $T=1.0$ sec, and (d) $T=4.0$ sec. The black crosses indicate the locations of the local V_S surveys.

much more varied, and we provide a method for mapping site response that is a weighted mean of the many site response estimates, where the weights are proportional to the variance of each estimate, thus accounting for both the period and spatial dependence of the uncertainty.

REFERENCES

- Borcherdt, R.D. (1994). Estimates of site-dependent response spectra for design (methodology and justification). *Earthquake Spectra* 10, 617–654.
- Joyner, W.B., Warrick, R.E. & Fumal, T.E. (1981). The effect of quaternary alluvium on strong ground motion in the Coyote Lake, California, Earthquake of 1979. *Bull. Seism. Soc. Am.* 71(4), 1333–1349.
- Wald, D.J. & Allen, T.I. (2007). Topographic slope as a proxy for seismic site conditions and amplification. *Bull. Seism. Soc. Am.* 97(5), 1379–1395.
- Wills, C.J. & Clahan, K.B. (2006). Developing a map of geologically defined site-condition categories for California. *Bull. Seism. Soc. Am.* 96(4), 1483–1501.
- Zhao, J., Irikura, K., Zhang, J., Fukushima, Y., Somerville, P., Asano, A., Ohno, Y., Oouchi, T., Takahashi, T. & Ogawa, H. (2006). An empirical site-classification method for strongmotion stations in Japan using H/V response spectral ratio. *Bull. Seism. Soc. Am.* 96(3), 914–25.

Reliability-based design of shallow foundations in cohesionless soils under compression loading: Ultimate limit state

S.O. Akbas

Gazi University, Ankara, Turkey

F.H. Kulhawy

Cornell University, Ithaca, NY, USA

1 INTRODUCTION

The ULS of a shallow foundation under compression loading is defined as the state in which the drained compression capacity is equal to the ultimate applied load. The foundation would not perform satisfactorily if the compression capacity is less than the applied load. Conversely, the foundation would perform satisfactorily if the applied load is less than the drained compression capacity. These three conditions can be described concisely by the following performance function, P :

$$P = Q_c - F \quad (1)$$

in which Q_c = compression capacity, and F = foundation load, which can consist of components such as the dead load and various live and transient loads. The conditions described above correspond mathematically to $P = 0$, $P < 0$, and $P > 0$, respectively.

2 RANDOM VARIABLES

Because of the variabilities in the load and soil parameters, the performance of a shallow foundation can not be evaluated with absolute certainty. The dead load is considered as normally distributed, with a bias equal to 1.05, and a coefficient of variation (COV) equal to 10%. The magnitude of the sustained live load is modeled by a gamma distribution, and its duration is modeled by an exponential distribution. The magnitude of the transient live load also is assumed to follow a gamma distribution, but its frequency is modeled as a Poisson distribution.

The variability of the snow load arises from two main sources. The first is the ground snow load, which is modeled by a lognormal random variable with a COV of 77%. The ground to roof conversion factor for the snow load also is a lognormally distributed random variable, with a mean of 1.09 and a COV of 44%. The occurrence of snow storms

is modeled by a Poisson process. The duration of each snow storm is assumed to be equal to the magnitude of the annual maximum ground snow load times an exponentially distributed constant, with a mean value of 25 days/kN/m².

The total load at any time was modeled conveniently as a sum of the individual load components. Each load effect was simulated separately, and then they were combined by superposition. The simulations for loads were performed in 50-year “subintervals”, i.e., if 20000 simulations are required, 400 simulations of these 50-year intervals were made. The maximum load for every year is calculated subsequently to be used in the reliability analyses as the value for a single simulation run.

On the capacity side, the main uncertain parameters are the effective stress friction angle and the shear modulus. The effective stress friction angle (ϕ') was modeled as a lognormal random variable. The range for the mean friction angle ($m_{\phi'}$) is between 30 and 45 degrees. The COV for the friction angle (COV $_{\phi'}$) is assumed to take values between 5 and 20%. The probability distribution for the shear modulus (G) is assumed to be lognormal. An approximate range for the shear modulus is between 4 and 40 MN/m². The probable range of COV for soil modulus has been estimated to be on the order of 30 to 90%.

3 PARAMETRIC STUDY AND SELECTION OF TARGET RELIABILITY INDEX

To evaluate the variation of the reliability index (β) with respect to each significant design parameter, a parametric study was conducted. The results of this study indicate the most influential design parameters, and accordingly the domains of calibration can be determined for the RBD equations.

It is determined that the reliability level varies significantly with the mean and COV of the effective stress friction angle and the ratio of 50-year mean recurrence interval snow load to total load. Thus, for non-snow areas, the mean and COV

of the effective stress friction angle are the only parameters for which the RBD equations need to be calibrated.

The results of the parametric study indicate that the following domains are appropriate for calibration of the simplified reliability-based design formats:

- a. $m_{\phi} = 30^{\circ}$ to 35° (loose sand), 35° to 40° (medium sand), and 40° to 45° (dense sand)
- b. $COV_{\phi} = 5$ to 10% , 10 to 15% and 15 to 20%
- c. 50-year snow load to total nominal load ratio (α) = 0 to 0.25 , 0.25 to 0.50 , and 0.50 to 0.75 .

Since their predictive equations differ, the general and local shear failure modes were calibrated separately, even though it was determined that the effect of shear modulus is minor in the resulting reliability index values.

Values of the reliability index (β) implicit in current designs were evaluated for a variety of design cases. It was determined that the reliability indices are highly variable, with an approximate range of 2.5 to 3.7. A target reliability index value of 3.2 is adopted.

4 CALIBRATION OF RBD EQUATIONS

The following simplified RBD format is selected for the calibration of the ULS of shallow foundations in cohesionless soils under compression loading:

$$F_{50} = \Psi_c^{ULS} Q_{cn} \quad (2)$$

in which F_{50} = 50-year return period total load on the foundation which consists of dead, live, and snow load components, Ψ_c^{ULS} = resistance factor in compression, and Q_{cn} = nominal net bearing capacity (or compression capacity). The ULS Ψ_c factor is calibrated to achieve a target reliability index of 3.2 for all of the domains selected, as consistently as possible. The resulting calibration factors, which range between 0.20 and 0.48, are tabulated for general and local shear failure modes, respectively. It was seen that the difference between the ULS Ψ_c factors for these two failure modes does not exceed 0.03 for any calibration point. Therefore, a single table of ULS Ψ_c factors could be used in practice without considering the failure mode.

The resistance factors are chosen so that they have the minimum average deviation from the target reliability index ($\Delta\beta$). A smaller value of average deviation from the target reliability index indicates that the reliability index generated in a given domain is more uniform. The average deviations from the target reliability index are rather small, with a maximum value of 0.255. Figure 1 illustrates the improvement in the uniformity of the reliability

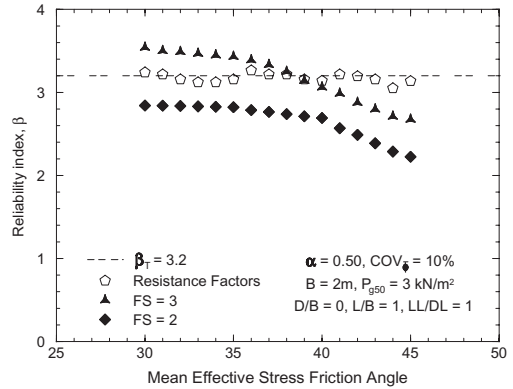


Figure 1. Comparison of uniformity of reliability levels using resistance factors and allowable stress design.

levels for a specific design problem by using the resistance factors from reliability analysis compared to allowable stress design by varying only the mean value of the effective stress friction angle.

5 SUMMARY AND CONCLUSIONS

The Reliability-Based Design (RBD) of shallow foundations under drained compression loading was examined. RBD equations for the ultimate limit state were developed to achieve a target reliability index of 3.2. The mean and COV of the effective stress friction angle and the ratio of the 50-year snow load to total load were determined to be the most influential parameters on the reliability index. The resulting resistance factors vary between 0.48 and 0.20. This wide range of resistance factors illustrates that use of a single factor of safety for different design and site conditions in traditional design practice clearly is both inadequate and inappropriate.

The insignificant difference between the resistance factors for the general and local shear failure modes suggests that a single set of resistance factors are adequate for design, without considering the failure type. The average deviations from the target reliability index using Equation 10 are between 0.151 and 0.255 and between 0.148 and 0.251 for the general and local shear failure modes, respectively. The uniformity of the reliability levels obtained by using the corresponding resistance factors also was illustrated.

Unlike conventional design based on FS, where indirect means of introducing safety by judgment and experience is common because of the large uncertainties inherent in the foundation performance predictions, RBD considers the uncertainties in the design process in a consistent and rational manner.

Effect of spatial variability on reliability evaluation of an earth slope

Y. Wang, Z.J. Cao & S.K. Au

Department of Building and Construction, City University of Hong Kong, Kowloon, Hong Kong

ABSTRACT: Various uncertainties exist in slope engineering, such as inherent spatial variability of soil properties and uncertainties induced by simplifications and approximations adopted in geotechnical models (e.g., geometry and location of slip surfaces in limit equilibrium methods). As noted in literature, a slope may fail along an unlimited number of potential slip surfaces, although evaluating the total failure probability along all potential slip surfaces are considered as a mathematically formidable task. Reliability evaluation of earth slopes is therefore frequently carried out only for one or a limited number of circular or non-circular slip surfaces. Effects of these uncertainties in reliability evaluation of earth slopes can be significant, and insight on these effects is of great value for understanding slope failure mechanisms and designing slope remedial measures.

This paper makes use of a cohesive soil slope example to illustrate the effects of inherent spatial variability of soil properties and the uncertainty associated with critical slip surfaces on reliability evaluation of slopes. The reliability evaluation is carried out using a practical approach to probabilistic slope stability analysis that implements an advanced Monte Carlo Simulation (MCS) method called Subset Simulation in a spreadsheet environment for improving the efficiency and resolution of MCS at relatively small probability levels.

To implement the MCS and Subset Simulation in a commonly available spreadsheet software EXCEL, a package of EXCEL worksheets and functions/Add-In have been developed, with the aids of Visual Basic for Applications (VBA) in EXCEL. A software architecture is proposed that deliberately divides the package into two parts: 1) deterministic analysis of slope stability, and 2) reliability analysis including uncertainty modeling, statistical analysis and Subset Simulation. It is of particular interest to decouple the development of EXCEL worksheets and VBA functions/Add-In for deterministic slope stability analysis and those for reliability analysis so that the reliability analysis can proceed as an extension of deterministic analysis in a non-intrusive manner. This allows

the deterministic analysis of slope stability and reliability analysis to be performed separately by personnel with different expertise and in a parallel fashion. This alleviates the geotechnical practitioners from digging into reliability computational algorithms so that they can focus on the slope stability problem itself.

Using the software package developed in this study, a series of simulations with different values of effective correlation length λ are performed to explore the effect of the inherent spatial variability of undrained shear strength S_u . Figure 1 summarizes the results in a plot of failure probability P_f versus normalized correlation length (λ/H), in which H is the height of the cohesive soil slope. As λ/H increases from 0.05 to 1 (or λ increases from 0.5 m to 10 m for $H = 10$ m), the value of P_f increases significantly from about 0.9% to 26%. When $\lambda/H > 1$ or λ is larger than the slope height H , the effect of λ on P_f begins to diminish, and P_f varies slightly as λ/H further increases. If the soil properties (e.g., S_u) are characterized by a single random variable or the spatial variability is ignored, the value of P_f is over-estimated significantly, particularly when the effective correlation length is smaller than the slope height.

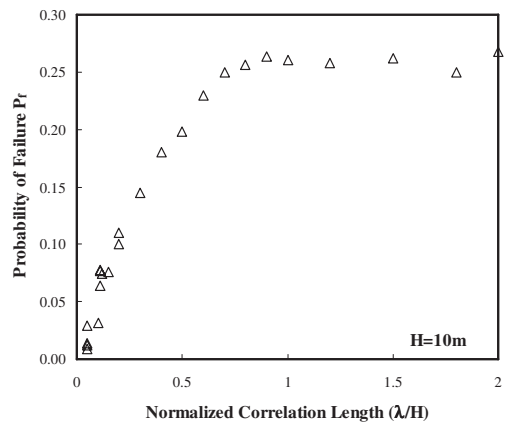


Figure 1. Effect of spatial variability of soil properties.

The simulation results further show that, when spatial variability is ignored by assuming perfect correlation (i.e., $\lambda = +\infty$), the variance of FS is over-estimated. However, the over-estimation may result in either over- (conservative) or under- (unconservative) estimation of P_f (i.e., probability of $FS < 1$). If $FS = 1$ occurs at the lower tail of the FS probability distribution, over-estimation of the FS variance leads to over-estimation of P_f , and it is therefore conservative. If the location of $FS = 1$ approaches to the center, or even the upper tail, of the FS probability distribution, (i.e., FS is relatively low), over-estimation of the FS variance leads to under-estimation of P_f , and it is therefore unconservative. Depending on the location of $FS = 1$ in the FS probability distribution, the over-estimation of the FS variance may result in contradicting results, as reported in literature.

The simulations performed in this study explicitly search a wide range of potential slip surfaces for obtaining the minimum FS in each random sample of \underline{S}_u . Figure 2 shows examples of different critical slip surfaces obtained from different random samples of \underline{S}_u . When $\lambda = +\infty$, the critical slip surface remains unchanged among different simulation samples, and it is the same as the one obtained from the deterministic analysis with all S_u values equal to their mean values of 40 kPa. On the other hand, when $\lambda = 0.5$ m, it is obvious that the critical slip surface changes significantly as the spatial distribution of \underline{S}_u changes among different random samples. Both center coordinates (x_c, y_c) and radius r for critical slip surfaces vary significantly. In particular, r varies from 21.0 m to 29.8 m and has a range of 8.8 m. It is evident that the inherent spatial variability of soil properties may result in significant uncertainty associated with critical slip surfaces. To further illustrate the effect of critical slip surface uncertainty on P_f ,

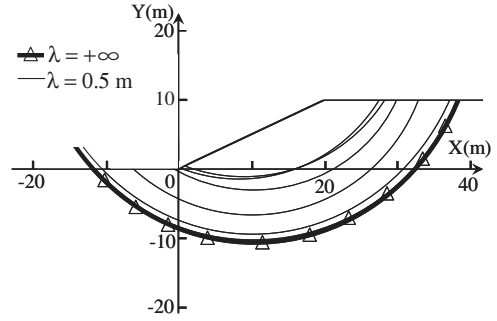


Figure 2. Examples of critical slip surfaces obtained from simulations.

simulations are also performed for $\lambda = 0.5$ m and with the fixed critical slip surface obtained from the deterministic analysis with all S_u values equal to their mean values of 40 kPa. The resulting P_f value decreases to about 0.13%, which is significantly smaller than 0.9% when the simulations include an explicit search of critical slip surfaces for each random sample.

When spatial variability is ignored or soil properties are characterized by a single random variable, location of critical slip surface is deterministic. This observation is consistent with the analytical results from previous study that, when spatial variability is ignored, location of critical slip surface is independent of the value of S_u , although the value of the minimum FS does vary as the S_u value changes. When spatial variability is considered, location of the critical slip surface changes significantly. Using only one given critical slip surface significantly under-estimates P_f , and it is unconservative. When spatial variability is considered, the critical slip surface uncertainty should therefore be properly accounted for.

Probabilistic characteristics of strip footing bearing capacity evaluated by random finite element method

J. Pieczyńska & W. Puła

Institute of Geotechnics and Hydrotechnics, Wrocław University of Technology, Poland

D.V. Griffiths

Division of Engineering, Colorado School of Mines, Golden, CO, USA

G.A. Fenton

Dalhousie University, Halifax, Nova Scotia, Canada

ABSTRACT: The Random Finite Element Method has been employed for calculating the random characteristics of bearing capacity of a strip foundation. The authors have focused on developing a formulation which includes anisotropic random fields of cohesion as well as the angle of internal friction. The influence of sub-soil self-weight has also been incorporated. Probability distributions of bearing capacity have been estimated.

1 INTRODUCTION

The influence of spatially random soil strength properties has been examined in a bearing capacity analysis. In this paper 2D numerical simulations are employed for the estimation of shallow footing bearing capacity in conjunction with the random finite element method (RFEM, e.g. Griffiths and Fenton 1993). RFEM connects random field theory and deterministic finite element methods by taking into account the mean, standard deviation, and correlation length of strength and load design parameters. In the present paper the authors focused their attention on:

- the role of anisotropy in random field analysis by analyzing different values of the correlation length in the vertical and horizontal directions;
- the influence of soil self-weight on probabilistic bearing capacity analysis.

2 BEARING CAPACITY EVALUATION

The bearing capacity analysis carried out in this paper uses an elastic perfectly plastic stress strain law with a classical Mohr Coulomb failure criterion. Plastic stress redistribution is accomplished using a viscoplastic algorithm. The finite element model incorporates five parameters: Young's modulus (E), Poisson's ratio (ν), dilation angle

(ψ), shear strength (c), and friction angle (ϕ). In the present study E , ν and ψ are held constant while c and ϕ are randomized. The Young's modulus governs the initial elastic response of the soil, but does not affect the bearing capacity.

Initially, a blue-grey clay has been considered. This kind of clay appears near Taranto in South East of Italy. The random field characteristics have been synthesized in Table 1 as a result of investigation over Taranto blue-grey clay (Cherubini et al. 2007). The friction angle has been defined as being a symmetric bounded distributed with lower limit $\phi_{\min} = 5^\circ$, upper limit $\phi_{\max} = 35^\circ$ and scale parameter $s = 2.27$ (Fenton and Griffiths 2008).

Secondly, a cohesionless sand has been considered with a bounded distribution of friction angle with minimum and maximum values of $\phi_{\min} = 14^\circ$, $\phi_{\max} = 51^\circ$, respectively and a scale parameter of $s = 2.21$. The sand characteristics (Table 2) are synthetic input data and they are not reflect any specific real situation. In order to compare results the values of vertical fluctuation scale has been assumed to be the same as in the case of Taranto clay. Computations within this study, have been

Table 1. Random characteristics of grey-blue clay.

Variable	Probability distribution	Mean	Standard deviation	Scale of fluctuation*
		μ	σ	θ_y
C	Lognormal	36 kPa	20 kPa	0.2; 0.5; 0.7; 1.0 m
ϕ	Bounded	20°	4.8°	0.2; 0.5; 0.7; 1.0 m
γ	Non-random	19 kN/m ³	–	–

*Horizontal fluctuation scale will be a subject of the parameter study.

carried out for anisotropic random fields. It means that the horizontal correlation length differs from the vertical one. In the vertical direction, four values of correlation length θ_y have been considered: 0.2; 0.5; 0.7 and 1.0 m. As reported in the literature, the horizontal correlation length is much greater than vertical. Therefore the following values of θ_x were used in the computations: 1; 5; 10; 50 m. It was assumed that the correlation lengths of cohesion and friction angle are the same.

Results for gray-blue clay are shown in Figure 1 and Figure 2. One can observe that the effect of horizontal fluctuation scale is important. However, for larger values that are realistic in natural soils, the bearing capacity coefficient of variations seems to be not very sensitive to the increase in the horizontal scale value (Figure 2). This result can be valuable if we are not able to precisely determine the horizontal fluctuation scale. In Figure 2 one can observe that the coefficients of variation for cases with and without self-weight almost coincide, for the same values of fluctuation scale. On the other hand bearing capacity coefficient of variation stabilizes with respect to horizontal fluctuation scale, when this scale reaches high values.

The results of computations carried out for sand are presented in Figure 3. An unexpected behavior is that the bearing capacity coefficients of variation may decrease with increasing value of horizontal fluctuation scale. This is quite different to the results for cohesive soil. It is recognized, however, that finite elements computation

Table 2. Random characteristics of sand.

Variable	Probability distribution	Mean	Standard deviation	Scale of fluctuation*
		μ	σ	θ_y
ϕ	Bounded	32.5°	4.8°	0.2; 0.5; 0.7; 1.0 m
γ	Non-random	19 kN/m ³	–	–

*Horizontal fluctuation scale will be the subject of parametric study.

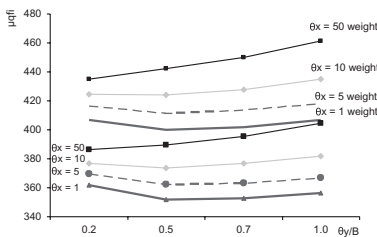


Figure 1. Mean value of bearing capacity versus ratio θ_y/B for different values of horizontal fluctuation scale. Curves denoted by “weight” result from computation where self-weight is included.

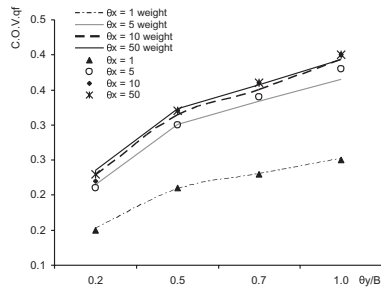


Figure 2. Coefficient of variation of bearing capacity versus ratio θ_y/B for different values of horizontal fluctuation scale. Curves denoted by “weight” result from computation where self-weight is included.

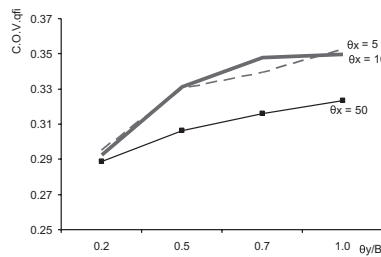


Figure 3. Coefficient of variation of bearing capacity versus ratio θ_y/B for different values of horizontal fluctuation scale. Results for cohesionless soil include self-weight.

of the bearing capacity of cohesionless soil is more challenging than cohesive soil, so this contrasting behavior needs further investigation and research.

3 CONCLUDING REMARKS

The RFEM method has been implemented in the investigation of probability characteristics of bearing capacity of a shallow spread foundation. The self-weight of soil and anisotropy of the random fields resulting from different vertical and horizontal correlation lengths has been taken into account. Results clearly show that the introduction of self weight and anisotropy into random fields is more realistic, and makes RFEM predictions more effective for design purposes.

REFERENCES

Cherubini, C., Vessia, G. & Pula, W. 2007. Statistical soil characterization of Italian sites for reliability analysis. *Proc., Characterization and Engineering properties of natural soils*, Tan et al. (eds.), Singapore: 2681–2706.

Fenton, G.A. & Griffiths, D.V. *Risk Assessment in Geotechnical Engineering*, John Wiley & Sons, New York, 2008.

Griffiths, D.V. & Fenton, G.A. 1993. Seepage beneath water retaining structures founded on spatially random soil. *Geotechnique*, 43, no. 4, pp. 577–587, (1993).

Evaluation of reliabilities of drilled shafts using bi-directional pile load test results

J.H. Park, D. Kim, K. Kwak, J.H. Lee & M. Chung

Geotechnolgy Eng'g Research Division, Korea Institute of Construction Technology,
Goyang, Republic of Korea

The use of drilled shafts is increasing due to its excellence, economic efficiency, and constructability in vertical and lateral behaviors according to the trend of enlargement and complex of structures, and especially, there are increasing applications as the foundation of long span sea bridge.

In this study, a reliability analysis was conducted on the side resistance of axially loaded drilled shafts in which bi-directional pile load test were carried out in order to develop LRFD design method. O-cell tests can measure the side and tip resistance separately, they can be used to calculate reliability index for side and tip resistance scrupulously. An analysis was conducted on the distribution of pile capacity regarding three representative bearing capacity equations by collecting and analyzing data from 24 bi-directional pile load test and geotechnical investigations on drilled shafts of 16 sites in South Korea. Evaluation on the reliability of each bearing capacity equation was conducted by first order reliability method (FORM) using the distribution of pile capacity.

To analyze the distribution of pile capacity of drilled shafts, the data of bi-directional pile load tests along with available geotechnical site investigation reports were collected and reviewed.

The selected test data represent general practice of large-size drilled shaft in South Korea. The diameter of the test piles was in the range of 800 mm to 3000 mm. Nine of the test piles were less than 30 m long and 15 were equal to or more than 30 m long. The test piles were embedded into weak rock within the range of 1.0–10.5 m. Unconfined compressive strength was computed and applied to estimate ultimate unit shaft resistance by taking a weighted average of the measured value at each depth regarding total weak rock layer. The maximum equivalent top-loaded test loads ranged from 20 MPa to 80 MPa, and the ratio of maximum equivalent top-loaded test load over allowable pile load was in the range of 2.0–2.9.

Load test data were compiled to determine the measured values of the unit side resistance. Unit side resistance was determined in two steps: (a) the average side resistance derived from the load test results, and (b) the unit side resistance in each soil section from the strain gauge data. Strain gauge measurements were used to calculate the load transfer distribution along the shafts. And the unit skin friction-displacement curve (f - w curve) were prepared for each stratum (weathered rock, soft rock). The equivalent top-loaded load-settlement curve was established by an approximate solution (LOADTEST 2000) using the pattern of developed side shear stress. The equivalent top-loaded curve of bi-directional pile load test is known to have relatively smaller settlements than the measured value for the result of conventional top-down static pile load test (Seol & Jeong 2009).

The Davisson criterion (1972) was chosen to determine the ultimate shaft resistance from the load test, which is called “measured capacity”. The selection of this criterion was based on the previous study performed by KICT (2008), in which four criteria (Davisson, FHWA 0.05D, ASCE 20-96, DeBeer) were used to estimate the nominal resistance of drilled shaft based on the static pile load test data.

The distribution of pile capacity is evaluated with statistical characteristics of resistance bias factors, the ratio of measured bearing capacity over

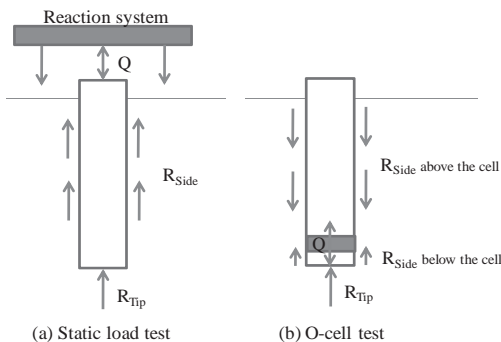


Figure 1. Comparison of (a) static load test and (b) O-cell test.

predicted bearing capacity. In order to calculate the predicated bearing capacity, three static bearing capacity equations (O'Neill & Reese 1999, Horvath & Kenney 1979, and Williams et al., 1980) were used to estimate the static shaft resistance of the 24 test piles. Static unit shaft resistances of the 24 test piles were calculated by these three methods and the computed values of resistance are called "predicted capacities". There does not seem to be a good correlation between the measured capacity and the predicted capacity by static analysis methods. In general, Williams et al. (1980) provides the most conservative prediction of unit shaft resistance among them.

The resistance bias factor ($R_{M/P}$) is defined as the ratio of the measured ultimate bearing capacity from a load test over the predicted ultimate bearing capacity by a static bearing capacity formula. The statistics of the filtered resistance bias factors are computed for reliability analysis and presented in Table 1. Horvath & Kenney (1979) equation appears to predict the bearing capacity the most closely to the measured capacity. As expected from the comparison of measured capacity and predicted capacity in Figure 2, Williams et al. (1980) equation, in general, underestimates the shaft resistance the most conservatively. However, the conservatism in the design method cannot

Table 1. Statistics of resistance bias factor ($R_{M/P}$).

Equation	Resistance bias factor ($R_{M/P}$)		
	Mean (μ)	COV*	Discarded data
O&R	1.18	0.59	No. 23
H&K	1.07	0.59	No. 23
Williams	1.62	0.59	No. 23

*COV = coefficient of variation (= standard deviation / mean).

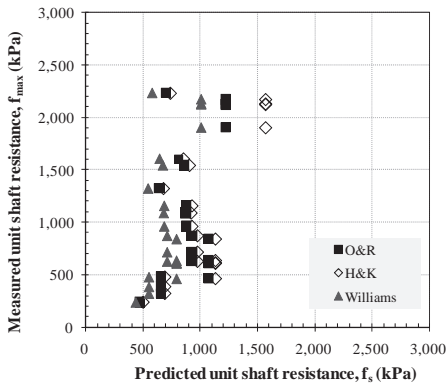


Figure 2. Correlation between measured and predicted shaft resistances.

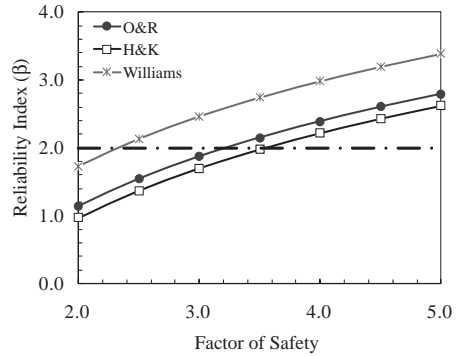


Figure 3. Calculated reliability indices.

be assured due to the large variation in the bias factors. Distributions of $R_{M/P}$ for the three bearing capacity methods were also examined and a lognormal distribution was found to most closely represent the bias factor ($R_{M/P}$) distributions for three methods.

This study employed the statistics of load bias factors used for the American Association of State Highway and Transportation Officials (AASHTO) LRFD bridge design specifications (2007). And two types of the First Order Reliability Methods (FORM), the Mean Value First Order Second Moment (MVFOSM) method and the Advanced First Order Second Moment (AFOSM) method were used to evaluate the reliability of the static bearing capacity design methods.

Reliability analysis was performed for safety factors in the range of 2.0–5.0. The computed reliability indices by both the MVFOSM and AFOSM methods are shown in Figure 3 for all 24 data.

The AFOSM method resulted in a little larger reliability indices than the MVFOSM method, but the difference was not significant (3.9% to 5.3% for O'Neill & Reese equation, 3.4% to 5.2% for Horvath & Kenney equation, and 4.7% to 5.5% for Williams et al. equation). The reliability indices of the three shaft resistance equations evaluated from AFOSM method for the FS in the range of 2.0–5.0 were in the ranges of 1.15–2.79 for O'Neill & Reese equation, 0.97–2.62 for Horvath & Kenney equation, and 1.73–3.38 for Williams et al. equation, respectively. The O'Neill & Reese equation and Horvath & Kenney equation showed similar level of reliability indices.

In Figure 3, the equivalent factors of safety corresponding to reliability index of 2.0 which is suggested as the required minimum safety level for deep foundations are in the range of 3.0–3.5 for O'Neill & Reese equation and Horvath & Kenney equation, 2.0–2.5 for Williams et al. equation, respectively.

*GS_336 — Recent advances in geotechnical
risk and reliability (2)*

This page intentionally left blank

Development of a computer-based evaluation system for soil parameters in the reliability design method

Y. Watabe & M. Tanaka

Port and Airport Research Institute, Yokosuka, Japan

T. Nishioka

Hozen Maintenance & Management Engineering Co., Ltd., Tokyo, Japan

I. Nozaki

Toa Research and Development Center, Toa Corporation, Yokohama, Japan

1 INTRODUCTION

The Japanese design code for port facilities was revised in 2007, and a performance-based reliability design method was introduced. This paper first briefly introduces a new practical method, which has been adopted in the annex of the design code, to evaluate soil parameters. The determination method of soil parameters in the code is called as “new port-design code” hereafter. Compared to the lower limit of 95% confidence interval, which is widely adopted in general design codes such as Eurocode 7 and JGS4001, the characteristic value determined by this method is slightly conservative when the number of data entries is larger than 10. The detail of the comparison will be described in this paper.

On the other hand, the geotechnical database for port and airport construction in Japan had been developed since 1983 by Port and Harbour Research Institute, Ministry of Transport, Japan, which has reorganized in 2001 to Port and Airport Research Institute, and the system is in operation since 1984. As of today, the geotechnical database contains 30,000 boring logs and those laboratory test results.

In this study, a computer-based evaluation system for the soil parameters in the new port-design code has been developed. This system can read the data stored in the Japanese geotechnical database for port and airport facilities. This system is programmed for both the new port-design code and arbitrary confidence interval corresponding to general design codes (such as 95% confidence level in Eurocode 7). The computer support system developed in this study is applied to a data set stored in the geotechnical database and its usability is demonstrated.

2 THE NEW PORT-DESIGN CODE

In order to evaluate the variation of the derived values x , it is convenient to use the coefficient of variation COV. In order to calculate the characteristic value x_k from the estimated value x^* , correction factor b_1 is introduced as a function of the COV, and then x_k is defined as Equation (1) with the correction factor defined as Equation (2).

$$x_k = b_1 \times x^* \quad (1)$$

$$b_1 = 1 \pm (\text{COV}/2) \quad (2)$$

In these definitions, the characteristic values correspond to either 30% (favorable) or 70% (unfavorable) fractile value. Because the simplification is aimed in this method, the values listed in Table A1 are to be used instead of the correction factors with detailed fractions.

If the number of data entries is not sufficient for statistical treatment, another correction factor b_2 is

Table A1. Value of correction factor b_1 .

Coefficient of variation COV	Correction factor b_1	
	Parameter for favorable side	Parameter for unfavorable side
COV < 0.1	1.00	1.00
0.1 ≤ COV < 0.15	0.95	1.05
0.15 ≤ COV < 0.25	0.90	1.10
0.25 ≤ COV < 0.4	0.85	1.15
0.4 ≤ COV < 0.6	0.75	1.25
0.6 ≤ COV	Reexamination of the data / Reexecution of the soil test	

introduced to correct b_1 . Then, the characteristic value is expressed as Equation (3).

$$x_k = b_1 \times b_2 \times x^* \quad (3)$$

About 10 or more data entries in the depth profile can be thought to be sufficient to reliably calculate COV. In the case with less than 10 data entries, the correction factor is defined as Equation (4).

$$b_2 = 1 \pm (0.5/n) \quad (4)$$

3 COMPUTER-BASED EVALUATION SYSTEM

3.1 Algorithm

A computer-based evaluation system for the soil parameters in the new port-design code is developed in this study. This system can read the data stored in the Japanese geotechnical database for port and airport facilities. This system is installed in MS-Excel file as macro functions programmed in MS-Visual Basic. The algorithm of the program is as follows:

1. Geological and geotechnical data obtained at the site concerned are read from the database. The program can read maximum 30 boring data sets.
2. The deposit is divided into soil layers corresponding to the soil types, i.e., gravel [G], sand [S], low-plastic silt [ML], high-plastic silt [MH], low-plastic clay [CL], and high-plastic clay [CH], based on the grain-size fractions and consistency. The program can integrate maximum 30 boring data sets. Then the depths of boundary of each layer are evaluated.
3. The depth profile of derived value in each soil layer is modeled as estimated value (regression line) by using least square method. If the regression line shows a tendency to decrease with depth, the depth profile is mandatorily modeled as uniform distribution with depth, because the depth profile of most soil parameters is positively correlated with depth.
4. Depth profile of the characteristic value is calculated from the depth profile of the estimated value in consideration of data variation (coefficient of variation COV) and number of data entries n .
5. Possibility of integration between two sequential layers is studied to achieve a higher characteristic value. Then, a depth profile of the characteristic value is proposed by the computer support system.
6. In order to obtain a rational depth profile of the characteristic value, integration or division of the soil layers are finally determined

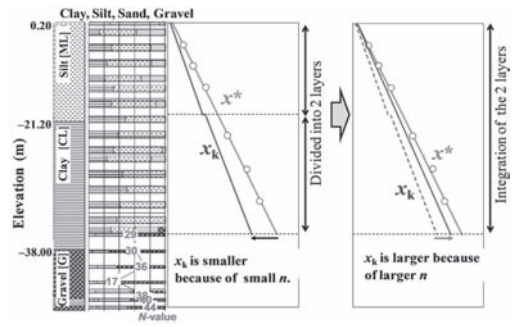


Figure A1. Illustration of a study on the possibility of integration or division of sequential clay layers (image).

by engineering judgment; and then the depth profile is recalculated.

The judgment whether two sequential layers should be integrated or divided is described here. In order to optimally determine the depth profile of mechanical properties such as consolidation yield stress p_c and undrained shear strength c_u , soil stratigraphy is divided into layers corresponding to the stress history. In order to interpret the mechanical properties of clay layers, stress history is a key factor. If COV does not significantly change in the integration process of the sequential clay layers, the characteristic value evaluated as the integrated soil layer results in a larger value than that evaluated as the discrete soil layers, because the number of data entries n significantly increases in each layer. This process is illustrated in Figure A1. By contrast, if COV significantly increases in the integration process, the characteristic value evaluated as the integrated soil layer may result in a smaller value than that evaluated as the discrete soil layers, because larger COV can strongly affect on the characteristic value rather than the number of data entries n .

The characteristic value of the soil parameters used in the reliability design should be objectively determined with the same confidence level based on a statistical treatment. However, the mere statistical treatment that is independent from empirical know-how based on soil mechanics is unrealistic to achieve a certain confidence level in practice; because both the engineering judgment and geological interpretation are strongly required to model the depth profile in association with the geological soil stratification, even though we have the computer-based evaluation system.

4 CONCLUSIONS

This paper first introduced the new practical method, which is adopted in the design code for

port facilities in Japan, to determine the depth profile of the characteristic values of soil parameter. In this method, the depth profile of the derived values is modeled as the profile of the estimated values, then the correction factors are multiplied to the estimated value according to the coefficient of variation (if $COV > 0.1$) and the number of the data entries (if $n < 10$).

In this study, a computer-based evaluation system for the soil parameters in the Japanese

design code for port facilities has been developed. Possibility of integration between two sequential soil layers is studied to achieve a higher characteristic value. In order to obtain a reasonable depth profile of the characteristic value, engineering judgment for integration or division of the soil strata is necessary, despite using the computer-based evaluation system.

On risk-based geotechnical site investigation of flood defenses

T. Schweckendiek

Department of Hydraulic Engineering, Delft University of Technology, Delft, The Netherlands
Unit Geo-engineering, Deltares, Delft, The Netherlands

P.H.A.J.M. van Gelder

Department of Hydraulic Engineering, Delft University of Technology, Delft, The Netherlands

E.O.F. Calle

Unit Geo-engineering, Deltares, Delft, The Netherlands

ABSTRACT: Site investigation planning in practice is largely based on intuition, engineering judgment, habits or the client's willingness to pay. Despite decision theory having been studied for geotechnical site investigation, for example by Baecher (1972), already in the early 1970's, applications seem to be restricted to academia. Elaboration of more specific examples close to practical questions and the provision of guidance and tools may aid the concept finding its way into practice, providing a framework for consistent decision-making. This paper applies decision theory to site investigation of flood defenses such as river dikes in order to demonstrate the usefulness and applicability to a common problem. After pointing out the specific requirements for assessing existing structures with explicit reliability requirements as opposed to design problems and pointing out the role of geotechnical site investigation herein, the framework is presented. A simplified example of the detection of an adverse geological detail by means of CPT illustrates the how an optimal inter-CPT distance is determined by the soil investigation strategy with the least expected cost. Even it cannot eliminate subjectivity from site investigation planning, the approach provides means of consistently deriving and justifying site investigation strategies based on prior information and accounting for the relevant costs and uncertainties involved.

1 INTRODUCTION

The current guidance material for determining the scope of Geotechnical Site Investigations (GSI) is mainly qualitative and relies mainly on engineering judgment. There is a lack of methods, guidance and examples of quantitative risk-motivated decision making, both, in practical guidance as well as in the literature. This paper proposes both,

a conceptual and a computational framework for determining the most cost-effective site inspection strategy in a safety assessment situation. The scope of a geotechnical investigation concerns choosing the techniques, the quality or the density or frequency of the measurements.

2 SAFETY ASSESSMENT OF FLOOD DEFENSES

The purpose of Safety Assessments (SA) of existing structures is to either extend their lifetime or to (re)define inspection and maintenance intervals. Flood defenses failing to meet the safety requirements have to be reinforced. A starting point for the methodology presented in this paper is the existence of an acceptable probability of flooding representing the safety requirement. Thus potential consequences of flooding are only treated implicitly.

3 GEOTECHNICAL INVESTIGATION

The vast majority of flood defenses are dikes, embankments and flood walls. Besides overtopping, the main threats are geotechnical failures like slope instability or internal erosion (e.g., piping).

These failure mechanisms are predominantly influenced by the composition of the subsoil, which is the result of natural deposition processes. The resulting heterogeneity is the main challenge in geotechnical investigations. Heterogeneity manifests itself in several ways: (a) in the stratification of the subsoil, (b) in the spatial variability of properties within the strata and (c) in the occurrence of adverse geological (or man-made) details. Detection of the latter is a key issue for flood defenses. From a reliability point of view, flood

defense systems can be characterized as serial systems where failure of any element leads to system failure. Hence, the weakest element of a flood defense determines its strength. Therefore, the role of geotechnical investigations in SA is principally the identification and characterization of weak spots.

4 CONCEPTUAL FRAMEWORK

The core concept and theory used in the presented approach is Bayesian Decision Analysis (Raiffa and Schlaifer (1961), Benjamin and Cornell (1970)). In this specific case, the often encountered difficulty of specifying an appropriate utility function has a simple solution, because the appropriate scope of geotechnical investigation for SA purposes is a cost-minimization question. As opposed to most risk-based decision problems, the cost of failure is out of the scope of the analysis, though still implicitly covered through the target reliability.

4.1 Decisions in safety assessments

The purpose of SA is to assess whether or not a structure is safe enough. We define safe enough in terms of an admissible probability of failure $P_{f,adm}$ (failure = unsatisfactory performance) or the equivalent target reliability:

$$\beta_{req} = \Phi^{-1}(1 - P_{f,adm}) \quad (1)$$

A negative SA outcome (i.e., unsafe or disapproval) implies that either reinforcement or more investigation (to reduce uncertainty) is required to achieve an acceptable state ($\beta > \beta_{req}$). The decision tree in Figure 1 illustrates the decision options *a*, possible outcomes (or states of nature)

θ and marginal cost *C* that are involved in the decision problem of getting to approval of an initially unsafe structure.

The main alternative actions are initiating a geotechnical investigation and directly reinforcing or replacing the structure. Within option (b) more choices to be made, such as the type and parameters (e.g., grid) of the geotechnical investigation. After the investigation, the result will be either approval or disapproval of the structure. The marginal cost for option (a) is mainly the cost of uncertainty reduction by means of analysis of readily available data. While the marginal cost for option (c) is simply the reinforcement cost, for option (b) it is either the inspection cost in case of approval or the cost of inspection plus the cost of reinforcement in case of disapproval. Notice that the required reinforcement after investigation might be less (in rare cases also more) extensive than option (c) due to additional information. For example, having identified weak spots in some reaches and excluded anomalies in other reaches, local reinforcements may be sufficient. Optimal inspection and maintenance strategies are regarded as the ones achieving the objective (a safe structure) with minimum cost:

$$s^* : \min_s E[C_I(s) + C_R(s, \varepsilon(s, \Theta))] \quad (2)$$

where *s* is the decision strategy (incl. the decision parameters) for the investigation (experiment) to be carried out. The cost of investigation $C_I(s)$ is assumed to be deterministic, while the cost of reinforcement $C_R(s, \varepsilon(\Theta))$ depends on the outcome $\varepsilon(\Theta)$ of the investigation (evidence), which itself depends on the state of nature Θ . In other words, the decision problem treats the question whether reinforcement (cost) can be either avoided or reduced by geotechnical site investigation and

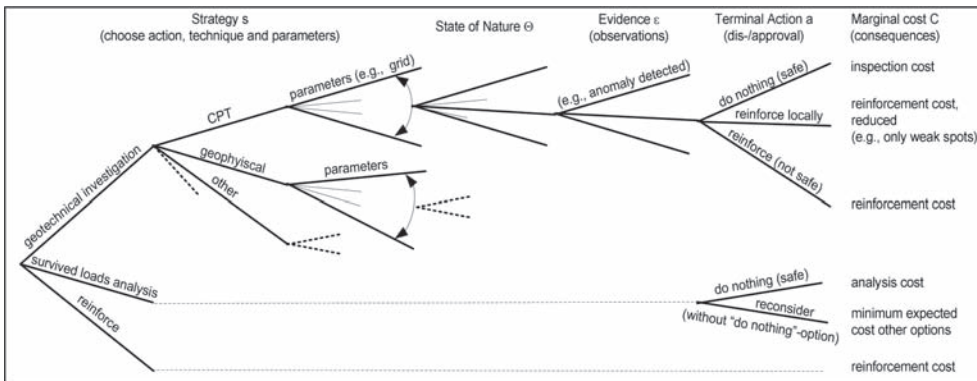


Figure 1. Decision tree for geotechnical investigation in safety assessments of flood defenses.

which type and setup can achieve this most cost-effectively.

5 MAIN RESULTS AND CONCLUSIONS

The paper demonstrates the usefulness of probability and decision theory for a specific application, the safety assessment of river dikes. It presents a decision framework and a simple but illustrative

simple example of detecting adverse geological details by CPT. has demonstrated the applicability of the framework. Using such a framework does not eliminate subjectivity from site investigation planning, since assessing prior probabilities still requires (subjective) expert judgment. Nevertheless, it provides a tool for consistent rational decision making. For practical application, the development of tools and guidance and the elaboration of examples are necessary.

Challenges in limit equilibrium based slope reliability problems

Jianye Ching

Department of Civil Engineering, National Taiwan University, Taipei, Taiwan

Kok-Kwang Phoon

Department of Civil and Environmental Engineering, National University of Singapore, Singapore

Yu-Gang Hu

Department of Civil Engineering, National Taiwan University, Taipei, Taiwan

This study addresses the challenges that may be encountered in slope reliability problems based on limit equilibrium methods (LEM). The main focus is on the existence of multiple failure modes that poses difficulty to many LEM-based slope reliability methods. In particular, when weak seams are present, the failure modes associated with those seams may be difficult to detect. A systematic way of searching the failure modes is proposed, and its robustness over slopes with or without weak seams is demonstrated. It is found that in the presence of weak seams, assuming circular slip surfaces may cause underestimation of slope failure probability. The conclusion of the study promotes the use of finite elements as the stability method for reliability evaluation because it is not necessary to search for failure surfaces in finite-element stability analysis.

Consider the slope containing a weak seam shown in Figure 1. The undrained shear strengths s_{u1} and s_{u2} of the two clayey layers are uncertain and independent and are lognormally distributed with mean values $\mu_{su1} = 30 \text{ kN/m}^2$ and $\mu_{su2} = 28 \text{ kN/m}^2$ and with c.o.v.s $\delta_{su1} = 30\%$ and $\delta_{su2} = 30\%$. The vertical line interval that the trial slip surfaces must pass through is chosen to be a-b-c in the figure.

In this example the failure mode involving the slip along the weak seam is difficult to detect. The main purpose of this example is to demonstrate the robustness of the proposed method over a slope with such a weak seam. The two trial slip surfaces obtained by the proposed method are shown in Figure 1 as ω_1 and ω_2 . Figure 2 shows the actual failure region F determined by the exhaustive

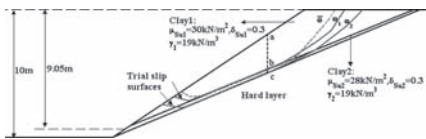


Figure 1. “Most probable” slip surface and trial surfaces in Example.

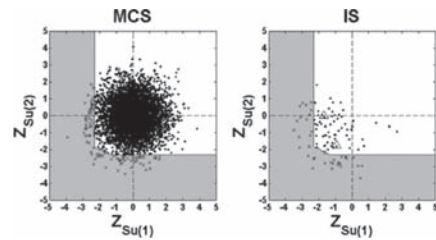


Figure 2. MCS (left-hand plot; $N = 5000$) and IS (right-hand plot; $N = 100$) samples in the standard Gaussian space (Spencer’s method).

analysis based on the Spencer’s method, where the locations of the OMS design points for the two trial slip surfaces are shown as the triangles. It is clear that both failure modes are captured. The FORM method, again, is only able to identify the first mode: the $\bar{\omega}$ surface in Figure 1 is the most probable failure surface found by FORM. It looks similar to ω_1 .

One hundred IS samples are plotted in Figure 2, showing that many of them are failure samples. The resulting P_F^{IS} is 0.022, and its c.o.v. is estimated to be 18.54%. The failure probability estimate for the MCS method ($N = 5000$) is found to be 0.020 with c.o.v. = 9.95%. These results are listed in Table 1 together with the FORM results for the Spencer’s method, simplified Janbu’s method and OMS. The FORM method underestimates the failure probability, and both the IS and MCS methods provide unbiased estimates, but the IS method is more efficient.

Since weak seams are present, the random search method may not work well. Also, the assumption of circular slip surfaces may be invalid. To investigate this, the random search method is taken to obtain circular trial slip surfaces for the IS analysis. Moreover, for the computation of failure probability in the IS analysis, circular slip surfaces are assumed and the simplified Bishop

Table 1. Analysis results from methods based on noncircular slip surfaces with the search method proposed in this study.

Method	Spencer		
	MCS	IS	FORM
Number of sample N	5000	100	
Estimated failure probability	0.020	0.022	0.0077
Estimator c.o.v. (%)	9.95%	18.54%	
Required N to achieve c.o.v. = 20%	1238	85	
Method	Simplified Janbu		
	MCS	IS	FORM
Number of sample N	5000	100	
Estimated failure probability	0.016	0.0078	0.0061
Estimator c.o.v. (%)	11.16%	22.10%	
Required N to achieve c.o.v. = 20%	1558	123	
Method	OMS		
	MCS	IS	FORM
Number of sample N	5000	100	
Estimated failure probability	0.019	0.023	0.0089
Estimator c.o.v. (%)	10.22%	18.4%	
Required N to achieve c.o.v. = 20%	1306	85	

method and OMS are applied. Table 2 shows the IS analysis results together with those obtained by the MCS and FORM methods. The failure probability estimates made by the two different stability methods are still similar. It is clear that all methods, including IS, MCS and FORM, significantly underestimates the actual slope failure probability. There are two reasons:

- Since circular slip surfaces are assumed, the second failure mode seen in Figure 2 may not exist since this failure mode pertains to non-circular slip surfaces passing through the weak seam. This is further verified by the results of the exhaustive analysis based on the simplified Bishop method: Figure 3 shows the actual failure region F determined by the exhaustive analysis as well as the approximate design points of the randomly generated circular trial slip surfaces (the triangles). The second failure mode clearly does not exist.
- Even if noncircular slip surfaces are generated in the random search, the second mode may still

Table 2. Analysis results from methods based on circular slip surfaces with the random search method.

Method	Simplified Bishop		
	MCS	IS	FORM
Number of sample N	5000	100	
Estimated failure probability	0.0048	0.0042	0.0046
Estimator c.o.v. (%)	20.36%	24.04%	
Required N to achieve c.o.v. = 20%	5182	144	
Method	OMS		
	MCS	IS	FORM
Number of sample N	5000	100	
Estimated failure probability	0.007	0.0024	0.0058
Estimator c.o.v. (%)	16.84%	29.66%	
Required N to achieve c.o.v. = 20%	3545	220	

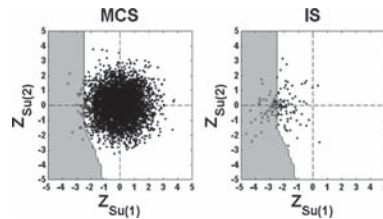


Figure 3. The MCS (left-hand plot; $N = 5000$) and IS (right-hand plot; $N = 100$) samples in the standard Gaussian space (simplified Bishop's method).

escape detection. This is because the slip surfaces generated by the random search method have negligible chance of passing through the weak seam when it is sufficiently thin.

REFERENCES

- Ang, A.H.S. and Tang, W.H. 1984. *Probability Concepts in Engineering Planning and Design, Volume II Decision, Risk, and Reliability*, John Wiley and Sons.
- Ching, J., Phoon, K.-K. and Hu, Y.-G. 2008. Efficient evaluation of reliability for slopes with circular slip surfaces using importance sampling. *ASCE Journal of Geotechnical Engineering*, 135(6), 768–777.
- Melchers, R.E. 1989. Importance sampling in structural systems. *Structural Safety*, 6, 3–10.
- Rosenblatt, M. 1952. Remarks on a multivariate transformation. *Ann. Math. Statist.*, 23, 470–472.
- Rubinstein, R.Y. 1981. *Simulation and the Monte-Carlo Method*, John Wiley & Sons Inc., New York.
- Shinozuka, M. 1983. Basic analysis of structural safety. *ASCE Journal of Structural Engineering*, 109, 721–740.

Spatial distributions of strength of an embankment based on synthesis of sounding tests and surface wave method

S. Nishimura, Y. Takayama & K. Fujisawa

Graduate School of Environmental Science, Okayama University, Japan

M. Suzuki

Institute of Technology, Shimizu Co., Koto-ku, Tokyo, Japan

A. Murakami

Graduate School of Agriculture, Kyoto University, Japan

1 INTRODUCTION

There are many earth-fill dams for farm ponds in Japan. Some of them are getting old and decrepit, and therefore, have weakened. The diagnosis of the embankments has been important to make the lifetime longer, and the investigation of the strength inside the embankment is required for the task. In this research, the spatial distributions of the strength parameters for the decrepit earth-fill dams are discussed, and the identification method of the distribution is proposed. Although, generally, the strength of the earth-fill is predicted from the standard penetration test (SPT) N-values, the Swedish weight sounding tests (SWS) are employed to obtain the spatial distribution of the N-values as the simpler method than SPT in this research. The SWS has the advantage to make the short interval exam possible, because of its simplicity. Furthermore, the results of surface wave investigation method are combined with the SWS results, and the synthesizing method of the two types of N-values is proposed based on the geostatistics herein.

Firstly, the statistical models of the N-values are determined from the SWS tests results. For this task, the MAIC (Minimizing Akaike's Information Criterion) method is employed (Akaike 1974), and the statistical model, which involves the mean function and the covariance function, is evaluated in an embankment. The spatial distributions of the N-values, can be identified based on the SWS test with high resolution, since the point estimations of the N-values are possible with the short testing intervals. However, the predicted N-values are supposed to involve great prediction errors at the parts, in which no point estimated data are included. To compensate this weak point, the surface wave method (SWM) is employed here, which is one of the geophysical exploration methods. By using the

method, the secondary wave (S-wave) distribution can be estimated easily as an averaged image in the wide area of a fill embankment, although the actual spatial fluctuations of the S-wave velocities are ignored throughout the inversion process. The S-wave has great correlations with the soil mechanical parameters, and is transformed into N-values in this research.

Secondly, two kinds of the N-value distributions derived from SWS and SWM are synthesized, and spatially interpolated with the indicator simulation, which is one of the geostatistical methods. In the method, the hard data (primary data) and the soft data (complementary data) can be used simultaneously. The SWS test and the SWM results are dealt as hard and soft indicator data, respectively. With synthesizing two kinds of data, the accurate spatial distribution of N-values is identified.

2 STATISTICAL MODEL OF N-VALUE

2.1 Determination method

The soil parameters that are obtained from the tests are defined here as $\Psi = (\Psi_1, \Psi_2, \dots, \Psi_M)$, where the symbol M signifies the number of test points. Vector Ψ is considered as a realization of the random vector $\psi = (\psi_1, \psi_2, \dots, \psi_M)$. If the variables $\psi_1, \psi_2, \dots, \psi_M$ constitute the M -variate normal distribution, the probability density function of ψ can be expressed as:

$$f_{\psi}(\psi) = (2\pi)^{-M/2} |C|^{-1/2} \exp \left\{ -\frac{1}{2} (\psi - \mu)^t C^{-1} (\psi - \mu) \right\} \quad (1)$$

By considering the logarithmic likelihood, Akaike's Information Criterion (AIC) is defined as

$$\begin{aligned}
AIC &= -2 \cdot \max \{ \ln f_{\Psi}(\Psi) \} + 2L \\
&= M \ln 2\pi + \min \left\{ \ln |C| + (\Psi - \mu)' C^{-1} (\Psi - \mu) \right\} + 2L
\end{aligned} \tag{2}$$

in which L is the number of unknown parameters included in the equation. These parameters are determined by numerically minimizing AIC (MAIC) for the unknown statistical variables included in Equation (2).

2.2 Relationship between SWS and SPT

Inada (1960) derived the relationship between results of SPT and SWS. Equation (3) shows the relationship for the sandy grounds.

$$N_{SWS} = 0.67 N_{SW} + 0.002 W_{SW} \tag{3}$$

in which N_{SWS} is N-value derived from SWS, N_{SW} is number of half rations, and W_{SW} is the total weight of loads. Considering the variability of the relationship, the SPT N-value is derived by

$$N_{SPT} = (1 + 0.354 \varepsilon_r) N_{SWS} \tag{4}$$

in which ε_r is $N(0,1)$ type reduced normal variables.

2.3 Statistical values of SWS N-values

The SWS tests were conducted at nine testing points with an the interval of 2 m. The mean function and covariance function of SWS N-value, N_{SWS} are determined with MAIC. The optimum mean and covariance functions are determined as Equations (5) and (6).

$$\mu = 1.98 + 0.816 \sin \left[\left(\frac{x}{5} - \frac{1}{2} \right) \pi \right] + 0.157z \tag{5}$$

$$\begin{aligned}
C_{ij} &= N_e \cdot \sigma^2 \exp \left(-|x_i - x_j| / 6.14 - |z_i - z_j| / 0.63 \right) \\
\begin{cases} N_e = 1 & (j = k) \\ N_e = 0.604 & (j \neq k) \end{cases} & \quad \sigma = 1.24
\end{aligned} \tag{6}$$

3 SYNTHESIS OF SWS AND SWM RESULTS

The surface wave has great correlation with the shear wave V_s , which has strong correlation with elastic modulus and N-values. In this research, the surface wave was measured in 40 m along the embankment axis with 2 m interval. The N-values are derived from the Equation (7) (Imai 1975).

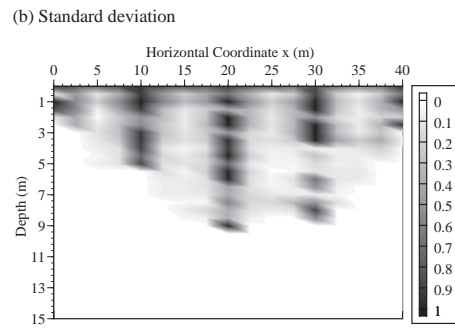
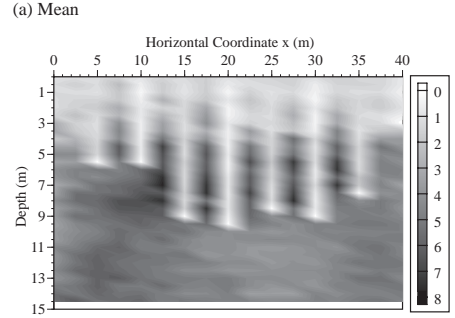
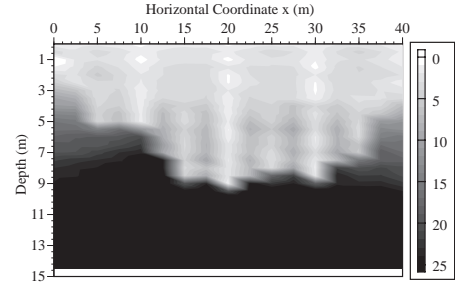


Figure 1. Spatial distribution of N-values. (Case of 9 points SWS with soft data.)

$$V_s = 89.8N^{0.341} \tag{7}$$

In this research, SWS and SWM results are considered as the hard and soft data, respectively, and then two results are synthesized with the indicator simulation method (Deutsch & Journel 1992). The synthesized results are shown in Figure 1. Since the mean and the standard deviation are strongly affected by the hard data, the periodic tendency is recognized in the mean, and the standard deviation is very small in the SWS measuring points. The probability that N-values are smaller than threshold value of 2.0, is great in the part where the mean value is small.

4 CONCLUSIONS

The results of SWS and SWM was synthesized conveniently by the indicator simulation method, which is one of geostatistical methods. The spatial distributions of the probability that the N-values are smaller than 2.0, which is essentially determined by the users, were estimated. The distributions can be referred for the decision making for the maintenance of embankments.

REFERENCES

- Akaike, H. 1974. A new look at the statistical model identification, *IEEE Trans. on Automatic Control*, AC-19(6): 716–723.
- Deutsch, C.V. and Journel, A.G. 1992. *Geostatistical Software Library and User's Guide*, Oxford University Press.
- Imai, T., Fumoto, H. and Yokota, K. 1975. Velocity of elastic wave and mechanical properties in Japanese grounds, *Proc. of 4th Symp. of Earthquake Eng.*: 89–96 (in Japanese).
- Inada, M. 1960. Usage of Swedish weight sounding results, *Geotechnical Engineering Magazine*, 8(1): 13–18 (in Japanese).

Evaluating model uncertainty of a CPT-based model for earthquake-induced soil liquefaction

Y.F. Lee

Department of Leisure Recreation and Travel Management, Toko University, Pu Tzu, Chiayi, Taiwan

Y.Y. Chi

Department of Land Management and Development, Chang Jung Christian University, Kway Jen, Tainan, Taiwan

C.H. Juang

Department of Civil Engineering, Clemson University, Clemson, SC, USA

ABSTRACT: The earthquake-induced liquefaction potential evaluation is one of the important topics in geotechnical engineering. In practice, the engineer most often employs simplified procedure to evaluate liquefaction potential of a soil. To account for uncertainties in the environmental parameters and model that are required in the calculation of soil liquefaction potential, the probabilistic approaches may be employed. Juang et al. (2006) suggested that this model uncertainty can be characterized with a single model bias factor (or model factor for short) that is applied to CRR (or the traditional “boundary curve” that separates liquefied cases from nonliquefied cases). Therefore, the F_s in a deterministic evaluation of liquefaction potential should be rewritten as:

$$F_s = c_1 \times \frac{CRR}{CSR} = c_1 \times \frac{f(\bar{x})}{f(\bar{y})} \quad (1)$$

where c_1 is the model factor of the adopted simplified model. However, the probability of liquefaction is calculated considering uncertainties of model and parameters by the Hasofer–Lind reliability index and the KCP (Lee et al., 2007).

In this paper a new CPT-based liquefaction triggering model (LTM) is arranged using field performance case histories of Moss et al. (2006). The model uncertainty, μ_{c_1} and $COV(c_1)$ of the LMT is determined by the sampling process taking proportional cases from the group of liquefied cases and the group of non-liquefied cases. The results of these analyses show that the μ_{c_1} value range from 0.79 to 0.85 and average value of $\mu_{c_1} = 0.81$; however, $COV(c_1)$ increases as the minimum percentage decreases. The largest variation can be extrapolated to be $COV(c_1) = 0.17$ where the sample size ranges from 0 to 100% of the database. In summary, the

process yields $\mu_{c_1} = 0.81$ and $COV(c_1) = 0.17$ for the LTM model.

Using the proposed LTM and the reliability index, the probability of liquefaction is calculated for case histories by the KCP (Lee et al., 2007). It is noted that the considering uncertainties of $COV(M_w)$, $COV(a_{max})$, $COV(\sigma_v)$, $COV(\sigma'_v)$, $COV(q_c)$, and $COV(R_f)$ is equal to 0.016, 0.162, 0.08, 0.08, 0.130, and 0.173, respectively. Under the environmental parameter uncertainty, there are two scenarios of $\mu(c_1)$ and $COV(c_1)$ in this paper. The first scenario of $\mu(c_1)$ and $COV(c_1)$ is equal to 1 and 0, respectively. That indicates only environmental parameters uncertainty is considered, the model uncertainty is not included. The first scenario is similar to Moss et al. (2006). The second scenario of $\mu(c_1)$ and $COV(c_1)$ is equal 0.81 and 0.17, respectively. As mentioned above, that

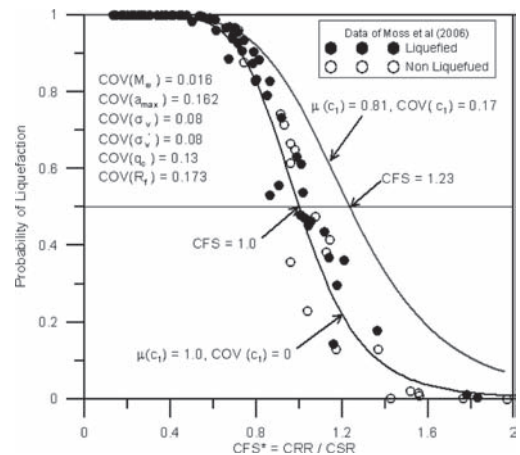


Figure 1. Regression results for two scenarios.

includes the results of the LTM model uncertainty analysis.

As shown Figure 1, the probability of liquefaction by Moss et al. (2006) are similar to the p_f under the first scenario curve, distinctly. The results verified the proposed LTM. It can be seen that the p_f by second scenario is higher than the p_f by the first scenario under the same CFS^* . In the same, the CFS^* by second scenario is higher than the CFS^* by the first scenario under the same p_f . For example, under $p_f = 0.5$, the CFS^* is equal to 1.23 and 1.0 for the second scenario and the first scenario, respectively.

The comparison of the results by Moss and results by the proposed model for the second

scenario is compared. During lower probability of liquefaction ($p_f \leq 30\%$), the probability by Moss is apparently less than the one by the proposed model considering model uncertainty. Near $p_f = 0.5$, the probability by the proposed model is close to the mean value of the results by Moss formula. On the contrary, the probability by Moss is apparently more than the one by the proposed model considering model uncertainty during $p_f \geq 80\%$. It is principally when evaluating probability of liquefaction that all (the model and parameter) uncertainty considered (as the second scenario) differs significantly from earlier and widely used only parameter uncertainty considered.

This page intentionally left blank

GS_312 — Reliability methods (1)

This page intentionally left blank

System reliability analysis of fatigue-induced, cascading failures using critical failure sequences identified by selective searching technique

Nolan Kurtz & Junho Song

University of Illinois at Urbana-Champaign, Urbana, IL, USA

Seung-Yong Ok

HanKyong National University, Anseong, Korea

Dong-Seok Kim

Interconstech, Inc., Seoul, Korea

Many structural systems are subjected to the risk of cascading system-level failures initiated by local failures. For efficient reliability analysis of such complex system problems, many research efforts have been made to identify critical failure sequences with significant likelihoods by an event-tree search coupled with system reliability analyses; however, this approach is time-consuming or intractable due to repeated calculations of the probabilities of innumerable failure modes, which often necessitates using heuristic assumptions or simplifications.

Recently, a decoupled approach was proposed by Kim (2009): critical failure modes are first identified in the space of random variables without system reliability analyses or an event-tree search. Then, an efficient system reliability analysis is performed to compute the system failure probability based on the identified modes. In order to identify critical failure modes in the decreasing order of their relative contributions to the system failure probability, a simulation-based selective searching technique was developed by use of a genetic algorithm as shown in Figure 1.

Points are randomly generated on the surface of a hypersphere with given radius. Each point's coordinates represent given values of the random variables once transformed into the standard normal uncorrelated space of random variables. These points were then treated as chromosomes and the points corresponding to system failures were treated as "elite" for the "mating pool." The genetic operator of crossover was used to search in the vicinity around the original failure modes. Then, the genetic operator of mutation was used to search far from these original failure modes. The system failure probability was then computed by a multi-scale system reliability method that

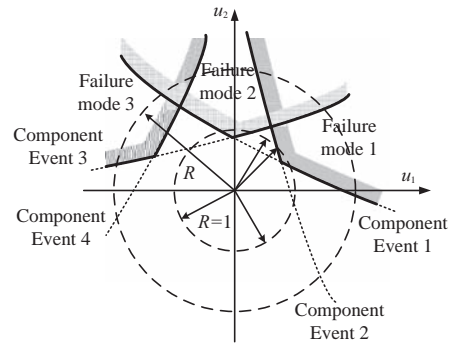


Figure 1. Three failure modes in the two-dimensional standard normal space.

can account for statistical dependence among the component events as well as among the identified failure modes.

This paper presents this decoupled approach in detail and demonstrates its applicability to complex bridge structural systems that are subjected to the risk of cascading failures induced by fatigue. Using a recursive formulation for describing limit-states of local fatigue cracking, the system failure event was described as a disjoint cut-set event (Lee & Song 2010). For example, the system failure event caused by the failure sequence $\{1 \rightarrow 2 \rightarrow \dots \rightarrow i\}$ for a given outcome $\mathbf{X} = \mathbf{x}$ is described by

$$\left[\bigcap_{\forall j \neq 1} (T_1^0 < T_j^0) \right] \cap \left[\bigcap_{\forall k \neq 1,2} (T_2^1 < T_k^1) \right] \cap \dots \cap \left[\bigcap_{\forall l \neq 1, \dots, i} (T_i^{1, \dots, (i-1)} < T_l^{1, \dots, (i-1)}) \right] \cap (T_1^0 + T_2^1 + \dots + T_i^{1, \dots, (i-1)} < T_{ins}^0) \quad (1)$$

where $T_i^{1, \dots, i-1}$ is the time until the i -th component fails after the sequence of local failures $\{1 \rightarrow 2 \rightarrow \dots \rightarrow (i-1)\}$ occurs and T_{ins} is the inspection cycle time. For all terms but the last term, the times at each step in the failure sequence were compared to assure that no other member failed earlier than the member of concern, guaranteeing a disjoint cut-set event. For example, if T_5^0 is smaller than $T_i^0, \forall i \neq 5$, and T_3^5 is smaller than $T_j^5, \forall j \neq 5, 3$, the failure sequence can be expressed as $\{5 \rightarrow 3\}$, the T_i^0 intersections guarantee member 5 fails first and the T_j^5 intersections guarantee member 3 fails second. The last intersection term guarantees that all members fail before the inspection cycle time.

These time terms can be obtained using fatigue crack growth models. For this application, the Paris-Erdogan crack growth model is used in conjunction with Newman's approximation of the stress intensity factor. If one integrates the Paris-Erdogan equation over the range of crack length values, one can find the time for particular member to fail for a given state of far-field stress range, i.e.

$$T_i^{1, \dots, i-1} = \frac{1}{C v_0 (S_i^{1, \dots, i-1})^m} \int_{a_i^0}^{a_{ci}} \frac{da}{[Y(a)\sqrt{\pi a}]^m} - \sum_{k=1}^{i-1} \left(\frac{S_k^{1, \dots, k-1}}{S_i^{1, \dots, i-1}} \right)^m T_k^{1, \dots, k-1} \quad (2)$$

where $S_i^{1, \dots, i-1}$ is the far-field stress range after the sequence of local, member failures $\{1 \rightarrow 2 \rightarrow \dots \rightarrow (i-1)\}$ has occurred, and $T_i^{1, \dots, i-1}$ is the time taken for the i -th member to fail given that the sequence of members failures $\{1 \rightarrow 2 \rightarrow \dots \rightarrow (i-1)\}$ has occurred, $Y(a)$ is the geometry function from Newman's approximation, a_{ci} is the critical crack length of the i -th member that leads to crack failure; a_i^0 is the initial crack length of the i -th members given that no members have failed, and C and m are the material parameters from the Paris-Erdogan equation, and v_0 is the annual frequency of loadings. All of these *sequential* system level failures were characterized by four criteria: local instability, global instability, excessively large values of the condition number of the global stiffness matrix, and excessive deflections at any given node.

These critical cut-sets, i.e. failure sequences with significant likelihood are identified by the selective searching technique using a genetic algorithm. Then, the probabilities of the cut-sets are computed by use of a sampling method. In this example, crude Monte Carlo Simulations (MCS) were used to tally the number of times a given system event occurred and then simply divided by the total number of samples to obtain estimates of the critical cut-set

probabilities. Crude MCS was used as opposed to more efficient methods to obtain estimates of individual component events in the disjoint cut-set formulation such as the first- or second-order reliability method (FORM or SORM) due to high nonlinearity in the limit state functions, preventing FORM and SORM from obtaining accurate estimates of the component probabilities for the individual events in Equation 1. Since these cut-sets are mutually exclusive, the lower-bound on the system cascading failure probability is then obtained by a simple addition of the probabilities of the identified cut-sets.

A numerical example of a bridge structure demonstrates that the proposed search method skillfully identifies dominant failure modes contributing most to the system failure probability, and the system reliability analysis method accurately evaluates the system failure probability with statistical dependence fully considered. An example bridge with 97 truss elements (see Figure 2) is considered to investigate the applicability of the method to realistic large-size structures.

Each bridge member was said to have three random variables: two material parameters C and m defined as lognormal, and an initial uncertain crack length a_i^0 defined as exponential. In addition to the 291 random variables, there was a stress range multiplier used to characterize randomness in the traffic loading that was defined as normal. The method identified 63 significant failure modes with similar reliability indices due to the high degree of redundancy and symmetry present in the system. All failure modes originate from the central 4 diagonals of the suspended truss. The nature of these "competing" failure modes made it necessary to identify 63 modes. Brute-force MCS, where many samples, \mathbf{x} , are repeatedly generated and checked whether or not a system failure has occurred within the inspection cycle time, with a c.o.v. of 3.4%, were then used to find an error of only 4.220%.

In this paper, an efficient and accurate method to identify dominant failure modes of a structural system subjected to the risk of fatigue-induced cascading failures and compute the over system and failure mode event probabilities was developed.

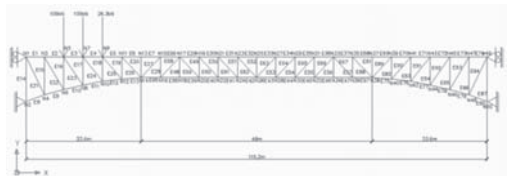


Figure 2. Truss bridge example.

Using the selective searching algorithm, dominant failure mode identification and system reliability analysis are decoupled, leading to lower computational costs. These dominant failure modes were formulated as disjoint cut-sets, permitting a simple summation of their probabilities for the overall system failure probability. The proposed method was applied to a 97 member planar-truss numerical example to show that it can compute the system failure probability accurately and efficiently.

REFERENCES

- Kim, D.-S. 2009. *Matrix-based System Reliability Analysis Using the Dominant Failure Mode Search Method*. Dept. of Civil and Environmental Engineering, Seoul National University, Seoul, Korea.
- Lee, Y.-J. & Song, J. 2010. Identification of critical sequences of fatigue-induced failures by branch-and-bound method employing system reliability bounds, *Proc. of AIAA SDM Conference*, April 12–15, Orlando, FL, USA.

Estimation of failure rates of crude product pipelines

Alex. W. Dawotola & P.H.A.J.M. van Gelder

Hydraulic Engineering Section, Delft University of Technology, Delft, The Netherlands

J.J. Charima

Operations Department, Nigerian National Petroleum Company, Abuja, Nigeria

J.K. Vrijling

Hydraulic Engineering Section, Delft University of Technology, Delft, The Netherlands

Pipelines are generally safe medium of transporting petroleum products from one part of the country to another. Majority of oil exploration and production companies rely on pipelines in transporting crude oil from rig to refinery, and from refinery to oil depot. Despite their relatively low failure probability, pipeline failures do occur. Failure of pipeline can be very disastrous, often carrying huge financial, life and environmental consequences. Risk safety assessment of pipelines is therefore a topic of prime interest to both regulators and operating companies.

Furthermore, in the research environment, the development of effective failure prediction models for oil pipelines continues to be a very active research area (Oke *et al.*, 2003). Many approaches have been presented to study the rate of occurrence of failures of operating pipelines depending on their types, and the trend of failures recorded. The times between failures could be independent or identical, with either a spontaneous or time dependent failure distribution. Pipelines are repairable systems, in general. That is, they can be restored or repaired after failure. Therefore, statistical methods for the reliability of repairable systems can be applied to model their failures (Rigdon and Basu 2000).

A number of researchers have worked on risk assessment and reliability of pipelines using different approaches. (Muhlbauer 2003) developed a qualitative index to rank pipelines based on level of risk. Semi quantitative methods such as Analytical hierarchy process (AHP) (Dey *et al.*, 2004 and Al-Khalil *et al.*, 2005) and AHP-FTA (Dawotola *et al.*, 2009) have been applied to subjectively estimate pipeline failures and provide risk management framework for operating pipelines. (Cagno 2000 & 2003) have utilized AHP as an elicitation method of expert opinion to obtain a priori distribution of failures of pipelines. The expert result was further combined with historical data of failures by Bayesian analysis. Probabilistic approaches, using

limit state models (Ahammed and Melchers 1997 & Caleyo *et al.*, 2002) have been applied with some success. Statistical approaches such as the work of (Sosa and Alvarez-Ramirez 2009) have studied the time distribution of hazardous materials pipeline incidents. Failures of both low and high severity index were analyzed using historical data obtained from the office of pipeline safety (OPS) of the US department of transport. Similarly, (Fa-si-oen and Pievatolo 2000) presents the analysis of 6-year ruptures incident in a metropolitan gas network using both HPP and power law process. Statistical analysis based on historical failures data can be particularly suitable to model pipeline failures owing to the use of real data.

In this paper, statistical methods for the reliability of repairable systems have been applied to provide an estimate for the failure rate of cross-country crude product pipelines based on historical failures. The pipelines are assumed to follow minimal repair models, and the failure data are tested against the homogenous Poisson process (HPP) and the non-homogenous Poisson process (NHPP). Two statistical tests, Laplace test and the MIL-HDBK 189 are used to test the null hypothesis that the process is an HPP against the alternative that the intensity is increasing, following a NHPP.

A case study is presented to illustrate the application of the proposed methodology. The studied data is obtained from the Nigerian National Petroleum Company (NNPC) and comprise three different API 5L X42 pipelines. The number of failures of the pipelines due to corrosion from 1999 to 2009 was collected.

The pipelines are assumed to follow minimal repair models. Trend test is applied to test whether HPP or NHPP is a suitable model to describe the failure records. The statistical tests conducted reveal that HPP is an acceptable model that describes the number of corrossions that occur in onshore crude product pipelines. The intensity

function (failure rate) and the Mean Time Between Failures (MTBF) of the pipelines are determined to study the dynamics of failures between pipelines installed at different periods.

The failure rate is obtained by multiplying the length of pipeline (km) by the computed λ . The result indicate that PPL2 pipeline exhibit the least MTBF which indicates that its propensity to failure is the highest among the three pipelines. PPL1 pipeline' propensity to failure is least among the three pipelines. Fig. 1 to Fig. 3 represent the plot of failure rate against time of operation in years.

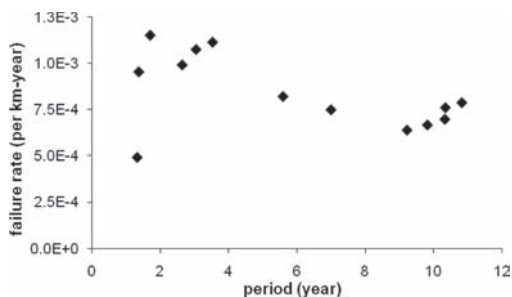


Figure 1. Failure rate against years of operation (1999 to 2009) for PPL1.

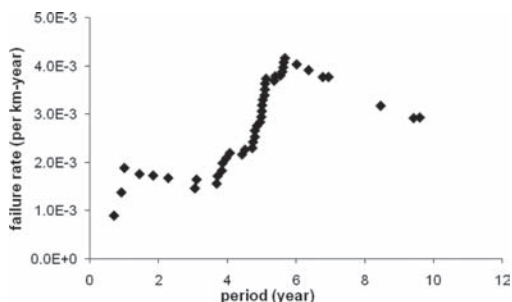


Figure 2. Failure rate against years of operation (1999 to 2009) for PPL2.

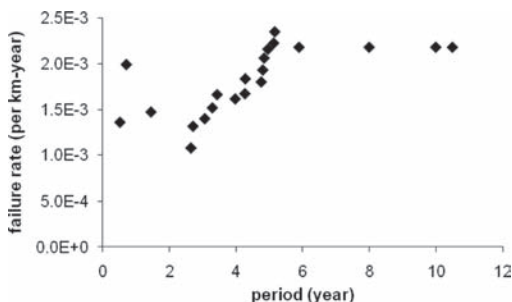


Figure 3. Failure rate against years of operation (1999 to 2009) for PPL3.

The plots indicate that there is little change in failure rate over 11 year period for each pipeline. This is consistent with the assumption of HPP. However, some variations can be seen in the plot for PPL1 this is due to the sudden jump in failure rates in the first 3 years from (1999 to 2002). PPL2 and PPL3 exhibit a similar trend in failure rate. The similarity is also observed in their MTBF and failure rate recorded in Table 3.

In conclusion, by carrying out a test of hypothesis, the research shows that the dynamics of corrosion incident can be described by Homogenous Poisson process. In addition, the analysis of the rate of failure shows that the curve of pipelines' rate of failure follows a similar trend for pipelines having relatively equal installation date.

The major contribution of the work is that it is can be used in making integrity maintenance decisions. Based on the calculated MTBF and failure rates, maintenance managers could be in the position to decide on most appropriate framework for maintainability (including design, redesign, construction, monitoring, inspection, maintenance, reconstruction and demolition) of crude product pipelines.

Future plans for the current work include development of a maintenance optimisation approach for the application of the failure rates to minimise pipeline risks. This will address such issues as suitability of HPP or NHPP for corrosion modelling, calculation of failure rates for different corrosion types, and using acceptable risk to determine optimum maintenance management framework for the pipelines.

REFERENCES

- Ahamed, M. & Melchers, R.E. 1997. Probabilistic analysis of underground pipelines subject to combined stresses and corrosion, *Eng Struct* 19(12), pp. 988–994.
- Al-Khalil, M., Assaf, S. & Al-Anazi, F. 2005. Risk-based maintenance planning of cross-country pipelines, *J of Performance of Constructed Facilities*. Vol. 19 No. 2 pp. 124–131.
- Cagno, E., Caron, F., Mancini, M. & Ruggeri, F. 2000. Using AHP in determining the prior distributions on gas pipeline failures in a robust Bayesian approach. *Reliab Eng Syst Safety*; 67: pp. 275–284.
- Cagno, E., Caron, F., Mancini, M., Pievatolo, M. & Ruggeri, F. 2003. Bayesian assessment of corrosion-related failures in steel pipelines, in *Safety and Reliability*, Bedford, T. & van Gelder, P.H.A.J.M. (eds.), Vol. 1, Balkema Pub., Lisse, The Netherlands.
- Caleyo, F., González, J.L. & Hallen, J.M. 2002. A study of the reliability assessment methodology for pipelines with active corrosion defects, *Int J Pressure Vessels Piping* 79, pp. 77–86.

- Dawotola, A.W., van Gelder, P.H.A.J.M. & Vrijling, J.K. 1999. Risk assessment of petroleum pipelines using a combined analytical hierarchy process-fault tree analysis (AHP-FTA). In proc., 7th Int. Prob. Work., Delft, Netherlands.
- Department of Defense, U.S.A. 1981. MIL-HDBK-189: Reliability Growth Management.
- Dey, P.K., Ogunlana, S.O. & Naksuksakul, S. 2004. Risk-based maintenance model for offshore oil and gas pipelines: a case study, *Journal of Quality in Maintenance Engineering*, Vol. 10 Number 3, pp. 169–183.
- Fa-si-oen, V. & Pievatol, A. 2000. The analysis of ruptures in metropolitan gas pipelines, *Qual. Reliab. Engng. Int.* 16, 17–22.
- Muhlbauer, W.K. 2003. Pipeline Risk Management Manual, third ed., Gulf Publishing.
- Oke, A., Mahgerefteh, H., Economou, I.G. & Rykov, Y. 2003. A transient outflow model for pipeline puncture, *Chem., Eng Sc.* 58 (2003) (20), p. 4591.
- Rigdon, S.E. & Basu, A.P. 2000. *Statistical Methods for the Reliability of Repairable Systems*, Wiley, New York.
- Sosa, E. & Alvarez-Ramirez, J. 2009. Time-correlations in the dynamics of hazardous material pipelines incidents, *J. Hazard. Mater.* 165, pp. 1204–1209.

Reliability analysis with probabilistic and interval variables

Kais Zaman, Mark McDonald, Sirisha Rangavajhala & Sankaran Mahadevan
Vanderbilt University, Nashville, TN, USA

Two forms of uncertainty are commonly considered in the literature—aleatory and epistemic. Aleatory uncertainty is typically irreducible; examples include inherent variations in physical processes, such as weather conditions. Epistemic uncertainty represents a lack of knowledge about the system due to limited data, measurement limitations, or simplified approximations in modeling system behavior. This type of uncertainty can be typically reduced by gathering more information. In some cases, the distribution for the input variable must be determined from imprecisely available data, such as intervals [1, 2]. Aleatory uncertainty is effectively handled by probabilistic analysis, whereas problems with interval uncertainty or a mixture of both aleatory and interval uncertainty have been handled by non-probabilistic methods [1, 3, and 5]. This paper develops and illustrates a probabilistic approach for uncertainty representation and propagation in reliability analysis, when the information on the uncertain input variables and/or their distribution parameters may be available either as probability distributions or simply intervals. Such an approach has the advantage of avoiding nested computation that results from handling probabilistic and interval variables separately. The issue of information addition/loss is handled through the use of a flexible family of distributions to represent the interval variables.

A unique aggregation technique is used to combine multiple interval data and to compute rigorous bounds on the system response CDF. The uncertainty described by interval data is represented through a flexible family of probability distributions. Conversion of interval data to a probabilistic format enables the use of computationally efficient methods for probabilistic uncertainty propagation. Two methods are explored for the implementation of the proposed approach, based on: (1) sampling and (2) optimization. The sampling based strategy

is more expensive and tends to underestimate the output bounds. The optimization based methodology improves both aspects, and estimates the distribution parameters of the input variables that minimize or maximize an output metric of interest, e.g., probability of failure or expectation of system response. We propose two types of optimization—percentile-based and expectation-based. The proposed methods are used to develop new solutions to challenge problems posed by the Sandia Epistemic Uncertainty Workshop [4]. Results for the challenge problems are compared with earlier solutions.

REFERENCES

- [1] Du, X., Sudjianto, A. & Huang, B. 2005 “Reliability based design with mixture of random and interval variables”, *Journal of Mechanical Design*, 127, pp. 1068–1076.
- [2] Ferson, S., Kreinovich, V., Hajagos, J., Oberkampf, W. & Ginzburg, L. *Experimental Uncertainty Estimation and Statistics for Data Having Interval Uncertainty*. Sandia National Laboratories Technical report SAND2007-0939, Albuquerque, New Mexico, 2007.
- [3] Mourelatos, Z.P. & Zhou, J. 2006. *A Design Optimization Method Using Evidence Theory*, *Journal of Mechanical Design*, ASME, 128(4), pp. 901–908.
- [4] Oberkampf, W.L., Helton, J.C., Joslyn, C.A., Wojtkiewicz, S.F. & Ferson, S. *Challenge Problems: uncertainty in system response given uncertain parameters*, *Reliability Engineering and System Safety*, 85 (2004) 11–19.
- [5] Rao, S.S. & Annamdas, K.K. 2009, *An Evidence-Based Fuzzy Approach for the Safety Analysis of Uncertain Systems*, *50th AIAA/ASME/ASCE/AHS/ASC Structures, Structural Dynamics, and Materials Conference*, Palm Springs, California, Paper number AIAA-2009-2263.

Dormant reliability analysis for dam spillways

M. Kalantarnia & L. Chouinard

McGill University, Montreal, Quebec, Canada

S. Foltz

U.S. Army Corps of Engineers, Champaign, IL, USA

ABSTRACT: Maintaining the safety of aging infrastructure is a major concern of owners and operators. Dams are no exception to this dilemma. Spillway gate systems are among the most critical for maintaining the safety of a dam and require assessments of both equipment and operational failure modes. Safety can be ensured by conducting regular inspections and tests of the facilities, by assessing the performance level of the various components and implementing a regular maintenance program. These tasks can be optimized by performing risk analyses and by identifying the components that are most critical to the operation of the facility.

The first part of this paper reviews these methodologies and their advantages and limitations. The approaches discussed herein may be summarized as:

1. Failure Mode, Effect and Criticality Analysis (FMECA): FMECA is a basic tool to evaluate the system design at the initial stage from a reliability aspect. In other words, it evaluates the need for and the effects of design change.
2. Fault Tree Analysis (FTA): Fault tree analysis is a deductive graphical design technique which is structured in terms of events rather than components. This approach identifies ways in which hazards may lead to accidents. The goal of using fault tree analysis for dam gates is to define a highly detailed representation of the fault environment so that the user can rapidly eliminate or accept branches on the basis of pre-screening and background knowledge of the specific dam project.
3. Indexing Approach (CI): A CI is a numerical rating, ranging from 0–100, that describes the condition of a structure at a specific point in time based on a series of observations by an inspector. Reliability of a spillway system may be determined over time by considering CI as a random variable. When an inspector assigns a condition state, it is assumed that the mean value of the CI is at the center of the range when

the condition state is first identified. As time goes by, the mean value will shift toward the lower end of the condition state. The structure will remain in the condition state until an inspection reveals that the component has deteriorated enough to transit to a lower condition state.

Although extensive work has been done in this area, little attention has been given to the dormant condition of the spillway gates. The second part of this paper addresses the dormancy issue of spillway gates by incorporating the effect of the dormancy period in the currently existing reliability and risk assessment approaches. Finally, the paper concludes by presenting a brief case study on a vertical gate to demonstrate the applicability of this approach.

Many components spend a portion of their serviceable life in a non-operating state. This state in which a system experiences little or no operational stress is defined as Dormancy. Reliability of such systems varies greatly between a dormant and active state. Although a dormant system is under less operational stress, dormant reliability is considered as important as active reliability and can sometimes become very complicated as failure in dormant state will not be identified until the system is re-activated.

Spillways are a good example of a dormant system as they spend most of their service life in dormancy and are activated occasionally either for normal use or periodic tests. Spillway gates are mainly used in emergency situations to discharge excess water from the reservoir. Failure to open the gate when required may lead to overtopping of the dam and possible dam breach. Therefore, determining the dormant reliability of such systems is critical. The second part of this paper will focus on introducing dormancy into existing methodologies to better represent the functionality of a spillway gate system. The application of this approach is finally demonstrated for a simple case study with a vertical gate.

Approaches which may be used to evaluate the performance of a dormant system are:

1. Markov Chain Analysis: This method is generally used to determine the reliability of a system as it transits between several states. The main application of this method is to model the behavior of stand-by/redundant systems or systems undergoing deterioration.
2. Dormant Availability Analysis: Availability is defined as the probability that a system performs as required at a specific point in time or over a period of time. Assuming idealized repairing conditions (system is restored to as good as new conditions after repair) availability of a dormant system with a dormant period of T , reliability of $R(T)$, inspection time of t_1 and repair time of t_2 may be written as:

$$A(T) = \frac{\int_0^T R(T) dt}{T + t_1 + t_2 [1 - R(T)]} \quad (1)$$

Using the equation above, the availability of a dormant system may be determined as a function of the dormant period.

The new approach discussed herein incorporates the availability analysis and the condition indexing approach. To best represent a dormant

system, the availability model will demonstrate the deterioration mechanism which occurs under dormancy while the condition index updates which are the results of periodic inspections of the system will improve the model after the end of each dormant period.

In other words, the availability analysis will model the behavior of the system under dormancy. After each inspection new data is obtained which may determine that the system is either functioning as expected by the model or deteriorating faster/slower than assumed. By integrating this data, the model will represent the behavior of the system more accurately.

A case study on a spillway system with a vertical gate discussed in the paper demonstrates the applications of this approach.

This study presents an approach to account for dormancy of spillways in a combination of 2 already existing methodologies which determine the availability of the dormant system given periodic inspection. Inspection data are used as inputs to improve the predictive abilities of the model. This new model has the advantage of accounting for the dormancy of a system while continuously updating itself from the scheduled inspections. An optimum inspection schedule may be determined by extending the results of this study to different dormancy periods.

On the utilization of monitoring data in an ultimate limit state reliability analysis

S. Thöns

Division VII.2 Buildings and Structures, BAM Federal Institute for Materials Research and Testing, Berlin, Germany
Institute of Structural Engineering, ETH Zurich, Switzerland

M.H. Faber

Institute of Structural Engineering, ETH Zurich, Switzerland

W. Rücker

Division VII.2 Buildings and Structures, BAM Federal Institute for Materials Research and Testing, Berlin, Germany

ABSTRACT: A current research challenge is the application of monitoring data for a reliability analysis in various fields of engineering (see e.g. Enright, Hudak et al. (2006), Liu, Frangopol et al. (2010) and Thöns, Faber et al. (2008)). An approach for the determination of uncertainties associated with monitoring data has been introduced in Thöns, De Sanctis et al. (2010) building upon two existing frameworks: The framework for the determination of measurement uncertainties based on ISO/IEC Guide 98-3 (2008) and the structural reliability analysis framework of the Joint Committee on Structural Safety (JCSS).

The basic formulation for the determination of measurement uncertainties represents the measurement equation which yields the measurand. For strain measurements with a strain gauge, which is a widely applied measurement technique, the measurand constitutes the mechanical strain. The mechanical strain is defined as the sum of the amplifier strain and the apparent strain.

Based upon the physical properties of the measurement process, physical equations are derived for the mechanical strain and the apparent strain. These process equations model the electrical measurement process with the strain gauge sensor and the amplifier. With probabilistic models for the associated random variables, the measurement uncertainty can be derived. The probabilistic models for the strain gauge and the amplifier take basis in product specification data, in specific guidelines and in the scientific literature. It is very important to note at this point, that the product information is usually valid for all strain gauges of the same type, all amplifiers of the same type and for all surrounding and application conditions

as documented in the manufacturer specifications according to standardized rules.

The observation based measurement uncertainty takes basis in the measurement equation and in observations of the measurement process. These observations are used for the determination of probabilistic models for the amplifier strain and the apparent strain applying the method of the maximum likelihood. An important point is that the measurement uncertainty obtained by observations has different boundary conditions associated with the probabilistic models. In contrast to the process equation based measurement uncertainty, the observation based measurement uncertainty applies to the utilized type of the sensor, the amplifier and to the specific application and surrounding conditions.

Based on the specific boundaries of both methods for the determination of measurement uncertainties the concept of the posterior measurement uncertainty is summarized (as introduced in Thöns, De Sanctis et al. (2010)). The posterior measurement uncertainty is based upon Bayesian updating and utilizes all available information and data, i.e. informative distributions for the prior and the likelihood. The process equation based measurement uncertainty is seen as the accumulation of the prior knowledge of the measurement process and therefore constitutes the prior measurement uncertainty. The measurement uncertainty derived from observations, constitutes the likelihood of the measurement uncertainty, i.e. the distribution of the observations given the prior knowledge. It is derived for the specific measurement application and surrounding conditions.

The framework for the determination of measurement uncertainties as introduced is applied for the utilization of monitoring data in the structural reliability analysis. The consideration of monitoring data as loading model information is discussed on the basis of an example. The example regards the ultimate limit state taking basis in the buckling reliability model. The structural reliability is calculated based upon design information and based upon monitoring information with strain gauges. For this example the probabilistic models are adjusted to account for the comparability of the design and monitoring structural reliability. With this example it is shown that the probability of failure can be reduced when monitoring data are utilized. The difference of the probability of failure is caused by the different probabilistic models. The design case involves a more complex structural model which results due to the model uncertainties in higher uncertainties of the loading than for the case where monitoring data and models are applied, despite the additional measurement uncertainties.

An alternative approach for the utilization of monitoring data in the reliability analysis is to consider monitoring data as resistance model information, i.e. as proof loading information. A new proof loading concept is introduced starting with a discussion of previous approaches and the characteristics of proof loading. Consecutive to the introduction of the concept it is applied to the introduced example and the influence of proof loading information on the probability of failure is quantified with parameter study. These results can serve as an orientation which loading event can be utilized as a proof loading event.

Most significant is the starting point of this paper as it contains the approach that the

application of monitoring data for a structural reliability analysis is subjected to measurement uncertainties. Monitoring data can then be utilized to update the loading or the resistance models. For both approaches it is shown that the specific modeling in a reliability analysis can result in a reduction of uncertainties and as a consequence in the reduction of the probability of failure.

The probabilistic models are consistent with the detailed and stringent modeling of the Probabilistic Model Code (JCSS (2006)). Herewith, the common association that monitoring procedures possess low uncertainties, can be modeled with the developed approaches. However, the effect of the reduced probabilities of failure depends on the specific probabilistic model uncertainties models and the measurement uncertainty.

The determination of the measurement uncertainty should integrally utilize the observations and the process equation of the measurement process. This constitutes the essence of the framework for the determination of the measurement uncertainty. Furthermore, the specific challenge of the dependency of the probabilistic model on the measurement datum, which itself represents a realization of a random process, is solved by explicitly accounting for the assignment uncertainty.

The introduced approaches and findings can be utilized for the assessment of structures in combination with monitoring aiming at life cycle extension. Furthermore the quantification of the measurement uncertainties facilitates the design of monitoring systems for improving the structural performance.

This page intentionally left blank

GS_322 — Reliability methods (2)

This page intentionally left blank

Identification of random variables via Markov Chain Monte Carlo: Benefits on reliability analysis

F. Lanata & F. Schoefs

GeM, Institute for Research in Civil and Mechanical Engineering, UMR CNRS 6183, University of Nantes, France

1 INTRODUCTION

The evaluation of failure probability in structural engineering is strongly dependent on the quantification of uncertainties associated with mechanical and model parameters. The uncertainties analysis can take advantage from the long-term monitoring of structural response that has shown to be the only way to understand complex interaction mechanisms and in-service structural behaviour, in particular when old designed structures need the definition of a new safety level due to the continuous evolution in loads and changes of environmental actions. Nowadays, the number of continuously monitored structures is increasing but the way to include this valuable information in a reliability analysis is not clear yet. Therefore, monitoring information is hardly used to improve the knowledge of involved parameters. Structural monitoring gives information on response quantities (displacements, strains, etc.) and not on input parameters of the structural model. Generally, an inverse analysis has to be performed to get the model parameters and/or the variables of interest from measurements (Schoefs et al., 2011). Uncertainties can be taken into account by considering the obtained parameters as random variables.

As for the long-term monitoring of a pile-supported wharf in the Great Maritime Port of Nantes-Saint Nazaire in France (see full article for details), a procedure of parameter identification has to be constructed when a limited number of data is available. This article proposes a Bayesian framework, based on the Markov Chain Monte Carlo (MCMC) approach, to introduce model uncertainties in the identification process when monitoring data are available (Ghanem & Doostan 2006). The prior densities of the model's parameters (called hyper-parameters in the following) are assessed from the available simulated measurements. The posterior densities are generated using a cascade Metropolis-Hastings algorithm. They are finally propagated through the model to obtain the probability density function of the mechanical parameter of interest.

The capability in evaluating the failure probability of the structure has been checked by comparing the obtained prediction density with the real simulated probability density function of a simple random parameter whose probabilistic structure was known.

2 NUMERICAL SIMULATION

The purpose of the numerical simulation is the evaluation of the algorithm convergence as a function of the number N of available observations and of the length M of the generated chains on the model's parameters. Due to the interest in characterizing extreme values of the random variable for a further failure probability analysis, the comparison between the true probability density function of the random variable $k(\omega)$ and the generated predictive one has been performed using a parameter representative of the distribution tails.

2.1 True population and sampling

The true distribution function of the random variable $k(\omega)$ has been generated by simulating 20,000 samples from a beta distribution of parameters $(\alpha, \beta) = (5, 2)$. The beta distribution has been chosen because it is particularly adaptable to represent a group of density functions simply adjusting the parameters. Moreover, its support is bounded (here between 0 and 1) and is suitable to represent physical processes. Five samples of reduced size have been randomly extracted from the true population to verify the accuracy of the proposed method for various values of N (in this article 20, 40, 60, 80 and 100). The real values of the parameters are always contained in the estimated confidence intervals due to the great uncertainty in the parameters even when the variance is reduced as larger samples are considered.

2.2 Metropolis-Hastings on sampled data

The best fitting of extracted samples being the beta distribution, the vector of the hyper-parameters

is constituted by the two parameters of the beta distribution, α and β . A normal prior distribution conditioned to the observations has been assumed for both parameters and it has been used as transition probability to generate a new state of the chain. The transition distribution has been inferiorly limited to 0 because the parameters can assume only positive values. Two independent Markov chains have been generated using the MCMC algorithm detailed in the full article. The final acceptance rate assessed from a 5000-sample Markov chain is around 50–55%. A 20,000-sample Markov chain has been also tested. The estimated values of the parameters are very close to the ones estimated from the 5000-sample chain, so to conclude that the shorter chain has already reached the stationary convergence to the posterior distribution (Perrin & Sudret 2008).

The generated posterior density functions of the hyper-parameters are close to the prior ones with a variance reduced by a factor 2 due to the increased number of samples. The parameters α have a greater influence on the uncertainties of the predictive probability density of the random variable $k(\omega)$.

3 RESULTS AND CONCLUSIONS

Each couple of parameters α and β from the two generated chains has been used to assess the predictive probability density function of the random variable under study. The collection of all these distributions has given an envelope of the final probability density function incorporating the uncertainty in its parameters. Figure 1 shows an example of the envelope in terms of cumulative density functions. A larger scatter is visible when few observations are available making impossible any consideration about the real distribution function (in dashed black). It has been shown in the full article that the choice of the prior information on the final estimation of the real distribution has gradually less influence on the results as the number of observations increases.

In view of a reliability analysis, the comparison has been further detailed and focused on the distribution tails. The critical value of the random variable k_{lim} associated to an assigned failure probability has been evaluated from the real population through the cumulative density function. This critical value has been then used to assess the failure probability for each distribution function obtained with the random parameters of the beta distribution.

Some reasonable values of the failure probability have been chosen, far from the probability of collapse for a civil structure but close to Service Limit States target probabilities. Thus, they are small enough to evaluate the reliability of the proposed procedure in

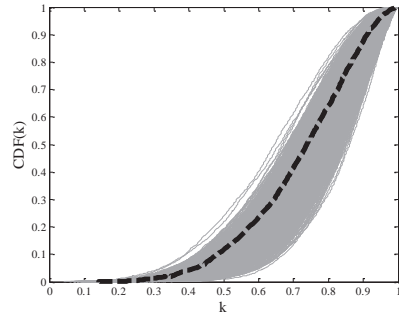


Figure 1. True population cumulative density function (dashed black) and cumulative density functions (continuous gray) assessed through the MCMC of α and β with a normal prior distribution ($N = 100$).

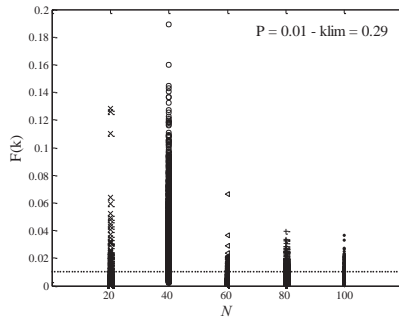


Figure 2. Failure probability for the true population (dotted line) and for the distributions assessed through the MCMC of α and β with a normal prior distribution as a function of observations N .

function of the number of available observations. Figure 2 shows the results associated to a failure probability of 1%. The introduction of model's uncertainties can strongly influence the results when only limited number of data is available. The method can only be taken into consideration starting with a number of measurements around 100.

REFERENCES

Ghanem, R.G. & Doostan, A. 2006. On the construction and analysis of stochastic models: characterization and propagation of the errors associated with limited data. *Computational Physics* 217: 63–81.

Perrin, F. & Sudret, B. 2008. Prise en compte des données expérimentales dans un modèle probabiliste de propagation de fissure. *Journées Fiabilité des Matériaux et des Structures: Proc. JFMS08*, Nantes, 26–28 March 2008.

Schoefs, F., Yañez-Godoy, H. & Lanata, F. 2011. Polynomial chaos representation for identification of mechanical characteristics of instrumented structures. *Computer-Aided Civil and Infrastructure Engineering* 26: 173–189.

Risk quantification of fatigue-induced sequential failures by Branch-and-Bound method employing system reliability bounds

Y.-J. Lee & J. Song

University of Illinois at Urbana-Champaign, Urbana, IL, USA

1 INTRODUCTION

Various structural systems are often subjected to the risk of fatigue-induced failures caused by repeated loading during their service (Karamchandani *et al.*, 1992). In order to quantify such risk, a new Branch-and-Bound method employing system reliability Bounds (termed the B³ method) has been proposed (Lee & Song 2010a, b). The method enables us to estimate the system risk and identify critical fatigue-induced failure sequences accurately and efficiently. It also identifies the critical failure sequences in the decreasing order of their likelihood.

However, the B³ method is not readily applicable to continuum structures because of its limitations. In order to overcome this challenge, this paper proposes a generalized B³ method. The performance of the proposed method is demonstrated by numerical examples of a continuum multi-layer Daniels system and an aircraft longeron structure.

2 GENERALIZED BRANCH-AND-BOUND METHOD EMPLOYING SYSTEM RELIABILITY BOUNDS (B³ METHOD)

The “original” B³ method is generalized in three phases: (1) the limit-state function is modified to deal with a general stress distribution instead of an assumed far-field stress distribution; (2) an external computer program is integrated with the B³ computational framework to estimate the stress intensity range with the general stress distribution without relying on analytical geometry function; and (3) an additional search termination criterion is introduced for efficient system reliability analysis of a continuum.

2.1 Generalization I: limit-state function formulations for general stress distribution

The probability that the progressive failure of a sequence $\{1 \rightarrow 2 \rightarrow \dots \rightarrow (i-1) \rightarrow i\}$ occurs within an inspection cycle $[0, T_s]$ is described as

$$P_i^{1, \dots, (i-1)} = P \left\{ \left[\bigcap_{\forall j \neq 1} (T_i^0 < T_j^0) \right] \cap \left[\bigcap_{\forall k \neq 1, 2} (T_2^1 < T_k^1) \right] \cap \dots \right. \\ \left. \cap \left[\bigcap_{\forall l \neq 1, \dots, i} (T_i^{1, \dots, (i-1)} < T_l^{1, \dots, (i-1)}) \right] \right. \\ \left. \cap (T_1^0 + T_2^1 + \dots + T_i^{1, \dots, (i-1)} < T_s) \right\} \quad (1)$$

where $T_i^{1, \dots, (i-1)}$ denotes the time required for the failure at the i -th component since the sequential failure $\{1 \rightarrow 2 \rightarrow \dots \rightarrow (i-1)\}$.

Note that the time terms introduced for damaged structures (such as $T_i^{1, \dots, (i-1)}$ in Equation 1) should be computed with the effects of load re-distribution considered. Through the derivations employing the Paris-Erdogan equation, the time terms are approximated by a recursive formulation:

$$T_i^{1, \dots, i-1} \approx \frac{1}{C v_0} \int_{a_i^0}^{a_{ci}} \frac{1}{[\Delta K_i^{1, \dots, i-1}]^m} da \\ - \sum_{k=1}^{i-1} \int_{a_i^0}^{a_{ci}} \frac{1}{[\Delta K_i^{1, \dots, i-1}]^m} T_k^{1, \dots, k-1} \\ \int_{a_i^0}^{a_{ci}} \frac{1}{[\Delta K_i^{1, \dots, k-1}]^m} da \quad (2)$$

where C and m are the material parameters that appear in the Paris-Erdogan equation, v_0 is the loading frequency, a is the crack length, a_i^0 and a_{ci} are respectively the initial crack length and the critical crack length at the i -th component, and $\Delta K_i^{1, \dots, (i-1)}$ is the stress intensity range at the i -th component after the sequential failure $\{1 \rightarrow 2 \rightarrow \dots \rightarrow (i-1)\}$.

2.2 Generalization II: evaluating stress intensity range using an external computer program

Figure 1 illustrates the computational framework of the generalized B³ method proposed in this paper. The main B³ analysis code in MATLAB® repeatedly calls ABAQUS® to obtain the stress distribution

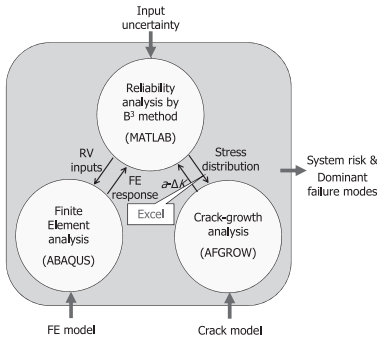


Figure 1. Computational framework of the generalized B^3 method.

from Finite Element (FE) analysis for given Random Variables (RVs) and damage conditions, and the stress distribution is transferred to AFGROW[®] for estimating the corresponding stress intensity range along crack length, which is the basic information for the estimation of the time terms in Equation 2.

2.3 Generalization III: additional termination criterion for systematic search scheme

The systematic search scheme of the generalized B^3 method is identical to that of the original B^3 method except for an additional analysis termination criterion and the crack-growth analysis process described in Section 2.2. In the proposed method, it is suggested to terminate the search process for risk quantification if any of the following conditions is satisfied: 1) gap of two bounds/upper bound < 0.05 ; and 2) lower-bound increment/upper bound < 0.001 .

3 NUMERICAL EXAMPLE I: MULTI-LAYER DANIELS SYSTEM

The generalized B^3 method is first tested by an example of a multi-layer Daniels system. By the generalized B^3 analysis, the upper and lower bounds are estimated as 1.010×10^{-2} and 9.608×10^{-3} for 30 FE simulations. On the other hand, by the original B^3 method, both bounds are estimated as 9.767×10^{-3} and 9.299×10^{-3} for 32 structural analyses. From Monte Carlo Simulations with 3×10^5 samples, the system failure probability is estimated as 9.807×10^{-3} (coefficient of variation = 1.83%) for more than 3×10^5 structural analyses. All the results from three different approaches match well. The slight difference between the results from the original and the generalized B^3 method is mainly due to the approximation introduced in Equation 2.

4 NUMERICAL EXAMPLE II: LONGERON

In order to test the applicability of the proposed method to continuum structures, an aircraft

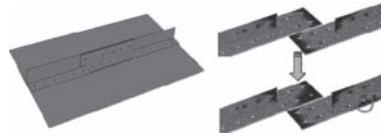


Figure 2. Longeron FE model (left); and the load-redistribution after a local failure (right).

longeron system is considered. Figure 2 shows an FE model (left) developed in ABAQUS[®] for the test and the load-redistribution (right) caused by local failure(s) (red circle). By the proposed method, the lower and upper bounds of system failure probability of the longeron are respectively estimated as 1.400×10^{-3} and 1.563×10^{-3} after only 151 FE simulations. In addition, various system failure modes on different locations and materials are identified in the decreasing order of their probabilities.

5 SUMMARY AND CONCLUSIONS

In this paper, the Branch-and-Bound method employing system reliability Bounds is generalized to overcome its limitations in risk analysis of continuum structures. To achieve this goal, (1) the limit-state function was modified to deal with general stress distribution instead of far-field stress; (2) an external computer program such as AFGROW[®] was incorporated into the B^3 computational framework to estimate the stress intensity range with the general stress distribution; and (3) the termination criteria of B^3 analysis was modified to avoid unnecessary simulations. The proposed method was demonstrated by a numerical example of multi-layer Daniels system, and the results were verified by the original B^3 method and Monte Carlo simulation. Furthermore, the generalized B^3 method was applied to an example of aircraft longeron system, and the merits of the proposed approach were successfully demonstrated.

REFERENCES

- Karamchandani, A., Dalane, J.I. & Bjerager, P. 1992. Systems reliability approach to fatigue of structures. *Journal of Structural Engineering*, 118(3): 684–700.
- Lee, Y.-J. & Song, J. 2010a. Risk analysis of fatigue-induced sequential failures by branch-and-bound method employing system reliability bounds. *IFIP WG7.5 Working Conference*, April 7–10, Munich, Germany.
- Lee, Y.-J. & Song, J. 2010b. Identification of critical sequences of fatigue-induced failures by branch-and-bound method employing system reliability bounds. *Proc. 12th AIAA NDA Conference*, April 12–15, Orlando, FL.

Reliability analysis of corroding RC members using adaptive Response Surface Method

A.N. Kallias & M.I. Rafiq
University of Surrey, Guildford, UK

1 SUMMARY

Rebar corrosion is currently a major research area due to the globally increasing number of deteriorating bridges and marine infrastructures. Corroding RC structures may exhibit premature in-service performance failures (e.g. excessive cracking, increased deflections) as well as reduced safety (i.e. loss of load capacity and ductility), placing additional stress to the scarce resources available to authorities and owners, responsible for their safe operation.

Effects of corrosion on RC elements include the loss of steel area, concrete cracking and spalling, bond deterioration and impaired mechanical properties in the affected rebars. Several studies have quantified the influence of each corrosion effects on the structural behavior of RC elements, e.g. (Du et al., 2007, Kallias & Rafiq 2010).

It is evident from the literature that quantifying the effect of corrosion on structural performance is a rather complex problem due to the interaction of various factors responsible for the observed behavior. For instance, the amount of bond degradation and its spatial distribution depends on the nature and extent of corrosion, yet both are equally important factors leading to increased deflections at the SLS (Kallias & Rafiq 2010). The complex behavior of corrosion-affected RC members is difficult to capture accurately using conventional sectional analysis adopting simplified assumptions; this leads to over-conservative assessments and undue repair works.

Non-linear finite element analysis (NLFEA) can be used for corroding RC structures to accurately predict the loss of strength and ductility and changes in the mode of failure due to corrosion. The RC member is treated as a structural system in NLFEA, by explicitly modeling concrete, steel rebars and their bond as well as considering changes in the material and bond behavior due to corrosion damage.

Reliability analysis is a widely proposed tool to assess corroding RC structures underpinning uncertainties in quantifying the deterioration processes. FORM/SORM are computationally

efficient methods for the probabilistic performance assessment of the structure especially when the performance function is expressed in explicit form. The performance function is only implicitly available when using NLFEA.

The Response Surface Method (RSM) is an attractive method for dealing with implicit functions. It uses a low-order polynomial to approximate the actual performance function, using a set of sampling points in the variable space, i.e. Experimental Design (ED), where the implicit function is evaluated.

In this paper, an adaptive method for reliability analysis is presented which utilizes NLFEA and RSM to approximate the performance functions of corroding RC members. FORM is then used through an iterative procedure to determine the reliability index β . The proposed procedure is demonstrated through a case study on corroding RC beams, considering the load-capacity and ductility limit states.

In this study, the 1st-order model which includes the two-factor interactions is initially fitted using data obtained from a two-level factorial ED. When the number of variables k is less than 4, a full 2-level factorial is used. In the case where $k \geq 5$ a 2-level fractional factorial of minimum resolution V is adopted. The quality of the fitted 1st-order model is checked by comparing its predictions with the predictions of the corresponding FE runs and an independent FE run at the center of the ED. If the differences between the predictions of the FE runs and those of 1st-order model are large, the model is augmented by adding the 2nd-order terms. To fit the 2nd-order model, axial points are added to the existing factorial design. The axial points are positioned to form a central composite design (CCD) or a faced centered cube design (FCC), depending on the limits imposed by the realistic variable space. The predictions of the 2nd-order model and the corresponding FE runs are compared; when large differences are observed the model is rejected and the design center and/or the variable ranges are redefined. The initial approximation is only used to facilitate the iterative procedure for the determination of the initial design point and reliability index β ; a sufficiently accurate initial

approximation leads to faster convergence of β . Once a suitable approximation is available, the FORM design point is searched and a new ED is defined to its proximity. The method is iteratively repeated until convergence of β is achieved.

A corroded beam (T-type) tested by (Du et al., 2007) is used to demonstrate the proposed methodology. Corrosion is assumed only over a 600 mm central portion of its tension rebars.

Two-dimensional (2D) non-linear finite element analysis (NLFEA) is used in this study. Concrete is modeled using 4-node plane stress elements with thickness equal to the beam's width. Rebars are modeled using truss elements. Bond of the tension rebars with concrete is modeled using interface elements, for details see (Kallias & Rafiq 2010).

Five basic random variables are considered in the reliability analysis, including concrete strength f_c^D , bond strength u_{max}^D , steel area A_{st}^D , yield strength f_y^D and ultimate strain ϵ_u^D of the corroded tension rebars. A 2^{5-1} fractional design (res V) is used to fit the 1st-order model, which includes two factor interactions. The initial ranges of the random variables are selected to consider up to roughly 20% corrosion loss in the tension rebars, assuming that f_c remains unaffected by corrosion. The effect of the initial variable ranges—which are larger than the ranges proposed in other studies e.g. (Wong et al., 2005)—is discussed. Finally, Crude Monte Carlo simulation (MCS) is used to obtain the first two moments (i.e. μ and σ), and distribution type of parameters f_y^D , ϵ_u^D and u_{max}^D , for the FORM analysis. The load capacity and ductility limit states in flexure are examined.

The results indicate that the fit of the 1st-order model for the yield-load capacity limit state is satisfactory, despite the large evaluation range considered for the variables. This is true, not only for the factorial points used to fit the model, but also for the center and axial points of the ED. The fitted 1st-order response surface is used for the reliability analysis of the yield load limit state using FORM. Two loads, 30 and 36 kN (60% and 72% of the yield-load of the uncorroded beam, respectively) are assumed in the FORM analysis to examine the evolution of reliability for increasing corrosion loss.

Figure 1a shows the convergence of the reliability index profiles for the two loads considered, for increasing corrosion damage. In all cases β converged within two iterations (following the initial approximation). Finally, the evolution of reliability index with time (years) can be seen in Figure 1b, for the two load cases analyzed, assuming a constant corrosion current, $i_{corr} = 1\mu A/cm^2$.

The results indicate that the large initial variable ranges did not produce satisfactory approximations (1st or 2nd order) of the ductility limit state, since large differences are observed between the predictions of the fitted model and the predictions

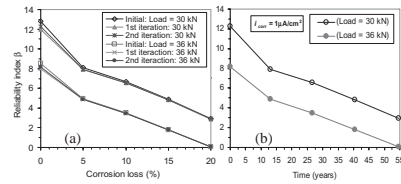


Figure 1. Reliability of yield-load capacity limit state: (a) convergence of β and (b) evolution of β with time.

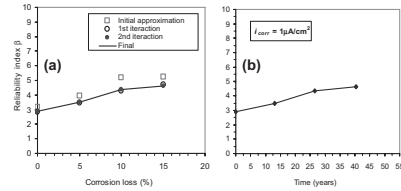


Figure 2. Reliability of ductility limit state: (a) convergence of β and (b) evolution of β with time.

of the corresponding FE runs. To improve the accuracy of the fitted model the variable space, is divided in smaller multiple overlapping regions, using 5% corrosion intervals. The 1st-order approximation produced satisfactory approximations for up to 10% corrosion loss (intervals 0%, 5% and 10%). At 15% corrosion interval, large differences are observed between the center and axial FE predictions and the predictions of the 1st-order approximation and the 1st-order model is augmented with the 2nd-order terms.

A displacement ductility factor is assumed for the reliability analysis and the initial design points are established for each corrosion interval. New design centers are selected close to the initial design points and iterations are performed until the convergence of β . Figure 2a shows the convergence of β , while Figure 2b shows the evolution of β with time (years) of active corrosion, assuming $i_{corr} = 1\mu A/cm^2$.

REFERENCES

- Du, Y.G. Clark, L.A. & Chan, A.H.C. 2007. Impact of reinforcement corrosion on ductile behaviour of reinforced concrete beams. *ACI Structural Journal* 104(3):285–293.
- Kallias, A.N. & Rafiq, M.I. 2010. Finite element investigation of the structural response of corroded RC beams. *Engineering Structures* 32(9): 2984:2994.
- Myers, R.H. Montgomery, D.C. & Anderson-Cook, C.M. 2009. *Response surface methodology: Process and product optimization using designed experiments*. John Wiley & Sons.
- Wong, S.M. Hobbs, R.E. & Onof, C. 2005. An adaptive response surface method for reliability analysis of structures with multiple loading sequences. *Structural Safety* 27:287–308.

Uncertain and unavoidable—reliability estimation in wave and tidal energy systems

J. Flinn & C. Bittencourt Ferreira
Det Norske Veritas, UK

The reliability of wave and tidal energy converters (collectively Marine Energy Converters—MECs) is a key issue that has to be addressed in order to make them a viable energy option. At this stage of early industrial development the reliability assessment of MECs is a challenging task, and the reliability of MECs is critical to the success of the industry. In other industries, such as wind energy, it has been possible to build up the reliability of the systems in an onshore, relatively accessible environment, prior to moving offshore. However, for most MECs it is necessary to work in an inherently hostile, less accessible environment from the start. For the industry-leading prototypes being deployed now it is important to demonstrate appropriate levels of reliability as this is linked directly to their potential Cost of Energy (CoE). This means an accurate assessment of the reliability (and the associated uncertainty) of the system is extremely useful, if not essential. More mature industries, such as the offshore oil and gas sector, have dealt with the problem and developed new methods as it became more critical to them (in terms of reducing maintenance requirements and lost revenue due to downtime of installations), and have implemented databases of historical failure data, such as OREDA.

Previous papers have investigated the application of existing reliability methods to a notional configuration of MEC in order to investigate the effectiveness of current methods and applicability of available data. It was found that the lack of readily applicable failure rate data meant that crude adjustments to often generic data were necessary, and results obtained were rather unfavorable and highly uncertain. This paper will: present the problem in the context of the wave and tidal energy industry; discuss the benefits to be gained from assessing reliability using a transparent and standardized method; identify the challenges of presenting results with associated uncertainty; describe the initial work carried out on a method of dealing with the issues of lack of failure rate data and application of existing data to a novel technology in a new environment; and identify

the work proposed to improve the assessment of reliability and availability in this industry through all stages of development of new devices.

Unlike many other offshore technologies, wave and tidal energy technologies are expected to operate in a harsh environment from the early stages of their development. Whereas wind and oil and gas technology could be developed onshore in a relatively accessible environment, most marine energy systems will have to be developed offshore, and any unforeseen reliability issues will be expensive and difficult to deal with.

For this reason, reliability can be considered more critical in this industry than in almost any other at a similar stage of development, particularly given the limited amount of funding available for development and the pressure from society for a fully functioning renewable energy sector. In order to ensure that public and private sources of funding are invested in the most effective ways, and that technology is developed using the most efficient routes, it is important to have a realistic and transparent estimation of concept reliability where the outputs satisfy the demands of the technology developer, their potential and existing investors, and other stakeholders in the industry.

Wave and tidal energy converters are required to operate from the early stages in a hostile environment. This environment makes accessing the devices for inspection and even minor maintenance both difficult and expensive. It is therefore desirable (and in most cases essential with respect to achieving a competitive cost of energy) to minimize the number of times the machine has to be accessed during its lifetime. By extension, this means that the reliability of the machine has to be maximized.

This provides a good illustration of why a realistic and systematic approach to early-stage reliability assessment is important, both in terms of providing a realistic estimate of cost of energy for a concept, and to allow more accurate targeting of less reliable and more critical aspects of the device.

There are difficulties with the availability of reliability data for wave and tidal energy systems,

and also with the uncertainty associated with the application of data from other industries to wave and tidal energy systems. The normal approach to these uncertainties and difficulties is to make some assumptions and simplifications to the estimation method in order to produce a result. There are two problems with this:

1. Different analysts will apply different sets of assumptions in their estimations. This makes comparison between different devices difficult to achieve on an equitable basis.
2. The simplifications and assumptions are unlikely to produce a representative estimation of the actual reliability of the system, without significant uncertainty.

By having a standardized method of analysis and adaptation of input data the results from different analyses can be repeated regardless of the analyst, and results for different concepts can be compared in an equitable manner. Additionally, the model can be structured such that reliability data from operation of prototypes and commercial installations can be fed back into the assessment to improve confidence in the result.

The results from a stochastic reliability analysis (for example, using a Monte Carlo simulation) should not be presented as a deterministic value, as this is not capable of providing an accurate representation of the situation. The actual representation of reliability of a marine energy converter must contain the result of combining the various sources of uncertainty included in the analysis. Some of the sources of uncertainty which are likely to be included in the analysis are uncertainty in the input data, and uncertainty in the application of existing data from other industries.

The uncertainty in the input data will, for the current early stages of development of the industry, remain significant, until several mature design concepts have been operated and monitored in the offshore environment and built up sufficient history to provide more confidence in the data.

The primary solution to this problem is the generation of new failure rate data from testing and monitoring. In the initial phase of development of the industry it is not realistic to expect an immediate mass deployment of MECs in real conditions, particularly not all using the same components

prior to further convergence of concepts. The solution to this is to run component lifecycle testing to produce failure mode and failure rate data for the components in their likely operating conditions.

A more immediate solution to the problem with lack of reliability data is to use data from other industries, principally the oil and gas industry, which has already run a large scale data collection exercise in the OREDA project. As discussed above, this data has normally been generated in a different operating environment from that of a MEC, with the result that inclusion of this data in the reliability assessment of a MEC should induce an increase in uncertainty in the result. The level and nature of this uncertainty will be different for the different applications, and a consistent assessment of the uncertainty is required to allow comparison of results.

Several factors will contribute to the uncertainty induced by the application of data from other industries:

- Experience: Total operating time for the component in question, across all installations
- Novelty: The extent to which the new system uses new ideas, or applies technology in new ways
- Complexity: The number of components included in the system, or the number of functions required to be performed
- Misfit: The potential gap in understanding that can exist when equipment is not specifically designed and built to the design specification, but instead the nearest existing equipment design is used

A qualitative or semi-quantitative scoring system is being developed to give a measure of the uncertainty induced by each of the factors above, and by combining these into an overall assessment of the data quality, the total uncertainty induced by the application of the data to the system in question can be assessed. This uncertainty can then be implemented quantitatively in the data being used by statistical manipulation of the failure rate distribution (e.g. by modifying the upper and lower boundaries of the failure rate distribution). The requirements of this system and the work done to date are discussed in more detail in this paper.

Post earthquake bridge damage assessment coupling field data and reliability tool

M. Torbol, R. Baghaei, J. Kang & M. Feng
University of California Irvine, USA

The health monitoring of the infrastructure of a region is a challenging topic, different field of engineering are involved from the mechanical/electrical engineering of the sensor on the structure to the computer science and the digital signal processing behind the data acquisition system, from the structural modeling of the structure to the risk analysis and decision making about its status. Bridge Doctor, the software object of this paper, has been developed to integrate all those different fields in a compact and efficient application for the health monitoring of bridges. It is composed by four main subroutines.

“Data acquisition”, where the field data gathered on the structure are loaded, common digital signal processing are implemented such as: baseline correction, filtering.

“Rapid damage detection”, where the processed digital signal are analyzed using an AR (autoregressive model) with time windows technique to retrieve a preliminary status of the structure after an earthquake (damage/no damage). In case that the AR can't give a unique answer on the structure status and a discrepancy is present between the different channels the user is supported a set of fragility curves developed for structure under analysis.

“Detailed damage assessment”, after establishing the presence of damage the next step is to assess the amount and location of this damage. This subroutine is divided in two parts. The modal identification composed by FDD (Frequency Domain Decomposition) and FRF (Frequency Response Function) used to obtain the damping ratio, natural frequency and mode shapes of the damaged structure. The structural damage detection composed by a GA (genetic algorithm) applied to a parametric Finite Element Model to calculate the amount of damage on the structure.

“Remaining capacity estimation” is the last step of Bridge Doctor and it give the decision maker valuable information about the total damage received by the structure, the ductility reached by its elements and their remaining capacity.

In Figures 1, 2 and 3 the different tab of the software are reported, while not necessary for the software functionality a small GUI generating the FE graphic model and sensor layout has been added to help while dealing with the different channel. A summary of the detailed damage assessment procedure is shown in Figure 4.

While bridge doctor is a health monitoring software under continuous development and evolution, the first prototype has shown good results in evaluating the health of the bridges under

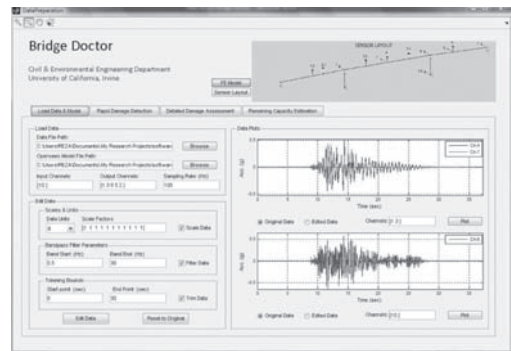


Figure 1. Data acquisition tab.

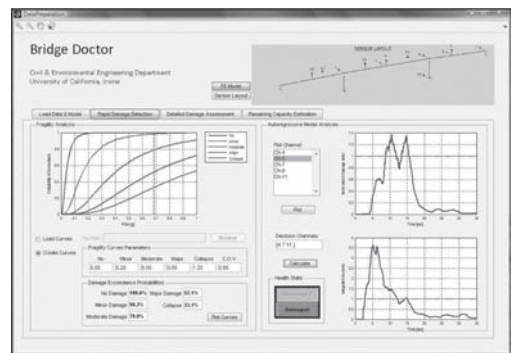


Figure 2. Rapid damage detection.

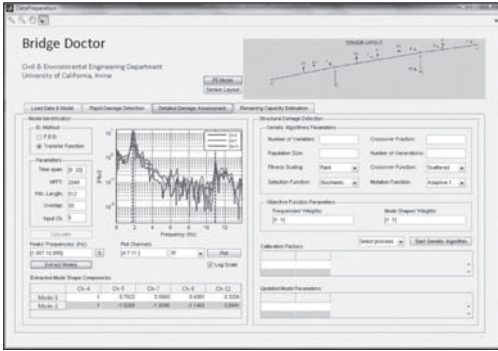


Figure 3. Detailed damage assessment.

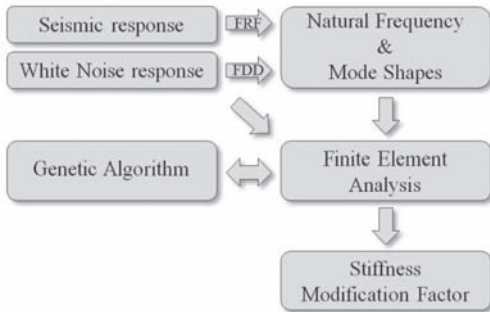


Figure 4. Detailed damage assessment procedure.

inspection. Its modularity: data acquisition, rapid damage detection, detailed damage assessment and remaining capacity estimation allows the possibility of changing and improving a single module without influencing those nearby as long as the input/output stay the same.

As previously stated a decision maker using this software can obtain the result damage/no damage from the “rapid damage detection” module in less than a minute after loading the channels data. For the more sophisticated “detailed damage assessment” results can take from 30 minutes to few hours on single core because of the computationally expensive GA. In any case the GA algorithm chosen can be parallelized and the first few results have shown a very good scalability.

The detailed damage assessment is capable of detecting location and amount of damage, but for a decision maker the last stage “remaining capacity estimation” is the key element, it evaluate the ductility reached by the structure and how much capacity is left.

Bridge doctor has still a lot of point that can be improved; for example the remaining capacity estimation is currently under revision and new methods are currently under implementation.

MS_235 — Reliability of marine energy converters

This page intentionally left blank

Reliability of tidal stream turbine blades

D.V. Val & L. Chernin

Heriot-Watt University, Edinburgh, UK

ABSTRACT: Tidal stream turbines are a new technology for extracting kinetic energy from tidal currents. Although a number of different concepts of tidal stream turbines have been proposed so far a majority of them are horizontal axis devices with an open rotor similar to a typical wind turbine (King & Tryfonas 2009). An important parameter for this type of turbines is the way their blades are connected to the rotor hub. The blades can be fixed (fixed-pitch) or being made rotatable about their axes (variable pitch). In the latter case the blades' orientation towards the current flow direction can be changed and by this the power take-off can be controlled (pitch-controlled turbine).

Figure 1 shows a power versus current speed curve for a horizontal axis pitch-controlled turbine with a rotor of 18-m diameter when the rated current speed is 2.5 m/s (the rated current speed is a speed at which the turbine reaches its rated power). The figure also shows the corresponding bending moments: flapwise, in-plane and total, at the blade root. The results in Figure 1 are calculated using the NWTC Subroutine Library (Buhl 2004), which is based on the blade element momentum theory. The Prandtl tip-loss factor is used to account for tip and hub losses. Up to stall values of the drag and lift coefficients for the blade elements are derived using the two-dimensional (2-D) vortex panel code XFOIL

(Drela 1989). Their post stall values are estimated by the Viterna method (Viterna & Corrigan 1981).

As can be seen from Figure 1, the flapwise and total bending moments at the blade root reach their maximum at the rated current speed and then decrease rapidly as the pitch angle increases to keep the power constant. It can also be seen that at the peak the difference between these two moments is insignificant. However, the pitch control does not react instantly to high frequency fluctuations of the current speed due to turbulence. The current speed fluctuations may cause much larger bending moments at the blade root than the peak values in Figure 1. To take this into account, a random variable ΔU representing fluctuations of the tidal current speed around its average value is introduced. Since it is clear that from a physical point of view the magnitude of ΔU should be limited, the latter is modelled by a beta random variable defined on $(-0.3U_r, 0.3U_r)$ with a zero mean, where U_r = rated current speed.

The spar of the blade is made of carbon fibre composite. The tensile strength of the composite laminate in the direction of fibres, f_f , is represented by a lognormal random variable with a coefficient of variation (COV) of 0.10.

There are numerous sources of uncertainty/error associated with the evaluation of forces acting on the turbine blades by the blade element momentum theory. In this study all these uncertainties are taken into account by a single random variable C_m . It has been estimated that for wind turbines the coefficient of variation of values of load effects (e.g., bending moments in rotor blades) due to the use of the blade element momentum theory for their calculation should be around 0.10–0.15. Thus, it is assumed herein that C_m is a normal random variable with a mean of unity and COV = 0.15.

To carry out reliability analysis a relationship between M_f and the tidal current speed, U (see Figure 2) needs to be established. The relationship obviously depends on the pitch angle of the blade. Since maximum values of the bending moment occur when the turbine is operating at a rated current speed the relationship between M_f and U is only needed for the pitch angle corresponding to this situation. It is found that the relationships are almost perfectly linear:

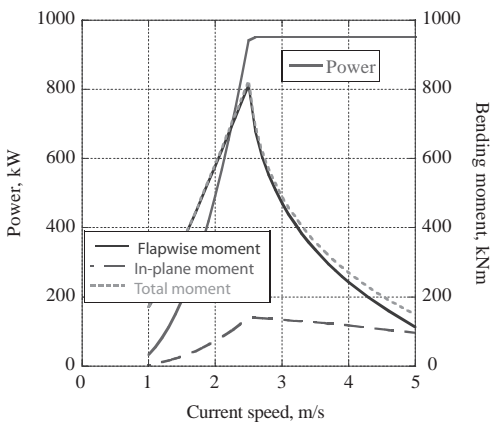


Figure 1. Power and bending moments at the blade root vs. tidal current speed.

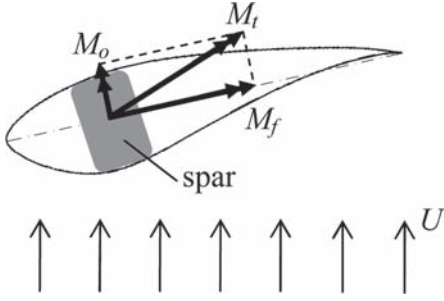


Figure 2. Blade cross-section at the root with acting bending moments.

$$\begin{aligned} M_f &= 438U - 306 \text{ (kNm)} \quad \text{for } U_r = 2 \text{ m/s} \\ M_f &= 464U - 338 \text{ (kNm)} \quad \text{for } U_r = 2.5 \text{ m/s} \end{aligned} \quad (1)$$

where U is in m/s. Thus, the limit state function for blade failure in bending can be written in the following form

$$G = f_t - \frac{C_m M_f}{Z} = f_t - \frac{C_m [A(U_r + \Delta U) - B]}{Z} \quad (2)$$

where Z = section modulus of the spar. The probability of failure, P_f , of the blade in bending is then

$$P_f = \Pr[G(f_t, C_m, \Delta U) \leq 0] \quad (3)$$

In ultimate limit state design the criterion to be satisfied is $S_d \leq R_d$, where R_d = design resistance and S_d = design load effect. In the context of bending failure of a tidal turbine blade

$$R_d = \frac{f_{t,k}}{\gamma_m}; \quad S_d = \gamma_f \frac{M_f}{Z} \quad (4)$$

where $f_{t,k}$ = characteristic tensile strength of the spar material; γ_m = partial factor for material; and γ_f = partial factor for load. The ultimate limit state design criterion can then be written as

$$SF = \gamma_f \gamma_m \leq \frac{f_{t,k}}{M_f/Z} \quad (5)$$

where SF = product of the partial factors, which is further referred to as the safety factor.

The reliability of a structural component is often expressed in terms of the reliability index β , which is related to the probability of failure by the following formula $\beta = -\Phi^{-1}(P_f)$, where Φ = cumulative function of the standard normal distribution. Using Monte Carlo simulation, values of the

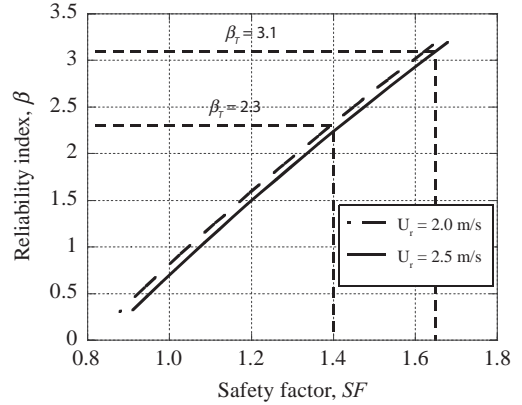


Figure 3. Reliability index vs. safety factor.

reliability index associated with bending failure of the tidal turbine blade are calculated for two rated current speeds (2 and 2.5 m/s) as a function of the safety index and the results are presented in Figure 3.

In order to select a required value of SF target reliability of a turbine blade in bending needs to be specified. If the target reliability index $\beta_r = 2.3$, the safety factor should be at least 1.4 (see Figure 3) that in terms of the partial factors can be achieved by setting, e.g., $\gamma_m = 1.1$ and $\gamma_f = 1.3$. If $\beta_r = 3.1$, SF should be at least 1.65 that in terms of the partial factors can be achieved by setting, e.g., $\gamma_m = 1.1$ and $\gamma_f = 1.5$.

ACKNOWLEDGEMENTS

This research has been carried out as part of the EPSRC-funded SuperGen Marine Energy Research Consortium. The financial support provided by the EPSRC is gratefully acknowledged.

REFERENCES

- Buhl, M.L. 2004. *NWTC Design Codes* (NWTC Subroutine Library), http://wind.nrel.gov/designcodes/miscellaneous/nwtc_sub/
- Drela, M. 1989. XFOIL: An Analysis and Design System for Low Reynolds Number Airfoils. In *Proc. Conference on Low Reynolds Number Aerodynamics, University of Notre Dame, Indiana, 5-7 June 1989*.
- King, J. & Tryfonas, T. 2009. Tidal stream power technology – state of the art. In *Proc. Oceans 2009 – Europe (Oceans'09), Bremen, 11-14 May 2009*.
- Viterna, L.A. & Corrigan, R.D. 1981. Fixed pitch rotor performance of large horizontal axis wind turbines. In *Proc. DOE/NASA Workshop on Large Horizontal Axis Wind Turbines, Cleveland, OH, July 1981*.

Reliability of power train components in tidal stream turbines

D.V. Val & C. Iliev

Heriot-Watt University, Edinburgh, UK

ABSTRACT: Tidal stream power is a major source of renewable energy, especially for an island country such as the UK. Since this is a new technology, almost no data are available at present on failures of tidal stream turbines and their components that creates difficulties in assessing the reliability of these devices. This, in turn, has a negative effect on the confidence of potential investors and hinders the commercial development of the technology.

The paper presents a method for estimating failure rates of power train components of a generic tidal stream turbine. The method is based on a Bayesian approach that uses generic failure data for similar components from other industries to construct a prior distribution. Generic failure data is represented by the base failure rate, λ_B , which is then adjusted to actual operating and environmental conditions of the component under consideration by multiplying it by the so-called “influence” factors, C_j

$$\lambda = \lambda_B \prod_j C_j \quad (1)$$

Uncertainties associated with the evaluation of the base failure rate and the influence factors are treated as random variables and the prior distribution of the component failure rate, $\pi_0(\lambda)$, is obtained by Monte Carlo simulation. Since the failure rate is expressed as the product of random variables, see Eq. (1), according to the central limit theorem it can be assumed that it has a lognormal distribution

$$\pi_0(\lambda) = \frac{1}{\sqrt{2\pi\xi\lambda}} \exp\left[-\frac{1}{2\xi^2} \ln^2\left(\frac{\lambda}{\lambda_p}\right)\right] \quad (2)$$

where λ_p and ξ = parameters of the distribution. It is also necessary to note that in addition to the influence factors, one more multiplier, C_m , representing uncertainty associated with the model itself is included into the product in Eq. (1).

A posterior distribution of the failure rate, $\pi(\lambda)$, is estimated as new information about the component performance in operating tidal turbines becomes available based on Bayes’ theorem

$$\pi(\lambda) = \frac{1}{c} \pi_0(\lambda) L(n|\lambda) \quad (3)$$

where $L(n|\lambda)$ = likelihood function representing new information and c = normalising factor. The likelihood of observing exactly n failures of the component over operating time T , when the failure rate is λ , is given by

$$L(n|\lambda) = \frac{(\lambda T)^n}{n!} \exp(-\lambda T) \quad (4)$$

The method is illustrated by assessing the failure rate of the main bearing of a tidal turbine power train. The main (locating) bearing is mounted on the main shaft right behind the main seal. For this component Eq. (1) can be written in the following form

$$\lambda = \lambda_B C_v C_c C_i C_{SF} C_m \quad (5)$$

where C_v = influence factor for lubricant; C_c = influence factor for contamination; C_i = influence factor for operating temperature; C_{SF} = influence factor for operating service conditions; and C_m takes into account model uncertainty.

To take into account various uncertainties associated with the determination of λ_B the latter is treated as a lognormal random variable with mean $0.14/L_{10}$ and coefficient of variation (COV) 0.20, where L_{10} = basic rating life of the main bearing.

The influence factor for lubricant, C_v , can be estimated as

$$C_v = \left(\frac{\nu_1}{\nu}\right)^{0.54} \quad (6)$$

where ν = actual kinematic viscosity of the lubricant at the operating temperature; and ν_1 = reference kinematic viscosity required to obtain adequate lubrication condition. Lubricant viscosity decreases exponentially with increasing operating temperature. Therefore, C_v is very sensitive to the operating temperature of the main bearing, which may vary significantly over the turbine operating time. It is estimated that the operating temperature

varies between 20°C and 100°C with mean 60°C. This variability of the operating temperature is described by a beta distribution with COV = 0.20. For illustrative purposes, a synthetic lubricant of ISO VG 1500 class with VI = 160 is selected for the main bearing. The relationship between the kinematic viscosity (in mm²/s) of this lubricant and the operating temperature (in °C), t_o , can be approximately described by the following formula

$$v(t_o) = 10000 \exp(-0.048t_o) \quad (7)$$

The influence factor for contamination takes into account both water and particle contamination and is expressed as

$$C_C = 1.176 \times 0.21^{0.01-cw} (FR)^{0.25} \quad (8)$$

where cw = percentage of water in the lubricant; and FR = oil filter rating in μm . The percentage of water in the lubricant is treated as a random variable. It is assumed that it can be described by a beta distribution defined on the interval (0.01,1.) with mean 0.2% and COV = 0.20.

The influence factor for operating service conditions accounts for a negative effect of shock and vibration on the failure rate of a rolling bearing. C_{SF} is modelled as a beta random variable defined on (1.,1.4) with mean 1.1 and COV = 0.05.

Finally, the multiplier C_m is introduced to represent other uncertainties associated with the modification method. In addition, since Eq. (5) is used in the context of Bayesian analysis, C_m can also be used to represent our degree of belief in this model and based on its prior distribution. The mean value of C_m is unity and it is described by a lognormal distribution in order to avoid negative values.

To illustrate the proposed method the prior distribution of the failure rate of the main bearing is constructed and then updated in accordance to various scenarios of the bearing performance. In order to construct the prior distribution values of the failure rate are generated by Monte Carlo simulation based on Eq. (5) and the above description of the random variables. Three values of COV of C_m representing different degrees of belief in the model given by Eq. (5) are considered in the analysis: 0.1—strong belief, 0.5—medium belief and 1.0—weak belief.

The effect of operating without failures for up to 20 calendar years is examined. The posterior distribution of the failure rate for a year T (≤ 20) is derived based on information that there have been no failures of the main bearing up to this year. Using this posterior distribution values of the mean μ_λ , and lower (5%) and upper (95%) confidence limits (denoted as $\lambda_{0.05}$ and $\lambda_{0.95}$, respectively) are then estimated. Results of the analysis

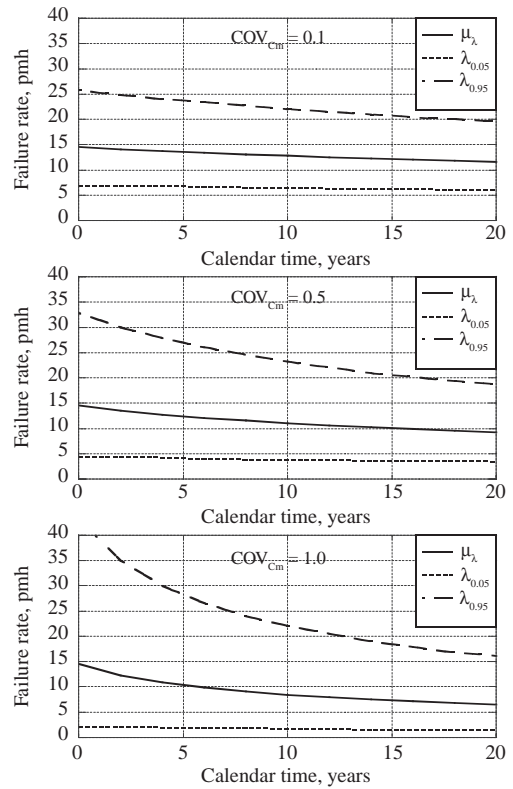


Figure 1. Change of the mean and lower and upper confidence limits of the failure rate with calendar time of operating without failure.

are shown in Figure 1. The failure rate is expressed per million hours (pmh) of operating time.

It should be noted that since the failure rate is assumed to be constant it is not important whether the information about failure-free operation comes from a single device or a group of devices, i.e., if one device has operated without failure of its main bearing for T years or T devices with identical main bearings have operated in similar conditions without such failure for one year.

According to the results, if belief in the prior estimate is strong (i.e., COV_{C_m} = 0.1) updating leads to relatively small changes in the failure rate characteristics. However, if belief in the prior estimate is weak (or at least medium) the use of the new information becomes much more beneficial.

ACKNOWLEDGEMENTS

This research has been carried out as part of the EPSRC-funded SuperGen Marine Energy Research Consortium. The financial support provided by the EPSRC is gratefully acknowledged.

Reliability methodology for evaluating tidal stream devices

T.M. Delorm & P.J. Tavner

School of Engineering and Computing Sciences, Durham University, UK

1 OVERVIEW

Tidal stream devices (TSDs) have the potential to satisfy rising energy demand. Unlike barrages, TSDs are modules installed incrementally; they are minimally intrusive to the environment. A TSD could be a horizontal or vertical turbine, or an oscillating hydrofoil, sub-categorised by seabed constraints and position in the water column (Mackie 2008), as shown in Figure 1.

Different TSD models have been proposed. TSDs, permanently installed at chosen tidal energy sites, face extreme climatic, current and wave load conditions, and their reliability and survivability are key challenges.

Information about TSD reliability is scarce because few prototypes have been built, so it is important to use reliability predictions to minimise the risks in prototyping. Reliability models for TSDs could reduce long-term risks and costs.

The intent of this study is to develop generic reliability models for TSDs in order to quantify reliability, make life-cycle predictions and permit comparisons. Reliability block-diagrams will describe the models proposed, and surrogate reliability data from marine, wind turbine, and electrical industries will predict TSD failure rates and survivor functions.

2 SURROGATE DATA SOURCES

The methodology of reliability studies of wave power devices done by Y-ARD Ltd. (1980) have not yet been applied to TSDs, nor has a comparison been made of different technologies

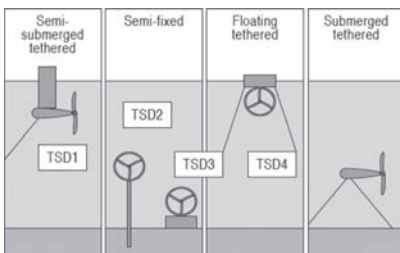


Figure 1. Types of horizontal axis TSDs. Adapted from Mackie (2008).

Although we lack operating data for TSDs, surrogate failure rate data are available in European onshore wind turbine (WT) databases: WMEP (Hahn et al., 2007) and LWK (Spinato et al., 2009) with most of the same subassemblies vital to TSDs—gearbox, generator and power electronics. The petrochemical industry has a reliability database OREDA (1984-2002), and generic databases NPRD-95 (1995) and MIL-HDBK 217F (1991), with extensive surveys of electrical equipment reliability in industrial plants and commercial buildings. These surrogate data were the backbone of this study. The problem is the relevance of these data for the TSD technology and operating environment, meaning that adjustments are needed. Surrogate data were adjusted for the more arduous marine environment.

The authors were unable to find a universal approach to representing the tidal environment. These uncertainties are crucial, so this research addresses two alternatives in reliability prediction that lead to worst-case scenarios: static Alternatives 1 and 2 (see Figs. 2 and 3, and full length paper).

3 TSD RELIABILITY ASSESSMENT METHOD

The proposed reliability prediction assessment method was applied to the 4 horizontal-axis TSDs illustrated in Figure 1.

Reliability Modelling and Predictions Analysis (RMPA) was chosen to quantitatively evaluate TSD design reliabilities because TSDs are new technology, and RMPA is applicable to all types of subassemblies, mechanical and electrical. The sequence used for reliability assessment is:

- Make a robust parts classification
- Establish a schematic diagram
- Derive a Functional Block Diagram (FBD)
- Use Surrogate Data Sources adjusted to the TSD tidal environment
- Use the Parts Count Reliability Prediction Technique (RIAC & DACS 2005) to evaluate total TSD reliability.

FBDs are complex mechanical, electrical, control, and structural systems, with dependen-

cies between systems, so they require advanced reliability modelling methods. Assuming subassembly times-to-failure are exponentially distributed, each subassembly is independent of others and all subassemblies operate in a single environment, the overall tidal TSD reliability based on surrogate data can be analyzed as series of subassemblies using the RBD.

The authors used the traditional method of reliability prediction. For a series reliability model based on Parts Count Reliability Prediction Technique, the equipment total predicted failure rate can be applied and expressed as in (RIAC & DACS 2005):

$$\lambda_{tot} = \sum_{i=1}^{N_S} \lambda_i \pi_{Ei} \pi_{Qi} \left(\frac{\text{failure}}{\text{year}} \right) \quad (1)$$

where: λ_{tot} = total predicted failure rate (failure/year); λ_i = surrogate or generic failure rate for the *i*th generic unit (failure/year); π_{Ei} = environmental adjustment factor; π_{Qi} = quality factor.

The latest Environmental Conversion Factors of MIL-HDBK 217F for electrical and electronic components are published in RIAC & DACS (2005).

Only critical equipment that directly contributes to power production has been analysed. Predicted survivor functions were calculated based on the assumption of a non-repairable system, of N_S independent subassemblies, for 1 or 0.2 calendar year, with a power output up to 100% for all TSDs

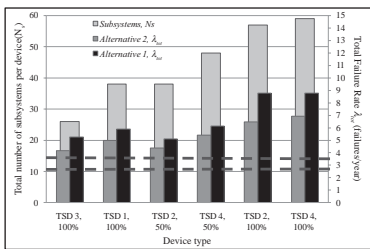


Figure 2. Predicted failure rates for TSD1 to 4, the dotted lines show measured failure rates for onshore WT of similar rating taken from Hahn et al. (2007).

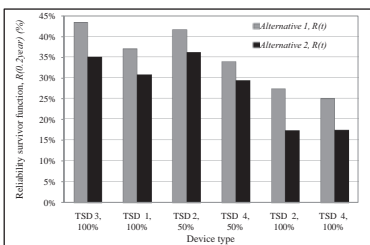


Figure 3. Predicted survivor functions for TSD1 to 4 after 0.2 year of operation.

(1–4) and up to 50%, for twin-axis TSDs (2 and 4). The technique was applied assuming that system redundant units are individual blocks. This technique was used as no specific product design and reliability information existed for these TSDs; however, this approach can lead to error.

4 RESULTS AND CONCLUSION

Predicted survivor rate results for the TSD reliability models are summarised in Figures 2–3, from which it can be seen that fixed TSDs without maintenance access will suffer poor survivor rates unless base failure rates are drastically reduced; TSDs with maintenance access (either by unmooring or the use of a sea-bed pile and turbine-raising) may achieve much better survivor rates.

A seabed bottom-mounted, ducted single-axis turbine TSD has the lowest failure rate because of its simple technology. Complexity increases for a TSD with twin-axis turbines; therefore so do failure rates. These TSDs show improved failure rates when only 50% power is required, due to the implicit redundancy of twin-axis technology.

Predicted TSD failure rates, 4–9 failures/turbine/year, are higher than measured for onshore WT at 2.5–3.5 failures/turbine/year. This is to be expected; TSD technology is in its infancy compared to WT technology.

Predicted reliability survivor values, based on these failure rates, after 1 year in the water are very low. However, after 0.2 years in the water the survivor rates become more respectable.

REFERENCES

Hahn, B., Durstewitz, M. & Rohrig, K. 2007. Reliability of wind turbines, Wind Energy—Proceedings of the Euromech Colloquium 464b 2005 Oldenburg, Germany: 329–332.

Mackie, G. 2008. Development for Evopod tidal stream turbine. Proceedings of the International Conference on Marine Renewable Energy, The Royal Institute of Naval Architects, London.

MIL-HDBK-217F, Notes 2. 1991. Military Handbook. Reliability Prediction of Electronic Equipment. USA Department of Defence.

NPRD-95 1995. Non Electronic Parts Reliability Data, Reliability Information and Analysis Center (RAC), Utica, New York, USA.

OREDA 1984-2002. *Offshore Reliability Data*.

RIAC & DACS 2005. System Reliability Toolkit, A Practical Guide for Understanding and Implementing a Program for System Reliability. US Department of Defence, Arlington, VA.

Spinato, F., Tavner, P.J., van Bussel, G.J. & Koutoulakos, W.E. 2009. Reliability of wind turbine subassemblies. IET Renewable Power Generation 3(4): 1–15.

Y-ARD Ltd 1980. Reliability study of wave power devices. Memorandum No. 3551/80, Report ETSU 1581. Energy Technology Support Unit, AEA Technology, Harwell.

Probabilistic design of wave energy devices

J.D. Sørensen & J.P. Kofoed

Department of Civil Engineering, Aalborg University, Denmark

C.B. Ferreira

Det Norske Veritas BV, London, UK

ABSTRACT: Wave energy has a large potential for contributing significantly to the production of renewable energy. However, the wave energy sector is still not able to deliver cost competitive and reliable solutions. But the sector has already demonstrated several proofs of concepts. It is possible to extract energy, and the sector has huge supply potential. The global wave power potential has been estimated to be of the same order of magnitude as world electrical energy consumption.

For wave energy devices (WED) the ratio between structural loadings in extreme and production conditions is in most cases very high. In comparison, for wind turbines the ratio is significantly smaller, as the turbine blades are pitched out of the wind in extreme conditions, making extreme loadings of the same order of magnitude as production loads. As extreme loadings and survivability drive the costs of the devices, and as income is only generated in everyday production conditions, it is of tremendous importance to increase reliability and reduce cost.

In traditional deterministic, code-based design, the structural costs are among other things determined by the value of the safety factors, which reflects the uncertainty related to the design parameters. Improved design with a consistent reliability level for all components can be obtained by use of probabilistic design methods, where explicit account of uncertainties connected to loads, strengths and calculation methods is made. In probabilistic design the single components are designed to a level of safety, which accounts for an optimal balance between failure consequences, material consumption and the probability of failure.

Probabilistic design can be used for direct design of the wave energy devices and thereby ensuring a uniform and economic design. Probabilistic design includes the following aspects described and illustrated in the paper: 1) definition of structural, electrical and mechanical components, 2) identification of important failure modes and stochastic models for the uncertain parameters,

3) recommendation of methods for estimation of the reliability, 4) recommendations for target reliability levels for the different groups of element and 5) recommendation for consideration of system aspects and damage tolerance. A probabilistic approach can also contribute to identification of reliability critical components.

Design of wave energy devices is a new and expanding technical area where there is no tradition for probabilistic design—in fact very little full scale devices has been build to date, so it can be said that no design tradition really exists in this area. For this reason it is considered to be of great importance to develop and advocate for a probabilistic design approach, as it is assumed (in other areas this has been demonstrated) that this leads to more economical designs compared to designs based on deterministic methods.

In the present paper a general framework for probabilistic design and reliability analysis of wave energy devices is presented. Considerations similar to those used for offshore wind turbines could be the basis for also for wave energy devices, see e.g. (Sørensen 2009) and (Sørensen & Toft 2010). The framework is illustrated on a generic level.

Describing wave energy devices in general terms is a challenging task, as a very large variety of device types exists. Over the years many different attempts have been made to categorize the various machines—but most of these have failed to include all of the devices which are being developed. However, a very general description of the various devices could be made by describing the various components of the devices, which in most cases have many similarities across the various devices. An attempt to make such a component based description is given in “EquiMar WP5, Luke” (Myers et al., 2011) where the device is divided into 4 subsystems:

- Reaction subsystem (foundation or moorings, the structural reference elements)
- Hydrodynamic subsystem (structural elements responsible for the primary power capture,

typically where the wave power is turned into mechanical/hydraulic/pneumatic power)

- Power take-off subsystem (mechanical and electrical elements responsible for conversion of the mechanical/hydraulic/pneumatic power into electrical power)
- Control subsystem (electronic elements including sensors and actuators needed for optimization and control of the power take-off subsystem).

A unique description of an individual wave energy device can then generally be described by a combination of a number of more common components within each of the subsystems. In this way a probabilistic system model for a wave energy device can be built, using a limited number of individual components, for which the probabilistic characteristics then should be known.

The important fact is that the structural integrity and reliability of a wave energy converter is normally related to the behavior of the PTO, and vice-versa. In addition, there are constraints regarding the limited amount of data and the need to achieve the required levels of integrity with low cost.

The overall methodology for assessment of the reliability and the optimum/minimum reliability level for WED can be described by the following items/questions:

1. Reliability modeling of a WED by structural, electrical and mechanical components
2. How to deal with structural reliability, definition of how to derive the safety levels based on risks (all from safety to reputation and costs) and uncertainties
3. Provide reward to the efforts performed by developer of technology to reduce uncertainties during the concept/planning/prototype/testing/pilot phases
4. How to model the reliability through the whole life cycle: fabrication/installation/operation/demolition taking into account information from tests, inspections and monitoring carried out for reduction of uncertainties. This includes how to address the impact of degradation (fatigue, localized stresses, corrosion) and life cycle costs/benefits including the impact of maintenance, inspection and repair philosophies.
5. How different types of calculations for stresses and the associated uncertainties impact on the required safety levels.

The reliability of one wave energy device can be estimated modeling it as a system of components. The model can be extended to include a group of wave energy devices in a larger system. The components are divided in two groups:

- Electrical and mechanical components where the reliability is estimated using classical reliability models, *i.e.* the main descriptor is the failure rate and the MTBF (Mean Time between Failure). Further, the bath-tub model is often used to describe the typical time dependent behavior of the hazard rate. Using e.g. FMEA (Failure Mode and Effect Analysis) or FTA (Failure Tree Analysis), system models can be established and the systems reliability can be estimated.
- Structural members such as steel beams, moorings and foundation (when relevant) where a limit state equation can be formulated defining failure or unacceptable behavior. Failure of the foundation could be overturning. The parameters in the limit state equation are modeled by stochastic variables and the reliability is estimated using Structural Reliability Methods.

Further, an important part of most wave energy devices is the control system which regulates the energy output and limits the loads on the wave energy device components. Failure of the control system can be critical for both the electrical/mechanical and the structural components since the loads on these can increase dramatically. Therefore the reliability of the control system should be included in a reliability assessment of the whole system.

REFERENCES

- Myers, L.E., Bahaj, A.S., Retzler, C., Pizer, D., Gardner, F., Bittencourt, C. and Flynn, J. Device Classification Template, Deliverable D5.2, EquiMar project, 2011.
- Sørensen, J.D. Framework for risk-based planning of operation and maintenance for offshore wind turbines. *Wind Energy*, Vol. 12, 2009, pp. 493–506.
- Sørensen, J.D. and Henrik, S. Toft: Probabilistic design of wind turbines. *Energies*, Vol. 3, 2010, pp. 241–257.

*MS_217 — Risk and reliability analysis for
interdependent infrastructure systems (1)*

This page intentionally left blank

Seismic risk and hierarchy importance of interdependent lifelines: Methodology and important issues

M.N. Alexoudi, K.G. Kakderi & K.D. Pitolakis

University of Macedonia, Thessaloniki, Greece

Department of Civil Engineering, Aristotle University of Thessaloniki, Greece

ABSTRACT: The strong dependence on lifeline and infrastructures is one of the distinctive characteristics of modern societies. Unfortunately, these systems are subjected to several hazards such earthquakes causing important physical damage, property loss, dysfunction to urban activities and serious socioeconomic consequences.

The variability of the type of the interactions (function/physical, collocation, recovery, substitute, cascade, general and logical) between the lifelines and infrastructures under investigation and their inherited complexity makes the assessment of interdependent systems' performance a very challenging issue for advanced seismic risk management solutions. An "efficient" seismic vulnerability analysis and a development of an optimum mitigation strategy requires firstly the quantification, in terms of hierarchy importance, of the interdependencies between lifeline systems in three different periods (prior, during and after the occurrence of a seismic event) and finally the production of the "systemic" fragility curves of interdependent elements.

The "systemic" vulnerability of interacting lifeline elements depends on the vulnerability of individual components, taking into account the way in which the components are connected, and the degree of their interdependency. Both "systemic" fragility curves and vulnerability curves of individual lifelines' components are described in terms of the probability of exceeding, in an independent or interdependent lifeline component, a specific limit state as a function of ground motion intensity.

The aim of the paper is to present appropriate methodologies for the estimation of the seismic risk of "interdependent" lifelines, to discuss the quantification of hierarchy importance of these complex systems comprised by several subsystems and to propose a method to produce "systemic" fragility curves of interdependent elements.

Three different methodologies are illustrated in the present paper to evaluate the "cross impact matrix" which represents the degree of corresponding impact of various "elements"

(lifelines, infrastructures). The proposed methodologies are based on (i) an economic approach (input-output model), (ii) a multi-criteria decision making procedure (Analytical Hierarchy Process: AHP) and (iii) a group decision making approach with linguistic preference relations. For each one of the three methodologies proposed, a description is briefly reported together with the basic assumptions, the important issues and the restrictions.

A major concern for the quantification of lifeline elements' interactions is the description of the typology and the functioning of systems involved, the nature of the reciprocal influence when the specific synergy is evolved (normal, co-seismic or restoration/recovery period) and the importance of the link (slight/strong) between components and systems.

An example of the application of the three methodologies in terms of hierarchy importance for the "interdependent" lifelines of port system facilities can be found in a companion paper in this conference.

The *Input-Output model* comprises a linear, deterministic, equilibrium approach and a framework capable to describe the degree of interconnectedness. One of its main assumptions is that the level of economic dependency is the same as the level of physical dependency. I-O model can be used in national or regional level and with some restrictions in city level if economical data is available. It gives better results in large systems, if coefficients are considered to be constant for a fixed unit of time (static approach); however it should be carefully used in "close systems". This model is better to use as a guideline to the potential cascading effects rather than as a forecasting model. Kakderi et al. (2007) give an application of the proposed methodology through an illustrative example.

The *Analytical Hierarchy Process (AHP)* is listed among the most popular multi-criteria decision making procedures, as with a theoretical robustness it employs simplicity, accuracy, can handle both intangible and tangible criteria and has the

capability to directly measure the inconsistency of the respondent's judgments. AHP combines subjective and objective alternatives into a single measure in a hierarchical framework. The pairwise comparisons of (sub)-criteria or alternatives and the use of Saaty (1989) table to convert verbal expression to numerical values are some of AHP's basic assumptions. Nevertheless, there is a restriction of a maximum number of criteria that can be used and number of lifelines or lifeline elements that can be involved. An early version of the methodology combined with an illustrative example is provided in Alexoudi et al. (2008) research.

The third methodology is based on linguistic (hybrid) geometric averaging operator, for *group decision making with linguistic preference relations*. It can be used in cases where the linguistic preference information provided by the experts does not take the form of precise linguistic variables. Value ranges can be obtained due to the experts' vague knowledge about the preference degrees of one alternative over another. This methodology exploits the opinion of every expert without losing information and precision. Important issues of this methodology are the flexibility to represent and analyse the imprecise/vague information and the easy to handle multiple perception-based judgment intervals instead of providing deterministic preferences. Moreover, no limit of indicators or criteria or size of the group of the experts exist and experts can express their preferences and their ratings using qualitative criteria as considered in linguistic or numerical terms. Using this methodology, the uncertainty of the opinion of the experts is transported in the estimated "systemic" fragility curve. The developed approach is described through a numerical example in Alexoudi et al. (2008, 2009) studies.

The optimum selection between the different approaches depends on available information, quality of data, experience of the experts and the type of lifeline systems involved and the desirable

level of reliability of the performed analysis. Each methodology has its own assumptions, advantages, disadvantages and restrictions that must be carefully accounted for and considered during the evaluation. The final outcome of this paper to give decision-makers the means and capacities to formulate effective risk management based on the quantification (hierarchy importance) of the interdependencies between lifelines and infrastructures and the "systemic fragility curves" for "interdependent" systems.

REFERENCES

- Alexoudi, M.N., Kakderi, K.G. & Pitilakis, K.D. 2008. Advanced fragility curves of Interdependent Lifelines Using Decision Making Process. *Proc. First International Symposium on Life-Cycle Civil Engineering (IALCC'E'08)*, Varenna, Lake Como, Italy, No. 129.
- Alexoudi M., Kakderi K. & Pitilakis K. 2008. Seismic risk of interdependent lifeline system using fuzzy reasoning" Proceedings of the 14th World Conference on Earthquake Engineering (14th WCEE), Beijing, China, No. 06-0122.
- Alexoudi, M.N., Kakderi, K.G. & Pitilakis, K.D. 2009. Seismic risk and hierarchy importance of interdependent lifeline systems using fuzzy reasoning. *Proc. 10th International Conference on Structural Safety and Reliability (ICOSSAR 2009)*, Osaka, Japan, No. ICOSSAR09-0484.
- Kakderi, K., Alexoudi, M. & Pitilakis, K. 2007. Seismic risk analysis of interdependent lifeline systems. *Proc. 4th International Conference on Geotechnical Earthquake Engineering*, Thessaloniki, Greece, No. 1578.
- Kakderi, K., Alexoudi, M. & Pitilakis, K. 2011. Seismic risk and hierarchy importance of interdependent lifeline and infrastructure components within port facilities. Application in Thessaloniki's Port (Greece). *Proc. 11th International Conference on Applications of Statistics and Probability in Civil Engineering (ICASP11)*, ETH Zurich, Switzerland.
- Saaty, T.L., (1989). Decision making, scaling, and number crunching. *Decision sciences*, 20: 404–409.

Modeling cascading failures in ‘systems of systems’ with uncertain behavior

E. Zio

Ecole Centrale Paris and Supelec, Paris, France
Energy Department, Politecnico di Milano, Milan, Italy

G. Sansavini

Energy Department, Politecnico di Milano, Milan, Italy

We consider critical infrastructures (CIs); these are large scale, man-made networked systems, mostly spanning long distances, which grant the continuous production and distribution of goods (e.g. fluids, energy, data) and services (e.g. banking, health care) essential for the welfare and security of modern Society. Such infrastructures are named critical, as any incapacity or destruction would have a debilitating impact on the health, safety, security, economics and social well being (Kröger and Zio 2011).

The full characterization of the vulnerability of CIs requires modeling the dynamics of flow of the physical quantities within the network. This entails considering the interplay between structural characteristics and dynamical aspects, which makes the modeling and analysis very complicated since the load and capacity of each component, and the flow through the network are often highly variable quantities both in space and time.

Functional models are, then, often used to capture the basic features of CIs networks within a weighted topological analysis framework, i.e. disregarding the representation of the individual dynamics of the CIs elements (Motter and Lai 2002; Dobson, Carreras et al., 2007; Zio and Sansavini 2009). These models can shed light on the way complex networks react to faults and attacks, evaluating their consequences when the dynamics of flow of the physical quantities in the network is taken into account. The response behavior often results in a dramatic cascade phenomenon due to avalanches of node breakings.

A characteristic of CIs is that they are highly interconnected and mutually dependent in complex ways, both physically and through information and communication technologies used for data acquisition and control, leading to the concept of “systems of systems” (Rinaldi 2004). This shifts the focus of the research on CIs from single, isolated systems to multiple, interconnected and mutually dependent systems with the additional objective of assessing the influences and limitations which interacting

infrastructures impose on the individual system operating conditions (Zimmerman 2001).

The modeling of interdependent CIs can be carried out in a cascading failure simulation framework which abstracts the physical details of the services provided by the individual infrastructures, while at the same time capturing their essential operating features and interdependencies, and examines the emergent effects of disruptions, with the associated downstream consequences (Newman et al., 2005; Zio and Sansavini 2011). Interdependencies are modeled as links connecting nodes of the interdependent systems; these links are conceptually similar to those of the individual systems and can be bidirectional with respect to the “flow” between the interdependent networks.

In this paper, the modeling of interdependent CIs is carried out in a cascading failure simulation framework which accounts for the physical specialization of the components and their interdependencies. The propagation of cascading failures in the 380 kV Italian power transmission network (TERNA 2002, Rosato, Bologna et al., 2007) is taken as reference example; its components are physically specialized in “generators” and “distributors”; the effects onto two interdependent CIs (communication and transportation networks) are investigated, whereby the interdependencies are modeled as “physical”, “cyber”, “geographic” and “logical” (Rinaldi et al., 2001). The analysis focuses on cascading failures triggered by the intentional removal of a single component, e.g. due to a malicious attack.

Inaccuracies in the values of the parameters of the cascading failure model may lead to erroneous estimations of the effects that a failure has on the system. Therefore, uncertainties in the model parameters are propagated through, within a probabilistic representation framework.

The influence of the systems operating safety margins on the consequences of the cascade is assessed. The knowledge gained from this analysis can help setting the value of the operating safety

margin so as to limit the consequences of cascading failures in the CI.

For the interdependent CIs case, the extent to which the interdependency parameter, i.e. the interdependency strength, affects the cascade propagation is assessed for various operating safety margins, μ_{α} . Once the operating safety margin is known, the systems can be designed or operated, tweaking the interdependency strength, μ_{cr} , to limit the maximum average connectivity loss, C_L or service loss, ΔE_{glob} .

The rankings of the most critical components in each one of the three considered CIs are provided, based on the magnitude of the disruption caused by the removal of the substations in the power transmission systems and of the communication nodes, respectively. It turns out that the nodes linking the northern and the Tyrrhenian sections of the networks and the Adriatic and the Tyrrhenian sections of the networks are the most critical. These rankings show that nodes which could be thought as most critical because of their high congestion or connectivity, are not always associated with the largest consequences following their removal. This points to the fact that the physical characterization of the components and interdependencies and the introduction of the uncertainties add a further level of complexity to the cascade propagation, so that the system bottlenecks cannot be identified though the static topological analysis alone but they require dynamical simulations.

Future developments of this work will be the modeling of active safety systems for preventing and mitigating cascading failures propagations and the analysis of interdependent CIs having their own individual cascade dynamics.

REFERENCES

- Albert, et al. 2004. Structural vulnerability of the North American power grid, *Physical Review E* 69, 025103.
- Batagelj, V. 1994. Semirings for social networks analysis. *Journal of Mathematical Sociology* 19(1): 53–68.
- Dobson, I., Carreras, B.A. et al. 2007. Complex systems analysis of series of blackouts: Cascading failure, critical points, and self-organization. *Chaos: An Interdisciplinary Journal of Nonlinear Science* 17(2): 026103.
- Duenas-Osorio & Vemuru, 2009. Cascading failures in complex infrastructures systems. *Structural safety* 31: 157–167.
- Freeman, L.C. 1978. Centrality in social networks conceptual clarification. *Social Networks* 1(3): 215–239.
- Freeman, L.C., S.P. Borgatti, et al. 1991. Centrality in valued graphs: A measure of betweenness based on network flow. *Social Networks* 13(2): 141–154.
- Johansson & Jonsson, 2009. A model for vulnerability analysis of interdependent infrastructure networks. *Safety, Reliability and Risk Analysis: Theory, Methods and Applications* – Martorell et al. (eds), Proceedings of ESREL 2008 and 17th SRA Europe Annual Conference, 22–25 September 2008, Valencia, Spain, Taylor & Francis Group, London, 2009.
- Kröger & Zio, 2011. *Vulnerable Systems*. Springer London Ltd., London, 2011.
- Latora & Marchiori, 2005. Vulnerability and protection of infrastructure networks. *Physical Review E* 71, 015103.
- Little, R.G. 2002. Controlling Cascading Failure: Understanding the Vulnerabilities of Interconnected Infrastructures. *Journal of Urban Technology* 9(1): 109–123.
- McDaniels, T., Chang, S., Peterson, K., Mikawoz, J. & Reed, D. 2007. Empirical Framework for Characterizing Infrastructure Failure Interdependencies. *Journal of Infrastructure Systems* 13(3): 175–184.
- Motter, A.E. & Lai, Y.-C. 2002. Cascade-based attacks on complex networks. *Physical Review E* 66(6): 065102.
- Newman, M.E.J. & Girvan, M. 2004. Finding and evaluating community structure in networks. *Physical Review E* 69(2): 026113.
- Newman, D.E. et al. 2005. Risk Assessment in Complex Interacting Infrastructure Systems, *Proceedings of the Thirty-Eight Annual Hawaii International Conference on System Sciences*, January 3–6, 2005, Computer Society Press.
- Nieminen, J. 1974. On the centrality in a graph. *Scandinavian Journal of Psychology* 15(1): 332–336.
- Rinaldi, S.M. et al. 2001. Identifying, understanding and analyzing critical infrastructures interdependencies, *IEEE Control System Magazine*, 21(6): 11–25.
- Rinaldi, S.M. 2004. Modeling and simulating critical infrastructures and their interdependencies, *Proceedings of the Thirty-Seventh Annual Hawaii International Conference on System Sciences*, January 5–8, 2004, Computer Society Press.
- Rosato, V., Bologna, et al. 2007. Topological properties of high-voltage electrical transmission networks. *Electric Power Systems Research* 77: 99–105.
- Sabidussi, G. 1966. The centrality index of graphs. *Psychometrika* 31(4): 581–603.
- TERNA. 2002. Dati statistici sull'energia elettrica in Italia. Technical Report. *Terna S.p.A. - Rete Elettrica Nazionale*. (in Italian) <http://www.terna.it/LinkClick.aspx?fileticket=PUvAU57MIBY%3d&tabid=418&mid=2501>
- Zimmerman, R. 2001. Social Implications of Infrastructure Network Interactions, *Journal of Urban Technology*, 8(3): 97–119.
- Zio, E. & Sansavini, G. 2009. Modeling failure cascade in network systems due to distributed random disturbances. *Proceedings ESREL 2008. Martorell et al. (eds): Safety, Reliability and Risk Analysis: Theory, Methods and Applications*. CRC Press, Taylor & Francis Group, London.
- Zio, E. & Sansavini, G. 2010. Modeling failure cascades in critical infrastructures with physically-characterized components and interdependencies. *Proceedings ESREL 2010. Ale et al. (eds): Reliability, Risk and Safety*. CRC Press, Taylor & Francis Group, London.
- Zio, E. & Sansavini, G. 2011. Modeling interdependent network systems for identifying cascade-safe operating margins, *IEEE Transactions on Reliability*, 60(1): 94–101.

Modeling of restoration process associated with lifeline systems and the interdependency due to a seismic disaster

G. Shoji & A. Toyota
 University of Tsukuba, Tsukuba, Japan

Economical and societal activities in a mega city strongly depend on the function of lifeline systems. Hence, physical failures and functional impairment induced in the systems due to a seismic disaster cause severe damage to activities. In order to reduce the damage, appropriate understanding of an overall structure of the related restoration process and improving of efficiency of the process is much important in addition to physical strengthening of the facilities. From the reasons, this paper analyzes scenarios of the restoration process on lifeline systems and the structures of the scenarios in the process are modeled as networks. Five lifeline systems are selected: electric power supply systems (EPSS), gas supply systems (GSS), communication networks (CN), water supply systems (WSS) and sewerage systems (SS).

For analyses, we select the scenarios due to the seismic damage by the North Tokyo Bay earthquake M7.3, which Central Disaster Prevention Council (2005) and Tokyo metropolitan government (2006) assume as one of severe seismic events in Tokyo metropolitan area. Emergency response phase and temporary restoration phase after an event are focused on. By analyzing the disaster prevention plans offered by Tokyo metropolitan government (2007) and the operational plans for disaster prevention by lifeline suppliers and managers (Tokyo Electric Power Company, Inc. 2006, Tokyo Gas Company, Ltd. 2008, Bureau of Waterworks Tokyo Metropolitan Government 2006, Bureau of Sewerage Tokyo Metropolitan Government 1998, and Nippon Telegraph and Telephone Corporation Group 2007), all related activities with sectors involved in the restoration process of the lifeline systems are detected in an order of the time series and the relations among their activities with the sectors are defined as scenarios in a table format.

Based on the analyses, we model the structures of the scenarios of restoration process as the network, assuming the restoration activity as a node and the relation of the activities as a link, shown in Figure 1. These network models can be numerically represented by adjacent matrices used in the graph

theory. When there is a relation from restoration activity i to j , the number of 1 is set in (i, j) component on the matrix, and when there is no relation from i to j , the number of 0 is set on the matrix.

Next, by referring the method based on Decision Making Trial & Evaluation Laboratory (DEMATEL) method (Fontela & Gabus, 1974), the sum of components in row i on the adjacent matrix is set as X_i and the sum of those in column i as Y_i . X_i means the total number of relations from restoration activity i to others (total number of ‘active’ relations), and Y_i means the total number of relations that restoration activity i has from others (total number of ‘passive’ relations). Hence, $(X_i + Y_i)$ indicates the degree of importance that activity i plays in an entire structure. We define it as related level R_i (RL) of activity i . On the contrary, $(X_i - Y_i)$ shows the difference between the number of active relations and that of passive ones. We define it as influence level I_i (IL). Then, the coordinates (R_i, I_i) is defined to visualize the network structure.

In order to clarify robustness and weakness of the connectivity of the networks, first, all combinations of the relations (links) from restoration activity (node) i to j are detected, second, the minimum

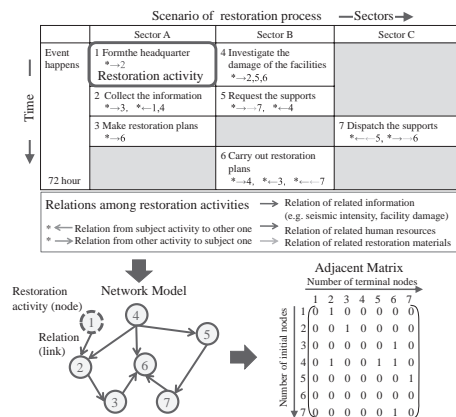
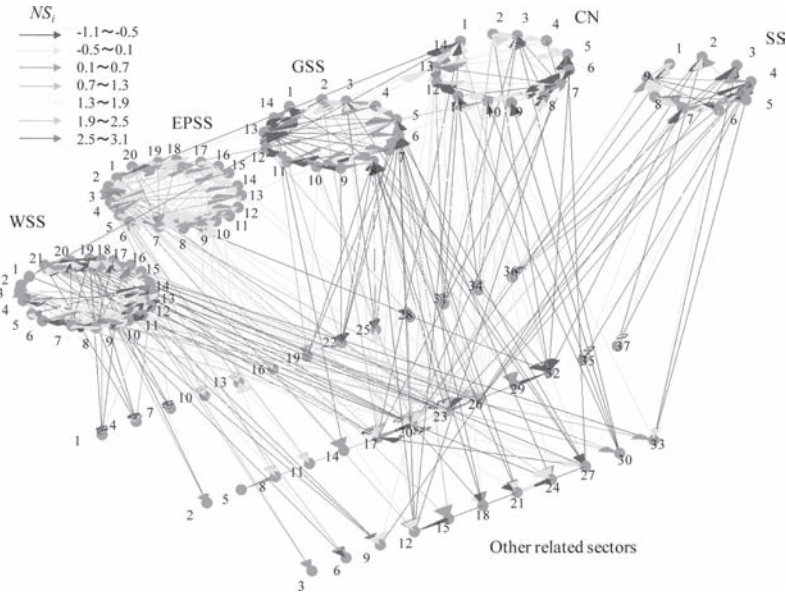


Figure 1. Quantitative modeling of scenarios.



Electric Power Supply System	11 Disaster Prevention Section	13 Construction Section	12 Other Electric Power Companies
1 Headquarters (Chairman)	12 Energy Resources & Production Section	14 Water Supply Operation Center	13 Tokyo Fire Department
2 Information Section	13 Plant	15 Water Quality Management Center	14 Ministry of Economy, Trade and Industry
3 Public Information Section	14 Information Technology Section	16 Emergency Water Service Squad	15 Electric Power System Council of Japan
4 Operational Section	Communication Network		16 Japan Meteorological Agency
5 Power System Section	15 Head Office	17 Water Resources Administration Office	17 Metropolitan Police Department
6 Logistics Section	16 Network Control Center	18 Branch Office	18 The Japan Gas Association
7 Welfare Section	3 Information Section	19 Service Station	19 Japan Coast Guard
8 General Affairs Section	4 Restoration Section	20 Purification Administration Office	20 Headquarters for Disaster Countermeasures of Tokyo Metropolitan Government
9 Branch Offices	5 Access System Section	21 Construction Office	21 Sewerage System
10 Nuclear Power Station	6 Station System Section	Sewerage System	
11 Thermal Power Office	7 Branch Office	1 Headquarters (Chairman)	22 Group Companies of Gas Supplier
12 Construction Office	8 Construction Section	2 Secretariat	23 Ministry of Land, Infrastructure, Transport and Tourism
13 Thermal Power Plant	9 Customer Section	3 Headquarters Meeting	24 Local Government
14 Transmission Office	10 General Affairs Section	4 Logistics Support Section	25 Tokyo Metropolitan Government Bureau of Port and Harbor
15 Remote Control & Maintenance Office	11 Information Section	5 Management Section	26 Cabinet Office
16 Sub Office	12 Sub Office	6 Construction Section	27 Self Defense Forces
17 Customer Center	13 Customer Section for repair	7 Sewerage Office	28 Tokyo Metropolitan Government Bureau of Construction
18 Central Load Dispatching Center	14 Mass User Section	8 Water Reclamation Center	29 Ministry of Internal Affairs and Communications
19 System Load Dispatching Center	15 General Affairs Section	9 Construction Office	30 Financial Sectors
20 Branch Office of Load Dispatching	Water Supply System		31 Transporters
Gas Supply System		Other Related Sectors	
1 Public Information Section	1 Headquarters (Chairman)	1 River Administrators	32 Press
2 General Affairs Section	2 Headquarters (Sub Chairman)	2 Material Manufacturers for Water Pipelines	33 Group Companies of Telecommunication Supplier
3 Personnel Affairs Section	3 Headquarters Meeting	3 Japan Water Works Association	34 Fuel Companies
4 Accounting Section	4 Emergency Mission Meeting	4 The Associated General Contractors of Tokyo	35 Sewerage Managers of Disaster Contract Cities
5 Logistics Section	5 Emergency Personnel	5 Ministry of Health, Labour and Welfare	36 Telecommunication Contractors
6 Local Administration Section	6 Information Section	6 Water Suppliers of Contracted Cities	37 Japan Sewerage Works Association
7 Customer Section	7 General Affairs Section	7 Water Works Contractors	38 Construction Companies contracted with Sewerage Supplier
8 Branch Office	8 Personnel Section	8 Conference of the Electric Power Supply in East Area	
9 Pipeline Network Section	9 Logistics Section	9 Group Companies of Electric Power Supplier	
10 Pipeline Management Section	10 Emergency Water Supply Section	10 Volunteer	
	11 Restoration Section of Purification Facilities	11 The Central Electric Power Council	
	12 Restoration Section of Distribution Facilities		

Figure 2. Model of interdependency among all sectors associated with the restoration process of lifeline networks.

path sets are computed for the combinations (node pairs). After carrying out the procedures for all node pairs of the activities, the frequency that the relation on the pair becomes the minimum path sets is computed for all node pairs. Finally, cumulative number S_i that the relation on the pair is selected as minimum path sets from the viewpoint of a link, is computed for all links.

From the analytical procedures above, the interdependency of the restoration process is modeled quantitatively as the network shown in Figure 2. The connectivity between the activities in the restoration process is measured by the following normalized index.

$$NS_i = \frac{S_i - \mu_{S_i}}{\sigma_{S_i}} \quad (1)$$

where, μ_{S_i} is the mean of S_i and σ_{S_i} is the standard deviation.

From the derived model strong and weak relations on information, human, and material resources in the restoration process between various sectors involved in management of lifeline systems are shown and interconnected.

A new modeling approach for resolving CI interdependency issues

Cen Nan & Wolfgang Kröger

Laboratory for Safety Analysis, ETH Zurich, Zürich, Switzerland

Critical Infrastructures (CI) deserve increased attention as our societies simply rely on most of the goods and services they are expected to continuously supply. Modern CI, such as systems for electricity generation/transmission/distribution, transportation, and information/communication are all large, complex and particularly interacting with each other. The interactions might trigger interdependency issues, which are hard to tackle, leaving CI ever more vulnerable. A failure within any CI or even loss of its continuous service may be damaging enough to society and the economy while cascading failures across CI-boundaries have the potential to cause multi-infrastructural collapse with unprecedented consequences. This has been demonstrated and highlighted by numerous major incidents such as several large-scale power black-outs (2001–2006). It is vital to get a clear understanding of CI interdependency issues and try to resolve them by applying advanced techniques.

The importance of minimizing cascading effects and identifying hidden vulnerabilities caused by interdependencies has been recognized and accepted, not only by governments but also by the public, as a topic of CI Protection (CIP). The purpose of the protection is not just to identify causes of failures and prevent them but also to halt ongoing cascading or escalating events before they affect other infrastructures. Hurricane Katrina, a natural disaster that occurred in August 2005 taking approximately 1,836 lives in the affected areas and resulting in more than \$100 billion US dollars damage loss, was not preventable [1]. However, the damage could have been minimized, possibly if interoperability problems had been recognized before Katrina and, therefore, less infrastructures had been affected.

In recent years a great effort has been devoted to study and analyze interdependencies between CI through a number of model/simulation approaches, e.g. [2] and [3]. Among these approaches, *Complex Network* (CN) theory and *Object-Oriented Modeling* (OOM) have been widely recognized as the two most promising approaches for performing interdependency analyses that primarily focus on complex systems such as CI. However, the CN theory approach alone lacks the ability to capture

uncertain characteristics of an infrastructure and is unable to model event-driven links such as an instant command sent from the *Supervisory Control And Data Acquisition* (SCADA) system to the *System Under Control* (SUC) in case of an emergency. The OOM approach demands a higher hardware configuration in order to achieve a faster simulation speed and increases the complexity of the simulation platform due to large number of parameters defined for each object. Models/Simulations based on both approaches have been challenged by two major technical difficulties: the lack of the performance and the lack of the simulation interoperability.

A new hybrid approach integrating different modeling/simulation techniques in an architecture of distributed network is presented in this paper. This approach will not just improve the efficiency/flexibility of each developed simulator but also decrease the complexity of the overall simulation platform. Each sector or infrastructure specific simulator will only be developed to represent its own system characteristics at the *application layer*. The information and control commands exchanged between simulators will be interpreted and processed at the *communication layer* over the network connection. The promise of this approach is to unveil relevant insights into causes of interdependency related vulnerability, cascading effects of system failures, and dynamic behavior of systems under abnormal situations. Better understanding of cascading infrastructure behaviors and negative impacts of system (infrastructure) interdependency can be achieved by observing simulations after setting up test scenarios at various domain-specific simulators. As a result, possible consequences of negative impacts and how a failure propagates from one system (infrastructure) to another system (infrastructure) can be visualized during the simulation. After analyzing simulation results, it is possible to improve the stability of systems in order to raise their resilience against cascading failures caused by interdependency and thus protect the infrastructure in the long run.

In order to implement the communication layer of the proposed approach, the HLA (High Level Architecture) simulation standard, which is

a general purpose high level simulation architecture/framework to facilitate the interoperability of multiple-types models and simulations, is adopted for the purpose of ensuring efficient information exchange between simulation components during the simulation.

To demonstrate the feasibility and the capability of the proposed hybrid modeling approach as a method to study and understand interdependencies within and between CI, an HLA-compliant experimental simulation platform, which is part of an ongoing broader-scale project in the area of CI vulnerability and interdependency studies at ETH Zurich, is being developed. Currently, the experimental platform consists of three major simulation components: EPSS (Electric Power Supply System) simulator, SCADA (Supervisory Control and Data Acquisition) simulator, and Central RTI (Run Time Infrastructure). Several experiments including a feasibility experiment and a failure propagation experiment have been designed and conducted on the experimental platform. According to the results gained from already completed

experiments, we conclude that the proposed modeling approach has the capability to represent interdependencies within and between infrastructure systems and therefore can be used as a method to analyze interdependency-induced vulnerabilities and resolve negative issues caused by them.

REFERENCES

- [1] *A FAILURE OF INITIATIVE: Final Report of the Select Bipartisan Committee to Investigate the Preparation for and Response to Hurricane Katrina*, Washington, 2006.
- [2] Apostolakis, G.E. and Lemon, D.M. "A Screening Methodology for the Identification and Ranking of Infrastructure Vulnerabilities Due to Terrorism," *Risk Analysis*, vol. 25, no. 2, pp. 361–376, 2005.
- [3] Setola, R. De Porcellinis, S. and Sforna, M. "Critical infrastructure dependency assessment using the input-output inoperability model," *International Journal of Critical Infrastructure Protection*, vol. 2, no. 4, pp. 170–178, 2009.

*MS_227 — Risk and reliability analysis for
interdependent infrastructure systems (2)*

This page intentionally left blank

Models of interdependence propagation for the fragility assessment of urban networks

Isaac Hernandez-Fajardo & Leonardo Dueñas-Osorio

Department of Civil and Environmental Engineering, Rice University, Houston, TX, USA

Urban service networks provide many of the utilities that allow live in modern society. Power, gas, and water networks, are examples of critical elements of urban infrastructure that citizens expect to perform adequately and continuously. In spite of these expectations, growing attention to the functionality, characteristics, evolution, and future of these systems is certainly recent. Concerns about emergent problematic global trends have put pressure on governments and private stakeholders for decisive action on the front of efficient management, and sustainable intervention on these infrastructure elements. When attempting to analyze these systems, an important situation has been highlighted: the presence of interdependence among systems. For stakeholders, the hovering possibility of dealing with potential impacts associated with the malfunction of components in other systems creates a brand-new challenge.

The issue of modeling interdependence is therefore a critical one. This paper focuses in one particular problem on the subject of interdependence models: the influence of a selected damage propagation scheme when the uncertainty of the transmission process is taken into account. The approach in this paper consists on comparing two damage transmission models. The first model is based on an instantaneous paradigm for damage transmission. The second model, a preferential action model, proposes that damage transmission follows specific rules regarding the order on which systems receive interdependent damage. Estimations of systemic fragility functions using both alternatives provide an initial ground for testing the influence of damage transmission methodologies.

In this work, interdependence is modeled using a dual deterministic and probabilistic characterization. The topology of systems' interdependence is described using a deterministic interdependence matrix, Im . In the simplest sense, Im is an modified adjacency matrix representing on its rows the nodes of the controlling (master) system, and on its columns the nodes of the influenced (slave) system. The interdependence representation is completed by a probabilistic parameter called

interdependence strength, I_{str} standing for the probability of damage transmission from a failed node in the master system to a healthy node in the slave network. This joint representation allows to model physical connections, while including the uncertainty associated to the functionality of a dependent node in the event of malfunction of its supply node in an external system.

The mechanisms of damage transmission play an essential role in the process of simulation of interdependence. The objective of a probabilistic systemic fragility assessment is to obtain probabilities of a system exceeding levels of global systemic performance. For interdependent systems, this process includes the fragility propagation from weaker systems to the system under study, in effect merging the inherent and external fragilities into a final interdependent estimate. In the process of Monte Carlo simulation, three steps are followed for determining the stable operational conditions of interdependent systems after perturbation. First, the direct action of the external perturbation is accounted; second, possible disconnection of surviving nodes is assessed; and third, the interdependent damage is identified and propagated among systems. It is in this third step that the damage propagation strategies play an essential role.

Figure 1 illustrates the instantaneous damage transmission. The key step in the procedure is stage 3, where interdependent-induced damage is acknowledged by all interacting systems at the same time. This behavior is essential on inducing instantaneous damage interchange with no account of order in the way that damage is transmitted or received.

In contrast, the preferential damage transmission attempts to reflect order, precedence, and hierarchy in the way interdependent systems manage their interactions. Figure 2 shows how sending and acknowledging damage does not occurs simultaneously, but following a preference rule. This rule will remain for the number of interaction cycles required to arrive to a global stable condition. Note that under this approach, it is possible to have a clique of systems strongly interacting

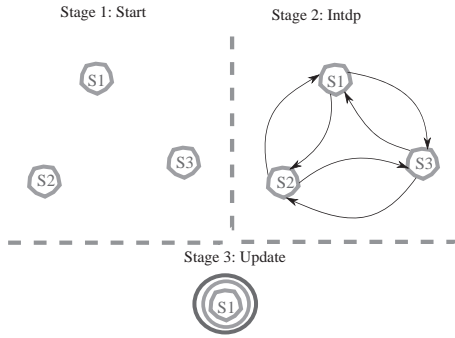


Figure 1. Representation of instantaneous damage propagation. Concentric circles represent systemic status updates taking place.

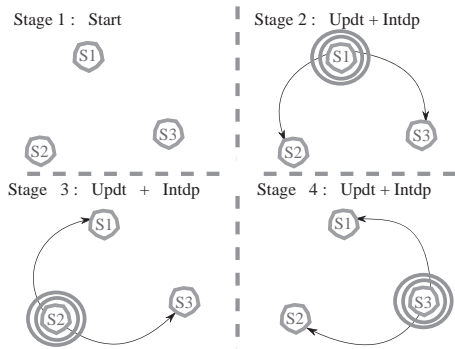
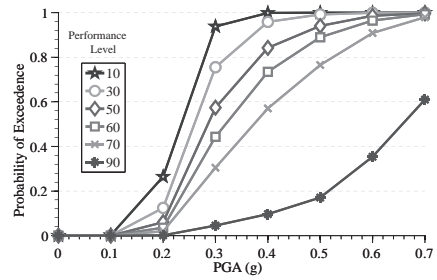


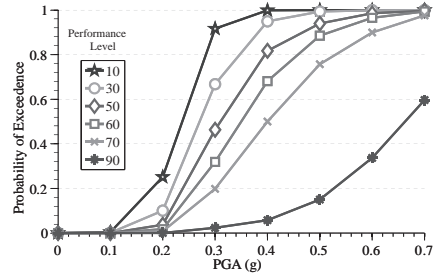
Figure 2. Representation of preferential damage propagation. The hierarchy/order that systems follow for updates is fixed, but it may be altered due to absence of external perturbation.

among themselves, arriving to a stable condition, and only after that, propagating damage to weakly interdependent ones. As a consequence, interdependence strength is affected by the established preference in systemic interactions.

The influence of the two alternatives on interdependence fragility is tested with a set of three interdependent systems. The test example involves a power (S1), water (S2), and gas (S3) networks of comparable size (in both, nodes and links), but different interdependence relationships. The example evaluates the interdependent fragility of the systems when perturbed by different intensities of earthquake hazard. The networks are represented as simple directed graphs, the fragility of the components to earthquake action is obtained from HAZUS-MH, and an integrity-based met metric,



(a) Instantaneous propagation



(b) Preferential propagation

Figure 3. Fragility estimates for water network (S2) under a) instantaneous propagation, and b) preferential propagation.

Table 1. Maximum absolute changes in estimated probabilities of exceedance.

	Interdependence strength, I_{str}				
	0.00	0.25	0.5	0.75	1.0
S1	0.00	0.00	0.04	0.04	0.00
S2	0.00	0.02	0.12	0.10	0.00
S3	0.00	0.02	0.13	0.06	0.00

connectivity loss (CL), is used to measure systemic performance. The two strategies rest on the core of a Monte Carlo simulation program involving 5 000 simulations of hazard action for each nominal intensity. Also, five values of interdependence strength, I_{str} made part of the analysis, 0.00, 0.25, 0.50, 0.75, and 1.00.

Figure 3 presents a sample of the results found. The general conclusion is that there is difference in the estimates produced by the alternative methodologies for damage propagation. Table 1 summarizes the absolute magnitudes of the changes in interdependent fragility found for each system. Noticeably, change is absent when interdependence is deterministic and reaches a peak when interdependence uncertainty is maximum. Explanations for this important trend and others obtained from this analysis are part of ongoing studies on the subject.

On robust decision-making in interdependent economic and infrastructure systems

R. Pant & K. Barker

School of Industrial Engineering, University of Oklahoma, Norman, OK, USA

ABSTRACT: In this paper, we address the problem of risk-based decision-making for interdependent infrastructure systems where uncertainties exist in describing model parameters and in describing the effects of disruptive events, potentially extreme in nature. Many of today's infrastructure systems are interdependent upon each other through exchange of money, information, goods and other important resources. Such interdependence increases the vulnerability of these infrastructures to disasters and man-made attacks. The interdependent nature of US infrastructure and industry sectors has prompted the Department of Homeland Security (DHS) to stress the need to protect infrastructures. Risk managers and decision-makers seeking to prepare for malevolent man-made events, accidents, and natural disasters must appropriately plan for the interdependent nature of today's complex infrastructure systems. Risk studies of infrastructures require the quantification of the disruptive events and the underlying interdependent complexities of the systems. While deterministic treatment of risk and interdependency can provide some initial answers, such analysis has limited scope. Uncertainties arising due to potentially unreliable data and limitations in disaster predictions need to be included in the analysis approach.

We make use of a risk-based interdependency model called the Inoperability Input-Output Model (IIM), which describes how the adverse impacts of a disruptive event propagate through several interconnected industry and infrastructure sectors by disruption-driven demand perturbations. The model provides a risk metric, inoperability, which defines the extent to which a system's functionality is lost, and in this study it helps us to quantify the loss of economic production due to a disruption in services. The IIM is a data-driven model based on economic input-output models that quantify equilibrium infrastructure interdependence in terms of the economic production of goods and services by industry sectors and their usage among other industries and end users. Using the IIM the flow of risk from one affected sector to all the other sectors can be effectively captured.

Since the IIM quantifies risk, we use it to inform risk-based decision-making. Namely, the model helps us quantify the efficacy of various preparedness options that seek to minimize the interdependent impacts of a disruptive event. The total economic loss quantified in terms of sector inoperabilities serves as a suitable metric for measurement of overall impact of inoperability on interdependent systems. One of the considerations of a risk planner is the minimization of the total economic loss resulting from a disruptive event. In this study, this objective is explored to compare different preparedness options that may be developed for interdependent systems. The risk preparedness planning question addresses in this study is

Given control over the upper and lower bounds of demand perturbations of sectors in static demand-loss risk reduction across directly and indirectly affected sectors, what is the best way to control the interdependent propagation of inoperability that minimizes total economic loss?

The lower and upper bounds on demand perturbations are dependent upon preparedness options and help in controlling the sum of losses in a certain number of sectors. The risk planning and management formulation developed in this paper is a linear programming problem that is easy to solve deterministically. We enhance the ability of the formulation to effectively address real-world systems by accounting for data and parameter uncertainties.

Since the IIM is a data-driven model, it contains uncertainties due to inaccuracies in data collection, including source data and assumptions inherent in input-output analysis, such as linearity or proportionality, allocation, and aggregation. In addition, the risk-based parameters such as demand perturbations and initial inoperabilities used in the IIM depend upon events that are often extreme in nature and difficult to understand *a priori*, thus introducing further uncertainty in the optimization problem. Instead of addressing the feasibility of the optimization problem for every possible type of uncertainty, we choose to examine the bounds

for convex uncertainty sets, and are convex. Such formulations allow us to explore robust solutions to the optimization problem in order to examine the extreme uncertainty conditions under which the optimization is feasible. Robust optimization has recently become a significant approach for addressing parameter uncertainty in mathematical programming problems. Often is the case in risk-based decision-making that we seek not the best option but rather to avoid making a bad decision, and decision-making driven by robust optimization can reflect such worst case scenarios.

We address data uncertainties by considering that realizations for each data point belong to an interval around the nominal value provided. This allows us to construct an infinity norm bounded uncertainty set that is convex, computationally tractable and preserves the linearity of the optimization problem. Modeling demand perturbation bounds reflect extreme events which are probabilistic. Hence, instead of being deterministic some of the inequalities have to be treated as probabilistic chance constraints that measure the probability of violating the given inequalities due to the extreme event uncertainties. In order to maintain computational tractability of the optimization problem we provide convex approximations of the probabilistic chance constraints that aim to find Gaussian distributions that bound the probability distribution measuring the chance constraint uncertainty. This allows us to construct a set of inequalities for which feasibility is maintained for

extremes. While, such an approximation leads to conic programming formulation, our problem is still linear because in its structure the data and parameter uncertainties are not coupled in the same inequalities. As such, we are able to formulate a robust counterpart to the optimization problem that is linear and provides us with extreme data and event analysis.

We apply the concepts developed to the study of disruptions to the inland Port of Catoosa in the U.S. state of Oklahoma. Risk-based interdependency analyses of inland port disruptions are notably sparse in the literature. The study is driven by publicly available data. The exports through the Port of Catoosa contribute towards the external demand of the industries in Oklahoma. Hence, in case of a disaster in the port resulting in the loss of exports there is a demand perturbation in the industries that use the port. Maximum demand perturbations are found for each industry as the ratio of that industry's mean estimate of exports to its industry output.

We show that data and parameter uncertainty provides us with a range within which the optimal objective function value will lie. As the uncertainty in the problem is increased, we see the predictive range of the model increases, which is useful for decision-makers as it provides them with an enhanced worst-case analysis.

Our study serves as a useful tool for predicting losses under extreme cases of uncertainty thereby increasing the scope of decision-making.

Broadening the discourse on infrastructure interdependence by modeling the “Ecology” of infrastructure systems

S. LaRocca, S.D. Guikema & J. Cole

Department of Geography and Environmental Engineering, Johns Hopkins University, Baltimore, MD, USA

E. Sanderson

Wildlife Conservation Society

Interdependencies among infrastructure systems arise for many reasons, including, among others, geographic proximity inducing common cause failures, direct dependence for physical flows of information, and common maintenance and repair actions. However, existing modeling of the risk and reliability of interdependent infrastructure generally deals with a limited subset of these sources of dependence, often focusing on only physical flows and geographic proximity. In this paper we show how a modeling construct recently proposed for ecological modeling can be used to give a much broader picture of dependencies between infrastructure systems and the elements of these systems and the effects of these dependencies on the reliability of interdependent infrastructure systems. This approach is based on Muir webs. Muir webs are a modeling approach first proposed for modeling complex, multi-faceted interdependence in a pre-European ecological-human community in the U.S. by Sanderson (2009). Traditional ecological network models focus on predator-prey relationships, the direct analogue to infrastructure interdependence models that focus on physical input-output dependencies. Muir webs generalize from predator-prey relationships to consider broader interactions such as dependencies on biotic but not directly consumed factors (e.g., shade for certain species of trees). They also

include interdependencies due to abiotic factors (e.g., soil types, moisture levels, and climate) and due to human management of the environment (e.g., fire-maintained meadows due to agricultural practices). These factors are considered through a multi-way dependency network describing (1) what factors a given organism depends on and (2) what other organisms and factors depend on a given organism performing its role in the environment. The end result is a directed graph together with probabilities of each of the organisms being present and performing its role as a function of the needed inputs. In this paper we show how a Muir web can be used to represent and model interdependent infrastructure system reliability. The analogy is that each organism in the infrastructure Muir web is either a component of the system (e.g., a pump or valve in a water distribution system) or is a factor needed by some element(s) of the system for it to perform its intended role (e.g., stable soil, a water supply, and proper maintenance, all for a water pump). We then use this expanded representation of the dependencies and interdependencies and demonstrate how to estimate system reliability through a simulation-based approach. This new approach provides a much broader representation and understanding of infrastructure interdependencies.

Geographical vulnerability analysis of interdependent critical infrastructures

J. Johansson

Department of Industrial Electrical Engineering and Automation, Lund University, Lund, Sweden
Lund University Centre for Risk Analysis and Management (LUCRAM)

H. Hassel

Department of Fire Safety Engineering and Systems Safety, Lund University, Lund, Sweden
Lund University Centre for Risk Analysis and Management (LUCRAM)

ABSTRACT: The services that technical infrastructures provide to our society are essential for its function, as highlighted by many infrastructure crises the last decades. These crises also clearly reveal the interconnectedness of technical infrastructures, where malfunction in one infrastructure can spread and cause disturbances in dependent infrastructures. Additionally, due to geographic co-locations, an external event may affect more than one infrastructure simultaneously and give rise to unanticipated consequences. Hence, it is important to proactively address interdependent systems' vulnerabilities in order to find weaknesses before a major crisis highlights them. Several methods are available that address the analysis of interdependent infrastructure vulnerabilities; however, due to the complexity of interdependent infrastructures, each method will only capture some of all relevant aspects of these systems. This coupled with the fact that the research field is rather young imply that different methods and perspectives are necessary to adequately characterize the vulnerability of these systems-of-systems.

An important area of this research field is the development new methods and perspectives for geographical vulnerability analysis. A geographic vulnerability analysis is here seen as an analysis of how well a system is able to withstand strains that expose some geographic area, creating a potential for several simultaneous component failures due to geographic interdependencies (co-locations) between infrastructures. Hazards that may exploit such vulnerabilities include for example flooding, hurricanes, earthquakes, explosions, snowstorms, solar flares and antagonistic threats.

The present paper argues that adopting several analytic perspectives is necessary if the purpose is to achieve a broad vulnerability analysis of interdependent infrastructure systems with respect

to events that may affect a geographical area. The main point of using different perspective is that they can give different and complementing information regarding the systems' vulnerability.

Two main perspectives are addressed and discussed in the present paper: Vulnerability to generic geographical strains, and vulnerability to hazard-specific geographical strains.

The first perspective is concerned with estimating the negative consequences that arise when geographical areas (of some spatial extent) are exposed to strains. This perspective is termed *generic* since no reference is made to specific threats or hazards; instead the focus is on identifying geographical areas, which if they are exposed to strains, independent on the specific hazard, give rise to large negative consequences. One part of this analytic perspective is concerned with single areas that are exposed to a strain. However, in an in-depth vulnerability analysis it may also be interesting to analyze combinations of geographical areas that give rise to large negative consequences if both are exposed to strains simultaneously. Therefore, the second part of this perspective considers vulnerability to multiple geographical strains.

The perspective assumes that all components in an exposed geographic area will fail. However, this is not always the case when considering specific hazards such as flooding, earthquakes, and hurricanes. For example, consider a power distribution system. A moderate flooding will probably not affect overhead lines, whereas strong wind is more likely to. The second perspective therefore aims to analyze the vulnerability of interdependent infrastructures to *specific* hazards (e.g. hurricanes, earthquakes, flooding, and explosion). This perspective of course requires extensive information and knowledge about the characteristics of potential hazards.

There are both benefits and drawbacks with the different perspectives. The purpose of the generic perspective is to enable more general conclusions to be drawn that are relevant to a wide array of underlying threats and hazards—for example identifying areas where several critical components are co-located. A benefit is thus that specific analyses do not need to be performed with respect to each possible hazard type (which may be insurmountable). A downside is that it is not entirely obvious to what extent the conclusions are valid with respect to specific hazards, since hazards not necessarily affect all infrastructures and components similarly.

A benefit of the hazard-specific perspective is that the conclusions of course become more valid with respect to the specific hazard type in focus. But the downside is that a large number of analyses must be performed in order to obtain a broad perspective of geographical vulnerability.

It is advantageous to combine the generic and specific perspectives. The generic perspective provides a broad, initial view of which areas that are most vulnerable to hazards that affect geographic areas. The identified areas can be targeted with in-depth vulnerability studies, for example by performing hazard-specific analyses with respect to the most relevant hazards (e.g. the most frequent ones) and especially targeting the areas previously identified as vulnerable.

A case study of a real interdependent railway system is performed in the paper, with the aim of exemplifying the generic perspectives. The case study makes use of a previously suggested modeling approach for interdependent systems. The modeling approach is based on a separation between the structural and the functional model of each infrastructure system. The structural model consists of the system components (nodes and edges between the nodes), which is essentially the way of modeling complex systems utilized in the field of network analysis. The functional model integrates knowledge about the behavior of the system into the modeling framework, which is essential in order to be able to use the models to draw conclusions about the actual systems of interest. Functional dependencies between infrastructures are captured by specifying dependency edges between the components of the infrastructures. When a failure occurs in a component all its outgoing dependency edges are removed, and the effect of this is evaluated in the dependent infrastructures. The modeling approach can thus capture both escalating and cascading effects. Geographical dependencies are captured by specifying the geographic coordinates of the components, which makes it possible to evaluate

whether a strain exposes several components simultaneously.

The railway system is located in southern Sweden and is owned and operated by the Swedish Transport Administration. It can be described as an interdependent infrastructure system that consists of seven interdependent systems (Train operation, Railway tracks, Signal, Telecommunication, Traction power, Internal power and External power) and dependencies among them. The Train operation represents the railway traffic and is the focus system of the study. The other systems are supporting systems since they provide no direct service to society. Instead the interest is in how strains to these supporting systems propagate to negative consequences in the Train operation—in terms of trains that cannot reach their final destinations.

In the case study, different types of information that can be derived from generic geographical vulnerability analysis are addressed and reflections regarding how this information can be used in vulnerability analyses are made.

There are several ways of developing the generic geographical vulnerability analysis. In the case study, only a single grid was imposed on the geographical area. However, this may be problematic since the criticality of a particular geographical point is sensitive to the exact placement of the grid. A point could be classified as very critical if it falls within a particular grid cell but when the grid is only slightly displaced, the point may not at all be classified as critical. One way to develop the generic vulnerability analysis is therefore to also perform analyses where the grid has been displaced which reduces the sensitivity of the result to the exact placement of the grid.

A common way to approach critical infrastructure protection is to start with addressing hazards that are likely to affect a geographic area of interest. Based on both the expected frequency and the possible severity of the hazards, decisions are made regarding what hazards to consider further. Hazards that have not been identified in the hazards identification phase will then of course not be addressed. This paper argues that perhaps we should start in the other end by looking at the systems' intrinsic vulnerabilities before we address specific hazards. In such an approach the goal is to identify single or multiple components, geographic areas, etc. that given they fail, independent on what particular hazard is the cause, large negative consequences will arise. It is argued that this is a more open-minded approach. Once a good understanding has been gained regarding system vulnerabilities and vulnerable states of the system, an analysis can be performed with the goal of identifying plausible hazards that can exploit these

vulnerabilities, thus expanding the vulnerability analysis into a risk analysis. At the same time, even though no plausible hazard can be imagined, there may be reasons for reducing a particular vulnerability, since in good risk and safety management systems ought to also be well protected against unknown or unidentified hazards. Note that this

paper has only addressed vulnerability analysis, but future research should further address how hazard analysis should be performed as a complement. The overall conclusion of the paper is that generic geographical vulnerability analysis can provide an important complement to more hazard-specific vulnerability analyses.

GS_219 — Risk assessment (1)

This page intentionally left blank

Revisiting risk management in major infrastructure projects— why a socio-technical systems approach makes sense

N.J. Smith & B. Aritua

School of Civil Engineering, University of Leeds, Leeds, UK

C. Clegg & R. Challenger

Leeds University Business School, University of Leeds, Leeds, UK

Earlier research sponsored by the Major Projects Association concluded that major projects are those which are particularly demanding either because of their size, complexity, schedule urgency or demand on existing resources or know-how. The term ‘major’ is relative. For example, a project may involve complex technology while not having high monetary demands. Alternatively, the technology demands may be low but due to schedule urgency and its relation to strategic drivers, it may be a major project in this sense. Inevitably however, major engineering infrastructure projects involve significant investment commitments, involve several organisations with complex relations, require challenging engineering/technological decisions and are often driven by schedule constraints. Moreover, the process of taking an infrastructure project from initial investment decision through to completion and into use is complex, generally bespoke, and fraught.

General systems theory provides the basis for understanding a variety of challenges. General systems theory defines a system ‘as a set of interconnected elements. In this sense, systems theory is a framework by which one can analyze and/or describe any group of objects that work in concert to produce a result. Fundamentally, the major project may be perceived as a system composed of socio-technical sub-systems. Socio-technical systems theory has at its core the notion that a systems can be improved, and indeed can only work satisfactorily, if the ‘social’ and the ‘technical’ are brought together and treated as interdependent subsystems of a wider system. The technical system is associated with the physical infrastructure, technology, processes and procedures while the social system includes issues associated with people and human behaviour, organisational culture and politics and the attitudes/expectations of stake holders. Thus, an endeavour can be thought of as comprising a wide range of interrelated sub-systems, all in a state of dynamic interplay. It is therefore critical

to focus jointly on and optimise both the technical and social subsystems as early as possible.

With regard to risk management in major infrastructure projects, the principle should apply to the entire life cycle. Major infrastructure projects are driven by strategic aspirations. It is therefore important to examine the socio-technical risk elements during the concept, design and construction phases as part of the risk management process. However operational risks should be seriously considered. In a study of major infrastructure in four principal sectors (energy, transport, waste and water), they concluded that operational risks have the potential to undermine the primary reasons for investment in major infrastructure. Society generally takes systems of infrastructure for granted, until they are either disrupted or fail to work. This view is reinforced by several recent events reported in popular media which draw attention to glitches in operation and the associated impact on everyday life of ordinary citizens. Therefore the arguments for a socio-technical approach apply equally, perhaps even more so, to the operational phase.

This is not to say that existing risk management approaches are flawed but to indicate that they are only effective in well defined situations with good quality data and limited uncertainty. The traditional view of project drivers of time, cost and quality being related to the engineering phase only do not seem to hold in major infrastructure projects. The predominant focus of most risk management research and guidance for engineering projects has been on delivering the implementation phase when the actual asset is built. Hence project risk management theory, the guidelines and tools and techniques are largely orientated towards processes and an implicit assumption of controlled environments.

The financial crisis which started having a global effect in 2007 is expected to heighten the role of risk management in most organisations. Some of the most substantial investments that many

organisations make are usually associated with capital infrastructure. Therefore organisations increasingly view risk management in major infrastructure as central to any investment in capital infrastructure. Moreover most major infrastructure projects are undertaken as part of a multi-project environment, hence the need to focus on a whole systems approach to risk management.

The authors believe that effective risk management is likely to result from the closer integration of

technical and engineering processes and the social sciences. The combination of engineering, organisational factors and cognitive systems offers a substantially wider and more appropriate approach to evaluating risk for major infrastructure projects. In developed countries the trend is towards a smaller number of more complex major projects and their strategic management relies upon an effective approach to risk management.

Building owners' requirement for seismic risk communication during structural design

K. Hirata & T. Ishikawa
Japan Women's University, Tokyo, Japan

1 OBJECTIVES

The purpose of decision making for the level of structural performance of a building is to determine the risk of failure in terms of human life and property. Building owners generally have to take the responsibility for the building performance as the buyer; they share this responsibility with professional engineers. However, in general, private building owners have poor experience and knowledge of risks or decision making for the level of structural performance. Structural engineers essentially need to initiate communication with owners about risk-related matters during the structural design procedure.

For establishing an effective risk communication process based on trust, professionals should understand the current requirement of owners and users and then support owners in decision making and improve owner skill.

This paper describes citizens' attitudes, gauged from questionnaires used to establish methods for communicating the risk requirements of houses between owners and structural engineers. Citizens are selected to understand a building owner's requirement because they are likely to become future building or house owners. This survey specifies the contents and requirements of communication to determine structural performance, focusing on owners' reliance on engineers. The goal of such communication is to make reasonable decisions regarding the safety levels required by owners.

A total of 1051 people responded to the web questionnaire survey. The respondents were chosen on the basis of residential location in three major metropolitan areas and eight rural areas in Japan, and their ages ranged from the thirties to the seventies.

2 CITIZEN'S ATTITUDE ABOUT RISK AND COMMUNICATION

This survey defines the developing process for citizens, with three steps in risk communication concerning a building's structural design in Fig. 1.

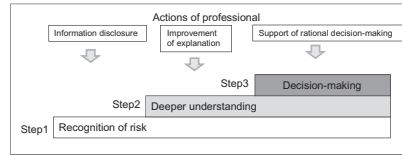


Figure 1. Owner's developing steps in risk communication.

The first step is recognition that risk information disclosure is needed. The second step is the owner's involvement during design procedure for a deeper understanding of risks. The third step is rational decision making on the part of the owners, supported by structural engineers.

The three steps of risk communication depend on the level of the owner's knowledge and involvement. In our previous study, we attempted to determine the current step at which each citizen was (Hirata & Ishikawa 2009, 2009b). This previous study indicated that Japanese citizens recognize the degree of seismic hazards with higher level of accuracy. People need to involve themselves in the decision-making process and receive a large amount of information about safety performances. Therefore, assistance in decision making is required in the future.

Over the 80% of respondents think ambivalent or information shortage. The 80 or 90% of people have positive impressions to understand content of performance and to communicate more with designer. Consequently, while citizens' willingness to be involved in a decision-making process is high, house owners still do not have sufficient rational criteria for making decisions regarding structural performance level or seismic safety level.

To resolve the current situation, the promotion of information disclosure and changes in the attitudes of structural engineers are first required. In particular, 90% of the respondents believe that risk communication is important, underlining its importance.

On the basis of the considerations, citizens require explanations on safety and future hazards or risk. In particular, they feel that there is a lack of

information about the structural performance of a building or house, and they need more information disclosure. In contrast, information on seismic safety performance is currently sufficient for owners in Japan. They have a positive impression of their dialogue with structural engineers. The feeling of reliability for citizens determines the success or failure of risk communication, and that feeling results from the explanations of the structural designer, as demonstrated in the previous step of dialogue. As a result, the respondents have no strong sense of conducting dialogue or decision making. Secondly, the respondents who did not sufficiently trust engineers required dialogue and to make decisions on their own.

Respondents with relief, trust, no relief, or no trust required more explanations or dialogue than all the respondents as a whole.

3 AWARENESS TYPES REPRESENTED BY REQUIREMENT OF DIALOGUE AND AUTONOMY

This figure shows the difference in results for the three groups divided by the high–low requirement for dialogue of respondents. Regardless of the high–low dialogue requirement, the difference in the decision-making ability or trust was small.

The high requirement of dialogue group needs better quality, has high interest and autonomy, and has a positive impression about information collecting during house purchase. The difference was greater for a positive impression of information, autonomy, and interest. On the other hand, for the group that needs dialogues, respondents collect information positively and have autonomy. The active commitment of the respondents is linked to risk communication dialogues.

4 CURRENT STATUS OF RECOGNITION FOR SATISFACTION BETWEEN SAFETY LEVEL AND INFORMATION DISCLOSURE

Current social requirements are shown by two axes: satisfaction with the seismic safety level regulated by law, and recognition of sufficient

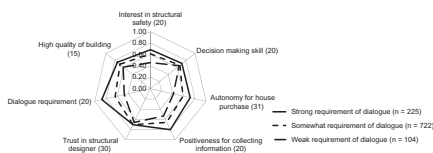


Figure 2. Characteristics of each awareness categorized as per three levels of requirement of dialogue.

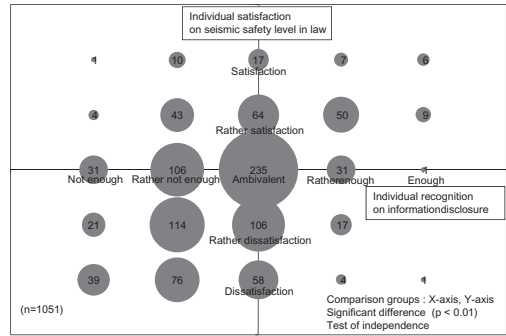


Figure 3. Individual recognition of relief and information disclosure.

information disclosure for understanding the structural performance of a building or house. The public feels less satisfied with safety and do not feel that enough disclosure has been shown; this can be seen from the lower left portion of Fig. 3. There are many people who do not have enough trust or satisfaction. Professionals have to improve public understanding for the people falling in the category shown in the lower left field to the upper right field in this figure. However, time-consuming or overly detailed explanations are not good for busy house buyers. The use of adequate explanations and sufficient communication will improve the current situation. Coordinating with the social needs for safety is important in helping house owners realize that risk communication about structural design is essential.

REFERENCE

- Hirata, K. & Ishikawa, T. 2009. Establishment of risk communication with owners in structural design stage: meeting owner's needs aimed at decision-making with regard to structural performance by consensus with engineers. *Journal of Structural and Construction Engineering (Transactions of AIJ)* 74(644): 1705–1713 (in Japanese).
- Hirata, K. & Ishikawa, T. 2009. Seismic risk communication with owners in structural design. *Safety, Reliability and Risk of Structure, Infrastructures and Engineering Systems, International Conference on Structural Safety and Reliability (ICOSSAR2009)*: 858–864.

Global flood risk assessment of major port cities

N. Lind & M. Pandey

Waterloo Institute for Sustainable Energy, University of Waterloo, Waterloo, ON, Canada
Department of Civil and Environmental Engineering, University of Waterloo, Waterloo, ON, Canada

J. Nathwani

Waterloo Institute for Sustainable Energy, University of Waterloo, Waterloo, ON, Canada
Department of Civil and Environmental Engineering, University of Waterloo, Waterloo, ON, Canada
Department of Management Sciences, University of Waterloo, Waterloo, ON, Canada

ABSTRACT: We consider the problem of assessing the hazards, exposures and risks of flood with respect to lives and assets in major port cities world-wide. Port cities have large concentrations of people and assets. They are a vital part of the global economy. Flood hazard presents an important civil engineering challenge, both in terms of potential loss of life and assets. Flood is among the most consequential problems in public risk management policy. Several recent floods, as in New Orleans in 2005, have illustrated the vulnerability of wealthy and poor societies.

The analysis builds on the study by Nicholls et al. (2007) who gave a global overview of the coastal flood hazard for 136 port cities with a population over 1 million. They produced rankings by hazard and social-economic vulnerability to weather extremes. The 100-year flood area assets were estimated as a function of the population exposed. Long-life assets were taken as five times the population's share of the GDP, losses from flood events five times greater than the GDP of the affected population.

Across all 136 cities about 40 million people are subject to a 100-year coastal flood event. When assets are considered, the distribution is weighted towards developed countries. Our analysis considers 28 of the most seriously affected port cities, each being among the top 20 with respect to assets or population subject to flood or both. The 28 cities span a very wide range of social and economic development.

The Life Quality Index LQI, deriving from the economics of human welfare (Nathwani et al. 2009), allows a comparison of risks on the background of such diversity. The LQI aggregates the expectancy of healthy life e with the GDP per person g calculated at purchasing-power parity. The Societal Capacity to Commit Resources (SCCR = $5\ g/e$ \$/year) to risk reduction, used here for simplicity to aggregate risks, is derived from the LQI.

The countries fall into two distinct groups: Bangladesh, China, Egypt, India, Ivory Coast, Vietnam and Thailand have normalized LQIs under 0.09. Canada, Germany, Japan, Netherlands, UK, and USA have LQIs greater than 0.9. The two groups differ markedly with respect to SCCR, flood protection and population loss rates. Yet, there is little group difference with respect to population, flood area population or asset loss rate.

The expected loss of life conditional upon flooding is the population in the area subject to flooding factored by the loss rate. Each fatality is taken to produce a loss of life years averaging one half of the life expectancy at birth. The total exposure is obtained by either expressing asset loss in terms of life loss equivalent or *vice versa*.

Exposure is not risk; the risk depends on the degree of flood protection and the emergency response capacity. Both must be carefully estimated by detailed analysis for each port city to determine the optimal level of flood protection. Such analysis is beyond the scope of this paper, but the available data provide a first assessment of the risk. The framework can readily serve with updated data for more accurate assessment and decision making.

Risk can be seen from the point of view of an individual exposed, or a member of the community, or the nation as a whole. All such viewpoints have their validity and application; there is no universal criterion to rank cities with respect to flood. The risk is assessed by six criteria: Annual expectation of (1) Fatalities, (2) Asset losses, (3) Annual expectation of life years lost (Figure 1), (4) Total of fatalities and asset losses in equivalent life years (Figure 2), (5) Same total per inhabitant in terms of purchasing-power, and (6) Same, as per cent of the GDP per person. We ranked the cities according to each criterion and determined the corresponding quartiles. Every criterion shows great diversity of risk. Guangzhou has the highest risk in terms

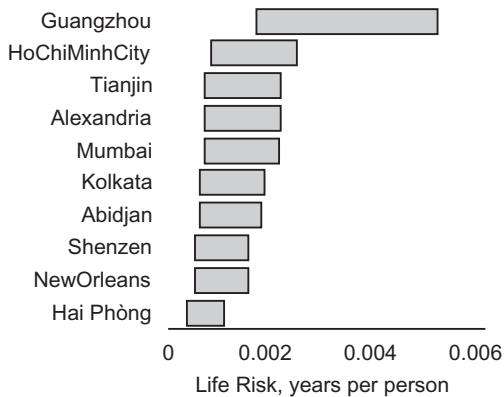


Figure 1. Annual life loss expectation, expressed as life years per year per inhabitant.

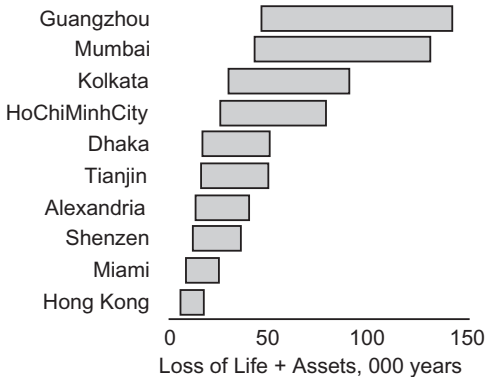


Figure 2. Expected value of the risk to life and asset equivalents per year for the ten urban areas of highest risk.

of total life and asset losses, loss of life years per person, or loss per person as per cent of the GDP per person. Guangzhou is in the highest quartile according to all six criteria. Ho Chi Minh City, Mumbai, New Orleans and Tianjin and are also at high risk according to more than half of the criteria. China has by far the largest population exposed to the flood hazard. Among the 28 cities studied, the quartiles of lowest risk comprise some nine cities. Amsterdam, Fukuoka-Kitakyushu, Hamburg, London, Rotterdam and Tokyo all exhibit low risk according to each of the six criteria.

All data in this study are uncertain, more uncertain than usual in engineering risk analysis for particular locations. Any measure of uncertainty

is itself uncertain. But it is useful to get a rough estimate of the uncertainty in the calculated risks, precisely because of the high uncertainty, to evaluate how robust the possible conclusions may be. The assigned coefficients of variation fall in two sets, with relatively low and high Coefficients Of Variation (COV). Since the latter set is large and dominant, the uncertainty in the former set is ignored if their COV is less than one third (17%) of the higher COVs. The reduced set of COVs used are then the same for all urban areas. To simplify the analysis further we assumed that the variables are approximately lognormally distributed, so that the aggregated risk variables will be approximately lognormal as well. The resulting COVs range for exposure variables from 54% to 59% and for risk variables from 74% to 77%. In spite of these wide error bands, the exposure and risk are concentrated on a few cities. The risk varies 300-fold over the set of 28 cities, from very serious to quite insignificant. Most high-risk locations are in Asia. The risks are generally small in the developed countries.

Flood area assets and flood area population are not good indicators of exposures and risks. Nicholls et al., cautiously call their study a “ranking” rather than exposure analysis. For the exposure analysis we had to make further assumptions, estimating some design return periods. When the accuracy has to be adequate for risk-based decision making, return periods can only be determined by detailed analysis for each urban area individually. The same applies to the loss rates for population and assets. Such estimates, and hence more accurate assessments of exposures and risks, are technically feasible. The risks obtained here are thus preliminary. Our triage (rather than a ranking) gives an indication of the relative and absolute magnitudes of flood hazard measures, indicating where further study is most urgent. If more accurate data become available, a revised set of values is readily calculated by the formulas presented.

REFERENCES

Nathwani, J.S., Lind, N.C. & Pandey, M.D. 2009. *Engineering Decisions for Life Quality: How Safe is Safe Enough?* London: Springer-Verlag.

Nicholls, R., Hanson, S., Herweijer, C., Patmore, N., Hallegatte, S., Corfee-Morlot, J., Chateau, J. & Muir-Wood, R. 2007. *Ranking port cities with high exposure and vulnerability to climate extremes: Exposure estimates*. OECD Environment Working Paper 1, ENV/WKP(2007)1. Paris: OECD.

Assessment of risk to life safety in fire compartments using an adaptive response surface methodology

C. Albrecht & D. Hosser

Institute of Building Materials, Concrete Construction, and Fire Protection, Technische Universität Braunschweig, Germany

INTRODUCTION

Protection of the health and life of the occupants in case of a hostile fire is the main safety objective of Fire Protection Engineering. This objective is achieved by providing for a safe evacuation from the building before the various effects of the fire inflict casualties on the occupants. This requirement of successful evacuation is manifested in nearly all of today's fire codes in countries all over the world. In Germany, this objective is satisfactorily shown by complying with the deemed-to-satisfy prescriptive codes and standards which contain basic material and constructional requirements. Yet, architecture has become increasingly complex during the last decades as advancements in structural engineering as well as material sciences have made it possible to realize such buildings. On many occasions, these advancements have outrun the prescriptive requirements as large atria and other complex geometries cannot not be realized in accordance with the codes. In such cases, shortcomings to the requirements are compensated with so-called performance-based engineering methods as part of a holistic fire safety concept on an individual basis to maintain the required safety level. This is usually shown if the required safe egress time (RSET) is smaller than the available safe egress time (ASET).

METHODOLOGY

As the approach described above is usually applied using deterministic values of an uncertain variable, engineers tend to estimate values on the safe side and thus might end up with overly safe and expensive solutions. The aim of this paper is to compute the reliability of a safe evacuation using a CFD model and a simple evacuation calculation. As a Monte Carlo simulation of a CFD model is not possible due to the high computational costs, a response surface method based on moving least

squares was chosen to minimize the number of necessary solver evaluations.

Reliability analysis

The approach followed herein is a moving least square (MLS) approach which is based on an enhancement of the above concept by Lancaster & Salkauskas 1981 of least squares by incorporating location information to increase the accuracy of the approximation. The approach utilizes a weighting of the Euclidian distance of each support point input vector \mathbf{x}_{mi} to the input parameters \mathbf{x} of the evaluation point so that

$$w_i(\mathbf{x}, \mathbf{x}_{mi}) = w_i(\|\mathbf{x} - \mathbf{x}_{mi}\|), \quad (1)$$

All weights are then compiled into a location dependent weighting matrix $\mathbf{W}(\mathbf{x})$ so that

$$\hat{\beta}(\mathbf{x}) = [\mathbf{H}^T \mathbf{W}(\mathbf{x}) \mathbf{H}]^{-1} \mathbf{H}^T \mathbf{W}(\mathbf{x}) \mathbf{y}. \quad (2)$$

Unfortunately, this leads to a location dependency of the coefficients $\hat{\beta}$ so that no global equation can be found. A MLS formulation has to be found for every evaluation point.

An approach outlined in Bucher 2009, Most & Bucher 2005 uses a nearly interpolating weighting function by introducing

$$w_i(\|\mathbf{x} - \mathbf{x}_{mi}\|) = \frac{\tilde{w}_R(\|\mathbf{x} - \mathbf{x}_{mi}\|)}{\sum_{j=1}^m \tilde{w}_R(\|\mathbf{x} - \mathbf{x}_{mj}\|)} \quad (3)$$

with

$$\tilde{w}_R(\|\mathbf{x} - \mathbf{x}_{mi}\|) = (\|\mathbf{x} - \mathbf{x}_{mi}\|^2 + \varepsilon)^{-2}, \quad \varepsilon \ll 1 \quad (4)$$

where ε is a regularization parameter to stabilize the problem numerically. In order to provide near-accurate solutions ε has to be chosen as small as possible but within machine precision. An ε in the range of 10^{-5} is usually sufficient (Most & Bucher 2005).

As described above, the fitted coefficients of an MLS approach are now location dependent and thus no closed-form global expression is available. Hence, Proppe 2008 recommends the use of adaptive importance sampling (AIS) instead of FORM.

APPLICATION TO A FPE PROBLEM

In the following, the described methodology will be applied to a simple, but representative example from Fire Protection Engineering. The main focus of the problem is to evaluate the reliability of a save evacuation from a simplified assembly room. This is usually shown if $ASET > RSET$ so the the limit state of the reliability problem can be simply taken as

$$g(\mathbf{x}) = t_{ASET} - t_{RSET} \quad (5)$$

which a failure domain $\Omega_f = g(\mathbf{x}) \leq 0$. Both times stem from an evacuation model and a CFD simulation, respectively, and will be evaluated with various random variables shown in the following.

The surrogate model will be constructed for both, fire and evacuation simulation using the response surface formulation described above. Even though a weighting matrix $\mathbf{W}(\mathbf{x})$ including all support points has to be constructed for every evaluation point the assessment is very fast so that a high number of samples can be evaluated with the surrogate—also leading to fast convergence of the AIS algorithm.

In a first step, random samples are drawn from the stochastic model using a random or pseudo-random number generator. The parameter sets are then fed into the surrogate to determine the response and subsequently evaluated with the AIS algorithm. Due to the high number of evaluation points on the surrogate and the high failure probability, a second step in AIS is not required in this calculation.

In a second step, a new design of experiments and thus additional support points are evaluated at the new mean and with the decreased variance of the adapted weighting function $h_2(\mathbf{x})$. Subsequently, an updated surrogate is constructed and a reliability analysis is carried out.

This process is repeated until the failure probability stabilizes, meaning that the difference between the current and the previous iteration is less than 2.5%.

All the steps applied for the visibility were repeated for assessment of the failure probabilities when a less conservative toxicity criterion is used instead of the visibility criterion. Usually,

visibility criteria are used for life safety design as a optical density of less than 0.1/m implies a very low level of toxic gases (Purser 2002) and thus can be regarded as a very conservative criterion.

Looking at the toxicity will provide us with information about the implicit level of safety between the two criteria as toxicity thresholds can be regarded as an ultimate limit state. They imply that upon reaching the threshold level, the remaining occupants are in great danger of becoming unconscious and thus are likely be severely harmed or even die in the fire.

RESULTS & DISCUSSION

The method presented allows for a very fast evaluation of the reliability using complex and numerically expensive computational models such as CFD tools with a very low number of necessary evaluation in comparison to other techniques like i.e. Monte Carlo simulation. The advanced and quasi-interpolating surrogate model allows for a precise approximation of the real limit state hyper-surface without loss of information due to global approximation. This technique also allows for all support points to be included in every iteration and thus will not omit previously evaluated supports in consecutive iterations. It should be noted that the algorithm will work quite well for many models and is even capable of a good representation of complex and noisy limit state hyper-surfaces—with the constraint that enough support points are present. The evaluation of support points is mostly limited by the high computational costs.

The failure probabilities should always be regarded as conditional probabilities, as the hostile fire is not a regular event for a building to be designed for. To compare the safety level against, for example, structural integrity, one has to look at the reference period—which for the latter is usually one year. The results using the optical density as a criterion has shown to be in the same range as the range as the find-ings of Magnusson, Frantzich & Harada 1996.

In conclusion, it should be noted that the results herein are based on very limited available data for the stochastic models; educated assumptions for some parameter uncertainties and distributions as detailed data is currently missing.

REFERENCES

- Bucher, C. (2009). *Computational Analysis of Randomness in Structural Mechanics*. Taylor & Francis Group, London, UK.

- Lancaster, P. & Salkauskas, K. (1981). Surfaces generated by moving least squares methods. *Mathematics of Computation* 37(155), 141–158.
- Magnusson, S.E., Frantzich, H. & Harada, K. (1996). Fire Safety Design Based on Calculations: Uncertainty Analysis and Safety Verification. *Fire Safety Journal* 27, 305–334.
- Most, T. & Bucher, C. (2005). A Moving Least Squares weighting function for the Element-free Galerkin Method which almost fulfills the essential boundary conditions. *Structural Engineering and Mechanics* 21(3), 315–332.
- Proppe, C. (2008). Estimation of failure probabilities by local approximation of the limit state function. *Structural Safety* 30, 277–290.
- Purser, D.A. (2002). *Toxicity Assessment of Combustion Products* (3. ed.). Chapter Section Two, Chapter 6, pp. 2–83–2–171. Quincy, MA: National Fire Protection Association (NFPA).

Effects of uncertainty on the seismic collapse risk of light-frame wood buildings

Yue-Jun Yin

Skidmore, Owings & Merrill LLP

Yue Li

Department of Civil and Environmental Engineering, Michigan Technological University, Houghton, Michigan, USA

ABSTRACT: In the 1994 Northridge Earthquake, the collapse of wood buildings caused about \$20 billion of losses and 24 deaths [1]. Since more than 90% of the residences are wood buildings in the United States (U.S.), it is important to evaluate the collapse risk of wood buildings.

Aleatory and epistemic uncertainties are involved in both the seismic demand and structural capacity. The uncertainty due to the inherent randomness is termed aleatory uncertainty. The uncertainty due to the limitation of human knowledge is termed epistemic uncertainty. A main source of uncertainty comes from the seismic demand. The aleatory uncertainty in earthquake demand exists between ground motions [2] and details of each ground motion [3], while the epistemic uncertainty exists in alternative seismic models. In this study, the uncertainty between ground motion is termed record-to-record uncertainty. The aleatory uncertainty of the structural capacity exists in characteristics of the structure, e.g., the damping, stiffness, mass, energy dissipation, etc, while the epistemic uncertainty represents how good the numerical model represents the actual structure as well as how good the models describe the real structure [4].

Recent studies [5–8] indicate that uncertainties in the structure capacity (termed resistance uncertainty later) have significant influence on the structural collapse risk of steel and reinforced concrete structures. However, it is unclear whether the uncertainty in resistance has a significant impact on the collapse risk of light-frame wood constructions. This topic is investigated in this study, in which both aleatory and epistemic uncertainties are propagated into seismic collapse risk assessment of light-frame wood constructions. A typical residence is assumed to be located at four sites in the U.S. Los Angeles, CA, Seattle, WA, and Boston, MA represent high, moderate and low seismicity areas, respectively. St Louis, MO represents sites in the Central and Eastern U.S.

where typically is referred to as low-to-moderate seismicity region [9].

Figure 1 shows a one-story light-frame wood building that is studied in this paper. The building located in Los Angeles has denser nailing schedule than buildings located in other three sites.

The incremental dynamic analysis (IDA) [10] is performed to examine the record-to-record uncertainty and its effect on the collapse risks of the buildings located at the four sites. Figure 2 shows a set of IDA curves of drift obtained for the one-story building subjected to a suite of 20 ground motions in Los Angeles. It is found that the record-to-record uncertainty caused capacity dispersion, β_{r2r} ranges from 0.31 to 0.5.

Assuming the dispersion of the collapse capacity due to the resistance uncertainty found in an individual shear wall is in the same level as that in the whole building, the south shear wall in the building B is chosen to examine the resistance uncertainty instead of the whole building so that the computational burden can be alleviated. The hysteresis parameters are assumed to be normally distributed. The median values of the hysteresis parameters are determined using the CASHEW program [11]. The coefficient of variation (COV) is assumed to be 0.5 for each parameter. Each hysteresis parameter is assumed to be independent from others. Finally, the resistance uncertainty



Figure 1. One-story light-frame wood building.

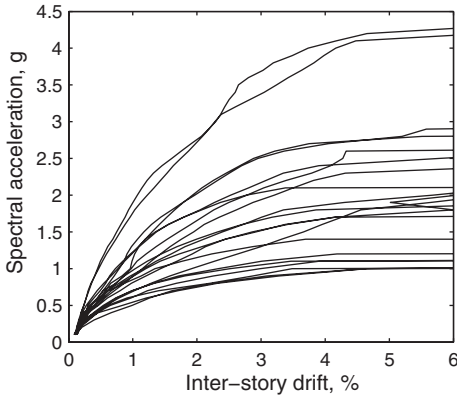


Figure 2. IDA curves of the one-story wood building subjected to the LA 2/50 ground motions.

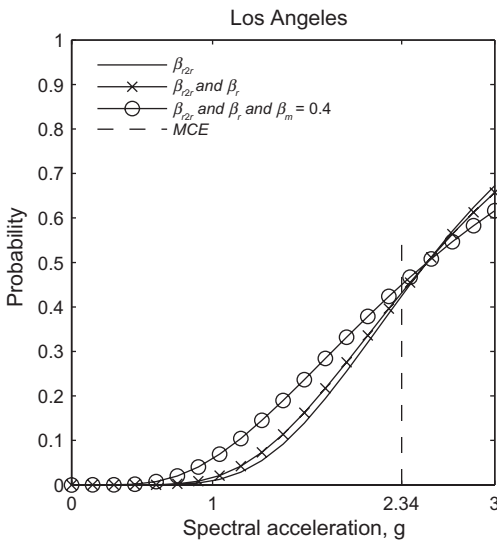


Figure 3. Collapse fragility of the building in Los Angeles.

caused collapse capacity dispersion is determined as $\beta_r = 0.18$.

Using the SRSS, the dispersion of the collapse capacity considering both aleatory and epistemic uncertainties can be determined as $\beta = \sqrt{\beta_{r2r}^2 + \beta_r^2 + \beta_m^2}$ where β_m is the modeling uncertainty. Three levels of modeling uncertainties are assumed in the paper, i.e., low ($\beta_m = 0.2$), moderate ($\beta_m = 0.4$), and high ($\beta_m = 0.6$).

Finally, the collapse risks are evaluated in terms of the collapse probability at the MCE event, the annual and 50-year collapse probabilities. Figures 3 shows the collapse fragilities of the one-story building located at Los Angeles, considering different sources of uncertainties.

REFERENCES

- [1] Yue Li and Bruce R. Ellingwood. Reliability of woodframe residential construction subjected to earthquakes. *Structural Safety*, 29(4):294–307, 2007.
- [2] Dimitrios Vamvatsikos and Michalis Fragiadakis. Incremental dynamic analysis for estimating seismic performance sensitivity and uncertainty. *Earthquake Engineering & Structural Dynamics*, 39:141–163, 2010.
- [3] Keith A. Porter, James L. Beck and Rustem V. Shaikhutdinov. Sensitivity of building loss estimates to major uncertain variables. *Earthquake Spectra*, 18(4):719–743, 2002.
- [4] ATC. Guidelines for seismic performance assessment of buildings, atc-58 50% draft report. <http://www.atcouncil.org/pdfs/ATC-58-50percentDraft.pdf>, 2009
- [5] L. Ibarra. *Global Collapse of Frame Structures under Seismic Excitations*. PhD thesis, Department of Civil and Environmental Engineering, Stanford University, 2003.
- [6] Abbie B. Liel, Curt B. Haselton, Gregory G. Deierlein and Jack W. Baker. Incorporating modeling uncertainties in the assessment of seismic collapse risk of buildings. *Structural Safety*, 31(2):197–211, 2009.
- [7] Bruce R. Ellingwood and Kursat Kinali. Quantifying and communicating uncertainty in seismic risk assessment. *Structural Safety*, 31(2):179–187, 2009.
- [8] Ozan Cem Celik and Bruce R. Ellingwood. Seismic fragilities for non-ductile reinforced concrete frames—role of aleatoric and epistemic uncertainties. *Structural Safety*, 32(1):1–12, 2010.
- [9] David V. Rosowsky, Weichiang Pang, Yue Wang, and Bruce R. Ellingwood. Fragility of conventional woodframe structures built in regions of low-to-moderate seismicity. In *10th International Conference on Structural Safety and Reliability*, 2009.
- [10] Dimitrios Vamvatsikos and C. Allin Cornell. Incremental dynamic analysis. *Earthquake Engineering & Structural Dynamics*, 31(3):491–514, 2001.
- [11] Bryan Folz and Andre Filiatrault. CASHEW—version 1.0: A computer program for cyclic analysis of wood shear walls. Technical report, Division of Structural Engineering, University of California, San Diego, 2000. Report No.: SSRP-2000/10.

This page intentionally left blank

GS_229 — Risk assessment (2)

This page intentionally left blank

Estimation of risk for design of structures exposed to combined effects of hurricane wind speed and storm surge hazards

Long T. Phan & Emil Simiu

National Institute of Standards and Technology, Gaithersburg, MD, USA

ABSTRACT: Hurricane wind speed and storm surge are coupled phenomena. The effects of these natural hazards on coastal structures are interdependent and are highly influenced by local bathymetry and topography. The design of structures in coastal high hazard areas is currently governed by ASCE 7-05 *Minimum Design Loads for Buildings and Other Structures* [ASCE, 2005] for wind and flood loading, and ASCE 24 *Flood Resistant Design and Construction* [ASCE, 2006] for resistance to flood, including high velocity wave action. ASCE 7-05 provides contours of basic wind speeds (3-s peak gusts at 33 ft (10 m) over open terrain) for both non-hurricane and hurricane winds. Non-hurricane winds are based on a nominal 50-year mean recurrence interval (MRI) and hurricane winds are based on longer MRIs dependent on location. ASCE 24 specifies mainly the elevation and foundation requirements for buildings and other structures. Neither ASCE 7 nor ASCE 24 addresses the joint probabilities of hurricane wind speed and storm surge.

Special design criteria that consider the combined effect of wind speed and storm surge have been developed and used in the past for special structures. The New Orleans flood protection system was designed on the basis of design criteria requiring that it resist the loads inherent in the Standard Project Hurricane (SPH). The SPH, developed in 1957 on the basis of analyses of hurricanes of record (from 1900 to 1956), is defined as the most severe hurricane that is considered reasonably characteristic of a region. However, the level of risk inherent in the SPH is not known. The fact that storm surges in Katrina were as high as 28 ft (8.5 m) shows that (1) the coupling between wind speed and storm surge height is highly dependent on local topography and bathymetry, and (2) the SPH is inadequate as a design criterion for protection against possible combinations of wind speed and storm surge height. Thus, at present there is a lack of risk-based design criteria for buildings and other structures in coastal regions subjected to hurricane winds and storm surge. Such risk-based design criteria should be developed by appropriately accounting for the risk posed by the combined effects of joint hurricane wind speed and storm surge events.

This requires consideration of the effects of local topography and bathymetry, on which storm surge at any specific location is highly dependent.

This paper describes a methodology for estimating risk due to combined effects of hurricane wind speed and storm surge. The proposed methodology is applied to the Tampa Bay, Florida region and entails the following three steps:

1. *Simulation and selection of hurricane storm tracks and characteristics:* A stochastic set of hurricane storm tracks is generated, each hurricane being characterized by a set of climatological parameters, including pressure defect, radius of maximum wind speeds, and its track.
2. *Hydrodynamic simulation to generate time histories of wind speeds and storm surge heights:* Time histories of wind speeds and storm surge heights at a site are generated using an appropriate storm surge model and software. For the case studies presented herein we used the software SLOSH (Sea, Lake, and Overland Surges from Hurricanes). The selected hurricanes in step 1 are used to prescribe the environmental conditions in the simulation. In addition to the time histories of wind speeds and storm surge heights, SLOSH also generates time histories of wind direction to allow for consideration of wind directionality. In this work the time histories were saved at 5-min intervals, so that no significant wind speed peaks were likely to be missed, without resulting in an unduly large amount of data. NOAA uses SLOSH to conduct real-time forecasts of potential storm surge from approaching hurricanes and includes these forecasts in periodic hurricane advisories. NOAA, in their advisories prior to Katrina's landfall, predicted based on SLOSH simulation "coastal storm surge flooding of 18 to 22 ft above normal tide levels ... locally as high as 28 ft along with large and dangerous battering waves ... can be expected near and to the east of where the center makes landfall." (Advisory 24 4 PM CDT Aug. 28, 2005), and "storm surge flooding of 10 to 15 ft near the tops of the levees is possible in the greater New Orleans area." (Advisory 26B 8 AM CDT Aug. 29, 2005). These predictions by

SLOSH, while likely to be underestimating the total water depth since SLOSH does not have wave effects represented, appear to be in general good agreement with the observed storm surge heights.

3. *Development of probabilistic descriptions of wind speed/storm surge height events and their effects:* Joint histograms of wind speeds and storm surge heights are developed using the simulated time histories of the wind speeds and storm surge heights. The joint histograms, and the historically-based mean annual hurricane arrival rate at the site, are used to estimate probabilities of exceedance of events associated with certain wind speed and storm surge height at that site, and corresponding MRIs.

The proposed methodology provides a state of the art approach for estimating risk due to combined effects of hurricane wind speed and storm surge with appropriate consideration for the influence of local topography and bathymetry, which could be used to underpin the development of risk-consistent design criteria for coastal structures or other engineering systems, including systems located in the coastal high hazard zones defined by the FEMA's FIRM map and subjected to the combined effect of hurricane wind speed and storm surge. However, the methodology has the following limitations:

The methodology is applicable only if a stochastic set of hurricane storm tracks and a current hydrodynamic model of the area of interest

(SLOSH basins) are available. For the State of Florida, both of these exist, thus design criteria can be developed for the State of Florida using the methodology developed here. Even for Florida the possible evolution in time of the bathymetry of the sites needs to be taken into consideration. Furthermore, changes to the terrain, including both dune building during beach restoration projects and destruction due to hurricane will impact the surge results. For other regions along the eastern seaboard and the Gulf coast, while hydrodynamic models of various basins exist, a public stochastic hurricane simulation model similar to the State of Florida FPHLM may not be available. The wind model simulations performed in this study did not consider variable radial pressure profile shapes that are known to affect the peak wind speed and the radial extent of damaging winds, and also used a relatively small storm motion asymmetry. Subsequent studies should investigate the sensitivity of results to wind models with more detailed physics.

The hydrodynamic simulations performed in this study using SLOSH did not consider the effect of waves and tides, both of which would increase the total water levels. Subsequent studies will need to investigate the feasibility of incorporating wave modeling and consider the effect of tides in the hydrodynamic simulation, and to compare results with other simulation tools such as the Advanced Circulation Model for Oceanic, Coastal and Estuarine Water (ADCIRC).

Risk assessment for road tunnels in Germany—development and application of quantitative methods

Frank Heimbecher

Federal Highway Research Institute (BASt), Bergisch Gladbach, Germany

Bernhard Kohl

ILF Consulting Engineers, Linz, Austria

The national implementation of the European Directive 2004/54/EC concerning the minimum requirements for the safety of tunnels in the trans-European road network (TERN) led to the development and application of quantitative methods for risk assessment of road tunnels in the individual European member states. It was intended to develop methods that facilitate a transparent and traceable analysis and evaluation of the accident risks for tunnel users.

In Germany, the requirements for the operational equipment of road tunnels are regulated in the “RABT” (guidelines for the equipment and operation of road tunnels). The European directive was implemented by an appropriate adaptation of the “RABT”. Risk assessment based on the method presented below now has to be used in specific cases. These include:

- road tunnels that have specific characteristics,
- determining the ventilation system for bidirectional tunnels and
- existing road tunnels, for which retrofitting according to the requirements would lead to disproportionately high costs.

Hence also in Germany a quantitative method for calculating monetarised expected risk values based on accident frequencies and fire simulations was developed. The German risk analysis method was published in the research report FE 03.378/2004/FRG in 2007. This method covers the risk due to the following initial events:

- risk due to car accident
- risk due to fires

The German risk model does not include the risk due to transport of dangerous goods through road tunnels. This risk is covered by a separate approach based on the international ADR tunnel regulations, which is not presented in this paper.

The German risk model allows to calculate two different risk indicators of societal risk for collision risk as well as for fire risk.

- *Expected risk value (EV)*: statistically (in a long term perspective) expected number of fatalities per year and per tunnel (or per tunnel km).
- *FN-curve*: graph depicting the relationships between frequency and consequences (in terms of number of fatalities per event) of the investigated accident scenarios in a double logarithmic scale.

For fire risk as well as for collision risk the frequencies of the individual consequence scenarios are calculated by event trees defined in the risk model. Whereas the consequence values for collisions are also defined in the method (based on statistical accident consequence data), the consequence values for fires have to be calculated individually for the tunnel under investigation.

The consequence model for tunnel fires consists of two elements:

- A smoke propagation model to calculate the propagation of smoke in the tunnel, taking fire development and fire size, air flow conditions (including ventilation) and geometrical conditions of the tunnel into account. For this step commercial CFD-models can be applied.
- A simplified consequence model to calculate the consequence values for fires based on the results of the smoke propagation model; this model applies defined lethality rates in dependence of smoke concentration (different visibility zones).

In order to investigate to what extent a unique specific safety level as reference for the evaluation of the results of a risk analysis could be specified additional research efforts were undertaken. Task of the research project “Sicherheitsbewertung von Straßentunneln auf Basis richtliniengerecht ausgestatteter Tunnel” was to determine the range of risk values for different tunnel types (model tunnels).

Based on results of the research work to the following conclusions can be drawn:

- The application of the German risk analysis method for road tunnels to 8 model tunnels showed comprehensible and traceable results.
- The interpretation and evaluation of the risk analysis results, specifically of FN-curves, is not easy; specific attention has to be paid whether the quantitative risk values represent the whole tunnel or are scaled according to tunnel length.
- Different model tunnels, all strictly designed and equipped according to RABT, show not equal risk levels; hence it is not possible to derive clear and unique quantitative risk reference criteria on that basis.
- Vice versa it can be concluded that some definitions in the guidelines (for instance length criteria for the application of different ventilation systems) could be discussed on the basis of the results of systematic risk assessment studies.
- Especially the sensitivity study of various ventilation parameters lead to interesting results.
 - Tunnels with natural ventilation and high traffic volume show a high fire risk.
 - The expected influence of various ventilation systems can be clearly demonstrated.
- If the implementation of a smoke extraction leads to the change of tunnel cross section (rectangular cross section due to intermediate ceiling instead of a vaulted profile) the positive effect of smoke extraction may be counterbalanced by the negative effect of a lower tunnel ceiling.

Risk assessment for the hazard scenario “Braking action on double track railway bridges”

Charles Fermaud, Frank Stenger & Vasiliki Malioka

Ernst Basler + Partner, Division of Safety and Security, Zollikon, Switzerland

Marcus Schenkel

Deutsche Bahn (DB), Germany

1 INTRODUCTION

The traffic route project Deutsche Einheit No. 8 (VDE 8) connects the cities of Nürnberg, Erfurt, Leipzig/Halle and Berlin with a new or upgraded railway line with an overall length of 500 km. Several sections of the line are already in use. Others are still under planning and construction. The layout of the newly built line includes a great number of viaducts, DB Projektbahn GmbH (2008).

In the course of the project realization, the German Federal Railway Authority (Eisenbahn-Bundesamt, EBA) raised the issue of a specific hazard scenario concerning viaducts: two trains braking with maximum power at the same time and place, while operating on parallel tracks and in the same direction. Additionally, one of the trains must be in the ultimate phase before standstill when the braking power reaches its maximum. As the newly built line allows a parallel train operation, the above hazard scenario cannot be excluded.

The present design of the viaducts accounts for the less demanding hazard scenario of a train braking on one track and of a train starting off in the opposite direction. However, in the previously mentioned scenario, it is expected that the superimposed maximum forces may exceed the resistance of the construction.

The design recalculation of the viaducts has shown that a small number of objects will probably not comply with the new requirements set by EBA. On the one hand, constructional options are being taken into consideration. On the other hand, a risk assessment aims to provide an answer to the question of how relevant, respectively how frequent, the hazard scenario could be.

The present paper aims to present the quantitative assessment of the annual probability of the aforementioned hazard scenario, accounting for the underlying uncertainties of the influencing factors, e.g. train velocity and deceleration, number of trains, train length, causes of braking action etc. For this purpose one of the route's

viaducts is examined, namely the Saale—Elster Viaduct with an overall length of 6.5 km.

The assessment of the frequency of the hazard scenario is, among others, based on the following consideration:

- Frequency of parallel operations, depending on the operational program and the local situation.
- Frequency of maximum braking action of one train as well as dependent and independent braking of a second train.
- Local and temporal occurrence of the braking action on the same considered bridge section.

It shall be noted that the input parameters and hence the results of the analysis presented in this paper hold for the time that the paper is written (October 2010) and are subjected to revision within 2011.

2 THE SAALE—ELSTER VIADUCT

2.1 Viaduct configuration and train movements

The Saale—Elster Viaduct consists of two parts as listed below and as shown in Figure 1:

- a. A two tracks bridge (main line) of 6.5 km in length and approximately 13.9 m in width, on which trains travel between Erfurt and Leipzig in both directions.
- b. A junction line of approximately 2.4 km, which branches off the main line at 2.9 km from Erfurt. Trains travel in the junction line between Erfurt and Halle in both directions. The viaduct's layout consists in principle of two—span sections, each with a length of 44 m between bearings. At some locations either the length of the span is larger or a three or more span section exists.

While most trains traveling on the parallel located tracks will travel in opposite directions, a small number of trains may be traveling parallel to each other. Such cases are not intended

according to the time schedule but could result if for example trains would need to overtake or due to a train delay.

2.2 Viaduct design and the Load case “Braking—Braking”

According to the specifications of the design codes, the viaduct has been designed to withstand horizontal forces imposed from the braking of individual trains on one track, accounting for the case that at the same time a train starts off in the opposite direction on the other track.

However, during a design recalculation process, the German Federal Railway Authority (Eisenbahn-Bundesamt, EBA) raised the issue of a specific hazard scenario (named “Braking—Braking”) relevant for viaducts where parallel train operations are possible: two trains braking with maximum power at the same time and place, while operating on parallel tracks. As the braking force for continuous braking differs from that at the ultimate phase of braking, four different scenarios need to be considered, Table 1. Scenario 4 corresponds exactly to the hazard scenario previously named as “Braking—Braking”. Scenario 1, namely “Ultimate phase—Ultimate phase”, refers to the situation where both trains reach the ultimate phase of braking at the same time and location on the bridge. Finally, scenarios 2 and 3 correspond to the situation of one train reaching the ultimate braking phase while the second train is braking. These cases will be herein referred to as “Ultimate phase—Braking”.

Following an estimation of the imposed forces resulting in the case that the above scenarios take place, see also DIN 1055-100 (2001), scenario 4 has been deemed as not critical and is not further examined. The scenarios though 1 to 3 may lead into forces that the viaduct would not withstand. The assessment of those scenarios in terms of an annual probability of occurrence is the scope of the project.

3 ASSESSMENT FRAMEWORK

The annual probability of the three hazard scenarios is assessed by consideration of the

Table 1. Load scenarios based on the possible braking scenarios.

Train Z1 (normal track)		
	Ultimate phase	Continuous braking
Train Z2 (parallel track)		
Ultimate Phase	Sc. 1	Sc. 2
Continuous Braking	Sc. 3	Sc. 4

events and parameters that are relevant for their occurrence. The general approach is based on the evaluation of event trees, which are built appropriately for the examination of the hazard scenarios. An illustration of the event trees employed is provided in the paper for the aforementioned scenarios.

Each event tree describes the logical series of events leading to the examined hazard scenario for a specific combination of parallel train operations. A combination is defined by the route of the trains during their parallel movement. In total there are eight such combinations examined. For each combination both cases of conditional and unconditional braking, of the train performing the parallel operation upon the braking of the first train, are assessed.

The hazard scenario is described with the help of a limit state function in which the uncertain parameters are modeled as random variables. The estimation of the expected annual probability of the hazard scenario follows from the employment of Monte Carlo simulation of the random variables in the defined limit state. The acceptability of the resulting probability is examined by comparison with acceptance criteria, formulated based on approaches commonly used in traffic safety, e.g. EN 50126 (1999) and Civil Aviation Authority (2006).

ACKNOWLEDGEMENTS

The authors would like to thank the Deutsche Bahn (DB) GmbH for allowing the publication of information regarding the Saale—Elster Viaduct based on the contracted to the Ernst Basler + Partner project “Wahrscheinlichkeit des Lastfalls Bremsen—Bremsen auf Brücken”, Ernst Basler + Partner (2010).

REFERENCES

- Civil Aviation Authority, Safety Regulation Group (UK) (2006). CAP 760 – *Guidance on the Conduct of Hazard Identification, Risk Assessment and the Production of a Safety Case For Aerodrome Operators and Air Traffic Service Providers.*
- DB Projektbau GmbH (2008). *Nürnberg – Berlin, Abschnitt Neubaustrecke Erfurt – Leipzig/Halle.* Streckenkarte, Dezember 2008.
- DB Projektbau GmbH (2008). *Neubaustrecke Erfurt – Leipzig/Halle, Eisenbahnüberführung Saale – Elster – Talbrücke.* 01.02.2008.
- DIN 1055-100 (2001). *Einwirkungen auf Tragwerke: Grundlagen der Tragwerksplanung, Sicherheitskonzept und Bemessungsregeln.*
- EN 50126, CENELEC (1999). *Railway applications—The specification and demonstration of reliability, availability, maintainability and safety (RAMS).*

Regional risk by reliability analysis

M. Mahsuli & T. Haukaas

University of British Columbia, Vancouver, BC, Canada

This paper takes a novel approach to regional risk analysis. Reliability methods are applied in conjunction with multiple probabilistic models for hazard, infrastructure, and loss. A state-of-the-art software is developed to carry out the multi-model reliability analysis. The software is named *Rt* and is freely available online at www.inrisk.ubc.ca. The methodology and the software are presented in another paper by the authors at this conference.

In the example presented in this paper, the seismic risk for the Metro-Vancouver is addressed. All sources of seismic activity that affect this region are considered. This entails three crustal, one subcrustal, and one subduction earthquake sources, each modelled as a separate hazard. Figure 1 is a depiction of these sources visualized in *Rt* by means of its Google Maps® widget. The multi-hazard analysis is carried out by means of two hazard-combination techniques. The first is a time-dependent sampling approach and the other is based on the load coincidence theory.

Each hazard is modelled with a set of probabilistic models that simulate the occurrence, magnitude, location, and intensity of the hazard. In the sampling-based analysis, the orchestrating algorithm establishes a list of time instants when hazards “turns on” or “turns off” during the time period under consideration. Subsequently, starting from time zero, a loss analysis is carried out whenever a hazard turns on. Importantly, the models in this analysis can be time-dependent, *i.e.*, they can account for deterioration and restoration.

The magnitude of the crustal and subcrustal sources is modelled using a doubly truncated exponentially distributed random variable with random parameters. The magnitude of the subduction source is modelled as a user-defined random variable derived from recurrence relations from the literature. A novel model for the location of earthquakes is developed and employed to model the crustal and subcrustal sources, as shown in Figure 1. Finally, the intensity of each source is modelled using the latest ground motion prediction equations available in the literature, which are implemented in *Rt*.

The infrastructure in focus in this paper is the buildings in the Metro-Vancouver region.

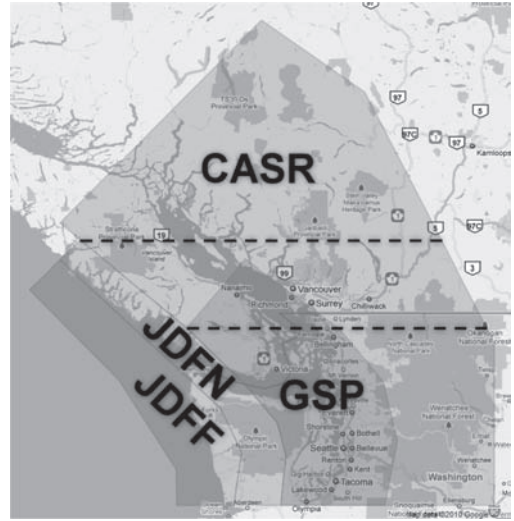


Figure 1. The three crustal earthquake hazard sources, CASR, JDFN, and JDFF, and the one subcrustal source, GSP, visualized in *Rt* through its Google Maps® widget.

Probabilistic models of varying levels of refinement are developed for the loss estimation of the buildings. These are Bayesian models that will be continuously updated as new data and knowledge becomes available. The least refined model computes the economic loss of an entire region (called sector). In a more refined set of models, the building response, damage, and losses are predicted given general characteristics of the building. In both approaches, structural as well as non-structural damage and loss are considered. The entire Metro-Vancouver region is modelled with 33 sector models. Figure 2 illustrates these sectors in *Rt*.

The output of the sampling-based load combination analysis is the probability-loss curve in Figure 3. The loss is accumulated over a time span of 50 years. Each point on this curve indicates the probability of exceeding a certain loss. For instance, the median loss is \$3.2 billion and the probability of exceeding \$54 billion in loss is 10%. In contrast, it is noted that the mean of the total value at stake is \$429 billion.

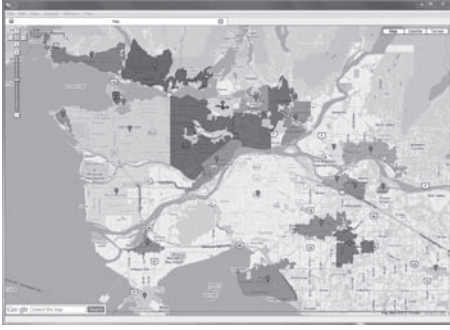


Figure 2. The sector loss models in this study visualized in the graphical user interface of *Rt*.

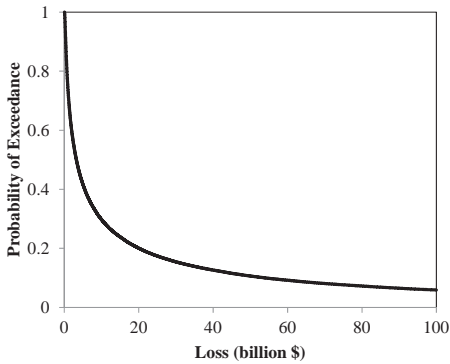


Figure 3. The loss exceedance probability curve from the time-dependent scenario sampling analysis.

The non-smoothness in some of the adopted models, *e.g.*, the ground motion relations, results in discontinuities in the derivative of the limit-state function with respect to certain random variables. In this work, smoothing techniques are employed and implemented in *Rt* to facilitate the use of the first-order reliability method (FORM) under such circumstances. Figure 4 illustrates one of these smoothed models. This facilitates FORM analysis and, subsequently, a load combination analysis based on the load coincidence theory. In this analysis, the failure probability due to all hazards is computed by reliability analysis. The selected limit-state function is $g = 10^{11} - \sum l_i$, where l_i denotes the total loss of the i -th sector. FORM analysis is carried out for all the hazard sources depicted in Figure 1. FORM results in a reasonably accurate reliability index and failure probability for all sources, except for the one that encompasses the Metro-Vancouver region. This hazard source requires second-order reliability method (SORM) to achieve a sufficiently accurate failure probability. The visualization of the limit-state function

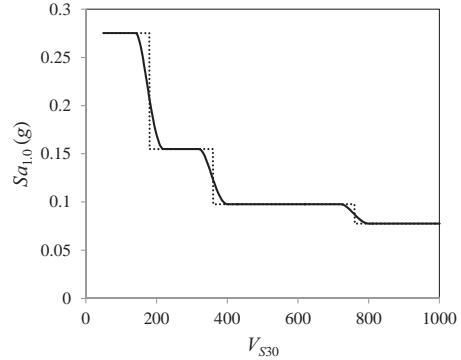


Figure 4. Smoothing the attenuation relation by Atkinson & Boore (2003) against shear wave velocity.

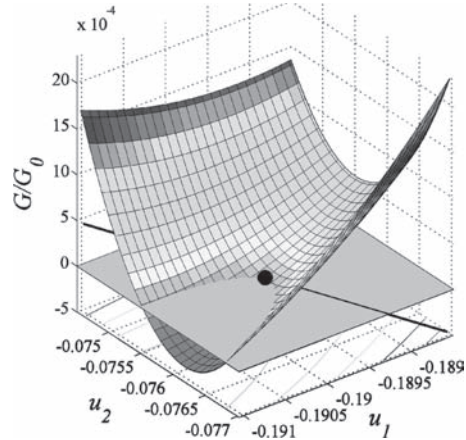


Figure 5. The 3D visualization of the limit-state function. The u_1 and u_2 are the input random variables to the location model of the middle part of the CASR crustal source.

in the standard normal space in Figure 5 shows a strong nonlinearity in the vicinity of the design point (black dot) for this source. This results in the overestimation of the failure probability by linearization (black line). From these FORM and SORM analyses, the probability of the 50-year maximum value of the loss exceeding \$100 billion is 0.0962, corresponding to a reliability index of 1.304.

In summary, the key contributions in this paper are the utilization of reliability methods in conjunction with probabilistic models in large-scale, multi-hazard risk analyses, and the proposition of probabilistic models for earthquake area sources and regional losses.

A probabilistic framework for generic fire risk assessment and risk-based decision making in buildings

G. De Sanctis, K. Fischer, J. Kohler, M. Fontana & M.H. Faber
Institute of Structural Engineering, ETH Zurich, Switzerland

The aim of fire safety engineering is to reduce the consequences, i.e. the human and financial losses, as much as reasonably possible. Risk assessment allows to perform this consistently. According to JCSS (2008) the methodological basis for a complete risk assessment comprises two parts, namely system definition and risk assessment. In the first part the relevant basic conditions are specified, e.g. representation of the system in terms of exposure, vulnerability and robustness (Fig. 1). In the second part there are two tasks, i.e. risk analysis and risk evaluation. Risk analysis includes the development of probabilistic models to calculate the occurrence rates and the consequences of events. Risk evaluation allows optimizing resource allocation related to economic purposes as well as life safety.

Risk indicators are any observable characteristic of a system containing information on the risk and can describe the exposure, the vulnerability as well as the robustness of a system. Identifying those risk indicators is necessary for a generic fire risk assessment for buildings. Other factors which influence the risk are fire safety measures. Passive and active fire safety measures can increase fire safety. Those measures can be regarded as decision alternatives in the context of fire safety management. Risk indicators and fire safety

measures may be associated with uncertainties due to the lack of knowledge and due to randomness. A probabilistic model allows to consider those uncertainties in a consistent way.

Because fires cannot be avoided completely, certain consequences always have to be expected. The expected consequences correspond to the fire risk and can be influenced by fire safety measures. Risk analysis corresponds to the quantification of the expected value of the consequences. To perform risk analysis probabilistic models for the occurrence rates of events and the consequences can be built. Physical probabilistic models describe physical processes in a system represented by parameters, i.e. risk indicators and decision parameters. Based on those physical models and the corresponding probabilistic parameters, the probability of events can be assessed using methods of structural reliability; see Madsen et al. (1986). In complex systems many of those events have to be modeled. Bayesian Probabilistic Nets (BPNs) can be utilized to consider several events together with their causal relations in complex systems; see Jensen & Nielsen (2007).

A basic issue in fire risk analysis is to describe the potential fire spread in a building and its consequences. Typically, in fire safety engineering

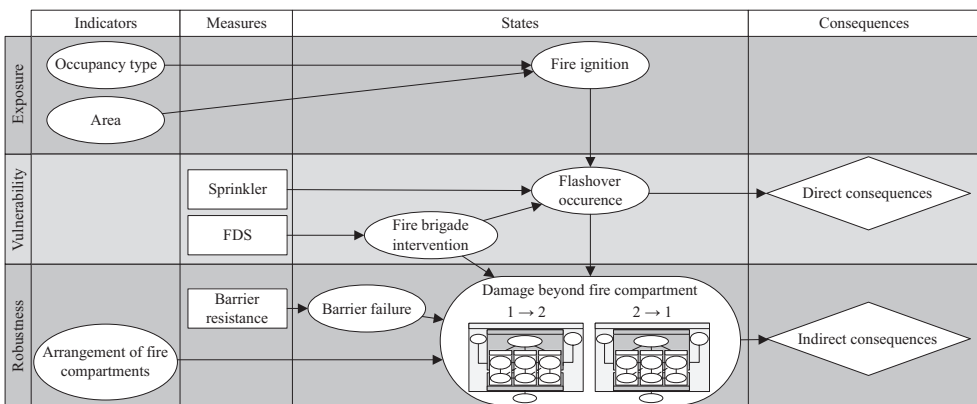


Figure 1. Levels of risk assessment and its causal relations—an example.

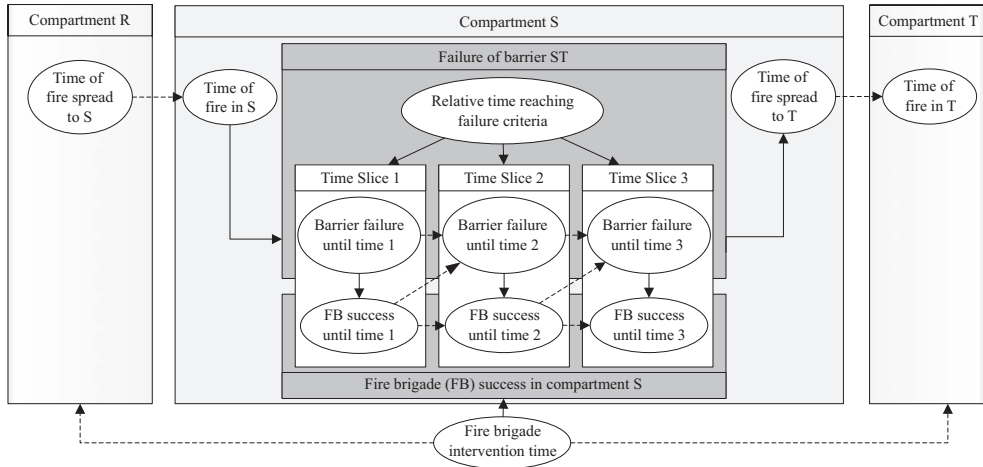


Figure 2. Compartment object and DBPN to model fire spread considering time effects.

scenarios are selected and the consequences for each scenario are estimated. In general scenarios that appear most likely or that may cause major losses are selected. For a quantitative risk assessment it is not sufficient to confine the evaluation to those few scenarios. The risk assessment method introduced in this paper takes into account all possible fire scenarios that may occur in a building. This is done by investigating all possibilities how a fire can spread in a building. Beside this, the presented model for fire spread considers time and space effects using BPNs (Fig. 2). Objects, which represent compartments and contain in- and output nodes are used to model the spread of fire in space. To consider time effects, time slices fulfilling the first-order Markov condition are introduced. Thus, in a time slice the events can be treated as stationary events. A Dynamic Bayesian Probabilistic Net (DBPN) is used to connect the time slices among each other.

Every measure or each combination of risk reducing measures is associated with costs and, due to the corresponding risk reduction, a certain benefit. If the acceptability of fire safety design in terms of risk to life is fulfilled, then it is reasonable to compare the costs of fire safety measures with its benefits, i.e. to perform an economic optimization of the overall costs. The acceptability regarding risk to life can be derived based on the Life Quality Index (LQI). This societal index can be seen as a utility function expressing societal preferences for

investments into life safety (Nathwani et al., 1997). The LQI principle derives acceptability regarding life safety from efficiency considerations. This assessment leads to a choice of efficient fire safety measures regarding risk to life.

The advantage of a generic fire risk model is that it can be applied without further modification for any building where the relevant risk indicators are known, at least within the population of buildings the model has been developed for. This makes generic risk modeling particularly useful for portfolio risk assessment. A fire risk model for a portfolio of buildings can be used for decision-making on a macro level, e.g. for the purpose of code development and calibration or in an insurance context.

REFERENCES

- JCSS. 2008. Risk Assessment in Engineering - Principles, System Representation & Risk Criteria. *JCSS Joint Committee on Structural Safety*.
- Jensen, F.V. & Nielsen, T.D. 2007. *Bayesian Networks and Decision Graphs*, Springer Verlag.
- Madsen, H.O., Krenk, S. & Lind, N.C. 1986. *Methods of Structural Safety*, Prentice-Hall. Inc. Englewood Cliffs, New Jersey.
- Nathwani, J.S., Lind, N.C. & Pandey, M.D. 1997. *Affordable Safety by Choice: The Life Quality Method*. Waterloo, University of Waterloo.

*MS_218 — Risk assessment and decision support systems
for interdependent lifeline infrastructures (1)*

This page intentionally left blank

Optimum interface topologies between urban infrastructure systems

M. Ouyang, L. Dueñas-Osorio & X. Min

Department of Civil and Environmental Engineering, Rice University, Houston, TX, USA

Modern societies are becoming increasingly dependent on critical infrastructures to provide essential services that support our economic prosperity and quality of life. These infrastructures include electric power, natural gas and petroleum production and distribution, telecommunications (information and communications), transportation, water supply, banking and finance, emergency and government services, agriculture, and other fundamental systems and services. Specially, these infrastructures are not alone but interconnected and interdependent at multiple levels. Interdependencies can enhance the overall service performance of infrastructure systems while they can also increase the potential for cascading failures and amplify the impact of small failure into events of catastrophic proportions.

To understand the damage propagation among infrastructures under natural hazards and man-made attacks, many researchers have proposed different methods on the modeling and simulation of interdependent infrastructure systems, such as Agent Based Methods, Inoperability Input-output Methods, System Dynamics Methods, Network or Graph Based Methods and Data Driven Methods. However, these studies mainly focus on the consequence analysis that the critical infrastructure systems undergo following a disruptive event and the analysis of results all show the importance of interdependencies. There are only a few studies on the inverse problem posed as the following question: how to design the interdependent topology (interface) between infrastructure systems to minimize the cascading failure effects as much as possible? To tackle this inverse problem, this paper proposes a flow-based interface design approach to find the optimum interface strategy. This approach includes the following several steps.

First, extract infrastructure topologies and select the operating models. Taking the power grid and gas transmission system as the illustrative example, for power grid, nodes are used to represent power generators and load substations, and links mimic electrical transmission lines between nodes. Due to lack of power injection and lines' susceptance

data, a complex network based betweenness model is used to describe its operating mechanism. For the gas pipeline system, nodes are used to represent gas compressors, gas storage facilities, gas delivery facilities, gas receipt facilities and gas pipeline connection points, and links represent the pipelines. To model the gas pipeline operating mechanism, the maximum flow model is used.

Second, model the hazards and initial failures confronted by each infrastructure. Infrastructure systems are subjected to different types of external or internal disturbances. However, available historical failure data are used to describe the hazards confronted by each infrastructure system. According to the real data, the number of initial failure components in power grid is described by a power-law distribution, and the probability that there is one initial failed pipeline segment is fixed as 1 in gas transmission system under failure cases. Due to the variety and the uncertainty of the disturbance types, the initial failure elements are assumed to randomly select from the system. Also, the hazards on different infrastructure systems are assumed to be independent under a given hazard intensity level (number of initial failure components).

Third, formulate interface design strategies and model interdependencies. Each power-dependent demand node in the gas infrastructure should connect to one or several power supply nodes in the power grid across infrastructure systems. Based on the available topological and geographical information of interdependent systems, three new strategies to design interfaces beyond cost considerations are listed as follows: $ITS_1(\delta)$: Each demand node d_j connects to $\text{floor}(\delta)$ supply nodes with the minimum Euclidean distance, while additional interface links are assigned to important demand nodes (defined in the following context) to realize the average interface link density δ . The δ parameter is also the average number of interface links for each demand node and floor is a function to get the maximum integer less than δ . $ITS_2(\delta, \gamma)$: Each demand node d_j connects to $\text{floor}(\delta)$ supply nodes with the maximum degree while the Euclidean distances between these supply nodes and the

demand node are less than $\gamma * \min_{i \in L_R} (dist(s_i, d_j))$. If the number of supply nodes within this range is less than $\text{floor}(\delta)$, the links are set according to minimum Euclidean distances. Additional interface links are assigned to important demand nodes to realize the average interface link density δ . **ITS₃(δ, γ)**: Each demand node d_j connects to $\text{floor}(\delta)$ supply nodes with the maximum betweenness (load or capacity) while the Euclidean distances between these supply nodes and the demand node are less than $\gamma * \min_{i \in L_R} (dist(s_i, d_j))$. If the number of supply nodes within this range is less than $\text{floor}(\delta)$, the links are set according to minimum Euclidean distances. Additional interface links are assigned to important demand nodes to reach the average interface link density δ . **ITS₄(δ, γ)**: Each demand node d_j connects to $\text{floor}(\delta)$ supply nodes with the maximum reliability based ranking metric while the Euclidean distances between these supply nodes and the demand node are less than $\gamma * \min_{i \in D_R} (dist(s_i, d_j))$. If the number of supply nodes within this range is less than $\text{floor}(\delta)$, the links are set according to their minimum Euclidean distance. Additional interface links are assigned to important demand nodes to reach the average interface link density δ . After determining the interdependent topologies, it is further required to model the interdependent mechanism. A demand node will fail when its attached interface links all fail. The interface links connecting the supply nodes and demand nodes can be out of service due to the collapse of the supply nodes and randomly fail at the same probability as the transmission lines in power grid.

Forth, assess interface effectiveness and find the optimum strategy. To compare different design strategies, an annual cascading failure effect (ACFE) metric is defined under the situation where there is damage passing through the interface and based on the functionality differences of the demand infrastructure between the cases considering only their own hazard intensity and the cases that additionally take into account the damage originating from the supply infrastructure and passing through the interface. However, this metric does not consider the design cost (measured by the interface line length) so that more interface links can obviously bring less CFE. To further consider the effectiveness of the increment of interface length, strategy ITS₁(1) which has the minimum interface length and also can ensure the normal operation of the demand infrastructure is taken as the reference strategy. Then a ACFE-based cost improvement (ACI) metric is defined to describe the decreasing magnitude of ACFE per kilometer increment of interface length.

Finally, taking the power grid and gas pipeline system in Harris County, Texas, USA as an

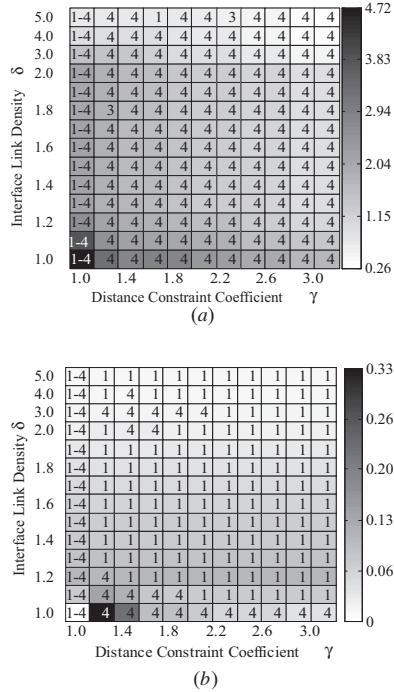


Figure 1. Optimum strategies assessed according to the *ACFE* and *ACI* under different combinations of interface link density δ and distance constraint coefficient γ . The number in each square denotes the index “ i ” of the optimum strategy and the color represents the global effectiveness value of the optimum strategy. “1–4” denotes the four strategies are equally effective. $tp = 1.05$; (a) *ACFE*; (b) *ACI*.

illustrative example, the optimum interface strategies are found and analyzed. Figure 1 shows the optimum strategy under different combinations of interface link densities δ and distance constraint coefficients γ and fixed tolerant parameter $tp = 1.05$ when different effectiveness metrics are used. The results show that if design cost is not considered, the reliability ranking based strategy is the optimum one under a wide variety of conditions; otherwise, the reliability ranking based strategy remains optimal but with specific interface link density $\delta = 1$ and distance constraint coefficient $\gamma = 1.2$. Compared to the reference strategy the reliability ranking based strategy can reduce *ACFE* by 0.9% – 14.3% per kilometer increment of interface length. In addition, assigning redundant interface links for around 20% important demand nodes is an optimum trade-off strategy between pursuing small value of cascading failure effect and large value of cost improvement metric. These results are verified to hold true when power grid operates under different safety margins.

Risk assessment of shutdown of water purification plant caused by Tohnankai-Nankai earthquakes tsunami surge

Masato Nakai

Planning and Coordination Bureau city of Osaka, Osaka, Japan

Masakatsu Miyajima

School of Environmental Design, Kanazawa University, Japan

This paper has reported on the risk of shutdown of water purification plant caused by tsunami induced by Tohnankai-Nankai earthquakes. First, the impact of tsunami surge on the deterioration of raw water quality was studied in an operation process of water purification. Second, an influence of shutdown of rapid sand filter process, and granular activated carbon absorption process was investigated by experimental approach in Osaka Municipal Waterworks Bureau (OMWB). Finally, a strategy of water treatment operation was discussed referring to the concept of Business Continuity Plan.

If the Tohnankai-Nankai earthquakes occur simultaneously, severe damage will be caused in the wide area in Japan. The height of tsunami is about 2.0 to 3.0 m. Moreover, tsunami runs up to the intake tower of water supply system of Osaka Municipal Waterworks Bureau. Therefore, when the Tohnankai-Nankai earthquakes occur, the water intake must stop as soon as possible. The maximum wave height is assumed about O.P. (Osaka Peil) + 5.0 m. The level of embankment in Osaka city is about O.P. + 5.7~7.2 m. The possibility of flood caused by the tsunami therefore seems to be low. However, there are 440 sliding gates to close the gates before reaching tsunami, tsunami will enter to inland area.

The maximum density of the chloride ion reaches 1,020 mg/L at vicinity of the intake of waterworks. The industrial water intake also faces a serious condition of the raw water quality in this case. The density of the chloride ion reaches 8,347 mg/L in the maximum, and the density of the chloride ion exceeds 200 mg/L for about nine hours. The above-mentioned result suggests that the run up of tsunami induced by Tohnankai-Nankai earthquakes seriously affects on the water quality of raw water.

The water treatment flow of OMWB is composed of 8 processes (Fig. 4). If the processing is stopped, a RSF and a GAC become anaerobic

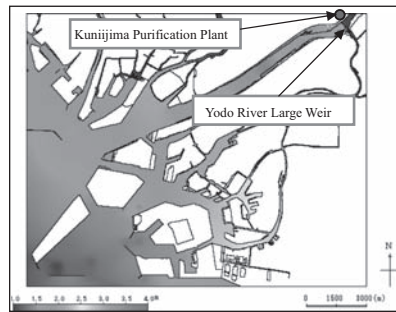


Figure 1. Wave height of Tohnankai-Nankai Tsunami.

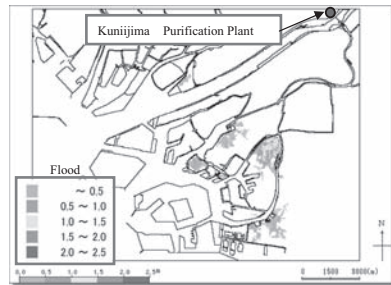


Figure 2. Assumed flood area of Tohnankai-Nankai Tsunami.

condition. Since the treated water quality in both processes deteriorates in this case, the level of deterioration must be studied. The actual plant and demonstration plant for advanced water treatment system (1,000 m³/day × 2 lines) were actually surveyed in order to clarify the influence of the intake stop.

Change of water quality of the stay water in the rapid sand filtration media was investigated in relation to processing stop time. The change of water quality in the filter media is shown in Figures 5 and 6. It is understood that denitrification treatment occurred and the environment of inside of filter media changed to the anaerobic

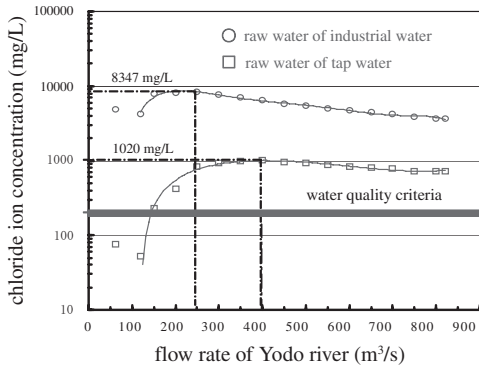


Figure 3. Damage to the raw water quality.

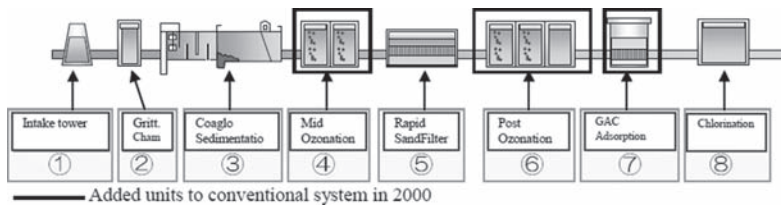


Figure 4. Process schematic of water treatment of OMWB (advanced water treatment system).

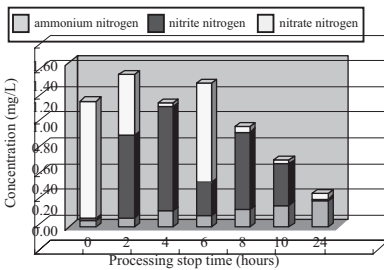


Figure 5. Changes of water quality in the filter media (Sampling depth: 10 cm from the surface, summer).

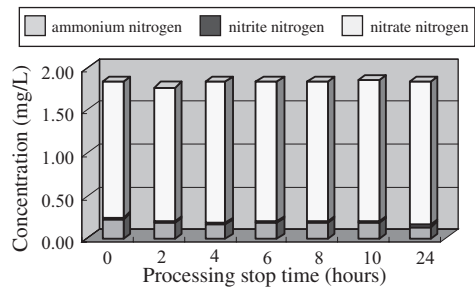


Figure 6. Changes of water quality in the filter media (Sampling depth: 10 cm from the surface, winter).

condition in summer but in winter the influence will be respectively low.

Influence of Tsunami: When Tohankai-Nankai earthquakes cause tsunami run up to the intake of waterworks and it is necessary to stop introducing raw water quickly before the tsunami surge reaches.

Influence to water treatment: If the intake stopped and each process is shutdown, the water quality inside the filter media such as Rapid Sand Filter and Granular Activated Carbon deteriorates and it is necessary to wash the filter media before restarting the treatment in the summer. In contrast to the summer condition, the result suggested the possibility of restart the treatment without washing medias and the lead-time of restarting can be shortened in winter.

Table 1. Three steps of this study.

Steps	Objective	Plant	Condition
Step 1	Grasp of influences on each process by intake stop	Actual plant	Summer, winter
Step 2	Grasp of influences on total system by intake stop (washing the media at the beginning)	Demo. plant	Winter
Step 3	Grasp of influence on total system by intake stop (without washing at the beginning)	Demo. plant	Winter

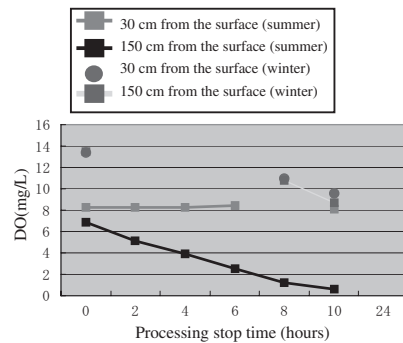


Figure 7. Dissolved oxygen concentration of stay water in filter media (GAC).

Disaster restoration support technologies for electric power distribution equipment

Y. Shumuta
 Central Research Institute of Electric Power Industry, Chiba, Japan

T. Todou
 Tohoku Electric Power Company, Miyagi, Japan

K. Masukawa
 The Chugoku Electric Power Company, Inc., Hiroshima, Japan

T. Ishikawa
 Central Research Institute of Electric Power Industry, Chiba, Japan

1 INTRODUCTION

When large-scale disaster such as a typhoon or an earthquake occurs, because a large number of distribution equipment is installed in all regions, damage is caused not only by the wind force or earthquake ground motion but also by damage to the surrounding facilities. Consequently, it is difficult to avoid equipment damage due to a large-scale disaster, and it is also difficult to accurately monitor and understand the equipment damage conditions while a typhoon is approaching or in the early stages after a large-scale earthquake. For this reason, highly accurate damage estimation technologies are desirable in order to support the emergency restoration work of electric power companies in Japan.

This paper describes a disaster damage estimation system for electric power distribution equipment. The predominant factors associated with the typhoon and seismic damage degree of electric power distribution equipment are clarified based on actual damage records. Based on the results, damage estimation functions for typhoons and earthquakes are proposed. The proposed system for a typhoon (RAMP-T) is actually applied to the Chugoku Electric Power Company. On the other hand, that for an earthquake (RAMP-Er) is actually applied to the Tohoku Electric Power Company. In this paper, two systems are introduced and their effectiveness is discussed.

2 TYPHOON DAMAGE ESTIMATION

Regarding typhoon damage, it was clarified that there was a high correlation between the equipment damage and the following factors: (1) wind velocity v , (2) *Microtopography* B , (3) *Land use condition* T , (4) *Line connectivity type* S , and (5) *Rainfall* $U(\alpha)$.

On the basis of the above results, a typhoon damage function for electric power distribution equipment ($F_{mijk}(z(v))$) is proposed as

$$F_{mijk}(z(v)) = L_m \cdot U_i(\alpha) \cdot B_j \cdot T_k \cdot S_l \cdot f_l(z(v)) \quad (1)$$

where $f_l(z(v))$ = the typhoon damage ratio of equipment with line connectivity type l and equipment dynamic performance $z(v)$ assuming that the maximum wind velocity v affects a 10 m height from the surface of the ground supporting the target equipment. Fig. 1 shows the line connectivity types of electric power distribution poles. This includes an edge pole, a line pole, a cross pole and a T-junction pole.

The details of $z(v)$ are described in this paper. S_j = the modification coefficient evaluated by the line connected type l · B_j = the modification coefficient for the microtopography division j · T_k = the modification coefficient for the land use condition k · $U_j(\alpha)$ = the modification coefficient for rainfall assuming 4 days of cumulative rainfall on the equipment i becomes α , L_m = the modification coefficient for local region m · m indicates an electric power supply area covered by a business branch office.

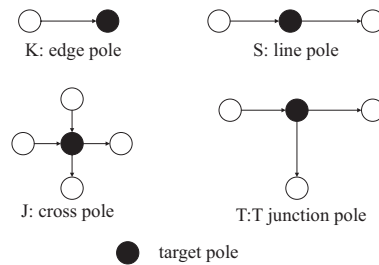


Figure 1. Line connectivity types of electric power distribution poles.

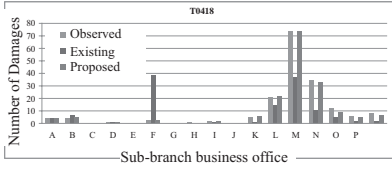


Figure 2. The number of damaged supports at each sub-branch business office due to T0418.

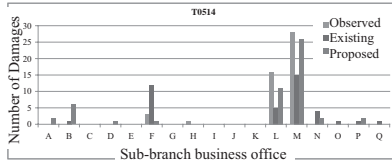


Figure 3. The number of damaged supports at each sub-branch business office due to T0514.

Figure 2 and Fig. 3 compare the number of damaged electric power distribution poles for every 17 sub-branch offices (shown as A to Q) at the Chugoku Electric Power Co. for the 2004 typhoon No. 18 (T0418) and the 2005 typhoon No. 15 (T0515), respectively. T0418 caused the most severe damage among recent typhoons within 10 years, and T0515 included buckets of rain. In Fig. 1 and Fig. 2, the numbers of damaged poles were estimated by the proposed function and the existing one. Both estimated values were compared with the actual numbers of damaged poles. Both figures show that the estimated numbers by the proposed function corresponds to the actual numbers better than that by the existing function. These results suggest that the proposed function enables us to more accurately estimate the damage degree for every sub-branch office.

3 EARTHQUAKE DAMAGE ESTIMATION

Regarding the earthquake damage, it was clarified that the equipment damage is highly correlated with (1) the seismic ground motion intensity including the measured seismic intensity e , (2) the microtopography division associated with the liquefaction potential B , (3) land use condition T , (4) line connectivity type l and (5) seismic countermeasure C .

In this paper, the relationship between the damage ratios of pole transformers with and without pole anchors is analyzed based on the actual damage

records from the 2007 Niigata-Ken Chuetsu-Oki Earthquake. In order to mitigate the seismic damage to the equipment, the Tohoku Electric Power Company has been taking some countermeasures against an earthquake for the electric power distribution equipment. As a result, it was clarified that a pole anchor was highly effective in mitigating the seismic damage to pole transformers.

On the basis of the above result, Eq. (2) is a seismic damage function for the electric power distribution equipment ($F_{mijkl}(z(e))$).

$$F_{mijkl}(z(e)) = L_m \cdot C_i \cdot B_j \cdot T_k \cdot S_l \cdot f_c(z(e)) \quad (2)$$

where $f_c(z(e))$ is the seismic damage ratio for the equipment with seismic countermeasures C and seismic performance $z(e)$ assuming that the seismic intensity e affects the surface ground supporting the target equipment. The seismic performance $z(e)$ indicates the seismic safety margin evaluated by the bending moment of the ground surface at the electric power distribution poles caused by the seismic intensity e defined by (Shumuta et al., 2010).

S_l is the modification coefficient evaluated by the line connected type l shown in Fig. 1. T_k is the modification coefficient for the land use condition k , B_j is the modification coefficient for the microtopography division j , C_i is the modification coefficient for the seismic countermeasure of equipment i , L_m is the modification coefficient for local region m . RAMP-Er produces a database associated with the surface ground condition at each distribution pole defined by the microtopography division, the land use condition correlated with the seismic damage to the surrounding facilities, and the line connectivity type.

The proposed model is applied to the jurisdiction area of Kashiwazaki and Nagaoka sub-branch offices of Tohoku Electric Power Company assuming that an earthquake of the same scale as the 2007 Niigata-Ken Chuetsu-Oki earthquake occurs.

Table 1 shows the comparison of the estimated and observed numbers of seismic-damaged electric power distribution poles. HNA(95) is the estimated result using the actual damage ratio under the seismic intensity 6 with and without liquefaction recorded during the 1995 Hyogo-ken Nambu Earthquake. Aomori(97), Tokyo(97) and Sapporo(97) are also the estimated results based on the damage estimation models using the Aomori, Tokyo, and Sapporo local governments, respectively.

As a result, Table 1 shows that the damaged pole numbers estimated by the proposed model is the closest to the observed damaged numbers.

Table 1. Comparison of estimated results.

	Obereved	HNA(95)	Aomori(97)	Tokyo(97)	Sapporo(97)	Proposed
Kashiwazaki	428	1076	221	259	873	430
Nagaoka	51	794	116	135	126	60

Ethical consideration for appropriate structural safety

J. Kanda

University of Tokyo, Kashiwa, Japan

D.G. Elms

University of Canterbury, Christchurch, New Zealand

1 INTRODUCTION

Structural safety criteria are usually specified in national or regional regulations. They are usually stated as minimum requirements, which could be seen as implying that building owners are encouraged to increase safety at their own expense.

As far as the safety is concerned, buildings are designed against natural environmental loadings such as strong wind, earthquake shaking and snow accumulation. These causes are of natural origin and the possibility always exists of higher values than those shown by past records. An exceedance probability of 1/500 per year is typically used as the minimum requirement criteria.

Since code values are regarded as minimum requirements, they may be neither sufficient nor appropriate for every application within a society. We have to consider the appropriate degree of safety for the client as well as the society, and the two may well be different.

2 THE CONCEPT OF SAFETY

A structure can be regarded as safe if it will not fail during its lifetime. There are two sources of failure: uncertainties in loads and resistances together with modeling uncertainties, and problems arising from errors in design or construction which have not been prevented by quality control procedures. Failure could be structural collapse, but it could equally well be economic damage or functional unserviceability. Typically, when a structure satisfies the design equations, that is, when the design resistance exceeds the design load effects, it is regarded as being safe. The quantification for safety measures always depends on mathematical models and a definition of terms, and the equations for resistance and load effects are based on such definitions. Analytic techniques, both static and dynamic, have been developed to carry out such procedures.

Structural standards have been developed in most countries through the long term efforts of

many engineers and researchers. The international standard *ISO2394: General Principles on Reliability of Structures* provides a common definition for structural safety in terms of the reliability index as a probabilistic measure.

Common mathematical models and physical conditions of structural components and systems are limited. Major approximations and simplifications have to be made, and in any case the reliability index take into account neither uncertainties arising from model limitations nor those deriving from errors. Because of this the reliability index must be regarded as a nominal value. Surveys of damage caused by major earthquakes, for example, indicate some conservatism in the design equation.

3 APPROPRIATENESS FOR SOCIETY

Although engineers can share engineering measures and the probabilistic safety measures, the safety designed into a structure differs between different countries. Economic conditions and cultural backgrounds certainly influence the quality of design and construction. If the client focuses more on money saving rather than on future seismic safety, it is easy to expect to have buildings with different degrees of safety even if they are designed with the same equation. The nominal values for safety measures have rather significant margins to allow for uncertainties and unknown effects which could differ for case by case. There is an underlying assumption that an increase in code factors will result in increased safety. This is by no means clear.

Although the role of engineers is to make a design meet the requirements of the client in one sense, he/she also has to make the structure acceptably safe for society or the surrounding environments. The client's demand is rather flexible as the client's duty to society when building is not clearly regulated or specified.

We believe that professional engineers have an ethical imperative to work to achieve results which are good, rather than merely adequate, and "good"

must include not only the client but also society as a whole, which includes all stakeholders involved with the structure.

We could bring in many issues beyond safety alone, such as cost, environmental issues, versatility, resilience, sustainability and so on, but to do so would lead to formulations which would be too general to apply easily to specific structures. Instead, we shall adopt a subjective utilitarian position and simply define the best solution as that which leads to the greatest overall happiness. Here, we follow the ideas first developed by Bentham who said: "*Ethics at large may be defined, the art of directing men's actions to the production of the greatest possible quantity of happiness, on the part of those whose interest is in view.*" (Bentham 1789, Chapter XVII. 4). In the context of structural safety, then, the aim should be to achieve the greatest possible happiness in all the stakeholders.

The implication here is that all stakeholders should have sufficient knowledge of the situation. Kant (1781) maintained that knowledge is information acted upon by understanding. Thus communication is a central issue, and it is more than simply conveying information. We can assume that engineers have a greater degree of knowledge concerning structural safety than either client or society generally. Even though this depends on the experience and quality of the engineers, nevertheless it is much wider than the scientific knowledge of the average citizen.

4 RISK COMMUNICATION

The first step is that all parties must agree as to what is good, and therefore, what is to be done. To achieve this, communication is central, and again following Kant, communication must involve a transferring of professional knowledge, rather than simply information. (Kanda and Elms, 2010)

In order to make a decision, information is needed which is reliable and pertinent, and the stakeholders must perceive it as being reliable. The professional engineer has to provide sufficient information for the safety decision making. Of course, some information is subjective and some is uncertain. Uncertainty, though, does not mean the information is worthless. However, the need to communicate uncertainty adds another dimension to the task of the engineer.

Accountability is an essential characteristic of the structural engineer as a professional. This being the case, the nature of the communication between the professional engineer and the client and community has to be considered seriously and

perhaps more so than usual, in order to achieve what society wants. Essentially, there needs to be a mutual understanding.

5 ENVIRONMENTAL ETHICS

The quality of building should be examined on a long term basis. The serviceable life may well be different for different buildings. The amount of occupancy and the nature of occupancy, in other words the degree of public use of a building also require different levels of safety. Based on the knowledge we as engineers can share, decisions on structural safety should be made from sustainable points of view.

Insightful investigations by responsible experts are necessary before and during the construction. In such a case, communications not only between engineer and client but also within and between organizations have to be ethically sound. This goes beyond the minimal requirements of the law. There is also an ethical imperative for a professional engineer to be a skilled communicator in a broad sense, an area in which many engineers are lacking.

6 CONCLUDING REMARKS

We have argued that in some cases, particularly when considering large and unusual structures, the design safety levels specified by national regulations and codes of practice may not be appropriate. In such a case the way forward is to achieve agreement between the client and the respective stakeholders within society as to what the safety level should be. It might be a matter of specifying a reliability index value, but in any case, agreement needs a mutual understanding of the issues by all parties. Achieving this is the responsibility of the professional engineer, and indeed, not only is it a responsibility but it is also an ethical imperative of the type that is part of the role of the professional.

REFERENCES

- Bentham, J. (1789). *An Introduction to the Principles of Morals and Legislation*. (1823 ed.) Oxford: Clarendon Press.
- I.S.O. (1998). *General Principles on Reliability for Structures*, ISO2394.
- Kanda, J. & Elms, D.G. (2010). *Communications in Structural Engineering from Ethical Aspects*, IABSE Symposium, Venice.
- Kant, I. (1781). *Critique of Pure Reason*. Trans. F.M. Muller (1966). New York: Anchor Books.

Risk assessment and maintenance of existing trunk lines with a new subsidiary system under seismic and deteriorating environments

T. Imai

JFE Engineering Corporation, Yokohama, Japan

T. Koike

Kyoto University, Kyoto, Japan

1 INTRODUCTION

The existing pipelines were designed to comply with the safety requirements based on the seismic design codes prevailing at that time, and have been safely operated by performing daily maintenance. Over many years, however, the original system will face not only severe loading conditions but also many business requirements, and therefore may be expanded with subsidiary systems which consist of a pipeline network and one shutoff valve to disconnect the subsystem from the main line when a leakage or breakage occurs in the subsystem or valve equipment. It is important to note that the original system and future subsidiary systems were separately designed based on their own probabilities of failure; the probability of failure for a future overall system was not considered at the initial stage.

If firms require the performance of the system to be improved each year, the present system must be expanded year by year, but the overall system then has a greater risk of potential defects as well as a higher probability of failure under seismic and deteriorating environments.

In order to keep the probability of failure for the overall system below the target level, potential defects must be minimized through daily patrols and periodic inspections. Especially, when the system is located in a seismically active area, repairs and retrofiting are also necessary to keep its seismic performance at the required level.

The present study considers that when a new subsidiary system is introduced into the existing system, the current maintenance scheme should be revised to comply with a new safety requirement which is based on the probability of failure for the existing system and that for the new subsidiary one.

It should be noted that the existing system is conditioned on the fact that the system actually exists and on the annual rate of occurrence of various types of damage including corrosion defects, dents and mechanically defective cracks produced under

deteriorating situations. Since the seismic damage to buried pipelines is often initiated at these deterioration—induced defects for severe ground motions and large peak ground displacements due to liquefaction and fault movements, maintenance activities should focus on these defects to ensure pipeline safety.

2 RELIABILITY ANALYSIS

Figure 1 shows the numerical model used in this study in which A is the source node and B is the demand node, and the k-th subsystem is constructed after the (k-1)-th subsystem was successfully operated.

1. Definition of performance damage modes

The performance damage modes of a lifeline system are defined as shown in Table 1.

The probability of performance damage modes means the probability that the seismic performance cannot be maintained in the event of seismic load EQ1 or EQ2.

2. Probability of performance damage modes

In the case of major damage mode, for instance, the probability of performance damage is given by:

$$P_{D_{EQ}}^{\text{major}} \equiv P[D_{EQ}^{\text{major}}(t)] = P[D_{EQ}^{\text{major}}(t) | Z^{\text{major}}(t) < 0] \cdot P[Z^{\text{major}}(t) < 0 | EQ2] P[EQ2] \quad (1)$$

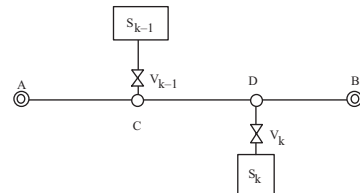


Figure 1. The numerical model of the k-th subsystem provided after the (k-1)-th subsystem which was successfully operated.

Table 2. Definition of performance damage modes.

Damage mode	Definition
Minor D_{EQ}^{minor}	The system serviceability is in the minor damage state by EQ1, and the probability of minor damage occurrence is defined as P_{fi}^D
Moderate $D_{EQ}^{moderate}$	The system serviceability is in the moderate damage state by EQ2, and the probability of moderate damage3 occurrence is defined as P_{fo}^D
Major D_{EQ}^{major}	The system serviceability is in the major damage state by EQ2, and the probability of major damage occurrence is defined as P_{fa}^D

The strength $R^{major}(C_S, t)$ of the lifeline system can be upgraded when the seismic disaster prevention investment C_S is adequately used for the retrofiting work. The probability of performance damage mode in various stages of the system can then be estimated with its corresponding resistance of the system as follows:

1. the initial strength:

$$R^{major}(0,0) \quad (2a)$$

2. the strength before the retrofiting:

$$R^{major}(0, T_p) = \psi(T_p) \cdot R^{major}(0,0) \quad (2b)$$

3. the strength after the retrofiting:

$$R^{major}(C_S, T_p) \quad (2c)$$

4. the strength in the future:

$$R^{major}(C_S, t) = \psi(t - T_p) \cdot R^{major}(C_S, T_p) \quad (2d)$$

where C_S is the seismic disaster prevention investment, and T_p is the present time, and $\psi(t)$ is a deterioration factor which is defined by

$$\psi(t) = 1 - \xi_1 \cdot \left(\frac{t}{T_D}\right)^{\xi_2} \quad (3)$$

where ξ_1 and ξ_2 are deterioration parameters and T_D is the service period of the system.

3. Design hazard function for the trunk line with the k -th subsystem

Now we introduce a design hazard function in which the probability of failure for the k -th expansion system should be less than the design value:

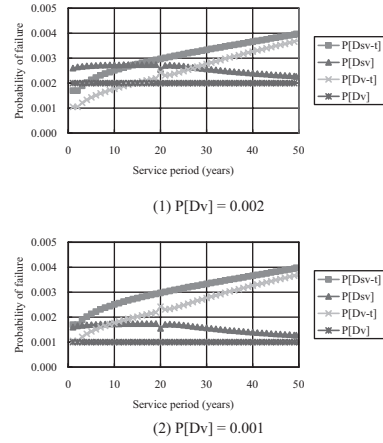


Figure 2. Required assurance quality of control valves.

$$P\left[D_k \mid \bar{D}_{k-1}\right] \leq p_{Hk}^{T_k} \quad (4)$$

Using the following definition of the subsystem with a control valve

$$D_{SV_k}(t) = D_{S_k}(t) \cup D_{V_k} \quad (5)$$

the probabilities of failure for the combined subsystem SV_k and the control valve V_k are given by:

$$P\left[D_{SV_k}(t)\right] \leq \frac{p_{Hk}^{T_k} - p_{Hk-1}^{T_{k-1}}}{1 - p_{Hk-1}^{T_{k-1}}} \quad (6)$$

and

$$P\left[D_{V_k} \mid EQ\right] \leq \frac{\frac{p_{Hk}^{T_k} - p_{Hk-1}^{T_{k-1}}}{1 - p_{Hk-1}^{T_{k-1}}} - P\left[D_{S_k}(t) \mid EQ\right]}{1 - P\left[D_{S_k}(t) \mid EQ\right]} \quad (7)$$

Figure 2 compares two different qualities of valve. $P[D_v] = 0.002$ means that the quality of this valve is less than that of $P[D_v] = 0.001$.

Valve (1) cannot satisfy the safety condition up to the 15th year, while valve (2) can maintain safety over the service period. This result suggests that the probability of failure for the control valve should be at least less than 0.001.

3 CONCLUSIONS

Procedures for assessing the risk of expanding the trunk line by subsystems were proposed, taking into consideration the seismic and deteriorating hazards.

*MS_228 — Risk assessment and decision support systems
for interdependent lifeline infrastructures (2)*

This page intentionally left blank

Seismic risk and hierarchy importance of interdependent lifelines and infrastructures within port facilities: Application in Thessaloniki's Port (Greece)

K.G. Kakderi, M.N. Alexoudi & K.D. Pitilakis

Department of Civil Engineering, Aristotle University of Thessaloniki, Greece
University of Macedonia, Thessaloniki, Greece

ABSTRACT: The strong dependence on lifeline systems and infrastructures is one of the distinctive characteristics of modern societies urban environment. Unfortunately, these systems are subjected to several hazards such earthquakes, causing physical damage, property loss, dysfunction to urban activities and serious socioeconomic consequences. Lifelines are complex systems comprising several subsystems integrated in an “urban lifeline network”. An example of a complex system of systems is a port facility, composed of different structural and non-structural components, utilities and infrastructures, thus concentrating various activities in a relatively limited area. In general, there is a strong level of interdependence between all components of a port facility. The aim of the paper is to discuss these synergies and to propose a method the estimate them in the general framework of risk assessment and management.

The present study focuses in the co-seismic and post seismic performance of interdependent lifeline and infrastructure components within port facilities, which are controlled by the vulnerability and the interconnectedness of the elements for a given level of earthquake intensity. The objectives of the research are (i) to quantify, in terms of hierarchy importance, the interdependencies between port system facilities and (ii) to propose appropriate methodologies to estimate the degree of impact of “inter-dependent” lifeline systems to the port system as a whole. Detailed description of the methodology, along with specific guidelines for the evaluation of the degree of corresponding impact of “inter-dependent” lifeline systems to the whole system, and the estimation of “systemic” fragility curves of interdependent elements can be found in a companion paper in this conference (Alexoudi et al., 2011).

Three different methodologies are proposed herein to evaluate a “cross impact matrix”, representing the degree of corresponding impact, composed of various “elements” (lifelines,

infrastructures). The proposed methodologies are using (i) an economic approach (input-output model), (ii) a multi-criteria decision making procedure (Analytical Hierarchy Process: AHP) and (iii) a group decision-making approach with linguistic preference relations.

The *Input-Output model* comprises a linear, deterministic, equilibrium approach and a framework capable to describe the degree of interconnectedness. It can be used in national or regional level and with some restrictions in city level if economical data is available. It gives better results in large systems, if coefficients are considered to be constant for a fixed unit of time (static approach); however it should be carefully used in “close systems”.

The *Analytical Hierarchy Process (AHP)* is listed among the most popular multi-criteria decision making procedures, as with a theoretical robustness it employs simplicity, accuracy, can handle both intangible and tangible criteria and has the capability to directly measure the inconsistency of the respondent's judgments. AHP combines subjective and objective alternatives into a single measure in a hierarchical framework. On the other hand, there is a restriction of a maximum number of criteria that can be used and number of lifelines or lifeline elements that can be involved.

The third methodology is based on linguistic (hybrid) geometric averaging operator, for *group decision making with linguistic preference relations*. It can be used in cases where the linguistic preference information provided by the experts does not take the form of precise linguistic variables. Value ranges can be obtained due to the experts' vague knowledge about the preference degrees of one alternative over another. This methodology exploits the opinion of every expert without losing information and precision. Using this methodology, the uncertainty of the opinion of the experts is transported in the estimated “systemic” fragility curve.

The optimum selection between the different approaches depends on available information, quality of data, experience of the experts and the type of lifeline systems involved. Each methodology has its own restrictions and disadvantages, that must be carefully accounted for and considered during the evaluation.

The methodology is applied in the port of Thessaloniki where we examine and evaluate the use of different approaches to quantify the degree of impact of interconnected lifelines for the normal, crisis and recovery period. The multiple interactions that exist between the different lifelines systems within port facilities are described for the three periods. The lifelines and infrastructures that were examined are: Electric Power System, Cargo Handling Equipment, Water System, Waste Water System, Telecommunication System, Natural Gas & Liquid Fuels, Roadway/Railway, Buildings, Ships/Wharves & Auxiliary Services.

The degree of the impact of interconnected lifelines in three operation periods is estimated using the methods described above for the estimation of the cross impact matrix. Different levels of accuracy are achieved for each case, based on the available data provided by the Thessaloniki Port Authority (THPA) and experts' opinions; the elements considered in the analysis and their interactions are described in the previous paragraph.

All three different approaches, have reached the same conclusion: "Electric Power System" is the most important system during the period of normal operations. Moreover, according to AHP and fuzzy logic approach the second more important system in normal period is "Telecommunication System", while "Buildings, Ships/Wharves & Auxiliary Services" is the least important element.

Unfortunately, there were no available data for Thessaloniki's Port to apply the economical approach for crisis and restoration period. Based only on Port's authority opinion for these periods, it is again proved that EPS is the most important in crisis and recovery periods as well. According to AHP and fuzzy logic approach, "Telecommunication System" and "Electric Power System" systems influence the most port operations in crisis-period as they are essential for the organization of restoration activities and the functioning of all utilities and lifelines inside the port. Major damages of such systems can lead to substantial port malfunction and important economic impacts.

In recovery period, AHP method and the group decision making approach infer that "Buildings, Ships/Wharves & Auxiliary Services" is the least important element and that "Electric

Power System" influence the most the operability of port facilities. Moreover, the two methodologies (AHP, fuzzy logic) agree also that after "Electric Power System" the next important systems affecting harbor global performance are the "Telecommunication System" and the "Roadway/Railway".

"Buildings, Ships/Wharves & Auxiliary Services" are the least important elements within port facilities in normal and restoration period; they can be characterized as rather "independent" elements with few interactions to the functionality of other systems, housing activities that can be easily transferred in case of catastrophic events. Of course their role is still very important for the port functionality.

A direct comparison of the estimated values of the "cross impact matrices" (in absolute terms) of the different methodologies is difficult, for several reasons i.e. the lack of detailed operational data under different conditions, inherent uncertainties in the evaluation of the performance of such a complex system etc.

The present methodology and discussion on the hierarchical importance of the different systems within the port complex system comes to assess indicators for each system through an efficient prioritization process of interdependent lifelines and infrastructures, in order to enhance the better development of pre-seismic and post-seismic restoration actions. When referring to particular lifeline systems within a system of systems, the methodology is able to identify the main sub-system affecting the global port performance.

Given the lack of well established methodologies to estimate the response of inter-dependent lifelines and utility systems as a whole, using systemic adequate vulnerability functions, a reasonable approach to estimate the induced direct losses for a certain level of seismic intensity, is to assume that the system performance could be approximated by the response of the most important single element within the system. For example, the functionality of the "Electric Power System" is simulated by the direct losses induced to the main substation within Thessaloniki's port, while the representative element for the "Buildings, Ships/Wharves & Auxiliary Services" is the newly constructed gravity-type wharf structures of the container terminal.

The final outcome of this study is to give decision-makers the means and capacities to formulate effective risk management, based on the quantification (hierarchy importance) of the interdependencies between port facilities. As a next step, the seismic risk of "inter-dependent" lifeline systems can be performed on the basis of a probabilistic

approach using “systemic fragility curves”. The development of appropriate methodologies to estimate the seismic risk of “interdependent” lifeline systems depends on available information and resources as well as the desirable level of reliability of the performed analysis.

REFERENCE

Alexoudi, M., Kakderi, K. & Pitilakis, K. 2011. Seismic risk of interdependent lifeline systems. Methodology and important issues. *Proc. ICASP11*, ETH Zurich, Switzerland.

A fuzzy comparative model for integrated risk ranking and mitigation prioritization of infrastructures; part 1: Methodology

M.B. Javanbarg, C. Scawthorn, J. Kiyono & B. Shahbodaghkhan
Graduate School of Engineering, Kyoto University, Japan

S. Takada
Department of Civil Engineering, University of Tehran, Iran

ABSTRACT: Decision making systems for risk-informed mitigation of infrastructure systems are often complex and multifaceted. Recently, tools for modeling decision making on improvement of infrastructures have improved significantly, and multicriteria decision making (MCDM) models are widely considered to be very useful in resolving conflicts related to the decision making process (e.g. Opricovic and Tzeng, 2002, Gauffre et al., 2007, Samsal et al., 2007, Javanbarg et al., 2008, and Caterino et al., 2009). Multicriteria decision making deals with the problem of choosing the best alternative, that is, the one with the highest degree of satisfaction for all the relevant criteria or goals. In order to obtain the best alternative a ranking process is required. Extensively adopted in MCDM, the Analytic Hierarchy Process (AHP) has successfully been applied to the ranking process of decision making problems (Saaty, 1988). The main advantage of the AHP is its inherent ability to handle intangibles, which are present in any decision making process. Also, the AHP less cumbersome mathematical calculations and, it is more easily comprehended in comparison with other methods. AHP is however ineffective when applied to ambiguous problems. Since the real world is highly ambiguous, some researchers apply fuzzy AHP as an extension of conventional AHP and employ fuzzy set theory to handle uncertainty and overcome this limitation (Mikhailov, 2003).

There are three objectives of this paper. First, structuring a risk ranking and mitigation prioritization procedure for infrastructures as a MCDM system, we propose a fuzzy optimization model to deal with shortfalls of the AHP method in handling the uncertainties and imprecision of MCDM systems. Secondly, we construct a fuzzy prioritization method which can derive exact priorities from consistent and inconsistent fuzzy comparison matrices. Thirdly, we apply an improved Particle Swarm Optimization (PSO) method to solve the

fuzzy optimization model as a system of nonlinear equations.

The main steps of decision making for risk ranking and mitigation prioritization using fuzzy AHP are as follows:

1. *Structuring decision hierarchy.* The first step is to break down the complex decision making problem into a hierarchical structure (Fig. 1).
2. *Developing pairwise fuzzy comparison matrices.*
3. *Consistency check and deriving priorities.* This step checks for consistency and extracts the priorities from the pairwise comparison matrices. In existing fuzzy AHP methods, only a few past studies have addressed the issue of checking for inconsistencies in pairwise comparison matrices. For consistency analysis, we follow the method proposed by Mikhailov (2003).
4. *Aggregation of priorities and ranking the alternatives.* The final step aggregates local priorities obtained at different levels of the decision hierarchy into composite global priorities for the alternatives based on the weighted sum method.

For an illustration and justification of our approach, we have performed a case study to compare our results with the existing fuzzy AHP methods. MATLAB is used for implementing the PSO

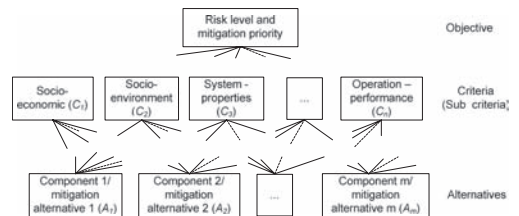


Figure 1. Hierarchical structure for risk ranking and mitigation prioritization.

Table 1. Exact solutions for illustrative example.

Criteria	MTY	FLX	ENC	RSK	QTY	Weight priority vector	
						Nonlinear FPP (Jaganathan et al., 2007)	PSO-fuzzy AHP
MTY	(1,1,1)	(1/6,1/5,1/4)	(1,2,3)	(2/5,1/2,2/3)	(2/7,1/3,2/5)	0.0871	0.0909
FLX	(4,5,6)	(1,1,1)	(7,8,9)	(5/2,3,7/2)	(1,2,3)	0.4141	0.4104
ENC	(1/3,1/2,1)	(1/9,1/8,1/7)	(1,1,1)	(1/4,1/3,1/2)	(1/8,1/7,1/6)	0.0472	0.0472
RSK	(3/2,2,5/2)	(2/7,1/3,2/5)	(2,3,4)	(1,1,1)	(1/2,2/3,1)	0.1582	0.1568
QTY	(5/2,3,7/2)	(1/3,1/2,1)	(6,7,8)	(1,3/2,2)	(1,1,1)	0.2934	0.2947

MTY: Monetary, FLX: Flexibility, ENC: Environment consciousness, RSK: Risk, QTY: Quality.

algorithm for solving the nonlinear optimization to derive the priorities from pairwise comparison matrices. A computer program namely PSO-fuzzy AHP has been developed. Consider the example given by Jaganathan et al. (2007). They applied nonlinear Fuzzy Preference Programming (FPP) method developed by Mikhailov (2003), to investment prioritization in new manufacturing technologies. They considered five criteria: Monetary; Flexibility; Environment consciousness; Risk; and Quality. The pairwise comparison matrix for criteria in the form of triangular fuzzy numbers is represented in Table 1. The local priority of criteria derived by both nonlinear FPP and proposed PSO-fuzzy AHP methods are also shown in Table 1 for comparison. The consistency index calculated by the the PSO-fuzzy AHP methods is 0.2335. As it can be observed from the illustrative example, the proposed PSO-fuzzy AHP method could be used as an efficient method for deriving priorities from fuzzy pairwise comparison judgments.

This study presents a simple fuzzy comparative model for multicriteria decision making of infrastructures risk ranking and mitigation prioritization. The method has the advantage of allowing for a more systematic handling of the subjective aspects of decision by integrating the specialist knowledge of infrastructure engineers and environmental experts into the process.

REFERENCES

Caterino, N., Iervolino, I., Manfredi, G. & Cosenza, E. (2009). Comparative analysis of multi-criteria decision-making methods for seismic structural retrofitting. *Computer-Aided Civil and Infrastructure Engineering*, 24(6), 432–45.

Gauffre, P., Laffrechine, K., Baur, R. & Schiatti, M. (2007). A multicriteria decision support methodology for annual rehabilitation programs of water networks. *Computer-Aided Civil and Infrastructure Engineering*, 22, 478–488.

Jaganathan, S., Jinson, J.E. & Ker, J. (2007). Fuzzy analytic hierarchy process based group decision support system to select and evaluate new manufacturing technologies. *International Journal of Advanced Manufacturing Technology*, 32, 1253–1262.

Javanbarg, M.B., Takada, S. & Kuwata Y. (2008). Priority Evaluation of Seismic Mitigation in Pipeline Networks Using Multicriteria Analysis Fuzzy AHP. In *Proc. of the 14th World Conference on Earthquake Engineering (14 WCEE)*, Beijing, China, No. 06-0015.

Mikhailov, L. (2003). Deriving priorities from fuzzy pairwise comparison judgments. *Fuzzy Sets and Systems*, 134, 365–385.

Oprićovic, S. & Tzeng, G.H. (2002). Multicriteria planning of post-earthquake sustainable reconstruction. *Computer-Aided Civil and Infrastructure Engineering*, 17(6), 211–220.

Saaty, T.L. (1988). *Multicriteria decision making: The analytic hierarchy process*. Pittsburgh PA: RWS Publications.

Samsal, S., Ramanjanyulu, K. & Lakshmanan, N. (2007). Priority ranking towards condition assessment of existing reinforced concrete bridges. *Structure and Infrastructure Engineering*, 3, 75–89.

A fuzzy comparative model for integrated risk ranking and mitigation prioritization of infrastructures; part 2: Application

J. Kiyono & M.B. Javanbarg

Department of Urban Management, Kyoto University, Japan

S. Takada

Department of Civil Engineering, University of Tehran, Iran

C. Scawthorn & M. Kobayashi

Kyoto University, Japan

ABSTRACT: Risk management of lifeline infrastructures is a process of weighting alternatives, selecting the most appropriate action, and integrating the results of risk assessment with engineering data, social, economic, and political issues to make an acceptable decision. Generally, the selection of different mitigation or preventative alternatives often involve competing and conflicting criteria, which requires the use of multicriteria decision making (MCDM). Multicriteria models have been recently considered to be very useful in resolving conflicts related to the decision making process for infrastructures (e.g. Opricovic & Tzeng 2002, Gauffre et al., 2007, Samsal et al., 2007, Javanbarg et al., 2008, and Caterino et al., 2009).

In the first part of this study (Javanbarg et al., 2011); we proposed a new fuzzy comparative model for MCDM problems related to risk management of infrastructures. The method has the advantage of integrating the engineering knowledge of an infrastructure and environmental aspects into the process. In the second part, herein, we examined the application of the proposed method to a case study of the risk ranking and replacement prioritization of an urban water pipeline network in Japan. Considering the importance rank of the pipelines as the main criteria and pipeline properties as the sub-criteria, we try to deal with uncertainty and imprecision in decision making for priority evaluation of pipeline renewal plan where the pipe segments groups are considered as the alternatives for replacement.

In this study, we have classified the importance rank of customers into three ranks; Rank A, very important; Rank B, important; and Rank C, others based on the contribution degree of each customer to post-earthquake response as a part of emergency preparedness plans. For instance, Figure 1 shows a classification of important rank

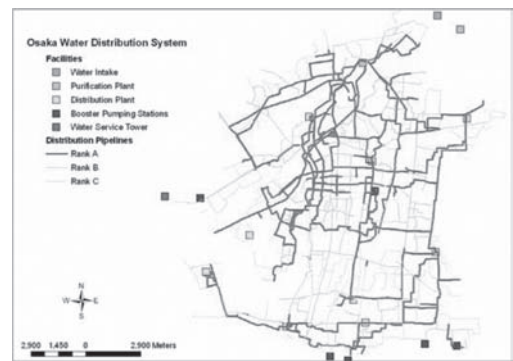


Figure 1. Classification of pipeline importance.

assigned to pipelines across the city selected for case study.

The hierarchy structure used for seismic risk ranking and priority evaluation of pipelines replacement across the water distribution network is represented in Figure 2. The hierarchy model includes five levels. It is worthy to mention that other appropriate hierarchy structures may also be adopted depending on the available data and the requirements for seismic mitigation of pipeline network.

It is then possible to assign a risk level rank to each pipe segments group based on the composite priority of the pipes. The higher composite priority the higher the risk level of pipeline could be. Considering the available annual budget for pipeline replacement, and knowing the length of pipelines, it is therefore possible to calculate the total annual length of pipelines with higher priority for mitigation based on their risk level. The results are represented in Figure 3. To illustrate the relation between spatial distribution of pipeline

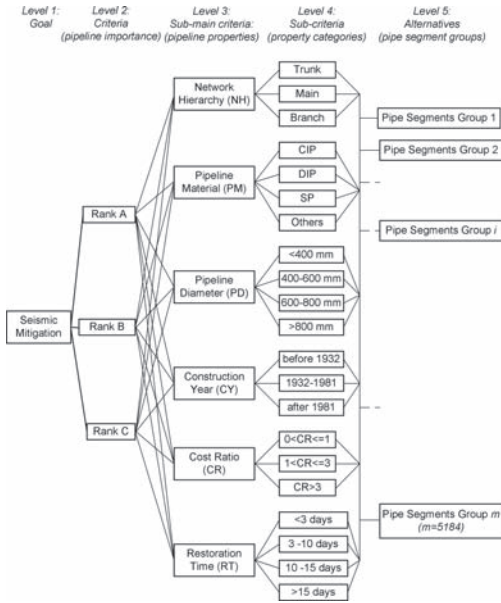


Figure 2. Hierarchical structure for seismic risk ranking and replacement prioritization of pipeline network.

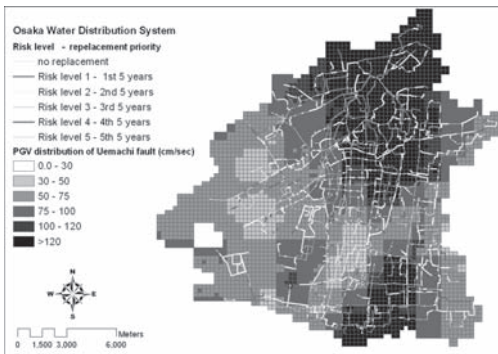


Figure 3. Seismic risk level and replacement priority of pipeline.

replacement and seismic hazard pattern, the layer of prioritized pipe replacement was overlaid with the Peak Ground Velocity (PGV) distribution of Uemachi scenario fault (the most causative scenario) as depicted in Figure 3. It is found that although most of pipelines located in higher PGV values have higher priority for replacement, but other criterions such as pipeline importance as well as pipeline properties affect the prioritization procedure.

To perform sensitivity analysis, the weights of the important criteria were separately altered and the relative nature of the weights, consistency degree, and overall priority ranking were observed. It was found that the primary assumption of relative importance of PM and PD as “about equal”, may not be relevant, since their variation sensitivities show different trends. Accordingly, we have tracked the variation of construction year and cost ratio. It was indicated that both construction year and cost ratio have the same sensitivity trend with different variation rate.

As a summary, in the first part of this study, we have presented a simple fuzzy comparative model for multicriteria decision making on risk ranking and mitigation prioritization of infrastructures. It proposes a novel fuzzy AHP method using Particle Swarm Optimization (PSO). In second part, we apply the proposed method to a case study of pipeline risk ranking and priority evaluation of pipeline replacement across the Osaka City water distribution network. The results demonstrate that the proposed fuzzy AHP can be used as an effective tool for tackling the uncertainty and imprecision associated with risk management of lifeline infrastructures.

REFERENCES

- Caterino, N., Iervolino, I., Manfredi, G. & Cosenza, E. (2009). Comparative analysis of multi-criteria decision-making methods for seismic structural retrofitting. *Computer-Aided Civil and Infrastructure Engineering*, 24(6), 432–45.
- Gauffre, P., Laffrechine, K., Baur, R. & Schiatti, M. (2007). A multicriteria decision support methodology for annual rehabilitation programs of water networks. *Computer-Aided Civil and Infrastructure Engineering*, 22, 478–488.
- Javanbarg, M.B., Scawthorn C., Kiyono, J., Shahbodaghkhan, B. & Takada, S. 2011. A Fuzzy Comparative Model for Integrated Risk Ranking and Mitigation Prioritization of Infrastructures; part 1: Methodology. In *Proc. ICASP11*, Zurich, Switzerland.
- Javanbarg, M.B., Takada, S. & Kuwata Y. (2008). Priority Evaluation of Seismic Mitigation in Pipeline Networks Using Multicriteria Analysis Fuzzy AHP. In *Proc. of the 14th World Conference on Earthquake Engineering (14WCEE)*, Beijing, China, No. 06-0015.
- Opricovic, S. & Tzeng, G.H. (2002). Multicriteria planning of post-earthquake sustainable reconstruction. *Computer-Aided Civil and Infrastructure Engineering*, 17(6), 211–220.
- Samsal, S., Ramanjanyulu, K. & Lakshmanan, N. (2007). Priority ranking towards condition assessment of existing reinforced concrete bridges. *Structure and Infrastructure Engineering*, 3, 75–89.

A questionnaire survey to customers on willingness to pay for earthquake countermeasures of water supply system by using risk communication

Yasuhiro Taniguchi

Graduate School of Science and Engineering, Kanazawa University, Kanazawa, Japan

Masakatsu Miyajima

School of Environmental Design, Kanazawa University, Kanazawa, Japan

Earthquake countermeasures including enhancing earthquake resistance which needs immeasurable costs are not enough implemented by the bad financial conditions in water suppliers and aged deterioration of water facilities in Japan. Over 20% of water suppliers have over 100% proportion of outstanding balance, which shows most of the water suppliers have the bad financial condition. The era when water facilities had spread is one of the reasons why enhancing earthquake resistant of water facilities is not enough implemented. The water supplier had expanded the water facilities especially in water pipelines from 1960s to 1970s, at the time Japan faced an age of high economic growth, according to the growth of population. It is said that the cost of replacing non-earthquake resistant facilities will be larger than the average from 2020 to 2040 as shown in Figure 1. So it is necessary to secure a source of revenue to replace aged pipes or equalize the amount of replace in each year.

It is necessary to win customer's understanding in order to progress the earthquake countermeasures.

The present paper deals with a questionnaire survey to customers of water supply system in order to clarify the costumers' willingness to pay to water charges for earthquake countermeasures when the relation between the investing to earthquake countermeasure and the risk of water suspension after the earthquake is shown.

The target cities of questionnaires are Osaka city as a large-scale city (population; about 2.65 million) and Kanazawa city as a moderate-scale city (population; about 0.46 million). One thousand samples were extracted by using the stratified sampling method, that can ensure statistical reliability of 5% level in significance, and questionnaires were sent by a post mail.

The date when we sent the sheet of questionnaire was November 17th, 2008 and we made the

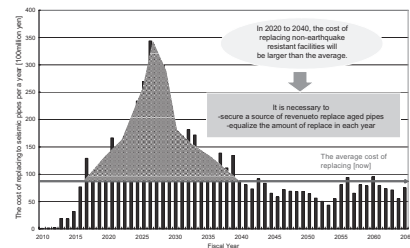


Figure 1. The amount of the revenue of replacing aged pipes to seismic one in each year in the case of Osaka city.

response until December 10th available in Osaka and the date we sent it was December 15th, 2009 and made it until 28th in Kanazawa.

The contents of questions were attributes (sex, generation, family structure and household income), the type of drinking water (way of drinking water, consciousness of saving water, experiences of water suspension and stock of water), knowledge of earthquake disaster and earthquake countermeasures, maximum permissible limit of water suspension in a disaster, understanding of earthquake countermeasures and willingness to pay (WTP) to water charges for earthquake countermeasures.

In order to clarify the effect of the information of the earthquake countermeasures by water suppliers on WTP and the maximum permissible limit of water suspension, two types of questionnaires were prepared, that is, one included the information of the earthquake countermeasures, and the other did not. As a result, we sent eight types of questionnaires that had each 125 copies in both Osaka and Kanazawa because we adopted double bound method of CVM (contingent Value Method.)

The number of valid responses was 216 (23.1%) in Osaka and 437 (45.7%) in Kanazawa except for address unknown.

The summary of the results of questionnaires is as follows;

- As for type of drinking water, we had supposed that the number of drinking water directly from faucet was less because water filter companies in Japan have conducted a negative campaign for direct water drinking from faucet, but it was larger than “only bottled water.”
- About 50% of respondents have consciousness of saving water. And also about 80% of respondents in Osaka and 50% in Kanazawa have the experience of water suspension.
- As for the knowledge of an earthquake disaster, we asked four questions, such as knowledge of the scenario earthquakes, knowledge of water suspension by an earthquake and knowledge of water delivering by a water supplier in disaster. Over 70% of the respondents in Osaka and 50% in Kanazawa have knowledge of water suspension and water delivering by a water supplier.
- Most Japanese water supplier set the goal to deliver 3 liters per a day to each person for drinking water till the 3rd day after an event, and 20 liters for drinking water, toilet and washing up till the 10th day. But the result of the maximum permissible limit of water suspension shows that the most intolerable usage is for toilet, in which over 90% of the respondents answered the maximum permissible limit was within 3 days in both Osaka and Kanazawa.
- As for an attitude of earthquake countermeasures, the number of the respondents who demanded countermeasures more by water supplier was larger than those who prepare water by themselves in disaster.

In the estimation of WTP to water charges to enhancing the countermeasures of anti-disaster, we used parametric model by Weibull distribution function.

The result of assumption of WTP was that most residents (also customers) have consciousness of paying more to earthquake disaster countermeasures. It was clarified that the WTP was 400–800 JPY (\$4.5–9USD) higher than that at present as shown in Figure 2 and Figure 3. These results agree with the result of an attitude of earthquake countermeasures. And WTP with information was not very different from that without information, so the problem seems to be the way to give information about earthquake disaster countermeasures to the customers.

We did chi-square tests in order to check the relevant among each question. Common tendency between Osaka and Kanazawa described below is expected from the result.

- The knowledge of a scenario earthquake, knowledge of water suspension by an earthquake and knowledge of water delivering by a

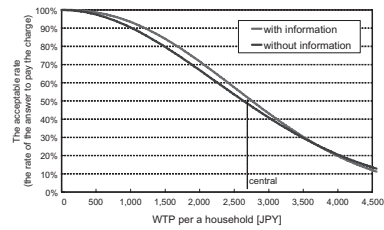


Figure 2. Cumulative distribution curves of WTP in Osaka.

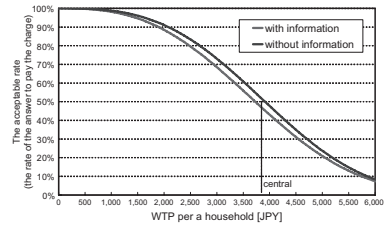


Figure 3. Cumulative distribution curves of WTP in Kanazawa.

water supplier in disaster are correlate, which is multicollinearity.

- Those who save water tend to have more knowledge of a scenario earthquake, water suspension by an earthquake and water delivering by a water supplier in disaster.
- Those who have experience(s) of water suspension tend to think they should prepare water by themselves in a disaster.
- Those who have the knowledge of water suspension by an earthquake and of water delivering by a water supplier in disaster tend to think they should prepare water by themselves in a disaster.

The tendencies which are differ from Osaka and Kanazawa as follows;

- Those who have experience(s) of water suspension tend to save water, have knowledge of the scenario earthquake and water delivering by a water supplier in disaster in Kanazawa, but there’s no correlation in Osaka.
- Those who save water tend to think they should prepare water by themselves in a disaster in Kanazawa, but there’s no correlation in Osaka.
- Those who have the knowledge of the scenario earthquake have shorter permissible limit of water suspension in a disaster in Osaka, but there’s no correlation in Kanazawa.
- Those who have the experience(s) of water suspension have the knowledge of water suspension by an earthquake in Osaka, but there’s no correlation in Kanazawa.

CVM is a calculation based on the virtual scenarios, so some kind of bias may be included. We’re now planning questionnaires to other cities which have different conditions.

This page intentionally left blank

*MS_131 — Risk-based assessment of climate change
adaptation strategies for infrastructure*

This page intentionally left blank

Deterioration of concrete structures in Australia under changing environment

M.G. Stewart

Centre for Infrastructure Performance and Reliability, The University of Newcastle, NSW, Australia

X. Wang

CSIRO Climate Adaptation Flagship and CSIRO Sustainable Ecosystems, Victoria, Australia

M. Nguyen

CSIRO Climate Adaptation Flagship and CSIRO Land and Water, Victoria, Australia

Concrete is the predominant construction type used in Australia's critical infrastructure. Its performance, therefore, is vital for the provision of the nation's essential services and the maintenance of its economic activities. The key performance requirements for the design, construction and maintenance of concrete structures relate to safety, serviceability and durability. The deterioration rate of such structures depends not only on the construction processes employed and the composition of the materials used but also on the environment. Changing climate may alter this environment, especially in the longer term, causing an acceleration of deterioration processes and consequently acceleration in the decline of the safety, serviceability and durability of concrete infrastructure, especially in coastal areas, which generally experience more severe environmental exposure.

The 2007 Intergovernmental Panel on Climate Change fourth assessment report indicated a significant increase of CO₂ concentration in the atmosphere from 280 ppm in 1750 to 380 ppm in 2005 with an increasing trend. In comparison with pre-industrial temperatures, the best estimation of the temperature increase is up to 4.4°C for 1000 ppm CO₂ by 2100. Increased temperature will increase rates of carbonation and chloride penetration, as well as corrosion rate.

Current levels of atmospheric CO₂ of about 380 ppm will, in many cases, not cause significant carbonation-induced corrosion. Stewart et al (2002) found that the ambient CO₂ concentration attributable to a typical urban environment is approximately 5–10% higher than CO₂ concentrations in a rural environment. Peng and Stewart (2008) used the latest CO₂ concentration data provided by the fourth assessment report of 2007 Intergovernmental Panel Climate Change (IPCC 2007) to predict the likelihood and extent

of carbonation-induced cover cracking and safety loss to RC and prestressed concrete beams in flexure and shear. Stewart and Peng (2010) then conducted a life-cycle cost assessment to assess the cost-effectiveness of increasing design cover as an adaptation measure to mitigate the effects of carbonation of concrete.

Investigation of concrete deterioration in Australian coastal cities under changing climate is being carried out as a part of the project funded by Department of Climate Change and CSIRO Climate Adaptation Flagship. It is based on the Monte-Carlo simulations that involve nine General Circulation Models (GCMs) with three emission scenarios, i.e. A1B, A1FI and 550 ppm stabilisation, representing medium, high and policy-intervened GHG emission scenarios. Two types of corrosion agents of concern are modelled: carbonation and chloride induced corrosion. The probabilistic analysis included the uncertainty of climate predictions, deterioration processes, material properties, dimensions, and predictive models. Deterioration of concrete structures is represented by the probability of reinforcement corrosion initiation and corrosion induced damage at a given calendar year between 2000 and 2100, and all of them are more or less affected by the changing climate depending on locations. The findings from the investigation provide a basis for the development of climate adaptation through the design of concrete structures.

Figure 1 describes the projection of CO₂ concentrations from 2000 for several emission scenarios: A1FI, A1B, 550 ppm by 2150, and no CO₂ increase above Year 2000 levels.

The carbonation depth without consideration of climate change (or called as a baseline), as well as their changes for A1FI emission scenario by 2100, are presented by Figure 2. The

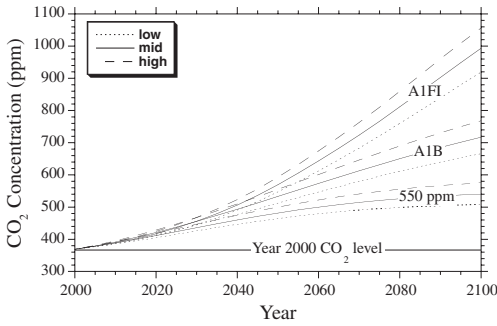


Figure 1. Predicted estimates of CO₂ concentrations.

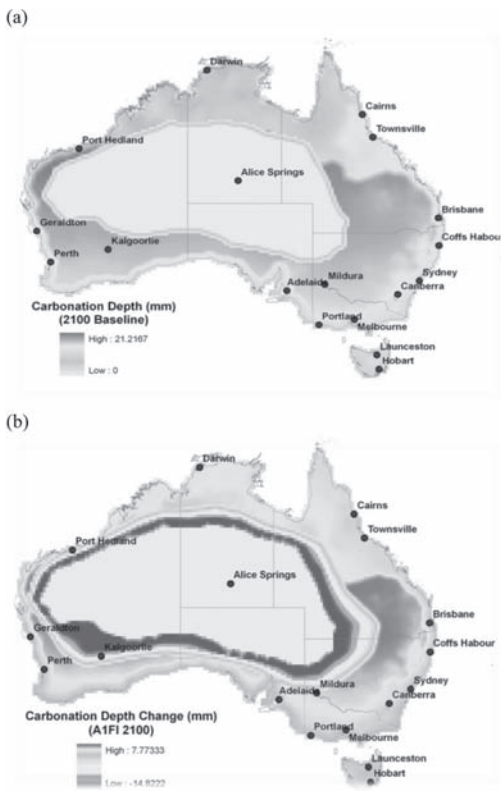


Figure 2. Carbonation induced corrosion of concrete structures by 2100: (a) mean carbonation depth without consideration of climate change, (b) change in carbonation depth for A1FI emission scenario.

carbonation depth for the baseline is in the range of 0 to 21 mm. Under climate change, the carbon depth can change in a range of 15 mm less than the baseline to 8 mm more than the baseline by 2100, depending on the location of the concrete structure. Within the area of the arid zone in central Australia, carbonation does not occur due

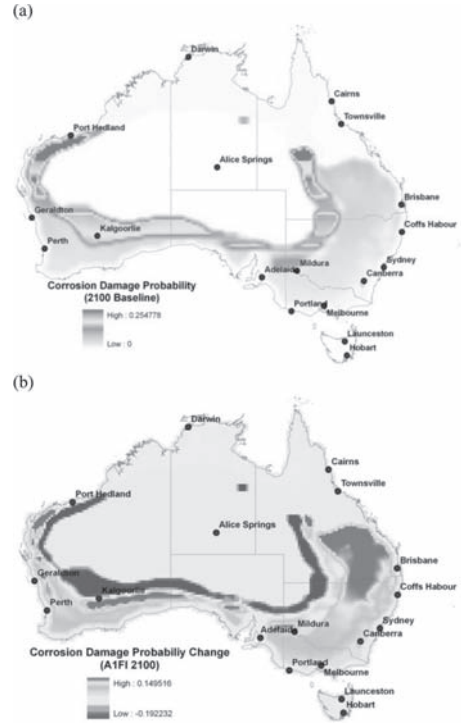


Figure 3. Carbonation induced probability of corrosion damage by 2100: (a) without consideration of climate change, (b) change in damage risks for A1FI emission scenario.

to a lack of moisture. The area is extended when the future climate becomes drier around central Australia. Meanwhile, around the border between New South Wales and Victoria, a relatively greater increase of temperature also pushes carbonation higher. In a small area in the west of Western Australia, the decrease in relative humidity is not sufficient to offset an increase in temperature, leading to an increase in carbonation.

In the absence of climate change, carbonation induced corrosion damage is in the range of 0 and 25%, depending on region (Figure 3). Under climate change, its probability varies regionally from a 19% decrease to a 15% increase in corrosion damage risk.

Chloride-induced corrosion initiation and damage risks are not influenced considerably by the emission scenario. For example, corrosion damage risks for the worst emission scenario (A1FI) are only 6% to 15% higher than the reference (best) emission scenario. This shows that while predicted increases in temperature will increase chloride diffusion coefficient and corrosion rate, that these increases will be relatively modest with relatively little influence on chloride-induced corrosion.

Probabilistic-based assessment of the impacts of climate change on hurricane loss and adaptation strategies

S.O. Bjarnadottir & Y. Li

Department of Civil and Environmental Engineering, Michigan Technological University, USA

M.G. Stewart

Centre for Infrastructure Performance and Reliability, The University of Newcastle, Australia

ABSTRACT: Hurricanes cause extreme damage around the world annually. In the United States (US), annual hurricane damage has increased by approximately 275% from the period 1950–1989 to 1989–1995, or from \$1.6 to \$6 billion dollars (Pielke and Pielke 1997). Even though that hurricane damages are increasing, the US coastal populations continue to grow. For example, insured coastal property values in Florida have increased by 55% from the year 1988 to 1993, from \$566 billion to \$872 billion (Stewart et al., 2003). In 2003, approximately 53% of the US population, or 153 million people, live in coastal counties (Crosset et al., 2004).

The Intergovernmental Panel on Climate Change (IPCC) issued a report in 2007 stated that increasing Sea Surface Temperatures (SST) are a

direct result of the changing global climate (IPCC 2007). Based on data from 1970–2004, SST have increased by approximately 5°C (IPCC 2007). It is a matter of debate whether increasing SST may alter hurricane intensity/frequency. Studies have suggested that hurricane intensity/frequency may change as a result of rising SST. Some studies concluded that there is a direct connection between rising SST and increasing hurricane intensity and suggested that every increase in temperature of 1°C could result in an increase of the peak wind speed of a tropical cyclone by 5% (Emanuel 2005). On the other hand, studies have stated that the increasing hurricane activity in the Atlantic Ocean is a result of the natural cycle of hurricane activity, therefore, not due to the changing climate (Klotzbach 2006).

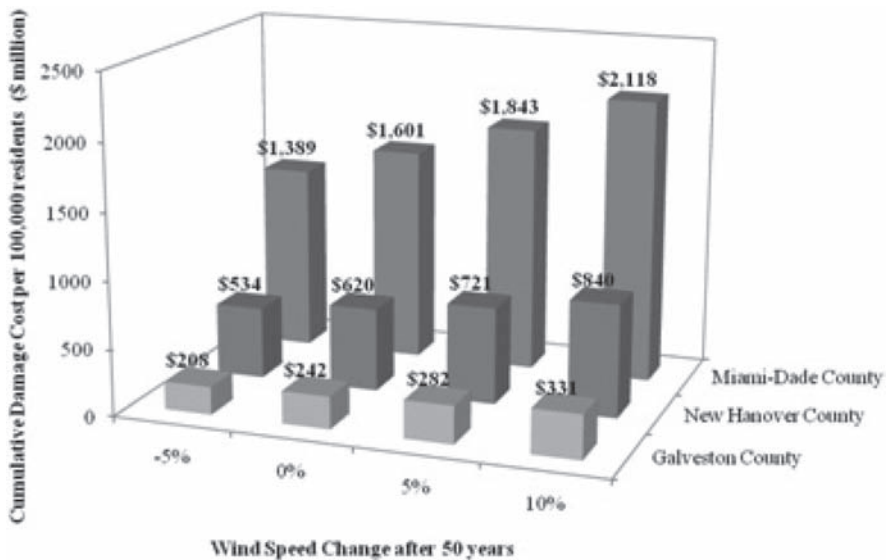


Figure 1. Cumulative damage cost per 100,000 residents to single-family units under different changes in wind speeds.

This paper will assess the potential impact of hurricane damage risks to buildings due to climate change and adaptation strategies. Three case study locations (Miami-Dade County, Florida, New Hanover County, North Carolina, and Galveston County, Texas) are presented to illustrate the framework under various scenarios of change in maximum annual wind speed over 50 years. The analysis will include a probabilistic hurricane wind field model and a hurricane vulnerability model. There is a great uncertainty on the change in hurricane hazard patterns. A recent study indicates that it can be expected that wind speeds may increase by 5–10% in the US (Vickery et al., 2009). Pryor et al. (2009) found that decrease in annual mean wind speeds is possible in the US. To represent this uncertainty and to investigate the potential impact of climate change, the paper will explore the scenarios of increases of –5–10% in mean annual maximum wind speed over 50 years. Figure 1 shows the cumulative damage cost after 50 years per 100,000 residents for all three counties under various scenarios of climate change.

Stewart et al. (2003) suggested that building vulnerability to hurricane damage can be decreased by retrofitting existing structures to current building standards. Four adaptation strategies are developed and the cost-benefit of these strategies is evaluated. This risk-cost-benefit analysis is vital in indentifying optimal and cost-effective adaption strategies to the potential adverse effects of enhanced greenhouse conditions. The effects of regional development dynamics, the rate of retrofit, cost of retrofit, reduction in vulnerability after retrofit, and discount rate will be investigated in this analysis.

It is possible that hurricane patterns and resulting damage losses may change as a result of climate change. The proposed framework provides a tool

to evaluate the potential impact of such change on hurricane damage risks assessment. This study finds that climate change may have a substantial impact on the damage and loss estimation in coastal areas, and that certain adaptation strategies can cost-effectively decrease the damage, even though the wind speed does not change.

REFERENCES

- Crosset, K.M., Culliton, T.J., Wiley, P.C. & Goodspeed, T.R. 2004. Population Trends along the Coastal United States: 1980–2008. *National Oceanic and Atmospheric Administration*. United States: Silver Springs.
- Emanuel, K. (2005). Increasing destructiveness of tropical cyclones over the past 30 years. *Nature*, 436: 686–688.
- IPCC (2007). Climate Change 2007: The Physical Science Basis. Contribution of Working Group I to the Fourth Assessment Report of the Intergovernmental Panel on Climate Change. Solomon, S., Qin, D., Manning, M., Chen, Z., Marquis, M., Averyt, K.B., Tignor, M. & Miller, H.L. (Eds.). Cambridge University Press, Cambridge.
- Klotzbach, P.J. 2006. Trends in global tropical cyclone activity over the past twenty years (1986–2005). *Geophys. Res. Letters*, 33.
- Pielke, R.A.J. & Pielke, R.A.S. (1997). *Hurricanes: Their nature and impacts on society*. Wiley, U.K.: Chichester.
- Pryor, S.C., Barthelmie, R.J. & Takle, G.S. 2009. Wind speed trends over the contiguous USA, *IOP Conference Series: Earth and Environmental Science*.
- Stewart, M.G., Rosowsky, D.V. & Huang, Z. 2003. Hurricane Risks and Economic Viability of Strengthened Construction. *Natural hazards review*, 4: 12–19.
- Vickery, P.J., Wadhera, D., Twisdale, L.A.Jr. & Lavelle, F.M. 2009. U.S. Hurricane Wind Speed Risk and Uncertainty. *Journal of Structural Engineering*, 135: 301–320.

Considerations for probabilistic assessment of the effect of global warming on durability of corroding RC structures

E. Bastidas-Arteaga & F. Schoefs

*LUNAM Université, Université de Nantes-Ecole Centrale Nantes, GeM,
Institute for Research in Civil and Mechanical Engineering, Nantes, France*

M.G. Stewart

Centre for Infrastructure Performance and Reliability, The University of Newcastle, NSW, Australia

1 INTRODUCTION

Chloride ingress and carbonation lead to corrosion of reinforcing bars that reduces the service life of reinforced concrete (RC) structures. Experimental evidence indicates that carbonation and chloride ingress are highly influenced by the weather conditions of the surrounding environment—i.e., temperature and humidity. According to the International Panel of Climate Change (IPCC, 2007), several changes in the future climate produced by global warming are expected. Consequently, the effect of global warming on both chloride ingress and carbonation should be considered for a comprehensive management of corroding RC structures. Within this context, the objective of this paper is to describe some considerations for estimating the effect of global warming on durability of corroding RC structures.

2 DURABILITY OF CORRODING RC STRUCTURES

The deterioration of RC induced by corrosion involves the interaction between three mechanisms: ingress of the corroding agent—i.e., chlorides or carbon dioxide, corrosion of reinforcing steel and concrete cracking. Chloride ingress is modeled by using a numerical approach that considers the interaction between three physical problems: chloride ingress, moisture diffusion and heat transfer. The carbonation model accounts for: larger carbon dioxide concentrations in urban areas, the effect of temperature and the increase of CO₂ concentration produced by global warming. Both models are used to determine the time to corrosion initiation. After corrosion initiation, the diameter reduction of reinforcing bars is controlled by the corrosion rate. This study considered a time-variant corrosion rate model

where the maximum corrosion rate depends on environmental corrosion aggressiveness.

3 MODELING GLOBAL WARMING ACTIONS

Chloride penetration and carbonation are governed by diffusion coefficients that depend, among other factors, on the surrounding humidity and temperature. Therefore, the assessment of the behavior of corroding RC structures should also include a comprehensive model of weather (humidity and temperature). A simplified model of climate is presented in this study. It accounts for the following aspects: (i) influence of global warming, (ii) seasonal variations, and (iii) random nature of weather. The change of temperature and humidity produced by global warming for the upcoming years is modeled by a linear time-variant function. A sinusoidal function is implemented to take seasonal variations of humidity and temperature into consideration. Taking into account the simplicity of the implementation and the computational time, Karhunen-Loève expansion is used to include the uncertainties related to weather parameters.

On the other hand, the increase of environmental CO₂ concentration produced by global warming will raise carbonation-induced corrosion risks. This phenomenon is difficult to model because it depends on several factors that differ for a particular problem. Therefore, this work uses the Model for Assessment of Greenhouse-gas Induced Climate Change (Wigley et al., 1996) that considers the influence of natural and anthropogenic forcings on CO₂ concentrations.

Global warming is influenced by several factors such as human activities, environmental protection measures, etc. Therefore there are important uncertainties related to the consequences of climate change that come mainly from the lack of knowl-

Table 1. Scenarios of global warming.

Scenario	Description
Without Expected	Climate change is neglected Use of alternative and fossil sources of energy, birthrates follow the current patterns and there is no extensive deployment of clean technologies
Pessimistic	Vast utilization of fossil sources of energy, appreciable growth of population and there are no policies to develop and extend the use of clean technologies

Table 2. Mean and standard deviation of the time to failure for the oceanic environment.

Corrosion aggressiveness	Scenario	Mean (yr)	σ (yr)	Reduction (%)
High	Without	62.2	9.4	0.0
	Expected	61.6	9.1	0.9
	Pessimist	61.4	8.9	1.4
Moderate	Without	124.8	20.3	0.0
	Expected	123.4	19.9	1.1
	Pessimist	122.6	19.7	1.7
Low	Without	411.2	75.5	0.0
	Expected	405.3	75.9	1.4
	Pessimist	401.7	76.3	2.3

edge about the societal policies and the response of the earth before global warming. To account for this uncertainty, this work defines three possible scenarios of global warming. These scenarios are called *without*, *expected* and *pessimistic* global warming (Table 1, Bastidas-Arteaga et al., 2010a).

4 NUMERICAL EXAMPLE

The influence of global warming on the reliability a simply supported RC girder placed in various chloride contaminated environments is illustrated with a numerical example. This analysis included: two environments (oceanic and tropical); three scenarios of global warming (without, expected and pessimistic) and three levels of corrosion aggressiveness (low, moderate and high). Structural reliability was evaluated in terms of the limit state of bending by using Monte Carlo simulations and Latin hypercube sampling. Table 2 presents the computed mean and standard deviation of the time to failure for the studied cases. The maximum reduction in time to failure is 2.3%. However, these results are non-conservative because the implemented corrosion model does not include the effect of global warming after corrosion initiation.

Corrosion rate can be influenced by temperature and humidity, and therefore, should be affected by global warming (Stewart and Peng, 2010). This effect should be taken into account to improve the prediction after corrosion initiation.

5 ADAPTATION STRATEGIES

Adaptation measures may be needed to ameliorate the increased damage risks due to climate change. Time of application is highly variable and dependent on extent and location of corrosion damage. Some adaptation strategies will be applied at time of construction (coatings/surface treatments, reinforcement), others at time of corrosion initiation (realkalization, chloride extraction). Clearly, it is preferable to use adaptation strategies that are implemented during design and construction rather than in-service (e.g., when corrosion damage occurs) as the latter will be much more costly in terms of direct costs and inconvenience/user delays and other indirect costs.

Stewart and Peng (2010) have conducted a preliminary life-cycle cost assessment to assess the cost-effectiveness of increasing design cover as an adaptation measure to mitigate the effects of carbonation of concrete. The preliminary analysis found that life-cycle costs for the current situation ('do nothing'—use existing covers) are lower than life-cycle costs for proposed increases in design cover. This suggests that although enhanced greenhouse conditions will lead to increased carbonation-induced corrosion of RC structures it may not be cost-effective to increase design covers. However, a more detailed assessment of risks, costs, benefits of adaptation measures and environmental impact may reveal a different conclusion.

6 CONCLUSIONS

This study presented some considerations to assess the effects of global warming on the durability of corroding RC structures subjected to chloride ingress or carbonation. This effect could be assessed by implementing deterioration models that take into account the changes in environmental factors (temperature, humidity and CO₂ concentration) produced by global warming. These environmental factors could be altered by climate change. Consequently, the computation of the changes in temperature, humidity and CO₂ concentration should also included in the analysis. All these points are treated in the paper and were illustrated with a numerical example that studies the effects of climate change on the reliability of a RC bridge girder placed in a chloride-contaminated

environment. The results showed that global warming could produce reductions in time to failure of up to 2.3%. Concerning to adaptation strategies that can be used to mitigate the effect of deterioration processes and global warming on structural safety, it is concluded that an optimal adaptation strategy should be selected by considering its risks, costs, benefits and environmental impact.

REFERENCES

- Bastidas-Arteaga, E. Chateauneuf, A., Sanchez-Silva, M., Bressolette, Ph. & Schoefs, F. 2010a. Influence of weather and global warming in chloride ingress into concrete: a stochastic approach. *Structural Safety* 32:238–249.
- IPCC, 2007. *Fourth Assessment Report of the Intergovernmental Panel in Climate Change*. Cambridge University Press, UK.
- Stewart, M.G. & Peng, J.X. 2010. Life-cycle cost assessment of climate change adaptation measures to minimise carbonation-induced corrosion risks. *International journal of Engineering Under Uncertainty* 2:35–46.
- Wigley, T.M.L., Richels, R. & Edmonds, J.A. 1996. Economic and environmental choices in the stabilization of atmospheric CO₂ concentrations. *Nature* 379: 240–43.

Development of adaptive flood risk management strategies under uncertainty

H. Harvey

School of Civil Engineering and Geosciences, Newcastle University, UK

J.W. Hall

Environmental Change Institute, University of Oxford, UK

ABSTRACT: The need for adaptive strategies to respond to uncertain long term processes of change in flooding systems is now well recognized. In the face of uncertainty, it is desirable to keep options open and enhance resilience. However, adaptive options are seldom achievable at zero marginal cost—in other words genuine ‘win-win’ solutions are rare. Therefore, appraisal frameworks are required that can evaluate adaptive strategies over extended timescales in the context of a wide range of alternative futures. In principle this may appear to be a relatively straightforward task. However, in practice, appraising flood risk management options, whose nature and cost will vary depending on which of many uncertain futures actually materializes, can be a computationally burdensome and conceptually taxing task. This paper describes a formal approach for specifying risk-based decision appraisal in the context of future uncertainties and long term processes of change. At the core of the analysis is a deterministic flooding model for estimating the severity and consequence of flooding, and cost model for computing the cost of flood risk management options. Around this kernel are layered risk calculations, simulations of long term change, comprehensive sensitivity analysis, decision analysis and analysis of the robustness of risk-based decisions to the ambient uncertainties. In the example presented here, processes of long term change include increasing relative mean sea level and increasing damage potential resulting from economic growth. In both cases the rates of increase are uncertain, as are the costs of implementing the interventions from which options are constructed. These various uncertainties are expressed as probability density functions (PDFs) over the variables in question. They are propagated through to option performance by means of a Monte Carlo experiment, allowing a PDF on performance to be constructed for each option.

1 OVERVIEW

Risk analysis, which involves the estimation of the statistical expectation of annual damage, EAD, using a damage model and a joint probability density function over the inputs to that model, is now a standard part of the flood risk management toolbox in the UK. Recent work has refined the structure of this analysis and made it possible to subject it to uncertainty propagation and sensitivity analysis methods. Strategic flood risk management interventions are planned and implemented over several decades. Where these interventions include physical infrastructure, as they surely will where large cities such as London are concerned, investments must be justified using cost benefit analysis over an appraisal period that includes the planning cycle and the design life of the infrastructure. This leads to the desire to evaluate management options in terms of their return on investment over a century or more. Climate, the economy and demography are but some of the more obvious sources of change that will influence estimates of flood risk on this time scale. First steps have been made towards the embedding of risk analysis within a framework enabling the examination of long-term change and the influence of possible flood risk management measures. In this paper we argue that these developments represent first steps in a process, the logical conclusion of which is *systematic decision analysis*. This goes beyond the status quo of modeling and risk analysis in a number of respects. We present a simple but general conceptual framework for decision analysis and illustrate its application to a simplified but representative strategic flood risk management decision.

Figure 1 depicts the conceptual framework in graphical form. It consists of five nested layers of analysis, as indicated by the nested boxes, each of which is labeled in the upper right hand

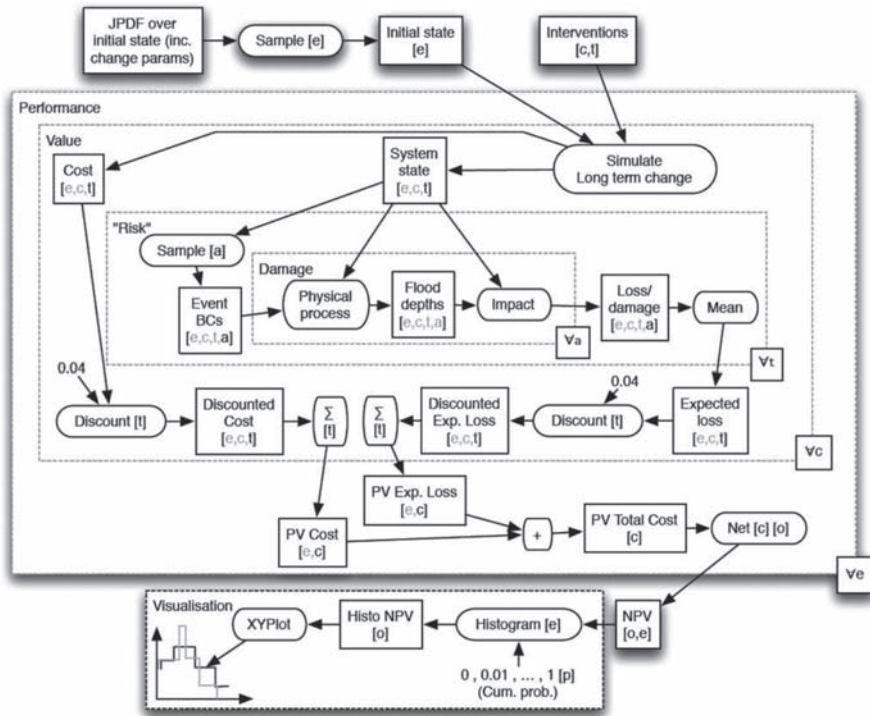


Figure 1. Overview of a conceptual framework for decision analysis. Larger boxes indicate the nested structure of the analysis. The computation itself follows the directed bipartite graph flowing from left to right. Unboxed nodes are data sets, while boxed nodes are transformations, where s stands for “sample”, m for “mean” and q for “estimate quantiles”. The dimensions of data sets are indicated by characters in square brackets beneath; these are *epistemic uncertainty* (e) *cases* (c), *options* (o), *time* (t), *aleatory uncertainty* (a), *cumulative probability level* (p).

corner. One way of thinking about the analysis is to consider these boxes as representing the nested loops of a naïve, sequential implementation. The layers of analysis are:

1. *Evaluate damage* using a deterministic model of the damage caused by a specific hydrological event. In the example set out below, damage is measured in money, however the framework can accommodate metrics for any undesirable outcome of system behaviour. Multi-criteria analysis has also been considered, but not yet demonstrated.
2. *Estimate Expected Annual Damage (EAD)*, for example following the RASP methodology now widely used within UK flood risk management. This involves many invocations of the layer 1 damage estimator.
3. *Simulate long-term change*. A possible future is specified as an initial system state, an option (a timed sequence of flood risk management interventions) and a set of parameters to a model of relevant long-term time-dependent processes (sea level rise, demographics, ...).
4. *Evaluate option performance*. The layer 3 computation is conducted for each of a set of *cases*, consisting of a “do nothing” base case and some number of “do something” *options*. For each option, a performance metric is evaluated, by comparison of the base case risk with the residual risk associated with each option.
5. *Apply computational experiments to performance estimator*. Both current system state and the parameters of change processes are uncertain, possibly highly so. Computational experiments, such as uncertainty and sensitivity analysis, can be applied to the layer 4 performance estimator to explore the impact of this uncertainty on decisions.

The paper presents and discusses the application of this decision analysis framework to the problem of strategic provision of flood protection. A prototype web-based user interface has been developed which allows the user to specify and run experiments on this example and explore and visualize the results from these experiments.

Probabilistic assessment of clay earthfill dams subject to variable precipitation

M.-C. Preziosi & T. Micic
 City University London, UK

ABSTRACT: Many uncertainties are associated with small earthfill dams that are not monitored in a comprehensive way. It is, a situation that may lead to significant threat of dam failure in case of extreme climate conditions. By applying probabilistic approach it becomes possible to assess such dams in more detail and obtain a clearer understanding of the risks associated with environmental threats, specifically different precipitation scenarios that may arise. This form of analysis is particularly useful when old, well established dams are considered for which new climate scenarios could not have been anticipated at the time of their design and construction.

The embankment model is based on a generic, small, homogenous earthfill dam for which steady seepage flow is considered and both upstream and downstream slope stability are selected as significant limit states governing the dam's long-term performance. The upstream and downstream sections of the dam behave, to a large extent, independently from one another. A specific area of the dam fill within the upstream section will become saturated and part of dam fill within the downstream section will become submerged to moist, over time, Figure 1. The residual embankment fill above the saturated and submerged parts will be deemed moist and/or dry depending on the current conditions at the dam site. Thus a more realistic model, analysing the overall stability of the upstream and downstream sections of the embankment, can be considered. This is important as the stability of the slopes will be greatly influenced by the type of the soil and its associated hydraulic conductivity.

The governing equations for the limit states are defined using sliding block methodology which incorporates the embankment's geometry,

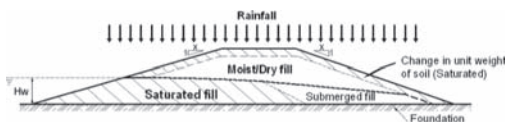


Figure 1. Modelling of embankment fill.

calculated position of the phreatic line and the specific soil conditions.

Climate scenarios rely on precipitation patterns for which historical data from the Met Office can be used. In order to establish slope instability due to precipitation and its infiltration through the embankment fill we use:

- The closed form van Genuchten method to establish hydraulic properties of the soil above the phreatic line.
- The standard and modified Green-Ampt method to establish the depth of infiltration and the time to ponding for the embankment segments.

To understand how different soil types can affect the reliability of the embankment's slopes, two types of London Clay were considered and exposed to the dam site conditions and short intensive and a prolonged less intensive rainfall. The modelling of the soil properties, presented in Table 1, had to be simplified to ensure that a broader set of data could be applied for various models under investigation.

For modelling of the precipitation effects on the embankment specific fill properties such as its degree of saturation (S_r), hydraulic conductivity

Table 1. LCA & LCB: Soil properties & unit weights of soil.

Soil properties	Units	Soil model	
		LCA*	LCB**
Void ratio (e)		0.79	0.69
Moisture content (θ)	%	27–29	24–39
Cohesion (c)	kN/m ²	7	5
Internal friction (ϕ)	°	20	20
Unit weight of soil	γ_d kN/m ²	14.9	16.1
	γ_m	16.0–16.6	17.0–17.6
	γ_{sat}	19.3	20.1
	γ_{sub}	9.5	10.3

*Extracted from (Davis et al., 2008)

** Extracted from (Kovacevic et al., 2001).

(K) and wetting front suction head (ψ) above the phreatic line need to be derived. We have implemented Van Genuchten method to derive the hydraulic conductivity and Green Ampt method to evaluate wetting front suction head.

As a result, the rainfall effects on unsaturated and saturated soils are evaluated and standard AFOSM applied. This allows for inclusion of deterministic and probabilistic site specific parameters. It is important to note that the probabilistic modelling, shown in Table 2 includes uncertainty in the soil properties, dam configuration and rainfall intensity. Thus the effects of environmental variables on the reliability index (β), probability of failure (P_f) and sensitivity factors for the upstream and downstream failure modes are obtained.

From the results in Table 3 it can be observed that when there is a high rainfall intensity over the short duration the slope's reliability is mostly influenced by the dam's geometry and the degree of saturation of its fill above the phreatic line.

Figures 2 & 3, show that the reliability indices for both upstream and downstream slope, for both soil models, steadily declines as the cumulative rainfall intensifies (rainfall intensity is assumed to be constant per hour). From the graphs, the decrease in the reliability indices for LCA and LCB follow the same pattern when subjected to the same conditions, but there is a clear difference between their values and the rate of decline. This implies that the soil properties of the fill clearly control the reliability of the embankment's slopes irrespective of the applied dam conditions.

From the results obtained we can identify the critical precipitation intensities and durations that can cause dam failure of either the upstream or downstream slope. Thus by implementing this form of probabilistic analysis, new management techniques and improved risk assessments for dams, with respect to precipitation scenarios can be established. This is of particular interest as the

Table 2. Probabilistic modelling of uncertain variables for clay embankment: All variables assumed to be normally distributed.

Variable	Unit	Mean (μ)	Standard deviation (σ)
Rainfall Intensity factor (RI_c)	mm	1.0	0.10
Height (H)	m	3.0	0.03
Crest Width (CW)	m	2.8	0.028
Foundation height (H_f)	cm	50.0	1.00
Headwater height (H_w)	m	2.0	0.10
Unit weight of soil factor (γ_{fc})	kN/m ²	1.0	0.10
Internal friction (ϕ)	°	μ_ϕ	$\mu_\phi \cdot 0.15$
Cohesion (c)	kN/m ²	μ_c	$\mu_c \cdot 0.30$

Flood and Water Management Act 2010 becomes the new regulatory document.

Table 3. Reliability indices for upstream and downstream collapse for soil A & soil B with varying degree of saturation Sr during 1 hr of rainfall.

Soil model	Sr %	Rainfall intensity mm	Reliability indices (β)			
			DG1		DG10	
			USlope 1:2.5	DSlope 1:2.5	USlope 1:4.0	DSlope 1:3.5
			β_{up}	β_{dwn}	β_{up}	β_{dwn}
A	56		2.53	1.47	3.94	2.61
	73	1-70	2.49	1.46	3.90	2.61
	86		2.45	1.44	3.85	2.59
B	59		2.01	0.45	3.63	1.80
	77	1-70	1.95	0.45	3.57	1.80
	88		1.85	0.43	3.47	1.78

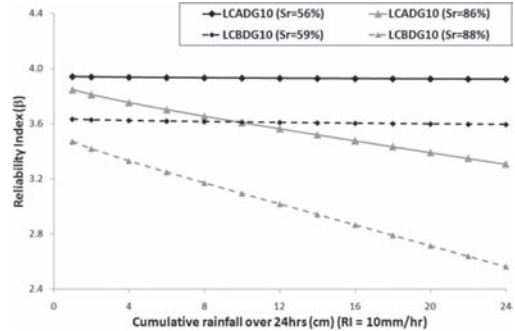


Figure 2. Reliability indices for two soil types with varying Sr for upstream slope failure with a constant rainfall of 10 mm/hr.

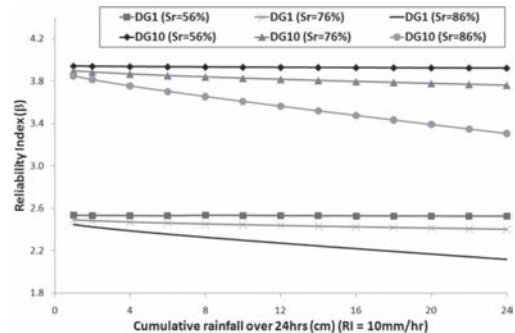


Figure 3. Variation in reliability indices for a single soil type for upstream slope failure for two dam geometries over 24 hours.

This page intentionally left blank

MS_323 — Robustness of structures (1)

This page intentionally left blank

Robustness of structures—a report on a joint European project

M.H. Faber

Technical University of Denmark, Lyngby, Denmark

A.C.W.M. Vrouwenvelder

TNO Building and Construction Research / Delft University of Technology, Delft, The Netherlands

J.D. Sørensen

Aalborg University, Aalborg, Denmark

M.K. Chryssanthopoulos

University of Surrey, Surrey, UK

H. Narasimhan

ETH Zurich, Zurich, Switzerland

1 BACKGROUND

Robustness of structures has been an issue of significant interest for the engineering profession over many years. It is generally agreed that robustness is a performance characteristic emerging from the structures as a system. The collapse of the World Trade Centre towers have substantially intensified research and efforts aiming to improve the robustness of structures, resulting in several useful recommendations on how to achieve robust structures. However, despite many significant theoretical, methodological and technological advances over the recent years, structural robustness is still an issue of controversy and poses difficulties with regard to its interpretation as well as regulation.

Modern structural design codes consider robustness through requirements which typically state that the consequence of damages to structures should not be disproportional to the causes of the damages. Despite the importance of robustness for structural design, such requirements are however still not substantiated in further detail; nor has the engineering profession been able to agree on an interpretation of robustness which facilitates its quantification.

It was with this starting point the Joint Committee on Structural Safety (JCSS) together with Working Commission (WC) 1 of the International Association of Bridge and Structural Engineering (IABSE) decided to organize a joint workshop in 2005 aiming for a consensus on how to deal with structural robustness in a more direct and explicit manner. One of the decisions resulting from this workshop was the initiation of a joint European

project on structural robustness titled ‘COST TU0601: Robustness of Structures’ in February 2007 under the COST (European Cooperation in Science and Technology) programme. A summary of the work carried out in this project and the major results achieved are described in this paper.

2 APPROACH FOR ASSESSING ROBUSTNESS

The Joint Committee on Structural Safety (JCSS) has developed a guideline document (JCSS 2008) that describes the framework and principles for risk based engineering decision making. An event tree representation for this framework is shown in Figure 1. The assessment begins with the modelling of exposures (EX) that have the potential to cause damage to the components of the considered structural system. Exposures could include extreme values of design loads, accidental loads and deterioration processes and also human errors in the design, execution and use of the structure. Damage refers to reduced performance or failure of individual components of the structural system. After the exposure event occurs, the components of the structural system either remain in an undamaged state (\bar{D}) as before or change to a damage state. Each damage state can then either lead to the failure of the structure (F) or no failure (\bar{F}).

Consequences are associated with each of the possible damage and failure scenarios, and are classified as either direct (C_{Dir}) or indirect (C_{Ind}). Direct consequences (C_{Dir}) are considered to result from damage states of individual component(s) of

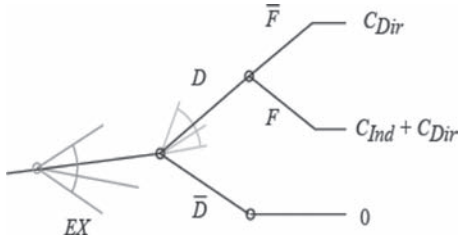


Figure 1. Event tree representation for quantification of robustness.

the structural system. Indirect consequences (C_{Ind}) are incurred due to loss of system functionality or failure and can be attributed to lack of robustness. With the event tree defined in Figure 1, the ensuing direct and the indirect risks may be assessed from:

$$R_{Dir} = \int \int C_{Dir}(D) P(D|EX) P(EX) dEX dD \quad (1)$$

$$R_{Ind} = \int \int C_{Ind}(F) P(F|D, EX) \times P(D|EX) P(EX) dEX dD \quad (2)$$

Using this approach, a robust system can be considered to be one in which indirect risks do not contribute significantly to the total risk, given that the ensuing direct risks have been determined to be acceptable. An index of robustness I_{Rob} can then be defined (Baker et al., 2008), which measures the fraction of total risk resulting from direct consequences:

$$I_{Rob} = \frac{R_{Dir}}{R_{Dir} + R_{Ind}} = \frac{R_{Dir}}{R_{Tot}} \quad (3)$$

3 THE PROJECT ORGANISATION

The main objective of the project is to provide the basic framework, methods and strategies necessary to ensure that the level of robustness of structural systems is adequate and sufficient in relation to their function and exposure over their life time and in balance with societal preferences in regard to safety of personnel and safeguarding of environment and economy. Research teams drawn from 24 countries representing both academia and industry are part of the project. The project has been running for a period of 4 years and is ending in October 2011. The major deliverables of the project are:

- A series of technical factsheets providing focused reporting on issues concerning robustness.

- A document on theoretical framework on structural robustness, which will serve as the basis to develop a probabilistic model code on design for robustness of structures.
- Educational material from a training school on robustness of structures for students, researchers and practicing engineers.
- A guideline document on robust structural design aimed at practicing engineers.

4 MAJOR RESULTS OF THE PROJECT

A theoretically sound framework for the assessment of robustness has been developed in this project which can facilitate the development of practice relevant methods for ensuring robust design as well as strategies for maintaining the robustness of existing structures throughout their service life and also form the basis for the development of pre-normative guidelines for robustness.

The project has seen extensive work being carried out related to the modelling of exposures and the representation of vulnerability and component failure modes relevant for robustness analysis. In addition to standard ultimate limit state design, the robustness assessment of a structure requires more advanced load as well as resistance models. In this project, various methods have been presented, differing in solution techniques, loading representations and member and joint modelling.

Work related to implementation aspect concerning robustness has also been carried out in the project. A common format for consequence evaluation in both building and bridge structures has been developed, and pertinent information on human, economic and environmental consequences has been collected and presented consistently both at component and system level. As part of risk mitigation and management, a categorisation of robustness enhancing measures and provisions in European standards has been described; this offers the opportunity to consider alternative strategies applicable to either new construction or existing structures.

5 CONCLUDING REMARKS

From the activities within the project and also from the outside of the project, it is becoming increasingly clear that the historically controversial theme of the project has been accepted and recognized as a key area in structural engineering. Moreover, the general approach to the assessment of robustness as forwarded by the project has been accepted in the research community of structural engineer-

ing. Building on these successes, future challenges primarily involve the establishment of a systems perspective in design and the codification of the set of principles and application rules for ensuring adequate and optimal robustness in structures. This will greatly enhance efficient and sustainable allocation of societal resources for structural safety and reliability.

ACKNOWLEDGEMENTS

The valuable and enthusiastic contributions of all the research teams involved in this project as well

as the strong support of the COST Office in Brussels are gratefully acknowledged.

REFERENCES

- Baker, J.W., Schubert, M. & Faber, M.H. 2008. On the Assessment of Robustness. *Structural Safety* 30: 253–267.
- JCSS 2008. Risk Assessment in Engineering. Internet Publication: http://www.jcss.ethz.ch/publications/JCSS_RiskAssessment.pdf.

A threat independent approach to evaluating the robustness of structures

S.M. Marjanishvili

Hinman Consulting Engineers, Inc, San Francisco, CA, USA

ABSTRACT: The term reliability, resilience, risk and redundancy are often used to convey similar or the same concept in the literature. Typically, none of these terms are defined in a computationally rigorous manner. Each of these terms has a unique mathematical meaning. However, resiliency and robustness have the special distinction of being particularly powerful because they are completely threat independent. Although it is possible to design structural systems to resist virtually any threat, it is impossible to design these systems to resist all possible threats. Even if all threats could be defined today, they cannot account for unknown future threats that may occur during the life of the structure. As a result robustness evaluation could be useful in prioritizing buildings and critical infrastructure for the purposes of allocating mitigation dollars potentially allowing for a way to optimize both sustainably and effectively. In this paper, the basic concepts used in probabilistic assessment approaches are described and an argument is made for using robustness and resiliency as the primary means for evaluating, repairing and replacing our structural systems in the 21st century.

1 RISK AND RELIABILITY

Risk of failure is a concept that can be universally understood by infrastructure stakeholders as well as engineers. A traditional definition of risk is that it is equal to the product of probability of failure (assuming that the threat has been executed) and cost of failure (i.e., consequence of failure). Hence, probability of failure needs to be computed to determine the risk. For the purpose of this paper let us assume an infrastructure type similar to a transportation or communication system, where performance is measured by the successful delivery of freight or data. This infrastructure will have a defined Capacity to perform (denoted as C) and a variable Demand (denoted as D).

It is intuitive that the infrastructure Demand and Capacity are dependent on each other. That is, if the infrastructure system is overloaded (i.e.,

the Demand is too great), its Capacity to perform goes down and nothing or very little freight or data gets successfully delivered (i.e., it fails). Similarly, if the infrastructure system is underutilized (i.e., the demand goes down) than its Capacity to successfully perform also decreases significantly (i.e., it has become obsolete)

Reliability techniques can be applied in engineering to compute the probability of failure based on a distribution of threats, or natural hazards, and a corresponding distribution of capacities to resist those threats. The probability of failure is determined based on the relative positions of the demand and capacity Probability Density Functions (PDFs) on a strength ordinate. Within the context of the definition of reliability, the probability of failure can be decreased by either: moving the relative positions of the PDFs to decrease overlap (decrease the load, increase the strength) or by decreasing the dispersion, or standard deviation of the PDFs (by increasing the certainty in the definition of either the load or the resistance).

2 RESILIENCY AND ROBUSTNESS

ASCE recommends promoting sustainability and resiliency as an integral part of its infrastructure report card. In Ref [4] ASCE presents a qualitative description of resiliency in context of each infrastructure sector. However it falls short in providing clear definition of resiliency. It is implied that resiliency is measured as elapsed time from the destructive incident until full operation of the infrastructure system is restored. Therefore, resiliency not only depends on the properties system (although it is unclear how) but it also depends on the system's operation and repair-time.

Another important quality of an infrastructure system is robustness, which is solely a property of the system. Robust infrastructure is insensitive to small deviations in assumed design parameters. The concept of robustness is illustrated on Figure 3. Despite System A and System B having the same Capacity values, System A is more robust

than Structure B, since the probability of failure for System A is less than that of System B. We may also note that System A is more reliable than System B without having more Capacity (i.e., the area under the curve for A and B is the same).

A subset of robustness is redundancy which is related to the existence of multiple and redundant sub-systems. These sub-systems may provide temporary and quick alternate way for the system to work around the damaged area and remain operational until full Capacity is restored.

3 PROTECTIVE DESIGN OF ROBUST SYSTEMS

Remarkably, there is little common ground regarding the definition of robustness. A quick look at the dictionary reveals five variations of the adjective with three of those five including the word “strong” or “strength”. So, it is natural that engineers, when asked about the meaning of robustness, would reply with words like “strong”, “resilient”, and “redundant”. There is currently no direct guidance out of the United States building codes standards that link robustness with a quantifiable definition. Be that as it may, other engineering and scientific disciplines have various specific definitions of robustness, and it is helpful to examine them here. Insight from outside of the structural engineering community combined with specific definitions of structural engineering metrics will lead to an adaptation to the definition of robustness and a novel way to evaluate infrastructure systems.

In Protective Design, the threat is unpredictable because the nature of the threat is always changing, evolving, and (usually) increasing in frequency and magnitude (TSWG, 2004). In this practice, it is difficult to predict any structure’s reliability given the great dispersion that is expected in the load scenario induced by the threat, though it is possible to determine and influence the dispersion of the resistance function. Increasing the certainty in the structural resistance by decreasing the standard deviation of the capacity—regardless of the expected value of the resistance (or strength)—increases the reliability for a constant threat PDF, and it also decreases the sensitivity of the system response to loading stimuli. The physical outcome of a narrow PDF for resistance is that the reliability of the structure will likely be unaffected by small perturbations in loading. This outcome is consistent with the Eurocode definition of robustness as well as the expected behavior of robust systems in various scientific fields.

A common approach to estimate resiliency and robustness is based on introduction of damages into the system and determination how sensitive the system is to this damage (robustness) and how soon

this system can recover (resiliency). Notable, these damages are almost universally related to damages due to a terrorist attack (i.e., a catastrophic event) and usually represented as an element removal (i.e., total destruction of the element). This approach requires enormous computational time as all damage scenarios as well as all response scenarios need to be determined and analyzed. This is a significant drawback of current approaches. Probabilistic techniques enable us to encompass all threats uniformly and as such will facilitate the design and improvement to infrastructure systems to withstand all threats, and natural hazards.

4 ALL HAZARDS APPROACH

The Fire Department of New York issued Terrorism and Disaster Preparedness strategy in 2007 [5], where it is strongly encouraged to “All-Hazard Preparedness”. The term all-hazard requires clarification to respond adequately to this challenge. How does one consider all hazards in the design and evaluation of our aging critical infrastructure? The table below provides examples of the assumptions made in the 20th century for the purposes of quantifying the effects of disasters are no longer accepted and are inconsistent with an all hazard approach.

In response to these shifts in our understanding of what a disaster is, the probabilistic concept of robustness provides a satisfying new approach, for it is a truly threat independent.

5 CONCLUSIONS

Today’s realities requires our critical infrastructure in the 21st century to achieve resiliency through sustainability and system robustness in response to a complex evolving threat and hazard environment.

Our infrastructure needs to be designed to be able to resist hazards and threats which are evolving and complex.

Robustness represents an infrastructure’s ability to absorb small failures (perturbations) without affecting the overall integrity, and can be measured as a standard deviation of the resistance probability density function.

Infrastructure robustness and resiliency represent interdependent qualities of system. Robust systems are inherently more resilient. Probabilistic approach to robustness and resiliency encompass all threats. As such robust and resilient design represent a true independence from threat.

Further research into the concepts of robustness and resiliency to explore how they may be used to evaluate our existing aging infrastructure and allocate our limited resources wisely for the demands of the 21st century.

Risk and robustness of road tunnels

D. Diamantidis

University of Applied Sciences, Regensburg, Germany

M. Holický

Klokner Institute, Czech Technical University, Prague, Czech Republic

ABSTRACT: The risk and the robustness of road tunnels are discussed in this contribution based on the experience of the author with industry projects. Minimum requirements for tunnels are reviewed first in this contribution such as those provided in the Directive of the European Parliament and of the Council of the European Union 2004/54/EU (EU, 2004). Risk and reliability acceptance criteria are presented in a so-called risk-matrix. For that purpose qualitative hazard probability levels have been defined as shown in Table 1 and hazard severity levels of accidental consequences as shown in Table 2. For the severity level human consequences are considered here. The hazard probability levels and the hazard severity levels are combined to generate the risk classification matrix as shown for example in Table 3. The classification scheme of Tables 1, 2 and 3 reflects also performance based engineering in which for specified hazards with given return period associated performance criteria are specified.

The lower bound values of Table 3 are more relevant as risk acceptance criteria for long tunnels.

Finally examples from case studies are provided demonstrating the applicability and the benefits from the risk analysis approach. The case studies deal with various types of tunnels i.e. bored, floating, immersed and different accidental actions such as fire, internal or external impact. For each accidental scenario associated performance criteria are defined and verified. The following conclusions are drawn:

1. A risk acceptance matrix offers a practical decision tool in order to evaluate the global performance of the tunnel system in case of accidental actions such as fire.
2. Current standards provide minimum requirements regarding tunnel safety and associated safety measures.
3. The safety measures should be verified and optimized based on a risk analysis.
4. The global failure should be checked based on system considerations.

Table 1. Hazard probability levels.

Class	Frequency	(Events per year)
A	Frequent	>10
B	Occasional	1–10
C	Remote	0.1–1
D	Improbable	0.01–0.1
E	Incredible	0.001–0.01

Table 2. Hazard severity levels.

Class	Severity category	Human losses
1	Insignificant	–
2	Marginal	Injuries only
3	Critical	1
4	Severe	10
5	Catastrophic	100

Table 3. Risk acceptability matrix.

	1	2	3	4	5
A	ALARP	NAL	NAL	NAL	NAL
B	ALARP	ALARP	NAL	NAL	NAL
C	AL	ALARP	ALARP	NAL	NAL
D	AL	AL	ALARP	ALARP	NAL
E	AL	AL	AL	ALARP	ALARP

Notes:

1–5: Hazard severity levels according to Table 2

A-E: Hazard probability levels according to Table 1

AL: Acceptable Level

ALARP: As Low As Reasonably Practicable (Level)

NAL: Not Acceptable Level.

REFERENCES

- Diamantidis, D. 2009. Robustness of buildings in structural codes, EU- COST workshop, Ljubljana, 21/22 September.
 EU, 2004. Directive 2004/54/EC, *Official Journal of the European Union*.

Progressive collapse in multi-storey steel frames: The effect of varying column spacing

V. Janssens & D.W. O'Dwyer

Department of Civil, Structural and Environmental Engineering, Trinity College, Dublin, Ireland

1 INTRODUCTION

On May 16, 1968, a small gas explosion triggered the partial collapse of the Ronan Point apartment tower. This event focused the intellectual debate on progressive collapse, and following the report of the Commission of Inquiry a number of countries introduced provisions to minimise the potential for progressive collapse. For the first time in the UK, it was required that “*structure[s] shall be designed and executed in such a way that [they] will not be damaged by events to an extent disproportionate to the original cause*” (CEN 2006).

The more recent attacks on the Murrah Federal Building (1995) and the World Trade Centre twin towers (2001) have highlighted the increased threat of terrorism worldwide. As a result, numerous publications on progressive collapse and extreme loading have appeared in the literature over recent years.

As building designers cannot possibly design for every hazard that a building may be subjected to in its lifetime, a general design approach is required to account for the risks associated with low-probability high-consequence events. This can be achieved through the provision of robustness:



Figure 1. Ronan point collapse.

where the authors consider robustness to be the ability of a structure to survive a certain degree of local damage without causing damage, to an extent disproportionate to the original cause. Current design codes and guidelines (ASCE 2005, CEN 2006, DoD 2009, GSA 2003) suggest three recommended approaches to provide a structure with an acceptable level of robustness. These are improved interconnection or continuity; key element design; and the notional element removal method. A review of these approaches is included in the full paper.

2 MODELLING PROGRESSIVE COLLAPSE

An analysis program capable of following the sequence of failures that occur during a progressive collapse has been developed by the authors (Janssens and O'Dwyer 2010). This program implements the finite element method, and is based on the notional element removal technique. This program models the progression of collapse through a structure, following the loss of one (or more) primary load carrying members. The dynamic effects associated with sudden member loss are included, and material nonlinearities are modelled using a plastic hinge approach. Additionally, the structural model is updated at each time step to account for geometric nonlinearities arising as a result of significant deformations in the structure. The algorithm developed removes individual elements from the structural model and computes the associated response. By systematically considering the effects of damage to all members in a structure, this algorithm can be used as both a design and an analysis tool to identify whether a structure is unduly sensitive to the effects of localised damage. The key features of this program are described further in this paper.

3 CASE STUDY

As part of the authors' research, the analysis program developed is being employed to study the

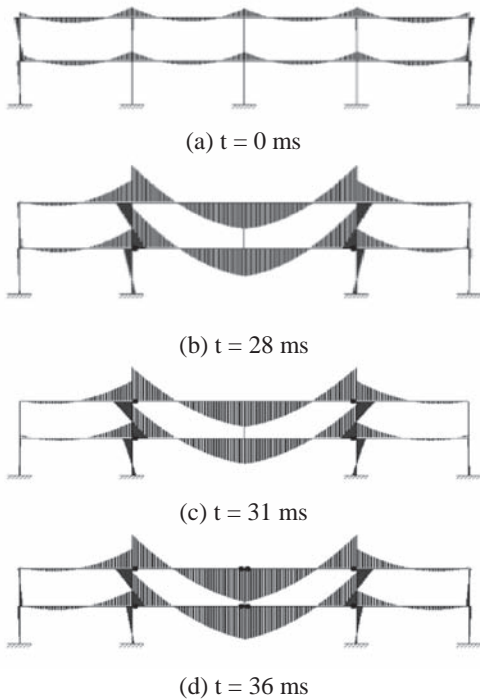


Figure 2. Response for column spacing = 10.5 m.

increased displacements and internal forces which may arise in steel-framed structures, following the sudden loss of a key element. By performing a series of parametric studies, the authors intend to quantify the increased displacements and internal forces which may arise following localised failure. The sensitivity of the response to variations in the material properties and the overall structural geometry will be assessed. The critical structural components in a collapse sequence will also be identified. This information may then be utilised by designers to ensure a structure possesses sufficient robustness to guarantee safety of its occupants if an extreme event were to occur. This paper presents the results of a preliminary study to determine the effect of column spacing on the response of a damaged structure.

The case study undertaken demonstrates the application of the progressive collapse program described. The behaviour of a two-storey frame is analysed, with a uniformly distributed load of 48,6 kN/m applied to the beams. The response of this structure, following the removal of the central ground floor column is shown in Figures 2(a)–(d). The results of this case study show significant bending moments in the columns, as well as large rotations and axial forces in the beams once their bending capacity has been exceeded. In particular, the duration of the ‘catenary phase’ has a significant influence in the peak values observed. Further work is currently being undertaken to develop developing relationships for these increased internal forces so that this information may be utilised by designers, to ensure the robustness of steel framed structures to accidental loading conditions.

ACKNOWLEDGEMENTS

This research is supported by the Irish Research Council for Science Engineering and Technology (IRCSET) Embark Initiative.

REFERENCES

- American Society of Civil Engineers 2005. *Minimum Design Loads for Buildings and Other Structures, ASCE 7-05*.
- Department of Defence (DoD) 2009. *Unified Facilities Criteria - Design of Building to Resist Progressive Collapse, UFC 4-023-03*. www.wbdg.org
- European Committee for Standardisation (CEN) 2006. *Eurocode 1: Actions on Structures - Part 1-7: General actions; Accidental actions, BS EN 1991-1-7:2006*.
- General Services Administration (GSA) 2003. *Progressive Collapse Analysis and Design Guidelines for New Federal Office Buildings and Major Modernization Projects*. www.buildingsecurity.us
- Janssens, V. & O’Dwyer, D.W. 2010. The Importance of Dynamic Effects in Progressive Collapse. *Proc. of 34th IABSE Symposium: Large Structures and Infrastructures for Environmentally Constrained and Urbanised Areas*, Venice.

Achieving robustness and mitigating risk of disproportionate collapse in building

Bruce R. Ellingwood

*The Raymond Allen Jones Chair in Civil Engineering, College of Engineering Distinguished Professor,
School of Civil and Environmental Engineering, Georgia Institute of Technology, Atlanta, GA, USA*

ABSTRACT: A disproportionate (or progressive) collapse is a catastrophic partial or total failure that initiates from local structural damage and propagates, by a chain reaction mechanism, into a failure that is disproportionate to the local damage caused by the initiating event. Such collapses can be initiated by many causes, including design and construction errors and extreme environmental or man-made events that are not considered explicitly in routine design. All buildings are susceptible to progressive collapse in varying degrees (Ellingwood and Leyendecker, 1978). A *robust* structural system is inherently capable of absorbing minor damage resulting from events outside the design basis. Although engineers generally recognize the need to engineer robust structural systems, specific design strategies and criteria for progressive collapse resistance have proved difficult to develop and implement in professional practice. At the same time, the public has become increasingly aware of building safety issues as a result of well-publicized collapses due to natural and man-made disasters. The decades following the Ronan Point collapse in 1968 saw numerous attempts in the following decade to develop criteria for progressive collapse resistance. Although the need to provide general structural integrity was (and is) widely recognized, specific practical codified design strategies and criteria for progressive collapse resistance have proved elusive. In the past decade, improved building practices to control the likelihood of progressive collapse have received renewed interest by the international professional engineering community and standards organizations. In the United States, the Federal government has implemented requirements for progressive collapse consideration in new buildings and major modernization projects (DOD, 2009; GSA, 2003).

Procedures for identifying specific threat scenarios, for assessing the capability of a damaged building

to withstand damage without the development of a general structural collapse, and for mitigating the risk of progressive collapse can be developed using concepts of structural reliability analysis and probabilistic risk assessment, supported by advanced computational tools (Ellingwood and Dusenberry, 2005; NIST, 2007). This paper summarizes current methods for assessing structural robustness, including recent provisions in *ASCE Standard 7-10, Minimum design loads for buildings and other structures* (ASCE, 2010) and identifies analytical and experimental research that is needed to advance risk-informed strategies for mitigating progressive collapse to the next level of professional practice.

REFERENCES

- ASCE, (2010). *Minimum design loads for buildings and other structures (SEI/ASCE Standard 7-10/ANSI Standard A58)*. American Society of Civil Engineers, Reston, VA.
- DOD, (2009). Design of buildings to resist progressive collapse. *Unified Facilities Criteria (UFC) 4-023-03*, Washington, DC, July, 2009.
- Ellingwood, B. & Leyendecker, E.V. (1978). Approaches for design against progressive collapse. *J. Struct. Div. ASCE* 104(3):413–423.
- Ellingwood, B.R. & Dusenberry, D.O. (2005). Building design for abnormal loads and progressive collapse. *Computer-aided Civil and Infrastruct. Engrg.* 20(5):194–205.
- General Services Administration (GSA). (2003). *Progressive collapse analysis and design guidelines for new federal office buildings and major modernization projects*, Washington, D.C.
- NIST, 2007. Best practices for reducing the potential for progressive collapse in buildings. *NISTIR 7396*, National Institute of Standards and Technology, Gaithersburg, MD (194 p).

This page intentionally left blank

MS_333 — Robustness of structures (2)

This page intentionally left blank

Probability based assessment of bridge exposed to extraordinary circumstances

I. Björnsson & S. Thelandersson

Lund University, Division of Structural Engineering, Lund, Sweden

K. Petersen

Lund University, Department of Fire Safety Engineering and Systems Safety, Lund, Sweden

1 INTRODUCTION

Considerations of robustness for structural bridge systems subject to accidental circumstances are discussed in this paper. An overview of the framework for the assessment of structural robustness is given highlighting the various features vital to its implementation. The application of probabilistic-risk based methodology for the investigation of system effects from rare exposure events is considered for a multi-span concrete bridge crossing multiple rail tracks as well as roads. Calculations are performed to ascertain and quantify these responses, specifically the investigation of impacts from derailed train traffic. The probability of such events occurring is estimated based on statistical data, an examination of subsequent propagating actions is carried out based on mechanical and structural considerations and the overall system response gauged. The potential consequences are then quantified and the corresponding risks associated with these events are assessed.

2 BRIDGE CASE

The bridge being considered is a multi span post-tensioned reinforced concrete bridge located in Sweden. The bridge crosses multiple rail tracks as well as a highway. A longitudinal section of the bridge is shown in Figure 1.

2.1 Modeling of bridge system

The bridge system is divided into two main constituent subsystems; (1) the physical load bearing structure and (2) the surrounding transport network. The transportation network is comprised of the infrastructure facilities such as roads and rail arteries in the region of the bridge. The system is bounded such that only traffic on roads and rail lines in direct proximity to the bridge are considered.

3 ASSESSMENT FRAMEWORK

The hazard event considered for the bridge case were train collision to supports 2, 3 & 4 as a result of derailment; refer to figure 1. These scenarios were chosen for the purposes of conducting a preliminary robustness assessment of the bridge system in an effort to provide an example of the application of the robustness assessment framework for an actual bridge.

The probabilities associated with train derailment near the bridge, on track adjacent to a support and in the direction of that support were determined. Then the corresponding impact force to the bridge support and the probability of support failure was found. Next, the behavior of the remaining bridge structure given support failure was evaluated. Finally, the consequences of the event sequences were assessed and the associated

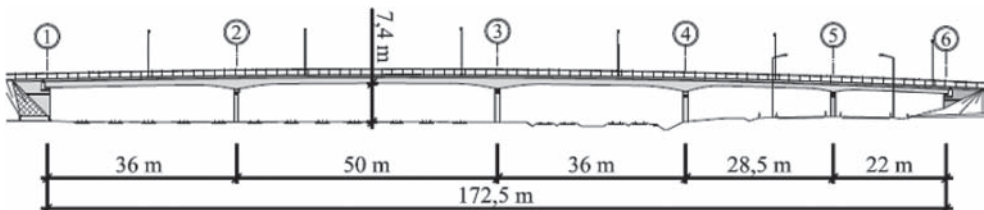


Figure 1. Longitudinal section of multi-span bridge crossing rail tracks and highway.

risks calculated. It was prescribed that system failure corresponds to loss of the bridges ability to maintain traffic on its superstructure.

The robustness of the system was evaluated using the robustness measure proposed by Baker et al. (2006); the index of robustness. The index of robustness is defined as the ratio of direct risks to the total risk for the system:

$$I_{Rob} = \frac{R_{Dir}}{R_{total}} = \frac{R_{Dir}}{R_{Dir} + R_{Ind}} \quad (1)$$

The definitions of the direct and indirect risks, R_{Dir} and R_{Ind} , are consistent with the JCSS (2008).

4 RESULTS

4.1 Structural response

The evaluation of train collision due to derailment for the bridge case determined an annual marginal probability of system failure at $3.7 \cdot 10^{-7}$. Table 1 shows a summary of the probabilities obtained including the extent of the bridge collapse given its failure.

4.2 Bridge system response

Given that the bridge collapses as a result of train collisions, the bridge system will incur negative consequences until the bridge is rebuilt.

The direct consequences included in the analysis were economic costs associated with damage to the supports. The indirect consequences included rebuild, human and traffic user costs. The human costs were comprised of fatalities and injuries for road vehicles on the bridge or running under it at the time collapse. Subsequent vehicle collisions to the collapsed bridge deck were also considered. Finally, the user costs were determined for short term, medium term and long term effects. As a result of actions taken after the hazard, the bridge system alters states gradually until full functionality

Table 1. Probabilities and intensities associated with event including the expected extent of bridge collapse.

Support	Collisions [per year]	Support failure*	Bridge failure**	Extent of collapse***
2	$9.89 \cdot 10^{-6}$	$7.30 \cdot 10^{-3}$	1.00	1-2, 2-3, 3-4
3	$1.04 \cdot 10^{-4}$	$3.42 \cdot 10^{-5}$	1.00	1-2, 2-3, 3-4
4	$1.00 \cdot 10^{-4}$	$2.94 \cdot 10^{-3}$	0.97	3-4, 4-5, 5-6

* Conditioned on collision

** Conditioned on support failure

*** i - j refers to failure of span between supports no. i and j

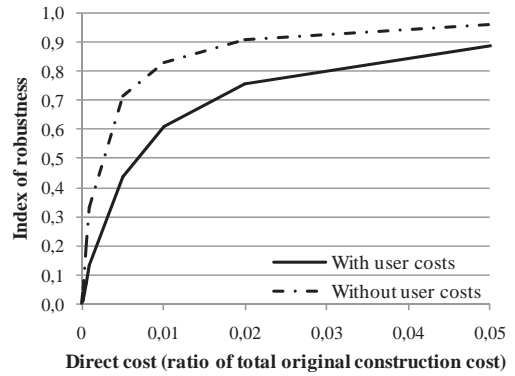


Figure 2. Index of robustness (conditioned on scenarios considered) in relation to the direct consequence.

is restored. Associated with each system state are consequences which were determined.

The traffic user costs and Value of a Statistical Life (VSL) were based on values recommended by the Swedish Institute for Transportation and Communication Analysis (SIKA 2008).

The robustness index according to equation (1) was determined to 0.14. Without taking into account the user costs, this value becomes 0.33. It was observed that these values depended largely on how large the minor repair costs were. Figure 2 shows the index of robustness plotted against the direct consequence costs in relation to the total original construction cost.

It is important to note that the obtained index of robustness is strictly conditioned on the scenarios considered. In the context of a decision analysis, the importance of these scenarios for the overall robustness of the system should be considered.

5 CONCLUSIONS

The overall conclusions based on the results of the probabilistic risk assessment and robustness calculation for the scenarios considered reveal that the structure is not very robust. On the other hand, the global system failure probability is, arguably, adequately low. The next step would then be to determine whether more robust promoting design strategies are required for this bridge or not. In order to do this, the contribution of other hazard scenarios not considered in the analysis, such as those resulting from road vehicle collisions or explosions, would have to be considered.

The important thing is to address robustness directly in the design procedure, prescribe the context of analysis, and provide clear indications of what is to be expected with regard to robustness.

REFERENCES

- Baker, J.W. Schubert, M. Faber, M.H. 2006. On the assessment of robustness. *Structural Safety*, 30: 253–267.
- JCSS 2008. *Risk Assessment in Engineering*. The Joint committee on Structural Safety. www.jcss.ethz.ch.
- SIKA 2008. Samhällsekonomiska principer och kalkylvärden för transportsektorn: ASEK 4. 2008:3.
- Stewart, M.G. & Melchers, R.E. 1997. *Probabilistic Risk Assessment of Engineering Systems*. Chapman & Hall, London.

Robust flood defences in a changing environment

H.G. Voortman & M. Veendorp

ARCADIS, Division Water, Amersfoort, The Netherlands

ABSTRACT: The paper investigates the application of robust design for levees and hydraulic structures. Robustness is in this paper defined as the ability of a structure to withstand future changes without the need for major modification. A basic economic framework for decision-making on robust design is developed.

1 INTRODUCTION

Safe, robust and long-lasting flood defence systems are a prerequisite for sustained development of deltas world-wide. It is not self-evident how such a system should be designed and managed.

The Joint Committee for Structural Safety (JCSS 2008) defines robustness as “The ratio between the direct risks and the total risks” with the total risks being equal to the sum of direct and indirect risks.

For flood defences, the direct risk is associated with failure to retain the water with flooding, economic losses and loss of life as a consequence. Indirect risk for a flood defence is very often associated with the need for (premature) refurbishment or modification of the structure due to the fact that the functionality of the structure is not up to current standards. Very often, such substandard performance is caused by changes in the environment of the flood defence, where environment is assumed to envelope the natural, societal and economical systems in which the defence is to function.

Modification of this type of infrastructure is time-consuming and costly. Designing the system with robustness decreases the likelihood that premature refurbishment becomes necessary. Therefore, a robust flood defence is in this paper defined as a defence that is designed and managed in such a way that it can deal with changes in its environment without the need for major modification.

The problem of providing sufficient safety in densely populated and heavily used Deltas appears to be a global one. The examples shown in this paper are taken from the Dutch part of the delta of the Rhine.

2 FLOOD DEFENCES IN A CHANGING ENVIRONMENT

2.1 *Overview of external influences*

Flood defence systems can not be seen separate from their environment. Environment is in this case taken in a wide context, namely the natural *and* societal environment of the system. Climate change, changes in the economy and changes in society influence the defence itself or the requirements imposed upon it.

2.2 *Economic and societal development*

Economic and societal development may have dramatic influence on the management of flood defences. Sad experience shows that societies generally respond after a disaster has caused considerable economic and societal damage.

Where physical measures follow disasters, the same is true for regulation. Thus, the legislation and safety standards for flood defences in the Netherlands were developed after the flooding of 1953 and, despite several rounds of updates, have been essentially unchanged ever since.

Also design philosophies follow a wave like pattern, sometimes even within a single project (see example below). After the 1953 flooding disaster dramatic measures were taken and robust design was considered more or less standard practice. Seeing the spatial and environmental consequences of (especially) the improvement of river dikes initiated in the 1990's the philosophy of “cunning design” which essentially meant applying no robustness at all. Several levees reconstructed in this period were already substandard as early as 2005. Robust design was reinvented around 2000 but under current economic conditions the tide is already shifting towards “sober” design.

3 ECONOMIC FRAMEWORK

The choice whether or not to adopt robustness in design is from a theoretical view point a cost benefit

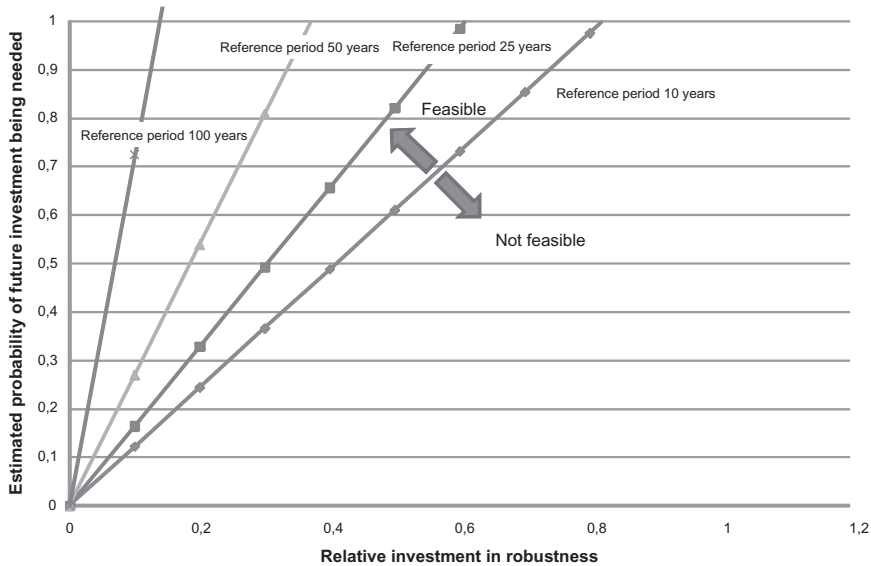


Figure 1. Graphical scheme for economic decision-making on robustness.

analysis, where the current extra investment is judged against the cost of a future reconstruction, where it is uncertain whether the future investment will ever be necessary.

The figure shows a graph for judging whether an investment in extra robustness is feasible. The economic model on which the graph is based is derived in the paper. The graph should be read as follows: consider a design which potentially needs reconstruction in 10 years. A modification of the design is available that increases the current cost, but avoids future investment in refurbishment. Based on estimates of the relative investment in robustness (cost of robustness as a fraction of the avoided future cost) and the likelihood of reconstruction in 10 years, the design option can be pinpointed in the graph. If the option is positioned above the line (marked reference period 10 years), it is an economically feasible option. If the option is positioned below the line, it is considered not economically feasible. The cost of the option is too high with respect to the avoided future cost or the likelihood of future reconstruction is considered low.

Because future developments are inherently uncertain, it is relevant to attach a probability to the need for reconstruction. In some special cases, it is possible to derive explicit estimates of the likelihood of future reconstruction. However, in a number of cases, estimating this likelihood needs

a lot of work or pinpointing options in the graph appears to be rather subjective. However, practical experience shows that, once a design is underway, the design team is very well capable of providing at least estimates of cost of robustness and likelihood of future reconstruction. Additionally, a number of special cases occur in practice, where rational decisions on robustness can be rapidly made based on this graph. The application of the decision framework is demonstrated in the paper in two example cases: robust design of levees and robust design of hydraulic structures.

SELECTION OF REFERENCES

- Joint Committee on Structural Safety 2008. Risk Assessment in Engineering, Principles, System Representation & Risk Criteria.
- Ministry of Public Works and Watermanagement, Royal Dutch Meteorological Institute. Report on the 1953 storm surge (in Dutch).
- Rooijendijk, C. 2009. Water wolves (in Dutch). *Atlas*.
- Van de Ven, G.P. 2003. Man-made lowlands, History of water management and land reclamation in the Netherlands. *Matrijs*.
- Voortman, H.G. 2002. Risk-based design of large-scale flood defence systems. *Phd-thesis Delft University of Technology*.
- Voortman, H.G. & Vrijling, J.K. 2004. Optimal design of flood defences in a changing climate. *Heron 4*.

Experimental and computational assessment of robustness of steel and reinforced concrete framed buildings

J.A. Main, Y. Bao, F. Sadek & H.S. Lew

Structures Group, Engineering Laboratory, National Institute of Standards and Technology, Gaithersburg, MD, USA

ABSTRACT: Since the destruction of the Alfred P. Murrah Federal Building in 1995, caused by a truck bomb attack, and the collapse of the World Trade Center towers in 2001, caused by the impact of large passenger jetliners, the engineering community, including codes and standards development organizations and public regulatory agencies, has paid greater attention to the performance of buildings subjected to damage from abnormal events. In the U.S. the American Society of Civil Engineers Standard 7, and the guidelines of the U.S. General Services Administration (GSA) and the Department of Defense (DoD) provide guidance to prevent disproportionate collapse (also known as progressive collapse). Disproportionate collapse occurs when an initial local failure spreads progressively, resulting in total collapse or collapse of a disproportionately large part of a structure. Resistance to disproportionate collapse is achieved either implicitly, by providing minimum levels of strength, continuity, and ductility; or explicitly, by (1) providing alternate load paths so that local damage is absorbed and major collapse is averted or (2) providing sufficient strength to structural members that are critical to global stability.

In the alternate path method, the structural integrity is assessed through analysis, to ascertain whether the structural system can bridge over failed structural members. For example, if a column is damaged, continuity of the beams adjacent to the top of the damaged column is required to redistribute the loads formerly carried by the damaged column. The analysis must demonstrate the adequacy of the beams and their connections to redistribute these loads, potentially through catenary action. An accurate characterization of the nonlinear, large-deformation behavior associated with the transfer of forces through the connections in such scenarios is critical in assessing the potential for disproportionate collapse. Physical tests are indispensable to validate the analytical models used to represent nonlinear connection behavior in such scenarios.

This paper describes both full-scale testing and finite-element based modeling of two beam-column

assemblies, including a steel and a reinforced concrete assembly. Each assembly comprises three columns and two beams, representing a portion of the second floor framing of a prototype ten-story building. Both assemblies represent a portion of an intermediate moment frame (IMF) designed for Seismic Design Category C (SDC C), typical of the Atlanta, Georgia area. The steel assembly incorporates welded unreinforced flange-bolted web (WUF-B) connections, while the concrete assembly was designed and detailed in accordance with ACI 318-02 requirements.

The beam-column assemblies are subjected to monotonically increasing vertical displacement of the unsupported center column to observe their behavior under a simulated column removal scenario, including the development of catenary action in the beams. Each test is continued until a collapse mechanism of the assembly is reached.

The steel assembly failed at a vertical column displacement of 495 mm, with a corresponding ultimate load of 890 kN. The vertical load versus displacement curves of the steel assembly exhibited an initial linear portion, a fairly well-defined yield point at a vertical displacement of about 50 mm, and a gradually increasing load beyond the yield point up to failure. The observed hardening behavior beyond the yield point was associated with the development of catenary action, and peak axial tension values of about 670 kN was measured in the beams of the steel assembly.

The reinforced concrete assembly failed at a vertical column displacement of 1090 mm, with a corresponding ultimate load of 547 kN. The vertical load versus displacement curve of the reinforced concrete assembly exhibited softening behavior, with an initial peak load at a vertical displacement of about 100 mm and reductions in load thereafter, up to a displacement of about 500 mm, at which point the load began to increase again up to the point of failure. The observed softening behavior was associated with softening and crushing of concrete, while the subsequent hardening behavior was associated with the development of catenary action. The initial peak load was about 300 kN,

and thus the ultimate load exceeded the initial peak load by a factor of 1.82.

Both detailed and reduced finite element models of the test specimens are developed, and the model predictions show good agreement with the experimental results, providing validation of the modeling approaches. The reduced models can be used for analysis of complete structural systems

to assess their vulnerability to disproportionate collapse. The tests and associated computational models help fill the gap in defining the response characteristics of the moment-resisting connections under collapse scenarios and contribute to establishing a library of validated connection models that can be used to assess the robustness of structural systems.

Fragility curve of steel containment failure due to hydrogen deflagration

Dirk Proske & Martin Richner

Axpo AG, Nuclear Power Plant Beznau, Switzerland

ABSTRACT: This paper describes the analyses and conclusions reached in regard to the ultimate pressure capacity of the free standing steel containment shell of the Swiss nuclear power plant Beznau during degraded core event. Such pressure capacities in terms of probabilities of failure are summarized in fragilities curves. The fragility curves for the containment have a strong influence on the results of the Probabilistic Safety Analysis (PSA) Level 2 in terms of Large Early Release Frequency (LERF) and therefore a detailed model is required, since goal values of LERF are given in laws.

As used herein the ultimate pressure capacity is defined as the dynamic internal pressure above the containment would be expected to have excessive leakage significantly beyond the design basis leakage (loss of function). Excessive leakage has been postulated to occur due to large deformations associated with yielding of main shell and/or penetrations, buckling of airlock structures, and failure of penetration/shell connections. The analyses were performed using actual material properties based on historical material test protocols. The room temperature test properties were adjusted to account for assumed accident temperature effects.

The dynamic structural computations were carried out as coupled field computation using first a thermodynamic computation to simulate the heating of the steel shell over time and space after the hydrogen deflagration energy release and secondly

the structural reaction to pressure caused by the hydrogen deflagration. The structural response analysis was carried out for simple analytical cases, in a two-dimensional finite element model and in a three-dimensional finite element model (Fig. 1). The finite element models consider non-linear material behavior and assume failure if a certain strain (Naus et al., 2004, Spencer et al., 2003, NUREG 6706) and deformation is reached. Several input parameters have been introduced as random variables. The application of random fields was investigated but later aborted due to missing data.

By application of advanced probabilistic and structural techniques it was possible to decrease the probability of failure of the steel containment under such loading in comparison to former investigations. On the other hand, further effects such as higher design temperatures, degradation effects and more restricted deformation capability by build-in components in the annulus have significantly decreased the capacity. In the end, both effects, positive and negative effects neutralized and therefore only a slight change in the load bearing capacity and a slight change in the probability of failure was achieved.

REFERENCES

- Naus, D.J., Ellingwood, B.R. & Graves, H.L. (2004): Methods for assessing NPP containment pressure boundary integrity. Nuclear Engineering and Design 28, pp. 55–72–Plant with NANO, 1989.
- NUREG/CR-6706-SAND2000-1735 (2001): Capacity of Steel and Concrete Containment Vessels With Corrosion Damage. Cherry & Smith.
- Spencer, B.W., Kunsman, D.S. & Graves, H.L. (2003): Risk-Informed Assessment of Degraded Containment Structures. Sandia Report, D455, Smirt 17 conference, 17–22 August 2003, Prague, Czech Republic.

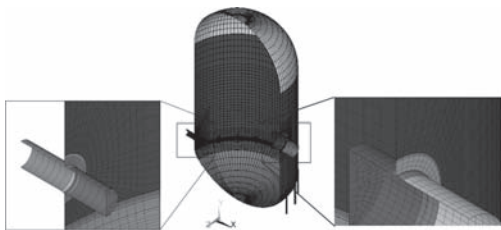


Figure 1. 3-D Finite element model of the steel containment of the nuclear power plant Beznau including main and emergency lock.

Seismic damage probabilities for segmented buried pipelines

S. Toprak, E. Nacaroglu & A.C. Koc
Pamukkale University, Denizli, Turkey

ABSTRACT: Having aging buried pipeline systems, many lifeline utility (e.g., water) companies worried about the performance of their systems against various hazards. For example, water distribution engineers of water utility companies need methodology that would assist in estimating the optimum time to replace water mains. Risk assessment of these systems provides a valuable tool for the mitigation studies. In seismic areas, pipelines are affected by earthquake loading and get some damage. The damage state is controlled by several parameters related to pipeline properties, geological and geotechnical characteristics of the locations where pipelines exist and seismic intensity. Because these parameters show substantial change for a pipeline system, which generally spreads over large areas, geographical information systems (GIS) are used for evaluations. In this study, the fragility relations relating the probability of buried pipeline damage within the pipeline system to the seismic intensity levels were presented. The seismic intensity is represented by peak ground velocity (PGV). The 1994 Northridge Earthquake and Los Angeles water supply system damage database were used to develop the fragility relations. By using the GIS, a grid of different sizes were superimposed on the pipeline damage and PGV maps. Effects of grid size on the damage probability curves were discussed.

1 INTRODUCTION

The earthquakes that occurred close to large urban areas caused significant damage. This was partly because of the relative size of buried pipeline systems that was exposed to earthquake and partly weaknesses in the systems. Some examples for weaknesses are aging of the pipelines, corrosion and inflexible joints. Risk assessment of buried pipeline systems provides a valuable tool for the mitigation studies. The basic equation for the risk calculation under extreme events is (e.g., Vrouwenvelder, 2009):

$$\text{RISK} = \sum P(H) P(D|H) P(S|D) C(S) \quad (1)$$

where H represents the hazard and $P(H)$ is the probability of exceedance of a given intensity over a given time period, D is the damage, $P(D|H)$ is the probability that the given facility get damage when subjected to the given hazard intensity, S is failure scenario, $P(S|D)$ is the probability that the given system fail when subjected to the given damage and C is the cost for the given failure scenario. The summation is over all relevant hazards, damage types and scenarios. The calculated risks can be used to calculate robustness index as proposed by Baker et al. (2008).

The objective of this study is to develop fragility relation relating the probability of pipe failure to the seismic ground motion parameter, namely peak ground velocity. In essence, a relationship to determine $P(D|H)$ for earthquake hazard is presented. The 1994 Northridge, USA earthquake pipeline damage was used to develop the relationships.

A similar approach was used by O'Rourke et al. (1999) to develop fragility relations relating the probability of pipe failure at a specified fault crossing location to the amount of fault offset.

2 FRAGILITY RELATIONSHIPS

2.1 Characterization of seismic hazard

Among the various seismic parameters, the most statistically significant correlations were found for PGV (O'Rourke et al., 1998; Toprak, 1998; ALA, 2001). PGV has a more direct physical interpretation in terms of its effects on buried pipelines.

2.2 The methodology

In order to develop fragility relation relating the probability of pipe failure to the seismic ground motion parameter, namely peak ground velocity, the study area is divided into $2 \text{ km} \times 2 \text{ km}$, $1 \text{ km} \times 1 \text{ km}$, $0.5 \text{ km} \times 0.5 \text{ km}$, and $0.25 \text{ km} \times 0.25 \text{ km}$ grids. Different grid sizes are used to evaluate the effect of grid size on the probabilities of pipe failure. Toprak et al. (1999) discussed the visualization of spatially distributed pipeline damage using GIS and emphasized the

effect of grid size on pipeline repair rate values. Figure 1 show the 2×2 km grid superimposed on the map of Los Angeles water supply system affected by the 1994 Northridge earthquake. The lines in the figure show the pipelines whereas the full circles show the pipeline repairs. The focus in this study is on distribution pipelines and particularly cast iron pipelines. The total length of the distribution lines is 10,750 km. About 76%, 11%, 9%, and 4% of the distribution lines are composed of cast iron (CI), steel, asbestos cement (AC) and ductile iron (DI), respectively. Out of 944 distribution line repairs, about 78%, 17%, 3%, 1%, and 1% are cast iron, steel, asbestos cement, ductile iron and other pipe type repairs, respectively (Toprak et al., 2008).

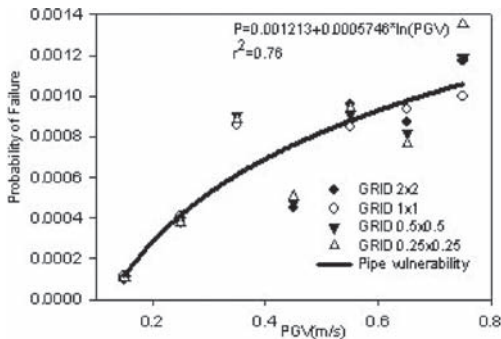
With GIS, the number of particular pipeline repairs and the length of pipelines are determined in each grid cell. The resulting pipe repair numbers and lengths are then grouped in such a way to correspond to 100 mm/s PGV intervals. In essence, corresponding values of the ground motion parameter based on the average ground motion to have occurred over the selected interval. The intervals are used in the following regression analysis. In order

to obtain the probabilities of pipe failure, number of pipelines which failed and did not fail should be determined. For this purpose, it is assumed that the pipe length is about 6 m and the total number of pipes in each PGV category is calculated by dividing the length of pipelines by 6. The number of pipes in each PGV category that failed is determined by assuming that each repair corresponds to one damaged pipe. This assumption is substantiated by checking the distances between the repairs are greater than 6 m by using GIS. The probability of failure is taken simply as the ratio of the number of damaged pipes to the total number of pipes in the same PGV category zone.

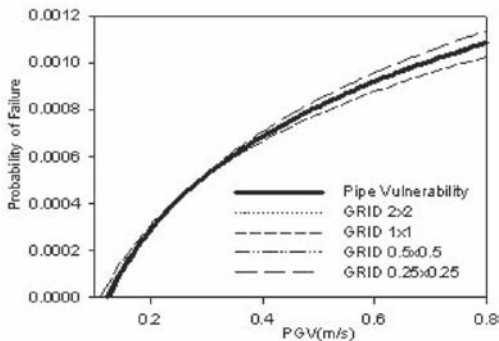
3 CONCLUSIONS

Data from four different grid sizes are shown in Figure 1. Also shown in the figure are the probability of failure curve obtained from all data and the equation for the curve. The effect of grid size on the curves are not so significant compared the results reported by Toprak et al. (1999). This may be the result of evaluating the probability of pipe failures over the PGV intervals of 100 mm/s.

The seismic fragility curves for pipeline damage presented herein can be useful for risk studies of segmented water utility systems. For example, water distribution engineers of water utility companies may combine them with risks from other hazards in estimating the optimum time to replace water mains. Because of the screening of data (PGV values greater than 0.8 m/s are not included in the analysis) similar to Toprak (1998), the curves should be applicable primarily to ground shaking hazard.



a. Data from various grid sizes



b. Comparison of probability of failure curves

Figure 1. Comparison of probability of failures for pipelines obtained from different grids.

ACKNOWLEDGEMENT

The research reported in this paper was supported by Scientific and Technological Research Council of Turkey (TUBITAK) under Project No. 106M252 and Pamukkale University Research Fund under Project Nos. 2010FBE031 and 2010FBE017. Partial Grant by PAU BAP to attend the conference is acknowledged.

REFERENCES

American Lifelines Alliance (ALA) (2001). Seismic Fragility Formulations for Water Systems, Part 1-Guideline, www.americanlifelinesalliance.org. 2001.
 Baker, J.W., Schubert, M. & Faber, M.H. (2008). On the Assessment of Robustness, Structural Safety 30 253–267.

- O'Rourke, M.J., Mitton, P. & Schiff, A. (1999). Pipeline Damage due to Fault Offsets in the Landers Earthquake, Optimizing Post-Earthquake Lifeline System Reliability, Proceedings, Fifth U.S. Conference on Lifeline Earthquake Engineering, Elliott, WM and McDonough, P, Eds., Seattle, WA, August, ASCE, 120–129.
- O'Rourke, T.D., Toprak, S. & Sano, Y. (1998). "Factors Affecting Water Supply Damage Caused by the Northridge Earthquake," Proceedings of the 6th US National Conference on Earthquake Engineering, Seattle, WA, USA, 1–12, 1998.
- Toprak, S. (1998). Earthquake effects on buried lifeline systems. PhD Dissertation, Cornell University; 1998.
- Toprak, S., Koc, A.C., Cetin, O.A. & Nacaroglu, E. (2008). Assessment of Buried Pipeline Response to Earthquake Loading by Using GIS. *The 14th World Conference on Earthquake Engineering*, Paper 06-0077.
- Toprak, S., O'Rourke, T.D. & Tutuncu, I. (1999). "GIS Characterization of Spatially Distributed Lifeline Damage", Optimizing Post-Earthquake Lifeline System Reliability, Proceedings, Fifth U.S. Conference on Lifeline Earthquake Engineering, W.M. Elliott and P. McDonough, Eds., Seattle, WA, August, ASCE, pp. 110–119.
- Vrouwenvelder, T. (2009). Probabilistic modelling of exposure conditions, Joint Workshop of COST Actions TU0601 and E55, September 21–22 2009, Ljubljana, Slovenia.

A reliability-based measure of robustness for concrete structures subjected to corrosion

E.S. Cavaco & L.A.C. Neves

Civil Engineering Department, Universidade Nova de Lisboa, Monte de Caparica, Portugal

J.R. Casas

Civil Engineering Department, Technical University of Catalonia, Barcelona, Spain

ABSTRACT: This work is a contribution to the definition and assessment of structural robustness. Special emphasis is given to reliability of reinforced concrete structures under corrosion of longitudinal reinforcement.

On this communication several proposals to define and measure structural robustness are analyzed and discussed.

In this paper the proposal of Cavaco et al. (2010) is adopted. Accordingly to the authors robustness can be defined as a measure of the degree of structural performance lost after damage occurrence. The structural performance can assume many forms, and can be related to service limit states or to ultimate limit states. Damage concept should also be considered with a broader sense, i.e., damage can vary from a simple degradation state to a more serious damage as a column or a beam failure. Errors during the design or the construction stage can also be seen as types of damages.

Associated to this definition the authors also propose a framework to assess robustness R_d obtained through equation (1), which gives the area above the curve defined by the normalized structural performance f subjected to a normalized damage d :

$$R_d = \int_{d=0}^{d=1} f(x) dx \quad (1)$$

where f is given by the ratio between the structural performances on the intact and damage states, and d is given by the ratio between actual and maximum possible damage.

In this paper the reliability index β is considered as the structural performance indicator since it is commonly used to assess the safety of existing structures. Corrosion level on longitudinal reinforcement, measured in terms of weight percentage, is considered as the damage indicator.

The proposed methodology is illustrated by means of an application example consisting on a simply supported beam with a rectangular cross

section subjected to self-weight g and live load q (Figures 1 and 2).

In order to consider the impact of reinforcement corrosion on failure probability growth, an advanced methodology based on the strong discontinuities approach and an isotropic continuum damage model for concrete, proposed by Sánchez et al. (2008), is adopted. The methodology consists on a two-step analysis: on the first step an analysis of the cross section is performed in order to capture phenomena such as expansion of the reinforcement due to the corrosion products accumulation and damage and cracking in the reinforcement surrounding concrete (Figure 3).

On the second step a 2D deteriorated structural model is built with the results obtained on the first step of the analysis (Figure 4). This model accounts also with reinforcement area reduction and bond strength deterioration between steel and concrete.

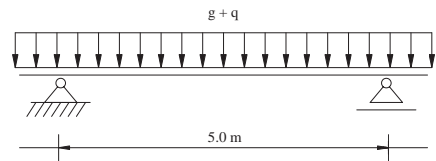


Figure 1. Simply supported RC beam under corrosion.

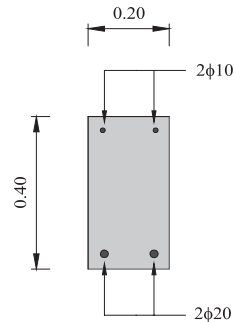


Figure 2. Cross section.

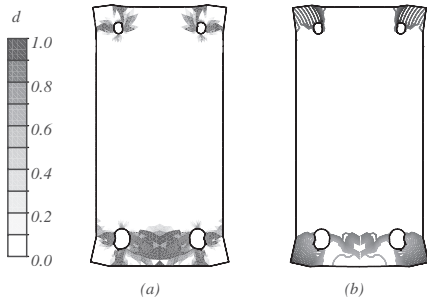


Figure 3. Cross section analysis results. (a) Concrete damage; (b) Concrete cracking.

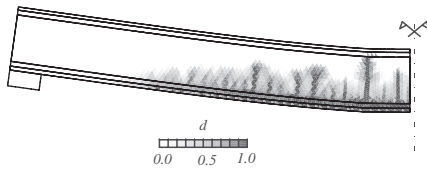


Figure 4. 2D longitudinal model results.

Table 1. Random variables distribution and parameters.

Random variable	Dist.	Mean	Std. dev.
f_c	logn	38.5 MPa	5.8 Mpa
f_y	norm	460 MPa	30 Mpa
g	norm	25k N/m ³	0.75 kN/m ³
q	gamma	1.25 kN/m ²	2.5 kN/m ²
θ_R	logn	1.2	0.15
θ_E	logn	1.0	0.10

In order to account with the uncertainties associated to the resistance R and load effect S , a reliability analysis is performed. Monte Carlo simulation, with $n = 10^8$ samples, is used to compute the failure probability and the reliability index of the structure for different corrosion levels. Due to complexity associated to the corrosion analysis methodology used, the number of random variables is limited to those presented in Table 1 and an approach to the resistance probability density function f_R is needed.

The resistance probability density function f_R is normally fitted accordingly to the maximum likelihood parameters estimation technique (Figure 5) for corrosion values varying from 0% to 100%, using results of Latin Hypercube sampling with 100 samples.

The fitting quality is guaranteed by performing a Kolmogorov-Smirnov hypothesis test.

The results obtained (Figure 6) show the evolution of the failure probability P_f and the reliability index β with corrosion level X_p .

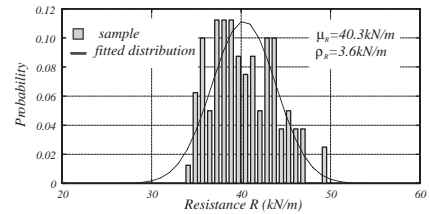


Figure 5. Fitting the resistance distribution for $X_p = 0\%$.

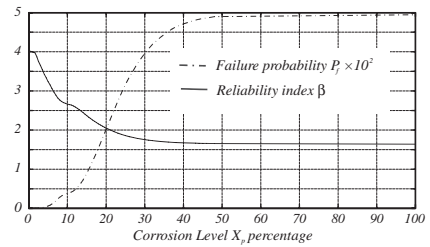


Figure 6. Failure probability P_f and reliability index β as function of the corrosion level X_p .

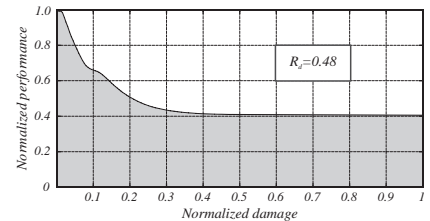


Figure 7. Robustness assessment.

Finally, robustness R_d is assessed accordingly to the methodology proposed by Cavaco et al. (2010) (Figure 7).

REFERENCES

- Cavaco, E.S., et al. (2010). Robustness of corroded reinforced concrete structures – a structural performance approach. *Structure and Infrastructure Engineering*. DOI:10.1080/15732479.2010.515597.
- Sánchez, P., Huespe, A., Oliver, J. & Toro, S. (2008). Numerical modelling of the load carrying capacity degradation in concrete beams due to reinforcement corrosion. In *8th World Congress on Computational Mechanics (WCCM8), 5th European Congress on Computational Methods in Applied Sciences and Engineering (ECCOMAS 2008)*.

This page intentionally left blank

MS_237 — Social perspectives for hazards decision

This page intentionally left blank

Making the case for resilience investments

E. Seville, J. Vargo, J. Stevenson & A. Stephenson
Resilient Organisations, University of Canterbury, New Zealand

1 INTRODUCTION

Our world is more technologically advanced and interdependent, risks are increasingly shared across local, regional and national boundaries and we are more culturally diverse than ever before. As a result, communities are increasingly confronted with emergencies and crises which challenge their social and economic stability.

While many organizational leaders agree with the need to improve resilience in principle; they appear to lack the commitment needed to drive through change. There always seems to be something more vital to address: either the organization is doing so well that they are working very hard to keep up, or the organization is already struggling and has nothing to spare. It is also very difficult to attract Board level buy-in or support for investments that have highly uncertain returns or quantifiable benefits.

In this paper we explore the realities of making decisions to invest in building resilience to natural hazard events.

2 THE GOAL OF RESILIENCE

A resilient organization is one that not only survives, but is also able to thrive in an environment of change and uncertainty. There are several dimensions to resilience for organizations. It is:

1. the ability to prevent negative consequences occurring,
2. the ability to prevent negative consequences worsening over time,
3. the ability to recover from the negative consequences of an event, and
4. the ability to find the ‘silver lining’—seeking out the opportunities that always arise during a crisis to emerge stronger and better than before.

Risk management provides an important mechanism for engaging organizations in proactively thinking about and managing the unexpected. As such, risk management is an important input to developing greater resilience (though it is not the only input). Also important for achieving greater

resilience is an organizational culture and ethos that promotes a capacity to adapt and respond positively to change and the unexpected.

3 MAKING THE CASE FOR RESILIENCE INVESTMENTS

The translation from the results of a risk assessment and evaluation process into investment in greater resilience can sometime be frustrating. While numerous studies are undertaken to identify vulnerabilities and methods for improving resilience, this growing body of knowledge does not always result in decisions makers willing to invest in risk mitigation and resilience initiatives. There are significant gaps in our understanding of how those in charge of making strategic investment decisions for organizations, factor resilience into their decision making processes. In the following section of this paper we use a recent event to explore the approach of some decision makers to the management of natural hazard risks before, during and after a major earthquake.

4 THE CANTERBURY EARTHQUAKE

At 4:35 am on a Saturday morning, the Canterbury region of New Zealand was struck by a major earthquake, 7.1 on the Richter scale and 11 km deep. There were no deaths from this earthquake and only three serious injuries, but these statistics mask the fact that there would have almost certainly been a substantial death toll had the earthquake occurred during the daytime. A description of the type and nature of the damage caused by the earthquake are given in the full paper.

5 REFLECTIONS ON RISK BASED DECISIONS

Prior to the September 4th Earthquake, Canterbury, had a well recognized seismic risk. The vulnerability of certain types of buildings and infrastructure to damage in earthquakes was also well understood.

In the New Zealand Building Code, a building is classed as an 'Earthquake Prone Building' if it has less than 33% of the strength required by the current building code. An earthquake prone building is at risk of collapse in a moderate sized earthquake. Many older buildings, particularly unreinforced masonry or concrete buildings built prior to modern building codes, would fall into the 'earthquake prone building' category unless they have already been seismically retrofitted.

Only 1 month prior to the earthquake, the Christchurch City Council had debated at length what its policy on Earthquake Prone Buildings should be. This debate was informed by detailed risk and impact assessments of the various policy options. It was decided for the policy to allow 15 years for buildings with special post-disaster functions to be brought up to a minimum of 33% of current code. Buildings that contain people in crowds or contents of high value were given 20 years to be brought up to the minimum of 33% of current code. Any significant alterations to the building within these timeframes would trigger an immediate requirement to strengthen the building up to the 33% threshold.

There had been a push from the engineering community for stronger requirements on building owners, but this had been outweighed by concern that more stringent requirements would result in the loss of many heritage buildings and reduced vibrancy in the central city business district (where many earthquake prone buildings are located).

Although this policy had already been the subject of significant analysis and debate in the year prior to the earthquake, within the first week after the earthquake, an Order of Council was passed to significantly change these requirements. Following the earthquake it was determined that all earthquake prone buildings that suffered damage in the earthquake would now need to be repaired to a minimum of 67% of current design code (up from the 33% requirement previously set out in the policy).

In the aftermath of the earthquake there was suddenly political will to make the change and that change was made extremely quickly. So why the change of heart?

The level of seismic risk had increased due to aftershocks and induced seismicity, but this shift in seismic risk is (relatively) short term and not of such a magnitude to explain this radical change. The nature of the vulnerability of the built

infrastructure had also changed, though some would say in a positive direction in that many vulnerable buildings had already collapsed and were in process of being demolished; so this too cannot account for the change. What had changed radically in the aftermath of the earthquake was the socio-political context of the decision making process. The community's awareness of the risk was heightened and the 'outrage' factors affecting the acceptability of the risk had altered significantly. The detailed analysis work prior to the earthquake did enable a rapid change in policy following the earthquake however, clearly the dominant influence on the decision making process was the shift in political will rather than the quality or nature of the information presented.

Further examples of risk based decision making behavior following the earthquake are given in the full paper.

6 CONCLUSIONS

Over the past decades there has been an increasing push for organizations to use risk based techniques for understanding their risks and prioritizing investment. In this paper we presented several examples from the recent Canterbury Earthquake that illustrate the radical shift natural hazard events can have on the way risk and resilience decisions are made. These examples highlight the importance of 'context' in the decision making process and point to the need to focus far greater attention on understanding and finding ways to influence this decision making context.

It seems that we have a better understanding of how to get that extra decimal point's worth of accuracy on our estimates of the level of risk, than we do on how to influence the social, political and organizational realities of how that information will be used to inform decisions. This is an area requiring greater research focus if we are to make a step-change in the level and quality of investment in resilience to natural hazard events for the future.

With just three months passed since the earthquake, now is an opportune time to explore with decision makers the key factors that influence their decision making over the recovery period. This will be a significant area of future research for the Resilient Organisations Research Programme.

Rebuilding L'Aquila following the 2009 earthquake: Priorities and perspectives

A.B. Liel & R.B. Corotis

Department of Civil, Environmental and Architectural Engineering, University of Colorado, Boulder, CO, USA

J. Sutton

Trauma Health and Hazards Center, University of Colorado, Colorado Springs, CO, USA

G. Camata & E. Spacone

University "G.D'Annunzio" of Chieti-Pescara, Italy

R. Holtzman

Meyer, Borgman and Johnson, Phoenix, AZ, USA

1 BACKGROUND

On April 6, 2009 at approximately 3:30 AM, an earthquake with magnitude (M_w) 6.3 struck the region of L'Aquila, Italy, approximately 120 km northeast of Rome, causing significant damage and killing more than 300 people.

This paper examines decision-making and progress in recovery and reconstruction in affected communities in the first year after the earthquake. Data were collected through face-to-face interviews with community leaders, public officials and building industry representatives involved in reconstruction activities. Interview responses characterize key stakeholder groups' priorities for recovery and reconstruction and the role of community groups, local and national politicians, building industry and others in shaping the recovery agenda. Analysis of recovery progress and process following the L'Aquila Earthquake provides a compelling case-study, because the Italian government undertook a new approach to disaster recovery, and decisions and organizations have evolved over time.

The study focuses on three communities impacted by the earthquake: L'Aquila, a small city and the provincial capital, Onna, a village that lost approximately 11% of its residents during the earthquake, and the nearby town of Poggio Picenze. These communities vary in terms of population, severity of ground-shaking and damage experienced, topography and dominant industry.

Semi-structured face-to-face interviews were conducted with key representatives in each community from each of three groups: grassroots community leaders (including journalists, religious leaders and community organizers), building industry leaders (including engineers, architects and

contractors), and government leaders (including public sector representatives). A total of 18 interviewees were identified on the basis of their leadership roles in the recovery and reconstruction process. All of the interview participants are men and range in age from their mid-forties to their mid-sixties.

Interview questions focused on three primary themes: (1) prioritization and process for post-earthquake reconstruction, (2) integration of local community organizations in decision-making and (3) awareness of seismic risk and building codes both before and after the earthquake. Interview guides differed depending on the leader's role in the community (i.e. community leader, industry leader or government leader). Each set of interview notes was then hand-coded to identify content related to each of the primary three themes.

2 DECISION-MAKING AND PRIORITIES BEFORE THE EARTHQUAKE

Community and industry leaders in all three communities expressed negative perceptions of political leaders. Local governments are mired by administrative and bureaucratic problems and their decisions are strongly colored by politics and political ambition. Leaders described that the citizens had experienced a sense of abandonment by the local authorities and that local government leaders were seen as dividers rather than as unifiers of the community. Building industry interviewees commented specifically on the lack of political leadership with regard to issues of seismic risk and risk mitigation. The regional Abruzzi authorities were generally viewed more positively.

Mayors and, to a lesser extent, city councils were responsible for decisions about built infrastructure and environment. Leaders from Onna emphasized that the decisions were made by the mayor of the municipality of L'Aquila (of which Onna is a part), not within their own village. Government leaders from Poggio Picenze emphasized their town's independence from L'Aquila. Most of the industry leaders stated that the building industry was not involved in important planning decisions.

The general public was not involved in decision-making related to planning and the built environment prior to the earthquake or was involved only at the end. The reasons given for the lack of community involvement included a lack of civic gathering spaces in which to hold meetings. In addition, one community leader told interviewers that no one is willing to make sacrifices for social or civic services.

3 RECONSTRUCTION PRIORITIES, DECISION-MAKING AND DECISION-MAKERS

The initial government response to the earthquake was viewed as essential, timely, and helpful. However, satisfaction with the national government response decreased in the months following the earthquake. Several leaders described the Civil Protection Agency's active work in April and May (the two months immediately following the earthquake), but lamented that there was a lack of a longer term government plan for reconstruction and rebuilding. They worked "without thinking of the future," according to one community leader.

Leaders in Onna expressed pride that their village had made important decisions about reconstruction locally, with a high level of community involvement. The degree of community engagement in recovery and reconstruction has been more varied in the larger communities of L'Aquila and Poggio Picenze. Community leaders in L'Aquila commented that all reconstruction decisions affecting L'Aquila had been made by the national government, leaving citizens no opportunity to provide input. Professionals from the building industry "are not considered at all." The general opinion was that the meetings that were held were not very useful because "everyone wants to operate separately" and because meetings did not focus on

the most important issues related to establishing priorities and planning for reconstruction.

4 AWARENESS OF SEISMIC RISK AND RISK MANAGEMENT

Many residents apparently did not know that the L'Aquila region was seismically active until just a few months before the April 2009 earthquake, when frequent smaller earthquakes began. This lack of awareness was attributed to poor communication by the government of past earthquakes and seismicity in the region. After the earthquake, residents were described as being very fearful of another earthquake and very aware of seismic risk. "People scream," even when there are just small earthquake shocks, one leader noted. "L'Aquila is like a ballerina," another said, and continued shaking is a frequent reminder of seismic safety.

The leaders interviewed cited changes to building codes, the use of innovative building technologies in new buildings, such as base isolation, and efforts to strengthen existing buildings as evidence of positive steps toward reducing seismic risk. Despite these positive signs and community demands for seismically safe structures, leaders expressed significant doubts about whether these concerns would have tangible effects on the rebuilding. Several said they saw little evidence that rebuilding would reflect increased consciousness about seismic risk. Real estate development and financial concerns were expected to be prioritized at the expense of construction quality. In addition, there is a lack of expertise in L'Aquila regarding building with timber because it is much different from the region's traditional building methods.

5 NEXT STEPS

This paper documents one part of a larger study on recovery and reconstruction in L'Aquila. In addition to those leaders whose responses are described here, we also interviewed four national leaders of the reconstruction. These responses will be analyzed to understand how decisions were made at a national level and differences between locals and national perceptions of priorities and progress. Some follow-up interviews with local industry, community and government leaders were conducted in April 2010.

The function of regulations and incentives for societal safety

A. Lentz & I.B. Kroon
 COWI A/S, Kongens Lyngby, Denmark

1 INTRODUCTION

The preferences of society with respect to safety often differ from those of its stakeholders—individuals, enterprises or entire industries. These differences can have objective as well as perceived causes. Society has two options for ensuring the implementation of its preferences. One is to make them part of binding regulations. The other option consists in manipulating the preferences of the stakeholders by means of positive or negative incentives. Incentives are typically used, whenever binding regulations are unwanted or even impossible.

Risk to human life is the most serious safety issue from a societal point of view, which is why it serves as a basis for all the considerations in this paper.

2 UTILITY-BASED DECISION MAKING

Cost-benefit analyses are the standard decision-making tool for many decisions. However, the decisions based on these tools are much dependent on the decision makers and their preferences. There is a tendency to reduce the value of human life to the amount of lost income in case of a fatality. Measuring the utility of one's future years of life is the most rational and consistent available decision-making tool for those cases.

For health-policy and engineering decisions, a common way of formulating lifetime utility is $L = L(l, g)$, where l is life expectancy and g is the average disposable income. A recent formulation of L , which takes both the health-policy orientated and engineering approaches into account (Pandey & Nathwani, 2004), is

$$L = g^a l_d \tag{1}$$

l_d denotes the average remaining life expectancy of all currently living members of society. The index d stands for 'discounting'.

If utility is made up of life expectancy l_d and disposable income g , it implies that life expectancy can be exchanged with income at a certain rate without

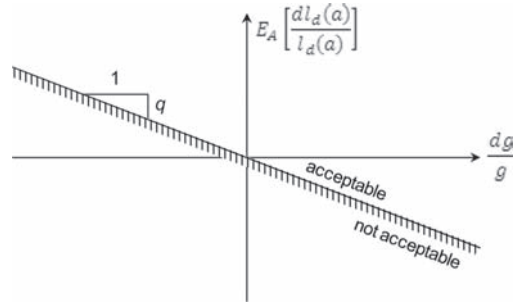


Figure 1. Societal willingness-to-pay function.

changing overall utility. The rate of exchange between income and life expectancy is referred to as willingness to pay (WTP). Engineering decisions have usually an effect upon safety levels and income at the same time, typically with opposed signs. A decision is judged acceptable, if the overall lifetime utility remains equal or rises. This is visualized by Figure 1, where the function represents the case $dL = 0$. Decisions that are placed precisely on the limit function are neutral with respect to lifetime utility and as such acceptable. Decisions that are located above the limit function are not only acceptable, but in fact recommendable.

3 THE FUNCTION OF REGULATIONS

The preferences of society as a whole (represented by the average citizen) and each of its stakeholders (individual citizens, enterprises or entire industries) are often different. The divergence from the societal preference function is presumably most pronounced for enterprises, while it can also be distinct for citizens with an economic situation far above or below the average.

Regulations are one of the options that society can choose in order to reduce or remove the gap between societal preferences and stakeholder preferences.

The effect of regulations is different for individuals and for enterprises. Individual citizens have their own utility functions, depending on their

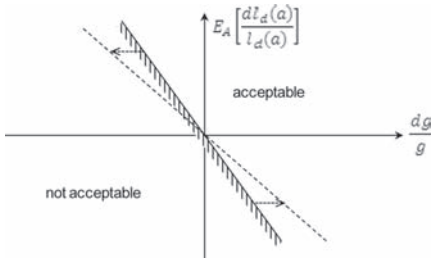


Figure 2. The effect of regulations upon the willingness-to-pay of an individual.

personal circumstances and risk perception. When an authority releases a safety-relevant regulation, e.g. by prescribing that every citizen has to invest in some specific safety equipment (in vehicles, houses or like), it essentially forces citizens to apply a certain utility function. Lacking risk awareness can necessitate regulative measures in order to avoid socio-economic damage. Figure 2 illustrates how regulations force individuals to adopt the utility function that is implied in the regulation.

The decisions of enterprises are not guided by willingness-to-pay considerations but are more likely to be governed by cost-benefit considerations. In the absence of regulations, most enterprises will choose the optimal safety level p^* , i.e. the level that leads to the maximum net expected benefit $Z(p^*)$. This can lead to decisions that do not respect the safety of employees, users and other citizens to a sufficient degree.

Safety regulations force enterprises to adopt the safety preferences of the surrounding society. From the cost-benefit perspective of the enterprise, this means that they are generally forced to respect a minimum safety level p_{lim} . If $p_{lim} \leq p^*$, the regulation does not have any effect on the decision of the enterprise. In the opposite case $p_{lim} > p^*$ the enterprise is forced to invest more into safety than it otherwise would have done or to abandon the project.

The minimum safety level p_{lim} can be defined in different ways. One is to prescribe a fixed maximum allowable fatality rate. Another is to use the precedents principle. Finally, it is possible to apply WTP considerations.

4 THE FUNCTION OF INCENTIVES

Similar to regulations, incentives are a means by which society can prompt stakeholders to act (more) in accordance with the societal safety preference. Incentives do not use legal force to the same degree as regulations. Instead, they

manipulate the stakeholder's utility or cost-benefit function, typically by artificially reducing the cost of safety measures. This is done for instance by giving financial subsidies to safety-increasing measures, by levying taxes on poor safety solutions or by prescribing high compensation payments in case of accidents.

Again, it is necessary to distinguish between individuals and enterprises. If individuals receive public financial incentives for making risk-reducing decisions in their daily life, this changes the pitch of their WTP function. This effect looks the same way as in Figure 2. However, incentives do not force the individual to behave according to other people's (i.e. society's) preferences. Instead, they change the preferences of the individual. Incentives to individuals are in principle a redistribution of income that is ideally aiming at creating a positive net benefit for society.

Enterprises tend to base their decisions on cost-benefit criteria. Incentives add an incentive to the expected revenues. This makes the optimum safety level p^* move further up relative to the situation without incentives. As with individuals, incentives do not force an enterprise to follow society's preferences, but manipulate the decision criterion instead.

Incentives are generally understood as something positive, i.e. a financial appreciation of a societal beneficial decision. All financial penalties fall into this category.

5 EXAMPLES

The first example concerns the Fehmarnbelt Fixed Link, which is currently under planning and will connect Denmark and Germany in 2020. Here, The governing principle for risk evaluation is a combination of precedents and ALARP (As Low As Reasonably Practicable). The ALARP principle is implemented making use of WTP considerations.

The second example deals with radon-exposed homes in Sweden. As an incentive, local authorities offer a 50 percent cost refund for risk-reducing investments within certain total cost limits.

REFERENCE

Pandey, M. & Nathwani, J. 2004. Life quality index for the estimation of societal willingness-to-pay for safety. *Structural Safety* 26(2): 181–199.

Political pitfalls in hazards planning

R. Corotis

University of Colorado, Boulder, CO, USA

Engineering risk professionals are well aware of the importance of a long-term view to address low probability, high consequence natural hazards. This means considering economic lifetimes of several hundred years, incorporating reasonable discounting policies, including intergenerational aspects, and selecting actions that maximize return on some logical basis such as expected utility. Engineering risk professionals are also not generally elected to office. Political leaders, however, have a two- to six-year time horizon, issues of intra-generational equity rather than intergenerational, and a constituency that doesn't want to hear about probabilities and uncertainties. They also know that reelection is related to the absence of perceived mistakes and the prevalence of tangible outcomes. Enter the world of the perfect storm between optimal policy and optimum politics.

The risk (mathematical or true risk) associated with a natural hazard is typically defined as the product of the likelihood of occurrence of the hazard (for some defined reference period) and a quantitative measure of the consequences given there is an occurrence. The perception of risk, however, also incorporates sociological and psychological attitudes and fears. Some of these are amenable to education, such as when people do not understand the accurate probabilities of occurrence, whereas other are buried within the psyche of the mind. The question for engineering risk decision making is how to handle the difference between mathematical risk and "accurate" perceived risk, and to do this in a way that reflects some societal norm across the affected population.

Some have argued persuasively that engineering risk managers should use only mathematical risk. This is the one quantity that can be utilized in an optimal utility sense to minimize the expected consequences to society. And the duty of engineers is to guide society's investments in an optimal manner (such as the least number of lives lost, maximum return on investment, highest quality of life, greatest sustainability, etc.).

Equally persuasive arguments can be made that feelings such as fear and dread are valid reactions, and that actions decreasing those emotions lead to

improved happiness and contentment, and thus a betterment of society. Since such feelings are personal, it is necessary to establish some sort of societal norm, but this is no different from the tradeoff of priorities across particular populations that are determined by voting on issues such as tax increases for schools and increased police protection.

Optimal decisions based on utility maximization dictate a risk-neutral approach. It is well known, however, that societies often prefer a risk-averse approach (and even upon occasion a risk-seeking approach) to public infrastructure decisions. Sometimes this may be a manifestation of the fact that risk perception rather than calculated mathematical risk is a very real consideration in the minds of elected or appointed decision makers. It may also reflect the political reality that re-election to office is more dependent on the minimax principle than one of optimality. That is, one increases his or her likelihood of re-election by minimizing the number and scale of events with widely observable negative outcomes.

One political solution to the quandary between true risk and perceived risk is presentation of choices in terms of options pricing. As a base price one uses the cost of making the (true) risk-neutral maximum utility decision. Then the utility risk premium can be computed for various risk-averse decisions (defined as the expected cost difference between the optimal risk-neutral approach and the risk-averse approach that has a reduced perceived risk). The risk premium thus serves the role of an options cost, reflecting the investment society must make in order to "purchase" the option with a lower perceived risk value.

In addition to the risk perception issue, this paper addresses the distortion on engineering risk decisions by governmental regulations, and the alternative goals of optimality between purely engineering solutions and political decisions. Several examples of correct decisions that have led the politically-elected decision maker into trouble are presented. These are followed by some alternatives that offer ways to address some of these issues.

One of these was used in ancient Greece, and is termed deliberative democracy. In this approach

a representative subset of society is selected (by democratic procedures) and agrees to become highly informed regarding the issues, including from discussions and presentations. This group then votes on behalf of the entire population. Another approach is that of options pricing, whereby risk associated with real capital is quantified through a market exchange, and one can purchase options that transfer the risk of outcomes from the original segment associated with the infrastructure to a secondary investment market.

Several recent events and attitudes have indicated that there are many positive factors that will bring improved alignment between political realities and hazards planning. The most important change is that engineering risk professionals are assuming a new leadership responsibility in bringing these issues to the attention of leaders, and the public at large. Another positive development is that the terrorist bombings in the United States in 2001 led people to recognize that there is structural risk in the built environment, and that it is not reasonable to devote a sufficient amount of society's resources to make this risk vanishingly small. A third positive sign comes from the increasing acceptance of life cycle costing, rather than simply initial investment. As newly effective ways to convey and contrast life cycle costs are developed, it will become easier to incorporate investment savings due to design consideration for low probability, high consequence natural hazard events.

Many infrastructure disasters can be classified as black swans, occurring essentially completely without precedence. In other words, predicting them from past history would have been a useless exercise. Therefore, these "anomalies" are not really anomalous from a practical viewpoint, just from the limited insight afforded by our restricted models. Since these unknowns cannot be designed against explicitly, and would be very difficult for political decision makers to effectively communicate to the public in any case. Instead, one can concentrate on the potential consequences of these extreme events, and how robustness and resilience can be built into a community, even without knowing in detail the likelihood of the events.

The practical usefulness of such an approach arises from the fact that it is often quite inexpensive to build in such robustness, even if some of the characteristics of the event are not quantified in detail. This is the concept introduced here of building ponds for black swans. Accommodating future demands, even when those demands are not completely described.

One of the hardest things to do in engineering risk analysis is to decide when existing infrastructure should be abandoned or removed. This may be the best course because development was not done in a sustainable manner, or that the consequences of some disaster dictate it (due either to greater than expected losses or the occurrence of a black swan).

The purpose of this paper is not to answer all the questions, nor to provide a definitive set of guiding principles for political leaders and public decision-makers. Rather it is to bring to the forefront of engineering risk decision theory and management an awareness of the very important real factors and rationalities that are ever present in the performance of their duties by such leaders.

Issues such as the incompatibilities of lifetimes, misunderstanding of probabilities and return periods, reality of risk perception and personal biases, role of government regulations, political motivation and distortion of policies are real and must be faced. On the other hand, engineering risk professionals who incorporate these issues into their approach stand a much better chance of being effective (even if they don't accept that some of these realities should be present). Tools and concepts such as options pricing for real capital investment, and deliberative democracy offer powerful methods to educate the public. Almost a decade ago this author introduced the concept of an infrastructure report card that would include not just the value of current infrastructure, but the future expected costs for maintenance, operation and probabilistically-estimated failures. Such a report card would be made available on election cycles, so that the public would be able to reward those political decision makers who invested for low probability, high consequence future hazards; in other words, those politicians who built ponds for black swans.

*MS_314 — Spatial probabilistic modeling
of deterioration and inspection (1)*

This page intentionally left blank

Optimization of inspection and monitoring of structures in case of spatial fields of deterioration/properties

F. Schoefs, T.V. Tran & E. Bastidas-Arteaga

LUNAM Université, Université de Nantes-Ecole Centrale Nantes, GeM,

Institute for Research in Civil and Mechanical Engineering, CNRS UMR 6183, Nantes, France

1 INTRODUCTION

In the general context of structural reliability of existing structures, the question of random variable updating has been widely addressed during the two last decades. Random variable updating is very useful when data from inspections or monitoring are collected for condition assessment and reliability updating (Straub et al., 2003; Schoefs et al., 2010a). Basically, the Bayes theorem and its derivative tools (Bayesian Networks) offer the theoretical context to deal with this issue. The so called Risk Based Inspection (RBI) generalizes these approaches in the case of non-perfect inspections by linking inspection and decisions (Faber, 2002; Sorensen et al., 2002; Schoefs et al., 2010b).

RBI methods are powerful once (i) there is no stochastic field involved into the problem, or (ii) the location of the most critical defect, from a reliability point of view, is known. In those cases, it can be assumed that the spatial distribution of defects in the neighboring zone does not affect the reliability assessment. Nevertheless, it has been showed that reality is more complex and that spatial randomness should be considered in several problems. For instance, in condition assessment, Schoefs (2009) has found that inspections should also account for stochastic fields of measured parameters.

The stochastic field could take several forms more or less complicated. The most simple is the stationary stochastic field that can be used, for instance, to model chloride distribution or other concrete properties (Bazant, 1991; 2000a; 2000b). A more sophisticated stochastic field is the piecewise stationary process that can integrate, for example, the variability of concreting materials by steps or the corrosion of structures located in contiguous environments with different characteristics.

During inspection, there are many factors that influence the quality of measurements—e.g, environmental conditions, error in the protocol, error due to material variability, and error induced by

the operator (Bonnet et al., 2009). These factors could lead, for a given inspection, under or overestimations of the measured parameter. If the parameter is underestimated and the owner could decide “do nothing” when repair is required. On the contrary, an overestimation generates a “wrong decision” where the early repair generates overcharges (Rouhan and Schoefs, 2003). On the whole, the stochastic nature of material properties and deterioration processes as well as the factors that reduce the quality of the inspections that can be used to quantify them, transform the management of deteriorating systems in a major challenge for owners and operators.

Within this context, the main objective of this work is to study influence of the noise of measurements on the reliability assessment. This paper focuses only on the inspection of stationary stochastic fields. Its description is outlined in section 2. Section 3 introduces the Karhunen-Loève decomposition for modeling the spatial variability and introduces the modeling of imperfect inspections. Section 4 describes the problem of measurement quality in the case of inspection of random fields and when only the objective of inspection is to determine a marginal probability distribution for reliability computation. Section 5 presents an illustrative example where we illustrate the effect of imperfect inspections on the reliability assessment.

2 MODELLING A STOCHASTIC FIELD WITH NON PERFECT INSPECTION

In terms of stochastic modeling, several approaches can be used to represent a stochastic field $X(x, \theta)$: Karhunen-Loève expansion, approximation by Fourier series, and approximation EOLE (Li and Der Kiureghian, 1993). In this paper, we used a Karhunen-Loève expansion to represent the stochastic field of resistance of a structure $R(x, \theta)$. This expansion represents a random field as a

combination of orthogonal functions on a bounded interval $[-a, a]$:

$$R(x, \theta) = \mu_R + \sigma_R \cdot \sum_{i=1}^n \sqrt{\lambda_i} \cdot \xi_i(\theta) \cdot f_i(x) \quad (1)$$

where, μ_R is the mean of the field R , σ_R is the standard deviation of the field R , n is number of terms in the expansion, ξ_i is a set of centered Gaussian random variables and λ_i and f_i are, respectively, the eigenvalues and eigenfunctions of the covariance function $C_{HH}(x_1, x_2)$. It is possible to analytically determine the eigenvalues λ_i and eigenfunctions f_i for some covariance functions (Ghanem and Spanos, 2003). For example, it can be determined if we assume that the field is second order stationary and we use an exponential covariance function:

$$C_{HH}(\Delta x = x_1 - x_2) = \exp\left(-\frac{|\Delta x|}{b}\right); 0 < b \quad (2)$$

where b is the correlation length and $\Delta x \in [-a, a]$. As stated in Schoefs et al. (2010a) a non-biased inspection can be modeled with a centered noise η around the exact value. In this paper, it is assumed that the noise is normally distributed $N(0, \sigma_\eta)$ without loss of generality.

This work considers that inspections will be used to determine the marginal probability distribution of a variable of interest that has the properties of a random field. If inspections are carried out on the same structural element, the distance between two consecutive measurements, L_c , should ensure independency between two results. In that case, we could build a statistically independent sample from equidistant inspections on a random field. This sample will be used to determine the marginal probability distribution.

3 PROBABILISTIC MODELLING AND RELIABILITY ASSESSMENT FROM INSPECTION

Assuming that the loading S is deterministic and that R_I is normally distributed, the probability of failure, P_f , is obtained as:

$$P_f = P(R \leq S) = \Phi\left(\frac{S - \mu_{R_I}}{\sigma_{R_I}}\right) \quad (3)$$

where μ_{R_I} and σ_{R_I} are, respectively, the mean and the standard deviation determined taking into account the considerations described in previous section. Equation (3) is also used to compute the

probability of failure P_f obtained with “perfect” inspection (without noise) that will be used here to study the influence of the noise of the measurement.

In the following results, we will compare the probability of failure computed from measurements with noise, $P_{f,I}$, with the probability of failure computed without noise, P_f , in terms of a confidence interval $[c, d]$. The lower and upper limits of this interval are defined according to the following conditions in the case without noise:

$$P(P_f < c) = 5\% ; P(P_f < d) = 95\% \quad (4)$$

Figure 1 shows the zone corresponding to this confidence interval for the case without noise (grey zone) that is used to determine the limits of the interval. Once these limits are defined, it is possible to determine the probability that $P_{f,I}$ (determined from noised inspections) belongs to the interval $[c, d]$, i.e., $P(c < P_{f,I} < d)$ (Figure 1) as:

$$P(c < P_{f,I} < d) = P(P_{f,I} < d) - P(P_{f,I} < c) \quad (5)$$

The hatched zone in Figure 1 presents the probability $P(c < P_{f,I} < d)$. The standard deviation of R_I is higher than σ_R because of the noise. Therefore, the area of $P_{f,I}$ between the interval $[c, d]$ is lower than the area computed without noise. The effect of noise on the assessment of the probability $P(c < P_{f,I} < d)$ will be more discussed in next section.

Discussion: From an application illustrated in the paper, it shown that the estimate of the quality of condition assessment i.e. $P(P_{f,I} \in [c, d])$ decreases strongly and regularly for a $\sigma_n > 5$.

It leads to conclude that for a given structure of the underlying stochastic field, an inspections

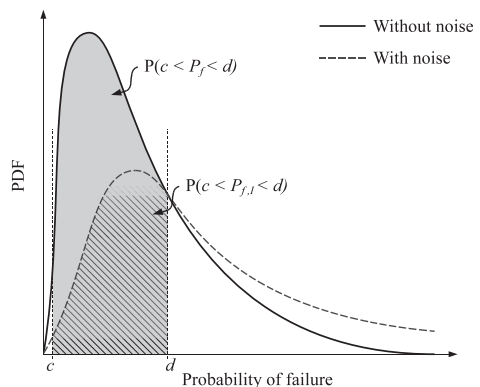


Figure 1. Determination of the limits of the confidence interval from the distribution of P_f .

quality can be required based on a acceptance criteria: $P(P_{f,t} \in [c,d]) > p$.

REFERENCES

- Bazant, Z.P. & Xi, Y. 1991. Statistical Size Effect in Quasi-brittle Structures: II. Nonlocal Theory. *ASCE J. of Engrg. Mech.* Vol. 117, No. 11, 2623–2640.
- Faber, M.H. 2002. Risk Based Inspection: The Framework. *Structural Engineering International (SEI)*, 12(3), August 2002, pp. 186–194.
- Schoefs, F., Clément, A., Boéro, J. & Capra, B. 2010a. The $\alpha\delta$ method for modeling expert Judgment and combination of NDT tools in RBI context: application to Marine Structures. *NSIE*, Jan. 2010, doi: 10.1080/15732479.2010.505374.
- Sørensen, J.D. & Faber, M.H. 2002. Codified Risk-Based Inspection Planning. *Structural Engineering International (SEI)*, 12(3), August 2002, pp. 195–199.
- Straub, D. & Faber, M.H. 2003. Modelling dependency in inspection performance, *Proc. ICASP 2003* pp. 1123–1130.

Repair efficiency and Life-Cycle Cost of RC bridge deck maintenance subjected to spatially variable corrosion damage

J.A. Mullard

Robert Bird Group, Hamilton, NSW, Australia

M.G. Stewart

Centre for Infrastructure Performance and Reliability, The University of Newcastle, NSW, Australia

The paper reviews a probabilistic reliability analysis which is used to predict the likelihood and extent of corrosion-induced damage to RC structures. Corrosion damage is deemed to occur when corrosion-induced crack widths of 1 mm are evident on the RC surface. The spatial time-dependent reliability model considers concrete properties, concrete cover and the surface chloride concentrations as spatially variable random fields. This allows for the calculation of the probability that a given extent of corrosion damage will occur for any time period. Three repair techniques will be considered: (i) patch repair, (ii) preventative repair, and (iii) complete rehabilitative overlay. Incorporated into each of the above maintenance strategies are two repair efficiency factors which take into account varying time to corrosion initiation and corrosion rate of the repair material. Maintenance strategies and repair efficiencies are incorporated in a Monte-Carlo event-based simulation analysis. Results are presented for a RC bridge deck subject to a marine environment. The life-cycle cost analysis considers repair and user delay costs which are both functions of extent (area) of damage.

See Table 1 for the ten maintenance strategies.

Repair and user delay costs for a typical RC bridge deck are given in Table 2.

The RC bridge deck considered is a 250 mm thick cast-in-situ slab. The deck span is a simply supported single span of 20 metres and the width of the deck is 20 metres, resulting in a total RC deck area of 400 m². The deck slab is reinforced longitudinally and transversely with 16 mm reinforcing bars and ‘fair’ durability design specifications are assumed (cover = 50 mm, $F'_c = 40$ MPa). The chloride environment is assumed to be ‘high marine’ and only the top surface of the bridge deck is modelled as it is assumed that the soffit of the RC deck is protected by the bridge girders and permanent formwork and will therefore not be subject to chloride induced corrosion as it is protected from wind borne chlorides. A discount rate of 5% is used to account for all future costs. Inspection interval is one year.

Table 1. Summary of maintenance strategy parameters.

Maintenance strategy	X_{repair}	Maintenance technique	Repair method	Repair efficiency	
				Δ_{T_i} (years)	γ_{corr} (%)
M1_0	2%	M1	Patch	0	0
M2_0	2%	M2	Patch	0	0
M3_0	12%	M3	Patch	0	0
M1_CST	2%	M1	Patch + CST	15	0
M2_CST	2%	M2	Patch + CST	15	0
M3_CST	12%	M3	Patch + CST	15	0
M1_CI	2%	M1	Patch + CI	7	-50
M2_CI	2%	M2	Patch + CI	7	-50
M3_CI	12%	M3	Patch + CI	7	-50
M3_CP	12%	M3	Patch + CP	0	-100

CST—Concrete surface treatment, CI—Corrosion inhibitor, CP—Cathodic protection.

Table 2. Summary of repair and user delay costs.

Maintenance strategy	Maintenance technique	Repair method	Costs	
			Repair	User delay
M1_0	M1	Patch	\$440/m ²	\$61,000
M2_0	M2	Patch	\$440/m ²	\$122,000
M3_0	M3	Patch	\$440/m ²	\$1.9 million
M1_CST	M1	Patch + CST	\$461/m ²	\$61,000
M2_CST	M2	Patch + CST	\$461/m ²	\$122,000
M3_CST	M3	Patch + CST	\$461/m ²	\$1.9 million
M1_CI	M1	Patch + CI	\$458/m ²	\$61,000
M2_CI	M2	Patch + CI	\$458/m ²	\$122,000
M3_CI	M3	Patch + CI	\$458/m ²	\$1.9 million
M3_CP	M3	Patch + CP	\$740/m ²	\$1.9 million

The economic performance of each of the maintenance strategies can be compared using the average LCC data presented in Table 3. The average LCC of repair is influenced by the cost of repair, the number of repair actions required over the service life and the time at which they occur.

Table 3. Summary of LCC.

Maint. Strategy	Average number of maint. actions (m)	Average area repaired (A_{repair})	Average LCC of repair costs	Average LCC of user delay costs	Average total LCC
M1_0	5.3	8.5 m ²	\$ 784	\$ 14,913	\$ 15,697 (0.72)
M2_0	2.8	54.5 m ²	\$ 2,552	\$ 18,889	\$ 21,441 (0.65)
M3_0	0.4	400 m ²	\$ 730	\$ 12,522	\$ 13,252 (1.57)
M1_CST	5.0	8.5 m ²	\$ 802	\$ 14,460	\$ 15,262 (0.71)
M2_CST	2.6	51 m ²	\$ 2,524	\$ 18,110	\$ 20,634 (0.63)
M3_CST	0.4	400 m ²	\$ 788	\$ 12,522	\$ 13,310 (1.57)
M1_CI	4.8	8.5 m ²	\$ 763	\$ 13,955	\$ 14,718 (0.7)
M2_CI	2.4	52 m ²	\$ 2,460	\$ 17,764	\$ 20,224 (0.62)
M3_CI	0.4	400 m ²	\$ 773	\$ 12,522	\$ 13,296 (1.57)
M3_CP	0.4	400 m ²	\$ 1,194	\$ 12,522	\$ 13,716 (1.57)

Notes: 1. Numbers in brackets are COVs. 2. The LCC's calculated in this study are in 2009 Australian dollars based on information and estimates from a number of sources.

Obviously repairs that occur later in the service life have a reduced influence on the average LCC due to the effect of the 5% discount rate. In terms of LCC of repair only, the maintenance strategies using maintenance techniques M1 and M3 are more economical than those using maintenance technique M2. Clearly, for economic optimisation there must be a balance between the length of delay in maintenance actions and the extent of damage repaired at that time (i.e. in terms of LCC of repairs, a longer delay in the timing of maintenance will more readily offset a larger repair area).

The influence of repair durability can also be seen in Table 3. For maintenance strategies using maintenance technique M1 (maintenance strategies M1_0, M1_CST and M1_CI) the use of no repair durability improvement, a concrete surface treatment and a corrosion inhibitor have life-cycle costs for repair of \$784, \$802 and \$763 respectively. For the case using the corrosion inhibitor, the effect of delayed maintenance (fewer average occurrences) offsets the cost of application and it has a lower LCC than for the case of no repair durability improvement. For the case of the concrete surface treatment, however, the cost of application outweighs the benefit of reduced maintenance actions and it has a higher LCC than for the case of no repair durability improvement. The influence of repair durability specifications is greater when maintenance technique M2 is used as a larger area of the RC surface is repaired. Maintenance strategies using maintenance technique M3 (maintenance strategies M3_0, M3_CST, M3_CI and M3_CP) do not benefit from repair durability improvements with the case of no repair durability improvements having the lowest LCC of repair.

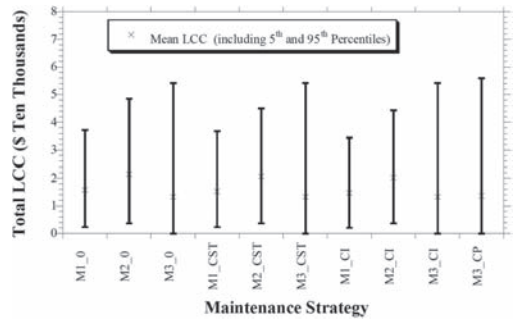


Figure 1. 90th confidence intervals for LCC.

This is because for strategies using maintenance technique M3, the probability of second repairs over a 120 year design life is 0.0 meaning that no benefit is achieved by the application of either a concrete surface treatment or a corrosion inhibitor. Table 3 shows that user delay costs dominate LCC. Clearly these results are sensitive to the discount rate, the cost of repair and the time and cost of user delay.

A measure of variability can be expressed by 5th and the 95th percentile values which can assist decision makers by providing the limits within which 90% of all outcomes will fall, see Figure 1. It can be seen that although maintenance strategy M3_0 has the lowest mean LCC, the variability is high and thus higher likelihood of incurring costs significantly higher than the mean. This information on the variability of performance and life-cycle costs clearly gives decision makers a more thorough basis for selecting maintenance strategies and may in fact alter the optimal solution from that

based on mean data alone if the decision maker is risk averse or risk prone. For example, a risk averse decision maker may be more concerned about the likelihood of large costs than mean values. This is particularly apt for individual assets. However, for a portfolio of many assets, the decision maker

should be risk neutral (use expected values) as this will provide the most cost-effective outcome across many assets. In other words, a risk neutral approach leads to decisions where the most benefit is achieved.

A unified probabilistic treatment for in-line inspection with respect to detectability, reportability, false call potential and depth sizing

M.A. Maes & M.R. Dann

Department of Civil Engineering, University of Calgary, Calgary, Canada

In-line inspections (ILIs) are periodically performed in pipeline systems to obtain information about the state of metal loss due to internal and external deterioration processes. The standard non-destructive measurement procedures, however, do not reveal directly the actual state of the system as measurement errors cause differences between the actual metal loss prevailing in the system and the reported metal loss by the inspection tool (IT). Defect related factors, IT-specific factors and environmental uncertainties such as the actual defect size and geometry, the IT design and signal processing, scanned material surface, and neighboring defects affect the results of ILI. All these factors express in four types of measurement uncertainties:

- The IT does not detect all existing defects. Some defects are ignored by the IT and it reports an intact pipe wall at that location.
- If the IT reports a defect having certain dimensions but the pipe wall is intact and the defect does not exist, this fictitious defect is referred to as a false call.
- ITs have a lower defect size threshold so that observed defects below that tool-specific threshold are reported as non-existing.
- If the IT detects a true defect, the actual defect size is subject to considerable sizing errors. The reported defect size differs from the actual defect size.

ILI data must be pre-processed to estimate the actual defect size using a probabilistic approach that accounts for all the uncertainties involved in the ILI process. As most available methods focus on some of the measurement uncertainties, the paper has the objective to present a comprehensive hierarchical Bayes model (HBM) that accounts for all four types of ILI measurement uncertainties.

Figure 1 provides a graphical representation of the populations of actual and observed defects where a cross represents schematically a defect. The first set AD consists of the actual existing defects in the pipeline, while the second set OD indicates

the defects detected by the IT. The intersection between the two sets $SD = AD \cap OD$ constitutes the defects which actually exist in the pipe wall and are successfully detected.

A false call ($FC = OD \setminus SD$) is referred to the anomaly where a non-existing or fictitious defect is wrongly identified and reported as a defect. On the other side, an actual existing defect that is ignored and not reported by the IT, is referred to as a non-detected defect ($ND = AD \setminus SD$). To describe to which set a defect belongs, two so-called detectability indicator D and true call indicator variable T are introduced. They take the values as shown in Table 1. An exact assignment of each defect to one of the three sub-groups in Figure 1 is not possible, thus, D and T are binary random variables following a Bernoulli distribution parameterized with the probability of detection (POD) and the probability of a true call (POTC), respectively.

Focusing only on the defect depth as the defect size, $POD(x)$ measures how likely it is to detect a defect having an actual depth x . But, it also depends on an uncertain and tool-specific detection threshold X_{DT} , which takes the other factors than x into account affecting the defect detection. ITs detect only defects having larger depths x than X_{DT} . The lower the detection threshold, the higher are the chances, expressed through $POD(x)$, that the defect with depth x will be detected.

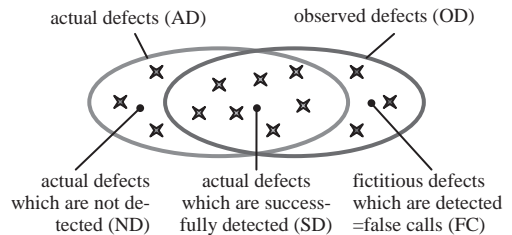


Figure 1. Set representation of actual defects (AD), defects observed by the inspection tool (OD) and their differentiation into successfully detected defects (SD), not detected defects (ND) and false calls (FC).

Table 1. Detectability and true call indicators for non-detected, successfully detected and false call defects.

Set of defects	Detectability indicator	True call indicator
Non-detected defects ND	$D = 0$	$T = 1$
Successfully detected defects SD	$D = 1$	$T = 1$
False calls FC	$D = 1$	$T = 0$

A similar approach is applied to the probability of a true call $POTC(x_R)$. It describes the probability that a defect having an observed defect depth x_R belongs to the set of successfully defects. $POTC(x_R)$ also depends on an uncertain IT-specific credible defect depth X_C . Again, X_C functions as a marginal value similar to the detection threshold X_{DT} .

The third type of ILI uncertainty is related to lower bound of the IT operating range. IT vendors provide lower operating thresholds in form of a minimum reportability threshold x_{RT} where both actual defects and noise effects with observed depth less than x_{RT} are reported as zero.

The fourth type of ILI uncertainty concerns about the sizing errors on top of the actual defect properties. If a defect is successfully detected and its depth remains above x_{RT} , then the reported defect depth differs to the actual defect depth due to sizing errors. A traditional approach applied in ILI data analysis for sizing errors adds to the actual unknown defect depth a random variable representing the sizing error.

The developed HBM combines the four individual approaches for ILI data uncertainty for a single inspection and consists of the following components (starting from the top level):

- Each defect has an unknown actual defect depth X .
- The second top level includes the random sizing error conditional on its known variance.
- $POD(X)$ and the defect indicator variable D indicate whether the defect is observable ($D = 1$) for the IT or not ($D = 0$) and provide the corresponding defect depth.
- The reportability threshold x_{RT} checks if the defect belongs to a pure noise effect and determines the reported defect depth x_R by the IT.
- The lowest level addresses the false call potential. The defect depth distribution of the actual defects consist of those defects having a true call indicator $T = 1$ only.

The complexity of the HBM prohibits closed form solutions. Instead Markov Chain Monte Carlo (MCMC) simulation techniques must be utilized to obtain the posterior pdfs of the defect

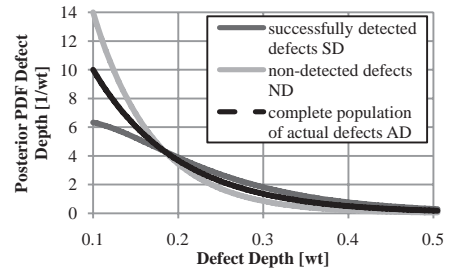


Figure 2. Posterior distribution of the actual defect depth for (1) the successfully detected defect population obtained from the HBM, (2) the non-detected defect population and (3) all actual defects.

depth of each individual defect and the population of successfully detected defects.

In a second analysis, a non-hierarchical Bayes approach estimates the posterior defect depth distribution of the population of non-detected defects conditional on the defect depth distribution of the successfully detected defects. Figure 2 shows the corresponding posterior results for an example provided in the paper.

The proposed methodology is then extended to adjust for two additional effects of results obtained from multiple inspections. First, typical pipeline deterioration increases monotonically over time in all defect locations. To take this condition into account, the inspections can not be analyzed independently. Each HBM for an inspection is linked together by a common stochastic deterioration model describing the increase of actual deterioration from one inspection to another for all defects. Second, the sizing errors at a specific defect location become correlated between all inspections due to the effects of neighbouring defects and algorithmic signal processing. Instead of using independent sizing errors, a random field represents the correlated sizing uncertainties for a defect and all its inspections.

The introduced two-step Bayesian approach for ILI data has several advantages. It accounts for all four types of ILI uncertainties within one comprehensive hierarchical approach to estimate effectively the defect size of the individual defects and the population of successfully detected defects. It also determines the defect size of the non-detected defects which play an important role in the reliability analysis and integrity assessment of pipeline systems. POD , $POTC$ and reportability threshold indicate high potential of ITs to identify correctly large defects which play a major role in reliability analysis and decision making. Small defects which suffer the most under ILI uncertainties, have larger probability to be ignored and, thus, be reported as zero by ITs.

Spatial hierarchical POD model for in-line inspection data

M.R. Dann & M.A. Maes

Department of Civil Engineering, University of Calgary, Calgary, Canada

Pipeline systems are subject to spatially and temporally varying corrosion processes affecting negatively their long-term reliability and integrity. In-Line Inspections (ILIs) are periodically performed to reveal the current state of corrosion using an Inspection Tool (IT) that moves through the pipeline and measures the loss of wall thickness along the pipe. However, the inspection procedure involves measurement uncertainties which express in different forms. For informed pipeline integrity assessment and decision making, the analysis of the inspection results must consider these measurement uncertainties. The paper focuses on one part of these uncertainties, the detection and non-detection of actual existing defects, and how its inherent spatial variability can be properly addressed in a Hierarchical Bayes Model (HBM).

Defects can be classified in two major groups as shown in Figure 1 (a cross represents schematically a defect) as a basis for the probabilistic analysis of defect detection uncertainties.

The first set AD consists of the actual existing but unknown defects in the pipeline, while the second set OD represents the defects detected by the IT. The intersection between the two sets $SD = AD \cap OD$ indicates the defects which actually exist in the pipe wall and are successfully detected. A false call ($FC = OD \setminus SD$) arises when a non-existing or fictitious defect is wrongly identified and reported as a defect. On the other side, an actual existing defect that is completely ignored and not reported by the IT, is referred to as a non-detected defect ($ND = AD \setminus SD$).

As we only focus on the non-detection problem in this paper, the set of actual defects AD and the corresponding subsets ND and SD are of interest.

Performing an ILI, an existing defect belongs to either the ND or the SD set in Figure 1 but the inspection result can not be estimated in advance due to uncertainties. IT-specific probability of detection (POD) curves describe usually as a function of the actual defect depth x , the reliability of an IT to detect successfully existing defects. The POD increases with x and varies from 0 for very small defects to (almost) 1 for very large defects. To indicate whether a defect belongs to set of successfully detected defects or not, a Bernoulli

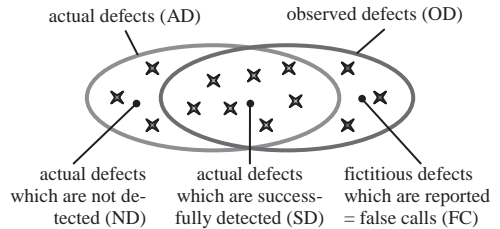


Figure 1. Representation of actual defects (AD), defects observed by the inspection tool (OD) and their differentiation into successfully detected defects (SD), not detected defects (ND) and false calls (FC).

distributed detection indicator variable D takes values either $D = 1$ or $D = 0$, respectively.

In order to achieve a stated POD, the actual defect depth x must exceed a detection threshold X_M , or, in other words, defects with depths below that uncertain marginal value X_M are not detectable. A common approach assumes $POD(x) = 1 - \exp(-x/\mu_M)$ where the mean detection threshold $E[X_M] = \mu_M$ controls the POD. The random variable X_M summarizes defect related, environmental-specific and IT dependent uncertainties (e.g. defect geometry, effect of neighbouring defects, scanned surface condition, IT vibration damping) affecting the successful detection of defects. Although these uncertainties vary spatially along the pipeline, the detection threshold does not consider their spatial effects and, thus, oversimplifies the POD approach.

To overcome this problem, a point-referenced spatial HBM is developed assuming a defect-specific detection threshold that takes the spatial uncertainties on the defect detection into account. In order to estimate and calibrate such spatial POD curves for an IT, a large set of actual machined defects needs to be considered. An independent measurement procedure first catalogues the various defects and their geometrical properties for verification. In the actual test phase, the IT moves in so-called pull-through tests (PTTs) several times through the pipeline and observes the defects. The results of a PTT reveal the set of successfully detected defects (SD) in Figure 1 and the

corresponding distinction between detected (SD) and non-detected (ND) defects as the basis for the POD calibration.

The introduced HBM consists of three levels. The bottom level contains the defect indicator variables for each defect and their (standard) PODs having now a defect-specific detection threshold. This detection threshold is conditional on the second level representing the spatial uncertainties on the defect detection with the following three components:

- Actual defect geometry properties other than depth, such as defect length, width, or volume of metal loss which may explain directly, using a regression model, the spatial variability on the defect level.
- A spatial random field accounts for the effects of environmental-specific uncertainties.
- A defect-specific random effect considers extra variability with respect to the detection threshold that is not covered by the regression model and the spatial random field.

The top level of the HBM contains a small set of governing model parameters, the so-called hyper-parameters, and their prior distributions to complete the Bayesian model specification. All model parameters in the HBM are updated in a Bayesian fashion, posterior = likelihood \times prior, conditional on the fixed parameters and the observed information obtained from the PTTs. After updating the entire HBM by means of Markov chain Monte Carlo simulation techniques, our interest lies in: (1) The posterior distributions of the hyper-parameters as they provide useful information about the explanatory variables, the systematic and the random errors in the analysis. (2) Obtaining the posterior detection thresholds of the tested inspection tool. (3) Drawing new (calibrated) posterior POD curves as a function of the defect depth x for given defect length and width. These POD curves are going to be applied as soon as the IT performs actual pipeline scans and the corresponding inspection results have to be processed in an integrity assessment of the inspected pipeline.

The approach is illustrated on a series of PTTs for a magnetic-flux-leakage IT for pipeline ILI. The following three models are considered. (1) A non-hierarchical model M1 usually applied in ILI. (2) A HBM (HBM1) with defect-specific detection thresholds based on the actual defect length and width. The longitudinal defect location is completely ignored. (3) The full HBM (HBM2) with defect-specific detection thresholds including fixed, random and spatial effects.

Figure 2 demonstrates the spatial variation of the posterior POD for a new defect with fixed

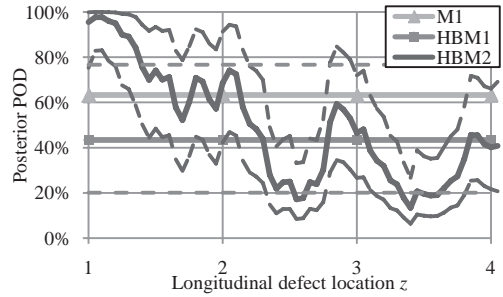


Figure 2. Spatial variation of the posterior POD for a defect ($L = W = 1$ wt) having defect depth $X = 0.20$ wt using M1, HBM1 and HBM2. Full lines show the posterior median and dashed lines indicate the 25% and 75%-quantiles.

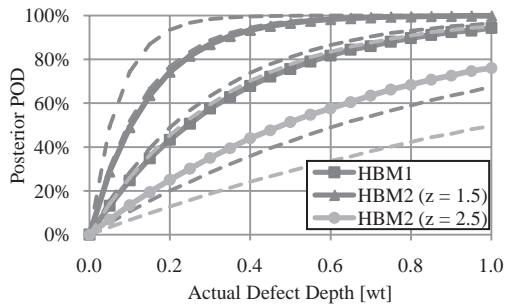


Figure 3. Posterior POD for a defect ($L = W = 1$ wt) using HBM1 and HBM2 at two different longitudinal locations. Full lines show the posterior median and dashed lines indicate the 25% and 75%-quantiles.

geometry. The defect detection clearly varies along the pipeline. Figure 3 shows the full posterior POD curves for a new defect at two different longitudinal locations z using the two hierarchical models. The regional differences become clearly noticeable using HBM2, while HBM1 provides results averaged out over the longitudinal axis.

The introduced HBM approach has several advantages for pipeline ILI. (1) It allows the estimation of more sophisticated POD curves for ITs and an improved understanding of the factors affecting the spatially varying defect detection. (2) Accounting for defect and location-specific effects, the posterior POD curves show less uncertainty than more generalized approaches. (3) IT users have the opportunity to calibrate their own POD curves based on PTTs and may compare it with information provided by vendors. (4) Future analyses of inspected pipeline systems rely on these results leading to more precise long-term reliability and integrity assessments.

*MS_324 — Spatial probabilistic modeling
of deterioration and inspection (2)*

This page intentionally left blank

Reliability of pipelines under corrosion and mechanical damage

F.A.V. Bazán & A.T. Beck

Department of Structural Engineering, São Carlos School of Engineering, University of São Paulo, São Carlos, SP, Brazil

1 INTRODUCTION

International databases (EGIG 2008, CONCAWE 2009, UKOPA 2009) show that mechanical damage due to third party interference and corrosion are two of the three most significant causes of failure (spills) in oil and gas pipelines. Risk management for such pipelines requires proper models to assess the influence of environmental and operating conditions on the likelihoods of failure. This paper assembles state-of-the-art failure models and uncertainty models for the reliability analysis of buried pipelines due to corrosion growth and mechanical damage.

2 UNCERTAINTY MODELS AND LIMIT STATE FUNCTIONS

2.1 Mechanical damage

Mechanical damage due to third party interference can cause pipe-wall dents and gouging. A general approach to this problem is to conservatively treat the gouge as a crack-like defect and to consider the dent as a stress-modifier (Francis et al. 2005).

Failure of the dented and gouged pipeline is modeled using the R6 elastic-plastic fracture mechanics model:

$$g_1 = \frac{\sigma_f}{\sigma_y} \left[\frac{8}{\pi^2} \ln \left\{ \sec \left(\frac{\pi \sigma_f}{2 \sigma_y} \right) \right\} \right]^{\frac{1}{2}} - \frac{K_I}{K_{IC}} \quad (1)$$

where K_I is stress intensity factor; K_{IC} is fracture toughness; σ_f is far field stress at fracture; and σ_y is yield strength.

Stress modifiers due to denting are given in Francis et al. (2005) and stress intensity factors for tension and bending are obtained from Rooke & Cartwright (1976) and Cheng & Finnie (1988).

2.2 Corrosion

For corrosion defects the limit state function suggested by DNV-RP-F101 (2004) is used:

Table 1. Mechanical damage and corrosion random variables.

Variable	Distribution	Parameter 1*	Parameter 2*
p	Gumbel	$\mu = 1.05$ MAOP	CoV = 3%
t	Normal	$\mu = t_n$	CoV = 3%
σ_y	Lognormal	$\mu = 1.08$ SMYS	CoV = 4%
K_{IC}	Weibull	$\mu = 100$ MPa · m ^{1/2}	CoV = 5%
L	Weibull	$\beta = 0.84$	$u_1 = 183.6$ mm
a	Weibull	$\beta = 0.63$	$u_1 = 0.73$ mm
F	Weibull	$\beta = 2.12$	$u_1 = 55$ kN
σ_u	Normal	$\mu = 1.09$ SMTS	CoV = 3%
l	Normal	$\mu = 25$ mm	$\sigma = 19.5$ mm
ν	Lognormal	$\mu = 0.15$ mm/yr	CoV = 50%
X_M	Normal	$\mu = 1.05$	CoV = 0.10

* μ = mean value; CoV = coefficient of variation; β = shape parameter; u_1 = scale parameter; t_n = nominal wall thickness.

$$g_2 = X_M \frac{2t \cdot \sigma_u}{(2R_0 - t)} \left(\frac{1 - \nu \tau/t}{1 - \frac{\nu \tau/t}{Q}} \right) - p \quad (2)$$

where the first term is the burst pressure capacity, R_0 is outer pipe radius; X_M is model uncertainty random variable; σ_u is ultimate tensile strength; ν is rate of growth of defect depth; and τ is time elapsed since pipeline commissioning.

Table 1 summarizes statistical distributions of the mechanical damage and corrosion random variables.

2.3 Distributed pipeline system

The limit state functions for mechanical damage (Eq. 1) and corrosion (Eq. 2) allow one to evaluate failure probabilities that are conditional to a single mechanical hit incident or to a single corrosion defect, respectively.

The actual reliability of a distributed pipeline also depends on the frequency of hits (per km · year), which has to be estimated from historical data, taking into account installation and

location conditions for the pipeline (depth of cover, nature of environment, use of warning and protection systems, and surveillance interval). Changes in these factors are likely to affect the frequency of hits and, therefore, the pipeline failure frequency.

On the same way, reliability of a distributed pipeline depends on the number of corrosion defects (or rate of defects per km · year) which is site-dependent and has to be estimated from in-line inspections.

The time-dependent failure probabilities (or rates per km) are evaluated as (Melchers 1999):

$$P_f(\tau) = 1 - \exp\left(-\int_0^\tau \eta P_f(\xi | defect) d\xi\right) \quad (3)$$

where $P_f(\tau)$ is a probability of failure accumulated over time for a reference pipeline length, η is a frequency of hits or of corrosion defects per km · year and $P_f(\xi | defect)$ is the conditional probability of failure given a single hit or corrosion defect. For corrosion, this conditional probability is time-dependent, whereas for mechanical damage it is constant.

3 NUMERICAL EXAMPLE

A grade X42 steel pipeline is considered, with the following main features: nominal outside diameter: 406.4 mm; nominal wall thickness: 6.4 mm; MAOP: 6.5 MPa; SMTS: 414 MPa and SMYS: 290 MPa.

Reliability analyses were performed, in order to calculate probabilities of failure conditional to a single mechanical damage incident. A first-order approximation (FORM) yielded $P_{f1} \approx 0.134$, and revealed that denting force (F) and crack (gouge) depth (a) are the random variables with most contribution to failure probability. Due to strong curvature of the limit state function, the first-order result is not accurate, and (crude) Monte Carlo simulation was performed, yielding $P_{f1} \approx 0.1$.

The probability of failure given a single corrosion defect was evaluated, as a function of time. This was initially performed by FORM, but some instability (and high curvature) of the limit state functions was observed. Figure 1 illustrates this instability in terms of the most probable point (MPP) trajectories to failure for $\tau = 11$ and $\tau = 13$ years. The MPP path to failure for $\tau = 11$ years starts at a very low “realization” of the model error random variable, and requires little defect growth until failure. On the other hand, for $\tau = 13$ years the MPP path to failure starts near the mean burst pressure (MPP path to failure for $\tau = 13$ years), but the defect grows very fast due to a large “realization” of the corrosion rate v .

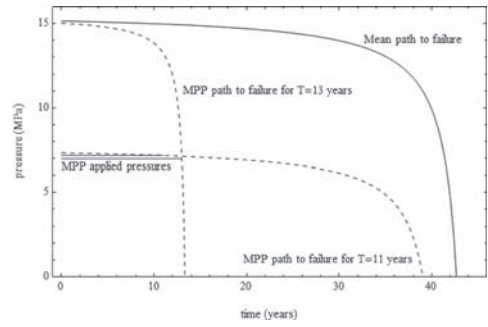


Figure 1. Burst pressure trajectories as a function of time: mean path to failure and most probable (MPP) paths to failure for $\tau = 11$ and 13 years.

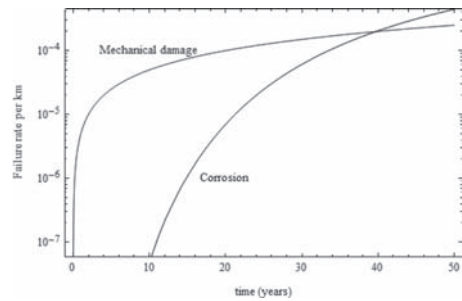


Figure 2. Failure rates (per km) for a pipeline subjected to mechanical damage and corrosion, as functions of time.

Statistics obtained by UKOPA (2009) were assumed for the frequency of hits and for the mean number of corrosion defects.

Figure 2 compares the evolution in time of the (time-integrated) failure rates (per km) for mechanical damage and corrosion. The rate of failure due to mechanical damage only increases due to integration over time, since the rate over time is constant. On the other hand, the rate of failure due to corrosion increases much sharply, as conditional failure probabilities also increase in time due to the growth of corrosion defects. The trend illustrated in Figure 2 does not include the effects of line inspection and repair, which should be included in a future extension of the present study.

4 FINAL REMARKS

This is an ongoing research project. In this first approach to the problem, little attention was dedicated to the actual modeling of the distributed pipeline system, nor to the effects of line inspection and repair. These issues will be addressed in a continuation of the present study.

The performance of sampling inspections for localized deterioration process

S.P. Kuniewski & J.A.M. van der Weide

Faculty of Electrical Engineering, Mathematics and Computer Science, Delft University of Technology,
The Netherlands

ABSTRACT: Risk Based Inspection (RBI) methodology for planning inspections have been used within the oil and gas industry for over the last several years. Using RBI methodology, inspection efforts are focused on the items with high risk which is the combination of the consequence of failure and the probability of failure. Some items are inspected partially with the aim to make a statement about the condition of the entire component. This strategy is of course costs saving but also risky as some defects may escape detection. (Terpstra 2009) describes some issues within the application of sampling inspection and also points out that a significant part of the oil and gas plants are actually inspected partially using the so called sampling inspection with Non-Destructive Testing (NDT).

An important issue in planning inspections is the effectiveness of a given inspection plan. In our case we are interested in the effectiveness of sampling inspection. To study and to understand the performance of sampling inspection we propose to investigate some relevant probabilities associated with the components failure and the performance of inspection. The first one is often defined by the probability of exceedance or more precisely the probability that at least one ‘defect’ exceeds corrosion allowance before a given time (for instance the next planned inspection time). The probability associated with the inspection performance is defined by the detection probability which is the probability of detecting at least one ‘defect’ that is detectable by a NDT technique used for inspection and that it is within the inspected part of the component. The last presented probability is the probability of exceedance and no detection, that is the probability that at least one defect exceeds corrosion allowance before next planned inspection and no detection of any defect in the inspected part of the component using a NDT technique occurs. By NDT technique we mean that the inspection technique is restricted to detect only defect with sufficient depths which is modeled by a detection threshold or the so called *Probability of detection* PoD curve.

The component is assumed to suffer from local defects that initiate in time at a particular location on the component’s surface and then grow following a monotonic process that represents a local wall penetration process (material loss). This deterioration process, also presented in (Kuniewski, van der Weide & van Noortwijk 2009), resembles pitting corrosion process. It is implicitly assumed to affect either interior or exterior of the component and is build on mainly of two elements. One is the defects initiation process and the other one is the growth process of each defect. These two are combined into one process that at each particular time t models the total number of defects that have initiated up to time t and the depths of all these defects. Defects initiation in time and space and consequently the total number of defects up to time t is modeled by a Poisson process. After defects initiate, they grow according to some monotonic (non decreasing) stochastic process. This stochastic process takes into account uncertainty in the evolution of the defects depths. Each defect grows according to an independent copy of the assumed stochastic process. That is, no interaction of growth depth between different initiation points in space occurs. In this article we consider the growth process to be a gamma stochastic process. Each defect receives an independent trajectory of the gamma process.

REFERENCES

- Kuniewski, S.P., J.A.M. van der Weide & J.M. van Noortwijk (2009). Sampling inspection for the evaluation of time-dependent reliability of deteriorating systems under imperfect defect detection. *Reliability Engineering and System Safety* 94, 1480–1490.
- Terpstra, S. (24–26 June 2009). Use of statistical techniques for sampling inspection in the oil and gas industry. *4th European-American Workshop on Reliability of NDE, Berlin*.

Influence of including spatial variability modelling on whole life management of concrete structures

A.J. O'Connor

Trinity College Dublin, Ireland

ABSTRACT: Reinforced concrete (RC) structures deteriorate considerably in chloride contaminated environments. Two main distinguished sources of chlorides are de-icing salts in cold countries and airborne slats in marine environments. Prediction of present and future deterioration states of these structures is important if proper planning for inspection and maintenance is to be made. The major aspect of such studies focuses on the diffusion process of chloride ions through the concrete cover and the prediction of time to corrosion initiation. To a lesser degree, focus is placed on prediction of the surface condition of the structure. A major shortcoming in the work carried out to date has been the neglect to model the spatial variability of the deterioration parameters, i.e. material and geometrical properties were treated as being homogeneous across the structure. This paper demonstrates the importance of consideration of spatial variability of concrete deterioration both at the serviceability and ultimate limit states.

1 INTRODUCTION

The number of deteriorating bridges due to chloride-induced corrosion increases annually as does the cost of inspection, maintenance, repair and where necessary replacement (Frangopol et al., 2001; Stewart and Rosowsky 1998). To optimise and manage budget spend; bridge owners/managers need to rely more on rational decision making methods rather than on subjective engineering judgment. In recognition of this, suggestions have been made that future Bridge Management Systems (BMS) will have to depend on probabilistic and reliability-based methods (Frangopol et al., 2001). Reliability-Based BMS (RBBMS) permits the inclusion of uncertainty of all parameters and models associated with the deterioration process. RBBMS will also have the advantage of using the reliability index ' β ' as a safety indicator, which provides clearer and better defined safety performance criteria. A major shortcoming in the work performed to date in this regard, (e.g. Enright and

Frangopol 1998; Val and Melchers 1997) is the neglect of the Spatial Variability (SV) of the deterioration parameters.

SV work which has been carried out has mainly focused on the prediction of the visual condition of the corroded structure over time (e.g. Li et al., 2004; Vu and Stewart 2005). However, due to the common parameters (material, environmental properties, etc.) positive correlations are expected between the times of damage initiation of the visual condition of the structure and the rate of degradation of structural safety. Therefore, in the provision of a comprehensive structure management methodology, it would be appropriate that the lifetime visual condition and safety were both predicted within the same framework using where possible the same material deterioration models and parameters. The main objective of this paper is to investigate the possibility of such integration and to highlight the importance of including SV in this modelling.

2 DETERIORATION MODELLING

The methodology for modelling deterioration of concrete structures employed in this paper is illustrated schematically in Figure 1. This is an extended version of Tutti's Standard model (Tutti, 1982).

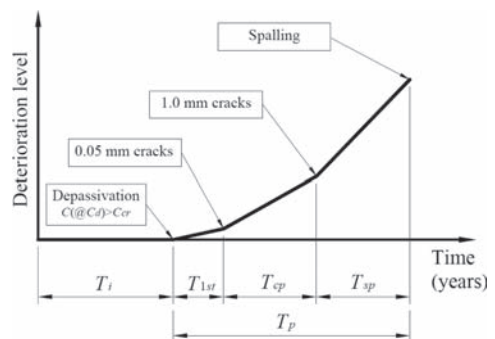


Figure 1. Concrete structure service life model.

Once initiated, two types of corrosion, general and pitting, are considered in the propagation phase.

3 SPATIAL VARIABILITY MODELLING

Early probabilistic analysis of RC deterioration typically modelled the material and geometrical uncertainty using a single random variable for the whole structure or component without considering SV. This assumes that material and geometrical properties are considered to be homogenous within a structure or a component. However, in reality, such properties vary in space. To account for this field variation, the surface of the structure can be discretised into number of small square elements following the SV approach described by Haldar and Mahadevan (2000); Vu and Stewart (2005).

4 STRUCTURAL RELIABILITY ANALYSIS

Three different (time-variant) LS's are considered in this paper; one, at the Serviceability Limit State—SLS, concerning the structure surface area condition (e.g. A_x) and the other two at the Ultimate Limit State—ULS, concerning the safety of the structure (i.e. flexure & shear capacities).

5 EXAMPLE

A hypothetical RC bridge, taken from Enright and Frangopol (1998), is considered in this paper to demonstrate the influence of considering/neglecting spatial variability on predicting optimal maintenance intervention strategies. Table 1 lists values of the parameter d for two key deteriorating variables, namely the Surface Chloride Content (C_s) and the Diffusion Coefficient (D_{app}).

5.1 Predicted safety profile

For both failure modes, flexure and shear, and for each of the two forms of corrosion, general and pitting, the annual reliability indices corresponding to the beam annual failure probabilities

Table 1. Scale of fluctuation (θ) and the corresponding correlation length (d).

Variable	θ (m)	d (m)	Reference
C_s	2.7	1.5	Kenshel, (2009)
$D_{app}, f_c', wc, i_{corr(1)}$	1.9	1.1	Kenshel, (2009)
Other RF variables	3.5	2.0	Li <i>et al.</i> (2004) & Vu and Stewart (2005)

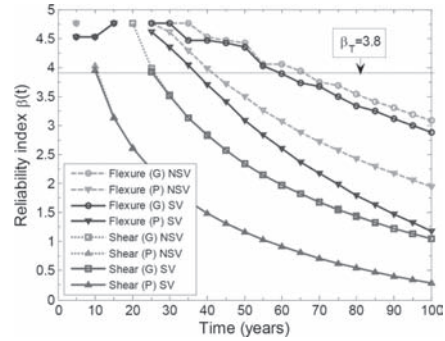


Figure 2. Influence of general (G) and pitting corrosion on safety profile for No SV and SV.

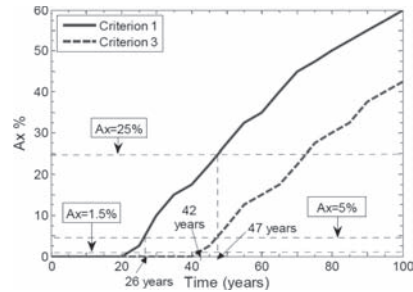


Figure 3. Time to first repair/maintenance based on SLS criteria.

are indicated in Figure 2 for two cases; (a) where spatial variability was not considered (b) where spatial variability was considered.

5.2 Time to maintenance action

Figure 3 indicates the computed time to first repair based upon SLS criteria.

6 CONCLUSION

A comprehensive spatial/temporal model for condition and safety deterioration prediction of corroding RC structures is developed in the paper using existing chloride-induced corrosion deterioration models. The model incorporates material, loading, geometrical and environmental uncertainties to identify the deterioration parameters most influencing the maintenance decision making process. Spatial variability, which has been neglected in many reliability based studies, has been shown to be of great importance when predicting the life-time condition and safety profiles. The importance of considering both the SLS and ULS in a unified framework to identify optimal whole life maintenance strategies is presented.

Reliability updating with inspection and monitoring data in deteriorating reinforced concrete slabs

Daniel Straub

Engineering Risk Analysis Group, Technische Universität München, Germany

ABSTRACT: Corrosion is a common phenomenon in engineering structures; examples include corrosion of the reinforcement in RC structures, corrosion of steel plates in ship hulls or localized corrosion in pipelines. These corrosion mechanisms are generally subject to random spatial variability, due to random changes in influencing factors over space. When assessing the effect of inspections and measurements on the reliability of such structures, it is essential to account for this spatial variability: Due to correlation among influencing factors at separate points, the measurement results obtained at one location contain information on the corrosion process at other locations. In this paper, a novel algorithm for reliability updating developed in (Straub 2011) is adopted to the spatial reliability analysis of RC corrosion conditional on measurements. The algorithm is computationally efficient and robust, thus facilitating the applications to reliability updating of large-scale structural systems subject to corrosion. The method is applied to an example concrete slab subject to chloride induced corrosion of the reinforcement, for which spatial measurements of concrete cover depth and chloride profiles are available.

Any information Z (e.g. measurements, observed performances) can be described by a likelihood function $L(\mathbf{x})$, whose arguments \mathbf{x} are the outcomes of the basic random variables describing the reliability problem (here: the random variables of the corrosion model). In Straub (2011) it has been shown that the conditional probability of the failure event F given the observed Z can be computed by solving the following structural reliability problem:

$$\Pr(F | Z) = \frac{\int_{\mathbf{x}, p \in \{\Omega_F \cap \Omega_{Z_e}\}} f_{\mathbf{X}}(\mathbf{x}) dx dp}{\int_{\mathbf{x}, p \in \Omega_{Z_e}} f_{\mathbf{X}}(\mathbf{x}) dx dp} \quad (1)$$

where $\Omega_F = \{g(\mathbf{x}) \leq 0\}$ is the failure domain in the outcome space of \mathbf{X} . $\Omega_{Z_e} = \{h_e(\mathbf{x}, p) \leq 0\}$ is a domain describing the information in the outcome space of \mathbf{X} and an additional auxiliary variable P , which has the standard uniform distribution.

As demonstrated in (Straub 2011), this domain is defined through the following limit state function:

$$h_e(\mathbf{x}, p) = p - cL(\mathbf{x}) \quad (2)$$

The constant c can be freely selected as long as it is ensured that $0 \leq cL(\mathbf{x}) \leq 1$.

As opposed to previous formulations of conditional probability in structural reliability theory (e.g. Madsen 1987, Schall et al., 1988), the above formulation can be evaluated using any structural reliability method (SRM), including FORM/SORM as well as sampling methods.

When considering spatial deterioration reliability, the conditional probability $\Pr(F|Z)$ must be computed for different locations in space. Therefore, a large number of evaluations of the integrals in Eq. (1) are potentially required. It is therefore important to employ a SRM that provides an optimal trade-off between computational robustness and efficiency. Robustness means that a method can be applied without problem specific adjustments and efficiency means that only a limited number of evaluations of the limit state functions are required.

As shown in (Straub 2011), FORM/SORM techniques are not generally suitable due to the fact that the limit state surfaces $h_e = 0$, which describe the information, can be highly non-linear. For the considered application to spatial corrosion reliability, the use of a simple importance sampling (IS) scheme is suggested, providing a good trade-off between robustness and efficiency. The IS estimator for the conditional probability $\Pr(F|Z)$ in Eq. (1) is

$$\Pr(F | Z) \approx \frac{\sum_{i=1}^{n_s} I[h_e(\mathbf{x}_i, p_i) \leq 0] I[g(\mathbf{x}_i) \leq 0] \frac{f_{\mathbf{X}}(\mathbf{x}_i)}{\psi(\mathbf{x}_i, p_i)}}{\sum_{i=1}^{n_s} I[h_e(\mathbf{x}_i, p_i) \leq 0] \frac{f_{\mathbf{X}}(\mathbf{x}_i)}{\psi(\mathbf{x}_i, p_i)}} \quad (3)$$

where in the samples \mathbf{x}_i and p_i are simulated from a distribution with sampling density $\psi(\mathbf{x}, p)$. As shown in the paper, Eq. (3) reduces to

$$\Pr(F|Z) \approx \frac{\sum_{i=1}^{n_s} I[g(\mathbf{x}_i) \leq 0] \frac{f_{\mathbf{X}}(\mathbf{x}_i)L(\mathbf{x}_i)}{\psi_1(\mathbf{x}_i)}}{\sum_{i=1}^{n_s} \frac{f_{\mathbf{X}}(\mathbf{x}_i)L(\mathbf{x}_i)}{\psi_1(\mathbf{x}_i)}} \quad (4)$$

where the sampling (proposal) distribution $\psi_1(\mathbf{x})$ is only on \mathbf{X} . Here, the prior PDF of \mathbf{X} is selected as its sampling density, i.e., $\psi_1(\mathbf{x}_i) = f_{\mathbf{X}}(\mathbf{x}_i)$, but more refined choices can be made (e.g. Straub 2010).

The algorithm is applied to the example of a reinforced concrete (RC) surface that is subject to corrosion of the reinforcement caused by chloride ingress. The method presented in the previous section is applied to compute the spatial probability of corrosion conditional on measurements of concrete cover depth and chloride penetration. The cover depth measurements are made on the entire surface using a continuous device (see Gehlen and Greve-Dierfeld 2010). Information on chloride penetration is obtained from cores taken at discrete locations of the surface. The considered surface area has size 10 m \times 20 m; For the purpose of the analysis, the surface is discretized in 800 elements of size 0.5 m \times 0.5 m. Results obtained with the algorithm are shown in Figure 1.

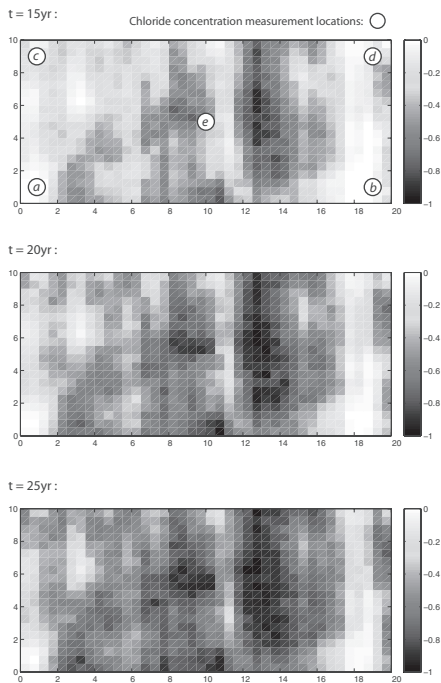


Figure 1. Probability of corrosion initiation at different times conditional on concrete cover depth measurements on the surface and on chloride measurements at locations (a) to (e).

CONCLUSIONS

The application presented in this paper demonstrates the potential of the method proposed in Straub (2011) for Bayesian updating of spatial probabilistic models of deterioration with information that is obtained at discrete points in space. In the presented application, this information is the measured chloride content at discrete points in the concrete surface. Additionally, when direct measurements of individual model parameters are available, the method can be combined with classical methods for Bayesian updating of random variables. In the presented example, such measurements were available on concrete cover depths.

The new updating method proceeds by transforming equality information into equivalent inequality information. In this way, Bayesian updating of the probabilistic model and the reliability estimate with any information can be performed using simple simulation techniques, such as importance sampling. These techniques have the advantage of being robust, which is of particular relevance in the context of spatially distributed systems, where a large number of conditional probabilities must be computed.

As the amount of information increases, the efficiency of the presented simulation techniques decreases, due to a decrease of $\Pr(Z_e)$, the probability of the equivalent inequality observation. This limitation becomes relevant when measurements, which are not directly on an input variable, are made continuously in space; an example being large-scale half-cell potential measurements. Further investigations are ongoing on how the efficiency of methods for Bayesian updating can be improved for such applications.

REFERENCES

- Gehlen, C. & Greve-Dierfeld, S. (2010). Optimierte Zustandsprognose durch kombinierte Verfahren. *Beton- und Stahlbetonbau*, **105**(5): 274–283. [In German].
- Madsen, H.O. (1987). Model Updating in Reliability Theory, in *Proc. ICASP 5*, Vancouver, Canada.
- Schall, G., Gollwitzer, S. & Rackwitz, R. (1988). Integration of multinormal densities on surfaces, in *Proc. 2nd IFIP WG7.5 Working Conference*, London.
- Straub, D. (2010). Reliability updating with measurements in spatially distributed systems using stochastic simulation. *Reliability and Optimization of Structural Systems* (ed. D. Straub), Proc. IFIP WG7.5 conference, Munich, Taylor and Francis/Balkema.
- Straub, D. (2011). Reliability updating with equality information. *Probabilistic Engineering Mechanics*, **26**(2): 254–258.

This page intentionally left blank

*MS_334 — Spatial probabilistic modeling
of deterioration and inspection (3)*

This page intentionally left blank

Spatial deterioration model updating of aging RC structures based on inspection information

K.G. Papakonstantinou & M. Shinozuka

Department of Civil and Environmental Engineering, University of California Irvine, Irvine, CA, USA

ABSTRACT: A spatial, stochastic, chloride induced corrosion model of reinforced concrete structures is briefly analyzed in this work. Modeling the spatial variability of model parameters gives one the ability, not only to quantify the probability of degradation, but the extent of damage as well. The model aspires to predict structures' extent of damage for their whole service life period. An efficient way of predicting reliable results, throughout the years, is by utilizing inspection information to update the model. This stochastic inverse problem, concerning the spatial extent of damage, presents many challenges however, in realistic applications, mainly due to computational intractability. To overcome this obstacle, a series of steps are taken in this work consisting of sensitivity analysis, quadrature techniques and the unscented transformation. The specific updating procedure allows the solution of the problem in reasonable computational time, even for large structures and sophisticated numerical models.

Given that deterioration processes are highly variable in space, it is of great importance to be simulated in a stochastic field context rather than a "point-in-space" probabilistic model. Accurately predicting the extent of damage for the whole service life period of a structure without inspection information is a fictional belief, to say at least. The importance of inspection information has been, indeed, widely identified by researchers and various inspection methods and techniques are available nowadays for corrosion induced damage monitoring.

Updating the parameters of a probabilistic computational model based on output information is a stochastic inverse problem with appearances in every engineering field. Standard, optimization-based as well as Bayesian methods can be utilized in solving it, with every method having positive and negative aspects of course. As far as corrosion deterioration problems are concerned, a very limited number of researchers has dealt by now with model updating issues. In majority these researches only update the output of the model, based on Bayesian principles, do not provide a systematic, algorithmic way to find the hidden, unobserved, input parameters of the model or do not address

the problem through a spatial perspective, which, self-evidently, greatly increases the required amount of computational effort. In this paper, all the aforementioned limitations have been resolved and a complete framework for solving the stochastic inverse problem of the extent of chloride induced corrosion deterioration of large structures is presented.

The model used for the direct simulation of the extent of damage has been described in more detail in Papakonstantinou & Shinozuka (2010). It can simulate all three stages of reinforced concrete corrosion, i.e. corrosion initiation, crack initiation and propagation. Nonetheless, just for clarity purposes, the extent of damage that refers to portion of the structure exceeding a certain crack width is not considered in this paper. Therefore, the crack propagation stage is not described.

Considering the spatial variation of the deterioration process, certain variables involved in the problem have been represented by uni-variate, two-dimensional, homogeneous, stochastic fields, simulated by the spectral representation method (Shinozuka & Deodatis 1996). In order to implement the probabilistic corrosion modeling, and determine some of the parameters involved in the problem, results from a field investigation on a port structure are used (Papakonstantinou & Shinozuka 2010) and the dimensions of the wharf deck slab under study in this paper are 24 m by 15.2 m.

Based on the output variables that have been considered in the paper, i.e. corroded and cracked extent of damage, a sensitivity analysis is performed using Sobol' indices. Sensitivity analysis results showed that the "full", spatial model used could be simplified in this case, without overlooking important information concealed in the input variables. Therefore, the time-consuming partial differential equation solver, used in the "full" model has been replaced by an adaptive Simpson's rule resulting in a drastic reduction of computational time. However, in an inverse analysis context, where many calls to the model are usually required, the computational time is still prohibitive.

In Papakonstantinou et al. (2009) it has been numerically showed that the extent of damage, in

the mean, is equal to the point-in-space probability of failure. The same conclusion can be seen in Sudret (2008), together with analytical expressions for calculating the variance of the extent of damage without discretizing the input random fields. Using a 5 point Lobatto quadrature rule and performing a few, carefully chosen, point-in-space analyses, the mean and variance of the extent of damage has been accurately computed without the need of an expensive, spatial solver. Results can be seen in Figure 1.

Regardless of the computational demands of the direct solver, using computationally low-cost inverse methods is still of paramount importance in a stochastic optimization context. Definition of stochastic optimization can have plenty interpretations. In this work randomness is present as measurement and process noise, as well as Monte Carlo simulations in the search procedure.

A very efficient, computationally inexpensive, Bayesian based method to solve the problem is available due to the unscented transform (Julier & Uhlmann 2004). The unscented transformation (UT) has been used, almost exclusively, in the literature in state estimation and identification of dynamic systems, by means of the Unscented Kalman Filter (UKF). However, its use can go beyond the vast amount of applications in this limited field, and it is surprising to the authors that no other works outside the aforementioned field could be found. In its broader essence, the UT is a method to propagate mean and covariance information through nonlinear transformations, without utilizing Jacobian matrices. Relying on the essence of the UT, an UKF has been used in this work to solve the inverse problem, in an out of the ordinary, modified framework, since the problem has not been casted in this case as a state estimation problem of a dynamic system. The UT resembles

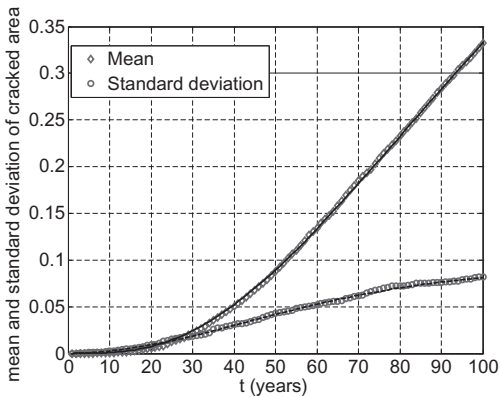


Figure 1. Evolution in time of the mean and standard deviation of cracked area percentage (black: stochastic field results).

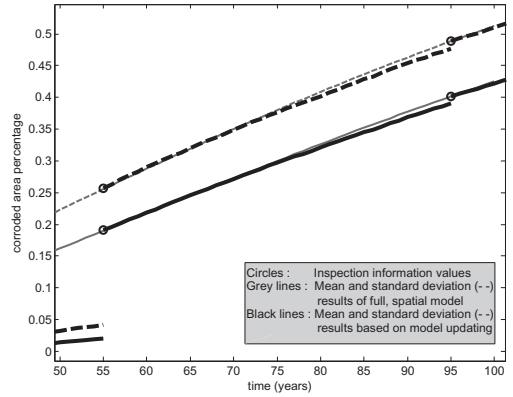


Figure 2. Model updating results.

quadrature based techniques; although it can be easily proven that it is much more than that.

To demonstrate the efficiency of the algorithm a numerical application has been performed. Supposing inspection information is available about the extent of corroded area at 55 and 95 years, the effect of the updating process can be seen in Figure 2. For the inspection information it is assumed that the extent of damage is given by the mean. The standard deviation resembles the uncertainty of the measurement. This is a very pragmatic approach since in reality only these two values are usually available. Just for crude comparison purposes, the presented inverse procedure terminated after approximately 30 minutes, for the first updating in 55 years, while a generic genetic algorithm program used, with a population of 20 chromosomes and the same termination criteria, required, in the mean, around 5.5 hours; a noteworthy difference.

REFERENCES

- Julier, S. & Uhlmann, J. 2004. Unscented filtering and nonlinear estimation, *Proceedings of the IEEE*, 92(3).
- Papakonstantinou, K., Kwon, S.J. & Shinozuka, M. 2009. Stochastic forecast analysis of the service life of reinforced concrete structures subjected to chloride penetration in *ICOSSAR*, CRC Press, Osaka, Japan.
- Papakonstantinou, K. & Shinozuka, M. 2010. Spatial stochastic and sensitivity analysis of steel corrosion in a RC port structure in *Computational Stochastic Mechanics (CSM6)*, G. Deodatis and P.D. Spanos (eds), Rhodes, Greece.
- Shinozuka, M. & Deodatis, G. 1996. Simulation of multi-dimensional Gaussian stochastic fields by spectral representation, *Applied Mechanics Review*, 49(1), ASME, 29–53.
- Sudret, B. 2008. Probabilistic models for the extend of damage in degrading reinforced concrete structures, *Reliability Engineering and System Safety* 93, 410–422.

Statistical analysis of the surfaces of corroded mild steel plates

R.E. Melchers, M. Ahammed, R. Jeffrey & G. Simundic

Centre for Infrastructure Performance and Reliability, The University of Newcastle, Australia

1 INTRODUCTION

For the management of large steel infrastructure exposed to marine environments, such as ships hulls and floating offshore platforms, the corrosion of the steel forming the main structure is of interest particularly for the assessment of structural safety but also for continued containment capability. Broad agreement exist between the leading international Classification Societies about the maximum average diminution that is acceptable. Typically plates are over-designed by at least 10% to provide a ‘corrosion allowance’.

An immediate question for owners and managers is the time expected to elapse before the corrosion allowance is likely to be used up and what factors and influences are involved.

Ship classification Societies have very extensive records of plate thickness measurements. There is doubt whether such data is useful for development of predictive corrosion loss models. One reason is that the environment to which a vessel has been subjected is seldom recorded or known and this may have a profound effect on corrosion losses. This variability has been ignored in a number of analyses. To assess the reliability of an individual ship ‘with-in plate’ corrosion losses are required.

Recent efforts to produce predictive models for the amount of corrosion or the depth of pitting to be expected in actual seawaters has focused on using, and obtaining, information derived from mass loss or maximum pit depth measurements on steel coupons of limited size exposed for realistic periods to natural seawaters. An important question is whether the corrosion losses and pit depths observed on small-scale coupons are sufficient to represent the corrosion characteristics for larger steel surfaces such as occur in actual steel structures.

Previous analyses of the correlation structure of the surfaces of corroded plates have used a Fast Fourier Transform (FFT) approach but only small plates were considered.

In the present investigation the results obtained from the corrosion of mild steel plates $1.2\text{ m} \times 0.6\text{ m}$ in size, exposed for up to 2.5 years in immersion, tidal and splash zone conditions in temperate

climate and seawater conditions are used to obtain estimates of the correlation structure of the surface. Only one set of results is described in some detail.

Estimates of the variability of the corroded surface of a plate can be obtained by estimating the variance of the amount of corrosion over a relatively small area and comparing each with similar variance estimates at other locations or for other plates or coupons. A more thorough analysis attempts to obtain the (auto-)correlation structure or, equivalently, its relative frequency distribution, through spectral analysis to produce a power spectrum from which the correlation structure can be estimated (de Silva 2000). The basic concepts for two-dimensional surfaces are summarized in the paper. Another possibility is to estimate the auto-correlation function for the corroded surface using repeated analysis of the corrosion depths for two (randomly chosen) points separated by a constant distance.

To obtain realistic data for the analysis, ten commercial mild steel plates each $1.2\text{ m} \times 0.6\text{ m} \times 3\text{ mm}$ thick were exposed in coastal seawater. One plate from two sets of 5 was recovered at 6, 12, 18, 24 and 30 months exposure. The plates were washed with a high-pressure water jet to remove marine growth and loose rusts. Typically this revealed a relatively regularly undulating metal surface (Figure 1).

The plates were guillotined into twelve equal $300 \times 200\text{ mm}$ plate pieces and the surfaces scanned on a 2 mm grid. The digitized scan results were processed. Figure 2 shows a typical result with expanded vertical scale (z-axis).

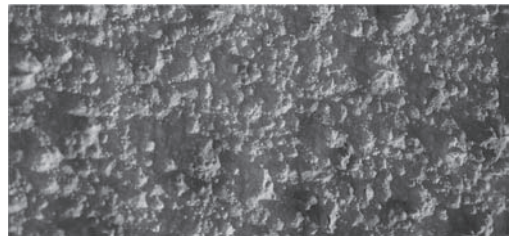


Figure 1. Close-up of corroded surface showing high degree of regularity of topography.

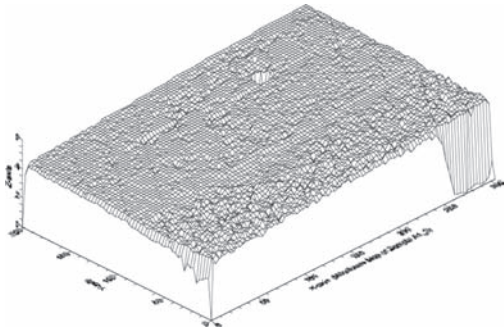


Figure 2. Wire frame map of the surface geometry of part of plate A, exposed in the splash zone for 6 months. The vertical axis is exaggerated. It reads 0, 2, 4 and 6 mm. The horizontal axes are 0, 50, 100, 150, 200 etc. mm. Note the fixing hole at top centre.

To obtain comparable power spectra, the data was in each case normalized to zero means. Figure 3 shows an example. It is clear that the frequencies along the two horizontal axes f_1 and f_2 are highly localized around 0.1 cycles/mm, with only minor amplitudes elsewhere. This highly restricted frequency content means that each exposure condition produced corroded surfaces that show a high degree of uniformity or regularity. Indeed, this is suggested already by visual examination of Figure 1. Moreover, the power spectra show that this high degree of regularity of the corroded surface is concentrated in the lower frequencies. The spectra show very little high frequency content in the topography of the corroded surfaces.

Similar results were found for all component plates exposed to the three exposure environments. In turn this means that there is negligible or at worst very little effect of surface area in the characteristic pattern of the corroded surface. This was found to be the case throughout the complete exposure period of 2.5 years. One practical outcome for statistical analyses is that this means that for any exposure condition small areas or (relatively) small samples can be taken as representative of the topography of the corroded surface and hence of its variability.

The above observations also allow an estimate to be made of the minimum size of coupon to obtain realistic results for the variability of a corroded surface. Moreover, it is sufficient, on the basis of the above observations, to represent the variability simply by the standard deviation or the coefficient of variation rather than the complete power spectrum or the auto-correlation function.

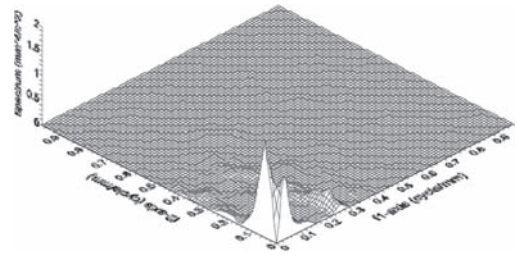


Figure 3. Power spectrum for sample plate piece A1 (side 1) exposed in the splash zone. The axis of the spectrum height, perpendicular to both frequency axes, has units of $\text{mm}^4/\text{cycle}^2$.

A matter of considerable practical interest is the probability of perforation of plates by corrosion pitting. In the conventional analyses, extreme value (EV) theory is employed, usually invoking the Gumbel distribution, although it has been shown recently that for longer term corrosion and pitting this may not be the most appropriate EV distribution. Extrapolation from small areas and from shorter-term exposures requires assumptions about continuity of the corrosion process and about the dependence structure. For situations where there is a non-trivial degree of dependence between observations, including perhaps some clustering, asymptotic independence can often be assumed to permit the use of one of the extreme value distributions. However, the possibility of asymptotic independence becomes increasingly less plausible as the data shows a higher degree of dependence. It would appear that the present results fall in this category. This suggests that conventional extreme value theory and in particular extrapolation from data and from interpretation of the data should be applied with great care.

The following conclusions may be drawn:

1. The surfaces of corroded steel plates are highly regular in topography for exposure in the one zone.
2. The results of the experiments show that this characteristic continues to be valid for exposures up to 2.5 years.
3. Relatively small corrosion coupons can be employed to capture the essential characteristics of the form of the corroded surfaces.
4. The minimum size of coupon to represent the character of the corroded surface was estimated to be in the range 15 mm to 150 mm square.

Random field modelling of spatial variability in FRP composite materials

Srinivas Sriramula

School of Engineering, University of Aberdeen, Aberdeen, UK

Marios K. Chryssanthopoulos

Faculty of Engineering and Physical Sciences, University of Surrey, Guildford, UK

ABSTRACT: The geometric and material properties of FRP composites exhibit an inherent uncertainty due to their complex manufacture and assembly processes. A wide range of stochastic analysis methods has been developed to account for this uncertainty at different scales. Researchers have shown interest in modelling uncertainty starting at a micro-scale (constituent level, fibre/matrix), meso-scale (ply level) or macro-scale (coupon/component level). The choice of micro-/meso-/macro-scale modelling depends on the objectives of the analysis, with each class having advantages and limitations. It is often desirable to fuse the different modelling levels in a multi-scale approach, either within a deterministic or, most importantly, within a stochastic framework.

It is recently being suggested that the advantages that stochastic analysis of composite structures may offer in terms of material efficiency and better utilisation can be best captured if uncertainty modelling accounts for spatial variation, preferably in conjunction with stochastic finite element analysis. However, the analytical and computational complexity arising from such modelling, and the scarcity of suitable experimental data, has so far limited the relevant investigations. These spatial variability models, if underpinned by experimental results, also assist in validating macro-level properties based on spatial micro-mechanics, while accounting for mathematical consistency across different scales.

As part of a research programme considering these options, this paper describes the experimental approach, and the associated modelling techniques, adopted for probabilistic spatial characterisation of two different sets of GFRP panels. The first is a set (*SET 1*) of GFRP panels obtained from Mondial House, a London building constructed in 1974 and demolished in 2006, with an average size of 1.5 m × 1.7 m. They were made from randomly placed chopped strand mat glass reinforcement in

a polymer matrix, resulting in isotropic in-plane properties. These panels had been exposed to varying ambient conditions, protected only by a fire retardant gel coat for self-cleaning. The second set (*SET 2*) comprises pristine factory made pultruded composite plates. These are structural grade GFRP products supplied in a standard size of 1.22 m × 2.44 m, made principally with unidirectional glass fibre bundles in one direction, thus exhibiting orthotropic properties.

The aged and weathered panels were expected to be indicative of the upper bound of spatial variability for FRP material systems, whereas the pristine pultruded composite plates were likely to be at the other end of the spectrum. Approximately 350 coupons were obtained in a pattern suitable for characterising the spatial variability of longitudinal tensile and compressive properties, as well as plate thickness. Spatial variability can be visualised in different ways. For example, for the *SET 2* plates, considering the longitudinal tensile modulus (E_{11}) value at reference locations 2 and 56, i.e., approximately at the start and end of the panel, the relative variation with respect to other locations is shown in Figure 1.

Experimental results were used to estimate the parameters of random fields, which are assumed to be spatially statistically homogeneous so that the primary and higher-order moments are independent of coupon location. The second-order information associated with the spatial variation of the considered variables is represented by covariance and appropriate correlation functions that are obtained by suitable normalisations. In all cases, the separation distance between coupons was treated as the index variable in random field modelling. The auto and cross-correlations among these variables were evaluated for various forms of correlation functions and typical results were discussed.

For a discrete set of n data points in the vector x , the auto-correlation function is given by

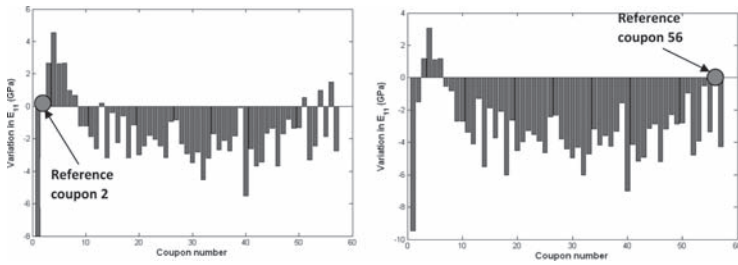


Figure 1. Variation of E_{11} with reference to coupons 2 and 56.

$$R_{xx}(\tau_j) = \frac{\gamma_{xx}(\tau_j)}{\sigma_x^2} = \frac{1}{n\sigma_x^2} \left(\sum_{i=1}^{n-j} (x_i - \mu_x)(x_{i+j} - \mu_x) \right) \quad j = 0, 1, \dots, n-1 \quad (1)$$

where μ_x and σ_x are the mean and standard deviation of variable x , $\gamma_{xx}(\cdot)$ is the auto-covariance function, and τ_j is the corresponding lag or separation distance between points. A wide range of functions satisfying the required mathematical conditions are available and could be explored with the available datasets. As a first attempt, functions belonging to the exponential class were chosen, partly because these have been referred to in previous studies based on theoretical models. Thus, the following functions were considered:

i. Exponential class

$$R(\tau) = \exp\left(-\frac{|\tau|}{b}\right) \quad (2a)$$

$$R(\tau) = \exp\left(-\left(\frac{|\tau|}{b}\right)^2\right) \quad (2b)$$

ii. Extended exponential class

$$R(\tau) = \left(1 - \frac{|\tau|}{b}\right) \exp\left(-\frac{|\tau|}{b}\right) \quad (3)$$

where b is the spatial correlation length.

Cross correlations between the variables can be obtained by a similar definition but with the functional forms being scaled by a power series to take care of the asymmetric patterns.

A typical auto correlation plot for the tensile strength of CSM GFRP panels is shown in Figure 2. The exponential correlation function in Eq. (2a) is found to give the best fit to the test data, leading to a b value of 92.1 mm. The auto-correlation plot

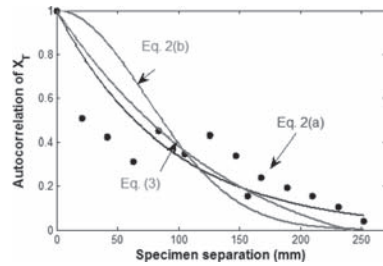


Figure 2. Autocorrelation models of X_T for SET 1 panels.

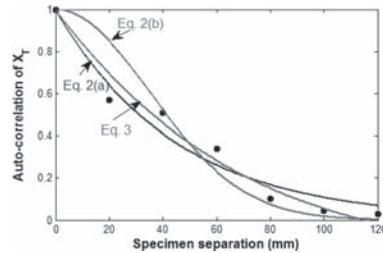


Figure 3. Autocorrelation models of X_T for SET 2 panels.

for the longitudinal tensile strength (X_T) for SET 2 panels is shown in Figure 3. Overall, both geometric and material properties were found to be well represented by autocorrelations from the exponential family, which has, in fact, been surmised in previous theoretical (rather than experimentally based) studies. It is concluded that manufacturing and in-service conditions play a major role in determining random field parameters, with correlation lengths in appropriately selected functions ranging from 20 to 100 mm. For any given FRP material, correlation lengths also vary depending on the property, which is pertinent to decisions made in SFEA. At present, further functional forms are explored, and correlation lengths for the remaining properties are being estimated.

Keywords: Uncertainty; Composite materials; Mechanical properties; Random fields; Spatial variability

Spatial variability of potential fields in reinforced concrete structures

S. Kessler & C. Gehlen

Centre for Building Materials, Technische Universität München, Germany

D. Straub

Engineering Risk Analysis Group, Technische Universität München, Germany

M. Huber

Institute of Geotechnical Engineering, University of Stuttgart, Germany

1 INTRODUCTION

For a realistic and accurate description of corrosion progress, spatial variability of corrosion processes must be accounted for particularly in the evaluation of existing structures. Corrosion of the reinforcement is one of the major deterioration mechanisms for reinforced concrete structures. The consequence of corrosion can be local loss of the reinforcement cross section in conjunction with sub-sequent cracking and spalling of concrete cover. This will impair the serviceability and eventually the load bearing capacity of the structure.

A main problem in estimating the spatial correlation structure of corrosion processes is the lack of data. In most studies, which focus on the spatial variability of concrete material properties, the values of the spatial correlation length and the associated discretisation scheme are based on practical considerations and experience. This paper presents an analysis of spatial variability of potential mapping results to support the modeling of spatially correlated concrete properties. Potential mapping is a widely used inspection method for detection of ongoing corrosion in reinforced concrete structures. With the aid of potential measurement results a structure can be divided into corroding and non-corroding areas. Therefore, the spatial variability of corroding areas can be described indirectly through the spatial variability of potential mapping, as demonstrated in this paper by the analysis of potential data obtained from bridge decks. Especially on structures with vast dimensions, decisions about further repair actions can be made and surveyed economically.

The paper focuses on the evaluation and comparison of the spatial variability of potential measurement results from several reinforced concrete

bridges. The approach can be performed without any additional assumptions for the post processing of the potential measurements.

2 EVALUATION OF SPATIAL VARIABILITY

Spatial variability of physical properties includes systematic spatial variation (variation of the mean value and standard deviation) and random spatial variation. The random spatial variability of the physical property can be captured via random fields as described, e.g. by Vanmarcke (1983) and Christakos (1992).

A first step in the evaluation of spatial variability is often the division of the structure into zones of comparable material resistances and environmental impact. The environmental impact depends on the exposure condition. The systematic spatial variation can be accounted for by this subdivision of the structure into zones. As a result of the systematic spatial variability, the probability of occurrence of a condition state will vary between different zones within the structure.

A second step is the subdivision of the zones into elements. The elements are represented by random variables. It is assumed that there is no spatial variation within a single element and so the individual elements behave statistically independent in terms of degradation.

To assess the size of these elements and their dependence structure, a study of the spatial correlation of the potential field measurement is carried out. The correlation length is commonly used to define the length of the elements. It is assumed that the potential field measurements can be described by a homogeneous random field, which is characterized by a mean value, a standard

deviation and a covariance function. Spatial correlation can also be described by the semivariance function γ_x and γ_y (Equation 1) as well as by the covariance function C_x and C_y , which are solely dependent on the vector of separation τ in x and y direction

$$\begin{aligned} \gamma_x(\tau_x) &= C_x(0) - C_x(\tau_x) \\ \gamma_y(\tau_y) &= C_y(0) - C_y(\tau_y) \end{aligned} \quad (1)$$

3 EXAMPLES

The evaluation of the spatial variability of potential fields of reinforced concrete structures is reasonable for structures with large dimension. For this reason potential measurements from six large bridges were analyzed.

The investigated bridges are between 35 and 50 years old. All bridges are exposed to spray containing chlorides and are subjected to cyclical wet and dry (exposure class XD3 according to EN 206). A high chloride impact and consequently chloride induced corrosion can be expected with time. Bridge 2a and bridge 2b refers to the same bridge, but two measurements made at different dates. The first measurement was in 2007 and the second in 2010. Segment 4a and segment 4b belong also to one bridge but the two different surfaces were measured with a time difference of three month.

The direction of traffic influences the distribution of the chloride and the humidity, in particular when it rains. Additional investigations are needed, e.g. the evaluation of the chloride and/or humidity distribution, to find the reason for the anisotropic behavior.

Table 1 gives an overview about the bridge data and the determined correlation lengths. The correlation lengths in the investigated bridges range from $\theta_x \approx 4$ m up to $\theta_x \approx 10$ m and show anisotropy of the correlation structure in two perpendicular directions. This anisotropy of the spatial correlation structure can be attributed to the construction process as well as to the influences of the traffic. The direction of traffic influences the distribution of the chloride and the humidity, in particular when it rains. Additional investigations are needed, e.g. the evaluation of the chloride and/or humidity distribution, to find the reason for the anisotropic behaviour.

Herein θ_x and θ_y are the correlation lengths in x and y direction. The correlation lengths of the bridges show comparable results. Bridge B4 and B2 have been measured twice. The segments B4a and B4b are different surfaces of Bridge B4 and

Table 1. Overview of bridge data and correlation length.

Bridge	Age [years]	measured area [m ²]	correlation length θ_x [m]	$\frac{\theta_x}{\theta_y}$
				[-]
B1	47	383	6	1
B2a	48	955	7	10
B2b	18	587	10	10
B3	42	2,360	10	5
B4a	39	818	4	10
B4b	39	570	6	10
B5	45	1,470	5	5
B6	39	500	7	8

were measured with a time difference of three month. Both segments of bridge B4 have a more or less similar value of the correlation length. It can be assumed that surfaces with the same material resistance, the same environmental condition and the same history will exhibit similar correlation lengths of the measured potential field. The bridge B2 was measured twice with a time difference of three years. Although the measured areas have different sizes, one can observe a dependence on time.

4 SUMMARY AND OUTLOOK

In this article, different case studies on the spatial variability of potential mapping of concrete bridges have been presented. The correlation lengths of the measured potential in the investigated bridges range from $\theta_{\text{parallel}} \approx 4$ m up to $\theta_{\text{parallel}} \approx 10$ m and from $\theta_{\text{perpendicular}} \approx 0.4$ m up to $\theta_{\text{perpendicular}} \approx 6$ m. The correlation structure is anisotrope.

Potential fields are influenced not only by corrosion processes but also by humidity and humidity differences in the concrete. The spatial evaluation of potential fields provides a first impression of the correlation structure of corrosion processes. But to obtain a complete understanding of the correlation structure it is necessary to account for the impact of humidity. If the humidity is uniform over the structure, then a high correlation between the spatial behaviour of corrosion processes and potential fields is expected. Additional research is needed to describe the correlation between corroding areas and potential fields.

Future research is needed to evaluate the time dependency of spatial correlation of reinforced concrete structures and to describe the relationship between corrosion processes, potentials field

and humidity in concrete. Also different reinforced concrete structures like parking garages or tunnels should be evaluated spatially with the same approach.

The results from the spatial variability of potential mapping provide important information about the actual condition state and the future performance of the concrete structure. The knowledge of the spatial distribution of corrosion damages support the calculation of the cost-consequences associated with further inspection and repair.

REFERENCES

- Chiles, J. & Delfiner, P. 1999. Modeling spatial uncertainty. *Wiley*, New York.
- Christakos, G. 1994. Random Field Models in Earth Science, *Dover Publications*, New York.
- Vanmarcke, E. 1983. *Random fields: analysis and synthesis*. M.I.T.-Press, Massachusetts.
- Wackernagel, H. 2003. Multivariate geostatistics: an introduction with applications. *Springer Verlag*, 3rd edition.

This page intentionally left blank

*GS_317 — Statistical investigations
and probabilistic modeling (1)*

This page intentionally left blank

Bayesian models for the detection of high risk locations on Portuguese motorways

S.M. Azeredo-Lopes & J.L. Cardoso

*Transportation Department, Planning, Traffic and Road Safety Division,
National Laboratory for Civil Engineering, Avenida do Brasil, Lisboa, Portugal*

ABSTRACT: Reducing road accident casualty frequency is an endeavor of extreme importance in Portugal due to this country's high rate of road fatalities. This reduction can be achieved in several ways, amongst which are engineering, enforcement, education and encouragement. Of these, road engineering improvements have been found to be highly cost-effective ways of improving road safety when they are targeted at sites where the risk of accident occurrence is unusually high relative to similar locations, due to the specific characteristics of those sites.

In order to apply engineering remedial interventions there is the need to identify those high risk road sites (also denoted by "hotspots", "blackspots" or "high risk locations"). For this identification to be efficient, it is convenient to develop accident prediction models in order to have a realistic estimate of the expected accident frequency as a function of traffic volume and roadway geometric characteristics over a road segment. Obtaining such estimates is also a critical component for transport engineers in the consideration of safety in other activities such as road planning and design.

In this study we illustrate an approach to obtain both accident prediction models and reliable high risk accident locations on the Portuguese motorway network employing methodology that has never been applied before to Portuguese accident data. It consists on a simulation methodology that considers two complete sets of bidirectional motorway sections with known safety status recorded over three and five years. The model parameters and probability distribution of mean accident frequency at each site (of the two bidirectional sets) are inferred from the data and used to establish the "true" high risk locations (hotspots) and to generate further accident data with known sample size (namely, 50, 100 and 400). The generated data is then used for identifying "new" or "detected" high risk locations after model fitting. The candidate models for fitting are hierarchical Bayesian regression models differing according to the types and distributions of the hyper-priors of the so-called dispersion

parameter. The Bayesian hierarchical models were implemented in WinBUGS in order to obtain the parameter estimates of the models by posterior inference using Markov chain Monte Carlo (MCMC) methods. The Gelman-Rubin statistic R (R_{hat}) was employed to certify that convergence was attained for the MCMC methods. A comparative performance between the different models that were fitted to the same samples of data was also made in terms of the deviance information criterion (DIC) values.

A ranking criterion was afterwards used for identifying the "detected" high risk locations, out of the posterior expected number of accidents obtained. The choice of a global critical value depended on the data under analysis and, for the purpose of the simulation employed, was chosen to be the 50% quantile of the list of posterior expected number of accidents.

Several scenarios were analyzed, including the type and distribution of hyper-priors, the sizes of the available accident data samples and the number of years of measured data.

The employment of various hyper-prior distributions had the purpose of investigating which type and distribution of hyper-prior (for the dispersion parameter) was better at detecting the "true" hotspots using a particular ranking criterion. The hyper-prior distributions involved in the study included the Gamma, Uniform and Christiansen's. The reason behind the choice of these distributions being their widely use on hierarchical Bayesian models fitted to accident data. Each of these distributions had parameters that had pre-incorporated available information from previous studies regarding Portuguese data; therefore, the hyper-priors were called informative. The Gamma distribution was also employed with parameters reflecting the absence of any kind of previous information (the non-informative or vague prior).

The performance of the alternative hyper-prior specifications, as well as the number of sites and number of years of measured data, were assessed according to the model's capacity to detect the

“true” high risk locations. This capacity was evaluated by the following measures: FDR (false discovery rate), the proportion of Type I errors among the “detected” hotspots; FNR (false negative rate), the proportion of Type II errors among the “detected” non-hotspots; SENS, the sensitivity or proportion of sites that have been correctly detected as hotspots and that can also be interpreted as the model’s capacity to detect a “true” hotspot in the group under analysis; SPEC, the specificity, representing the proportion of non-hotspots that have been correctly classified as “non-hotspots”; Risk, the proportion of the total number of errors (Type I and Type II) and the number of sites under analysis; PMD, the Poisson mean differences test with the aim of differentiating various false identifications; Percentage Deviation Value, adapted in the present study to quantify the effects of changing the hyper-prior specifications when a given criteria to detect dangerous accident locations is used; the Spearman correlation coefficient, employed to measure the degree of association between the “true” and the “simulated” ranked lists of accident frequencies. A comparison in terms of the accuracy of the estimation of the coefficient parameters (made

between the “true” model and the model fitted to the simulated data) was also performed. To make sure that statistically reliable estimates were obtained, each scenario was replicated 25 times and the results were presented by the mean values of these 25 simulations.

The study showed that when developing hierarchical Bayesian prediction models with the aim of using some of its outcomes for hotspot detection in Portuguese motorways, it is best to employ informative hyper-priors, namely Gamma and Christiansen’s, when small samples are considered (with sizes between 50 and 100). The use of informative hyper-priors when the available samples are greater (around size 400) is also preferable in particular obtaining more reliable estimates of the so-called dispersion parameter rather than being more accurate at detecting high accident high risk locations; as it was observed that for greater sample sizes (i.e. 400) no relevant differences were found amongst the hyper-prior types and distributions employed. The overall results showed that more accurate outcomes were obtained when more years (five, in the present study) of aggregated data were analyzed as in comparison with three years of data.

Statistical analysis of mechanical properties of prestressing strands

L. Jacinto

Instituto Superior de Engenharia de Lisboa, Lisbon, Portugal

M. Pipa & L.O. Santos

Laboratório Nacional de Engenharia Civil, Lisbon, Portugal

L.C. Neves

Faculdade de Ciências e Tecnologia da Universidade Nova de Lisboa, Caparica, Portugal

1 INTRODUCTION

This study deals with the statistical analysis of three groups of samples of strands with nominal diameters of 13.0, 15.2 and 15.7 mm, which correspond to the nominal cross sectional areas of 100, 140 and 150 mm², respectively. All strands have nominal tensile strength of 1860 MPa and are all composed by 7 wires. These have been the most commonly used in Portugal.

The samples refer to tensile tests performed between 2001 and 2009 in *Laboratório Nacional de Engenharia Civil* (LNEC), Portugal. During this period, over 500 tensile tests were carried out for the 3 families of strands mentioned above. However, several of these tests refer to strands produced from the same heat. As it is well known, the variability within a single heat is lower than the variability between different heats. Thus, for the purpose of statistical analysis, only one test from each heat was chosen (at random), which reduced the sample to 131 tests.

For each of the 3 families of strands, the following mechanical properties were studied: tensile strength (f_p), 0.1% proof stress ($f_{p0.1}$), total elongation at maximum force (ϵ_u) and modulus of elasticity (E_p). However, it was found that the difference in the mean of those properties between families was of the same order of magnitude of its standard deviations, which allowed us to consider the 3 families as belonging to the same population. The 3 families were thus merged into a single population.

The strands tested came from manufacturers of different countries, including Portugal, Spain, Thailand and Italy. However, as it will be seen, the variability of the studied mechanical properties is relatively small, not justifying a separated analysis by manufacturer.

As said above, the studied strands are all of the Y1860 grade, which has been clearly the most

commonly used in Portugal. The value 1860 (which designates the grade) is termed *nominal tensile strength*, expressed in MPa (prEN 10138-1, 2009) and can be interpreted as the quantile 0.05 of the probability distribution of the tensile strength f_p , known generally by characteristic value and denoted usually by f_{pk} .

This paper analyzes the variability of the most important mechanical properties of the prestressing strands and compare it with the corresponding recommendations of the *Probabilistic Model Code* (JCSS, 2001).

2 STATISTICAL ANALYSIS

This section presents a statistical analysis of the 0.1% proof stress. In the full paper, all the above mentioned parameters are studied, including a Bayesian analysis concerning the characteristic tensile strength.

The 0.1% proof stress $f_{p0.1}$ is a parameter of great importance for the structural safety and, to some extent, more decisive than the tensile strength f_p . In fact, the tensile strength is only achieved for large strains, hardly reached even for ultimate limit states. Figure 1 shows the histogram of the 0.1% proof stress and its temporal variation (131 tests), which does not reveal any trend during the period observed (2001 to 2009).

The 0.1% proof stress has greater variability ($\sigma_{f_{p0.1}} = 51$ MPa) than the tensile strength ($\sigma_{f_p} = 35$ MPa). In fact, the 0.1% proof stress is more sensitive than tensile strength, because it depends on the measured modulus of elasticity and even the curvature of the stress-strain diagram where yielding starts. This finding raises a comment on the model $f_{p0.1} = 0.85f_p$ proposed by PMC (JCSS, 2001). In fact, according to this model, the standard deviation of the 0.1% proof stress is smaller than that of the tensile strength, contrarily to the results

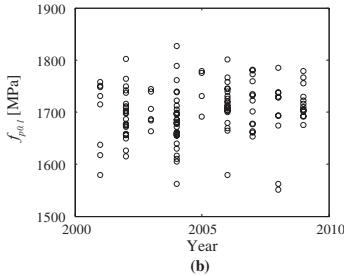
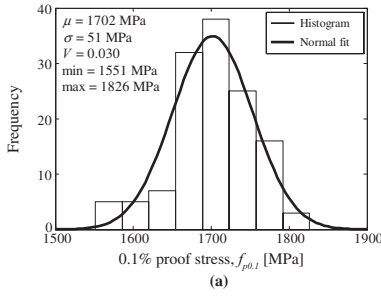


Figure 1. The 0.1% proof stress $f_{p0.1}$. (a) Histogram. (b) Values of $f_{p0.1}$ by year. Each dot corresponds to a tensile test.

obtained. In the full paper, a model for obtaining $f_{p0.1}$ from f_p based on regression analysis will be proposed, which allows overcoming this issue.

3 CONCLUSIONS

The present study made it possible to appreciate the low variability of the mechanical properties of prestressing strands, which, of course, benefits the safety of structures. The highest variability was obtained for the elongation at the maximum force, which revealed a coefficient of variation of about 0.06. For the remaining properties, the coefficient of variation obtained was lower than 0.03.

The Bayesian analysis showed that the estimate of the characteristic tensile strength can be considered accurate. Since the standard deviations for other mechanical properties are also small, this conclusion can be also applied to those properties. In addition, it is believed that the sample at hand has a reasonable representativeness, so that it can be proposed probabilistic models for the main mechanical properties of prestressing strands. Table 1 summarizes the models proposed.

The proposed models were based on the results obtained for strands of the Y1860 grade, where the value 1860 refers to the characteristic tensile strength f_{pk} . However, taking into account the quality control typical for this kind of product, we believe the same model can be applied to strands of other grades.

Table 1. Proposed probabilistic models for prestressing strands of the Y f_{pk} grade (f_{pk} = characteristic tensile strength).

Variable	Unit	Mean	Std. dev.	V	Distrib.
f_p	MPa	$f_{pk} + 1.645 \times 35$	35	–	Normal
$f_{p0.1}$	MPa	$0.89 \mu_{f_p}$ *	50	–	Normal
ϵ_u	–	5%	0.4%	–	Normal
E_p	GPa	195	5	–	Normal
A_p	any value	Nominal	–	0.01	Normal

* When it is necessary to model simultaneously $f_{p0.1}$ and f_p , the full paper provides a model based on regression analysis.

It was demonstrated that the correlation between the 0.1% proof stress and tensile strength is strong. In fact, these parameters cannot be considered independent from each other. On the other hand, the correlation between tensile strength and total elongation at maximum force can be neglected.

Finally, as a last comment, it should be emphasized that the proposed models were the result of tests performed between 2001 and 2009. During this period the mechanical properties studied did not show any trend. However, for purposes of assessment of existing structures, the models should be verified, especially if the steel have been produced in a period outside the period analyzed.

REFERENCES

- Ang, A. & Tang, W.H. 2007. *Probability Concepts in Engineering*, John Wiley & Sons, Chichester, 2nd edition.
- Bernardo, J.M. & Smith, A.F.M. 2000. *Bayesian Theory*. John Wiley & Sons.
- E453:2002. *Prestressing steel strands. Characteristics and tests* (in Portuguese). Especificação LNEC.
- EN 1992-1-1:2004. *Eurocode 2: Design of concrete structures – Part 1–1: General rules and rules for buildings*, CEN, Brussels.
- ISO 12491:1997. *Statistical methods for quality control of building materials and components*. International Organization for Standardization, Switzerland.
- JCSS. 2001. *Probabilistic Model Code. Joint Committee on Structural Safety*, <http://www.jcss.ethz.ch>, 12-th draft.
- Montgomery, D.C. & Runger, G.C. 2007. *Applied Statistics and probability for engineers*. John Wiley & Sons, fourth edition.
- Paulino, C.D., Turkman, M.A. & Murteira, B. 2003. *Bayesian Statistics* (in Portuguese). Fundação Calouste Gulbenkian, Lisboa.
- prEN10138-1:2009. *Prestressing steels - Part 1: General requirements*. CEN, Brussels.
- prEN10138-3:2009. *Prestressing steels - Part 3: Strand*. CEN, Brussels.

Probabilistic model for damage accumulation in concrete tunnel lining and its application to optimal repair strategy

Hiroaki Tanaka

Department of Applied Analysis and Complex Dynamical Systems, Kyoto University, Kyoto, Japan

Osamu Maruyama & Atsushi Sutoh

Department of Urban and Civil Engineering, Tokyo City University, Tokyo, Japan

1 PURPOSE OF THIS STUDY

In this paper, we focus on modeling uncertainties of structural performance and failures under environmental loadings, we propose a new probabilistic model for describing variation of damage accumulation in concrete tunnel linings. The proposed model is based upon a stochastic differential equation driven by a Poisson white noise, whose solution process represents a damage accumulation. Next, we discuss an optimal repair strategy for road tunnels by applying the stochastic control theory.

2 PROBABILISTIC MODEL FOR DAMAGE ACCUMULATION

Letting $X(t)$ be a quantified damage degree in an objective concrete tunnel lining at time t , we assume that its temporally random variation is described by the following stochastic differential equation of Itô type;

$$dX(t) = \mu X(t)dt + X(t-)dC(t), \quad (1)$$

where $C(t)$ is a compound Poisson process defined as

$$C(t) = \sum_{k=1}^{N(t)} Y_k, \quad (2)$$

in which $N(t)$ is a Poisson process with an intensity λ , and $\{Y_k\}_{k=1,2,\dots}$ is a family of i.i.d. (identically and independently distributed) positive random variables, whose probability distribution function $F(y) = P(Y_k \leq y)$ is known.

The first term of Eq. (1) represents continuous growth of the damage degree according to the effect of rainfalls, salt or other usual effects. On the other hand, the second term represents large-scale growth of the damage caused by unusual effects such as large-scale earthquakes, serious frost damage etc. In this study we call the former growth *small scale growth* and the later *large scale growth*.

3 FORMULATION OF REPAIR STRATEGY AND ITS OPTIMIZATION

We basically suppose the following repair strategy;

- The inspection-repair program starts at time s [year] and terminates at time T [year] ($0 \leq s \leq T$).
- When the damage degree is known to be x by an inspection at time t , we execute a repair of the damage so that the damage degree is reduced from x to $x - a(t)$, where $a(t)$ is a control variable in our optimization procedure. A cost required for such a repair as well as an inspection is given as

$$R(s, x, a(t)) = e^{-rs} \left(R_I + C_R x^m \frac{a(t)}{x} \right), \quad (3)$$

in which R_I is an inspection cost, C_R is a repair cost parameter and r is a riskless interest ratio that is introduced based upon the discounted cash flow method.

- The control $a(t)$, i.e., amount of repair is supposed to be generally a stochastic process taking on a value in $\mathcal{D}(x) = \{a; 0 \leq a \leq \max\{x - 1, 0\}\}$ provided that the detected damage degree is x at time t . Here we only discuss the so-called Markov control, i.e., $a(t)$ is expressed as $a(t) = \alpha(t, X(t))$ by the use of a deterministic function $\alpha(s, x)$.
- The tunnel concrete liner is supposed to fail when the damage degree exceeds a prespecified critical level denoted by x_c . A cost incurred by a failure of the tunnel lining provided that the failure takes place at time t after the damage degree grows to $x (> x_c)$, is given as

$$\varphi(s, x) = e^{-rs} C_F \frac{x}{x_c}, \quad (4)$$

- where C_F represents a failure cost parameter.
- The inspection-repair program is here assumed to terminate when the tunnel lining fails before the terminal time T .

Let $J^a(s, x)$ be an expected total cost up to the terminal time $t = T$ under the condition that $X(s) = x$, with a control $a = \{a(u); s \leq u \leq T\}$. Based upon our repair strategy, we can formulate it as follows:

$$J^a(s, x) = E^{s,x} \{K^a(s, x)\}, \quad (5)$$

$$K^a(s, x) = \int_s^{\min\{T, \tau^a\}} R(u, X^a(u-), a(u-)) dN_R(u) + \varphi(\tau^a, X^a(\tau^a)) \mathbf{1}_{\{\tau^a \leq T\}} \quad (6)$$

where $X^a(t)$ is a damage growth process under the control a , $\tau^a(s, x)$ is a failure time defined as $\tau^a = \inf\{t; X^a(t) > x_c\}$, $\mathbf{1}_{\{\cdot\}}$ is an indicator function and $E^{s,x}$ is an operator to take expectation under the condition that $X(s) = x$. That is, the first term represents total repair cost and the second term represents a failure cost respectively in (s, T) . The optimal control, i.e., optimal repair strategy a^* is defined as

$$\inf_{a \in \mathcal{D}(x)} J^a(s, x) = J^{a^*}(s, x) \equiv V(s, x). \quad (7)$$

It should be noted that the optimal value function $V(s, x)$ satisfies a terminal condition $\lim_{s \rightarrow T} V(s, x) = 0$.

4 HJB EQUATION

By applying the stochastic control theory, we can derive the Hamilton-Jacobi-Bellman (HJB) equation, which gives a necessary and sufficient condition for the optimality, as follows:

$$\inf_{a \in \mathcal{D}(x)} [\mathcal{L}^a V(s, x) + \lambda_R R(s, x, a)] = 0, \quad (8)$$

$$\begin{aligned} \mathcal{L}^a V(s, x) = & -(\lambda + \lambda_R)V(s, x) + \frac{\partial}{\partial s} V(s, x) \\ & + \mu x \frac{\partial}{\partial x} V(s, x) + \lambda_R V(s, x - \alpha) \\ & + \lambda \int_0^{x_c/x-1} V(s, (1+y)x) dF(y) \\ & + \lambda \int_{x_c/x-1}^{\infty} \varphi(s, (1+y)x) dF(y), \end{aligned} \quad (9)$$

The solution of the HJB equation $\alpha^*(s, x)$ gives an optimal control $a^*(t)$ as $a^*(t) = \alpha^*(t, X(t))$ and $V(s, x)$ gives a corresponding optimal value function.

5 NUMERICAL EXAMPLES

Figures 1 and 2 show the numerically solved solution of the HJB equation $\alpha^*(s, x)$ and $V(s, x)$ for several values of s , where parameters are set as $\mu_0 = 0.03$ [year⁻¹], $\lambda = 0.5$ [year⁻¹], $q_1 = 0.05$, $T = 50$ [year], $x_c = 15$, $R_l = 1$, $C_R = 10$, $m = 2$, $r = 0.014$, $C_F = 3000$ and $\lambda_R = 0.1$ [year⁻¹].

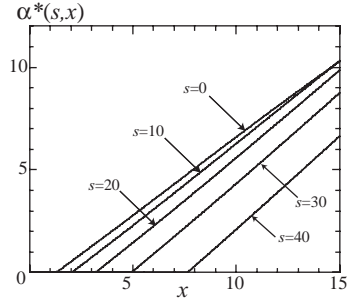


Figure 1. Optimal repair $\alpha^*(s, x)$ for several values of s .

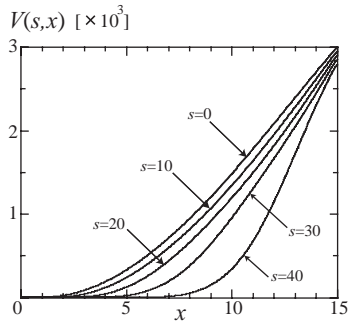


Figure 2. Optimal value function $V(s, x)$ for several values of s .

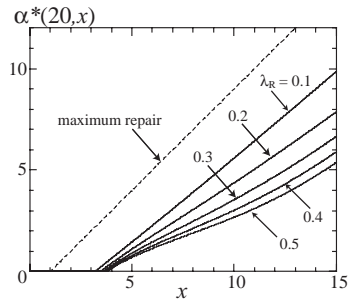


Figure 3. Effects of λ_R on the optimal repair $\alpha^*(20, x)$.

We can see that the optimal amount of repair almost linearly increases when the detected damage degree exceeds a certain threshold value for each s and that the effect of time s is gradually weakened as s becomes small. Especially, if the rest time $T - s$ is greater than 30 [years] and the detected damage is large, the optimal amount of repair is almost independent of time s .

Figure 3 shows the optimal repair $\alpha^*(20, x)$ for several values of the inspection intensity parameter λ_R , in which the dashed line shows the maximum amount of repair in our setting.

Application of extreme value theory to discriminate between failure modes

R.E. Melchers

Centre for Infrastructure Performance and Reliability, The University of Newcastle, Australia

1 INTRODUCTION

In the study of the factors that influence the long-term durability of Reinforced Concrete (RC) structures it has become increasingly apparent that laboratory studies, even those extending over many years, are unable to provide sufficiently convincing evidence. Mostly these studies are useful to show the effect of a potential influencing factor given a hypothesis about its likely effect. Already over many years it has been found that corrosion of reinforcement is not necessarily related closely to the rate at which chlorides diffuse into the concrete. For example, completely uncorroded reinforcement has been found even in the presence of very high chloride levels (Melchers & Li 2009a). For example, completely uncorroded reinforcement has been found even in the presence of very high chloride levels (Melchers & Li 2009b). This does not accord with the conventional wisdom.

The timing of corrosion initiation depends the rate at which the buffering capacity of the concrete matrix against pH drop (i.e. its alkalinity) deteriorates. Conventionally the buffering capacity of concrete has been considered in terms of the alkalinity provided by the cement in the process of setting the concrete. This has been equated with the concentration of alkalis present, that is with the concentration of hydroxide ions $[\text{OH}^-]$ and this in turn is related directly to pH. The commonly quoted criterion for corrosion initiation under chloride conditions, namely $[\text{Cl}^-]/[\text{OH}^-]$, stems from this approach (e.g. Gjorv 2009).

Alkalis always are introduced into the concrete by the cement reaction. They also may arise from the addition to the concrete of various admixtures (such as retarders, water reducers, pore blockers, etc.). Significant quantities of aggressive alkalis may be released from the aggregates themselves, particularly the volcanic aggregates, such as basalts and these alkalis can cause the break-up of the aggregates and hence the concrete. Estimates of time before there are visible signs that there is an alkali-aggregate problem range from 9 months to several years. Importantly, the loss of

effective concrete cover in such a short time should not be attributed to a failure of the concrete cover to provide a sufficient barrier to the diffusion of aggressive ions (such as chlorides) into the concrete and towards the reinforcement bars, or its ability to retain the alkalis that are protective against reinforcement corrosion. These are two quite different failure mechanisms. In statistical terms there are two different populations from which samples (i.e. failure cases) may be drawn.

A recent review of many cases of failures of RC structures reported in the literature showed that it is likely that where the concrete aggregates had the ability to provide a buffer of alkalis that did not cause damage to the aggregate themselves, the time to initiation of reinforcement corrosion appeared to be considerable greater than for concretes without such aggregates. Limestones and dolomites appeared to have this property. However, in some cases structures with these aggregates were found to have very short initiation times t_i . The influence of alkali aggregate reactivity was found also for the time to active corrosion t_{ac} (Melchers 2010).

The present paper is concerned with attempting to discern which data for t_i and t_{ac} should be attributed to alkali aggregate reactivity and which to conventional corrosion initiation and progression with sound concrete cover.

To do the analysis more than 30 data sets, ranging from just one structure to others comprising more than 300 complete structures were considered for (i) the chloride content immediately adjacent to the reinforcement, (ii) the time to corrosion initiation, such as indicated by minor rust staining and minor cracking and (iii) the time to active corrosion as judged by the onset of severe cracking, severe spalling and concrete cover delamination.

Many other aspects conventionally considered to be important in estimates of durability of reinforced concrete structures under marine or similar conditions were not considered owing to the lack of sufficient data and considered simply add to 'noise' in the conclusions. They were found not to be crucial in the outcomes. What was considered, however, was the type of aggregates used in the concretes.

Analysis showed that t_i and t_{ac} are only moderately influenced by chloride concentration. Thus, for the purposes of the statistical analysis the effect of chloride concentration was ignored so that the data could be grouped together, for each of t_i and for t_{ac} each considered as individual populations. Of interest is the probability of first occurrence of t_i and of t_{ac} . This is a matter for extreme value analysis.

Figure 1 shows a Weibull plot with data for both the normal concretes and the ‘alkali-buffered’ concretes. The data are not linear as would be expected if all data in each set were from the same population. Both data sets consist of 3 distinct groups, suggesting three different (sub-) populations. A generally similar plot arises for t_{ac} .

The trend lines for the lower values of t_i in Figures 1 may be interpreted as showing the influence of Alkali-Aggregate Reactivity (AAR) and Alkali-Silicate Reactivity (ASR).

This interpretation allows data that can be identified as influenced by AAR and ASR to be disregarded in analyses for reinforcement corrosion initiation, permitting a better estimate of the influence of chloride induced corrosion on t_i and also on t_{ac} , once corrosion has initiated.

As expected from eliminating early t_i and t_{ac} values, the trend curves show longer corrosion initiation times and longer times to active corrosion for both normal and alkali buffered concretes. In contrast the conventional EV approach would discard all data except those forming the trend for the lower values of t_i in Figure 1. However, this is not appropriate since there is ‘a priori’ knowledge that (i) the population for t_i is not homogeneous, (ii) there are three potential failure modes and the two of these, with low values of t_i , are not of primary interest. Considering only the lower values

of t_i would not be appropriate since these most likely represent failures resulting from AAR.

Only part of the trends are likely to be the result of chloride related reinforcement corrosion within a sound concrete structure. It follows that all data are relevant. Each trend in the data explains some part of the observed structural and material response—not just the data in the extreme region (i.e. the left tails for the minima). Generally similar comments apply to t_{ac} .

The use of cumulative distribution functions herein, including the extreme value distributions, is an artifice to discern the possibility of the data being non-homogeneous and, if possible, to assign meaning to the component distributions. No particular meaning should be attached to the probabilities associated with these plots. They are not necessarily related to the frequency of occurrence of AAR, ASR or chloride induced reinforcement corrosion in the general community of reinforced concrete structures.

The present analysis shows how to use probability theory to discriminate data corresponding to different failure modes for reinforcement corrosion in concrete. In particular it permitted the times to structural failure resulting directly from AAR and ASR and consequent reinforcement corrosion to be separated from the data for the failure mode of most interest, that is, the time to failure as governed by chloride and oxygen diffusion through concrete cover not damaged by alkali-aggregate reactivity.

REFERENCES

- Gjorv, O.E. 2009. *Durability design of concrete structures in severe environments*, London, Taylor & Francis.
- Melchers, R.E. 2010. Observations about the time to commencement of reinforcement corrosion for concrete structures in marine environments, Consec 2010, Concrete under severe conditions, Mexico, CRC Press, Boca Raton, 617–624.
- Melchers, R.E. & Li, C.Q. 2009a. Reinforcement corrosion in concrete exposed to the North Sea for over 60 years, *Corrosion* 65(8): 554–566.
- Melchers, R.E. & Li, C.Q. 2009b. Reinforcement corrosion initiation and activation times in concrete structures exposed to severe marine environments, *Cement and Concrete Research*, 39: 1068–1076.

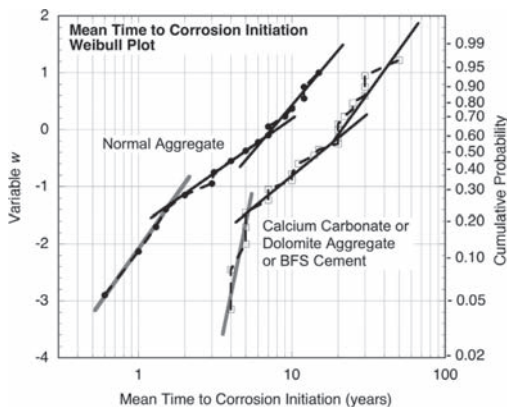


Figure 1. Weibull plot showing sharp change in trends in data for time to initiation.

Development of state-based Markovian transition probabilities for bridge condition estimation

T.M. Reale & A.J. O'Connor
 Trinity College Dublin, Ireland

1 INTRODUCTION

The derivation of transition probabilities has traditionally been derived using one of two primary methods—expert judgement or percentage prediction. The latter relies on observations made from historical data, but the former is purely subjective and varies from inspector to inspector. To this end, in this paper, two other methods of obtaining appropriate transition matrices based on the original data are outlined. The first uses the regression curve of the observed data in its performance function and the second uses the distribution of condition rating data in its objective function. Different optimisation solvers are utilised to obtain these matrices and in particular the use of Cross-Entropy as an optimisation method for use in infrastructure management and bridge management systems specifically is investigated.

Markovian transition probabilities have been used extensively in the field of infrastructure management to provide forecasts of facility condition and thus enable the relevant authorities to optimize maintenance and repair decisions over time.

Following a few basic assumptions, such as the structure is only allowed deteriorate at most one condition state per time period and ignoring the effects of maintenance and repair, a transition probability matrix for use in a Markovian process looks as depicted in Figure 1.

$$\begin{bmatrix} T_{00} & 1-T_{00} & 0 & 0 & 0 & 0 \\ 0 & T_{11} & 1-T_{11} & 0 & 0 & 0 \\ 0 & 0 & T_{22} & 1-T_{22} & 0 & 0 \\ 0 & 0 & 0 & T_{33} & 1-T_{33} & 0 \\ 0 & 0 & 0 & 0 & T_{44} & 1-T_{44} \\ 0 & 0 & 0 & 0 & 0 & T_{55} \end{bmatrix}$$

Figure 1. Example of transition matrix whereby the element is only allowed to deteriorate one state at a time and where maintenance and repair are not considered.

2 APPROACHES TO THE DERIVATION OF TRANSITION PROBABILITY MATRICES

Transition probability matrices are often populated by one of two methods—either that of expert judgement or percentage prediction. In this paper however, combinatorial optimisation is used to minimise various objective functions in order to derive the infrastructure transition probabilities.

3 DIFFERENT OPTIMISATION ALGORITHMS INVESTIGATED

By large, combinatorial optimisation is a complex and computationally intensive problem, generally requiring the exploration of large, multidimensional search spaces in order to obtain an answer. Many different methods exist to solve such problems but since the main purpose of this paper was to investigate whether or not Cross Entropy could be used as a viable alternative to traditional optimisation solvers in the context of estimating transition probability matrices for infrastructure deterioration, two Matlab solvers were chosen for comparative purposes. These were Fmincon and Global Search.

In order to test the various objective/performance functions and compare and contrast the efficiency of the different solvers, a normally distributed random database was generated. This database comprised of an assigned annual condition rating to 2000 bridges over a 25 year period.

4 DIFFERENT OBJECTIVE/ PERFORMANCE FUNCTIONS FOR COMPUTING TRANSITION MATRICES

To assess the various algorithms mentioned above and thereby investigate the applicability of cross-entropy as a suitable optimisation solver in, two different objective functions were utilised:

$$\text{Minimize: } \sum_{t=1}^N |S(t) - EX(t)| \quad (1)$$

subject to: $0 \leq p_{ij} \leq 1$ for $i = 1, 2, \dots, n$

$$\sum_{j=1}^n p_{ij} = 1$$

This is based on minimising the difference between a polynomial 4th order regression curve $S(t)$ and the expected value of condition state as predicted by a Markov process.

The second performance function to be examined then is based on a minimisation of the expected condition rating at time t as computed by a Markov process versus the actual probability distribution of condition rating as defined in the database. This is represented as follows:

$$\sum_{t=1}^{25} \sum_{n=0}^5 |P(t) - P'(t)| \quad (2)$$

where $P(t)$ = the probability distribution of condition rating as defined in the database and $P'(t)$ = The probability distribution of condition rating as computed by the Markov process.

5 RESULTS

Both objective functions were computed at year number 15 and year number 25 in order to assess whether or not either method became more appropriate as structures aged and underwent further deterioration.

Histograms of condition rating spread were developed at both years 15 and 25 respectively

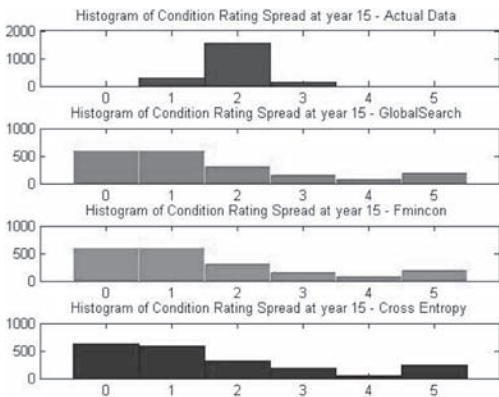


Figure 2. Condition rating spread at year 15 under objective function 1.

Table 1. Transition probabilities as determined by objective function 1.

	Transition probabilities					Obj. func.
FM	0.9254	0.899	0.820	0.701	0.515	3.5701
GS	0.9256	0.899	0.819	0.702	0.527	3.5698
CE	0.9282	0.898	0.810	0.692	0.478	3.5684

under both objective functions and using all three solvers.—See Figures 2 for an example.

However, as can be seen, while the three algorithms themselves all give relatively the same answer, this answer or expected condition rating spread is significantly different to the actual condition rating spread—irrespective of the objective function or algorithm in question.

Table 1 gives the transition probabilities obtained under the first objective function using the three different solvers. As shown above in Figures 2, it can be seen that the three solvers give approximately the same solutions and results but that again as shown and discussed above, the objective functions are not sufficiently minimised.

6 CONCLUSION

The purpose of this paper was to investigate if Cross Entropy could be used as a viable alternative to traditional optimisation solvers in the context of estimating suitable transition probabilities for infrastructure deterioration. Although as previously stated, the probabilities obtained are not as yet sufficiently exact, judging from the similarity in the shape of the histograms and in the transition probabilities obtained with the different optimisation solvers, regardless of the objective function under consideration, the algorithm appears to be at least as suitable as others in use at the present time.

*GS_327 — Statistical investigations
and probabilistic modeling (2)*

This page intentionally left blank

A model for the failure probability of components of electrical substations under seismic load

M. Raschke

Laboratory for Safety Analysis, ETH, Zurich, Switzerland

ABSTRACT: Power grids are very complex systems and disruptions of their elements can affect all human activities in a large region. Disruptions of this kind can be caused by earthquakes. The failure probability of the substations' components of a power grid has to be modelled for the estimation of the earthquake risk of the whole power grid. A model for the relation of local earthquake intensity to the failure probability of substation elements is presented in this paper. The relation between local earthquake intensity and failure probability is not functional but stochastic. The failure probability is also a random variable in this approach. Only the expectation of the failure probability is determined by a functional relation to the local earthquake intensity in the model. A special regression method is used for the estimation of model parameters. It includes a kind of conditional likelihood estimation. Empirical data are often censored because, in many cases, it is neglected that "no observation" is in fact an observation. The influence of this unconscious censoring on the parameter estimation is shown. Methods concerning the reduction of the influence of the censoring are presented. The results of the regression analysis are presented and compared with already published functions.

Following research results are described: That the CDF of the Weibull distribution is more appropriate for the modelling of functional failure of substation elements is justified by the physical basic, the mechanical failure of parts of the elements. This is a classical problem of minima what leads to the Weibull distribution. Furthermore the hazard rate of the log normal and log logistic model is not plausible. That's why the approach with the Weibull distribution should be applied for the failure functions.

The beta binomial distribution and the function $V(E)$ of P describe the randomness of P appropriate and flexible. But there exist more variants for $V(E)$ than considered here. The approach of Straub et al. (2008) is complicate but can be replaced by the equivalent approach with the beta binomial model (biased transformation, Raschke 2009).

It should be distinguished between a real correlation of the failure of substation elements with a determined failure probability and the apparent correlation, caused by a random failure probability. Beside this the influence of a measurement error of x to the randomness of P should be considered in the estimation when it is possible. This measurement error could be neglected in risk analysis wherein the local shaking intensity is determined and not estimated.

The possibilities of the statistical inference like the goodness-of-fit test and the model selection should be applied whenever possible in the estimation of failure functions. Former researches have ignored this field of inference. The lack of an appropriate test has to be stated.

The estimations for the circuit breaker CB9 and the transformer TR1 lead to different results (s. Fig. 1). The relation $V(E)$ of the beta-binomial model does not follow a clear tendency. Furthermore the randomness of P does not need to be relevant according to the estimation of circuit breaker CB9. The estimated exponent seems to be too small what could be caused by the uncontrolled censoring. The functions of model A are compared with other published functions (based on empirical data) of Oikawa et al. (2001), Shinozuka et al. (2004) and Straub et al. (2008, Tab. 4) in Fig. 2. The new function for the transformer is similar to the function of Straub et al. (2008) because the data base is similar. But the new function for the circuit breaker differs much from the function of Straub (2008) although the data base is similar. The failure function for the circuit breaker of Shinozuka et al. (2004) does not seem to be realistic compared with the other functions although it is based on data of the Northridge earthquake (1994, California) and the data base used here contains data of the earthquake too. The large differences between the functions indicate a poor quality of data. The new functions are not recommended for a risk analysis because they seem to be biased strongly. The uncontrolled censoring causes probably a large part of the bias. The randomness of P could have influenced the estimation also negatively. The quality of

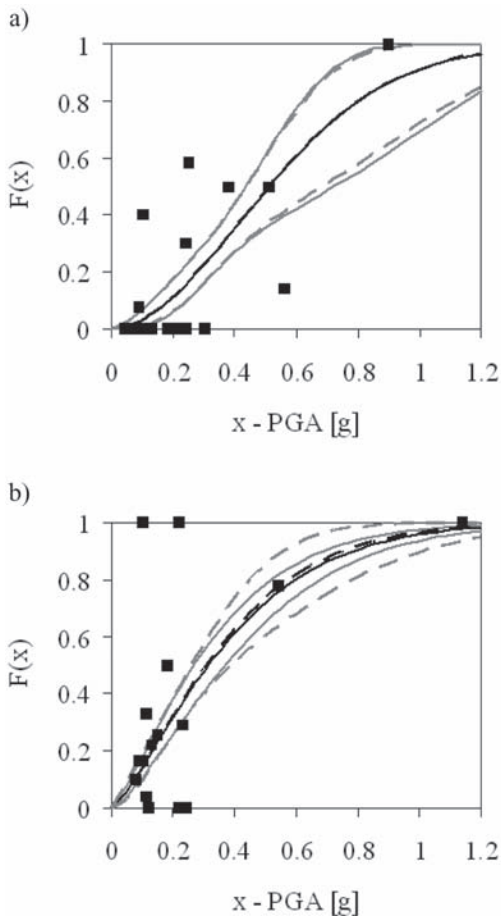


Figure 1. Estimation results: a) transformer TR1 (solid line—case D, broken line, case C), b) Circuit breaker CB9 (solid line—model A, broken line, model B), black lines— $F(x)$, gray lines—confidence intervals 5–95% of $F(x)$, black points—observations Tab. 1: Estimation results for the transformer TR1.

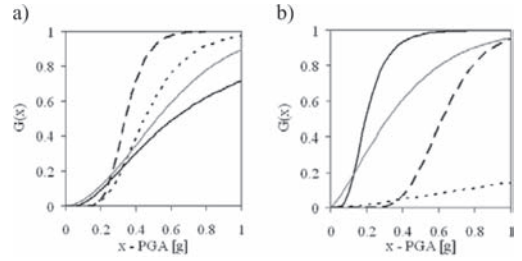


Figure 2. Comparison of failure functions: a) transformer, b) circuit breaker (black, solid—Straub et al., 2008, Tab. 4, black, broken—Oikawa et al., 2001, black, dotted—Shinozuka et al., 2004, gray—new estimation, model A).

an estimation for a random P is not so high as for a determined probability.

Last but not least it should be noted in all fields of engineering that “no observation” is often an important observation. And a good data collection is the basic for a good model.

Details of the research can be found in the paper.

A study of the stochastic properties of auto-correlation coefficients for microtremor data simultaneously observed at two sites

H. Morikawa

Tokyo Institute of Technology, Yokohama, Japan

K. Iiyama

Tokyo University of Science, Tokyo, Japan

M. Otori

Japan Agency for Marine-Earth Science and Technology, Yokohama, Japan

ABSTRACT: We discussed stochastic properties of the spatial-correlation (SPAC) coefficients for microtremor data which are observed simultaneously at two sites. Usually, the SPAC method can provide the phase velocities using the data observed simultaneously on circular array with more than four sites. The method, however, suggests analytically the possibility that we can estimate the phase velocities using only the data observed simultaneously at two sites. To clarify the limitation of this idea, some mathematical analyses are performed and stochastic properties of SPAC coefficients are derived. Furthermore, some real data of microtremors are applied to the above analytical results and the validity is discussed.

1 INTRODUCTION

The information about the ground structure is very important to estimate earthquake ground motions. The microtremor survey, is very useful for the purpose, because the microtremors can be observed anywhere and anytime. Generally speaking, to estimate the ground structure, we estimate phase velocities from the data of microtremors. Since the phase velocities depend on the ground structures, we can obtain a model of the ground structure, which is shear wave velocities of horizontally layered medium through an inversion technique.

There are some techniques to estimate the phase velocities from microtremors: for example, frequency wave number (F-K) method, and spacial autocorrelation (SPAC) method. To apply these methods, we have to observe microtremors simultaneously at more than four sites on a circular array. This means that many resources are required for the observation, such as personnel, instruments, any other costs.

To reduce this kind of difficulties relating to the observations, we will try to propose a simpler procedure to estimate the phase velocities based on the SPAC method (Aki 1957), that is, the proposed method requires simultaneous observation at only two sites.

2 METHOD

As a first step of our research, we discuss stochastic properties of the spatial auto-correlation (SPAC) coefficients for microtremor data which are observed simultaneously at two sites. The SPAC method suggests analytically the possibility that we can estimate the phase velocities using the data observed simultaneously at only two sites instead of at more than four sites. In the discussion, we assume that the microtremors are stationary processes and their propagation direction is stochastic variable with uniform distribution.

The SPAC coefficients are obtained from the follows:

$$\rho(\omega; r) = \frac{1}{2\pi} \int_{-\pi}^{\pi} \frac{\Re[S_{0r}(\omega, \theta)]}{\sqrt{S_{00}(\omega)S_{rr}(\omega, \theta)}} d\theta, \quad (1)$$

where $S_{00}(\omega)$ and $S_{rr}(\omega, \theta)$ are power spectrum density function at center of the array and a site with azimuth θ on a circle, respectively, and $S_{0r}(\omega, \theta)$ is cross spectrum density function between these two sites. $\Re[\cdot]$ denotes real part of complex value.

Equation 1 requires the azimuthal averaging, which is the integral with respect to θ . In a case where we carry out the simultaneous observation at only two sites, the azimuthal averaging cannot be calculated. Thus, we assume that the microtremors propagate from various directions instead of the azimuthal averaging. To represent this condition,

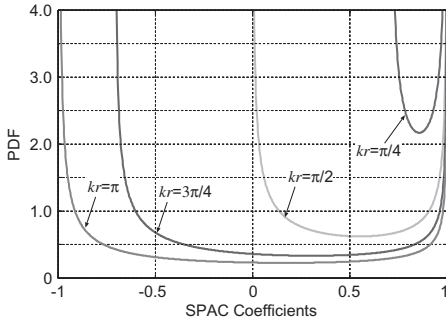


Figure 1. Examples of PDF for $\rho_{\mathfrak{R}}, f_{F_{\mathfrak{R}}}(\rho_{\mathfrak{R}})$.

we consider that the propagating direction φ is a stochastic parameters and it distributes uniformly in $[-\pi, \pi]$. Under this assumption, we can obtain same representation as Equation 1 from the correlation between the microtremor data at two sites.

Furthermore, some statistical properties are derived analytically: probability density function (PDF), expectation, and variances for SPAC coefficients. For example, the PDF of SPAC coefficients are obtained as shown in Figure 1. In this figure, $\rho_{\mathfrak{R}}$ is a SPAC coefficient, k wavenumber, and r distance between two sites.

3 APPLICATION TO REAL DATA

To discuss the availability of the analysis in the previous sections, real data of microtremors are used. Microtremor observation was carried out at a site, where the velocity structure is available.

We estimate the phase velocities using the proposed technique as shown in Figure 2. In this figure, the solid line shows the dispersion curve obtained analytically from the velocity structure at the site. The estimated values agree with analytical line. This suggests that the proposed technique can be applied to the real data, though we do not have enough information about the condition of applicability.

To provide the information, statistics of SPAC co-efficients are discussed. For example, the histogram of SPAC coefficients are calculated. As shown in Figure 3, the statistics agree with the analytical results under some cases. On the other hand, we find some cases whose statistics does not agree with the analytical results but the phase velocities are reasonable. This means that the statistics is not the necessary and sufficient condition for our assumptions.

Furthermore, physical approaches are discussed for the assumption with respect to the microtremors. Physical properties of Rayleigh wave are

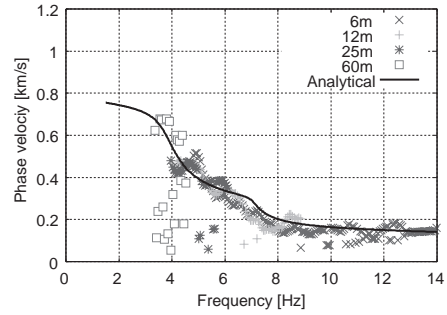


Figure 2. Phase velocities for Rayleigh wave estimated from the microtremors and analytical dispersion curve obtained from the available velocity structure at the site.

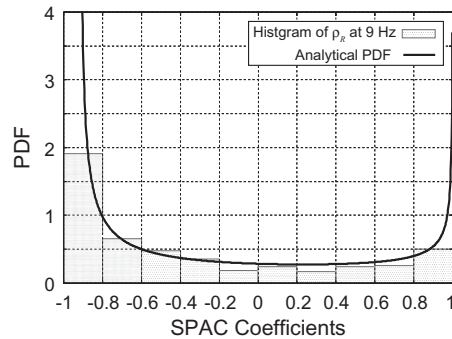


Figure 3. Histogram of $\rho_{\mathfrak{R}}$ and its PDF (9 Hz; $E[\rho_{\mathfrak{R}}] = -0.15240 \cdot kr = 2.722712$).

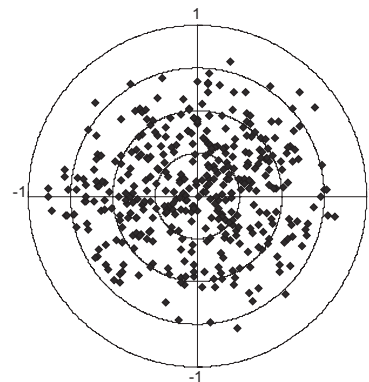


Figure 4. The propagating direction of microtremors. The plots in outer side of the chart denote more Rayleigh-wave-like waves.

introduced and the propagating directions are roughly estimated from the microtremor data. Figure 4 shows the propagating directions and the radii of the plots correspond to the similarity to Rayleigh wave. We can consider that plots at

outer side of the chart are Rayleigh waves. From this figure, it is observed that Rayleigh waves are included and their propagating direction scattered in whole the range.

4 CONCLUSIONS

We derived the stochastic properties of the SPAC co-efficients analytically under some assumptions: (1) the vertical component of microtremors consists of Rayleigh wave mainly, (2) they propagate evenly to various directions, (3) the propagating directions are stable during a short portion, and (4) they are plane wave. The analysis suggests that we can estimate phase velocities using the microtremor data observed simultaneously at only two sites.

From the analysis of the real data, we obtained appropriate phase velocities and discussed the conditions to obtain the appropriate results on the basis of statistical and analytical approaches. We confirmed a part of the adequacy of our assumption and analysis, though some problems are still remaining. At least, however, we can conclude that the phase velocities can be estimated reasonably if Rayleigh wave propagates without directionality.

REFERENCES

- Aki, K. (1957). Space and time spectra of stationary stochastic waves, with special reference to microtremors. *The Bulletin of Earthquake Research Institute* 35, 415-456.

A Bayesian approach to analysing structural uncertainties in flood inundation models

L. Manning

School of Civil Engineering and Geosciences, Newcastle University, UK

J.W. Hall

Environmental Change Institute, University of Oxford, UK

ABSTRACT: Analysis of uncertainties in hydraulic models of flooding processes is a perennial area of investigation. Here our concern is with (i) combining prior knowledge about model parameter values with information from calibration exercises to generate well justified posterior distributions on model parameters, whilst (ii) at the same time also using observations to understand the structural uncertainties that separate model predictions from hydraulic processes in reality. Bayesian methods provide a statistically coherent approach to dealing with both of these issues, but entail a number of technical issues, not least the need to do a large number of model runs in calibration exercises based upon Markov Chain Monte Carlo methods. We circumvent this latter difficulty by constructing a dynamical emulator of the flood inundation model in the form of a transfer function model with a non-linear state-dependent transformation of the inputs. A similar approach is adopted for the observed data, so that the structural uncertainty is reflected in the discrepancy between the non-linear state-dependent functions. The approach is shown to enhance the accuracy of models with known deficiencies at the same time as providing well justified uncertainty estimates.

1 INTRODUCTION

It is important to understand the uncertainty associated with any prediction of flood risk. However, methods for establishing this uncertainty depend on the end use for the flood prediction system. Real-time flood forecasting starts from a known river state, and can be updated in real time by assimilation of water level observations as they become available; the problem is one of extending the usable forecast to give an adequate lead time for protection measures to be taken. By contrast, flood risk analysis does not have to be performed in real time, but must take into account a much

broader range of uncertainties, not only those that affect the predicted flood probability, but also the probability of failure of flood defences and the consequences of flooding.

This study is motivated by the need to provide uncertainty estimates in the prediction of flood depths for use in flood risk analysis. In common with other approaches, a distinction is made between different sources of error, that is, between input, model structural error or inadequacy, and output measurement error. The objective is to be able to formulate the uncertainty estimates in such a way that they can be used within a risk analysis, where the risk is formed from an integral, over all forcing scenarios and the entire range of modeling errors, of the product of the probability of flooding and the damage caused.

2 STEADY STATE FORMULATION

The emphasis in this study is placed on model inadequacy. The calibration formulation used is derived from that of Kennedy and O'Hagan (2001). Distinction is made between the contributions of model inadequacy and downstream measurement error to observed data by considering the covariance associated with the values of the model inadequacy, describing it as a Gaussian process; that is, the values at the locations (in time or space) where data are measured are considered to jointly vary as a stochastic process with a multivariate Normal distribution. Further, in a hierarchical description, the mean of this Gaussian Process is itself a regression on some suitable basis. Formally, the observed quantity y , given as a function of location x , is described as

$$y(x) = M(x, \theta) + \delta(x) + \varepsilon \quad (1)$$

where $M(x, \theta)$ is the model output at location x , subject to parameter values θ , ε represents observation error, assumed to be Gaussian, with

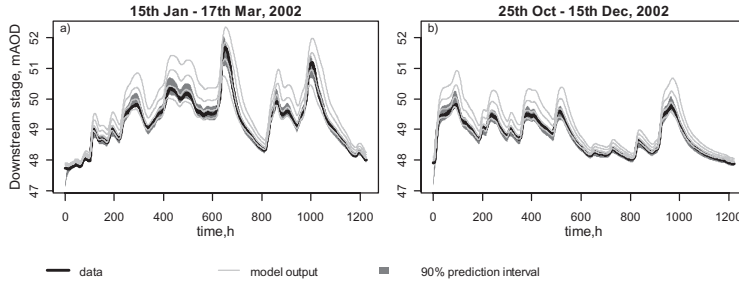


Figure 1. Calibrated prediction for stage at Welsh Bridge at Shrewsbury compared with model predictions and observed data: a) time period used in calibration, b) validation time period.

variance σ_8^2 , and $\delta(x)$ is the Gaussian process representing model inadequacy, described as $N(m(x), V(x, x'))$, where $m(x)$ is the mean discrepancy.

3 EXTENSION TO DYNAMIC MODEL CALIBRATION

We use a transfer function to represent the dynamic response of our flood model. The transfer function consists of an autoregressive moving average (ARMA) transfer function, applied to the output of a nonlinear transformation of the upstream stage measurement. Formally, assuming an ARMA(1,1) transfer function, this can be described as:

$$\tilde{x}_t = b(x_t) \cdot x_t \quad (2)$$

$$y_t = ay_{t-1} + \tilde{x}_{t-l} + \varepsilon_t \quad (3)$$

where x_t and y_t are upstream and downstream stage at time t , l is the lag between the upstream and downstream response, ε_t is observation noise, α is the autoregressive coefficient of the transfer function and z^{-1} is the backwards shift operator; $z^{-1}x_t = x_{t-1}$.

4 CASE STUDY

The methodology has been demonstrated with respect to a 1-D model of a 22 km reach of the river Severn, UK, immediately upstream of Shrewsbury. The model has been run using measured hourly stage and flow data at Montford for 15th Jan–7th Mar 2002, with uniform channel Manning's n (θ in the above) of 0.02, 0.03, 0.04 and 0.05. For each Hec-Ras run, the input and model output stage time series were used in an optimization routine to estimate the transfer function emulator describe above.

Prior probability distributions for the variables were chosen as follows. The prior for Manning's n was chosen as a Normal distribution,

encompassing the range for which solutions were achievable with the hydraulic model. Priors for the various modeling error parameters were chosen as lognormal distributions, taking them to be as diffuse as possible.

Calibrated prediction yields distributions for the nonlinear function and autoregressive coefficient for the observed data, and for Manning's n . These distributions can then be used to provide calibrated predictions for downstream stage in the time domain for both calibration and validation input series (Figure 1). The calibrated output shows good agreement with the downstream data in both calibration and validation periods, and the prediction interval is reasonably small, while taking into account uncertainty in the parameter and the modeling process.

5 CONCLUSIONS

A workable method has been demonstrated for the estimation of uncertainty in modeled flood predictions, taking into account model structural uncertainty. The methodology is shown to be suitable, after calibration, to estimate downstream stage with associated uncertainty for upstream hydrographs that are different to those used in calibration, and thus, to be useable for flood risk management planning, where responses may be required from many simulated input hydrographs.

While the methodology demonstrated here is focused on model structural error, errors due to upstream data measurement and uncertain lateral inflows should be incorporated into the analysis, in order to fully incorporate all sources of uncertainty. This is the subject of continued work.

REFERENCE

Kennedy, M.C. & O'Hagan, A. 2001. Bayesian calibration of computer models *J. Roy. Stat. Soc.* B63(3): 425–464.

Seismic loss modeling of two building portfolios using generalized Pareto model and copula

K. Goda

University of Bristol, Bristol, UK

J. Ren

University of Western Ontario, London, Canada

ABSTRACT: A large earthquake affects multiple structures simultaneously and causes catastrophic loss to urban cities. Vulnerability to extreme seismic events is a serious concern for many stakeholders. To assess potential impact of future destructive earthquakes accurately and to implement risk mitigation measures effectively, it is essential to have a tool for quantitative seismic loss estimation and decision-making. For instance, the HAZUS-Earthquake, developed by FEMA & NIBS (2003), is capable of assessing gross regional seismic loss to a number of buildings and infrastructure due to a scenario earthquake, and serves as a critical risk management tool for both pre-disaster planning and post-disaster relief activities. Nevertheless, there is an urgent research need to further develop more rigorous tools/methods that can be applied to complex risk management problems, such as insurance/reinsurance portfolio analysis subject to earthquake risks (Kleindorfer et al., 2005, Bazzurro & Park 2007).

A key aspect in modeling seismic loss of a portfolio of buildings and infrastructure is the adequate consideration of uncertainty and dependence of physical seismic effects to structures. Goda & Hong (2008) demonstrated the importance of accounting for spatiotemporally correlated seismic excitations in seismic loss estimation. Recently, Bazzurro & Park (2007) investigated the effects of “portfolio relocation and aggregation” on the accuracy of seismic loss estimation for multiple properties, and found that such artificial manipulation, which is routinely done in insurance portfolio analysis, could bias the assessment. Aiming at avoiding such inaccuracy in portfolio aggregation, Goda & Ren (2010) investigated a copula-based approach to combine seismic losses from two building portfolios probabilistically, by taking seismic loss dependence of the portfolios into account, and showed that seismic losses from geographically close portfolios can be nonlinearly correlated in the upper tail. A failure to account for this correlation might result in biased seismic loss evaluation.

In this study, an alternative statistical approach is proposed to model seismic losses of two building portfolios by focusing on the upper tail characteristics. The approach is based on the generalized Pareto (GP) model to approximate seismic loss data that exceed some large threshold value for marginal distribution modeling, and employs the copula technique to combine two marginal probability distributions. The GP model for describing the upper tail of data has well-established statistical foundation (Coles 2001). Moreover, the copula technique effectively separates dependence modeling from marginal distribution modeling (McNeil et al., 2005). The above method is suitable, if our focus is primarily on large seismic losses due to rare events, and is especially useful for assessing earthquake risk exposure for insurers and reinsurers. To demonstrate the method, two groups of existing wood-frame houses located in southwestern British Columbia are considered. An earthquake-engineering-based seismic loss model by Goda et al. (2011) is employed to generate seismic loss samples for two groups of wood-frame houses; these seismic loss data are then used to develop a statistical model based on the GP model and copula function. The developed statistical models are applied to calculate several risk measures for a reinsurance portfolio, such as value-at-risk and tail value-at-risk. The comparison of the estimated risk measures based on the earthquake-engineering-based model with those based on the fitted statistical models indicate that the proposed statistical approach can achieve good accuracy in approximating large seismic loss data.

REFERENCES

- Bazzurro, P. & Park, J. 2007. The effects of portfolio manipulation on earthquake portfolio loss estimates. In *Proc ICASP10*, Tokyo, Japan.
- Coles, S. 2001. *An introduction to the statistical modeling of extreme values*. London: Springer.

- Federal Emergency Management Agency (FEMA), & National Institute of Building Sciences (NIBS). 2003. *HAZUS-Earthquake - Technical Manual*. Washington DC: FEMA & NIBS.
- Goda, K., Atkinson, G.M., & Hong, H.P. 2011. Seismic loss estimation of wood-frame houses in south-western British Columbia. *Struct. Safety* 33 (10.1016/j.strusafe.2010.11.001).
- Goda, K. & Hong, H.P. 2008. Estimation of seismic loss for spatially distributed buildings. *Earthquake Spectra* 24: 889–910.
- Goda, K. & Ren, J. 2010. Assessment of seismic loss dependence using copula. *Risk Analysis* 30: 1076–1091.
- Kleindorfer, P., Grossi, P. & Kunreuther, H. 2005. The impact of mitigation on homeowners and insurers: an analysis of model cities. In *Catastrophe modeling: a new approach to managing risk*: 167–188. New York: Springer.
- McNeil, A.J., Frey, R. & Embrechts, P. 2005. *Quantitative risk management: concepts, techniques, and tools*. Princeton, NJ: Princeton University Press.

ACER function plots as a diagnostic tool for extreme value prediction

A. Naess

Centre for Ships and Ocean Structures & Department of Mathematical Sciences
 Norwegian University of Science and Technology, Trondheim, Norway

O. Gaidai

MARINTEK A/S Trondheim, Norway

1 INTRODUCTION

Recently a new method for estimation and prediction of extreme values based on available time series of recorded or simulated data was proposed (Naess & Gaidai 2009). This method is based on the concept of average conditional exceedance rate (ACER), which enables the estimation of the empirical extreme value distribution inherent in the available time series assumed to represent a realization of a stochastic process. In particular, the emphasis is on the use of the ACER functions to reveal the effect of dependence in the data time series on the final predictions of extreme response. The ACER method, when correctly implemented, will provide an estimate of the exact extreme value distribution. This is achieved by constructing a cascade of conditioning approximations, which are referred to as the ACER functions. When this cascade of approximations have converged, we are left with an estimate of the exact distribution.

A disadvantage of going down the cascade of approximations is that the higher the order of the approximation, the less data are available for the estimation phase, potentially increasing the statistical uncertainty of the corresponding estimates. In this paper it will be shown how the ACER function plot can be used to decide on the order of the approximation that is needed to get accurate extreme response predictions. As an example, among several others, it will be demonstrated that it is possible to assume that the time series of hourly maxima of wind speed consist of independent data for the purpose of prediction of 100 year wind speed levels despite the fact that such data are strongly dependent. It turns out that for these data the plot of the ACER functions reveals that the effect of dependence diminishes toward the tail sufficiently rapidly to allow us to assume independent data for the purpose of extreme value prediction. This makes it possible to increase the amount of data available for analysis and thereby the accuracy of the predictions. However, as another example

we shall present the case of tether tensions for a tension leg platform used for oil production offshore. It will be demonstrated that for these data the dependence structure is such that an assumption of independent data would lead to inaccurate extreme value predictions.

2 THE ACER METHOD

Consider a stochastic process $Z(t)$, which has been observed over a time interval, $(0, T)$ say. Assume that values X_1, \dots, X_N , which have been derived from the observed process, are allocated to the discrete times t_1, \dots, t_N in $(0, T)$. This could be simply the observed values of $Z(t)$ at each t_j , $j = 1, \dots, N$, or it could be average values or peak values over smaller time intervals centered at the t_j 's. Our goal in this paper is to accurately determine the distribution function of the extreme value $M_N = \max\{X_j; j = 1, \dots, N\}$. Specifically, we want to estimate $P(\eta) = \text{Prob}(M_N \leq \eta)$ accurately for large values of η .

The following cascade of approximations to the exact extreme value distribution can be derived (Naess and Gaidai 2009),

$$P(\eta) \approx P_k(\eta) = \exp\left(-\sum_{j=k}^N \alpha_{kj}(\eta)\right), \quad (1)$$

for $N \gg 1$, and where

$$\alpha_{kj}(\eta) = \text{Prob}\{X_j > \eta \mid X_{j-1} \leq \eta, \dots, X_{j-k+1} \leq \eta\} \quad (2)$$

denotes the exceedance probability conditional on $k-1$ previous non-exceedances, $k = 1, 2, \dots$

For the empirical estimation of the requisite quantities in the $P_k(\eta)$, it is expedient to introduce the concept of average conditional exceedance rates (ACER) as follows,

$$\varepsilon_k(\eta) = \frac{1}{N-k+1} \sum_{j=k}^N \alpha_{kj}(\eta), \quad k = 1, 2, \dots \quad (3)$$

With the ACER functions available, we now have a unique opportunity to reveal in a simple manner the importance of dependence in the time series on the extreme value statistics. As will be illustrated in the section on numerical results, this makes the ACER function plot a very useful tool in practical extreme value prediction.

3 PREDICTION

For most prediction problems it is necessary to go beyond the reach of the data available. Such data may cover only 10 to 20 years of operation, while the desired return period level may correspond to 100 years. This necessitates some form of extrapolation of the empirical extreme value distribution if the prediction is to be based on the data. In several papers (Naess and Gaidai 2009, Naess et al., 2010, Naess and Haug 2010) we have argued that this can be done by assuming the following parametric class of functions for the ACER, provided the asymptotic extreme value distribution is of Gumbel type:

$$\varepsilon_k(\eta) \approx q_k(\eta) \exp\{-a_k(\eta - b_k)^{c_k}\}, \quad \eta \geq \eta_1 \quad (4)$$

where a_k , b_k , c_k , and q_k are suitable constants, that in general will be dependent on k . Note that the values $c_k = 1$ and $q_k = 1$ correspond to the assumed asymptotic form. The values of the parameters q , a , b , c is obtained by an optimization procedure (Naess et al., 2010, Naess and Haug 2010).

4 NUMERICAL RESULTS

We shall illustrate the use of the ACER function plot as a diagnostic tool for extreme value prediction by studying two particular cases. The first case is the prediction of extreme wind speeds based on 7 years of recorded hourly maxima, which are strongly dependent data. The second example deals with the extreme tether tension for a tension leg platform (TLP) in heavy seas. The time series of the peak values of the tether tension will also constitute a time series of strongly dependent data. However, the ACER function plot will reveal that the importance of the statistical dependence for the prediction of extreme values will be quite different for the two cases. For the wind speed data, it is seen that the first ACER function can be used for prediction since the ACER functions seem to coalesce in the far tail, that is, the strong statistical dependence for the low wind speed levels is vanishing for the very large levels. For the tether tension data this is not so. Even at the very high tension

levels the statistical dependence is sufficiently strong to preclude confluence of the first ACER function with the other ACER functions. Hence, prediction of extreme tether tension should be based on higher order ACER functions.

Case 1—Wind speed data

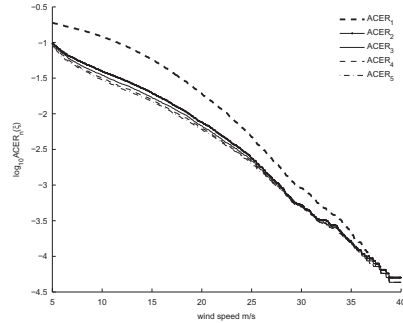


Figure 1. Ørland wind speed statistics, 7 years hourly data. Comparison between ACER estimates for different degrees of conditioning on the decimal log scale.

Case 2—TLP tether tension data

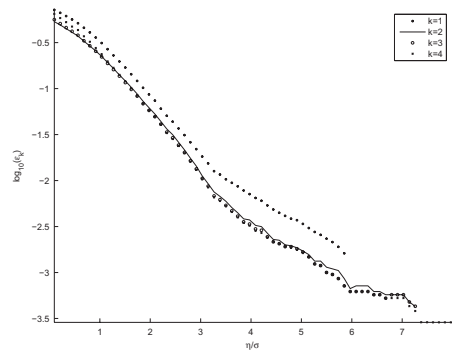


Figure 2. Log plot of empirical ACER $\varepsilon_k(\eta)$, $k = 1, 2, 3, 4$, Sea state I.

REFERENCES

Naess, A. & Gaidai, O. (2009). Estimation of extreme values from sampled time series. *Structural Safety* 31, 325–334.

Naess, A., Gaidai, O. & Batsevych, O. (2010). Prediction of extreme response statistics of narrow-band random vibrations. *Journal of Engineering Mechanics* 136(3), 290–298.

Naess, A. & Haug, E. (2010). Extreme value statistics of wind speed data by the POT and ACER methods. *Journal of Offshore Mechanics and Arctic Engineering, ASME* 132, 041604-1-7.

This page intentionally left blank

*MS_337 — Statistical investigations
and probabilistic modeling (3)*

This page intentionally left blank

Statistical analysis of NDT results for analysing the efficiency of repair techniques of wharves: The MAREO project

F. Benmeddour, G. Villain, X. Dérobert & O. Abraham

Laboratoire Central des Ponts et Chaussées, LCPC, centre de Nantes, Route de Bouaye, Bouguenais, France

F. Schoefs, M. Perrin, S. Bonnet & M. Choinska

Institute in Civil and Mechanical Engineering (GeM), UMR 6183, Nantes Atlantic University, CNRS, Nantes cedex, France

1 INTRODUCTION

The MAREO project was developed with two objectives. The first one is to compare the efficiency of repairing techniques on concrete structures in coastal regions within the global context of reassessment of repaired structures. The project therefore relies on global methodologies for risk analysis and assessment. The second one is to identify and quantify uncertainties and hazard sources in assessing the performance functions. The project research work was performed at several levels. Firstly, identify the performance indicators of structures. Secondly, investigate exhaustively the evaluation chains of these indicators and compare them in terms of risk analysis. Thirdly, outline experimental devices and protocols, in laboratory or on site with controlled conditions of measurement.

The paper focuses on the developments around the use of non-destructive testing (NDT) techniques and destructive testing (DT). Beams placed in natural exposure and slabs specimens in accelerated conditions in laboratory are considered. For all the beams, the contaminated concrete was removed using high-velocity water jets. The selected repair techniques were wet shotcrete, dry shotcrete, formed concrete and manual repair. This paper focuses on the ability of the NDT techniques to evaluate the changes of properties related to the chloride ingress in concrete both on site and on specimens in laboratory. The interest of each technique and its sensitivity to several physical factors are highlighted. The need of the combination of different NDT techniques is illustrated.

2 EXPERIMENTAL PROCEDURE

2.1 *Materials and specimens description*

In this work four repaired beams of $200 \times 34 \text{ cm}^2$ and 75 cm of height are considered. These beams

arise from the demolition in 2006 of a wharf made of reinforced concrete at the Lorient port in the west of France. Ten slabs ($45 \times 45 \times 12 \text{ cm}^3$) were fabricated during the repair of beams with the same materials and the same techniques.

2.2 *Destructive testing techniques*

Results of the destructive tests (DT) can be used as inputs or outputs of actual models of the prediction of structures life-time in reinforced concretes. The DT measurement techniques used in this work are proven, standardised or during normalisation. These techniques concern the mechanical characteristics and durability indicators and the determination of the chloride profiles (Perrin et al., 2010).

2.3 *Non-destructive testing techniques*

The NDT techniques are not commonly used for the diagnostics of structure performances. However, NDT methods are well correlated with durability indicators and provide valuable information for diagnosis on porosity, mechanical properties and water content of reinforced concrete structures. Furthermore, it is particularly interesting to combine non-destructive methods (Villain et al., 2009a). The used NDT techniques are: the impact-echo method (Gibson, 2005 and Villain et al., 2009b), the surface waves method (Chekroun et al., 2009 and Abraham et al., 2009), The multi-offset radar method and the capacitive method (Dérobert et al., 2008).

3 RESULTS AND DISCUSSIONS

The sensitivity analysis of each method is called S and can be expressed as:

$$S = \frac{\Delta M}{6 STD}, \quad (1)$$

Table 1. Weighted means, standard deviations, variance coefficients and the sensitivity of the NDT methods.

Methods		Means	STD	CoV (%)	STi				
					I	II	III	IV	
Impact-Echo	B	2534,67	99,01	3,97	0,07	0,14	0,21	0,07	
	S	16639,70	340,65	2,09	0,20	0,10	0,17	0,43	
Surface waves	B	2385,63	72,27	3,12	0,03	0,00	0,25	0,17	
	S	2325,84	74,02	3,24	0,10	0,11	0,03	0,30	
Multi-Offset Radar	B	-	-	-	-	-	0,67	-	
	S	8,68	0,52	6,05	1,18	0,75	0,91	0,69	
Capacitive	S	B	7,42	0,79	10,41	0,65	0,02	0,58	0,07
		S	8,37	1,35	16,88	0,40	0,39	0,24	0,53
	M	B	8,45	0,62	6,73	0,09	0,17	0,24	0,15
		S	10,80	1,23	11,78	0,78	0,02	0,03	0,50
	G	B	10,36	0,77	7,03	0,22	0,17	0,01	0,08
		S	11,34	0,50	4,79	1,65	0,91	0,57	0,28

where: ΔM is the difference between two measured results of the same technique at two times (STi). *STD* designates the standard deviation. Assuming that this uncertainty follows a normal distribution in a range containing 97.74%, the probable scatter due to the uncertainty of the technique is 6 times the *STD* wide. Results of the computation of STi of the NDT are shown on Table 1. In this table, the weighted means, standard deviations and coefficients of variance were also computed and presented.

We can consider that only the STi values higher than or equal to 0.5 can be considered for the analysis. At this stage of the project, it is shown that only 13 from 45 cases (28.88%) and 2 from 5 methods correspond to this condition (see boldface values in Table 1). The majority of these values (10) were those of slabs. Note that the CoV varies in a wide range [2.09; 16.88] depending on the technique. The CoV is very low (less than 10%) for the impact-echo, surface waves and multi-offset radar methods. It is also very low for the case of beams (ME “middle electrodes” and GE “great electrodes”) and slabs (GE) of the capacitive method. However, the CoV is very high for SE (small electrodes) and slabs of the ME.

4 CONCLUSION

In this paper, several repair techniques applied to the tidal zone were carried out and analysed. The study was performed by destructive testing techniques (DT) and non-destructive ones (NDT). The DT methods were used to evaluate the mechanical characteristics: the compressive strength R_c , the static Young’s modulus E_{stat} and the coefficient of Poisson ν , and the durability indicators: the global porosity accessible to water ϕ and the dry density of concretes ρ_{dry} . The NDT can evaluate: the first symmetrical Lamb mode frequency (f_{s1}), the surface

phase velocities ($V_{\phi(\lambda = 3, cm)}$) and the permittivity (ϵ_r). In addition, an inversion algorithm was applied to the impact-echo method to obtain the dynamic Young’s moduli E_{dyn} and the Poisson coefficients ν . Experiments were carried out to repaired beams, placed in natural exposure, and fabricated slabs, placed in accelerated conditions. Four different concretes of repairation were considered: wet shotcrete (I), dry shotcrete (II), formed concrete (III) and manual repair (IV). It was shown that the majority of NDT techniques have the ability to be sensitive to the change of properties related to the chloride ingress. Besides, the comparison of mechanical characteristics and durability indicators between concretes having the same constituent (I and II) reveals that the dry shotcrete has the best mechanical and durability performances. The obtained results on slabs are better than those obtained for beams due to the natural conditions nature of the latter.

These aspects are further developed in the following section, where predictions from the probabilistic corrosion model are used to carry out a time-dependent reliability analysis to evaluate the structural safety of corroded harbor structures.

ACKNOWLEDGEMENTS

This work is funded by Région Pays de la Loire. Authors are grateful to B. Bigourdan (IFREMER, Brest, France) for controlling ageing of beams in the tidal basin and to F. Jacquemot (CERIB, Epernon, France) for the accelerated tests on slabs.

REFERENCES

- Abraham, O., Villain, G., Lu, L., Cottineau, L-M. & Durand, O. 2009. A laser interferometer robot for the study of surface wave sensitivity to various concrete mixes. *NDTCE’09*, 30th june-3rd july 2009, pp. 597–608. Nantes, France.
- AFPC-AFREM, 1997. Méthodes recommandées pour la mesure des grandeurs associées à la durabilité. Recommended methods for measurement of quantities associated to sustainability. *Journées techniques sur la durabilité des bétons*, 11–12 december 1997. Toulouse, France.
- Chekroun, M., Le Marrec, L., Abraham, O., Durand, O. & Villain, G. 2009. Analysis of coherent surface wave dispersion and attenuation for non destructive testing of concrete. *Ultrasonics*, 49 (8), 2009, pp. 743–751.
- Dérobot, X., Iaquina, J., Klysz, G. & Balayssac, J.P. 2008. Use of capacitive and GPR techniques for non-destructive evaluation of cover concrete. *NDT&E Int.*, Vol. 41, 2008, pp. 44–52.
- Gibson, A. & Popovics, J. 2005. “Lamb wave basis for impact-Echo method analysis”, *J. of Eng. Mech.*, April 2005, pp. 438–443.

- Perrin, M., Choinska, M., Bonnet, S., Boukhouna, A. & Gaillet, L. 2010. Repair materials durability of structures in marine environment. 2nd conference on Marine Environment Damage to Coastal and Historical Structures. *MEDACHS 2010*. 28–30 April 2010, La Rochelle, France.
- Villain, G., Dérobert, X., Abraham, O., Coffec, O., Durand, O., Laguerre, L. & Baltazart, V. 2009a. Use of ultrasonic and electromagnetic NDT to evaluate durability monitoring parameters of concrete. *NDTCE'09*, 30th june-3rd july 2009, pp. 343–348, Nantes, France.
- Villain, G., Abraham, O., Le Marrec, L. & Rakotomanana, L. 2009b. Determination of the bulk elastic moduli of various concrete by resonance frequency analysis of slabs submitted to impact echo. *NDTCE'09*, 30th june-3rd july 2009, pp. 881–886, Nantes, France.

The $\alpha\delta$ method for reliability modeling and improvement of NDT-tools for Risk Based Inspection (RBI): Application to corroded structures

F. Schoefs

LUNAM Université, Université de Nantes-Ecole Centrale Nantes, GeM,
Institute for Research in Civil and Mechanical Engineering, CNRS UMR 6183, Nantes, France

J. Boéro

Oxand S.A, Avon, France

1 INTRODUCTION

Replacement of engineering structures results in high economic and environmental costs, thus increasing the interest in maintaining these structures with efficient management plans. Therefore, the challenge for the owners consists in guaranteeing the operation and safety of ageing structures, while ensuring reasonable costs and availability conditions. Harbor structures meet all these stakes.

Reassessment of existing structures generates a need for updated material properties. In a lot of cases, on-site inspections are necessary and in some cases visual inspections are not sufficient. Non Destructive Testing (NDT) tools are required for the inspection of coastal and marine structures where marine growth acts as a mask or where immersion gives poor conditions for inspection (visibility, ...). In these fields, the cost of inspection can be prohibitive and an accurate description of the on-site performance of NDT tools must be provided. Inspection of existing structures by a NDT tool is not perfect and it has become a common practice to model their reliability in terms of probability of detection (PoD), probability of false alarms (PFA) and Receiver Operating Characteristic (ROC) curves (Rouhan & Schoefs 2003, Straub & Faber 2003, Pakrashi et al., 2008). These quantities are generally the main inputs needed by owners of structures who are looking to achieve Inspection, Maintenance and Repair plans (IMR) through Risk Based Inspections methods (RBI). The assessment of PoD and PFA is even deduced from inter-calibration of NDT tools or from the modeling of the noise and the signal. Both due to their great economic interest and the cost (direct and indirect) of inspection, authors have selected steel harbor structures for the application (not detailed in this paper).

First, on the basis of several previous works, this paper reviews the theoretical aspects coming from detection theory and probabilistic modeling of inspections results. The objective is to provide inputs in the computation of mathematical expectation of RBI cost models. It is shown how these models highlight the role of the probability of defect presence. Expert judgment or the knowledge of ageing laws allows quantifying this probability (Rouhan & Schoefs, 2003). The paper introduces the polar coordinates of NDT-BPP for characterizing ROC curves, which allows us to perform parametric studies and improve NDT techniques with various assumptions on costs. The application concerns corroded steel sheet-piles in harbours.

2 PROBABILISTIC MODELING OF INSPECTION BASED ON DETECTION THEORY

The most common concept which characterizes inspection tool performance is the probability of detection. Let a_d be the minimal defect size, under which it is assumed that no detection is done. Parameter a_d is called detection threshold. Thus, the Probability of Detection (PoD) is defined as Eq. 1:

$$PoD = P(\hat{d} \geq a_d) \quad (1)$$

where \hat{d} is the measured defect size.

Let's assume that noise and the signal amplitude are independent random variables, then PoD and PFA have the following expressions:

$$PoD = \int_{a_d}^{+\infty} f_{signal}(\hat{d}) \partial \hat{d} \quad (2)$$

$$PFA = \int_{a_d}^{+\infty} f_{noise}(\eta) d\eta \quad (3)$$

where f_{signal} and f_{noise} are respectively the probability density functions of ‘signal + noise’ (or measured defect) and ‘noise’.

Thus, PoD is a function of the detection threshold, the defect size and the noise, while PFA depends on the detection threshold and noise only. Noise is due to the decision-chain “physical measurement-decision on defect measurement transfer of information”, the harsh environment of inspection and the complexity of testing procedure (link diver-inspector for underwater inspections for instance).

The ROC (Receiver Operating Characteristic) curve links the Probability of Detection and the Probability of False Alarm. For a given detection threshold, the couple (PFA, PoD) allows defining NDT performance. This couple can be considered as coordinates of a point in \mathbf{R}^2 with axes representing PFA and PoD. Let us consider that a_d takes values in the range $[-\infty; +\infty]$, these points belong to a curve called Receiver Operating Characteristic (ROC) which is a parametric curve with parameter a_d and defined by equations (2) and (3).

3 THE α - δ METHOD

A simple geometric characterization of ROC curves is the distance δ between the curve and the Best Performance Point (BPP) of coordinates (PFA = 0, PoD = 1). By definition, the greater the distance is, the worse the performance. The corresponding point on the ROC curve is called the performance point of the NDT tool (NDT-BPP). However as the configuration of ROC curves for the same distance are varied due to the ‘noise’ and ‘signal + noise’ pdf, we extend this measure of performance by using the polar coordinates of the NDT-BPP. The $\alpha\delta$ -method lies on this characterization. The NDT-BPP polar coordinates are then defined by:

- the radius δ_{NDT} is the performance index (NDT-PI) (distance between the best performance point and the ROC curve) (Schoefs & Clément 2004, Schoefs et al., 2007);
- the angle α_{NDT} between axis (PFA = 0) and the line (BPP, NDT-BPP).

The first objective of the $\alpha\delta$ -method was to perform parametric studies lying on these two parameters to analyze the effect of the shape of ROC curves on the decision process relating to

inspection, maintenance and repair. To achieve this goal, the influence of the performance of ROC curves, represented by δ_{NDT} and α_{NDT} , was appreciated through the costs and (Schoefs et al., 2010). It was shown that these parameters were sufficient to describe the effect of the ROC curve on the costs.

4 α - δ METHOD

Figure 1 presents mappings of extra cost of no detection according to the position of NDT-BPP in polar (δ_{NDT} , α_{NDT}) coordinates, for $\gamma = 0.9$ and following cost assumptions: Failure 1, Repair 0.1, Inspection 0.01. For this large probability of defect presence ($\gamma = 0.9$), extra costs of no detection for increase when α_{NDT} decreases and δ_{NDT} increases. Note that when considering extra costs of detection, they are maximum in the zone defined by values of δ_{NDT} higher than 0.3 and α_{NDT} higher than 50° . Outside this area, extra cost of detection increases mainly with δ_{NDT} .

Maximum extra costs of detection are located in zone with high values of δ_{NDT} and α_{NDT} . It is also interesting to note that for values of δ_{NDT} lower than 0.1, the influence of α_{NDT} is negligible. In addition, extra costs of no detection for $\gamma = 0.1$ are maximum for values of δ_{NDT} superior than 0.1 and for values of α_{NDT} minor than 30° . When α_{NDT} is higher than 30° , extra costs of no detection increase mainly with δ_{NDT} . Let us consider NDT-BPP A in the following ($\alpha = 30^\circ$, $\delta = 0.5$) for $\gamma = 0.9$.

Then if the cost of inspection is negligible in comparison to cost of repair several strategies of improvement (reduction of risk) can be compared in terms of “displacement” of the original position A of the NDT-BPP on the mapping (see positions of A', A'', and A''' on Figure 1).

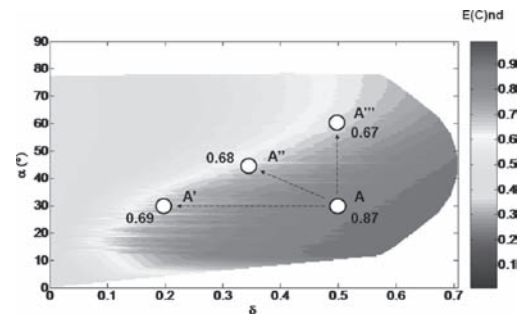


Figure 1. Mapping of extra cost of no detection $\overline{E(C)}_{nd}$ in polar plane for $\gamma = 0.9$.

REFERENCES

- Pakrashi, V., Schoefs, F., Memet, J.B. & O'Connor, A. (2010). "ROC dependent event isolation method for image processing based assessment of corroded harbour structures", NSIE, vol. 6(3), pp. 365–378.
- Rouhan, A. & Schoefs, F. (2003). "Probabilistic modeling of inspections results for offshore structures", Structural safety, vol. 25, pp. 379–399, 20 pages, Elsevier Ltd.
- Schoefs, F., Clément, A., Boéro, J. & Capra, B. (2010). "The $\alpha\delta$ method for modeling expert Judgment and combination of NDT tools in RBI context: application to Marine Structures, NSIE, accepted January 26th 2010, in Press.
- Straub, D. & Faber, M.H. (2003). "Modelling dependency in inspection performance", Proc. Application of Statistics and Probability in Civil Engineering, ICASP 2003 – San Francisco, Der Kiureghian, Madanat and Pestana eds., Millpress, Rotterdam, ISBN 90 5966 004 8. pp. 1123–1130.

Fluctuation Analysis of stochastic physical systems based on Probability Density Evolution Method

W.L. Sun, J. Li & J.B. Chen

State Key Laboratory of Disaster Reduction in Civil Engineering & School of Civil Engineering, Tongji University, Shanghai, P.R. China

1 INTRODUCTION

The parameters of structure, such as the material properties, geometrical parameters and the boundary conditions, are usually not exactly available. As a result, in some occasions variance of the parameters may lead to considerable random fluctuation in the responses (Li, 1996). Therefore, dynamic response analysis considering randomness of the parameters is of paramount importance. The dynamical characteristics of a single-degree-of-freedom (SDOF) linear and non-linear system are investigated and fluctuation of the displacement response caused by randomness of the natural circular frequency is studied by the probability density evolution method in this paper.

2 NONLINEAR DYNAMICAL SYSTEM

The equation of motion of a non-linear SDOF system is given by

$$\ddot{x} + 2\xi\omega\dot{x} + \alpha\omega^2x + (1-\alpha)\omega^2z = f(t) \quad (1)$$

The hysteretic force z is related to x through the following first-order nonlinear differential equation

$$\dot{z} = h(z) \frac{A\dot{x} - v(\beta|\dot{x}||z|^{n-1}z + \gamma\dot{x}|z|^n)}{\eta} \quad (2)$$

where v, η varying with the energy dissipation, are the strength and stiffness degradation parameter, respectively. The function relationships between v, η and ε are chosen as

$$v = 1 + \delta_v\varepsilon, \quad \eta = 1 + \delta_\eta\varepsilon \quad (3)$$

where

$$\varepsilon(t) = \int_0^t z\dot{x} dt \quad (4)$$

$h(z)$ is the pinching function

$$h(z) = 1.0 - \zeta_1 e^{-[z \operatorname{sgn}(\dot{x}) - qz_u]^2 / \zeta_2^2} \quad (5)$$

in which

$$\zeta_1(\varepsilon) = \zeta_s(1 - e^{-p\varepsilon}) \quad (6)$$

$$\zeta_2(\varepsilon) = (\psi + \delta_\psi\varepsilon)(\lambda + \zeta_1(\varepsilon)) \quad (7)$$

If $\zeta_s = 0$, the model does not exhibit pinching.

3 PROBABILITY DENSITY EVOLUTION METHOD

The response of a MDOF system is governed by

$$M\ddot{\mathbf{X}} + C\dot{\mathbf{X}} + f(\boldsymbol{\Theta}, \mathbf{X}) = \mathbf{F}(\boldsymbol{\Theta}, t) \quad (8)$$

where $\boldsymbol{\Theta} = (\Theta_1, \Theta_2, \dots, \Theta_s)$ is an s -dimensional random vector involved with known joint probability density function $p_\theta(\boldsymbol{\theta})$.

In a general sense, if there are a set of physical quantities $\mathbf{Z} = (Z_1, Z_2, \dots, Z_m)$ associated with the system in Equation (8), then \mathbf{Z} can usually be determined by its connection with the state vector, for instance by

$$\dot{\mathbf{Z}} = \mathbf{G}(\mathbf{h}_X(\boldsymbol{\Theta}, t), \mathbf{H}_X(\boldsymbol{\Theta}, t)) \quad (9)$$

The generalized probability density evolution equations is given by

$$\frac{\partial p_{\mathbf{Z}\boldsymbol{\Theta}}(\mathbf{z}, \boldsymbol{\theta}, t)}{\partial t} + \sum_{j=1}^m \dot{Z}_j(\boldsymbol{\theta}, t) \frac{\partial p_{\mathbf{Z}\boldsymbol{\Theta}}(\mathbf{z}, \boldsymbol{\theta}, t)}{\partial z_j} = 0 \quad (10)$$

The instantaneous PDF of the response and its evolution, where the randomness in such structural parameters as physical and/or geometric parameters as well as the randomness in excitation is involved, is available by the probability density method exactly and efficiently.

4 FLUCTUATION ANALYSIS OF STOCHASTIC STRUCTURES

4.1 SDOF dynamical system analysis

From the response spectrum of a linear dynamical system excited by El Centro accelerogram with the damping from 0.01 to 0.07, it is obviously that as the damping increases, the value of response spectrum decreases. Under some conditions, actual structure based on present design theory may be unsafe under dynamic load.

4.2 Fluctuation index based on variance

The response of the dynamical system described by Equation (8) is a stochastic process. The index of fluctuation is defined by the mean $E[x(\Theta, t)]$ and the variance $D[x(\Theta, t)]$ as:

$$F_2 = \frac{\| \sqrt{D[x(\Theta, t)]} \|_2}{\| E[x(\Theta, t)] \|_2} \quad (11)$$

$$F_{\max} = \frac{\| \sqrt{D[x(\Theta, t)]} \|_{\max}}{\| E[x(\Theta, t)] \|_{\max}} \quad (12)$$

where $\| \cdot \|_2$ means 2-norm and $\| \cdot \|_{\infty}$ means ∞ -norm.

4.3 Fluctuation analysis of stochastic structures

The fluctuation of displacement response of the SDOF system excited by El Centro accelerogram with the random parameter ω is investigated. ω is a random variable distributed normally with the coefficient of variation δ_ω . The parameters of BWN model are shown in Table 1 and the damping ratio ξ is 0.05.

4.3.1 Fluctuation with ω

The fluctuations at different coefficients of variation ($\delta_\omega = 0.1, 0.2$ and 0.3) are investigated when the mean of nature frequency ω are set to 3.0, 6.0, 9.0 and 12.0 rad/s. Figure 1 shows the value of Fluctuation index F_{\max} increases as δ_ω increases.

Displacement fluctuation of the non-linear dynamical system increases as the coefficient of variation increases and small variation of the natural circular frequency of the structure induces large fluctuation of the structural responses.

Table 1. Parameters of BWN model.

α	A	β	γ	n	δ_v	δ_n
0.01	1	28	17	1	0.005	0.025
q	p	ψ	δ_ψ	λ	ζ_s	
0	25	0.2	0.006	0.34	0.05	

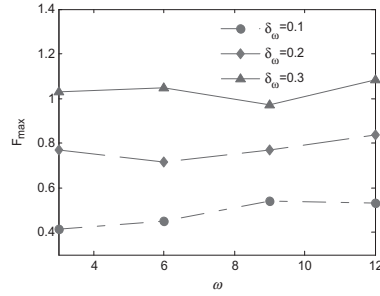


Figure 1. Fluctuation index with respect to the natural circular frequency.

4.3.2 Fluctuation comparison between linear versus nonlinear system

The mean of nature frequency ω is 6.0 rad/s. Both the fluctuation index F_2 and F_{\max} increase with increasing δ_ω , almost linearly. Comparing the fluctuation index between linear versus nonlinear system with the coefficient of variation δ_ω increasing, the fluctuation index of linear system are larger than that of nonlinear system. The fluctuations of both linear and nonlinear system is extreme large compared with the coefficient of variation δ_ω .

5 CONCLUSION

With the increase of coefficient of variation, the displacement fluctuation of nonlinear dynamical systems will increase and the value of fluctuation index is much larger than that of coefficient of variation. Due to the characteristics of dynamical systems and the fluctuation, an actual structure based on present design theory may be unsafe under dynamic load. More investigations are needed for fluctuation of general MDOF system. The concept of entropy evolution may also be an important index to be further studied.

ACKNOWLEDGEMENT

The support of Natural Science Foundation of China for Young Scholars (Grant No. 10872148), National Hi-Tech Development Plan (863 Plan) (Grant No. 2008AA05Z413), and Systematic Research Project of State Key Laboratory of Disaster Reduction in Civil Engineering are greatly appreciated.

REFERENCE

Li, J. 1996. Stochastic structural systems: analysis and modeling (in Chinese). Beijing: Science Press.

The use of quasi-symmetric point method in probability density evolution method

J. Xu, J.B. Chen & J. Li

State Key Laboratory of Disaster Reduction in Civil Engineering & School of Civil Engineering,
 Tongji University, Shanghai, P.R. China

1 INTRODUCTION

In the past years, a family of probability density evolution method (PDEM) has been proved to be effective for stochastic response analysis of linear/nonlinear structures. The PDEM has achieved very good results in linear/nonlinear dynamic response analysis and dynamic reliability assessment, and it is being extended to the field of structural stochastic optimal control.

In the PDEM, the selection of representative points in random-variate space is of paramount importance for probability density evolution analysis. Though some strategies have been developed, the approach applicable to very high-dimensional problems is still to be studied. In the present paper, the adaption of quasi-symmetric point method (Q-SPM) is studied.

2 THE PROBABILITY DENSITY EVOLUTION METHOD FOR GENERAL STOCHASTIC SYSTEMS

Generally, the equation of motion of n -DOF structure can be rewritten as a stochastic state equation in $2n$ -dimension. Without loss of generality, let the stochastic state equation be

$$\dot{\mathbf{X}} = A(\mathbf{X}, \Theta, t) \quad (1)$$

where Θ is the random vector contained in structural parameters and external excitations. The probability density function $p_{\Theta}(\theta)$ of the random vector is known.

The generalized density evolution equation (GDDE) (Li & Chen, 2009) could be derived from the principle of preservation of probability from random event description.

$$\frac{\partial p_{Z\Theta}(\mathbf{z}, \theta, t)}{\partial t} + \sum_{j=1}^m \dot{Z}_j(\theta, t) \frac{\partial p_{Z\Theta}(\mathbf{z}, \theta, t)}{\partial z_j} = 0 \quad (2)$$

where Z_j denotes physical quantities of interest.

3 NUMERICAL ALGORITHM FOR PROBABILITY DENSITY EVOLUTION METHOD

The numerical algorithms for probability evolution method could be explained as: The representative points in random-variate space with assigned probability are determined firstly. Then the physical equation Eq. (1) are numerically solved to provide the value of the velocity required in Eq. (2). After that, the probability density function of interest could be captured by finite difference method such as LW scheme or TVD scheme.

4 QUASI-SYMMETZRIC POINT METHOD

There is some similarity between the selecting representative points for PDEM and the high-dimensional numerical integration. Therefore, investigation to high-dimensional numerical integration may be a significant reference to point selection for PDEM.

Several numerical strategies have been developed for the normally weighted high-dimensional integration. Victoir (2004) constructed two class cubature formulae by invariant theory and orthogonal arrays with 5th polynomial degree for some special regions, which can keep balance between positive weights and computational efficiency.

First solution

When the dimension $d\psi$ is in the form of $d\psi = 3k-2$, the integration points and the weights are given as follows:

$$\mathbf{x}_0 = (0, \dots, 0), \mathbf{x}_1 = (l\sqrt{3}, \dots, l\sqrt{3}, 0, \dots, 0) \quad (3)$$

where l is the permutation of ± 1 , k is the number of $l\sqrt{3}$ in \mathbf{x}_1 , part of the points in \mathbf{x}_1 are selected for contribution to the integration. The sum of the weights read

$$a_0 = \frac{2}{d+2}, a_1 = \frac{d}{d+2} \quad (4)$$

The second solution

The integral points read

$$\mathbf{x}_0 = (lr, \dots, 0), \mathbf{x}_1 = (ls, \dots, ls) \quad (5)$$

where

$$r^2 = \frac{d+2}{2}, s^2 = \frac{d+2}{d-2} \quad (6)$$

l is also the permutation of ± 1 , \mathbf{x}_0 denotes the symmetric set with $2d$ points and \mathbf{x}_1 refers to the total or part of points in the other symmetric points. The sum of the weights read

$$a_0 = \frac{8d}{(d+2)^2} l, a_1 = \frac{(d-2)^2}{(d+2)^2} \quad (7)$$

The integral points are adopted to be the representative points in high-dimensional random-variate space, and the assigned probability could be constructed according to the characteristic of cubature formulae.

$$P_k = a_k f(\mathbf{x}_k), k = 1, 2, \dots, N \quad (8)$$

let $f(\mathbf{X}_k) = 1$, the integral value over the normally distributed random-variate space equals to 1, which means the sum of the probability is 1. Then the assigned probability reads

$$P_k = a_k, k = 1, 2, \dots, N \quad (9)$$

Because the assigned probability must be positive, the counterpart in high-dimensional integration is that weights should be all positive. Eq. (9) means that the positive weights can be taken as the assigned probability directly. For more detailed discussion, refer to Xu et al. (2011).

5 NUMERICAL EXAMPLE

Seismic Response analysis of a 2-span 9-story shear frame structure is carried out. The lumped masses from top to bottom are 3.442, 3.278, 3.056, 2.756, 2.739, 2.739, 2.739, 2.739 and 2.692 ($\times 10^3$ kg), respectively. The lateral inter-story stiffness are 0.89, 0.96, 1.85, 1.92, 1.60, 1.60, 1.62, 1.63 and 1.47 ($\times 10^8$ N/m) in turn. Rayleigh damping is adopted such that $\mathbf{C} = a\mathbf{M} + b\mathbf{K}$, where \mathbf{C} , \mathbf{M} and \mathbf{K} are the damping, mass and stiffness matrices, respectively, and $a = 0.2643 \text{ s}^{-1}$, $b = 0.0071 \text{ s}$. The El-Centro acceleration records in the W-E direction are adopted as the ground motion. In the case nonlinearity involved in the restoring forces,

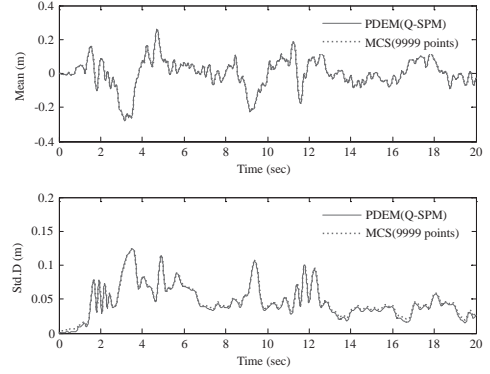


Figure 1. The mean and variance of response.

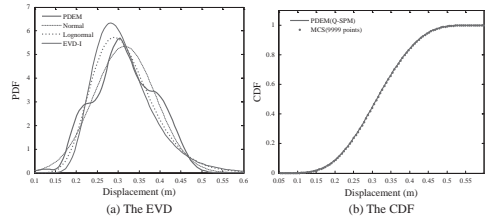


Figure 2. The EVD and CDF of extreme values ($T = 20 \text{ s}$).

the Bouc-Wen model (Wen, 1976) is adopted. The parameters in the hysteretic model are: $\alpha = 0.04$, $A = 1$, $n = 1$, $q = 0.25$, $p = 1000$, $d_w = 5$, $\lambda = 0.5$, $\psi = 0.05$, $\beta = 100$, $\gamma = 20$, $d_v = 2000$, $d_\eta = 2000$ and $\zeta = 0.99$, respectively.

The results evaluated through the probability density evolution method employing the Q-SPM are shown in Figures 1 and 2 where 552 representative points are selected via Q-SPM. Perfect accordance between the PDEM via Q-SPM and the MCS is seen, demonstrating fair accuracy of the proposed strategy. As far as the efficiency of the proposed strategy is concerned, the expected purpose is achieved: the computational effort of the stochastic dynamical problem involving 20 random parameters is just about 1/20 of the MCS.

6 CONCLUDING REMARKS

The proposed strategy is indeed efficient and accurate not only in response analysis but also in dynamic reliability analysis of general MDOF nonlinear structures. The proposed strategy—quasi-symmetric point method is an effective method for PDEM in high-dimensional problems.

Supports of the National Natural Science Foundation of China (Grant Nos. 90715083 and 10872148), National Hi-Tech Development Program (863 Plan) (Grant No. 2008AA05Z413), and the State Key Laboratory of Disaster Reduction in Civil Engineering (Grant Nos. SLDRCE08-A-01 and SLDRCE10-B-02) are greatly appreciated.

Victoir, N. 2004. Asymmetric cubature formulae with few points in high dimension for symmetric measures, *SIAM J. Numer.*, 42(1): 209–227.

Wen, Y.K. 1976. Method for random vibration of hysteretic systems. *J Eng Mech.* 1976, 102(2): 249–263.

Xu, J., Chen, J.B. & Li, J. 2011. Probability density evolution analysis of nonlinear structures via cubature formulae. *Computational Mechanics*, submitted.

REFERENCES

Li, J. & Chen, J.B. 2009. *Stochastic Dynamics of Structures*. John Wiley & Sons.

This page intentionally left blank

*MS_331 — Stochastic models and simulation
of earthquake ground motions*

This page intentionally left blank

Seismic risk sensitivity analysis focusing on stochastic ground motion modeling

A.A. Taflanidis & C. Vetter

University of Notre Dame, Notre Dame, IN, USA

1 INTRODUCTION

Evaluation of seismic hazard in structural engineering requires (i) adoption of appropriate models for structural systems, for their performance quantification, and for the natural hazard itself, and (ii) characterization and propagation of the uncertainty in these models. Undoubtedly the most important component of this process is the description of the earthquake hazard since significant variability is expected in future excitations. Moreover for a complete characterization of this hazard a model of the entire ground motion history is needed. This can be established using stochastic ground motion models (Boore 2003; Rezaeian and Der Kiureghian 2008), which are based on modulating a stochastic sequence Z through functions that address spectral and temporal characteristics of the excitation and whose parameters can be correlated to earthquake and site characteristics by appropriate predictive relationships. Description of the uncertainty for the earthquake characteristics and the predictive relationships leads then to a complete stochastic description of potential future ground-motion time-histories and ultimately to quantification of seismic risk. To formalize this idea, let $p(Z)$ denote the probability model for the stochastic sequence Z , θ the augmented vector of all uncertain model parameters, $p(\theta)$ its respective probabilistic description, and $h(\theta, Z)$ the performance measure for the structural system which represents the utility-loss from a decision-theoretic point of view. Seismic risk is ultimately expressed by the *stochastic integral*

$$H = \int_{\Theta} \int h(\theta, Z) p(\theta) p(Z) d\theta dZ \quad (1)$$

This paper discusses a probabilistic sensitivity analysis for this risk with particular emphasis on stochastic ground motion modeling. This analysis aims to identify the uncertain model parameters that have higher importance to the overall seismic risk.

2 SENSITIVITY ANALYSIS

The sensitivity analysis approach is based on the novel ideas discussed initially in (Taflanidis 2009). Foundation of this methodology is the definition of an auxiliary probability density function that is proportional to the integrand of the risk integral

$$\pi(\theta, Z) = \frac{h(\theta, Z) p(\theta) p(Z)}{H} \propto h(\theta, Z) p(\theta) p(Z) \quad (2)$$

where \propto denotes proportionality. Comparison between $\pi(\theta, Z)$ and the prior probability model $p(\theta) p(Z)$ expresses the sensitivity of the performance measure to the various model parameters; bigger discrepancies between these distribution indicate greater importance in affecting the system performance, since they ultimately correspond to higher values for $h(\theta, Z)$. This idea can be implemented to a specific group of parameters (or even to a single parameter), denoted y herein, by looking at the marginal distribution $\pi(y)$. Comparison between this distribution $\pi(y)$ and the prior distribution $p(y)$ expresses the probabilistic sensitivity with respect to y . Uncertainty in all other model parameters and stochastic excitation is explicitly considered by appropriate integration of the joint probability distribution $\pi(\theta, Z)$ to calculate the marginal probability distribution $\pi(y)$. Different grouping of the parameters, for defining y , will provide information for each group separately. In this process the stochastic sequence Z should be always considered as a separate group since it represents a fundamentally different type of uncertainty in the hazard description.

A quantitative metric to characterize the sensitivity based on the definition (2) is the relative information entropy, which is a measure of the difference between probability distributions $\pi(y)$ and $p(y)$

$$D(\pi(y) \| p(y)) = \int \pi(y) \log(\pi(y) / p(y)) dy \quad (3)$$

Smaller, i.e. close to zero, values for $D(\pi(y)||p(y))$ indicate minor impact of the group of parameters y in influencing seismic risk. The relative importance of each parameter, or sets of them, may be then directly investigated by comparison of the relative information entropy value *for each of them*.

An analytical expression, though, is not readily available for the marginal distribution $\pi(y)$. An alternative stochastic-sampling approach is discussed next, based on generation of samples from the joint distribution $\pi(\theta, Z)$. Such samples may be obtained by any appropriate stochastic sampling algorithm. Projection of this sample set from $\pi(\theta, Z)$ to the y space, provides then samples for the marginal distribution $\pi(y)$. Projection of the same set of samples to different subspaces (different definitions for the group y) provides information for the marginal distributions for each of them separately. Thus this approach allows for efficient exploration of the sensitivity for various groups y using the same set of samples. For scalar quantities, $y = \theta$, the relative entropy (3) may be then efficiently calculated by establishing an analytically approximation for $\pi(\theta)$, based on the available samples, through Kernel density estimation. A Gaussian Kernel density estimator may be used, for example, for this purpose.

Extension of this approach for calculation of the relative information entropy to vector variables is inefficient due to numerical problems associated with the Kernal density estimation and alternatives are currently under investigation. For the stochastic sequence Z the relative entropy is calculated in this study by direct evaluation of (3) through stochastic simulation, which simplifies in this case to

$$D(\pi(Z)||p(Z)) \approx \frac{1}{n_{sz}} \sum_{j=1}^{n_{sz}} \frac{\hat{h}(Z_j)}{\hat{H}} \log \left(\frac{\hat{h}(Z_j)}{\hat{H}} \right) \quad (4)$$

where the following two quantities were introduced

$$\begin{aligned} \hat{h}(Z_j) &= 1/n_{s\theta} \sum_{i=1}^{n_{s\theta}} h(\theta_i, Z_j) \\ \hat{H} &= 1/(n_{s\theta} n_{sz}) \sum_{i=1}^{n_{s\theta}} \sum_{j=1}^{n_{sz}} h(\theta_i, Z_j) \end{aligned} \quad (5)$$

and $Z_j \sim p(Z)$, $\theta_i \sim p(\theta)$. Note that the samples used for evaluation of (4) can be used as candidate samples for the stochastic sampling algorithm used to generate samples from $\pi(\theta, Z)$. Since the sample sets are identical, no additional evaluations of the augmented model response are needed for estimation (4) compared to the evaluations already performed for the stochastic sampling process.

This methodology ultimately leads to an efficient approach for identifying the importance of each of the model parameters and of the stochastic sequence Z in affecting seismic risk. Furthermore direct comparison of samples from the distributions $\pi(\theta_i)$ and $p(\theta_i)$ can provide additional insight about what specific values for each parameter contribute more to the risk.

3 ILLUSTRATIVE EXAMPLE

The framework is illustrated in a simple example involving the response of a single degree of freedom (SDOF) system with damping 3% and variable period T_s , and a source-based stochastic ground motion model. Five different risk quantifications are considered, three of them refer to the ground motion history itself, (i) average Peak Ground Acceleration (PGA), (ii) average Peak Ground Velocity (PGV), and (iii) probability that PGA will exceed a threshold β_a (RA), and the last two to the response of the SDOF, are the (iv) average maximum displacement (x_m) and (v) the probability that the maximum displacement will exceed a threshold β (R). Thresholds β_a and β are selected so that the corresponding probability of failure is 1% for each case. Sample results are shown in Figure 1 below.

From all different cases investigated, the seismic hazard characteristics, i.e., the magnitude and epicentral distance, are identified as the most important parameters influencing seismic risk. Dependence of the sensitivity analysis results on the chosen probability models for characterizing the ground motion uncertainties and on the response selection for quantifying risk is also illustrated. The natural period, T_s , of the SDOF also has an important impact on the sensitivity analysis results. Overall the results presented in this study provide useful insight in understanding the dependence of seismic risk on the ground motion modeling.

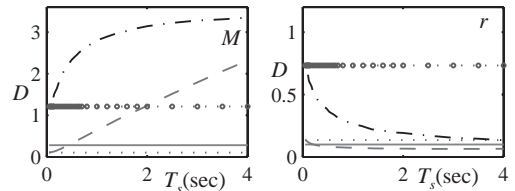


Figure 1. Sample results of the study. Different curves correspond to PGA(···), PGV(-), x_m (-·-·-), R(-·-·-), RA (°). Here M corresponds to the moment magnitude and r to epicentral distance of seismic events.

REFERENCES

- Boore, D.M. 2003. Simulation of ground motion using the stochastic method. *Pure and Applied Geophysics* 160: 635–676.
- Rezaeian, S. & Der Kiureghian, A. 2008. A stochastic ground motion model with separable temporal and spectral nonstationarities. *Earthquake Engineering & Structural Dynamics* 37: 1565–1584.
- Taflanidis, A.A. 2009. Stochastic subset optimization with response surface methodologies for stochastic design. In, *1st International Conference on Soft Computing Technology in Civil, Structural and Environmental Engineering, Madeira, Portugal, 1–4 September*.

Simulation of seismic ground motion time histories from data using a non Gaussian stochastic model

I. Zentner

Laboratory for the Mechanics of Aging industrial Structures, LaMSID UMR EDF-CNRS, France

F. Poirion

Department of Structural Dynamics and Aeroelasticity, ONERA, France

P. Cacciola

School of Environment and Technology, University of Brighton, UK

This paper addresses the modelling and the simulation of seismic ground motion time histories. When time-domain “best-estimate” seismic analyzes have to be performed, for example in the context of margin assessment or when evaluating fragility curves, then accurate modeling of seismic load is crucial in order to determine realistic structural responses. In this context, seismic ground motion has to be modelled by a non stationary stochastic process. It has to be stressed that seismic ground motion exhibits non stationarity as well in frequency content and as in amplitude (standard deviation is time-dependant). A convenient mathematical framework for this is the description by evolutionary, non separable power spectral densities (PSD), see for example [9] [10], [11]. However, the commonly used methods based on Gaussian processes [10], [9] are not always capable of reproducing variability observed for natural earthquakes [5].

We propose a new method for simulating seismic ground motion based on Karhunen-Loeve expansion. The idea behind this approach is to use recorded ground motion data coming from the constantly growing international strong motion databases in order to feed an appropriate probabilistic model. The generated ground motion time histories then exhibit properties equivalent to natural accelerograms. The scope of the method proposed in this paper is the enrichment of an existing database. The number of ground motion time-histories available for a given scenario and site-condition is limited and generally not sufficient for carrying out more advanced probabilistic structural response analysis. The proposed method enables the analyst to upgrade the size of a given database by adding artificial accelerograms having same properties as the natural ones. In order to evaluate the accuracy of the proposed method, we

compare simulated ground motion time histories to natural ones contained in a given database. We construct both Gaussian and non Gaussian time histories in order to demonstrate the superiority of the non Gaussian model. Ground motion parameters considered here are PGA, CAV, Arias intensity and strong motion duration. We furthermore analyse response spectra of natural and artificial accelerograms. It is shown that the natural variability of ground motion parameters is much better matched by the proposed non Gaussian model than by standard Gaussian simulation. Moreover, the actual fractiles of ground response spectra (evaluated here from an existing data base) are well reproduced. In order to keep computation times handy, time-domain responses and fragility curves were computed only for a linear structure. In future applications, we will evaluate the performance of the proposed method for nonlinear response computations.

REFERENCES

- [1] F. Poirion & C. Soize, Numerical methods and mathematical aspects for simulation of homogeneous and non homogeneous Gaussian fields. *In: P. Krée and W. Wedig, Editors, Probabilistic Methods in Applied Physics, Lecture Notes in Physics 451* Springer, Berlin, 17–53, 1995.
- [2] P. Krée & C. Soize, *Mathematics of random phenomena*. Reidel, Dordrecht, 1986.
- [3] L. Guikhman & A. Skorokhod, *The theory of Stochastic Processes*. Springer Verlag, Berlin, 1979.
- [4] C. Soize, *Méthodes Mathématiques de l'Analyse du Signal*. Masson, 1993.
- [5] E. Viallet & N. Humbert, Considerations on the use of natural and artificial time histories for seismic transient non-linear analyses of structures and variability assessment. *Proceedings of SMiRT 19, Toronto, Canada*, 2007.

- [6] G. Pousse G., L.F. Bonilla, F. Cotton & L. Margerin, Nonstationary Stochastic Simulation of Strong Ground Motion Time Histories Including Natural Variability: Application to the K-Net Japanese Database, *Bulletin of the Seismological Society of America*, 96(6), 2103–2117, 2006.
- [7] C. Berge-Thierry, F. Cotton, O. Scotti, A.A. Griot-Pommerer & Y. Fukushima, New empirical response spectral attenuation laws for moderate european earthquakes. *J. Earthquake Eng. 7(2)*, 193–222, 2003.
- [8] European Strong Motion Database: <http://www.eaee.boun.edu.tr/bulletins/v19/SM.HTM>
- [9] S. Rezaeian & A. Der Kiureghian, A stochastic ground motion model with separable temporal and spectral nonstationarity. *J. Earthquake Eng. & Struct. Dyn 37(13)*, 1565–1584, 2008.
- [10] A. Preumont, The generation of non-separable artificial earthquake accelerograms for the design of nuclear power plants. *Nuclear Eng. Design 88*, 59–67, 1985.
- [11] J.P. Peng & B.F. Conte, Fully nonstationary analytical earthquake ground-motion model *J Eng. Mech. 123(1)*, 15–24, 1997.
- [12] D. Wakefield, M. Ravindra, K. Merz & G. Hardy, Seismic Probabilistic Risk Assessment Implementation Guide. *Final Report 1002989, EPRI*, 2003.
- [13] B.R. Ellingwood & K. Kinali, Quantifying and communicating uncertainty in seismic risk assessment. *Structural Safety 31(2)*, 2009.
- [14] I. Zentner, Numerical computation of fragility curves for NPP equipment. *Nuclear Eng Design 240(6)*, 2010.
- [15] S. Lermite, T. Chaudat, T. Payen, D. Vandeputte & E. Viallet SMART 2008: Seismic design and best-estimate methods assessment for RC buildings subjected to torsion. *Proceedings of WCEE, World conference of earthquake engineering*, Beijing, China, 2008.

Stochastic model for earthquake ground motion using wavelet packets

Y. Yamamoto & J.W. Baker

Department of Civil & Environmental Engineering, Stanford University, CA, USA

ABSTRACT: For performance-based design, non-linear dynamic structural analysis for various types of input ground motions is required. Stochastic (simulated) ground motions are sometimes useful as input motions, because unlike recorded motions they are not limited in number and because their properties can be varied systematically to understand the impact of ground motion properties on structural response. Here a stochastic ground motion model with time and frequency nonstationarity is developed using wavelet packets. Wavelet transform is a tool for analyzing time-series data with time and frequency nonstationarity, as well as simulating such data. Wavelet packet transform is an operation that decomposes time-series data into wavelet packets in the time and frequency domain, and its inverse transform reconstructs a time-series from wavelet packets. The characteristics of a nonstationary ground motion therefore can be modeled intuitively by specifying the amplitudes of wavelet packets at each time and frequency. In the proposed model, 13 parameters are sufficient to completely describe the time and frequency characteristics of a ground motion. These parameters can be computed from a specific target ground motion recording or by regression analysis based on a large database of recordings. The simulated ground motions produced by the proposed model reasonably match the target ground motion recordings in several respects including the spectral acceleration, inelastic response spectra, significant duration, significant bandwidth, and time and frequency nonstationarity. In addition, the median and logarithmic standard deviation of the spectral acceleration of the simulated ground motions match those of the published empirical ground motion prediction. These results suggest that the synthetic ground motions generated by our model can be used for the non-linear dynamic structural analysis as the input ground motions.

1 INTRODUCTION

Nonlinear dynamic structural analysis generally requires the use of large numbers of input ground

motions, but the number of available recorded ground motions is limited and may not be sufficient for characterizing a particular analysis condition. In order to obtain enough numbers of the ground motions, ground motion scaling and spectral matching are widely used to adjust recorded ground motions and make them more representative of particular analysis conditions, however, the results from these operations could have the characteristics different from those of the actual recordings (Luco and Bazzurro 2007, Bazzurro and Luco 2006). Therefore the artificial ground motions that are consistent with both the physical condition and the characteristics of the actual ground motion recordings are needed.

The model proposed here is based on Thráinsson and Kiremidjian (2002) and we extend their model using wavelet packet transform (WPT) in order to approximate the EPSD since the WPT has the advantages of being able to control amplitudes in the time and frequency domain with constant resolution and of allowing reconstruction of the original time series from the wavelet packets.

The proposed model has the following advantages: a) the temporal and the spectral nonstationarity can be controlled by adjusting the parameters describing amplitudes of wavelet packets, b) the model is empirically calibrated and produces motions that are consistent in their important characteristics with recorded ground motions and ground motion prediction models, and c) the procedure is extremely computationally inexpensive (1000 simulations can be produced per hour on a standard desktop PC), so obtaining large numbers of ground motions is efficient.

2 GROUND MOTION SIMULATION USING OUR STOCHASTIC MODEL

Our stochastic ground motion model employs a linear combination of two independent groups of wavelet packets (a major and minor group) because the wavelet packet transform is compressive.

To determine the wavelet packets in both groups, 13 parameters are required in this model: one each

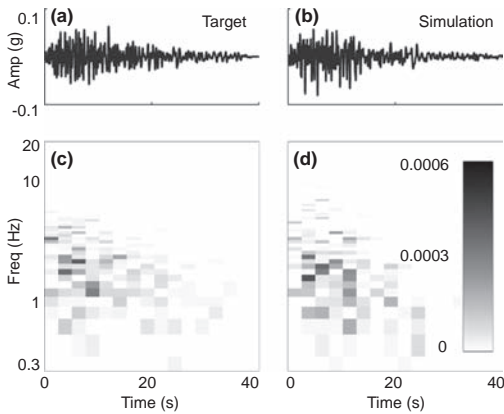


Figure 1. Recording (target) and simulation for the Northridge earthquake Santa Barbara UCSB Goleta recording ($R_{RUP} = 123 \text{ km}$, $V_{S30} = 339 \text{ m/s}$) (a), (c) time series and wavelet packets of the target recording, and (b), (d) time series and wavelet packets of the simulation.

of temporal centroid and variance, spectral centroid and variance, and correlation between time and frequency for both groups median of amplitude for major group, total energy, and the standard deviation of residuals from time and frequency modulating function.

Figure 1 shows a recorded ground motion at far distances, and our simulation. For the target recordings, in the far field, PGA is smaller, duration is larger, correlation of wavelet packets between time and frequency is larger, and bandwidth is smaller than those in the near field. The simulations obtained from our model reflect these characteristics, which are observed empirically and expected theoretically.

3 COMPARISON WITH GROUND MOTION PREDICTION MODELS

To connect the 13 parameters to a particular earthquake scenario, two-stage regression analysis (Joyner and Boore 1993) is employed with moment magnitude (M_w), hypocentral distance (H_{HYP}), rupture distance (H_{RUP}), and average shear wave velocity within 30 m depth (V_{S30}) as predictors.

The following parameters are computed by our model with predicted parameters from the regression analysis and by appropriate ground motion prediction models (GMPM): S_a and inelastic S_a , duration (t_{95-5}), mean period (T_m , Rathje et al., 2004), Arias intensity (I_a , Arias 1970), and the prediction errors of S_a (ϵ , Baker and Cornell

2005) for $M_w = 7$, vertical strike-slip fault, and $V_{S30} = 270 \text{ m/s}$ with various range of distances.

All of these parameters from our simulations reasonably match those from GMPM predictions except S_a in long period. This discrepancy occurs in part because the wavelet packets at low frequencies have low frequency resolution, and so the fluctuation of the amplitude and frequency of wavelet packets at long periods cause large variations in S_a .

4 CONCLUSIONS

A stochastic model for simulating earthquake ground motions with time and frequency non-stationarity using wavelet packets has been developed. This model can simulate the target ground motion recordings having PGA, t_{95-5} , T_m , significant bandwidth, I_a , S_a , and the inelastic S_a values that are comparable to those same properties observed in recorded ground motions. Furthermore, this model can simulate a ground motion with a specified M_w , H_{HYP} , H_{RUP} , and V_{S30} . Additionally, ϵ are seen to be normally distributed and have correlation that is consistent with observations in recorded ground motions. These results suggest that the synthetic ground motions generated by our model can be used for the non-linear dynamic structural analysis as the input ground motions. Current work is studying whether these simulations do in fact produce appropriate levels of response in nonlinear structural models.

Source code and documentation are available at stanford.edu/~bakerjw/gm_simulation.html.

ACKNOWLEDGEMENT

This material is based in part upon work supported by the National Science Foundation under NSF grant number CMMI 0726684. Any opinions, findings and conclusions or recommendations expressed in this material are those of the authors and do not necessarily reflect the views of the National Science Foundation.

REFERENCES

- Arias, A. (1970). A measure of earthquake intensity. *Seismic Design for Nuclear Power Plants*, Hansen RJ (ed.). MIT Press: Cambridge, MA, 438–483.
- Baker, J.W. & Cornell, A. (2005). A vector-valued ground motion intensity measure consisting of spectral acceleration and epsilon. *Earthquake Engineering & Structural Dynamics* 34(10), 1193–1217.

- Bazzurro, P. & Luco, N. (2006). Do scaled and spectrum-matched near-source records produce biased nonlinear structural responses? *Conference, National Engineering, Earthquake Engineering 94111*.
- Joyner, W.B. & Boore, D.M. (1993). Methods for regression analysis of strong-motion data. *Bulletin of the Seismological Society of America 83*(2), 469–487.
- Luco, N. & Bazzurro, P. (2007). Does amplitude scaling of ground motion records result in biased nonlinear structural drift responses? *Earthquake Engineering and Structural Dynamics 36*, 1813–1835.
- Rathje, E.M., Faraj, F., Russell, S. & Bray, J.D. (2004). Empirical relationships for frequency content parameters of earthquake ground motions. *Earthquake Spectra 20*(1), 119.
- Thráinsson, H. & Kiremidjian, A.S. (2002). Simulation of digital earthquake accelerograms using the inverse discrete Fourier transform. *Earthquake Engineering & Structural Dynamics 31*(12), 2023–2048.

Simulation of non-stationary differential support motions accounting for varying soil conditions

Katerina Konakli & Armen Der Kiureghian

Department of Civil and Environmental Engineering, University of California, Berkeley, CA, USA

Earthquake design of extended structures, such as bridges, requires accounting for the spatial variability of the ground motion. Non-linear response history analysis of such structures requires as input sets of consistent closely-spaced earthquake motions, recordings of which are rare. The characterization of spatially varying ground motions is based on the notion of the coherency function, which models the ground motion variability in the frequency domain. The coherency function is defined for stationary time-series, which is an unrealistic assumption for earthquake motions. However, typical ground motions that do not contain a directivity pulse can be segmented in nearly stationary parts which can be propagated in time and space, consistently with an assumed coherency model, using the method of conditional simulation.

Based on the theory of Gaussian distributions, Kameda & Morikawa (1992) derived expressions for the conditional means and variances/covariances of the Fourier coefficients used for the representation of a ground motion random field. These expressions are employed in an interpolating process that simulates arrays of time-series conditioned on one or more deterministic time functions. Vanmarcke & Fenton (1991) used the equivalent method of Kriging for the conditioned simulation of ground accelerations after an arbitrary division of the original record into small segments to achieve a more accurate representation of the non-stationarity of the field. Liao & Zerva (2006) used the interpolating process introduced by Kameda & Morikawa (1992) in conjunction with the concept of segmentation to simulate an array of non-stationary ground motions consistent with target recorded or synthetic accelerograms. Their study provides a more thorough investigation of the problem by incorporating the necessary post-processing to obtain physically compliant motions, and by additionally examining the velocities and displacements of the simulated motions, as well as the corresponding response spectra and coherency characteristics. However, as in the previous works, their study is limited to the case of uniform soil conditions.

Variations in local soil profiles can significantly contribute to the spatial variability of ground motions and, therefore, influence the response of multiply supported structures. By incorporating the site-response effect, the present paper provides an important extension of the previously developed method of conditional simulation.

When the Fourier coefficients at the first station are obtained for a recorded ground motion, we obtain sets of spatially varying ground motions that inherit the characteristics of that motion. However, the variance of the simulated motions increases with increasing distance from the initial station, which is an undesirable characteristic in statistical analyses of earthquake response. This problem is overcome if we condition the simulated array of motions on the power spectral densities of the segmented target accelerogram rather than its specific realization. Vanmarcke & Fenton (1991) used this approach to simulate accelerograms, but did not examine the physical compliance of the simulated motions in terms of displacement time-histories and response spectra.

In this paper, we simulate arrays of ground motions under spatially varying soil conditions using two approaches. In the first approach, we condition the simulated array on the power spectral density of a given accelerogram (unconditioned simulations). In the second, the array of motions is conditioned on an observed realization (conditioned simulations). The unconditioned simulation method involves sampling from a zero-mean joint Gaussian distribution, the covariance matrix of which is determined in terms of the auto-power spectral densities of the segmented observed record, the assumed variability of the local soil profile and a prescribed coherency function. The conditioned simulation method involves sampling from a conditional joint Gaussian distribution, specification of which additionally involves the Fourier coefficients of the observed realization. This approach is statistically equivalent with the iterative process used by Kameda & Morikawa (1992) and Liao & Zerva (2006) but is computationally superior. The non-stationary extension of the above methods, based on the concept of segmentation, is described

and details of the implementation are discussed. Criteria for the segmentation are introduced and applied for the division of an observed accelerogram in nearly stationary segments. The same accelerogram is used in an example application in which we simulate conditioned and unconditioned support motions for an existing bridge in California, accounting for the effects of incoherence, wave-passage and site-response, for an assumed variation of the local soil profile. The assumed coherency function incorporates the incoherence and spatially varying site-response effects, whereas the wave-passage is applied as a deterministic time-shift. Example simulations are shown to verify the physical compliance of the motions. The simulation methods are validated by the excellent agreement of estimated coherency characteristics from an ensemble of realizations with the target theoretical model. Response spectra at all support motions are also investigated and the variability with distance from the point of the observed motion is compared for the two approaches.

We note that the segmentation and post-processing involved in the non-stationary extension of the conditioned simulation method alters the

low-frequency content, and thus the displacement waveform of the original record. A method of preserving the original low-frequency content has been introduced by Liao & Zerva (2006) and is further developed by Konakli & Der Kiureghian (2011).

REFERENCES

- Kameda, H. & Morikawa, H. 1992. An interpolating stochastic process for simulation of conditional random fields. *Probabilistic Engineering Mechanics* 7: 243–254.
- Konakli, K. & Der Kiureghian, A. 2011. Simulation of spatially varying ground motions including incoherence, wave passage and differential site response effects. *Earthquake Engineering and Structural Dynamics* (to appear).
- Liao, S. & Zerva, A. 2006. Physically compliant, conditionally simulated spatially variable seismic ground motions for performance-based design. *Earthquake Engineering and Structural Dynamics* 35: 891–919.
- Vanmarcke, E.H. & Fenton, G.A. 1991. Conditioned simulation of local fields of earthquake ground motion, *Structural Safety* 10: 247–264.

Stochastic simulation of near-fault ground motions for specified earthquake and site characteristics

Mayssa Dabaghi, Sanaz Rezaeian & Armen Der Kiureghian
University of California, Berkeley, CA, USA

A procedure for stochastically simulating an ensemble of near-fault strong ground motion time histories for a specified set of earthquake and site characteristics (earthquake magnitude, location of the site relative to the fault, shear wave velocity, etc.) is presented. Use of simulated motions is of particular interest in performance-based earthquake engineering due to scarcity of near-fault recordings. The simulated motions can be used in addition to or in place of recorded motions.

We first develop a parameterized stochastic model of near-fault ground motion in the fault-normal direction, including the forward directivity pulse, and fit the model to a database of near-fault ground motions. The stochastic model consists of two sub-models, one for the directivity pulse and one for the residual motion, i.e., the total motion minus the directivity pulse. An existing wavelet-based method by Baker (2007) is used to characterize the directivity pulse and extract it from the total motion for recorded accelerograms. A modified version of the idealized pulse model by Mavroeidis and Papageorgiou (2003), which ensures zero displacement at the end of the pulse, is employed and fitted to the extracted pulses (see Figure 1 for a sample fit), thereby generating a sample of data for the five parameters of the model. For the residual, the non-stationary filtered white noise model by Rezaeian and Der Kiureghian (2008, 2010) is employed and its six parameters are identified by fitting to the database of residual motions. Regression analysis is performed to construct predictive equations for the $5 + 6 = 11$ model parameters, while accounting for correlations between the parameters and non-normal behaviors of the underlying distributions. Using these predictive equations and correlation coefficients, for a given set of earthquake and site characteristics, we generate a sample set of model parameters. These are used to generate a synthetic pulse and a corresponding residual motion. The residual motion is high-pass filtered to make sure that it also has zero velocity and displacement at the end of the motion. Adding the derivative of the simulated velocity pulse to the high-passed residual, we obtain a synthetic near-fault ground

motion having a forward directivity pulse. One can repeatedly generate sets of model parameters and use them to generate an ensemble of synthetic near-fault ground motions. The resulting synthetic motions have the same statistical characteristics as the motions in the database, including the record-to-record variability for the given set of earthquake and site characteristics.

To illustrate the proposed procedure, we simulate samples of fault-normal ground motion components with forward directivity pulses for the earthquake and site characteristics of the NGA record number 459, which is recorded at the Gilroy Array #6 station during the 1984 Morgan Hill earthquake. The solid black line in Figure 1 shows the extracted directivity pulse of this record. The solid black line in Figure 2 shows one of the simulated pulses. Figure 3 shows the recorded ground acceleration time history (bottom), the derivative of the velocity pulse extracted from it (top), and the corresponding residual motion (middle). Figure 4 shows the same components for the simulated motion. The acceleration, velocity and displacement time histories of the synthetic motion are plotted in Figure 5. These recorded and simulated motions should be regarded as random realizations of the fault-normal component of the ground motion resulting for an earthquake and site with the characteristics of the recorded

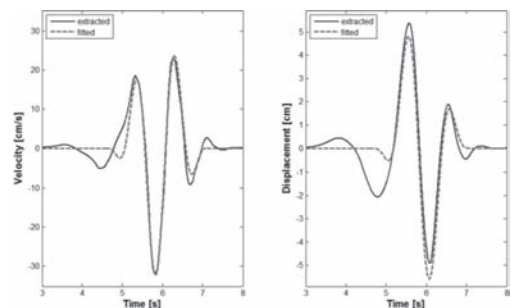


Figure 1. Extracted and fitted velocity pulses and corresponding displacement waveforms for NGA record 459.

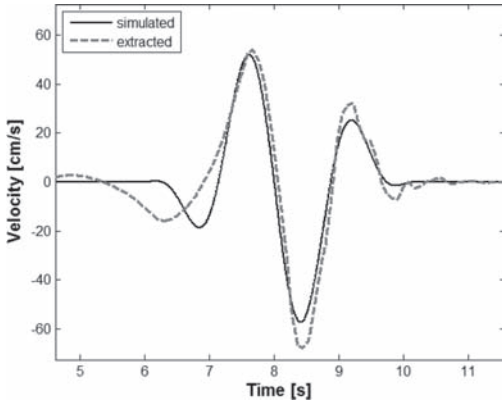


Figure 2. Simulation; simulated velocity pulse and pulse extracted from total synthetic ground motion.

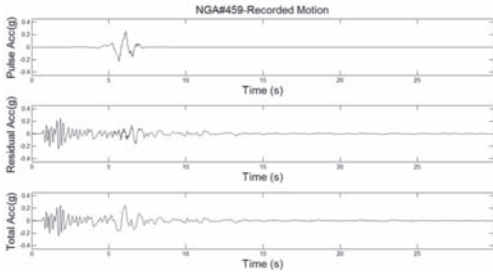


Figure 3. Recorded motion: derivative of extracted pulse (top), residual motion (middle) and total acceleration record (bottom).

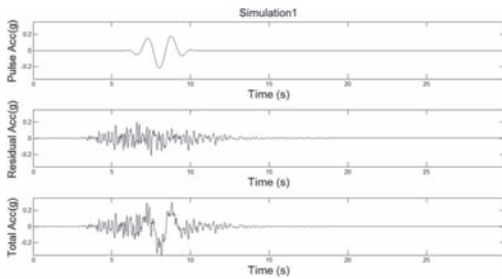


Figure 4. Simulated motion 1: derivative of simulated pulse (top), simulated residual motion (middle) and total simulated acceleration record (bottom).

earthquake. The full paper shows two additional simulations, demonstrating the natural variability of near-fault ground motions for a given set of earthquake and site characteristics.

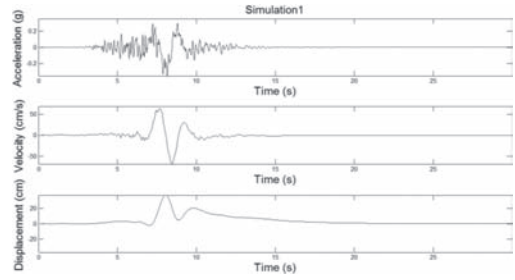


Figure 5. Simulated motion 1: acceleration, velocity and displacement time histories.

Finally, Baker's algorithm is applied to the synthetic ground motion to check if it detects the presence of a forward directivity pulse. The motion is indeed identified as pulse-like with the extracted velocity pulse having a period of 1.93 s. The extracted pulse is shown in Figure 2 as a red dashed lines.

The procedure described in this paper is for simulating near-fault ground motions that contain a velocity pulse. Not all near-fault ground motions at a given site contain velocity pulses, even those that are located in the forward directivity region. A refinement to account for this effect is currently under development. Moreover, we have not accounted for the variable number of records used from the same earthquake. This can be done by using random effects regression and is also a work in progress. Until then, the results reported in this paper should be regarded as preliminary in nature.

REFERENCES

- Baker, J.W. (2007). Quantitative classification of near-fault ground motions using wavelet analysis, *Bulletin of the Seismological Society of America*, 97:1486–1501.
- Mavroeidis, P. & Papageorgiou, A.S. (2003). A mathematical representation of near-fault ground motions, *Bulletin of the Seismological Society of America*, 93:1099–1131.
- Rezaeian, S. & Der Kiureghian, A. (2008). A stochastic ground motion model with separable temporal and spectral nonstationarities, *Earthquake Engineering & Structural Dynamics*, 37:1565–1584.
- Rezaeian, S. & Der Kiureghian, A. (2010). Simulation of synthetic ground motions for specified earthquake and site characteristics, *Earthquake Engineering & Structural Dynamics*, 39:1155–1180.

GS_222 — Structural reliability (1)

This page intentionally left blank

Variance reducing capacity of concrete conformity control in structural reliability analysis under parameter uncertainties

R. Caspeele & L. Taerwe

Magnel Laboratory for Concrete Research, Department of Structural Engineering,
 Ghent University, Ghent, Belgium

1 INTRODUCTION

Conformity control is often used in order to verify whether the delivered product, i.e. concrete, complies with the specifications. Due to this quality control, certain batches of concrete are accepted and some are rejected, resulting in a filtering effect with respect to the concrete strength distribution. As a consequence, conformity control increases the achieved safety level in comparison to production without conformity verification. Further, also the dependency of the reliability index with respect to parameter uncertainties reduces due to the quality verification, resulting in an increase of the predictive reliability index.

2 THE FILTER EFFECT OF CONFORMITY CONTROL

Using a numerical algorithm (see Caspeele & Taerwe 2009b), the ratios μ_o/μ_i (average outgoing strength after conformity control to the average incoming strength) and σ_o/σ_i (standard deviation of the outgoing strength distribution to the standard deviation of the incoming strength distribution) can be calculated in function of the fraction defectives θ_i (from the incoming strength distribution). The filter effect of 3 conformity criteria is given in Figure 1 in case of auto correlated test results.

Due to this filter effect, conformity control also influences the reliability index, as illustrated in Figure 2 in case of an example axially loaded concrete column under compression. These results illustrate that the filtering effect of conformity control with respect to the reliability index increases with an increasing fraction defectives. However, it is even more important to notice that due to conformity control a more or less homogeneous reliability index is obtained, i.e. the dependency of the reliability index with respect to the parameter uncertainties of concrete strength distributions decreases.

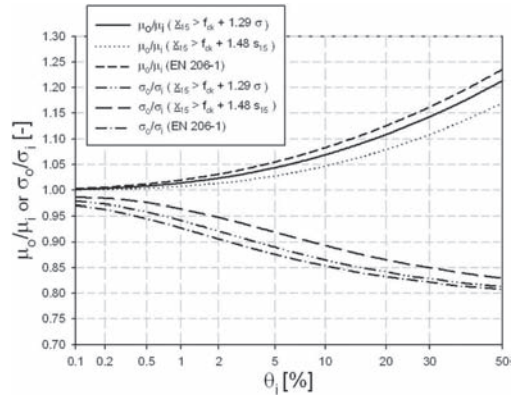


Figure 1. Filter effect corresponding to criteria $\bar{x}_{15} \geq f_{ck} + 1.29\sigma_i$, $\bar{x}_{15} \geq f_{ck} + 1.48s_{15}$ and EN 206-1 for continuous production control (auto correlated observations).

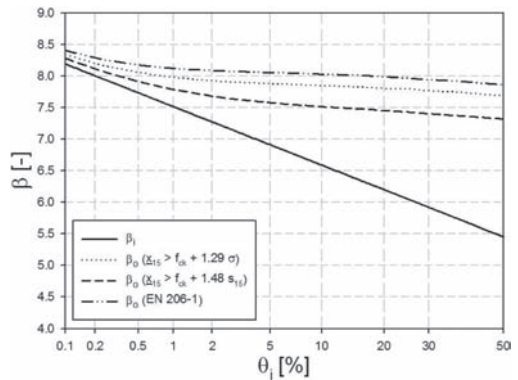


Figure 2. Reliability index for the example concrete column before and after conformity control according to criteria $\bar{x}_{15} \geq f_{ck} + 1.29\sigma_i$, $\bar{x}_{15} \geq f_{ck} + 1.48s_{15}$ and the EN 206-1 conformity criteria (auto correlated observations).

3 VARIANCE REDUCING CAPACITY OF CONFORMITY CONTROL

Based on Taylor approximations and making use of the Simplified Level II method (König & Hosser 1982), the ratio of the outgoing predictive reliability index (corresponding to accepted concrete lots) to the incoming predictive reliability index (corresponding to incoming lots) can be approximated by the following formula:

$$\frac{\beta_o}{\beta_i} = \frac{\mu_{\mu_{f_{c,o}}} - \frac{f_{ck}}{\gamma_c}}{\mu_{\mu_{f_{c,i}}} - \frac{f_{ck}}{\gamma_c}} \times \dots \frac{\mu_{\sigma_{f_{c,o}}}}{\mu_{\sigma_{f_{c,i}}}} \quad (1)$$

$$\sqrt{1 + \left(\frac{\alpha_{f_c}}{\mu_{\sigma_{f_{c,i}}}} \right)^2 \sigma_{\mu_{f_{c,i}}}^2 + \left(\frac{\alpha_{f_c} \left(\mu_{\mu_{f_{c,i}}} - \frac{f_{ck}}{\gamma_c} \right)}{\mu_{\sigma_{f_{c,i}}}^2} \right)^2 \sigma_{\sigma_{f_{c,i}}}^2} \Bigg/ \sqrt{1 + \left(\frac{\alpha_{f_c}}{\mu_{\sigma_{f_{c,o}}}} \right)^2 \sigma_{\mu_{f_{c,o}}}^2 + \left(\frac{\alpha_{f_c} \left(\mu_{\mu_{f_{c,o}}} - \frac{f_{ck}}{\gamma_c} \right)}{\mu_{\sigma_{f_{c,o}}}^2} \right)^2 \sigma_{\sigma_{f_{c,o}}}^2}$$

This equation enables to quantify the increase of the reliability index of concrete structures, based on the filter effect with respect to the strength distribution, which on its turn can be calculated based on the numerical algorithm as described in (Caspele 2010) in case prior information is available.

4 EVALUATION OF THE VARIANCE REDUCING CAPACITY OF CONFORMITY CONTROL ACCORDING TO EN 206-1

As an example, this approach is used to quantify the variance reducing capacity of the EN 206-1 conformity criteria in case of different concrete classes.

The results of the filter effect of the conformity criteria mentioned in EN 206-1 (2000) on the mean and standard deviation of the unknown reliability index and the effect on the predictive reliability are given in Table 1 for different concrete classes.

Table 1. Filter effect of conformity control according to EN 206-1 for different concrete classes.

Characteristics	Concrete grade			
	C15	C25	C35	C45
μ_{μ_i} [MPa]	28.93	37.46	46.32	52.84
σ_{μ_i} [MPa]	4.60	5.10	4.50	3.65
μ_{σ_i} [MPa]	5.02	5.45	5.01	4.42
σ_{σ_i} [MPa]	1.53	1.58	1.53	1.40
μ_{μ_o} [MPa]	29.96	38.97	47.58	54.28
σ_{μ_o} [MPa]	3.49	3.55	3.23	2.39
μ_{σ_o} [MPa]	4.79	5.13	4.69	4.00
σ_{σ_o} [MPa]	1.37	1.41	1.32	1.11
μ_{B_o}/μ_{B_i} [-]	1.105	1.140	1.127	1.175
$\sigma_{B_o}/\sigma_{B_i}$ [-]	0.950	0.953	0.967	0.975
β_o/β_i [-]	1.137	1.171	1.151	1.195

5 CONCLUSIONS

- The filtering effect of conformity control on concrete strength distributions consists of an increase in mean concrete strength and decrease in standard deviation of the predictive strength distribution.
- An example of an axially loaded concrete column was used in order to illustrate the filter effect in function of absolute values of the reliability index. This example enabled to notice that due to conformity control a more or less homogeneous reliability index is obtained in function of the incoming fraction defectives. Thus, conformity control reduces the dependency of the reliability index with respect to the parameter uncertainties of concrete strength distributions.
- The filter effect with respect to the concrete strength distribution was translated into a variance reducing effect on the unknown structural reliability index, using an approximate quantification approach based on the Simplified Level II method.
- The variance reducing effect of the EN 206-1 conformity criteria was analyzed based on the suggested method, taking into account prior strength distributions from literature.

REFERENCES

- Caspele, R. 2010. *Probabilistic Evaluation of Conformity Control and the Use of Bayesian Updating Techniques in the Framework of Safety Analyses of Concrete Structures*. PhD thesis, Ghent University, Ghent, Belgium.
- EN 206-1. 2000. *Concrete-Part 1: Specification, performance, production and conformity*. European Standard, CEN.
- König, G. & Hosser, D. 1982. *The simplified level II method and its application on the derivation of safety elements for level I*. CEB Bulletin no. 147.

Corrosion effects onto the safety of steel sheet pile walls in marine environment

P. Osório, C. Odenbreit & M. Greger
University of Luxembourg, Luxembourg

Ton Vrouwenvelder
Delft University of Technology, Delft, The Netherlands

ABSTRACT: Corrosion of steel sheet piles in a marine environment is a highly complex phenomenon that is dependent on many different parameters, which mainly are: a) endogenous parameters, that define the properties of the steel material, like for example, chemical composition and microstructure, b) exogenous parameters, which are defined by the properties of the marine environment, like for example the ionic content of the water and c) a dynamic parameter, which is the effect of time on the thickness loss (Houyoux, C. 2004).

The model of corrosion given in the EN 1993, Part 5—Piling, defines zones of different aggressiveness, and suggests values that depend on the temporal horizon of the structure. Although of easy and practical application, the model is made to be applied to any structure in marine environment, independently of the specific conditions that may be present in each case.

In this paper, a new multi-factorial model of corrosion in marine environment, that takes into consideration the water properties, the steel class, the age of the structure, the existence of currents, berth and tide, is applied in a probabilistic way to determine the effect of corrosion in the safety of steel sheet piles.

Two different structural systems were defined, with different retaining heights and the position of the anchor, having necessarily different cross-section profiles. The structures were designed according to the specifications of the Eurocodes and the verification to corrosion was made according to EN 1993-5.

The multi-factorial model was applied for two different scenarios—one having low water currents and the other having high currents. Figure 1 shows the difference between the corrosion loss distribution for both cases and compares it with the model of EN 1993-5.

The performance of reliability analyses had the objective of determining the level of safety associated to the structures, after the effect of

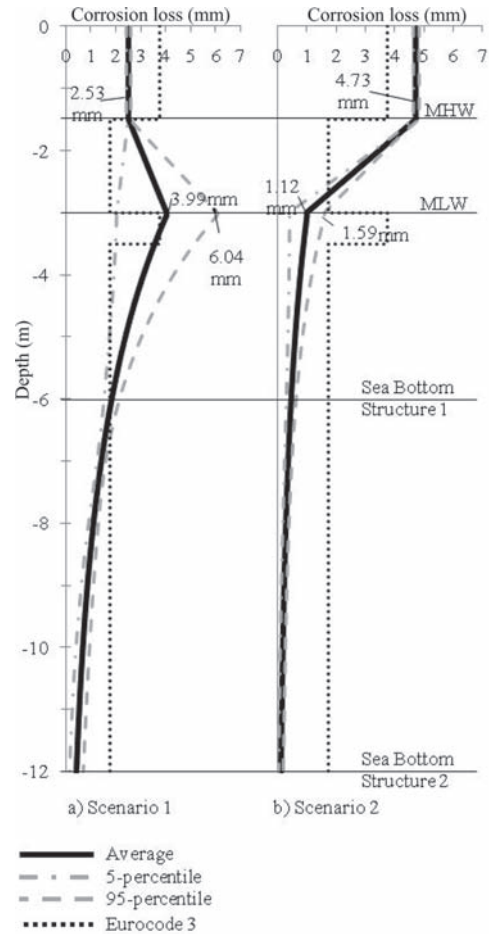


Figure 1. Distribution of corrosion loss for structures 1 and 2 in scenario 1 and 2 in comparison with the Eurocode model.

corrosion, and compare it to the level of safety of the non-corroded state.

The reliability analyses were performed using a probabilistic program called Prob2B, developed at TNO, Netherlands, coupled with the program that performs the structural analysis, MSheet, and with Microsoft Excel, that is used to apply the corrosion model into the structure. All the reliability analyses were performed with the First Order Reliability Method (FORM).

The values of the stochastic properties of the geotechnical parameters were withdrawn from the literature (JCSS 2001 and Rackwitz 2000). It was considered that there was homogeneity in the properties of the soil, and therefore the soil variability was not taken in consideration. Some of the soil properties are strongly correlated, like the soil unit weight and the internal friction angle (Fenton et al., 2005). It is also known that soils with higher compaction show higher stiffness (Smolczyk, U. 2002), i.e., there is also a correlation between the soil unit weight and the stiffness. For this study, a factor or $\rho = 0,5$ was defined by for the correlation between the unit weight and the friction angle, as suggested by (Rackwitz 2000), as well as between the unit weight and the sub-grade reaction modulus. All the soil properties are considered to have a lognormal distribution, as recommended in the literature (JCSS 2001 and Rackwitz 2000).

In order to assess the effect that the corrosion model of EN 1993-5 has in the level of safety and compare it with the new multi-factorial model, a third scenario was added, where that corrosion model was introduced.

The results of all the reliability analyses are summarized in Figure 2.

If for the other situations there is no significant reduction of level of safety, for the case of the

scenario 1 (low currents), system 1 has a reliability index $\beta = 2.1$, which is considerably smaller than the limit of $\beta = 3.8$ for structural safety. The model of corrosion given in EN 1993-5 is, therefore, of simple and practical application, but it must be applied by structural engineers with caution and with knowledge that it has limitations, as shown in this paper.

REFERENCES

- European Committee for Standardization, European Standard EN 1993-5:2003, Brussels, 2003.
- Fenton, G.A., Griffiths, D.V. & Williams, M.B. 2005. Reliability of traditional retaining wall design, *Géotechnique* 55, No. 1, 2005.
- Houyoux, C. 2004. *Design Method for Steel Structures in Marine Environment Including the Corrosion Behaviour*, Report, ESCS, 2004.
- JCSS 2001. *Probabilistic Model Code*, Joint Committee for Structural Safety, Zurich.
- MSheet 2007. *MSheet Manual - Design of Diaphragm and Sheet pile Walls*, MSheet Version 7.7, Geodelft, Delft, 2007.
- Rackwitz, R. 2000. Reviewing probabilistic soils modeling, *Computers and Geotechnics*, 26, Elsevier.
- Smolczyk, U. 2002. *Geotechnical Engineering Handbook*, Ernst & Sohn, Berlin.

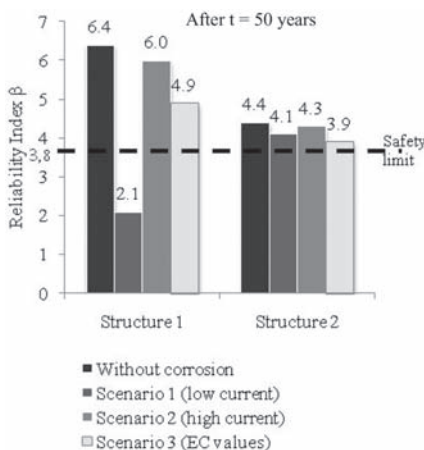


Figure 2. Reliability indices obtained for the different scenarios.

Robustness analysis of structural systems considering accidental actions

N. Kagho

IFSTTAR, Paris, France

A. Orcési

IFSTTAR, France

C. Cremona

Directorate for Research and Technology, Ministry of Sustainable Development, La Défense, France

Robustness of structural systems with respect to accidental loads (e.g., bomb blast, impact and human errors) has gained recently the attention of researchers and stakeholders, following several structural failure events in recent decades. Quantifying robustness of structural systems under uncertainty is a crucial issue. EN 1991-1-7 (2006) considers identified and unidentified accidental actions and defines robustness as “the ability of a structure to withstand events like fire, explosions, impact or the consequences of human error, without being damaged to an extent disproportionate to the original cause.”

Under uncertainty in spoiling phenomena and structural analyses, a probabilistic approach is justified. This paper presents a reliability-based framework for assessing robustness of structural systems. In this approach, robustness quantifies the impact of relatively small damage on major structural consequences, by identifying the failure mechanism with the largest probability of occurrence (the “reference” structural system failure mechanism). Since identifying all failure paths may be computationally tricky for structures with a high degree of redundancy, stochastically dominant failure paths are identified by using the branch-and-bound method (Okada et al., 1984a, b, Thoft-Christensen & Murotsu 1986).

Considering the most probable failure path (reference path) q_c , with performance functions $g_{c_1}, g_{c_2(c_1)}, \dots, g_{c_n(c_1, c_2, \dots, c_{n-1})}$, where $n = \text{length of } q_c$, and $g_{c_n(c_1, c_2, \dots, c_{n-1})}$ is the performance function associated with structural element c_n knowing that elements c_1, c_2, \dots, c_{n-1} have already failed, respectively. A measure of structural robustness is proposed by comparing the probability of failure of the first failure element c_1 in the failure path with the probability of occurrence of the failure mechanism. Knowing that all complete failure mechanisms are parallel systems, and that the sequential order

of failure elements that failed is c_1, c_2, \dots, c_n , the robustness index is expressed as

$$I_r = \frac{P_{local}}{P_{global}} \quad (1)$$

where $P_{local} = P[g_{c_1} \leq 0]$ = probability of failure of the first failure element in the reference path, and $P_{global} = P\left[\bigcap_{i=1}^n g_{c_i(c_1, \dots, c_{i-1})} \leq 0\right]$ = probability of occurrence of the failure mechanism, where $g_{c_i(c_1, \dots, c_{i-1})} = g_{c_i}$ for $i = 1$. Obviously, I_r is greater than or equal to 1.

Numerical examples are considered to illustrate the impact of structural design on the robustness index. The variation of the robustness index with the cross-sectional area of the structural members (IPE and IPN cross-sections are considered), for a portal frame subjected to combined loads (a horizontal load acting on the top of the left column and a vertical load acting on the mid-section of the horizontal beam), is shown in Figure 1. It clearly appears that the larger the cross-sectional area is, the greater the robustness.

When a loading coefficient is applied to those loads (α_1 for the horizontal load and α_2 for the vertical load), the variation of I_r with α_1 and α_2 is shown in Figure 2. It appears that α_2 is the factor with the largest impact on I_r .

The impact of structural redundancy on robustness index is shown in Table 1. These results show that, for this type of loading conditions, right bracing B_3 produce a higher robustness index than the left one B_2 . It can be seen in Table 1 that the more there are bracings the longer the reference path is, and the larger the robustness index I_r is. These results lead to conclude that, V-shaped bracing can efficiently increase the robustness of frame structures.

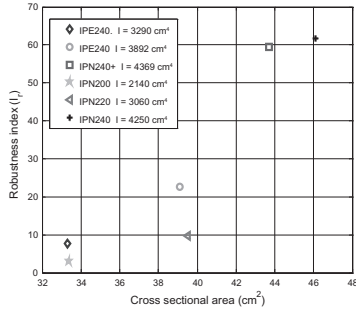


Figure 1. Robustness index versus cross sectional area.

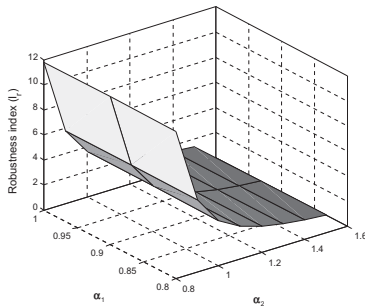


Figure 2. Robustness index versus loading coefficients α_1 and α_2 .

To evaluate the efficiency of the proposed robustness indicator, a number of numerical simulations have been carried out with frame structures. The results demonstrate that redundancy is a key factor for progressive failure and robustness. Frangopol & Curley (1987) have shown that structural redundancy depends on many factors, such as structural topology, materials properties, member size, applied loads, etc. The results obtained in this analysis confirm the dependence of structural robustness to these parameters. Even though redundancy is not the only key factor for robustness, it is a crucial one when designing against propagation of failure throughout the overall system.

The approach proposed in this paper aims at quantifying the structural robustness of a system by means of reliability theory. The proposed robustness index quantifies the impact of a local damage on major structural damage. As disproportionate failure, progressive collapse, and structural robustness are tied, failure mechanisms analysis of a structure can help assessing efficiently the robustness of a structure by considering the stochastically most dominant failure path. The proposed examples show that robustness is affected by static indeterminacy as well as redundancy, loads, material properties and the cross sectional characteristics of the structural members as shown by Frangopol & Curley (1987).

Table 1. Variation of degree of indeterminacy (h) and redundancy with robustness index (I_r).

Structural Design				
h	3	6	6	9
Reference Failure path	4-7-2	7-5-8-9-1	2-1-4-7-10-8	—
Probability of failure	4 3.19×10^{-2} 7 2.98×10^{-2} 2 1.03×10^{-2}	7 1.53×10^{-2} 5 1×10^{-3} 8 9×10^{-4} 9 2×10^{-4} 1 1×10^{-4}	2 2.98×10^{-7} 1 2.40×10^{-8} 4 1.59×10^{-9} 7 7.98×10^{-10} 10 3.95×10^{-10} 8 9.38×10^{-11}	$\rightarrow 0$
I_r	3.095	150.75	3174.9	$\rightarrow \infty$

REFERENCES

- Baker, J.W. Schubert, M. & Faber, M.H. 2008. On the assessment of robustness. *Elsevier, Structural Safety* 30(3): 253–267.
- Biondini, F. Frangopol, D.M. & Restelli, S. 2008. On Structural Robustness, Redundancy and Static Indeterminacy. *ASCE Structures Congress 2008*. Vancouver, April 24–26. Canada.
- Canisius, T.D.G. Sorensen, J.D. & Baker, J.W. 2007. Robustness of structural systems—a new focus for the Joint Committee on Structural Safety (JCSS). In Kanda, Takada & Furuta (eds). *Applications of Statistics and Probability in Civil Engineering*. London.
- Ditlevsen, O. 1979. Narrow reliability bounds for structural systems. *Mechanics based design of structures and machines*. Taylor & Francis 7(4): 453–472.
- EN 1990. 2002. Basis of Structural design. *Eurocode 0: CEN 2002*.
- EN 1991-1-7. 2006. Actions on Structures: Part 1–7: Accidental Actions. *Eurocode 1: CEN 2006*.
- Frangopol, D.M. & Curley, J.P. 1987 “Effects of Damage and Redundancy on Structural Reliability”, *ASCE Journal of Structural Engineering*, 113(7): 1533–1549.
- Madsen, H.O. Krenk, S. & Lind, N.C. 1986. Methods of structural safety. *Englewood Cliffs (NJ): Prentice-Hall, Inc.*
- Melchers, R.E. 1999. Structural Reliability Analysis and Prediction. (*Second Edition*) John Wiley & Sons. Chichester.
- Murotsu, Y. Okada, H. Yonezawa, M. Martin, G. & Taguchi, K. 1982. Automatic Generation of Stochastically Dominant Modes of Structural Failure in a Frame Structure. *Bulletin of University of Osaka Prefecture. Series A, Engineering and natural sciences*. 30(2): 85–101.
- Okada, H. Matsuzaki, S. & Murotsu, Y. 1984. Safety Margins for Reliability Analysis of Frame Structures. *Bulletin of University of Osaka Prefecture. Series A, Engineering and natural sciences*. 32(2): 155–163.
- Thoft-Christensen, P. & Murotsu, Y. 1986. Application of structural Systems Reliability Theory. *Springer-Verlag, Berlin*.

A coupling Bayesian/reliability approach for robust updating applications

B. Richard, L. Adelaide & A. Orcési

French Public Works Laboratory University Paris Est, France

C. Cremona

Ministry of Energy, Ecology, Sustainable Development and Sea, Paris, La Défense, France

1 AIM AND SCOPE

Reinforced concrete structure are becoming old and therefore, the constitutive materials change with respect to the time. It is important and necessary to evaluate their performance level to check if design code requirements are fulfilled (service ability, structural safety). Therefore, the material parameters (Young's modulus, tensile strength, compressive strength, ...) related to the constitutive materials can be estimated. In this paper, the authors present a methodology aiming to update a given structural model by using the available experimental information at the structural scale (displacement, rotations, ...). The proposed approach is based on the used of (i) the reliability theory and (ii) of Bayesian networks. This tool has been considered because (i) it allows updating a large number of variable and (ii) it allows updating not only the structural response of a model but also the input variables, what would not have been possible if basic Bayesian approach had been used. Thanks to the proposed approach, destructive tests can be avoided since the structural measurements can be used to update the mechanical parameters of a model. The updated parameters can be seen as the true material parameters of the structure.

2 PROPOSED UPDATING METHODOLOGY

The proposed approach can be seen as a four-step sequence. The **first step** lies in identifying the most interesting variables. Two criteria are proposed herein to identify the most important variables. First, engineering considerations can be used. Such considerations can be invoked to carry out a first sorting, leading to decrease the total number of the input variable included in the analysis. Second, the reliability theory (Melchers 1999) can be advantageously used. This efficient framework allows providing quantitative indicators related to the sensitivity of the structural response of a model

with respect to each input variable. The **second step** lies in building the Bayesian network (Lauritzen 1988). In the present study, this step has been realized by means of Monte Carlo Simulations (Metropolis 1949). Although this approach is not optimal from a computational point of view, it is simple and robust. The **third step** lies in updating the statistical parameters related to the input variables by including the observations in the Bayesian network. The updating process is based on the use of the well known Bayes' theorem. Based on the knowledge of the updated material parameters, the corresponding structural response can be computed again. This **fourth and last step** is carried out by a reliability analysis, what allows computing the cumulative probability function related to the structural response in a straightforward way.

3 CASE STUDY: A PRESTRESSED REINFORCED CONCRETE BEAM

The VIPP (*Viaducs travees Indépendantes Poutres préfabriquées en béton Précontraint par post-tension*) are simple span viaducts made of precast concrete girders prestressed by post-tension. This type of construction was largely developed between the years 1955 to 1970, thanks to its girders launching system which allowed the crossing of non classical obstacles with reasonable height. This technique is no longer used, largely completed by other construction techniques making it possible to carry out more economic and safer redundant structures with respect to failure. The enthusiasm which reigned at the construction time of the first VIPP generation resulted in many design and execution mistakes. The French ministry of Energy, Ecology, Sustainable Development and Sea decided to carry out an extensive experimental campaign to estimate the residual carrying capacity of such structures. Therefore, prestressed beam was experimentally studied. Its cross section is depicted in Figure 1. In order to capture the mean structural behaviour

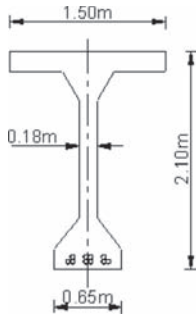


Figure 1. Girder cross section.

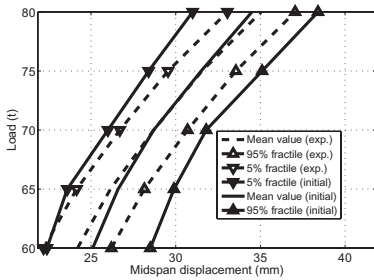


Figure 2. Initial mean values and 90% confidence interval.

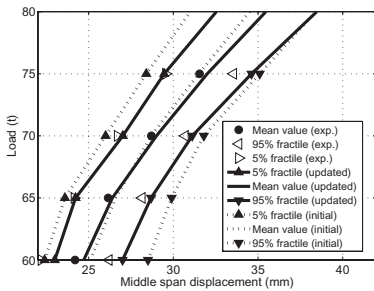


Figure 3. Updated mean values and 90% confidence interval.

of the prestressed girder, a mechanical model has been developed based on linear elastic software classically used by civil engineers. The beam is supposed to be a simply supported beam subjected to a concentrated load, applied at mid-span. The calculation principle is to increase the applied load in order to obtain a tensile stress at the bottom part of the beam. As soon as the cracked cross-sections are identified, the modelling lies in modifying the inertia of cracked components. Based on the structural reliability theory (Der Kiureghian 2005), a probabilistic model has been developed in order to take into account parameters uncertainties. The most preponderant variables have been

identified by means of a sensitivity analysis. This probabilistic analysis allows quantifying not the mean structural response but also the 90% confidence interval. The results are exposed in Figure 2. It can be noticed that the numerical confidence interval are wider than the experimental ones. Therefore, the uncertainty level has been chosen too high and does not seem to be representative of the experience. This point has motivated by the use of an updating analysis to obtain better standard deviation related to input variables. Monte Carlo Simulations have been carried out to build the corresponding Bayesian network. The experimental information was included in the network in terms of load/midspan displacement. The final results are given in Figure 3. As expected, the numerical confidence interval has been reduced on the basis of available experimental information. This enables to conclude that the proposed updating methodology can handle problems where standard deviations (and not only mean values) have to be updated.

4 CONCLUDING REMARKS

This paper is devoted to present a coupling reliability/Bayesian approach aiming to estimate the true material parameters of an existing reinforced concrete structure. It is based on the use of (i) the reliability theory and (ii) the Bayesian networks theory. The main steps have been presented and a structural case has been exposed in order to illustrate their capability to handle practical engineering problems. Especially, it has been shown that the proposed approach could be used in order to update a probabilistic model that has been initially designed in a too pessimistic way. These results seem to be satisfactory and promising for further developments. The authors are convinced that this approach could be used by civil engineers to avoid carrying out insite destructive tests since structural information is used to estimate the true material characteristics.

REFERENCES

Der Kiureghian, A. (2005). *First and second order reliability methods*. CRC Press, Boca Raton, FL.

Lauritzen, B. & Spiegelhalter, H. (1988). Local computations with probabilities on graphical structures and their application to expert systems (with discussion). *Journal of the Royal Statistical Society (Series B)* 50(2), 157–224.

Melchers, R. (1999). *Structural reliability analysis and prediction*. John Wiley and Sons.

Metropolis, N. & Ulam, S. (1949). The monte carlo method. *Journal of the American Statistical Association* 247(44), 335–341.

Comparative study of safety formats for nonlinear finite element analysis of concrete structures

H. Schlune, M. Plos & K. Gylltoft
 Chalmers University of Technology, Gothenburg, Sweden

ABSTRACT: For the design of concrete structures a consistent safety format that leads to good agreement with the target reliability level is needed. This article describes how the safety format for nonlinear analysis according to EN 1992-2, CEN (2005), and the safety format according to Schlune *et al.* (2011) were tested on short columns and beams subjected to shear. At first, the safety formats were used to calculate design resistances for example structures. Then, Monte-Carlo simulations were used to calculate the probability that the resistances are below the design resistances. The safety format according to EN 1992-2 led to a reliability level that was far below the target reliability when it was used in combination with the shear model, with a high model uncertainty. Design according to the safety format by Schlune *et al.* (2011) led to better agreement with the target reliability.

1 INTRODUCTION

Nonlinear finite element analysis (FEA) is increasingly being used to design and assess reinforced concrete structures. In contrast to linear elastic FEA, nonlinear FEA account for the nonlinear material behavior of concrete structures which allows for a more realistic simulation of the structural response. The employed material laws automatically guarantee equilibrium in all parts of the structures. This allows computing the maximum resistance directly as a result of the nonlinear analysis without time consuming, manual component checks. This article describes how the safety format according to EN 1992-2, CEN (2005), and Schlune *et al.* (2011), both intended for nonlinear FEA, were tested on short columns loaded in compression and beams loaded in shear.

The safety format according to EN 1992-2 is based on the semi-probabilistic approach with a target reliability for the design resistance for a reference period of 50 years of $\beta_R = \alpha_R \beta = 3.04$, CEN (2002). The material strengths that are to be used in the nonlinear analysis are

$$\tilde{f}_y = 1.1 f_{yk} \tag{1}$$

$$\tilde{f}_c = 1.1 \frac{\gamma_s}{\gamma_c} \alpha_{cc} f_{ck} \tag{2}$$

where f_{yk} is the characteristic yield strength of the reinforcement steel, and f_{ck} is the characteristic design concrete compressive strengths, α_{cc} is a coefficient taking into account long term effects and the way the load is applied and $\gamma_s = 1.15$ and $\gamma_c = 1.5$ are the partial factors for steel and concrete. By inserting the material strengths, \tilde{f}_y , and, \tilde{f}_c , and nominal geometrical parameters, a_{nom} , into the nonlinear analysis, the ultimate load $q_{ud} \{ \tilde{f}_y, \tilde{f}_c, a_{nom} \}$ can be calculated. The design resistance is obtained by division of the obtained ultimate load by the safety factor, γ_θ , and using the associated resistance.

An alternative safety format for nonlinear analysis was proposed by Schlune *et al.* (2011) and led to improved agreement with the target reliability when tested on beams in bending. According to this safety format, mean *in-situ* material strengths, $f_{ym, is} = f_{ym}$ and $f_{cm, is}$, and nominal geometrical parameters, a_{nom} , are to be used in the nonlinear analysis to calculate the resistance $R_m = R \{ f_{ym}, f_{cm, is}, a_{nom} \}$. The design resistance is obtained by division by a resistance safety factor, γ_R , to yield

$$R_d = \frac{R_m}{\gamma_R} = \frac{R \{ f_{ym}, f_{cm, is}, a_{nom} \}}{\gamma_R} \tag{3}$$

Under the assumption of a log-normal distributed resistance, the resistance safety factor can be calculated as

$$\gamma_R = \exp(\alpha_R \beta V_R) \tag{4}$$

where, $\alpha_R = 0.8$ is the weight factor of the resistance side according to the semi-probabilistic approach, β is the target reliability i.e. 3.8 according to EN 1990 CEN (2002), and V_R is the coefficient of variation

of the resistance. The coefficient of variation of the resistance can be calculated as

$$V_R = \sqrt{V_G^2 + V_M^2 + V_F^2} \quad (5)$$

where V_G , V_M and V_F are the coefficient of variation used to account for the geometrical-, model-, and material uncertainty, respectively.

Schlune *et al.* (2011) recommended to use $V_G = 5\%$ for structures that are insensitive to geometrical imperfections.

The model uncertainty is dependent on the modeling approach and the failure mode and can vary significantly between different types of analysis. Hence, it was suggested to chose a problem specific value to account for the model uncertainty, which depends on the modeling approach, the failure mode and the complexity of the structure. Based on a review of round robin analysis and modeling competitions typical values for the model uncertainty of nonlinear models were found to be in the range of $V_M = 5 - 30\%$, Schlune *et al.* (2011).

To estimate the material uncertainty Schlune *et al.* (2011) suggested using a sensitivity study which required two additional nonlinear analysis—one with reduced concrete compressive strength and one with reduced steel strength.

2 TESTING OF THE SAFETY FORMAT ON EXPLICIT LIMIT STATE FUNCTIONS

The safety formats were tested on explicit limit state functions which correspond to the sectional resistance of short columns loaded in compression and beam section subjected to shear forces according to EN 1992-1-1, CEN (2004). First the design resistance using the safety format according EN 1992-2 and Schlune *et al.* (2011) were calculated. Then Monte-Carlo simulations were used to calculate the probability $P(R < R_d)$ and the corresponding reliability indexes.

2.1 Short column

The safety formats were tested on 72 different column sections, covering nine reinforced ratios ($\rho = 0.2 - 3\%$), four concrete compressive strength classes (C20, C40, C60 and C80) and two column widths (200 and 500 mm). The safety format according to EN 1992-2 led to a mean reliability index of $\bar{\beta}_{EN} = 2.51$ with a coefficient of variation of $V_{\beta_{EN}} = 5.2\%$. The application of the safety format according to Schlune *et al.* (2011) led to a better agreement with the target reliability index of $\beta_R = 3.04$

and led to a mean reliability index of $\bar{\beta}_{new} = 3.05$ with a coefficient of variation of $V_{\beta_{new}} = 4.9\%$.

2.2 Shear

To test the safety formats on beams loaded in shear 96 beam configurations were analyzed, covering twelve shear reinforced ratios ($\rho = 0.1 - 1.2\%$), four concrete compressive strength classes (C20-C80) and two effective depths ($d = 300$ and 500 mm). The safety format according to EN 1992-2 led to a mean reliability index of $\bar{\beta}_{EN} = 1.07$ with a coefficient of variation of $V_{\beta_{EN}} = 25.0\%$. This was far below the target reliability index of $\beta_R = 3.04$. The safety format according to Schlune *et al.* yielded a mean reliability index of $\bar{\beta}_{new} = 3.04$ with a coefficient of variation of $V_{\beta_{new}} = 1.9\%$.

3 CONCLUSIONS

When the safety format according to EN 1992-2 was applied on structural models with a high model uncertainty, it led to a reliability level that was far below the target reliability.

The safety format according to Schlune *et al.* (2011) led to much better agreement with the with the target reliability.

ACKNOWLEDGEMENTS

The authors would like to express their gratitude to Rikard Möse and Mikael Furu for their help. The Swedish Research Council, FORMAS, and the Swedish Transport Administration, Trafikverket, are gratefully acknowledged for their financial support.

REFERENCES

- CEN (2002). *EN 1990, Eurocode - Basis of structural design*. European Standard EN 1990, CEN, European Committee for Standardization, Brussels, Belgium.
- CEN (2004). *EN 1992-1-1, Eurocode 2: Design of concrete structures - Part 1-1: General rules and rules for buildings*. European standard EN 1992-1-1, CEN, European Committee for Standardization, Brussels, Belgium.
- CEN (2005). *EN 1992-2, Eurocode 2: Design of concrete structures - Part 2: Concrete bridges. Design and detailing rules* CEN European Committee for Standardization, Brussels.
- Schlune H., Plos M. & Gylltoft K. (2011). Safety Formats for Nonlinear Analysis of Concrete Structures. *Submitted to Magazine of Concrete Research*.

GS_232 — Structural reliability (2)

This page intentionally left blank

Probabilistic analysis of iced structures

J. Marková

Klokner Institute CTU, Prague, Czech Republic

ABSTRACT: The paper is focused on the reliability assessment of specific structures as masts of electric power lines, guided towers and various members of high-rise structures which may be significantly sensitive to atmospheric icing. Presently for the design the CEN standards EN 1993-3-1 (2006), EN 1993-3-2 (2006), CENELEC standard EN 50341 (2001) and also international standard ISO 12494 (2001) may be applied. A considerable difference between the rules for design of masts, towers and other specific structures provided in the above introduced standards currently exists including terminology and definitions, rules for load combinations, reliability differentiation of structures, target reliability levels and definition of the characteristic value of climatic action. It should be noted that the models of wind actions recommended in EN 50351-1 (2001) are currently based on the preliminary ENV Eurocode for wind actions only.

Overview of the partial factors for permanent actions, wind and icing provided in EN 50351-1 (2001) and EN 1993-3-1 (2006) for individual reliability classes is given in Table 1.

Reduction factors ψ_0 for accompanying values of wind and icing are given in Table 2. The last two rows of the table indicate the national decision currently accepted in the National Annexes (NA) of implemented standards in the Czech Republic. The

reduction factor k is used in ISO 12494 (2001) and also in EN 1993-3-1 (2006) to decrease wind pressure assuming a reduced probability for simultaneous 50 year actions combined with heavy icing.

The different definition of ice regions and classes may require the development of different national icing maps for practical applications as it has been decided in the Czech Republic (see Table 3).

The probabilistic methods of the theory of structural reliability are applied for the reliability analysis of a steel member designed according to above introduced CEN and CENELEC prescriptive documents. The probabilistic reliability analysis is based on the design condition given as

$$\theta_R R(X) > \theta_E E(X) \quad (1)$$

where $R(X)$ denotes random resistance and $E(X)$ random action effects for the vector of random variables. The probability of failure P_f determined from the reliability analysis describes likelihood that the condition (1) is not met. Instead of the failure probability P_f , the reliability index $\beta = \Phi^{-1}(1 - P_f)$ is considered in the following analyses where Φ is a standardised normal distribution function. The probabilistic models of basic variables are given in the full paper. The probabilistic model for atmospheric ice load is based here on Wichura (2009) where the maximum loads in Germany having caused serious structural damage were analyzed. The densities of ice accretions at overhead lines were estimated to $3 \pm 0,5 \text{ kN/m}^3$ and the diameter of ice accretion $0,15 \pm 0,03 \text{ m}$. Time dependent and time independent load components are recognized as indicated by Holicky (2009).

It is assumed that the icing I is a leading variable action and the wind W is an accompanying variable action. The target reliability level $\beta_t = 3,8$

Table 1. Partial factors for actions.

Action	EN 50351-1			EN 1993-3-1		
	RC1	RC2	RC3	RC1	RC2	RC3
Permanent	1	1	1	1	1,1	1,2
Wind	1	1,2	1,4	1,2	1,4	1,6
Icing	1	1,25	1,5	1,2	1,4	1,6

Table 2. Reduction factor ψ_0 in different standards.

Action	EN 50351-1	EN 1993-3-1	ISO 12494
Wind	0,4	0,5 k	0,6 k
Icing	0,35	0,5	0,3
Wind in NA	0,5 to 0,25	0,5 k	0,5 k
Icing in NA	in project	0	0,5 k

Table 3. Comparison of ice regions in EN 50341-3 (2003) and ice classes in ISO 12494 (2001).

Region	N0	N1	N2	N3	N5	N8
Weight [N/m]	6	12	23,9	35,9	60	95,7
Class	IR1	IR2	IR3	IR4	IR5	IR6
Weight [N/m]	10	16	27	35	49	65

for common type of structures as recommended in EN 1990 (2002) is indicated in Figures 1 and 2 by the horizontal dashed line.

In design of a simple steel member the partial factors γ for actions and combination factors ψ_0 are accepted following the recommendation of relevant prescriptive documents.

Figure 1 indicates significantly low values of the reliability index β as a function of the load ratio χ between characteristic variable to total loads assuming the design of a steel member according to EN 1993-3-1 (2006), alternative load combinations (6.10) and (6.10a,b) given in EN 1990 (2002) and a set of partial factors for actions recommended for the reliability class RC2 ($\gamma_G = 1,1$, $\gamma_I = \gamma_W = 1,4$).

Figure 2 shows the reliability index β versus the load ratio χ for a steel member assuming the design according to EN 1993-3-1 (2006), EN 50541 (2001),

nationally implemented ISO 12494 (2001) and also EN 1990 (2002), considering here exp. (6.10).

The reliability of steel members, designed according to EN 1993-3-1 (2006) and EN 50341 (2001) seems to be significantly lower than the target reliability level recommended in EN 1990 (2002). No recommendations for the target reliability level of steel masts, towers and other similar structures are provided in EN 1993-3-1 (2006) and EN 50341 (2001).

The models for actions and their combinations introduced in CEN and CENELEC standards should be further calibrated and harmonized. The target reliability levels for three reliability classes should be analysed and optimised. For the assessment of the target reliability index not only the safety of people should be considered but also potential economical losses due to the failure should be taken into account.

For specification of models of icing further research and data collection is needed.

ACKNOWLEDGEMENT

This study is a part of the project LG11043 Probabilistic reliability and risk assessment of structures.

REFERENCES

- EN 50341. 2001. Overhead electrical lines exceeding AC 45 kV – Part 1: General requirements – Common specifications. CENELEC.
- EN 1990. 2002. Basis of structural design, CEN.
- EN 1993-3-1. 2006. Design of steel structures - Part 3-2: Towers, masts and chimneys - Towers and masts. CEN.
- EN 1993-3-2. 2006. Design of steel structures - Part 3-2: Towers, masts and chimneys - Chimneys. CEN.
- ISO 2394. 1999. General requirements on structural reliability.
- ISO 12494. 2001. Atmospheric icing on structures.
- JCSS Probabilistic Model Code, www.jcss.ethz.ch. 2001.
- Fikke, S.M. 2009. Review of results, COST Action 727 WG2. In: IWAIS XIII. Andermatt.
- Holicky, M. 2009. Reliability analysis for structural design. Stellenbosch.
- Holicky, M. & Markova, J. 2005. Calibration of Reliability Elements for Steel Members. In: *Eurosteel 2005*. pp. 1.7–33–38. Volume A.
- N 512. 2010. On inconsistencies between the structural design part of CLC standards and the Eurocodes. CEN/TC/250/SC1 document.
- Wichura, B. & Makkonen, L. 2009. Evaluation of a wet snow accretion model for the Münsterland event in November 2005. In: *IWAIS XIII*, Andermatt.

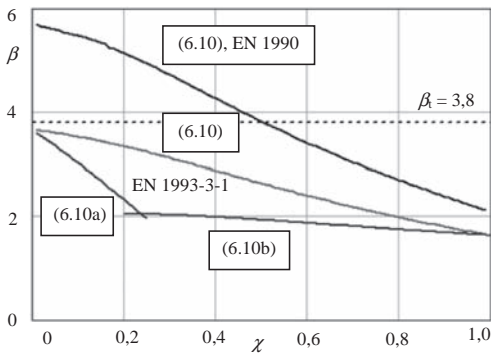


Figure 1. Variation of the reliability index β with the load ratio χ , the load combination based on alternative expressions (6.10) and (6.10a,b) and on a set of partial factors given in EN 1993-3-1 (2006) and EN 1990 (2002) for the reliability class RC2.

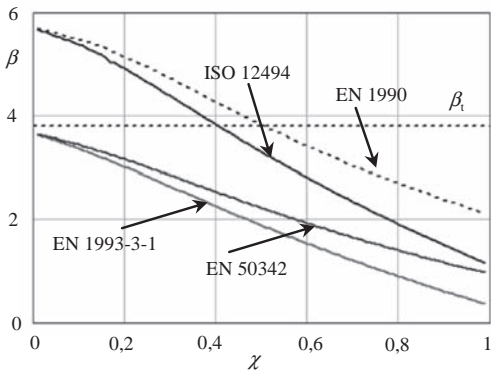


Figure 2. Reliability index β versus the load ratio χ considering reliability elements for structural class RC2 in EN 50541 (2001), EN 1993-3-1 (2006), EN 1990 (2002) and nationally implemented ISO 12494 (2010).

Probabilistic durability assessment of power-producing facilities

M. Holický & J. Marková

Klokner Institute CTU, Prague, Czech Republic

ABSTRACT: The paper is focused on the probabilistic durability assessment of existing structural components of power-producing facilities and their remaining working life in selected hydroelectric power plant of the Czech Republic.

For estimation of the residual working life t_{res} of a structural component, the following expression is applied

$$P_f(t_{res}) = P\{R(t_{res}) - E(t_{res}) < 0\} \approx P_{f,t} \quad (1)$$

when it may be decided about repair or replacing of the component (see Figure 1).

The general requirements for the assessment of structural serviceability were applied for the reliability analysis of many years safely running quick-closing steel valves in a power-plant. The inspection revealed deterioration of the components including their steel cover plates (pitting corrosion with pits up to 2 mm).

It is assumed that the time-dependent depth of corrosion $d_{corr}(t)$ in the steel cover plate of quick-closing valves may be estimated on the basis of the relationship

$$d_{corr}(t) = A t^B \quad (2)$$

where A and B are the parameters of analytical model, which are considered for parameter A in ranges from 0,03 to 0,13 and for parameter B from

0,6 to 0,7, Val et al. (1998). It may be considered here for non-uniform corrosion

$$A = 0,06 \text{ mm} \text{ a } B = 0,7 \quad (3)$$

based on the results of inspection of the actual state.

It is assumed that the steel cover plate of quick-closing valves (old about 50 years) is gradually deteriorating due to non-uniform corrosion with average one-side decrease up to 1 mm and about 30% probability of simultaneous weakening at opposite side of the cover plate. Therefore, the model of corrosion introduced in expression (2) considering parameters in expression (3) leads after 50 years to the actual average depth of corrosion of 1,3 mm.

The ultimate limit state is expressed as the difference $\Delta M(t)$ of the time-dependent resistance moment and the bending moment due to the water pressure

$$\Delta M(t) = \xi_R b (d - 1,33 d_{corr}(t))^2 f_y / 4 - \delta q L^2 / 12 \quad (4)$$

The theoretical models of all variables are listed in Table 1.

Some of the basic variables entering expression (4) are assumed to be deterministic values denoted DET (steel cover plate of span L , width b , parameter of corrosion B and dynamic enhancement

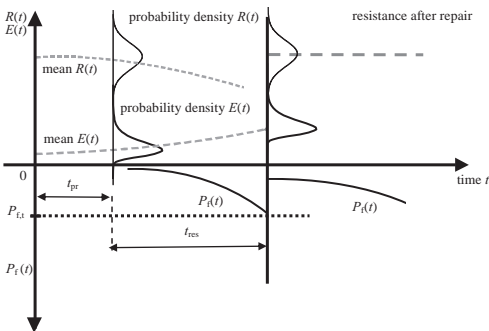


Figure 1. Probabilistic assessment of remaining working life.

Table 1. Probabilistic models of basic variables.

Basic variable	Symbol	Distr.	Mean μ	C.V. V
Yield strength [MPa]	f_y	LN	280	0,08
Plate span [m]	L	DET	0,75	–
Plate thickness [m]	d	N	0,018	0,03
Plate width [m]	b	DET	1	–
Parameter A [mm]	A	N	0,06	0,10
Parameter B	B	DET	0,7	–
Water pressure [kN/m ²]	q	N	157,6	0,1
Dynamic factor	δ	DET	1,3	–
Resistance uncertainty	ξ_R	DET	0,85	–

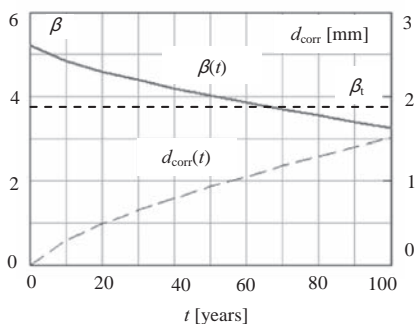


Figure 2. Time-dependent reliability index $\beta(t)$ and one-side corrosion depth $d_{\text{corr}}(t)$.

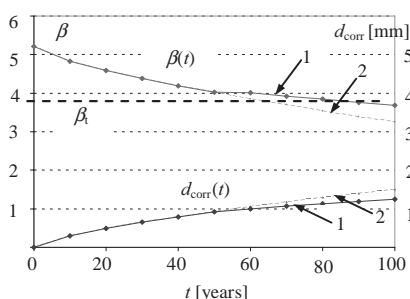


Figure 3. Time-dependent reliability index $\beta(t)$ and one-side corrosion depth $d_{\text{corr}}(t)$ for considered increased maintenance level (case 1). Case 2 indicates common level of maintenance.

factor δ) while the others are considered as random variables having normal (N) or lognormal (LN) distributions.

The reliability of the steel cover plate decreases in time due to the corrosion leading to reduction of its thickness $d_{\text{corr}}(t)$. The value of the target reliability index $\beta(80) = \beta_t = 3,7$ for considered 80 year working life of the cover plate is specified on the basis of required reliability index for a reference period of one year $\beta(1) = 4,7$ given as

$$\Phi(\beta(80)) = (\Phi(\beta(1)))^{80} = (\Phi(4,7))^{80} = \Phi(3,7) \quad (5)$$

The probabilistic reliability assessment of the steel cover plate is based on own software tool developed in software Mathcad.

Initial reliability of the cover plate non-affected by corrosion (reliability index $\beta = 5,2$ corresponding to failure probability $P_F = 9,4 \times 10^{-8}$) satisfies the target reliability level for considered reference period of 80 years ($\beta_t = 3,7$). For one-side corrosion of 1 mm and cover plate 53 years old (current state), the reliability index decreases to $\beta = 4$ (failure probability $P_F = 3,6 \times 10^{-5}$), see Figure 2.

It appears that the working life of the cover plate may be estimated to approximately 70 years when the reliability index $\beta(t)$ decreases to 3,7. Thus, the residual working life of a cover plate is considered to be about 20 years.

In case that a more effective protection level of cover-plate is provided (currently planned) then lower rate of corrosion may be considered (e.g. parameter $B = 0,6$ only, case 1 in Figure 3). New estimation of the residual working life is illustrated in Figure 3 leading to extended residual working life from 70 to 90 years.

The probabilistic assessment of existing structures make it possible to estimate remaining working life of the quick-closing valves and to plan their regular maintenance and required economic resources. The assessment of the quick-closing valves has shown that its residual life-time is about additional 20 years provided that regular maintenance will be made. Protective layers should be renovated and regularly inspected. When the reliability index would decrease below the target reliability index 3,7 (estimated to 20 years), a new reliability assessment of cover plates should be made on the basis of updated material characteristic and corrosion models.

ACKNOWLEDGEMENT

This study is a part of the project No. 103/09/0693 Assessment of Safety and Risks of Technical Systems supported by GACR.

REFERENCES

- CEB Bulletin d' Information No. 238, 1997, New Approach to Durability Design. An example for carbonation induced corrosion, p. 152.
- EN 1990. 2002. Basis of structural design. CEN, p. 87.
- EN 1993-1-1. 2005. Eurocode 3: Design of steel structures - Part 1-1: General rules and rules for buildings.
- Fib Bulletin 34. 2005. Model Code for Service Life Design.
- Holický, M. 2009. Reliability Analysis for Structural Design. Stellenbosch, p. 199.
- Holický, M. & Marková, J. 2007. Probabilistic Design of Structures for Durability. In: ESREL 07, pp. 1757-1762, Taylor & Francis, Balkema.
- ISO 2394. 1998. General principles on reliability for structures.
- ISO 13822. 2001. Bases for design of structures - Assessment of existing structures, ISO, p. 35.
- ISO 13823. 2008. General principles on the design of structures for durability, ISO, p. 39.
- Val, V.D. et al. 1998. Effects of Reinforcement Corrosion on Reliability of Highway Bridges, *Engineering Structures, Vol. 20, No. 11, pp. 1010-1019.*

Uncertainty effects on dynamic response evaluations of wind energy offshore platform

K. Kawano, Y. Kimura, K. Nagafuchi & T. Takahashi

Department of Ocean Civil Engineering, Kagoshima University, Kagoshima, Japan

1 INTRODUCTION

The great challenge is placed on the development of energy without the greenhouse gas emission in these days. The reduction of greenhouse gas emission is great interesting challenge to development of industry. It is appear that the wind energy platform is one of the effective methods on the development of the clean energy. The offshore platform has great possibilities because it is essential to implement the development of the offshore wind energy production.

In the present study, the dynamic response is carried out with the substructure method to an idealized model of the offshore wind energy platform with pile soil foundation, and it is examined about the dynamic response evaluation of the offshore wind energy platform subjected to wave force and seismic force with uncertainty. For uncertain parameters on the wave and seismic force, the Monte Carlo Simulation (MCS) method is applied to carry out the maximum response characteristics of the offshore wind energy platform, which can be evaluated with the second moment approach. Applying the simulation results, it is suggested that uncertainty effects of the dynamic response evaluations including the aging effect could be evaluated with the reliability index for the offshore wind energy platform. For the offshore platform subjected to seismic forces, the reduction effects on the seismic response are examined with the base isolation system equipped under the deck of the structure. It is suggested that the uncertainty effects on the wave and seismic forces play important roles on the reliable estimation of the dynamic response of the offshore platform and the aging effects could be essential for the reliable estimation. Moreover, it is shown that the effective reduction of the seismic response could be carried out with the base isolation for the offshore platform with wind energy generation tower.

2 SUMMARY OF RESULTS

For the idealized two-dimensional offshore platform with wind energy tower subjected to wave and

seismic forces, the dynamic response evaluation is carried out with the time domain analysis. The idealized offshore platform with soil-pile foundation system as shown in Figure 1 has the base isolation system. The height of the offshore platform is 60 m, and the wind energy production tower has 30 m height. The depth of water is 50 m. The offshore platform is made of steel, and is equipped with the large diameter member near the sea surface, which can be helpful to perform effective reduction of the reaction force to the sea bed.

Figure 2 shows the reliability index of the offshore platform with the deterioration effects. The abscissa denotes the aging year and each line corresponds to the reliability index for the typical member.

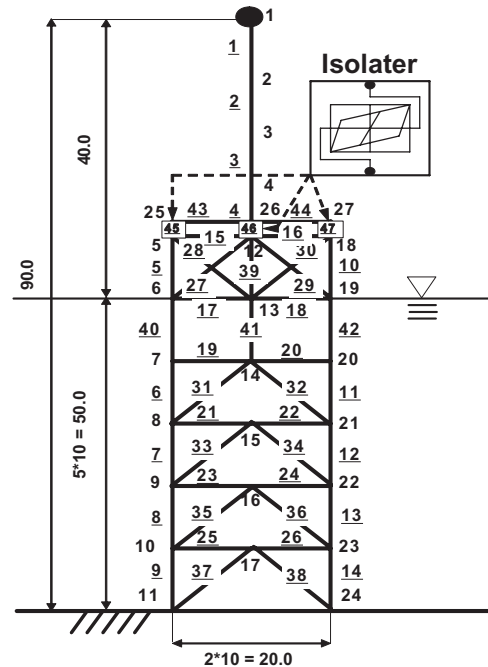


Figure 1. A idealized offshore platform with wind power generation system.

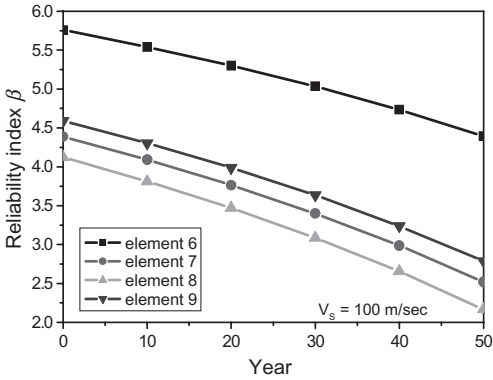


Figure 2. Reliability index of offshore platform due to aging effects (Wave force simulated).

The limit state function is the bending stress that the strength of the yield bending stress has 240 MPa and the coefficient of variation is 10%. The reliability index gradually declines for increase of aging. The difference on the reliability index to these nodal points is closely related with the stress response induced by the structural properties. The reliability index on the random sea wave situation is considerably influenced by the deterioration due to the aging. It is suggested that the deterioration of the strength as well as the random property of wave forces plays important roles on the reliability estimation for the dynamic forces.

Figure 3 shows the reliability index for the deterioration effect due to the aging. The limit state function is the bending stress at the nodal point 3, which is caused to most severe responses on the seismic force. The seismic motion is Taka-ns with the maximum input acceleration 300 gal. The abscissa denotes the reduction ratio of the member due to the aging effect. Comparisons are made for the situation of both the fixed foundation and the soil-structure interaction. It is assumed that the mean value of the yield bending stress is 240 Mpa and its coefficient of variation 20%. It is noted that the considerable decline of reliability index is brought about for the aging, and it plays important roles on the response evaluation. Especially, for the reduction factor over about 60%, taking into account the results that the reliability index becomes relatively small value for the aging situation, it is necessary for the safety of the structure to enhance the strength of the structure against the seismic force.

Figure 4 shows the time history of displacement responses due to severe seismic force of which the maximum acceleration is adjusted to 800 gal. Comparisons are made for the responses with the base isolation and without the

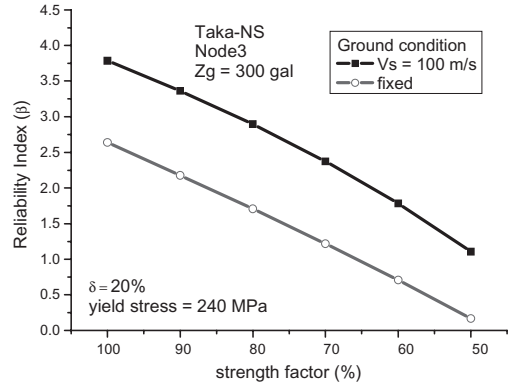


Figure 3. Reliability index for deterioration due to aging.

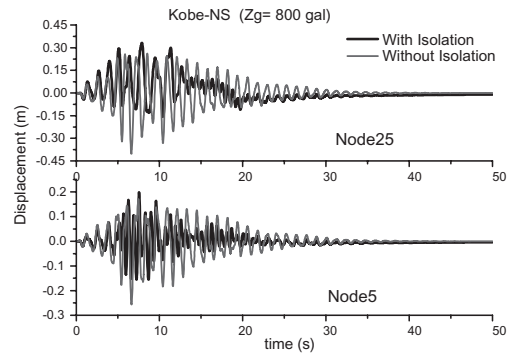


Figure 4. Comparisons of time history of displacement response with base isolation and without base isolation.

base isolation at the nodal point 5 and 25. The displacement response at the nodal point 5 under the deck is effectively reduced by the base isolation. It is expected for the base isolation to play important roles on the response reduction against the seismic force.

3 CONCLUSIONS

The dynamic response evaluation of the offshore platforms with wind energy generation tower is examined. In the present study, it is suggested that the uncertainty effects on the wave and seismic forces play important roles on the reliable estimation of the dynamic response, and the aging effects could be essential for the reliable estimation of the offshore platform. Moreover, it is shown that the effective reduction of the seismic response could be carried out with the base isolation for the offshore platform with wind power generation tower.

Seismic risk assessment of building-elevator systems based on simulated ground motion considering long period components and phase characteristics

M. Kohiyama

Keio University, Yokohama, Japan

T. Kita

TOTO, Ltd., Kitakyushu, Japan (Formerly, Keio University)

To address the problem of elevator rope sway in a high-rise building, a method to evaluate the seismic damage risk of a building-elevator system is proposed using a model of group delay time of ground motion. The response of the system is evaluated by the response spectrum method for a non-classically damped system.

A building site is assumed at Shinjuku, Tokyo in Japan and possible earthquake source zones are considered in the Chuetsu District, Niigata Prefecture, the northwest of Chiba Prefecture, Miyagi Offshore region and Tonankai region.

For 50, 100, 150, 200 and 250-meter-high buildings, models of building-elevator systems are constructed. In this study, only suspension rope is considered for simplicity. The suspension rope is modeled by finite elements.

The response is modeled by the lognormal distribution, and the damage probabilities of the elevator rope is obtained considering the seismic event occurrence, the probability distribution of the earthquake magnitude and probability of elevator rope damage due to synthesized seismic ground motions.

The method to synthesize seismic ground motion using observed records is proposed. The Fourier amplitude spectrum is evaluated based on a method proposed by Zama (2000). With respect to phase characteristics, the following regression curve of group delay time, T_{gr} , is proposed:

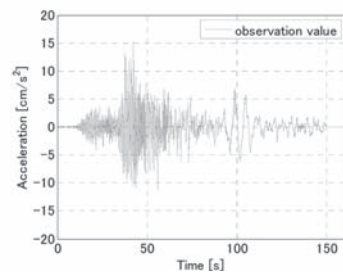
$$T_{gr} = \begin{cases} \frac{\ln(A_0(f)/A)}{a_g(f + f_b) + c_g} & (f \leq f_b) \\ \frac{\ln(A_0(f)/A)}{c_g} & (f > f_b) \end{cases} \quad (1)$$

where A_0 is an initial amplitude and A is a constant for normalization, which can be 1. Parameters, a_g and c_g are regression coefficients and f_b predominant frequency of the surface layer.

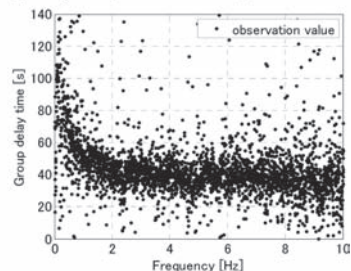
Figure 1 shows accelerograms and group delay times of an observed record (K-NET Shinjuku NS component of the 2004 Niigataken Chuetsu earthquake) and the wave synthesized by the proposed method. In both waves, long period components predominate after short period component. Duration of long period components of the synthesized wave is as long as that of the observed record.

The length of the suspension rope of a counterweight can be obtained by the building height minus the length of rope of a car, approximately. Figure 2 shows the damage probability of rope of both a car and a counterweight in 50 years for the five building models, in which all sources are considered. The models and the model names correspond to the height of the building, e.g. Model H50 stands for the height of the building is 50 m.

a) Accelerogram (observed record)



b) Group delay time (observed record)



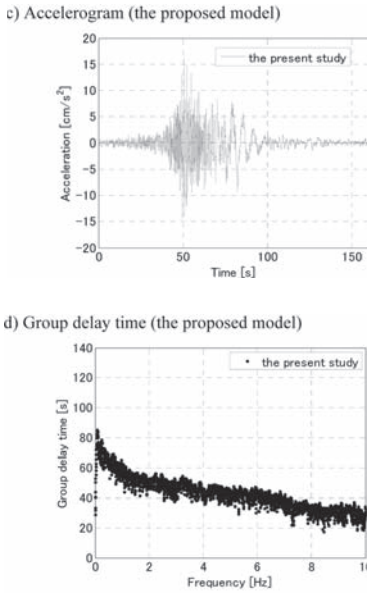
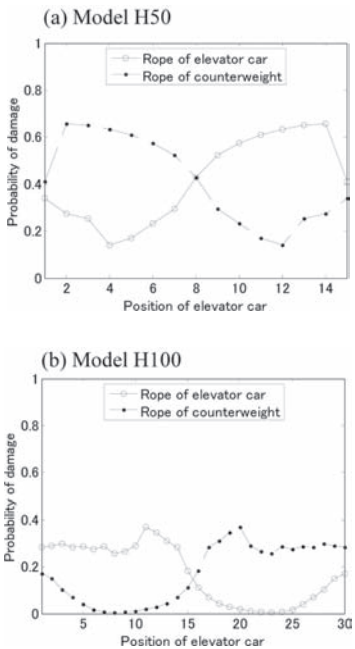


Figure 1. Comparison of group delay times and accelerograms between an observed record (K-NET Shinjuku NS component of the 2004 Niigataken Chuetsu earthquake) and a wave synthesized by the proposed method.



For each building model, the probability of rope damage changes significantly depending on the car position. When elevator rope resonates, i.e. the natural period of rope is close to the predominant period of an input wave or the natural period of a

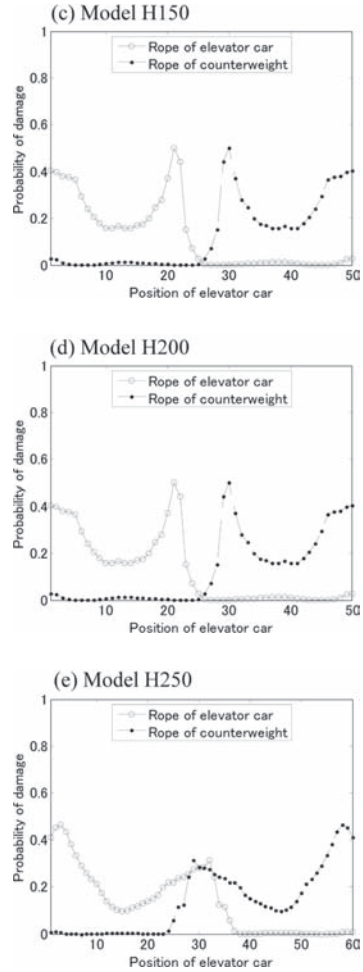


Figure 2. Probability of the rope damage in 50 years considering ropes of both a car and a counterweight. The damage threshold of the rope is 0.2 m.

building at low order of the modes, the response of a building-elevator system grows large. Thus, to reduce the probability of rope damage, it is important to avoid resonance of the rope.

It is clarified that damage risk of a building-elevator system can be evaluated and safer car position can be sought based on the proposed method. It is recommended to move and park an elevator car at lower risk positions when few people use the elevator such as in nighttime.

REFERENCE

Zama, S. 2000. Semi-Empirical Expression for Acceleration Spectrum of Long-Period Ground Motion. *Report of National Research Institute of Fire and Disaster* 89: 1–10 (in Japanese).

Structural reliability analysis of steel sheet-pile seawalls subjected to corrosion in harbour environment

J. Boéro, H. Yáñez-Godoy & B. Capra
OXAND S.A., Avon, France

F. Schoefs
*LUNAM Université, Université de Nantes-Ecole Centrale Nantes, GeM,
Institute for Research in Civil and Mechanical Engineering, Nantes, France*

1 INTRODUCTION

This article summarizes research carried out in the framework of the GEROM (risk management of marine and river harbor structures) project with the Scientific Interest Group MRGenCi (www.mrgenci.org). The main objective of the project is to develop a risk management methodology to assist owners in establishing decision-making procedures through maintenance master plans. The project is split into two phases: the initial phase consists of a study into maintenance management practices for harbor infrastructure and a preliminary risk analysis to identify vulnerable structures (ageing and stakes); the second phase then consists in quantifying the risks associated with the vulnerable structures identified in the initial phase.

The initial phase has been described in several papers (Boéro et al., 2009a, b). The present article is concerned only with the second phase, specifically the reliability analysis of steel sheet-pile seawalls undergoing uniform corrosion.

For this purpose, a stochastic (spatial-temporal) model of steel corrosion is proposed, based on a statistical analysis of data collected from several French ports in multiple zones that have been exposed to marine environment for varying lengths of time. At the preliminary stage, an in-depth understanding of the following issues is necessary:

- interpretation of the experimental data and physico-chemical phenomena which allow spatial corrosion to be treated essentially as a one-dimensional problem, according to the depth of the structures under consideration (Boéro et al., 2009c). An analysis of corrosion mechanisms shows that the process can be modeled by 5 independent random variables corresponding to 5 different exposure zones, each one based on a different random context;
- probabilistic modeling for taking into account the variability of the phenomena. Having taken the preceding points into consideration, the stochastic

time-dependent corrosion model presented in this paper is based on the temporal evolution of the probability distribution parameters defining steel loss of thickness in each exposure zone.

Predictions resulting from the corrosion model are then used to perform a time-function reliability calculation for corroded harbor structures. A coupled approach between a FORM-algorithm and deterministic finite element model (Cast3M) is used to assess the β index. An analysis of the effect of the basic variables with time concludes the paper.

2 MODELLING OF STOCHASTIC CORROSION FIELDS IN STEEL HARBOUR STRUCTURES BASED ON FEEDBACK FROM FRENCH PORTS

The proposed corrosion model takes into account the spatio-temporal aspects of corrosion on steel sheet piles seawalls or cofferdams. It is based, after data cleansing, on a statistical analysis of over 35000 measurements taken from several French ports (Boéro et al., 2009c).

The model is based on the general hypothesis that corrosion can be considered to be a decoupled phenomenon on the R^2 plane of a structure; that is, in the length direction x and along the depth z .

The spatial aspect of corrosion in the x -direction is represented by the deterministic tendency $T(x, z_p, t)$ which evolves in time t and depends on the exposure zone z_j (tidal zone, immersion zone, etc.). Corrosion may be considered as being uniform in the z -direction within a given exposure zone z_j (tidal zone, immersion zone, etc.). The corrosion distribution $c(z_p, t, \theta)$ is therefore assumed to be independent of x , dependent on the time t and discretized along the depth z by exposure zone z_j . Thus the predictive corrosion model takes the following form (1):

$$c(x, z_p, t, \theta) = T(x, z_p, t) + c(z_p, t, \theta) \quad (1)$$

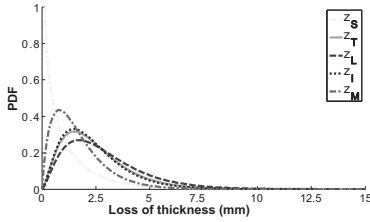


Figure 1. Steel thickness loss distributions obtained from the corrosion model for the different zones over a time period $t = 25$ years.

where $c(x, z_j, t, \theta)$: loss of thickness as a function of the x -coordinate and the time t , for the exposure zone z_j (mm); $T(x, z_p, t)$: deterministic tendency with respect to a constant mean corrosion level throughout the x -direction; $c(z_p, t, \theta)$: random variable representing the loss of thickness with time t for the exposure zone z_j (mm).

The Gamma probability distribution is used to characterize the variability of the corrosion $c(z_p, t, \theta)$, since it is the theoretical probability law that can be best fitted, in terms of maximum likelihood, to the empirical distribution of steel loss of thickness. The Gamma distribution is characterized by a shape parameter α and a scale parameter β which depends on the mean and standard deviation of steel loss of thickness and which evolves, according to the present model and in the absence of other information on the stochastic structure, in a spatio-temporal manner. Steel thickness loss distributions obtained from the corrosion model for a 25 year exposure period in the marine environment are shown in Figure 1 ($z_S =$ Splash; $z_T =$ Tidal; $z_L =$ Low seawater level; $z_I =$ Immersion; $z_M =$ Mud).

The paper presents the complete model, including the piece-wise stationary stochastic field with depth.

3 TIME-DEPENDENT STRUCTURAL RELIABILITY OF A CORRODED STEEL SHEET PILES SEAWALL

Based on the previous corrosion model, a time dependent reliability analysis is carried out on a sheet-pile wall (Figure 2). For simplicity and in view to simplify the analysis of results we consider in this paper that U piles are uniformly corroded with the “out-pans” kinetics. Moreover, if the corrosion has been shown to be stationary, the identification correlation length along x is still a challenge (Boéro 2010): we assume here that the correlation is negligible after 20 meters and that the wall can be modeled with a 2D model (Figure 2). Thus we consider the stability of a sheet pile 2 meter wide, the distance between tie-rods. Finally, the tie-rods

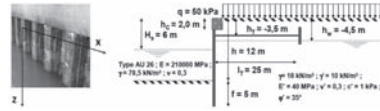


Figure 2. Geometrical and mechanical characteristics of the quay.

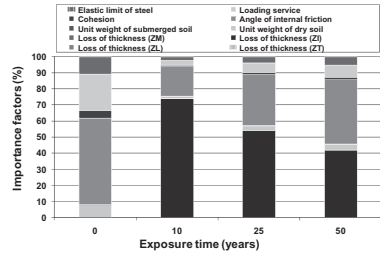


Figure 3. Evolution of importance factors with time (point of the section towards the seaside excavation).

are protected (galvanization) and are considered not to be affected by corrosion.

Let us focus only on sensitivity factors. Figure 3 reports the values of these factors obtained when computing the reliability index in the most critical section at time $t = 0, 10, 25$ and 50 years. The results are very interesting. At the beginning of the lifetime, dominant random variables are angle of internal friction, loading service (operating excess load) and steel yield stress with a pro-eminent role of the first (55%). After 10 years, the role of the corrosion in zone Z_I is already pro-eminent (more than 70) and angle of internal friction follows. This role of corrosion decreases with time and is the same than the role of angle of internal friction after 50 years (almost 40%). Note that of course this trend depends on the position of the steel section under consideration. If we focus on the section near the tie-rod (see figure 9), the role of corrosion random variable, here in area Z_T increases with time.

REFERENCES

Boéro, J., Schoefs, F., Capra, B. & Rouxel, N. 2009a. Technical management of French harbour structures. Part 1: Description of built assets. *PARALIA*, Published on line December 21th 2009, 2: 6.1–6.11.

Boéro, J., Schoefs, F., Capra, B. & Rouxel, N. 2009b. Technical management of French harbour structures. Part 2: Current practices, needs – Experience feedback of owners. *PARALIA*, Published on line December 21th 2009, 2: 6.13–6.24.

Boéro, J., Schoefs, F., Melchers, R. & Capra, B. 2009c. Statistical Analysis of Corrosion Process along French Coast. In: Furuta, Frangopol & Shinozuka (eds), *ICOSSAR'09; Proc. int. conf., Osaka, Japan, 13–19 September 2009*. London: Taylor & Francis Group.

GS_311 — Structural reliability (3)

This page intentionally left blank

Reliability-based design optimization via a concurrent process

K.W. Liao

National Taiwan University of Science and Technology, Taipei, Taiwan

This paper presents a new approach to evaluate the Reliability-Based Design Optimization (RBDO) via a concurrent calculation process. RBDO considers variability in design variables/parameters, searching an optimum point with higher robustness and lower probability of failure. A traditional way for RBDO is a nested double-loop approach where the outer loop conducts optimization and the inner loop deals with probabilistic analysis. The computational cost for this double-loop procedure is prohibitive for most practical problems. Many algorithms have been developed to overcome this issue (Myers and Montgomery 2002; Qu and Haftka 2002; Du and Chen 2003; Youn and Choi 2004; Liao and Ha 2008).

In development/search of a concurrent approach, one of the major concerns is the computational efficiency. As introduced, RBDO analysis is a nested double-loop calculation, in which the reliability analysis and deterministic optimization are coupled. For a concurrent approach, techniques used to decouple these two analyses are similar to those utilized in a Multidisciplinary System (MS), which composes two or more coupled subsystems. Thus, analyses of MS are briefly reviewed to help the built of a concurrent algorithm of RBDO.

Multidisciplinary analysis or system level analysis is the process of searching a feasible design in a MS. Finding an optimal feasible design for a MS is then called Multidisciplinary Design Optimization (MDO). Although many approaches have been proposed to solve MDO problem, they may be categorized into two major groups: including the system level analysis or not. It is obvious that system analysis may take most of computational time in MDO problem. Therefore, many proposed approaches attempt to decompose the MS into several subsystems (e.g., distributed systems) to save the computational time. In this regard, the distributed system approaches are utilized in our proposed RBDO approach to avoid the system level analysis, which is a series of coupled analyses (e.g., the nested double-loop approach). One of the keys to utilize MDO on RBDO problem is the two major operations in RBDO (i.e., the reliability analysis and optimization) must be decomposed. The Most Probable Point (MPP) obtained from

inverse reliability analysis plays a key role in the process of decomposing. Details are given in the following sections.

The original MS is an integrated system giving that many feedback and feed-forward activities among subsystems. In order to lessen the burden of the feedback and feed-forward computation, auxiliary design variables and compatibility constraints are introduced in the distributed system approach. The auxiliary design variables are “copies” of the computed linking variables from upper-level to lower-level or vice versa (Kroo et al., 1994). Inconsistency exists among these sharing variables and responses among each distributed systems in the middle of optimization process. The measure of such inconsistency is called discrepancy functions and the compatibility constraints are used to ensure convergence is achieved. Once MS is decomposed into several subsystems in MDO, the goal of upper-levels is to minimize the system overall objective function, while the lower-levels (i.e., subsystems) attempt to minimize discrepancy functions that are the inconsistency (i.e., deviations between targets and responses) among the original variables (i.e., linking variables) and the auxiliary variables.

Note that unlike the typical MDO approach described above, in our proposed concurrent RBDO approach, the objective of the upper level is to minimize the discrepancy of the linking variables obtained from each analysis in the lower level. The lower level has two sub-analyses such as the deterministic optimization and the inverse reliability analysis. Through the proposed approach, the optimization and reliability analysis need not to be conducted sequentially. Instead, these two analyses can be executed simultaneously to accelerate the analysis procedure and therefore, the computational cost is reduced.

Several important topics, which play critical roles in our proposed evaluation process of RBDO, are introduced in the following manner. Existing multidisciplinary optimization approaches are reviewed first; followed by the introduction of the difference between Deterministic Optimization (DO) and RBDO. The major idea of the proposed approach is then described and the general formulation of the

proposed method is given. In the end, numerical examples are provided, demonstrating the concepts of the proposed method. RBDO of a cantilever beam is first used to examine the accuracy of the proposed approach by comparing the results of the double-loop RBDO approach. Details of

RBDO solved by bi-level optimization technique are revealed through other numerical example.

Keywords: optimization, reliability analysis, concurrent process

Efficient method for the probability assessment of ellipsoidal limit state surface

S.D. Koduru

University of California, Berkeley, CA, USA

1 INTRODUCTION

Performance-based earthquake engineering (PBEE) requires simulation of the structural response under extreme loading conditions, and involves detailed numerical modeling of the structure. In order to measure the structural performance, the quantities of interest are damage, monetary loss, and down-time, which include *nonlinear* structural response under a dynamic loading event. Hence, the structural reliability methods that address the nonlinear dynamic problems have been a major research focus in the recent years. For addressing such problems, the *peak* response measures, such as peak deformations, are often considered as the performance measures that enter the limit state function. Conversely, *cumulative* response measures may provide an improved measure of structural performance for the structures subjected to long duration, large magnitude earthquakes.

Cumulative response measures include the effects of the total number as well as the amplitude of load cycles on the structural behavior over the duration of a dynamic loading. Thus, the characteristics of the limit state surface with the

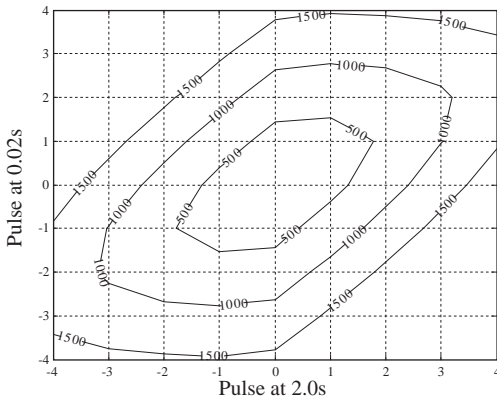


Figure 1. Behaviour of the energy limit-state surface (in Nmm) of the SDOF with random pulses in the loading spaced at 0.02s and 2.0s (Koduru 2008).

cumulative response measures, in the presence of stochastic dynamic loading, are recently studied (Koduru 2008).

The results indicate that the limit-state surface has a closed shape (Figure 1), and may not be easily amenable to traditional reliability methods, such as the first order reliability method (FORM) and the hyper-parabola approximation of the second order reliability method (SORM). The presence of large number of random variables due to the stochastic load model prevents the response surface methods from being computationally efficient. Previously, probability bounds are proposed to estimate the probability content inside the closed limit-state surface. In this paper, an improved method for the estimation of the probability content is proposed.

2 BINNING METHOD

The proposed method involves an approximation of the limit state surface as a hyper-ellipsoid (Figure 2). The traditional methods to estimate the probability content of an ellipsoid require a complete second order derivative (Hessian matrix) of the limit state function. The computational effort to assess the derivative is considerable in a high-dimensional problem with significant number of

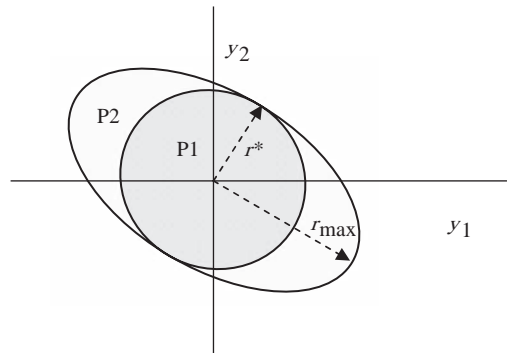


Figure 2. Idealization of the limit state surface in the standard normal space.

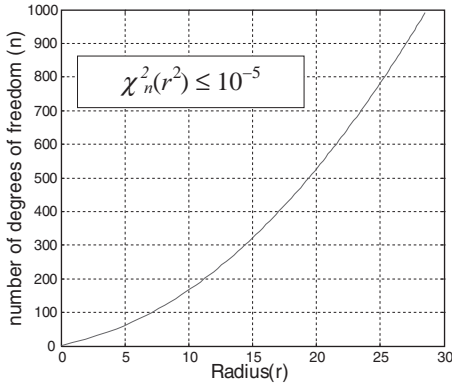


Figure 3. Variation of probability content from Chi-square distribution depending on the number of degrees of freedom.

the random variables. Furthermore, the performance assessments in PBEE are performed on large finite element models of the structure with nonlinear time history analysis. Thus, the computational cost increases with the number of evaluations of the limit state function.

In the present study, the probability content of the hyper-ellipsoid is estimated by modifying the numerical method known as “binning method” in (Somerville 2001). The modified numerical method in the present study employs only the maximum (r_{\max}) and the minimum (r^*) semi-axis lengths of the hyper-ellipsoid. Instead of the intermediate semi-axis lengths and the full Hessian matrix, the distance of the limit-state surface from the origin is estimated along each of the random variable axis. This significantly reduces the computational effort in the evaluation of limit state function gradient that is employed for the search of limit state surface. Furthermore, in a high-dimensional random space, the minimum semi-axis length of the hyper-ellipsoid is approximated by the minimum radius of the ellipsoid along the random variable axes. This approximation is proposed due to the nature of chi-square distribution. At large number of degree of freedom, the contribution of probability content from the smaller radii is practically negligible as shown in Figure 3.

Hence, this approximation further reduces the computational cost and makes the proposed method especially advantageous to the high-dimensional problems with stochastic ground motion models. However, for high probability values, the hyper-ellipsoid approximation of the limit state surface may no longer be valid and a cylindrical-ellipsoid may become valid. In such cases, the proposed method results in an underestimation of the probability content.

Table 1. Probability content of the ellipsoid for SDOF with 500 random variables.

Method	Value	$g(\mathbf{x})$ Evaluations
Monte Carlo Simulation	0.7416	50000
Hyper-sphere approximation	1.0000	8010
Proposed method mean	0.7322	3000
Upper bound	0.8179	–
Lower bound	0.6575	–

3 EXAMPLE

The numerical examples are presented with a single degree of freedom (SDOF) model with hysteretic energy as the performance measure and two-storey two bay reinforced concrete frame with the monetary loss as the performance measure. The results from the proposed method are compared to those from the mean-centered Monte Carlo sampling method. The results (Table 1) for the SDOF show that the proposed method provides accurate probability estimates for the hyper-ellipsoid in a high-dimensional space with considerable computational efficiency.

4 CONCLUSION

An efficient method for the probability estimation is proposed for the reliability problems with cumulative performance measures and stochastic dynamic loading modeled by Gaussian white noise. The proposed method takes advantage of the high-dimensional random space, and the closed point-symmetric shape of the limit state surface for the cumulative performance measures, in order to reduce computational cost by several orders of magnitude. However, the efficiency of the proposed method is reduced at high probability values and for the cylindrical-ellipsoid shape of the limit state surface.

REFERENCES

Koduru, S.D. 2008. *Performance-based Earthquake engineering with the first-order reliability method*, Ph.D Dissertation, University of British Columbia, Vancouver, Canada.

Somerville, P.N. 2001. Numerical computation of multivariate normal and multivariate-t probabilities over ellipsoidal regions. *Journal of Statistical Software* 6 (8): 1–10.

Modeling structural degradation of RC bridge columns subjected to cumulative seismic damage and their fragility estimates

R. Kumar & P. Gardoni

Texas A&M University, College Station, TX, USA

ABSTRACT: Bridges should have a minimum safety level at all times during their design lives. One of the major concerns for bridges is the deterioration in their performance during their service life. Work has been undertaken to predict the performance of as-built bridges when subjected to earthquakes. However, for a design based on long-term seismic performance it is imperative to be able to predict the deterioration in the reliability due to cumulative seismic damage.

The current seismic design practices focus primarily on the ability of as-built bridges to withstand the design earthquake. Major contributions have been made by researchers to quantify structural degradation due to cumulative seismic damage. However, the increase in vulnerability of bridges due to structural degradation has not been investigated.

This paper develops a probabilistic model for the deformation capacity of reinforced concrete (RC) bridge columns subject to cumulative seismic damage. The proposed model accounts for the degradation in the ultimate curvature capacity associated to low-cycle fatigue. The proposed model is then used to assess the fragilities of RC bridge columns for given deformation demand. The novelty of this research lies in the development of the

probabilistic models for curvature capacity, and its implementation in a degradation-dependent deformation capacity, which is used to assess the fragility of three example columns subject to seismic degradation. The proposed probabilistic models can be used to assess the effects of structural degradation on the safety of bridges.

The probabilistic model is calibrated based on data generated from pushover and cyclic load analysis using finite element method (FEM). The FEM model accounts for the cracking and pinching of RC sections to properly simulate the degradation process. Presently, laboratory data on the capacity of damaged columns is unavailable and thus the model must be recalibrated when the data is available.

It is found that the cumulative seismic damage can significantly affect the vulnerability of bridge columns. Thus the proposed probabilistic model is useful for a seismic design that properly accounts for long-term safety and reliability. It is found that the deformation capacity of RC columns deteriorates due to low-cycle fatigue when damage exceeds a specific transition value. As a result, the fragilities of RC columns for given deformation demand increases once the value of damage exceeds the threshold value.

Calibration of reliability-based load rating method for New York State

Michel Ghosn

The City College of New York/CUNY, New York, USA

Bala Sivakumar

HNTB Corporation, New York, USA

Feng Miao

The City College and the Graduate Center/CUNY, New York, USA

The American Association of Highway and Transportation Officials (AASHTO) has recently adopted the Load and Resistance Factor Rating (LRFR) Specifications which were calibrated to provide uniform reliability levels represented by a target reliability index $\beta = 3.5$ for Inventory Ratings and $\beta = 2.5$ for Operating Ratings. The calibration process was based on a generic database that was considered to be representative of truck weight and traffic spectra at typical U.S. bridge sites. Recognizing the limitations of this generic data set, the LRFR specifications provide sufficient flexibility and allow state agencies to adjust the LRFR load factors based on their individual conditions and site-specific or state-specific information. The goal would be to develop an LRFR process that is compatible with current state procedures while considering their particular loading conditions.

Recent observations made on truck weight data collected from Weigh-In-Motion stations (WIM) at representative NY State sites have shown that truck weights in New York can be significantly heavier than assumed during the calibration of the AASHTO LRFR specification. Therefore a recalibration of LRFR provisions was considered necessary.

This paper develops a Load and Resistance Factor Rating (NYS-LRFR) methodology for New York bridges. The methodology is applicable for the rating of existing bridges, the posting of under-strength bridges, and checking Permit trucks. The proposed LRFR methodology is calibrated to provide uniform reliability index values for all applications. The reliability calibration of live load factors is based on live load models developed using Truck Weigh-In-Motion (WIM) data collected from several representative New York sites. The live load models provide statistical projections of the

maximum live load effects expected on New York bridges.

The safety evaluation of existing New York bridges can be executed using a LRFR equation that takes the form:

$$R.F. = \frac{\phi_c \phi_s \phi R_n - \gamma_{DC}(D_{C1} + D_{C2}) - \gamma_{DW} D_W}{\gamma_L L_n} \quad (1)$$

where R.F. is the rating factor, R_n is the nominal resistance, D_{C1} is the dead load effect of pre-fabricated components, D_{C2} is the dead load effect of cast-in-place components and attachments, D_W is the nominal dead load effect for the wearing surface, L_n is the live load effect of the nominal load used to calculate the Rating Factor including dynamic allowance and load distribution factor, ϕ is the resistance factor, ϕ_c is the condition factor, ϕ_s is the system factor, and γ are the load factors. A Rating Factor $R.F. \geq 1.0$ indicates that the trucks whose live load effects can be modeled by L_n can safely cross the bridge.

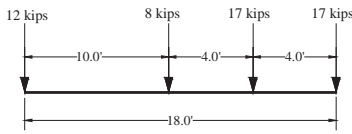
1 LEGAL TRUCK RATING

A new set of NYS Legal Trucks along with appropriate live load factors are proposed for performing Operating Level Ratings of existing bridges. Figure 1 provides the proposed NYS Legal Trucks while Table 1 lists the proposed NYS Live Load factors for Legal Truck Load Operating Rating.

2 PERMIT TRUCK RATING

Permit load factors are calibrated for divisible loads and non-divisible loads for single crossings as well

a) SU4 Legal Load (27 tons)



b) Type 3S2 Legal Load (36 tons)

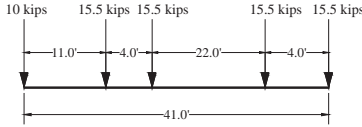


Figure 1. Proposed New York State Legal Trucks for bridge rating.

Table 1. NYSDOT live-load factors, γ_L for Legal Loads.

Traffic volume (one direction)	Load factor for multi-lane bridges (use LRFD load distribution factor for multi-lanes)	Load factor for single-lane bridges (use LRFD load distribution factor for a single lane without removing the multiple presence factor)
ADTT \geq 5000	1.95	2.65
ADTT = 1000	1.85	2.50
ADTT \leq 100	1.65	2.20

Table 2. NYSDOT permit load factors, γ_L .

Permit type	Frequency	Loading condition	Distribution factor	ADTT (one direction)	Permit load factor, γ_L
Annual Divisible Load	Unlimited trips	Multi-lane bridges Mix with traffic	Multi-lane	ADTT \geq 5000	1.20
				ADTT = 1000	1.15
				ADTT \leq 100	1.10
Annual Divisible load	Unlimited trips	Single lane bridges	Single Lane DF after dividing out MP = 1.2	ADTT \geq 5000	1.20
				ADTT = 1000	1.15
				ADTT \leq 100	1.10
Non-Divisible loads	Unlimited trips	Multi-lane bridges Mix with traffic	Multi-lane	All ADTT	1.10
Non-Divisible loads	Unlimited trips	Single lane bridges	Single Lane DF after dividing out MP = 1.2	All ADTT	1.10
Special Hauling and Superloads	Single Crossing	Multi-lane bridges Mix with traffic	Single Lane DF after dividing out MP = 1.2	All ADTT	1.10
Special Hauling and Superloads	Single Crossing	Single lane bridges	Single Lane DF after dividing out MP = 1.2	All ADTT	1.10

as unlimited crossings of bridges. The calibration of the permit load factors was based on the analysis of multiple presence probabilities and on the uncertainties associated with estimating the load effects of the permit trucks and those of the random trucks that may cross simultaneously with the permit. Accordingly, lower permit load factors are recommended than those in the AASHTO LRFR. The permit load factors are listed in Table 2.

3 LOAD POSTING

An equation is proposed for determining Posting weight limits for bridges with low Rating Factors as a function of the effective span length. The posting equation was calibrated so that posted bridges

will meet the same target reliability $\beta_{\text{target}} = 2.0$ used for the Legal Load Ratings and the Permit weight checks. The posting weight calibration however was based on several assumptions regarding the probability of having overweight trucks cross posted bridges. It is proposed that two different posting weights should be provided one for single unit trucks and the other for semi-trailer trucks. The proposed equation is given as:

$$\text{Posting Load} = W [RF + 0.00375(L - 110)(1 - RF)] \quad (2)$$

where W = Weight of Rating Vehicle (54 kips for Single Trucks, or 72 kips for semi-trailers)

RF = Legal Load Rating Factor for the governing NYS-Legal Truck

L = Effective span length in feet.

Structural reliability in the fire situation, the effect of active fire safety

Jean-Baptiste Schleich

Engineering Office E.A.S.E., Luxembourg

Keywords: Fire design situation in buildings, Risk of fire activation, Active fire safety measures, Natural fires, Structural reliability, Eurocode on Actions on Structures exposed to fire EN1991-1-2

1 INTRODUCTION

This contribution describes the present state of the art in fire engineering developments according to EN1991-1-2 (DAV 20.11.2002). Essential theoretical relations in the field of the probability of getting a severe fire, when regarding the positive effect of active fire safety, are laid down and discussed, as well as the consequence on structural failure probability is investigated.

2 ACTIVE FIRE SAFETY

Furthermore in the following described buildings, instead of paying for protection materials in order to fulfil ISO fire requirements of 90 minutes and more, this money was used for the installation of active fire safety measures. Active fire safety produces real safety for people, f.i. by adequate partitioning, by safe escape routes, by proper smoke venting or by conveniently designed & maintained sprinkler systems. But at the same time active fire safety contributes in helping the structure resist realistic heating conditions, as the potential severity of a fire and its probability of occurrence are cut down.

A first step consists in accepting the global structural analysis in the fire situation, in considering the accidental combination rule for actions during fire exposure and in designing according to natural fire conditions. A second step consists finally in considering Performance Based Requirements i.e. the fire safety of occupants and firemen, the protection of property and environment, a realistic required fire resistance period, and a realistic structural fire design including active fire safety.

The main objective is given by the acceptable safety level, which may be defined by comparison to the different existing risks in life including the structural collapse of a building in normal

conditions of use. The target failure probability not to be exceeded in normal conditions is given by $7, 23 \cdot 10^{-5}$ for the building life of ~55 years. Hence the objective for the fire situation should be

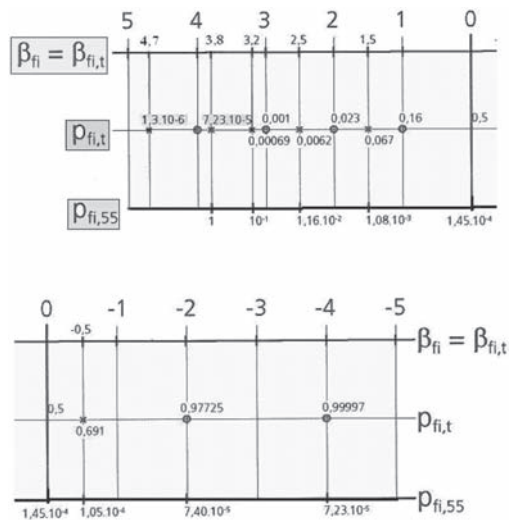
$$p_{f,55} \text{ (probability of failure)}$$

$$\leq p_{t,55} \text{ (target failure probability)} = 7, 23 \cdot 10^{-5}$$

$$p_{f,55} = p_{fi,55} \text{ (probability of severe fire)}$$

$$\cdot p_{f\bar{fi}} \text{ (failure probability in case of fire)}$$

This allows to create a connection between the reliability index β_{fi} , related to the probability of structural failure in case of fire p_{fi} , and the probability $p_{fi,55}$ of getting a fully fire engulfed compartment during the life time of the building, which depends on the compartment size, the type of occupancy and the active fire safety measures.



It has to be mentioned, that negative values of the reliability index β_{fi} correspond to quite low values for the probability $p_{fi,55}$ of getting a severe fire, which is the case when active fire safety measures exist.

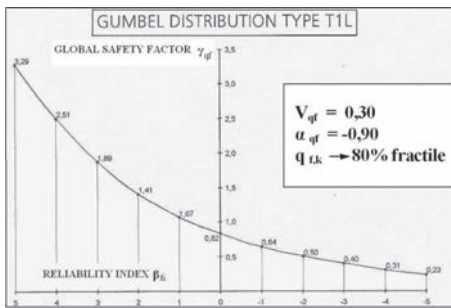
Reliability calculations have shown that the weighing factor for the main action at room temperature is strongly reduced in case of fire and may therefore be considered as a secondary action, whereas the fire load becomes the main action. This leads to a global factor γ_{qf} , giving the design fire load

$$q_{f,d} = \gamma_{qf} \cdot q_{f,k} \text{ [MJ/m}^2\text{]}.$$

Finally a connection may be established between the reliability index β_{fi} related to the probability of structural failure in case of fire p_{fi} , and the global factor γ_{qf} affecting the characteristic value $q_{f,k}$ of the fire load according to equation

$$\gamma_{qf} = \frac{\gamma_{sd} \left\{ 1 - V_{qf} \left(\frac{\sqrt{6}}{\pi} \right) \left(0,577216 + \ln[-\ln \Phi(-\alpha_{qf} \cdot \beta_{fi})] \right) \right\}}{\left\{ 1 - V_{qf} \left(\frac{\sqrt{6}}{\pi} \right) \left(0,577216 + \ln[-\ln \Phi(\beta_k)] \right) \right\}}$$

That equation is illustrated by the following graph



The previously described procedure was announced through various publications of the author since 1992 and was clearly developed during the years 1994 to 2000 by an European Research Group comprising various competent Research Institutes from eleven European countries, also under the leadership of the same author.

3 ARCHITECTURE AND PRACTICAL DESIGN

Following conclusions may be drawn on the basis of the design performed, in the fire situation, for the described structures. For all of them the real fire, function among others of the ventilation conditions and the fire load, was considered. Furthermore the effect of active fire safety measures on the design fire load was also taken into account.



Under these conditions the following amazing result could be obtained, which consists in finally having conceived and realized a tower building, 75 m high, with steel columns and steel beams kept visible and unprotected. It is for the first time that such an innovative step has been undertaken, not forgetting that the active fire safety implemented brings even people's safety to the highest possible level.

- The design results indicate that, under natural heating, no failure nor any critical deformation will occur. This is due to the fact that structures are in fact best protected by the active fire safety measures, as the potential severity of a fire and its probability of occurrence are cut down.
- All static calculations in the fire situation have been done through a two dimensional analysis, which is completely sufficient in connection to every day design. Indeed the aim according to EN1991-1-2 is clearly to show that, under natural heating and by considering the active fire safety measures as proposed in the global fire safety concept, no failure occurs and deformations are limited to acceptable levels.
- It is the author's opinion, that fire is to be considered as a load like wind or earthquake, which will lead to a robust structural design of buildings. Indeed the global behaviour of the structure has to be activated in the fire situation, as was underlined for the first time by the author in 1988. Of course this also highlights the fact that, in a two dimensional analysis, floor beams may move into catenary action, pulling columns back inwards etc. This means that a redistribution of internal load actions takes place in the fire situation and that a.o. connections may be submitted to much higher load effects than in normal conditions of use.

This page intentionally left blank

GS_321 — Structural reliability (4)

This page intentionally left blank

Seismic fragility of RC bridges using the data obtained from nondestructive testing

Q. Huang, P. Gardoni & S. Hurlebaus
Texas A&M University, College Station, TX, USA

ABSTRACT: Seismic fragility reflects the ability of a structure to withstand future seismic demands. It is defined as the conditional probability that a structural demand quantity attains or exceeds a specified capacity level of the bridge for given the characteristics of an earthquake. In order to obtain an accurate assessment of the fragility of a bridge, it is critical to incorporate information about the current structural properties, which reflects the possible aging and deterioration. This paper describes a probabilistic framework to identify the actual conditions of reinforced concrete (RC) bridges in the field using nondestructive testing (NDT) and to develop the corresponding fragility estimates for the bridge.

In this study, a probabilistic capacity model for RC bridge column is built considering the possibility of non-uniform flexural stiffness over the column height to account for the possible effects of non-uniform deterioration. A probabilistic seismic demand model is developed to fully consider the prevailing uncertainties associated with the structural demands on RC bridges due to seismic excitations. Such uncertainties include uncertainties in the ground motions and the structural properties, model error, and statistical uncertainties in the model parameters.

The proposed probabilistic framework combines global and local NDT methods to identify the in situ structural properties of RC bridges. A combination of these two NDT methods takes advantage of the complementary strengths of both. Global

NDT uses the modal data of an existing bridge to assess its global/equivalent structural properties and to detect potential damage locations. Modal data can be easily extracted from the time-history dynamic response of the bridge that can be obtained from a vibration test, making the global NDT of practical value. Measurement and modeling errors are considered in the application of the global NDT and the analysis of the NDT data. Local NDT uses local measurements to identify the local characteristics of the structure. Particularly, this paper uses the SonReb technique (a combination of ultrasonic pulse velocity test and rebound hammer test) to estimate the concrete compressive strength. The quantities assessed by SonReb are expressed in probabilistic manner to account for the material variability, measurement error, and environmental influence.

As an illustration, the proposed probabilistic framework is used to assess the fragility of an example RC bridge with one single-column bent. The result of the illustration shows that the proposed framework can successfully provide the up-to-date structural properties and more accurate fragility estimates than by using assumed/typical values for the bridge properties. The result of this research will help bridge owner optimize the allocation of resources for maintenance, repair, and/or rehabilitation of bridge systems, therefore increase the safety of national transportation networks. The proposed framework can be extended to other civil engineering systems as well.

Use of BWIM data for bridge assessment

M. Petschacher

PEC ZT-GmbH, Feldkirchen/Carinthia, Austria


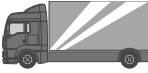
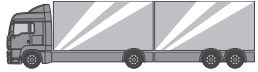
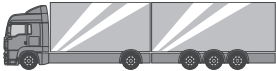

ABSTRACT: The object of this paper will describe the way from Bridge-Weigh-In-Motion (BWIM)-data to the assessment of bridge structures under consideration of the real traffic. It is obvious that the load assumptions are of importance. The evaluation of existing bridges regarding remaining life is an important issue. The bridge stock shows an increasing ageing combined with a deterioration of the state on the one hand and an increase of the traffic load on the other hand. Simple recalculations can lead to sub-optimal results, which lead to cost-intensive claims like reconstruction of a bridge. Using BWIM-data as calculation basis proofed as a probate approach in practice, see (Petschacher 2010, Grundy & Bouilly 2004). Load models for the recalculation and evaluation of existing objects basing on BWIM-measurements will be shown, where the construction site traffic guidance, short 4–0, is regarded. The reason for choosing 4–0 is that this traffic guidance will be occurring more often in the future and lead to higher loads as a strong increase of the heavy traffic would.

BWIM is a special form of weigh in motion, where a bridge is used to collect data like speed or load of vehicles. Sensors that record data are installed under the bridge and connected to a electronic device. Results of measurements are traffic and load statistics as well as the influence of the



Bridge under view.

Table 1. Some frequent vehicle classes.

VC	Symbol	pVC
113		0.312
40		0.131
61		0.107
74		0.078
62		0.077

traffic on the pavement expressed as equivalent single axle loads (ESAL).

Generally stochastic problems are solved by use of analytical methods, where amongst others the forecast of extreme load effects needs to be solved (Vrouwenvelder & Waarts 1993). After an appropriate solution for this question was found, a simple form of the stochastic description of the loads was chosen.

$$Z \sim (q_1 (f_1 \text{ Lane}_1) + q_2 (f_2 \text{ Lane}_2))^N \quad (1)$$

The mixed distribution describes the amount of empty, partial and fully loaded trucks of a class. The form of the distribution and the partial chances p_i are found with the EM algorithm or the Gibbs-simulation method (VaP 2010).

With given vehicle class and gross weight the mean of an axle load is defined by:

$$\mu_i(Q_i|W) = \beta_i + \alpha_i W \quad (2)$$

The simulation basis is formed by the load step method (LSM) in which an action takes place n times and the statistical analysis is the basis for further

extrapolations. The result of this is an arbitrary point in time distribution of structural responses. Employing the extreme value theory leads to the necessary distributions for further analyses.

The following steps depend on the particular structural situation and will be demonstrated on a typical Austrian highway bridge, where corrosion problems have been detected, (JCSS 2001).

BWIM-measurements were carried out which resulted in an amount of data used to establish a stochastic axle load model. On that a simulation of realistic traffic has been carried out. In the next step an extreme value distribution of loading at the critical section, namely the field joint could be defined. The assessment of the bridge was carried out with probabilistic methods of this field joint.

It is obvious in reevaluation of bridge structures that traffic loading assumptions are

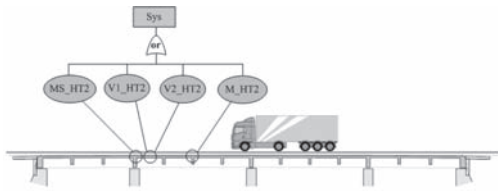


Figure 1. A fault tree applied on a bridge.



Figure 2. Corrosion shortcoming.

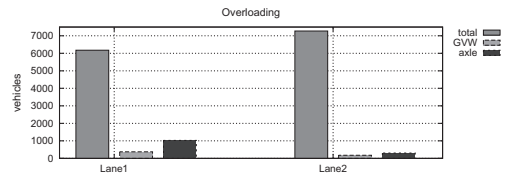


Figure 3. Number of overload vehicles in one direction.

of high importance. Therefore BWIM is strongly recommended to be done in that circumstance. The results of such an investigation should be used further in a fully probabilistic analysis where extreme value theory takes place. Additionally, deterioration processes have to be taken into account in order to get the time variant behavior of the structure.

The approach described here tries to give a path through an analysis where BWIM stands at the beginning providing valuable data. The following data analysis process fills an axle load and traffic flow model used in simulation or a simplified approach based on GVW. The outcome from the static analysis process is an arbitrarily Point-In-Time distribution of the structural response. This information can be transformed to the considered time horizon and traffic class at the bridge of interest. Finally, the engineering part employs probabilistic methods to come up with a decision basis for the client.

REFERENCES

- Grundy, P. & Bouilly, G. (2004). Assessment of bridge response using weigh-in-motion data. Technical report, 5th Austroroads Bridge Conference.
- JCSS (2001). PMC - Probabilistic Model Code. Technical Report 1, Joint Committee on Structural Safety.
- Petschacher, M. (2010). Bridge-Weigh-in-Motion. FSV, Wien.
- VaP (2010). User Manual - Variables Processor VaP 3.0. Technical Report 3, www.petschacher.at
- Vrouwenvelder, A. & Waarts, P. (1993). Traffic Loads on Bridges. *Structural Engineering International* 3, 169–177.

Harmonic wavelet-based statistical linearization of the Bouc-Wen hysteretic model

P.D. Spanos

Rice University, L.B. Ryon Endowed Chair in Engineering, Houston, TX, USA

I.A. Kougiumtzoglou

Rice University, Department of Civil and Environmental Engineering, Houston, TX, USA

ABSTRACT: Random excitations such as seismic motions, winds or ocean waves inherently possess the attribute of evolution in time. For instance, earthquake ground motions are almost invariably non-stationary with time-varying intensity and frequency content due to the dispersion of seismic waves. Thus, the mathematical theory of non-stationary random processes and the related concept of the Evolutionary Power Spectrum (EPS) are perhaps indispensable to model realistically these phenomena (e.g. Priestley, 1965; Dahlhaus, 1997; Nason et al., 2000).

Further, structures can become nonlinear and inelastic with restoring forces depending on the time history of the response under severe dynamic excitation. This memory-dependent relationship between force and deformation is generally described in the literature by the term hysteresis. A mathematical description of various existing models of hysteresis can be found in Macki et al. (1993). Therefore, several research attempts have focused on determining response statistics of hysteretic oscillators under evolutionary excitation (e.g. Kougiumtzoglou and Spanos, 2009).

The introduction of the versatile Bouc-Wen hysteretic model (Bouc, 1967; Wen, 1976) was followed by its successful application to numerous structural dynamics related fields. For instance, the model has been used for base-isolation studies and for the response analysis of soil deposits. One of the reasons for the popularity of the model, besides its versatility in efficiently capturing a wide range of hysteretic behaviors, is the option of explicitly computing equivalent linear elements. A detailed presentation of the applications and the extensions of the Bouc-Wen model can be found in review papers and books, such as the ones by Ikhouane and Rodellar (2007) and by Ismail et al. (2009).

Focusing next on the response analysis of structures under evolutionary excitation it can be argued that a wavelet-based formulation is capable of

rendering a joint time-frequency response analysis possible. Early attempts towards determining the response of a linear system in terms of its wavelet representation when the excitation admits a wavelet expansion include the works by Basu and Gupta (1998), and by Tratskas and Spanos (2003). It is noted that the aforementioned literature deals with the wavelet representation of realizations of random processes or, in other words, with representing deterministic functions. In fact, as it is pointed out in Priestley (1996), unless a rigorous mathematical model exists for representing non-stationary random processes via wavelets, questions are raised concerning any kind of wavelet-based analysis.

In this paper, a harmonic wavelet-based statistical linearization method, initially developed in Spanos and Kougiumtzoglou (2010), is modified and extended to determine the response EPS of a Bouc-Wen hysteretic oscillator subject to evolutionary excitation. The method is applicable not only for separable but non-separable in time and frequency excitation EPS as well. Specifically, employing the generalized harmonic wavelet properties and relying on a locally stationary wavelet-based representation of non-stationary random processes (Nason et al., 2000), wavelet scale (frequency)- and wavelet translation level (time)- dependent equivalent stiffness and damping elements are derived. This novel concept is next incorporated in the resulting system of equations of motion which is solved in an iterative manner to determine the response EPS. The accuracy of the method is demonstrated by pertinent Monte Carlo simulation data.

REFERENCES

- Basu, B. & Gupta, V.K. 1998. Seismic response of SDOF systems by wavelet modeling of non-stationary processes, *Journal of Engineering Mechanics*, vol. 124: 1142–1150.

- Bouc, R. 1967. Forced vibration of mechanical system with hysteresis, *Proceedings of 4th Conference on Non-linear Oscillation, Prague*.
- Dahlhaus, R. 1997. Fitting time series models to non-stationary processes, *The Annals of Statistics*, vol. 25: 1–37.
- Ikhoulane, F. & Rodellar, J. 2007. Systems with hysteresis: analysis, identification and control using the Bouc-Wen model, John Wiley and Sons.
- Ismail, M., Ikhoulane, F. & Rodellar, J. 2009. The hysteresis Bouc-Wen model, a survey, *Archives of Computational Methods in Engineering*, vol. 16: 161–188.
- Kougioumtzoglou, I.A. & Spanos, P.D. 2009. An approximate approach for nonlinear system response determination under evolutionary stochastic excitation, *Current Science, Indian Academy of Sciences*, vol. 97: 1203–1211.
- Macki, J.W., Nistri, P. & Zecca, P. 1993. Mathematical models for hysteresis, *SIAM Review*, vol. 35: 94–123.
- Nason, G.P., von Sachs, R. & Kroisand, G. 2000. Wavelet processes and adaptive estimation of evolutionary wavelet spectra, *Journal of the Royal Statistical Society*, vol. 62: 271–292.
- Priestley, M.B. 1965. Evolutionary spectra and non-stationary processes, *Journal of the Royal Statist. Soc., Series B*, 27: 204–237.
- Priestley, M.B. 1996. Wavelets and time-dependent spectral analysis, *Journal of time series analysis*, vol. 17: 85–103.
- Spanos, P.D. & Kougioumtzoglou, I.A. 2010. An approximate approach for nonlinear system evolutionary response spectrum determination via wavelets, *Proceedings of the IUTAM Symposium on Nonlinear Stochastic Dynamics and Control, Hangzhou, China, 10–14 May*.
- Spanos, P.D., Kougioumtzoglou, I.A. & Soize, C. 2011. On the determination of the power spectrum of randomly excited oscillators via stochastic averaging: An alternative perspective, *Probabilistic Engineering Mechanics*, vol. 26: 10–15.
- Tratskas, P. & Spanos, P.D. 2003. Linear multi-degree-of-freedom system stochastic response by using the harmonic wavelet transform, *Journal of Applied Mechanics*, vol. 70: 724–731.
- Wen, Y.K. 1976. Method for random vibration of hysteretic systems, *Journal of the Engineering Mechanics Division*, vol. 102: 249–263.

Reliability analysis of stresses in prestressed concrete girder under service live load

E.-S. Hwang

Kyung Hee University, Yongin, Korea

I.-R. Paik

Kyung Won University, Seongnam, Korea

S.H. Nguyen

Kyung Hee University, Yongin, Korea

1 INTRODUCTION

The objective of this paper is to perform the reliability analysis of stresses in prestressed concrete girder subject to service live load. To establish statistical characteristics of concrete tension strength, splitting tension tests and bending tension tests are performed for various specified strength of concrete. The live loads characteristics are established from various field data. Other statistical characteristics are collected from related studies and references. Reliability analysis is performed on typical prestressed concrete I-shaped girder and box type girder using first-order reliability method. Results are compared with reliability level of ultimate limit states and target reliability indices from various codes.

Reliability indices for ULS of prestressed concrete girders are also calculated to compare with those for SLS. Since the first reliability-based design code are under development now in Korea, reliability indices for current live load and proposed live load model are calculated and compared. Reliability indices are calculated from actual sections designed by Korean Bridge Design Code. Sensitivity on the reliability index of random variables is examined through parametric study.

2 LIMIT STATE FUNCTIONS

The limit state functions for SLS for the compression and tension stress are formulated based on design and working principle of prestressed concrete girder. These functions have been used to calculate the reliability index at the initial stage and service load stage.

At the initial stage, the limit state functions at the top and bottom fiber are given as in Eqs. (1) and (2), respectively.

$$g_1 = f_{sp} + \frac{P_i}{A_{ci}} - \frac{P_i e_{pi}}{I_{xi}} y_{ti} - \frac{M_{DC}}{I_{xi}} y_{ti} \quad (1)$$

$$g_2 = 0.6 f_{ci} + \frac{P_i}{A_{ci}} + \frac{P_i e_{pi}}{I_{xi}} y_{bi} - \frac{M_{DC}}{I_{xi}} y_{bi} \quad (2)$$

where f_{ci} = compressive strength of concrete at initial prestress, f_{sp} = splitting tensile strength of concrete, P_i = prestressing force before time-dependent losses, A_{ci} = cross-sectional area of a girder, I_{xi} = moment of inertia of the section, e_{pi} = eccentricity of tendon, y_{ti} and y_{bi} = distance from neutral axis to top fiber and bottom fiber of a girder, respectively, M_{DC} = moment due to self weight of structural component.

When girder is subjected to live load, the limit state functions at service load stage are given as in Eqs. (3) and (4), respectively.

$$g_3 = 0.4 f_{ck} + \frac{P_e}{A_c} - \frac{P_e e_p}{I_x} y_t - \frac{M_{DC} + M_{DW}}{I_x} y_t - \frac{M_{LL}}{I_x} y_t \quad (3)$$

$$g_4 = f_{sp} + \frac{P_e}{A_c} + \frac{P_e e_p}{I_x} y_t - \frac{M_{DC} + M_{DW}}{I_x} y_b - \frac{M_{LL}}{I_x} y_b \quad (4)$$

where f_{ck} = specified design strength of concrete, M_{DW} = moment due to dead load of wearing surfaces, M_{LL} = moment due to live load and impact load (if any), meanwhile, remaining component are calculated at the service load stage.

3 TYPICAL PSC BRIDGE GIRDERS

This paper considers five typical I-shape girder with span length of 20, 25, 30, 35 and 40 m and four typical box type girder with span length of 40,

50, 60 and 100 m. These girders have been widely used for PSC bridges in Korea and were designed based on Korean Bridge Design Code (KBDC).

4 ANALYSIS OF TEST DATA

Statistical parameters for concrete properties are determined through analysis of test data obtained from experiments at the laboratory combined with data from previous domestic researches. Statistical parameters includes mean value μ , standard deviation σ , coefficient of variation COV and bias factor λ for compressive strength and splitting tensile strength of concrete cylinder. The values of bias factor and coefficient of variation for compressive strength of concrete are also compared to those of Nowak and Szersen (CPA R&D-2849, 2008) in this paper.

5 STATISTICAL PROPERTIES OF RANDOM VARIABLES

It is assumed that all the variables in limit state functions are independent. Statistical parameters of concrete are taken from analyzing of test data in the previous section and other variables are referred from the other sources as shown in table below.

Table 1. Statistical description of random variables.

Variable	λ	COV	Distribution	Reference
f_{ci} (MPa)	1.02	0.180	Normal	Al-Harthy
f_{ck} (MPa)	1.22	0.15	Normal	This study
Pe (kN)	1.03	0.015	Normal	N & S*
A_c (m ²)	1.04	0.070	Normal	N & S*
I_x (m ⁴)	1.04	0.070	Normal	N & S*
e_p (m)	1.00	0.065	Normal	Mirza (1996)
y_t (m)	1.04	0.070	Normal	N & S*
y_b (m)	1.04	0.070	Normal	N & S*
M_{DC}	1.05	0.100	Normal	NCHRP (1999)
M_{DW}	1.00	0.250	Normal	NCHRP (1999)
M_{LL}	1.05	0.200	Normal	KBRC (2008)

*Nowak & Szersen (CPA R&D-2849, 2008).

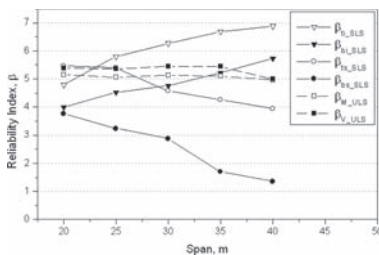


Figure 1. Comparison between SLS and ULS of PSC I-shape girder.

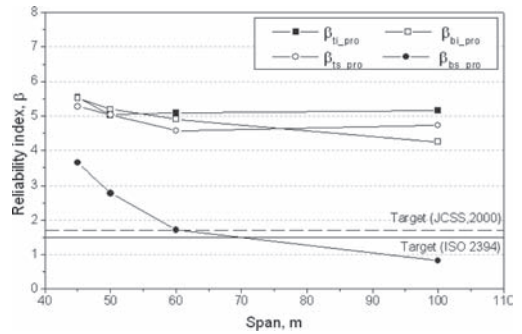


Figure 2. Comparison with target reliability level of international standard for SLS of PSC box type girder.

6 CALCULATION RESULTS

In this paper, First Order Reliability Method (FORM) is applied to calculate the reliability index. An iteration procedure developed by Rackwitz and Fiessler (1978) is programmed and performed by Matlab program.

Generally the reliability indices for current load model show a little higher values than those for proposed live load. The reliability indices for ULS show consistent values, but the reliability indices for SLS show more variable values. Comparison between target and calculated reliability indices for SLS shows that the reliability indices for longer span are less than target value.

7 CONCLUSION

This paper deals with the reliability analysis of stresses in prestressed concrete girder subject to the initial and service load stage. Reliability analysis is performed on typical prestressed concrete I-shape girder and box girder for SLS and ULS. Comparisons of reliability index have been done between SLS and ULS together with target reliability level from international standards. Results pointed out that all reliability indices are higher than target values, except tension stresses of long span girder at service load stage. As span becomes longer, the reliability index for tension stress of girder bottom fiber becomes smaller and less than target values suggested by ISO2394 or JCSS(2000). Also reliability indices for serviceability limit states show more variability than for ultimate limit states. More detailed research and calibration for stresses in PSC girder and adequate target reliability level for serviceability limit states are required.

Fragility analysis for sensor fault detection of smart structures

Yeeseock Kim

Department of Civil and Environmental Engineering, Worcester Polytechnic Institute, MA, USA

Jong-Wha Bai

Department of Civil Engineering, California Baptist University, Riverside, CA, USA

ABSTRACT: This paper investigates the impact of sensor fault/failures within smart control systems under a variety of earthquake signals using seismic fragility curves. Seismic fragility analysis can be used as a tool for evaluating the performance and vulnerability of smart structures under earthquake events. It would play an important role in estimating seismic losses and in the decision making process based on control performance during seismic events. The seismic fragility curves are developed using a closed form equation. Seismic demand model is constructed with a Bayesian updating approach while seismic capacity of smart structures is estimated based on the approximate structural performance of semi-active control structures. Peak ground acceleration (*PGA*) of ground motion is used as a measure of earthquake intensity. To demonstrate the proposed

methodology, a three-story building employing a highly nonlinear hysteretic magnetorheological (MR) damper is analyzed to estimate seismic fragility of smart control system. Then the developed fragility curves for the smart structure are compared with those for the control system with faulty sensing information while the responses of the uncontrolled structure are used as a baseline. It is shown from the simulations that the proposed methodology is effective in quantifying the impact of sensor fault/failures within smart structures.

Keywords: Smart structures; sensor fault detection; semi-active control; seismic fragility analysis; fragility curves; magnetorheological (MR) dampers; Bayesian updating; structural control

*MS_315 — The treatment of uncertainties
in large-scale stochastic systems (1)*

This page intentionally left blank

Stochastic responses of Navier-Stokes equations computed with dynamically orthogonal field equations

T.P. Sapsis & P.F.J. Lermusiaux

Massachusetts Institute of Technology, Cambridge, MA, USA

Dynamical systems play a central role in applications of mathematics to natural and engineering sciences. However, dynamical systems governing real processes always contain some elements characterized by uncertainty or stochasticity. Uncertainties may arise in the system parameters, the boundary and initial conditions, and also in the ‘external forcing’ processes. Also, many problems are treated through the stochastic framework due to the incomplete or partial understanding of the governing physical laws. In all of the above cases the existence of random perturbations, combined with the complex dynamical mechanisms of the system itself can often lead to a rapid growth of the uncertainty in the dynamics and state of the system. Such rapid growth can distribute the uncertainties to a broadband spectrum of scales both in space and time, making the system state particularly complex.

In the past decades an increasing number of problems in continuum theory have been treated using stochastic dynamical theories. Such problems are mainly described by stochastic partial differential equations (SPDEs) and they arise in a number of areas including fluid mechanics, elasticity, and wave theory, describing phenomena such as turbulence, random vibrations, flow through porous media, and wave propagation through random media. This is but a partial listing of applications and it is clear that almost any phenomenon described by a field equation has an important subclass of problems that may profitably be treated from a stochastic point of view.

Probably the most characteristic representative from this family of problems are turbulent flows. In turbulence the spatial and temporal dependence of the instantaneous values of the fluid dynamics fields have a very complex nature. Moreover, if turbulent flow is setup repeatedly under the same conditions, the exact values of these fields will be different each time. However, even though the details of the flow maybe different over various runs, it has been observed that their statistical properties remain similar, or at least coherent over certain finite-time and space scales. These

observations lead to the natural conjecture that statistical modeling or statistical averaging over appropriate spatial and temporal scales maybe more efficient for the description of these phenomena.

In this work, we use a new methodology for the representation and evolution of the complete probabilistic response of infinite-dimensional, random, dynamical systems. More specifically, in Sapsis & Lermusiaux (2009) and Sapsis (2010) an exact, closed set of evolution equations for general nonlinear continuous stochastic fields described by a Stochastic Partial Differential Equation (SPDE) was derived. By hypothesizing a decomposition of the solution field into a mean and stochastic dynamical component that are both time and space dependent, a system of field equations consisting of a Partial Differential Equation (PDE) for the mean field, a family of PDEs for the orthonormal basis that describe the stochastic subspace where the stochasticity ‘lives’ as well as a system of Stochastic Differential Equations that defines how the stochasticity evolves in the time varying stochastic subspace was derived. These new Dynamically Orthogonal (DO) evolution equations are derived directly from the original SPDE, using nothing more than a dynamically orthogonal condition on the representation of the solution. This condition is the ‘key’ to overcome the redundancy issues of the full representation used while it does not restrict its generic features.

Therefore, without assuming any a priori representation neither for the stochastic coefficients, nor for the spatial structure of the solution; all this information is obtained directly by the system equations, boundary and initial conditions. If additional restrictions are assumed on the form of the representation, it was shown that both the Proper-Orthogonal-Decomposition (POD) equations and the generalized Polynomial-Chaos (PC) equations are recovered.

For the efficient treatment of the strongly transient character on the systems described above, adaptive criteria for the variation of the stochastic dimensionality that characterizes the system response were derived in Sapsis (2010) and

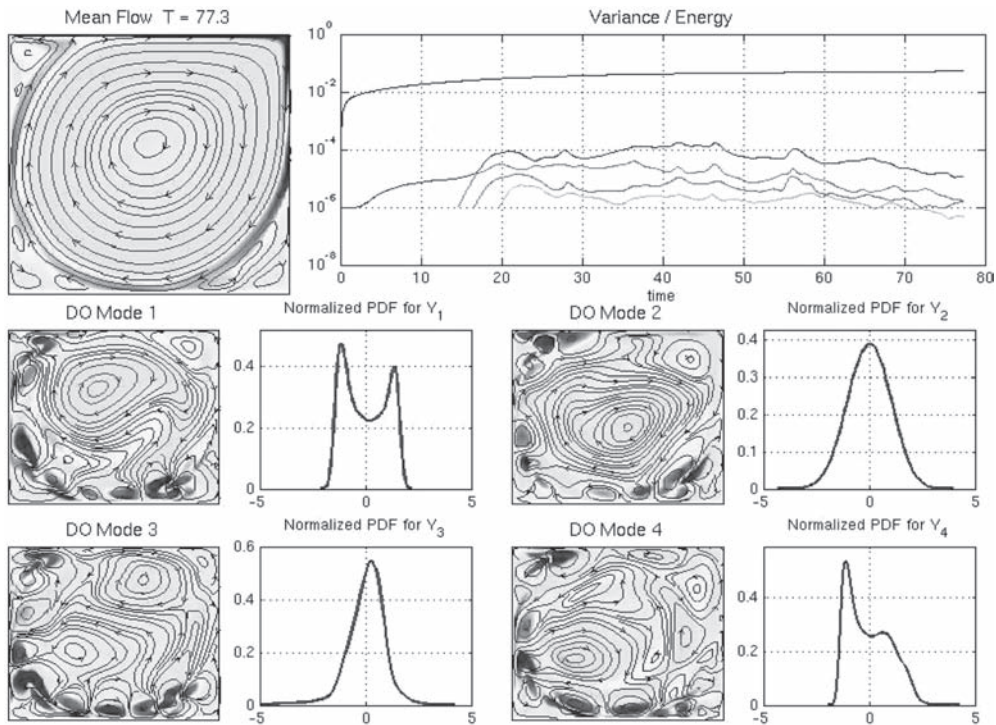


Figure 1. Strongly non-Gaussian responses for the lid-driven cavity flow with $Re = 10000$.

Sapsis & Lermusiaux (2010). Those criteria follow directly from the dynamical equations describing the system.

Here we use this computational framework to compute the complex responses of stochastic Navier-Stokes equations initiated with a very small stochastic perturbation. In low Reynolds number regimes this stochastic perturbation decays exponentially. However, for larger Re numbers internal instabilities cause rapid growth of these small perturbations leading to strongly non-Gaussian responses (Figure 1). We present the response of the lid-driven cavity flow for a Reynolds number $Re = 10000$. The system is initiated with a very small stochastic perturbation having 4–5 orders of magnitude smaller energy (or variance) from the energy of the mean flow.

Using the DO framework we are able to characterize completely the statistics of these stochastic responses and also prove that those will live in a finite dimensional space. More specifically, since the basis of the stochastic subspace is evolving according to the system SPDE, fewer modes are needed to capture most of the stochastic energy relative to the classic POD method that fixes the

form of the basis a priori, especially for the case of transient responses. On the other hand, since the stochasticity inside the dynamically varying stochastic subspace is described by a reduced-order, exact set of SDEs, we avoid the large computational cost of PC methods to capture non-Gaussian behavior. Therefore, by allowing the stochastic subspace to change we obtain a better understanding of the physics of the problem over different dynamical regimes without having the well known cost or divergence issues resulted from irrelevant representations of spatial (in POD method) or stochastic structure (in PC method).

REFERENCES

- Sapsis, T.P. Dynamically orthogonal field equations for stochastic fluid flows and particle dynamics, Doctoral Thesis, MIT 2010.
- Sapsis, T.P. & Lermusiaux, P.F.J. Dynamically criteria for the evolution of stochastic dimensionality in flows with uncertainty, *submitted*, 2010.
- Sapsis, T.P. & Lermusiaux, P.F.J. Dynamically Orthogonal field equations for continuous stochastic dynamical systems, *Physica D*, **238**, 2347–2360, 2009.

Seismic reliability of frame structures with non-Gaussian system properties

G. Stefanou & M. Fragiadakis

Institute of Structural Analysis & Seismic Research, National Technical University of Athens, Greece

ABSTRACT: Over the last few years, the efficient prediction of the stochastic dynamic response and reliability of structures with uncertain system properties has been the subject of extensive research. The majority of existing methods are usually limited to linear elastic analysis considering only monotonic loading. In the framework of the stochastic finite element method (e.g. Stefanou 2009), a novel approach has been recently introduced by the authors for the analysis of realistic structures subjected to transient seismic actions (Stefanou & Fragiadakis 2009). This approach is used here to assess the nonlinear stochastic response and reliability of a steel moment-resisting frame combining Monte Carlo simulation (MCS) and translation process theory (Grigoriu 1998). The frame is modeled with a mixed fiber-based, beam-column element, whose kinematics is based on the natural mode method. The adopted formulation leads to the reduction of the computational cost required for the calculation of the element stiffness matrix, while increased accuracy compared to traditional displacement-based elements is achieved (Papachristidis et al., 2010). The uncertain parameters of the problem are the stiffness and strength, both described by homogeneous lognormal translation stochastic fields that vary along the element (Figure 1). The frame is subjected to natural seismic records corresponding to three levels of increasing seismic intensity.

The response variability (mean, coefficient of variation (COV) and skewness) of the frame is

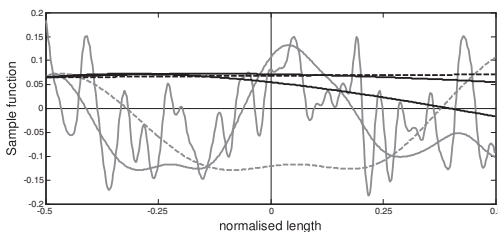


Figure 1. Sample functions of lognormal stochastic fields of the Young modulus of the beams for different values of the correlation length parameter.

computed using MCS. Probabilities of the demand, expressed in terms of the maximum interstorey drift θ_{\max} exceeding a given threshold, are calculated. Moreover, the effect of correlation structure of the stochastic fields that describe the two uncertain parameters on the response variability is investigated using two spectral density functions with spectral power concentrated at zero frequency and also shifted away from it. The issue of stochastic field discretization (related to the finite element mesh) is also examined. Finally, useful conclusions are provided regarding the influence of the correlation length of the stochastic fields on the response variability and reliability. In contrast to the static case where the response variability shows always the same trend, starting from small values for small correlation lengths up to large values for large correlation lengths, the COV of θ_{\max} is found to vary significantly not only with the correlation length but also in many different ways among the records of the same intensity level. The reliability of the frame is substantially reduced for large correlation lengths.

REFERENCES

- Stefanou, G. 2009. The stochastic finite element method: past, present and future. *Computer Methods in Applied Mechanics and Engineering* 198: 1031–1051.
- Stefanou, G. & Fragiadakis, M. 2009. Nonlinear dynamic analysis of frames with stochastic non-Gaussian material properties. *Engineering Structures* 31: 1841–1850.
- Grigoriu, M. 1998. Simulation of stationary non-Gaussian translation processes. *Journal of Engineering Mechanics (ASCE)* 124: 121–126.
- Papachristidis, A., Fragiadakis, M. & Papadrakakis, M. 2010. A 3D fiber beam-column element with shear modeling for the inelastic analysis of steel structures. *Computational Mechanics* 45: 553–572.

Pile settlement analysis on spatially random soil

G. Stefanou, G. Pittos & M. Papadrakakis

Institute of Structural Analysis & Seismic Research, National Technical University of Athens, Greece

ABSTRACT: The topic of foundation settlement is of particular interest to practicing engineers as excessive settlements often lead to problems of structural integrity or serviceability. Soil properties present an inherent random spatial variation even within homogeneous layers. Stochastic models are thus needed for an accurate description of soil variability and for the development of new perspectives concerning the risk and reliability of soil-foundation systems. With the spectacular increase of computing power and the advances in simulation methods, it is now possible to investigate realistic geotechnical problems in the framework of the stochastic finite element (SFE) method (e.g. Stefanou 2009).

In this paper, a 2D pile settlement problem is treated considering uncertainty with respect to the stiffness of the soil. The response variability is computed using Monte Carlo simulation (MCS) and translation process theory (Grigoriu 1995). The pile is modeled with beam elements while the soil is modeled with four-node quadrilateral plane strain elements. The spatial variability of the elastic modulus of the soil is described by a homogeneous non-Gaussian stochastic field with assumed statistical characteristics. The settlement variability is computed using MCS. Statistical convergence is achieved within a reasonable number of simulations, as shown in Figure 1. Parametric investigations are carried out examining the effect of probability distribution, coefficient of variation (COV) and correlation length b of the stochastic field on the response variability. The settlement COV starts from small values for small correlation lengths (wide-banded stochastic field) and tends to large values for large correlation lengths (random variable case). Substantial magnification of uncertainty is observed in the case of large input COV (>50%) as shown in Figure 1b. Finally, spectral-distribution-free upper bounds of the settlement variability are obtained using a SFE

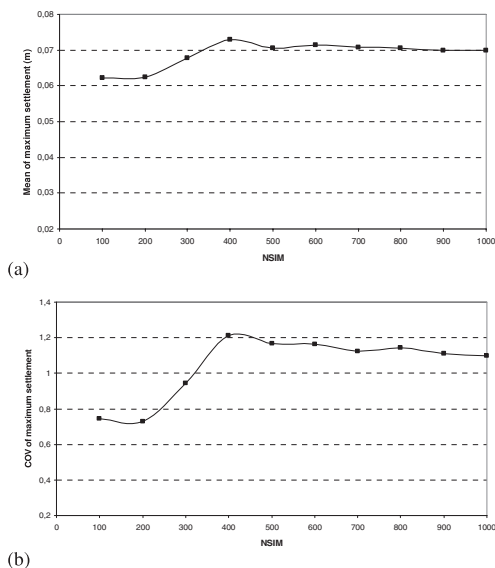


Figure 1. (a) Mean value and, (b) COV of pile settlement for lognormal stochastic field ($\sigma_f = 0.8$, $b_1 = b_2 = 1,000$ m).

approach based on variability response functions (Wall & Deodatis 1994) and compared with the results of MCS.

REFERENCES

Stefanou, G. 2009. The stochastic finite element method: past, present and future. *Computer Methods in Applied Mechanics and Engineering* 198: 1031–1051.
 Grigoriu, M. 1995. *Applied non-Gaussian processes*, Prentice-Hall, Englewood Cliffs, N.J.
 Wall, F.J. & Deodatis, G. 1994. Variability Response Functions of stochastic plane stress/strain problems, *J. of Engineering Mechanics (ASCE)* 120: 1963–1982.

A response surface method for nonlinear stochastic dynamic analysis

U. Alibrandi

Department of Civil Engineering, University of Messina, Italy

ABSTRACT: The aim of the stochastic dynamic analysis is the evaluation of the response of dynamic systems subjected to stochastic input. If the stochastic excitation follows a Gaussian distribution and the dynamic system is nonlinear, then the response follows a non-Gaussian distribution, and its determination is a very complicated task to be accomplished. To this aim, promising results are given from the application to the nonlinear stochastic dynamic analysis of the tools of structural reliability analysis (Der Kiureghian 2000). At first, the stochastic input is discretized into a large number of standard normal random variables. Define the tail probability as the probability that the response of the dynamic system is greater than a chosen threshold x at fixed time instant t . In this way, for given x and t the dynamic problem is reduced to a time-invariant structural reliability problem, where FORM can be applied.

However, in high-dimensional spaces, as the one here analyzed, the evaluation of the design point requires a great computational effort. Indeed, it is obtained as a solution of a constrained optimization problem (Liu & Der Kiureghian 1991); usually gradient-based procedures are adopted, which require repeated numerical evaluations of the response gradient, and then of several nonlinear dynamic computations. To reduce the computational cost an alternative strategy is given from the Response Surface Methodology (RSM), which builds a surrogate model of the target limit state function, defined in a simple and explicit mathematical form (Bucher & Burgund 1990). Once the Response Surface (RS) is built, it is possible to substitute the RS with the target LSF, and

then it is no longer necessary to run demanding dynamic computations.

In this paper, at first, a novel response surface based on the High Dimensional Model Representation (HDMR) (Li et al., 2001) is adopted to build a preliminary simple model of the dynamic system. Then, a variant of Model Correction Factor Method for nonlinear stochastic dynamic analysis (Alibrandi & Der Kiureghian 2010) is used to determine a close approximation of the design point with a relatively reduced number of dynamic computations. The presented approach is finally applied to a simple hysteretic oscillator.

REFERENCES

- Alibrandi, U. & Der Kiureghian, A. 2010. The Model Correction Factor Method in Nonlinear Stochastic Dynamic Analysis, 6th Computational Stochastic Mechanics Conference, Rhodes, Greece.
- Bucher, C. & Burgund, U. 1990. A fast and efficient response surface approach for structural reliability problems. *Structural Safety* 7: 57–66.
- Der Kiureghian, A. 2000. The geometry of random vibration and solutions by FORM and SORM, *Probabilistic Engineering Mechanics*, 15: 81–90.
- Fujimura, K. & Der Kiureghian, A. Tail-equivalent linearization method for nonlinear random vibration, *Probabilistic Engineering Mechanics*, 22: 63–76.
- Li, G., Rosenthal, C. & Rabitz, H. 2001. High dimensional model representation, *Journal of Physical Chemistry A*, 105: 7765–77.
- Liu, P-L. & Der Kiureghian, A. 1991. Optimization algorithms for structural reliability, *Structural Safety*, 9(3): 161–177.

Estimating seismic performance uncertainty using IDA with progressive accelerogram-wise latin hypercube sampling

D. Vamvatsikos

School of Civil Engineering, National Technical University, Athens, Greece

The accurate estimation of the seismic demand and capacity of structures stands at the core of performance-based earthquake engineering. While guidelines have emerged (SAC/FEMA 2000) that recognize the need for assessing epistemic uncertainties by explicitly including them in estimating seismic performance, this role is usually left to ad hoc safety factors, or, at best, standardized dispersion values that often serve as placeholders. Still, seismic performance is heavily influenced by both aleatory randomness, e.g., due to natural ground motion record variability, and epistemic uncertainty, owing to modeling assumptions, omissions or errors. While the first can be easily estimated by analyzing a given structure under multiple ground motion records, for example via incremental dynamic analysis (IDA, Vamvatsikos & Cornell 2002), estimating the uncertainty effects remains a little-explored issue.

Recently, several researchers (Liel et al., 2009, Dolsek 2009, Vamvatsikos & Fragiadakis 2010) have proposed applying IDA combined with Monte Carlo simulation to quantify the uncertainty effects for structural models with non-deterministic parameters. Therein, each model realization out of a predetermined sample size is subjected to a full IDA under multiple ground motion records. However, applying this method is severely restricted due to two important issues. First of all, it is not possible to determine a priori the required number of samples that one should use to perform the simulation. As the LHS design size cannot be changed at will, if such a need arises it is not possible to arbitrarily reduce or increase it. Second, there is a large overhead in the number of analyses per sample, as a full IDA with multiple ground motion records needs to be performed for each case. This essentially prohibits its use for large systems with more than a handful of random variables.

To mitigate these issues, we propose using the same fundamental blocks of IDA and LHS but essentially redefine the way that they are implemented by incorporating two important changes. First, latin hypercube sampling is applied

Table 1. The format of the iLHS sample for N parameters and M records.

No.	X_1	X_2	...	X_N	X_{N+1} ¹	X_{N+2} ²
1	$x_{1,1}$	$x_{1,2}$...	$x_{1,N}$	ang ₁	Rec ₁
2	$x_{2,1}$	$x_{2,2}$...	$x_{2,N}$	ang ₂	Rec ₂
...
M	$x_{M,1}$	$x_{M,2}$...	$x_{M,N}$	ang _{M}	Rec _{M}
$M + 1$	$x_{M+1,1}$	$x_{M+1,2}$...	$x_{M+1,N}$	ang _{$M+1$}	Rec ₁
$M + 2$	$x_{M+2,1}$	$x_{M+2,2}$...	$x_{M+2,N}$	ang _{$M+2$}	Rec ₂
...

¹incident angle.

²record index.

incrementally by starting with a small sample that is doubled successively until adequate accuracy has been achieved. This is perhaps the only way that one can reuse the results of a previous LHS design, since doubling the size allows a simple way to insert new observations within the existing ones while maintaining all the properties and advantages of LHS. Thus, by comparing the convergence of the sample properties in successive generations of the LHS design the development of a rational stopping rule becomes possible. This essentially offers an intuitive way to determine a reasonable sample size, minimizing the waste of runs over repeated tries or the tendency to overestimate the size to “get it right” in one step.

Furthermore, by taking advantage of the fact that the IDA is itself a sampling process at equiprobable points (or records) we propose that LHS is performed simultaneously on the structural properties and on the ground motion records. Instead of maintaining the same properties for a given model realization over an entire record suite, sampling is performed on a record-by-record basis, efficiently expanding the number of observations without increasing the number of nonlinear dynamic analyses, a concept that has also been proposed in a different context by Schotanus & Franchin (2004). An example of such a sampling design appears in Table 1, where each row is one model observation that also corresponds to a single ground motion

record on which IDA is performed. As a further bonus, the incident angle of the record may also be varied to allow for including its effect as well. In the customary application of such a procedure, each row of the table would be subject to IDA for the entire record suite, multiplying the number of dynamic analyses by a factor of 20–60.

The end result is iLHS, a general algorithm that efficiently upgrades the original to be applicable to large models with hundreds of random variables and without any need of pre-determining sample sizes in any way. On the other hand, iLHS is not without some minor disadvantages that can be easily remedied. Perhaps the most important is that due to the small size of the first generation samples, one cannot use some standard algorithms (Iman & Conover 1982) for imposing the desired correlation structure on the sample. Instead, genetic or evolutionary algorithms need to be employed, such as the one by Charmpis & Panteli (2004). These are more time-consuming but they offer the ability to fine-tune the correlation structure. Another issue is that we cannot use some “accelerated-IDA” techniques, e.g., priority lists (Azarbakht & Dolsek 2007), or SPO2IDA (Fragiadakis & Vamvatsikos 2010). Finally, we cannot distinguish the model uncertainty effects from the record-to-record variability unless additional analyses are performed for the mean-parameter model.

To showcase iLHS we use a steel moment-resisting frame building whose plastic hinges have uncertain parameters. Having a total of 270 random variables, the incremental iLHS algorithm is applied with a starting size of 10 and reaches a fairly stable distribution of IDA results after only 4–5 generations, at 160 or 320 samples, respectively. In comparison to a typical analysis considering only the mean-parameter model, the dispersion is found to be similar (Figure 2) but the mean response itself has a prominent bias, which, due to the details of the correlation imposed, appears to be a conservative one (Figure 1). All in all, the method proposed

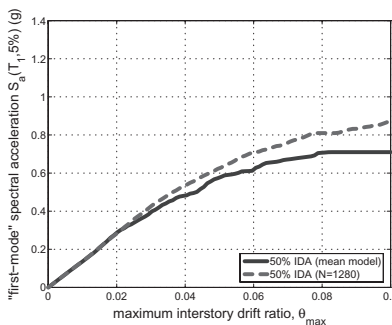


Figure 1. Comparison of median IDAs: iLHS versus the mean model.

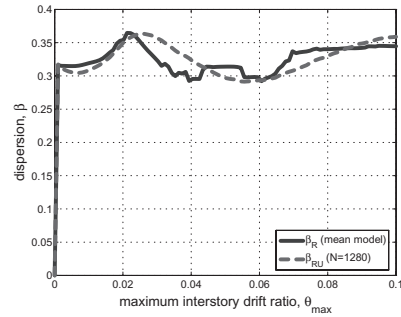


Figure 2. Comparison of dispersion of $S_a(T_1, 5\%)$ capacity: iLHS versus the mean model.

is shown to be amenable to parallelization and automated application while it allows excellent scalability and extends the original methodology to be easily applicable to realistic large-scale applications with hundreds of random variables.

REFERENCES

- Azarbakht, A. & Dolsek, M. (2007). Prediction of the median IDA curve by employing a limited number of ground motion records. *Earthquake Engineering and Structural Dynamics* 36(15), 2401–2421.
- Charmpis, D.C. & Panteli, P.P. (2004). A heuristic approach for the generation of multivariate random samples with specified marginal distributions and correlation matrix. *Computational Statistics* 19, 283–300.
- Dolsek, M. (2009). Incremental dynamic analysis with consideration of modelling uncertainties. *Earthquake Engineering and Structural Dynamics* 38(6), 805–825.
- Fragiadakis, M. & Vamvatsikos, D. (2010). Fast performance uncertainty estimation via pushover and approximate IDA. *Earthquake Engineering and Structural Dynamics* 39(6), 683–703.
- Iman, R.L. & Conover, W.J. (1982). A distribution-free approach to inducing rank correlation among input variables. *Communication in Statistics Part B: Simulation and Computation* 11(3), 311–334.
- Liel, A.B., Haselton, C.B., Deierlein, G.G. & Baker, J.W. (2009). Incorporating modeling uncertainties in the assessment of seismic collapse risk of buildings. *Structural Safety* 31(2), 197–211.
- SAC/FEMA (2000). Recommended seismic design criteria for new steel moment-frame buildings. Report No. FEMA-350, SAC Joint Venture, Federal Emergency Management Agency, Washington, DC.
- Schotanus, M. & Franchin, P. (2004). Seismic reliability analysis using response surface: a simplification. In *Proceedings of the 2nd ASRANet Colloquium*, Barcelona, Spain, pp. 1–8.
- Vamvatsikos, D. & Cornell, C.A. (2002). Incremental dynamic analysis. *Earthquake Engineering and Structural Dynamics* 31(3), 491–514.
- Vamvatsikos, D. & Fragiadakis, M. (2010). Incremental dynamic analysis for estimating seismic performance sensitivity and uncertainty. *Earthquake Engineering and Structural Dynamics* 39(2), 141–163.

This page intentionally left blank

*MS_325 — The treatment of uncertainties
in large-scale stochastic systems (2)*

This page intentionally left blank

The use of homotopy WHEP algorithm for solving stochastic differential equations

M.A. El-Tawil

Cairo University, Faculty of Engineering, Engineering Mathematics Department, Giza, Egypt

ABSTRACT: The Wiener-Hermite expansion and perturbation technique (WHEP) showed a great efficiency in introducing the average and covariance solution for perturbative stochastic differential equations. This technique has been greatly extended by the use of homotopy perturbation to yield what is called Homotopy WHEP. In this technique the homotopy technique replaces the ordinary perturbation technique which enables the application of the technique on non-perturbative problems. This means that an efficient algorithm can introduce an average and covariance solution for almost general stochastic differential equations. The solution proposed by the algorithm is sufficient for many applicants, e.g. engineers, to better handle a random system described by a stochastic differential equation when having an average solution and a variance as a measure of an error in the average solution. Better design is obtained when having this knowledge. In this paper, the algorithm is particularly applied on some nonlinear stochastic differential equations.

- El-Tawil, M.A. The Application of WHEP technique on stochastic partial differential equations, *International Journal of Differential Equations and its Applications*, 2003: 7(3): 325–337.
- El Tawil, M.A. & Mahmoud, G.M. The Solvability of Parametrically Forced Oscillators using WHEP Technique, *J. Mechanics and Mechanical Engineering*, 1999: 3(2): 181–188.
- Magdy, A. El-Tawil and Amna, S. El-Jihany. Approximate solution of a mixed nonlinear stochastic oscillator, *J. Computer and mathematics with applications*, 2009: 58, 2236–2259.
- Magdy A. El-Tawil. The Homotopy Wiener-Hermite expansion and perturbation technique (WHEP), *Trans. on Comput. Sci. I, LNCS 4750 (Springer Verlag)* 2008: 159–180.
- Magdy A. El-Tawil. The average solution of a stochastic nonlinear Schrodinger equation under stochastic complex non-homogeneity and complex initial conditions, *Trans. on Comput. Sci. III, LNCS 5300 (Springer)* 2009: 143–170.
- Magdy A. El-Tawil and Noha El-Mulla. Using Homotopy-WHEP Technique in Solving Nonlinear Diffusion Equation with Stochastic non Homogeneity, *Trans. on Comput. Sci. VII, LNCS 5890 (Springer)* 2010: 51–67.

REFERENCES

- Abdel Gawad, E.F. & El Tawil, M.A. General Stochastic Oscillatory Systems, *Applied Mathematical Modeling*, 1993: 17(6): 329–335.

Efficient sensitivity analysis of complex engineering problems

Thomas Most

DYNARDO—Dynamic Software and Engineering GmbH, Weimar, Germany

1 INTRODUCTION

In the assessment of computational engineering models sensitivity analysis has played an increasing role during the last two decades. For probabilistic models variance based sensitivity methods are very common. In this paper classical variance based methods are improved by using approximation techniques. With global and local polynomial regression methods the efficiency of the sensitivity analysis can be significantly increased which enables the application for complex engineering problems. For this purpose the assessment of the approximation quality is required. Several quality measures are investigated.

2 VARIANCE BASED SENSITIVITY ANALYSES

Assuming a model with a scalar output $Y=f(X_1, X_2, \dots, X_m)$ as a function of a given set of m random input parameters X_i the first order sensitivity measure was introduced by Sobol' (1993) as

$$S_i = \frac{V_{X_i}(E_{X_{\sim i}}(Y | X_i))}{V(Y)}, \quad (1)$$

where $V(Y)$ is the unconditional variance of the model output and $V_{X_i}(E_{X_{\sim i}}(Y | X_i))$ is named the *variance of conditional expectation* with $X_{\sim i}$ denoting the matrix of all factors but X_i . $V_{X_i}(E_{X_{\sim i}}(Y | X_i))$ measures the first order effect of X_i on the model output.

Since complex engineering models contain not only a first order (decoupled) influence of the input variables but also coupled, which are called higher order, effects on the model output, total sensitivity indices have been introduced by Homma & Saltelli (1996)

$$S_{Ti} = 1 - \frac{V_{X_{\sim i}}(E_{X_i}(Y | X_{\sim i}))}{V(Y)}, \quad (2)$$

where $V_{X_{\sim i}}(E_{X_i}(Y | X_{\sim i}))$ measures the first order effect of $X_{\sim i}$ on the model output which does not contain any effect corresponding to X_i .

In order to compute the first order and total sensitivity indices using sampling methods a matrix combination approach following Saltelli et al. (2008) is very common in sensitivity analysis. In this procedure two independent sampling matrices **A** and **B** are generated according to the joint probability density function of the input parameters and recombined.

3 REGRESSION BASED METHODS

In order to decrease the numerical effort of a probabilistic analysis often surrogate models are used to approximate the model output instead of evaluating the real sophisticated model. For this purpose the model output is replaced mainly by a continuous function, which can be evaluated quite fast compared to a real model call. A very common method is polynomial regression, where the model response is generally approximated by a polynomial basis function of linear or quadratic order with or without linear coupling terms. The model output y_j for a given sample x_j of the input parameters **X** is estimated as $\hat{y}_j(x_j) = \mathbf{P}^T(x_j)\hat{\beta}$ where $\hat{\beta}$ is a vector containing the estimated regression coefficients which are obtained by the least squares solution (Myers & Montgomery 2002)

$$\hat{\beta} = (\mathbf{P}^T \mathbf{P})^{-1} \mathbf{P}^T \mathbf{y} \quad (3)$$

where **P** is a matrix containing the basis polynomials of the support point samples.

In order to verify the approximation model the coefficient of determination R^2 has been introduced (Myers & Montgomery 2002). In order to penalise overfitting the adjusted coefficient of determination R_{adj}^2 can be applied. More general is the estimation of the surrogate model prediction using cross validation. There the set of support points is mapped to q subsets. Then the surrogate model is built up by removing subset i from the support points and approximating the subset model output using the remaining point set. The predictive coefficient of determination R_{cross}^2 can finally be formulated as the squared linear correlation coefficient between the approximated and true model outputs. In Figure 1 the convergence of the different coefficients is shown for a linear

approximation of a two-dimensional quadratic model ($Y=2X_1+4X_2+0.5X_1^2+X_1X_2$) with standard normally distributed input variables. The figure indicates, that R_{adj}^2 and R_{cross}^2 converge to a coefficient of 0.93, whereby only R_{cross}^2 gives an accurate prediction estimate which increases with an increasing number of support points.

Generally R^2 is interpreted as the fraction of the variance of the true model represented by the approximation model. This can be used to estimate total sensitivity indeces based on the regression model (Bucher 2009) $S_{T_i}^R = R_X^R - R_{X_{-i}}^2$ where R_X^R is obtained using the complete parameter set to build up the regression model and $R_{X_{-i}}^2$ originates from a regression model with the reduced parameter set X_{-i} . In Figure 2 the computed total sensitivity indeces are given depending on the number of support points for the coupled nonlinear model. The figure indicates that the usage of the R_{adj}^2 converges faster then using R_{cross}^2 . Another approach for regression based sensitivity analysis is to apply the matrix method according to Saltelli et al. (2008) directly on the regression model using the complete parameter set X and scale the obtained first order or total indeces with the corresponding predictive coefficient of determination R_{cross}^2 . In figure 2 the estimated total sensitivity indeces are shown additionally which converge significantly faster then the other estimates.

In order to represent a complex coherence between model input and output local regression methods can be used instead of global polynomial regression. In this study Moving Least Squares (Lancaster & Salkauskas 1981) is applied, where a position depending radial weighting function is used to obtain a local character of the regression. The approximation function reads

$$\hat{y}(\mathbf{x}) = \mathbf{p}^T(\mathbf{x})(\mathbf{P}^T \mathbf{W}(\mathbf{x}) \mathbf{P})^{-1} \mathbf{P}^T \mathbf{W}(\mathbf{x}) \mathbf{y} \quad (4)$$

where the diagonal matrix $\mathbf{W}(\mathbf{x})$ contains the weighting function values corresponding to each

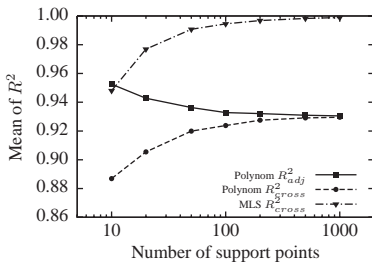


Figure 1. Convergence of coefficient of determination (mean of 1000 sampling sets) depending on the number of support points of a linear polynomial and MLS approximation of a coupled nonlinear two-dimensional model.

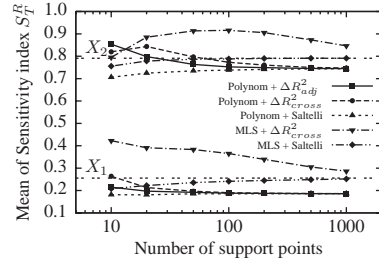


Figure 2. Convergence of the regression based total sensitivity indeces (means of 1000 sampling sets) for the nonlinear two-dimensional model.

support point. The MLS approximation converges always to the exact model function for continuous models if the weighting function radius is chosen appropriately. In the figures 1 and 2 the predictive coefficient of determination and the estimated sensitivity indeces are given additionally for the simple nonlinear model which are obtained by using only a linear MLS basis.

4 CONCLUSIONS

In the present paper classical methods for sensitivity analysis have been improved by global and local polynomial approximation techniques. It could be shown, that the proposed method is much more efficient as the evaluation of the original model. Based on a multisubset cross validation the accuracy of the approximation could be derived. From the investigated methods the combination of the matrix approach with the approximation models gave the most accurate estimates for a certain number of available model evaluations. With the proposed extension variance based sensitivity measures can be estimated even for complex models with moderate computational effort.

REFERENCES

Bucher, C. (2009). *Computational Analysis of Randomness in Structural Mechanics*. London: CRC Press, Taylor & Francis Group.

Homma, T. & Saltelli, A. (1996). Importance measures in global sensitivity analysis of nonlinear models. *Reliability Engineering and System Safety* 52, 1–17.

Lancaster, P. & Salkauskas, K. (1981). Surface generated by moving least squares methods. *Mathematics of Computation* 37, 141–158.

Myers, R. & Montgomery, D.C. (2002). *Response Surface Methodology* (2 ed.). John Wiley & Sons, Inc.

Saltelli, A. et al. (2008). *Global Sensitivity Analysis. The Primer*. Chichester, England: John Wiley & Sons, Ltd.

Sobol', I.M. (1993). Sensitivity estimates for nonlinear mathematical models. *Mathematical Modelling and Computational Experiment* 1, 407–414.

Simulation of strongly non-Gaussian stochastic vector processes using translation process theory

M.D. Shields

Weidlinger Associates, Inc., New York, USA

G. Deodatis

Department of Civil Engineering and Engineering Mechanics, Columbia University, New York, USA

ABSTRACT: The theory of non-Gaussian translation processes imposes certain conditions on the compatibility between the cross-spectral density matrix (CSDM) and the marginal probability density functions (PDFs) of the non-Gaussian vector process (Grigoriu 1995, Gioffre et al., 2000). When these two quantities are compatible, it is straightforward to estimate the CSDM of the underlying Gaussian vector process according to translation process theory (the CSDM of the underlying Gaussian vector process is necessary for simulation purposes). However, when the non-Gaussian CSDM and the PDFs are incompatible, the problem is considerably more challenging. For the incompatible case, a number of techniques have been proposed with differing levels of success.

In this paper, a new methodology is developed which has the following objective. Given a pair of incompatible $m \times m$ CSDM $S_N^T(\omega)$ and non-Gaussian CDFs $F_{X_j}(\cdot), j=1, 2, \dots, m$, find a compatible CSDM $S_N(\omega)$ which resembles, as closely as possible, the prescribed incompatible CSDM (compatibility/incompatibility is defined here with respect to translation process theory). Also produced through this procedure is the corresponding compatible underlying Gaussian CSDM $S_G(\omega)$ which may be used for simulation purposes. The proposed technique utilizes an iterative scheme which is devised to automatically ensure, at each iteration, that all four compatibility conditions imposed by translation process theory are satisfied.

The proposed methodology follows the following general outline:

1. Guess the initial Gaussian CSDM and compute its corresponding non-Gaussian CSDM through translation mapping;
2. Decompose both the Gaussian CSDM and the non-Gaussian CSDM using Cholesky's Method;
3. Sequentially upgrade the terms of the Gaussian CSDM;

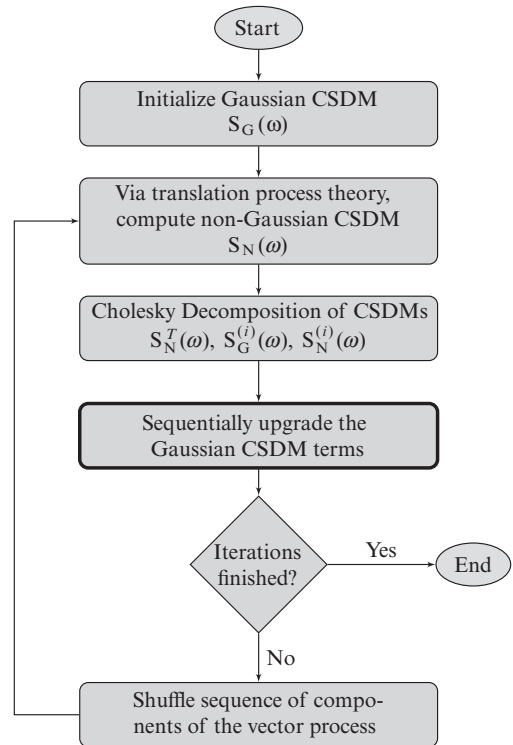


Figure 1. Flow-chart of proposed methodology.

4. Shuffle the sequence of components of the vector process;
5. Iterate back to step 2.

These general steps are shown schematically in Figure 1.

The proposed iterative technique uses a sequential upgrading of the Cholesky decomposed form of the underlying Gaussian CSDM to ensure its compatibility at every iteration. The Cholesky decomposed form of each CSDM term $H_{Gjk}^{(i+1)}(\omega)$ at iteration $(i + 1)$ is upgraded by multiplying

the Cholesky decomposed term $H_{Gjk}^{(i)}(\omega)$ at the previous iteration (i) by the ratio of the target non-Gaussian Cholesky decomposed term $H_{Njk}^{(T)}(\omega)$ to the non-Gaussian Cholesky decomposed term $H_{Njk}^{(i)}(\omega)$ at the previous iteration (i) raised to a power β . At each iteration, the upgrading begins with the top-left term of the CSDM and progresses row-wise (from left to right within each row) through the matrix. This sequential upgrading is necessary in order to account for previously upgraded terms within the current iteration. Finally, the sequence of components within the vector process should be shuffled to allow all terms to converge with a similar level of accuracy. The upgrading scheme is repeated until sufficient convergence is achieved.

This iterative scheme converges rapidly and with high computational efficiency. A numerical example is provided demonstrating the capabilities of the methodology involving a tri-variate non-Gaussian vector process with prescribed CSDM and non-Gaussian CDFs which are incompatible according to translation process theory.

REFERENCES

- Gioffre, M., Gusella, V. and Grigoriu, M. (2000). Simulation of non-Gaussian Field Applied to Wind Pressure Fluctuations. *Probabilistic Engineering Mechanics* 15, 339–345.
- Grigoriu, M. (1995). *Applied non-Gaussian Processes*. New Jersey: Prentice Hall.

Computational reliability analysis of Soil-Foundation-Structure Interaction (SFSI) systems

Q. Gu

School of Architecture and Civil Engineering, Xiamen University, Fujian, P.R. China

M. Barbato

Civil and Environmental Engineering Department, LSU, Baton Rouge, LA, USA

J.P. Conte

Structural Engineering Department, UCSD, La Jolla, CA, USA

1 INTRODUCTION

A challenging task for structural engineers is to provide a structure with the capability of achieving a target performance over its design life-time. In order to fulfill this task successfully, all pertinent sources of aleatory and epistemic uncertainties must be rigorously accounted for during the design process. Thus, proper methods are required for propagating uncertainties from model parameters to structural response quantities used in defining performance limit states. These methods need also to be integrated with methodologies already well-known to engineers, e.g., the finite element (FE) method.

This paper presents recent developments in FE response sensitivity and reliability analyses of structural and geotechnical systems. Necessary extensions of the direct differentiation method (DDM) are presented for accurate and efficient computation of FE response sensitivities of structural and/or soil-foundation-structure interaction (SFSI) systems. Taking advantage of the presented advances in FE response sensitivity analysis, existing time-invariant and time-variant reliability methods are applied for reliability analysis of structural/geotechnical systems based on realistic models thereof. Importance sampling (IS) and orthogonal plane sampling (OPS) techniques are adopted and implemented into the considered FE software frameworks for accurate computation of failure probabilities.

2 FINITE ELEMENT RESPONSE SENSITIVITY ANALYSIS (FERSA)

FERSA represents an essential ingredient for gradient-based optimization methods required in various subfields of structural and geotechnical

engineering. In addition, FE response sensitivities are invaluable for gaining insight into the effects and relative importance of system and loading parameters on system response.

Several methodologies are available for response sensitivity computation. Among them, the DDM is a general, efficient and accurate method (Kleiber et al., 1997). In the DDM, the consistent FE response sensitivities are computed at each time step, after convergence is achieved for the response computation. This requires the exact differentiation of the FE algorithm for the response calculation with respect to each sensitivity parameter. In this paper, recent DDM advancements are presented, including the DDM-based response sensitivity algorithm for force-based and three-field mixed formulation elements, and the extension of the DDM to geotechnical and SFSI systems.

3 FINITE ELEMENT RELIABILITY ANALYSIS

In general, a structural reliability problem consists of computing the probability of failure P_f of a given structure, which is defined as the probability of exceeding a specified limit state (or damage state) when the loading(s) and/or structural properties and/or parameters in the limit state functions (LSFs) are uncertain quantities and modeled as random variables. This paper focuses on component reliability problems, which are described by a single LSF. The LSF g is chosen such that $g \leq 0$ defines the failure domain. Thus, the failure probability corresponds to the probability content of the failure domain. In time-variant reliability problems, the objective is computing the time-variant failure probability, $P_f(T)$, defined as the probability of occurrence of at least one outcrossing of the LSF during the time interval $[0, T]$. The time

integral of the mean down-crossing rate, $v_g(t)$, of level zero of g provides an upper bound of $P_f(T)$.

Often, time-invariant reliability problems are solved in the standard normal space (SNS), after introducing a one-to-one mapping between the physical space of the random variables and the SNS (Ditlevsen and Madsen 1996). An optimum point at which to approximate the limit state surface $g = 0$ is the “design point” (DP), which is defined as the most likely failure point in the SNS. Finding the DP is a crucial step of semi-analytical approximate methods, such as FORM and SORM. However, these methods may give inaccurate results when the LSF in the SNS is highly nonlinear. Instead, advanced sampling techniques, such as importance sampling (IS) and orthogonal plane sampling (OPS) are adopted and further improved in this study.

4 APPLICATION EXAMPLE

A two-dimensional (2-D) SFSI system consisting of a reinforced concrete building founded on layered soil modeled with random/uncertain material parameters is considered here as a benchmark (Figure 1). Both time-invariant and time-variant reliability analysis of the benchmark example are considered in this paper.

In the time-invariant reliability analysis example, after static application of the gravity loads, the structure is subjected to a quasi-static pushover analysis. The material parameters and the applied horizontal loads are considered as random variables. The LSF is defined as $g(\theta) = \Delta_{limit} - \Delta_1$, where Δ_1 = first interstory drift and Δ_{limit} = critical threshold. FORM, IS and OPS failure probability estimates are compared to crude MCS results (using 10,000 simulations) in Table 1. The coefficients of variation (c.o.v.) of the estimates of P_f obtained by MCS, IS, and OPS are also given in Table 1. It is observed that, for high thresholds,

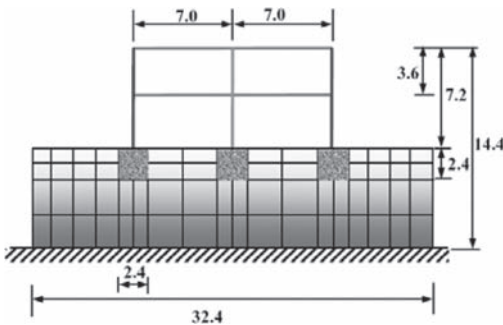


Figure 1. Benchmark SFSI system (unit: meter).

Table 1. Reliability analysis of the benchmark SFSI system: time-invariant reliability analysis results.

Δ_{limit} (cm)		2.5	5.0	7.5
P_f (c.o.v.)	FORM	8.94e-2	8.19e-4	1.59e-4
	MCS	9.03e-2 (0.032)	5.0e-4 (0.447)	0
	IS	8.62e-2 (0.100)	8.27e-4 (0.100)	1.42e-4 (0.100)
	OPS	8.85e-2 (0.100)	7.01e-4 (0.100)	1.05e-4 (0.100)

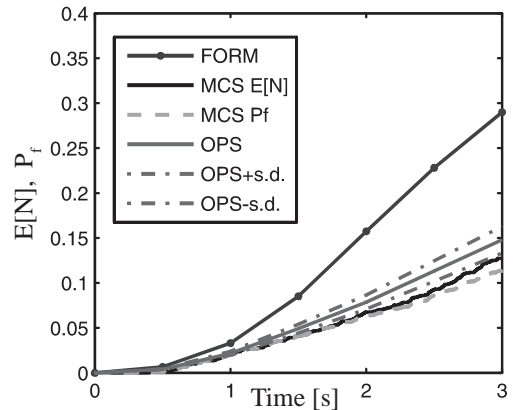


Figure 2. Reliability analysis of the benchmark SFSI system: time-variant reliability analysis results.

MCS becomes very inaccurate, while FORM, IS and OPS provide consistent results. The same 2-D SFSI example is used for time-variant reliability analysis. The stochastic excitation is modeled as a white noise. The material parameters are considered to be deterministic. The LSF is the same as for the time-invariant case with $\Delta_{limit} = 3.6$ cm. In Figure 2, the MCS estimates of the expected cumulative number of upcrossings, $E[N]$, and the failure probability, P_f , are compared with the upper bound approximation of the P_f obtained by OPS and FORM. OPS results are much more accurate than FORM results, considering MCS results as reference solution.

5 CONCLUSIONS

This paper presents recent advances in FE response sensitivity and reliability analyses of structural and/or geotechnical systems. These advances are integrated into general-purpose software frameworks for nonlinear FE response analysis. The objective is to extend analytical/numerical tools

familiar to structural/geotechnical engineers, such as nonlinear FE response analysis, in order to obtain probabilistic estimates of structural performance. Extensions of the DDM for accurate and efficient computation of system response sensitivities are shown. Time-invariant and time-variant reliability analyses, based on classical reliability methods (FORM and SORM) and sampling techniques (IS and OPS) are presented and illustrated through a benchmark SFSI system. From the application examples shown, it is observed that the computational reliability methods used here provide, at a

reasonable computational cost, reliability analysis results that are sufficiently accurate for engineering purposes.

REFERENCES

- Ditlevsen, O. and Madsen, H.O. 1996. *Structural Reliability Methods*, Wiley, New York.
- Kleiber, M., Antunez, H., Hien, T.D. and Kowalczyk, P. 1997. *Parameter Sensitivity in Nonlinear Mechanics: Theory and Finite Element Computations*, Wiley, New York.

*MS_213 — Uncertainty and imprecision in geotechnical
and structural engineering (1)*

This page intentionally left blank

Error proneness in construction

Franz Knoll

Nicolet, Chartrand, Knoll, Montreal, Quebec, Canada

ABSTRACT: Construction industry is one of the foremost endeavours man has undertaken, in numerous respects: Economic turn-over, effect on the physical, chemical and perceptible environment, our lifestyle and well-being, mobility and so on. It is one of the prerequisites which has allowed the human population to expand from a few isolated bands to numbers which are turning out to be difficult if not impossible to manage, to feed, to keep peaceful, and to limit.

As in most human activities, the tendency is to produce results which maximally satisfy anticipation and hope in exchange for a minimal investment of time, money and energy. This brings with it the consequence that perfect quality can seldom be achieved, and it has been one of man's major challenges to control that lack of perfection to an acceptable degree. This acceptance varies greatly with geographical, social, political and historical background, from the high quality expectations found in western and northern Europe, to the misery in other parts of the world, or in past ages. Perfection includes, among other aspects, the absence of faults, defects and mishaps, in other words, errors.

Evaluation and perception of perfection or its lack also varies with context. Thousands of fatal road accidents hardly raise an eyebrow and are accepted as a fact of life while the failure of an element of construction leading to a single fatality becomes newsworthy for days or weeks, occupying front pages, editorials and TV time, and waking up public authorities who launch themselves into a frenzy of investigation and new regulation.

Traditionally, and going back to the distinction Gauss made for the "errors" affecting measurement, three classes are being held apart, each one having been the subject of research and efforts to reduce it in magnitude and frequency.

- Stochastic deviations having to do—when measuring reality—with the limits of precision of the measuring mechanism, including human perception. Stochastic deviations can be treated and assessed with mathematical methods as witnessed by the great quantity of papers that are currently published, using different approaches,

hypotheses, semantics and terminologies relating to uncertainty.

- Systematic deviations, sometimes called bias, or epistemic uncertainty, occur in the translation of data into different forms as for example when an engineer "errs on the safe side", in other words converts a quantity he has determined by calculation or measurement into something he considers more appropriate. Modeling of data usually implies a similar deviation, through simplification, regulation (building codes are systematically biased toward a "safe side"). "Robust" assessment of data introduces a bias as well where, among several plausible methods of interpretation, one adopts the one bringing the more or most unfavorable results, based on the hypothesis that if the worst case scenario is used for decisions, all other possible scenarios are secure. The acquisition of data may itself be "infested" by epistemic or systematic deviations if it is perceived through proxy-type methods. Systematic or epistemic deviation can often be quantified and the data adjusted if so desired.
- Gross errors are of a different nature altogether as recognized by Gauss. A mathematical treatment has not been found so far and academic research has been curiously abstaining from touching this subject. Two efforts, in the late 1960's and early 1980' have produced some literature of little consequence. On a recent conference on the treatment of uncertainty there were, among over 700 papers dealing with stochastic or "epistemic" type uncertainties, two (2) contributions on gross error. The real problem with this is that neither the stochastic nor the epistemic/systematic uncertainties are the real problem of the construction industry, but the gross errors are. Almost invariably they are the only or main reason of mishaps, accidents and loss.

In this paper the attempt shall be made to review, eclectically, the elements and circumstances which make a building process error prone. At this time very little evidence that can be called scientific has been found or analyzed to prove that this or that type of scenario favours the genesis and

perpetuation of gross errors, beyond common sense. It is hoped that such evidence can eventually be assembled, based on real life scenarios.

Nevertheless this author believes it to be worthwhile to review the construction process and its circumstances as they relate to the genesis and perpetuation of errors, and eventually, mishaps, accidents and lack of quality. A methodology aimed at improving the situation must be based on the available knowledge, however incomplete and qualified it may be. Wherever in the process information is being created, translated, transferred, modeled and made into physical expression, it can be misconceived, misunderstood, mistaken, distorted or lost, amounting to erroneous information.

Among the features favoring error genesis and perpetuation, the following shall be examined without any claim to completeness. Also, many of the elements of a building scenario are correlated with each other which needs to be remembered when drawing conclusions and eventually, or so this author hopes, when data can be assembled and mathematical methods be found to treat it.

For the discussion of error proneness, six different groups of parameters may be distinguished, each one comprising several aspects, in a somewhat arbitrary array:

- 1 Management and organization
- 1.1 Coordination, trades and disciplines
- 1.2 Subdivision of responsibility
- 1.3 Communication
- 1.4 Modifications

- 1.5 Delays
- 1.6 Quality control, verification, checking and testing
- 2 Constraints and pressures
- 2.1 *Economy*
- 2.2 *Time*
- 3 Personnel
- 3.1 *Competence, experience*
- 3.2 *Attitude*
- 3.3 *Change of personnel*
- 4 Work culture
- 4.1 *Trust, cooperation*
- 4.2 *Protectionist measures*
- 4.3 *Equitability, fairness*
- 5 The product
- 5.1 *Innovation, novelty*
- 5.2 *Complexity*
- 6 Special problems
- 6.1 *Computer glitches*
- 6.2 *Metric vs. imperial system*
- 6.3 *Allowable stress vs. limit states*
- 6.4 *Mixing of codes and standards*

The role of uncertainty in the political process for risk investment decisions

H. Bonstrom, R. Corotis & K. Porter
University of Colorado, Boulder, Colorado USA

ABSTRACT: The cost of natural disasters continues to rise around the world, in part due to the direct and indirect effects of population growth, urbanization, and the pressures they place on land use. In 2005, the United States ranked third among countries most often hit by natural disasters and it led the world in the cost of these events (EM-DAT, 2005). One of the primary factors contributing to the rise in US disaster losses is the steady increase in the population of high-hazard areas, such as the US hurricane-prone Gulf and Atlantic coasts, and the earthquake-prone west coast. Furthermore, the growth in these high-hazard areas is concentrated in urban areas. For example, while the US population has been growing by an average of 12% each decade since 1950, 89% of the population growth has been in urban areas (Olshansky, 1999). Unfortunately rapid urban growth can outpace prudent planning and the realistic assessment and management of hazards. This chasm between short-term growth and long-term sustainability must be addressed in order to integrate the necessary hazard issues into current and future development plans. Many of the tools necessary to reverse this trend are known, but their implementation faces political and public roadblocks.

Increasing societal natural-disaster costs will increase demands for engineers to help reduce the vulnerability of the built environment to earthquakes and extreme weather. That is, after each major natural disaster, engineers will find it increasingly important to make new and existing infrastructure more disaster-resistant, so as to offset the increased quantity of what is out there to be damaged. To reduce the vulnerability of infrastructure, especially existing infrastructure, will require that engineers bring more than technical capabilities to bear. Engineers also need to know *which* measures of risk are most meaningful or relevant to decision makers, and then be able to communicate those risks, and the costs and benefits of mitigation, in concise, credible, meaningful terms.

While California cities have recently incorporated seismic safety into development plans, there has been limited success in convincing communities to integrate natural hazards issues into their

planning for future growth (Burby, 1998). This can be attributed at least in part to the lack of effective public education on natural hazard risk. Much of the difficulty associated with public education can be related to the inability of individuals as a whole to extrapolate to un-experienced low-probability, high-consequence events. There are specific psychological barriers related to this issue that must be assessed and overcome in order to successfully educate the public toward risk mitigation. If engineering professionals are to be effective with public education, they will need to understand the bases by which the public at large and elected officials in particular, make decisions with respect to risk management (Corotis, 2003).

If it is desired to communicate risk as credible and relevant to the interested parties, it must address what these parties believe may be at risk in the particular situation, and it must incorporate their specialized knowledge. Often, the best way to do this is by the active involvement or representation of the parties affected (National Research Council, 1996). When the public is involved in decision making, they are more likely to understand the issue at hand, and develop a sense of accountability for the issue. Without public involvement, people may develop opposition to risk-related issues as a result of lacking education and responsibility for the issue.

A challenge that may arise in addressing what the affected parties believe may be at risk, is the insensitivity to community heritage. By quantifying risk in general probabilities, and even high-level costs, the very essence of what is important to a community may be neglected. Communities want to know how they will be affected. It is important to identify what a community values, and speak to those values when communicating risk. Focusing on assets specific to communities will elevate the understanding of risk to a direct and personal level, and create the ambiance of immediacy for the taking of action.

Beyond public education and involvement, however, are the basic pressures and incompatibilities between the motivating rationale of elected decision makers and optimal policies for

long-term sustainability. The political system is based on lifetime cycles of approximately 4–8 years, whereas the lifetime of infrastructure, and similarly, the return period of a low-probability, high-consequence natural-hazard events may be 100 years or more. Therefore, the probability of a major disaster occurring during a specific elected official's term in office is low. As a result, a political leader may rightfully conclude that spending resources on definite decisions with immediate effects instead of investments in long-term sustainability is the best way to satisfy his or her constituents. While such justification may work for a particular decision maker, Tversky and Bar-Hillel (1983) note that consecutive short-term decision making may not result in what is best for the long-term.

Finally, financial tools are often used as a method of allowing the public and their political leaders to understand the balance between risk and return. The public uses multiple standards to assess future benefits and risks, and these must be taken into account in order to establish a system that will be effective in involving the public in the political decision making process. There are several comparison methods used in comparing risk and rewards, including the cost-benefit method. A limitation to the cost-benefit analysis is the increased sensitivity to discounting in rare events, such as natural hazards, where the timeframe of reference should be many decades. While discounting is largely based on economic theory, there are also many psychological issues which must be taken into consideration when developing an appropriate discount rate (Corotis and Gransberg, 2005). Unlike pure economic discounting, which has a constant discount rate, the discount rate associated with social or psychological factors tends to decrease with time. It is inherent in humanity to want immediate benefits, and as a result, discount the value of those same benefits in the future, but not at a constant rate. The applications to time varying discounting may be utilized in infrastructure decision making to significantly increase projected benefits for addressing natural hazard risk. Since a discount rate tells the amount of future benefits which will justify spending a dollar today, it can be seen why there is considerable debate regarding the appropriate discount rate to apply to a cost-benefit analysis conducted over longer lifetimes.

When presenting alternatives of financial-based methods for quantifying risk, challenges also arise regarding the time period associated with costs and benefits. A widely shared public rationale during the course of decision making is “what does it cost me now?” Solely focusing on the initial cost of risk mitigation does not align properly with the

objective of long-term sustainability. As discussed earlier, this is often the case in the political arena, where politicians tend to be persuaded against long-term sustainability decisions due to the higher initial costs. When presenting financial-based methods it is beneficial to focus on the total cost of a hazard mitigation investment over the lifetime of infrastructure, and view it as investing money now so that it can pay off in the long run.

Engineering risk analysis is currently developing from a purely mathematical field to one that incorporates the psychological rationale that drives the political decision maker, and more importantly the public. This paper presents current knowledge and analysis that focus on the issues of: (1) public risk perception, (2) public participation in hazard mitigation planning, (3) incorporation of community values, (4) incompatibility of political motivation and long-term planning, and (5) finances of risk and return. It is hoped that developing effective risk communication strategies based on an understanding of the framework of these issues will promote optimal long-term sustainable policy with recognizable benefits to society. A case study reviewing the work done by the San Francisco Community Action Plan for Seismic Safety (CAPSS) team is presented as an example that effectively implements methods presented in this paper. The approaches and concepts presented in this paper are intended to provide an important next step for incorporating natural hazard risk into long-term development plans.

REFERENCES

- Burby, R., ‘Involving Citizens in Hazard Mitigation Planning: Making the Right Choices’, *The Australian Journal of Emergency Management*, 2001, 16(3), 45–52.
- Corotis, R. (2003). “Risk-Setting Policy Strategies for Hazards,” *Life-Cycle Performance of Deteriorating Structures*, D. Frangopol, E. Bruhwiler, M. Faber and B. Adey, Editors, ASCE:1–8.
- Corotis, R. and Gransberg, D. ‘Discount Rate Issues for Life-Cycle Decision-Making’, in *Advances in Life-Cycle Cost Analysis and Design of Civil Infrastructure Systems*, A. Nowak, D. Frangopol, D. and Laumet, P. Editors, Proceedings of the International Workshop, May 8–11, 2005, Cocoa Beach, Florida.
- EM-DAT: The OFDA/CRED International Disaster Database. <http://www.em-dat.net>, UCL—Brussels, Belgium.
- National Research Council (1996). *Understanding Risk: Informing Decisions in a Democratic Society*. Washington, D.C: National Academy Press.
- Olshansky, R. (1999). Urbanism and its Legacy of Vulnerability. *Building Disaster Resilient Communities*. FEMA Training, 1999.

Evaluation of the safety criteria of Brazilian Standard NBR 6118 for slender members based on reliability analyses

F.R. Stucchi

Polytechnic School of São Paulo State University (USP)/EGT Engenharia, São Paulo, Brazil

S.H.C. Santos & R.M. Franco

Polytechnic School, Federal University of Rio de Janeiro (UFRJ), Rio de Janeiro, Brazil

ABSTRACT: The Brazilian Standard for concrete design defines its safety criteria in a deterministically, through partial safety factors. It is now a days recognized that a rational basis for the safety evaluation is only achieved through probabilistic analyses. An alternative to the application of these methods is the definition of safety factors that could assure to a structure designed deterministically, an adequate safety level when evaluated through reliability analyses. One of the issues for defining these safety factors is the influence of geometric deviations in slender members, such as slabs and columns. From the presented reliability analyzes, it is shown that some changes in the Brazilian Standard are necessary for attaining acceptable levels of safety.

1 INTRODUCTION

A new revision of the Brazilian Standard NBR6118 (2007) is under way. Some points, in which the Reliability Analysis can be applied, are presented in this paper.

One of the main issues for defining partial safety factors is the influence of geometric deviations in slender members. These deviations include the variations in the thickness of the structural members and in the effective values of the concrete cover.

Slender elements are analyzed herein. The uncertainties present in the design variables are taken into account, including the ones due to actions, resistances, design processes and geometric deviations.

2 PERFORMED RELIABILITY ANALYSES

2.1 Reliability analyses for beams and slabs

The considered data for the analyzed slabs and beams are given in Table 1. Two extreme levels of reinforcement (minimum and maximum) are

Table 1. Data for the analyzed elements, $f_{ck} = 25$ Mpa.

Elements	Width (cm)	Height (cm)	$A_{s\min}$ (cm ²)	$A_{s\max}$ (cm ²)
Beams	15	50	1.57	8.61
	20	75	2.36	18.84
	20	100	3.14	24.55
Slabs	100	10	1.56	7.85
	100	15	2.5	16.40

defined, as well as two values of concrete compressive strength, $f_{ck} = 25$ MPa and $f_{ck} = 35$ MPa.

Data for the adopted reinforcement corresponding to $f_{ck} = 25$ MPa are also given in Table 1. The steel has characteristic yielding stress $f_{yk} = 500$ MPa.

The deterministic design of NBR 6118 considers partial factors for resistance, $\gamma_c = 1.40$ for the concrete and $\gamma_s = 1.15$ for the steel and partial factors for actions $\gamma_f = 1.40$ for both permanent and variable loads.

Typical results for beams and slabs are shown in Figures 1–2 ($A_{s\max}$, $f_{ck} = 25$ MPa), respectively, as a function of the parameter ξ (fraction of the live loads in the total loads). The value $\beta = 3.8$ is the reference parameter in the Eurocode EN1990 (2001) for the Consequence Class CC2.

Obtained values of the coefficient β are practically independent of the value of the concrete resistance f_{ck} and of the amount of reinforcement.

Adequate values for the reliability coefficients are obtained only for the coefficient $\xi \leq 0.5$, i.e., for live loads not superior to dead loads.

For comparison with the results obtained for slabs, the ones obtained for the beams of 15×50 are also shown in the Figure 2.

Geometric deviations affect the slabs more negatively than they affect beams. The coefficients β are consistently smaller for slabs than for beams.

Another set of results is obtained for the slabs of 10 cm, applying an additional safety factor

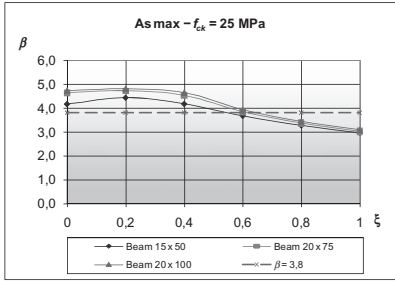


Figure 1. Results for beams $A_{s \max} - f_{ck} = 25$ MPa.

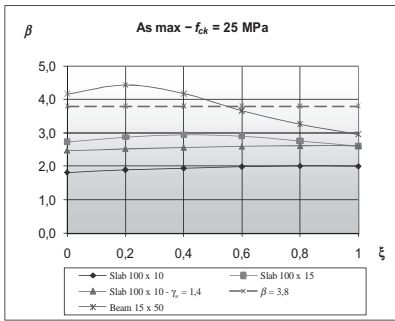


Figure 2. Results for slabs $A_{s \max} - f_{ck} = 25$ MPa.

$\gamma_n = 1.4$. Using this factor, the obtained values of β increase for values of around 3.0, that are similar to the ones obtained for the slabs of 15 cm.

2.2 Reliability analyses for columns

The Brazilian Standard NBR 6118 defines an additional increase factor γ_n for forces acting in slender columns (with thickness between 12 and 19 cm), as given below (h is the column thickness in cm):

$$\gamma_n = 1.95 - 0.05h \quad (1)$$

The analyses are done for columns of 12×60 , 15×60 and 20×60 cm², for concretes with $f_{ck} = 25$ MPa and $f_{ck} = 35$ MPa, and steel with $f_{yk} = 500$ MPa.

Among the several situations analyzed by the authors, results of the following one are presented:

$$\eta = \frac{N_d}{b \cdot h \cdot f_{cd}} = -1.00; \quad \mu = \frac{M_d}{b \cdot h^2 \cdot f_{cd}} = 0.20 \quad (2)$$

N_d and M_d are the design values of the acting normal forces and bending moments; b and h are the columns widths and thicknesses.

Typical results for columns are shown in Figure 3. Adequate values for the reliability coefficients

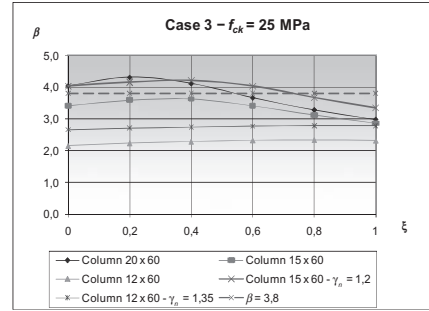


Figure 3. Results for columns $- f_{ck} = 25$ MPa.

are obtained for the 20×60 column and for the 15×60 column, in this case considering the additional factor $\gamma_n = 1.2$. For the 12×60 column, even considering the additional factor $\gamma_n = 1.35$, the obtained reliability coefficients are much lower than the required one.

3 CONCLUSIONS

Regarding the partial safety factors defined in NBR 6118, for actions of both permanent and variable character ($\gamma_f = 1.40$), it was shown that more adequate values for these safety factors have to be defined.

Regarding the slabs, the following is proposed:

- increase the lower limit of thickness of cantilever slabs from the present value of 7 cm to 10 cm;
- consider the following additional safety factor γ_n for cantilever slabs with thickness between 10 cm and 15 cm, where h is the slab thickness in cm:

$$\gamma_n = 2.20 - 0.08h \quad (3)$$

Regarding columns, it is proposed to increase the minimum thickness of columns from the present value of 12 cm to 15 cm.

These conclusions have been already transmitted by the authors to the Commission in charge of the future revision of NBR 6118.

REFERENCES

- Brazilian Association of Technical Standards (ABNT) 2007. *Design of structural concrete. Procedure. (NBR 6118)*. Rio de Janeiro: ABNT (in Portuguese).
- European Committee for Standardization (CEN) 2001. *EN 1990 – EUROCODE: Basis of Structural Design*.

Uncertainty analysis in geotechnical engineering—a comparative study of selected approaches

M. Beer

Centre for Engineering Sustainability, School of Engineering, University of Liverpool, Liverpool, UK

Y. Zhang, S.T. Quek & K.K. Phoon

Department of Civil & Environmental Engineering, National University of Singapore, Singapore

In this paper common probabilistic methods for dealing with uncertainty in geotechnical engineering are investigated and compared with an alternative approach based on interval analysis. The selected methods are examined in view of (i) an appropriate modeling of the information actually available in practical cases, (ii) the transfer of the uncertainty to the computational results, and (iii) the interpretation of the results. A simple nonlinear settlement problem is used for the study and considered as known in a deterministic form. This describes the input-to-output transformation of the available information in all cases. Representative available information about the parameters of the settlement model is taken from literature, and typical practical specifications for the parameters are considered.

Practical problems in geotechnical engineering are frequently associated with severe uncertainty. In order to consider this uncertainty in a numerical analysis, a traditional probabilistic uncertainty model is usually employed. The required probabilistic modeling, however, can be associated with difficulties due to the lack of information typical in geotechnical engineering. The data needed for utilization of mathematical statistics are frequently not available to a sufficient extent and quality. This problematic situation is investigated in (Phoon & Kulhawy 1999). The selection of a specific probabilistic model then involves subjective decisions with several options. But for specific geotechnical problems, a meaningful application of probabilistic methods can even be achieved based on scarce information. For example, the prediction of displacements of piles based on small sets of test data is investigated in (Ching & Chen 2010). In (Fellin et al. 2010) the stability of a tunnel face structure is analyzed, and sensitivities are investigated on the basis of limited data from small-scale experiments.

If the lack of information is more severe, it is questionable whether a probabilistic model can be specified for certain parameters. This applies,

for example, when only bounds are known for parameters involved in the mechanical problem. In those cases, alternative, non-probabilistic methods provide a framework for quantification and processing. In this context, interval modeling is frequently adopted. Intervals do not imply any scheme for the occurrence of values between the interval bounds. In contrast to this, a probabilistic model is associated with a certain expected frequency of occurrence (from the statistical point of view) or with a subjectively specified likelihood of occurrence (from the subjectivistic point of view) of realizations. That is, the information content of an interval is lower compared to a random variable, and the information is of a different nature. This difference has immediate consequences for the propagation of uncertainty, and for the interpretation of the results for deriving engineering decisions. An application of interval analysis in geotechnical engineering is reported, for example, in (Degrauwe et al. 2010) to analyze the ground water flow under a dam. Fuzzy modeling, as a generalized form of interval modeling, is discussed in (Hanss & Turrin 2010) and applied to investigate landslide failure.

In practical problems with various different parameters both random variables and interval variables may occur simultaneously in the mechanical problem. This mixed problem can be solved with concepts of imprecise probabilities (Walley 1991). The results are then obtained in form of bounds on probability; see (Ferson & Hajagos 2004) and (Beer 2009). In geotechnical engineering, random set approach has attracted particular attention. Recent applications on this basis are mainly focused on reliability analysis including a consideration of sensitivities. Examples for investigated structures concern a sheet pile wall in (Oberuggenberger & Fellin 2008), a tunnel in (Nasekhian & Schweiger 2010), as well as a slope in view of stability in (Rubio et al. 2004).

In the present study, interval models imprecise probabilities are investigated and compared to probabilistic approaches in view of propagation of uncertainty and interpretation of the results. To keep the investigation transparent, a simple nonlinear settlement problem is considered as example. In the investigation it is revealed that interval modeling and fuzzy modeling provide certain advantages if the available information is very limited. Covering the worst case of possible models for the input parameters, the results are quite conservative. The degree of conservatism is comparable with conclusions based on Chebyshev's inequality, however, requiring even less information. For cases in which probabilistic models can be specified for a part of the input parameters, imprecise probabilities show some advantageous features. This combination of probabilistic modeling with interval/fuzzy modeling is adjustable to the specific situation and admits the consideration of only as much conservatism as is suggested by the degree of indeterminacy of the input information. Feasibility of the analysis regarding numerical effort is demonstrated for all cases.

REFERENCES

- Beer, M. 2009. Fuzzy Probability Theory In: Meyers, R. (ed.), *Encyclopedia of Complexity and Systems Science*, Vol. 6, 4047–4059, New York: Springer.
- Ching, J.Y. & Chen, J.R. 2010. Predicting displacement of augered cast-in-place piles based on load test database, *Structural Safety*, 32(6): 372–383.
- Degrauwe, D., Lombaert, G. & De Roeck, G. 2010. Improving interval analysis in finite element calculations by means of affine arithmetic. *Computers and Structures*, 88(3–4): 247–254.
- Fellin, W., King, J., Kirsch, A. & Oberguggenberger, M. 2010. Uncertainty modelling and sensitivity analysis of tunnel face stability. *Structural Safety*, 32(6): 402–410.
- Ferson, S. & Hajagos, J.G. 2004. Arithmetic with uncertain numbers: rigorous and (often) best possible answers, *Reliability Engineering & System Safety* 85(1–3): 135–152.
- Hanss, M. & Turrin, S. 2010. A Fuzzy-Based Approach to Comprehensive Modeling and Analysis of Systems with Epistemic Uncertainties, *Structural Safety*, 32(6): 433–441.
- Nasekhian, A. & Schweiger, H.F. 2010. Random Set Finite Element Method Application to Tunneling, In: Beer, M., Muhanna, R.L. and Mullen, R.L. (eds), 2010, *Proceedings of the 4th International Workshop on Reliable Engineering Computing (REC2010), Robust Design – Coping with Hazards, Risk and Uncertainty*, Research Publishing, Singapore, 369–385.
- Oberguggenberger, M. & Fellin, W. 2008. Reliability bounds through random sets: nonparametric methods and geotechnical applications, *Computers & Structures*, 86: 1093–1101.
- Phoon, K.K. & Kulhawy, F.H. 1999. Characterization of geotechnical variability, *Canadian Geotechnical Journal*, 36: 612–624.
- Rubio, E., Hall, J.W. & Anderson, M.G. 2004. Uncertainty analysis in a slope hydrology and stability model using probabilistic and imprecise information, *Computers and Geotechnics*, 31: 529–536.
- Walley P. 1991. *Statistical reasoning with imprecise probabilities*. Chapman & Hall.

Debris flow impact uncertainty modeling with Grey numbers

Dirk Proske

Institute of Mountain Risk Engineering, University of Natural Resources and Life Sciences, Vienna, Austria

ABSTRACT: In this paper an investigation about extreme debris flow impact pressures at debris flow breakers considering different types of uncertainty is presented. The paper is based on some earlier works using statistical and mixed methods for the estimation of probabilities of extreme debris flow impact pressures and debris flow volumes (e.g. Suda et al., 2009). In contrast to earlier work, this paper partially uses Grey system models according to Deng (1988) to describe uncertainty in the data available (see also Liu & Lin 2005). Such techniques have already been used for extreme surge water levels on the Dutch coast by the author (Proske & van Gelder 2006).

First, Grey system models are introduced and applied to historical data sets of extreme debris flow levels. This so-called exponential Grey model is used to investigate systematical changes inside the data provided. In addition, this model is also used to estimate low probability values of extreme debris flow levels. Such achieved values can then be compared to an application of the exponential distribution. Some work has been carried out to identify the type of the distribution of extreme debris flow levels. Furthermore, we have in contrast to such works considered the logistic distribution. The logistic distribution based on the Verhulst differential equation has been applied successfully to the estimation of low probability values recently. Therefore in the next step the Grey Verhulst model is used. The Verhulst differential equation forms the basis for the Grey Verhulst model as well as for the logistic distribution. This permits a comparison of the gained extreme values.

In the final step, the Grey debris flow variables are combined with the random variables of the resistance of debris flow breakers made of reinforced concrete. To compute the loading on the breakers caused by debris flows, certain debris flow impact pressure models have been discussed recently (Proske et al., 2008) and are used. However, it can be seen that further research is required for the combined application of Grey numbers and random numbers in a joined safety system for structures.

REFERENCES

- Deng, J. (1988). *Essential topics on Grey Systems – Theory and Application*. China Ocean Press, Beijing.
- Liu, S. & Lin, Y. (2005). *Grey Information: Theory And Practical Applications* (advanced Information And Knowledge Processing), Springer, London.
- Proske, D. & van Gelder, P. (2006). Analysis about extreme water levels along the Dutch north-sea using Grey Models: preliminary analysis. In *Safety and Reliability for Managing Risk – Guedes Soares & Zio (eds.)*, Taylor & Francis Group, London, pp. 1385–1392.
- Proske, E., Kaitna, R., Suda, J. & Hübl, J. (2008). Abschätzung einer Anprallkraft für murenexponierte Massivbauwerke. *Bautechnik*, Volume 85, Issue 12, December 2008, pp. 803–811.
- Suda, J., Strauss, A., Rudolf-Miklau, F. & Hübl, J. (2009). Safety assessment of barrier structures, *Structure and Infrastructure Engineering*, Volume 5, Issue 4 August 2009, pp. 311–324.

This page intentionally left blank

*MS_223 — Uncertainty and imprecision in geotechnical
and structural engineering (2)*

This page intentionally left blank

Evaluation and implications of soil variability in tunneling

M. Huber, P.A. Vermeer & C. Moormann

Institute of Geotechnical Engineering, University of Stuttgart, Germany

1 INTRODUCTION

According to prognoses of the European Commission, the growth in traffic between member states is expected to double by 2020. To meet the challenges connected with the increased requirements for efficient traffic infrastructure the use of underground space often constitutes an efficient and environmentally friendly solution. But there can be also one essential disadvantage in building tunnels because especially in urban environment large settlements due to tunnelling can cause tremendous consequences.

2 CONTENT

This contribution investigates the consequences of soil variability in connection with tunnelling. The Random Finite Element Method (RFEM) is used to take soil variability into account. Within this method, random fields are used to simulate the spatial variability of the stiffness of soil. The influences of soil variability are evaluated within a case

study on the surface settlements due to tunnelling. The influencing factors on the probability of damage due to differential settlements are identified and compared to each other.

The results of this case study help to understand the influence of soil variability within this specific problem.

3 CONCLUSIONS

It is shown in this case study that the variability of stiffness has a bigger influence on the surface settlements than the spatial variability. The width and the location of the building have also a very strong influence on the probability of damage. On top of these influencing factors is the anisotropy of the random field, which asks for more investigation. Therefore additional investigation will be carried out focusing on soil layering in order to simulate different soil types as homogeneous zones. In order to go one step further, experimental evaluation on the stochastic soil properties should be carried out in order to describe soil variability in a better way.

Risks of analyses with lateral earth pressure load

P. Koudelka

Czech Academy of Sciences—Institute of Theoretical and Applied Mechanics

ABSTRACT: Earth pressure in general and lateral earth pressure in particular doubtless can be considered as the load. However, it is not an ordinary load like others (weight, wind, snow etc.) since earth pressure is a very special one. (This fact is caused by other physical matters, i.e., *action* (or also *reaction*) of an *interacting soil/rock mass*). More over, the consequential acting of the mass on the retaining structure is very complex and non-linear. European standard rules (e.g. EC 7-1, ČSN 73 0037—see Chapter 7 References in the paper) solve this problem on the basis of the Ultimate Limit State Design theory using *material partial factors*. Unluckily due to a linearity supposition of the theory base, this solution is not adequate and its reliability cannot be assumed. The paper presents the results of a comparative numerical analysis of earth pressure according to average values, i.e., EC 7-1 design values and residual values, applying a reliable database of Czech soils. Further, the paper uses the results of a number of physical experiments with lateral pressure of granular masses and also deals with the effects of an incorrectness of the theory for the geotechnical design and a calibration of EC 7-1 (EUROCODE 7-1, Geotechnical design—Part 1: General rules). Some recommendations according to contemporary research knowledge are suggested for design practice and the National Annex.

1 INTRODUCTION

EC 7-1 using the Ultimate Limit State Design theory considers several types partial factors and between them also *material partial factors for the soil/rock mass*. The interaction between a hand-made analyzed structure and touching and acting soil/rock mass is an extraordinarily complex geotechnical task of which the object is characterized by very complicated non-linear behaviour. In mechanics in general, it is well-known that application of coefficients and factors for non-linear tasks or tasks of the 2nd order and similar ones is incorrect. The application of any *material factors* for these cases appears to be a rejection of the principles of mechanics. This theoretical principal

error of course has caused significant uncertainty and risk for design practice.

Applying a code derivation procedure of soil properties leads usually to another and very different soil with very unfavourable properties, which should be considered and then active earth pressure is too high and passive earth pressure is too low. A design based on these earth pressure values is very conservative and in particularly for retaining walls, design property values often have to be chosen directly on the basis of experience. This frequent necessity raises designer risk.

The presented comparative analysis of earth pressure according to the differently derived inputs is based on code (EC 7-1) Annex C and its graphs of coefficients *K*. The analysis should in a quantitative evaluation show differences between results of the average, design (EC 7-1) and residual input sets.

This analysis is based on a rather wide database of identification and the shear strength data of soils. The database was created over long time taking out results of reliable tests by certified laboratories.

Regrettably the above mentioned uncertainty and risk about earth pressure is not unique and a number of risks flow from the incorrectness of the contemporary earth pressure theory. The paper especially targets *lateral* earth pressure (not tunneling) and risks are presented from the point of view of excavated and retaining structures.

2 DATABASE OF SOIL PHYSICAL PROPERTIES

The database has data of 258 soils in Bohemia to date and it is structured in accordance with standards of gravel, sandy and fine-grained soils. The gravels are not considered due to a low number of soils. The comparative analysis is based on sandy (S) and fine grained materials (F). Groups of the categories are numbered and indicate materials as follows. S2 = SP (12 samples), S3 = S-F (9 samples), S4 = SM (29 samples), S5 = SC (11 samples); F3 = MS (32 samples), F4 = CS (35 samples), F5 = ML-MI (21 samples),

F6 = CL-CI (50 samples), F7 = MH-MV-ME (10 samples), F8 = CH-CV-CE (11 samples).

Except of international identification data, for the analysis was used data of unit weight and effective and residual shear strength. More detailed information about the database is included in a second paper “Shear strength variability of sandy and fine grained soils”.

3 RISK OF CODE DESIGN

For this task of soil mechanics as well the (EC 7-1) code’s statistical definition of mass characteristic values and the code definition of mass material design values using *material* partial factors is matter of ineffective designs. The risk follows due to exigency to apply the direct assessment of design input values. Detailed discussion of the problem is presented in the paper. The ineffective results of the code design are shown in a number of graphs comparing the code design results (index *d*) with results of average input sets, i.e. averages including top shear strength (index *m*) and averages including residual shear strength (index *r*). Here are shown two reduced graphs of pressure coefficients $K_{a\phi}$ and $K_{p\phi}$ sandy soils (active and passive pressure) and a respective couple figures on earth pressure (from many others in the paper and the complete analysis). Three calculated coefficients according to the kinds of input data (average effective shear strength, EC 7-1 design, average residual shear strength) for the given soil groups are mottled together to make it possible better comparison.

The graph in Fig. 1 and others show uniform relations between three analyzed input data sets of both *active* and *passive* coefficients $K_{a\phi}$ and $K_{p\phi}$ even for sandy soils. However, there should be noticed relative differences between the input results. The maximal relative differences according to the EC 7-1 procedure come on results of the average shear strength sets of which ratios are shown in the Table 2 in the paper. The table also

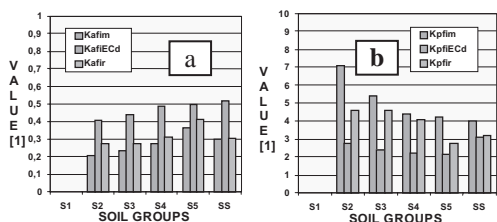


Figure 1. Pressure coefficients of internal friction K_{ϕ} for sandy soils with input sets $\phi_{ef,m}$, $\phi_{ef,d}$, $\phi_{ef,r}$: a—active $K_{a\phi}$; b—passive $K_{p\phi}$.

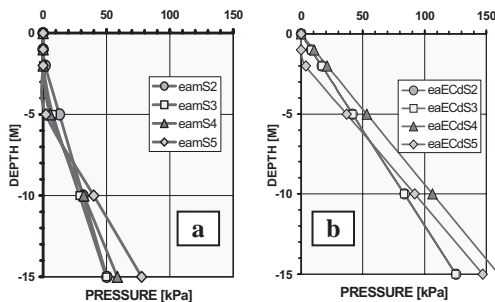


Figure 2. Active pressure of sandy soils as per individual soil groups using different input sets: a—average values including top effective shear strength, b—design values according to EC 7-1 (Annexes A and C).

shows ratios between the results of the average residual shear strength.

The analysis of earth pressure has been carried out on a base of the active and passive pressure coefficients upper presented and according to the equation (C.1) and (C.2) of the Annex C, EC 7-1. Results of the analysis are summed in a number figures of which here are Figs. 2a,b.

Histories of *active* earth pressure of both sandy and fine-grained soils of all considered groups show that the minimal values correspond to the average values and top shear strength values. The maximal values are given by the EC 7-1 input set, the differences between them are high. Active pressure of input set with the average residual values remains a bit lower between both extremes to the pressures of average values with top effective shear strength.

4 RISKS OF EARTH PRESSURE THEORY

Conventional earth pressure theory has several serious discrepancies of which have been mentioned problems of pressure at rest, mobilisation of the extreme pressure values, neglecting of residual shear strength, time pressure instability except others. Also risks of these problems should be involved in earth pressure solutions of the codes and standards.

5 CONCLUSION

The design values stipulated by EC 7-1 appear to be too conservative. The presented analysis prefers to consider the average values with residual shear strength and values pressure at rest on the average value base. The procedure should be modified according to the recent results of earth/lateral pressure research.

Uncertainty correlation in structural performance assessment

James-A. Goulet & Ian F.C. Smith

Swiss Federal Institute of Technology (EPFL), Lausanne, Switzerland

ABSTRACT: Uncertainties as well as their correlations play a major role in inverse tasks such as structural identification. In this paper, the importance of uncertainty correlation is described and an approach is proposed for its evaluation based upon the Model Filtering (MOFI) algorithm. This methodology builds on a probabilistic framework to support model-based data interpretation. The methodology explicitly includes uncertainties coming from measurements, modelling and uncertainties themselves. However, the methodology did not previously account for the uncertainty in the correlation input. Uncertainty correlations can be included in the system identification process using qualitative reasoning. It increases the applicability of MOFI methodology to the identification of real structures through accounting for knowledge of uncertainty correlations. The new methodology is applied to a beam example in order to show the influence of correlations on the identification results.

1 INTRODUCTION

An increasing number of structures that are measured have led to important challenges related to data interpretation. Structural performance assessments and structural identification tasks are intrinsically dependent on uncertainties and on their correlations. The Model Filtering (MOFI) algorithm (Goulet and Smith 2010; 2011) builds on a probabilistic framework to support model-based data interpretation. The methodology explicitly includes uncertainties originating from measurements, modelling and uncertainties themselves. However, the uncertainty in the correlation input was not included. The evaluation of uncertainties related to uncertainty and correlation is necessary because their estimation is often based on user judgment, which is also subject to uncertainties.

In this paper, the importance of uncertainty correlation is described and an approach is proposed for its evaluation. The uncertainty on correlations is included in a methodology based on qualitative reasoning. The approach applicability

is demonstrated through a case study. The second section presents a summary of the Model Filtering (MOFI) proposed by Goulet and Smith.

2 MODEL FILTERING (MOFI)

MOFI methodology is intended to help identify the behaviour of a system. The methodology is designed in a way that when uncertainties are adequately evaluated and a right model is present in the initial model set, this model should be included in the candidate model set with a reliability φ .

Rather than finding plausible models, the approach aims to discard models for which predictions are sufficiently different from measurements so that the right model is retained in the candidate model set. Candidate models are the models which are able to explain the measured behaviour while accounting for uncertainties. Each step of the methodology is detailed in the full paper.

3 UNCERTAINTY CORRELATION

Figure 1 shows two types of possible errors: independent and correlated. Uncertainties such as those related to the resolution of measuring devices are

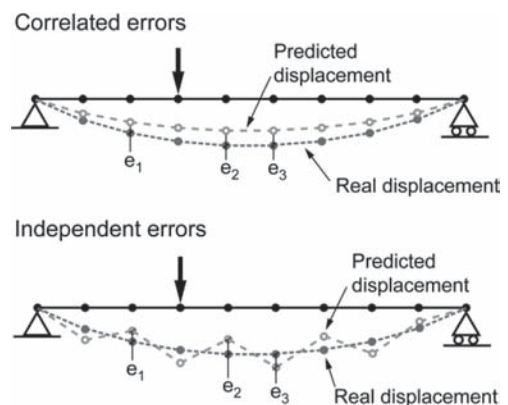


Figure 1. Error dependency in deterministic modelling.

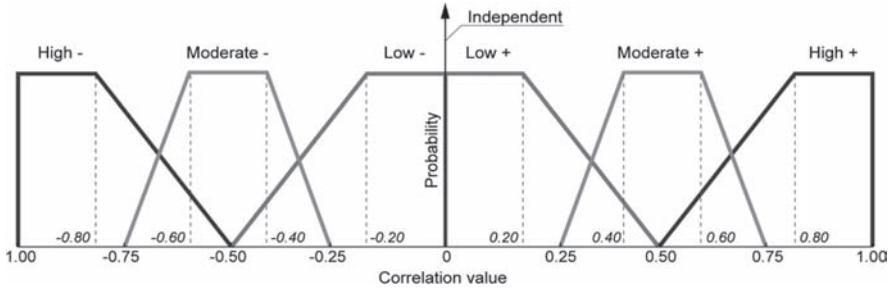


Figure 2. Qualitative reasoning decision scheme.

independent. Correlated errors correspond to cases where for different locations, errors are dependent. Errors related to results from deterministic finite element models are often correlated. Common model-updating techniques are applied to cases where errors are assumed to be independent with zero mean because they involve residual minimization (minimizing the difference between prediction and measurement). This limitation underlines the need for a method such as MOFI, in order to account for systematic uncertainties.

As mentioned in Section 2 the MOFI methodology overcomes limitations associated with residual minimization. In addition to accounting for uncertainties, it can use uncertainty correlations to define the threshold bounds that separate rejected and candidate models. Nevertheless, evaluating the correlation between uncertainties remains a cumbersome task since little information based on user judgment is available.

In this paper, a method based on qualitative reasoning is proposed to estimate correlation values in a stochastic process. Qualitative Reasoning (QR) has been introduced by Kler et al. (1977) as a method to treat uncertainties when more detailed statistical analysis cannot be justified. It uses common sense reasoning to support complex decisions. QR is often used in the field of modelling, control and to support decision when limited information is available. Figure 2 show the qualitative reasoning scheme used for correlation definition. In this figure, the correlation value is presented on the horizontal axis. The vertical axis corresponds to the probability to have a given correlation value depending on its qualitative description. It is hard for users to provide exact correlation values. Indicating whether the correlation between error types is low, moderate or high and whether the correlation is positive or negative is easier than providing numerical values. In most structural applications, the correlation is positive. This means, for example, that if at a given location the error is high, it should also be high at surrounding locations. Note that this proposal should not be confused with fuzzy logic

since there is no causal link. Qualitative reasoning is used as a representation of our knowledge.

4 LIMITATIONS

The methodology presented in this paper extends the applicability of the approach to the identification of full-scale structures where uncertainties are correlated. However, when little information on the level of correlation between uncertainties is available, the reliability of identification remains to be studied.

5 CONCLUSIONS

The challenge of defining uncertainty correlation can be addressed using qualitative reasoning when more detailed statistical analysis cannot be justified. The approach defines correlation values in a framework which accommodates imprecise knowledge of exact values.

This approach is included in the Model Filtering algorithm which can now account for the uncertainty of uncertainties and of correlations.

ACKNOWLEDGEMENTS

This research is funded by the Swiss National Science Foundation under contract no. 200020-117670/1.

REFERENCES

- Goulet, J.-A. and I.F.C. Smith (2010). Predicting Usefulness of Measuring Structures during Load Tests. *Structural Faults & Repairs*. Edinburgh.
- Goulet, J.-A. and I.F.C. Smith (2011). *Overcoming the limitations of traditional model-updating approaches*. ICASP-ISUMA conference, Maryland, US.
- Kler, J.d., Doyle, J. et al. (1977). AMORD explicit control of reasoning. *Proceedings of the 1977 symposium on Artificial intelligence and programming languages*, ACM.S.

Seismic response evaluations of ground pavement system with uncertainty

K. Nagafuchi, K. Kawano & Y. Kimura

Department of Ocean Civil Engineering, Kagoshima University, Kagoshima, Japan

1 INTRODUCTION

The dynamic response evaluation of surface layer of ground plays important roles on seismic damage evaluations for pavement system. From the seismic design point of views on structures, a number of researches on the seismic response of the surface layer have been carried out to clarify the dynamic characteristics. It is well known that the seismic performance evaluation of the structure is closely depended upon the ground situation and seismic motion characteristics. The ground condition of the surface layer can be represented with various quantities such as the shear wave velocity, friction angle, and density of soil, etc. While these quantities have been estimated by observation data and various experiments, it is likely to involve various uncertainties that are supposed to have important effects on the seismic responses.

In the present study, the uncertainty effects on the seismic response evaluation of the ground pavement system are examined with the Monte Carlo Simulation (MCS). The ground pavement system is represented with the finite element method of two-dimensional plain strain situation. The nonlinear dynamic characteristic of the ground and pavement are represented with a flow rule model. The uncertainty of the shear wave velocity of the ground is represented with a normal distribution. Otherwise, the uncertainty on the maximum acceleration of the seismic motion is possibly evaluated with a log normal distribution. Applying the MCS on the dynamic response estimation of the ground pavement system, the damage evaluation can be carried out with the maximum response characteristics such as the maximum displacement, the maximum principal stress and shear strain. It is suggested that for the damage evaluation of the ground pavement system due to seismic forces, it is essential to clarify the effect of the uncertainty with respect to the maximum seismic response quantities.

2 SUMMARY OF RESULTS

In the present study, the seismic response evaluation is carried out with the two-dimensional

ground pavement system as shown in Figure 1. The ground pavement system has horizontal width, 400 m and depth of the ground about 25 m. The pavement is settled on the surface layer between the points A and the point C as denoted in Figure 1. The seismic response evaluation on the pavement is carried out for the two cases of the ground conditions. The pavement is treated with as asphalt concrete of which the dynamic properties such as the shear wave velocity and the strength of the shear stress are strongly depended upon temperature.

Figure 2 shows the time history of seismic displacements in the nonlinear situation to kobe-ns component at the ground condition c. Comparison is made for the maximum acceleration of seismic motion of 2 m/s² and 3 m/s², respectively. For the maximum acceleration of seismic motion 3 m/s², it is understood that it leads to considerably increase of the displacement response and causes the drift displacement, which may be brought about some damages on the pavement system.

Figure 3 similarly shows the cumulative probability distribution on maximum displacement response of point A for the ground c. Two symbols stand for cumulative probability distributions on the maximum displacement for the uncertainty on

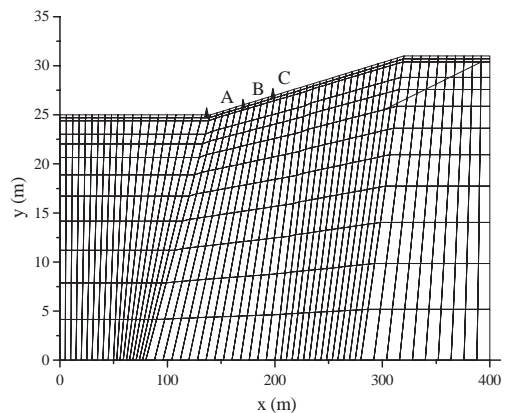


Figure 1. Ground pavement system in two—dimensional model.

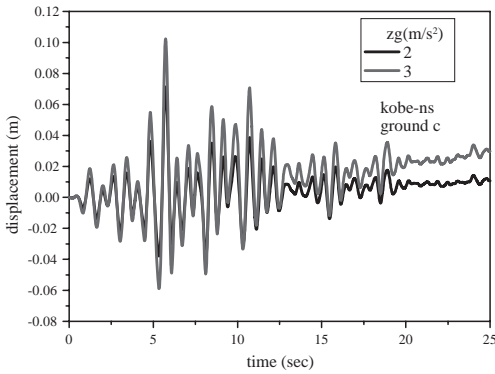


Figure 2. Time history of displacement responses in the nonlinear situation (kobe-ns).

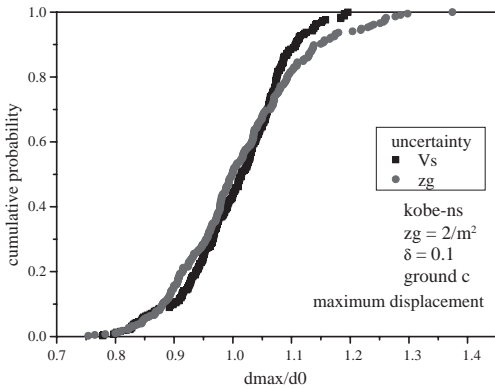


Figure 3. Cumulative probability distributions on maximum displacement to V_s and Z_g .

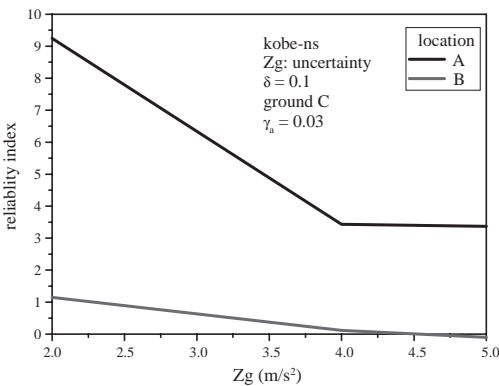


Figure 4. Reliability index for uncertainty on the maximum acceleration of seismic motion.

the maximum acceleration of seismic motion and the shear wave velocity of the ground pavement system. The coefficient of variation is assumed to be 10% for each uncertainty. The uncertainty of the shear wave velocity of the ground pavement system is assumed to be a normal distribution. The abscissa denotes the ratio of the maximum displacement response to its mean value. It is noted that the distribution of the maximum displacement have same tendency for the uncertainty on the shear wave velocity of ground and the maximum acceleration of seismic motion, but the extreme response due to the maximum acceleration of seismic motion leads to broader response than that due to the shear wave velocity. The maximum response distributions become considerably different from the normal distribution due to the nonlinear situation.

Figure 4 shows the reliability index on the uncertainty of the maximum acceleration of the seismic motion. The abscissa denotes the mean value of the maximum acceleration of input seismic motion with the coefficient of variation, 10%. Two lines denote the reliability index on the location A and B indicated in Figure 1. The limit state function is evaluated with the shear strain and the allowable shear strain is assumed to be 0.03, which may be suitable to severe damage on the pavement. The reliability index is considerably related to location of the pavement and the intensity of seismic motions because complicated response characteristics on shear strain are brought about nonlinearity.

3 CONCLUSIONS

The effects of uncertainty on the seismic response are examined for the ground pavement system in the present study.

It is shown that the seismic response characteristics play important roles on damage evaluations for ground pavement system. In order to clarify the maximum response characteristics on the seismic response, it is essential to examine the uncertainty effects due to the maximum acceleration of seismic motion and shear wave velocity of the ground pavement system. Moreover, it is suggested that reliability evaluation plays important roles on the damage estimation with nonlinear situation of ground pavement system with some uncertainties to various seismic motions.

Resolution and uncertainty analysis in Bayesian FE model updating applied to the damage assessment in a reinforced concrete beam

E. Simoen, E. Reynders, G. Lombaert & G. De Roeck

Structural Mechanics Division, Department of Civil Engineering, K. U. Leuven, Leuven, Belgium

1 INTRODUCTION

FE model updating allows for a calibration of FE models based on observed data. Structural FE model updating often makes use of vibration data, i.e. time histories obtained from forced, ambient or hybrid vibration testing, as well as modal characteristics identified from these vibration tests. In many cases, the updating process is applied for structural damage assessment, where damage is identified as a local reduction of structural stiffness.

The actual determination of FE model parameters based on experimental data involves solving an inverse problem, which is often formulated as a constrained optimization problem, where the objective is to minimize the discrepancy between measurements and predictions by calibrating some FE model stiffness parameters. In many cases, however, the inverse problem is ill-posed, meaning that uniqueness, stability and even existence of the solution cannot be guaranteed. Therefore, the quantification of uncertainties due to measurement and modeling error poses an important issue in FE model updating.

In this paper, a probabilistic method for Bayesian inference is applied to account for uncertainty in the FE model updating problem. A Bayesian inference scheme is used to update information about the FE model parameters based on observed data (Beck and Katafygiotis 1998). The results of the Bayesian scheme are investigated using a thorough resolution/uncertainty analysis. Furthermore, the Bayesian FE model updating process and resolution analysis are applied to the vibration-based damage assessment of a reinforced concrete beam.

2 BAYESIAN INFERENCE

Bayesian FE model updating The Bayesian approach makes use of probability theory to represent uncertainty; the plausibility or degree of belief attributed to the values of uncertain parameters is represented by modeling the FE model

stiffness parameters as well as the measurement and modeling error as random variables. A “prior” PDF reflects the prior knowledge about the parameters, i.e. the knowledge before any observations are made. Using Bayes’ theorem, this prior PDF is then transformed into a “posterior” PDF, accounting both for uncertainty in the prior information as well as for uncertainty in the experimental data and FE model predictions. This is done through the “likelihood function”, which reflects the contribution of the experimental data and expresses how good a certain FE model is in explaining the observed data. This function can be calculated based on the probabilistic models for the measurement and modeling error.

Resolution analysis Many posterior statistics can be calculated such as posterior mean values and Maximum A Posteriori (MAP) estimates. Additionally, standard deviations as well as covariance and correlation coefficient matrices may be computed to inspect basic resolution and correlation of the estimated parameters. In this paper, an eigenvalue analysis is proposed to examine the directions in the parameter space which show the highest and lowest reduction from prior to posterior variability.

3 APPLICATION: RC BEAM

The Bayesian method and the resolution analysis are applied for the vibration-based damage assessment in a 6 m long Reinforced Concrete (RC) beam. The experimental data consist of eigenfrequencies and mode shapes of the first four bending modes of the beam, which were measured in laboratory conditions after a load of 25 kN was applied at two thirds of the length of the beam (further referred to as “load step 5”).

Identification methods allowed for the estimation of the measurement error (Reynders et al., 2008); for the modeling error assumed values were adopted. These errors cause uncertainty on the measured data and the FE model predictions.

Deterministic FE model updating A 2D 30 beam-element FE model is constructed to represent the beam, with a constant Young's modulus of 37.5 GPa. 10 updating parameters are defined corresponding to the stiffness of 10 substructures of the beam. A least squares cost function is constructed and the optimization problem is solved using a Trust-region Reflective algorithm. The updated bending stiffness distribution is shown in Figure 1. The damage induced by the static load at about 4 m is clearly reflected in a decrease of the bending stiffness by about 50% at this location.

Application of the Bayesian approach Wide log-normal prior PDFs are appointed to the 10 stiffness parameters, which are a priori assumed to be statistically independent. The likelihood function is computed based on the assumption of zero-mean Gaussian measurement and modeling error. The joint posterior PDF is sampled using a Markov Chain Monte Carlo method, the results are shown in Figure 2.

The Bayesian scheme succeeds in identifying and locating the damage at about 4 m. Figure 2 shows larger uncertainty bounds towards the outer ends of the beam and smaller uncertainty bounds in the damaged area. This is explained by the fact that the damage induces higher modal curvatures in the damaged zone; the experimental data are more

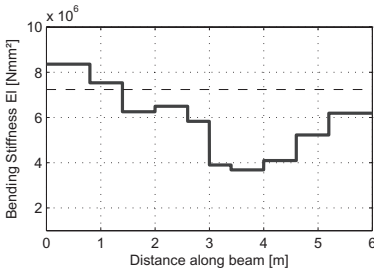


Figure 1. Updated bending stiffness distribution for load step 5.

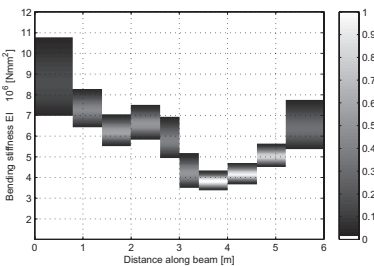


Figure 2. Resulting 99% confidence bounds on the bending stiffness distribution for load step 5. The color scale reflects the values of the normalized marginal PDFs.

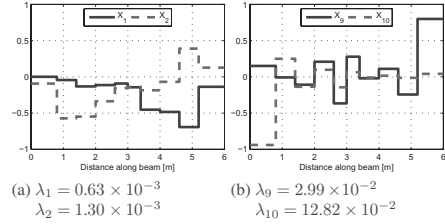


Figure 3. (a) Two best resolved and (b) two least resolved directions in the parameter space, with corresponding eigenvalues.

sensitive to stiffness changes in these areas and provide more information.

Resolution analysis The correlation coefficient matrices are calculated, and the eigenvalue analysis allows for the calculation of a set of directions in the parameter space ranked according to decreasing reduction of variance. In Figure 3a, the two best resolved directions in the parameter space are shown, and it is clear that they are very “global” vectors in the sense that they incorporate almost all parameters to some extent. The low eigenvalues corresponding to these vectors indicate that the variance in these directions is reduced substantially in the Bayesian scheme. Figure 3b shows the least resolved directions, which show very localized behavior at the outer areas of the beam. The much higher corresponding eigenvalues indicate that at the free ends of the beam very little information can be obtained from the data.

4 CONCLUSIONS

In this paper, a probabilistic approach based on Bayesian inference is elaborated for uncertainty quantification in vibration-based FE model updating and a resolution analysis is proposed to examine the results of the Bayesian scheme in a comprehensive manner. The approach is applied to the vibration-based damage assessment of a reinforced concrete beam, where it was found that the method provides a comprehensive insight into the resulting uncertainties and their underlying causes.

REFERENCES

Beck, J. & Katafygiotis, L. (1998). Updating models and their uncertainties. I: Bayesian statistical framework. *ASCE Journal of Engineering Mechanics* 124(4), 455–461.

Reynders, E., Pintelon, R. & De Roeck, G. (2008). Uncertainty bounds on modal parameters obtained from Stochastic Subspace Identification. *Mechanical Systems and Signal Processing* 22(4), 948–969.

This page intentionally left blank

*MS_233 — Uncertainty and imprecision in geotechnical
and structural engineering (3)*

This page intentionally left blank

An extension of limit state functions by parameterized probability measures

Thomas Fetz

Unit for Engineering Mathematics, University of Innsbruck, Austria

ABSTRACT: In reliability analysis the probability p_f of failure of a system is obtained by

$$p_f = \int_{\{x \in \mathbf{x}; g(x) \leq 0\}} f^X(x) dx$$

where $x = (x_1, \dots, x_n) \in \mathbf{x}$ are the basic variables of the system such as material properties and loads and where f^X is a probability density function describing the uncertainty of the variables x . The function g is the limit state function of the system telling us for which x the system fails ($g(x) \leq 0$) or not ($g(x) > 0$).

In the case of scarce information about the values of the basic variables x and the behavior of the system it may be neither sufficient to model the uncertainty of the variables x by a single probability density f^X nor to describe the system's reliability by a single deterministic limit state function g . To overcome such difficulties, fuzzy sets (Zadeh 1965), random sets (Dempster 1968), credal sets (Levi 1980) or sets of parameterized probability measures (Fetz 2007) have been used to model the uncertainty of the variables x , cf. also (Fetz 2001, Fetz 2004, Fetz & Oberguggenberger 2004, Fetz & Tonon 2008). Uncertainties in the limit state function g have been modelled using additional random variables (Ditlevsen 1982), fuzzy sets, random sets (Hall & Lawry 2003) or fuzzy probabilities (Möller, Graf & Beer 2003).

Here in this paper we will extend the limit state function to have imprecise or uncertain output also in the case of precise deterministic input values x and define a function $p_f(a, b)$ resulting in probabilities of failure depending on parameters a and b :

$$p_f(a, b) = \int_{x=-\infty}^0 \int f_{b(x)}^{Y_x}(y) dy f_a^X(x) dx.$$

In the integral two parameterized probability density functions f_a^X and $f_{b(x)}^{Y_x}$ appear. The probability density f_a^X is again needed to describe the uncertainty of the basic variables $x = (x_1, \dots, x_n) \in \mathbf{x}$. The probability density $f_{b(x)}^{Y_x}$

is the density of a random variable Y_x describing the uncertain output of the limit state function given a deterministic value x . The parameter a is a vector of parameters controlling the form of the density function f_a^X and the parameter b provides parameters for each value of x for the shape of $f_{b(x)}^{Y_x}$.

Example:

Let $b(x) = (\mu(x), \sigma)$ and

$$f_{b(x)}^{Y_x}(y) = f_{(\mu(x), \sigma)}^{Y_x}(y) = \frac{1}{\sigma\sqrt{2\pi}} e^{-\frac{1}{2}\left(\frac{y-\mu(x)}{\sigma}\right)^2}$$

the density of a Gaussian distribution with mean values $\mu(x) = g(x)$ at each x and constant variance σ^2 replacing the function values of an ordinary limit state function g depending on one variable x . The variable x is assumed to be Gaussian distributed too with parameters μ' and σ' and density

$$f_a^X(x) = f_{(\mu', \sigma')}^X(x) = \frac{1}{\sigma'\sqrt{2\pi}} e^{-\frac{1}{2}\left(\frac{x-\mu'}{\sigma'}\right)^2}.$$

A realisation of such a probability of failure

$$p_f(a, b) = p_f((\mu', \sigma'), (g, \sigma))$$

may look like Figure 1.

By means of the function $p_f(a, b)$ we have an interface for controlling the behavior of the probability distributions used for modelling the uncertainty of the basic variables x and the uncertainty of the output of the limit state function. In a further step the two parameters a and b are assumed to be uncertain too using intervals, sets or random sets which results in an upper probability \bar{p}_f of failure.

The plan of the full paper is as follows:

In Section 2 we develop the function $p_f(a, b)$. In Section 3 we show how to deal with uncertain parameters a and b and in the last section we use a simple engineering example with one uncertain basic variable x to exemplify different cases and models of uncertainty of a and b and

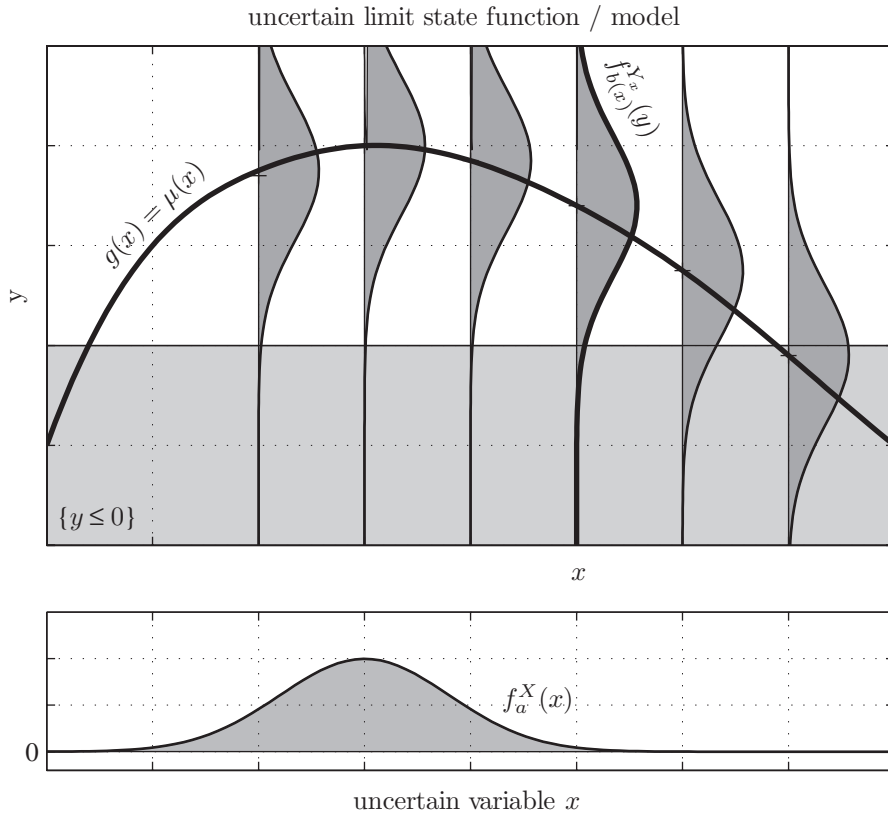


Figure 1. Uncertain limit state function and variable x .

the computation of the upper probability \bar{p}_f of failure by means of $p_f(a, b)$.

REFERENCES

- Dempster, A. (1968). Upper and lower probabilities generated by a random closed interval. *Ann. Math. Stat.* 39, 957–966.
- Ditlevsen, O. (1982). Model uncertainty in structural reliability. *Structural Safety* 1(1), 73–86.
- Fetz, T. (2001). Sets of joint probability measures generated by weighted marginal focal sets. In *G. de Cooman, T. Fine, T. Seidenfeld (Eds.), ISIPTA'01, Proceedings of the Second Symposium on Imprecise Probabilities and Their Applications*, Maastricht, pp. 171–178. Shaker Publ. BV.
- Fetz, T. (2004). Multiparameter models: rules and computational methods for combining uncertainties. In *W. Fellin, H. Lessman, R. Vieider, and M. Oberguggenberger (Eds.), Multiparameter models: rules and computational methods for combining uncertainties*. Berlin: Springer.
- Fetz, T. (2007). Multiparameter models: Probability distributions parameterized by random sets. In *G. de Cooman, J. Vejnarova, M. Zaffalon (Eds.): ISIPTA '07, Proceedings of the Fifth International Symposium on Imprecise Probabilities and Their Applications*, Action M Agency, SIPTA, Prague, 317–326.
- Fetz, T. & Oberguggenberger, M. (2004). Propagation of uncertainty through multivariate functions in the framework of sets of probability measures. *Reliability Engineering and System Safety* 85(1–3), 73–87.
- Fetz, T. & Tonon, F. (2008). Probability bounds for series systems with variables constrained by sets of probability measures. *Int. J. Reliability and Safety* 2(4), 309–339.
- Hall, J. & Lawry, J. (2003). Fuzzy label methods for constructing imprecise limit state functions. *Struct. Saf.* 28, 317–341.
- Levi, I. (1980). *The Enterprise of Knowledge*. London: MIT Press.
- Möller, B., Graf, W. & Beer, M. (2003). Safety assessment of structures in view of fuzzy randomness. *Comput. Struct.* 81, 1567–1582.
- Zadeh, L.A. (1965). Fuzzy sets. *Inf. Contr.* 8, 338–353.

On the optimal scaling of the Modified Metropolis-Hastings algorithm

K.M. Zuev & J.L. Beck

*Division of Engineering and Applied Science,
California Institute of Technology, Pasadena, CA, USA*

L.S. Katafygiotis

*Department of Civil and Environmental Engineering,
Hong Kong University of Science and Technology, Hong Kong, China*

Estimation of small failure probabilities is one of the most important and challenging problems in reliability engineering. In cases of practical interest, the failure probability is given by a high-dimensional integral. Since multivariate integration suffers from the curse of dimensionality, the usual numerical methods are inapplicable. Over the past decade, the civil engineering research community has increasingly realized the potential of advanced simulation methods for treating reliability problems. The Subset Simulation method, introduced by Au & Beck (2001), is considered to be one of the most robust advanced simulation techniques for solving high-dimensional nonlinear problems. The Modified Metropolis-Hastings (MMH) algorithm, a variation of the original Metropolis-Hastings algorithm (Metropolis et al., 1953, Hastings 1970), is used in Subset Simulation for sampling from conditional high-dimensional distributions. The efficiency and accuracy of Subset Simulation directly depends on the ergodic properties of the Markov chain generated by MMH, in other words, on how fast the chain explores the parameter space. The latter is determined by the choice of one-dimensional proposal distributions, making this choice very important. It was noticed in Au & Beck (2001) that the performance of MMH is not sensitive to the type of the proposal PDFs, however, it strongly depends on the variance of proposal PDFs. Nevertheless, in almost all real-life applications, the scaling of proposal PDFs is still largely an art. The issue of optimal scaling was realized in the original paper by Metropolis (Metropolis et al., 1953). Gelman et al. (1996) have been the first authors to publish theoretical results about the optimal scaling of the original Metropolis-Hastings algorithm. They proved

that for optimal sampling from a high-dimensional Gaussian distribution, the Metropolis-Hastings algorithm should be tuned to accept approximately 25% of the proposed moves only. This came as an unexpected and counter-intuitive result. Since then a lot of papers has been published on the optimal scaling of the original Metropolis-Hastings algorithm. In this paper, in the spirit of Gelman et al. (1996), we address the following question which is of high practical importance: what are the optimal one-dimensional Gaussian proposal PDFs for simulating a high-dimensional conditional Gaussian distribution using the MMH algorithm? We present a collection of observations on the optimal scaling of the Modified Metropolis-Hastings algorithm for different numerical examples, and develop an optimal scaling strategy for MMH when it is employed within Subset Simulation for estimating small failure probabilities.

REFERENCES

- Au, S.K. & Beck, J.L. (2001). Estimation of small failure probabilities in high dimensions by subset simulation. *Probabilistic Engineering Mechanics* 16(4), 263–277.
- Gelman, A., Roberts, G.O. & Gilks, W.R. (1996). Efficient metropolis jumping rules. *Bayesian Statistics* 5, 599–607.
- Hastings, W.K. (1970). Monte carlo sampling methods using markov chains and their applications. *Biometrika* 57(1), 97–109.
- Metropolis, N., Rosenbluth, A.W., Rosenbluth, M.N., Teller, A.H. & Teller, E. (1953). Equation of state calculations by fast computing machines. *J. Chemical Physics* 21(6), 1087–1092.

Non-specificity modeling of concrete cracking strength using possibility theory

Jung J. Kim, Mahmoud M. Reda Taha & Timothy J. Ross

Department of Civil Engineering, University of New Mexico, USA

1 INTRODUCTION

Inherent randomness of microstructure in concrete makes it difficult to determine concrete properties. Concrete cracking strength can be determined by various test methods including flexural strength test, splitting tensile strength test and direct tension test. Moreover, the computational models proposed by design codes have variations among themselves. Therefore, it can be stated that there exist a number of alternatives to represent concrete cracking strength due to the different cracking criteria of concrete according to the stress regime on concrete cracking. As the flexural reinforced concrete (RC) members are subjected to combined tensile stresses due to bending and restrained concrete shrinkage respectively, it is difficult to select a single cracking criterion for practical RC serviceability calculations. This difficulty in choosing from many alternatives of concrete cracking strength criteria can be modeled as an uncertainty known as “non-specificity” (Dubois et al., 1993, Ross 2010), an epistemic uncertainty.

In this study, confidence intervals are used to model non-specificity in concrete cracking strengths. The confidence intervals are extracted from three types of experimental tests and three different computational models to predict concrete cracking strength. Three types of tests, flexural, splitting and direct tension tests, are conducted. The concrete compressive strength test is also conducted and the results are used to predict concrete cracking strengths through three different computational models. A possible concrete cracking strength interval is determined from the intervals using possibility theory. A case study to predict the RC deflection interval using the possible concrete cracking strength interval is presented to show the effectiveness of the proposed approach.

2 METHODS

Six concrete cracking strength intervals were used to generate the corresponding possibility

distribution. Based on our test results, three intervals of the flexural tensile strength, the splitting tensile strength and the direct tensile strength were developed. Moreover, the three computational models of the concrete cracking strength proposed by design codes, the ACI 318M-08 (2008), the CEB-FIP MC-90 (1993) and the CSA-CHBDC (2006), are computed as intervals based on the compressive strength confidence interval.

When each interval has its weight m , a possibility distribution for the consonant set of intervals can be generated using the relationship between π and m as

$$\pi(x) = \sum_{x \in H_i} m(H_i) \quad (1)$$

where H_i is a interval of a consonant set, $m(H_i)$ is the corresponding weight based on supporting evidence. To generate a consonant set of intervals from a completely disjoint set of intervals, an anchor interval needs to be defined first (Donald 2003) and a weighted anchor (Kim 2008) can be used for a practical alternative.

Deflections of RC beams are calculated using cracked plane frame (CPF) analysis. Full details of CPF analysis can be found elsewhere (Ghalli & Favre 2002).

3 CASE STUDY AND DISCUSSIONS

The third-point bending tests (Washa 1947) of a simple support RC beam with different concrete compressive strengths (the average of 29.5 MPa with the standard deviation of 1.6 MPa) was selected for the application of a possible concrete cracking strength interval to deflection calculation of RC beams. The average of the deflection is 40.3 mm and the corresponding 95% confidence interval is determined as [37.2, 43.5] mm.

Using the six concrete cracking strength intervals for the case study, the possibility distribution was generated as shown in Figure 1. The possible

concrete cracking strength interval at π of 25%~50% is determined from Figure 1 as

$$f_{cr}^{\pi=25\% \sim 50\%} = [1.74 \ 3.45] \text{ MPa} \quad (2)$$

The deflection interval of the RC beam according to the concrete cracking strength interval in Eq. (2) was calculated using CPF analysis as

$$\Delta^{\pi=25\% \sim 50\%} = [37.1 \ 48.7] \text{ mm} \quad (3)$$

When the calculated deflection interval is compared with deflection observations of RC beams, the calculated deflection interval in Eq. (3) includes all deflection observations of RC beams.

The possibility distribution of the deflection can be generated as shown in Figure 2. Using dual monotone measures, the *certainty* and the *possibility*, in possibility theory, uncertainty information in possibility distribution can be examined. For the 95% confidence interval [37.2, 43.5] mm, “the actual deflection being in the interval [37.2, 43.5] mm is possibly 100% but certainly 0%” is evaluated. This means that there is no evidence for the actual deflection to be in the interval when non-specificity of the concrete cracking strength is considered.

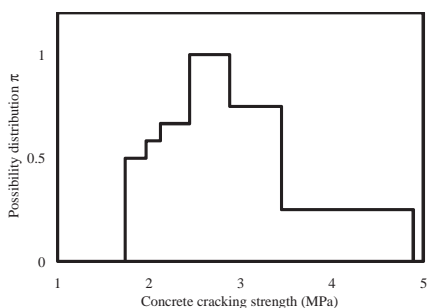


Figure 1. Possibility distribution of concrete cracking strength for the case study.

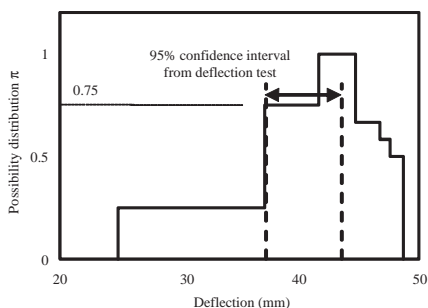


Figure 2. Possibility distribution of the deflection generated from the possibility distribution of concrete cracking strength in Figure 1.

4 CONCLUSIONS

It was shown through a case study that the possible concrete cracking strength interval can be used to quantify deflection intervals of RC beams. The deflection intervals are compared with the confidence interval of the deflection test results, which can be an interval by considering only random uncertainty. The results show the necessity of epistemic uncertainty consideration to the deflection predictions of RC beams. Moreover, it is shown that the use of interval for the RC deflection could be appropriate for the epistemic uncertainty assignment to the deflection calculation.

ACKNOWLEDGEMENTS

Financial support to the authors by US Defense Threat Reduction Agency (DTRA) basic research grant on uncertainty quantification is appreciated.

REFERENCES

- American Concrete Institute (ACI) 2008. Building code requirements for structural concrete, ACI 318M-08, and commentary. Farmington Hills: ACI.
- CEP-FIP Model Code (MC) 90 1993. Model code for concrete structures, Comité Euro- International du Béton. CEB. Fédération Internationale de la Précontrainte. FIP. London: Thomas Telford Ltd.
- Canadian Standards Association (CSA) 2006. Canadian Highway Bridge Design Code (CHBDC). Toronto: CAN/CSA-S6-06.
- Donald, S. 2003. Development of empirical possibility distributions in risk analysis. Ph.D. Thesis. Albuquerque (NM, USA): Department of Civil Engineering, UNM.
- Dubois, D., Prade, H. & Sandri, S. 1993. On possibility/probability transformations. In: Lowens et al., editors. Fuzzy Logic. Kulwer Academic Publishers.
- Ghali, A. & Favre, R. 2002. Concrete Structures: Stresses and Deformations. 3rd ed. UK: Spon Press.
- Helton, J.C., Johnson, J.D. & Oberkampf, W.L. 2004. An exploration of alternative approaches to the representation of uncertainty in model predictions. *Reliability Engineering & System Safety* 85(1–3): 39–71.
- Kim, J.J. 2008. Uncertainty quantification in serviceability of reinforced concrete structures. Ph.D. Thesis. Albuquerque (NM, USA): Department of Civil Engineering, UNM.
- Ross, T.J. 2010. Fuzzy logic with engineering applications. 3rd ed. Chichester (UK): John Wiley and Sons.
- Washa, G.W. 1947. Plastic Flow of Thin Reinforced Concrete Slabs. *ACI Journal Proc.* 44: 237–258.

Likelihood-based representation of imprecision due to sparse point data and/or interval data

Shankar Sankararaman & Sankaran Mahadevan
Vanderbilt University, Nashville, TN, USA

ABSTRACT: This paper presents a likelihood-based methodology for a unified probabilistic representation of an uncertain quantity for which only sparse point data and/or interval data may be available. While probabilistic methods are readily available for treatment of point data, interval data are usually handled by non-probabilistic approaches such as evidence theory, interval theory-based methods, fuzzy logic, etc. Hence, existing methods are not directly applicable when information is available in both forms. In this paper, the concept of likelihood is used to construct probability distributions for quantities for which data may be available in the form of sparse point data and interval data, thereby enabling the combined treatment of both forms of evidence.

In the case of point data, the likelihood is evaluated from the probability density function of the random variable. This paper extends this approach to construct the likelihood function when the data on a random variable is available in the form of single or multiple intervals, or even as a mixture of point and interval data. The likelihood-based approach is then adapted to calculate the entire probability distributions of the distribution parameters of the input random variables; this information is propagated through the system model to compute the probability distribution of the output. Non-parametric probability distributions are used to represent the interval data, wherein the entire distribution is discretized at a finite number of points and the probability density values at these points are inferred using the principle of maximum likelihood, thus *avoiding the assumption of any particular distribution*. The entire probability density function of the quantity of interest can be interpolated using the maximum likelihood estimate of the probability density values at the discretization points. If a higher number of discretization points are used, then the dimension of the optimization problem increases; however, the resulting probability density function is more accurate. Further, different interpolation

methods lead to different results. This paper studies three different interpolation techniques—linear interpolation, spline-based interpolation, and Gaussian process interpolation. While the linear interpolation method is a simple but useful approximation, splines and Gaussian processes are advanced and flexible interpolation techniques. As mentioned earlier, any of these interpolation techniques may be used for construction of the probability density function of the quantity of interest.

Using challenge problems from the Sandia Epistemic Uncertainty Workshop (Oberkampf et al., 2004), the proposed method is investigated and compared with previous studies that have pursued other approaches to represent and propagate interval description of input uncertainty. While other researchers have used computationally intensive interval analysis methods, fuzzy sets, evidence theory, etc. for uncertainty propagation of imprecision due to interval data, this paper uses purely probabilistic methods; this enables the use of adaptive Monte Carlo methods, first and second order reliability methods, etc. for uncertainty propagation. The proposed approach significantly reduces the computational cost by avoiding the nested computation that is encountered when some variables are treated using a probabilistic method and some other variables are treated using a non-probabilistic method.

Keywords: Interval data, likelihood, probability distribution, distribution parameters, epistemic uncertainty, Gaussian process interpolation

REFERENCE

- Oberkampf, W.L., Helton, J.C., Joslyn, C.A., Wojtkiewicz, S.F. & Ferson, S. 2004. Challenge Problems: uncertainty in system response given uncertain parameters. *Reliability Engineering and System Safety* 85:11–19.

Response bounds for structures with interval stiffness

N. Impollonia & S. Zito

Dipartimento di Architettura, Università di Catania, Catania, Italy

G. Muscolino

Dipartimento di Ingegneria Civile & C.I.Di.S., Centro Interuniversitario di Dinamica Teorica e Sperimentale
 Università di Messina, Messina, Italy

F. Saitta

ENEA, Centro Ricerche di Bologna, Bologna, Italy

1 INTRODUCTION

In this paper the uncertainties present in many engineering problems are modeled as interval variables, which seems today the most suitable analytical tool in the framework of non-probabilistic methods (Elishakoff & Ohsaki 2010). The interval model is derived from the interval analysis, in which a parameter is treated as an interval variable with lower and upper bounds (Moore et al., 2009). However, the application of the interval analysis in classical form, to solve the algebraic equations governing the equilibrium conditions, can result in a severe overestimation of the uncertainty of the output (Moens & Vandepitte 2005). Moreover, in the evaluation of the element stress tensor, because one or several variables occur more than once in an interval expression, the overestimation increases and the result becomes physically unacceptable. This is a consequence of the so-called *dependency phenomenon* (Moens & Vandepitte 2005, Moore et al., 2009). The major drawback, of this phenomenon is its repeated vulnerability to conservatism (Moens & Vandepitte 2005).

Aim of the paper is to develop a method to evaluate the static response of structures with interval stiffness. The procedure overcomes the drawback of the dependency phenomenon, in the inversion of the assembled interval stiffness matrix, by means of an approximate, but very accurate, interval-valued Sherman-Morrison-Woodbury (SMW) formula (Impollonia & Muscolino, 2011), which leads to more sharp solution than traditional interval analysis. Numerical results evidence the accuracy and the effectiveness of the proposed approach in the evaluation of the bounds of the response.

2 MAIN STEPS OF THE PROPOSED APPROACH

The main steps of the proposed approach are:

- i. The adoption of a procedure based on a factorization of the single element stiffness matrix, following the *unimodal components* concept (Fuchs 1992) in order to assemble the stiffness matrix by a non conventional approach:

$$\mathbf{K}(\alpha) = \mathbf{K}_0 + \sum_{i=1}^N \alpha_i \phi_i \phi_i^T \quad (1)$$

- ii. The definition of the *i*-th unimodal uncertain component α_i as an interval variable:

$$\alpha_i^I = \alpha_{0,i} + \lambda_i e_i^I = \lambda_i e_i^I \equiv [-\lambda_i + \lambda_i] \quad (2)$$

where $\alpha_{0,i}$ is the reference value assumed equal zero and λ_i is the fluctuation around the reference value.

- iii. The inversion of the assembled interval stiffness matrix, by means of an approximate, but very accurate, interval-valued SMW formula (Impollonia & Muscolino, 2011):

$$\begin{aligned} \mathbf{K}^{-1}(\alpha) &= \left(\mathbf{K}_0 + \sum_{i=1}^N \lambda_i e_i^I \phi_i \phi_i^T \right)^{-1} \\ &\approx \mathbf{K}_0^{-1} - \sum_{i=1}^N \frac{\lambda_i e_i^I}{1 + \lambda_i e_i^I a_i} \mathbf{A}_i; \quad \alpha_i \in \alpha_i^I \end{aligned} \quad (3)$$

In Eq. (3), \mathbf{K}_0 is the reference stiffness matrix (where the parameters take their reference value):

$$\mathbf{K}_0 = \sum_{i=1}^N \alpha_{0,i} \phi_i \phi_i^T \quad (4)$$

and

$$a_i = \phi_i^T \mathbf{K}_0^{-1} \phi_i > 0; \quad \mathbf{A}_i = \mathbf{K}_0^{-1} \phi_i \phi_i^T \mathbf{K}_0^{-1} \quad (5)$$

iv. The evaluation of the narrowest interval $\mathbf{u}(\alpha)$ containing all possible solution vectors:

$$\begin{aligned} \mathbf{u}(\alpha) &= \mathbf{K}(\alpha)^{-1} \mathbf{f} = \left(\mathbf{K}_0 + \sum_{i=1}^N \lambda_i e_i^l \phi_i \phi_i^T \right)^{-1} \mathbf{f} \\ &\approx \mathbf{A}_0 \mathbf{f} + \sum_{i=1}^N \frac{\lambda_i e_i^l}{1 - (\lambda_i a_i)^2} (\mathbf{A}_i \mathbf{f}); \quad \alpha_i \in \alpha_i^l \end{aligned} \quad (6)$$

v. The derivation an alternative approach, qualified for the evaluation of internal forces problems, to avoid the dependency phenomenon.

3 NUMERICAL APPLICATION

The plane stress problem given by the arch of thickness t modeled by constant strain triangles shown in Figure 1 has been analyzed assuming a fixed value of the Poisson ratio, $\nu = 0.3$, and of the nominal elastic modulus, E_0 . The structure, composed of $N_e = 48$ elements, has $n_{dof} \times N_n = 66$

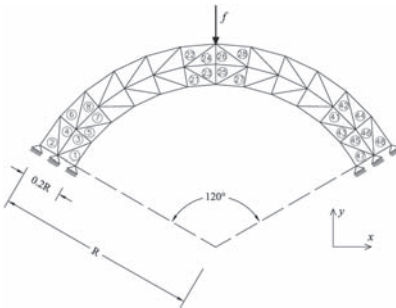


Figure 1. Arch structure modeled by 2-D constant strain triangles with plane stress assumption.

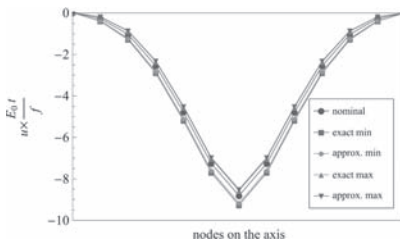


Figure 2. Vertical displacements of the nodes on the axis of the arch. Nominal solution, exact and approximate bounds when elements 1–4 and 45–48 have the elastic modulus defined by interval variables with radius $\Delta E = 0.3E_0$.

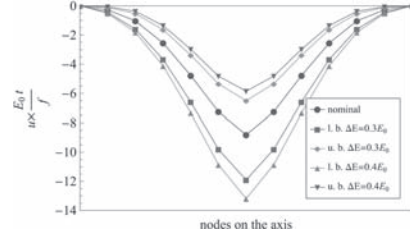


Figure 3. Vertical displacements of the nodes on the axis of the arch. Nominal solution and approximate bounds when all the elements have the elastic modulus defined by interval variables with radius $\Delta E = 0.3E_0$ and $\Delta E = 0.4E_0$.



Figure 4. Range variability of nodal displacements, represented by tick segments, when all the elements have the elastic modulus defined by an interval variables with radius $\Delta E = 0.3E_0$.

degrees of freedom, so that $N_\lambda = 144$ unimodal components are present.

In order to assess the accuracy of the proposed solution, the lower and upper bounds of the response are compared in Figure 2 with the exact ones for the case where the elements 1–4 and 45–48 have the elastic modulus defined by interval variables with radius $\Delta E = 0.3E_0$.

The case when all the elements have uncertain elastic modulus with $\Delta E = 0.3E_0$ and $\Delta E = 0.4E_0$ is considered in Figure 3. Finally, Figure 4 shows the variability of all horizontal and vertical displacements for the case $\Delta E = 0.3E_0$.

REFERENCES

Elishakoff, I. & Ohsaki, M. 2010. *Optimization and anti-optimization of structures under uncertainty*. Singapore: Imperial College Press.

Fuchs, M.B. 1992. The explicit inverse of the stiffness matrix. *International Journal of Solids & Structure*, 29: 2101–2113.

Impollonia, N. & Muscolino, G. In press. Interval analysis of structures with uncertain-but-bounded axial stiffness *Computer Methods in Applied Mechanics and Engineering*. doi:10.1016/j.cma.2010.07.019.

Moens, D. & Vandepitte, D. 2005. A survey of non-probabilistic uncertainty treatment in finite element analysis. *Computer Methods in Applied Mechanics and Engineering* 194: 1527–1555.

Moore, R.E., Kearfott, R.B. & Cloud, M.J. 2009. *Introduction to interval analysis*. Philadelphia: SIAM.

*MS_313 — Uncertainty and imprecision in geotechnical
and structural engineering (4)*

This page intentionally left blank

Stochastic optimal structural control

K. Marti

Aerospace Engineering and Technology, Federal Armed Forces University Munich,
Neubiberg/Munich, Germany

ABSTRACT: In order to omit structural damages and therefore high compensation (recourse) costs, active control techniques are used in structural engineering. The structures usually are stationary, safe and stable without considerable external dynamic disturbances. Thus, in case of heavy dynamic external loads, such as earthquakes, wind turbulences, water waves, etc., which cause large vibrations with possible damages, additional control elements can be installed in order to counteract applied dynamic loads, see [2,13].

The structural dynamics is modeled mathematically by means of a system of first order differential equations for the state vector $z = z(t)$ consisting of the vector $q = q(t)$ of displacements and their time derivatives $\dot{q} = \dot{q}(t)$. The system of differential equations involves random dynamic parameters, random initial values, the random dynamic load vector and a control force vector depending on an input control function $u = u(t)$. Robust optimal feedback controls u^* are determined in order to cope with the stochastic uncertainty involved in the dynamic parameters, the initial values and the applied loadings. In practice, the design of controls is directed often to reduce the mean square response (displacements and their time derivatives) of the system to a desired level within a reasonable span of time.

The performance of the resulting structural control problem under stochastic uncertainty is evaluated therefore by means of a convex quadratic cost function $L = L(t, z, u)$ of the state vector $z = z(t)$ and the control input vector $u = u(t)$. While the actual time path of the random external load is not known at the planning stage, we may assume that the probability distribution or at least the moments under consideration of the applied load and other random parameters are known. The problem is then to determine a robust (open-loop) feedback control law by minimization of the expected total costs, hence, a stochastic optimal control law.

1 STOCHASTIC HAMILTON-JACOBI APPROACH

Using a stochastic version, see [10], of the deterministic *Hamilton-Jacobi Theory*, cf. [4], necessary and sufficient optimality conditions for the resulting optimal control problem under stochastic uncertainty may be formulated in terms of a) the *stochastic Hamiltonian* of the control problem, and b) the related canonical (Hamiltonian) Two-Point Boundary Value problem with random coefficients. Stochastic optimal regulator parameters $V^* = V^*(t)$ of the feedback control law, or a stochastic optimal open-loop feedback control law $u^* = u^*(t)$ may be represented by means of a *H-minimal control* \tilde{V}^*, \tilde{u}^* , resp., which is obtained by solving a certain *finite dimensional stochastic programming problem*. Several methods are available, see [9,10], for solving the related canonical system of differential equations with random parameters for the optimal state and co-state trajectory $(z^*, y^*) = (z^*(t, \omega), y^*(t, \omega))$.

2 OPTIMAL FEEDBACK CONTROL

Assuming here that at each time point t the state $z_t := z(t)$ is available, the control force $f_a = \Gamma u$ is generated by means of a *PD*-controller. Hence, for the input n -vector function $u = u(t)$ we have

$$u(t) := \varphi(t, q(t), \dot{q}(t)) = \varphi(t, z(t)) \quad (1a)$$

with a feedback control law $\varphi = \varphi(t, q, \dot{q})$. Finding an optimal feedback control law—insensitive as far as possible with respect to random parameter variations—means that besides optimality of the control law also its insensitivity with respect to stochastic parameter variations should be guaranteed.

Efficient approximate feedback control laws are constructed here by using the concept of **open-loop feedback control**. Open-loop feedback control

is the main tool in *model predictive control*, cf. [7,8,11], which is very often used to solve optimal control problems in practice. The idea of *open-loop feedback control* is to construct a feedback control law quasi *argument-wise*, see [1,5].

3 STOCHASTIC OPEN-LOOP FEEDBACK CONTROL

Having to cope with stochastic uncertainty, we proceed with the following new stochastic version of open-loop feedback control: At each intermediate time point $t_b \in [t_0, t_f]$, based on the observed state $z_b = z(t_b)$ at t_b , a stochastic optimal open-loop control $u^* = u^*(t|(t_b, z_b))$, $t_b \leq t \leq t_f$, is determined first on the remaining time interval $[t_b, t_f]$, see Fig. 1, by stochastic optimization methods, cf. [6].

Having a stochastic optimal open-loop control $u^* = u^*(t|(t_b, z_b))$, $t_b \leq t \leq t_f$, on each remaining time interval $[t_b, t_f]$ with an arbitrary starting time t_b , $t_0 \leq t_b \leq t_f$, a stochastic optimal open-loop feedback control law is then defined by

$$\varphi^* = \varphi(t_b, z(t_b)) := u^*(t_b|(t_b, z_b)), \quad t_0 \leq t_b \leq t_f. \quad (1b)$$

Hence, at time $t = t_b$ just the “first” control value $u^*(t_b) = u^*(t_b|(t_b, z_b))$ of $u^*(\cdot|(t_b, z_b))$ is used only. For each other argument $(t, z_t) := (t, z(t))$ the same construction is applied.

For finding stochastic optimal open-loop controls, on the remaining time intervals $t_b \leq t \leq t_f$ with $t_0 \leq t_b \leq t_f$, the stochastic Hamilton function of the control problem is introduced. Then, the class of H —minimal controls is determined by solving a finite-dimensional stochastic optimization problem for minimizing the conditional expectation of the stochastic Hamiltonian subject to the remaining deterministic control constraints at each time point t . Having a H —minimal control, the related two-point boundary value problem with random parameters is formulated for the computation of the robust optimal state—and costate—trajectory. Due to the linear-quadratic structure of the underlying control problem, the state and costate trajectory can be **determined analytically** to a large extent. Inserting then these trajectories into the H -minimal control, robust optimal open-loop controls are found on an arbitrary remaining time interval. These controls yield then immediately a robust open-loop feedback control law. Moreover, it is possible to realize the obtained controls **real-time**. This is already applied to applications in optimal control of industrial robots, cf. [12].



Figure 1. Remaining time interval.

Summarizing, we get *optimal feedback controls under stochastic uncertainty* minimizing the effects of external influences on system behavior, subject to the constraints of not having a complete representation of the system, cf. [3]. Hence, robust optimal active controls are obtained by **new** techniques from *Stochastic Optimization*, see [9]. Of course, the construction can be extended also to *PID—controllers*.

REFERENCES

- [1] Aoki, M. 1967. Optimization of Stochastic Systems - Topics in Discrete-Time Systems. (New York - London: Academic Press).
- [2] Block, C. 2008. Aktive Minderung personeninduzierter Schwingungen an weit gespannten Strukturen im Bauwesen. Fortschrittberichte VDI, Reihe 11, Schwingungstechnik, Nr. 336. (Düsseldorf: VDI-Verlag GmbH).
- [3] Dullerud, G.E. & Paganini, F. 2000. A Course in Robust Control Theory - A convex approach. (New York [etc.]: Springer-Verlag).
- [4] Kalman, R.E., Falb, P.L. & Arbib, M.A. 1969. Topics in Mathematical System Theory. (New York [etc.]: McGraw-Hill Book Company).
- [5] Ku, R. & Athans, M. 1973. On the Adaptive Control of Linear Systems Using the Open-Loop-Feedback-Optimal Approach. IEEE Transactions on Automatic Control, AC-18, 489–493.
- [6] Marti, K. 2008. Stochastic Optimization Problems, 2nd edition. (Berlin-Heidelberg: Springer-Verlag).
- [7] Marti, K. 2008. Approximate Solutions of Stochastic Control Problems by means of Convex Approximations. In: B.H.V. Topping, M. Papadrakakis (Eds.) *Proceedings of the 9th Int. Conference on Computational Structures Technology (CST08)* (Stirlingshire, UK: Civil-Comp Press), paper No. 52.
- [8] Marti, K. 2008. Stochastic Nonlinear Model Predictive Control (SNMPC), 79th Annual Meeting of the International Association of Applied Mathematics and Mechanics (GAMM), Bremen 2008, PAMM, Volume 8, Issue 1, Wiley-VCH, 10775–10776.
- [9] Marti, K. 2010/11. Optimal Control of Dynamical Systems and Structures Under Stochastic Uncertainty: Stochastic Optimal Feedback Control. Accepted for publication in *Advances in Engineering Software (AES)*, Elsevier, DOI information: 10.1016/j.advengsoft.2010.09.008.
- [10] Marti, K. 2010/11. Continuous-Time Control Under Stochastic Uncertainty. Accepted for publication in the *Wiley Encyclopedia of Operations Research and Management Science*, Wiley.
- [11] Richalet, J., Rault, A., Testud, J.L. & Papon, J. 1978. Model Predictive Heuristic Control: Applications to Industrial Processes. *Automatica*, **14**, 413–428.
- [12] Schacher, M. 2010. Stochastisch Optimale Regelung von Robotern. (PhD Thesis, submitted to the Faculty for Aerospace Engineering and Technology, Federal Armed Forces University Munich).
- [13] Soong, T.T. 1990. Active Structural Control: Theory and Practice. (New York: Longman Scientific and Technical, J. Wiley).

Risk acceptance criteria based on uncertain estimates of structural failure probabilities

S.G. Reid

School of Civil Engineering, The University of Sydney, Australia

ABSTRACT: Calculated probabilities of structural failures commonly have significant uncertainties associated with the possible estimation errors relative to the ‘true’ failure probabilities. The ‘true’ failure probabilities may be defined as the failure probabilities that arise from the real (aleatory) variability of structural loads and resistances, whilst possible estimation errors may arise from epistemic uncertainties associated with imperfect knowledge and imperfect understanding of the load and resistance mechanisms.

The influence of an underlying uncertainty on the ‘true’ value of the probability can be assessed with regard to the conditional value of the ‘true’ probability, dependent on the value of the underlying variable. Hence, uncertainty in a probability estimate can be expressed in terms of a probability distribution of the conditional ‘true’ probability.

For a probability distribution of a failure probability p_f , an associated measure of ‘probabilistic confidence’ has been proposed to reflect the concern that uncertainty about the true probability of failure could result in a structure that is unsafe (in relation to a target level of safety) and could subsequently fail.

Accordingly, a probabilistic measure of ‘lack of confidence’ (C) that a structure is safe with regard to a target probability of failure p_{fi} can be determined from the probability distribution of the probability of failure $f_{p_f}(p)$ and the complementary measure of ‘probabilistic confidence’ C that a structure is safe (in relation to p_{fi}) is then given by:

$$C_{p_{fi}} = 1 - C'_{p_{fi}} = 1 - \int_{p_{fi}}^1 (f_{p_f}(p) \cdot p) dp \quad (1)$$

Also, it has been proposed that the level of probabilistic confidence required when dealing with uncertain failure probabilities should match the level of probabilistic confidence that is implicit in the specification of a target reliability for structures with well-defined probabilities of failure.

The paper describes how the concept of probabilistic confidence can be applied to evaluate and appropriately limit the probabilities of failure

attributable to particular uncertainties such as design errors that may critically affect the dependability of risk-acceptance decisions. It is argued that the concept of probabilistic confidence provides a rational and ‘objective’ basis for dependable risk acceptance criteria, not only to match the probabilistic confidence required for decisions based on well-defined risks, but also to ensure appropriate (higher) levels of probabilistic confidence are provided in relation to risks attributable to uncertainties that may critically affect the dependability of risk-acceptance decisions.

The concept of probabilistic confidence is applied to the evaluation of structural safety, considering examples of uncertain probability distribution functions of the probability of failure p_f for designs based on prototype testing (with uncertainty attributable to sampling variability). In this context, the probabilistic confidence is evaluated in relation to the probability of failure attributable to a loss of safety (with respect to the target probability of failure p_{fi}) due to the influence of sampling variability in the design process.

Standard procedures for structural design based on prototype testing include fully-probabilistic procedures (in which the sampling uncertainty is included in the reliability model) and statistical procedures (in which the sampling uncertainty is taken into account with regard to the concept of statistical confidence). A fully-probabilistic procedure specified in a North American Standard (AISI) and a statistical procedure specified in Australian Standards are reviewed. The AISI procedure is intended to achieve an overall (average) target safety index β_o , whilst the Australian Standard procedure is intended to achieve a target safety index β_o with a statistical confidence level of 90% for each application. Uncertainty in the probability of failure for structures designed in accordance with these procedures has been evaluated with regard to the risks attributable to sampling variability.

To illustrate the influence of sampling variability, prototype test results have been simulated for a population of structures with a LogNormal distribution of strengths and a coefficient of

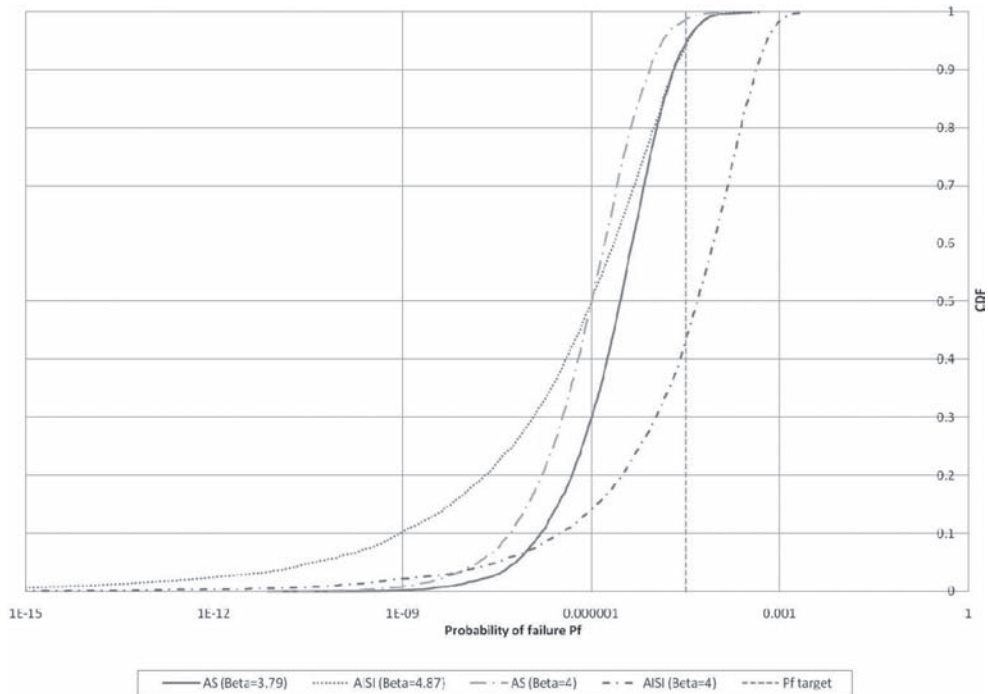


Figure 1. Distributions of the uncertain probability of failure p_f for structures designed on the basis of prototype testing procedures.

variation V_R that is itself LogNormally distributed with a mean value of 0.15 and a standard deviation of 0.03.

Considering samples of size $n = 5$, design strengths were obtained by simulation in accordance with the AISI procedure and the Australian Standard procedure for a target safety index β_o of 4.0 (considering a LogNormal distribution of loads with a coefficient of variation V_S of 0.3). The distributions of the corresponding nominal probabilities of failure p_f for AISI ($\beta_o = 4$) and AS ($\beta_o = 4$) are shown in Figure 1.

The level of fiducial confidence that a structure would be ‘safe’ in relation to the target probability of failure ($p_{ft} = 3.17 \times 10^{-5}$) has been evaluated for each prototype testing procedure with regard to the probabilistic confidence $C_{p_{ft}}$ and the complementary lack of confidence $C_{p_{ft}}^c$ which takes values of 1.46×10^{-4} and 2.75×10^{-6} for the AISI and AS procedures, respectively. Thus the probability of failure attributable to ‘unsafe’ results is very high (roughly an order of magnitude greater than p_{ft}) for the AISI procedure whilst it is much lower (roughly an order of magnitude less than p_{ft}) for the AS procedure.

To ensure that the prototype testing procedures produce results that are sufficiently dependable for the purposes of structural design, it is proposed that the probability of failure attributable to sampling variability $C_{p_{ft}}^c$ should be limited to a value that is one tenth of the conventional target value of the notional failure probability p_{ft} . This has been achieved by changing the nominal values of β_o to 4.87 and 3.79 for the AISI and AS procedures, respectively, and the corresponding results are shown in Figure 1.

It is shown that probabilistic confidence provides a convenient integrated measure of the risks associated with the sampling variability, and provides a rational and objective basis for comparison of the dissimilar results obtained from the two different design procedures. Furthermore, it is demonstrated that recalibration of the prototype testing procedures to ensure an appropriately high level of probabilistic confidence is a practicable option that produces sensible results. It is concluded that differentiated levels of probabilistic confidence can provide a practicable basis for dependable decision-making.

Interval finite elements for nonlinear material problems

M.V. Rama Rao

Vasavi College of Engineering, Hyderabad, India

R.L. Mullen

University of South Carolina, Columbia, SC, USA

R.L. Muhanna

Georgia Institute of Technology, Atlanta, GA, USA

1 INTRODUCTION

Structural analysis without considering uncertainty in loading or material properties leads to an incomplete understanding of the structural performance. Structural analysis using interval variables has been used by several researchers to incorporate uncertainty into structural analysis. To the authors' knowledge, applications of interval methods for the analysis of structures with material nonlinearity do not exist anywhere in literature. In this paper, we present an initial investigation into the application of interval finite element methods to non-linear problems of structural mechanics. In this work, we will consider two dimensional truss structures with a deformation theory form of plasticity as a constitutive model of the material response. Critical to our development is the computation of element strains that do not have the large overestimation of derived quantities (or secondary quantities) that has plagued displacement based interval finite element methods. We will incorporate a mixed/hybrid formulation to simultaneously calculate the interval strains and displacements (Rama Rao, Mullen and Muhanna, 2010).

2 INTERVAL FINITE ELEMENT METHODS

Interval finite element methods have been developed for the last twenty years to handle the analysis of systems for which uncertain parameters described as intervals. A variety of solution techniques have been proposed for interval FEM, including the combinatorial method, perturbation method, sensitivity analysis method, and interval analysis. In this paper, the interval FE analysis is formulated as an interval analysis problem. A natural idea to implement interval FEM is to apply the interval extension to the deterministic

FE formulation. Unfortunately, such a naïve use of interval analysis in FEM yields meaningless and overly wide results. The reason is that in interval arithmetic each occurrence of an interval variable is treated as a *different, independent* variable. It is critical to the formulation of the interval FEM that one identifies the dependence between the interval variables and prevents the overestimation of the interval width of the results. In this paper, an element-by-element (EBE) technique is utilized for element assembly. We will incorporate a mixed/hybrid formulation to simultaneously calculate the interval strains and displacements (Rama Rao, Mullen and Muhanna, 2010). This linear formulation results in the interval linear system of equations given in Eq. (1) which can be introduced in the form of the following system:

$$(K + B \mathbf{D} A) \mathbf{u} = a + F \mathbf{b} \quad (1)$$

where bold font represents intervals, with interval quantities in \mathbf{D} and \mathbf{b} only. The term $(K + B \mathbf{D} A)$ represents the interval structural stiffness matrix and the $a + F \mathbf{b}$ term, the structural loading. The solution is obtained by performing the following Neumaier's iterative

$$\begin{aligned} \mathbf{v} &= \{(ACa) + (ACF)\mathbf{b} + (ACB)\mathbf{d}\} \cap \mathbf{v}, \\ \mathbf{d} &= (D_0 - \mathbf{D})\mathbf{v} \cap \mathbf{d} \end{aligned} \quad (2)$$

until no more improvement in values of \mathbf{d} , and then the following enclosure is obtained:

$$\mathbf{u} = (Ca) + (CF)\mathbf{b} + (CB)\mathbf{d} \quad (3)$$

where

$$\begin{aligned} C &:= (K + B D_0 A)^{-1} \\ \mathbf{u} &= Ca + CF\mathbf{b} + CB\mathbf{d} \\ \mathbf{v} &= ACa + ACF\mathbf{b} + ACB\mathbf{d}, \\ \mathbf{d} &= (D_0 - \mathbf{D})\mathbf{v} \end{aligned} \quad (4)$$

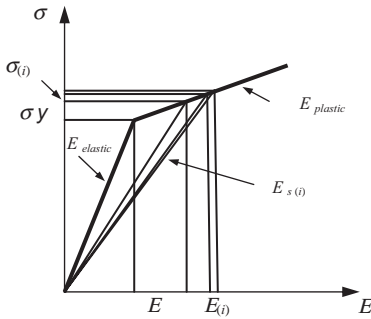


Figure 1. Nonlinear stress strain relation.

3 NONLINEAR SECANT METHOD

The method chosen for solving the system of non-linear interval equations resulting from the interval finite element method is the secant method. While incremental tangent stiffness methods are more common in finite element applications, the tangent stiffness methods use an incremental approach and therefore require the summation of a number of interval incremental solutions. Such a summation may lead to overestimation of the width of the solutions. The secant method does not require an incremental solution with its potential for overestimation.

For each element in the structure, a tri-linear constitutive relationship antisymmetric with respect to the origin using a yield strain and hardening modulus is assumed as shown in Figure 1. When the absolute value of the strain, ϵ , in an element is below the yield strain, ϵ_y , the secant modulus is taken as the elastic modulus, E . In subsequent iterations, a secant modulus is calculated from the current element strain. If the load is given as an interval value, the resulting element strain will also be an interval quantity. This may lead to an interval value for the secant modulus with the bounds on secant modulus calculated from the bounds on the element strain.

4 FORMULATION

The formulation provides the strains along with displacements and forces. Solution of conventional interval finite elements provides interval bounds of displacements, the calculations of strains from displacements result in significant overestimation. In the current formulation, the strains are not calculated from displacements but are obtained simultaneously with the displacements and forces avoiding any additional *overestimation*. These sharp interval strains' bounds are used in an iterative algorithm for calculating the updated interval values of the secants.

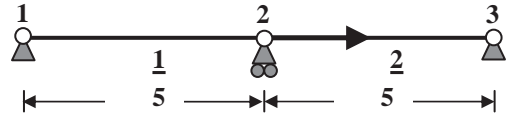


Figure 2. Two bar assembly.

Table 1. Two bar assembly—variation of nonlinear strain and secant modulus with load uncertainty in member 1.

α	Strain $\times 10^{-3}$		Secant modulus $\times 10^7$	
	Lower	Upper	Lower	Upper
0.000	6.249	6.249	4.800	4.800
0.002	6.185	6.310	4.7646	4.840
0.004	6.109	6.370	4.728	4.887
0.006	6.018	6.430	4.694	4.947
0.008	5.903	6.490	4.660	5.023
0.010	5.747	6.550	4.626	5.133

Example 1—two bar assembly

The two bar assembly shown in Figure 2 is subjected to a nominal point load of 6000 kN at the node 2 in the horizontal direction. The value of Young's modulus of each element is $E_i = 2 \times 10^{11}$ N/m², $i = 1, 2$ while the cross sectional area is 0.01 m². The structure is subjected to nonlinear deformation as a result of application of the above load.

Table 1 presents the values of strain and secant modulus in member 1 for various levels of load uncertainty. Figure 3 shows the variation of strain in member 1 with the variation of uncertainty of load.

5 CONCLUSIONS

A non-linear finite element method for structural analysis with uncertainty is presented. In this paper, uncertainty is represented as interval numbers. An interval secant stiffness method is presented. Example problems illustrate the application of the method to truss problems. Further study of non-linear interval finite elements methods that use alternative equation solving strategies is still needed to provide a more complete understanding of nonlinear interval finite element methods.

REFERENCE

- Rama Rao, M.V., Mullen, R.L. & Muhanna, R.L. 2010. "A New Interval Finite Element Formulation With the Same Accuracy in Primary and Derived Variables", International Journal of Reliability and Safety, *in press*.

Reliability-based design for steel drive-in racks under forklift truck impact

Hao Zhang

School of Civil Engineering, University of Sydney, NSW, Australia

Benoit P. Gilbert

School of Engineering, Griffith University, QLD, Australia

Kim J.R. Rasmussen

School of Civil Engineering, University of Sydney, NSW, Australia

Steel drive-in racks are susceptible to structural failure due to accidental impact by the operating forklift trucks. The impact forces the bay to open by pushing on the upright. If the bowing of the impacted upright is sufficiently large, the pallets can drop through as shown in Fig. 1. Therefore, the system limit state function g can be defined as $g = \delta - \Delta$, in which δ = pallet bearing width, and Δ = actual bay opening under the impact load. Structural failure occurs when $g < 0$. This mode of failure defines a limit state that forms the basis for evaluating the safety of drive-in racks under forklift truck impact. Recently, a simple equation to calculate the equivalent static impact force was proposed, based on full-scale rack/truck impact tests and 3D dynamic FE analysis (Gilbert et al., 2009). In this study, an impact load factor is developed on the basis of structural reliability assessment, taking into account the uncertain nature of the impact force, structural resistance and computational models. In design practice, the bay opening is determined from the factored impact loads, and is not to exceed specified limits.

The probability of structural failure developing from an accidental impact event can be written as

$$P_f = P(\text{Fail}|\text{I})P(\text{I}) \quad (1)$$

in which P_f = probability of structural failure, I = event of accidental impact, $P(\text{I})$ = probability of impact, and $P(\text{Fail}|\text{I})$ = probability of structural failure given that the impact occurs. The risk of structural failure can be mitigated by strategies to reduce the incidence of impact, or to reduce its effect on structural performance through structural design if the impact does occur (Ellingwood 2007). From a structural design point of view, the focus is on controlling the conditional failure probability $P(\text{Fail}|\text{I})$, i.e., to compensate for impact in design.

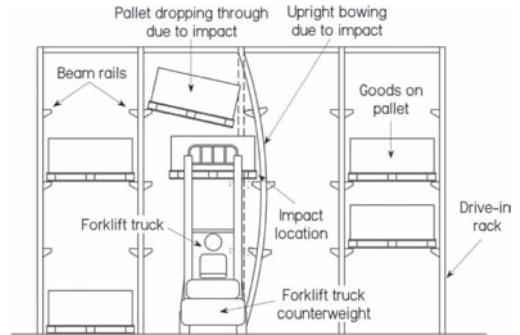


Figure 1. Pallet drop-through due to forklift truck impact.

In the modern probability-based design specifications for steel structures, the target failure probability for various structural members under gravity loads are about 1.24×10^{-4} to 2.7×10^{-5} /yr. The acceptable overall failure probability, P_f , for rack structures is assumed to be 2.0×10^{-4} /yr, a value comparable to that of a typical steel member.

The frequency of occurrence of impact needs to be estimated to calculate the conditional failure probability. Impact event may be modeled as occurring in time as a Poisson process, with a mean occurrence rate of ν (the average number of occurrence per unit time interval). There are little statistical data to define ν . In deriving the impact load factor, a range of ν will be considered, i.e., from 10^{-2} to 2/rack/yr.

The impact force is characterized by high uncertainty. The uncertainty arises from two sources: the model uncertainty and the inherent randomness of the basic variables (e.g., the bending stiffness of the impacted upright, and the forklift truck body rotation). The model uncertainty was

estimated by comparing the dynamic FE results to those predicted by the design equation. The statistical data for the forklift truck body rotation were collected from a total of 116 experiments (Gilbert et al., 2009). It is found that α has a mean of 0.023 rad and a COV of 0.46. In the present study, the nominal (design) value for truck body rotation is taken as its mean value, i.e., $\alpha_n = 0.023$ rad. With known statistical properties for the basic random variables and the model uncertainty, Latin Hypercube sampling method is used to obtain the statistics for impact load. The impact force was found to have a mean-to-nominal value of 1.0 and a COV of 0.49.

There is an apparent lack of statistical data for the pallet bearing width in the literature. However, the bounds of the pallet bearing width can be readily obtained based on the manufacturing specifications. In typical Australian industry practice, the design bearing width for pallet is around 60 mm. If the pallet is not positioned evenly between the two rails, the bearing width varies between 40 mm to 80 mm. In general, let $\delta_{n,min}$ and $\delta_{n,max}$ denote the design minimum and maximum pallet bearing width. The pallet bearing width is assumed in this study to be uniformly distributed between these two extreme values. The assumption of uniform probability distribution is conservative because it possesses maximum uncertainty.

The bay opening under the impact force can be calculated with sufficient accuracy by using a first/second order elastic analysis. Since the second order effect is relatively insignificant, the bay opening and impact force can be assumed as linearly related, i.e., $\Delta = fF$, in which f = flexibility coefficient, and F = impact force. The limit state function thus can be expressed as

$$g = \delta - fF. \quad (2)$$

If a rack is designed at the limit, one has

$$\delta_\alpha = \gamma f_n F_n, \quad (3)$$

in which δ_α = allowable bay opening, f_n and F_n are the nominal values for f and F . In the present study, the allowable bay opening δ_α is taken to be the design minimum pallet bearing width, $\delta_{n,min}$, specified by the manufacturer.

Galambos & Ellingwood (1986) studied the reliability implication of serviceability (drift) limit states for steel rigid frames under lateral wind load. It was found that $f_m/f_n = 1.0$, and V_f is mainly due to the variabilities in the bending stiffness of the column and is of the order of 0.10. Values of f_m/f_n and V_f for a steel rack structure would not be dissimilar to those of a rigid frame. This paper thus adopts the values $f_m/f_n = 1.0$ and $V_f = 0.1$.

Table 1. Impact load factor γ .

ν (/yr)	$P(g \leq 0 I)$	β	γ^a	γ^b	γ^c
10^{-2}	2.01×10^{-2}	2.05	1.77	1.61	1.52
10^{-1}	2.10×10^{-3}	2.86	2.21	2.09	2.02
0.5	5.08×10^{-4}	3.29	2.43	2.33	2.27
1	3.16×10^{-4}	3.42	2.49	2.40	2.35
2	2.31×10^{-4}	3.50	2.53	2.44	2.39

Values are based on a target risk $P_f = 2 \times 10^{-4}/\text{yr}$.

^a $\delta_{n,max}/\delta_{n,min} = 1.5$.

^b $\delta_{n,max}/\delta_{n,min} = 2.0$.

^c $\delta_{n,max}/\delta_{n,min} = 2.5$.

With known statistics for f and F , the conditional reliability index β for a given load factor γ can be evaluated by first-order reliability method (FORM). As discussed earlier, an appropriate target value for the overall failure probability P_f is estimated as $2.0 \times 10^{-4}/\text{yr}$. Under this assumption, Table 1 presents $P(g \leq 0|I)$, conditional reliability index β , and the required impact load factor γ for impact occurrence rate ν varying from 10^{-2} to 2/rack/yr. Three sets of impact load factors are listed in the table, with $\delta_{n,max}/\delta_{n,min} = 1.5, 2.0$ and 2.5, respectively. As can be expected, for a given target reliability index the required impact load factor decreases as $\delta_{n,max}/\delta_{n,min}$ increases. However, the difference is not significant and the general trends are the same. This implies that the load factor γ is relatively insensitive to $\delta_{n,max}/\delta_{n,min}$. Although a designer can choose the impact load factor from Table 1 if the information on ν and $\delta_{n,max}/\delta_{n,min}$ is available, it is desirable in the practice to use a single load factor to simplify the design process. It may be observed that γ falls within a range of 2.0 to 2.5 for ν varying from 10⁻¹ to 1/yr. A single factor, $\gamma = 2.3$, appears to be satisfactory across a large range of impact occurrence rate, though it could be over-conservative if ν is less than or equal to 10⁻²/yr.

REFERENCES

- Ellingwood, B.R. (2007). Strategies for mitigating risk to buildings from abnormal load events. *Int. J. Risk Assessment and Management* 7(6/7), 828–845.
- Galambos, T.V. & Ellingwood, B.R. (1986). Serviceability limit states: deflection. *J. Struct. Engrg., ASCE* 112(1), 67–84.
- Gilbert, B.P., Rasmussen, K.J.R. & Zhang, H. (2009). Impact tests and parametric impact studies on drive-in steel storage racks. Research Report No R903, Centre for Advanced Structural Engineering, School of Civil Engineering, University of Sydney.

Reliability analysis of steel scaffold shoring structures

Hao Zhang

School of Civil Engineering, University of Sydney, NSW, Australia

Kim J.R. Rasmussen

School of Civil Engineering, University of Sydney, NSW, Australia

Bruce R. Ellingwood

School of Civil and Environmental Engineering, Georgia Institute of Technology, Atlanta, GA, USA

Steel scaffolds are commonly used in reinforced concrete construction as shoring systems to support formwork. At present, industry practice for the design of steel scaffold structures are based on the working load limit (WLL) philosophy. The factor of safety, typically ranging from 2.0 to 2.5, is judgmental in nature. The reliability associated with current steel scaffold design practice is unknown.

This paper presents a reliability assessment of a typical steel scaffold structure designed in accordance with the WLL design format. The reliability implications for the scaffolds designed by advanced nonlinear structural analysis and the customary elastic analysis are compared. The probabilistic load models for scaffolds were obtained from the load survey data published in the literature. The statistical characteristics of the structural resistance were derived using simulations and an advanced nonlinear structural analysis. The simulation studies also provide useful information on the relative significance of different sources of uncertainty to the overall variability in structural strength.

The vertical loads acting on a scaffold can be categorized as dead and live loads. The dead load is due to the weight of concrete and formwork. It increases as the concrete placement progresses, and reaches its maximum at the end of the placement. The live load consists of the weight of construction personnel, equipment, stacked material, and the effects of any impact during concrete placement. The magnitudes of the live loads depend on the stages of construction, i.e., before, during, and after placement of concrete. Fig. 1 shows a typical history of a shore load (a combination of the dead and live load effects). The maximum shore load typically occurs during the period of concrete placement, at the point when the dead load is fully developed while the live load assumes its instantaneous value. This stage of construction represents the critical condition for scaffold design, and it is

this stage of construction that the present paper addresses.

The live load of interest in this study is the companion live load when the dead load reaches its maximum at the end of the pour. This companion live load was examined by Fattal (1983) and Ikäheimonen (1997). It was found that: 1) the load due to the weight of workmen and equipment is very small in comparison with the dead load; 2) when concrete is placed by pumping, the impact load is insignificant; 3) when the crane-and-bucket method is used for concreting, the COV V_L ranges from 0.5 to 0.7, and the mean live load \bar{L} equals approximately $0.3 L_n$ if the nominal live load L_n is calculated using a design formwork live load of 2.4 kPa (50 psf) as specified in ACI 347. Based on this limited data, it is assumed in the present study that the live load on scaffolds has a Type I extreme distribution, with $V_L = 0.7$ and $\bar{L}/L_n = 0.3$ for a design formwork live load of 2.4 kPa (50 psf).

Theoretically, the dead load transmitted to the uprights of a scaffold can be calculated with reasonable accuracy as the variability in concrete weight is relatively low. However, many studies have shown that the measured-to-calculated value for the dead load applied to scaffolds has a relatively large variation (Fattal 1983, Rosowsky et al., 1994, Ikäheimonen 1997, Puente et al., 2007). The survey

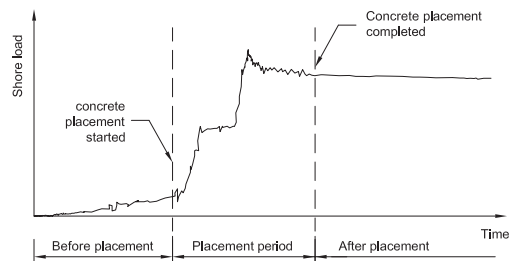


Figure 1. Typical shore load history.

results suggest that $\bar{D} \approx D_n$, and V_D ranges from 0.25 to 0.3. The reason for this relatively high uncertainty is not fully understood but it might be related to differential settlement of the uprights, or imperfections in the scaffold installations such as lack of bearing between the uprights and the formwork/bearer beams (Fattal 1983, Rosowsky et al., 1994, Ikäheimonen 1997). Also, the tributary area concept might be a source of the discrepancy. It appears that under current normal construction practice, a COV of 0.30 is representative for the dead load effect on the scaffolds. Thus, it is assumed in this study that the dead load is normally distributed, with $\bar{D}/D_n = 1.0$ and $V_D = 0.30$.

A typical 3-story 1 bay \times 1 bay steel scaffold tower as shown in Fig. 2 was considered. The uprights and ledgers are connected via cuplok joints. The jacks at the bottom and top of the frame are adjustable and are assumed to be of the same length. Two extreme values for the jack extensions are considered, i.e., 100 and 600 mm. The corresponding frames are referred to as Scaffold 1 and 2, respectively. The uprights, ledgers and braces are steel circular hollow sections (CHS). The jacks are solid steel rods.

Seven basic random parameters were identified in the present study: (1) yield stress of the uprights, (2) yield stress of the jacks, (3) initial out-of-straightness of the uprights, (4) load eccentricity, (5) thickness of the CHS of the uprights, (6) diameter of the jacks, and (7) joint stiffness of the semi-rigid cuplok joints.

Statistics of system strengths were simulated using the Latin Hypercube sampling method and a three-dimensional second-order inelastic finite element model. The inelastic FE model provides accurate theoretical predictions of system strength.

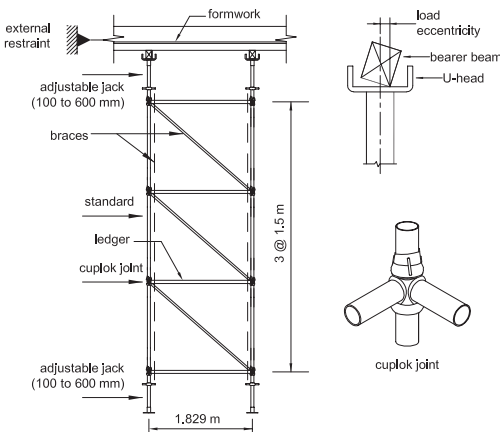


Figure 2. A steel scaffold tower with cuplok joints.

Simulation studies showed that for scaffolds with short jack extensions (100 mm), the failure of the system is due to inelastic flexural buckling of the upright members. The variability in structural strength mainly arises from the uncertainties in load eccentricity, the yield strength and thickness of the CHS uprights. The mean strength R equals $1.02R_n$ with a COV of 17%. The histogram is noticeably skewed to the left. The strength of Scaffold 1 can be best fitted by a three-parameter Weibull distribution.

For scaffolds with long jack extension (600 mm), a different failure mode, in which the lateral deformations were essentially confined to the jacks and the scaffolding in between shows little deformation, was observed. The uprights and ledgers experienced only small curvature and remained elastic. The system strength is governed by the buckling of the jacks. The jack diameter and load eccentricity become dominant influences on the structural strength. Other random parameters have inconsequential effects on V_R . The strength of Scaffold 2 has a mean-to-nominal ratio of 1.0 and a COV of 16% when all random variables are considered simultaneously. Its strengths are relatively evenly distributed on both sides of the mean.

For a typical loading ratio $L_n = D_n = 0.5$, the reliability index for Scaffold 1 is found to be 2.6 if its nominal ultimate strength is determined by the advanced nonlinear structural analysis. If the nominal system strength is computed using the customary elastic methods, the reliability index ranges from 2.6 to 2.93, depending on the modelling of the cuplok joints and the method for determining the effective length factor. For Scaffold 2, the elastic analysis appears to be sufficiently accurate for evaluating the system strength, as the design is controlled by the elastic buckling of the jacks. The reliability indices for the designs by advanced nonlinear analysis and by elastic analysis are similar, all being approximately 3.0.

REFERENCES

- Fattal, S. (1983). Evaluation of construction loads in multistory concrete buildings. NBS building science series 146, National Bureau of Standards, Washington D.C.
- Ikäheimonen, J. (1997). *Construction loads on shores and stability of horizontal formworks*. Ph. D. thesis, Royal Institute of Technology, Stockholm, Sweden.
- Puente, I., Azkune, M., & Insausti, A. (2007). Shore-slab interaction in multistory reinforced concrete buildings during construction: An experimental approach. *Eng. Struct.* 29, 731–741.
- Rosowsky, D.V., Huang, Y.L., Chen, W.F. & Yen T. (1994). Modeling concrete placement loads during construction. *Struct. Engrg. Rev.* 6(2), 71–84.

GS_111 — Uncertainty, statistics and probability (1)

This page intentionally left blank

Robust simulation for sensitivity analysis of catastrophe risk losses

R.J. Murnane

OpenRisk, LLC, Belmont, MA, USA
RPI/BIOS, St. Georges, BDA

C.E. Taylor

Torrance, CA, USA
University of Southern California, Los Angeles, CA, USA

T. Jagger

Climatek, Denver, CO, USA

Z. Hu

ImageCat, Long Beach, CA, USA

1 INTRODUCTION

Multiple model runs permit a “robust simulation” approach for catastrophe risk modeling. Here we use the term in the sense that multiple results from a robust simulation approach will account for exogenous model uncertainty (where exogenous refers to any non-modeled factor that results in divergent results) and produce a range of possible outcomes (Taylor et al., 2010). As an example of robust simulation, we present multiple results for estimates of probable loss from hurricane landfall along the US coastline. The poorly constrained impact of climate variability on hurricane hazard provides an instructive example of the sensitivity of a portfolio’s sensitivity to different views of hurricane hazard. The sensitivity is quantified using the expected Average Annual Loss (AAL) and return period losses from the portfolio’s loss exceedance curve.

Prior to 2006 the typical approach for hurricane hazard in the US was to use climatology to determine hurricane hazard in the US. In 2006 vendors of commercial risk models released new versions of their hurricane risk models that accounted for multi-decadal variability in the number of hurricanes in the Atlantic Ocean (Goldenberg et al. 2001). We are currently in a period associated with higher hurricane activity. The new model results based on the higher hurricane activity are described as a “near-term” view. Expected AAL and long return period losses (e.g., annual exceedance probabilities of 0.01, 0.004, and 0.002, or the 100, 250, and 500 year return periods) for the near-term view were significantly higher than losses associated with climatology. However, variations

in climate are not limited to the multi-decadal variability associated with the near-term view.

The results from a number of model simulations are used to illustrate the concept of robust simulation in the context of our understanding of how climate influences hurricane hazard. An idealized portfolio of exposure is run through a hurricane catastrophe risk model using multiple views of climate to assess the sensitivity of loss to different catalogs of hurricane events. The portfolio consists of single residential structures with identical construction at each population-weighted ZIP Code centroid in the domain of the hurricane model. In addition, the idealized portfolio is run through a single view of hurricane hazard using different levels of knowledge of the structure’s construction.

2 THE HURRICANE MODEL

The hurricane catastrophe risk model used for this analysis, and provided by Baseline Management Company, Inc., is a version of the HURLOSS model produced by Applied Research Associates (ARA). Details of HURLOSS can be found on the FCHLPM website (<http://www.sbafla.com/methodology/>).

Below we examine how four sources of climate variability influence the hurricane hazard: the El Niño-Southern Oscillation (ENSO), the North Atlantic Oscillation (NAO), sea surface temperature (SST) in the tropical North Atlantic, and sun spot numbers. Elsner and Bossak (2004) describe a statistical technique that can be used to model the response of US hurricane landfall to changes in climate. This approach is used in the Baseline

model to account for how changes in climate would influence hurricane hazard.

3 MODEL SIMULATIONS

Two sets of simulations are discussed. The first set is designed to assess how plausible variations in climate influence the hurricane hazard and the associated expected loss. For these simulations the structure's construction is coded as an unknown wood frame structure less than 4 stories tall, and its occupancy is set as a detached, single unit residential structure. Four climate scenarios are discussed: 1) climatology, 2) warm SST, 3) low activity, 4) high activity. The low and high activity scenarios are defined by the four climate variables.

The second set of simulations is designed to assess how changes in construction influence expected loss. For these simulations the hurricane hazard is consistent with climatology. The first two scenarios examine the influence of year built on expected loss. The years 1991 and 2008 are used because they are one year prior to Hurricane Andrew in 1992 and several years after the active 2004 and 2005 hurricane seasons. The years between 1991 and 2008 saw a number of code improvements that have made structures significantly more resistant to hurricane winds. The second two scenarios were used to assess the potential range of losses assuming the structures in urban/suburban terrain were poorly built or well built.

A summary of the ground-up losses from the different model runs is given in Table 1. The AAL ratio varies by over a factor of three between the low and high activity climate scenarios. There is an even larger difference in AAL for the weak and strong construction scenarios, but this is an "idealized"

scenario for illustrative purposes. Nevertheless, it shows that it is possible to dramatically reduce losses through changes in building practices.

4 DISCUSSION AND CONCLUSIONS

Hazard catalogs for hurricane catastrophe risk models start with the same set of historical information: the best-track data. The historical record is then expanded through a variety of techniques. Cat-model users are aware that although the scientists and engineers that develop catastrophe risk models put their best efforts forward, there is a significant amount of uncertainty associated with a model. In fact, despite the expense, companies license multiple cat models in order to assess better the variability in model results. The use of multiple models is essentially a simple version of robust simulation that attempts to characterize aspects of exogenous uncertainty through independently developed models.

Here we provide an example of robust simulation using a hurricane catastrophe risk model for the mainland US. Robust simulation entails following a set of coherent assumptions for a model simulation. A "preferred model" is chosen and other alternatives are used to examine the exogenous uncertainties not captured by the preferred model.

There is a significant amount of interannual and interdecadal variability in the historical record. It is unclear from the limited historical sample of hurricane activity what type of hurricane catalog adequately captures the true variability in hurricane activity. Our two "end-member" scenarios of low and high activity produce a significant amount of variation in simulated loss (Table 1).

In addition to variations in hazard one also should consider uncertainties in terrain, vulnerability functions, and the exposure data that is run against a model. The impact of uncertainty in vulnerability functions is not assessed through this exercise, instead the range of results from the different construction scenarios suggests how uncertainty in exposure data might bias results from what would be expected in reality.

An advantage of robust simulation is that it forces us to confront the limitations and uncertainties of our catastrophe models. It is better to acknowledge and tolerate this uncertainty, rather than using methods that conceal or suppress uncertainty. Acknowledging the limitations in models will highlight the value of improved exposure data (age and quality of construction) and encourage efforts to gather and manage exposure data to reduce the impacts of exposure uncertainty.

Table 1. Ground-up losses from model simulations.*

Scenario	AAL	100 year	500 year
Climatology	7.3	52	77
Warm SST	8.7	56	82
Low Activity	4.3	40	63
High Activity	14	71	97
1991	7.4	53	79
2008	5.5	41	59
Weak	12	79	114
Strong	3.1	26	38

*All simulations assumed that the occupancy was permanent single family. One- and five-hundred-year return period losses are for the annual aggregate loss. All losses are millions of dollars.

REFERENCES

- Elsner, J.B. & Bossak, B.H. 2004. Hurricane landfall probability and climate. I.R.J. Murnane and K.-B. Liu (eds.), *Hurricanes and Typhoons: Past, Present and Future*: 333–353. New York: Columbia University Press.
- Goldenberg, S.B., Landsea, C.W., Mestas-Nuñez, A.M. & Gray, W.M. 2001. The recent increase in Atlantic hurricane activity: Causes and implications. *Science* 293: 474–479.
- Li, I.J., Zhao, Y.-G., Chen, J. & Peng, Y. (eds.), *Reliability Engineering and Risk Management: Proceedings of the International Symposium on Reliability Engineering and Risk Management*: Shanghai: Tongji University Press.
- Taylor, C., Lee, Y.J., Graf, W., Hu, Z.H. & Huyck, C. 2010. Robust simulation and cat diagnostics for treating uncertainties in catastrophe risk analysis.

Propagation of aleatoric uncertainty in light-frame wood shear walls

Seyed Masood Hassanzadeh Shirazi & WeiChiang Pang
 Department of Civil Engineering, Clemson University, USA

The objective of this study was to develop a probabilistic shear wall model for estimating the inherent (*aleatoric*) uncertainty in light-frame wood shear walls using Monte Carlo simulation technique. Using the probabilistic shear wall model developed in this study, one may further investigate the propagation of uncertainty from the wall-level to the building-level and quantify the uncertainty in the lateral capacity of the buildings. In light-frame wood construction, the nonlinear response of wood shear walls is mainly attributed to the nonlinear shear-slip response of the sheathing nails (Gupta and Kuo 1985). On the other hand, the bearing between the sheathing panels and slip in the framing members have a lesser influence on the overall response of shear walls. In this study, the inherent randomness in material properties, such as the modulus of elasticity (MOE) of the framing members and shear-slip response of the sheathing nails, were explicitly considered and modeled as random variables.

A series of cyclic nail tests were conducted to investigate the inherent variability in the shear slip response of sheathing and framing nail connections. The hysteretic response of the framing and sheathing nails was modeled using the 10-parameter Modified Stewart Hysteretic Model (MSTEW) developed as part of the CUREE project (Folz and Filiatrault 2001). Two probabilistic nail models were developed (i.e., correlated and uncorrelated). The uncorrelated nail model assumes no correlation between the 10 modeling parameters, while the

correlated nail model specifically considers the correlation of the nail parameters. A method of moments approach was used to determine the statistical distributions of each MSTEW parameter. Table 1 summarizes the distribution parameters for the 10d common framing nails and 8d common sheathing nails, assuming no correlation among the parameters. Using the cyclic test data, the correlation coefficient matrices were computed (Table 2)

Table 1. Distribution parameters for uncorrelated 8d common nails.

MSTEW parameters	Distribution parameters		
	First*	Second†	Distribution type
K_0 (N/mm)	7.2826	0.42076	Lognormal
r_1	0.05000	2.8142	Weibull-Smallest
$ r_2 $	2.9441	0.02820	Frechet-Largest
r_3 -I	0.8322	0.01216	Frechet-Largest
r_4	0.00842	2.5916	Weibull-Smallest
F_0 (N)	876.750	7.6069	Weibull-Smallest
F_i (N)	170.32	26.0981	Gumbel-Largest
Δ (mm)	1.9612	0.28937	Lognormal
α	40.336	20.2397	Beta
β -I	0.37619	5.9887	Weibull-Smallest

* Gumbel-Largest (μ_n) & Frechet-Largest (μ_l) = location parameter, Weibull-Smallest (u) = Scale Parameter.

† Gumbel-Largest (β_n) = scale parameter, Frechet-Largest (k) = shape parameter, Weibull-Smallest (k) = Shape parameter.

Table 2. Final coefficients of correlation for 10d common nails.

	K_0	r_1	r_2	r_3	r_4	F_0	F_i	Δ	α	β
K_0	1.00	0	0	0	0	0	0	0	0.43	0
r_1	0	1.00	0	0	-0.43	0	-0.59	0	0	0
r_2	0	0	1.00	0.40	0	0	0	-0.48	0.55	0
r_3	0	0	0.40	1.00	0	0	0	0	0	0
r_4	0	-0.43	0	0	1.00	0.56	0	0	0	0
F_0	0	0	0	0	0.56	1.00	0.41	0	0	0
F_i	0	-0.59	0	0	0	0	1.00	0.40	0	0
Δ	0	0	-0.48	0	0	0	0.40	1.00	0	0
α	0.43	0	0.55	0	0	0	0	0	1.00	0.51
β	0	0	0	0	0	0	0	0	0.51	1.00

and used to generate sets of correlated MSTEW parameters. Figure 1 shows an example scatter plot for selected nail parameters and a simulated nail hysteresis for the correlated nail model.

As an illustrative example, a nonlinear mechanistic shear wall program, M-CASHEW2 (Pang and

Shirazi 2006), was used to analyze the variability in the lateral capacity of a 2.44 × 2.44 m wood shear wall (Figure 2) tested by Johnston et al. (2006). The frames were constructed of nominal 51 × 102 mm spruce-pine-fir studs spaced at 406 mm on-center and the wall was sheathed with two 11.11 mm thick 1.22 × 2.44 m oriented strand board placed vertically and fastened to the framing members using 8d nails.

Table 3 shows the summary of all simulation combinations under monotonic and cyclic loadings. The backbone curves of 86 simulated wood shear walls under monotonic loading with random frame modulus of elasticity and randomly generated correlated nails are given in Figure 3.

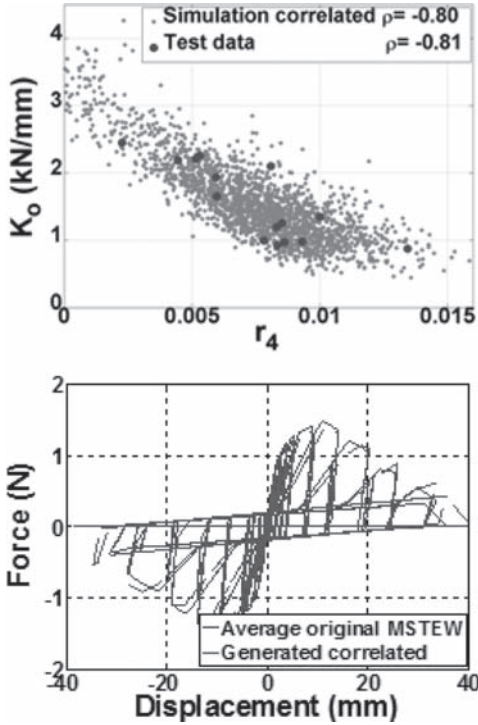


Figure 1. Example simulated correlated parameters and hysteretic loops.

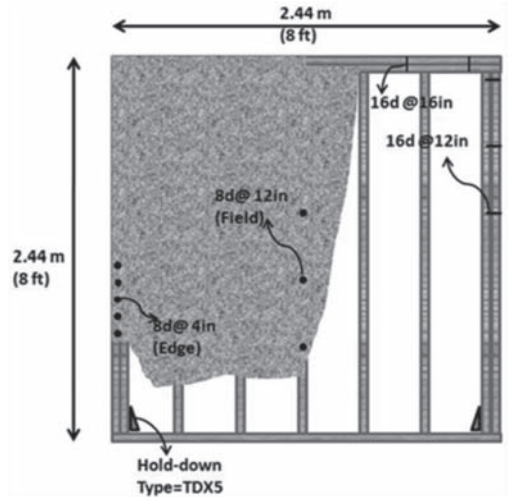


Figure 2. Example wall configuration.

Table 3. Summary of simulation results.

Simulation	Loading Type	Force (kN)				
		Max	Min	Mean	STD	COV
CSP*	Monotonic	31.37	28.95	30.03	0.53	0.017
CSP	Cyclic	31.60	29.25	30.00	0.66	0.022
NCSP†	Monotonic	31.68	27.76	29.63	0.72	0.024
NCSP	Cyclic	30.63	28.17	29.48	0.64	0.022
MOE‡	Monotonic	30.99	30.67	30.88	0.05	0.001
MOE	Cyclic	30.60	30.17	30.51	0.11	0.003
CSP + MOE	Monotonic	31.93	28.59	30.02	0.59	0.019
CSP + MOE	Cyclic	31.05	28.70	29.73	0.62	0.021
NCSP + MOE	Monotonic	31.35	27.62	29.56	0.73	0.024
NCSP + MOE	Cyclic	30.86	27.72	29.53	0.78	0.026

* Correlated MSTEW Parameters for All Connectors.

† Not-Correlated MSTEW Parameters for All Connectors.

‡ Modulus of Elasticity.

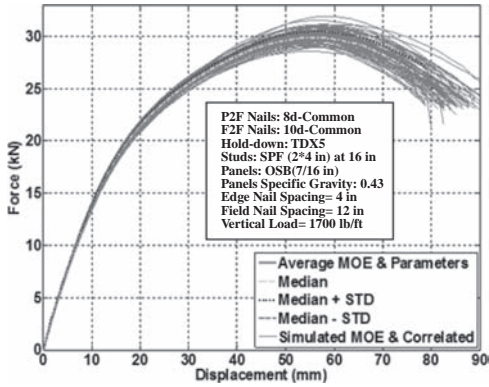


Figure 3. Shear wall backbone curves (random frame MOE and correlated nails).

The average peak force was about 30 kN with a standard deviation of 0.59 kN (CoV = 0.02). According to the results, the frame MOE had the less influence on the results and the CoVs were approximately 0.001 and 0.003 for monotonic and cyclic simulations, respectively. Considering both the nail and MOE as random variables, the COVs ranged from 0.020 for the uncorrelated nail model to 0.025 for the correlated nail model. These values were very close to the COVs of the peak forces observed in experimental shear wall tests.

Based on the simulation results, the variability of the frame MOE only had about a 0.2 percent influence on the overall shear strength response. On the other hand, when both the uncertainty of the frame MOE and nails were considered, the CoV of the simulated peak backbone forces was about 2.5 percent. The presented simulation framework can easily be extended to the house-level to estimate the lateral shear capacity uncertainty of the buildings.

REFERENCES

- Folz, B. & Filiatrault, A. (2001). "Cyclic analysis of wood shear walls." *J. Struct. Eng.*, 127 433.
- Gupta, A.K. & Kuo, G.P. (1985). "Behavior of wood-framed shear walls." *J. Struct. Eng.*, 111(8), 1722–1733.
- Johnston, A.R., Dean, P.K. & Shenton III, H.W. (2006). "Effects of Vertical Load and Hold-Down Anchors on the Cyclic Response of Wood Framed Shear Walls." *J. Struct. Eng.*, 132 1426.
- Pang, W. & Shirazi, S.M.H. (2010). "Next Generation Numerical Model for Non-Linear In-Plane Analysis of Wood-Frame Shear Walls." *Proc. of World Conference on Timber Engineering*, Italy.

Shear strength variability of sandy and fine-grained soils

P. Koudelka

Czech Academy of Sciences—Institute of Theoretical and Applied Mechanics

ABSTRACT: The soil and rock variability is a constitutive characteristics of geotechnical materials and it is important to know utmost on it. This knowledge is necessary for a regular and solid calibration both the LSD theory and, of course designs according to EC 7-1. The most important in-put data for the Ultimate Limit State Design are data of shear strength and unit weight. The mentioned reasons led to the establishment of a database of physical properties of soils in solid and reliable laboratories tested and to concentrating on shear strength and unit weight. The database is supported continuously a number of years at the Institute of Theoretical and Applied Mechanics of the Czech Academy of Sciences. The paper brings summed database data and deals with the statistical analysis of the single soil groups taking use of the database to date. The analysis could provide a better quantitative view at a possible influence of soil variability in geomechanics and in geotechnical design.

1 INTRODUCTION

Soil and rock mechanics research and design have a great disadvantage according to other civil engineering ranges, i.e. examined materials are natural, very variable and knowledge both of materials and their location is not perfect but, on the contrary often very low. The strong material variability occurs not only between different layers and their location but also usually variability characterizes material into a layer. This fact is well-known but it causes fundamental difficulties both for design theories and practice. The greatest difficulty appears for the geotechnical Limit State Design (LSD) where a partial *material* factor application (probably B. Hansen 1953) has led to a fatal theoretical error. Videlicet, almost all geotechnical tasks are not linear but, on the contrary they distinguish from tasks of the other ranges by a marked non-linearity. The application of any material factors appears to be a hard “crime” against the principles of mechanics at all. Due to it the basic European geotechnical directive, i.e. EUROCODE 7-1

“Geotechnical design—Part 1: General rules” (EC 7-1), could not be and has not been satisfactorily and uniformly drafted.

Nevertheless, the soil and rock variability is a constitutive characteristics of geotechnical materials and it is important to know utmost on it. This knowledge is necessary for a regular and solid calibration both the LSD theory and, of course designs according to EC 7-1. The most important in-put data for the Ultimate Limit State Design are data of shear strength and unit weight. The upper mentioned reasons led to the establishment of a database of physical properties of soils in solid and reliable laboratories tested and concentrating on shear strength and unit weight. The database is supported continuously a number of years at the Institute of Theoretical and Applied Mechanics of the Czech Academy of Sciences. Information on the database and its statistical analysis to date are subject of the paper.

2 CONCEPT OF THE DATABASE

The paper targets the database of shear strength, i.e. except of deformation characteristics. System of the database is created from point of view of demands of the Ultimate Limit State Design.

The shear strength database system is compounded from an identification block (38 data fields) and a block of physical properties (98 data fields). The database is divided according to soils up three parts: fine-grained and sandy soils and gravels regarding to the Czech standard ČSN 73 1001 “Subsoil under shallow foundations”. The standard distinguishes five gravel groups (G), five sandy groups (S) and eight fine-grained groups (F). Denotation of soil kinds keeps international usances as they follow in the Chapter 4.

3 APPLIED DATA OF SOILS

The database does not contain to date samples of groups F1 (MG), S1 (SW), G1 (GW), G4 (GM) and G5 (GC) thus, these groups could not be analysed.

Also the numbers of gravel samples are too low for statistical evaluation and because also the groups F2 (CG), G2 (GP) and G3 (G-F) were not analysed.

The database contains also some samples of fill soils. It concern 4 samples (CV) in the group F8 and 5 samples (SP) in the group S2. It is necessary to evaluate fill soils independently and so these samples have been excluded from input data of the statistical analysis, other samples are considered.

4 STATISTICAL ANALYSIS

The presented statistical analysis has been carried out on the base of altogether 224 samples. Sizes of single sets are as it follows:

Fine grained soils:

F3 = MS (32 samples), F4 = CS (35 samples),
F5 = ML-MI (21 samples), F6 = CL-CI (50 samples),

F7 = MH-MV-ME (10 samples),

F8 = CH-CV-CE (11 samples).

Sandy soils:

S2 = SP (12 samples), S3 = S-F (13 samples),

S4 = SM (29 samples), S5 = SC (11 samples).

In total amount the analysis contains 159 samples of fine-grained soils and 65 samples of sandy soils.

Results of the statistical analysis are summed in the Table 1 below:

Denotation of statistical quantities in the table is presented and others are: n —number of samples, γ —unit weight, ϕ_m —average value of shearing resistance angle, c_m —average value of cohesion.

5 DISCUSSION OF RESULTS

Table 1 makes it possible to compare differences between quantities the single soil groups and their

Table 1. Statistical quantities of single groups of the sandy and fine-grained soils (shear strength in effective values).

TABLE OF STATISTICAL QUANTITIES OF SOIL DATABASE										
Group	Samples	Average values			Medium deviations			Variability coefficients		
	n	π_m	π_m	c_m	s_σ	s_σ	s_c	v_σ	v_σ	v_c
-	1	kNm ³	°	kPa	kNm ³	°	kPa	1	1	1
SANDY SOILS										
S1	-	-	-	-	-	-	-	-	-	-
S2	12	1810	39,1	7,3	112,96	5,01	4,57	0,062	0,128	0,627
S3	13	1793	36,7	13,8	60,15	5,91	10,99	0,034	0,161	0,794
S4	29	1927	33,8	19,9	150,35	6,59	17,11	0,078	0,195	0,860
S5	11	2115	24,5	18,0	91,24	2,57	8,01	0,044	0,096	0,272
FINE GRAINED SOILS										
F1	-	-	-	-	-	-	-	-	-	-
F2	1	-	-	-	-	-	-	-	-	-
F3	32	1955	27,6	33,9	99,58	4,029	20,00	0,051	0,146	0,590
F4	35	2003	23,9	44,9	133,65	3,831	28,74	0,067	0,160	0,640
F5	21	1993	22,4	38,0	99,81	3,035	22,27	0,050	0,135	0,586
F6	50	2021	22,4	41,7	92,94	3,107	20,47	0,046	0,139	0,491
F7	10	1982	19,5	74,6	137,14	2,95	53,93	0,069	0,151	0,723
F8	11	1953	16,8	47,8	137,29	1,894	17,03	0,070	0,113	0,356

variability. Statistical weight of the results is given by size of the statistical set. Detailed discussion of the results can found in the Paper.

6 CONCLUSION

The presented database has made it possible the statistical analysis of the most of groups of soils in the categories of sandy soils and fine-grained soils. The analysis results have different statistical weights according to the respective numbers of samples but all analysed sets are statistically sufficient and reliable.

The variability of the analysed fine-grained soils (F) in single quantities (γ , ϕ , c) appears surprisingly uniform, the differences of the group averages appear low. The variability of the analysed sandy soils (S) in these quantities appears higher but respectively not much.

Samples of the database are chosen accidentally according data full-scale and quality of the tests. The mentioned uniformity of the quantity results obviously is not an effect of a single sample site.

The database and its statistical analyses are and will be very useful. The database and the analysis results to date have been exploited for another paper “Risk of analyses with lateral earth pressure load” of the Conference.

A further development and stocking of the database appears very desirable.

ACKNOWLEDGEMENT

The Grant Agency of the Czech Republic and the Grant Agency of the Czech Academy of Sciences provided financial support of the connected research (GP Nos.103/2002/0956, 103/2005/2130, 103/07/0557, 103/08/1617 and No. A2071302 resp.). The author would like to thank them all for support.

REFERENCES

- ČSN 73 1001 Foundation of structures - Subsoil under shallow foundations 1987, ps. 75. Prague: ÚNM.
- EN 1997-1 - Eurocode 7, Geotechnical design – Part 1: General rules (Final draft), [11/2004]. Brussels, CEN/TC 250/SC7-WG1, ps. 168.

Correlation in probabilistic simulation

M. Vořechovský

Brno University of Technology, Brno, Czech Republic

ABSTRACT: The objective of this paper is twofold. Firstly to deliver theoretical bounds for performance of simulation techniques of Monte Carlo type measuring the ability to fulfill prescribed correlation matrices. Secondly, we study the performance in correlation control of recently proposed procedure for sampling from a multivariate population within the framework of Monte Carlo simulations [10–12] (especially Latin Hypercube Sampling). In particular, we study the ability of the method to fulfill the prescribed marginals and correlation structure of a random vector for various sample sizes. Two norms of correlation error are defined, one very conservative and related to extreme errors, other related to averages of correlation errors. We study behavior of Pearson correlation coefficient for Gaussian vectors and Spearman rank order coefficient (as a distribution-free correlation measure).

The paper starts with theoretical results on performance bounds for both correlation types in cases of desired uncorrelatedness. Firstly, the correlation errors (distance between the target and the actual correlation matrices) are studied for the case of random ordering of samples. The results for both correlation errors are based on the fact that a random correlation coefficient for a pair of random variables approximately follows Gaussian distribution. The errors for random vectors are then extension to multivariate case. These errors are understood to be the upper bounds on the mean performance of any algorithm because no algorithm should perform worse than just a random permutations (shuffling) of samples.

Lower bounds on the error are initially obtained by analyzing attainable values of correlation as they follow from analysis of the correlation estimation formulas.

For the cases when the sample size is less than the number of random variables, it is shown that the correlation matrix must be singular. Studies on spectral properties of these matrices helped us to derive lower bounds on the mean square error of the correlation in a closed form. Matrices that fulfill this optimality are shown to be non-unique and from all the possible solutions the one with

minimal absolute correlation is shown to be preferable. The paper also proposes a simple mechanical model for dynamical simulations that is used to automatically deliver the lower bound on the matrix errors. Moreover, they deliver the whole optimal matrices. As an alternative, the task is also redefined as optimization problem and a numerical procedure of imposing a spectrum is used to solve the problem, too. The typical convergence of the correlation error for a fixed number of variables and increasing sample size is shown in Fig. 1.

As for the performance for cases when the sample size exceeds the number of random variables, the following observations have been made. It is shown that, under some circumstances, a very high rate of convergence can theoretically be achieved.

These rates are compared to performance of other developed techniques for correlation control, namely the Cholesky orthogonalization as applied by Iman and Conover [3,4]; and Owen's method [8] using Gram-Schmidt orthogonalization. We show that *the proposed technique* based on combinatorial

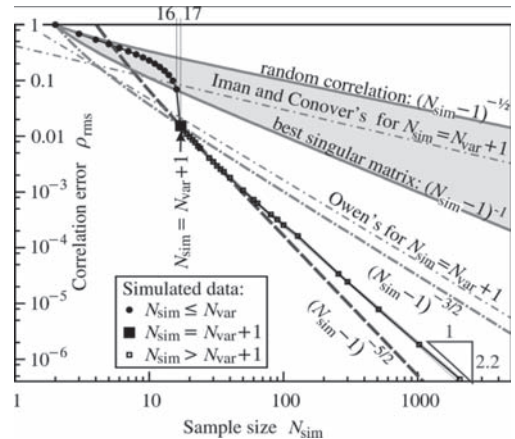


Figure 1. Typical performance plot obtained for $N_{var} = 16$. Simulated data (averages are denoted by symbols and a solid line, minima and maxima by thin solid lines) are compared to theoretical bounds and results of other techniques.

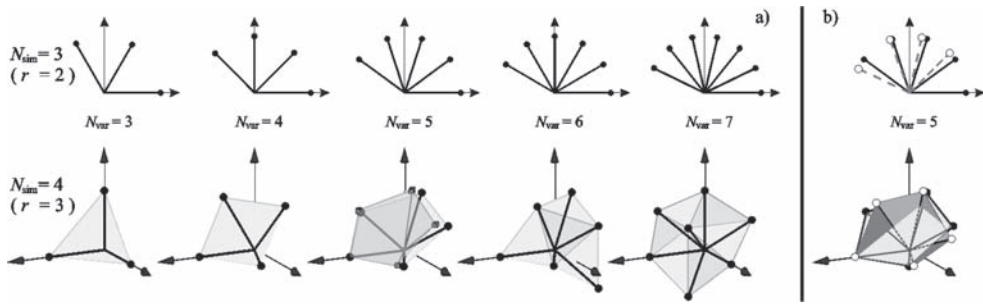


Figure 2. Visualization of optimal singular correlation matrices. a) \mathbf{R}^M (solid circles). All of these solutions are also \mathbf{M} matrices except for $N_{\text{var}} = 5$ and $N_{\text{sim}} = 4$ (visualized with solid boxes). b) Examples of optimal correlation matrices \mathbf{R} (empty circles) used compared with those from (a). Top row: $N_{\text{sim}} = 3$ (dimension $r = 2$). Bottom row: $N_{\text{sim}} = 4$ (dimension $r = 3$).

optimization [10–12] yields much better results than the other known techniques.

When correlated vectors are to be simulated, the proposed technique exhibits nearly the same excellent performance as in the uncorrelated case provided the desired vector exists. It is shown that the technique provide much wider range of acceptable correlations than the widespread Nataf [7] model [5] (known also as the Li-Hammond model [6] or the NORTA model [1]) and that it is also much more flexible than the Rosenblatt model [2,9].

ACKNOWLEDGEMENT

The presented work was supported by The Grant Agency of the Academy of Sciences of the Czech Republic under project KJB201720902 and the Czech science foundation under project number GACR P105/11/1385.

REFERENCES

- [1] Ghosh, S. & Henderson, S.G. (2003). Behavior of the NORTA method for correlated random vector generation as the dimension increases, *ACM Transactions on Modeling and Computer Simulation* 13(3): 276–294.
- [2] Hohenbichler, M. & Rackwitz, R. (1981). Non-normal dependent vectors in structural safety, *Journal of Engineering Mechanics*, ASCE 107(6): 1227–1238.
- [3] Iman, R.C. & Conover, W.J. (1980). Small sample sensitivity analysis techniques for computer models with an application to risk assessment, *Communications in Statistics: Theory and Methods* A9 (17), 1749–1842.
- [4] Iman, R.C. & Conover, W.J. (1982). A distribution free approach to inducing rank correlation among input variables, *Communications in Statistics B11*, 311–334.
- [5] Liu, P. & Der Kiureghian, A. (1986). Multivariate distribution models with prescribed marginals and covariances, *Prob Eng Mech* 1(2): 105–111.
- [6] Li, S.T. & Hammond, J.L. (1975). Generation of pseudo-random numbers with specified univariate distributions and correlation coefficients, *IEEE Transactions on Systems, Cybernetics* 5, pp. 557–560.
- [7] Nataf, A. (1962). Détermination des distributions de probabilités dont les marges sont donnés, *Comptes Rendus de L'Académie des Sciences* 225: 42–43.
- [8] Owen, A.B. (1994). Controlling Correlations in Latin Hypercube Samples, *Journal of the American Statistical Association (Theory and methods)* 89(428): 1517–1522.
- [9] Rosenblatt, M. (1952). Remarks on multivariate analysis, *Annals of Statistics* 23: 470–472.
- [10] Vořechovský, M. (2007). *Stochastic computational mechanics of quasibrittle structures*. Habilitation thesis presented at Brno University of Technology, Brno, Czech Republic.
- [11] Vořechovský, M. & Novák, D. (2002). *Correlated random variables in probabilistic simulation*. In: Schießl, P. et al. (Eds.), 4th International Ph.D. Symposium in Civil Engineering, Vol. 2. Millpress, Rotterdam. Munich, Germany, pp. 410–417. Awarded paper. ISBN 3-935065-09-4.
- [12] Vořechovský, M. & Novák, D. (2009). Correlation control in small sample Monte Carlo type simulations I: A simulated annealing approach, *Probabilistic Engineering Mechanics*, 24(3): 452–462. doi: 10.1016/j.probengmech.2009.01.004.
- [13] Vořechovský, M. & Novák, D. (2009). Performance of Correlation Control by Combinatorial Optimization for Latin Hypercube Sampling, In ICOSAR 2009, 10th Int. Conf. on Struct. Safety and Reliability, 3844–3851.
- [14] Vořechovský, M. (2010). Correlation control in small sample Monte Carlo type simulations II: Theoretical analysis and performance bounds, *Probabilistic Engineering Mechanics*, in review.
- [15] Vořechovský, M. (2011). Correlation control in small sample Monte Carlo type simulations III: Algorithm performance and relevance to copulas and multivariate modeling, *Probabilistic Engineering Mechanics*, in review.

Computational intelligence techniques with modern applications of fuzzy pattern classification

I.F. Iatan

Department of Mathematics and Computer Science, Technical University of Civil Engineering,
 Bucharest, Romania

The specialists think that the genetic algorithms are a computational intelligence application as well as the expert systems, the fuzzy systems, the neural networks, the intelligent agents, the hybrid intelligent systems, the electronic voice.

Since the specialists think that the genetic algorithms are a computational intelligence application we shall use in this paper a complex mathematical model, which include both the genetic algorithms and the fuzzy logic and the classification elements.

The fuzzy logic is used for our data fuzzification. The genetic algorithms are necessary for solving an optimal control problem.

The classification helps us to determine the pattern membership to a class. The originality of this paper consists in the generalization of the Ishibuchi method in the aim of the proposed theme achievement and its adaptation to the proposed theme. There are three stages in order to achieve our paper objectives:

The first stage: We shall describe a method for the generation of fuzzy IF-THEN rules.

The fuzzy number can be represented using the following two methods:

1. The method proposed by Umano and Ezawa (Umano M., Ezawa Y. 1991) according to which a fuzzy number is represented by a finite number of membership values;
2. The method of Uehara and Fujise (Uehara K., Fujise M. 1990) regarding the representation of a fuzzy number by a finite number of α level sets.

For obtaining a set of fuzzy *if-then* rules from a database with K vectors having n components we have to represent each component of a vector by three values which constitutes the component membership to the three linguistic properties: *small*, *medium* and respective *big*.

In order to generate the terms which appears in the consequent of the rule we shall suppose that the membership to a class of a pattern from the training set one computes using the formula:

$$\mu(y_i) = \frac{1}{1 + \left(\frac{z_{ik}}{F_d} \right)^{F_c}}, \quad i = \overline{1, M}, k = \overline{1, K}, \quad (1)$$

where: M means the number of classes, K is the number of vector from the training lot, z_{ik} represents the weighted distance from a training vector and the mean vector of each class; F_d , F_c are some real parameters.

The second stage: We use a fuzzy neural network in order to: train the generated rule set in the view of in adjustment the weights and to classify a new pattern.

The third stage: We shall use the genetic algorithms in the view of solving the problem to select a compact rule system from the entire rule set. The problem tackled in this stage can be formulated as a combinatorial optimization problem with two objectives: to maximize the number of correctly classified patterns and to minimize the number of fuzzy *if-then* rules and it can be solved using the genetic algorithms. A set of fuzzy *if-then* rules is coded as an individual in genetic algorithms. That is, a rule set S should be represented by a string.

Encoding of chromosomes is one of the problems, when you are starting to solve problem with genetic algorithms. We shall use the binary encoding in order to encode the chromosomes. In binary encoding, every chromosome is a string of bits, 0 or 1.

Let us denote a rule from the set of all fuzzy if-then rules corresponding to K , that are generated from the training patterns x_p , $p = \overline{1, K}$. (i.e. a chromosome) by a string $s_1 s_2 \dots s_M$, where:

- M is the number of classes, namely the number of the terms which appear in the consequent of a rule,
- for each chromo some $k = \overline{1, K}$, $s_i = 1$ if the pattern k belongs to the class i and $s_i = 0$ otherwise.

A string 010 ... 0 is decoded as the respective pattern is in the two class. The initial population containing $N_{pop} = K$ strings, where K is the number of fuzzy if-then rules in S .

A compact fuzzy classification system based on a small number of fuzzy if-then rules has the following advantages:

- it does not require a lot of storage;
- the inference speed for new patterns is high;
- each fuzzy if-then rule can be carefully examined by users.

The last advantage suggests the possibility of knowledge acquisition. When a small number of

fuzzy if-then rules are selected, it is possible that a user acquires new knowledge by carefully examining the selected rules.

On the contrary, if a lot of fuzzy if-then rules are included in a fuzzy classification system, it is a quite troublesome task to examine all the rules.

I intend to extend in the future this paper with a new stage which has to consist in the achievement of a software for testing the performances corresponding to the method used for a database.

GS_121 — Uncertainty, statistics and probability (2)

This page intentionally left blank

Reliability analysis of a brittle fracture due to crack instability using sequential Monte Carlo simulation

L.E. Garciano & I. Yoshida

Department of Urban and Civil Engineering, Tokyo City University, Tokyo, Japan

Built structures gradually deteriorate over time. Extreme loads, harsh environment and day-to-day load can cause cracks or micro-fissures on any structure. Monitoring and maintenance, especially critical ones, becomes a necessity to detect possible deterioration or degradation either to halt its progress or slow it down. Retrofitting or maintenance therefore can help avoid loss of lives and property.

Assessing the present state of a structure is necessary and important. One way to assess the present state is to compare the reliability index (or probability of failure) of a structure or its component just after construction and T years later. Data from inspections gathered at specific times during the life of the structure can be used to assess the present state of the structure. This scenario is ideal in employing a Bayesian updating approach since it is desired to update the prior density of the state using observation data to obtain a posterior density of the state.

Sequential Monte Carlo Simulation (SMCS) (Gordon et al., 1993) is a tool that can be used for this purpose. SMCS has been applied to diverse fields, e.g. model parameter estimation (Yoshida and Sato 2002), reliability estimation (Yoshida et al., 2009), risk assessment (Garciano and Yoshida, 2008) etc.

In this paper a brittle crack failure due to crack instability is considered as the failure mode of a structural component. This can be considered a time-dependent reliability problem if the resistance deteriorates over time. The limit state exceeding probability in this case can be calculated using ordinary Monte Carlo Simulation (MCS).

However if inspections are conducted at specific times of the life of the structure and observation data can be gathered, e.g. crack lengths, then it is possible to update the state variables using SMCS. Subsequently the limit state exceeding probabilities (p_j) for those years are also updated.

Consider the following system model

$$x_k = F(x_{k-1}, w_k) \quad (1)$$

with system transition function F and process noise w .

$$z_k = H(x_k, v_k) \quad (2)$$

At discrete times, measurements become available and are related to the state vector through the observation equation with measurement function H and measurement noise v . The probability density functions (pdf) are assumed known and independent and F and H can be linear as well as nonlinear functions. The prior distribution of the state at $t = 0$ is assumed to be distributed according to the density $p(x_0)$. To obtain an optimum estimate of the state x_k at time step k given the observations Z_k , the following conditional probabilities are required: the time updating process and the observation updating process.

In the time updating process, the state $p(x_k | Z_{k-1})$ at time step k considering all the observations up to time step $k-1$ is determined. While in the observation updating process the posterior distribution of the state $p(x_k | Z_k)$ using measurements Z_k is determined using Bayes' rule as shown below

$$p(x_k | Z_k) = \frac{p(z_k | x_k)p(x_k | Z_{k-1})}{\int p(z_k | x_k)p(x_k | Z_{k-1})dx_k} \quad (3)$$

The above equation shows an optimal Bayesian solution to the filtering problem. If F and H are linear and all other densities are Gaussian the Kalman Filter is an optimal solution. For nonlinear problems other techniques can be used, e.g. Extended Kalman Filter or the Unscented Kalman Filter. In this paper SMCS is used since the observation equation is nonlinear so that a closed-form solution is not possible.

Consider a reliability problem where S is the random load and $R(S)$ is the resistance. For each load S the resistance decreases until such time failure will occur as the random load outcrosses the deteriorating resistance. Specifically consider a semi-infinite plate under variable-amplitude loading (Lentz et al., 2003).

The limit state function in this case (brittle fracture due to crack instability) is given as

$$g_{k/k} = \frac{K_{k/k}}{Y_{k/k} \sqrt{\pi a_{k/k}}} - S_{k/k} \quad (4)$$

where S is the stress history, K is the fracture toughness and Y is the geometry correction factor. The crack length $a(t)$ (accumulated damage) equation is given as

$$z_{k/k} = a_{o,k/k} \exp \left[C_{k/k} (Y_{k/k} \sqrt{\pi})^2 v T \times (2\sqrt{2})^m \sigma_S^m \Gamma \left(1 + \frac{m}{2} \right) \right] + v_k \quad (5)$$

where C and m are crack propagation parameters, a_o is the initial crack length, N is the number of load cycles up to time t and ΔS is the cumulative dynamic stress range acting on the structure during a given time period. This equation is also the observation equation since crack lengths can be observed at any time t .

The density of ΔS is related to S if the latter is a narrow-band Gaussian process. It can be shown that the stress ranges from (peak amplitudes) rain-flow counting methods are twice compared the peak amplitudes from the stress history. Therefore if S is a narrow-band Gaussian process then ΔS can be written as

$$\sum_{i=1}^{N(t)} \Delta S_i^m = N(t) (2\sqrt{2})^m \sigma_S^m \Gamma \left(1 + \frac{m}{2} \right) \quad (6)$$

where the number of stress cycles $N(t)$ in the time interval T is $N(t) = v \cdot T$. The variables in the equations shown above are as follows: σ_S is the standard deviation of the narrow-band Gaussian process and $\Gamma(\cdot)$ is the gamma function and v is the stress cycle rate.

To evaluate this example problem the statistics of the random variables are assumed. Reliability analyses are performed using ordinary MCS and the p_f of brittle crack failure due to crack instability is calculated as

$$p_{f,k/k-1} = p(g_{k/k-1} < 0) = 1 - \frac{1}{n} \sum_{i=1}^n U \left(g \left(\mathbf{x}_{k/k-1}^{(i)} \right) \right). \quad (7)$$

The above equation describes limit state exceeding probability at the k -th step before updating, where U is the step function. To update p_f at specific years the vector $\mathbf{x}_{k/k-1}^{(i)}$ is replaced with $\mathbf{x}_{k/k}^{(i)}$.

To update the state random variables observation data are required. Four cases were considered in the paper. In cases A and B the p_f is updated only once corresponding to observation data, $z = 7$ or 12 mm, on the 30th year for case A and $z = 10$ or 15 mm on the 40th year for Case B.

For cases C and D the p_f is updated twice corresponding to observation data, $z = 7$ mm to 12 mm, for not-so-severe case and $z = 12$ mm to 17 mm for severe case. However for case D it was assumed that the observed cracked length (severe case) is $z = 12$ mm and the not-so-severe case is $z = 7$ mm. This observation is the same at $t = 30$ and 40 .

To start the analysis samples as many as 10,000 points were generated from all random variables. The sample realization determines the prior distribution. Subsequently these particles were used to estimate limit state exceeding probability using ordinary MCS. With inspection data available the p_f were updated at this particle observation year.

For Case A, random variables are updated using crack length observations on the 30th year. Based on these updated variables the p_f is also updated. After updating an ordinary MCS of the re-sampled particles is used to estimate the p_f for the succeeding year. The p_f is calculated by calculating the ratio of samples found above the 45° line and the total number of sample realization. The results showed that p_f increased as R deteriorates over time. In Case B, the p_f is updated on the 40th year. Afterwards an ordinary MCS of the re-sampled particles is used to estimate the p_f on the 50th year.

Cases C and D illustrates updating at two different years. More data means better assessment of the structure. After each update, an ordinary MCS using the re-sampled particles is done to estimate the p_f for the succeeding year.

In all cases, the results show that SMCS can be used to assess the present state of the structure if observation data are available. The state of the structure is determined through its p_f .

As a summary, it has been shown that SMCS can be utilized to update the present state of a deteriorating structure thorough the limit state exceeding probability. This is possible if inspection or observation data are available and can be used to update the state equation. This updated index can be a signal (depending on the severity) to owners, building officials or stakeholders to perform retrofitting or maintenance measures to prevent or stop further deterioration of the structure.

For future work, the authors would want to apply SMCS to a deteriorating structure which exhibits strong nonlinearities in both state and observation equations. It is also desired to update the state equation using multiple observation data.

Life-cycle assessment and uncertainty in modelling: Introduction of a possible “aid” index

E. Garavaglia

Politecnico di Milano, Department of Structural Engineering, Milano, Italy

The life-cycle assessment of structural system over time suffers from uncertainty and therefore probabilistic modelling is required. If a system is new, its performance is high, but, over time, different random attacks can reduce its performance capability. Each time the system capability reaches lower or dangerous values the system suffers a “failure” and it moves from the current state of performance into another that is characterised by a lower level of performance. This kind of process can be approached as a stochastic transition process, where the random variable assumed is the waiting time spent by the system in each performance state before transition. The modelling of the waiting times requires a probabilistic approach. In this paper, the approach proposed is a semi-Markov (SM) approach in connection with a Monte Carlo (MC) simulation.

In other words, a SM process (SMP) describes the evolution of the system’s life through different service states with different waiting times, transitions occur each time a certain loss of performance is recorded, or each time maintenance is carried out.

If the SMP is defined and t_0 is the time already spent by the system in the current state i before a transition, the probability of transition from state i , into state k can be defined as follows:

$$\Pr(\text{next state } k, \tau_{ik} \leq t_0 + \Delta t \mid \text{current state } i, \tau_{ik} > t_0) = \mathbf{P}_{\Delta t | t_0}^{(ik)} \quad (1)$$

where τ_{ik} is the waiting time spent by the system in state i before transition into k , and Δt is the discrete time in which the prediction will happen. If the distribution functions, $F_{ik}(t)$, modelling the waiting times are defined and $\tau_{ik} = t_0$, Eq. (1) can assume the following form:

$$\mathbf{P}_{\Delta t | t_0}^{(ik)} = \frac{[F_{ik}(t_0 + \Delta t) - F_{ik}(t_0)] p_{ik}}{\sum_{j=1}^s [1 - F_{ij}(t_0)] p_{ij}} \quad (2)$$

where the probabilities p_{ik} can be obtained by experimental observation.

As all the probabilistic models, the SMP also suffer from uncertainty. The influence of the epistemic uncertainty on the probabilistic modelling will be analysed and discussed, extending the criterion of validation introduced by Grandori et al. (1998) in their seismic hazard life-cycle assessment. This criterion is based on an index able to compare two models and decide which is the most reliable (Grandori et al., 1998, 2003; Guagenti et al., 2003):

$$\Delta_{rs}^{\circ} = \Delta_r^{\circ} - \Delta_s^{\circ} \quad (3)$$

The procedure proposed by Grandori was extended to consider reliability in the modelling of waiting times in the deterioration transition process. Where:

$$\Delta_r^{\circ} = \Pr \left\{ P^{\circ} - h < P_r \leq P^{\circ} + h \right\} \quad (4)$$

is the probability that P_r , obtained from Eq. (2) using a given r – model (e.g. Gamma), falls in a given interval around the “true” value P° obtained by Eq. (2) using the larger dataset obtained by MC simulation (h defines a conventional interval around P°). In the same way Δ_s° is defined, it is connected with the probability of transition P_s obtained by using a given s —model (e.g. Weibull). In this paper, modelling of the deterioration process is carried out, and comparison is made between the Gamma and Weibull distributions. Their reliability will be evaluated assuming the results obtained from the MC simulation as the *true* transition times.

The process to be analysed was the deterioration of a steel truss subjected to environmental attacks and ageing (Fig. 1).

The deterioration over time of the system was measured by a time-variant damage index $\delta = \delta(t) \in [0;1]$ following an appropriate damage model (see Biondini et al., 2008). Through the Monte Carlo simulation the true F_{ik}° was established, and by using Eq. (2) the true \mathbf{P}_{ik}° was evaluated.

The states assumed were: *State 1* relating to low damage ($\sigma \leq 1100$ MPa), *State 2* relating to

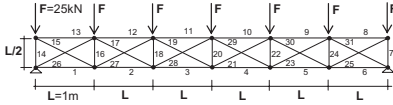


Figure 1. Statically indeterminate truss system: total area of members $A = 2500 \text{ mm}^2$ and total volume $V = 0.0723 \text{ mm}^3$.

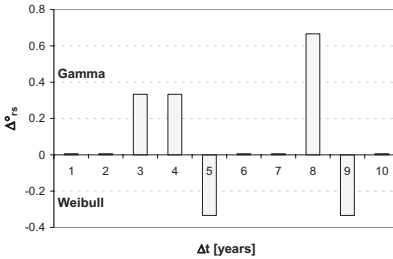


Figure 2. Probability of transition $P_{\Delta_{it}(t)}^{(12)}$; comparison of Gamma and Weibull models through the behaviour of the relative index Δ_{rs}° .

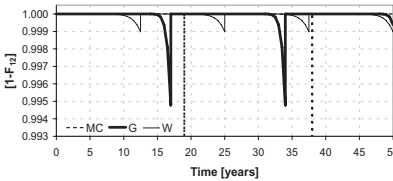


Figure 3. Comparison between the survivor functions of scenario (1)-MC, (2)-G and (3)-W, over the service life. When maintenance is carried out the system renews itself.

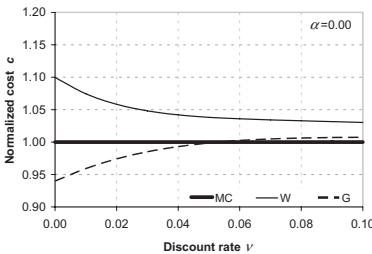


Figure 4. Total cost C , calculated as the sum of initial cost C_0 and maintenance cost C_m , of scenarios (2) Gamma, and (3) Weibull, normalised to the cost C of the scenario (1) MC, the true process, versus the discounted rate ν .

moderate damage ($1100 < \sigma \leq 1250$), and *State 3* relating to heavy damage ($\sigma > 1250$).

The true process F_{ik}° was modelled with Gamma and Weibull, and by applying Eq. (3) and Eq. (4) the aid index, Δ_{rs}° , was created. The index has

put into evidence the similar behaviour of the two distributions being compared, highlighting a slight preference for Gamma over Weibull (Fig. 2).

The consequence of the choice of one distribution over another has also been investigated in terms of maintenance actions and costs of maintenance. Therefore, the comparison between the maintenance scenarios obtained from Weibull, Gamma and MC was considered. In each scenario maintenance was carried out when the system reached the *State 2* and was applied to the whole system; after every maintenance action, the system is reclassified as the undamaged *State 1* (Fig. 3). The scenarios were also compared in terms of the cost of maintenance following the approach proposed by Kong and Frangopol, (2003) (Fig. 4).

The results prove that the choice between Gamma and Weibull lead to similar results in terms of reliability of the modelling, the cost analysis shows that modelling with the Weibull method leads to the most prudent, but expensive, maintenance planning.

The application of the credibility index, proposed here, highlights the importance of having information concerning which, between two models, is the most reliable in the assessment of a given process, because choice of the wrong model can have an influence on the lifetime prediction and on the cost of maintenance.

REFERENCES

- Biondini, F., Frangopol, D.M. and Garavaglia, E. 2008. Life-Cycle Reliability Analysis and Selective Maintenance of Deteriorating Structures. in: Biondini, F. and Frangopol, D.M. (eds.) *First International Symposium on Life-Cycle Civil Engineering (IALCCE'08)*, Varenna, Lake Como, Italy, June 10–14, 2008, CRC Press, Taylor & Francis Group, London, UK, I: 483–488.
- Grandori, G., Guagenti, E. and Tagliani, A. 1998. A proposal for comparing the reliabilities of alternative seismic hazard models, *Journal of Seismology*, 2: 27–35.
- Grandori, G., Guagenti, E. and Tagliani, A. 2003. Magnitude distribution versus local seismic hazard, *BSSA, Bull. of Seismological Society of America*, June 2003, 93: 1091–1098.
- Guagenti, E., Garavaglia, E. and Petrini, L. 2003. Probabilistic Hazard Models: is it Possible a Statistical Validation? in: “System – based Vision for Strategic and Creative Design” in: F. Bontempi (ed.) *2nd Int. Structural Engineering and Construction Conf (ISEC02)*, Rome, Italy, U.E., September 23–26, 2003, A.A. Balkema Publishers, Lisse, The Netherlands, II: 1211–1216.
- Kong, J.S. and Frangopol, D.M. 2003. Life-Cycle Reliability-Based Maintenance Cost Optimization of Deteriorating Structures with Emphasis on Bridges. *J. of Structural Engineering*, ASCE 129: 818–824.

Mechanical characterisation of lacustrine clay by interpreting spatial variability in CPTU measurements

Giovanna Vessia

Visiting researcher at ETSI de Caminos, Canales y Puertos (UCLM), Ciudad Real, Spain

Francesca Casini & Sarah Springman

Institute for Geotechnical Engineering, ETH, Zurich, Switzerland

1 INTRODUCTION

The deposits of lacustrine clays in Switzerland are mainly concentrated in the Mittelland (Fig. 1), which is located between the Alps and the Jura mountains. This region is the most densely populated and fastest developing area in terms of infrastructure and construction, so the lacustrine clay represents one of the most challenging soils with respect to foundations and construction (Messerklinger 2006).

Swiss practice is focusing more on serviceability limit state design for infrastructure (e.g., roads, retaining walls), with the intent to achieve optimal (i.e., more economic) design. To this end, cone penetration tests (CPTU) have been widely performed within lacustrine clays in Switzerland in order to get detailed information about the stratigraphy, mechanical and hydraulic properties. Nonetheless, measurements from CPTU continuous readings are strongly affected by inherent spatial variability and heterogeneity.

Thus, statistical tools have been introduced to improve the soil profiling and to establish characteristic values of undrained shear strength

s_u (by means of its spatial trend and variability structure) for optimal design of geo-structures in such varved clays.

2 A CASE STUDY: WAUWIL SILTY CLAYS

Extensive site and laboratory investigations were carried out on a small area in Wauwil in a thick deposit of varved Swiss lacustrine clay about 70 km SW of Zurich (Springman et al., 1999, Hird & Springman 2006). Eight CPTUs at the Wauwil site have been performed with two cone dimensions: cross-sectional areas of 10 cm² and 5 cm²; the data were saved at the rate of 25 readings per second and the standard rate of penetration was 20 mm/s. Therefore, spatial lags of measurements are about 0.5 mm on average. Statistical methods have been employed to develop a more precise prediction of both anomalies and layer boundaries at a centimetre scale. Moreover, a comparison between statistical information, derived from CPTUs, with a cross sectional area of 10 cm² and 5 cm², has been presented.

The study undertaken aims at achieving the following objectives:

1. to develop a statistical procedure for detecting layer boundaries and determine the depth of anomalies, which can be attributed to lenses or local heterogeneities;
2. to calculate a representative mean trend, standard deviation and the scale of fluctuation for lacustrine clay from the Wauwil site;
3. to investigate the differences between data for piezocones with cross sectional areas of 10 cm² and 5 cm², which can be exploited for statistical analyses.

Normalised cone resistance Q_t , that is:

$$Q_t = \frac{q_{T,net}}{\sigma'_{v0}} \quad (1)$$



Figure 1. Swiss lacustrine clay distribution (source: Hydrogeological map of Switzerland, after Trausch Giudici 2004).

has been considered as the primary parameter because it reflects mobilisation of a spherical volume ahead of the penetrometer and can be used in all stages of soil characterisation, from lithological to mechanical. The authors focused on the Q_t readings from CPTUs reported in Fig. 2, namely: A201, A202, A303, A304.

The following steps are necessary in order to derive the spatial random structure of this parameter:

1. To recognise homogeneous soil layers;
2. To de-trend the measurement profiles in order to determine residuals;
3. To verify the weak stationarity of residuals and calculate their standard deviation;
4. To calculate the autocorrelation function and to fit it by means of autocorrelation models;
5. To derive the fluctuation scale from the best fitting autocorrelation model.

Such tasks can be accomplished by means of different methods. The authors present a combination of the intraclass correlation coefficient RI (Wickremesinge & Campanella 1991), the modified Bartlett method (Phoon et al., 2003) and the moment method (Fenton 1999).

Furthermore, the de-trending step (step 2) has been undertaken over the original Q_t readings by means of the ‘most likelihood’ rule. The s_u trend functions have been derived for each layer from these results by means of the following equation:

$$s_u = \frac{Q_t}{N_{kt}} \cdot \sigma'_{v0} \quad (2)$$

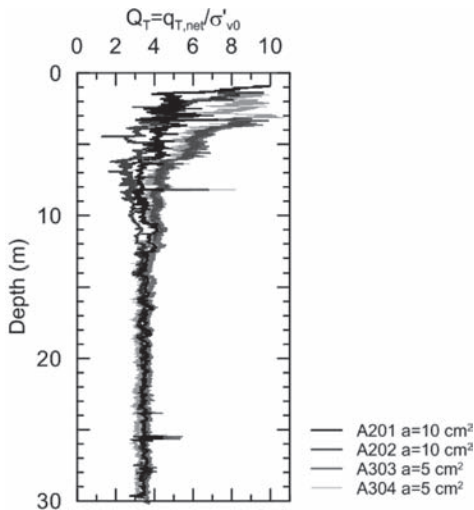


Figure 2. Q_t profiles from Wauwil site.

where N_{kt} is the cone factor assumed to be equal to 17. Figure 3 reports the trend functions calculated by this study on the A201 s_u profile (which is representative of the studied readings) at the Wauwil site and the one derived from Springman et al. (1999) at Kreuzlingen, on the shores of Lake Constance. Table 1 shows results from a statistical standpoint.

Table 1. Statistics of spatial variability of s_u derived from CPTUs conducted at A201.

Depth [m]	Autocorrelation fitting model	s_u Standard deviation [kPa]	Scale of fluctuation [m]
A201			
0.8 ÷ 3.4	Cosine exponential	0.79	0.3
3.4 ÷ 15.5	Cosine exponential	0.96	0.9
15.5 ÷ 24.4	Cosine exponential	0.88	0.16
24.4 ÷ 28	Binary noise	1.5	0.06
28.0 ÷ 31	Cosine exponential	1.35	0.071

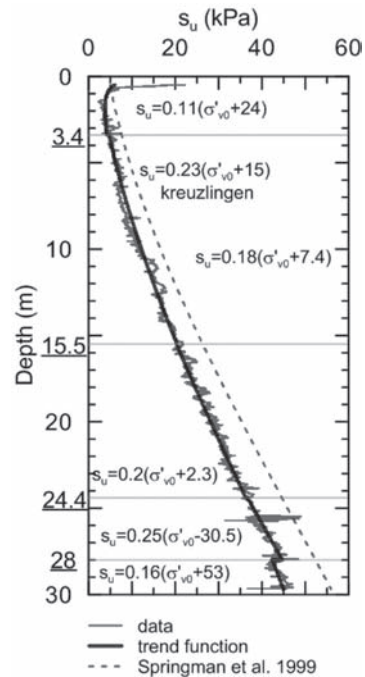


Figure 3. Comparison between s_u trend functions calculated for the A201 CPTU by this study at Wauwil and at Kreuzlingen by Springman et al. (1999).

3 CONCLUDING REMARKS

A statistical investigation at the Wauwil site has been developed. Accordingly, the following conclusions can be drawn:

1. Up to a depth of 28 m, s_u values increase with depth with an almost linear and continuous trend, as expected in a normally consolidated clay; at 28 m depth, a discontinuity in s_u values has been deduced from the data.
2. A more variable statistical structure for the s_u values has been found below 15.5 m depth. Further results show that the deterministic profiling must be improved. Moreover, for

design purposes, s_u values below a depth of 15.5 m shall be taken with less confidence with respect to the values related to the shallower layers.

Finally, differences have been highlighted on the capacity for detection of the layering between Q_t readings from piezocones with 10 cm² and 5 cm² cross sectional areas: these outcomes seem to be due to the relative dimension of the soil volume mobilised during the cone penetration with respect to the fabric of the soil and the lens/boundary thickness and stiffness. Further study is needed to demonstrate conclusive evidence of this hypothesis.

Dynamic response variability of a small span bridge for high speed rail traffic

J. Rocha, A.A. Henriques & R. Calçada
University of Porto—Faculty of Engineering, Porto, Portugal

1 OBJECTIVES/ DESCRIPTION

The main purpose of this work is to evaluate the sensitivity of small span bridges in high speed railway lines to the resonance phenomena bearing in mind the real variability of the parameters that influence the bridge dynamic response. Simulation techniques, namely the Monte Carlo and Latin Hypercube methods, were applied as they allow an accurate consideration of the randomness of structural parameters that influence the bridge dynamic response. Several simulations scenarios with different sample sizes were analysed and, with those results, a safety assessment of the bridge was performed.

As a case study, the railway bridge of Canelas, located in the Northern line of the Portuguese railway, was selected. The bridge has six simply supported spans of 12 m each leading to a total length of 72 m. The bridge deck is a composite structure and has two half concrete slab decks with nine embedded rolled steel profiles HEB 500, each supporting one rail track. This is a very common structural solution for small span bridges in the European high speed railway lines, especially in France and Germany.

After selecting the random variables that allow the definition of the problem in study, and before

proceeding to the analysis of the several simulation scenarios, a variable screening procedure based on a sensitivity analysis was carried out. The objective of this procedure is to assess the importance that each random variable has on the structural dynamic response. The variables which relevance is smaller than a pre-established value (10%) are considered as deterministic in further analysis.

Furthermore, a safety assessment of the bridge was done based on the results obtained in the simulations in order to evaluate the train speed limits on the bridge.

2 RELEVANT RESULTS

The structure acceleration is, among the other variables, the parameter with a higher relevance for the studied problem and is shown in Figure 1.

As it can be seen in Figure 1 the obtained results in terms of mean values and standard deviation values are consistent for different simulation methods applied in the study and for the different sample sizes analyzed.

However, when comparing the maximum acceleration response values obtained for the two simulation methods a higher dispersion of the results can be observed.

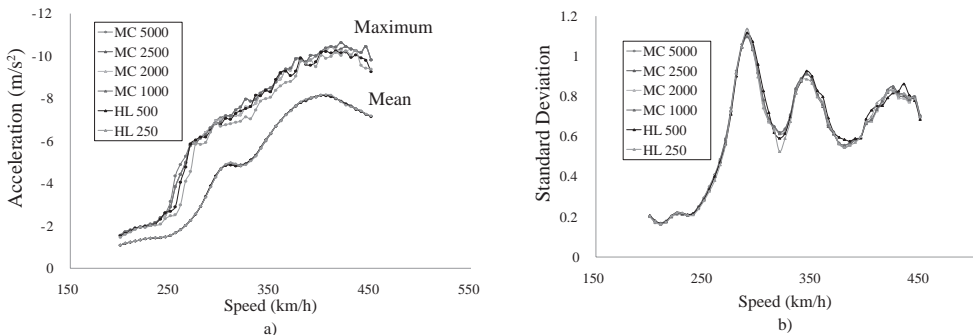


Figure 1. Comparison of the accelerations for the different simulation scenarios: a) mean and maximum values; b) standard deviation values.

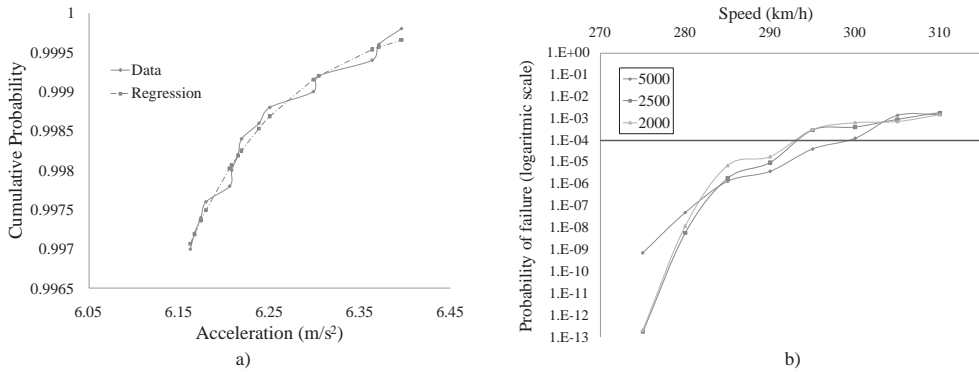


Figure 2. Safety assessment: a) Regression function; b) Probability of failure.

This turns out to be a key issue for the analysis since the maximum values are the ones that have a higher importance in the assessment of structural safety.

In order to establish speed limits for the high speed trains that might pass on the bridge a safety assessment of Canelas bridge was performed based on the obtained results for the several simulation scenarios. This analysis was based on the acceleration values registered at mid span of the bridge which turned out to be the most restrictive aspect of the response.

A curve was fitted to the upper extremity of the cumulative probability function in order to perform a safety assessment of the bridge. For this safety assessment several types of regression functions were used, namely sigmoidal and exponential functions. One of the performed regressions is shown in Figure 2 as well as the probability of failure evaluated for the analysed train speeds and for different sample sizes.

3 CONCLUSIONS

By comparing the results from the two applied simulation methods it can be confirmed that the Latin Hypercube method is more efficient than the

Monte Carlo method. It can be seen that with only one quarter of the simulations the mean values and the scatter of the bridge response obtained by Latin Hypercube is very similar to the results obtained by the Monte Carlo method.

However, the analysis of the maximum response values obtained for the two simulation methods shows a significant difference between them. Since these are the values that have a higher importance in structural reliability problems this turns out to be a relevant aspect and does not allow the applicability of the Latin Hypercube method to this problem due to the inadequate representation of the interest zone. Furthermore, and since one of the goals of this paper was to perform a safety assessment of the bridge, it was observed that only for samples with more than 2000 simulations the probabilities of failure obtained are reliable because they allow to represent accurately the upper extremity of the of the response distribution.

Taking into account the type of the studied problem, probability values up to 10^{-4} are considered to be acceptable to measure admissible failure due to the instability of the ballast layer. Analysing Figure 2, it can be seen that this value is not exceeded for speeds lower than 290 km/h, making this the train speed limit on the bridge.

This page intentionally left blank

Under the pressure of harsh environmental conditions and natural hazards, large parts of the world population are struggling to maintain their livelihoods. Population growth, increasing land utilization and shrinking natural resources have led to an increasing demand of improved efficiency of existing technologies and the development of new ones. Additionally, growing complexities of societal functionalities and interdependencies among infrastructures and urban habitats amplify consequences of malfunctions and failures. Malevolence, sustainable developments and climatic changes have more recently been added to the list of challenges. Over the last decades, substantial progress has been made in assessing and quantifying risks. However, with regard to the broader utilization of risk assessment as a means for societal strategic and operational planning, there is still a great need for further development.

Applications of Statistics and Probability in Civil Engineering

contains the proceedings of the 11th International Conference on Applications of Statistics and Probability in Civil Engineering (ICASP11, Zürich, Switzerland, 1-4 August 2011). The book focuses not only on the more traditional technical issues, but also emphasizes the societal context of the decision making problems including the interaction between stakeholders. This holistic perspective supports the enhanced and sustainable allocation of limited resources for the improvement of safety, environment and economy. The book is of interest to researchers and scientists working in the field of risk and reliability in engineering; to professionals and engineers, including insurance and consulting companies working with natural hazards, design, operation and maintenance of civil engineering and industrial facilities; and to decision makers and professionals in the public sector, including nongovernmental organisations responsible for risk management in the public domain, e.g. building authorities, the health and safety executives, the United Nations and the World Economic Forum.



6000 Broken Sound Parkway, NW
Suite 300, Boca Raton, FL 33487
Schipholweg 107C
2316 XC Leiden, NL
2 Park Square, Milton Park
Abingdon, Oxon OX14 4RN, UK

